iJERGS International Journal of Engineering Research And General Science

Journal which deals with research, Innovation and Originality

International Journal Of Engineering Research and General Science

ISSN 2091 - 2730

Table of Content

CHIEF EDITOR BOARD

Message from Associate Editor In Chief

Let me first of all take this opportunity to wish all our readers a very happy, peaceful and prosperous year ahead.

This is the sixth Issue of the Third Volume of International Journal of Engineering Research and General Science. A total of 118 research articles are published and I sincerely hope that each one of these provides some significant stimulation to a reasonable segment of our community of readers.

In this issue, we have focused mainly on the Global challenges and its innovative solutions. We also welcome more research oriented ideas in our upcoming Issues.

Author's response for this issue was really inspiring for us. We received many papers from many countries in this issue but our technical team and editor members accepted very less number of research papers for the publication. We have provided editors feedback for every rejected as well as accepted paper so that authors can work out in the weakness more and we shall accept the paper in near future. We apologize for the inconvenient caused for rejected Authors but I hope our editor's feedback helps you discover more horizons for your research work.

I would like to take this opportunity to thank each and every writer for their contribution and would like to thank entire International Journal of Engineering Research and General Science (IJERGS) technical team and editor member for their hard work for the development of research in the world through IJERGS.

Last, but not the least my special thanks and gratitude needs to go to all our fellow friends and supporters. Your help is greatly appreciated. I hope our reader will find our papers educational and entertaining as well. Our team have done good job however, this issue may possibly have some drawbacks, and therefore, constructive suggestions for further improvement shall be warmly welcomed.

Er. Pragyan Bhattarai,

Associate Editor-in-Chief, P&REC,

International Journal of Engineering Research and General Science

E-mail -Pragyan@ijergs.org

International Journal of Engineering Research and General Science Volume 3, Issue 6, November-December, 2015
ISSN 2091-2730

Wavelet Analysis of Meteorological Data Collected by an Automated Microcontroller-Weather Station System

Maria Teresa Caccamo, Antonio Cannuli, Salvatore Magazù

Dipartimento di Scienze Matematiche e Informatiche, Scienze Fisiche e Scienze della Terra, Messina University, Messina, Italy,
Email: mcaccamo@unime.it, +390906765025

Abstract — The present paper reports the findings obtained through a wavelet analysis, applied to meteorological data collected by means of a LSI-LASTEM weather-station, connected to a microcontroller. For the data collection, the station was located at the Polo Papardo of Messina University (38° 15' 35.10'' N latitude and 15° 35' 58.86'' E longitude), while a multi-scale wavelet approach was employed for the data analysis. The first part of the work is addressed to the data acquisition system description, which also includes the sensors and the remote microcontroller. Then, the wavelet protocol is introduced and applied by means of both continuous and discrete wavelet transforms; this method provides a time frequency representation of the analyzed signals, capable of highlighting the correlation among the registered meteorological parameters. The analysis through the evaluated wavelet scalograms shows that for all the months a positive correlation between maximum temperature and minimum temperature exists whereas, contrarily to what in most cases occurs, a constant negative correlation exists between daily rainfall and maximum temperature as well as daily rainfall and minimum temperature.

Keywords — Weather monitoring, Automatic weather station, Meteorological parameters, Weather meters, Weather analysis, Continuous and Discrete wavelet transforms, Wavelet data analysis.

INTRODUCTION

An automated weather station is a meteorological device, which is able to collect climatic data and through a specific microcontroller to register and to send them to a remote control system. It is often used to satisfy several needs ranging from simple weather monitoring to data acquisition addressed to model development for weather forecasts, to support air pollution analyses and to provide useful information in many fields such as, for example, agriculture, renewable energy and building automation [1]. As a rule, it is possible to classify such devices into two different groups: weather stations that provide data in real-time and others, classified as offline, that do not record data in real-time. A real-time weather station can provide data to users at programmed times, in emergency conditions so allowing to monitor possible critical warning states such as storms, river or tide levels on particular requests. An offline station records data on internal or external data storage devices, or on a website. Accuracy and specifications should adhere to the standards of the World Meteorological Organization (WMO) [2]. In the present work, the meteorological physical parameters collected by a meteorological station sat at Messina University are analyzed by means of both Discrete Wavelet Transform (DWT) and Continue Wavelet Transform (CWT). In particular, the analyzed quantities are the maximum and minimum temperatures and the total daily rainfall for the three years: 2012, 2013 and 2014. As we shall see, the analysis shows that a positive correlation between maximum temperature and minimum temperature exists whereas a negative correlation exists between daily rainfall and maximum temperature as well as daily rainfall and minimum temperature [3]. The obtained findings are discussed in the framework of current theories.

DATA ACQUISITION SYSTEM

The data acquisition system is a LSI LASTEM weather station able to capture typical meteorological parameters such as temperature, relative humidity, wind speed, wind direction, barometric pressure, solar radiation and rainfall [4]. Such a station is integrated by a microcontroller for the remote connection. It is well known that, as far as sensors are concerned, they can be classified as analogue, digital and intelligent depending on their output characteristics: in analog sensors, the output is commonly in the form of voltage, current, charge, resistance or capacitance and signal conditioning converts these basic signals into voltage signals; digital sensors contain the signal in a bit or bit group and sensors with pulse or frequency output; finally intelligent sensors or transducers include a microprocessor performing basic data acquisition and processing functions and provide an output in serial digital or parallel form [5].
The employed weather station consists of a 12 inputs data logger, a sensors kit and a software for acquisition programming and data transfer. Each component is specifically designed for long-term operation in extreme conditions. The heart of the system is the data logger in which the values are stored. The data logger is housed within an IP65 box, together with a barometer, data communication systems and power supply. The E-Log data logger, whose characteristics are reported in Table 1, allows the signals acquisition from the meteorological sensors, the processing and the storing of statistical values and the typical calculations of the weather applications with a particularly low power consumption. Different types of communications equipment are possible, such as GPRS or TCP/IP;

these can be used to data transfer on the LSI LASTEM web application, where it is possible to view the latest measurement values, to download and produce reports at any time and from any platform. The system is also equipped by standard MODBUS or TTY serial outputs to connect the weather station to other devices (see Fig.1). In our case, the station is remotely connected via microcontroller [6]. The results will be a series of observations which are representative over limited area and which can be analyzed through multiresolution approaches such as those offered by wavelet methods. In the recent years, the wavelet analysis methods have become a useful and a powerful tool for characterizing the variations, the periodicities, the trends of a time series of meteorological parameters.

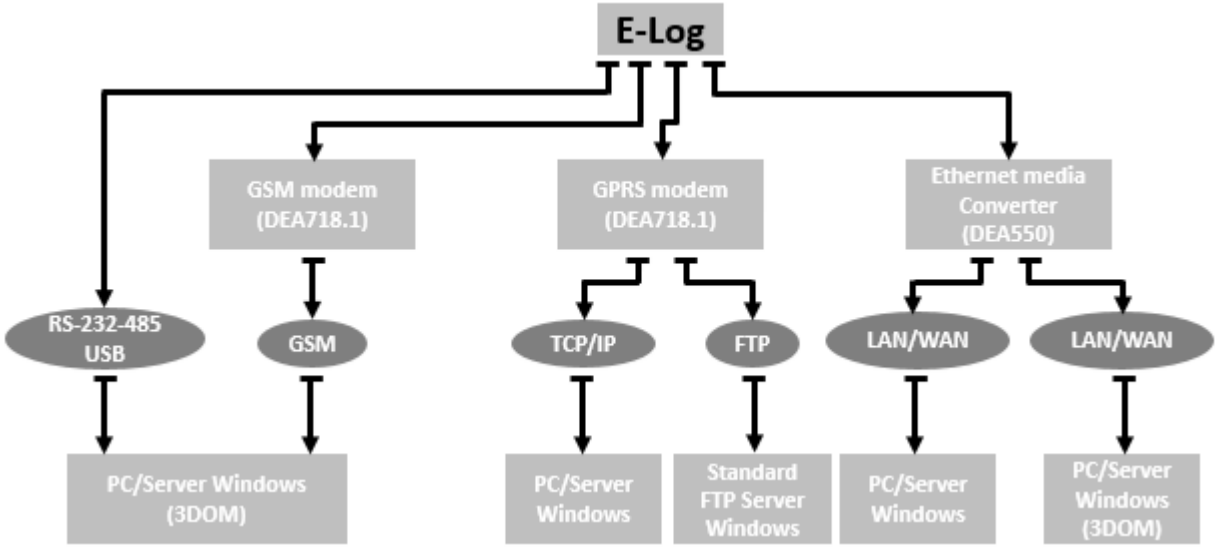

Fig. 1: Type and communications protocols scheme

E-log Environmental Data Logger		Field	Resolution	Uncertainty
Analog inputs	Voltage	-300 ÷ 1200 mV	40 µV	± 160 µV
		± 78 mV	5 µV	± 30 µV
		± 39 mV	1.5 µV	± 15 µV
	Pt100	-50 ÷ 70 °C	0.003 °C	± 0.1°C
		-50 ÷ 600 °C	0.011 °C	± 0.3°C
		0 ÷ 4000 Ω	0.1 Ω	± 1.5 Ω
	Thermo-couples	E-IPTS 68	< 0.1 °C	± 0.6 °C
		J-IPTS 68	< 0.1 °C	± 0.6 °C
		J - DIN	< 0.1 °C	± 0.6 °C
		K-IPTS 68	< 0.1 °C	± 0.6 °C
		S-IPTS 68	0.22°C	± 2.0 °C
		T-IPTS 68	< 0.1 °C	± 0.6 °C
	Inputs number	n. 8 differential (16 single-ended)		
	ESD protection	± 8 kV contact discharge IEC 1000-4-2		
	Max input signal	1.2 V		
	EMC filters	on all inputs		
	Temperature error (0 ÷10+30 °C)	300 ÷ 1200 mV = ± 0.01% FSR ± 39 mV < ± 0.01% FSR ± 78 mV < ± 0.01% FSR		
Digital inputs	Inputs number	n. 4		
	Function	n. 4 inputs frequency/counters/logic state On/Off (signals 0 ÷ 3 Vcc); n. 2 for optoelectronic sensors, max 10 kHz n. 2 max inputs 1 kHz		
	Uncertainty	3 Hz @ 5 kHz		
	Protection	Transient voltage suppressor 600 W, <10 µs		
Digital outputs	Outputs number	n. 7 (n. 6 for sensor/events, n. 1 for power supply commutation apparatus)		
	Max current available	700 mA for each output, 1.2 A max. for all outputs		
	Protections	Thermal and overcurrent		
Power supply	Power supply	8 ÷ 14 Vcc		
	Consumption	< 140 mW display on Stand-by display off: < 4 mW		
	Protection	Transient voltage suppressor: 600 W, t < 10 µs; on polarity inversion		
Radio	Type	ZigBee		
	Frequency	ISM 2.4 GHz direct sequence channels		
	Power	10 mW (+10 dBm)		
Other	Internal clock	Accuracy 30 s/month (T amb. = 25 °C)		
	Display	LCD 4 x 20 car		
	Keyboard	n. 8 buttons		
	Processor	1 RISC 8 bit, clock 16 MHz		
	ADC resolution	16 bit		
	Acquisition time	80 ms (rejection 50 Hz)		
	Data memory	Flash EEPROM 8 Mb		
	Environmental limits	-20 ÷ 60 °C, 15 ÷ 100 % RH		
	Protection	IP 40		
	Weight	500 g		
	Dimension	140 x 120 x 60 mm		
RS232 port	Speed	1200 ÷ 115200 bps		
	Type	DB 9 pin female/DCE		

Tab. 1: E-log Environmental Data Logger characteristics

Weather meters consist of a wind speed meter, a direction meter, a thermo-hygrometer, a barometer, a radiation sensor, a rain gauge and an atmospheric pressure sensor. The speed wind meter is a DNA202 sensor, characterized by compact size and a robust structure and of rotor and it is suitable to acquire low and high speeds up to 75 m/s. The sensing element is a high efficiency and durability relay-reed. The sensor body is made of anodized aluminum, while the rotor is made of carbon fiber reinforced. The direction wind meter is a DNA212 sensor; it is very compact, sturdy and suitable both in very low and strong wind conditions; it is up to durability applications without maintenance. The measuring element is a Hall Effect transducer and the sensor body is composed of anodized aluminum. The above two sensors are completed of a cable L= 3m with connector IP65. The thermos-hygrometer is a temperature and relative humidity sensor. It is specifically dedicated to meteorological applications where there may be rapid thermo-hygrometric variations and there may be long periods of hygrometric saturation. An anti-radiation shield protects the sensor from solar radiation by ensuring the best accuracy of the temperature measurement. The sensor used to measure barometric pressure has an accuracy of 1hPa; it is housed in the same box (IP65), where the data logger is fit. The sensor for the solar radiation measurement obeys the requirements of Class 2 of the standard ISO9060 and specific WMO No. 8; it is lightweight and compact. The rain gauge is characterized by an exterior part of anodized aluminum. The measurement system consists of a collector cone and a teeter connected to a magnet, which activates a reed relay, each teeter corresponds to 0.2 mm of rain. The rain gauge is mounted on a base positioned on a flat surface. Power supply is a key component of this system, because a continuous power supply is necessary to make the system work continuously. A rechargeable battery is connected with a solar panel. The software used to configure the data logger, diagnostic and data download is 3DOM. It allows to import and export configurations through serial cable to connect the E-log to a PC. The results will be a series of observations, which are representative over limited area which can be analyzed through multiresolution approaches such as that offered by the wavelet method.

RESULTS AND DISCUSSION

It's well known that wavelet transforms are a powerful tool for approaching complex problems in various fields such as engineering, mathematics, physics, meteorology and spectroscopic data analyses [7-12]. From a general viewpoint the wavelet analysis allows to decompose a signal into its wavelets component, highlighting the correlation between the primitive signal and the set of the scaled and translated mother functions; furthermore wavelet analysis, in respect to Fourier transform, shows which frequencies are present and where, or at what scale, they are; finally wavelets are also widely employed for the compression or de-noising of a signal, often without appreciable degradation. In order to analyze the meteorological parameters collected by means of a meteorological station, located at 38° 15' 35.10'' N latitude and 15° 35' 58.86'' E longitude, i.e. Messina University, both Discrete Wavelet Transform (DWT) and Continue Wavelet Transform (CWT) were applied. The registered meteorological quantities are maximum temperature, minimum temperature and total daily rainfall, for a period of three years between 2012 and 2014. Following the Köppen-Geiger classification, Messina has a Mediterranean climate with dry hot summers and mild winter; in particular, summers are dry and hot due to the domination of subtropical high-pressure systems while winters experience moderate temperatures and changeable, rainy weather due to the polar front and the annual mean temperature is 21, 71°C. In Fig. 2, the average of low temperature and the average of high temperature for the year 2014 are reported. As can be seen, the warmest months are July and August, with a value of 27,63°C and 28,90° respectively, on the other hands, the coolest months are January (11,72 °C) and February (11,69 °C).

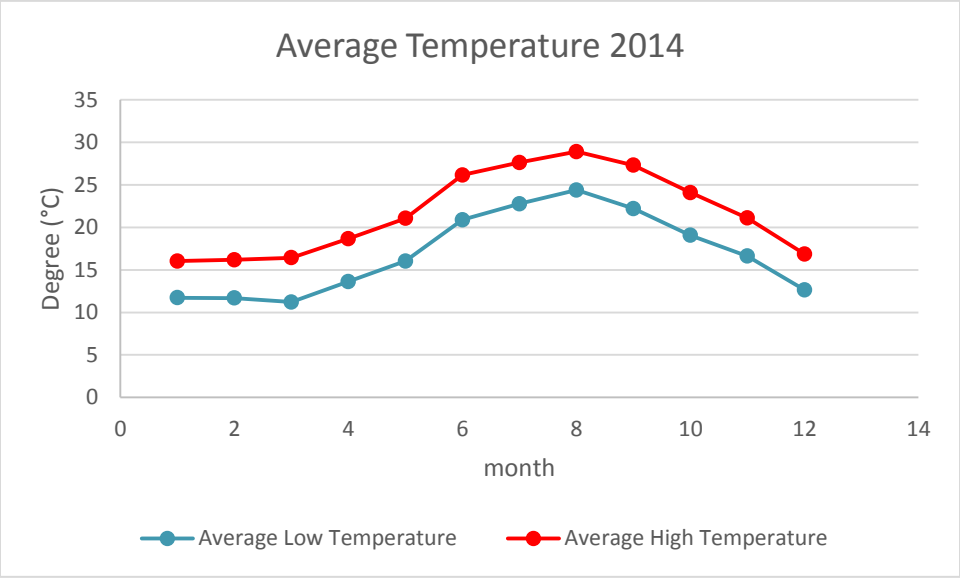

Fig. 2: Average low temperature and average high temperature for the year 2014

In Fig. 3, the annual rainfall for Messina in the year 2014 is shown. It can be seen that total annual precipitation averages 843.8 mm (33.2 inches) and the most rainfall is seen in January, November and December. November is the wettest month and August is the driest month.

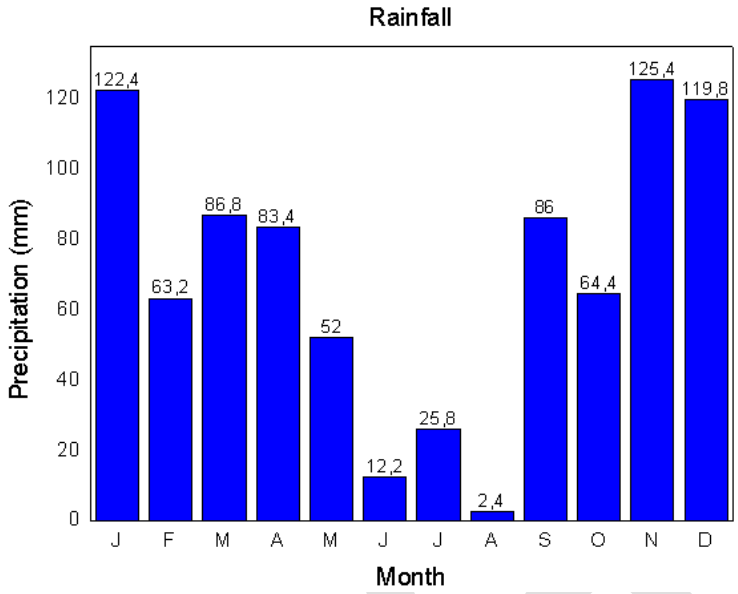

Fig. 3: Rainfall for the year 2014

As far as DWT is concerned, Daubechies (Db) wavelets, introduced by Ingrid Daubechies [13-14] were taken into account. It is well known that Db wavelet allows to split the investigated meteorological parameters into approximation coefficients, which correspond to the signal's low frequency components and into detail coefficients that represent the signal's high-frequency counterpart. In Figg. 4-6 the decomposition of maximum temperature, minimum temperature and total daily rainfall, as obtained by means of Daubechies transform at level 5 (Db5), using MATLAB Wavelets Toolbox, are shown. Such an analysis parameter set has been chosen in order to guarantee a good enough approximation coefficient a_5 which is connected to the general parameter trends, i.e. on a large time scale, whereas the detailed coefficients give account of the parameter variation on a short time scale [15]. In the Figg. 4-6 the first row represents the input investigated signal; the second raw reports the approximation coefficient: a_5 for db5, while d_1, d_2, d_3, d_4 and d_5 correspond to detail coefficients for five different levels.

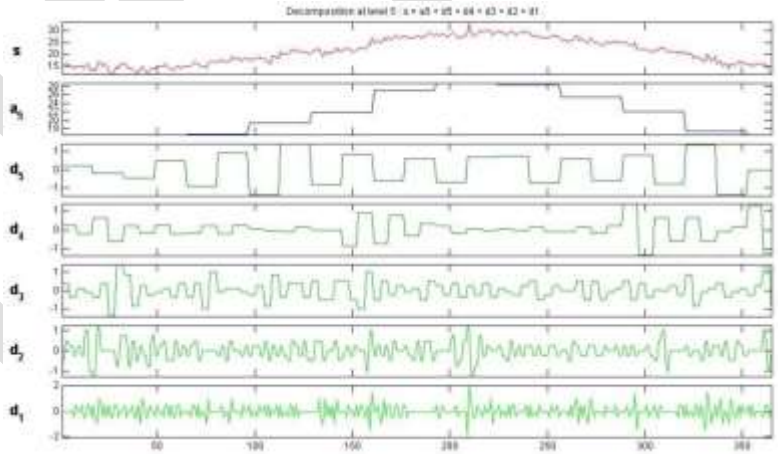

Fig. 4: Decomposition of maximum temperature data by means of the mother wavelet Daubechies at level 5

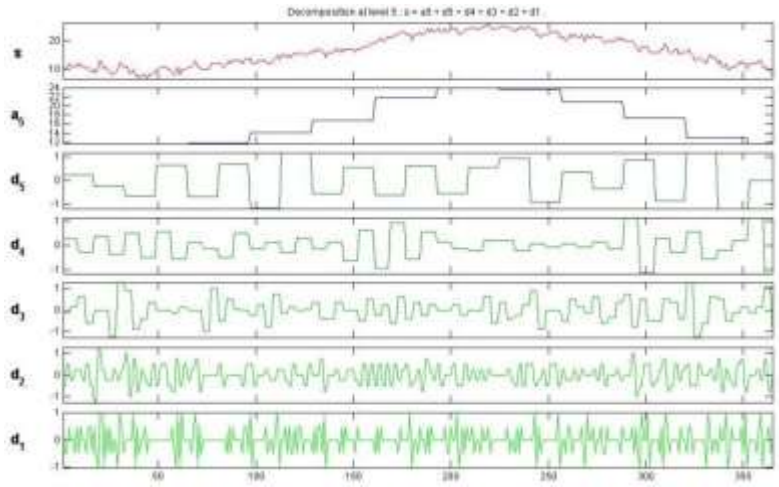

Fig. 5: Decomposition of minimum temperature data by means of the mother wavelet Daubechies at level 5

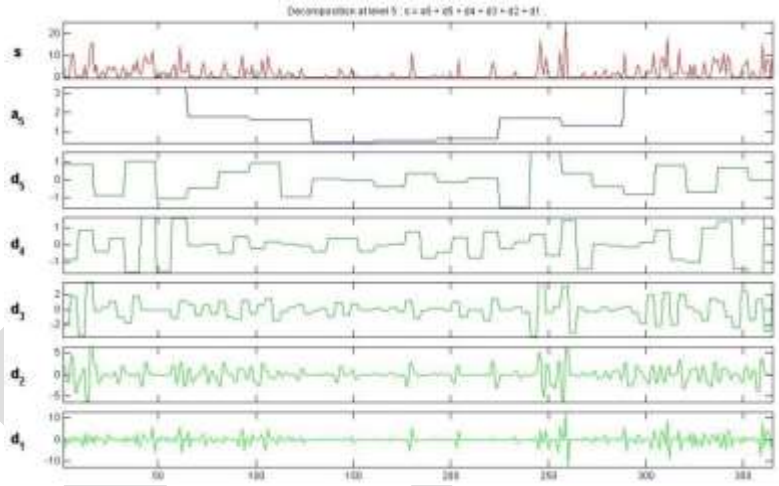

Fig. 6: Decomposition of rainfall data by means of the mother wavelet Daubechies at level 5

The analysis, performed by means of DWT, shows, through the evaluated approximation coefficients, i.e. a_5, of the two quantities, i.e. the maximum and minimum temperatures, and the detail coefficients, i.e. $d_1 \div d_5$, that, for each x-axis partition (i.e. time windows), a positive correlation between maximum temperature and minimum temperature exists for all the years, since a similar behavior is registered for such quantities; in particular the approximation and the detail coefficients as a function of time are in most the cases each other in phase. On the contrary, the evaluated approximation coefficients of the maximum and minimum temperatures and of the daily rainfall parameter, and the detail coefficients, for each time windows shows that a negative correlation (opposite correlation) exists between daily rainfall and maximum temperature as well as daily rainfall and minimum temperature; in fact the approximation and the detail coefficients as a function of time are in most the cases each other out-of-phase.
As far as CWT is concerned, the Mexican hat wavelet [16], whose name is due to the shape of the function that is like an upside-down Mexican hat, has been considered:

$$\psi(t) = \frac{2}{\pi^{1/4}\sqrt{3\sigma}}\left(\frac{t^2}{\sigma^2} - 1\right)\exp\left(-\frac{t^2}{\sigma^2}\right)$$

Its form represents the second derivative of a Gaussian function $\exp\left(-\frac{t^2}{2\sigma^2}\right)$. In Figg. 7-9 the Mexican Hat wavelet transforms for the maximum temperature, minimum temperature and total daily rainfall are shown. In particular, on the top of the figure the investigated signal is reported; in the second raw, the scalogram is shown. In the third row the daily variation of coefficients is reported and, finally, at the bottom figure, one finds the local maximum of the analyzed meteorological parameters; in all the figures the horizontal axis represents the number of days while the vertical axis shows the frequency values. From such an analysis, in respect to the

previous approach, it is possible to better appreciate the parameter variations both on an intermediate and on a fine time scales where a strong positive correlation between the two extreme temperatures is observed whereas the daily rainfall parameter emerges at low scale, i.e. fine time window, suggesting that it influences both the extreme temperature with a negative correlation [17-18].

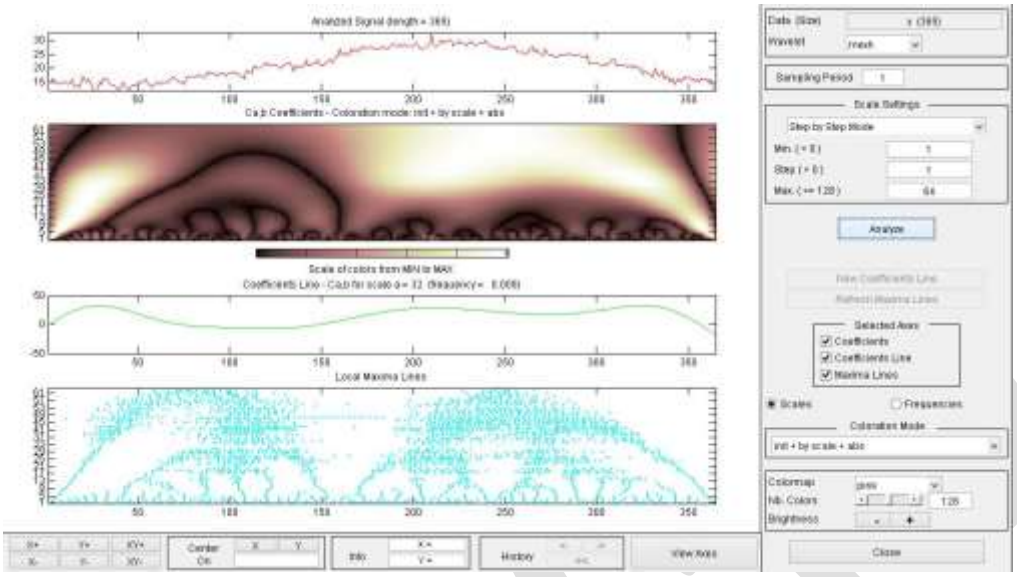

Fig. 7: Mexican hat Continuous Wavelet analysis of Maximum Temperature

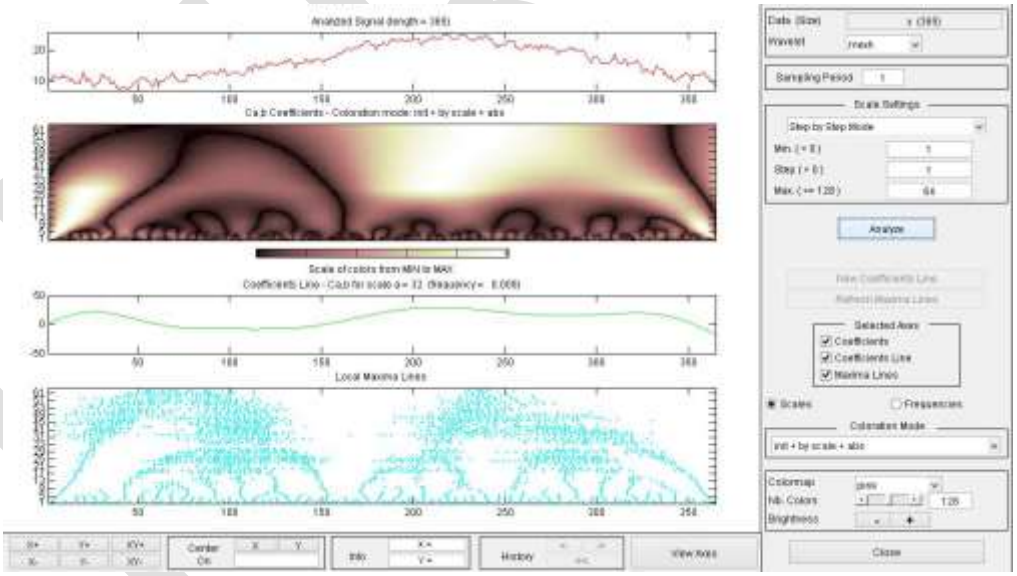

Fig. 8: Mexican hat Continuous Wavelet analysis of Minimum Temperature

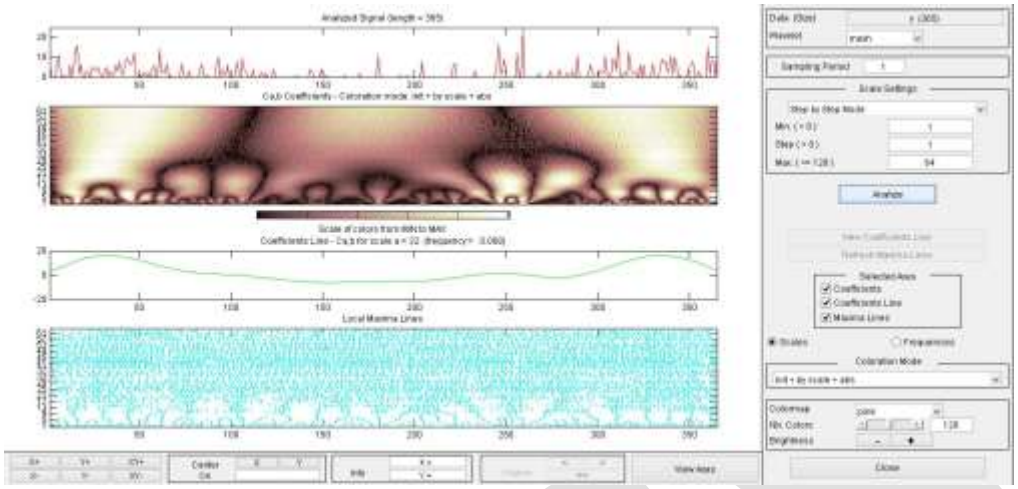

Fig. 9: Mexican hat Continuous Wavelet analysis of Rainfall

The analysis, performed by means of CWT, confirms, through the evaluated wavelet scalograms (second row), coefficient profiles values (third row) and local maxima (forth row) that a positive correlation between maximum temperature and minimum temperature exists for all the years, since a similar behavior is registered for such quantities. From a general point of view, a negative correlation is most frequent in summers, while negative and positive correlation appear about equally in other seasons. On the contrary, the same quantities reveal that a negative correlation exists between daily rainfall and maximum temperature as well as daily rainfall and minimum temperature all over the year.

CONCLUSION

In present work the results obtained by means of DWT and CWT to data collected by means of the LSI-LASTEM automatic weather station are reported. In particular, the weather station was interconnected to a microcontroller for the remote connection and was able to monitor weather and environmental parameters. The data acquisition system, the employed sensors and the remote connection microcontroller are described in the first section of the paper while, in the second part a wavelet approach, addressed to analyze the collected data series, is applied. From the analysis, it emerges that the maximum and minimum temperature parameters show a positive correlation for all the investigated years whereas a negative correlation is registered between rainfall and maximum temperature as well as rainfall and minimum temperature.

REFERENCES

[1] G. Booch, C. Robert, M. and J. Newkirk "Case Study: Weather Station." In Object Oriented Analysis and Design with Applications, 2d. ed. (1998) 59-112.

[2] "Geneva: World Meteorological Organization Geneva: World Meteorological Organization" Measurements at Automatic Weather Stations, WMO-No. 8, 2nd ed., (2010).

[3] K. M Lau, H. Weng, "Climate signal detection using wavelet transform: how to make a time series sing", Bulletin of the American Meteorology Society, 76 (1995) 2391-2406.

[4] G. Hoogenboom, D.D Gresham, "Auto weather station network ", Proceeding of the 1997 Georgia water resource Conference. Athens, vol.1 (1997) 483-486.

[5] K. Montgomery, K. Chiang, "A New Paradigm for Integrated Environmental Monitoring", ACM International Conference Proceeding Series (2010).

[6] Y. Zhengtong, Z. Wenfeng, "The research of environmental pollution examination system based on the Cloud Computing", International Conference on Communication Software and Networks, (2011) 514-516.

[7] S. Magazù, F. Migliardo, M.T. Caccamo, "Innovative Wavelet Protocols in Analyzing Elastic Incoherent Neutron Scattering", J.Phys. Chem. B, 116 (2012) 9417-9423.

[8] S. Magazù, F. Migliardo, B.G. Vertessy, M.T. Caccamo, "Investigations of Homologous Disaccharides by Elastic Incoherent Neutron Scattering and Wavelet Multiresolution Analysis" Chemical Physics. Chem. Phys, 424 (2013) 56-61.

[9] F. Migliardo, M.T. Caccamo, S. Magazù, "Elastic Incoherent Neutron Scatterings Wavevector and Thermal Analysis on Glass-forming Homologous Disaccharides" Journal of Non Crystalline Solids, 378 (2013) 144–151.

[10] F. Migliardo, M.T. Caccamo, S. Magazù, "Thermal Analysis on Bioprotectant Disaccharides by Elastic Incoherent Neutron Scattering" Food Biophysics, 9 (2014) 99-104.

[11] S. Magazù, F. Migliardo, M.T. Caccamo, "Upgrading of Resolution Elastic Neutron Scattering (RENS)", Advances in Materials Science and Engineering, 2013 (2013) 1-7.

[12] F. Migliardo, M.T. Caccamo, S. Magazù, "Innovative Signal Processing of Neutron Scattering Data through Multiresolution Wavelet Approach", International Journal of Advanced Computer Science & Application, 5 (2014) 50-53.

[13] Ingrid Daubechies, "Ten Lectures on Wavelets", Society for Industrial and Applied Mathematics. Beijing, 2004.

[14] Ingrid Daubechies, "The wavelet transforms time-frequency localization and signal analysis", Society for Industrial and Applied Mathematics. Beijing, 2004.

[15] S. G. Mallat, "A theory for multiresolution signal decomposition: the wavelet representation", IEEE Transactions on Pattern Analysis., 2 (1989) 674-693.

[16] Enders A. Robinson and Sven Treitel, "Geophysical Signal Analysis", Prentice-Hall, New Jersey, 1980.

[17] P. Kumar, E. Foufoula-Georgiou, "Wavelet analysis for geophysical applications", Reviews of Geophysics, 35 (1997) 385-412.

[18] R. Bhardwaj, "Wavelet & Correlation Analysis of Weateher Data", International Journal of Current Engineering and Technology, 2 (2012) 178-183.

International Journal of Engineering Research and General Science Volume 3, Issue 6, November-December, 2015
ISSN 2091-2730

Experiments with Fusion of Images with Use of Wavelet Transformation in Problems of the Text Information Analysis

Vyacheslav V. Lyashenko[1], Mohammad Ayaz Ahmad[2], Oleg A. Kobylin[3]

[1]The chief of the laboratory "Transfer of Information Technologies in the risk reduction systems", Kharkov National University of RadioElectronics, Ukraine, lyashenko.vyacheslav@mail.ru

[2]Physics Department, Faculty of Science, P.O. Box 741, University of Tabuk, 71491, Saudi Arabia, mayaz.alig@gmail.com

[3]Department of Informatics, Kharkov National University of RadioElectronics, Ukraine, oleg.kobylin@gmail.com

Abstract— An analysis of images is the powerful tool of research in various fields of knowledge. One of directions of application of such analysis is a computer processing of text information. There is defined a number of problems among existing variety of methods of image processing of a text, where a wavelet procedure of fusion of images is in the basis. There is carried out a number of experiments for the purpose of a substantiation of possibility and expediency of application of wavelet procedure of fusion of images for the computer processing and the analysis of text information. As a result of the carried out experiments, a complexity of a choice of a fusion method of investigated images and an estimation of quality of such fusion are shown. Necessity of use of adaptive procedures is proved at a choice of a fusion method of approximating and detailing coefficients of wavelet expansion.

Keywords— pattern recognition, Image, wavelet analysis, image fusion, approximating coefficients of wavelet expansion, detailing coefficients of wavelet expansion, computer analysis of text information.

1. INTRODUCTION

A computer processing and an analysis of text information is one of directions of the general theory of pattern recognition. A complexity of practical realization of such direction consists in necessity of the solution and the account of:

– traditional problem aspects which are inherent to the general problematics of the solution of problems by means of the pattern recognition theory [1, 2],

– specificity of recognition of text information which is connected, first of all, with specificity of concrete language representation of such information [3, 4].

Nevertheless, among such problem aspects it is possible to define the general problems which are necessary for solving in the course of computer processing and the analysis of text information. There are following problems:

– restoration of a fragment of the lost text,

– restoration of the text by means of fusion of several fragments,

– improvement of quality of perception of the text by computer system on the basis of removal of noise or increase of dearness of the analyzed text,

– identifications of the considered test on the basis of carrying out of the comparative analysis of the initial text with a database of various texts.

Thus as the tool which is used for the solution of the considered problems, it is possible to use separate procedures of wavelet analysis. Such choice is based on, that a wavelet analysis is a quite powerful device used in pattern recognition and processing of images. It is connected with that the use of procedures of wavelet analysis gives:

– possibility of the account for various aspects of investigated images from the point of view of a way of their representation,

– possibility of use of various approaches for underlining of any aspects of representation of visual images in the course of their the subsequent processing.

It, finally, defines the interest in a choice of a considered subject of research.

2. WAVELET TRANSFORMATION AS METHODOLOGY OF PROCESSING OF IMAGES

The wavelet transformation is an expansion of a signal on system of wavelets. Wavelets are made by shift and scaling of one function – a generating wavelet [5]. In this case a wavelet is a function which rapidly decreases on infinity and its average value is equal to zero. If the signal has a gap then high amplitudes will be present only in those wavelets which maximum appears next to a gap point. A gap is a sharp discontinuous transition during any process. Quantitatively it can be estimated in size of the first derivative

of such process. There, where the jumps take place, the first derivative is very great. If jump has a gap form, the first derivative aspires to infinity. However, the real processes which are measured by physically real devices cannot have ideal gaps. Actually, measured fractural transitions are characterized by final value of a derivative. The more sharply gap, the greater value of a derivative. Smooth transitions will have small values of a derivative. Because of this fact, it is possible to define presence of features of a signal as well as a point where it is shown.

Thus, the main idea of the wavelet transformation – time-and-frequency representation of a signal [5]. From the formalized point of view under a wavelet transformation (W) we understand expansion by means of functions, where each of them is the shifted and scaled copy of one function – a parent wavelet [5, 6].

Continuous wavelet transformation of function $f(t)$ is defined by expression:

$$W[f(t)] = \frac{1}{\sqrt{a}} \int_{-\infty}^{+\infty} f(t) \cdot \varphi\left(\frac{t-b}{a}\right) dt, \qquad (1)$$

where a – scale;

b – centre of time localization;

function $\varphi(t)$ is a parent wavelet and it satisfies to a condition:

$$\int_{-\infty}^{+\infty} \varphi(t)dt = 0. \qquad (2)$$

Function of continuous wavelet transformation is applicable for one-dimensional signals, and the image is a two-dimensional signal. Therefore the discrete wavelet transformation is applied to processing of images in the assumption, that [7]:

values a, b accept only discrete values,

accordingly integration is replaced with summation which is separately conducted for every line and every column of the analyzed image.

If we have some input image B which is presented in the form of a matrix $B(x,y) \in L_2(R)$ then its wavelet expansion at each level of decomposition can be presented in the form of the scheme [8] shown on figure(1) (sign $2\downarrow$ – image decimation, L – low-frequency filter, H – high-frequency filter).

x, y – current co-ordinates of the matrix of the values of image B which displays co-ordinates of a line and a column, and $B(x,y)$ – quantitative value of an element of the image with co-ordinates (x,y).

i ($i = 1,2,...j$, $N = 2^j$ N – a linear size of the initial analyzed image) is a level of wavelet expansion of the initial (input) image (the image which is exposed to wavelet expansion or decomposition in future).

vv – an input image in the form of the matrix $B(x,y)$. Target images are designated accordingly – $v1^{(i)}, v2^{(i)}, v3^{(i)}, v4^{(i)}$ where $v1^{(i)}$ – the reduced copy of the initial image, and, $v2^{(i)}, v3^{(i)}, v4^{(i)}$ – images of wavelet expansion of the initial image across, verticals and diagonals for the certain level of expansion i.

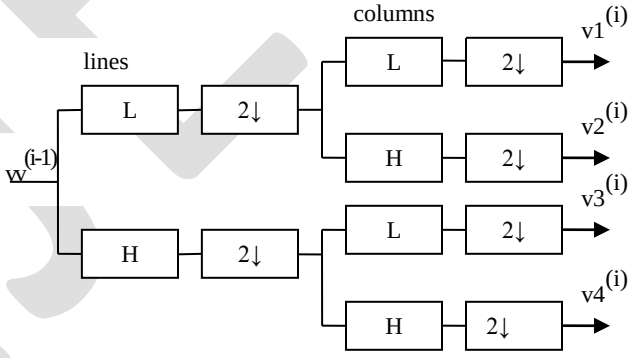

Figure (1): Two-dimensional discrete wavelet transformation

Thus, the result of consecutive wavelet expansion of some image is its multilevel representation in the form which is represented on figure (2). Figure (2) as an example shows schematic two-level wavelet expansion of the initial image B, where B2 – the reduced copy of the initial image B on the second level of expansion; H, V and D – accordingly images of wavelet expansion of the initial image across, verticals and diagonals for the certain level of expansion.

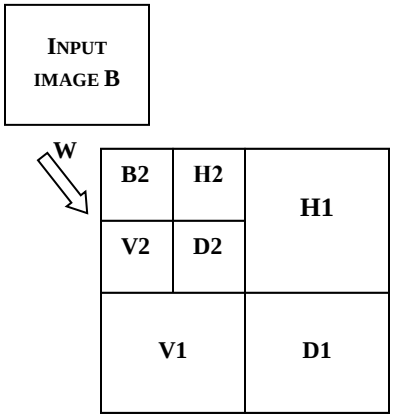

Figure (2): Schematic representation of wavelet expansion

Expansion of the initial image with the help of wavelet transformation, in particular, allows to compress the initial image for its subsequent transfer through communication channels and in the subsequent to restore, using the reverse wavelet transformation (W^{inf}) [9]. Thus, application of updating procedure which is used taking into account separate levels of wavelet expansion is possible before restoration of the compressed image. The essence of such updating consists in use of image fusion procedure for separate levels of expansion of initial images therefore the new and modified wavelet expansion of some investigated image has appeared. Figure (3) shows schematic representation of process of updating of some wavelet expansion of the initial image B by means of wavelet expansion of the auxiliary image C where in the result we'll get the modified image A [10].

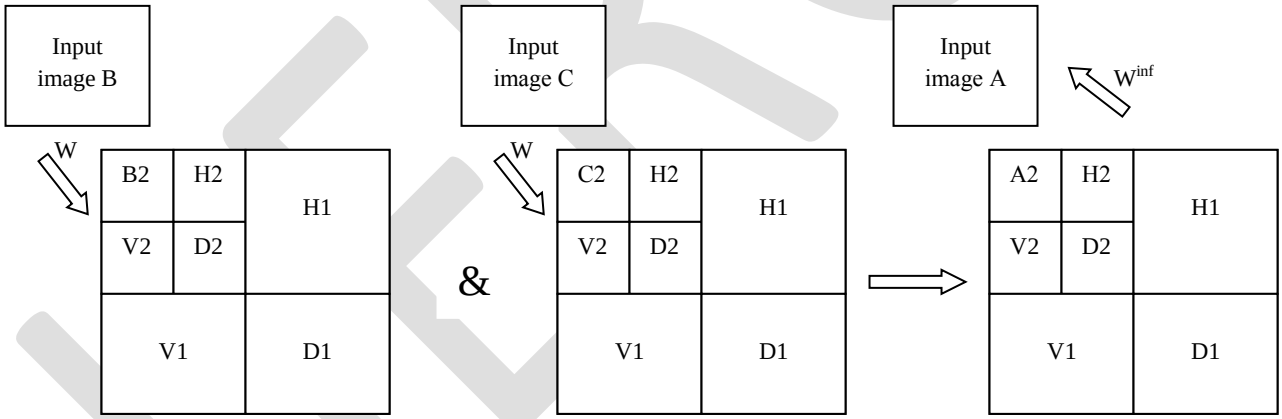

Figure (3): Schematic representation of the image updating by means of its wavelet expansion and the reverse wavelet transformation

Symbol & designates a way of fusion of the images which essence consists in application of certain procedure of fusion of approximating and detailing coefficients [9, 10] which are the result of wavelet transformation (expansion) of input images B and C [7, 8].

3. WAVELET IMAGE FUSION PROCEDURE AS A BASIS OF THE SOLUTION OF PROBLEMS OF COMPUTER PROCESSING AND THE ANALYSIS OF TEXT INFORMATION

The considered procedure of image fusion for their updating can be used both in problems of computer processing, and the analysis of text information. It is connected with that the wavelet image fusion procedure does not limit a spectrum of considered

initial images. The key moment in use of such procedure is the substantiation of the way of fusion of two images (&) depending on complexity of representation of the considered text, a context of a solved problem and various noise on images.

Thus it is necessary to notice, that questions of possible use of the wavelet image fusion procedure are considered in works of different authors:

in research of K. Amolins, Z. Yun, and D. Peter variety of different methods, ways and schemes of association of images in comparison with the wavelet image fusion procedure where achievement of the most desirable characteristics undertakes a basis of an estimation of quality of such fusion in the general image which are inherent in initial images [10] are in detail considered;

in research of W. Shi, C. Zhu, Y. Tian and J. Nichol at consideration of wavelet image fusion procedure, the emphasis is placed on an estimation of quality of the obtained image after fusion of initial images. Thus as such estimation it is offered to use coefficient of an average and standard deviation for the values of initial and processed images, and correlation coefficient between initial and processed images as a measure of distortion of the analyzed information [11];

P. R. Hill, C. N. Canagarajah and D. R. Bull investigate quality of fusion of images depending on wavelet functions which are applied to such procedure [12];

Z. Wang, D. Ziou, C. Armenakis, D. Li and Q. Li analyze productivity of different procedures of fusion, placing thus emphasis on a preliminary filtration of initial images for the purpose of reduction of influence of noise by fusion process at reception of the final image [13];

S. Li and B. Yang study possibility of combined use of different methods and approaches at image fusion [14].

Thus, there is a set of different researches where the analysis and research of existing procedures of image fusion is carried out. At the same time the estimation of quality of image fusion depends on its concrete application. In different applications various aspects of the account of quality of the image can be demanded. At the same time it is necessary to notice, that the main objective of image fusion, in particular at processing of text information, consists in increase of visibility of the initial text. It is necessary to have possibility to read and work with a text. Finally, it defines the objective of this research.

4. RESULTS AND DISCUSSION

For the purpose of realization of the object in view of research, there has been carried out the analysis of quality of wavelet image fusion procedure which assumes the solution of the following problem – restoration of the initial image on the basis of fusion of two images with loss of separate fragments of the text.

For this purpose it is considered:

The initial image (figure (4)) – the original of the text which has been lost,

Two images with partial loss of various fragments of the text (figure (5), figure (6)) which are used in fusion procedure.

Figure (4): The initial image of the text

Figure (5): The image 1 from the partial fragment loss

Figure (6): The image 2 with partial fragment loss

Thus, the experiment essence consists in fusion of the images presented on figure (5) and figure (6) and comparison of some image obtained at such fusion with the image which is presented on figure (4).

Each of the presented images is the binary image which characteristics are:

the general number of points of the image (N),

the number of points of the text (I) –they are marked with black color on figures,

the number of background points (F) –they are marked with white color on figures.

Characteristics of considered images are presented in table (1) according to figure (4), figure (5) and figure (6).

Table 1: Statistical characteristics of analyzed images

Images	Characteristics		
	N	I	F
Figure (4)	64616	13376	51240
Figure (5)	64616	10410	54206
Figure (6)	64616	10819	53797

As we can see from the table 1 for the image 1 (figure (5)) the loss of a fragment of points of the text makes 22,17 % from points of the original text or 4,6 % from the general number of points of the original image (figure (4)). For the image 2 (figure (6)) the loss of a fragment of points of the text makes 19,12 % from points of the original text or 3,96 % from the general number of points of the original image (figure (4)). Total loss of fragments of the text which are necessary for restoring makes 5523 points.

Wavelet fusion procedure of two images was carried out by means of wavelet Dobeshi-2 function and wavelet expansion on three levels. As a whole, the choice of concrete family of wavelets is dictated by applied problems and type of the initial information. Nevertheless, use of Dobeshi wavelets creates more smooth approximation of investigated input data, and it has formed a basis for its application in the given research, being based on work conclusions «Properties of wavelet coefficients of self-similar time series» [15]. The number of levels of expansion has been chosen based on the sizes of images and insignificant separately by each of parts of the lost fragments in relation to a total square of all original image.

Result of research was ascertainment of quality of fusion of two images (figure (5) and figure (6)) on the basis of use of various ways of fusion of two images (&).

For ascertainment of quality of fusion of considered images, in particular, it was considered:

the opinion of seven experts which compared the restored image with the original one (figure (4)). Each of experts on five-grade scale (from 1 – the worst quality to 5 – the best quality) estimated quality of fusion of two images. As a result the average estimation has been obtained;

quantity of points of the text of the restored image in relation to quantity of points of the text of the original image.

Results of estimation of quality of fusion of images are presented in table (2) on the basis of opinion of experts.

Table 2: An expert estimation of quality of fusion of images

Experiment number	Way of fusion of coefficients		Average estimation of experts
	approximating	detailing	
1	max	mean	2,86
2	max	rand	2,43
3	max	linear-0,5	2,71
4	max	Up-down fusion-1	2,57
5	max	Down-up fusion-1	2,57
6	max	Left-right- fusion-1	2,71
7	max	Right-left fusion-1	1,86
8	max	img1	1,57
9	max	img2	1,57
10	mean	max	3,57
11	rand	max	3,29
12	linear-0,5	max	3,71
13	Up-down fusion-1	max	3,86
14	Down-up fusion-1	max	3,86
15	Left-right- fusion-1	max	4,00
16	Right-left fusion-1	max	3,57
17	img1	max	3,71
18	img2	max	3,71
19	mean	rand	3,86
20	min	max	4,71
21	mean	mean	4,43

22	max	max	3,57
23	linear-0,5	max	4,57
24	max	min	1,00
25	min	min	3,57

As we can see from the table (2) the restoration of the lost fragments of the text by means of procedure of fusion of images is quite challenge, from the point of view of achievement of quality of the total image. It allows to speak about necessity of a careful choice of a way of fusion of images by means of the wavelet analysis. A basis of such conclusion is the fact, that estimations of experts were based on a common view of fusion of images. Result of such common view of process of fusion is restoration of separate points of the lost fragments, however thus such points cannot be identified unequivocally as a point of a fragment of the text. In particular the given type of restoration concern:

the restored contour of the lost fragment,

points of the lost fragment which have numerical values in the matrix of the restored image distinct from the matrix of values of the original image.

The made remark proves to be true given table (3) where the corresponding estimation of quality is presented by percentage of quantity of the restored points of the lost fragments to number of such points in the original image.

When we compare data from table (2) and table (3) we can see some discrepancy in estimations of quality of fusion of images. The explanation of such discrepancy has been specified above.

Table 3: An estimation of quality of fusion of images on the basis of calculation of the restored points which have been lost

Experiment number	Way of fusion of coefficients		Percent of the restored points which have been lost, %
	approximating	detailing	
1	max	mean	23,54
2	max	rand	21,73
3	max	linear-0,5	22,63
4	max	Up-down fusion-1	19,92
5	max	Down-up fusion-1	20,82
6	max	Left-right- fusion-1	21,91
7	max	Right-left fusion-1	9,05
8	max	img1	12,67
9	max	img2	10,14
10	mean	max	63,37
11	rand	max	54,32
12	linear-0,5	max	66,99
13	Up-down fusion-1	max	65,18
14	Down-up fusion-1	max	61,56
15	Left-right- fusion-1	max	72,42
16	Right-left fusion-1	max	62,47
17	img1	max	61,56
18	img2	max	57,94
19	mean	rand	76,05
20	min	max	96,74
21	mean	mean	86,91
22	max	max	25,35
23	linear-0,5	max	83,29
24	max	min	0,00
25	min	min	74,24

Hence, at consideration the wavelet procedure of fusion of images it is necessary to consider, both a way of such fusion, and a way of estimation of quality of fusion of images. At the same time a necessary condition of improvement of quality of fusion of investigated images is application of adaptive procedures of a choice of a way of fusion of approximating and detailing coefficients of wavelet expansion of such images based on a context of a task. The given conclusion is based on possibility of use of different ways of

fusion of approximating and detailing coefficients of wavelet expansion of investigated images and ambiguity in an ascertainment of a total estimation of quality in the course of use of considered procedure of fusion of images.

5. CONCLUSION

Thus, the work considers the results of experiments on application of wavelet procedure of fusion of image for computer processing and the analysis of text information. Revealing of complexity of carrying out of wavelet procedure of fusion of image was the purpose of carrying out of such experiments and it consists of:

necessity of a choice and a substantiation of procedure of fusion of images on the basis of consideration of different variants of possible fusion of approximating and detailing coefficients of wavelet expansion of investigated images,

consideration of separate estimations of quality of fusion of images.

As a result of the carried out research different ways of fusion of approximating and detailing coefficients of wavelet expansion of investigated images are considered. The estimations of the obtained results of fusion are resulted.

The conclusion is drawn on necessity of use of adaptive procedures for a choice of a way of fusion of approximating and detailing coefficients of wavelet expansion. Nevertheless, the obtained results can be used for construction of the automated systems of the computer analysis of text information.

REFERENCES:

[1] Zhang, Dengsheng, and Guojun Lu. "Review of shape representation and description techniques." *Pattern recognition*, 37.1: 1-19, 2004.

[2] Nieddu, Luciano, and Giacomo Patrizi. "Formal methods in pattern recognition: A review." *European Journal of Operational Research*, 120.3: 459-495, 2000.

[3] Chen, D., Odobez, J. M., & Bourlard, H. "Text detection and recognition in images and video frames. " *Pattern Recognition*, *37*(3): 595-608, 2004.

[4] Lu, Yi. "Machine printed character segmentation—; An overview." *Pattern Recognition*, 28.1: 67-80, 1995.

[5] Kingsbury, N. "Image processing with complex wavelets." *Physical and Engineering Sciences*, 357(1760): 2543-2560, 1999.

[6] Heil, C. E. and Walnut, D. F. "Continuous and discrete wavelet transforms. " *SIAM review*, 31(4): 628-666, 1989.

[7] Kobylin, O., and Lyashenko, V. "Comparison of standard image edge detection techniques and of method based on wavelet transform." *International Journal of Advanced Research*, *2*(8): 572-580, 2014.

[8] Lyashenko V., Kobylin O., and Ahmad M. A. "General Methodology for Implementation of Image Normalization Procedure Using its Wavelet Transform." *International Journal of Science and Research (IJSR)*, 3(11): 2870-2877, 2014.

[9] Averbuch, Amir, Danny Lazar, and Moshe Israeli. "Image compression using wavelet transform and multiresolution decomposition." *Image Processing, IEEE Transactions on*, 5.1: 4-15, 1996.

[10] Amolins, Krista, Yun Zhang, and Peter Dare. "Wavelet based image fusion techniques—An introduction, review and comparison." *ISPRS Journal of Photogrammetry and Remote Sensing*, 62.4: 249-263, 2007.

[11] Shi, W., Zhu, C., Tian, Y., & Nichol, J. "Wavelet-based image fusion and quality assessment. " *International Journal of Applied Earth Observation and Geoinformation*, *6*(3), 241-251, 2005.

[12] Hill, P. R., Canagarajah, C. N., & Bull, D. R. "Image fusion using complex wavelets. " *In BMVC* : 1-10), 2002.

[13] Wang, Z., Ziou, D., Armenakis, C., Li, D., & Li, Q. "A comparative analysis of image fusion methods. " *Geoscience and Remote Sensing, IEEE Transactions on*, *43*(6): 1391-1402, 2005.

[14] Li, S., & Yang, B. "Multifocus image fusion by combining curvelet and wavelet transform. " *Pattern Recognition Letters*, *29*(9): 1295-1301, 2008.

[15] Lyashenko, V., Deineko, Zh., and Ahmad, M. "Properties of wavelet coefficients of self-similar time series." *International Journal of Scientific and Engineering Research,* 6 (1): 1492-1499, 2015.

International Journal of Engineering Research and General Science Volume 3, Issue 6, November-December, 2015
ISSN 2091-2730

EVALUATION OF FLUXCTURAL PROPERTIES OF ALUMINIUM, BORASSUS FLABELLIFER FIBER AND POLYESTER COMPOSITES

A.VENKATA DINESH [1],U.RAMESH [2],DEMISE.M[3]
[1]Department of Mechanical Engineering, Debre Tabor University, Debre Tabor, Ethiopia
[2]Department of Mechanical Engineering, Dire Dawa University, Ethiopia.
[3] Department of Mechanical Engineering, Demise.M, Debre Tabor University, Debre Tabor, Ethiopia.
E- Mail Address: venkatadinesh.avvari@gmail.com

Abstract- The use of natural fibres like borassus flabellifer fiber, flax, sisal, jute, kenaf, etc. as replacement to manmade fibres in fibre-reinforced composites have increased now a days due to advantages like low density, low cost and biodegradability. But the natural fibres have poor compatibility with the matrix and they have relatively high moisture sorption. In this research, the standard test method of ASTM D638M-89is used to prepare specimens as per the dimensions for testing tensile properties of fiber-resin composites. The test specimen has a constant cross section with tabs bonded at the ends. The specimens were incorporated with borassus flabellifer fiber. Five identical specimens were prepared for each weight by varying fiber content in grams i.e. 0.5, 1.0, 1.5, 2.0, 2.5. Tensile strength of fabricated composites increases with increase in weight of fiber. The tensile properties of pure polyesters are also determined experimentally. The tensile strength of pure polyester is 35.2 N/mm².The tensile strength of a fibered composite is 64.51 N/mm^2 (for maximum loading fiber that is at 2.5 grams).

Keywords: Composite, Natural Fibre, Tensile strength

1. Introduction

With the increased trend for sustainable and environmentally friendly materials, polymer composites industries has lead towards bio degradable polymers from renewable resources such as PVA (polyvinyl alcohol).Biopolymers offer environmental benefits such as biodegradability, greenhouse gas emissions, and renewability of the base material. Bio-composites are usually fabricated with biodegradable/ non-biodegradable polymers as matrix and natural fibers as reinforcement. Many lignocellulosic fibers, such as jute, hemp, sisal, abaca etc. are used as reinforcement for biodegradable bio-composites because of their good mechanical properties and low specific mass. has received much attention of biodegradable polymers. PVA is linear aliphatic thermoplastic polyester, produced from renewable agricultural resources. PVA has properties that are competitive to many commodity polymers (e.g. PP, PE, PLA, PS) such as high stiffness, clarity, gloss, and UV stability. A way to improve the mechanical and thermal properties of PVA is the addition of fibers or filler materials. Combining PVA with natural fibers which are abundantly, readily available such as kenaf, jute, sisal etc. can lead to a totally bio degradable composite made only from renewable resources.

1. Bast or Stem fibres (jute, mesta, banana etc.)

2. Leaf fibres (Palmyra palms, Elephant grass, sisal, pineapple, screw pine etc.)

2. Fruit fibres (cotton, coir, oil palm etc.).

3. EXPERIMENTAL PROCEDURE

2.1 Materials:

Palmyra palms are economically useful and widely cultivated in tropical regions. The Palmyra palm has long been one of the most important trees of Cambodia and India where it has over 800 uses. The leaves are used for thatching, mats, baskets, fans, hats, umbrellas, and as writing material and PVA (polyvinyl alcohol).

- Aluminum
- Borassus flabellifer fiber
- Polyester

2.2 Extraction of Fiber

Fiber is available in the form of bract on a Palmyra tree .First collect dried bracts from the Palmyra tree then after segregate fibers from the bract then after Fibers are cleaned and dried under sun for two days to remove moisture content. Further, the fibers were kept in oven for 2 hours at 70^0 C to ensure that maximum moisture was removed. The above fibers extracted by different methods are used for making composite specimens. In this work I took Palmyra bract fiber these are generally 40 cm long.

2.3 Composite Fabrication

The test specimen has a constant cross section with tabs bonded at the ends. The specimen is prepared by hand layup process in the form of a rectangular strip of 160x13x3 mm thick and ground to conform to the dimensions. The mould is prepared on smooth ceramic tile with rubber shoe sole to the required dimension. Initially the ceramic tile is cleaned with shellac (NC thinner) a spirituous product to ensure clean surface on the tile. Then mould is prepared keeping the rubber sole on the tile. The gap between the rubber and the tile is filled with mansion hygienic wax. A thin coating of PVA (polyvinyl alcohol) is applied on the contact surface of specimen, using a brush. The resulting mould is cured for one hour.

2.3 FLUXCTURAL Test

FLUXCTURAL Tests were conducted according to ASTM D638 using a 2 ton capacity - Electronic Tensometer, METM 2000 ER-I model, supplied by M/S Microtech Pune, with a cross head speed of 2mm/min.

3. Results and Discussion

The Fluxctural strength and modulus of ***borassus flabellifer fiber*** /PVA as a function of the ***borassus flabellifer fiber*** content are presented in figure 3.1&3.2.

From figures 3.1&3.2, it was observed that the Fluxctural strength of composite increased with increase in the fibre loading up to 2.5 grams weight and the Modulus is given maximum at 2.5 grams of borassus flabellifer fiber/PVA composites.

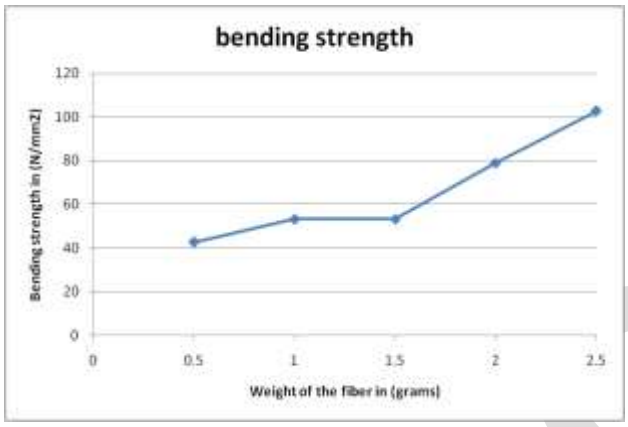

*Figure 3.1: Variation of Bending strength of **borassus flabellifer fiber** /PVA composite with fiber loading.*

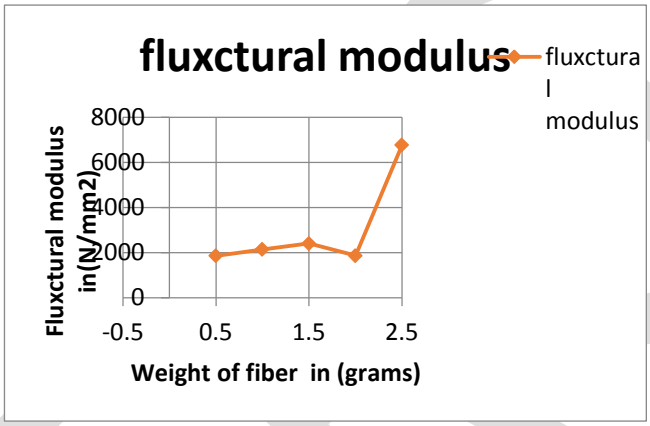

*Figure 3.2: Variation of Fluxctural modulus of **borassus flabellifer fiber** /PVA composite with fiber loading.*

4. Conclusions

1. By using chemical treatment we can increase the Tensile, flexural and impact strengths.

2. It can be seen that by varying volume of fiber the mechanical properties of the composite also change. by increase in volume of fiber in composite mechanical properties also increased up to maximum loading.

3. It can be seen that there is an appreciable increase in Tensile properties of chemically treated composite when compared to un treated fibered composites which can be observed from the results below
   - The flexural strength of a fibered composite is 102.73 N/mm^2 (for maximum loading fiber).And The Flexural strength of pure polyester is 110.10 N/mm^2.
   - The Flexural module of pure polyester is 355.7N/mm^2.The flexural module of a fibered composite is 6767.18 N/mm^2 (for maximum loading fiber)

REFERENCES:

[1] Xue Li Æ Lope G. Tabil Æ Satyanarayan Panigrahi: Chemical Treatments of Natural Fiber for Use in Natural Fiber-Reinforced Composites: A Review: J Polym Environ (2007) 15:25–33.

[2] X. Y. Liu, G. C. Dai.: Surface modification and micromechanical properties of jute fiber mat reinforced polypropylene composites: eXPRESS Polymer Letters Vol.1, No.5 (2007) 299–307

[3] Eastham J. : Natural fibres for the automotive industry in 'Seminar of The Alternative Crops Technology Interaction Network, Manchester, UK' **16**, 142–146 (2001).

[4] Han S. O., Defoort B., Drzal L. T., Askeland P. A.: Environmentally friendly biocomposites for automotive applications in '33rd ISTC Conference, Seattle, USA' **33**, 1466–1477 (2001).

[5] Marsh G.: Next step for automotive materials. Materials Today, **6**, 36-43 (2003).

[6] Chen Y., Chiparus O., Sun L., Negulescu I., Parikh D. V., Calamari T. A.: Natural fibers for automotive nonwoven composites. Journal of Industrial Textiles, **35**, 47–62 (2005).

[7] Gassan J., Bledzki A. K.: Possibilities for improving the mechanical properties of jute/epoxy composites by alkali treatment of fibres. Composites Science and Technology, 59, 1303–1309 (1999).

[8] Gassan J., Bledzki A. K.: Effect of cyclic moisture absorption desorption on the mechanical properties of silanized jute-epoxy composites. Polymer Composites, 20, 604–611 (1999).

[9] Gassan J., Gutowski V. S.: Effects of corona discharge and UV treatment on the properties of jute-fibre epoxy composites. Composites Science and Technology, 60, 2857–2863 (2000).

[10] Karmaker A. C., Youngquist J. A.: Injection moulding of polypropylene reinforced with short jute fibers. Journal of Applied Polymer Science, 62, 1147–1151 (1996).

[11] Wei-ming Wang; Zai-sheng Cai; jian-yong Yu: Study on Chemical Modification Process of jute. Journal of Engineering fibers and fabrics Volume 3, Issue 2, 2008.

[12] Mohd Zuhri Mohamed Yusoff; Mohd Sapuan Salit; Napsiah Ismail; Riza Wirawan: Mechanical Properties of short random oil palm fiber reinforced epoxy composites. Sains Malaysiana 39(1)(2010): 87-92.

[13] Morsyleide F. Rosa, Bor-sen Chiou, Eliton S. Medeiros: Effect of fiber treatments on tensile and thermal properties of starch/ethylene vinyl alcohol copolymers/coir biocomposites: Bioresource Technology 100 (2009) 5196–5202.

[14] Amel El Ghali, Imed Ben Marzoug: Separation and characterization of new cellulosic fibers from the Juncus acutus L Plant: Bio Resources 7(2), 2002-2018, 2002.

[15] Md Nuruzzaman Khan, Juganta K. Roy, Nousin Akter, Haydar U. Zaman: Production and Properties of Short Jute and Short E-Glass Fiber Reinforced Polypropylene-Based Composites: Open Journal of Composite Materials, 2012, 2, 40-47.

[16] Dipa Ray, B K Sarkar, A K Rana And N R Bose: Effect of alkali treated jute fibres on composite properties: Bull. Mater. Sci., Vol. 24, No. 2, April 2001, pp. 129–135.

[17] H.M.M.A Rashed, M.A. Islam and F.B. Rizvi: Effects of process parameters on tensile strength of jute fiber reinforced thermoplastic composites. Journal of naval architechture and merine engineering, 3(2006) 1-6.

[18] Beckerman G.W., Pickering, K.L., and foreman. N.J.: The Processing, Production and Improvement of hemp fibre reinforced polypropylene composite materials: proceedings of SPPM, 25-27 feb.2004. pp 257-265.

[19] Dieu. T.V., Phai L.T.,Ngoc P.M.: Study on preparation of polymer composites based on polypropylene reinforced by jute fibers: JSME International journal, Series A: Solid mechanics & Material engineering, Vol. 47, No.4, pp 547-550.

[20] Razera I.A.T., and Frollini.E.: Composites based on jute fibers and phenolic matrices: Properties of fibers and composites: Journal of applied polymer science Vol.91, No.2, pp 1077-1085.

[21] Ray D., Sarkar B.K., Rana A.K., Bose N.R.: Effect of alkali treated jute fibres on composite properties, Bulletin of materials science, Vol.24, No.2, pp. 129-135.

[22] M Alamgir Kabir, M. Monimul Huque: Mechanical Properties of Jute fibre reinforced Polypropylene composite: effect of benzenediazonium salt inalkaline edium: bio resources 5(3), 1618-1625

International Journal of Engineering Research and General Science Volume 3, Issue 6, November-December, 2015
ISSN 2091-2730

An Instant-Fuzzy Search Using Phrase Indexing and Segmentation with Proximity Ranking

Ramesh S. Yevale[1]
Dept. of Computer Engineering,
ICOER,Wagholi.
Pune, India
ryevale33@gmail.com

Prof.Vinod S. Wadne[2]
Dept. of Computer Engineering,
ICOER,Wagholi
Pune,India
vinods1111@gmail.com

Abstract— An Instant search is said to be effective when it gives faster retrieval of answer set with minimum computational time. Fuzzy search needed for queries that are mistypes due to several reasons. Fuzzy search used to improve user search experiences by finding relevant answers with keywords similar to query keywords. We are using phrase threshold value which is used to limit the answer set generated by instant fuzzy search. For that main challenge is that to improve the speed of performance as well as minimize answer set to retrieval of desired documents for the user query. At the same time, we also need better ranking functions that consider the proximity of keywords to compute relevance scores. In this paper, we study how to compute proximity information into ranking in instant-fuzzy search while achieving efficient time and space complexities. A phrase base indexing technique is used to overcome the space and time limitations of these solutions, we propose an approach that focuses on common phrases and trie indices in the database. We study how to index these phrase threshold value and compare user threshold for effective answer set and develope an computational algorithm for efficiently segmenting a query into phrases and computing these phrases using algorithm to find relevant answers to the user query.

Keywords— Instant search,fuzzy search,trie indices

Introduction

Finding relevant answers within time limit to a user query. Fuzzy logic is useful to retrieve exact documents to a user query while there may be misspelling in query. Instant search will helpful to lookup expected results while user typing a query.Searching to the target document is much easier and fast. Proximity ranking is responsible for getting relevant answer set to user query.Auto-completion of a query reduces time limit to retrieve relevant answer set to user query.Instant search faster retrieval of answer set with minimum computational time. It is known that to achieve an instant speed for humans, from the time a user types in a character to the time the results are shown in answer set, the total time should be less than 100 milliseconds. It is needed to consider time goes in network delay, time on the search server to find relevant documents to the query, and the time of running code on the device of the user such as web browser. Thus the amount of time the server can spend is even less. At the same time, compared to traditional search systems, instant search can result in more queries on the server since each keystroke can invoke a query, thus it requires a higher speed of the search process to meet the requirement of a high query throughput. What makes the computation even more challenging is that the server also needs to retrieve high-quality answers to a query given a limited amount of time to meet the information need of the user.

It is needed to consider time goes in network delay, time on the search server to find relevant documents to the query, and the time of running code on the device of the user such as web browser. Thus the amount of time the server can spend is even less.Text related interfaces have been undergoing a sea change in the last few years. An auto completion mechanism unobtrusively prompts the user with a set of suggestions, each of which is a suffix, or completion, of the user's current input. This allows the user to avoid unnecessary typing, hence saving not just time but also user cognitive burden.

Instant search is said to be effective when it gives faster retrieval of answer set with minimum computational time. It is known that to achieve an instant speed for humans, from the time a user types in a character to the time the results are shown in answer set, the total time should be less than 100 milliseconds [7]. It is needed to consider time goes in network delay, time on the search server to find relevant documents to the query, and the time of running code on the device of the user such as web browser. Thus the amount of time the server can spend is even less. At the same time, compared to traditional search systems, instant search can result in more queries on the server since each keystroke can invoke a query, thus it requires a higher speed of the search process to meet the requirement of a high query throughput. What makes the computation even more challenging is that the server also needs to retrieve high-quality answers to a query given a limited amount of time to meet the information need of the user.[8]

Using trie index tree an improved fuzzy logic can be applicable to the words even though that mistypes. When user mistypes a query, even though system will retrieve most of the relevant answer set. Fuzzy searching is specially useful when researching unfamiliar, foreign-language, or sophisticated terms, the accurate spellings of which are not widely known. Fuzzy searching can also be used to locate individuals based on imperfect or partially inaccurate identifying information.

PROBLEM STATEMENT :

It is needed return proper results to an user query even user mistypes due to small interface just like mobile phones, lack of english spelling knowledge to user, etc. So, we study how to integrate proximity information into ranking in instant-fuzzy search to compute relevant answers to the query[8]. User mistypes a query due to small keyboards, mobile phones, spelling mistake or lack of subject knowledge, etc. The proximity of matching keywords in answers is an important function to determine the relevance of the answers. User queries typically contain correlated keywords, as well as some pattern based phrases and to answers to these keywords or phrases together are more likely what the user is looking for. [15]

Finding relevant answers within time limit to a user query. Fuzzy logic is useful to retrieve exact documents to a user query while there may be misspelling in query.For example, if the user types in a search engine as a search query “Sachin Tendulkar”, the user is most likely looking for the records containing information about the cricketer Sachin Tendulkar, while documents containing “Sachin Pilgaonkar”.Existing system have limitation to respond to user query, as it requires mostly three phrases to enter for proximity instant search and it is time consuming. To achieve exact matches needed to user, we adapt instant fuzzy search. There is a need to minimize time and space tradeoff for retrieval of user query while user typing a query. Eventhogh user mistypes from at the start of query fuzzy search needed to calculate similarity as well as edit distance by considering trie index tree structure to get proper results.

LITERATURE SURVEY

In [1], In this paper, a document is altered to a pseudo document form, means containing long form, short forms or any related data to it. Also, a term count is propagated to other nearby terms, so that nearness among the words is find. Then they consider three heuristics, i.e., the distance of two query term occurrences, their order, and asigned term weights, which can be viewed as a pseudo term frequency.

In [2], author studied the problem of auto completion by considering different words. There are two main challenges: one is that the number of phrases (both the number possible as well as the number actually observed in a corpus) is combinatorially larger than the number of words; the second is that a “phrase”, unlike a “word”, does not have a well-defined boundary, so that the auto completion system has to decide not just what to predict, but also how far way these phrases indeed. For that implementation they introduced a FussyTree structure to address the first challenge and the concept of a significant phrase to address the second challenge. They developed a probabilistically driven multiple completion choice model, and exploit features such as frequency distributions to improve the quality of our suffix completions. They experimentally demonstrate the practicability and value of our technique for an email composition application and show that we can save approximately a fifth of the keystrokes typed.

In [3], author studied how to identify existing indexes, search algorithms, filtering strategies, selectivity estimation techniques and other work, and comment on their respective merits and limitations.

In [4], the author uses new early termination techniques for efficient query processing for the case where term proximity is integrated into the retrieval model. They implemented new index structures based on a term-pair index, and study new document retrieval strategies on the resulting indexes. They have performed a detailed experimental evaluation on new techniques and compare

them with the existing approaches. Experimental results on large scale data sets show that their techniques can significantly improve the efficiency of query processing.

In [5], author proved the results of lower ranked auto completion is basically receive lower engagement than the higher one. They suggested that users are most likely to engage with auto-completion after typing about half of the query, with particular at word boundaries. They also noticed that the auto-completion varies with the distance of query characters on the keyboard. Finally, the results indicates user engagement with auto completion is effective.

In [6], author implemented log linear model is indicating as conditional probability distribution of an output string and a rule set for the transformation conditioned on an input string. The learning method employs maximum likelihood estimation for parameter estimation. The string generation algorithm based on pruning is used to generate only important documents in answer set. Author also worked with error correction in query to provide effective answer set to the query.

In our work, we are using effective phrase indexing and also want the use of trie index structure to improve speed of performance to instant query search.

IMPLEMENTATION DETAILS

Proposed System Architecture

Fig. 1 shows proposed architecture of system indicating computation of dictionary and valid phrases to the user query continuously when user interacts. An trie indices are also generated for each of the valid phrases with an incremental approach.These collected phrases are will be stored in dataset for further use of comparison when user enters keywords as a query.We are preparing valid phrase based indexing and making tree based structure to store these phrases to fast retrieval when user enters a query. Next step is to develop effective query plan that helps to generate valid segmentation and ranking only top-k answers to the query. Proposed system will overcome limitation of existing system as we are dealing with minimizing top-k answers by effective phrase indexing and segmenting those phrases in proper order.

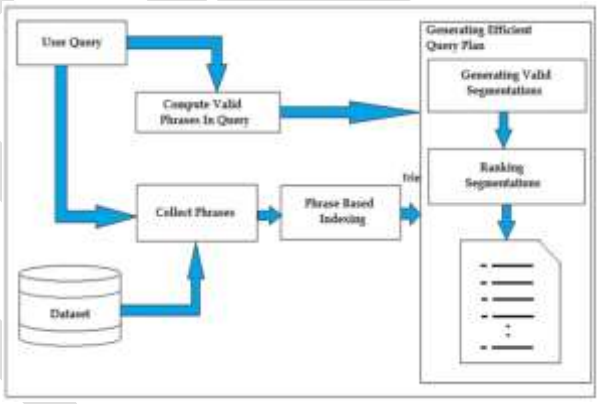

Fig.1 Proposed System Architecture

MATHEMATICAL MODEL

- **Finding Cosine Similarity Between Words :**

$$C.S. = \frac{\sum(Q_{wi}) * (P_{wi})}{\sqrt{\sum(Q_{wi})^2}. \sqrt{\sum(P_{wi})^2}}$$

Were,

C.S. = Cosine Similarity

Q = User query

W_i = Each word in the document

P = No. of occurrences of W_i in the document

- **Finding Edit Distance Between Keywords** :

e.g. "cats"

"ckats"

Edit Distance = 2

A DFA is mathematically represented as a 5-Tuple

(Q,∑, ∂, Q0, F)

The function ∂ is a transition function.

Fig.2 Shows mathematical model,

Were,

X1:User query

X2:Database

X3:Phrase Index Identification

X4:Collected Phrases

X5:Valid Phrases

X6:Effective Query Plan

X7: Gathering Valid Segmentation

X8:Ranking Segmentation

X9:Instan-Search Ranked Documents Choosen with Threshold Value

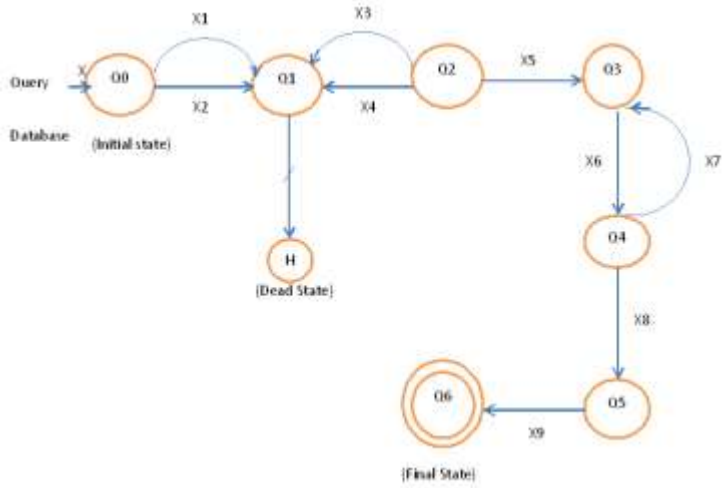

Fig.2 Mathematical Model for Proposed System

Modules

1. Module I: Loading Database to Instant Fuzzy Search

In this module, we are loading dataset of movies which is created in XML. XML document is loaded in to Instant Fuzzy Search for preparing overall dictionary to given dataset. Dataset is prepared from IMDB, were 2000 movies dataset is collected for real time processing.

2. Module II: Collection and preparation of Dictionary

After loading dataset, we are preparing dictionary which involves all the uniqe keywords from the XML document. Basically dictionary involves valid keywords after removal of stopwords. This prepared dictionary is passed to next phases of Instant fuzzy search.

3. Module III: Preparation Of Valid Phrases

Previous module stores unique keywords from dataset. On the basis of given dictionary, we prepare valid phrases. These phrases are important to retrieve relevant answer set to the user. These prepared valid phases are then forwarded to next phase for the preparation of Trie tree.

4. Module IV: Preparing Trie tree for Collected Valid Phrases

In this phase, we are preparing trie nodes which involves root and their various inserted childs depending on valid phrases. Basically, there is a possible chain of keywords which involves single parent node and multiple or single child to an active node. So, for the given valid phrases there are several active nodes involves several possible combination of childs.

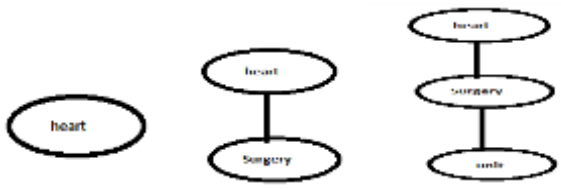

Fig 1. Trie Index Tree

RESULTS

The IMDB dataset is used for the experimental setup that includes movies related information which is stored in structural format i.e. in XML format. We are using 2000 movies information from the IMDB dataset for our project. The given dataset is structured using separation of movie name, year of releasing and basic information.

TABLE I Movie Dataset

Dataset	IMDB(Movies Related Information)
No. of distinct keywords	5000
Average record length	40
Data Size	184 KB

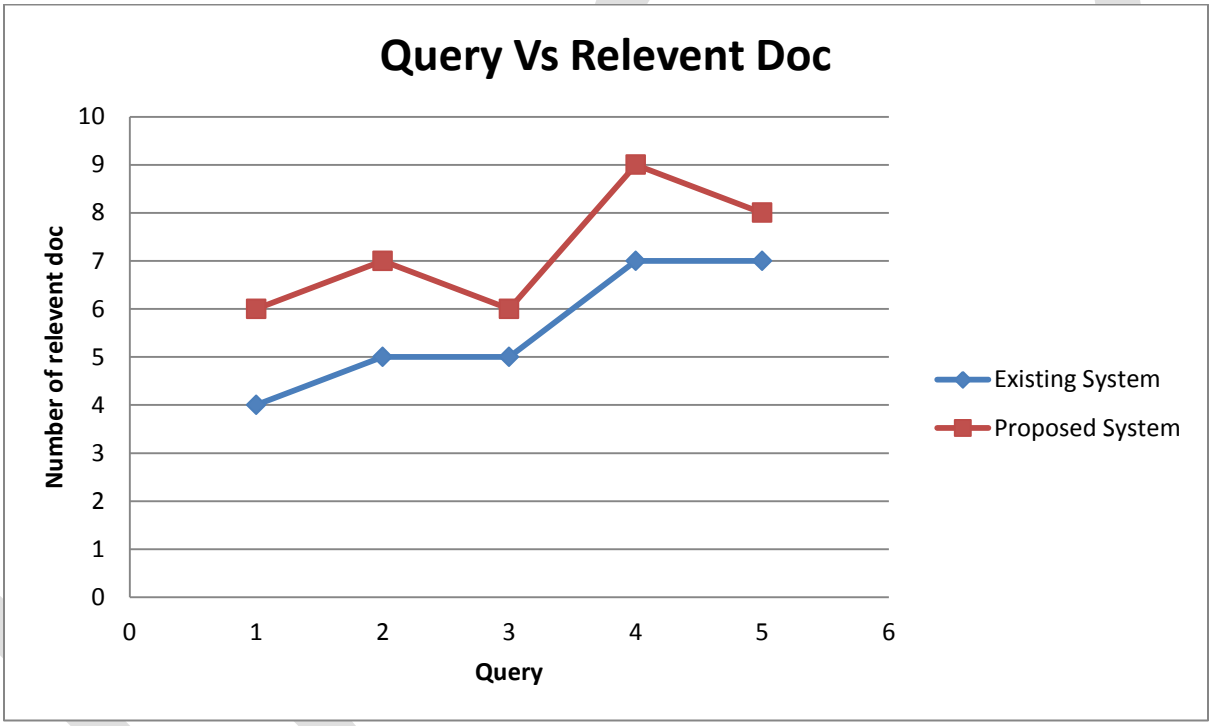

Fig. 3 Relevent documents to user query

The results obtained from the traditional Instant fuzzy search framework and implemented proposed system are taken on different sets of data. Both results are then compared to find out the conclusion. For both traditional and proposed system the same environment is used. The setup used for Instant fuzzy search and the results obtained are discussed below.

Figure 3 shows number for relevant document set is retrieved for given user queries. We are showing there are for five user queries as a input to the search engine and for each user query, search engine instantly gives responses. Figure 3 shows for the first user query, search engine gives us 6 relevant answer set from 10.(i.e. Total length of retrieved answer set to the user query). Similarly when user enters second query, that returns 7 relevant answer sets as shown in figure. Basically our proposed system will apply fuzzy logic from the first alphabet of the query as compared with existing system requires at least 3 characters.

CONCLUSION

In this paper we study how to improve instant-fuzzy search by effective phrase index identification and segmenting those phrases with proper indexing by considering proximity information when we need to compute top-k answers. We compared our techniques to the instant fuzzy adaptations of basic approaches. We conducted a very thorough analysis by considering space, time, and relevancy tradeoffs of these approaches.

In particular, our experiments on real dataset movies will show the efficiency of the proposed technique for retrieval of maximum no. of relevant document when user partially types a query. Even though user mistypes a query our proposed architecture retrieves maximum number of relevant answer set.

REFERENCES:

[1] Ruihua Song, Liqian Yu, Ji-Rong Wen, and Hsiao-Wuen Hon "A Proximity Probabilistic Model for Information Retrieval", Microsoft Research Asia, Beijing, 100190, China.

[2] A. Nandi and H. V. Jagadish, "Effective phrase prediction," in *VLDB*,2007, pp. 219–230.

[3] M. Hadjieleftheriou and C. Li, "Efficient approximate search on string collections," *PVLDB*, vol. 2, no. 2, pp. 1660–1661, 2009.

[4] H. Yan, S. Shi, F. Zhang, T. Suel, and J.-R. Wen, "Efficient term

proximity search with term-pair indexes," in *CIKM*, 2010, pp. 1229–1238.

[5] Bhaskar Mitra, Milad Shokouhi, Filip Radlinski, Katja Hofmann,"On User Interactions with Query AutoCompletion", Microsoft Cambridge, UK.

[6] A. Meenahkumary, V. Manjula, B. Divyabarathi, V. Nirmala," Top K Pruning Approach to String Transformation", 2014.

[7] M. Zhu, S. Shi, N. Yu, and J.-R. Wen, "Can phrase indexing help to process non-phrase queries?" in *CIKM*, 2008, pp. 679–688.

[8] Inci Cetindil, Jamshid Esmaelnezhad, Taewoo Kim and Chen Li," Efficient Instant-Fuzzy Search with Proximity Ranking", 2014.

[9] R. B. Miller, "Response time in man-computer conversational transactions," in *Proceedings of the December 9-11, 1968, fall joint computer conference, part I*, ser. AFIPS '68 (Fall, part I). New

York, NY, USA: ACM, 1968, pp. 267–277. [Online]. Available:http://doi.acm.org/10.1145/1476589.1476628

[10] M. Zhu, S. Shi, M. Li, and J.-R. Wen, "Effective top-k computation in retrieving structured documents with term-proximity support," in *CIKM*, 2007, pp. 771–780.

[11] S. B¨uttcher, C. L. A. Clarke, and B. Lushman, "Term proximity scoringfor ad-hoc retrieval on very large text collections," in *SIGIR*, 2006, pp.621–622.

[12] H. Zaragoza, N. Craswell, M. J. Taylor, S. Saria, and S. E. Robertson,"Microsoft cambridge at trec 13: Web and hard tracks," in *TREC*, 2004.

[13] A. Arampatzis and J. Kamps, "A study of query length," in *SIGIR*,2008, pp. 811–812.

[14] D. R. Morrison, "Patricia - practical algorithm to retrieve information coded in alphanumeric," *J. ACM*, vol. 15, no. 4, pp. 514–534, 1968.

[15] C. Silverstein, M. R. Henzinger, H. Marais, and M. Moricz, "Analysis of a very large web search engine query log," *SIGIR Forum*, vol. 33,no. 1, pp. 6–12, 1999.

[16] G. Li, J. Wang, C. Li, and J. Feng, "Supporting efficient top-k queries in type-ahead search," in *SIGIR*, 2012, pp. 355–364.

[17] R. Schenkel, A. Broschart, S. won Hwang, M. Theobald, and G. Weikum, "Efficient text proximity search," in *SPIRE*, 2007, pp. 287–299.

[18] M. Zhu, S. Shi, N. Yu, and J.-R. Wen, "Can phrase indexing help to process non-phrase queries?" in *CIKM*, 2008, pp. 679–688.

[19] A. Jain and M. Pennacchiotti, "Open entity extraction from web search query logs," in *COLING*, 2010, pp. 510–518.

[20] Z. Bao, B. Kimelfeld, and Y. Li, "A graph approach to spelling correction in domain-centric search," in *ACL*, 2011.

[21] J. R. Herskovic, L. Y. Tanaka, W. R. Hersh, and E. V. Bernstam, "Research paper: A day in the life of pubmed: Analysis of a typical day's query log," *JAMIA*, vol. 14, no. 2, pp. 212–220, 2007.

[22] H. C. Ozmutlu and F. _Cavdur. Application of automatic topic identi_cation on excite web search engine data logs. Inf. Process. Manage., 41:1243,1262,

September 2005.

[23] S. Ozmutlu. Automatic new topic identi_cation using multiple linear regression. Inf. Process. Manage., 42:934,950, July 2006

International Journal of Engineering Research and General Science Volume 3, Issue 6, November-December, 2015
ISSN 2091-2730

Fault Classification and Phase Selection Using Sequential Components

Athira Rajan[1] , Jisha James[2]

PG Student [Power System], Dept. of EEE, Saintgits College of Engineering, Kottayam, Kerala, India,

Email: athiracem@gmail.com, Contact no:9497325836[1]

Assistant professor, Dept. of EEE, Saintgits College of Engineering, Kottayam, Kerala, India[2]

Abstract— A new steady state based fault classification and faulted phase selection technique is proposed using the symmetrical components of reactive power. After extracting the symmetrical components of voltage current from sending end and receiving end the symmetrical components of reactive power are calculated. Based on these values we can classify single phase to ground, double phase and double phase to ground fault and also to select the faulted phase. The proposed method is a setting-free method because it does not need any threshold to operate. The simulation studies of different fault cases reveal the capability of the proposed method.

Keywords— Symmetrical Components, Fault classification, Faulted phase selection, Single phase to ground fault, Double phase fault, Double phase to ground fault.

INTRODUCTION

In power systems, protective devices detect fault conditions and operate circuit breakers and other devices to limit the loss of service due to a failure. Fast and reliable fault detection and fault classification technique is an important requirement in power transmission systems to maintain continuous power flow. Identifying the type of fault, e.g., single-phase grounding fault, phase-to-phase fault, etc. will help the relay to select different algorithm elements to deal with different fault situations. Identifying the faulted-phase helps to satisfy single-pole tripping and auto reclosing requirements and it becomes possible to only disconnect the faulted phase(s). This will increase the stability margin of the power system and probably avoid unnecessary loss of electricity in some regions.

A new steady-state-based approach to fault classification and faulted phase selection for single-circuit transmission lines is proposed by using the sequential reactive power components. Using the symmetrical components of voltage and current symmetrical reactive power components are calculated. Based on these values single phase to earth fault, phase to phase fault and double phase to earth fault can be identified. Also the faulted phase can be selected by analyzing the sequential reactive power components.

PROPOSED METHOD

The symmetrical components of reactive power are given by

$$Q_1 = \mathrm{Im}\{V_1 * I_1^*\} \rightarrow (1)$$

$$Q_2 = \mathrm{Im}\{V_2 * I_2^*\} \rightarrow (2)$$

$$Q_0 = \mathrm{Im}\{V_0 * I_0^*\} \rightarrow (3)$$

where Q_1, Q_2, and Q_0 are, respectively, called positive-, negative-, and zero-sequence component of reactive power. Also, V_1 ,V_2 ,and V_0 are, respectively, positive-, negative-, and zero-sequence component of voltage measured at relay point (either sending or receiving end of Fig.1). Similarly, I_1 ,I_2 ,and I_0 are, respectively, positive-, negative-, and zero-sequence component of current measured at relay point. In this work, Q_2 and Q_0 will be utilized to develop the proposed method.

Fig. 1. Single-circuit transmission line protected by sending and receiving end relays.

A. Fault classification and faulted phase selection

- Single phase to ground fault

If the ratio Q_0/Q_2 is greater than 1 in any of the relay then it is a single phase to ground fault. $|Q_{20}|$ will have maximum value in the faulted phase.

- Double phase to ground fault

If the ratio Q_0/Q_2 is between 0 and 1 for both relays it is double phase to ground fault. For ABG fault $|Q_{20}|$ is maximum in phase C. If $|Q_{20}|$ is maximum in phase A it is BCG fault. For CAG fault $|Q_{20}|$ is maximum in phase B.

- Phase to phase fault

ΔQ_{12} is zero in healthy phase and non-zero for the faulty phase. Q_{12} is given by

$$Q_{12} = \mathrm{Im}\{(V_1 + V_2) * (I_1 + I_2)^*\} \rightarrow (4)$$

.

B. Logical Pattern

Fig. 2 illustrates a flowchart of the proposed method in a logical pattern. Three phase currents and three phase voltages are sampled . Sequential reactive powers are calculated by using the sequential components of voltage and current. In Fig. 3, Q_{0S} and Q_{0R} stand for zero-sequence reactive power at sending and receiving ends, respectively. Similar definition holds for Q_{2S} and Q_{2R}.

After a fault inception is declared, the relays will firstly check if ΔQ_{12} is zero on one phase to identify phase-to-phase faults and to find the healthy phase. At this stage, the relays can either share their information or decide individually. If ΔQ_{12} not equal to zero on all three phases, ratio Q_0/Q_2 will be examined. From the view point of both relays, if $0< Q_0/Q_2<1$, a double-phase-to-earth fault will be declared and if $Q_0/Q_2>1$ from the view point of at least one relay, a single-phase-to-earth fault will be declared. Here, both relays should share their own measurement by a pilot scheme. Faulted phase selection, however, is done locally, that is, each relay selects the faulted phase(s) by using its own measurement $|Q_{20}|$ as previously outlined.

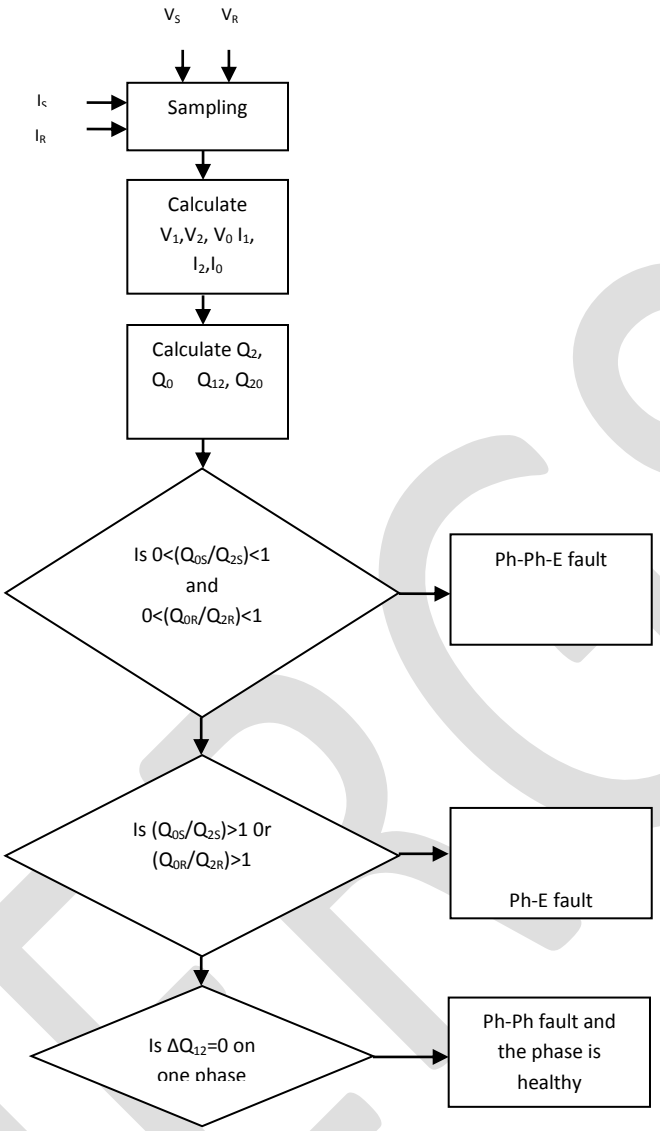

Fig. 2. Proposed method in a logical pattern.

RESULT AND DISCUSSION

The transmission line model is implemented in the PSCAD 4.2.1 professional version. The 50-Hz, 400-kV simulated system is shown in Fig. 3.

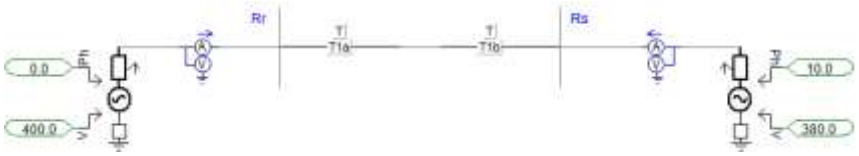

Fig. 3. PSCAD model of transmission line

The length of the transmission line was chosen 200 km. Sending end and receiving end sources are implemented using three phase voltage source model with base voltage level of 400kV and 380kV. The phase angles are set at 0^o and 10^o for sending end and receiving end respectively.

The fault classification and faulted phase selection algorithm was implemented using the MATLAB program. Various fault cases have been considered as tabulated in different tables. To avoid large numbers, Q_{20} and ΔQ_{12} are given in per unit (pu) with the base power of 100 MW.

Table I: Values measured by sending end for different single line to ground faults

Sl No.	**Fault type**	**Fault resistance (Ω)**	**Fault distance (km)**	**Q_0/Q_2**	**$\lvert Q_{20}^A \rvert$ (pu)**	**$\lvert Q_{20}^B \rvert$ (pu)**	**$\lvert Q_{20}^C \rvert$ (pu)**
1	AG	10	10	1.6116	5.2957	1.1380	1.5655
2	AG	10	100	1.3742	0.4361	0.0913	0.1259
3	AG	10	190	0.4564	0.1022	0.0265	0.0288
4	BG	50	10	1.6116	0.1533	0.5189	0.1114
5	BG	50	100	1.3742	0.0346	0.1201	0.0251
6	BG	50	190	0.4564	0.0032	0.0114	0.0029
7	CG	100	10	1.6116	0.0299	0.0412	0.1394
8	CG	100	100	1.3742	0.0083	0.0114	0.0396
9	CG	100	190	0.4564	0.0008	0.0008	0.0031

Table II: Values measured by receiving end for different single line to ground faults

Sl No.	**Fault type**	**Fault resistance (Ω)**	**Fault distance (km)**	**Q_0/Q_2**	**$\lvert Q_{20}^A \rvert$ (pu)**	**$\lvert Q_{20}^B \rvert$ (pu)**	**$\lvert Q_{20}^C \rvert$ (pu)**
1	AG	10	190	0.4987	0.1622	0.0305	0.1197
2	AG	10	100	1.4010	0.5199	0.1152	0.1501
3	AG	10	10	1.5895	5.2787	1.1968	1.1354
4	BG	50	190	0.4987	0.0033	0.0117	0.0131
5	BG	50	100	1.4010	0.0403	0.1431	0.0319
6	BG	50	10	1.5895	0.1684	0.5885	0.1260
7	CG	100	190	0.4987	0.0008	0.0008	0.0125
8	CG	100	100	1.4010	0.0104	0.0133	0.0487

9	CG	100	10	1.5895	0.0363	0.1058	0.1002

As Tables I and II show, the ratio of Q_0/Q_2 was more than 1 at either one end or both ends in case of single-phase-to-earth faults. This confirmed a single-phase-to-earth fault inception. For the AG faults, the maximum $|Q_{20}|$ occurred on Phase A. For BG and CG faults, maximum $|Q_{20}|$ occurred on Phases B and C, respectively. Therefore, the faulted phase was selected. It is clear that the method can cope with high fault resistance and any fault location.

Table III: Values measured by sending end for different double line to ground faults

Sl No.	**Fault type**	**Fault resistance (Ω)**	**Fault distance (km)**	**Q_0/Q_2**	**$\|Q_{20}^A\|$ (pu)**	**$\|Q_{20}^B\|$ (pu)**	**$\|Q_{20}^C\|$ (pu)**
1	ABG	10	10	0.6290	0.9808	2.2587	6.1416
2	ABG	10	100	0.1852	0.2261	0.3239	0.7478
3	ABG	10	190	0.1821	0.0425	0.0580	0.1364
4	ACG	50	30	0.9479	0.1646	0.3986	0.0463
5	ACG	50	100	0.5769	0.0631	0.1346	0.0148
6	ACG	50	175	0.5293	0.0089	0.0225	0.0035
7	BCG	100	70	0.9947	0.0656	0.0079	0.0264
8	BCG	100	100	0.8991	0.0412	0.0048	0.0169
9	BCG	100	130	0.8396	0.0233	0.0019	0.0093

Table IV: Values measured by receiving end for different double line to ground faults

Sl No.	**Fault type**	**Fault resistance (Ω)**	**Fault distance (km)**	**Q_0/Q_2**	**$\|Q_{20}^A\|$ (pu)**	**$\|Q_{20}^B\|$ (pu)**	**$\|Q_{20}^C\|$ (pu)**
1	ABG	10	190	0.1946	0.0476	0.0685	0.7118
2	ABG	10	100	0.1888	0.2740	0.3768	0.9303
3	ABG	10	10	0.6343	1.0867	2.1257	3.2993
4	ACG	50	170	0.6020	0.0123	0.0308	0.0125
5	ACG	50	100	0.5881	0.0734	0.1607	0.0199
6	ACG	50	25	0.9931	0.1916	0.4919	0.0576
7	BCG	100	130	0.8773	0.0278	0.0037	0.0154
8	BCG	100	100	0.9167	0.0492	0.0063	0.0203

9	BCG	100	70	0.9910	0.0779	0.0105	0.0248

For double-phase-to-earth faults, Q_0/Q_2 was less than 1 at both ends, as seen in Tables III and IV. This confirmed a double-phase-to-earth fault. For ABG faults, $|Q_{20}|$ was the maximum on Phase C. For BCG and CAG faults, was the maximum on Phases A and B respectively. This disclosed the faulted phases. But the fault classification technique fails when fault location is on the extreme ends of the transmission line for high fault resistance case. As the fault resistance increases the span of length of transmission line in which the proposed method works reduces.

Table V and VI presents ΔQ_{12} on each phase measured by relays R_S and R_R for different phase-to-phase fault cases as tabulated, ΔQ_{12} were nearly zero on the healthy phase while they were not zero on the faulted phases.

Table V:Values measured by sending end for different phase to phase faults

Sl No.	**Fault type**	**Fault resistance (Ω)**	**Fault distance (km)**	**$\|\Delta Q_{12}^A\|$ (pu)**	**$\|\Delta Q_{12}^B\|$ (pu)**	**$\|\Delta Q_{12}^C\|$ (pu)**
1	AB	10	20	3.4504	19.3470	0.0009
2	AB	10	100	5.6532	10.3340	0.00006
3	AB	10	180	2.5493	6.3656	0.0006
4	AC	50	20	8.4356	0.0009	4.3539
5	AC	50	100	5.7786	0.00005	0.5113
6	AC	50	180	2.2233	0.0007	0.8158
7	BC	100	20	0.0009	3.0066	4.1922
8	BC	100	100	0.00004	1.2527	2.8809
9	BC	100	180	0.0007	0.7324	0.9828

Table VI:Values measured by receiving end for different phase to phase faults

Sl No.	**Fault type**	**Fault resistance (Ω)**	**Fault distance (km)**	**$\|\Delta Q_{12}^A\|$ (pu)**	**$\|\Delta Q_{12}^B\|$ (pu)**	**$\|\Delta Q_{12}^C\|$ (pu)**
1	AB	10	180	3.1383	5.8105	0.0013
2	AB	10	100	5.5453	8.7675	0.00005
3	AB	10	20	2.0256	14.1510	0.0010
4	AC	50	180	2.1911	0.0013	0.2853

5	AC	50	100	5.4187	0.00007	0.0270
6	AC	50	20	7.2563	0.0010	3.9583
7	BC	100	180	0.0013	0.3789	1.0404
8	BC	100	100	0.00004	0.8215	2.8416
9	BC	100	20	0.0010	2.7709	3.7155

CONCLUSION

A new fault classification and faulted phase selection technique in single-circuit transmission by using the symmetrical components of electrical quantities lines was proposed. It is setting-free since it works with constant thresholds, that is, 1 and 0. Since setting these functions always requires struggles this feature of protective functions is very attractive. Another advantage is that it utilizes Q_0/Q_2 at each end and, thus, data of each end are not required to be synchronized since Q0 and Q2 are scalar quantities. This eliminates any concern about data synchronization. Moreover, the proposed method will not act on any symmetrical conditions which resemble faults, such as power swings and overloading since only zero-sequence and negative-sequence reactive power are used. The simulation results show that the capability of the system with high fault resistance.

But the fault classification technique for double phase to earth fault fails when fault location is on the extreme ends of the transmission line for high fault resistance case. As the fault resistance increases the span of length of transmission line in which the proposed method works reduces. Future work will expand to resolve this problem.

REFERENCES:

[1] A. Jamehbozorg and S. M. Shahrtash, "A decision-tree-based method for fault classification in single-circuit transmission lines," IEEE Trans.Power Del., vol. 25, no. 4, pp. 2190–2196, Oct. 2010.

[2] O. A. S. Youssef, "New algorithm to phase selection based on wavelet transforms," IEEE Trans. Power Del., vol. 17, no. 4, pp. 908–914, Oct.2002.

[3] Z.He,L.Fu,S.Lin,and Z.Bo, "Fault detection and classification in EHV transmission line based on wavelet singular entropy," IEEE Trans. Power Del., vol. 25, no. 4, pp. 2156–2163, Oct. 2010.

[4] [X. Dong,W. Kong, and T. Cui, "Fault classification and faulted-phase selection based on the initial current traveling wave," IEEE Trans. Power Del., vol. 24, no. 2, pp. 552–559, Apr. 2009

[5] G.BenmouyalandJ.Mahseredjian, "A combined directional and faulted phase selector element based on incremental quantities," IEEE Trans. Power Del., vol. 16, no. 4, pp. 478–484, Oct. 2001.

[6] T. Adu, "An accurate fault classification technique for power system monitoring devices," IEEE Trans. Power Del.,vol.17,no.3,pp.684–690, Jul. 2002

[7] X.-N. Lin, M. Zhao, K. Alymann, and P. Liu, "Novel design of a fast phase selector using correlation analysis," IEEE Trans. Power Del.,vol. 20, no. 2, pt. 2, pp. 1283–1290, Apr. 2005.

[8] P.K.Dash, S.R.Samantaray, and G.Panda, "Fault classification and section identification of an advanced series compensated transmission line using support vector machine," IEEE Trans. Power Del., vol. 22, no. 1, pp. 67–73, Jan. 2007.

[9] R. Salat and S. Osowski, "Accurate fault location in the power transmission line using support vector machine approach," IEEE Trans. Power Syst., vol. 29, no. 2, pp. 979–986, May 2004.

[10]. Wang and W. W. L. Keerthipala, "Fuzzy-neuro approach to fault classification for transmission line protection," IEEE Trans. Power Del., vol. 13, no. 4, pp. 1093–1104, Oct. 1998.

[11] Behnam Mahamedi and Jian Guo Zhu, "Fault Classification and Faulted Phase Selection Based on the Symmetrical Components of Reactive Power for Single-Circuit Transmission Lines," IEEE Trans Power Del, vol. 28, no. 4, October 2013.

[12] Abouzar Rahmati and Reza Adhami, "A Fault Detection and Classification Technique Based on Sequential Components," IEEE Trans. Industry Applications, vol. 50, no. 6, December 2014

International Journal of Engineering Research and General Science Volume 3, Issue 6, November-December, 2015
ISSN 2091-2730

Study of the Light Weight Deflectometer and Reviews

Shivamanth A., Pramod K. Kolase, Shama P S.
Mayank K. Desai, Atul K. Desai

(Applied Mechanics Department, SVNIT, Surat-395007
Email: shiva05cv@gmail.com Ph. No. 9408216712)
(Applied Mechanics Department, SVNIT, Surat-395007
Email : pramodkolase@gmail.com)
(Department of Computer Science & Engineering, CUK, Kalaburagi –585367
Email : shm.san1@gmail.com)
(Applied Mechanics Department, SVNIT, Surat-395007
Email : mkd@amd.svnit.ac.in)
(Applied Mechanics Department, SVNIT, Surat-395007
Email : akd@amd.svnit.ac.in)

ABSTRACT- The lightweight deflectometer (LWD) is currently essential instrument for further characterization of soil and their properties like modulus of elasticity (E) and deflection values. There are a number of commercially available LWD designs that yield different deflection and elastic modulus values. This provides good data to prescribe target deflections and elastic modulus values during earthwork construction analyses, this result gives the proper design for the given location. This paper presents on detailed study of LWD instrument and some of the review papers. The influence of the accelerometer versus geophone, measurement of base plate versus ground surface, LWD rigidity, and applied load pulse were investigated through field-testing. Several Researchers have used stress sensors to measure in-situ stress levels from various loading conditions and devices are shown in literature revive.
The use of a portable light weight deflectometer (LWD) for construction quality control and material investigation for earthworks and road construction. In the field of non-destructive testing of soil, the portable deflectometer devices have discovered , in the modern years, a wide use for in-situ assessment of elastic properties of soils, sub-grade and pavement foundations. The LWD- induced surface wave strain levels at a1m offset from the LWD were found to be on the order of 10.2 to 10.3% compared to the10.3 to 10.4% strain levels associated with conventional small hammer-induced surface waves. The measured low and high strain modulus compares well with published modulus reduction functions. The minimum LWD modulus value was obtained for sand-1, sand-2 and sand-3 layer, which was represents 19.0, 41.7 and 21.6 MPa respectively. The highest coefficient of variation was obtained for sand layers which goes up to 55.8% for sand-1 layer.

Keywords **–** LWD, Geophone, sub-grade, Deflection, Modulus of elasticity, rigidity, Stiffness.

INTRODUCTION

The Light Weight Deflectometer (LWD) is a portable it was developed in Germany especially as an alternative in-situ device to the plate load test with the ability to overcome accessibility problems for soil investigations and roads under construction. In the recent year, different types of LWD have been introduced in the market, including the German dynamic plate, the Transport Research Laboratory (prototype) foundation tester, and the Prima LWD.
The LWD is a field device that is increasingly being used for quality control/quality assurance (QC/QA) of compacted unbound materials. A falling weight (5-10–15kg) impacts a 200–300- mm-diameter (D) base plate and the resulting peak surface deflection (d0) and impact force are measured. The impact force and base plate diameter is designed to deliver a peak contact stress level (s0) of about100–200kPa to mimic the approximate stress pulse on a typical sub-grade or base layer due to traffic loading on top of a finished pavement. The resulting peak stress and deflection combined with homogeneous, isotropic, linear- elastic half-space theory yields a deformation modulus (Evd) of the soil. In the conventional LWD test a static loading condition (Livneh & Goldberg, 2001; Nazzal et al., 2004; Puppala, 2008; Ryden & Mooney, 2009; Vennapusa & White, 2009).

REVIEWS ON DIFFERENT PARAMETERS USING LWD

The research work is concerned with the compaction of the sub-grade and sub-base layers that comprise a pavement system. While the number and thickness of pavement layers varies generally, the typical structure is shown in “Fig.” 1.

Fig. 1 Typical Layer of pavement structure (Christopher et al., 2006).

Christopher et al., 2006, had provides the two purposes of sub-grade system; firstly, it provides a platform during the construction of the pavement structure; and secondly, it ensures that excessive deflection of the natural soil does not negatively influence the pavement structure. The sub-base strength shall be considers in the design of the pavement system. Therefore, the estimated bearing strength needs to be assuring during construction.

N. Ryden, and M. A. Mooney, 2009, were conducted field experiments on clay, silt and gravel soils to characterize the nature of LWD induced surface waves and to determine both low and high strain moduli. The usable high frequency limit was found to be 300Hz for LWD induced surface waves, enabling the low strain modulus characterization of the top 0.3–0.5m thick soil layer and finally, the measured low and high strain modulus.

Lambert et al., 2008, The portable devices are quick to implement and have been shown to adequately mimic the transient nature of wheel load forces, qualities that make them more appropriate for practical application. Typically, these devices usually measure a single deflection on the center of a bearing plate or on the surface of the prepared material being tested. The measured deflection may relate to the influence of one or more layers of material and could be used to determine the field values of parameters relevant in quality control and quality assurance.

METHODOLOGY AND MEASURING PRINCIPLE

A center geophone sensor measures the deflection caused by dropping a 10 kg hammer freely onto the loading plate. The falling mass impacts load produces pulse of 15-20 milliseconds. The diameter of the loading plate used in this research is 200 mm. Alternatively 100 mm and 300 mm plates are available. The load range of the LWD is 1 to 15 kN. It measures both force and deflection. The measured deflection of the ground is combined with the applied load to calculate the stiffness using conventional Bossiness static analysis. The load cell used in Prima 100 LWD has a resolution of 0.1 kN. The velocity transducer (geophone), which is mounted to the center of loading plate, has a resolution of one µm and range between 1-2200 µm. The standard model has one geophone sensor but models with three geophones, which can provide a simple deflection bowl, are also available Fleming (2000). The measured center deflection is used to estimate the dynamic deformation modulus as follows:

$$E_{LWD} = \frac{K \times (1 - u^2) \times P \times r}{d_c}$$

Where,

E_{LWD} = LWD dynamic modulus

K = p/2 and 2 for rigid and flexible plates, respectively.

d_C = Center deflection

P = Applied Stress

r = Radius of the plate

EQUIPMENT AND TEST PROCEDURE

A. LWD Equipment:

There are several types of LWDs. The LWD measures the deflection of the test layer produced from a given drop weight, drop height, and load according to the American Society for Testing and Materials (ASTM) Specification 2583–07, ‘‘Standard Test Method for Measuring Deflections with a Light Weight Deflectometer.’’ The built-in load cell and geophone measure the time history of the load pulse and soil velocity. Sensors may be of several types such as displacement transducers, velocity transducers, or accelerometers. The consequential integration provides a measure of the material displacement, which can be used with a measure of the peak load to determine the modulus values (Tehrani & Meehan, 2010). The following is a general description of the LWD will be Moving from top to bottom, the handle is used to keep the shaft vertical. Next along the shaft is a release trigger, which holds the mass in place prior to dropping, thereby, ensuring a standard drop height (720mm). The mass is dropped to provide an impact force. Buffers, made of either rubber pads or steel springs, catch the falling mass and transfer the impact force to the loading plate. Below the buffers is a measurement device that measures the deflection, and for some models the force. On the bottom, there is a loading plate, which must be in full contact with the ground. Impact load imposed to the plate are measured by a load cell and a geophone sensor mounted at the bottom of the plate measures the resulting deflection. Singh N et al (2010).

B. LWD test procedures:

The testing area should be levelled so that the load plate can be placed on an even surface. Loose particles on the surface should be removed and the load plate must be in contact with the material being tested. The diameter of the test area should be at least 1.5 times larger than the plate diameter Alshibli K (2005).

Table 1 LFWD test results

LAYER ID	LWD (Mpa)	Std.Deviation(Mpa)	CV (%)
Clay 1	181.3	18	11.4
Clay 2	-	-	-
Clay 3	51.5	11.3	18.7
Clay 4	133.9	64	45.7
Clay 5	47.6	8.4	18.4
Clay 6	313.9	38.5	13.5
Clay 7	227.6	73.3	32.5
Clay 8	33.2	0.8	2.5
Clay 9	172.4	2.1	1.5
ClayeySilt-1 (opt.)	32.4	4.6	14.9
ClayeySilt-2 (dry)	48.8	8.6	16.1
ClayeySilt-3 (wet)	29.5	14.2	47.3
Sand-1	19	6.7	56.8
Sand-2	41.7	3.8	14.9
Sand-3	21.6	5.4	28.6
		Average	23.15

THE LIGHT WEIGHT DEFLECTOMETER (LWD)

The LWD dynamic modulus values, corresponding standard deviation and coefficient of variation (CV) values are given in Table 1. There are total of fifteen test cases were conducted for each layer and it was represented by an average value of dynamic modulus. However, the LWD data for clay-2 layer is questionable. The LWD dynamic modulus readings for clay-2 layer were highly incompatible and ranged from 400 MPa to 700 MPa, which is also too high compared to strength results obtained from other tests. The minimum LWD modulus value was obtained for sand-1, sand-2 and sand-3 layer, which was represents 19.0, 41.7 and 21.6 MPa respectively. The highest coefficient of variation was obtained for sand layers, which goes up to 55.8% for sand-1 layer. Summary of Statistics result of the LWD Sample profiles tests as show table 2. Graphical represented in “Fig” 2.

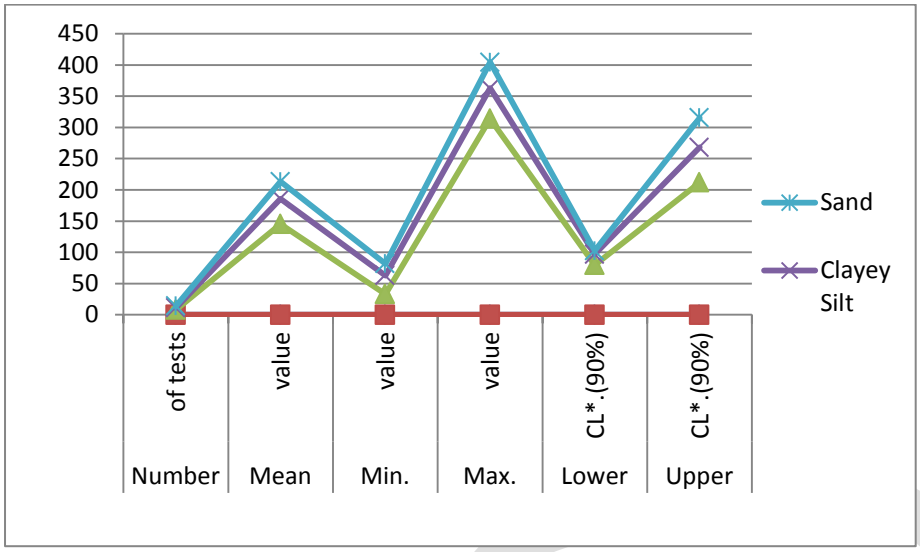

Fig 2 Typical Statistics result of the LWD Sample profiles tests

Table2. Descriptive Statistics of the LWD Results

LWD Dynamic Modulus (MPa)	No. of tests	Mean value (MPa)	Min. value (MPa)	Max. value (MPa)	Lower CL*. (90%)	Upper CL*. (90%)
Clay	8	145.17	33.2	313.9	79.8	212.0
Clayey Silt	3	40.6	29.5	48.8	17.1	56.1
Sand	3	27.43	19.0	41.7	5.5	47.4

LIMITATIONS

This paper reviews the LWD as a field evaluation tool and discusses the test variables and data quality. This concludes that its usefulness and its limitations for a variety of earthwork and road assessment scenarios. Many factors that influence LWD values and these should be considered while designing a quality assurance process in any agency/company. These factors include, but are not limited to, the following: size of loading plate, plate contact stress, type and location of deflection transducer, plate rigidity, loading rate, and buffer stiffness. Again, the moisture content of the material being tested has been reported to significantly influence the field modulus-based measurements. There is also an inverse relationship between water content and soil moduli (Hossain & Apeagyei, 2010; Ryden & Mooney, 2009). Also, in some cases, it is reported that the actual depth of the material being tested is greater than the single layer of material under consideration and therefore is measuring a composite layer composed of the material under consideration and underlying subbase and subgrade materials. The resulting modulus is therefore a composite rather than the modulus of the single layer under consideration (Benedetto & Di Domenico, 2012).

CONCLUSIONS

Light weight deflectometer (LWD) devices are newly established tools for estimating moduli during quality control and quality assurance. LWD devices are used because of they provide a somewhat accurate estimation of a soil modulus from a mechanically simple test.

An investigation was conducted to determine the influence of LWD design characteristics on the measured deflection and, by inference, estimated modulus.

The LWD is a versatile and portable stiffness measuring tool. From the published literature it appears to be increasingly used on a variety of materials/constructions including during construction and in service (on thinly surfaced roads) around the world.

The usable surface wave frequency content at 100–200Hz enables the low strain modulus characterization of the top 0.3–0.5 m thick soil layer, consistent with the measurement depth for the high strain modulus determined by conventional LWD testing.

REFERENCES:

[1] Livneh, M., & Goldberg, Y. (2001). Quality assessment during road formation and foundation construction: Use of falling-weight deflectometer and light drop weight. Transportation Research Record, 1755, 69–77.

[2] Nazzal, M., Abu-Farsakh, M., Alshibli, K., & Mohammad, L. (2004). Evaluating the potential use of a portable LFWD for characterizing pavement layers and subgrades. In M. K. Yegian & E. Kavazanjian, Geotechnical Engineering for Transportation Projects: Proceedings of Geo-Trans 2004, July 27–31, 2004, Los Angeles, California. Reston, VA: American Society of Civil Engineers.

[3] Puppala, A. (2008). Estimating stiffness of subgrade and unbound materials for pavement design. NCHRP Synthesis 382. Washington, DC: Transportation Research Board.

[4] Ryden, N., & Mooney, M. (2009). Analysis of surface waves from the light weight deflectometer. Soil Dynamics and Earthquake Engineering, 29, 1134–1142.

[5] Vennapusa, P., & White, D. (2009). Comparison of light weight deflectometer measurements for pavement foundation materials. Geotechnical Testing Journal, 32(3), 1–13.

[6] Christopher, B., Schwartz, C., & Boudreau, R. (2006). Geotechnical aspects of pavements (Report No. NHI-05- 037). Washington, DC: National Highway Institute, Federal Highway Administration, U.S. Department of Transportation.

[7] Lambert, J., Fleming, P., & Frost, M. (2008). The assessment of coarse granular materials for performance based pavement foundation design. International Journal of Pavement Engineering, 9(3), 203–214.

[8] Fleming, P.R. (2000). "Small-scale Dynamic Devices for the Measurement of Elastic Stiffness

[9] Modulus on Pavement Foundations." Nondestructive Testing of Pavements and Back calculation of Moduli, Volume 3, ASTM STP 1375

[10] ASTM (2011)Specification 2583–07 Standard Test Method for Measuring Deflections with a Light Weight Deflectometer (LWD)

[11] Tehrani, F. and Meehan, C. (2010).The effect of water content on light weight deflectometer measurements. Proceedings from GeoFlorida 2010: Advances in Analysis, Modeling & Design, 930–939. http://dx.doi.org/10.1061/ 41095(365)92.

[12] Singh, N., Mejia, C., Martison, T., Shah, F., Fleming, C., & Fitzpatrick, J. (2010). Use of the light weight deflectometer (LWD) at Highland Valley Copper Mine. Proceedings from the 63rd Canadian Geotechnical Conference, Sept. 12–16, Alberta, Canada.

[13] Alshibli, K., Abu-Farsakh, M., & Seyman, E. (2005). Laboratory evaluation of the geoguage and light falling weight deflectometer as construction control tools. Journal of Materials in Civil Engineering, 17(5), 560–569.

[14] Hossain, M., & Apeagyei, A. (2010). Evaluation of the lightweight deflectometer for in-situ determination of pavement layer moduli (Publication No. FHWA/VTRC 10-R6). Charlottesville, VA: Virginia Transportation Research Council Research.

[15] Benedetto, A., & Di Domenico, F. (2012). Elliptic model for prediction of deflections induced by a light falling weight deflectometer. Journal of Terramechanics, 49, 1–12.

International Journal of Engineering Research and General Science Volume 3, Issue 6, November-December, 2015
ISSN 2091-2730

Android Based Healthcare System Using Augmented Reality

Vaishnavi Chidgopkar[1], Raksha Shelar[2,] Shweta Patil[3]

1,2,3 Department of Computer Engineering, Padmashree. Dr. D. Y. Patil Institute of Engineering

Management and Research, Pune, India.

rakshashelar3@gmail.com , contact no: 9011545966

Abstract— Android mobile phone most important part of today's lifestyle. Currently people use their mobile for calling as well as for other purpose like searching information or any location using internet and GPS, playing games, etc. It observed that people in unknown area face difficulties to find hospital quickly. In emergency cases even single minute is important so this smart application helps person to quickly locate the healthcare utility. The aim of this paper is to build Intelligent Healthcare Management system using Android OS and Augmented Reality concept [4]. So any person can access medical information, like Hospital's contact details and address, contact details of Ambulance service and also can find out nearer hospital and medical store at anytime from anywhere. We must ensure that a person when visiting places need not have to worry about, where is the hospital or medical store and the contact number of ambulance .Using this application all the information is accessible on the android device and also in user customized format. We are using JSON parsing to keep updated record about doctor's contact details and their location.
.

Keywords— Android operating system, Augmented Reality, JSON, GPS, Google map, GPRS, SQLite.

INTRODUCTION

In this growing age of technology it is necessary to have a proper healthcare management system. This application runs on Android device. It helps patient to query their symptoms and get the hospital location and also it helps user to get the location of medical stores and ambulance. Patient can easily access all the healthcare utility regardless of their current location. We are using Augmented Reality concept using android phone [5]. Healthcare application uses camera of phone to access location. Augmented reality is One type of virtual reality. It can be used on any type of screen and connected devices. It is related to mediated reality, in this, view of reality is modified by computer. AR is used in many applications like entertainment, military training, engineering design, manufacturing, robotics etc [4]. First this application ask to select location , after selecting location, application accepts the symptoms from the user, process the data, identifies the particular disease and provide appropriate hospital's contact details using JSON parsing. The advantage of application is user can also search the exact location of hospital or medical store. This technology utilizes various sensors embedded in the mobile device.

Existing system

Existing system only provides the information about doctor, and it just provides contact number, but it fails to provide exact location of hospital. In existing system user can access only predefined location, it cannot access the location other than previously stored location provided in the application.

Proposed system

In this application user can access hospital regardless of his location, and can also locate the nearby medical store and ambulance service provider. The key feature of this application is using augmented reality on android platform. This is done by AR (Augmented Reality). This AR Technology makes use of various sensors embedded in the mobile device, like Location sensors i.e.; GPS, the location sensor determine user's current location [1]. Google Map is used to find particular location or to trace the route between any

two locations but it simply provides the top view of the map so it make confusing situation for user between the mobile standard north that is fixed, and the frequent position changing of the user in real time .To address this problem we are developing an application that allows user to select location and then provides options to select parameters like hospital , medical store or ambulance .If user selects parameter as hospital then application provides list of doctor's type then user can select the type of doctor from list like dentist, cardiologist, orthopedic, Dermatologist etc, and it automatically finds your current location and plots it on a map using an marker and provide an short description on it about the hospital. If user selects Ambulance as parameter then application provides list of the phone numbers of ambulance services provided in that particular area. In this application all data is link through Google. There is no need to manage separate data base. This data base is redirect as per user requirement.

System Architecture

Fig shows architecture of proposed system. It consists of GPS, Google Server, Data base, LBS (Location Base Sensor).

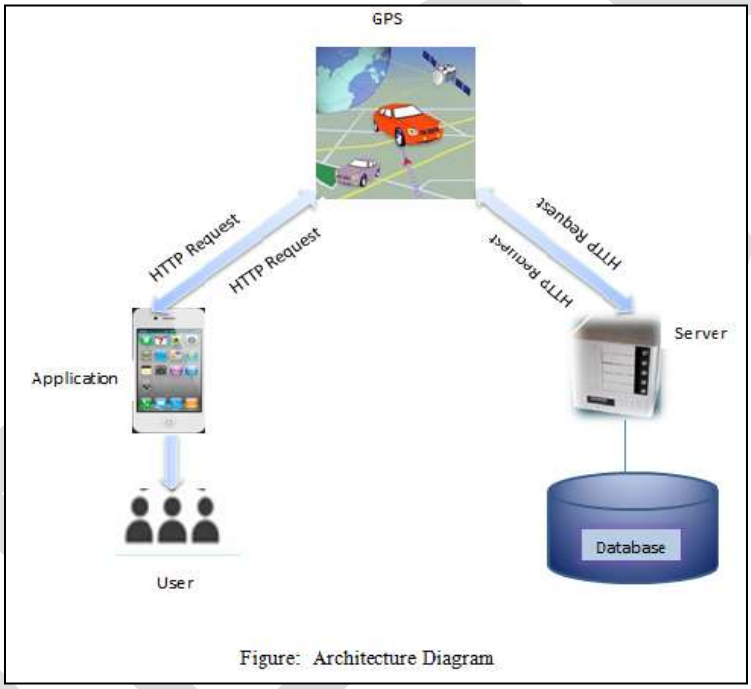

Figure: Architecture Diagram

a) GPS (Global Positioning System)

It is a space based navigation system. It provides location at any time in any weather situation. this concept is based on clock. The current GPS system consists of 3 major segments, 1) space segment (ss) 2) control segment (cs) 3) user segment (us). GPS compute difference between time and signal from different satellites to trace the user's exact location. A-GPS (Assisted GPS) is new technology which is used to integrate the mobile network with GPS to give better accuracy.

b) Data base

SQLite - SQLite is relational database management system which implements server less, zero configuration (means no setup or administration needed), self-contained (no external dependency), transactional SQL database engine. It is used to reduce the latency in database access. It is very small and light weight. It is written in ANSI-C and provides easy way to use API. Separate server process or system to operate is not required by SQLite. To create database, define tables in it, insert and change rows and run queries a standalone command line program is used. To create new SQLite database 'sqlite3' command is used, there is no need to have any special privilege to create new SQLite database.

c) LBS (Location Base Sensor)

This service is offered through mobile phone. Location-based services or LBS refer to a set of applications that accomplish the knowledge of the geographical location of a mobile device in order to provide services based on that information [2]. It is depend on location of mobile devices.

Uses of LBS: -

- Store location
- Travel information
- Roadside assistance
- Fraud prevention

5. Technology & Concept

I. Augmented Reality

1. Augmented reality is one type of virtual reality [1]. It can be used on any type of screen and connected devices. It is related to mediated reality, in this, view of reality is modified by computer. AR is used in many applications like, military training, engineering design, robotics, manufacturing, entertainment, medical application, wearable technology etc [7]. Components of AR are GPS, POI (Points of Interest).

POI: - It provides location information of any place. This information includes POI titles, description. It interacts with environment.

II. JSON

JSON means JavaScript Object Notation. It is an independent data exchange format and is the best alternative for XML. It is easy to read and write for human. It is language independent, self-describing, easy to understand.

Android provide four different classes to manipulate JSON data:

1. JSONArray.
2. JSONObject.
3. JSONStringer.
4. JSONTokenizer.

Component of JSON:

1. Array ([): Square ([) bracket represent JSON Array.
2. Objects ({): Curly ({) bracket represent JSON Objects.
3. Key: It is just a string. Pairs of key-value make up a JSON Object.
4. Value: Each Key has value that could string, integer, double.

Acknowledgement

It gives us great pleasure in presenting the paper on 'Android Based Healthcare System Using Augmented Reality Concept'.

We would like to take this opportunity to thank our internal guide Prof. Suvarna Patil for giving us all the help and guidance we needed. We are really grateful to them for their kind support. Their valuable suggestions were very helpful.

Conclusion

In this paper we have presented an android based healthcare management system with augmented reality. In this paper we take advantage of augmented reality on an android platform to address the location tracing problem. User can access the correct information at exact location in real time. The aim of this paper is to build Intelligent Healthcare Management system using Android OS and Augmented Reality concept [4]. So any person can access medical information, like Hospital's contact details and address, contact details of Ambulance service and also can find out nearer hospital and medical store at anytime from anywhere.

REFERENCES:

[1] Global Illumination for Augmented Reality on Mobile Phones: Yong Beom Lee§ Samsung Advanced Institute of Technology Samsung

[2] Amit Kushwaha, Vineet Kushwaha _Location Based Services using Android Mobile Operating System'International Journal of Advances in Engineering & Technology, © IJAET ISSN: 2231-1963.

[3] M. Alcaniz, D. C. Perez- Lopez, and M. Ortega, "Design and Validation of an Augmented Book for Spatial Abilities Development in Engineering Students", Computers & Graphics, 2010, 34(1), pp. 77-91.

[4] J. Joachim, R. Newcombe, and A. Davison. Real-time surface lightfield capture for augmentation of planar specular surfaces. In Proceedings of the 2012 IEEE International Symposium on Mixed and Augmented Reality (ISMAR), pages 91–97, Atlanda, USA, Oct. 2012.

[5] Francois Andry, Lin Wan and Daren Nicholson, "A Mobile Application Accessing Patients' Healthcare Records Through a Rest API,"IEEE 2012.

[6] Onlive. Onlive. Last accessed: 28 March 2013. http://www. onlive.com/.

[7] Hand-held Mobile Augmented Reality for Collaborative Problem Solving: A Case Study with Sorting: 2014 47th Hawaii International Conference on System Science.

[8]. AndrzejPodziewski, KamilLitwiniuk, JarosławLegierski,"Emergency Button – a Telco 2.0 application in the e-health environment", 978-83-60810-48- 4/$25.00 c 2012 IEEE.

[9]. Baviskar Rahul Nandkishor Mrs. Aparna Shinde Mrs. P. Malathi, "Android Smartphone Based Body Area Network for Monitoring and Evaluation of Medical Parameters", 978-1-4799-3486-7/14/$31.00_c 2014 IEEE.

[10]. Vandana Rohoakale, Neeli Prasad, "Receiver Sensitivity in Opportunistic Cooperative Internet of Things (IoT)", Second International Conference on Ad Hoc Networks, August 2010, Victoria, British Columbia, Canada

[11]**.** DINESH B. RAUT. PRAGATI PATIL," RESEARCH ON EMERGENCY CALL AND LOCATION TRACKING SYSTEM WITH ENHANCED FUNCTIONALITY FOR ANDROID", VOLUME 3, ISSUE 5, MAY 2015

[12]. Chao-Lin Chen; Kai-Ten Feng, "Hybrid Location Estimation and Tracking System for Mobile Devices" Vehicular Technology Conference, 2005. VTC 2005- Spring, 2005 IEEE 61st Volume4

International Journal of Engineering Research and General Science Volume 3, Issue 6, November-December, 2015
ISSN 2091-2730

Effects of Kingiodendron *Pinnatum Leaves*(KPL) on Zinc in Natural sea water

P. Deivanayagam[1*], I. Malarvizhi[1,] S. Selvaraj[1]D.P. Rufus[2]

[1]Postgraduate and Research Department of chemistry Sri Paramakalyani College, Alwarkurichi – 627 412, Tamil Nadu, India.

[2]Principal, Department of mechanical engineering, FX Polytechnic College, Tharuvai - 627356

Corresponding author: deivam1101@gmail.com

Abstract -The inhibition efficiency of kingiodendron pinnatum leaves extract on Zinc in Natural Sea Water environment. It has been investigated on various concentrations of inhibitor as well as temperature by mass loss measurement. The observed results indicate that the percentage of inhibition efficiency is increased with increase of inhibitor concentration as well as temperature. Thermodynamic parameter viz (E_a, Q_{ads}, ΔG_{ads}, ΔH and ΔS) suggests that the adsorption of inhibitor is chemisorptions, exothermic and Spontaneous process. The Corrosion product on the metal surface in the presence and absence of inhibitor is characterized by UV, FT-IR and SEM-EDX Spectral techniques.

Keywords: Zinc, KPL inhibitor, Natural Sea Water, Mass Loss, Adsorption

1. INTRODUCTION

Corrosion is defined as destruction or deterioration of a material (metal) because of its reaction with environment[1]. Zinc metal has a numerous industrial applications and is mainly used for the corrosion protection of steel. Because steel exhibits a wide range of useful forms and mechanical properties. Due to these facts steel is almost used in all industries[2]. The zinc-coated steel materials provide a greater resistance to corrosion, but they undergo rapid corrosion, when exposed to humid atmosphere leading to the formation of a corrosion product known as white dust[3]. Zinc is an industrially important metal and is corroded by many agents, of which aqueous acids are the most dangerous one[4]. Due to the increasing usage of zinc, the study of corrosion inhibition is most important one. Every year, billions of dollars are spent on capital replacement and control methods for corrosion infrastructure[5]. The inhibitor must be eco-friendly to replace the older, which is more toxic and harmful to the environment. The recent years literature reveals that the study of corrosion inhibition of different metals with various green inhibitor have been reported. A few investigations are Red Peanut Skin[6], Musa species peels[7], *Vernonia Amygdalina*[8] , *Piper guinensis*[9], Henna extract[10], *Delonix regia* extracts[11], Rosemary leaves[12], natural honey[13], *opuntia* extract[14], khillah (*Ammi visnaga*) seeds[15], *Carica Papaya* and *Camellia Sinensis* Leaves[16], *Ricinuscommunis* Leaves[17], *Justicia gendarussa*[18], *Vitis vinifera*[19],*Punica granatum* peel[20], Leaves of *Genus Musa*, *GenusSaccharum* and *Citrullus Lanatus*[21] have been studied onvarious metals and alloys. However only a limited number of literatures is available for the corrosion inhibition by green inhibitor with zinc metal surface. Some investigators have been reported with zinc metal is *Ocimum tenuiflorum*[22], Red onionskin[23], *Nypa fruticans Wurmb*[24], *Aloe vera*[25], henna (*lawsonia*) Leaves[26]. Thus, our present attention is to study the effect of adsorption and corrosion resistant behavior of Kinglodendron pinnatum leaves on zinc metal surface with natural sea water environment [27-36].

2 MATERIALS AND METHODS

2.1 Specimen preparation

Zinc specimen were mechanically pressed cut to form different coupons, each of dimension exactly 20cm^2 (5x2x2cm), polished with emery wheel of 80 and 120, and degreased with trichloroethylene, then washed with distilled water cleaned, dried and then stored in desiccator for the use of our present study.

2.2 Preparation of *Kingiodendron Pinnatum Leaves (*KPL) Extract:

About 3 Kg of *Kinglodendron Pinnatum,* leaves was collected from in and around Western Ghats and then dried under shadow for 5 to 10 days. Then it is grained well and finely powdered, exactly 150g of this fine powder was taken in a 500ml round bottom flask and a required quantity of ethyl alcohol was added to cover the fine powder completely, and left it for 48 hrs. Then the resulting paste was refluxed for about 48 hrs, the extract was collected and the excess of alcohol was removed by the distillation process. The

obtained paste was boiled with little amount of activated charcoal to remove impurities, the pure plant extract was collected and stored.

2.3 Properties of Kingiodendron pinnatum leaves:

Kingiodendron pinnatum leaves belongs to *Euphorbiaceous* family and it is an annual herbaceous climbing plant with a long history of traditional medicinal uses in many countries, especially in tropical and subtropical regions. The common Name is Kolavu. The peel extract of this plant is used to regulate thyroid function and glucose metabolism. The phytochemicals present in this plant is flavonoids, alkaloids, saponins and triterpenes

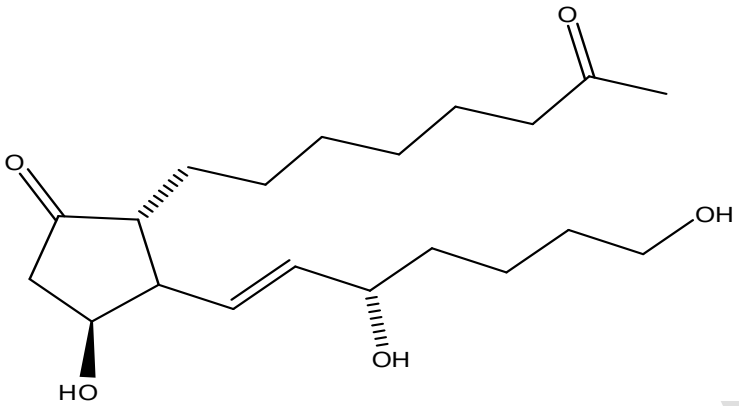

Figure 1: Chemical structure of the main active compounds present in *Kingiodendron pinnatum* leaves extract.

2.4 Mass loss measurement

In the mass loss measurements on Zinc in triplicate were completely immersed in 100ml of the test solution in the presence and absence of the inhibitor. The metal specimens were withdrawn from the test solutions after an hour at 313K to 333K and also measured 24 to 360 hrs at room temperature. The Mass loss was taken as the difference in weight of the specimens before and after immersion using LP 120 digital balance with sensitivity of ±1 mg. The tests were performed in triplicate to guarantee the reliability of the results and the mean value of the mass loss is reported.

From the mass loss measurements, the corrosion rate was calculated using the following relationship.

$$\text{Corrosion Rate}(\text{mmpy}) = \frac{87.6 \times W}{DAT} \qquad \text{---------- (1)}$$

Where, mmpy = millimeter per year, W = Mass loss (mg), D = Density (gm/cm^3),

A = Area of specimen (cm^2), T = time in hours.

The inhibition efficiency (%IE) and degree of surface coverage (θ) were calculated using the following equations.

$$\%IE = \frac{W_1 - W_2}{W_1} \times 100 \qquad \text{---------- (2)}$$

$$\theta = \frac{W_1 - W_2}{W_1} \qquad \text{---------- (3)}$$

Where W_1 and W_2 are the corrosion rates in the absence and presence of the inhibitor respectively.

2.5 Adsorption studies

2.5.1 Activation energy

The activation energy (E_a) for the corrosion of Copper in the presence and absence of inhibitors in natural sea water environment was calculated using Arrhenius theory. Assumptions of Arrhenius theory is expressed by equation (4).

$$CR = A\exp(-E_a/RT) \quad \text{---------- (4)}$$

$$\log(CR_2/CR_1) = E_a/2.303\ R\ (1/T_1 - 1/T_2) \quad \text{---------- (5)}$$

Where CR_1 and CR_2 are the corrosion rate at the temperature T_1 (313K) and T_2 (333K) respectively.

2.5.2 Heat of adsorption

The heat of adsorption on the surface of various metals in the presence of plant extract in natural sea water environment is calculated by the following equation.

$$Q_{ads} = 2.303\ R\ [\log(\theta_2/1-\theta_2) - \log(\theta_1/1-\theta_1)] \times (T_2T_1/T_2-T_1) \quad \text{---------- (6)}$$

Where R is the gas constant, θ_1 and θ_2 are the degree of surface coverage at temperatures T_1 and T_2 respectively.

2.5.3 Langmuir adsorption isotherm

The Langmuir adsorption isotherm can be expressed by the following Equation-4.10 is given below.

$$\log C/\theta = \log C - \log K \quad \text{---------- (7)}$$

Where θ is the degree of surface coverage, C is the concentration of the inhibitor solution and K is the equilibrium constant of adsorption of inhibitor on the metal surface.

2.5.4 Free energy of adsorption

The equilibrium constant of adsorption of various plant extract on the surface of copper, mild steel and zinc is related to the free energy of adsorption ΔG_{ads} by equation (8).

$$\Delta G_{ads} = -2.303\ RT \log(55.5\ K) \quad \text{---------- (8)}$$

Where R is the gas constant, T is the temperature, K is the equilibrium constant of adsorption**.**

3. RESULT AND DISCUSSION

3.1 Mass loss measurements

The dissolution behavior of Zinc in Natural sea water environment containing in the absence and presence of KPL extract with various exposure times (120to 480 hrs) are shown in Table-1**.** The observed values are clearly indicates that in the presence of MEL inhibitor the corrosion rate significantly reduced from 0.2556to 0.0408 mmpy (120 hrs) and 0.1380 to 0.0332 mmpy (480 hrs) with increase of inhibitor concentration from 0 to 1000 ppm. The maximum of 84 % of inhibition efficiency is achieved even after 120 hrs exposure time. This achievement is mainly due to the presence of active phytochemical constituents present in the KPL extract which is adsorbed on the metal surface and shield completely to prevent further dissolution from the aggressive media of chloride ion (Cl^-).

Table -1: The corrosion parameters of Zinc in Natural Sea Water containing different concentration of KPL extract after 120 to 480 hours exposure time

Con. of	120 hrs	240 hrs	360 hrs	480 hrs

inhibitor (ppm)	C.R	% I.E	C.R	% I.E	C.R	% I.E	C.R	% I.E
0	0.2556	--	0.1840	--	0.1397	--	0.1380	--
10	0.1942	24.00	0.1508	18.05	0.1022	26.82	0.1022	25.92
50	0.1635	36.00	0.1226	33.33	0.0954	31.70	0.0920	33.33
100	0.1431	44.00	0.0996	47.83	0.0886	36.53	0.0843	38.89
500	0.1022	60.00	0.0971	47.22	0.0783	43.90	0.0626	54.62
1000	0.0408	84.00	0.0511	72.22	0.0477	67.85	0.0332	75.93

3.2 Temperature Studies

The corrosion parameters of copper in Natural Sea Water containing various concentration of KPL extract with different temperature in range from 313 to 333K is shown in Table-2. In the absence of inhibitor, the corrosion rate increased from 23.3102 to 48.4621 mmpy at 313 to 333K, but in the presence of inhibitor, the value of corrosion rate decreased from 23.3102 to 4.9075mmpy and 48.4621 to 5.5210 mmpy with increase of inhibitor concentration at 313and 333K. The maximum of 88.60 % inhibition efficiency is achieved at 333K respectively. The value of inhibition efficiency is increased with rise in temperature (313-333K). This results clearly reflects that component present in the inhibitor on the metal surface is higher than the desorption process. It clearly shows that the inhibitor follows chemisorptions process

Table -2: The corrosion parameters of Zinc in Natural Sea Water containing different concentration of KPL extract at 313,323 and 333 K

Con. of inhibitor (ppm)	313 K		323 K		333 K	
	C.R	% I.E	C.R	% I.E	C.R	% I.E
0	23.3102	68.42	25.7647	--	48.4621	--
10	7.3614	89.47	19.6305	23.80	16.5632	65.82
50	2.4537	92.10	7.9747	69.04	8.5882	82.27
100	1.8403	76.31	2.4537	90.47	5.5210	88.60
500	5.5210	78.94	11.0421	57.14	13.4957	72.15
1000	4.9075	68.42	9.8512	61.64	11.6554	75.94

3.3 Effect of Temperature

3.3.1 Activation energy:

The observed values of activation energy are ranged from 35.1417 – 54.2894 kJ/mol for Zinc in natural Sea Water containing various concentration of inhibitor. The average value of E_a obtained from the blank (31.71581) is lower than that in the presence of inhibitor and clearly suggest that there is a strong chemical adsorption bond between the KPL inhibitor molecules and the Zinc surface.

Table -3: Calculated values of Activation energy (E_a) and heat of adsorption (Q_{ads}) of KPL extract on Zinc in Natural Sea Water environment**.**

S. No	Conc. of inhibitor(ppm)	% of I.E		E_a ($KJmol^{-1}$)	Q_{ads} ($KJmol^{-1}$)
		40^o	60^o		
1.	0	--	--	31.7158	--
2.	10	68.420	65.822	35.1417	-1.0063
3.	50	89.473	82.278	54.2894	-0.0990
4.	100	92.105	88.607	47.6093	-0.3158
5.	250	76.315	72.151	38.7343	-1.1649
6.	500	78.947	75.949	37.4853	-0.7106

3.3.2 Heat of adsorption:

The value of heat of adsorption (Q_{ads}) on Zinc in Natural Sea Water containing various concentration of KPL extract is calculated and the values of Q_{ads} are ranged from -0.0990 to -1.1649 kJ/mol (Table- 3). These negative values reveals that the adsorption of KPL extract on the surface of Zinc may follows exothermic process.

3.3.3 Adsorption studies:

The adsorption isotherm is a process, which are used to investigate the mode of adsorption and it characteristic of inhibitor on the metal surface. In our present study the Langmuir adsorption isotherm is investigated. The straight line (Fig-1) indicates that the inhibitor follows Langmuir adsorption isotherm.

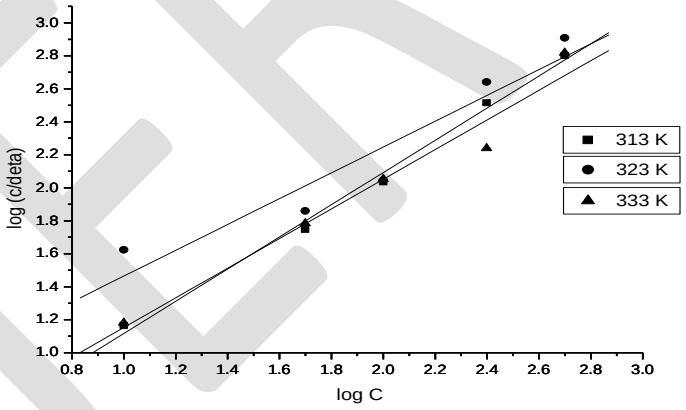

Figure-2: Langmuir isotherm for the adsorption of KPL inhibitor on Zinc in Natural Sea Water Environment

3.3.4 Free energy of adsorption:

The standard free energy of adsorption (ΔG_{ads}) can be calculated using the Equation- (8) and the observed negative values are (Table-1) ensure that the spontaneity of the adsorption process and the stability of the adsorbed layer is enhanced.

Table-4: Langmuir adsorption parameters for the adsorption of KPL inhibitor on Zinc in Natural Sea Water

Adsorption isotherms	Temperature (Kelvin)	Slope	K	R2	Gads kJ/mol
Langmuir	313	0.97585	0.14107	0.9966	-5.356

	323	0.78254	0.68212	0.9061	-9.760
	333	0.8987	0.25447	0.9662	-7.331

3.3.5 Thermodynamics parameters

The another form of Transition State equation which is derived from Arrhenius equation as below (4)

$$CR=RT/Nh \exp(\Delta S/R) \exp(-\Delta H/RT) \text{ ----- (4)}$$

Where h is the Planck's constant, N the Avogadro's number, ΔS the entropy of activation, and ΔH the enthalpy of activation. A plot of log (CR/T) vs. 1000/T gives a straight line (Fig. 4) with a slope of (−ΔH/R) and an intercept of [log(R/Nh)) + (ΔS/R)], from which the values of ΔS and ΔH were calculated and listed in Table-5. The observed positive values of enthalpy of activation suggest that the endothermic nature of the metal dissolution process is very difficult. The increase of ΔS is generally interpreted with disorder may take place on going from reactants to the activated complex.

Table -5: Thermodynamic parameters of zinc in natural sea water obtained from weight loss measurements

S.No	Concentration of KPL (ppm)	ΔH (kJ mol^{-1})	ΔS (J k^{-1} mol^{-1})
1	0	13.6787	-51.9717
2	10	15.4953	-49.3507
3	50	22.3972	-26.8013
4	100	20.4333	-39.0817
5	250	15.7525	-49.7643
6	500	15.2221	-51.8623

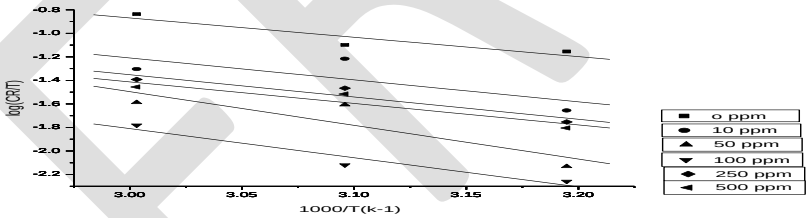

Figure- 3: The relation between log (CR/T) and 1/T for different concentrations of KPL extract.

3.4 UV SPECTROSCOPY:

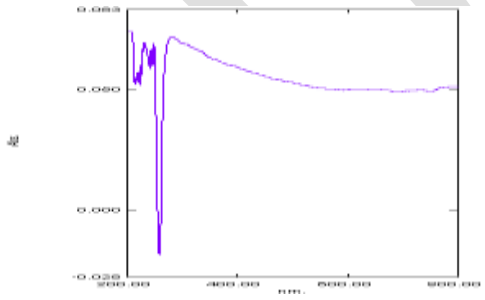

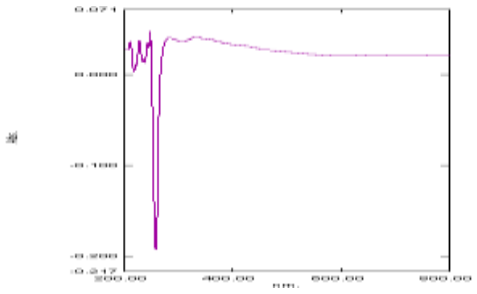

Figure 4 **Figure 5**

Figure- 4: UV spectrum of ethanolic extract of KPL**, Figure -5:** Corrosion product on Zinc in Natural Sea Water in the presence of KPL extract

The Figures 4 and 5 shows that the UV visible spectrum of ethanolic extract of KPL and the corrosion product on the surface of mild steel in the presence of KPL extract in natural sea water respectively. In this spectrum, one peak is appeared around 300nm (Fig 3) and in the presence of inhibitor the band was disappeared. This change of absorption band may confirm that the strong co-ordination bond between the active group present in the inhibitor molecules and the metal surface.

3.5 FT-IR SPECTROSCOPY

FT-IR studies of KPL extract on Zinc surface in Natural Sea Water:

The figures- 6 and 7 reflect that the FTIR spectrums of the ethanolic extract of inhibitor and the corrosion product on Zinc in the presence of KPL extract in Natural Sea Water. On comparing both of these spectra the prominent peak such as, the -O-H stretching frequency for alcohol is shifted from 2926.45 to 2927.41cm^{-1}, the C-O stretching in acid is shifted from 1117.55 cm^{-1} to 1108.87cm$^{-1.}$ and 1632.45 cm^{-1} corresponds to C-O stretching frequency for carbonyl compounds is shifted to 1612 cm^{-1}. These results also confirm that the FTIR spectra support the fact that the corrosion inhibition of KPL extract on Zinc in Natural Sea Water may be the adsorption of active molecule in the inhibitor and the metal surface.

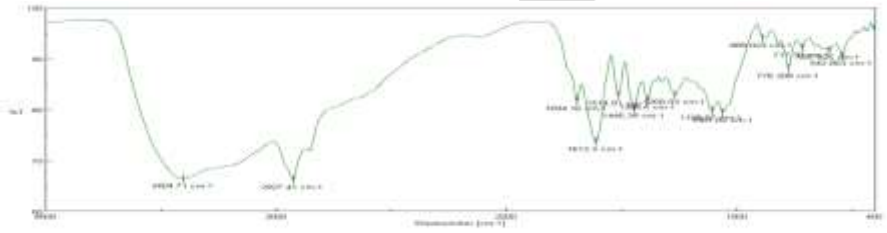

Figure-6: FT-IR spectrum of ethanolic extract of *Kingiodendron pinnatum* leaves (KPL)

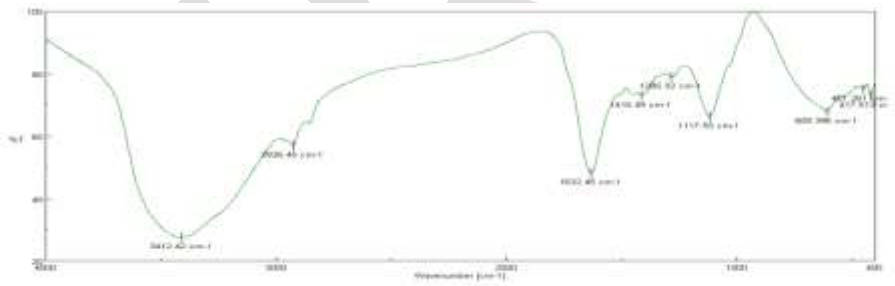

Figure-7: FT-IR spectrum for the corrosion product on Zinc in the presence of KPL extract with Natural Sea Water

3.6 EDX ANALYSIS

EDX spectroscopy was used to determine the elements present on the zinc surface before and after exposure to the inhibitor solution. Figures 8 & 9 represents the EDX spectra for the corrosion product on metal surface in the absence and presence of optimum concentrations of KPL extract with Natural sea water environment. In the absence of inhibitor molecules, the spectrum may confirms that the existence of zinc, iron, silicon, carbon, stannum. However, in the presence of the optimum concentrations of the inhibitors, oxygen atom is found to be present on the metal surface. It clearly indicates that the hetero atom such as oxygen present in the inhibitor molecules may involve the adsorption process with metal atom and hence it may protect the metal surface against the corrosion.

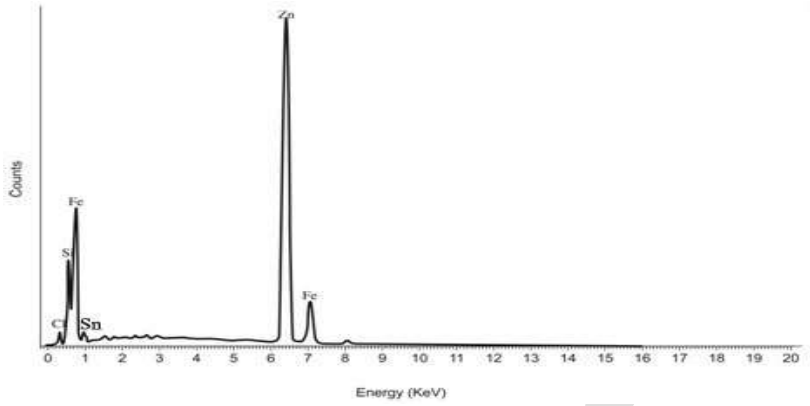

Figure -8: EDX spectrum of the corrosion product on zinc surface in Natural seawater**.**

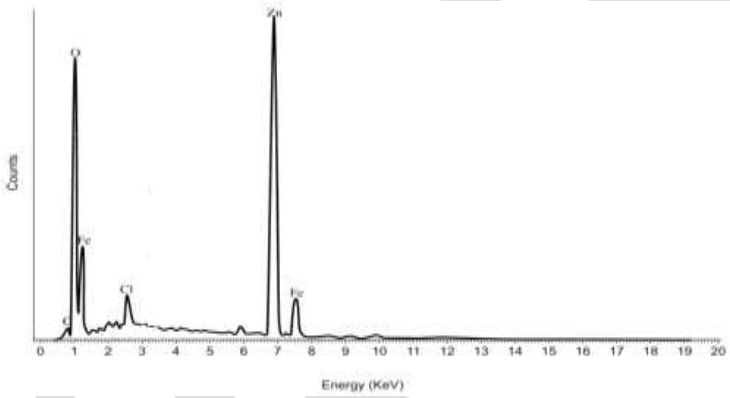

Figure- 9: EDX spectrum of the corrosion product on zinc surface with the presence of KPL extract in Natural seawater.

3.7 SEM ANALYSIS

The surface morphology of zinc surface was studied by scanning electron microscopy (SEM). The Figures-10 (a) and (b) shows the SEM micrographs of zinc surface before and after immersed in Natural seawater, respectively. The SEM photographs showed that the surface of metal has a number of pits with layer type, but in presence of inhibitor they are almost minimized by the formation of spongy mass covered on the entire surface of the metal.

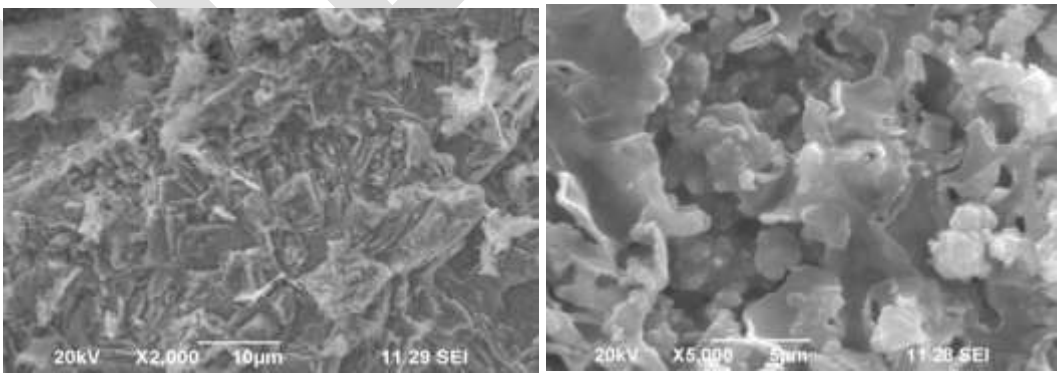

(a) (b)

Figure 10: SEM images of the zinc surfaces: (a) immersed in Natural sea water (b) immersed in natural sea water with KPL extract.

ACKNOWLEDGMENT

The authors would like to thank to the management of sri paramakalyani college, alwarkurichi, for providing the lab facilities. The spectral studies (UV & FT-IR) were taken in psn college of engineering and technology, tirunelveli. The SEM and EDX were taken in karunya university coimbatore

4. CONCLUSION

Using *Kingiodendron pinnatum* leaves (KPL) extract on zinc in natural sea water

Using KPL extract on zinc, the corrosion rate markedly reduced with increase of concentrations from 0 to 500ppm. Even though we attained the maximum 84% inhibition efficiency after 120 hours exposure time. This is due to strong bindings between the inhibitor molecule and ions from the metal surface. In temperature studies, the percentage of inhibition efficiency increased with rise of temperature ranges from 313 to 333K is due to the adsorption of active inhibitor molecules on the metal surface is higher than desorption process. The maximum 92% inhibition efficiency is attained and follows chemisorptions. The thermodynamic parameters namely activation energy (E_a), heat of adsorption (Q_{ads}), Standard free energy adsorption (ΔG_{ads}), enthalpy (ΔH) and entropy (ΔS), suggests that, strong chemical bond, exothermic, spontaneous process respectively. The KPL inhibitor obeys Langmuir adsorption isotherm. The film formation may also confirm UV, FTIR, SEM, EDX, spectral studies

REFERENCES:

[1] US Report on "Corrosion Costs and Preventive Strategies in the United States", www.corrosioncost.com, July 2002
[2] Popoola A.P.I. and Fayomi O.S.I., "Electrochemical Study of Zinc Plate in Acid Medium, Inhibitory Effect of Bitter Leaf (Vernonia Amygdalina)", *Int. J. Electrochem. Sci.,* 6(8), 4581–4592 2011
[3] Rajappa S.K., Venkatesha T.V. and Praveen B.M., "Chemical treatment of zinc surface and its corrosion inhibition studies", *Bull. Mater. Sci.,* 31(1), 37–41 2008
[4] Shanthamma Kampalappa rajappa Thimmappa V.Venkatesha., "Inhibition Studies of a Few Organic Compounds and their condensation products on the corrosion of Zinc in Hydrochloric Acid Medium", *Turk. J. Chem.,* 27, 189-196 2003
[5] Cherry B.W. and Skerry B.S., Clayton Vic. "Corrosion in Australia: the report of the Australian National Centre for Corrosion Prevention and Control feasibility Study" Department of Materials Engineering, Monash University: Australia (1983)
[6] James A.O., Akaranta O. and Awatefe K.J., Red PeanutSkin, "An Excellent Green Inhibitor for Mild Steel Dissolution in Hydrochloric Acid Solution", *An Int. J. of Chem.,* 2(2), 133-139 2011
[7] Eddy N.O., Odoemelam S.A. and Odiongenyi A.O.,"Ethanol extract of musa species peels as a green corrosion inhibitor for mild steel: kinetics adsorption and thermodynamic considerations", *EJEAFChe.,* 8 (4), 243- 253 2009
[8] Nwabanne J.T. and Okafor V.N., "Inhibition of the Corrosion of Mild Steel in Acidic Medium by Vernonia Amygdalina, Adsorption and Thermodynamics Study", *JETEAS,* 2(4), 619-625 2011
[9] Ebenso E.E., Eddy N.O. and Odiongenyi A.O., "Corrosion inhibitive properties and adsorption behaviour of ethanol extract of Piper guinensis as a green corrosion inhibitor for mild steel in H_2SO_4", *Afr. J. Pure Appl. Chem,* 2(11), 107-115 2008
[10] Ostovari A., Hoseinieh S.M., Peikari M., Shadizadeh S.R. and Hashemi S.J., "Corrosion inhibition of mild steel in 1M HCl solution by henna extract, A comparative study of the inhibition by henna and its constituents (Lawsone, Gallic acid, α-d-Glucose and Tannic acid)" *Corros. Sci.,* 51(9), 1935 2009
[11] Abiola O.K., Oforka N.C., Ebenso E.E. and Nwinuka N.M., Eco-friendly corrosion inhibitor: "The inhibitive action of Delonix Regia extract for the corrosion of aluminium in acidic media", *Anti-Corrosion Methods and Materials,* 54(4), 219-224 2007
[12] Kliskic M., Radoservic J., Gudic S. and Katalinic V "Aqueous extract of Rosmarinus officinalis L. as inhibitor of Al- Mg alloy corrosion in chloride solution", *J. Appl. Electrochem.,* 30(7), 823-830 2000
[13] El-Etre A Y., "Natural honey as corrosion inhibitor for metals and alloys. I. Copper in neutral aqueous solution", *Corros. Sci,* 40(11), 1845-1850 1998
[14] El-Etre A.Y., "Inhibition of aluminum corrosion using Opuntia extract", *Corros. Sci.,* 45(11) 2485–2495 2003
[15] El-Etre A.Y., "Khillah extract as inhibitor for acid corrosion of SX 316 steel", *Applied Surface Science.,* 252(24), 8521–8525 2006

[16] Loto C.A., Loto R.T. and Popoola A.P.I., "Inhibition Effect of Extracts of Carica Papaya and Camellia Sinensis Leaves on the Corrosion of Duplex (α β) Brass in 1M Nitric acid", *Int. J. Electrochem. Sci.*, 6, 4900 – 4914 2011
[17]Saratha R., Kasthuri N. and Thilagavathy P., "Environment friendly acid corrosion inhibition of mild steel by Ricinus communis Leaves", Der Pharma Chemica., 1 (2), 249-257 2009
[18] Satapathy A.K., Gunasekaran G., Sahoo S.C. and Kumar Amit Rodrigues P.V., "Corrosion inhibition by Justicia gendarussa plant extract in hydrochloric acid solution",*Corros. Sci.*, 51, 2848–2856 2009
[19] Deepa Rani P. and Selvaraj S., "Inhibitive action of vitis vinifera (grape) on copper and brass in natural sea water environment", *Rasayan J. Chem.*, 3(3), 473-482 2010
[20] Deepa Rani P. and Selvaraj S., "Inhibitive and adsorption properties of punica granatum extract on brass in acid media", *J. Phytol*., 2(11), 58-64 2010
[21] Mohammad Ismail A. and Abdulrahman S. Mohammad Sakhawat Hussain, "Solid waste as environmental benign corrosion inhibitors in acid medium", *International Journal of Engineering Science and Technology.*, 3(2), 1742- 1748 2011
[22]. Sribharathya V, Susai Rajendran and Sathiyabama, J. "Inhibitory action of Phyllanthus amarus extracts on the corrosion 2-thiophene carboxaldehyde as corrosion inhibitor for zinc in phosphoric acid solution of mild steel in seawater", Chem. Sci Trans, 2, 315-321 2013
[23]. Ayeni F.A, et.al, "Effect of aqueous extracts of bitter leaf powder on the corrosion inhibition of Al-Si alloy in 0.5 M caustic soda solution", Advanced Mater. Res, 367: 319-325 2012
[24] Dris Ben Hmamou et.al, "Carob seed oil: an efficient inhibitor of C38 steel corrosion in Hydrochloric acid", Inter. J. of Industrial Chem, 3:25 2012
[25] Ambrish Singh et.al, "Stem extract of brahmi (Bacopa Monnieri) as green corrosion inhibitor for aluminum in NaOH solution", Int. J. Electrochem. Sci, 7: 3409 – 3419. 2012.
[26] Petchiammal A, Deepa Rani P, Selvaraj S, and Kalirajan K. "Corrosion Protection of Zinc in Natural Sea Water using *Citrullus Vulgaris* peel as an Inhibitor", Res. J. of Chem. Sci, 2, 24-34 2012
[27] Petchiammal A, Selvaraj S, and Kalirajan K. "*Albizia lebbeck* seed extract as effective corrosion inhibitor for Mild steel in acid medium". Bio interface res. in App. Chem, 3, 498-506 2013
[28] Petchiammal A, Selvaraj S, and Kalirajan K. "Influence of *Hibiscus Esculenta* leaves on the corrosion of stainless steel in acid medium", Inter. J. of Univ. Pharm. and Bio Sci, 2, 242-252 2013
[29] Deepa Rani P and Selvaraj S.."Comparitive account of *Jatropha curcas* on Brass(Cu- 40Zn) in acid and Natural sea water environment", Pacific J. of Sci. and Technol, 12, 38- 49 2011
[30] Sharma Sanjay K., Ackmez Mudhoo, Jain Gargi and Sharma Jyoti, "Inhibitory effects of Ocimum tenuiflorum (Tulsi)on the corrosion of Zinc in Sulphuric acid A Green approach", *Rasayan.J.Chem*., 2(2), 332-339 2009
[31] James A.O. and Akaranta O., "The inhibition of corrosion of zinc in 2.0 M hydrochloric acid solution with acetone extract of red onion skin", *African Journal of Pure and Applied Chemistry.*, 3(11), 212-217 2009
[32] Orubite Okorosaye K. and Oforka N.C., "Corrosion Inhibition of Zinc on HCl using Nypa fruticans Wurmb Extract and 1,5 Diphenyl Carbazone", *J. Appl. Sci. Environ. Mgt.*, 8(1), 57–61 2004
[33] Aboia O.K. and James A.O., "The effects Of Aloevera extract on Corrosion and Kinetics of Corrosion process of zinc in HCl Solution", *Corrosion Science*, 52(2), 661-664 2010
[34] El-Etre A.Y., Abdallah M. and El-Tantawy Z.E., "Corrosion inhibition of some metals using lawsonia extract", *Corros. Sci*., 47(2) 385-395 2005
[35] P. Deivanayagam, I,Malarvizhi, S. Selvaraj and P. Deeparani "Corrosion inhibition efficacy of ethanolic extract of mimusops elengi leaves(MEL) on copper in Natural Sea Water", International Journal of multidisciplinary research and development 2(4): 100-107 2015
[36] P. Deivanayagam, I.malarvizhi,S. Selvaraj and P. Deeparani "Corrosion behavior of Sauropus androgynus leaves(SAL) on mild steel in Natural Sea Water", International Journal of Advances in pharmacy, biology and Chemistry 4(3) 574-585 2015

International Journal of Engineering Research and General Science Volume 3, Issue 6, November-December, 2015
ISSN 2091-2730

Experimental analysis of thermal contact resistance across different composite material pair using different interface material in ambient pressure condition

Er. Bipin G. Vyas[1], Prof. Nilesh R. Sheth [2], Prof. Mukesh P. Keshwani[3] and Prof. Nirmal Parmar[4]

[1] PG Student, Government Engineering College, Valsad, Gujarat, India
bipinvyas00@gmail.com
[2]Assistant Professor, Government Engineering College, Valsad, Gujarat, India
nileshsheth2001@gmail.com
[3]Assistant Professor, Neotech Institute of Technology, Vadodara, Gujarat, India
mukeshkeshwani@gmail.com
[4]Assistant Professor, Neotech Institute of Technology, Vadodara, Gujarat, India
nirmalparmar88@gmail.com

Abstract— The Practical study of heat transfer through surface contact resistance is very essential for advancement of thermal applications. It is required to understand the heat transfer between composite pair having same as well as different interface material. The outcomes will be very essential for design of different heat transfer thermal applications. The sole objective of this research work is to reduce the Thermal Contact Resistance (TCR) and increases thermal efficiency of the application. To minimize thermal contact resistance, the study of heat transfer with composite material pair & Thermal Interface Material (TIM) has been carried out experimentally in absence of pressure (ambient) condition.

The Experimental work includes effective pairs of circular plates of aluminum (HE30/6082) and copper (EC101) alloys. To avoid radial losses during experiments, plates are designed and manufactured in circular disc form 184 mm diameter with 5mm thickness each. Each of plate having four groove, Pencil k type thermocouple (Tip length: 70mm & diameter: 3mm) placed inside that grove which measured average temperature of surfaces with the help of 8 channel temperature indicator. The various effective pair of metal alloys disc has been considered during practical where air and brass foil are used as TIM for particulate pair. The average temperature of plate surface is measured under the steady state condition at 40^{o}C-70^{o}C temperature interval. An experiment has been conducted with some specific conditions to achieve ideal results.

With experiment, it is possible to analyze and identify suitable thermal interface material with minimum thermal contact resistance between two plates. Selection of proper TIM will lead towards higher heat transfer rate.

Keywords- Heat transfer, thermal applications, thermal contact resistance, thermal interfacial material, ambient pressure, temperature, circular plate and radial heat losses

1. INTRODUCTION

Heat transfer across a contact interface formed by any two solid bodies is usually accompanied by a measurable temperature difference because there exists a thermal resistance to heat flow in the region of the interface. The temperature difference at the contact interface is obtained by extrapolating the steady state unidirectional temperature distribution from regions far from the contact plane.

When two surfaces come into contact as shown in Figure1.1, they remain separated by their roughness elements. A gas or a liquid may also fill the spaces between the surfaces, and if the interface fluid has a lower thermal conductivity than the surface materials a contact resistance may exist that can become a design consideration.Figure1.1 also illustrates the type of temperature distribution that is encountered in such situations where a sharp temperature gradient across the small interfacial separation distance is caused by the contact resistance.

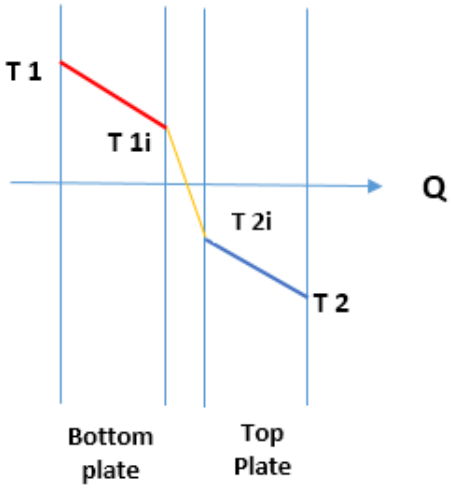

Figure 1.1 Interfacial Contact

Thermal resistance is thermal property of a material and it indicates how it resists heat at a specific thickness. As shown below, thermal resistance is proportional to the thickness of the material, but it can be affected by gaps that occur between contact surfaces. These gap create contact resistance, contributing to additional thermal resistance.

A) Methods to Reduce Contact Resistance [28]

For solid of high thermal conductivity, the contact resistance may be reduced by the following two methods:

1) Increasing the area of contact spots, accomplished by

-Increasing contact pressure which will "flatten" the peaks and valley of the micro roughness

-Reducing the roughness & waviness and increasing the flatness of surface

2) Using the Thermal interface material (TIM) of high thermal conductivity. Any interfacial material that fill the gap between contacting two surfaces, whose thermal conductivity exceed that of air

B) Various Types of Interface Material [28]

1) No fluidic interfacial material:

-Metallic Foils i.e., brass, copper, tin, lead, gold, indium etc.

-Metallic and Nonmetallic Coatings

-Polymers i.e. thermosets, thermoplastic, elastomers etc.

-Cements, Adhesives

2) Fluidic interfacial material:

- Phase change material, silicon **(**Thermal grease)

3) **Gases i.e.** hydrogen, nitrogen, Helium, carbon dioxide, argon, mixture of helium + argon etc.

4) Vegetable oil

C) Ideal Thermal Interface Material (TIM) Characteristics [28]

1) Minimum thickness is required.
2) It should have high thermal conductivity
3) It should be Non-toxic
4) It would not leak out of the interface zone
5) Easily deformed by small contact pressure so that uneven areas of both contacting surface become a flat

6) Manufacturing friendly means easy to apply and remove

7) It would maintain performance indefinitely

2. REVIEW OF PUBLICATIONS

A comprehensive literature review of thermal contact resistance has been provided in references [1-27]. Thermal contact resistance is very essential for design of heat transfer industrial applications. Various parameter influences on thermal contact resistance i.e. thermal interface material, surface morphology, pressure, metal thermal conductivities, material hardness etc. Surface morphology such as flatness, roughness and waviness have a maximum impact on the thermal contact resistance. It decrease with increasing flatness and decrease with waviness & roughness. Many investigator worked associated with two solid surfaces pressed together under ambient as well as applied load. C.V. Madhusudana [2] found out the effect of various interstitial fluid on thermal contact resistance. He concluded contact resistance improves in presence of good conducting medium in between two surfaces. P.W. O'Callaghan et al. [3] developed computer based mathematical model for interface material which will minimize the thermal contact resistance. A.M. Khounsary et al. [8] measured the thermal contact resistance across silicon-copper interface by using various interface foil and also concluded softer the interface material, lower the thermal contact resistance. D.D.L Chung [11] reviewed material for thermal conduction include materials exhibiting high thermal conductivity as well as thermal interface materials and Carried out materials of high thermal conductivity are needed for the conduction of heat for the purpose of Heating or cooling. J.P. Gwinn et al. [13] carried out performance and testing of interface material and surface characteristic & interface material most critical parameter affecting on thermal contact resistance.

The objective of this study was to experimental analysis of thermal contact resistance across different composite (Al-Al, Al-Cu) material pair using different interface material (Air, Brass foil). Experimental variables including ambient condition, position of top and bottom plate, temperature interval, interfacing material etc. Finally, experimentally investigated the composite metallic pair most suitable to minimize thermal contact resistance.

3. METHOD OF APPROACH

3.1 Apparatus

Experimentations has been conducted to find out the thermal contact resistance for same and different form of composite & thermal interface materials. The experimental setup is illustrated in Figure 2.1 and 2.2. Experimental setup consists of various components i.e. circular type electric heater (diameter: 200 mm, Height: 110 mm from the datum), pair of test specimen Copper (Grade: EC101), Al (grade: HE30/6082) (diameter: 184 mm & thickness: 0.5mm), 8 channel Temperature indicator (Model: MS1208, 4 digit-LED, 0.56'',3 digit-LED, 0.4''), Continuous variable autotransformer (Temperature Variac, ISO 9001:2000), Digital Multimeter (DMM, 200-300V), 8 no of pencil K type Nickle-Cronel thermocouple (-270^{o}C-1260^{o}C), Brass foil (thickness: 0.1mm) as thermal interface material etc.

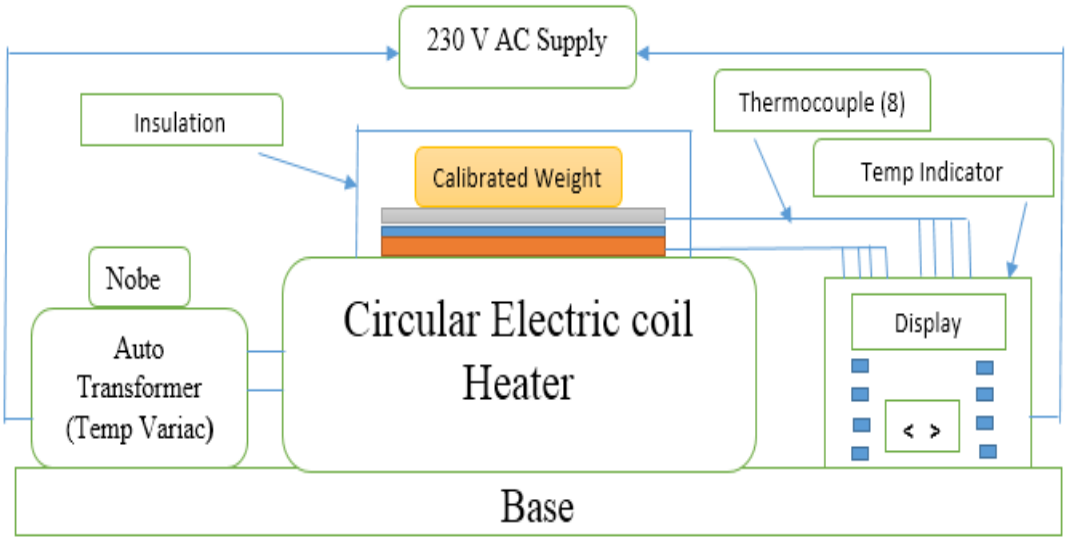

Figure 3.1 Schematic line diagram of experimental setup

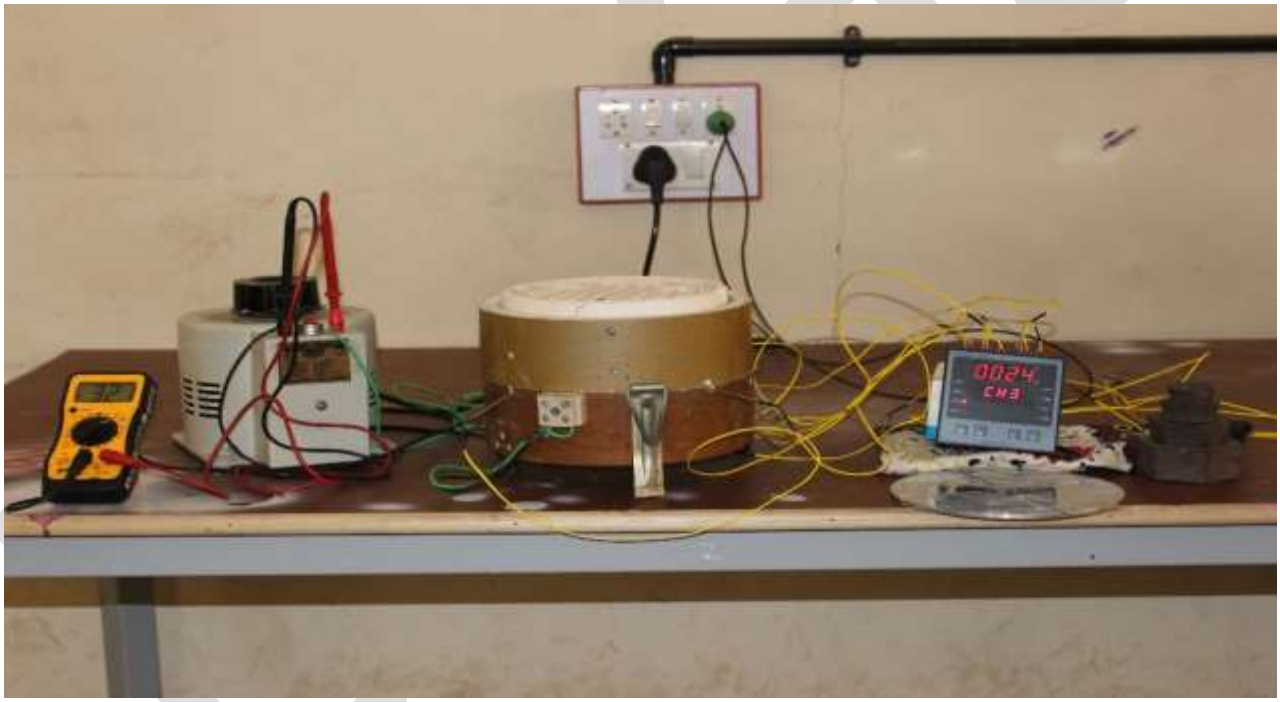

Figure 3.2 Schematic actual diagram of experimental setup

3.2 Experimental Test Procedure

A circular form of Copper (EC 101) and Aluminum (HE30/6082) plate of size (diameter: 184 mm & thickness: 0.5mm) are taken for experimentation. A circular form of copper plate is placed on heat source of circular type electric heater (diameter: 200 mm, Height: 110 mm from the datum) having ceramic alloys material (insulation) which prevents the losses. In which, Cu (Bottom) - Al (Top) composite pair with interface material is placed on electric coil heater. Each of plates has four grooves, 'k' types thermocouple are placed inside that grove which measures the temperature difference (T1i-T2i) between top surface of copper plate and bottom surface of aluminum plate with the help of 8 channel temperature indicator.

One more thermocouple is also placed at bottom surface of Copper plate its temperature (T1) remains constant 40°C–70°C means constant heat flow is maintained by varying voltage of continuous variable autotransformer which is directly connected with electric coil heater. Also, one thermocouple is mounted on top surface (T2) of Al top plate. Both of these temperatures (T1 & T2) are also measured with the help of temperature indicator.

The average temperature of plate surface is measured under the steady state condition at 40°C-70°C temperature interval. An experiment has been conducted with some specific conditions i.e. steady state conditions**,** one dimensional heat transfer**,** assuming constant Environment Temperature**,** avoiding convection losses**,** avoiding Radiation losses**,** minor Experimental errors avoided**,** proper Insulation**,** surfaces are clean and contact is static**,** thermal conductivities are uniform etc. to achieve ideal results. Same experiments are performed orientation wise in which changes the position of top & bottom plate with different interface material in ambient pressure condition. Same experiments test procedure was repeated for Al-Al composite pair with different interfacial material in ambient condition.

4. RESULTS AND DISCUSSION

Based on experimental work on TCR, Five experiments were performed with same and different composite material pair using different interface material in absence of pressure conditions as well as same experiments were performed orientation wise. In which Source temperature (T1) remains constant at 40°C -70°C interval. When upper surface of bottom plate (T1i) and lower surface of top plate temperature (T2i) attained the steady state condition, average temperature (T1i, T2i and T2) was measured. Outcome of these experiment results are illustrated graphically & in tabular form. Considering,

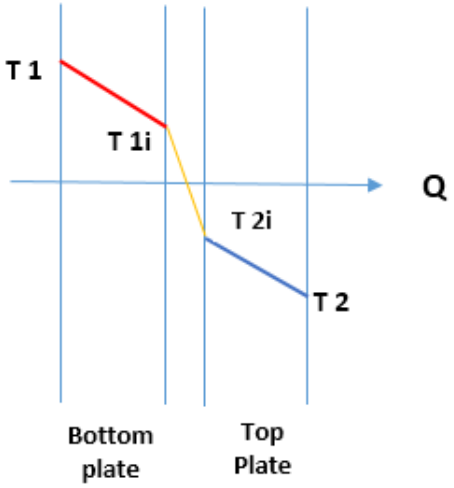

Figure 4.1 Composite metallic pair

Where;

Q = Total Heat Flow (W),

T1 = bottom surface temperature of bottom plate (°C)

T1i =Top surface of bottom plate (°C),

T2i =bottom surface of top plate (°C),

T2 =Top surface of top plate (°C)

Table 4.1. Experimental Results at 40°C-70°C

Experimental Results at 40°C-70°C						
	Experiment	**Exp-1**	**Exp-2**	**Exp-3**	**Exp-4**	**Exp-5**
	Temp. Range	**Al-Air-AL**	**Cu-Air-AL**	**Al-Air-Cu (O)**	**Cu-Brass-AL**	**Al-Brass-Cu(O)**
	40	40	40	40	40	40
T1	**50**	50	50	50	50	50
	60	60	60	60	60	60
	70	70	70	70	70	70
	40	38	34.33	41	39.66	36.66
T1i	**50**	45	42.66	48.66	49.66	47.33
	60	53	49.33	56.66	59.33	56.33
	70	59.33	54.66	66.33	68.33	63.33
	40	33	33.66	37.66	39.33	34.33
T2i	**50**	38	42.33	44.66	40	44.33
	60	42	48	52.33	46	51.66
	70	50	54.33	60.66	51	58.33
	40	31	31	33	32	33
T2	**50**	36	37	40	37	41
	60	42	42	45	38	46
	70	48	47	51	49	52

Note: (O) indicates orientation Wise (Changes the position of top and bottom plate)

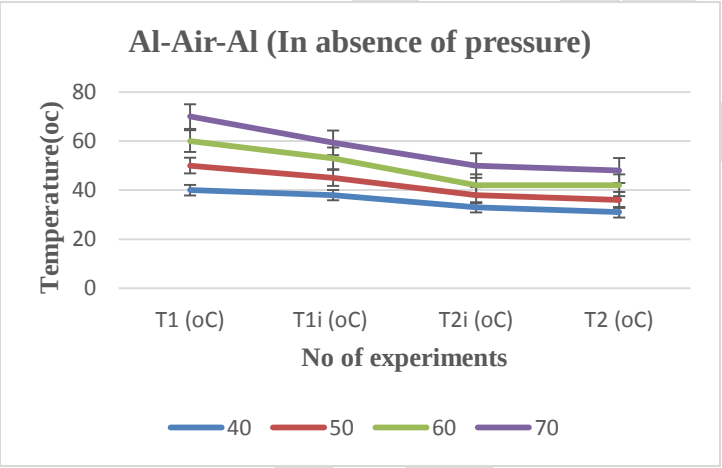

Experiment: 1 Al-Air-Al (In absence of Pressure)

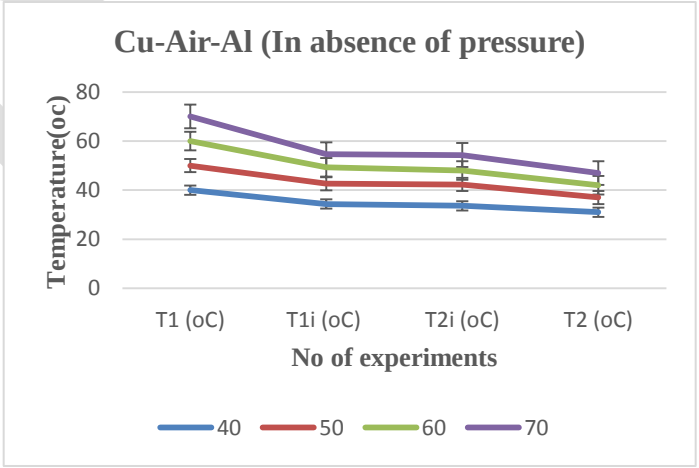

Experiment: 2 Cu-Air-Al (In absence of Pressure)

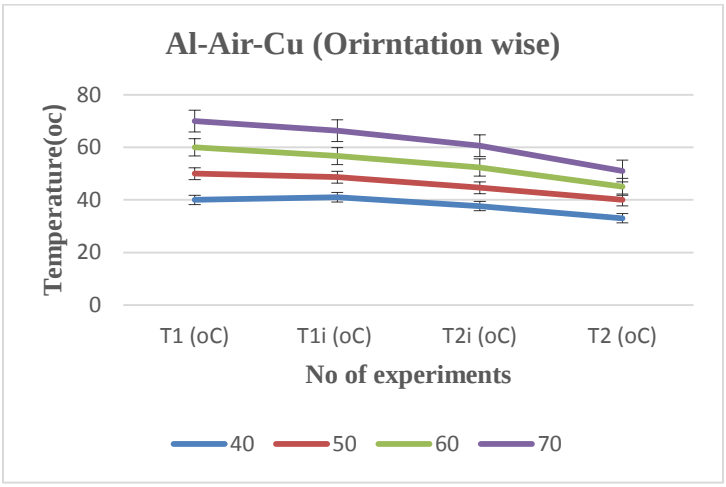

Experiment: 3 Al-Air-Cu (O) (In absence of Pressure)

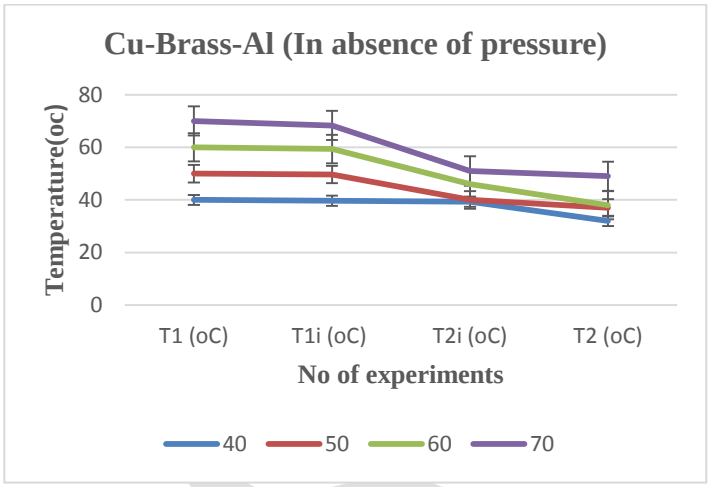

Experiment: 4 Cu-Brass-Al (In absence of Pressure)

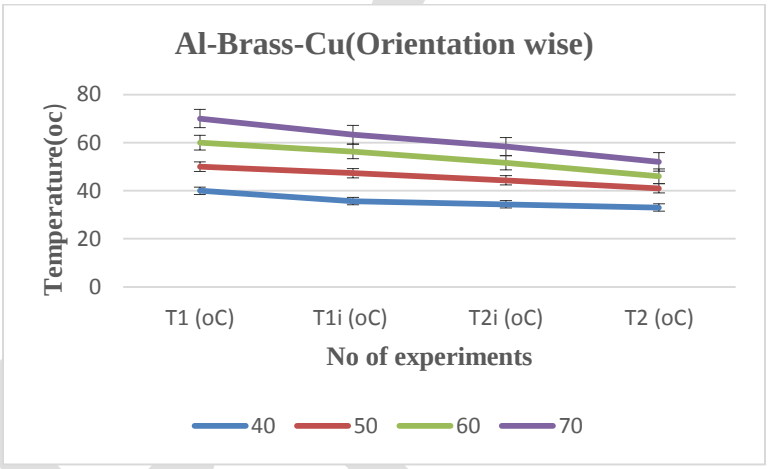

Experiment: 5 Al-Brass-Cu (O) (In absence of Pressure)

OBSERVATIONS:

Experiment 1: From the outcome results of Al-Air-Al pair in absence of pressure condition, it was observed that, Al was taken as bottom and top plate and air was taken as thermal interface material, Temperature drop of bottom Al plate & air gap increased with increase in temperature however temperature drop of top plate remains constant.

Experiment 2 In case of Cu-Air-Al composite pair, when Cu was taken as bottom plate and Air was taken as thermal interface material, Temperature drop of bottom Cu plate and top Al plate increased with increase in temperature. However, temperature drop of interface material (air) remained constant. It was clearly seen that high Cu thermal conductivity has significant effect on heat transfer.

Experiment 3. In Al-Air-Cu (Orientation wise) composite pair, Al was taken as bottom plate and Air was taken as thermal interface material same as previous first experiment (Al-Air-Al). In this case temperature drop of bottom Al plate, intermediate zone & top Cu plate is increased with increase in temperature it was observed that temperature drop for Al-Air-Cu (Orientation) composite pair is high compared to previous experiment Cu-Air-Al (2).

Experiment 4. In case of Cu-Brass-Al pair was taken as bottom, interface and top plate, results were become very interesting. Temperature drop for copper plate remains constant but temperature drop for intermediate zone and top plate increased with increase in temperature. As previous results and ideal conditions, when increasing the temperature, temperature drop supposed to be decreased

at intermediate zone but this phenomena did not occurred due to unevenness of brass foil which created the air gap on both side of brass foil in experimental setup**.**

Experiment 5. It was observed that when Al-Brass-Cu (Orientation wise) pair were taken as bottom, interface and top plate, graphical presentation showed that temperature drop for Al, brass and Cu plate increasing with increase in temperature. Also, observed that Intermediate temperature drop for Al-Brass-Cu was less compare to experiment: 4 (Cu-Brass-Al).

5. VALIDATION:

Based on performing five experiments with same and different composite material pair & interface material, Brass foil offered minimum thermal contact resistance compared to air. Experimental 4 & 5 results were validated in ANSYS workbench'12 software through static thermal analysis. Outcomes results are illustrated graphically and in tabular form which are very close to experimental results

Table 5.1 Validated Experimental and ANSYS results of Cu-Brass-Al and Al-Brass-Cu (O)

Source Temp	Cu-Brass-AL		Al-Brass-Cu(O)	
T1	**T2 Exp**	**T2 ANSYS**	**T2 Exp**	**T2 ANSYS**
40	32	32.204	33	33.468
50	37	37.886	41	39.89
60	38	43.579	46	46.347
70	49	49.281	52	52.838

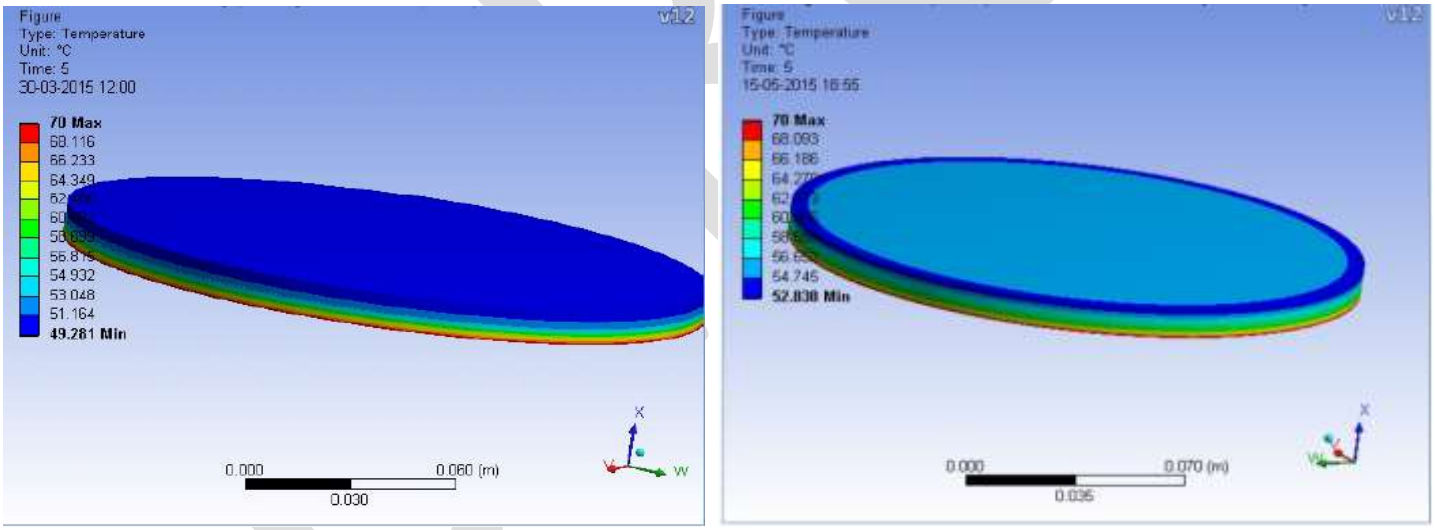

Figure 5.1 Temperature distribution profile Cu-Brass-Al (Left) and Al-Brass-Cu (O) (Right)

The figure 4 shows variation of temperature distribution pattern for Cu-Brass-Al (Left) and Al-Brass-Cu (O) (Right) composite pair. It depicts how to temperature distribution profile gradually occurs from bottom plate to top plate which are obtained in ANSYS workbench'12. The red color regions indicates bottom source plate temperature which identify higher (Maximum) value of temperature. The dark (left) & light (right) bluish regions indicates top sink plate temperature depicts lower (minimum) value of temperature. In case of Cu-Brass-Al (left) pair, top plate attained dark bluish color whereas Al-Brass-Cu (O) pair attained light bluish

color. This phenomena occurred because of source plate. It can be observed from graphical temperature distribution profile, outcomes ANSYS workbench results very close to experimental results in both cases.

6. MICRO OBSERVATION:

Comparison between Al-air-Al, Cu-Air-Al, Al-Air-Cu (Orientation Wise), Cu-Brass-Al, Al-Brass-Cu (Orientation wise) pairs in absence of pressure at 70°C temperature with orientation wise are illustrated in tabular as well as graphical representation in following ways respectively

Table 6.1 Experimental results of Al-air-Al, Cu-Air-Al, Al-Air-Cu (Orientation Wise), Cu-Brass-Al, Al-Brass-Cu (Orientation wise) at 70°C

EXPERIMENTAL RESULTS				
Composite pair	T1 (°C)	T1i (°C)	T2i (°C)	T2 (°C)
Al-Air-Al	70	59.33	50	48
Cu-Air-Al	70	54.66	54.33	47
Al-Air-Cu(O)	70	66.33	60.66	51
Cu-Brass-Al	70	68.33	51	49
Al-Brass-Cu (O)	70	63.33	58.33	52

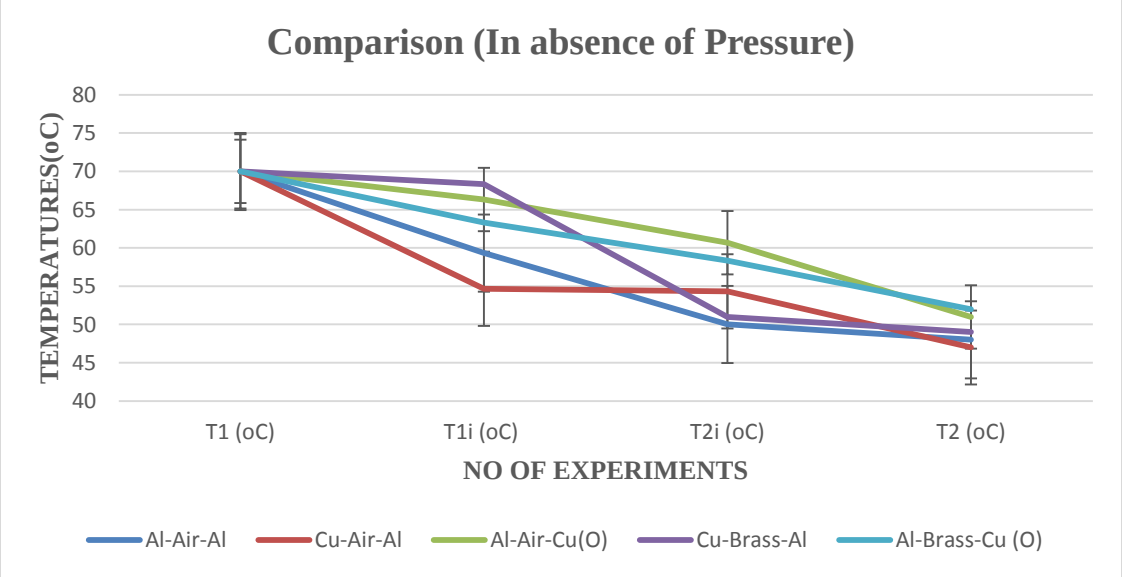

Figure 6.1 comparison of composite pair in absence of pressure condition

Table 6.2 Temperature difference overall, bottom, intermediate and top zone

Composite pair	T1-T2 (°C)	T1-T1i (°C)	T1i-T2i (°C)	T2i-T2 (°C)
Al-Air-Al	22	10.67	9.33	2
Cu-Air-Al	23	15.34	0.33	7.33
Al-Air-Cu(O)	19	3.67	5.67	9.66
Cu-Brass-Al	21	1.67	17.33	2
Al-Brass-Cu (O)	18	6.67	5	6.33

Table 6.3 Best pair results of air and brass as interface material in ambient condition

Sr No	Temperature Drop Zone Application	Best Pair	
		Air (interface material)	Brass (interface material)
1	Bottom to Top Zone (ΔT)	Al-Air-Cu(O)	Al-Brass-Cu (O)
2	Bottom Plate (ΔT1)	Al-Air-Cu(O)	Cu-Brass-Al
3	Intermediate Zone (ΔTi)	Cu-Air-Al	Al-Brass-Cu (O)
4	Top Plate Zone (ΔT2)	Al-Air-Al	Cu-Brass-Al

After performing five experiments in absence of pressure & orientation conditions, it was observed from the outcome of the results listed in table and graph,

- When temperature drop is required minimum for particular bottom to top overall application (ΔT) in case of air was used as interface material, best results obtained through Al-Air-Cu pair (Orientation wise) whose temperature drop is minimum compare to others in which Al-Air-Cu were taken as bottom, interface and top plate respectively. Thus, Al-Air-Cu is the best composite pair compare to others.
- When temperature drop is required minimum for particular bottom to top overall application (ΔT) in case of brass foil was used as interface material, best results obtained through Al-Brass-Cu pair (Orientation wise) whose temperature drop is minimum compare to others in which Al-Brass-Cu were taken as bottom, interface and top plate respectively. Thus, Al-Bras-Cu is the best composite pair compare to others.

It was also observed at micro level from the graph and outcome results in absence of pressure conditions, Heat transfer phenomena is effected not only overall temperature drop (ΔT) but also effected on all intermediate temperature drop zone i.e. ΔT1, ΔTi, and ΔT2. Thus, there is relationship between the same & different composite metal pair and used different interface material. In short, there is relationship between bottom plate - interface material and interface material - top plate.

- When temperature drop is required minimum for particular base plate application (ΔT1) in case of air was taken as interface material, better results obtained with Al-Air-Cu pair (Orientation wise) in which Al should be preferred as bottom and Air should be preferred as interface material. In case of brass foil was taken as interface material, better results obtained with Cu-Brass-Al pair in which Copper should be used as bottom and Brass should be preferred as interface material.
- When temperature drop is required minimum for particular interface contact zone application (ΔTi) in case of air was taken as interface material, better results obtained with Cu-Air-Al pair in which Cu-Air-Al should be preferred as bottom, interface and top plate respectively. In case of brass foil was taken as interface material, better results obtained with Al-Brass-Cu (Orientation wise) pair in which Al-Brass-Cu should be preferred as bottom, interface and top plate respectively.
- When temperature drop is required minimum for particular top zone application (ΔT2) in case of air was taken as interface material, better results obtained with Al-Air-Al pair. Thus, Air should be chosen as interface material & Al plate should be chosen as top plate. In case of brass foil was taken as interface material, better results obtained with Cu-Brass-Al pair. Thus, brass should be preferred as interface material and Copper should be preferred as top plate.

7. CONCLUSION:

- It was concluded from (experiment :1) when both top and bottom plate kept as aluminum, Temperature drop of bottom Al plate & air gap increased with increase in temperature however temperature drop of top plate remains constant. This happened due to heat transfer from the bottom Al plate to the air in the intermediate zone, thus heating the air. Now this heated air due to high temperature goes out of the gap & cold air from outside gets in thus filling the intermediate zone.
- Also when Cu was taken as source (Bottom) plate instead of aluminum plate (experiment: 2), Temperature drop of bottom Cu plate and top Al plate increased with increase in temperature. However, temperature drop of interface material (air) remained constant. It was clearly seen that high Cu thermal conductivity has significant effect on heat transfer. It absorbs maximum heat due to its high thermal conductivity.
- Besides, when changes the position of bottom and top plate (orientation wise) as Al & Cu respectively, temperature drop of bottom Al plate, intermediate zone & top Cu plate is increased with increase in temperature. It was observed that temperature drop for Al-Air-Cu (Orientation) composite pair is high compared to experiment Cu-Air-Al (2). This phenomena happened due to properties of Al plate which was taken as heat source or base bottom plate. Temperature drop is less compare to Al-Air-Al (Exp: 1) pair. This happened due to copper was taken as top plate.
- Finally, It was concluded that from observation of five experiments, two specific conditions i) When Air was taken as interface material & copper was taken as bottom plate.2) When brass was taken as interface material & Aluminum was taken as bottom plate transferred the maximum heat at minimum thermal contact resistance.

REFERENCES:

[1] M.M.Yovanovich, "Thermal Contact Conductance of turned surfaces," Aerospace science SEMI, pp. 71-80, 1971.
[2] C.V.Madhusudana, "The Effect of interface fluid on thermal contact conductance," International Journal Heat and mass Transfer, ISSN-0017-9310, vol. 18, pp. 989-991, 1974.
[3] P.W.O'Callaghan, S.D.Probert, "Reducing the Thermal Resistance of a Pressed Contact," Applied Energy, vol. 30, pp. 53-60, 1988.
[4] S.Lee, S.Song & K.P.Moran, M.M.Yovanovich, " Analytical modeling of thermal resistance in bolted joint", Enhanced cooling Techniques for Electronics Applications ASME, pp. 115-122, 1993
[5] Koichi Nishino, Shigemasa Yamashita and Kahoru Torii, " Thermal contact conductnace under low applied load in a vacuum environment" Experimental Thermal and Fluid Science, pp. 258-271, 1995.
[6] Marcia B.H. Mantelli, M.R. Sridhar and M.M.Yovanovich, " Influence of elastic and plastic contact models on the overall thermal resistance of bolted joints", Eleventh IEEE SEMI, pp.39-47.
[7] Seri Lee, Kevin P. Moran, Seaho song, Van Au "Constriction/Spreading Resistance Model For Electronics Packaging," ASME/JSME Thermal Engineering Conference, vol. 4, pp. 199-206, 1995.
[8] A.M.Khounsary,D. Chojnowski, L. Assoufid, "Thermal Contact Resistance across acopper -silicon interface," SPIE, vol. 3151, pp. 45-51, 1997.
[9] E.G.Wolff, D.A. Schneider "Prediction of thermal contact resistance between polished surfaecs," International Journal Heat and mass Transfer, ISSN-0017-9310, vol. 41, pp. 3469-3482, 1998
[10] Syed M.S.Wahid, C.V.Madhusudana "Gap Conductance in contact heat transfer," International Journal Heat and mass Transfer, ISSN-0017-9310, vol. 43, pp. 4483-4487, 2000.
[11] D. D. L. Chung, "Materials for thermal conduction," Applied Thermal Engineering, vol. 21, pp. 1593-1605, 2001.
[12] V.Satre, M. Lallemand "Enhancement of thermal contact conductance for electronic systems," Applied Thermal Engineering, vol. 21, pp. 221-235, 2001.
[13] J.P.Gwinn, R.L.Webb "Performance and testing of thermal interface materials," Microelectronic Journal, vol. 34, pp. 215-222, 2002.
[14] C.L.Yeh, Y.F.Chen, C.Y. Wen, K.T. Li "Measurement of thermal contact resistance of aluminum honeycombs," experimental Thermal and Fluid Science, ISSN-0894-1777,vol. 27, pp. 271-281, 2003.
[15] I.SAvija, J. R. Culham, M.M.Yovanovich, "Review of thermal contact conductance models for joints incorporating enhancement materials," Journal of thermophysics and heta transfer, SSN-0887-8722, vol. 17, pp. 43-52, 2003.
[16] M.Rosochowska, K.Chodnikiewicz, R. Balendra, "A new method of measuring thermal contact conductance," Journal of materials and processing technology, ISSN-0924-0136, vol. 145, pp. 207-214, 2004.

[17]S.Sunil Kumar, K. Ramamurthi, "Thermal Contact Conductance of Pressed contacts at low temperature," Cryogenics, ISSN-0011-2275, vol. 44, pp. 727-734, 2004.
[18]V.V.Rao, M. V. Krishna Mrthy, J. Nagaraju, "Thermal Conductivity and thermal contact conductance studies on Al_2O_3/Al-AlN metal matrix Composite," Composites Science and Technology, vol. 64, pp. 2459-2462, 2004.
[19] Vishal Singhal, Paul J.Litke, Anthony F. Black, Suresh V. Garimella, "An Experimentally validated thermo-mechanical model for the prediction of thermal contact conductance," Internatiional Journal Heat and mass Transfer, ISSN-0017-9310, vol. 48, pp. 5446-5459, 2005.
[20] Ruiping Xu, Lie Xu "An Experimental Investigation of thermal contact conductance of stainless steel at low temperatures," Cryogenics, ISSN-0011-2275,vol. 45, pp. 694-704, 2005.
[21] Majid Bahrami, M.Michael yovanovich, J.Richard Culham, "Thermal Contact resistance at low contact pressure: Effect of elastic deformation," International Journal Heat and mass Transfer, ISSN-0017-9310, vol. 48, pp. 3284-3293, 2005.
[22] G.P.Voller, M. Tirovic "Interface pressure distributions and thermal contact resistance of a bolted joint," Mathematical Physical & Engineering Sciences, ISSN-0017-9310, vol. 461, pp. 2339-2354, 2005.
[23] C.Fieberg, R.Kneer, "Determination of thermal contact resistance from transient temperature measurement," International Journal Heat and mass Transfer, ISSN-0017-9310,vol. 51, pp. 1017-1023, 2007.
[24] Prashant Misra, J.Nagaraju, "Thermal gap conductance at low contact pressure(<1MPa): Effect of gold plating and plating thickness," International Journal Heat and mass Transfer, ISSN-0017-9310, vol. 53, pp. 5373-5379, 2010.
[25]Wang Zongren, Yang Jun, Wang Shung, Zhang weifang, "Compensation Heating Technique for experimental investigation of thermal contact conductance across GH4169/K417 interface," Sciencedirect vol. 42, pp. 1572-1575, 2013.
[26] Donghuan Liu, Yan Luo, Xinchun Shang, "Experimental Investigation of high temperature thermal contact resistance between high thermal conductivity C/C material and Inconel 600," International Journal Heat and mass Transfer, ISSN-0017-9310,vol. 80, pp. 407-410, 2014.
[27] Larry Pryor P.E, Rick Schlobohm P.E, and Bill Brownell P.E, " A Comparison of Aluminum Vs. Copper as used in Electrical Equipment"
[28] Bipin G. Vyas, Nilesh R. Sheth and Mukesh P. Keshwani, " Review: thermal contact resistance of metallic composite pair", International journal of application or Innovation in Engineering & Management, vol.4, pp. 193-200, 2015

BOOKS

[29] F.P.Incopera,D.P. Dewitt, Fundamental, Fundamentals of Heat and mass Transfer, Sixth edition, willey, New york, pp 57-101,2005
[30] Y. A. Cengel, Heat Transfer: A Practical Approach, Second Edition., McGraw-Hill publication, pp 2-40 & 128-143, 2003
[31] Holman J.P. Heat Transfer, Tenth Edition, McGraw Hill Publication,pp 1-57, 2010
[32Lienhard IV & V John H. A Heat transfer textbook, Third Edition, Phlogiston press, Cambridge, U.S.A, pp 3-96, 2008
[33] T.F.Irvine Jr. Themal contact resistance, Hemisphere publishing corporation, pp 2.4.6.1-2.4.6.4, 1983

International Journal of Engineering Research and General Science Volume 3, Issue 6, November-December, 2015
ISSN 2091-2730

Survey Paper For Detection Of Malicious Nodes In Routing Of Mobile Ad-Hoc Network

Bhavik Panchal (M.E Wireless And Mobile Computing)

GTU PG School Ahmedabad, bhavik_panchal17@yahoo.com and +919429457971

Abstract — To find method of detecting selfish and misbehaving node for providing better security in routing of adhoc network. First of all generate the adhoc network. In Adhoc network nodes are mobile so the network topology may change rapidly and unpredictably over time. The network is decentralized, where all network activity including discovering the topology and delivering routing messages is executed by the nodes themselves, so one or more of them may misbehave and disturb the network. The misbehavior or attack can be of many types.

In the network the node can work in two ways by exhibiting selfishness or misbehaviour and cause disturb once in the network by using different type of attack. To identify or detecting malicious or selfish node Intrusion Detection System (IDS) system is developed. It has different architecture for to detect malicious or selfish node. One is Stand Alone architecture and other is Distributed and co-operative architecture.

I will use Watch-Dog mechanism to detect selfish and misbehaving node that agree to forward packet but fails to do so. Path-rater is mechanism used for removing path from cache that contain malicious or selfish node.

Keywords— Ad-Hoc Network ,Watch-Dog , Intrusion Detection System (IDS),Security , Distributed , Stand Alone Architecture , Pathrater.

INTRODUCTION

During the last few years we have all witnessed a continuously increasing growth in the deployment of wireless and mobile communication networks. Mobile ad hoc networks consist of nodes that are able to communicate through the use of wireless mediums and form dynamic topologies. The basic characteristic of these networks is the complete lack of any kind of infrastructure, and therefore the absence of dedicated nodes that provide network management operations like the traditional routers in fixed networks. In order to maintain connectivity in a mobile ad hoc network all participating nodes have to perform routing of network traffic. The cooperation of nodes cannot be enforced by a centralized administration authority since one does not exist. Therefore, a network layer protocol designed for such self-organized networks must enforce connectivity and security requirements in order to guarantee the undisrupted operation of the higher layer protocols.

Security is an essential service for wired and wireless network communications. The success of mobile ad hoc networks (MANET) strongly depends on peoples confidence in its security. However, the characteristics of MANET pose both challenges and opportunities in achieving security goals, such as confidentiality, authentication, integrity, availability, and non-repudiation. We

provide a survey on attacks and countermeasures in MANET in this paper. The countermeasures are features or functions that reduce or eliminate security vulnerabilities and attacks. First, we give an overview of attacks according to the protocols stacks, and to security attributes and mechanisms.

Literature Review

S. Martiet [1]. provides the information of DSR Routing algorithm. The paper also describe two techniques that improve throughput in an adhoc network in the presence of nodes that agree to forward packet but fails to do so. To mitigating this problem we propose categorizing the nodes based upon their dynamically measured behavior. We use watchdog that identifies misbehavior node and pathrater that helps routing protocols avoid these misbehavior of nodes. Through simulation we evaluate watchdog and pathrater using packet throughput, percentage of overhead(routing) transmission and the accuracy of misbehaving node detection.

Network Security

A security protocol for ad hoc wireless networks should satisfy the following requirements. The requirements listed below should in fact be met by security protocols for other types of networks also.

Confidentiality: The data sent by the sender (source node) must be comprehensible only to the intended receiver (destination node). Though an intruder might get hold of the data being sent, he/she must not be able to derive any useful information out of the data. One of the popular techniques used for ensuring confidentiality is data encryption.

Integrity: The data sent by the source node should reach the destination node as it was sent: unaltered. In other words, it should not be possible for any malicious node in the network to tamper with the data during transmission.

Availability: The network should remain operational all the time. It must be robust enough to tolerate link failures and also be capable of surviving various attacks mounted on it. It should be able to provide the guaranteed services whenever an authorized user requires them.

Non-repudiation: Non-repudiation is a mechanism to guarantee that the sender of a message cannot later deny having sent the message and that the recipient cannot deny having received the message. Digital signatures, which function as unique identifiers for each user, much like a written signature, are used commonly for this purpose.

Authentication: Enables a node to ensure the identity of the peer node it is communicating with. Without authentication, an adversary could masquerade a node, thus gaining unauthorized access to resource and sensitive information so it is interfering with the operation of other nodes. [2]

Issues And Challenges For Security

Hao yang [3] covers basic challenge and issues related to secure routing. Designing a foolproof security protocol for ad hoc wireless is a very challenging task. This is mainly because of certain unique characteristics of ad hoc wireless networks, namely, shared broadcast radio channel, insecure operating environment, lack of central authority, lack of association among nodes, limited availability of

resources, and physical vulnerability. A detailed discussion on how each of the above mentioned characteristics causes difficulty in providing security in ad hoc wireless networks is given below.

Issues And Challenges For MANET Security

Shared broadcast radio channel: Unlike in wired networks where a separate dedicated transmission line can be provided between a pair of end users, the radio channel used for communication in ad hoc wireless networks is broadcast in nature and is shared by all nodes in the network. Data transmitted by a node is received by all nodes within its direct transmission range. So a malicious node could easily obtain data being transmitted in the network. This problem can be minimized to a certain extent by using directional antennas.

Insecure operational environment: The operating environments where ad hoc wireless networks are used may not always be secure. One important application of such networks is in battlefields. In such applications, nodes may move in and out of hostile and insecure enemy territory, where they would be highly vulnerable to security attacks.

Lack of central authority: In wired networks and infrastructure-based wireless important central points (such as routers, base stations, and access points) and implement security mechanisms at such points. Since ad hoc wireless networks do not have any such central points, these mechanisms cannot be applied in ad hoc wireless networks.

Lack of association: Since these networks are dynamic in nature, a node can join or leave the network at any point of the time. If no proper authentication mechanism is used for associating nodes with a network, an intruder would be able to join into the network quite easily and carry out his/her attacks.

Limited resource availability: Resources such as bandwidth, battery power, and computational power (to a certain extent) are scarce in ad hoc wireless networks. Hence, it is difficult to implement complex cryptography-based security mechanisms in such networks.

Physical vulnerability: Nodes in these networks are usually compact and handheld in nature. They could get damaged easily and are also vulnerable to theft. [2]

Issues And Challenge For Routing In MANET Security

Detection of malicious node Node is participant in route and do the misuse of information.

Guarantee of correct route discovery We have to check the correctness of route.

Confidentiality of network topology Topology discover by malicious node so it create traffic or DOS attack.

Stability against attacks one node first participant in network. After some time it is work as a malicious node and disturb the routing process. Node must be stable not change the state.

Security Scheme

There are two main approaches in securing ad hoc environments currently utilized.

The first approach is the intrusion detection approach that aims in enabling the participating nodes to detect and avoid malicious behaviour in the network without changing the underlined routing protocol or the underling infrastructure. Although the intrusion detection field and its applications are widely researched in infrastructure networks it is rather new and faces greater difficulties in the context of ad hoc networks.

The second approach is secure routing that aims in designing and implementing routing protocols that have been designed from scratch to include security features. Mainly the secure protocols that have been proposed are based on existing ad hoc routing protocols like AODV and DSR but redesigned to include security features. In the following sub sections we briefly present the two approaches in realizing security schemes that can be employed in ad hoc networking environments.

Intusion Detection System (IDS)

Intrusion is defined as "any set of actions that attempt to compromise the integrity, confidentiality, or availability of a resource". Intrusion protection techniques works as the first line of defense. However, intrusion protection alone is not sufficient since there is no perfect security in any system, especially in the field of ad hoc networking due to its fundamental vulnerabilities.

Therefore, intrusion detection can work as the second line of protection to capture audit data and perform traffic analysis to detect whether the network or a specific node is under attack. The two type of nodes are in under attack on a network. [8]

Selfish nodes: It doesn't cooperate for selfish reasons, such as saving power. Even though the selfish nodes do not intend to damage other nodes, the main threat from selfish nodes is the dropping of packets, which may affect the performance of the network severely.

Malicious nodes: It has the intention to damage other nodes, and battery saving is not a priority. Without any incentive for cooperating, network performance can be severely degraded.

Once an intrusion has been detected then measures can be taken to minimize the damages or even gather evidence to inform other legitimate nodes for the intruder and maybe launch a countermeasure to minimize the effect of the active attacks.

Stand Alone IDS

In this architecture, each host has a IDS and detect attacks independently. There is no cooperation between nodes and all decision is based on local nodes (Figure 1). This architecture is not effective enough but can be utilized in an environment where not all nodes are capable of running IDS

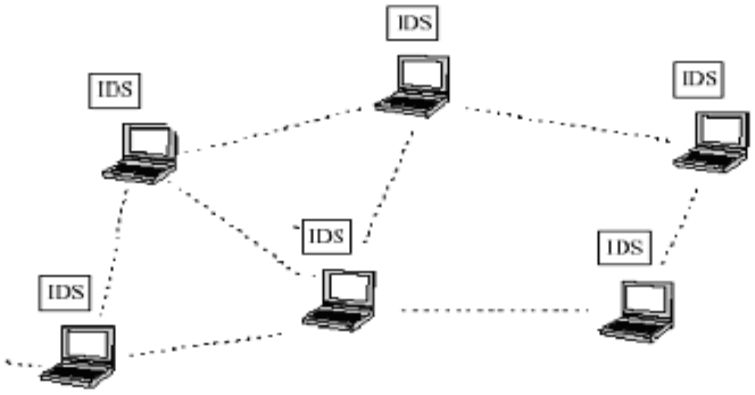

Figure 1: Stand Alone Architecture

Mechanism

Xia Wang [11] describes the various IDS system with different mechanism that used for detection of node.

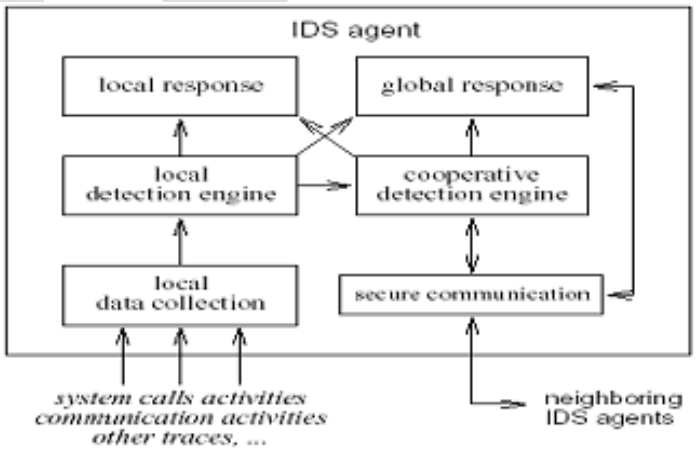

Figure 2: Distributed and cooperative architecture component

In the IDS system the mechanism is used to identify or detect the node in network. The different mechanisms are used with different architecture and according to different routing protocol mechanism is change. We have to first check that which architecture used in network for IDS and also which routing protocol is used in network In that stand alone architecture we are using Watchdog and Pathrater.[12]

Watchdog

The watchdog and pathrater scheme consists of two extensions to the DSR routing protocol that attempt to detect and mitigate the effects of nodes that do not forward packets although they have agreed to do so. This misbehavior may be due to malicious or selfish intent, or simply the result of resource overload. Although the specific methods proposed build on top of DSR. The watchdog extension is responsible for monitoring that the next node in the path forwards data packets by listening in promiscuous mode. It identifies as misbehavior nodes the ones that fail to do so.

Every node that participates in the ad hoc network employs the watchdog functionality in order to verify that its neighbors correctly forward packets. When a node transmits a packet to the next node in the path, it tries to promiscuously listen if the next node will also transmit it. Furthermore, if there is no link encryption utilized in the network, the listening node can also verify that the next node did not modify the packet before transmitting it.

The watchdog of a node maintains copies of recently forwarded packets and compares them with the packet transmissions overheard by the neighboring nodes. Positive comparisons result in the deletion of the buffered packet and the freeing of the related memory. If a node that was supposed to forward a packet fails to do so within a certain timeout period, the watchdog of an overhearing node increments a failure rating for the specific node.

This effectively means that every node in the ad hoc network maintains a rating assessing the reliability of every other node that it can overhear packet transmissions from. A node is identified as misbehaving when the failure rating exceeds a certain threshold bandwidth. The source node of the route that contains the offending node is notified by a message send by the identifying watchdog. [5]

Watchdog example

In given figure 3 is a packet is traveling from S to D. A can overhear B and tell whether B has forwarded the packet. Buffer is maintained for recently sent packets. The overheard packet is compared with the sent packet. If there is a match, discard the packet. If the packet stays till a timeout, increment the failure tally for the node. If tally exceeds a threshold, declare the node as misbehaving.[1].

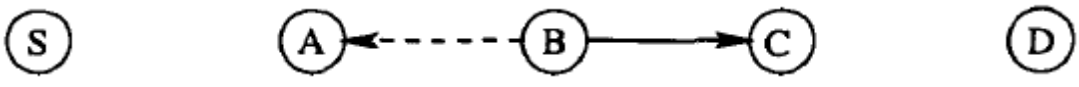

Figure 3: A Example of WatchDog

Pathrater

The pathrater assesses the results of the watchdog and selects the most reliable path for packet delivery. One of the base assumptions of this scheme is that malicious nodes do not collude in order to circumvent it and perform sophisticated attacks against the routing protocol.

The pathrater extension to DSR selects routes for packet forwarding based on the reliability rating assigned by the watchdog mechanism. Specifically, a metric for each path is calculated by the pathrater by averaging the reliability ratings of the nodes that participate in the path. This path metric allows the pathrater to compare the reliability of the available paths, or to emulate the shortest path algorithm when no reliability ratings have been collected. The pathrater selects the path with the highest metric when there are multiple paths for the same destination node.

The algorithm followed by the pathrater mechanism initially assigns a rating of 1.0 to itself and 0.5 to each node that it knows through the route discovery function. The nodes that participate on the active paths have their ratings increased by 0.01 at periodic intervals of 200 milliseconds to a maximum rating of 0.8. A rating is decremented by 0.05 when a link breakage is detected during the packet forwarding process to a minimum of 0.0. The rating of -100 is assigned by the watchdog to nodes that have been identified as misbehaving. When the pathrater calculates a path value as negative this means that the specific path has a participating misbehaving node.

The watchdog and pathrater extensions facilitate the identification and avoidance of misbehaving nodes that participate in the routing function. The identification is based on overheard transmissions and the selection of reliable routes is based on the calculated reliability of the paths.

ACKNOWLEDGEMENT

Though only my name appears on the cover of this Report, a great many people have contributed to its production. I owe my gratitude to all those people who have made this dissertation possible and because of whom my Dissertation experience has been one that I will cherish forever.

I am extremely grateful to my coordinator **Mr. Gardas Naresh Kumar (C-DAC)** for being a source of inspiration and for their constant support in the Design and Evaluation of the Dissertation. They have been the constant constructive force throughout my pursuit of Masters Degree at GTU-CDAC and I am sure that their active and passive teachings will always inspire me throughout my life.

I will always remain indebted to my guide at Shankersinh Vaghela Bapu Institute of Technology, Gandhinagar, Honorable **to Mr. Nitin Pandya.** I am thankful to him for him constant constructive criticism and invaluable suggestions, which benefited me a lot while doing research on Detection Of Malicious Nodes In Routing Of Mobile AdHoc Network. He has been always there to support me whenever I felt down or lost my way and always led me on right path.

I also express my gratitude to **Mr. Bhadreshsinh Gohil (GTU PG School)**, for providing me the infrastructure to carry out the Dissertation and to all staff members who were directly and indirectly instrumental in enabling us to stay committed.

I would like to thank my parents & my friends for always giving me full support, inspiring advices and courage to always follow righteous path whenever my steps have faltered.

CONCLUSION

After doing parametric study for different architecture of IDS system for adhoc wireless network we get the different mechanism to detect the malicious or selfish node. On that Watchdog is used in Stand Alone architecture for detect in malicious or selfish node. In Distributed and Cooperative architecture we have CONFIDANT Protocol, Probing algorithm mechanism used for detection. Stand Alone architecture Watchdog mechanism made for forwarded packet drop misbehavior done by node.

REFERENCES:

[1] S. Martiet, "Mitigating routing misbehavior in mobile ad hoc networks," ACM Mobicom, pp. 255–65, Auguest 2000.

[2] C. Murthy and B. Manoj, Ad Hoc Wireless Networks: Architectures and Protocols. New Delhi: Prentice Hall India, second ed., 2005.

[3] H. yang, "Security in mobile ad hoc networks: Challenges and solutions," IEEE Wireless Communications magazine, October 2000.

[4] K. Inkinen, "New secure routing in ad hoc networks," tech. rep., Helsinki University of Technology. kai.inkinen@hut.fi.

[5] D. O. Patroklos G. Argyroudis, "Secure routing for mobile ad hoc networks,"

[6] E. J. Caballero, "Vulnerabilities of intrusion detection systems in mobile ad-hoc networks - the routing problem," erjica@gmail.com.

[7] B. A. Jean-Marie Orset and A. Cavalli, "An efsm-based intrusion detection system for ad hoc networks," Institut National des Telecommunications GET-INT. Evry, France fjean-marie.orset, baptiste.alcalde, ana.cavallig@int-evry.fr.

[8] S. S. Frank Kargl, Andreas Klenk and M. Weber, "Advanced detection of selfish or malicious nodes in ad hoc networks," Auguest 2004.

[9] R. D. Ningrinla Marchang, "Intrusion detection system for wireless networks," Collaborative techniques for intrusion detection in mobile ad-hoc networks, pp. 508–523, June 2008.

[10] Y. X. G. S. Bo Sun, Osborne L, "Intrusion detection techniques in mobile ad hoc and wireless sensor networks," Wireless Communications, IEEE, vol. 14, pp. 56–63, October 2007.

[11] X. Wang, "Intrusion detection techniques in wireless ad hoc networks," Computer Software and Applications Conference, vol. 2, pp. 347–349, Sepetemer 2006. COMPSAC apos;06. 30th Annual International.

[12] T. W. Mike Just, Evangelos Kranakis, "Resisting malicious packet dropping in wireless ad hoc networks,"

International Journal of Engineering Research and General Science Volume 3, Issue 6, November-December, 2015
ISSN 2091-2730

Comparison of Remote Monitoring Systems - A Review

Swathi.K[1] , Kishore Balasubramanian[2] and Muthuvel V[3]

[1]PG scholar, Applied Electronics, Dr.Mahalingam College of Engineering and Technology, Pollachi
swathi.k0905@gmail.com

[2]Assistant Professor, Department of EEE, Dr.Mahalingam College of Engineering and Technology, Pollachi
bkishore1979@gmail.com

[3]Assistant Professor, Department of EEE, Dr.Mahalingam College of Engineering and Technology, Pollachi
muthuvelhve@gmail.com

Abstract— This paper presents a detailed study on comparison of different remote monitoring systems. There are many systems for remote monitoring and control, designed as either commercial products or experimental research platforms. It is noticed that most of the research are carried out in categories such as Internet based Monitoring via Servers, GPRS modems, etc. There are different other approaches for GSM-SMS protocols using GSM module individually or in combination besides using Wireless technologies such as Sensor Networks, Bluetooth, Wi-Fi, Zigbee and RF. For choosing the appropriate monitoring system for an application, a number of characteristics are important. A review of different monitoring systems with their characteristics is presented.

Keywords— Remote monitoring, internet-based monitoring, , Wireless technologies, Bluetooth, Zigbee, Wi-Fi, General Packet Radio Service (GPRS).

INTRODUCTION

Remote monitoring includes data from gauges and sensors like soil moisture, pressure, environmental, etc. It is used to know the status of farm gates and building doors (open/close), irrigation valves and pumping equipment. It helps to view the video of operation in live mode, monitoring of greenhouses, livestock enclosures and storage facilities.

Conventional wired monitoring system provides reliable solution in data transmission but suffers from several limitations. Apart from the physical constraints during laying of the data cables, the use of these cables also increases installation and maintenance cost. Besides, for outdoor application such as PV systems, continuous exposure to sun beam and rains may reduce the lifespan of the system (Spertino & Corona, 2013). To overcome these issues, wireless monitoring system is favoured over its cable-based counterpart. In this project, a Zigbee-based wireless monitoring system is designed and built as a replacement to the conventional cable-based monitoring system for a grid-tied PV system. Various aspects of the system, from design to construction and testing, are detailed here. Besides that, a PC-based application integrated with web-based function is designed and implemented in order to allow remote control of the system as well as easy access of the data over the internet.

CLASSIFICATION OF REMOTE MONITORING SYSTEMS

In a monitoring system, it is important to choose a method through which the users can access the monitored data effectively. For the monitoring of a system, users should have easy and prompt access to the data, in order to provide timely evaluation on the system performance, as well as to provide counter measures should any failure is detected. Based on the previous works surveyed, it is found that web-based monitoring system can be an attractive monitoring method,as it enables data to be distributed among remote users and userscan view data from any device with internet connectivity.

INTERNET BASED MONITORING

Internet monitoring is one of the common approaches for remote monitoring. Many researchers have worked in field of Internet based remote monitoring. They developed home gateway system for interconnecting home network consisting of IEEE 1394 AV network and X10 power line home automation network with Internet. This provided remote access functions from Internet for digital AV appliances like Digital Video Camera, Digital VCR connected to IEEE 1394 network and home appliances like TV, desk lamp, electric fan connected to X10 controller.

Java based home automation system via World Wide Web were developed. The home appliances were controlled from ports of embedded system board connected to PC based server at home. X10 controller interfaced through serial port to PC server for control of devices was invented. The Common Gateway Interface (CGI) is used to interface between the browser and the X10 protocol via http connection. The server executes CGI programs in order to satisfy a particular request from the browser, which expresses its request using the http.

Model of web services based email extension for remote monitoring of embedded systems which integrates web services into emails. It uses a general purpose email messaging framework to connect devices and manipulators. This low cost model fits for systems with low connection bandwidth, small data transportation volume and non-realtime control, e.g., monitoring of home appliances and remote meter-reading.

A system for controlling home electrical appliances over the internet uses Bluetooth wireless technology to provide a link from the appliance to the Internet and Wireless Application Protocol (WAP) to provide a data link between the Internet and a mobile phone. However, technical details relating controller are not revealed.

Design and implementation of an Internet home automation system was made available. The design uses an embedded controller based on C8051F005 microcontroller which is connected to a PC-based home Web server via RS232 serial port. The home appliances are connected to the input/output ports and the sensors are connected to the analog/digital converter channels of the embedded controller. The software of the system is based on the combination of Keil C, Java Server Pages, and JavaBeans, and dynamic DNS service (DDNS) client. Password protection is used to block the unauthorized user from accessing to the server [5].

A remote wireless monitoring system for off grid Wind turbine based on the GPRS and the Internet was developed. The remote monitoring system is made up of three parts: controlling terminal, central monitoring computer and communication network. Controlling terminal consists of microcontroller ARM7 LM3S1138, data acquisition module and GPRS communication module WAVECOM Q2406B connected to ARM7 system using serial port. GPRS module sends parameters relating wind turbine to central monitoring computer. The client can access central monitoring computer server through Internet and know parameters of different wind turbines[12].

Key Press Markup Language (KPML) and SIP Event Package was introduced to control devices in the home environment remotely without the need for specialized hardware in the home devices. KPML provides an efficient, reliable protocol for the remote control of consumer devices using plain old telephones with 12-digit keypads using Internet transport technologies. Figure 1 shows Key Press Markup Language (KPML) with two sites.

The architecture of embedded remote monitoring system based on Internet has been developed by the researchers. The system adopts embedded web server as a central monitoring node and results in improvement in stability and reliability of system. Moreover, utilization of dynamic monitoring web based on Java Applet improves the response capability and brings convenience for complex monitoring web design.

Wireless remote monitoring system based on the GPRS (General Packet Radio Service) and the MCU (Micro programmed Control Unit) was designed. System is based on 89C58 microcontroller and PIML GPRS-MODEM as the core, can collect data from

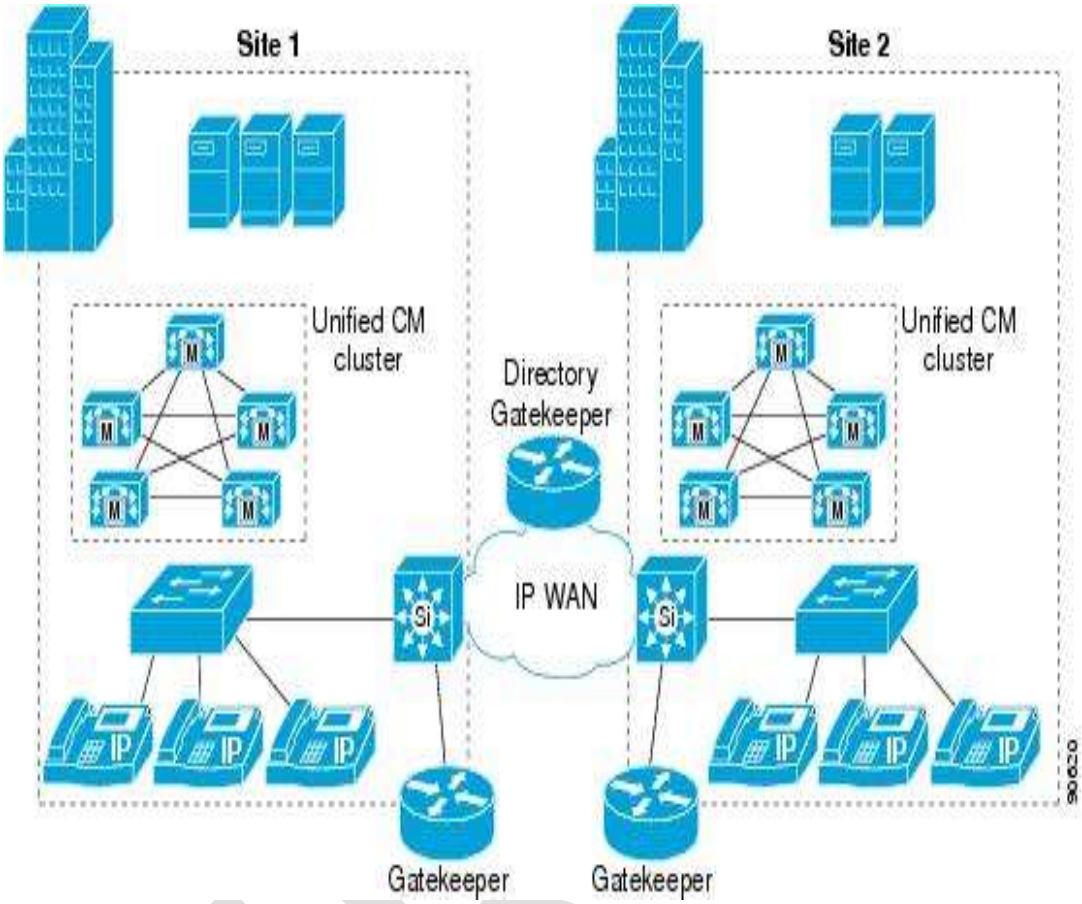

Figure 1: Key press markup language (KPML)

Eight sensors control two-way Data Acquisition, in the local real-time display and support remote Internet monitoring. The data from sensors are encoded, sent to the WEB server (fixed IP address or fixed domain name website) through the GPRS channel. The system also accepts commands from remote monitoring centre.

Table 1: Comparison of different remote monitoring systems

Sl.no	Techno logy	Processor	Monitoring Station	Modules Interfaced	Tools	Programming Code
1.	Internet	8051 family	PC	None	Keil IDE	Java, Interactive C
2.	Internet	PIC16	PC	None	MPLAB IDE	UML, C
3.	Bluetooth	Atmega64	PC	TDK Blu2i	AVR Studio	C
4.	Bluetooth	Atmega168	Mobile	Bluegiga WT11	AVR Studio, Symbian	Interactive C, Pythan
5.	Bluetooth	Atmega32	Mobile	CBOEMSPA312	AVR studio, Eclipse 3.2.2	C, Java
6.	RFID	Parallex P8X32A	PC	RFID Reader, ENC 28J60	Propeller tool, Spin compiler	Spin
7.	RF	Atmega 48	PC	RDM-A4FZ	AVR Studio	C

8.	RF	8051 family	PC	nRF905, Si4421	Keil IDE	C51
9.	GSM	8051 family	Mobile	Sony Ericsson GM47	Keil IDE	Visual C++
10.	GSM-FPGA	8051	Mobile	MAXON MM-6854	Xilinx ISE 6.2i	VHDL
11.	GSM	MSP430F149	PC	Siemens TC35	C430 IDE	C
12.	GSM	ARM7	PC, Mobile	Siemens TC35	Flashmagic	C
13.	GSM-Internet	Atmega128, PIC 18	PC, Mobile	Siemens TC35	AVR Studio, MPLAB IDE	C
14.	GSM	8051 family	PC	Nokia FBUS	Keil IDE, Linux	C, Java
15.	GSM-Internet-speech	PIC16	Mobile	Siemens TC35	MPLAB	C
16.	GSM-WSN	8051 family	PC, Mobile	Siemens TC35, CC1100	Keil IDE	C51
17.	GSM-Zigbee	Atmega 128	Mobile	Sony Ericsson T290i, EM357	IDE & C compiler	C
18.	GSM-Zigbee	8051	Mobile	GM862QUAD-PY, CC2430	Keil IDE, Symbian	C, Pythan
19.	GSM-Zigbee	8051	PC/Mobile	Siemens TC35	Keil IDE	C/C++
20.	GPRS	ARM7		CC2430 nRF24E1	µC/OS-II	
21.	GPRS	8051 family	PC	SIM300, SN65LBC184	Keil IDE	Visual C
22.	RF	Atmega128, APXA271	PC	CC2420	AVR Studio, TinyOS	C
23.	RF	APXA271	PC	CC2420	TinyOS	nesC

Table 1 explains the comparison of different remote monitoring systems with respect to its technology, processor used, Monitoring station, Modules Interfaced, tools and programming code.

Wireless remote image monitoring system based on GSM/GPRS and ARM_Linux developing environment was developed. The monitoring system uses S3C2410 RISC MCU -ARM920Core, USB Web camera, SD Card and UART GPRS module. ARM Linux operating system is loaded on SD Card. APIs of Video4Linux kernel are used to realize image acquisition of the system, through PPP dial-up to access the GPRS, through network programming to realize the transmission of the image.

Application on remote monitoring system of reservoir based on GPRS was developed. GPRS data terminal hardware includes the intelligent processing module, remote communication module, serial interface module and display module. Intelligent processing module contains two chips AT89C55 microcontroller and serial E2PROM X25045. AT89C55 is used to transmit data between remote communication module, A/D conversion module and display module. To ensure that data will not be lost because of power outages, serial E2PROM X25045 devices is adopted for data storage. Remote communication module includes GPRS wireless module, SIM card and serial module MAX3238. Database mainly stores various parameters of the flood accommodation procedures for the user and reservoir historical hydrological data, such as electric power generated, relation curve of water level flows, the water storage capacity curve, and discharge curve, unit's efficiency curve of different conditions, historical flood data and flood information.

A system composed of server which interfaces several video surveillance cameras including several microphones for audio surveillance is designed. This server captures video and audio streams from the video cameras and microphones and operates on these streams according to the configuration of the local control software module. This module can store the video and audio streams on local hard-disks, index video and audio captures by time and place, retrieve images and sound based on user specified time intervals and deliver them to the user via Internet, or deliver (streaming) live images and sounds from a predefined camera. The system is connected to the building power supply and can be connected to the Internet via several communication solutions based on their availability. In case of power grid failure the system is provided with a secondary power supply based on rechargeable batteries which can keep the system functional for several hours. The main weaknesses of this system are the power supply and the Internet connection. To improve the reliability of this system, an autonomous diagnosis system has been added to the main monitoring server. The system will detect any change in the functioning state of the main system, like communication link failure, power grid failure or internal power source depletion and will report these events by sending a short message (SMS).

Wireless home automation system by merging communication technologies of GSM, Internet and speech recognition was developed GSM and Internet methods were used for remote access of devices of house whereas speech recognition was designed for users inside the house. The communication between the user and the home is established by the SMS (Short Message Service) protocol. A GSM modem is connected to the home automation server. The communication between the home automation server and the GSM modem is carried out by the AT (Attention) commands. To accomplish Internet connectivity, a web server is built to take requests from remote clients. The clients can send requests to the home appliances. The home appliances can send their statuses to be displayed for the remote client through the server. A web page is constructed as an interactive interface where commands can be submitted by the client to change and also monitor the status of the devices. A speech recognition program is written to control the house by means of human voice. Dynamic Time Warping (DTW) algorithm is used for speech recognition [5].

The mobile telephone is then configured with a mobile-to-host GPRS connection (GPRS attachment and PDP context activation). Patient data are recorded and stored in the processor's memory module, typically for 10 min. Then the processor transmits an AT-command to the mobile phone to initiate data transmission via the GPRS network [12].

GSM-SMS BASED MONITORING

With the wide spread use of cellular networks, this approach is also popular when small amount of data is to be transferred through the network. Extensive work has been carried out by researchers using this approach especially in medical field.

A remote monitoring system based on SMS of GSM was described. The system includes two parts which are the monitoring center and the remote monitoring station. The monitoring centre consists of a computer and a TC35 GSM communication module. The computer and TC35 are connected by RS232. The remote monitoring station includes a TC35 GSM communication module, a MSP430F149 MCU, a display unit, various sensors, data gathering and processing unit.

A tele-monitoring system, based on short message service (SMS), to remotely monitor the long-term mobility levels of elderly people in their natural environment was developed. Mobility is measured by an accelerometer-based portable unit, worn by each monitored subject. [3] The portable unit houses the Analog Devices ADuC812S microcontroller board, Falcon A2D-1 GSM modem, and a battery-based power supply. Two integrated accelerometers are connected to the portable unit through the analog inputs of the microcontroller. Mobility level summaries are transmitted hourly, as an SMS message, directly from the portable unit to a remote server for long-term analysis. Each subject's mobility levels are monitored using custom-designed mobility alert software, and the appropriate medical personnel are alerted by SMS if the subject's mobility levels decrease.

A system for early diagnosis of hypertension and other chronic diseases was proposed. The proposed design consists of three main parts: a wrist Blood Pressure (BP) measurement unit, a server unit and a terminal unit. Blood Pressure is detected using data acquired by sensors intelligently using DSP microchip. The data is then transmitted to the remote server unit located at Community Healthcare Centres/Points (CHC/P) by using Short Messaging Service (SMS), and notification information is sent to the terminal unit to inform users if patient's BP is abnormal.

Home security system by means of GSM cellular communication network using microcontroller 89X52 and Sony Ericsson GM-47 GSM module was developed. This system enables far end user through SMS facility to monitor the state of home door, provide password facility for key based door lock and control home lighting system.

A remote medical monitoring system based on GSM (Global System for Mobile communications) network was described. This system takes advantage of the powerful GSM network to implement remote communication in the form of short messages and uses FPGA as the control centre to realize the family medical monitoring network. The system is made up of user terminal equipments, GSM network and hospital terminal equipments. Hospital terminal equipments can be a personal computer (connected with GSM modules) or other receiving equipment's such as the mobile phone of the related doctor, while user terminal equipments are used to collect, demonstrate and transmit kinds of physiological parameters. User terminal devices include the temperature acquisition module, blood pressure/heart rate acquisition module, FPGA of Actel Fusion series, information-sending and information-receiving module --Siemens TC35 GSM module, LCD displays and expansion modules [11].

A mobile-based home automation system that consists of a mobile phone with Java capabilities, a cellular modem, and a home server was designed. The home appliances are controlled by the home server, which operates according to the user commands received from the mobile phone via the cellular modem.[50]

Figure 2 shows short message service/ General Packet Radio Service consists of GPRS modem, GPRS network, and base station Ervice. Here, the home server is built upon an SMS/GPRS (Short Message Service/General Packet Radio Service) mobile cell module Sony Ericsson GT48 and a microcontroller Atmel AVR 169, allowing a user to control and monitor any variables related to the home by using any java capable cell phone [5].

A role-based intelligent mobile care system with alert mechanism in chronic care environment was proposed and developed [12]. The roles included patients, physicians, nurses, and healthcare providers. Each of the roles represented a person that uses a mobile phone to communicate with the server setup in the care. For mobile phones with Bluetooth communication capability attached to chronic patients, physiological signal recognition algorithms were implemented and built-in in the mobile phone without affecting its original communication functions. Several front-end mobile care devices were integrated with Bluetooth communication capability to extract patients' various physiological parameters [such as blood pressure, pulse, saturation of hemoglobin (SpO2), and electrocardiogram (ECG)], to Monitor multiple physiological signals and to upload important or abnormal physiological information to healthcare centre for storage and analysis or transmit the information to physicians and healthcare providers for further processing. An alert management mechanism has been included in back-end healthcare centre to initiate various strategies for automatic emergency alerts after receiving emergency messages or after automatically recognizing emergency messages.

A remote data collection and monitoring system was designed and implemented. The system communication is based on GSM short messages from cell phones using Siemens cell phone module TC35. The serial interface of TC35 is directly connected to the serial interface of PC computer. The system hardware includes remote client monitoring hardware, central monitoring module, and 0809 A/D converter.

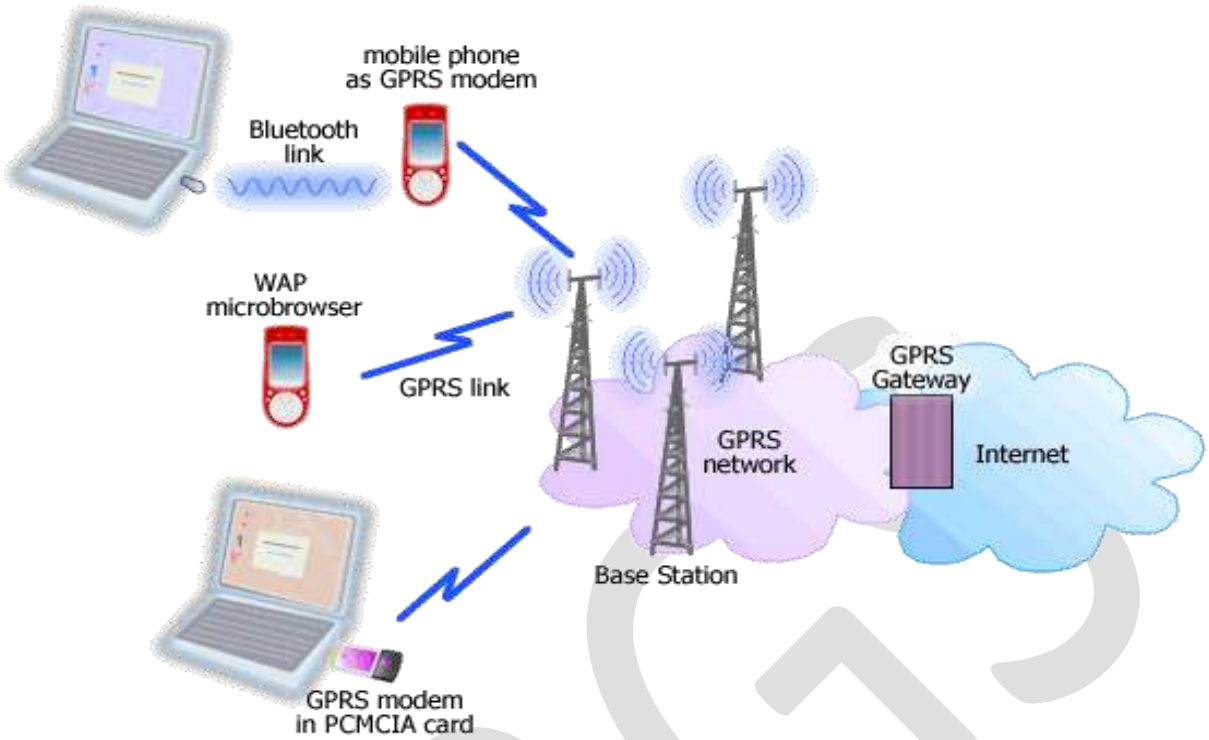

Figure 2: Short Message Service/General Packet Radio Service

The central monitoring module sends commands via channel 1. Data collection commands are sent out through TC35 to collect all sorts of data. After data are collected they are processed by remote clients and sent back to the central monitoring module by GSM short messages via channel 2. Each monitoring module can connect up to 128 sensors and equipment within the range of 1000 meters via RS485 interface. The server hardware consists of 8031 microprocessor, 74LS373, one 8 kB 2764 E2PROM, one 2 kB 6116 extended memory, and one 8155 programmable serial interface chip. One 4×4 keyboard is connected to the PI port and 8 LED displays are connected to PA and PB ports of 8155.

SMS based system for controlling of home appliances remotely was developed and providing security when the user is away from the place. Home appliance control system (HACS) consists of PC which contains the software components through which the appliances are controlled and home security is monitored and GSM Modem that allow the capability to send and receive SMS to and from the system. The communication with the system takes place via RS232 serial port.

ADVANTAGES OF WIRED NETWORKS:

Conventional wired monitoring system provides reliable solution for data transmission.

DISADVANTAGES OF WIRED NETWORKS:

Use of these cables also increases installation and maintenance cost. For outdoor application such as PV systems, continuous exposure to sun beam and rains may reduce the lifespan of the system

REMOTE MONITORING USING WIRELESS SENSOR NETWORKS (WSN), BLUETOOTH, WIFI, ZIGBEE TECHNOLOGIES

Many Wireless Technologies like RF, Wi-Fi, Bluetooth and Zigbee have been developed and remote monitoring systems using these technologies are popular due to flexibility, low operating charges, etc. Today Wireless Sensor Network are used into an increasing number of commercial solutions, aimed at implementing distributed monitoring and control system in a great number of different application areas. Figure 3 shows three network topologies which are supported by Zigbee devices; centralized star, cluster-tree-based and mesh network Zigbee devices have two types of capabilities which are reduced-function device (RFD) and full-function device (FFD).

A general purpose controlling module was designed with the capability of controlling and sensing up to five devices simultaneously. The communication between the controlling module and the remote server is done using Bluetooth technology. The server can communicate with many such modules simultaneously. The controller is based on ATMega64 microcontroller and Bluetooth communication TDK Blu2i (Class 1) modulewhich provides a serial interface for data communication. The designed controller was deployed in a home automation application for a selected set of electrical appliances [3].

A home appliance control system over Bluetooth with a cellular phone was developed, which enables remote-control, fault-diagnosis and software-update for home appliances through Java applications on a cellular phone. The system consists of home appliances, a cellular phone and Bluetooth communication adapters for the appliances. The communication adapter hardware consists of a 20MHz 16bit CPU, SRAM and a Bluetooth module. The communication adapter board is connected to the home appliance and to the cellular phone through serial ports. The appliances can communicate with the cellular phone control terminal via Bluetooth SPP [3].

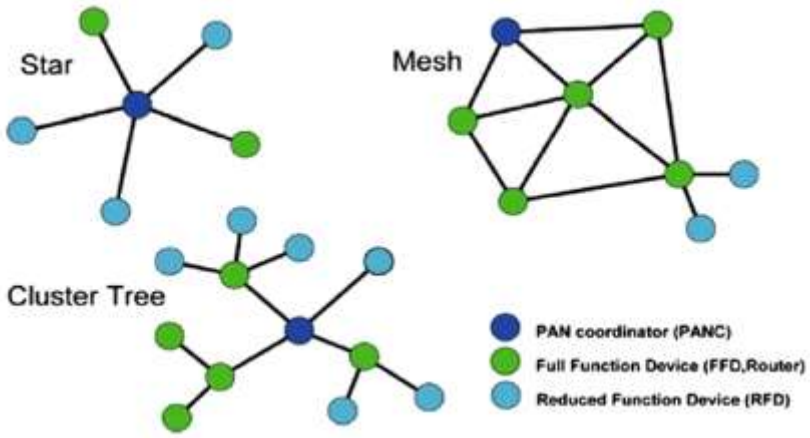

Figure 3: Topology of Zigbee wireless networks

A wireless patient monitoring system which integrates Bluetooth and Wi-Fi wireless technologies was introduced. This system consists of the mobile unit, which is set up on the patient's side to acquire the patient's physiological signals, and the monitor units, which enable the medical personnel to monitor the patient's status remotely. The mobile unit is based on AT89C51 microprocessor. The digitized vital-sign signals are transmitted to the local monitor unit using a Bluetooth dongle. Four kinds of monitor units, namely, local monitor unit, a control centre, mobile devices (personal digital assistant; PDA), and a web page were designed to communicate via the Wi-Fi wireless technology [6].A novel architecture for environmental tele-monitoring that relies on GSM for sampling point delocalization was suggested, while on-field nodes implement local subnets based on the DECT technology.

Table 2: Comparison of Bluetooth, WIFI, Zigbee

Standard	Range	Number of Nodes	Frequency Band	Data Protection	Power use
Bluetooth	10 m	8	2.4GHz	16-bit CRC	High
Wi-Fi	100 m	32	3.1-10.6 GHz	32-bit CRC	High
Zigbee	10-200 m	More than 25400	868/915 MHz 2.4 GHz	16-bit CRC	Low

Table 2 explains the comparison of Bluetooth, Wi-Fi, Zigbee with respect to its range of distance, Number of nodes, Frequency band, Data protection and power use.

A novel architecture for environmental tele-monitoring that relies on GSM for sampling point delocalization was suggested, while on-field nodes implement local subnets based on the DECT technology. Local subnets contain two major blocks; Acquisition Station (AS) where sensors and actuators are located and Transmitting Module (TM), i.e., the module that handles several measurement stations and sends data to the control center (CC). Each AS acts as a data logger, storing in its internal memory device field data; communications between AS and TM are cyclic (round robin), with a cycle time of about 1–10 min. On the contrary, (personal digital assistant; PDA), and a web page were designed to communicate via the Wi-Fi wireless technology. Figure 4 shows IBSS and ESS configuration of WI-FI networks consisting of distribution system.

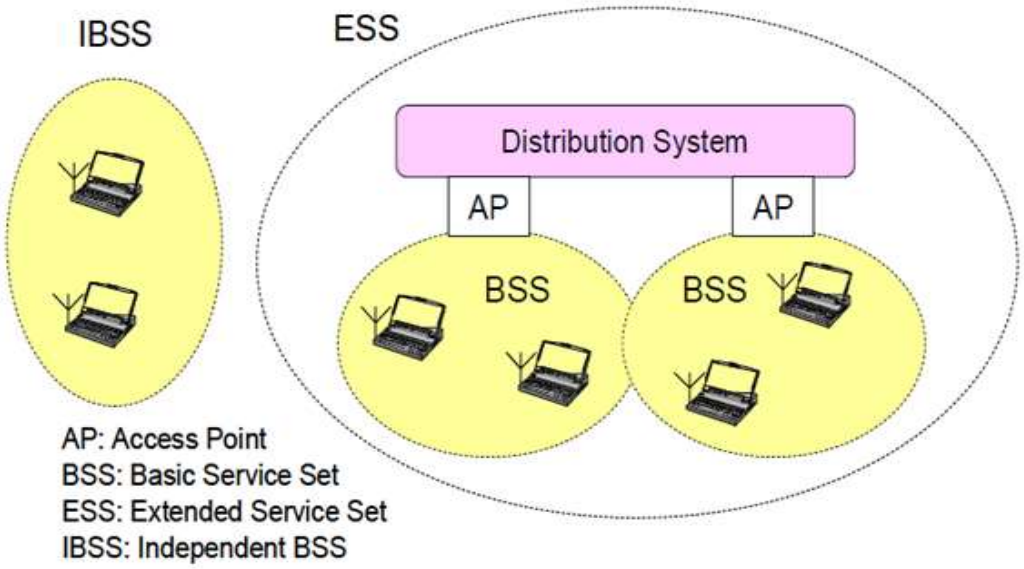

Figure 4: IBSS and ESS Configuration of Wi-Fi networks

Design and instrumentation of variable rate irrigation, a wireless sensor network, and software for real-time in-field sensing and control of a site-specific precision linear-move irrigation system was done. Field conditions were site-specifically monitored by six in-field sensor stations distributed across the field based on a soil property map, and periodically sampled and wirelessly transmitted to a base station. An irrigation machine was converted to be electronically controlled by a programming logic controller (Siemens S7-226 with three relay expansion modules activated electric over air solenoids to control 30 banks of sprinklers) that updates geo-referenced location of sprinklers from a differential Global Positioning System (GPS) (17HVS, Garmin) and wirelessly

communicates with a computer at the base station. Communication signals from the sensor network and irrigation controller to the base station were successfully interfaced using low-cost Bluetooth wireless radio communication through Bluetooth RS-232 serial adaptor (SD202, Initium Company).Figure 5 shows power observing structure via Bluetooth, Ethernet and GSM.

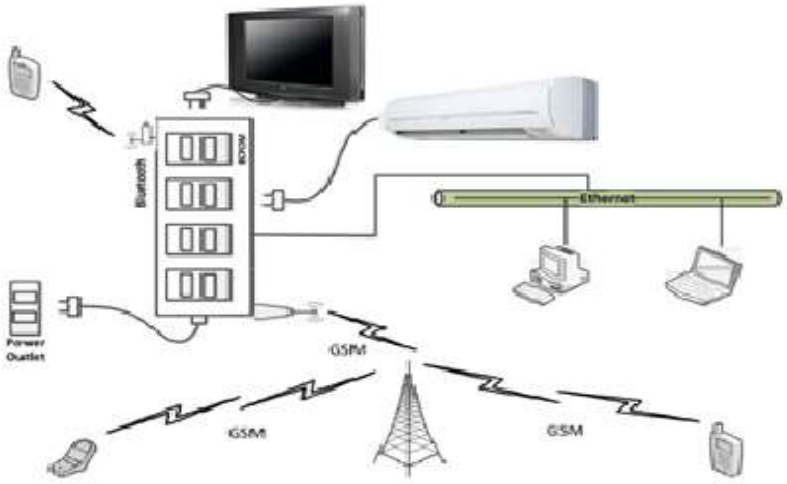

Figure 5: Power Observing structure via Bluetooth, Ethernet and GSM

A WSN based system for monitoring a series of physiological parameters in the vineyard to prevent plant vine diseases was developed. Sandy soils have very different behaviour to irrigation in respect to clayey ones; water retention capacity is completely different and measuring it exactly where it is needed can help in controlling the irrigation system and saving water. Monitoring air temperature and humidity in different parts of a vine can help in preventing and Fighting plants diseases, reducing the amount of pesticides only when and where they are necessary.

The master node of the Wireless Sensor Network is connected to a GPRS gateway board, forwarding data to a remote server, using the TCP-IP standard protocol. It included 11 nodes with a total of 35 sensors distributed on 1 hectare area; monitor common parameter using simple, unobtrusive, commercial and cheap sensors.

Forwarding their measurements by the means of a heterogeneous infrastructure, consisting of WSN technology, GPRS communication and ordinary Internet data transfer (TCP-IP protocol). Data coming from sensors are stored in a database that can be queried by users everywhere in world, only using a laptop or a PDA: the Smart User Interface also allows to read and to analyze data in an easy way. (Harms et al., 2010) describe the emerging wireless sensor networks (WSN) for autonomous Structural Health monitoring SHM systems for bridges. In SmartBrick Network, the base station and sensor nodes collect data from the onboard and external sensors. The sensor nodes communicate their data from quasi-static sensors, e.g., temperature sensors, strain gauges and seismic detectors to the base station over the ZigBee connection. The base station processes these data and communicates them, along with any alerts generated, to a number of destinations over the GSM/GPRS link provided by the cellular phone infrastructure. The data are reported by email and FTP to redundant servers, via the Internet, at regular intervals or on an event-triggered basis. The alerts are sent directly by SMS text messaging and by email. Wireless sensor networks are the key enabler of the most reliable and durable systems for long-term SHM and have the potential to dramatically increase public safety by providing early warning of impending structural hazards [1].

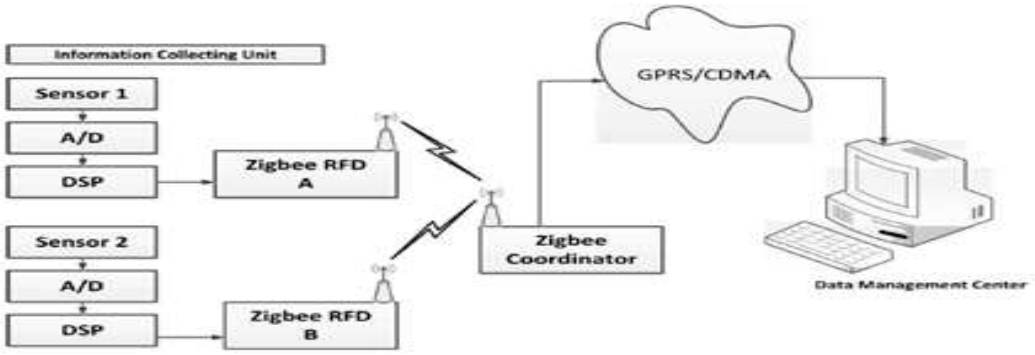

Figure 6: Zigbee-based Transmission Line Monitoring

Forwarding their measurements by the means of a heterogeneous infrastructure, consisting of WSN technology, GPRS communication and ordinary Internet data transfer (TCP-IP protocol). Data coming from sensors are stored in a database that can be queried by users everywhere in world, only using a laptop or a PDA: the Smart User Interface also allows to read and to analyze data in an easy way. (Harms et al., 2010) describe the emerging wireless sensor networks (WSN) for autonomous Structural Health monitoring SHM systems for bridges. In SmartBrick Network, the base station and sensor nodes collect data from the onboard and external sensors. The sensor nodes communicate their data from quasi-static sensors, e.g., temperature sensors, strain gauges and seismic detectors to the base station over the ZigBee connection. The base station processes these data and communicates them, along with any alerts generated, to a number of destinations over the GSM/GPRS link provided by the cellular phone infrastructure. The data are reported by email and FTP to redundant servers, via the Internet, at regular intervals or on an event-triggered basis. The alerts are sent directly by SMS text messaging and by email. Wireless sensor networks are the key enabler of the most reliable and durable systems for long-term SHM and have the potential to dramatically increase public safety by providing early warning of impending structural hazards [1].

A wireless medical interface based on ZigBee and Bluetooth technology. The purpose is to acquire, process, and transfer raw data from medical devices to Bluetooth network. The Bluetooth network can be connected to PC or PDA for further processing. The interface comprises two types of device: MDIZ and MDIZB. MDIZ acquires data from medical device, processes them using microcontroller, and transmit the data through ZigBee network through UART. MDIZB receives data from several MDIZs and transmit them out to PC through Bluetooth network. MDIZB comprises of ZigBee module, two processors, RAM, and Bluetooth module. It receives data from ZigBee network through its ZigBee module is shown in Figure 6. The data are then sent to processor 1. Processor 1 decides priority of MDIZs. In processor 1, the data frame is added with Start byte and End byte to mark the beginning and the end of data frame. After being processed in processor 1, the data are then sent to processor 2 through SPI (Serial Peripheral Interface). Processor 2 transmits data to PC throgh Bluetooth network [2]. Processor 2 controls Bluetooth module. It also receives commands given by PC through Bluetooth network.

Table 3 explains the comparison of Bluetooth, Wi-Fi, Zigbee and UWB with respect to their Standards such as IEEE spec, Frequency band, maximum signal rate, nominal range, nominal Tx power, number of RF channels, Channel bandwidth, modulation type,spreading,co-existance mechanism, basic cell, extension of basic cell, maximum number of cell nodes , encryption, authentication and Data protection.

Table 3: Comparison of Bluetooth, UWB, Zigbee and Wi-Fi

Standard	Bluetooth	UWB	Zigbee	Wi-fi
IEEE spec	802.15.1	802.15.3a*	802.15.4	802.11a/b/g
Frequency band	2.4GHz	3.1-10.6GHz	868/915 MHz;2.4GHz	2.4GHz;5GHz
Max signal rate	1Mb/s	110Mb/s	250Kb/s	54Mb/s
Nominal range	10m	10m	10-100m	100m
Nominal Tx power	0-10 dBm	-41.3dBm /MHz	(-25)-0 dBm	15-20 dBm
Number of RF channels	79	1-15	1/10;16	14(2.4GHz)
Channel bandwidth	1MHz	500 MHz-7.5GHz	0.3/0.6 MHz;2MHZ	22MHz
Modulation type	GFSK	BPSK;QPSK	BPSK(+ASK), O-QPSK	BPSK, QPSK COFDM,CCK,OFDM
Spreading	FHSS	DS-UWB,MB-OFDM	DSSS	DSSS,CCK,M-QAM
Coexistence mechanism	Adaptive freq. hopping	Adaptive freq. hopping	Dynamic freq. selection	Dynamic freq. selection, transmit power control. (802.11h)
Basic cell	piconet	Piconet	star	BSS
Extension of basic cell	scattement	Peer-to-peer	Cluster tree, mesh	ESS
Max number of cell nodes	8	8	>65000	2007
Encryption	E0 Stream clipher	AES block clipher (CTR counter mode)	AES block clipher (CTR counter mode)	RC4 block clipher (WEP) AES block clipher
Authentication	Shared secret	CBC-MAC(CCM)	CBC-MAC(ext of CCM)	WPA2(802.11i)
Data protection	16-bit CRC	32-bit CRC	16-bit CRC	32-bit CRC

The interface is connected with four different medical devices through UART and analog port at 42 kbps of data rate. Table 3 explains the comparison of Bluetooth , UWB, Zigbee and Wi-Fi based on IEEE spec , frequency band, Nominal range, Channel bandwidth, modulation type etc.

CONCLUSION

In this paper, Web-based wireless system for remote monitoring is presented. Besides having control function which can monitor the system remotely, the system is also equipped with web-based function which made it accessible at any place and any time via the internet. We use both wired and wireless networks for remote monitoring. Wired network has some limitations to which we prefer wireless networks due to its reduced cabling costs and installation time. It lets you move your measuring device from place to place and remotely monitor conditions. You can log data from your existing devices wirelessly by adding appropriate adaptors or routers.

Here, from the above analysis we find both Wi-Fi and Zigbee are better than other monitoring systems. When data protection is considered as first priority, Wi-Fi is preferred over Zigbee. Zigbee is preferred to other monitoring systems due to the advantages such as security, long battery lifetime due to low duty cycle and low cost .It has large number of nodes up-to 65000 in a network. It is easy to deploy and is used globally

To improve on the monitoring system, some future works are suggested here. Firstly, the data obtained from the monitoring system is useful for future reference to determine the efficiency and stability of the PV system as it may reduce over times. Secondly, the data collected can also be used for fault detection. Thirdly, faulty notification to user by using messaging system may become an added value to the system. Lastly, sensors failure detection may be added to the developed system to improve its robustness.

REFERENCES:

1. N. Javaid, A. Sharif, A. Mahmood, S. Ahmed, U. Qasim, Z. A. Khan "Monitoring and Controlling Power using Zigbee Communications" , Aug- 2012.
2. Jin-Shyan Lee, Yu-Wei Su, and Chung-Chou Shen "A Comparative Study of Wireless Protocols: Bluetooth, UWB, ZigBee, and Wi-Fi", Nov- 2007.
3. ViniMadan , S.R.N Reddy "GSM-Bluetooth based Remote Monitoring and Control System with Automatic Light Controller", Volume 46– No.1, May 2012.
4. Purnima, S.R.N. Reddy, PhD. "Design of Remote Monitoring and Control System with Automatic Irrigation System using GSM-Bluetooth",Volume 47– No.12, June- 2012.
5. Van Der Werff, M , ; Gui, X., Xu, W.L . "A mobile-based home automation system", Nov-2005.
6. E. Ferro and F. Potorti, "Bluetooth and Wi-Fi wireless protocols: A survey and a comparison", Volume 12, Issue 1, Pages 12-26,Feb-2005.
7. Baker, N. "ZigBee and Bluetooth: Strengths and weaknesses for industrial applications" Volume 16, Issue 2,Pages 20-25, April-May 2005.
8. P. S. Neelakanta and H. Dighe, "Robust factory wireless communications: A performance appraisal of the Bluetooth and the ZigBee collocated on an industrial floor", 2003.
9. Cheng, J.Y. and Hung, M.H. and Chang, J.W., "A Zigbee-based power monitoring system with direct load control capabilities" , Pages 895-900,April-2007.
10. M. Gagliarducci, D.A. Lampasi, L. Podesta, "GSM-based monitoring and control of photovoltaic power generation", Volume 40, Issue 3, Pages 314–321, April-2007.
11. Jifeng Ding, JiyinZhao,Biao Ma, "Remote monitoring system of temperature and humidity based on GSM ", Pages 1-4, Oct-2009.
12. Stanley Liu, "Overcoming IP Address Issues with GPRS Remote Monitoring and Alarm Systems", April-2009.
13. FarihahShariff , Nasrudin Abd Rahim , Hew Wooi Ping "Zigbee-based data acquisition system for the online monitoring of grid-connected photovoltaic system", Oct-2014.

International Journal of Engineering Research and General Science Volume 3, Issue 6, November-December, 2015
ISSN 2091-2730

A Study on Concrete Properties by Partial Replacement of Sand by Pond Ash

Tushar G. More[1], Pankaj B. Autade[2] .

1 Student, Dept. of Civil Engineering, PDVVP College of Engineering, Ahmednagar 414111 (India), email-tushargmore27@gmail.com, contact-08055568220. 2 Assistant Professor, Dept. of Civil Engineering, PDVVP College of Engineering, Ahmednagar 414111 (India).

Abstract—Pond ash is wastes and by-products of Thermal power plant, have been introduced into Indian concrete industry to conserve natural resources of ingredients of concrete. In India, most of the Thermal power plants adopt wet method of ash disposal. Pond ash is collected from Thermal power plant at the bottom, in that it contains significant amount of relatively coarser particles (spanning from 150 microns to 2.36 mm). Pond ash utilization helps to reduce the consumption of natural resources. Also it is help to solve the problem of disposal of Pond ash because it contains huge amount of chemical compounds such as SiO_2, Al_2O_3 etc. These chemical compounds (SiO2, Al2O3) are plays an important role in hydration reaction and helps to produce bond between two adjacent particles. Use of Pond Ash in concrete is an important eco efficiency drive. It is necessary to find the exact suitable percentages of pond ash so that it is decided to use in varying percentage as 0%, 5% 10%, 15%, 20%, 25%, 30%. And to check the properties of fresh concrete and hardened concrete such as slump and compressive strength, tensile strength, flexural strength respectively. Also concrete plays an important role in long life period of structure so it is also important to check effect on durability by using sulphate attack, chloride ion penetration, drying shrinkage.

Study shows the basic properties of Pond ash. It also compares these properties with natural sand. Partial replacement does not cause any adverse effect on properties of fresh concrete. The result shows that concrete giving good strength with partial replacement of fine aggregate. As well as Pond ash is the good if used as filler material in concrete. Thus, it is suitable to use pond ash as fine aggregate or partial replacement with natural sand.

Keywords— pond ash, concrete, natural recourses, wet method, SiO_2, Al_2O_3, hydration, bond, eco friendly, compressive, tensile, flexural, durability, sulphate, chloride.

INTRODUCTION

Waste and by-products have been introduced into Indian concrete industry to conserve natural resources and environment as well as to reduce the cost of concrete (Kasemchaisiri et.al)[1]. As an example, fly ash, a by-product from thermal power plants, has been widely used in Indian concrete industries as a pozzolanic material for replacing a part of cement due to its main benefits on workability and durability. The idea of using by-products to replace natural aggregates is another alternative solution to achieve environmental conservation as well as to obtain a reasonable concrete cost.

Unused fly ash and bottom ash (residue collected at the bottom of furnace) are mixed in slurry form and deposited in ponds which are known as pond ash (Bhangale et.al)[2]. Pond fly ash and contains relatively coarse particles. The coal fly ashes contain toxic metals in much higher concentrations that are released into the environment by thermal power plants based on coal combustion. Bottom ash is the companion to fly ash in process of coal-burning with an approximate amount of 20 % by volume of the total ash, depending on the type of boiler, dust collection system, burning temperature and the type of coal. Its particle is porous, irregular, and coarser than that of fly ash but its chemical composition is not much different (Cheriaf et.al)[3]. Some studies on the usage of bottom ash in concrete had been focused on its potential to replace or partially replace fine aggregate due to its similar particle size to that of normal sand (Bai et.al)[4]. Various attempts to apply bottom ash as a pozzolanic material had also been reported (Targan et.al)[5].The fly ash produced annually in India, with an estimated amount of 110 million tonnes(Central Electricity authority of India)[6], has been mostly dumped in landfill sites. Though, fly ash had been proved to enhance various properties of Concrete. In this research work an attempt is made to find out the possibility of using pond ash in conventional concrete. The part of the sand is replaced by pond ash in different composition and the concrete is made in conventional method.

Most of the Thermal Power plants in Indian adopt wet methods of disposal and storage of the ash in large ponds and dykes. In the wet method, both the fly ash collected from electrostatic precipitators and the bottom and grate ash are mixed with water and

transported to the ponds in a slurry form. Pond ash is being produced at an alarming rate and efforts are required to safely dispose it and if possible find ways of utilizing it. Fly ash collected through hoppers has been widely accepted as pozzolonic and is being used by the construction industry. Pond ash being coarser and less pozzolonic is not being used, or more importantly in places where the fine aggregate is contaminated with harmful chemicals such as sulphates and chlorides and pond ash accumulation posing environmental problems. The partial replacement of sand by pond ash in concrete is attempted. It is found that it is possible to use only pond ash as fine aggregate without compromising on strength and durability. This study opens up a major avenue for utilization of pond ash.

With a growing content of pond-ash, there has been are relatively greater increase in compressive strength, compared to normal concrete, and such trend might be a consequence of decreased water/cement ratio induced by the absorption of mixing water. (Lee Bong Chun et.al, 2008)[15]. The purpose of this study is to investigate the possibility of using alternative fine aggregates such as Pond ash. The disposal of fly ash will be a big challenge to environment, especially when the quantum increases from the present level to high. Hence worldwide research work was focused to find alternative use of this waste by product and its use in concrete industry is one of the effective methods of utilization in proper manner. Increase in demand of fine aggregate and decrease in natural resource of fine aggregate for the production of concrete has resulted in the need of identifying a new source of fine aggregate. It is also very important to study the effect of this partial replacement of sand on concrete, to find the optimum replacement of fine aggregate. energy generation is increasing day by day due to rapid industrialization. Energy generation through thermal power plants is very typical now days. Pond ash from these thermal plants is available in large quantities. Pond ash utilization helps to reduce the consumption of natural resources. In current time natural sand are using and a it is costly so it's require to replace by Pond Ash. Use of alternative material in concrete such as industrial by product coal Ash (Fly Ash and Pond Ash) is an important eco efficiency drive. It is also the social responsibility of researchers to encourage the "beneficial use of industrial by products in order to preserve resources, conserve energy and reduce or eliminate the need for disposal of industrial waste in landfills. This research paper reports the basic properties of Pond ash. It also compares these properties with natural sand. Basic changes in both type of aggregate properties were determined by various test as per require IS code, thus, it is a suitable to use pond ash as fine aggregate or partial replacement with natural sand.. Concrete is a construction material composed mainly of Cement, Fine Aggregate (Sand), Coarse Aggregate, Water and Admixture. River sand is the most commonly used Fine aggregate in many parts of the world. The huge demand for concrete has made this natural resource to get impoverished. On one side extraction of river sand in excess has conspicuous environmental impacts, on the other side, large quantity of coal ash is being produced every day in Thermal Power Plants, leading to many environmental problems. It is of prime importance to carry out research works on the feasibility of using alternative materials like Pond Ash, a waste by product and its suitability for potential utilization in concrete constructions, which can replace sand partially or fully as an alternative construction material contributing to sustainability and reducing burden on environment.

OBJECTIVES

To develop the conventional concrete of grade M25, and investigates the influence of the use of Pond ash as a replacement for natural fine aggregates on the properties of concrete in the fresh and hardened state and also on durability. Use of Pond Ash in concrete is an important eco efficiency drive to conserve natural recourses of sand. Ash is the residue after combustion of coal in thermal power plants. Fly ash and Bottom ash (residue collected at the bottom of furnace) are mixed in slurry form and deposited in ponds which are known as POND ASH. Most of the Thermal Power plants in Indian adopt wet methods of disposal and storage of the ash in large ponds and dykes. In the wet method, both the fly ash collected from electrostatic precipitators and the bottom and grate ash are mixed with water and transported to the ponds in a slurry form. Pond ash is being produced at an alarming rate and efforts are required to safely dispose it and if possible find ways of utilizing it. As it is very important to do disposal of this waste product of Thermal Power Plant, this study gives some ideas to utilization of Pond ash. Natural sand is commonly used as fine aggregate in concrete. There is scarcity of natural sand due to heavy demand in growing construction activities which forces to find the suitable substitute, also due to extensive construction activity natural sand is becoming expensive and scarce. The purpose of this study is to investigate the possibility of using alternative fine aggregates such as Pond ash. The disposal of fly ash will be a big challenge to environment, especially when the quantum increases from the present level to high. Hence worldwide research work was focused to find alternative use of this waste by product and its use in concrete industry is one of the effective methods of utilization in proper manner. Increase in demand of fine aggregate and decrease in natural resource of fine aggregate for the production of concrete has resulted in the need of identifying a new source of fine aggregate. The possibility of utilization of thermal power plant by-product pond ash as replacement to fine aggregate in concrete is taken into consideration for work. Disposal of coal fly ash in open and unlined ash ponds causes serious adverse environmental impacts due to its elevated metals concentrations and its leaching into soils and groundwater. (Lokeshappa B, Anil Kumar Dikshit)[7]

It is also very important to study the effect of this partial replacement of sand on concrete, to find the optimum replacement of fine aggregate. Therefore the study of properties of concrete with different proportion of replacement of sand by pond ash is covered in this project work. It is not just the study of concrete properties by partial replacement of sand but also one eco friendly drive to do disposal of waste product of Thermal Power Plant that is Pond ash, because by using pond ash in concrete we are not going to disturb environment any way.

POND ASH

Ash is the residue after combustion of coal in thermal power plants. Particle size of the ash varies form around one micron to around 600 microns. The very fine particles (fly ash) collected from this ash generated by electro static precipitators are being used in the manufacture of blended cements. Unused fly ash and bottom ash (residue collected at the bottom of furnace) are mixed in slurry form and deposited in ponds which are known as pond ash (Bhangale et.al)[8]. Among the industries, thermal power plants are the major contributor of pond ash. Be sides, this steel, copper and aluminum plants also contribute a substantial amount of pond ash. During the combustion of pulverized coal at the thermal power station the product formed are bottom ash, fly ash and vapors. The bottom ash is that part of the residue which is fused into particles and is collected at the bottom of the furnace.

ADVANTAGES OF USE OF POND ASH

Following are the main advantages of Pond ash while using in Concrete.

- Use of Pond ash as partial replacement of Sand is Eco-friendly drive.
- Pond ash acts as filler material as well as bonding agent as it shows the bonding property also.
- Use of pond ash in concrete can save the thermal industry disposal costs and produce a 'greener' concrete –for construction.
- Environmental effects from wastes and residual amount of cement manufacturing can be reduced through this way.
- Pond ash can be use to form various higher concrete grades.
- The cement content can be reduced a lot by increasing the fly ash content to make it more economical and also we can achieve designed compressive strength .
- Use of Pond ash as partial replacement of Sand is help to solve issue of ash disposal.
- Use of pond ash is good Option for natural Sand.
- Partial replacement of natural sand is does not change original strength of concrete.
- Manufacturing of cement mortar also possible.
- The cement content can be reduced a lot by increasing the fly ash content to make it more economical and also we can achieve designed compressive strength.
- The quantity of pond ash is available enormously at thermal power stations at free of cost.
- It is easy to investigate the properties of pond ash.
- When pond ash is used in brick construction the compressive strength of brick is increase with increase in lime content.

LIMITATIONS OF STUDY

As the famous phrase says that, every coin has two sides. Till this moment we saw only the easy way of use of pond ash as replacement of natural sand but from the another side there are some limitations on such replacement. This study is work on the concept of partial replacement of sand (one of the important ingredient of concrete) by pond ash (waste byproduct of thermal power plant), with different proportions. The investigation of previous research paper shows that, if the partial replacement of sand exceeds some limit that affects the properties of concrete on large scale, it will prove dangerous or it is not possible to use such concrete practically.

- While adding pond ash in concrete it will need skilled supervision. At the time of replacing the sand in concrete, it is very important to replace the sand in desired proportions only, therefore it is required skilled supervision. This is also one of the limitation of this study.
- This replacement is suitable only for mass concreting projects as like construction of dam structures. This partial replacement is not economical if the concreting is on small scale.
- Also pond ash may not available easily, availability of pond ash depends upon the distance of construction site and ash ponds.
- The CaO content is less in the pond ash so that the plasticizer property of pond ash is decreased. Hence, the compressive strength is decreased(after some limit only).
- The water absorption of pond ash is on large scale and
- is generally dependent on which type of coal is used in its manufacturing. Pond ash cannot be used in large proportions for replacement (Prof. Jayeshkumar Pitroda, Gaurav Patel, Dr F S Umrigar)[9]
- While the pond ash is used the workability is reduced. For obtaining the required workability, superplasticizers are added while preparing the concrete. **(Arumugam et.al (2011)[10]**

PROBLEM STATEMENT AND METHODOLOGY

This study investigates the interpretation of tests results on concrete in which fine aggregate (natural sand) is partially replaced by pond ash. Pond ash is wastes and by-products of Thermal power plant, have been introduced into Indian concrete industry to

conserve natural resources of ingredients of concrete. In India, most of the Thermal power plants adopt wet method of ash disposal. In wet method of disposal of ash, bottom ash and fly ash are mixed with water and the slurry is disposed on vacant land to reduced the excess water from that slurry. After the drying of that slurry clinkers are formed and that can be collected as Pond ash. Sometimes it becomes the problem of such ash disposal because it requires the large vacant land to disposal of ash. Bottom ash is collected from Thermal power plant at the bottom, in that it contains significant amount of relatively coarser particles (spanning from 150 microns to 2.36 mm). Pond ash utilization helps to reduce the consumption of natural resources. Also it is help to solve the problem of disposal of Pond ash because it contains huge amount of chemical compounds such as SiO_2, Al_2O_3 etc. These chemical compounds (SiO_2, Al_2O_3) are plays an important role in hydration reaction and helps to produce bond between two adjacent particles. Also sand does not use only to fill gap between two particles of aggregate but also to increase the volume of concrete. Pond ash plays this both role very well.

Thermal Power Plants using coal is chief source of energy in our country and it is likely to remain so in near future. The total production of fly ash per annum has already crossed 100 million tones and the disposal of the fly ash is causing several challenges. Utilization of fly ash has picked up but till the percentage utilization is far below satisfaction and power plants are no option but to dispose the fly ash in ash pond

Pond ash is cheaply available and is available on large scale. Use of Pond Ash in concrete is an important eco efficiency drive. It is necessary to find the exact suitable percentages of pond ash so that it is decided to use in varying percentage as 0%, 5% 10%, 15%, 20%, 25%, 30%. And to check the properties of fresh concrete and hardened concrete such as compacting factor, slump and compressive strength, tensile strength, flexural strength respectively. Also concrete plays an important role in long life period of structure so it is also important to check effect on durability by using sulphate attack, chloride ion penetration, drying shrinkage.

PROBLEM OF COAL ASH DISPOSAL

It is becoming very major problem of generated coal ash disposal Presently, out of 110 million tonnes of total ash generated, about (55%) is being utilized and remaining 45% remains dumped. Therefore it is very important to do utilization of coal ash. Presently majority of the coal ash generated is being handled in wet form and disposed off in ash ponds which is harmful for the environment and moreover ash remains unutilized for gainful applications. Nearly, 73% of India‟s total installed power generation capacity is thermal of which coal based generation are nearly 90% (by diesel, wind, gas and steam adding about 10%). Indian coal gives 35 to 45% ash which is responsible for large volumes of pond ash. Thermal Power Plants using coal is chief source of energy in our country and it is likely to remain so in near future Construction of large ash disposal areas results in resettlement issues and loss of agricultural production, grazing land and habitat as well as other hand use impacts from diversion of large areas of land to waste disposal. (Alok Sharan),[21].

The total production of fly ash per annum has already crossed 100 million tones and the disposal of the fly ash is causing several challenges. Utilization of fly ash has picked up but till the percentage utilization is far below satisfaction and power plants are no option but to dispose the fly ash in ash pond. Presently Bhusawal Thermal Power Station (M.S.) has 1500 MW capacity of thermal power station and BTPS alone, nearly 1000 MT. of pond ash is produced every day. Effective utilization of pond ash is very essential to reduce the environmental problems caused by the accumulation of pond ash. If it is found suitable for construction industry, large scale utilization of pond ash would be possible and this will become a major contribution factor for reducing pollution. Future more a precious Natural resource as sand is becoming scare and quarrying of sand has been restricted in many places near BTPS. This has lead to look for possibility of partial replacement of sand by pond ash without compromising on strength (Prof. P. P. Bhangale, Prof. P. M. Nemade)[8]. The coal fly ashes contain toxic metals in much higher concentrations that are released into the environment by thermal power plants based on coal combustion. Disposal of coal fly ash in open and unlined ash ponds causes serious adverse environmental impacts due to its elevated metals concentrations and its leaching into soils and groundwater. (Lokeshappa B, Anil Kumar Dikshit)[7].

The fly ash gets mixed with bottom ash and disposed off in large pond or dykes as slurry. It is also termed as ponded fly ash and contains relatively coarse particles. The large areas of land are used to store such a mixture of pond ash resulting in land degradation near the thermal power plants. As the pond ash is being produced at an alarming rate, hence the efforts are required to safely dispose it and if possible find ways of utilizing it. In the pond ash the dissolvable alkalies present are washed with water. The metal oxides, sulphur, siliceous & aluminous materials with less pozzolonic properties than fly ash, are some main constituents of pond ash. These ash produced, if disposed off unscientifically, can cause environmental risks i.e. air pollution, surface water and groundwater pollution and thus its safe disposal is indispensable. In fact, the pond ash is a mixture of fly ash and bottom ash. The main difference between pond ash and fly ash is in their particle size. The pond ash being coarser and less pozzolonic and hence is not being accepted as pozzolona. (Prashant G. Sonawane, Dr. Arun Kumar Dwivedi)[19]

Though fly ash is known to be an inert material, there is an appearansion about certain soluble chemicals in the decanted water which can have adverse effect if such decanted water is let into a river body or ground water. For this purpose, the norms of Pollution Control Board insist on providing a plastic liner over the entire bottom of the pond and upstream face of the ash dyke. New ash ponds being constructed have to provide the plastic liner to prevent pollution of ground water. Due to the presence of plastic liner, provision

of the drainage becomes difficult and as result the deposited sediments could not get consolidated to the same extent as that anticipated in the pond without plastic liner. For this reason, whenever plastic liner is provided, it is important to check the adequacy of strength parameters for the deposited ash for supporting the next section of the dyke if upstream method of construction is adopted.

Apart from pollution to ground water, another major concern is dust pollution in the surrounding area during heavy wind. To prevent dust pollution, water sprinklers shall be arranged in the beach area which is in dry condition. The dust pollution is more from the pond which is not in operation and where construction is in progress by excavating the fly ash. For the pond which has reached the ultimate height and no further extension of height is warranted, the surface shall be covered with a 300mm thick soil layer. Suitable vegetation shall be grown over the area which ensures no dust pollution.

TESTS ON CONCRETE SPECIMEN

In this chapter the description of experimental tests investigation carried out on M25 grade concrete to determine its fresh state properties, hardened state properties and durability of concrete when natural sand is replaced by pond ash are presented. The following tests were conducted to assess the various properties.

Fresh property test on concrete-

1) Slump cone test.

Hardened concrete tests-

2) Compressive Strength Test.
3) Split tensile strength test.
4) Flexural strength test.

Durability tests-

1) Weight loss due to SULPHATE ATTACK.
2) Weight loss due to ACID ATTACK.
3) Loss of Compressive Strength due to immersion in MgSO4 solution.
4) Loss of Compressive Strength due to immersion in HCl solution.

TEST RESULTS AND DISCUSSION

This chapter gives the interpretation of various test results as below, also present the short discussion on respective results as stated

1) SLUMP CONE TEST

The higher the slump flow (SF) value, the greater its ability to fill formwork. Test results are tabulated as below:

Table 1) Slump flow value

Sr. No.	% Pond ash	Slump (mm)
01	0	113
02	5	105
03	10	100
04	15	96
05	20	90
06	25	80
07	30	75

Discussion on test results- As percentage of pond ash is increased the workability is reducing. Main reason for this is the water absorption of pond ash.

2) COMPRESSION STRENGTH TEST

Compressive strength of concrete mixes made with various percentage of partial replacement of sand by pond ash was determined at curing period of 3rd, 7th, 28th and 56th days. The results are as follows:

Table 2 Average Compressive Strength

Sr no	Replacement of Pond Ash	Average Compressive Strength			
		3 days (N/mm^2)	7 days (N/mm^2)	28 days (N/mm^2)	56 days (N/mm^2)
1	0%	13.36	17.15	26.78	28.59
2	5%	9.66	17.07	27.05	29.13
3	10%	9.07	16.74	27.44	30.28
4	15%	8.68	16.36	27.94	30.71
5	20%	8.00	16.06	28.24	31.20
6	25%	7.41	15.20	24.95	27.20
7	30%	6.81	14.99	23.17	25.57

Discussion on test results- Experimental results proves that, as percentage of pond ash increases in concrete it leads to the increase in compressive strength of concrete only up to partial replacement of 20% of natural sand by pond ash and beyond that percentage of pond ash there is reduction in strength of concrete. Also the pond ash concrete gains strength at slower rate in the initial period and acquires strength at faster rate beyond 28 days, due to pozzolonic action of pond ash. The graphical representation of results is shown in respective figures:

Figure 1) **3 days** Compressive strength of concrete with varying % of pond ash

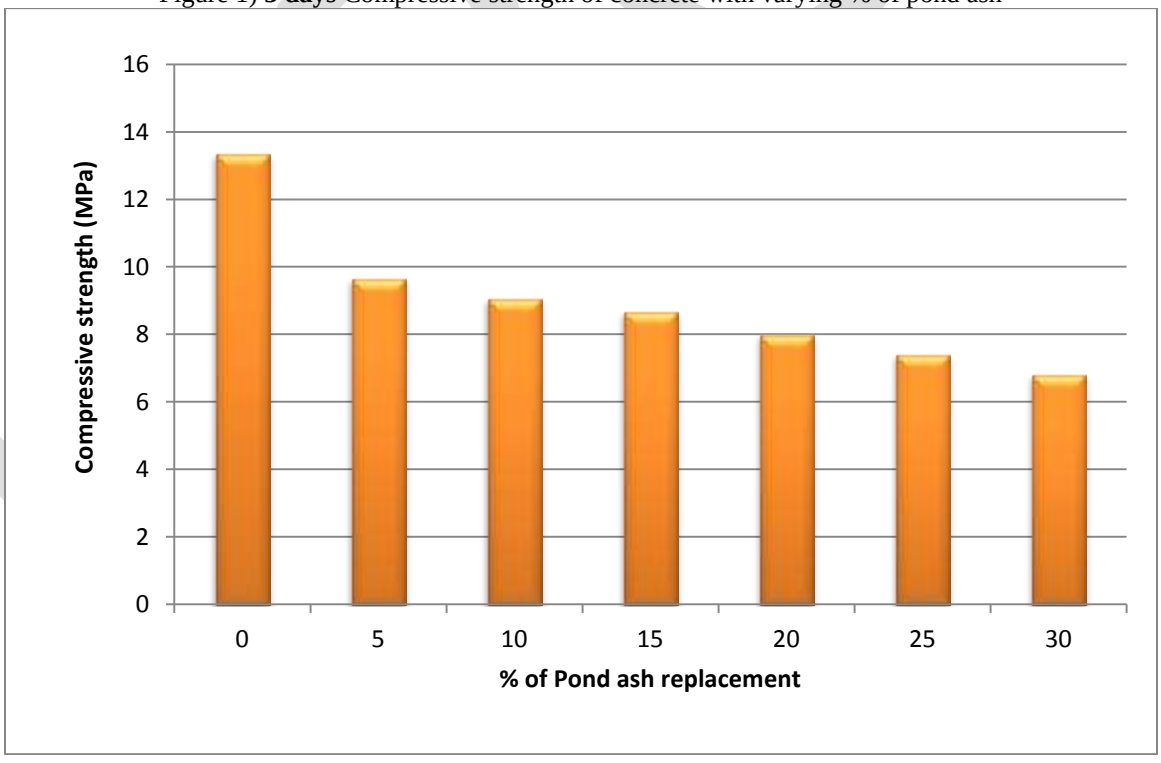

Figure 2) **7 days** Compressive strength of concrete with varying % of pond ash

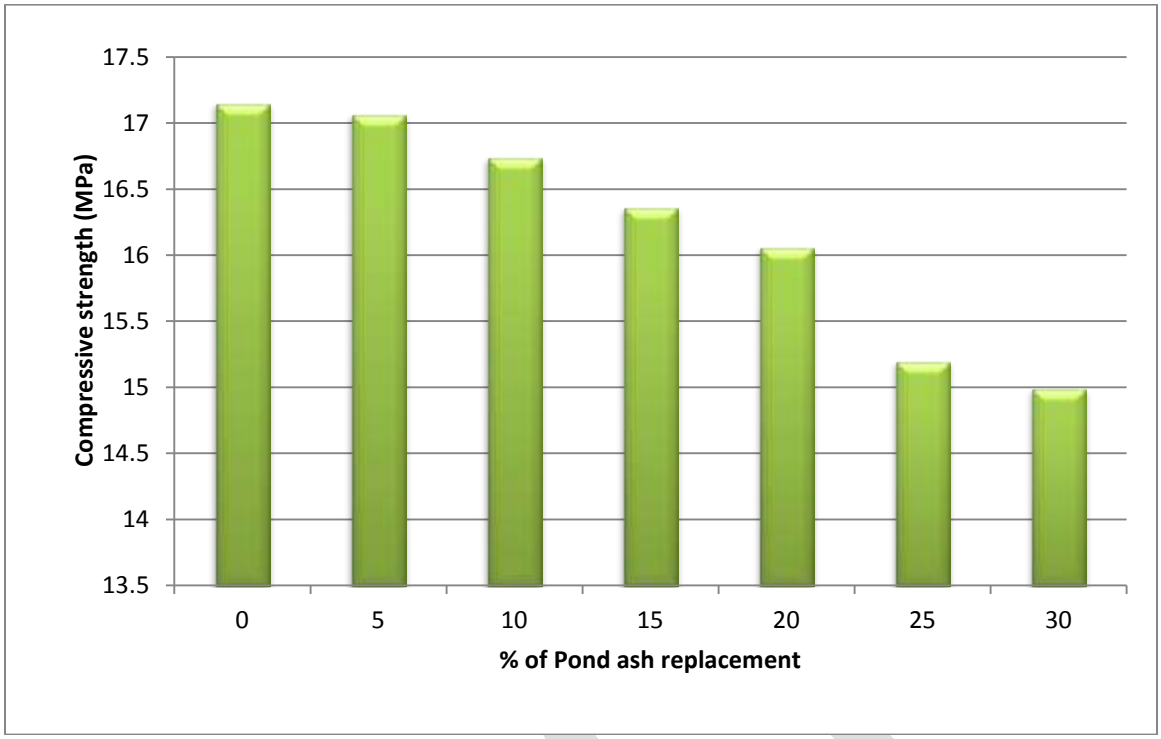

Figure 3) **28 days** Compressive strength of concrete with varying % of pond ash

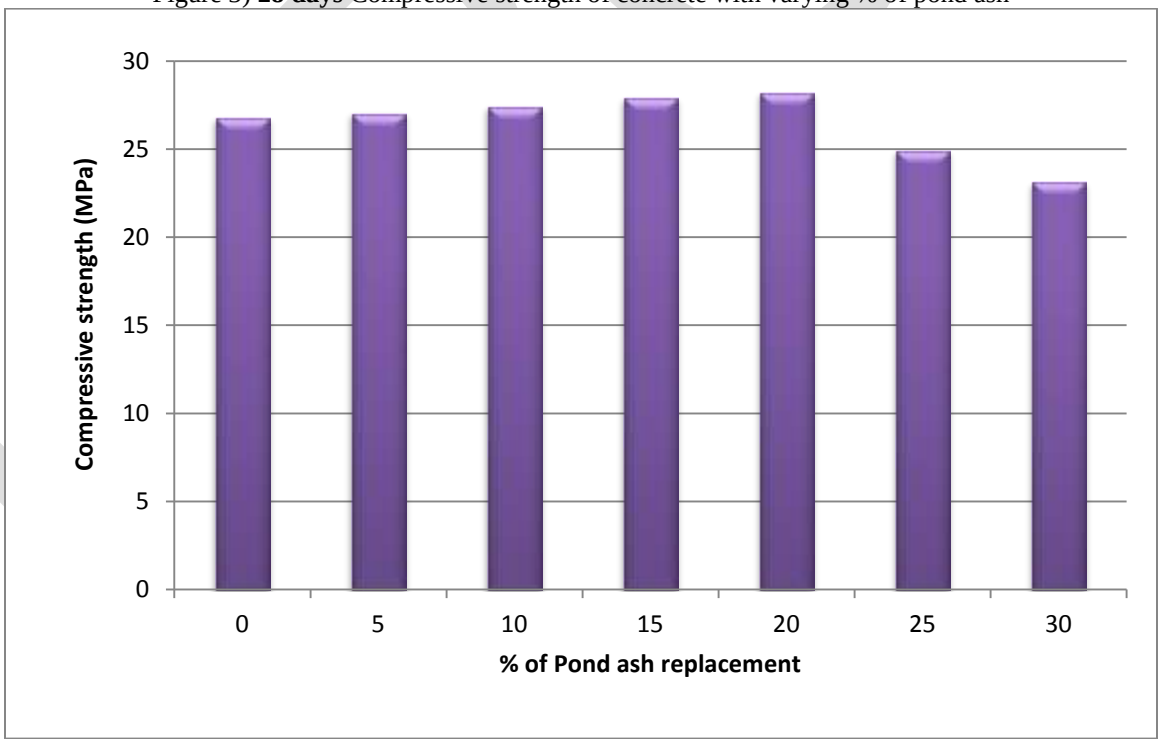

Figure 4) **56 days** Compressive strength of concrete with varying % of pond ash

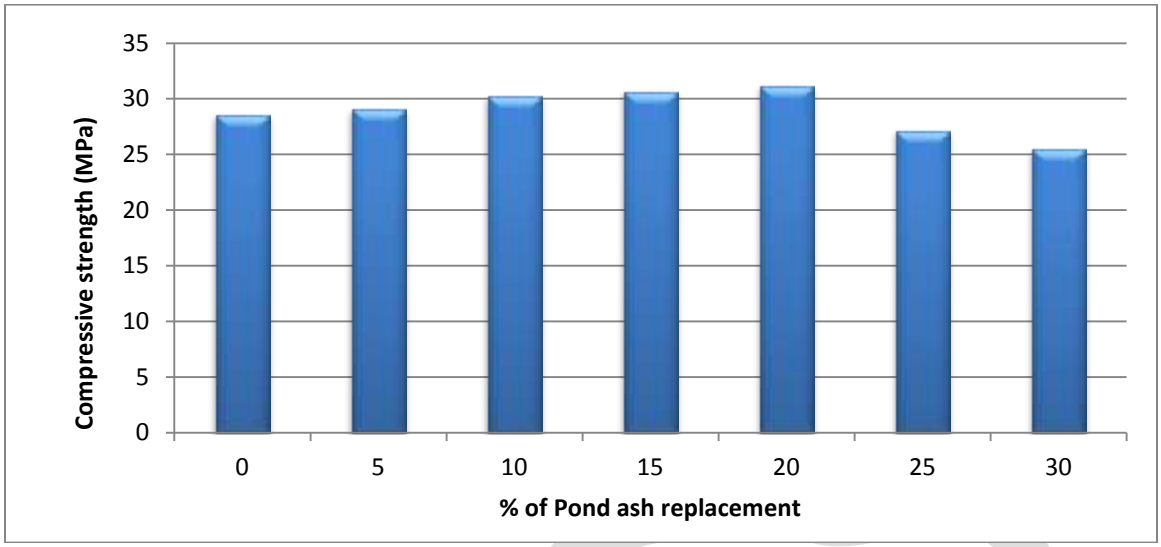

3) SPLIT TENSILE STRENGTH TEST:

The results of split tensile strength for various replacements of partial replacement of natural sand by pond ash are as follows:

Table 3) Average Split tensile Strength

Sr no	Replacement of Pond Ash	Average Split tensile Strength (N/mm^2)
1	0%	3.55
2	5%	3.59
3	10%	3.60
4	15%	3.66
5	20%	3.71
6	25%	3.48
7	30%	3.38

Discussion on test results- It is observed from results that the splitting tensile strength of concrete increases only up to partial replacement of 20% of natural sand by pond ash, beyond that it decreases with the increase in the percentage of fine aggregates replacement with the pond ash.

Figure 5) 28 days Split tensile strength of concrete with varying % of pond ash

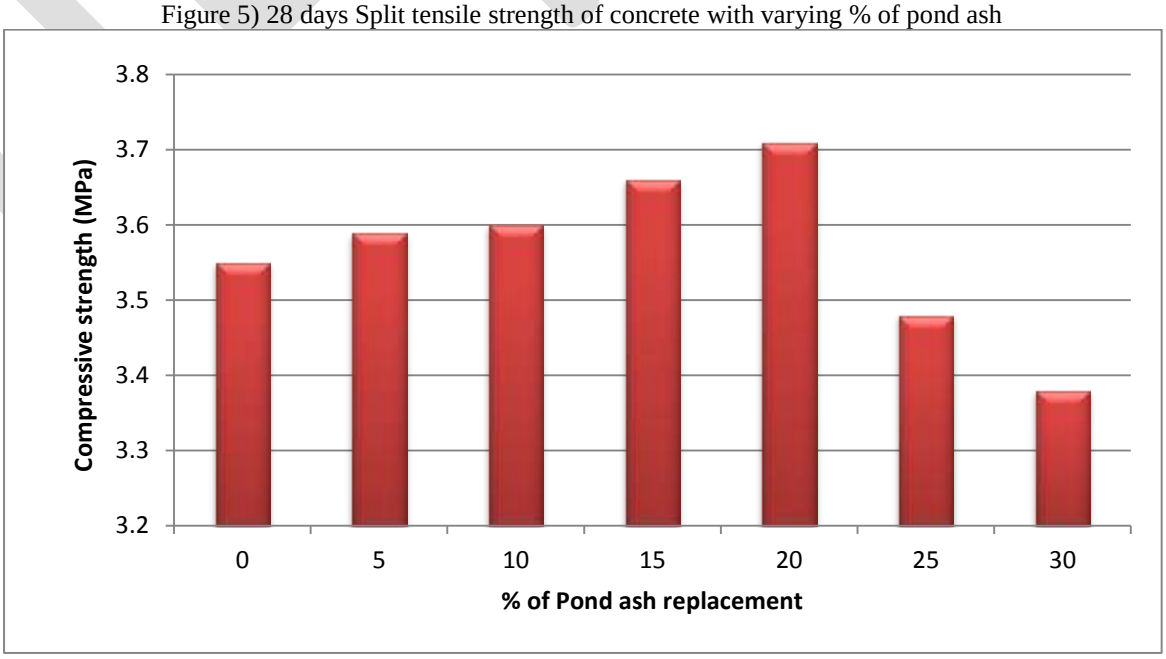

4) **FLEXURAL STRENGTH TEST**:

The results of flexural strength strength for various replacements of partial replacement of natural sand by pond ash are as follows:

Table 4) Average Flexural Strength

Sr no	Replacement of Pond Ash	Average Flexural Strength (N/mm^2)
1	0%	7.14
2	5%	7.23
3	10%	7.28
4	15%	7.46
5	20%	7.6
6	25%	6.64
7	30%	5.94

Discussion on test results- It is observed from results that the splitting tensile strength of concrete increases only up to partial replacement of 20% of natural sand by pond ash, beyond that it decreases with the increase in the percentage of fine aggregates replacement with the pond ash.

Figure 6) 28 days flexural strength of concrete with varying % of pond ash

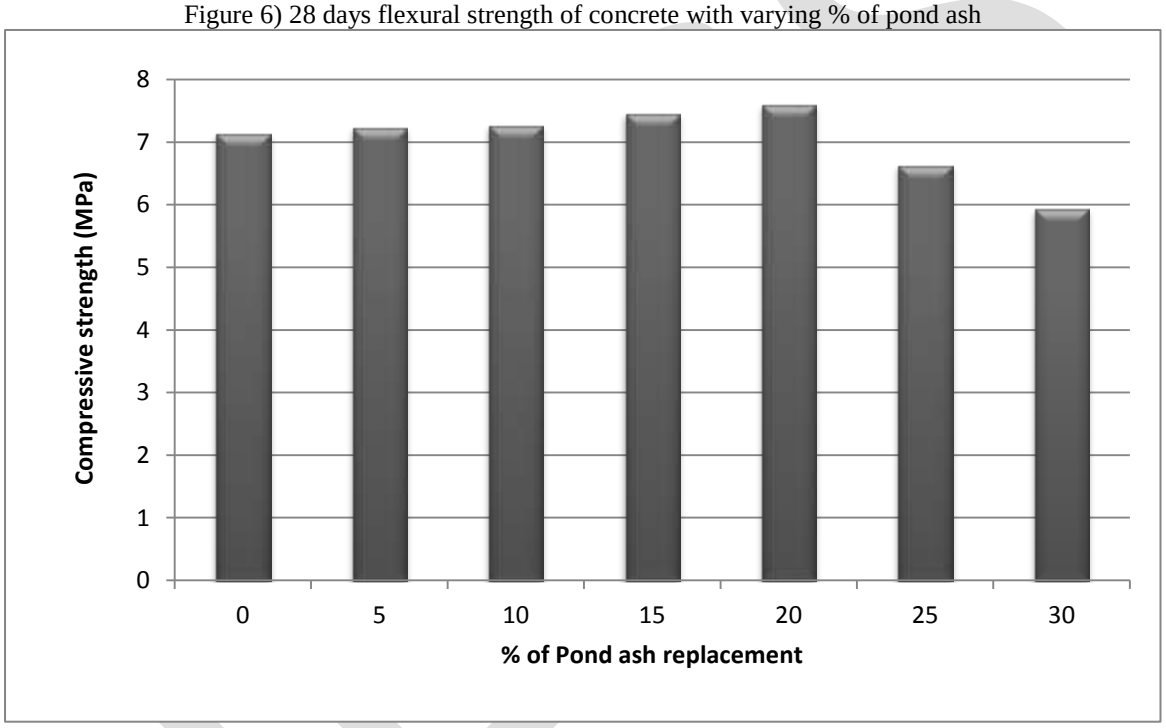

5) RESISTANCE TO SULPHATE ATTACK ON CONCRETE:

Average % weight loss and compressive strength results are listed below:

Table 5) Weight loss and Compressive strength variation due to Sulphate attack on Concrete after **28 days:**

Pond ash %	Initial wt.	Final wt.	% wt. loss	Compressive strength (Mpa)
0	7.882	7.896		27.11
	7.736	7.748		27.47
	7.96	7.975		26.84
Average	**7.859**	**7.873**	**-0.18%**	**27.14**
5	7.746	7.76		27.20
	7.816	7.831		27.56
	7.534	7.55		27.91
Average	**7.698**	**7.713**	**-0.19**	**27.56**
10	7.404	7.426		28.00
	7.882	7.902		27.91
	7.754	7.776		28.18
Average	**7.68**	**7.701**	**-0.27%**	**28.03**
15	7.444	7.464		28.36
	7.806	7.828		28.09
	7.606	7.63		27.91
Average	**7.618**	**7.64**	**-0.29%**	**28.12**
20	7.882	7.908		28.53
	7.736	7.76		28.89
	7.642	7.668		28.09
Average	**7.753**	**7.778**	**-0.32%**	**28.50**
25	7.49	7.499		25.33
	7.653	7.665		24.98
	7.872	7.882		24.80
Average	**7.671**	**7.682**	**-0.14%**	**25.04**
30	7.288	7.292		23.38
	7.564	7.568		23.20
	7.414	7.42		23.02
Average	**7.422**	**7.426**	**-0.05%**	**23.20**

Discussion on test results- Experimental results show that there is no effect of sulfate solution on concrete when partial replacement of natural sand by pond ash is used in concrete. The solution is not affect on the compressive strength of concrete also. That mean when natural sand is replaced by pond ash then there is no any adverse effect on durability of concrete.

6) RESISTANCE TO CHLORIDE ATTACK ON CONCRETE:

Average % weight loss and compressive strength results are listed below:

Table6) Weight loss and Compressive strength variation due to Chloride attack on Concrete after **28 days**:

Pond ash %	Initial wt.	Final wt.	% wt. loss	Compressive strength (Mpa)
0	7.404	7.416		28.18
	7.526	7.536		28.80
	7.366	7.378		28.89
Average	**7.432**	**7.443**	**-0.15%**	**28.62**
5	8.162	8.176		29.24
	8.206	8.218		29.42
	7.986	8.001		30.22
Average	**8.118**	**8.131**	**-0.16%**	**29.63**
10	7.526	7.538		29.78
	7.404	7.413		30.31
	7.422	7.436		30.58
Average	**7.45**	**7.462**	**-0.16%**	**30.22**
15	7.67	7.688		30.76
	7.356	7.374		30.58
	7.876	7.892		31.02
Average	**7.634**	**7.651**	**-0.22%**	**30.79**
20	7.67	7.696		31.56
	7.356	7.38		32.09
	7.495	7.514		31.58
Average	**7.507**	**7.53**	**-0.31%**	**31.68**
25	8.062	8.07		27.02
	7.894	7.904		27.56
	8.1	8.11		27.82
Average	**8.018**	**8.028**	**-0.12%**	**27.47**
30	7.894	7.904		26.67
	8.062	8.07		26.49
	7.975	7.983		25.78
Average	**7.977**	**7.985**	**-0.10%**	**26.31**

Discussion on test results- Experimental results show that there is no effect of chloride solution on concrete when partial replacement of natural sand by pond ash is used in concrete. The solution is not affect on the compressive strength of concrete also. That mean when natural sand is replaced by pond ash then there is no any adverse effect on durability of concrete.

CONCLUSIONS

The conclusions based on experiments conducted and observations from the present study are listed below

1. Indian Standard method is easy method for the mix design of M25 grade concrete.
2. Pond ash shows the more water absorption as compared to natural sand.
3. As percentage of pond ash is increased the workability is reducing.
4. 20% of pond ash as sand replacement is found to be the optimum amount in order to get a favorable strength.
5. The pond ash concrete gains strength at slower rate in the initial period and acquires strength at faster rate beyond 28 days, due to pozzolonic action of pond ash.
6. Strength of pond ash concrete decreases with increase in percentage of replacement of sand by pond ash.
7. The compressive strength of concrete with pond ash increases with increased curing period.

8. It is observed from results that the splitting tensile strength of concrete increases only up to partial replacement of 20% of natural sand by pond ash, beyond that it decreases with the increase in the percentage of fine aggregates replacement with the pond ash.
9. It is observed from results that the splitting tensile strength of concrete increases only up to partial replacement of 20% of natural sand by pond ash, beyond that it decreases with the increase in the percentage of fine aggregates replacement with the pond ash.
10. There is no any adverse effect of sulfate solution on concrete when partial replacement of natural sand by pond ash is used in concrete.
11. The sulfate solution is not affect on the compressive strength of concrete also. That mean when natural sand is replaced by pond ash then there is no any adverse effect on durability of concrete.
12. There is no any adverse effect of chloride solution on concrete when partial replacement of natural sand by pond ash is used in concrete.
13. The chloride solution is not affect on the compressive strength of concrete also. That mean when natural sand is replaced by pond ash then there is no any adverse effect on durability of concrete.

REFERENCES:

[1]Ratchayut Kasemchaisiri and Somnuk Tangtermsirikul, "Properties of Self Compacting Concrete in Corporating Bottom Ash as a Partial Replacement of Fine Aggregate", ScienceAsia 34, pp. 087-095 (2008).

[2]Prof. P. P. Bhangale, Prof. P. M. Nemade, "Study of Pond Ash (BTPS) "Use as a Fine Aggregate in Cement Concrete- Case Study", Shri SantGadge Baba College of Engineering & Technology, Bhusawal, Maharashtra, India.

[3]Cheriaf M, Cavalcante J and Pera J (1999) Pozzolanic properties of pulverized coal combustion bottom ash. Cement and Concrete Research Vol. 29, No. 9, 387-1391.

[4]Bai Y and Basheer P A M (2003) "Influence of furnace bottom ash as fine aggregate on properties of concrete". Structures and Buildings Vol. 156, No. 1, 85-92.

[5]Targan S, Olgun A, Erdogan Y and Sevinc V (2004) Mineralogy and Organic Matter Content of Bottom Ash Samples from Agios Demitrios Power Plant, Greece. Bulletin of the Geological Society of Greece Vol. 36, Proceeding of the 10th international Congress, Thessaloniki, 321-6.

[6]Central Electricity authority of India, 2013 www.cea.nic.in

[7]Lokeshappa B [a,b], Anil Kumar Dikshit [c,d,e] Behaviour of Metals in Coal Fly Ash Ponds.

[8]Prof. P. P. Bhangale, Prof. P. M. Nemade.(2012) "Study of Pond ASH (BTPS) Use as A Fine Aggregate in Cement Concrete - Case Study".

[9]Prof. Jayeshkumar Pitroda, Gaurav Patel, Dr F S Umrigar "Pond Ash: Opportunities For Eco-Friendly Material (As Fineaggregate) In Green Concrete". JiarmVolume 1Issue 8 (2013) .

[10]Arumugam , Ilangovan , James Manohar, "A study on characterization and use of Pond ash as fine aggregate in concrete"International journal of civil and structural engineering Volume 2, No 2, 2011.

[11] Lee Bong Chun Kim Jin Sung, Kim Tae Sang and Chae SeongTae, "A study on the fundamental properties of concrete incorporating pond-ash in korea", The 3rd ACF International Conference-ACF/VCA, pp.401-408, (2008).

[12]Arumugam K, Ilangovan R and James Manohar, "A study on characterization and use of Pond Ash as fine aggregate in Concrete", International Journal of Civil And Structural Engineering Vol 2, No 2, pp.466-474, (2011).

[13]Kondaivendhan B, Velchuri, Sairam and K. Nandagopal, "Influence of pond ash as fine aggregate on strength and durability of concrete", The Indian Concrete Journal.

[14]Ratchayut Kasemchaisiri and Somnuk Tangtermsirikul, "Properties of Self Compacting Concrete in Corporating Bottom Ash as a Partial Replacement of Fine Aggregate", ScienceAsia 34, pp. 087-095 (2008).

[15]Lee Bong Chun Kim Jin Sung, Kim Tae Sang and Chae SeongTae, "A study on the fundamental properties of concrete incorporating pond-ash in korea", The 3rd ACF International Conference-ACF/VCA, pp.401-408, (2008).

[16]Virenda Kumar, (May, 2004), "Compaction and permeability study of pond ash". Journal of The Institution of Engineers (India), pp 31-3.

[17]Bai Y. and Basheer P. (2003) "Influence of furnace bottom ash as fine aggregate on properties of concrete." Structures and Buildings Vol. 156, No. 1, 85-92.

[18]Prashant G. Sonawane, Dr. Arun Kumar Dwivedi "Technical Properties of Pond Ash - Clay Fired Bricks – An Experimental Study".

[19]Ranganath.R.V, Bhattarcharjee B. and krishnamoorthy S.,"Influence of size fraction of ponded ash on its pozzolonic activity", Cement and Concrete Research, Vol.28, No.5, pp. 749-761, (1999)

[20]P.V.V. Satyanarayana, N. Pradeep, N. Sai Chaitanya Varma, "A Study on the Performance of Pond Ash In Place of Sand and Red Soil as A Subgrade and Fill Materia", International Journal of Engineering and Advanced Technology (IJEAT) ISSN: 2249 – 8958, Volume-3, Issue-1, (2013).

[21]Alok Sharan, "strength characteristics of fibre reinforced compacted pond ash", National institute of technology, rourkela odisha-769008. (2011).

[22]Gaurav Kantilal Patel, Prof. Jayeshkumar Pitroda "Assessment Of Natural Sand And Pond Ash In Indian Context", International Journal of Engineering Trends and Technology (IJETT) – Volume 4 Issue 10 –(2013)

[23]www.google.com.

International Journal of Engineering Research and General Science Volume 3, Issue 6, November-December, 2015
ISSN 2091-2730

ANALYSIS OF DELAYS IN CONSTRUCTION PROJECTS

Aedwin Regi Varghese[1], Shibi Varghese[2]
[1]PG student,Structural Engineering & Construction Management, M A College Of Engineering
[2]Associate Professor, Civil Engineering Department, M A College Of Engineering
[1]aedwinr@yahoo.com
[2]shibi_chelattu@rediffmail.com

Abstract:- Time , quality and economy constitute the three main factors in a construction project, of which time plays a significant role in construction. Delay in any task or operation is a time overrun which influences the completion of the work. The common problems in civil engineering projects all around the world are mainly due to delay in construction. These problems occur frequently during project duration leading to disputes and litigation. Thus it's essential to study and analyse causes of construction delays.This study is based on a list of construction delay causes retrieved from literature reviews. The feedback of construction experts was obtained through interviews. Subsequently, a questionnaire survey was prepared. The questionnaire survey was distributed to construction experts who represents consultants, and contractor's organizations. A case study is analyzed and compared to the most important delay causes in the research. Statistical analysis is carried out to test delay causes, obtained from the survey.

Keywords:- Questionnare, Likert Scale, Frequency Index, SPSS, Chronbach's alpha

INTRODUCTION

A typical construction project suffers from high risks associated with schedule delays and time-based disputes, since time is of the essence of the construction contract. For example, the unique nature of construction makes the work susceptible to unforeseen site conditions and severe weather changes. In addition, a construction plan created for a project relies on the performance of owners, designers, contractors, subcontractors, and suppliers, as well as the co-ordination among them. A single event that deviates from the plan, such as a change in the scope of the project, can disturb the overall performance and can create turbulence among the parties.

Delay in construction can have a number of consequences in a project, such as late completion, lost productivity, acceleration, consequential damages, increased cost and contract termination. The party experiencing damages from delays needs to be able to recognize the delays and the parties responsible for them in order to recover time and cost.
A number of methodologies have been developed to assess delays and their impacts, but honourable courts and administrative boards have not specified any standard method to evaluate delay impacts. Delay analysis can be conducted in a cursory manner or in such detail as to exceed the value of the underlying dispute. Each delay analysis method adopts a different approach to identify delay impacts and may yield different results. The most sophisticated delay analysis method using the highest level of detail does not guarantee success.

Delay Analysis

The objective of delay analysis is to calculate the project delay and work backwards and tried to identify how much of it is attributable to each party (contractor, owner, or neither) so that time and/or cost compensation can be decided.
The most widely used delay analysis techniques are

- Schedule Review/ Discussion
- As Planned Versus As Built Analysis
- Impact As Planned Analysis
- Collapsed As Built Analysis
- Time Impact Analysis
- Productivity Method

Schedule Review/ Discussion

Schedule review/discussion is the simplest method that involves arguing a claim with or without using a schedule, but relying mostly on the strength of the evidence and testimony. The method is an easy and inexpensive way to argue time-based claims when detailed

calculations cannot be conducted. But the results of such an analysis are not acceptable to most analysts because it ignores the nature of each delay event and assumes that every delay has an equal impact on the project duration.

As Planned versus as Built Analysis

The as-planned versus as-built schedule delay analysis involves comparing the baseline, or as-planned, construction schedule against the as-built schedule or a schedule that reflects progress through a particular point in time. This analysis method is typically utilized when reliable baseline and as-built schedule information exists.

Impact as Planned Analysis

The impact as-planned method of delay analysis is a technique which forecasts or predicts a delay's effect on a project's completion date. This delay analysis method involves the insertion or addition of activities representing delays or changes into the baseline schedule to determine the impact of those delay activities. Use of the impact as-planned schedule analysis method is generally restricted to the quantification of delays for contemporaneous requests for time extensions.

Collapsed as Built Analysis

The collapsed as-built delay analysis methodology is a retrospective technique that begins with the as-built schedule and then subtracts activities representing delays or changes to demonstrate the effect on the completion date of a project but for the delay or change. Generally, this method is applied in cases where reliable as-built schedule information exists, but baseline schedule and/or contemporaneous schedule updates either do not exist or are flawed to the extent that they are not reliable to support a delay analysis.

Productivity Method

The productivity method compares the productivity achieved in an activity against normal productivity rates. The intent is to seek damages on the grounds that site productivity has been negatively affected by a delay. However, historically speaking, courts and boards have often arbitrarily reduced claims based on published impact standards because of the uncertainty as to their accuracy

QUESTIONNARE ANALYSIS

A questionnaire is a research instrument consisting of a series of questions and other prompts for the purpose of gathering information from respondents. Although they are often designed for statistical analysis of the responses, this is not always the case.

When developing a questionnaire, items or questions are generated that require the respondent to respond to a series of questions or statements. Participant responses are then converted into numerical form and statistically analysed. These items must reliably operationalize the key concepts detailed within specific research questions and must, in turn, be relevant and acceptable to the target group. There are a range of scales and response styles that may be used when developing a questionnaire.

Within researches Likert-type or frequency scales are most commonly used. These scales use fixed choice response formats and are designed to measure attitudes or opinions.

The questionnaire designed for use in the survey comprised demographic information about respondents and 39 delay causes which were grouped to six categories: owner related, consultant related, contractor related, labor and equipment related, external related. The respondents were requested to choose one degree of frequency for each delay cause which is completely disagree, disagree, neither agree nor disagree, agree, completely disagree. The questionnaire was distributed to firms mainly under Builders Association of India Cochin Centre. The size of the sample required from the targeted population i.e. respondents was determined statistically.

The sample size required for the Questionnaire survey is determined from Taro Yamane Sample size Formula given by

$$n=\frac{Z\alpha\times Z\alpha\times p\times(1-p)\times N}{Z\propto\times p\times(1-p)+N\times e\times e}$$

- n – sample Size
- p – proportion of favourable result in the population (0.5)
- e – Standard error(0.1)
- N – Population(150)
- Z_α -Critical Value of desired confidence level (95%-1.96)

Thus the sample size required for the survey is set at **60** Sample.

The respondents were asked to determine the frequency of occurrence of each cause as follows: Completely disagree = 1, Agree = 2, Neither agree nor disagree = 3, Agree= 4, Completely agree. Reliability test for Questionnaire is conducted with the pilot survey response. Cronbach's alpha is the most common measure of internal consistency or reliability. It is most commonly used when there are multiple Likert questions in a survey/questionnaire that form a scale and to determine the reliability of the scale. Cronbach's alpha will generally increase as the inter-correlations among test items increase, and is thus known as an internal consistency estimate of reliability of test scores. Generally, a questionnaire with $\alpha > 0.7$ is considered reliable.

The test is conducted with the help of SPSS software, the Cronbach's Alpha value – **0.909** is obtained which is well above 0.7. Thus the questionnaire is proved to be reliable. Figure 3.1 shows the output of reliability test performed in SPSS

Reliability

```
[DataSet1] E:\AEDWIN\MTECH\PROJECT RESULTS\chronbchs test.sav
```

Scale: ALL VARIABLES

Case Processing Summary

		N	%
Cases	Valid	20	100.0
	Excluded[a]	0	.0
	Total	20	100.0

a. Listwise deletion based on all variables in the procedure.

Reliability Statistics

Cronbach's Alpha	N of Items
.941	39

Fig 1:- Cronbach's alpha in SPSS

Table 1 Delay causes of construction projects.

OWNER RELATED	20. Inexperience
1.Slow decision making	21. Poor qualification of staff
2. Delay in delivering the site	22. In effective planning
3. Payment delay	23. Frequent change of subcontractor
4. Improper Planning and Scheduling	LABOUR & EQUIPMENT RELATED
5. Owner interference	24. Shortage of labours
6. Change in orders	25. Low productivity level OF labours
7. Suspension of work	26. In-experienced work force
8. Lack of communication	27. Delay in material delivery
9. Late decision making	28. Shortage of materials
10.Conflicts among partners	29. Shortage of equipment
CONSULTANT RELATED	30. Equipment break down
11.Inadequate experience	31. Low productivity & efficiency
12. Delay in approving drawings and samples	32. Poor operator skill
13. Inadequate detailing and clarity in drawings	33. Lack of communication
14. Quality assurance control	EXTERNAL FACTORS
15. Mistakes & discrepancies in design documents	34. Change in government regulations
CONTRACTOR RELATED	35. Poor soil conditions
16. Delay in payment	36. Delay in obtaining permits
17. Delays in sub- contractor work	37. Climatic factors

18. Poor site management and supervision	38. Accidents during construction
19. Rework due to errors	39. Delay in commissioning

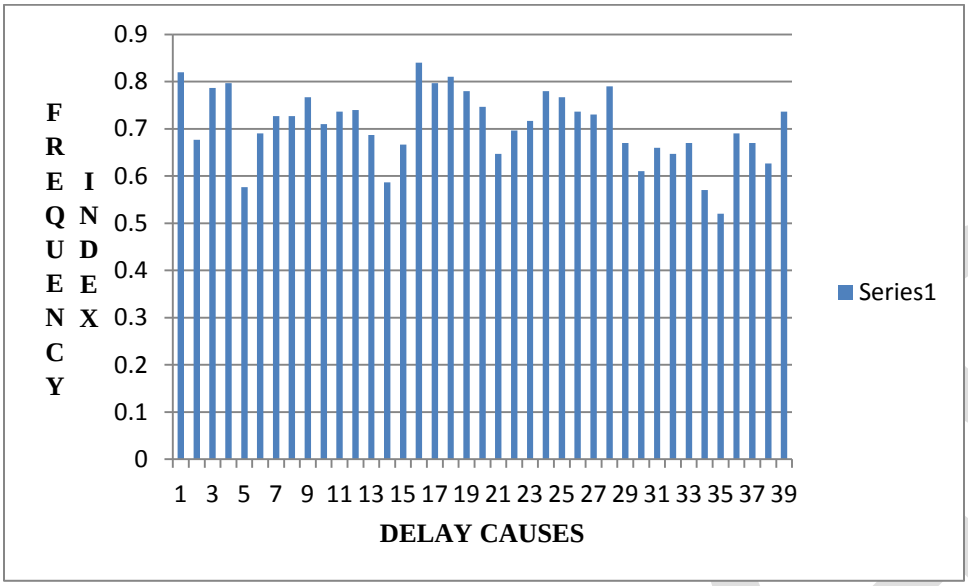

Fig 2:- Frequency Index of Delay Related Causes

Table 2: Top ten delay causes according to frequency index

Delay group	Delay causes
Contractor related	Delay in payment
Owner related	Slow decision making
Contractor related	Poor site management & supervision
Contractor related	Delays in subcontractor work
Labour & equipment related	Shortage of materials
Contractor related	Rework due to errors
Labour & equipment related	Low productivity level of labours
Owner related	Payment delay to contractors
Labour & equipment related	Delay in obtaining permits
External factors	Delay in commissioning

CASE STUDY

A contract was signed between the claimant (contractor) and the defendant (owner) to construct a commercial building including utilities and landscape in of 27000square feet plinth area at Ernakulam. The project was delayed for the following reasons:

- There was a six month delay from the authorities to obtain permits. Authorities are less aware of the rules and regulations of buildings and constructions, which created a huge role in the construction of the building.
- Strike of quarries in kerala affected the construction process a lot as it caused a delay in material supply tto the site.
- There was an accidental during concreting phase of one floor, as the formworks were not tightened properly it resulted in the collapse of formworks and further delayed the work for two weeks.

DISCUSSIONS

- Project parties should preview the site. Complete planning on how the works should be made before the start of project.
- Formal relationships among project parties should be identified, as well as roles and responsibilities.

CONCLUSION

This paper analysed causes of construction delays in Ernakulam (Cochin). The feedback of construction experts was obtained through interviews and questionnaire surveys. Frequency Index is calculated according to the highest values of them the top ten delay causes of construction projects in Ernakulam are determined.

REFERENCES:

[1]. David Arditi and Thanat Pattanakitchamroon, **"**Analysis Methods in Time-Based Claims", J.Constr.Eng.Manage, ASCE, Vol.134, April, 2008, 242-252.

[2]. Tarek Hegazi; and Wail Menesi, "Delay Analysis under Multiple Baseline Updates", J.Constr.Eng.Manage. ASCE, Vol.134, August, 2008, 575-582.

[3]. Mohamed M Marzouk, "Analysing delay causes in Egyptian construction projects", Journal of Advanced Research, Cairo University, May, 2014, 49-55

[4]. Michael J Cunningham, "Comparison of Delay Analysis Methodologies", J.Constr.Eng.Manage. ASCE, Vol.124, August,1998, 315-322.

[5]. Jonghyun Kim, " Construction schedule delay risk assessment by using combined AHP-RII methodology for an international NPP project" Nucl Eng Technol,47, 2015, 362-379

[6]. Janice Rattray, "Essential elements of questionnaire design and development" Journal of Clinical Nursing,Vol16, April 2005, 234-243

[7]. Nasrin Parsian," Developing and Validating a Questionnaire to Measure Spirituality: A Psychometric Process", Global Journal of Health Science, Vol 1,No 1, April 2009.

[8] Meera V, " Study on Time Delay Analysis for Construction Project Delay Analysis", IJERT, Vol 4, Issue 3, March 2015.

[9] Aditi Dinakar,"Analysis of Delays in Construction Projects", IJETAE , Vol 4, Issue 5, May 2014.

[10] C R Kothari, " Research Methodology, Methods & Techniques" Second Revised Edition.

[11] Robert F Devilis, " Scale Development Theory & Applications", Applied Social Research Methods Series, Vol 26.

[12] Henry Alinaitwe, Ruth Apolot and Dan Tindiwensi," Investigation into the Causes of Delays and Cost Overruns in Uganda's Public Sector Construction Projects", Journal of Construction in Developing Countries,Vol 18(2), Pages 33–47, 2013

International Journal of Engineering Research and General Science Volume 3, Issue 6, November-December, 2015
ISSN 2091-2730

Provision of Credential Based Security in broker-less publish/Subscribe System

Shital S. Biradar , Sushilkumar N. Holambe

pursuing ME at College of Engg,Osmanabad. Email- Sbiradar999@gmail.com. , contact no- 9422033718.

Abstract— Publish/Subscribe system is a system used for sharing data between the users of the system. Here we are considering content based Publish/Subscribe [9] System. In Content based Publish/Subscribe [9] System messages are routed according to the content of the message. This System can also be called as messaging System. This paper presents an approach to provide security in the publish/subscribe system by using the credentials of the user and it uses broker-less network for the dissemination of the message. Here we are providing identity based encryption [1] for the security purpose and message can be decrypted by only those subscribers who are having credentials with the message. In this system users are divided into two classes .The user can be Publisher of the system (who is providing information to the system in the form of messages or events) and second is subscriber (who is consuming information provided by the publisher according to their subscriptions). This paper presents mechanism for providing authentication, Confidentiality and Scalability.

Keywords— content based, security, publish/subscribe, identity based encryption, confidentiality, broker-less, peer-to-peer.

INTRODUCTION

In Publish/Subscribe system there is a loose coupling between two types of users that is publishers and subscribers. Therefore this system has been very popular and also these can be used with many distributed applications due to the loose coupling. In the existing system there is a use of broker architecture. In that message is passed or forwarded towards the subscribers by the publishers through the broker. It means every application is connected to the central broker and there is communication with the help of intermediate broker for each communication, therefore there is no authentication and confidentiality. To avoid such problems in a broker-less content based publish subscribe system [2]; we are using Pairing based cryptography mechanism.

Publisher publishes events/messages over the network, and subscriber subscribes interested messages. These published messages can be decrypted by subscribers who are having match between credentials of subscriptions and published messages or events.

To provide security hear we are supporting basic security mechanisms such as confidentiality and access control [11]. In case of confidentiality it requires that the content of message should not be disclosed to the routing infrastructure and subscribers should get messages off all interested subscriptions without disclosing its subscription to the system. In case of access control ,It require only authenticated publishers are allowed to publish the message in the network and only those published messages are provided only to the authorized subscribers.

Our traditional Public key Infrastructure (PKI) will not maintain loose coupling between publishers and subscribers so here we are using Identity based mechanism for encryption. In this system all subscribers maintain credentials for their relevant subscriptions and specific private key is provided to the subscribers by the key server depending on the credential. publisher also maintain credential with the encrypted messages and that private key can decrypt only that cipher text whenever there is a match between credential of the subscriptions and credential of the message event.

LITERATURE SURVEY

The Publisher/Subscriber communication technique has become very popular because of its natural loose coupling between publishers and subscribers related to the time, space and synchronization. Publisher disseminate information into the publish/subscribe system, and subscribers can receive that published information by making the interested subscriptions. Published information / messages / events are routed over the network and provided to the relevant subscriber. Publisher having no any knowledge about the group of subscribers who are subscribing their events or messages, and subscribers are also unknown about the publishers. This system is useful for large scale distributed applications such as stock exchange prize information, news feed, traffic control, environmental monitoring etc.

It is very important to provide security supports such as access control [11] and confidentiality. It is the requirement of every user of the Content based Publish/Subscribe system [9]. So there is a requirement to route the event /messages without knowing each

other (publishers and subscribers) for the security purpose. Existing mechanism for the secure publish/subscribe system [10] depend only on the traditional broker network. By using such traditional mechanism it is very difficult to achieve fine grained access control and scalability. This paper presents new approach to provide confidentiality and authentication in publish/subscribe system with broker-less infrastructure.

METHODOLOGY

In content based publish/subscribe system [9], for the routing of events from the publishers to the specific subscriber we are considering event space. It is denoted by Ω and consist of ordered set of n attributes(Ai): Ω={A1,A2,A3,……..,An}. Every attribute is having unique name, its data type and its domain. Data type can be any one of the following types: integer, floating point and character strings. The domain is nothing but the range of attribute values bounded by two values that is lower and upper value.

A subscription function f is nothing but the equation that contains predicates combined with and operator that is,

f = {p1^p2^…..^pj}

p1,p2,….,pj – are the predicates.

Predicate is nothing but the combination of the three items that is attribute A, operator (op) and value. Predicate pi can be denoted as (Ai, opi, vi). Operators consist of equality and range operations for the numeric attributes and prefix or suffix for the string attributes. Events include attributes and its related values. The event is said to be matched with the subscription f is nothing but the value of attribute in the event satisfy the constraints provided by subscriptions.

Here we are using attribute base d encryption [3] [5], so for our implementation we require that at first we have to create credentials as this can be done in following way.

1. Numeric attributes-

   Here we are considering event space as a data, and each time this space is divided into two halves. These two halves are indicated as 0 and 1. Then first half part is again divided into two halves and it is denoted as 00 and 01. Second half part after division is denoted as 10 and 11. For example consider two attributes in terms of space means it is two dimensional space and its division is as follows.

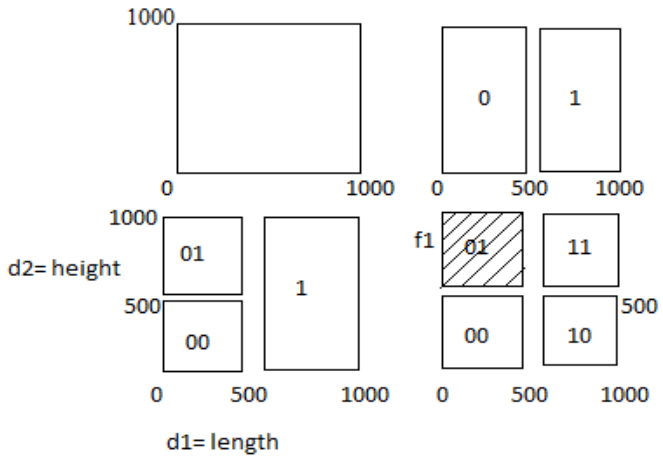

Fig1. Numeric attributes

Function f1={ length = [0,500], height = [500,1000] }

2. String attributes-

   In this technique we are creating credentials for string operation such as prefix matching can be generated using a trie. Trie is like a tree in which each node is labeled with a string. Each node is considered as a prefix string that is common to all its descendants. For example operation prefix matching tree is generated as,

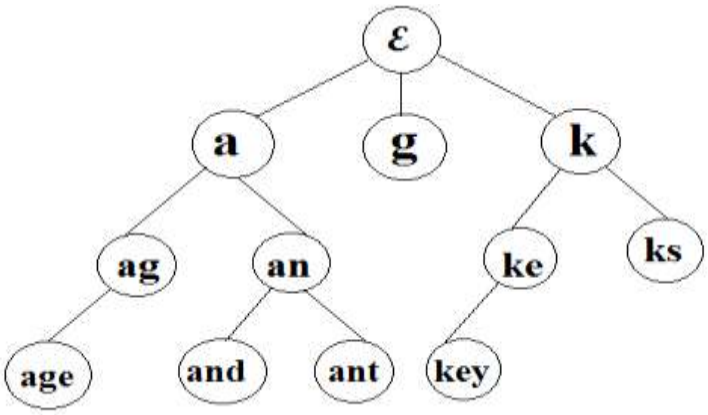

Fig2 . Prefix matching

3. Range attributes-
In case of this attribute, separate credentials are provided to a subscriber along with the keys for each attribute. In the network specific range is described. Data or event is sent in the specific range of the subscribers.

Here with the help of Identity based encryption [1] over the broker-less infrastructure, we are going to provide scalability, authentication and confidentiality.
These security issues can be implemented by creating four modules in our project, these are as follows.

I. Content Based Publish/Subscribe module-
Publishers and subscribers participate as peers in the overlay structure for the maintenance. For the routing of the events from publisher to the specific subscriber we are using content based publish/subscribe system [9]. In this system event is routed according to the content of event. The publisher must be authenticated and this is done by the use of advertisements in which publisher announces set of the events which he wants to publish.

II. Identity based Encryption module-
In this project we are using Identity based encryption [1] and it is implemented in this module. Publisher and Subscriber communicate with the key server. They provide credentials to the key server and then receive keys according to their credentials.
Credential is nothing but it is having two parts.
I) Capability of peer

II) Proof of its identity.

Event is encrypted with identity of the receiver. Identity [7] is nothing but the public key and there is no need to transfer the public keys. Private keys are used to decrypt the encrypted event and it is done only if the credentials of the event and the key are same. That is the credential becomes authorized by the key server. Here cipher text is also labeled with credentials. For each authorized credential private keys are maintained by the publishers and subscribers. Here we are using searchable encryption [8] for the routing of the event since our system is content based publish/subscribe system.

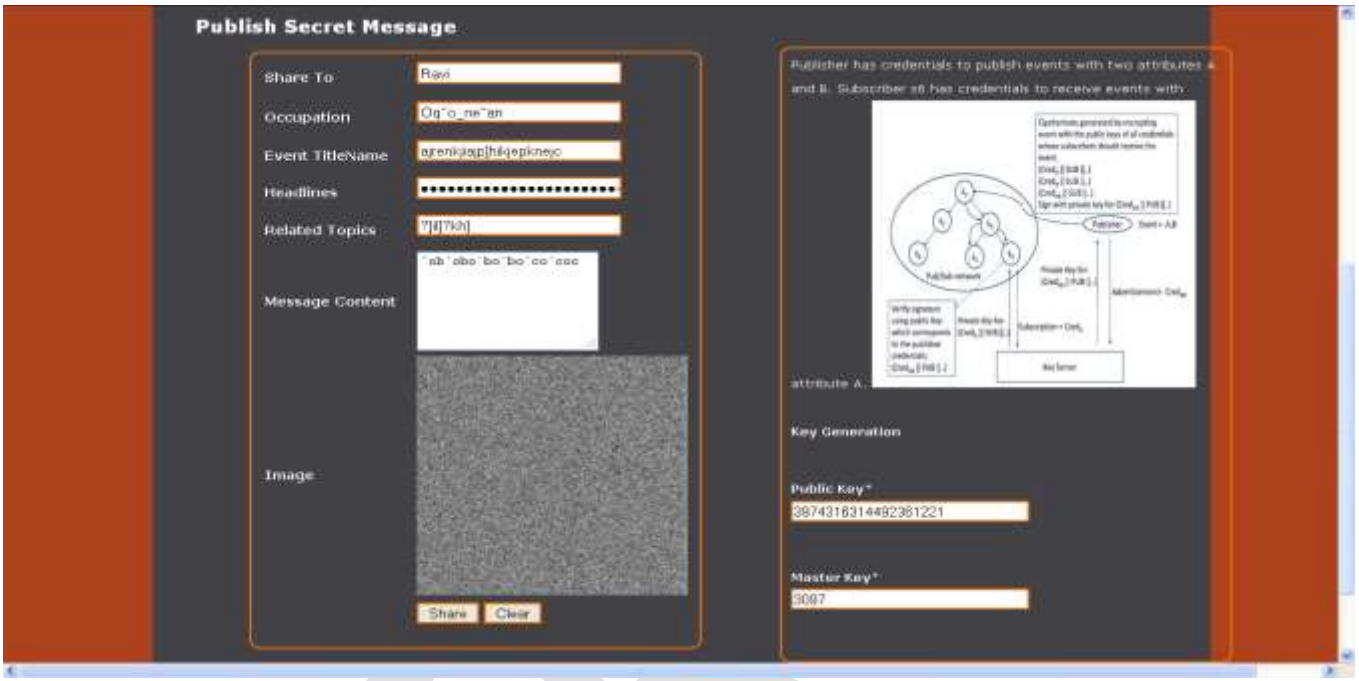

III. Key generation for publisher/Subscriber module-

Publisher keys:

Before publishing events over the content based publish/subscribe system, a publisher has to communicate with key server. Publisher passes credentials for each attribute in its events of advertisement to the key server.

If publisher is authenticated then he can publish events according to the credentials, and that events are encrypted by using the private keys generated by the key server [4]. Key server generates separate private key for each credential. Public key for a publisher for credi,j is generated as,

$Pui,j := (Credi,j \| Ai \| PUB)$

PUB is nothing but the identity of publisher. Credi,j is notation of credential j of attribute Ai.

Subscriber keys:

In the same manner, before receiving the event , subscriber communicate with the key server and only those private keys are received by them which are having matching credentials with the subscriptions of the subscribers. Credentials are associated with each attribute A. in case of subscriber Public key is given as,

$Pui,j := (Credi,j \| Ai \| SUB)$

SUB is nothing but the identity of subscriber.

In our implementation private keys for publishers and subscribers are generated by using advanced encryption standards (AES) [12]. It is described in following sections.

IV. Secure overlay maintenance module-

In this module we are implementing secure overlay maintenance protocol is used for maintaining tree of subscribers. In this tree subscribers are connected to each other according to their containment relationship. It means that subscriber is connected to subscriber having coarser credentials. In other words subscriber generates cipher text by using private keys and cipher text is attached with the connection request(CR) and that request is passed to the random node in the tree, that node is nothing but subscriber(peer). A connection is allowed only if the peer can decrypt any of the cipher text using its private keys.

Algorithm for secure overlay maintenance protocol-

1. on receiving connection request of new subscriber (Sn) from any subscriber (Sp)do
2. If(credential of Sn == credential of Sp)
3. Event is decrypted.
4. If decrypt (CR) is successful
5. If degree is available
6. Then establish a connection
7. Else CR is forwarded to other node excepting Sp.
8. If decryption is failed then
9. If Sp is parent then
10. Sn receives CR from Sp
11. Else
12. Move CR towards parent
13. If any node is not suitable for establishing connection with Sn.
14. Then there is no containment relationship.

METHODS FOR EVENT DISSEMINATION

Here we are describing two methods for event dissemination.

i) One-hop flooding-
In this method parent forward each successfully decrypted event to all child assuming that they have same credentials. All children also forward each successfully decrypted event to their children and so on. In this method child may receive false positives because child may have finer credentials than its parent.

ii) Multicredential routing-

In this method there are no false positives. It is done by restricting parents to forward events to all nodes on each attribute tree. Events are forwarded only to the child who is having matching credentials with the parent.

ADVANCED ENCRYPTION STANDARDS

In this project, we are using AES algorithm [12] [4] for the key generation. It is a block cipher intended to replace DES. It uses 128-bit block size and a key size of 128,192 or 256 bits. AES structure consists of full round having 4 functions: byte substitution, permutation, arithmetic operations over a finite field and Xor with a key. Depending on number of rounds length of the key is determined as follows.

No. of rounds	Key length (bytes)
10	16
12	24
14	32

It is a symmetric key encryption standard.

RESULTS AND DISSCUSION

In this project, we are considering security of the publish/subscribe system. As we are using Identity based encryption [1], so this content based publish/subscribe system became very powerful because every publisher and subscriber is authenticated. Before publishing events publisher have to login into the system using its own id and password. Only that publisher can login into the system who is already registered, so illegal publisher cannot publish vulnerable events over the network.

To subscribe event, subscriber also have to login into the system and then they can get the message or event, if it is allowed by the publisher. If subscriber is eligible for accessing the message, then key is provided for the decryption of the message because message is in encrypted form. Message can be translated into the plaintext if that key is correct. The correct key is provided only if subscriber is authorized. Therefore as compared to simple content based publish/subscribe system this project implements secure content based publish subscribe [9] system. Here with the encryption message is routed [6] properly because we are using searchable encryption [8]. In this project some delay occurs due to the tasks like encryption, decryption and for the connection of new subscriber at proper position in the attribute tree. The delay is normally 150 to 200 milliseconds as compared to the system that is not having security mechanism. So our performance is also better and it is with the security, it doesn't take very long time to do security related tasks. So this project is very useful for the secure event dissemination over the network. System is also having scalability that is any number of subscribers and publishers can use the system.

CONCLUSION

This paper gives a new approach to provide security in content based publish/subscribe system. Our system became secure as we are using identity based encryption to provide security and also using advanced encryption standards (AES) algorithm [12] for the key generation. Event can be decrypted by the subscriber only if there is a match of credential.

REFERENCES:

[1] D. Boneh and M.K. Franklin, "*Identity-Based Encryption from theWeil Pairing*," Proc. Int'l Cryptology Conf. Advances in Cryptology, 2011.

[2] Muhammad Adnan Tariq, Boris Koldehofe, and Kurt Rothermel" *Securing Broker-Less Publish/Subscribe Systems Using Identity-Based Encryption*" IEEE transactions on parallel and distributed systems, vol. 25, no. 2, February 2014.

[3] V. Goyal, O. Pandey, A. Sahai, and B. Waters, "*Attribute-Based Encryption for Fine-Grained Access Control of Encrypted Data*,"Proc. ACM 13th Conf. Computer and Comm. Security (CCS), 2010.

[4] Sean O, Mealia and Adam J.Elbirt "*Enhancing the Performance of Symmetric –key cryptography via Instruction set instruction*" IEEE transactions on very large scale integeration vol.18 no.11 November 2011.

[5] Ming li,Shucheng Yu.Yao Zheng,Kui Reng, Weiging Lou "*Scalable and secure sharing of personal data in cloud computing using attribute-based encryption*"IEEE transaction on parallel and distributed computing 2013.

[6] Legathaux Martins and Sergio Duarte "*Routing Algorithms for Content based publish/subscribe system*"IEEE commm-unications and tutorials first quarter 2010.

[7] Karl aberer, Aniwitaman datta and Manfred Hauswirth "*Efficient Self Contained Handling of Identity in Peer to Peer System*"IEEE transaction on know- ledge and data engineering, 2004.

[8] D. Boneh, G.D. Crescenzo, R. Ostrovsky, and G. Persiano, "Public Key Encryption with Keyword Search," Proc. Int'l Conf. Theory and Applications of Cryptographic Techniques on Advances in Cryptology (EUROCRYPT), 2004.

[9] A. Shikfa, M. O ¨ nen, and R. Molva, "Privacy-Preserving Content- Based Publish/Subscribe Networks," Proc. Emerging Challenges for Security, Privacy and Trust, 2009.

[10] M. Srivatsa, L. Liu, and A. Iyengar, "EventGuard: A System Architecture for Securing Publish-Subscribe Networks," ACM Trans. Computer Systems, vol. 29, article 10, 2011.

[11] J. Bacon, D.M. Eyers, J. Singh, and P.R. Pietzuch, "Access Control in Publish/Subscribe Systems," Proc. Second ACM Int'lConf.Distributed Event-Based Systems (DEBS), 2008.

[12] F.P. Miller, A.F. Vandome, and J. McBrewster, Advanced Encryption Standard. Alpha Press, 2009.

International Journal of Engineering Research and General Science Volume 3, Issue 6, November-December, 2015
ISSN 2091-2730

Effective Bug Triage and Recommendation System

Manisha Bedmutha [1], Megha Sawant [2], Sushmitha Ghan[3]
Department of Computer Engineering,
P.E.S. Modern College of Engineering,
Pune University (MH), India.
[1]m.bedmutha13@gmail.com
[2]meghasawant93@gmail.com
[3]sushghan11@gmail.com

Abstract— Dealing with the bugs is an important thing in software industry. For fixing these bugs lots of time is required and each developer have to go through bug report which aims at wasting the time and ultimately the money. To solve this problem an important step which we can take is bug triage, which aims as correctly assign a developers to new bug. As well as to decrease time cost in manual work of developer text classification technique is applied to conduct the automatic bug triage. Ultimatum is to reduce scale and improve the quality of bug data. After donning with triage process, we are recommending bugs to the respective developers depending on their profile and previous work history which will help the system to predict which bug to assign to which developer. If any particular developer failed to fix the bug in the given time the triage method will be used to predict the new developer.

Keywords— Mining Software Repositories, Data Management in bug Repositories, Bug Data Reduction, Feature Selection, Instance Selection, Bug Triage, Bug Report ,Prediction for assigning bugs , Frequent item selection, Recommendation of bugs.

1. INTRODUCTION

Bugs are the programming errors that cause significant performance degradation. Bugs lead to poor user experience and low system throughput. Large open source software development projects such as Mozilla and Eclipse receive many bug reports. They usually use a bug tracking system where users can report their problems which occurred in their respective projects. Each incoming bug report needs to be triaged. For example, as of October 2012, the Mozilla project had received over 80,000 reports, averaging 300 new bug reports each day [2].

In appropriate developers may delay the bug resolution time as In manual bug triage in Eclipse, 44 percent of bugs are assigned by mistake while the time cost between opening one bug and its first triaging is 19.3 days on average [1], [16].

Selecting the most appropriate developer to fix a new bug report is one of the most important stages in the bug triaging process and it has a significant effect in decreasing the time taken for the bug fixing process [16] and the cost of the projects [2], [11]. Software companies spend over 45 percent of cost in fixing bugs [1], [8], and [17]. In traditional bug triage systems, a developer who is dominant in all parts of the project as well as the activities plays the role of bug triager in the project. The triager reads a new bug report, makes a decision about the bug, and then selects the most appropriate developer who can resolve the bug. Fixing bug reports through the traditional bug triage system is very time consuming and also imposes additional cost on the project [2].

One of the important reasons why bug triaging is such a lengthy process is the difficulty in selection of the most competent developer for the bug kind. The bug triager, the person who assigns the bug to a developer, must be aware of the activities (or interest areas) of all the developers in the project. Bug triaging normally takes 8 weeks to resolve a bug if the developer, to whom the bug report is assigned, could not resolve it, it is assigned to another developer. This would consume both time and money. Thus, it is really important on part of bug triager to assign the bug report to a developer who could successfully fix the bug without need of any tossing. Hence, the job of bug triager is really crucial [2].

In this paper, we present an approach for automatically recommending the bugs to the respective developers. The goal is to reduce the bug report and analyze it using bug instance selection and Feature Selection. To use the term frequency mining technique to predict the most suitable developer for new bug report depending upon the information available from historical bug reports and the profile of the developer. The term extracted from previously fixed bug reports and area in which developer is expertise are used for updation of profiles of developers. The frequency of each term corresponding to each topic indicates the expertise factor of each developer relating that particular topic. If the frequency of solving a bug based on particular topic is more, then system should

recommend the bugs related to that topic first to the developer.

2. RELATED WORK

Xuan et al. [1] combined feature selection with instance selection to reduce the scale of bug data sets as well as improve the data quality. To determine the order of applying instance selection and feature selection for a new bug data set, they have extracted attributes of each bug data set and train a predictive model based on historical data sets. They empirically investigate the data reduction for bug triage in bug repositories of two large open source projects, namely Eclipse and Mozilla.

Matter et al. [3] proposed an information retrieval based technique that computes the expertise of developers based on vocabulary used in source code. They extracted the vocabulary of developers from the version control repository of the project. Their approach finds a relationship between the vocabulary extracted from new bug reports and the vocabulary extracted from source code and then uses the relationship between them for recommendation purpose.

Hu el al. [4] they have proposed Bug Fixer, an automated bug report assignment method that utilizes historical bug fix data. Bug Fixer adopts a new method for computing bug report similarity. Bug Fixer also constructs a novel network structure, called Developer-Component-Bug (DCB), to model the relationship between the developers and the source code components they worked on, as well as the relationship between the components and the associated bugs. For a new bug, Bug Fixer calculates its similarity to existing bugs, and recommends developers based on the structure of DCB network.

Hosseini et al. [10] proposed an auction based bug allocation mechanism. When a new bug report comes, the bug triager extracts some basic information such as type, severity, etc. and then auctions off the bug. The developers place their bids on the bugs. The bug triager receives the bids and based on the developer's experience, expertise, historical preferences and current work queue, he announces the final decision and assigns the bug report to the winner developer.

Park el al. [14] they proposed a new bug triaging technique, COSTRIAGE, by (1) treating the bug triage problem as a recommendation problem optimizing both accuracy and cost and (2) adopting CBCF combining two recommender systems. A key challenge to both techniques is the extreme sparseness of the past bug fix data. They addressed the challenge by using a topic model to reduce the sparseness and enhanced the quality of CBCF.

Bhattacharya et al. [15] employed a fine grained incremental learning approach. They constructed multi feature tossing graphs and used it for predicting the relevant developers for the bug report. Their results showed high prediction accuracy for recommending developers and high reduction in tossing path lengths.

3. PROPOSED ARCHITECTURE

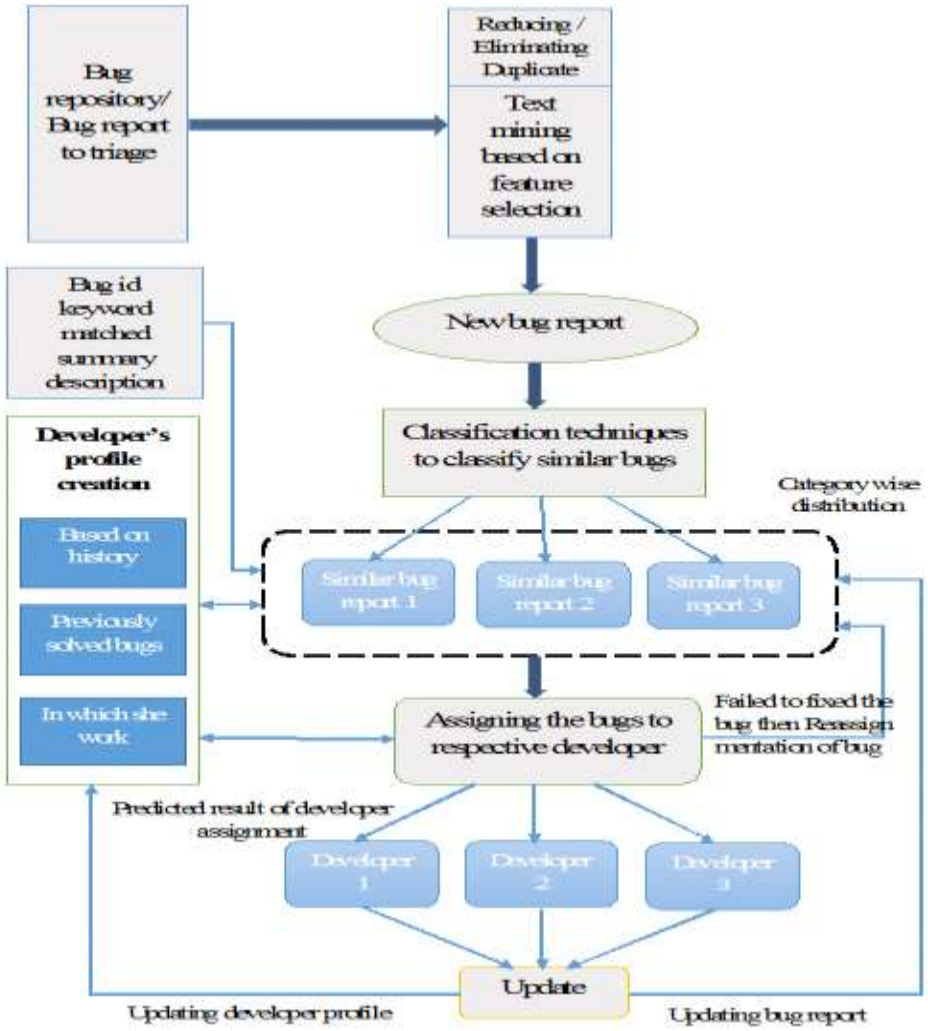

Figure 3.1: Architecture diagram of proposed system

3.1 Bug Triage

Bug Triage refers to assuring quality of bug reports. Bugs are inevitable in software development. The situation arise when we have certain number of bugs to be fixed and don't know their priority so, some standards are used in company that when certain number of bugs reached and not fixed then there should be meeting held and decided on the priorities of the bugs, so all the team members will gather and decided about each and every bug and finalize the priorities.

In daily testing and maintenance, bug reports are accumulated and stored in projects' bug tracking system. In our proposed system bug tracking system provides a platform for tracking the status of bug reports. Once a bug report is created, through the bug tracking system, developers can also collaborate on reproducing and fixing bugs. A bug report should be assigned to an appropriate developer before the process of bug fixing. The step of assigning bug reports to developers is called bug triage.

3.2 Bug Reduction

Here we are reducing the bug data by using instance selection and feature selection which will give low scale data and the qualitative data. Instance selection associated with data mining tasks such as classification and clustering. Feature selection is to choose a subset of input variables by eliminating features with little or no predictive information.

3.3 Profile Updation

The reduced bug report will be automatically assigned to the developer based on his previous work history and experience. After the bugs get solved by the developer the developer's profile will get update.

3.4 Bug Recommendation

If the frequency of solving a bug based on particular topic is more, then system will recommend the bugs related to that topic first to the developer.

3.5 Reassignment of bugs

If a particular developer failed to solve the bug in the given time then that bug will be reassign to the other developer.

4. CONCLUSION

In this paper we have focused on reading the bug report which will remove the redundant and noisy data. The system will automatically recommend the bugs to the developer which will save the time and cost in finding the bugs for fixing. As the system is time based if particular developer failed to solve the bug in given time the bug will be reassign to the other developer, so ultimately the project will get complete prior to the dead line. Also it will be easy to find out which developer is expertise in which area.

REFERENCES:

[1] Jifeng Xuan, He Jiang, Yan Hu, Zhilei Ren, Weiqin Zou, Zhongxuan Luo, and Xindong Wu, "Towards Effective Bug Triage with Software Data Reduction Techniques," IEEE Transactions, Volume 27, NO. 1, JANUARY 2015.

[2] Anjali, Sandeep Kumar Singh, "Bug Triaging: Profile Oriented Developer Recommendation", International Journal of Innovative Research in Advanced Engineering (IJIRAE) ISSN: 2349-2163, Volume 2, Issue 1, January 2015.

[3] D. Matter, A. Kuhn, and O. Nierstrasz, "Assigning bug reports using a vocabulary- based expertise model of developers," in Mining Software Repositories, 2009. MSR '09. 6th IEEE International Working Conference on, May2009, pp. 131 –140.

[4] Hao Hu, Hongyu Zhang, Jifeng Xuan, Weigang Sun, "Bug Triage based on Historical Bug-Fix Information". ISSRE - The 25th IEEE International Symposium on Software Reliability Engineering, 2014, Naples, Italy, Nov 2014.

[5] C. Sun, D. Lo, S. C. Khoo, and J. Jiang, "Towards more accurate retrieval of duplicate bug reports," in Proc. 26th IEEE/ACM Int. Conf. Automated Softw. Eng., pp. 253–262, 2011.

[6] ZHANG Jie, WANG XiaoYin , HAO Dan1, XIE Bing, ZHANG Lu and MEI Hong, "A survey on bug-report analysis", Science China, Information Sciences, Vol. 58 021101:2, February 2015.

[7] Henrique Rocha, Guilherme de Oliveira, Humberto Marques-Neto, and Marco Tulio Valente, "NextBug: a Bugzilla extension for recommending similar bugs", Rocha et al. Journal of Software Engineering Research and Development , 2015.

[8] Pankaj Gakare, Yogita Dhole,Sara Anjum, "Bug Triage with Bug Data Reduction", International Research Journal of Engineering and Technology (IRJET) e-ISSN: 2395 -0056,Volume 02 Issue 04, July 2015.

[9] Mamdouh Alenezi, Kenneth Magel, and Shadi Banitaan, "Efficient Bug Triaging Using Text Mining", ACADEMY PUBLISHER, 2013.

[10] H. Hadi, N. Raymond , and G. Michael, " A market based bug allocation mechanism using predictive bug lifetimes", in 16th European Conference on Software maintenance and Reengineering, pp. 149-15, 2012.

[11] J. Anvik and G. C. Murphy, "Reducing the effort of bug report triage: Recommenders for development-oriented decisions," ACM Trans. Softw. Eng. Methodol., vol. 20, no. 3, pp. 10:1–10:35, Aug. 2011.

[12] Philip J. Guo, Thomas Zimmermann, Nachiappan Nagappan, and Brendan Murphy, " "Not My Bug!" and Other Reasons for Software Bug Report Reassignments", ACM, 2011.

[13] J. Anvik and G. C. Murphy, "Reducing the effort of bug report triage: Recommenders for development-oriented decisions," ACM Trans. Soft. Eng. Methodology., vol. 20, no. 3, article 10, Aug. 2011.

[14] Jin-woo Park, Mu-Woong Lee, Jinhan Kim, Seung-won, and Hwang Sunghun Kim, "COSTRIAGE: A Cost-Aware Triage Algorithm for Bug Reporting Systems", in Twenty-Fifth AAAI Conference Artificial Intelligence, year 2011.

[15] Bhattacharya P, Neamtiu I., "Fine-grained incremental learning and multi-feature tossing graphs to improve bug triaging", In: Proceedings of the IEEE International Conference on Software Maintenance, Timisoara, 2010.

[16] G. Jeong S. Kim, and T. Zimmermann, "Improving bug triage with bug tossing graphs", in Proceedings of Seventh joint meeting of European Software Engineering Conference & ACM SIGSOFT symposium on Foundations of software engineering, ser. ESEC/FSE '09. New York, NY, USA: ACM, pp. 111–120, 2009.

[17] R. S. Pressman, "Software Engineering: A Practitioner's Approach", 7th ed. New York, NY, USA: McGraw-Hill, 2010.

International Journal of Engineering Research and General Science Volume 3, Issue 6, November-December, 2015
ISSN 2091-2730

A STUDY ON CONSTRUCTION SAFETY ISSUES AND DEVELOPMENT OF A GENERAL SOLUTION FRAMEWORK

Nikhil Roy[1], Jeevan Jacob[2]

[1]PG Student, Structural Engineering and Construction Management, M A College Of Engineering
[2]Assistant Professor, Civil Engineering Department, M A College Of Engineering
[1]nikhil05101991@gmail.com
[2]jeevanjacob@mace.ac.in

Abstract: - Safety in an inevitable factor to be considered in construction industry. Absence of safety measures can cause accidents in construction sites leading to injuries or even fatality. On the other hand, modern technologies have the potential to improve construction safety. In this context, the Objective of this study is to identify the construction safety issues and develop technical solutions for that. For the purpose, (1) extensive literatures survey was conducted to get insight into the problem and (2) questionnaire survey in construction sites was conducted to establish the major safety issues. Based on these studies solution concepts based on radio frequency identification (RFID) was proposed. Personal Protection Unit (PPU) checking system and a proximity alert system were developed using RFID and tested. Also a Building Information Modeling (BIM) based fall protection plan and a proactive safety plan to be submitted to authorities was developed.

Keywords:- Safety, Personal Protection Unit(PPU), Proximity Alert System, Fall Protection Plan, Questionnaire, Proactive safety plan, General Solution Framework

1. INTRODUCTION

Safety can be defined as the absence of danger at sites or eliminating the situations which will be fatal. Thousands of construction workers are injured or killed in construction accidents each year. Construction companies provide safety equipments and training, but unfortunately accidents still happen. When a construction site accident occurs, the owners, architects, designers and manufacturers of equipment are held responsible for inadequate safety provisions. Use of modern technologies may be used in construction sites. Construction companies are slow in adapting automated technologies that have proven to work in other industries. Radio Frequency identification is a technology which can revolutionize safety prevention. Once tested successfully in the construction environment, these emerging technologies could be adapted.

Building Information Modelling (BIM) is gaining importance in the construction industry. If we have information we can model it. These technologies are handy in the planning stages. Fall protection plans can be developed using BIM. This will give an idea to the safety officer in advance where to provide the necessary fall prevention measures like hand rails, nets etc.

2. OBJECTIVE SCOPE AND METHODOLOGY

Objective

The objective of this project is to study construction safety issues and to develop a general solution framework.

- To identify the safety issues by conducting a questionnaire survey.
- To develop technical solutions and safety plans.

Scope

The scope of the project is limited to

i. Development of technical solutions for
   a. Fall related accidents,

b. Accidents related to moving equipment's,
c. Accidents due to careless behaviour of workers

ii. Development of a proactive safety plan

Methodology

The initial phase of the project consists of a questionnaire survey. This is to analyse the conditions in the site and find out the safety issues. Questionnaires are given to various reputed firms in Ernakulam .Information obtained from questionnaire was analysed to identify the safety issues.

Technical solutions include development of a Personal Protective Equipment checking system, a proximity Alert System and fall protection plans. Personal Protective Equipment checking system and proximity Alert System based of RFID were developed in Matlab environment.

A 3D Model based fall protection plan was developed. 3D model of a building was prepared in Revit. The fall prone zones were identified in the 3D model and safety rails were provided.

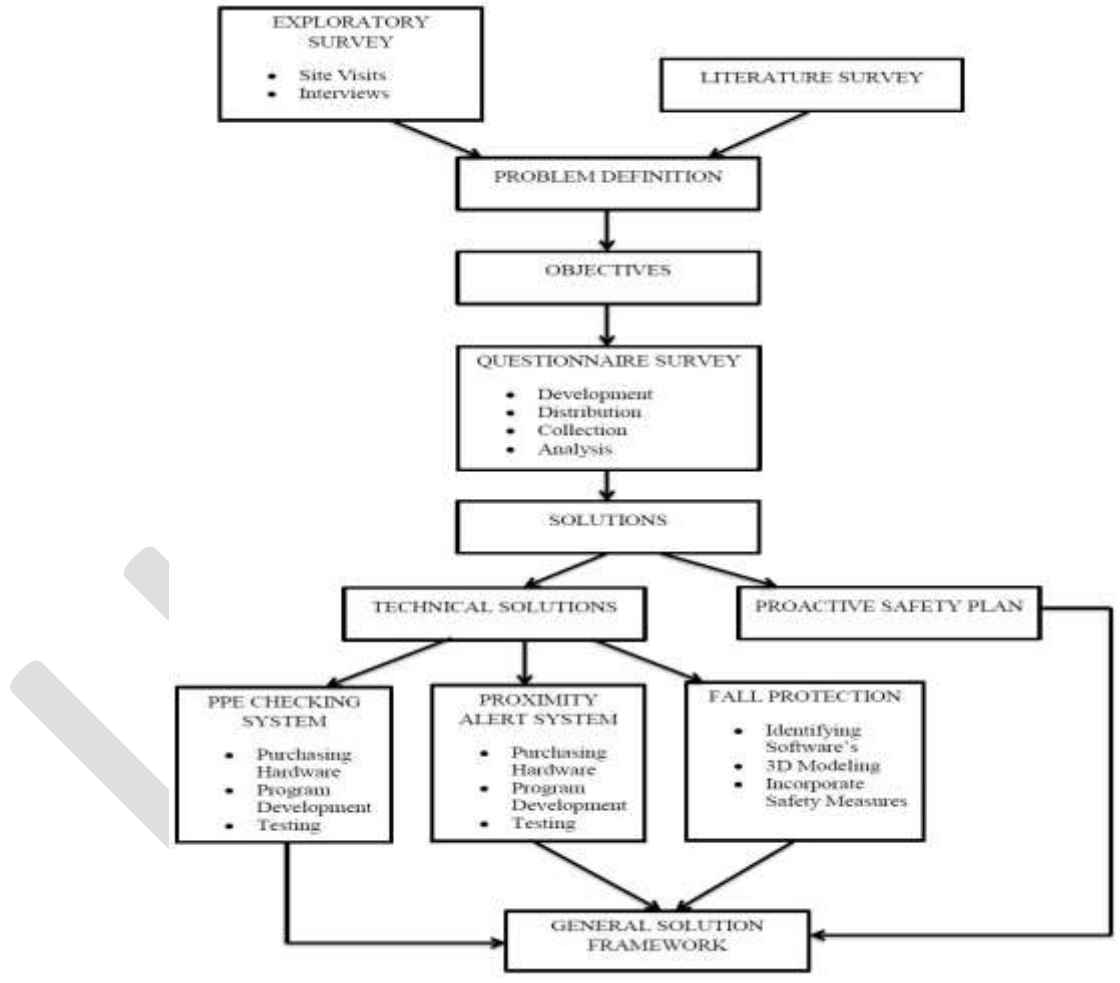

Fig 1:Methodology

3. QUESTIONNAIRE ANALYSIS

To understand the various safety issues in construction sites and to find remedies a questionnaire survey was conducted. Questionnaires were distributed to various design, contracting and other firms. The collected questionnaires were analysed to get an idea about safety issues and the possible remedies in the opinion of experts. Questionnaire consisted of 2 parts. 'A' part containing multiple choice questions (10 questions A1 A2…A10). 'B' part consists of scale based questions (12 questions B1, B2…B12). The number of respondents was 35.

Some of the conclusions from multiple choice questions of questionnaires are as follows:

- Accidents on construction sites are due to Lack of safety knowledge as shown in Fig 2.
- The major reasons of accidents on sites are that the workers are short of Safety training as shown in Fig 3.
- The most common type of accident in construction sites are fall related accidents as shown in Fig 4

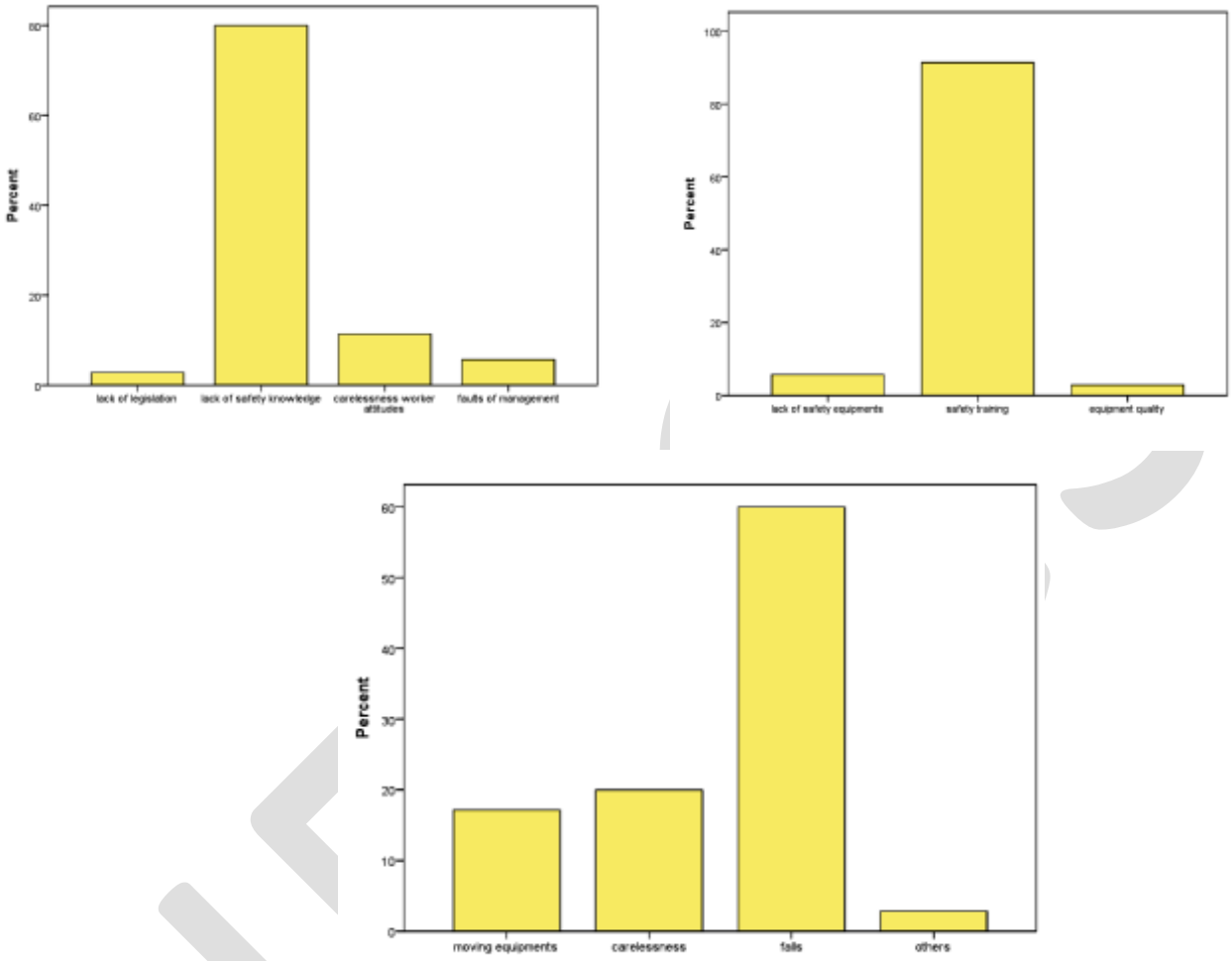

Fig 4: Major types of accidents in sites

The bar charts give the percentage distribution of votes for different questions.

When developing a questionnaire, items or questions are generated that require the respondent to respond to a series of questions or statements. Participant responses are then converted into numerical form and statistically analyzed. Likert scale was used for the analysis. The frequency index (FI) was calculated (Table 1).

FI= Sum of weights x 100

(Highest Weight x Number of Questionnaires)

The conclusions obtained from the scale based questions are as follows:

- Accidents in sites are due to lack of safety knowledge.
- Engineers must have knowledge of current safety regulations, rules, and standards and update this knowledge.
- Construction professionals should form an alliance to share experience and set code practice to promote and assure safety in sites.
- The government should set up a construction safety council with members from constructional professionals to study strategy and establish common safety working practices in the construction industry.

Table 1: Frequency Index

Scale	Strongly Agree	Agree	Disagree	Strongly Disagree	Don't Know	Total	Frequency Index	Rank
	1	2	3	4	5			
Weight	5	4	3	2	1			
B1	18	16	1	-	-	157	89.7	5
B2	7	27	1	-	-	146	83.4	8
B3	30	5	-	-	-	170	97.1	1
B4	1	27	5	-	2	130	74.2	12
B5	9	14	9	2	1	133	76.0	11
B6	27	8	-	-	-	167	95.4	2
B7	16	18	1	-	-	155	88.6	6
B8	15	18	2	-	-	153	87.4	7
B9	26	9	-	-	-	166	94.5	3
B10	7	20	8	-	-	139	79.4	10
B11	18	17	-	-	-	158	90.3	4
B12	9	18	8	-	-	141	80.6	9

4. TECHNICAL SOLUTIONS

The construction process is associated with accidents. Sometimes this may be fatal. Measures should be taken to guarantee a safe working environment for the workers. Modern technologies may be useful in ensuring safety. Technical solutions were developed for the following safety issues

- Fall Related
- Equipment Related and
- Carelessness of workers

Personal Protective Equipment checking system

In order to ensure that the workers use all personal protective equipment's (PPE) a program was developed. It is based on radio frequency identification. RFID cards are attached to all the PPE's. The workers are asked to move through an RFID gate. It is provided with RFID antennas. As they pass the gate the details of the RFID cards attached to their PPE's will be retrieved by the antennas. The PPE details of employees are stored in a database. The program compares the card details provided by antenna with the workers PPE details in the database. If the workers carries all the PPE required for his safety he will be allowed to work else alert will be given.

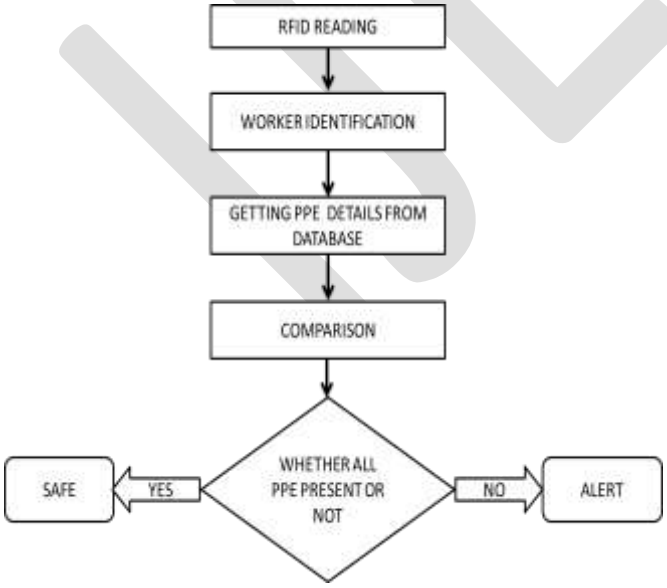

Fig 5: PPE checking system

Fig 6: Prototype-RFID Reader and Cards

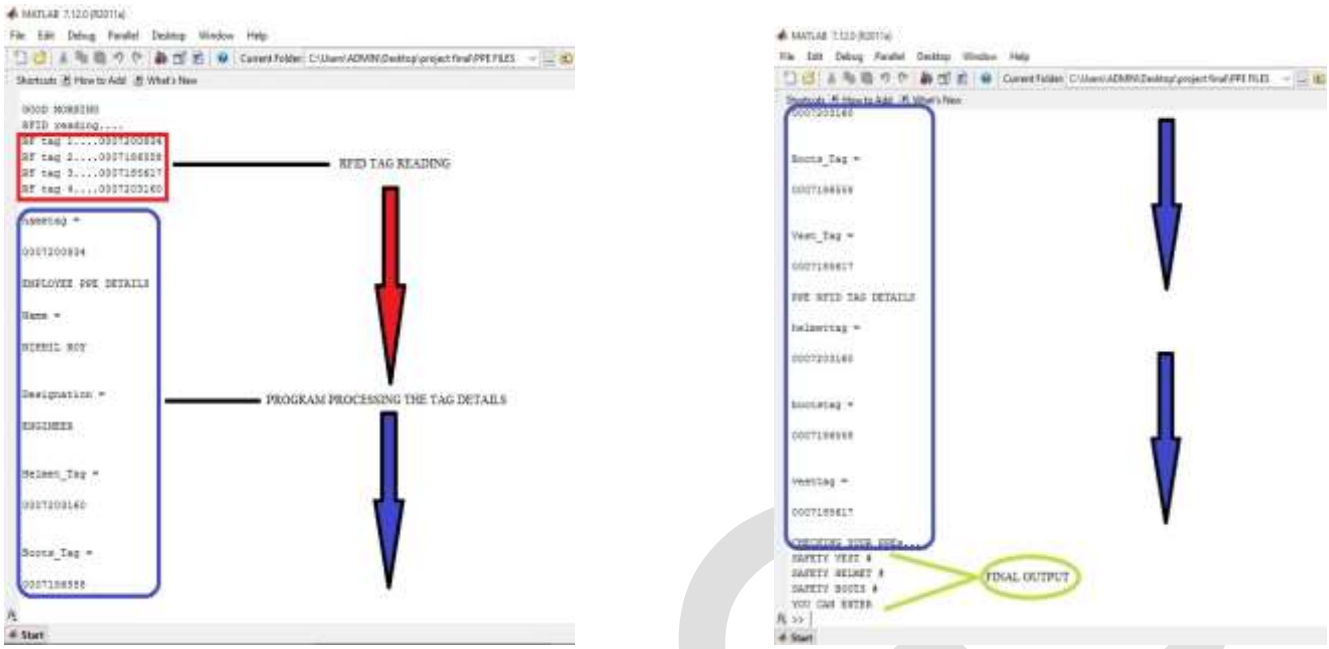

Fig 7:Working of PPE checking system

Proximity Alert System

To prevent equipment related safety issues like run over by trucks, a proximity alert system was developed. This is also based on RFID. A single or a group of Radio frequency antennas are provided on the equipment. The works and others vehicles carry RFID tags. The antennas continuously scan for RF tags in its range. Once the antennas detect a tag alert will be given.

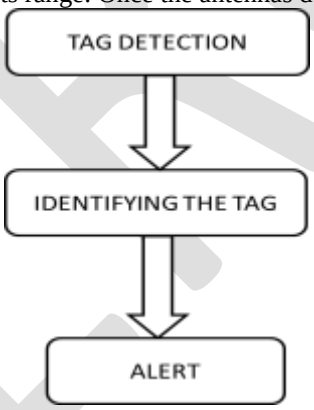

Fig 8:Proximity Alert System

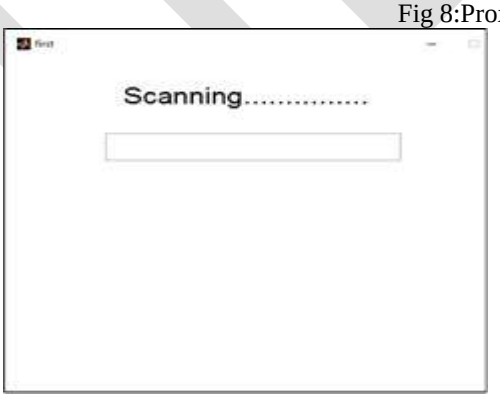

Fig 9: Program Scanning for RFID Tags

Fig 10: Program detecting a Tag

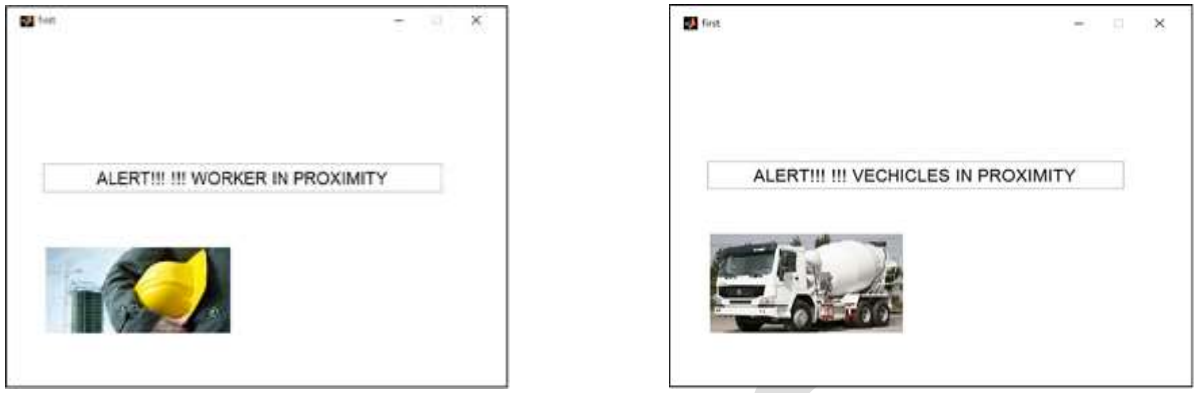

Fig 11: Output of Program

Fall Protection Plan

Falls from building is a common site accident. Reasons may be careless worker attitude, alcohol consumption or lack of safety equipments. 3D model based fall protection plan which are developed during the planning stage of the project can prevent accidents. They can give a better idea to the safety officer on where to provide safety rails and nets. Such plans can be linked with the schedule. A 3D BIM based fall protection plan was developed. It was linked with construction schedule and a simulation video was developed.

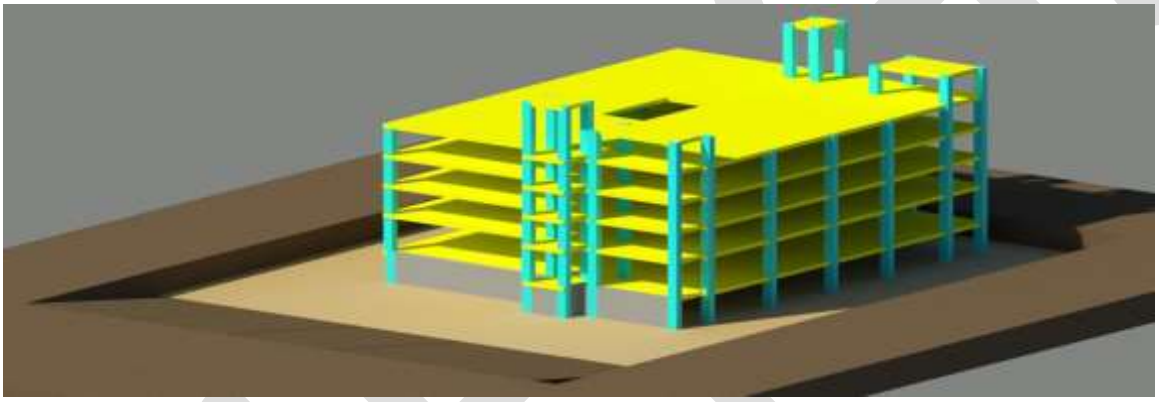

Fig 12: 3D model of building without fall protection

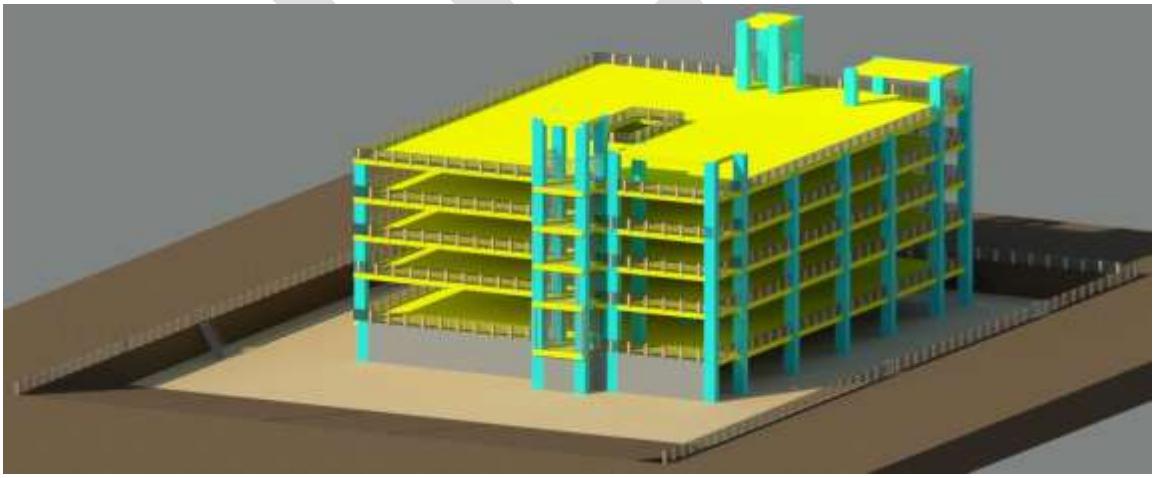

Fig 13: 3D model of building with fall protection

Proactive Safety Plan

A proactive safety plan was developed. It contains details about possible safety issues, remedies, medical help details, safety officer details etc. This plan can help in accident prevention during construction phase.

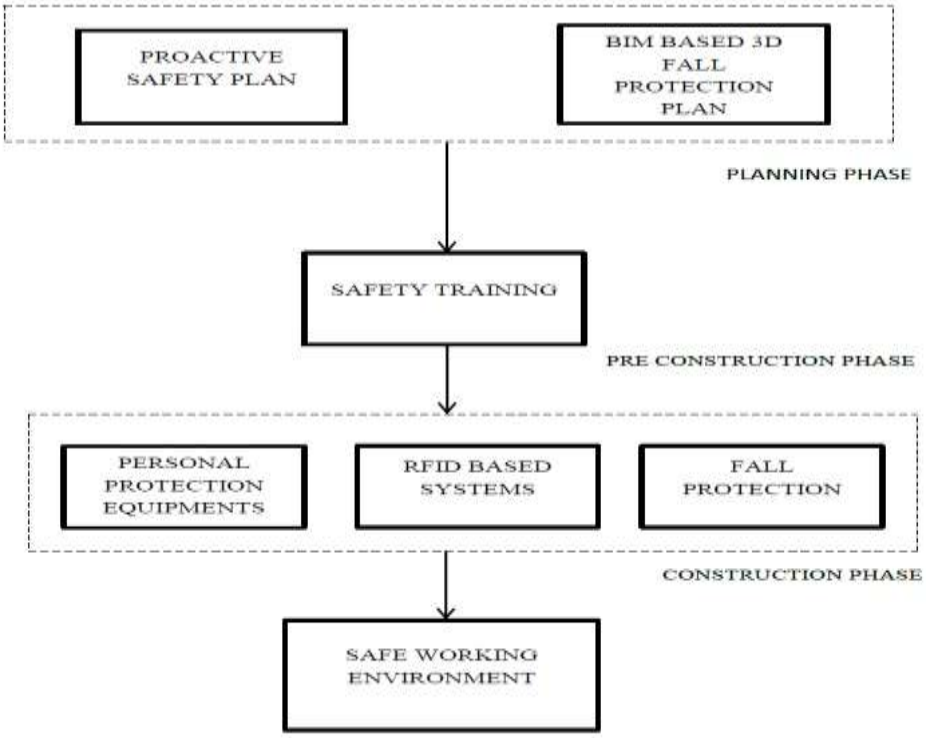

Fig 14: General Solution Framework

5. CONCLUSION

The safety issues in construction sites were studied and steps to prevent accidents were identified. Lack of safety Knowledge and safety training are the major reasons for accidents. The management, safety officers and workers should join hands and work towards the goal of ensuring 100% safety in sites. It is recommended that the workers get proper safety training and personal protection equipments. The proposed radio frequency identification based personal protection equipment checking and proximity alert systems were tested successfully. If implemented the proposed RFID based systems can prevent accidents in sites. It is recommended that importance is given to safety in the planning stage itself. If implemented the proposed fall protection plan and proactive safety plan can prevent fall related and other accidents.

REFERENCES:

1. Jochen Teizer ,Ben S. Allread , Clare E. Fullerton , Jimmie Hinze “Autonomous pro-active real-time construction worker and equipment operator proximity safety alert system” Automation in construction 19 (2010) 630–64. Www.elsevier.com
2. M. Abderrahim, E. Garcia, R. Diez, C. Balaguer “A mechatronics security system for the construction site” Automation in Construction 14 (2005) 460-466. Www.elsevier.com
3. Satish Kumar,V.K. Bansal " Construction Safety Knowledge for Practitioners in the Construction Industry" Journal of Frontiers in Construction Engineering (2013) 34-42

4. Zubaidah Ismail, Samad Doostdar, Zakaria Harun "Factors influencing the implementation of a safety management system for construction sites" Safety Science 50 (2012) 418-423
5. Agnes Kelm, Lars Laubat, Anica Meins-Becker, Daniel Platz, Mohammad J. Khazaee, Aaron M Costin, Manfred Helmus "Mobile RFID portal for automated and rapid control of Personal Protective Equipment in Construction Sites" Automation in Construction 36 (2013) 38-52
6. Sijie Zhang, Jochen Teizer, Manu Venugopal " Building information modeling and safety: Automatic safety checking of construction models and Schedules " Automation in Construction 29 (2013) 183-195
7. David Dagan, Shabtai Isaac "Planning safe distances between workers on construction sites" Automation in construction 50 (2015) 64-71
8. Sijie Zhang, Kristiina Sulankivi, Markku Kiviniemi, Ilkka Romo, Charles M. Eastman,Jochen Teizer "BIM-based fall hazard identification and prevention in construction safety planning" Safety Science 72 (2015) 31–45
9. Joonoh Seo, SangUk Han , SangHyun Lee , Hyungkwan Kim "Computer vision techniques for construction safety and health monitoring" Advanced Engineering Informatics (2015)
10. Abdulkadir Ganah, Godfaurd A. John "Integrating Building Information Modeling and Health and Safety for Onsite Construction" Safety and Health at Work (2014) 1-7

International Journal of Engineering Research and General Science Volume 3, Issue 6, November-December, 2015
ISSN 2091-2730

Physio-Morphological Characterization of *Mycobacterium spp.* followed by substrate selection (Phytosterol) for 9-OH-AD Production

Dr. Umesh Luthra*, Dr. Nishtha K. Singh, Archana Tripathi and Sejal Vora
Ipca Laboratories Ltd., Biotech R&D, Kandivali (W), Mumbai-400067, Maharashtra, India

Abstract— *Mycobacterium spp.* was used for the biotransformation of phytosterol to 9*α*-hydroxyandrost-4-ene-3,17-dione (9-OH-AD). Fast growing *Mycobacterium spp.* rapidly and completely degrades sterols by simultaneously attacking the steroid ring nucleus and 17-alkyl side chains. The 3-ketosteroid 9α-hydrolyase has been reported as a key enzyme in production of 9-OH-AD. The present study signifies the importance of culture characterization and selection of phytosterol. Physio-morphological Characterization of *Mycobacterium* revealed that the microorganism is Gram-positive, non motile and acid-fast rod; colonies varies in size 5-15mm on different agar media and appear as non-pigmented, rough with opaque aspect. Statistical design was used to screen the most suitable source of phytosterol for 9-OH-AD production by *Mycobacterium spp*. Quality of phytosterol plays a crucial role in the biotransformation process. Six different types of phytosterols were studied by Fraction factorial design (FFD). Maximum yield of 9-OH-AD (5.58 mg/g) was obtained with the use of substrate- vendor (A) Micronized phytosterol - 10 g/l. The FFD was very effective in screening of substrate for 9-OH-AD production.

Keywords— Phytosterol, Bioconversion, Characterizaton, *Mycobacterium spp.*, 9*α*-hydroxyandrost-4-ene-3,17-dione, Statistical design and Fraction factorial design.

INTRODUCTION

The Steroids are natural, organic compounds widely distributed in eukaryotic organism. Steroids are terpenoid,lipids of specific structure that contain the gonane nucleus of four cycloalkane rings.The steroid drug production industry demands more than 2000 tons of natural sterols annually and there is an increasing need for cheap and available sterol containing raw materials [1]. A majority of steroid drugs as anti-inflammatory, anti-allergic, cardiotonic, geriatric, progestational, anabolic, immunosuppressive and contraceptive agents have been successfully introduced in the allopathic system of medicine. The commercial production of these pharmaceutically active steroidal drugs depends upon three C-17-ketosteroid precursors namely, androst-4-ene-3,17-dione (AD), androsta-1,4-diene-3,17-dione (ADD) and 9α-hydroxyandrost-4-ene-3,17- dione (9-OH-AD) [2,3]. 9-OH-AD is the key precursor in the synthesis of various glucocorticoids.

Microbial steroid transformation which exploits the metabolic and biocatalytic potential of the microorganisms, is a powerful tool for generation of novel steroidal drugs, as well as their key intermediates. Selective side chain degradation of sterols to 17-ketosteroids is one of the most widely used bio transformation reactions of steroids. It is well-known that phytosterols (PSs) are suitable raw materials for microbial degradation to 17-ketosteroids because of low cost and easy availability [4].

Phytosterol is a collective term for plant sterols and stanols. The most common plant sterols are sitosterol, campesterol, and stigmasterol, and the most common plant stanols are sitostanol, campestanol, and stigmastanol [5]. Phytosterols, which are structurally and physiologically similar to cholesterol, are a large group of steroidal triterpenes. The pharmaceutical industry has a long history of converting phytosterols to therapeutic steroid hormones by microbial transformation. However, some functions of phytosterols are often limited because of their poor solubility in aqueous media.The bioavailability of phytosterols can be improved by micronizing the particles.

Micronization means transfer of the coarse drug powder to an ultrafine powder with a mean particle size being typically in the range of 2-5 μm, size distributions normally ranges from approximately 0.1 to 25 μm by very simple technique i.e. wet milling or jet milling.The basic principle of micronization is to increase the dissolution velocity by increasing the surface area. After micronization, the particles have greater specific surfaces which lead to better solubility. Reducing the particle size by the rapid expansion of supercritical solutions (RESS) can enhance the solubility and so improve the bioavailability of phytosterols [6].

Media optimization and strain improvement are two important methods for the enhancement of the yield by biotransformation. Usually media optimization is done to obtain maximum yield from minimum possible inputs, thus minimizing the amount of non utilized components at the end of fermentation.The conventional method involves varying one parameter at a time while keeping the others at a fixed level. It is very time consuming and expensive. The statistical approach enables evaluation of various components at a time thus making it cost effective and time saving process [7].

The present study describes the bioconversion using *Mycobacterium species* of phytosterols to 9α-hydroxyandrost-4-ene-3,17-dione (9-OH-AD), a key intermediate for the production of steroidal drugs and hormones, by designing a suitable production medium using statistical optimization. The gene cluster of *Mycobacterium species* involved in sterol catabolism reported as a new starting point for the biotransformation of phytosterols [8]. *Mycobacterium spp.* rapidly and completely degrades sterols such as sitosterol and cholesterol by simultaneously attacking the steroid ring nucleus and 17-alkyl side chains [9, 10].

MATERIALS AND METHODS

Microorganism and Cultivation

Mycobacterium spp. was used for the biotransformation of phytosterol to 9α-hydroxyandrost-4-ene-3,17-dione. The strain was cultivated in culture media comprising of Yeast Extract-12.00 g/l, Potassium dihydrogen phosphate-0.50 g/l, Dipotassium hydrogen phosphate-0.70 g/l, Ferrous sulphate-0.0050 g/l, Zinc sulphate-7- hydrate-0.0020 g/l, Magnesium sulphate-0.25 g/l, Glycerol-12.50 g/l, Polypropylene Glycol-2-5.0 g/l and Antifoam-1.0 ml with pH - 7.00 and agar-25.0 g/l. The slants were incubated at 30ºC for 8 days. Grown culture was perserved with 20% glycerol for further use.

Morphophysiological characterization

Mycobacterium spp. is a non-tuberculous species of the phylum actinobacteria, belonging to the genus mycobacterium. It is a chemoheterotroph and obligate anaerobe. It is also a saprophyte whose natural habitat includes soil, water and dust. Its optimal growing temperature is 30-37°C, making it a thermophile. It was grown on different media for characterization (Table 1) and incubated for 10 days at 30°C. The colony morphology of isolates was observed with the use of a stereomicroscope (10×). Gram and acid-fast stains were used for studies of microscopic morphology and acid-fast stain respectively [11]. *Mycobacterium spp.* morphology was studied further by Scanning electron microscopy. *Mycobacterium spp.* was one of the first bacterial species to be examined using the technique of electron microscopy (EM) [12]. Culture was fixed in a solution of 2.5% glutaraldehyde in 0.1M phosphate buffer, pH 7.4, overnight at 4.0 °C. The samples were rinsed once in the same buffer and dehydrated by increasing concentrations of ethanol (30, 50, 70, 90 and 100%). The samples were dried in a fume hood and fixed on to stubs with conductive self-adhesive carbon tapes, coated with gold film sputtering and used for analysis with scanning electron microscopy (SEM).

Sr. No.	Agar Media	Composition
1	I	L-Asparagine-5 g/l, Potassium dihydrogen phosphate-5.9 g/l, Potassium dihydrogen sulphate-5 g/l, Citric Acid-1.5 g/l, Magnesium Carbonate-0.6 g/l, Glycerol-20 ml, Tween 80-2 ml and agar - 25 g/l, pH - 7.2.
2	II	Peptone-10g/l, Sodium Chloride-5 g/l, Beef Extract-5g/l,Tween 80-2 ml and agar - 25 g/l, pH - 7.4.
3	III	Yeast extract-11.50 g/l, Diammonium Hydrogen Phosphate-1.73 g/l, Potassium Dihydrogen Phosphate-0.58 g/l, Dipotassium Hydrogen Phosphate-0.64g/l, Ferrous sulphate-0.0058g/l, Zinc sulphate-7-hydrate-0.0023g/l, Magnesium Sulphate-0.23 g/l, Glycerol-11.67g/l, Tween 80 -3.50 g/l and Antifoam-1 ml and agar - 25 g/l with pH - 7.00.
4	LA	Dextrose-10 g/l, Malt Extract-20g/l, Yeast Extract-3 g/l, Bacteriological Peptone-10 g/l and agar - 25 g/l with pH - 7.00 .
5	SA	Yeast Extract-5g/l, Ammonium sulphate-1g/l, Potassium Dihydrogen Phosphate-1g/l, Soyaflour-5 g/l, Soya Oil-5g/l, Tween 80-10 g/l and agar - 25 g/l, pH - 7.00 .
6	TRSA (Tryptic Soya Agar)	Casein Enzymic Hydrolysate-15.00 g/l, Papaic digest of Soyabean meal-5.00 g/l, Sodium chloride-10.00g/l, Agar 15.00g/l with Final pH (at 25°C) 7.3±0.2.
7	NA (Nutrient Agar)	Peptic digest of animal tissue-5.00 g/l, Sodium Chloride-5.00 g/l, Beef extract-1.50g/l, Yeast extract-1.50g/l, Agar-15.00g/l with final pH (at 25°C) 7.4±0.2.
8	SFMA (Sautons Fluid Medium Agar)	Ferric Ammonium Citrate-0.0167 g/l, L-Asparagine-1.33 g/l, Citric Acid-0.66 g/l, Magenium Sulphate 7 hydrate-0.166 g/l, Dipotassium hydrogen Phosphate-0.177g/l, Sodium Dihydrogrn Phosohate-0.056 g/l, Sodium Chloride-0.035 g/l, Polysorbite 80-0.833g/l and Agar-20 g.l, pH 7.2.
9	BHIA (Brain Heart Infusion Agar)	Calf brain, infusion from-200.00g/l, Beef heart, infusion from -250.00 g/l, Proteose Peptone-10.00 g/l, Dextrose-2.00g/l, Sodium chloride-5.00g/l, Disodium phosphate-2.50g/l, Agar-15.00 g/l with Final pH (at 25°C) 7.4±0.2.
10	LJ (Lowenstein Jensen Agar)	L-Asparagine-6.0g/l, Monopotassium Phosphate -4.0g/l, Magnesium Sulphate-0.4g/l, Magnesium Citrate-1.0g/l, Potato starch, soluble-50.0g/l, Malachite green-0.6g/l.
11	AV3 Agar	Dextrose-22 g/l, Soyaflour-10g/l, Yeast Extract-2.5 g/l, Citric Acid-2.2 g/l, Urea-0.5 g/l, Diammonium Sulphate-1g/l, Potassium Dihydrogen Phosphate-0.5 g/l, Magnesium Sulphate-0.5 g/l, Ferrous Sulphate-0.05 g/l, Calcium Carbonate-2 g/l, Polypropylene Glycol-0.1 ml and agar - 25 g/l, pH - 6.2.
12	AA2	Dextrose-10 g/l, Soyaflour-3 g/l, Citric Acid-2.2 g/l, Potassium dihydrogen Phosphate-0.5 g/l, Urea-0.5 g/l, Magensium Sulphate-0.5 g/l, Ferrous sulphate-0.05 g/l, Calcium Carbonate-1.5 g/l, Ammonium Chloride-1 g/l and agar - 20 g/l, pH - 6.9
13	Middlebrook 7H9 Agar Base	Ammonium Sulphate-0.50 g/l, Sodium glutamate-0.50g/l, Sodium citrate-0.10g/l, Pyridoxine-0.001g/l, Biotin-0.0005g/l, Disodium phosphate-2.500g/l, Monopotassium phosphate -1.000g/l, Ferric ammonium citrate-0.040g/l, Magnesium sulphate-0.050g/l, Calcium chloride-0.0005g/l, Zinc sulphate -0.001g/l, Copper sulphate-0.001g/l, Malachite green-0.001g/l, Agar-15.00g/l with Final pH (at 25°C) 6.6±0.2.
14	Middlebrook 7H10 Agar Base	Ammonium sulphate-0.500g/l, L-Glutamic acid-0.500g/l, Monopotassium phosphate-1.500g/l, Disodium phosphate -1.500g/l, Sodium Citrate-0.400g/l, Ferric Ammonium Citrate -0.040g/l, Magnesium Sulphate-0.025g/l, Calcium chloride -0.0005g/l, Zinc sulphate-0.001g/l, Copper sulphate-0.001g/l, Pyridoxine hydrochloride-0.001g/l, Biotin-0.0005g/l, Malachite green-0.00025g/l, Agar-15.000g/l with Final pH (at 25°C) 6.6±0.2.

Table 1: Media and their composition

Biotransformation process

Mycobacterium spp. was used for the biotransformation of phytosterol to 9-hydroxyandrostenedione. The grown slant was harvested with normal saline and was used to inoculate the seed medium. This medium is composed of Yeast Extract-12.00 g/l, Potassium dihydrogen phosphate-0.50 g/l, Dipotassium hydrogen phosphate-0.70 g/l, Ferrous sulphate-0.0050 g/l, Zinc sulphate 7 hydrate-0.0020 g/l, Magnesium sulphate-0.25 g/l , Glycerol-12.50 g/l, Polypropylene Glycol-2-5 g/l and Antifoam- 1.0 ml with pH - 7.0. Inoculum flasks were incubated at 30ºC at 240 rpm on shaking incubator for 24±4 hrs.

Transformation medium (production medium) comprises of the basal components like Phytosterol-10 g/l, Tween 80-3.50 g/l,

Ammonium acetate-2.50 g/l, Potassium dihydrogen phosphate-0.75 g/l, Dipotassium hydrogen Phosphate-4.00 g/l, Yeast Extract-2.50 g/l, Ferrous Sulphate-0.002 g/l, Zinc Sulphate-0.0008 g/l, Glycerol-12.50 g/l and Magnesium sulphate-0.50 g/l with pH 7.0. 10% of the grown seed medium was transferred to production medium in 250 ml conical flasks containing 30 ml of medium. Flasks were incubated at 30ºC and 240 rpm for 120 hrs. The process parameters such as pH, PCV were checked and yield was assessed through HPLC at an interval of 24 hrs.

9-OH-AD estimation by HPLC

9*α*-hydroxyandrost-4-ene-3,17- dione (9-OH-AD) produced in the culture broth was determined by HPLC. The culture broth of 2.5 gm was taken in 25 ml volumetric flask with 10 ml methanol and sonicated for 20 minutes.The extract was filtered and diluted with methanol and injected in the system. The HPLC (Waters 2496) having C-18 column (Betasil) was used for the estimation of 9-OH-AD at 238nm. The mobile phase was composed of Water: Acetonitrile, the flow rate was 0.8 ml/min and column temperature at 30°C. Concentration of 9-OH-AD was calculated by comparison of peak areas with the standard 9-OH-AD and subsequently 9-OH-AD activity was calculated.

Substrate (Phytosterol) Selection for 9-OH-AD production

Phytosterols (PSs) are suitable raw material for microbial biotransformation. The effect of different phytosterols on the biotransformation process for production of 9-OH-AD was studied. Six different types of phytosterols from different vendors were used. The applied phytosterol constitute of 2-sitosterol, campesterol, brassicasterol, stigmasterol , sitostanol, campestanol, and stigmastanol. Depending on the vendor, this composition of phytosterol may vary. A list of different Phytosterols is given in Table 2.

Sr.No.	Different Types of Phytosterol	Code
1	(A)- Micronized	A
2	(B)- Micronized	B
3	(C)- Non micronized	C
4	(D)- Non micronized	D
5	(E)- Non micronized	E
6	(F)- Non micronized	F

Table 2: Variation of Phytosterol

Experimental design

In order to optimize the conditions of biotransformation for 9-OH-AD yield and phytosterol conversion, a set of statistically designed experiments were conducted. All the statistical analysis was done using the Design expert software (Stat-Ease Inc., Version 8.0.7.1). First, fractional factorial design (FFD) was used to identify the significant factors affecting 9-OH-AD yield and phytosterol conversion rate by *Mycobacterium spp*. The coded values of variables are given in Table 2. A 2^{5-1} FFD which included 16 sets of trials with four replicates at center point was carried out in duplicate to screen the critical parameters influencing 9-OH-AD yield and phytosterol conversion rate [12].

The 9-OH-AD yield and PS conversion rate are considered as responses (R1) 9-OH-AD. After the analysis of FFD, a first-order model was gained [13].

RESULTS AND DISCUSSION

Isolation and morphological characterization

The colony morphology of *Mycobacterium spp.* on different media (Figure 1) were observed regularly upto 10 days with the use of a stereomicroscope-10× (Figure 2 & Table 3). Morphological studies of culture showed that size of *Mycobacterium spp.* varies from 5-15mm.

Colony Characteristics	Different Plate Media						
	I	**II**	**III**	**LA**	**SA**	**TRSA**	**NA**
Size	5mm	9mm	9mm	10mm	10mm	7mm	15mm
Shape	Round	Round	Round	Round	Round	Round	Round
Color	Off-white	Cream	Off-white	Off-white	Off-white	Off-white	Off-white
Margin	Irregular	Irregular	Irregular	Irregular	Irregular	Irregular	Irregular
Elevation	Convex	Convex	Convex	Flat	Convex	Convex	Flat
Opacity	Opaque	Opaque	Opaque	Opaque	Opaque	Opaque	Opaque
Morphology	Granulated	Grooved	Rough Furrow	Centrally Furrow	Rough granulated	Shiny granulated	Shiny Furrow

Colony Characteristics	Different Plate Media						
	SFMA	**BHIA**	**LJ**	**AV3 Agar**	**AA2**	**7H9 Agar**	**7H10 Agar**
Size	6mm	7mm	6mm	9mm	9mm	9mm	10mm
Shape	Round	Round	Round	Round	Round	Round	Round
Color	Pale Yellow	Off-white	Buff brown	Off-white	Cream	White	White
Margin	Irregular	Irregular	Irregular	Irregular	Irregular	Irregular	Irregular
Elevation	Convex	Flat	Convex	Flat	Convex	Convex	Flat
Opacity	Opaque	Opaque	Opaque	Opaque	Opaque	Opaque	Opaque
Morphology	Rosette cluster	Rough Furrow	Lobular	Shiny center	Rough Furrow	Glossy appearance	Shiny granulated

Table 3: Morphological Characterization

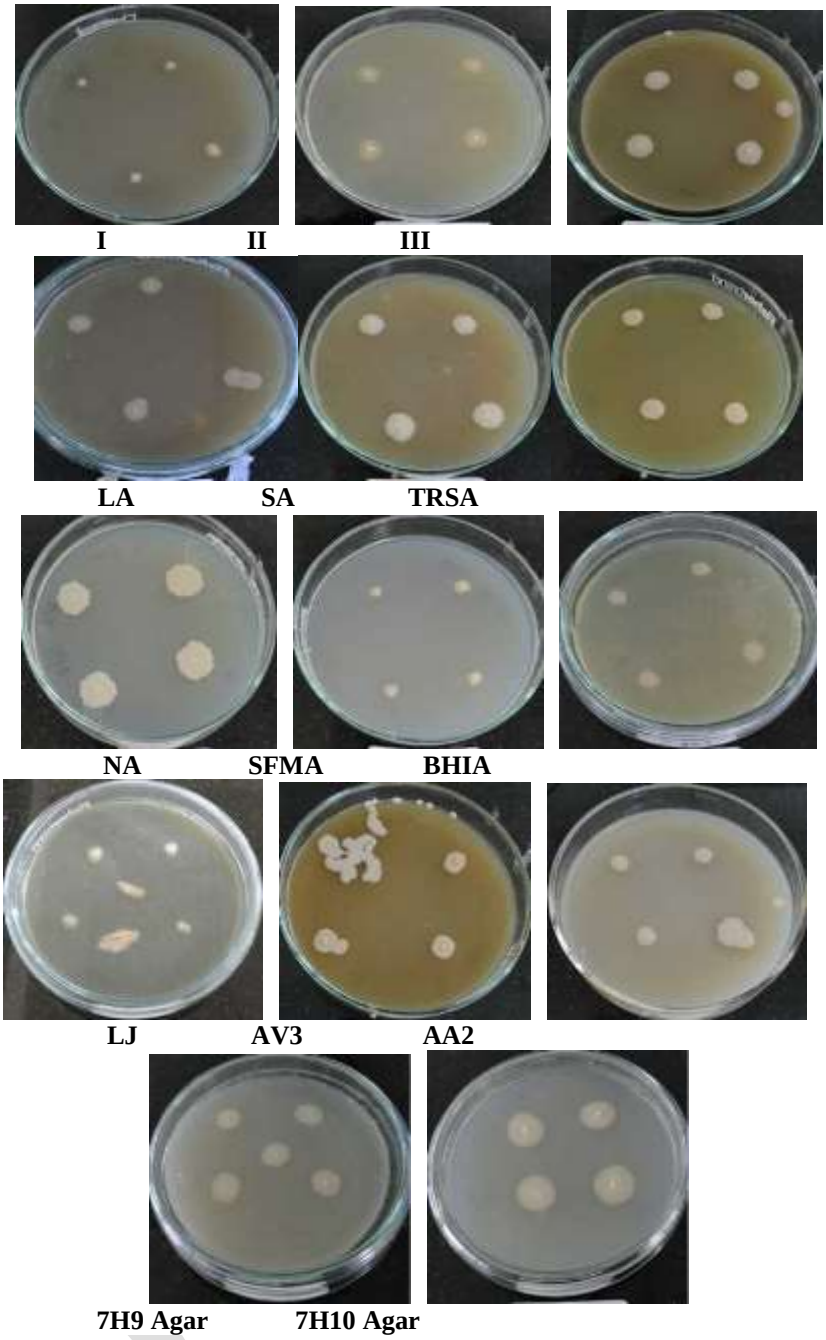

Figure 1: Morphology of *Mycobacterium spp.*on different Agar media

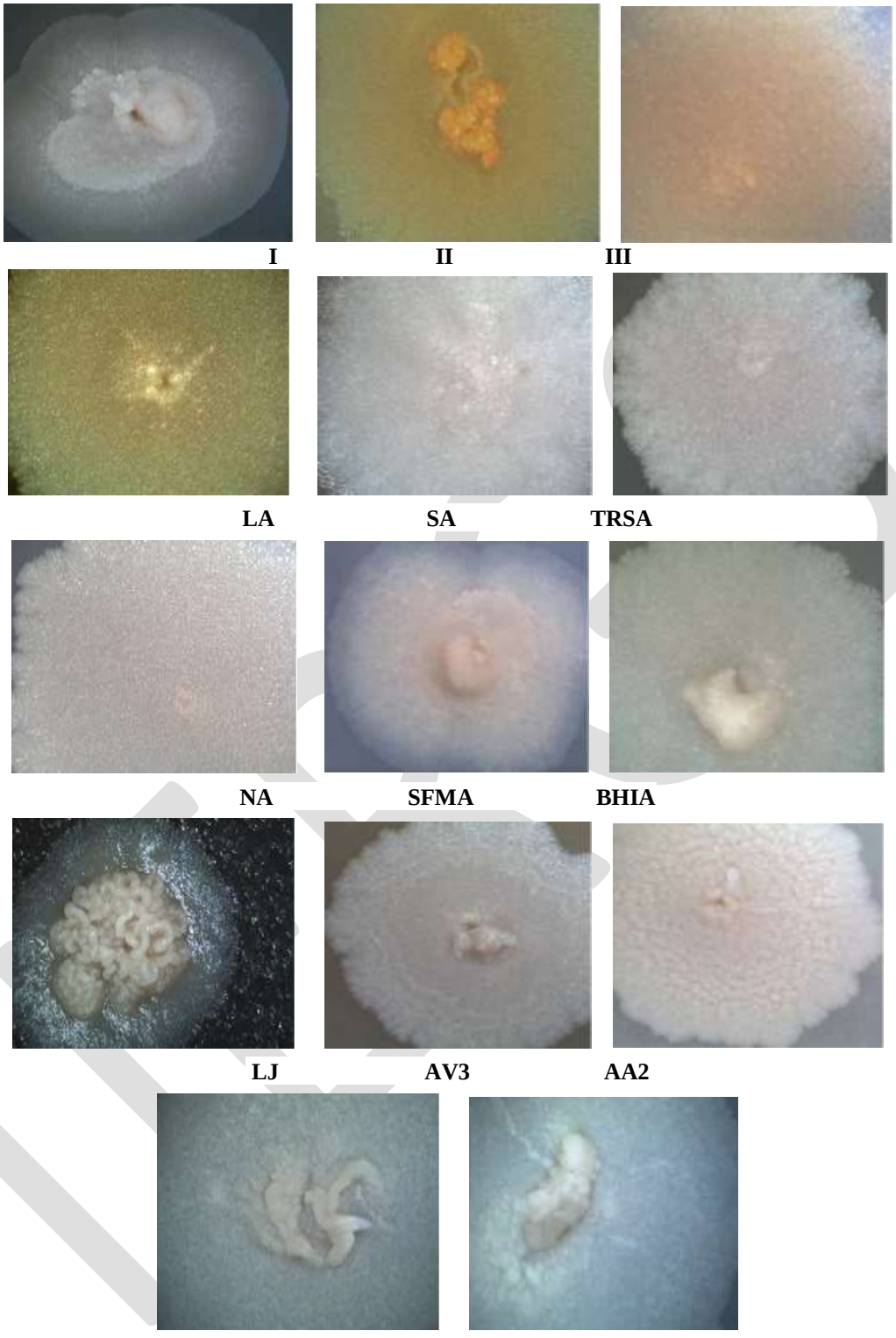

Figure 2: Stereomicroscopic images of colonies on different Agar media

Microscopic Observation During Bioconversion Process

Microscopic studies of culture during bioconversion process showed that *Mycobacterium spp.* is a Gram-positive bacilli (in Gram Staining). In live slide, it was observed that it is non motile rod (1-3 µm x 0.2-0.4 µm). Acid fast staining revealed that it is acid fast organism, sometimes long rods with occasional beaded or swollen cells having non-acid-fast ovoid bodies at one end (Figure 3). Scanning electron microscopy of *Mycobacterium spp.* revealed some of the ultrastructural morphologic details exhibited by a number of "rod-shaped", *Mycobacterium spp.* bacteria (Figure 4).Long filamentous structures are often observed, but spores and capsules are absent.

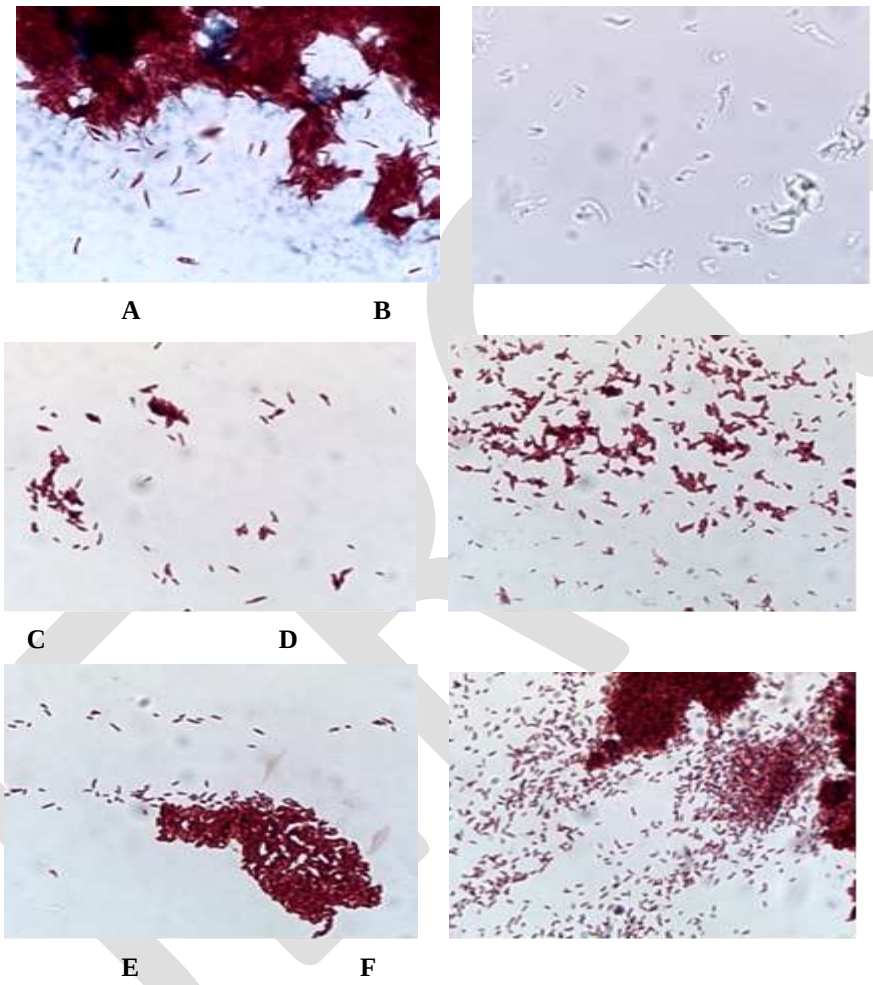

Figure 3: A-Stain image of seed culture, B-Live image of seed culture, C-F: Culture image in Production media at different Hrs:- C-24 Hrs, D-24 Hrs, E-24 Hrs and F-24 Hrs

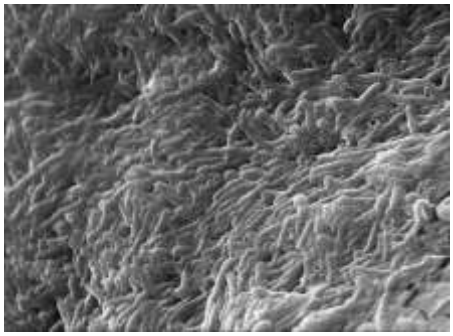

Figure 4: Scanning Electron Micrograph of *Mycobacterium spp.*

Bioconversion Process

It was established that *Mycobacterium spp.* degrades specifically only the side hydrocarbon chain in phytosterols molecules and uses it as a carbon source. In bioconversion medium inoculated with *Mycobacterium spp.* (Figure 5), phytosterol was transformed into product 9*α*-hydroxyandrost-4-ene-3,17- dione (9-OH-AD). The maximum yield of 9-OH-AD was obtained at 96-120 hrs.

A **B**

Figure 5: A- Grown Seed broth , B- Grown Production Broth

FFD analysis for process variables affecting 9-OH-AD yield and PS conversion

A screening design was performed to estimate the effects of six phytosterol. The design and results of FFD are indicated in Table 4. Effects of the six variables were analyzed by multiple regression analysis method and are illustrated in Table 5. The results indicated factor A and factor E are significant but comparatively (A)- Micronized Phytosterol (factor E) was most significant factor (P<0.0001). Thus, use of vendor: (A)- Micronized phytosterol would lead to the increase of 9-OH-AD yield (5.58 mg/g). The analysis of variance (ANOVA) of FFD was carried out and the results are shown in Table 5. P values for 9-OH-AD yield using vendor (A)- Micronized phytosterol was 0.0057. The higher values of determination coefficient (R2=0.7510 for 9-OH-AD yield) further confirmed the effectiveness of the models.

Std	Factor 1 A.A	Factor 2 B.B	Factor 3 C.C	Factor 4 D.D	Factor 5 E.E	Factor 6 F.F	Response 1 R1
1	-1	-1	-1	-1	-1	-1	2.962
2	1	-1	-1	-1	1	-1	5.581
3	-1	1	-1	-1	1	1	2.066
4	1	1	-1	-1	-1	1	3.211
5	-1	-1	1	-1	1	1	4.881
6	1	-1	1	-1	-1	1	2.596
7	-1	1	1	-1	-1	-1	2.348
8	1	1	1	-1	1	-1	5.561
9	-1	-1	-1	1	-1	1	2.248
10	1	-1	-1	1	1	1	5.121
11	-1	1	-1	1	1	-1	4.986
12	1	1	-1	1	-1	-1	5.248
13	-1	-1	1	1	1	-1	3.164
14	1	-1	1	1	-1	-1	5.516
15	-1	1	1	1	-1	1	2.005
16	1	1	1	1	1	1	5.216

Table 4: Design and results of FFD

Verification of significant factors

The analysis of variance (ANOVA) was applied to evaluate the statistical significance of the design and to verify the above results (Table 5). The Model F-value of 4.83 implies the model is significant. There is only a 1.79% chance that a "Model F-Value" this large could occur due to noise. Values of "Prob > F" less than 0.0500 indicate model terms are significant.

Source	Sum of Squares	df	Mean Square	F Value	P-value Prob>F	
Model	23.33	6	3.89	4.52	0.0218	Significant
A-A	11.21	1	11.21	13.04	0.0057	
B-B	0.13	1	0.13	0.15	0.7091	
C-C	1.156E-003	1	1.156E-003	1.345E-003	0.9715	
D-D	1.15	1	1.15	1.34	0.2763	
E-E	6.81	1	6.81	7.93	0.0202	
F-F	4.02	1	4.02	4.68	0.0588	
Residual	7.74	9	0.86			
Cor Total	31.06	15				

Table 5: ANOVA analysis for FFD model

Abbreviations: df: degree of freedom

R-squared 0.7510 Pred R-Squared 0.2129

Adeq Precision 5.936 Adj R-squared 0.5859

In this case A, E are significant model term. Values greater than 0.1000 indicate the model terms are not significant. Here model terms B, C and D are not significant. Adeq Precision measures the signal to noise ratio. A ratio greater than 4 is desirable. The ratio of 5.936 indicates an adequate signal and thus model can be used to navigate the design space.

CONCLUSION

Present study reveals characterization of *Mycobacterium spp.* on different plate agar media and selection of phytosterol source by using fraction factorial design (FFD). This work has demonstrated the importance of statistical approach to maximize the bioconversion to 9-OH-AD from phytosterol by using *Mycobacterium spp*. FFD analysis showed that vendor: (A)- Micronized phytosterol is the most suitable source of phytosterol for 9-OH-AD production. Validation results by ANOVA indicates that vendor (A)- Micronized phytosterol is the most appropriate among all studied phytosterols. Data obtained in this study, overall depicts that statistical technique can be used to select the most suitable source for phytosterol.

REFERENCES:

[1] Szentirmai, A. (1990). Microbial Physiology of Sidechain Degradation of Sterols. Journal of Industrial Microbiology and Biotechnology, 6: 101-115.
[2] Fernandes, P., Cruz, A., Angelova, B., Pinheiro, H. M. And Cabral, J. M. S. (2003). Microbial conversion of steroid compounds: recent developments. Enzyme Microb. Technol., 32(6): 688-705.
[3] Malaviya, A. and Gomes, J. (2008). Androstenedione production by biotransformation of phytosterols. Biores. Technol., 99(15): 6725-6737.
[4] Fernandes, P., Cabral, J. M. S. (2007). Phytosterols: applications and recovery methods. Biores. Technol., 98(12): 2335-2350.
[5] Dutta PC, Appelqvist L. (1996). Saturated sterols (sta-nols) in unhydrogenated and hydrogenated edible vegetable oils and in cereal lipids. J Sci Food Ag-ric 71: 383-391.
[6] Tom, J.W. and Debenedetti, P.G. (1991). Particle formation with supercritical fluids, Journal of Aerosol Science, 22:555–584, .
[7] Khan, S., Misra, A. K., Tripathi, C. K. M., Misra, B. N. And Bihari, V. (2006). Response surface optimization of effective medium constituents for the production of alkaline protease from a newly isolated strain of Pseudomonas aeruginosa. Ind. J. Exp. Biol., 44: 151-156.
[8] Van der Geize, R.; Yam, K.; Heuse,r T.; Wilbrink, M.H.; Hara, H.; Anderton, M.C.; Sim, E.;Dijkhuizen, L.; Davies, J.E.; Mohn, W.W. & Eltis, L.D. (2007). A Gene Cluster Encoding Cholesterol Catabolism in a Soil Actinomycete Provides Insight into Mycobacterium tuberculosis Survival in Macrophages. Proceedings of the National Academy of Sciences of the United States of America, 104: 1947-1952.
[9] Da Costa Cruz, J. 1938. Mycobacterium fortuitum urn novo bacilo acido-resistente patogenico para o homen. Acta Med. (Rio de Janeiro) 1:298-301.
[10] Marina, A., Waldburger, C.D., and Hendrickson, W.A. (2005). Structure of the entire cytoplasmic portion of a sensor histidine-kinase protein. EMBO J 24, 4247-4259.
[11] Berd, D. (1973). Laboratory identification of clinically important aerobic actinomycetes. Appl Microbiol 25, 665–681.
[12] Werner, G.H. (1951) Electron-microscopic studies of the cellular morphology of tubercle bacilli. Bibl. Tuberc. 5, 53–90.
[13] Chen, Q.H., He, G.Q., Mokhtar, A.M.A., (2002). Optimization of medium composition for the production of elastase by Bacillus sp. EL31410 with response surface methodology. Enzyme Microb. Technol., 30(5):667-672.
[14] Chen, Q.H., Fu, M.L., Liu, J., Zhang, H.F., He, G.Q., Ruan, H., (2008). Optimization of ultrasonic-assisted extraction (UAE) of betulin from white irch bark using response surface methodology. Ultrason. Sonochem., 16(5):599-604.

International Journal of Engineering Research and General Science Volume 3, Issue 6, November-December, 2015
ISSN 2091-2730

Sentiment Analysis of Twitter Data Using Hadoop

Ajinkya Ingle, Anjali Kante, Shriya Samak, Anita Kumari

PES's, MCOE Department Of Computer Engineering, Pune-05, ajinkyaingle05@gmail.com, Mob.:8793646961

Abstract—In today's highly developed world, every minute, people around the globe express themselves via various platforms on the Web. And in each minute, a huge amount of unstructured data is generated. This data is in the form of text which is gathered from forums and social media websites. Such data is termed as big data. User opinions are related to a wide range of topics like politics, latest gadgets and products. These opinions can be mined using various technologies and are of utmost importance to make predictions or for one-to-one consumer marketing since they directly convey the viewpoint of the masses. Here we propose to analyse the sentiments of Twitter users through their tweets in order to extract what they think. Hence we are using hadoop for sentiment analysis which will process the huge amount of data on a hadoop cluster faster.

Keywords— Opinion Mining, Sentiment analysis, Hadoop Cluster, Twitter, Unstructured data, Movie review analysis, Tokenisation.

INTRODUCTION

Sentiment Analysis:

Sentiment analysis also known as opinion mining. The process of computationally identifying and categorizing opinions expressed in a piece of text, especially in order to determine the writer's attitude towards a particular topic or product. Sentiment Analysis is the process of detecting the contextual polarity of text. In other words, it determines whether a piece of writing is positive, negative or neutral.

Twitter Data:

Twitter, one of the largest social media site receives tweets in millions every day in the range of Zettabyte per year. This huge amount of raw data can be used for industrial or business purpose by organizing according to our requirement and processing.

About this Project:

In this project, we are going to implement a system in Hadoop which analyses twitter data where cluster of nodes will be formed. Twitter data is in the form of comments which are nothing but sentiments that is opinions, feelings of people. This data will be collected by using Twitter API. By analysing this data, our system will give output in the form of positive, negative and neutral tweets. In this case, it makes the use of data dictionary for classifying the data. This data can be used further according to particular application. And this analysed data can be represented in the form of pie-charts.

Motivation:

Today we are living in the world which is surrounded by 99% of data. There are different microblogging sites where users express their views about different products these views are nothing but opinions of people and it will go waste if it is not used in proper way so there is a need to use opinions of people in improving productivity, usefulness, functionality of particular product or application or technique or any entertainment resource. Hence, there is a need to develop a product which can analyse opinions of people. This product will be useful in increasing market value of industries as well as satisfy needs of customers.

BRIEF DESCRIPTION

Need of Sentiment Analysis:

Sentiment analysis is extremely useful in social media monitoring as it allows us to gain an overview of the wider public opinion behind certain topics. Social media monitoring tools like Brand-watch Analytics make that process quicker and easier than ever before. The applications of sentiment analysis are broad and powerful. The ability to extract insights from social data is a practice that is being widely adopted by organizations across the world. Shifts in sentiment on social media have been shown to correlate with shifts in the stock market. The Obama administration used sentiment analysis to gauge public opinion to policy announcements and campaign messages ahead of 2012 presidential election.

The ability to quickly understand consumer attitudes and react accordingly is something that Expedia Canada took advantage of when they noticed that there was a steady increase in negative feedback to the music used in one of their television adverts.

The core objective of the project is:-
1) Content Retrieval: The large amount of data is collected using java Twitter streaming API.
2) Storage: This data is stored in a certain format (HDFS: Hadoop Distributed File system) so as to form key value pair which is needed to feed to mapper in map-reduce programming approach. The data is stored in Hadoop Distributed File System.
3) Data Processing: Data collected over a period of time is processed by using java and distributed processing software framework developed by Apache Hadoop and using map reduce programming model and Apache hive frame work.
4) Data Analysis: The output obtained from reducer phase is analysed.
5) Data Representation: Representation of classified data in the form of pie charts.
6) At the end we will get the outcome in the form of classified tweets that is Positive, Negative and Neutral tweets.

This project will mainly analyse the predefined stored twitter data and classify it based on polarity.
Analysis of data consist following steps:

1. Tokenization:
All the words in a tweet are broken down into tokens. This is the tokenization process. For example, '@Jack That is an awesome car!' is broken down into individual tokens such as '@Jack', 'That', 'is', 'an', 'awesome', 'car'. Emoticons, abbreviations, hashtags and URLs are recognized as individual tokens. Each word in a tweet is separated by a space. Therefore, on encountering a space, a token is identified.

2. Normalization:
The normalization process verifies each token and performs some computing based on what kind of token it is.

- If the token is an emoticon, its corresponding polarity is taken into account by searching the emoticon dictionary.
- If the token is an acronym, it is checked in the acronym dictionary and the full form is stored as individual tokens.
- Intensifiers such as 'AWESOME' are converted into lowercase and the token is stored as 'awesome'.
- Spelling of character repetitions such as 'veryyyyy' are first corrected into 'very' and then stored as 'very'.
- The normalization process also discards all those tokens which, in no way, contribute to the sentiment of a tweet such tokens are called stop word. It also discards URL's.

For analyzing the tweets, we have to take polarity into consideration using various types of dictionaries.

1) Lexical Dictionary:

It mainly consists of most of the English words which will help us to analyze the tweets by matching the word in the tweet with the words in the lexical dictionary. It also consists of idioms, phrases, headwords and multiwords.

2) Acronym Dictionary:

It is used to expand all the abbreviations and acronyms which will further generate words which can be analyzed using lexical dictionary.

3) Emoticon Dictionary:

A tweet containing emoticons can be analyzed by using this dictionary. Emoticons are basically the textual portrayal of the tweeter's mode which conveys some meaning.

4) Stop Words Dictionary:

These are the words in the tweet which do not have any polarity and they need not be analyzed. So they are eliminated and tagged as stop words. We maintain a dictionary with the list of all stop words for example able, are, both, etc.

Sentiment Classifier:

The tweets are broken down into tokens where each token is assigned polarity which is a floating point number ranging from 1 to -1.

A. Positive Tweets:

Positive tweets are the tweets which show a good or positive response towards something. For example tweets such as "It was an inspiring movie!!!" or "Best movie ever".

B. Negative Tweets:

Negative tweets can be classified as the tweets which show a negative response or oppose towards something. For example tweets such as "Waste of time" or "Worst movie ever".

C. Neutral Tweets:

Neutral tweets can be classified as the tweets which neither show a support or appreciate anything nor oppose or depreciate it. It also includes tweets which are facts or theories. For example tweets such as "Earth is round".

3. Part-of-speech Tagging:

The valid tokens are then passed to the part-of-speech tagger which attaches a tag to each token, specifying whether it's a noun, verb, adverb, adjective etc. Part-of-speech tagging helps determine the sentiment of the overall tweet because words have different meanings when represented as different parts of speech.

4. Classification**:**

At the end system will classify the twitter data into Positive, Negative, Neutral reviews with the help of data dictionary.

System Architecture:

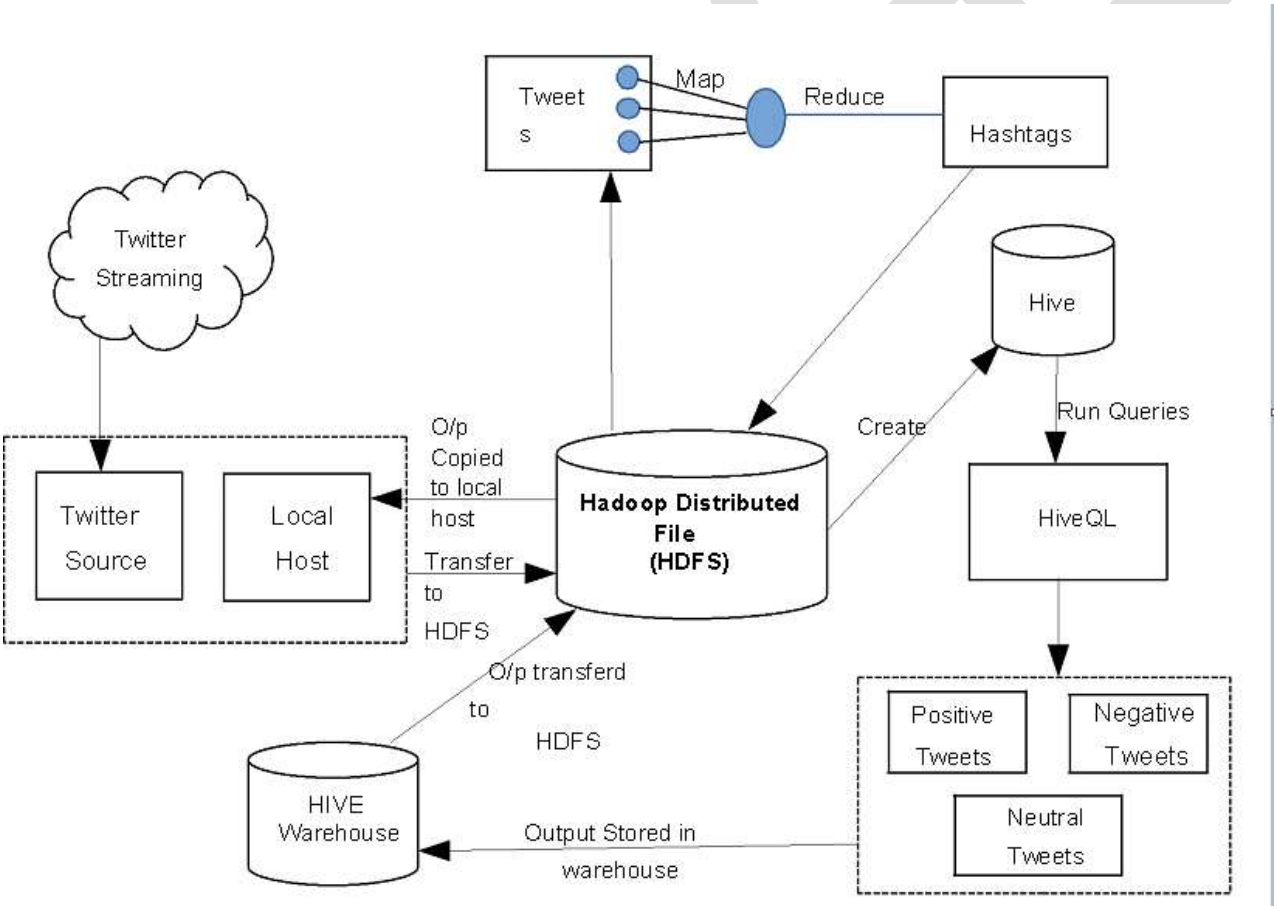

CONCLUSION

This project will give us hands on experience of handling and parallel processing of huge amount of data. Data collection process will introduce us to Java twitter streaming API. We will get exposure to work with prominent parallel data processing tool: Hadoop.

Apache Hadoop framework is gaining significant momentum from both industry and academia as the volume of data to analyse growth rapidly. This project will help us not only to gain knowledge about installation and configuration of hadoop distributed file system but also map reduce programming model. Amongst the many fields of analysis, there is one field where humans have dominated the machines more than any – the ability to analyse sentiment, or sentiment analysis.
The future of this data analysis field is vast. This project not only analyses the sentiments of the user but also computes other results like the user with maximum friends/followers, top tweets etc. hence hadoop can also be effectively used to compute such results in order to determine the current trends with respect to particular topics. This can be very useful in the marketing sector.

REFERENCES:

[1] Changbo Wang, Zhao Xiao, Yuhua Liu, Yanru Xu, Aoying Zhou, and Kang Zhang, "SentiView: Sentiment Analysis and Visualization for Internet Popular Topics", IEEE Transactions On Human-Machine Systems, Vol. 43, No. 6, November 2013

[2] Apoorv Agarwal, Boyi Xie, Ilia Vovsha, Owen Rambow and Rebecca Passonneau, "Sentiment Analysis of Twitter Data", Department of Computer Science, Columbia University

[3] Jianshu Weng, Ee-Peng Lim, Jing Jiang, Qi He, "TwitterRank: Finding Topic-sensitive Influential Twitterers", WSDM'10, February 4–6, 2010, New York City, New York, USA Copyright 2010 ACM

[4] Efthymios Kouloumpis, Theresa Wilson, Johanna Moore, "Twitter Sentiment Analysis: The Good the Bad and the OMG!", Proceedings of the Fifth International AAAI Conference on Weblogs and Social Media Rushabh Mehta, Dhaval Mehta, Disha Chheda, Charmi Shah and Pramila M. Chawan, "Sentiment Analysis and Influence Tracking using Twitter" in International Journal of Advanced Research in Computer Science and Electronics Engineering, Vol 1, Isuue 2, May 2012

[5] Bo Pang and Lillian Lee, "Opinion Mining and Sentiment Analysis", Foundations and Trends in Information Retrieval Vol. 2, No 1-2 (2008) Aditya Pal & Scott Counts, "Identifying Topical Authorities in Microblogs", WSDM'11, February 9–12, 2011, Hong Kong, China, Copyright 2011 ACM

[6] Hive kiwi at http://www.apache.org/hadoop/hive.

[7] Hadoop Map-Reduce Tutorial at http://hadoop.apache.org/common/docs/current/mapred_tutorial.html.

[8] Hadoop HDFS User Guide at http://hadoop.apache.org/common/docs/current/hdfs_user_guide.html.

[9] Hive Performance Benchmark. Available at http://issues.apache.org/jira/browse/HIVE-396

[10] Running TPC-H queries on Hive. Available at http://issues.apache.org/jira/browse/HIVE-600

[11] Luciano Barbosa and Junlan Feng. 2010. Robust sentiment detection on twitter from biased and noisy data. Proceedings of the 23rd International Conference on Computational Linguistics: Posters, pages 36–44.

[12] Bakliwal, A., Arora, P., Madhappan, S., Kapre, N., Singh, M., Varma, V.: Mining sentiments from tweets . Proceedings of the WASSA 12 (2012)

[13] A. Bifet, E. Frank, Sentiment Knowledge Discovery in Twitter Streaming Data, Springer-Verlag, Berlin, Heidelberg, 2010, pp. 1–15.

[14] A. Cui, M. Zhang, Y. Liu, S. Ma, Emotion Tokens: Bridging the Gap among Multilingual Twitter Sentiment Analysis, Springer-Verlag, Berlin, Heidelberg, 2011, pp. 238–249.

Role of Synchronised Phasor Measurement Units in Power System

Sumeetpal kaur[1], Baljeet Singh, Jaswinder Singh Sra

[1]Student (M.tech. Power Engg.)

Guru Nanak Dev Engineering College, Ludhiana, India, sumeet.garcha8@gmail.com, 9501373475

Abstract— In the present era, with the expansion of power system the complexity and challenges in terms of grid stability, security and safety is increased. So more accurate, reliable monitoring and control systems are required. SCADA system is capable only to provide steady state view of the power system with high data latency. Synchronised phasor measurement unit is one of the important equipment in this regard. This paper presents a review of phasor measurement units in power system and smart grids. PMUs have great potential in the power system monitoring, control and protection. The historical development, principle working, applications and other related aspects are discussed in this paper.

Keywords— PMU-Phasor measurement unit, PDC-Phase data concentrator, SCADA-supervisory control and data acquisition system, GPS-global positioning system, WAMS-Wide area measurement system, RTDS- Real time digital simulator, GSM-Global system for mobile.

INTRODUCTION

In mid 1980s PMUs were developed. Phasor measurement unit (PMU) is a device or a function in a multifunction device that produces synchronized phasor, frequency, and rate of change of frequency (ROCOF) estimates from voltage and/or current signals and a time synchronizing signal [7].

The Bonneville Power Administration (BPA) is the first utility to implement comprehensive adoption of synchrophasors in its wide-area monitoring system. WAMS is one or more networks of measuring devices that may include phasor measurement unit (PMUs), local recorders, legacy equipment, or advanced technologies that are GPS-synchronized over a geographically diverse area [7].

PMU technology provides phasor information (both magnitude and phase angle) in real time [4].It is possible to obtain synchronized phasor measurements using PMU. The advantage of referring phase angle to a global reference time is helpful in capturing the wide area snap shot of the power system. Whenever any disturbance or fault occur the protection or control system has to be initiated for power system degradation, minimize the impact of disturbance, isolates the unhealthy part and restores the power system to normal healthy state.

1. *Phasor Basics*

A pure sinusoidal waveform can be represented by a unique complex number known as a phasor. Consider a sinusoidal signal[8]

$$\boldsymbol{x(t) = X_m cos(\omega t + \theta)} \dots\dots\dots\dots\dots\dots\dots\dots. (\mathbf{1})$$

where,

X_m is the peak value of the signal

$\boldsymbol{\omega}$ is the frequency of the signal in radians per second

Θ is the phase angle in radians

The phasor representation of this sinusoidal is given by where,

$X = X_r + jX_t = (X_m/\sqrt{2})\, e^{j\theta}$

$= x_m/\sqrt{2}(cos\Theta + jsin\Theta)$ ……………………………………………………………………………….(2)

where

$x_m / \sqrt{2}$ is the magnitude of the phasor i.e. the r.m.s. value of sinusoid
The sinusoidal signal and its phasor representation given by (a) and (b) are illustrated in Fig. 1.

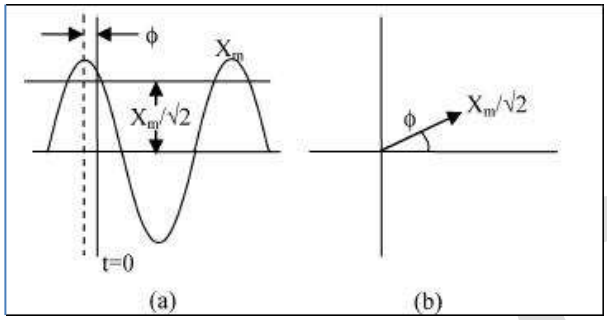

Fig 1. (a)Sinusoidal signal and (b) its phasor representation

2.Block diagram of PMU

The main elements of Phasor Measurement Unit (PMU) are as shown in Fig. 2.[8]

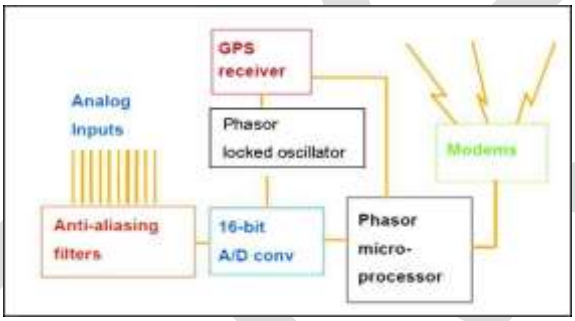

Fig 2. Basic block diagram of PMU

Analog inputs- Current and voltage transformers are employed at substation for measurement of voltage and current. The analog inputs are the voltages and currents obtained from the secondary winding of the three phase voltage and current transformers.
Anti-aliasing filters- The analog inputs go into an anti-aliasing filter. It limit the bandwidth to satisfy the Nyquist criterion. As per Nyquist theorem, to reconstruct signal after sampling, without introducing error, sampling frequency must be greater than twice the maximum frequency of the signal to be sampled. Thus they are used to filter out the input frequencies that are higher than the Nyquist rate [8].
A/D converter-It converts the analog signal to the digital one.
Phase lock oscillator and GPS reference source -Phase lock oscillator along with Global Positioning System reference source provides the needed high speed synchronized sampling, Global Positioning System (GPS) is a satellite-based system for providing position and time. The accuracy of GPS-based clocks can be better than 1 μs [7] . It consists of 24 satellites orbiting in 6 geo-synchronous orbits such that at any given instant 4 satellites are visible from any point on the earth surface.
Phasor microprocessor -The phasor microprocessor calculates the phasor using digital signal processing technique and uploads to phasor data concentrator.
Phasor data concentrator (PDC) -The electrical parameters measured by a number of PMUs are to be collected by some device either locally or remotely, this function is performed by Phasor Data Concentrator (PDC). A PDC forms a node in a system where phasor data from a number of PMUs is collected, correlated and fed as a single stream to other applications. Phasor Data Concentrator (PDC) is a function that collects phasor data and discrete event data from PMUs and possibly from other PDCs, and transmits data to other applications. PDCs may buffer data for a short time period but do not store the data[7].
In a hierarchal set up the PDCs can also be used to collect the data from number of down stream PDCs.[13]
PDC is differentiated into:-

- Nodal PDC(NPDC)
- Master PDC (MPDC)
- Super PDC (SPDC)

3.Synchrophasor standards

1. Standard IEEE 1344

The concept of synchronized phasor with the power system was introduces in the 1980s and the first synchrophasor standard, IEEE 1344 was introduced in 1995 [8]. It was created to introduce synchrophasors to the power industry and set basic concepts for the measurement and methods for data handling.

2. Standard IEEE C37.118-2005

This standard defines synchronized phasor measurements used in power system applications. It provides a method to qualify the measurement, tests to be sure the measurement conforms to the definition, and error limits for the test. It also defines a data communication protocol, including messages formats for communicating this data in a real time system. The concept of (PDC) which included data from several PMUs introduced [8]. In India this standard is mainly used [13].

APPLICATIONS OF PMU

The various applications of PMU are as follows [13]:-

1. Real time monitoring and Control
2. State estimation[1]
3. Real Time Congestion Management
4. Post-Disturbance analysis
5. Power System Restoration
6. Automated control

The measurement obtained through PMUs installed in the grid helps to calculate the complete view of current state of the power system. State estimation measurements run at fixed interval of time gives a snapshot of the system at that time [10].

If we are able to predict dynamic changes of the power system one step ahead it will be very beneficial for security analysis and allows more time for the grid operator to take quick, timely control decisions in case of an emergency. Most reports on blackouts show that majority of the blackouts were preventable and PMU helps to achieve this objective. The accuracy of state estimation is largely dependent on the accuracy of measuring devices. PMUs are much more accurate than SCADA.

PMU can measure both voltage and current phasors at the installed bus. The measurement of voltage angle along with voltage magnitude was not possible with SCADA but PMU can directly measure it.

Detection of imbalance in three phase system

PMU can also be used for the detection of imbalance in three phase power system[6]. Frequency deviation s& imbalances causes serious contingencies leading to blackout. Ill effects of voltage imbalances are :-

1. Increase in losses
2. Overheating of machinery
3. Insulation degradation
4. Reduced life of motors and transformers

A generalized likelihood ratio test (GLRT) is developed and shown to be a function of the negative-sequence phasor estimator and the acceptable level of imbalances for nominal system operations [6]. In [6] a statistical model that captures characteristics of imbalance from PMU output is developed. For a perfectly balanced power system the PMU output is a single complex sinusoid, whereas under imbalance the symmetrical components at PMU output have two related frequencies. Detection of imbalance is done using negative sequence in addition to positive sequence component. Under perfectly balanced conditions only positive sequence component is present while negative & zero components are absent.

For Industrial applications

The industrial area is also prone to disturbances and contingencies. The potential of PMU can also be used in industrial areas for fault localisation. It is very important to develop methods to locate faults quickly and to take appropriate protective measures to reduce the impact of fault. In[2] a fault localisation method is proposed based on the online monitoring of the duration of signal which is needed to get from one point to other, where length of cable is known to us. As PMU measurements are time synchronised, they should observe differences in time of occurrence of significant disturbances in the grid & localise the disturbance source.

Identification of faults

Whenever any fault occurs in the power system for monitoring and detection of the faults basically there are two components [14]:-

1. The first component tis the voltage reduction due to the occurrence of the fault or contingency.
2. The second component is that the power flow direction reverses due to fault occurrence.

Phase angle measured by PMU is used for the determination of fault current with respect to the reference quantity. The nominal power flow will result in phase angle between voltage & current around its power factor angle $\pm\phi$. [14]. When power flow direction reverses due to fault it becomes $(180\pm\phi)$.

It is concluded that minimum voltage value indicates the nearest area to the fault and maximum absolute angle difference is selected to identify the faulted line in the power system [14].

Comparison between SCADA and PMU [8]

TABLE1 Comparison between SCADA and PMU

.

Factors	SCADA	PMU
Measurement	Analog	Digital
Resolution	2-4 samples per cycle	Up to 60 samples per cycle
Phasor angle measurement	No	Yes
Monitoring	Local	Wide-area
Observability	Steady state	Dynamic/Transient state
Analogy	X-Ray	MRI

It is concluded that PMUs are much more accurate than the SCADA system and helps in dynamic state monitoring. But in the present power system it cannot completely take place the SCADA system. But the combination of both technologies is used.

RELATED ASPECTS

Testing of PMU and PDC with RTDS

Real time digital simulator tests the performance requirements of PMU & PDC according to IEEE standards. In [5] the tests are created in RSCAD software of RTDS. It can also be used for testing of protection and control devices. It examine the PMU compliance with frequency range, signal magnitude range, phase angle range, harmonic distortion. Using the PMU-PDC platform with RTDS the steady state and dynamic state tests are developed and performed for the SEL-451 PMU. For both test categories the synchrophasor measurements captured by the PMU under test are evaluated over the Total Vector Error (TVE), Frequency Error (FE) and Rate of Change of Frequency Error (RFE). For the step change tests of dynamic state, the response time, delay time and maximum overshoot are also calculated. SEL-451 PMU conforms to the limits defined by the standards for both the steady and dynamic state tests. The tests are conducted at 50 Hz frequency and at 50 frames per second sampling rate for the PMU under test [5].

Failure of communication link

The goal of PMU installation is to do real time monitoring of the power system. Various PMUs in the power system send its data to PDC & further monitoring and control actions are taken. This network configuration is prone to failure in the event of damage to the dedicated communication path between PMUs and PDC. In [4] usage of GSM/GPRS (Global system for mobile) communication between PMUs to establish alternate pathways of communication to ensure smooth operation until the original communication path is established, is proposed. It allows use of dedicated monitoring of PMU using smart phone. Spider follows a variant of mesh topology to achieve this objective [4].

Optimal PMU placement

For complete observability optimal placement of PMU is mandatory. As PMUs are costly equipment so judicial use important. It decided contingency cases along with base operating conditions. Two methods are used for the determination of optimal placement are [11]:--

1. Numerical observability
2. Topological observability based methods
3. Numerical observability based approach utilizes the information matrix or the measurement jacobian reflecting theconfiguration of the system and measurement set[11]. It involves huge matrix manipulation and computationally expensive. Various techniques based on this concept are, simulated annealing [A. B. Antonio and R. A. TorreBo], Tabu search[H. Mori and Y. Sone], Genetic Algorithm[B. Milosevic and M. Begovic] based methods. These techniques require large convergence time. However topological based methods utilize the graphic theoretic concept e.g. Depth Search method[R. F. Nuqui and A. G. Phadke], Spanning tree method[T. A. Baldwin, L. Mili, M. B. Boisen, and R. Adapa], Integer linear programming methods[B. Xu and A. Abur].In [11] a voltage stability based contingency ranking has been carried out to screen flow critical contingencies. This has been tested on IEEE 14 bus system, New England 39 bus system and Northern Region Power grid-246 Indian bus system.

In [12] based on greedy heuristic & relaxation, a branch and bound algorithm to find the globally optimal location is proposed. The optimal location is obtained in at most 19 iterations.

If acknowledgement is there wishing thanks to the people who helped in work than it must come before the conclusion and must be same as other section like introduction and other sub section.

CONCLUSION

This paper presented a brief review on phasor measurement unit & its related aspects in the power system. PMU is a promising device for smart grids to provide protection, monitoring and control. Many utilities including India are employing power projects to install PMUs in their existing power systems. Due to its features it is clear that most transmission networks will be employing it in the future. It can be used for numerous applications as discussed above, like fault detection, imbalance detection, voltage sags and swells, in industrial enterprises. But optimal placement is mandatory to completely fulfil our objectives, only then we can completely visualise power system effectively. Overall

the power system security, reliability increases manifolds with the introduction of PMUs.

REFERENCES:

[1] Jitender kumar, J.N.Rai, Naimul Hasan; Use of Phasor Measurement Unit (PMU) for Large Scale Power System State Estimation
[2] M. Gurbiel, P. Komarnicki, Z. A. Styczynski SM, M. Kereit, J. Blumschein, B. M. Buchholz; Usage of Phasor Measurement Units for Industrial Applications
[3] Vipin Krishna, R,S. Ashok, Megha G Krishnan; SYNCHRONISED PHASOR MEASUREMENT UNIT
[4] Mijaz Mukundan, Jayaprakash P.; SPIDER: A GSM/GPRS Based Interconnected Phasor Measurement Unit (PMU) System for Prevention of Communication Failures
[5] Konstantinos Diakos, Qiuwei Wu, Arne Hejde Nielsen; Phasor Measurement Unit and Phasor Data Concentrator test with Real Time Digital Simulator
[6] Tirza Routtenberg, Yao Xie, Rebecca M. Willett and Lang Tong; PMU-Based Detection of Imbalance in Three-Phase Power Systems
[7] IEEE Guide for Synchronization, Calibration, Testing, and Installation of Phasor Measurement Units (PMUs) for Power System Protection and Control, 6 March 2013
[8] Rohini P. Haridas; GPS Based Phasor Technology in Electrical Power System; International Journal of Electronics and Electrical Engineering Vol. 3, No. 6, December 2015
[9] Amit jain,Shivakumar;Phasor measurements in dynamic State Estimation of power systems ; TENCON 2008. IEEE Region 10 Conference 19-21 Nov. 2008 Page(s):1 to 6, Digital Object Identifier 10.1109/TENCON.2008.4766698;Report No: IIIT/TR/2009/44
[10] Emilie Brunsgård Ek; Utilization of Phasor Measurements as Basis for System State Estimation
[11] Ranjana Sodhi, S. C. Srivastava and S. N. Singh; Optimal PMU Placement to Ensure System Observability under Contingencies
[12] Yue Zhao, Andrea Goldsmith and H. Vincent Poor; On PMU Location Selection for Line Outage Detection in Wide-area Transmission Networks
[13] Report on URTDSM; Power grid corporation of India LTD.Gurgaon;Feb'12
[14] C.Anil Kumar, K.Lakshmi; Monitoring and detection of fault using Phasor Measurement Units

International Journal of Engineering Research and General Science Volume 3, Issue 6, November-December, 2015
ISSN 2091-2730

Web Integrated Smart Home Infrastructure Using Internet of Things

Manveer Joshi, Bikrampal Kaur

Department of IT, Chandigarh Engineering College, Landran, Mohali, Punjab, India

Email: joshi.manvir@gmail.com

Abstract— Internet of Things is an evolving concept with an ever increasing range of applications leading to development of new technologies and methods for the development of IoT environment. A smart home is one such application of IoT. In this paper a framework for smart home is proposed using Constrained Application Protocol which provides a method to control sensors and actuators remotely over the Internet. An application using Constrained Application Protocol is developed to demonstrate the smart home concept by incorporating light, temperature and humidity sensors. The application is developed using Contiki and simulated with the help of Cooja simulator. Also an experimental evaluation of the suitable medium access layer protocol and radio duty cycle protocol for smart home infrastructure.

Keywords—Internet of Things, Smart Home, Constrained Application Protocol, Zigbee, Contiki, IPv6, WSN

INTRODUCTION

Internet has changed human's life by providing anytime, anywhere connectivity with anyone. Recent innovations in the information communication and technology field are strongly focused towards the Internet of Things (IoT), which will definitely lead to an enhancement in the home environments. Internet of Things (IoT) offers us a world in which one will be connected with every kind of object around us [1][2]. In IoT world one can access information about anything from anywhere at any time but there exists many challenges to interface these object with the Internet.

A smart home is one such application. It is basically a home or living environment where all the things such as home appliances to be controlled automatically or remotely [3]-[6]. In this paper, we present a home automation framework where things are controlled remotely through Internet.

The applications of an interconnected IoT ecosystem are so extensive that they challenge our preconceptions of interfacing with the Internet. The embedded and resource-constrained devices central to the IoT ecosystem provides highly specific functions for sensing and actuating. These low power and low cost devices forms a network of interconnected objects to transform our home to smart home. In this context, the home automation system/devices are getting popular both in industry and among researchers due to their ability to change our homes by increasing the safety, energy efficient and comfort of our homes.

In this paper the objective is to provide a versatile, low-cost and flexible automated home infrastructure for use in private homes which can be controlled remotely through internet. A basic idea for such type of Smart Homes using loT is shown in figure 1.

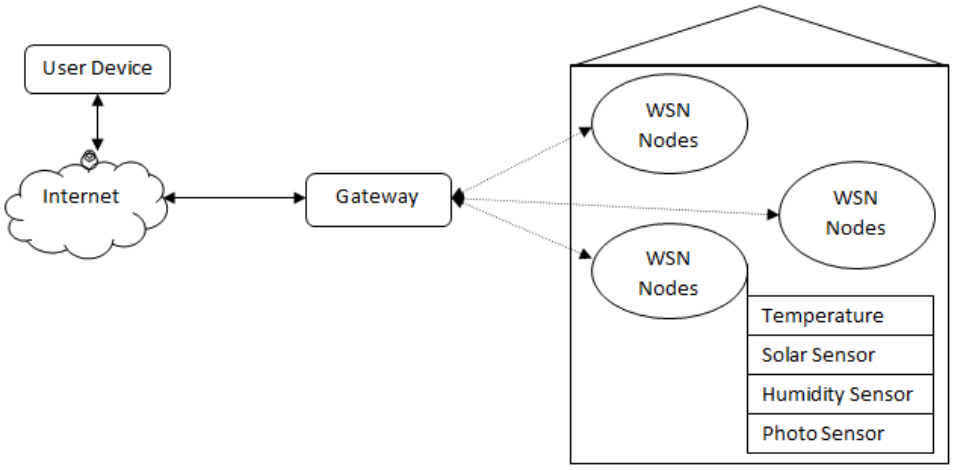

Figure 1: Smart Home Framework

As shown in the figure 1, this type of home automation system will consist of a number of smart nodes in a network, incorporating several sensors. In this paper for consideration only four sensors: light, solar, temperature and humidity sensors are shown but in reality any number of sensors can be connected depending on the technology and hardware used. The objective here is that non-

technical user should be able to use the system easily. These sensors nodes are easy to install and cable free, easy to use and maintain. These sensors nodes are connected to a gateway device by ZigBee which connects them to Internet through Ethernet or Wi-Fi. The gateway device basically acts as a bridge for sending data from wireless sensor network to Internet. A simple, secure web based system is used to read node and sensor data from the internal database and display in an easily interpreted graphical fashion. The website can be accessed through the internet by any suitable browser but is optimized for Mozilla Firefox.

A low-end implementation of a home automation network will subject to the same design considerations as bigger networks for instance those used for urban traffic control and power-grid management networks. One primary design consideration, for the selection of hardware, is to choose networking and routing protocols which must offer a scalable, versatile, and auto management solution. Second important choice is the selection of a set of parameters which are suited for the purpose and size of the smart node network. As home automation network is much smaller and simpler than its above-mentioned counterparts, it is more than likely that a set of networking and routing parameters can be optimised for such a situation. As a physical network is hard to evaluate for network and routing parameters, a software simulator/emulator is used to obtain the required data. The use of web services on the simulated network is tested and found to be feasible. Web services provide a flexible and reliable way to remotely obtain sensor and network data and are easy to program once the underlying system firmware is available. Finally, to access web based services Constrained Application Protocol is used to demonstrate its utility in network consisting of resource constrained nodes.

RELATED WORK AND METHODOLOGIES USED

Gaikwad et al. surveyed the smart home systems based on Internet-of-Things [7]. He discussed the IoT architecture along with the problems and challenges faced by IoT concept as applicable to smart homes. He also proposed the solutions for some of the problems and challenges faced.

Kamilaris and Pitsillides discussed the web of things architecture application for smart homes with the help of a case study [8]. They discussed the idea of energy-aware smart homes which have the potential to offer solution for energy awareness and integration in addition to their integration in smart electricity grids. They proposed the idea of combining sensor devices with residential smart power outlets.

Wang et al. builds a smart robot consisting of two parts: a smart phone acting as brain and a robot car as body [6]. While user is away from home, he can monitor different parameters of home measured by different sensors in robot body while robot brain acted by smart phone is with him.

Wang et al. proposed a smart home control system solution consisting of smart central controller and wireless sensor and actuator network (WSAN) to manage and control home appliances [9]. They developed different control modules in the WSAN to control varied type of home appliances. Any number of home appliances can be added or removed thereby giving the required flexibility.

Ventylees remotely monitored the smart home and provided biometrics and public key encryption based security system and SMS based alarm system while authenticated user is away from the home [5]. He used a gateway which uses ZigBee IEEE 802.15.4 based Sensor Network, GSM and Wi-Fi wireless networks to control the wireless communication in smart home systems.

Ye and Huang presented a Cloud based smart home framework for home automation, household mobility and interconnection without the need of high performance computers [4]. Bing presented smart home system architecture by using gateway, 3G and ZigBee.

Bergmann used CoAP and the proprietary FS20 protocol for the demonstration of home automation concept [10]. The FS20 device addresses was mapped to path segments of CoAP URIs whereas its commands to the basic CoAP operations.

Han and Lim designed a smart light control system based on sensor network for smart home and energy control production. ZigBee based smart home architecture is proposed by them for control of different appliances by assigning them coordinator, router and control device roles [11]. In another paper, they proposed an IEEE802.15.4 and ZigBee based Smart Home Energy Management System (SHEMS) [12]. They proposed Disjoint Multi Path based Routing protocol to improve the performance of Zigbee sensor network.

PRESENT WORK

In this paper, we present a smart home framework concept based on CoAP and Zigbee. Not many researchers have covered this though many design concepts and framework exists in the literature as discussed in previous section. Moreover, the paper offers to manage all the home appliances monitored and controlled by different sensors and actuators using any device capable of running a web browser. The framework is easily extendable to large number of wireless sensor network nodes supporting the ZigBee protocol. Also, Internet connectivity can be provided to smart home network through Ethernet or Wi-Fi.

As shown in the Figure 1 it consists of three principal parts: ZigBee network, IP network and a gateway device. The ZigBee wireless sensor network forms a IEEE 802.15.4 6lowpan network where all the sensor and actuator nodes exists. To provide Internet connectivity to these nodes or 6lowpan network, we need some mechanism to connect them to Internet. This is done by a device known as border router or gateway, the purpose of which is to interface IP network to the 6lowpan network. The data packets are routed through this device to both the networks.

The software framework selected for development is Contiki OS which is an open source operating system designed for memory constrained networked systems with special emphasis on low power IoT devices. It only needs 10KB RAM and 30KB ROM for proper operation, therefore a lot of hardware options exists for its implementation. In this paper, we have selected Tmote sky mote as the hardware for sensors and actuator connectivity to support ZigBee based 6lowpan network.
The smart home framework concept is proved by simulation using Contiki OS provided Cooja simulator with Tmote sky nodes. The Cooja also offers the opportunity to emulate the Tmote sky nodes. The Contiki software architecture is shown in Figure 2 as shown by Shelby & Bormann [13].

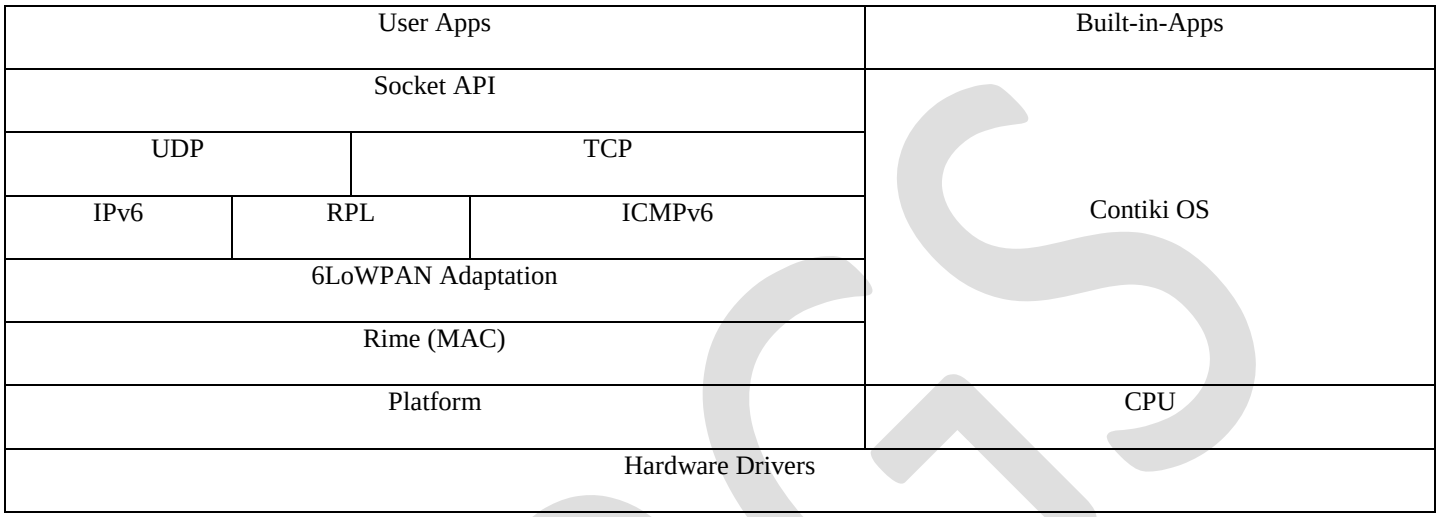

Figure 2: Contiki Software Architecture

As shown in the Figure 2, at the top layer of software architecture is user apps. In the proposed framework at the application layer CoAP (Constrained Application Protocol) is used for interaction with 6lowpan network. CoAP is a light-weight application layer protocol based on UDP transport intended to be used for resource constrained devices which need to be controlled remotely over the internet. CoAP offers multicast, low overhead and simplicity which are advantageous for IoT networks.
To further reduce the memory footprint and energy consumption we have evaluated Contiki OS medium access layers protocols available. Media access control (MAC) layer algorithms play a vital and crucial role in optimizing communications to increase battery life. The prime goal of a MAC algorithm is to reduce contention in the wireless medium between simultaneously communicating devices, which must both back off , retry later time if any another node is transmitting already.
Contiki MAC consists of three layers: MAC, Radio Duty Cycle (RDC) and framer. The MAC used is CSMA and nullmac. An experimental evaluation and optimization is done to select the best MAC. Radio duty cycling (RDC) algorithm a part of MAC algorithms is also optimized. These algorithms determine how often a radio of a device 'wakes up' to check whether there are any other devices trying to communicate with it. RDC layers implemented in Contiki are ContikiMAC, xmac, Low Power probing (lpp), nullrdc-noframer, nullrdc and sicslowmac.

RESULTS AND DISCUSSIONS

Since sensor nodes are constrained for computing power, memory and energy, it is very important that proposed framework implementation should have very low memory footprint as well as low energy consumption so that nodes can have longer operational life with no maintenance since they can be used at places that could be hard to reach. Therefore, several optimizations in Contiki IPv6 stack and application code size is done to fit the firmware in the selected sensor node memory. Furthermore, optimization at the MAC and RDC layer of Contiki is done to increase the power efficiency of the network and reduce the firmware size.
As stated in previous section an experimental evaluation is done at Contiki MAC layer to select best option for home automation network and it is found that ContikiMAC and CSMA is the best choice for the network. ContikiMAC with CSMA average radio duty cycle is found minimum as shown in Figure 3 at 10.94 % as compared to other options with CSMA MAC for 30 client and one server node. The first, second and third part of the Figure 3 corresponds to ContikiMAC, xmac and nullmac average radio duty cycle tables while CSMA is selected as MAC.
Also the PRR statistics were also analyzed for all 30 sensor nodes and the average PRR of ContikiMAC is found **50.48%** and it is concluded that as compared to other MAC ContikiMAC implementation is more energy and throughput efficient. Therefore Contiki MAC is selected as RDC layer for home automation system.

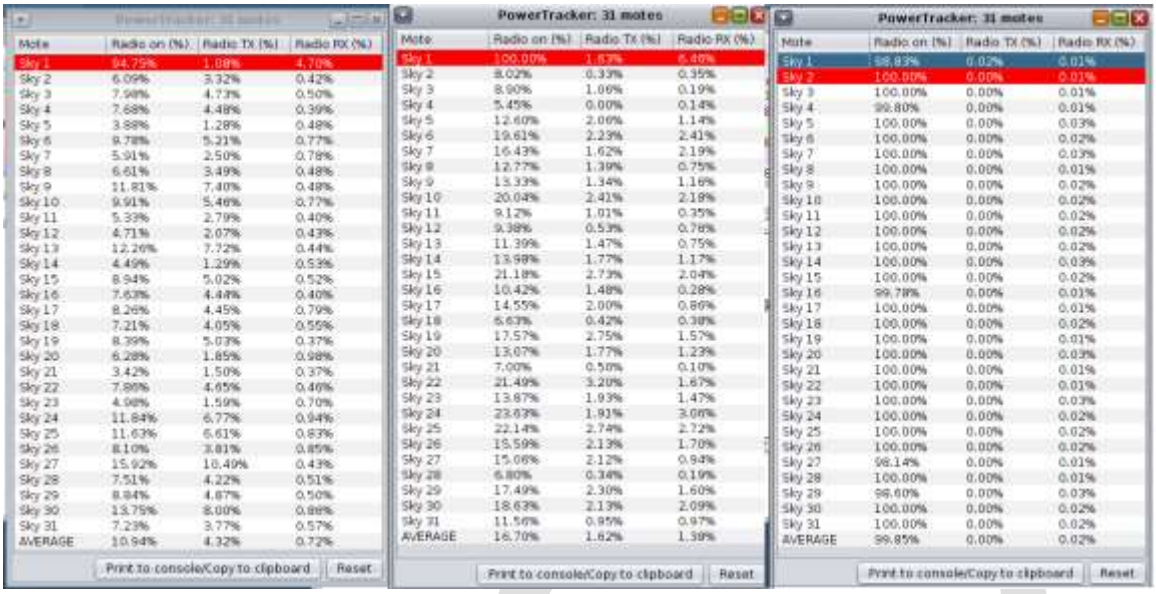

Figure 3: RDC layers comparison

A comparison is also done with respect to channel listen frequencies of 16 Hz, 8 Hz and 4 Hz. It is found that the average listening power consumption increases with the RDC frequency whereas the average transmission power decreases with a net result of increase in total average power consumption frequency. The lowest RDC frequency of 4 Hz is found most appropriate in our case for battery-powered nodes. Figure 4 shows the Instantaneous Power Consumption at RDC frequency of 4 Hz.

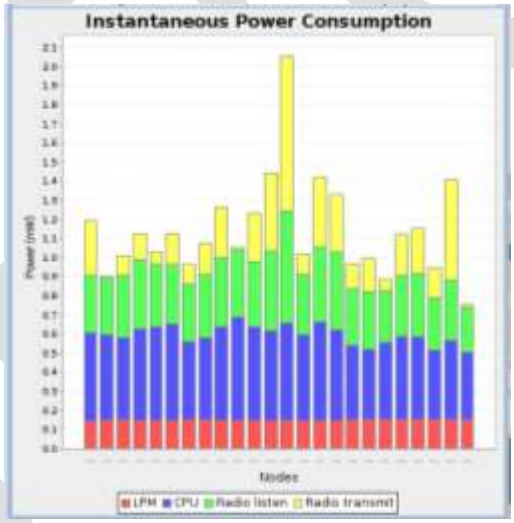

Figure 4: Instantaneous Power Consumption at RDC frequency of 4 Hz

After selection of the suitable protocols CoAP is used to control different sensors mounted on sensor nodes interfaces with Copper add on running on the Mozilla web browser over the Internet. The sensor node resources are mapped to CoAP uniform resource identifiers (URI) which can be accessed by the CoAP methods defined as GET, POST, PUT and DELETE. CoAP makes use of GET, PUT, POST, and DELETE methods in a same manner to HTTP and are used to manipulate the resources. A CoAP URI used in this example is coap://[aaaa::212:740b:b:b0b]5683/sen/humidity for humidity sensor. The user enters URI in browser and requests for a resource. The browser displays the result. Figure 5 and 6 shows the browser snapshots of the application while copper add on is working as client. In figure5 humidity sensor returns the value of 150.62 while accessing this resource with CoAP GET method. Similarly in the Figure 6 temp sensor is accessed via CoAP URI coap://[aaaa::212:740b:b:b0b]5683/sen/temp to get a value of 24.00^{o}C.

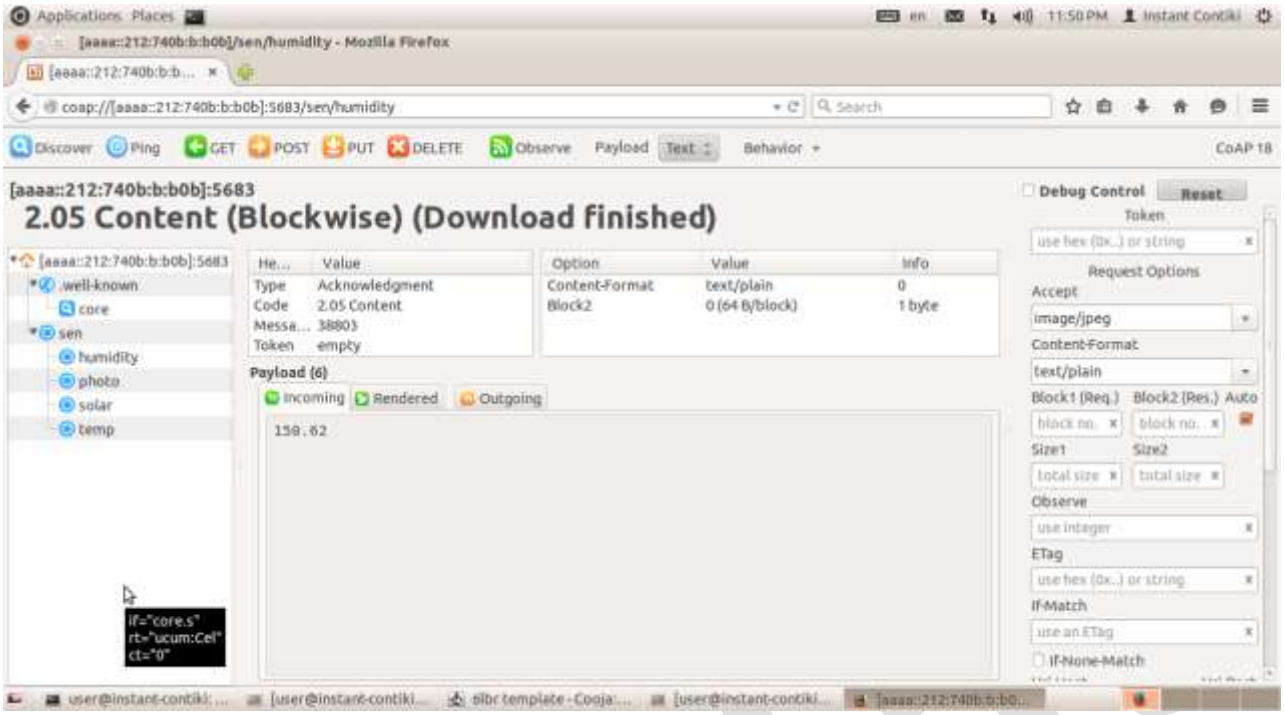

Figure 5: A successful response from a CoAP server to a request for its '/sen/humidity' resource, which returned the value "150.62"

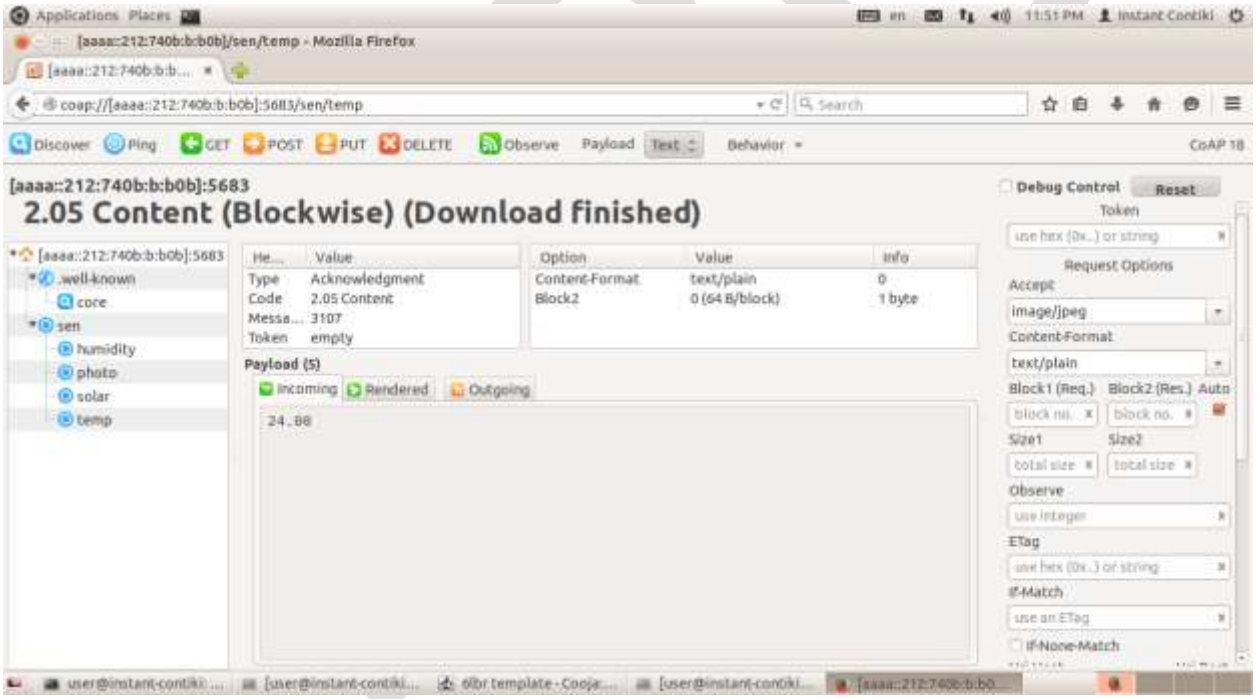

Figure 6: A successful response from a CoAP server to a request for its '/sen/temp' resource, which returned the value "24.00"

CONCLUSION

A smart home infrastructure is proposed which can be monitored and controlled over the Internet using CoAP. Since the wireless sensor nodes are constrained devices in terms of processing power and memory, it is essential to use suitable technologies and to achieve this Contiki OS is selected. Furthermore, an experimental evaluation is done to find the most suitable MAC and RDC layer protocols of Contiki OS MAC layer. In addition to it, variable, stack and application size optimization is done to fit the firmware in the

sensor nodes memory. Further studies can be carried out to propose new low memory footprint protocols which will enhance the life of sensor nodes.

REFERENCES:

[1] Dhananjay Singh, Gaurav Tripathi and Antonio J. Jara "A survey of Internet-of-Things: Future Vision, Architecture, Challenges and Services" IEEE Proc. of the IEEE World Forum on Internet of Things (WF-IoT), pp. 287-292, 2014

[2] Moataz Soliman, Tobi Abiodun, Tarek Hamouda, Jiehan Zhou1 and Chung-Horng Lung "Smart Home: Integrating Internet of Things with Web Services and Cloud Computing" IEEE International Conference on Cloud Computing Technology and Science, vol. 2, pp. 317 – 320, 2013

[3] Kang Bing, Liu Fu, Yun Zhuo, and Liang Yanlei "Design of an Internet of Things-based Smart Home System" 2nd International Conference on Intelligent Control and Information Processing (ICICIP), vol. 2, pp. 921 – 924, 2011

[4] Xiaojing Ye and Junwei Huang "A Framework for Cloud-based Smart Home" International Conference on Computer Science and Network Technology (ICCSNT), vol. 2, pp. 894 – 897, 2011

[5] Ventylees Raj.S "Implementation of pervasive computing based high-secure smart home system" IEEE International Conference on Computational Intelligence & Computing Research (ICCIC), pp. 1-8, 2012

[6] Haidong Wang, Jamal Saboune and Abdulmotaleb El Saddik "Control your smart home with an autonomously mobile smartphone" IEEE International Conference on Multimedia and Expo Workshops (ICMEW), pp. 1-6, 2013

[7] Pranay P. Gaikwad, Jyotsna P. Gabhane and Snehal S. Golait "A Survey based on Smart Homes System Using Internet-of-Things" IEEE International Conference on Computation of Power, Energy Information and Communication (ICCPEIC), pp. 0330 – 0335, 2015

[8] Andreas Kamilaris and Andreas Pitsillides "Towards Interoperable and Sustainable Smart Homes" 1ST IEEE Africa Conference and Exhibition (1ST-Africa), pp.1 -11, 2013

[9] Ming Wang, Guiqing Zhang, Chenghui Zhang, Jianbin Zhang, Chengdong Li "An IoT-based Appliance Control System for Smart Homes" Fourth International Conference on Intelligent Control and Information Processing (ICICIP), pp. 744-747, 2013

[10] Olaf Bergmann, Kai T. Hillmann, Stefanie Gerdes "A CoAP-Gateway for Smart Homes" International Conference on Computing, Networking and Communications, Communication Software and Services Symposium, pp.446 -450, 2012

[11] Dae-Man Han and Jae-Hyun Lim "Smart Home Energy Management System using IEEE 802.15.4 and ZigBee" IEEE Transactions on Consumer Electronics, vol. 56, no. 3, pp. 1403-1410, August 2010

[12] Dae-Man Han and Jae-Hyun Lim "Design and Implementation of Smart Home Energy Management Systems based on ZigBee" IEEE Trans. Consum. Electron, vol. 56, no. 3, pp.1417 -1425, 2010

[13] Z Shelby and C Bormann, "6LoWPAN: The Wireless Embedded Internet", John Wiley & Sons, November 2009

International Journal of Engineering Research and General Science Volume 3, Issue 6, November-December, 2015
ISSN 2091-2730

Dark - Side of TORRENT

Gaurav Kumar Roy

(Bachelor of Computer Application [BCA], C|EH, CCNA, Web Developer, Penetration Tester)

Email : gauravkxj62@gmail.com,

Abstract— In today's world, Internet has become the most indispensable part of human life & it's impossible to deny the advantages of internet after its changing the whole globe. The benefits are introduced in facilitating communications, decreasing the distances around the globe, emerging an easier life and surely many other benefits that one cannot deny. With the new move, the human mind is more connected to its surroundings and what lays beyond. For instance, anyone can communicate with anybody anywhere whenever they want. The history of internet began in 1950s with the development of electronic computers. Initial concepts of packet networking were originated in United-States, Great Britain & France. Among them, the Department Of Defense of US awarded contracts for packet network systems in early 1960s, including the development of the ARPANET (which become the first network to use the Internet Protocol.) The first message was sent over the ARPANET from computer science Professor Leonard Kleinrock's laboratory at University of California, Los Angeles (UCLA) to the second network node at Stanford Research Institute (SRI). Access to the ARPANET was expanded in 1981 when the National Science Foundation (NSF) funded the Computer Science Network (CSNET). In the 1980s, the work of Tim Berners-Lee in the United Kingdom, on the World Wide Web, theorized the fact that protocols link hypertext documents into a working system,[4] marking the beginning the modern Internet. Since then, all the legal internetwork we use today is based on ARPANET (Advanced research Project Agency Network). But other then ARPANET, there lies another networking technological architecture which primarily uses the internet but not to a full extent. It's the **torrent network**.

Keywords— Programming language, Server, P2P, Torrenting, IP address, Hackers, program, download/upload

INTRODUCTION

Torrent networking and its sharing feature was debuted in 2001. A Python-language programmer, **Bram Cohen**, who created this torrent - technology with the intent to share files with everyone across the globe by downloading it through the use of internet. Now what a **torrent-file** is? Basically, a **torrent file** is a computer file (*having extension* ***.torrent***) that contains metadata about files and folders to be distributed, and usually in a list of the network locations of trackers; which are computers, that help participants in the system find each other and form efficient . These groups are called "swarms". Torrent files does not contain the content to be distributed but only contains information about those files, such as their names, sizes, folder structure, and cryptographic hash values for verifying file-integrity.

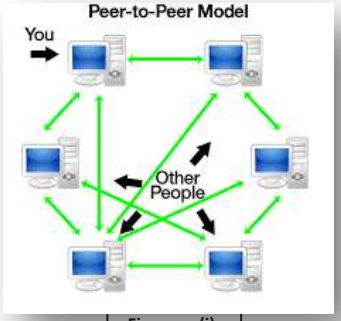

Figure :- (i)

Now, what **Torrenting** is basically a peer-to-peer (P2PP2P) or for easy understanding people-to-people file sharing system, where people upload and people download but from within the computer (& not from the server) via internet using a '.torrent' file. In case of Google Drive or Drop-box, the downloading is done from a single source, ie. where the files have been uploaded, only from that location (or we can say - single server) users can download the file and the speed is dependent on both single server's (DropBox's) and the ISP also. Torrenting is different method to solve sharing large data files from a single source or multiple sources. In the *figure (ii),*we have uploaders (who could be any-one) who upload that single file/folder & the downloader's who is getting help from uploader to download that file directly as torrenting works on peer-to-peer file sharing system. If there are lots of people uploading the same file,it becomes helpful to those downloaders' (people who are downloading) to easily fetch those chunks and parts of the file from different pc from around the world at the same time, maintaining the speed.

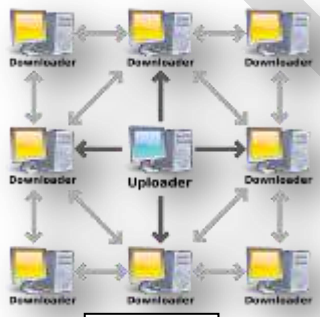

Figure :- (ii)

Figure :- (iii)

In the above *figure (iii)*, I'm downloading an OS(.iso file) which is getting downloaded from other two PCs residing one at Brazil and another at America also using uTorrent Mac with versions 1.8.7 & 1.8.6. This shows that the files which gets downloaded from torrent network are files residing at other's PCs. Now, with Torrent comes another two terms –

- *Seeders (Seeds)*
- *Leechers (Peers)*

Seeders are uploaders or those who have already downloaded the files & are currently uploading them, the more seeders a file have – the faster file gets uploaded (each seeder uses a minimum of 10kbps to upload); & accordingly spend their bandwidth to help a file get downloaded to the downloaders. Leechers are downloaders who doesn't have the entire file & is using torrent network to download any specific file. During this file sharing procedure, you will be able to know people's IP-address and the same case happens with us too. Other torrent users are also getting my IP-address. In short, every torrent users on torrent network share their IPaddress during the process called download.Unlike other download methods, Torrent maximizes transfer speed by gathering pieces of the file you want and downloading these pieces simultaneously from people/other torrent users who already have them. This process makes popular and very large files, such as videos and television programs, download much faster than is possible with other protocols. There is another term Pieces which refers to the torrented files being divided into equal specific sizes(eg. 64kB,128kB, 512kB, 1MB, 2MB, 4MB). The pieces are distributed in a random sequence among peers in order to optimize trading efficiency.

Is torrent legal? - Many of the torrent users think that it is not legal. But the truth is, "Torrent is Legal" which is simply sharing files from one device to another via internet where one person share files with other(or with the world) following the Peer-topeer (P2P) architecture. But those files (songs, games, software) which are uploaded on the internet with cracks & patches are illegal, and downloading those cracked games & software (which costs money) using the torrent network is illegal. If we are sharing copyrighted content with other people,that is considered illegal. We can use torrent for legal purposes by sharing large Open-Source files faster & easier. No (Internet Service Providers) ISP will put you in jail for using torrents, but some Internet providers don't like torrents & hence they slower the speed while users browse torrent sites or sometimes block users from accessing those sites. In gist, the programs or technologies behind torrent based file-sharing are not illegal. It's the data being shared that may be illegal. Using Bit-Torrent or other file sharing programs to download software (trial), a game demo, movie trailer, or similar is legal. However, using that same program to download a new hit song or a movie still in theaters is illegal.

How is Torrent Dangerous? - There are many disadvantages while normal users do torrenting, but most of the torrent users are unaware of it. Firstly, as said earlier, while downloading any file using the torrent, your IP-address gets shared and others can track you using trackers (which keeps tracks of which seeds & peers are in the swarm) . Secondly, if someone (hackers) does social engineering or even get access to your system(s) using backdoors (trojans & botnets) or using other penetration technique, they may use those torrent programs (such as uTorrent, Bit-Torrent, Vuze etc),to create a torrent file (which could be your sensitive data, project, personal photos and videos).The steps for doing this are :-

(i) Search in victim's PC the directory where his/her sensitive files are stored.

(ii) We can create our own torrent using any of the torrent downloader program (such as : uTorrent, Bit-Torrent, Vuze).

(iii)

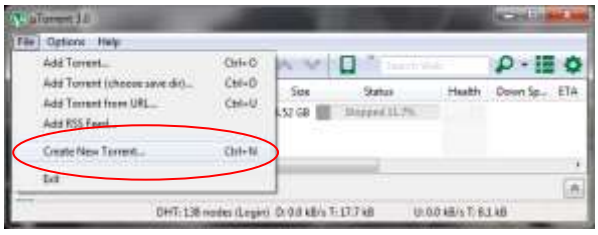

(iv) "Add File" is for selecting any specific file & "Add Directory" is for selecting

an entire folder.

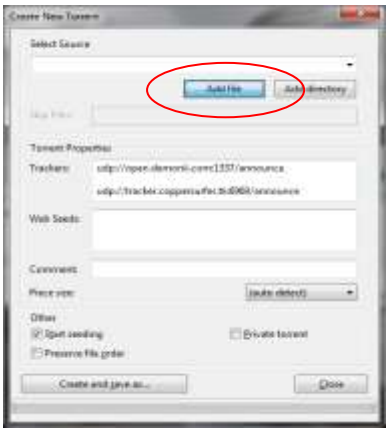

(v) After clicking “Add File” button , select the file you want to make as torrent.

(vi) Click on “Create & Save As” button

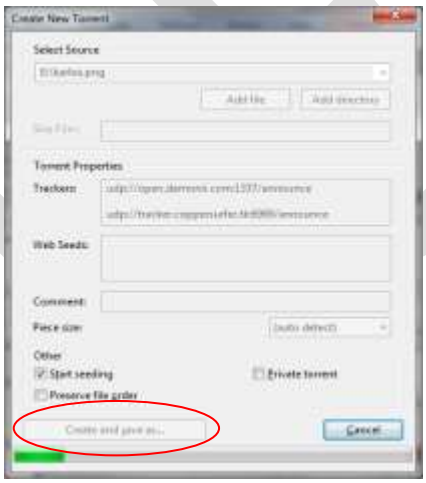

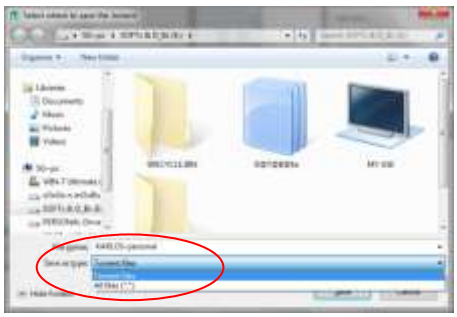

(vii) Give the .torrent file a name (here : KARLOS-personal) and file type as – ‘Torrent files’ give the file a location where it
will be created and click the ‘Save’ button.

(viii) Now, your torrent file is ready on that saved location.
(ix) After the .torrent file gets created, it will show its “seeding” stage in any torrent downloading software (that is installed in your PC)

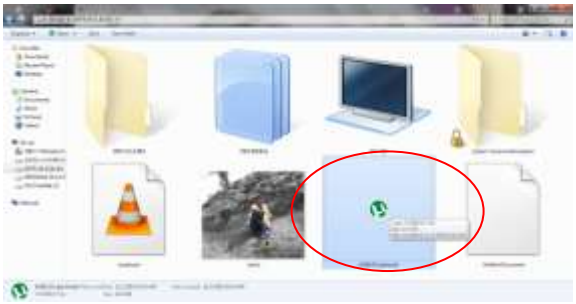

(x) Grab that .torrent file and somehow upload it in any torrent site. The steps for uploading .torrent files are :-

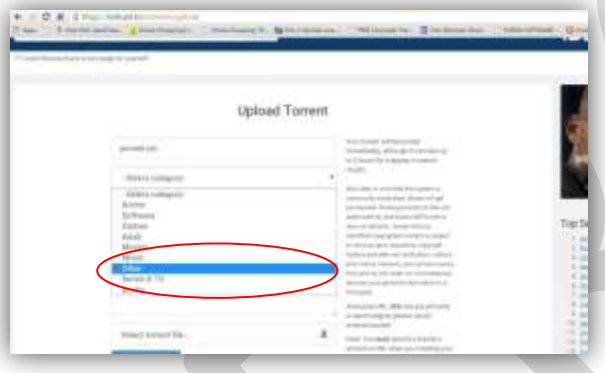

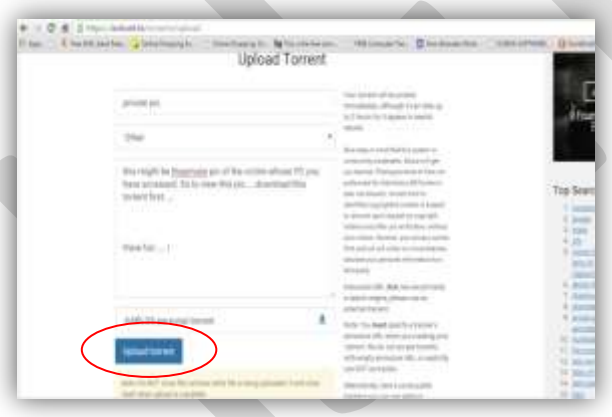

(xi) After the torrent is being uploaded, it has seeders but need 2-4 days to gradually increase the peers. In this way anyone can make your (victim's) personal photos, videos, projects and other files open to the world.

How to make Torrent users Secure? – As told earlier, torrent users can be tracked down using the IP address, since this a peer-to-peer system (people know your IP & you know people's IPs). So there is an extra tool (for Windows) available called *PEER-BLOCK*; what peer block does is : it lets you control who your computer 'talks to' on the internet by selecting appropriate lists of 'known bad' computers- you can block communication with other users (peers), advertising or spyware oriented servers, computers monitoring your P2P activities, computers those have been hacked etc. This tool becomes a precious shield when you become a seeder. This tool restricts access and henceforth can't

get others into your computer & your computer won't try to send anything either. To download the tool, visit : www.peerblock.com . There is also another tool called *Peer-Guardian* for MAC users also.
We can also take other precautions such as keep all our private/personal photos, videos, projects, files in a separate external hard disk or we can run these torrent programs in a virtual environment.

ACKNOWLEDGMENT

I, the author would like to thank those anonymous readers and reviewers who found this topic fruitful. I would also like to thank the
Department of Computer Science and Application of Karimganj College and Assam University & Byte-Code Cyber Security Pvt. Ltd who supported me, encouraged me to perform such research work.

CONCLUSION

Now-a-days security has become the prime issue for computer users. Torrent based file stealing and broadcasting that file to the entire world
can lead the victim to a dangerous situation and so torrent users must remain cautious while accessing torrent network using torrent programs.

REFERENCES:

[1] G. B. Shelly, T. J. Cashman and M. E. Vermaat, "Discovering Computers 2005: A Gateway to Information," Course Technology, Boston, 2004.

[2] Cache logic, Bit Torrent bandwidth usage http://www.cachelogic.com/research/2005_slide06.php

[3] Multitracker specification http://home.elp.rr.com/tur/multitracker-spec.txt

[4] Additional information on the Bit Torrent Protocol http://wiki.theory.org/BitTorrentSpecification

[5] Investigation into the extent of infringing content on Bit Torrent Network by Robert Layton & Paul Watters

[6] L. Wang and J. Kangasharju, "Monitoring bittorrent mainline dht," Department of Computer Science, University of Helsinki, Tech. Rep., 2012, available at http://www.cs.helsinki.fi/u/jakangas/Papers/BTReport. pdf.

[7] J. Liang, N. Naoumov, and K. W. Ross, "The index poisoning attack in p2p file sharing systems," in Proc. of IEEE Infocom, 2006.
[8] D. Stutzbach and R. Rejaie, "Understanding churn in peer-to-peer networks," in Proceedings of ACM SIGCOMM Internet measurement conference, 2006.

International Journal of Engineering Research and General Science Volume 3, Issue 6, November-December, 2015
ISSN 2091-2730

Anthropomorphic Robotic Arm

Parasdeep Singh [i], Prashant Saxena [ii]

[i]Independent Reasearcher, parasdeep@protnmail.ch -9921674762

[ii]Independent Reasearcher, prashant.saxena@sitpune.edu.in-7387492617

Abstract- Our project basically deals in mechatronics, which aims to integrate mechanical, electrical and biological systems. In this report we will look at development of an anthropomorphic robotic arm that will mimic actions of a human arm.

Search and Rescue vehicle are used for a myriad of tasks in the 21st century. They are designed to do particular tasks that humans can but will not do, or even things humans cannot do. Our objective is to design and construct a vehicle to be used in an emergency response mission that will be able to venture into terrain and environments that are otherwise too dangerous for human responders.

The main function of the Rescue vehicle is to detect survivors using real time video transmission and send robot location via Bluetooth GPS receiver mounted on robot. The video camera will also be connected to PC wirelessly for real time video transmitting. The GPS will also send location data to PC and it will have the location where rescuers are to be sent. The vehicle is manually controlled by an operator and will be driven via looking at real-time video feedback received on PC.

The Mechanical Engineering part of this project is to design the actual platform for the robot to travel. Vehicle has 6 wheels, each wheel powered individually by an electric motor similar to many bomb disposal robots, so that it can traverse rough terrain. Motors with appropriate torque and speed have been selected based on weight and performance parameters. Two basic factors have been considered while designing the vehicle, first is vehicle performance and second is cost.

We aim to create an affordable robotic arm that is lightweight, easy to use, and performs as similar as possible to a natural arm. Our first task is to detect myoelectric signals from hand movements, process them and convert them to a form suitable as input to a microcontroller. We also plan to make a functional elbow joint and a palm with fingers capable of independent movement, minimizing weight and construction cost while maintaining structural strength.

Also, in order to improve its user efficiency, we have mounted the slave arm on top of a vehicular mobile unit. This enables us to move the slave arm to different locations too to perform multiple tasks and to even reach to areas which are difficult for a human physically. This vehicular mobile unit is remote controlled and is very user friendly. It has been designed keeping in mind all the needful and expected ergonomics and can even bear the weight upto 50kg for a possible situation where the slave arm is expected to lift something heavy and move it. This vehicle also has the ability to cross considerable size of obstacles without getting disbalanced or toppling.

Constraints like weight, dimensions, sensitivity of the arm and mobile vehicle will be verified at each stage of development.

Keywords- Mechatronics, microcontroller.Bionic arm,master slave, potentiometer, degree of freedom, servo motor ,Aurdino.

INTRODUCTION

Our project basically deals in mechatronics, which aims to integrate mechanical, electrical and biological systems. In this report we will look at development of an anthropomorphic robotic arm that will mimic actions of a human arm.

We aim to create an affordable robotic arm that is lightweight, easy to use, and performs as similar as possible to a natural arm. Our first task is to detect myoelectric signals from hand movements, process them and convert them to a form suitable as input to a microcontroller. We also plan to make a functional elbow joint and a palm with fingers capable of independent movement, minimizing weight and construction cost while maintaining structural strength.

Also, in order to improve its user efficiency, we have mounted the slave arm on top of a vehicular mobile unit. This enables us to move the slave arm to different locations too to perform multiple tasks and to even reach to areas which are difficult for a human physically. This vehicular mobile unit is remote controlled and is very user friendly. It has been designed keeping in mind all the needful and expected ergonomics and can even bear the weight upto 50kg for a possible situation where the slave arm is expected to lift something heavy and move it. This vehicle also has the ability to cross considerable size of obstacles without getting disbalanced or toppling.

Constraints like weight, dimensions, sensitivity of the arm and mobile vehicle will be verified at each stage of development.

CHAPTER 2: LITERATURE SURVEY

2.1 ROLE OF ELECTRONICS ENGINEERING

The role of electronic engineers in this project is to detect and receive the signals from the master arm .The signals sent by the master arm are carried through to the slave arm. The concept is that when movement is made in master arm, there is a voltage variation of some order in the connected potentiometers. This variation can be easily sent to the slave arm to copy the actions. The signals once detected have to be treated and transmitted using a micro controller.

We have used potentiometers which will be attached to the master arm. These will then send the signals and these signals are interpreted by the microcontroller which drives the servo motor in slave arm.

2.2 ROLE OF MECHANICAL ENGINEERING

The field of mechanics plays a very crucial part in the project. The signals received by the controller are used to control the arm. The design of the arm is thus very important.

The arm provides 7 DOF i.e it can copy most of the human arm movements easily including holding and grasping.

The mechanical engineering plays a very crucial part in selection of motor and chassis designing of the mobile vehicle. We had to choose the motors for both, vehicle and the arms based on different torque requirements and various calculations for it had to be performed. Various comparisons between different types of motors were done to finally decide the servo motor and DC motors which would be used in our project.

And the arm was designed using a 4-bar linkage to produce clamping motion. The pressure of the clamp is derived from a Hitech HS-311 servo motor. The servomotor produces up to a ±90° rotation based on the programming of the microcontroller. Inside the servo motor is a simple potentiometer. The potentiometer, or variable resistor, will allow the motor to rotate until the intended position is reached. Once the position is reached the motor will stop rotating. It will only be prompted to move again if a new signal is provided by the microcontroller.

CHAPTER 3: METHODOLOGY

3.1. ROBOTIC ARMS

3.1.1 ARDUINO

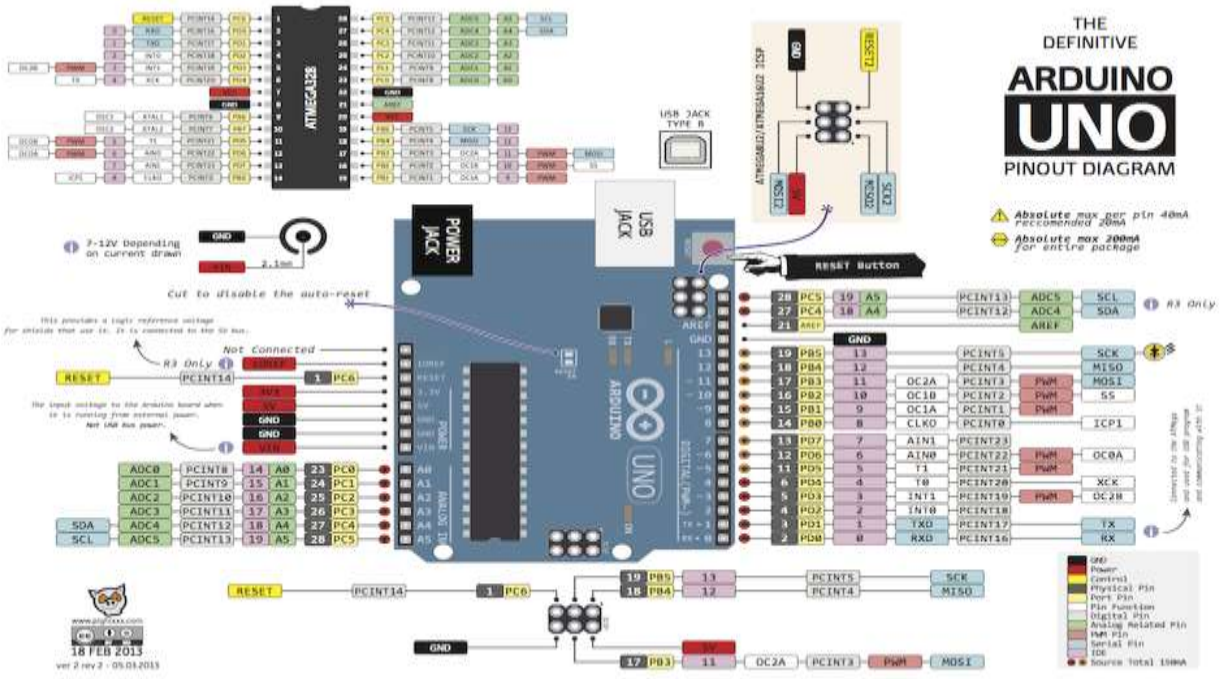

Arduino can sense the environment by receiving input from a variety of sensors and can affect its surroundings by controlling lights, motors, and other actuators. The microcontroller on the board is programmed using the Arduino programming language (based

on Wiring) and the Arduino development environment (based on Processing). Arduino projects can be stand-alone or they can communicate with software running on a computer (e.g. Flash, Processing,MaxMSP).

The boards can be built by hand or purchased preassembled; the software can be downloaded for free. The hardware reference designs (CAD files) are available under an open-source license, you are free to adapt them to your needs.

Arduino received an Honorary Mention in the Digital Communities section of the 2006 Ars Electronica Prix. The Arduino founders are: Massimo Banzi, David Cuartielles, Tom Igoe, Gianluca Martino, and David Mellis. Credits.

ARDUINO ATmega

- This is a microcontroller board based on the ATmega328 (datasheet).
- It has 14 digital input/output pins (of which 6 can be used as PWM outputs)
- 6 analog inputs.
- A 16 MHz ceramic resonator
- USB connection
- Power jack
- ICSP header
- reset button.

It contains everything needed to support the microcontroller; simply connect it to a computer with a USB cable or power it with a AC-to-DC adapter or battery to get started.

The Uno differs from all preceding boards in that it does not use the FTDI USB-to-serial driver chip. Instead, it features the Atmega16U2 (Atmega8U2 up to version R2) programmed as a USB-to-serial.

Revision 2 of the Uno board has a resistor pulling the 8U2 HWB line to ground.

Revision 3 of the board has the following new features:

- 1.0 pinout: added SDA and SCL pins that are near to the AREF pin and two other new pins placed near to the RESET pin, the IOREF that allow the shields to adapt to the voltage provided from the board. In future, shields will be compatible with both the board that uses the AVR, which operates with 5V and with the Arduino Due that operates with 3.3V. The second one is a not connected pin, that is reserved for future purposes.
- Stronger RESET circuit.
- Atmega 16U2 replace the 8U2.

"Uno" means one in Italian and is named to mark the upcoming release of Arduino 1.0. The Uno and version 1.0 will be the reference versions of Arduino, moving forward. The Uno is the latest in a series of USB Arduino boards, and the reference model for the Arduino platform; for a comparison with previous versions, see the index of Arduino boards

SUMMARY

Microcontroller	ATmega328
Operating Voltage	5V
Input Voltage (recommended)	7-12V
Input Voltage (limits)	6-20V
Digital I/O Pins	14 (of which 6 provide PWM output)
Analog Input Pins	6
DC Current per I/O Pin	40 mA
DC Current for 3.3V Pin	50 mA
Flash Memory	32 KB (ATmega328) of which 0.5 KB used by bootloader
SRAM	2 KB (ATmega328)
EEPROM	1 KB (ATmega328)
Clock Speed	16 MHz

EAGLE files: arduino-uno-Rev3-reference-design.zip (NOTE: works with Eagle 6.0 and newer)

Schematic: arduino-uno-Rev3-schematic.pdf

Note: The Arduino reference design can use an Atmega8, 168, or 328, Current models use an ATmega328, but an Atmega8 is shown in the schematic for reference. The pin configuration is identical on all three processors

POWER

The Arduino Uno can be powered via the USB connection or with an external power supply. The power source is selected automatically.

External (non-USB) power can come either from an AC-to-DC adapter (wall-wart) or battery. The adapter can be connected by plugging a 2.1mm center-positive plug into the board's power jack. Leads from a battery can be inserted in the Gnd and Vin pin headers of the POWER connector.

The board can operate on an external supply of 6 to 20 volts. If supplied with less than 7V, however, the 5V pin may supply less than five volts and the board may be unstable. If using more than 12V, the voltage regulator may overheat and damage the board. The recommended range is 7 to 12 volts.

The power pins are as follows:

- VIN. The input voltage to the Arduino board when it's using an external power source (as opposed to 5 volts from the USB connection or other regulated power source). You can supply voltage through this pin, or, if supplying voltage via the power jack, access it through this pin.
- 5V.This pin outputs a regulated 5V from the regulator on the board. The board can be supplied with power either from the DC power jack (7 - 12V), the USB connector (5V), or the VIN pin of the board (7-12V). Supplying voltage via the 5V or 3.3V pins bypasses the regulator, and can damage your board.
- 3V3. A 3.3 volt supply generated by the on-board regulator. Maximum current draw is 50 mA.
- GND. Ground pins.

- IOREF. This pin on the Arduino board provides the voltage reference with which the microcontroller operates. A properly configured shield can read the IOREF pin voltage and select the appropriate power source or enable voltage translators on the outputs for working with the 5V or 3.3V.

MEMORY

The ATmega328 has 32 KB (with 0.5 KB used for the bootloader). It also has 2 KB of SRAM and 1 KB of EEPROM (which can be read and written with the EEPROM library).

INPUT AND OUTPUT

Each of the 14 digital pins on the Uno can be used as an input or output, using pinMode(), digitalWrite(), anddigitalRead() functions. They operate at 5 volts. Each pin can provide or receive a maximum of 40 mA and has an internal pull-up resistor (disconnected by default) of 20-50 kOhms. In addition, some pins have specialized functions:

- Serial: 0 (RX) and 1 (TX). Used to receive (RX) and transmit (TX) TTL serial data. These pins are connected to the corresponding pins of the ATmega8U2 USB-to-TTL Serial chip.
- External Interrupts: 2 and 3. These pins can be configured to trigger an interrupt on a low value, a rising or falling edge, or a change in value. See the attachInterrupt() function for details.
- PWM: 3, 5, 6, 9, 10, and 11. Provide 8-bit PWM output with the analogWrite() function.
- SPI: 10 (SS), 11 (MOSI), 12 (MISO), 13 (SCK). These pins support SPI communication using the SPI library.
- LED: 13. There is a built-in LED connected to digital pin 13. When the pin is HIGH value, the LED is on, when the pin is LOW, it's off.

The Uno has 6 analog inputs, labelled A0 through A5, each of which provide 10 bits of resolution (i.e. 1024 different values). By default they measure from ground to 5 volts, though is it possible to change the upper end of their range using the AREF pin and the analogReference() function. Additionally, some pins have specialized functionality:

- TWI: A4 or SDA pin and A5 or SCL pin. Support TWI communication using the Wire library.

There are a couple of other pins on the board:

- AREF. Reference voltage for the analog inputs. Used with analogReference().
- Reset. Bring this line LOW to reset the microcontroller. Typically used to add a reset button to shields which block the one on the board.

See also the mapping between Arduino pins and ATmega328 ports. The mapping for the Atmega8, 168, and 328 is identical.

COMMUNICATION

The Arduino Uno has a number of facilities for communicating with a computer, another Arduino, or other microcontrollers. The ATmega328 provides UART TTL (5V) serial communication, which is available on digital pins 0 (RX) and 1 (TX). An ATmega16U2 on the board channels this serial communication over USB and appears as a virtual com port to software on the computer. The '16U2 firmware uses the standard USB COM drivers, and no external driver is needed. However, on Windows, a .inf file is required. The Arduino software includes a serial monitor which allows simple textual data to be sent to and from the Arduino board. The RX and TX LEDs on the board will flash when data is being transmitted via the USB-to-serial chip and USB connection to the computer (but not for serial communication on pins 0 and 1).

A SoftwareSerial library allows for serial communication on any of the Uno's digital pins.

The ATmega328 also supports I2C (TWI) and SPI communication. The Arduino software includes a Wire library to simplify use of the I2C bus; see the documentation for details. For SPI communication, use the SPI library.

PROGRAMMING

The Arduino Uno can be programmed with the Arduino software (download). Select "Arduino Uno from the Tools > Board menu (according to the microcontroller on your board). For details, see the reference and tutorials.

The ATmega328 on the Arduino Uno comes preburned with a bootloader that allows you to upload new code to it without the use of an external hardware programmer. It communicates using the original STK500 protocol (reference,C header files).

You can also bypass the bootloader and program the microcontroller through the ICSP (In-Circuit Serial Programming) header; see these instructions for details.

The ATmega16U2 (or 8U2 in the rev1 and rev2 boards) firmware source code is available . The ATmega16U2/8U2 is loaded with a DFU bootloader, which can be activated by:

- On Rev1 boards: connecting the solder jumper on the back of the board (near the map of Italy) and then resetting the 8U2.
- On Rev2 or later boards: there is a resistor that pulling the 8U2/16U2 HWB line to ground, making it easier to put into DFU mode.

You can then use Atmel's FLIP software (Windows) or the DFU programmer (Mac OS X and Linux) to load a new firmware. Or you can use the ISP header with an external programmer (overwriting the DFU bootloader). See this user-contributed tutorial for more information.

AUTOMATIC (SOFTWARE) RESET

Rather than requiring a physical press of the reset button before an upload, the Arduino Uno is designed in a way that allows it to be reset by software running on a connected computer. One of the hardware flow control lines (DTR) of the ATmega8U2/16U2 is connected to the reset line of the ATmega328 via a 100 nanofarad capacitor. When this line is asserted (taken low), the reset line drops long enough to reset the chip. The Arduino software uses this capability to allow you to upload code by simply pressing the upload button in the Arduino environment. This means that the bootloader can have a shorter timeout, as the lowering of DTR can be well-coordinated with the start of the upload.

This setup has other implications. When the Uno is connected to either a computer running Mac OS X or Linux, it resets each time a connection is made to it from software (via USB). For the following half-second or so, the bootloader is running on the Uno. While it is programmed to ignore malformed data (i.e. anything besides an upload of new code), it will intercept the first few bytes of data sent to the board after a connection is opened. If a sketch running on the board receives one-time configuration or other data when it first starts, make sure that the software with which it communicates waits a second after opening the connection and before sending this data.

The Uno contains a trace that can be cut to disable the auto-reset. The pads on either side of the trace can be soldered together to re-enable it. It's labeled "RESET-EN". You may also be able to disable the auto-reset by connecting a 110 ohm resistor from 5V to the reset line; see this forum thread for details.

USB OVERCURRENT PROTECTION

The Arduino Uno has a resettable polyfuse that protects your computer's USB ports from shorts and overcurrent. Although most computers provide their own internal protection, the fuse provides an extra layer of protection. If more than 500 mA is applied to the USB port, the fuse will automatically break the connection until the short or overload is removed.

PHYSICAL CHARACTERISTICS

The maximum length and width of the Uno PCB are 2.7 and 2.1 inches respectively, with the USB connector and power jack extending beyond the former dimension. Four screw holes allow the board to be attached to a surface or case. Note that the distance between digital pins 7 and 8 is 160 mil (0.16"), not an even multiple of the 100 mil spacing of the other pins.

DESIGNING THE ARM

In manipulator structures, stiffness-to-weight ratio of a link is very important since inertia forces induce the largest deflections. Therefore, an increase in the Elastic modulus, E would be very desirable if it is not accompanied by an unacceptable increase in specific density, γ. The Elastic modulus is an indication of the material's resistance to breakage when subjected to force. The best properties are demonstrated by ceramics and beryllium but ceramics have a problem of brittleness and beryllium is very expensive. Structural materials such as magnesium (Mg), aluminium (Al), and titanium (Ti) which are light have about the same E/γ ratios as steel and are used when high strength and low weight are more important than E/γ ratios. Factors like ageing, creep in under constant loads, high thermal expansion coefficient, difficulty in joining with metal parts, high cost and the fact that they are not yet commercially available make the use of fibre-reinforced materials limited though they have good stiffness-to-weight ratios. However, with advances in research, some of the mentioned setbacks have been significantly reduced.. Aluminumlithium alloy have better processing properties and is not very expensive. Alloyedmaterials such as Nitinol (nickel – titanium – aluminium), aluminium incramute (copper -manganese – aluminium) are also commercially available. Therefore the materials recommended for use in this project are

•Al-Li alloys

• Nitinol (nickel-titanium-aluminium)

•Incramute (copper-manganese-aluminum)

•Glass-reinforced Plastic (GRP)The links have an internal hollow area, which provides conduits for power transmitting components i.e. gears in this case, and the stepper motors. At the same time, their external dimensions are limited in order to reduce waste of the usable workspace. They are as light as possible to reduce inertia forces and allow for the highest external load per given size of motors and actuators. For a given weight, links have to possess the highest possible.

Bending (and torsional) stiffness. The parameter to be modified to comply with these constraints is the shape of the cross-section. The choice is between hollow round and hollow rectangular cross-section. From design standpoint of view, the links of square or rectangular cross-section have advantage of strength and machinability ease over round sections. Despite the recommendations mentioned above as regards choice of materials, our options were narrowed down to a choice between steel, GRP, and aluminium based on feasibility studies carried out. Current trend in robotics (especially industrial robotics) shows a quest to achieve lighter designs with reasonable strength. This design goal has always meant a trade-off in terms of cost. Composite materials are generally more expensive than most metals used in industrial robots fabrication. For the particular case of our project, we narrowed our options down to composite material – glass reinforced plastic – otherwise known as GRP and aluminium. The original project, upon which we are building, was fabricated with steel sheets. The sheets cost practically nothing because metal scraps were used, but there was a setback of the motors not being able to cope with the weight of the metal .We figured out at least three ways of overcoming the setback mentioned above. One option would have been to redesign the gear trains and increase torque amplification, so that the motors can support the load. The torque amplification here would have been limited by the real estate on the arm for the gear train and the maximum speed we would be able to give to the motors, as output speed would reduce with increase in torque. We discarded this idea based on long-term considerations. This would mean that much of the energy expended by the robot would go to lifting its own weight thereby reducing the effective load it can lift.

Another option would have been to replace the motors with others having higher torque ratings. This, for us, would almost be as expensive as re-fabricating the arm with a lighter material, and the problem of effective load, as mentioned previously, would still be there. A third option was to re-fabricate the arm, or at least part of it, with a lighter material of reasonable strength, and that was the option we went for. It certainly involved increased short-term costs but then we foresaw a pay off in the long term. We would no longer be constrained to jeopardize the speed or maximum effective load of the robot while trying to increase torque; instead, any torque amplification would directly translate to increased effective load the robot can lift.After more research and consultations with our supervisor and some lecturers in the Mechanical Engineering department, who are experts in the field, we settled for aluminium mainly on grounds of cost and workability.

THE GEAR SYSTEM

In this work, we have chosen the bevel, spur and spiral types of gears. These were readily available from scrap machines (photocopiers). Spiral gears have the advantage of high torque amplification within a relatively small space. The necessary data for the selection and choice of the gear arrangements at each joint

i.Power transmitted, P = TW

ii.Transmitted speed, ω (rad/s)

iii.Torque developed , T (Nm)

iv.Lewis form factor, Y

v.Bending stress, σ ,(ultimate tensile strength)

vi.Ultimate tensile strength

vii.Factor of safety, n

viii.Module of gear, m

ix.Number of teeth, N

CHAPTER:4

EXPERIMENT WORK

4.1 BLOCK DIAGRAM OF EMG HAND

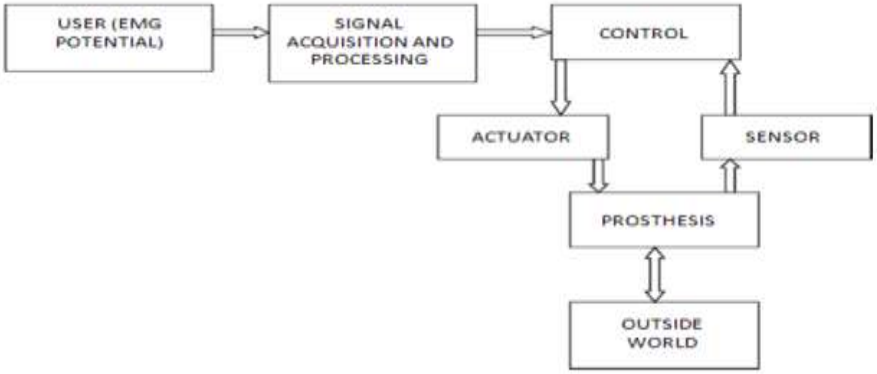

4.1.2 MICROCONTROLLER

The EMG signals are fed to the microcontroller. According to the voltage levels, the Servo motor is controlled. The controller converts the analog signals into the PWM(Pulse Width Modulated)signal for driving the motor.

4.1.3 SERVO MOTOR

The signals sent to the motor control and rotate it in the clockwise or anti-clockwise direction. The servo motor that is being used has the drivers and negative feedback position control loop hard- wired.

4.4 SERVO LIBRARY

This library allows an Arduino board to control RC (hobby) servo motors. Servos have integrated gears and a shaft that can be precisely controlled. Standard servos allow the shaft to be positioned at various angles, usually between 0 and 180 degrees. Continuous rotation servos allow the rotation of the shaft to be set to various speeds.

The Servo library supports up to 12 motors on most Arduino boards and 48 on the Arduino Mega. On boards other than the Mega, use of the library disables analogWrite() (PWM) functionality on pins 9 and 10, whether or not there is a Servo on those pins. On the Mega, up to 12 servos can be used without interfering with PWM functionality; use of 12 to 23 motors will disable PWM on pins 11 and 12.

4.4.1 CIRCUIT CONNECTIONS

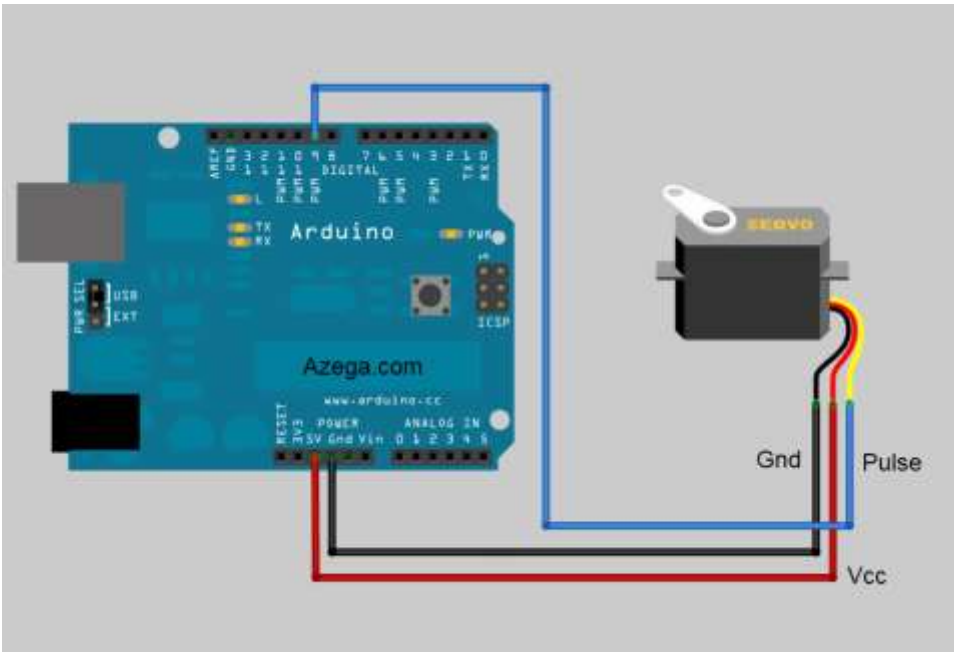

Fig: Interfacing Servo Motor with Arduino

Servo motors have three wires: power, ground, and signal. The power wire is typically red, and should be connected to the 5V pin on the Arduino board. The ground wire is typically black or brown and should be connected to a ground pin on the Arduino board. The signal pin is typically yellow, orange or white and should be connected to a digital pin on the Arduino board. Note that servos draw considerable power, so if you need to drive more than one or two, you'll probably need to power them from a separate supply (i.e. not the +5V pin on your Arduino). Be sure to connect the grounds of the Arduino and external power supply together.

4.4.2 FUNCTIONS USED

4.4.2.1 attach ()

- Description

Attach the Servo variable to a pin. Note that in Arduino 0016 and earlier, the Servo library supports only servos on only two pins: 9 and 10.

- Syntax

servo.attach(pin)

servo.attach(pin, min, max)

- Parameters

servo: a variable of type Servo

pin: the number of the pin that the servo is attached to

min (optional): the pulse width, in microseconds, corresponding to the minimum (0-degree) angle on the servo (defaults to 544)

max (optional): the pulse width, in microseconds, corresponding to the maximum (180-degree) angle on the servo (defaults to 2400).

4.4.2.2 write()

- Description

Writes a value to the servo, controlling the shaft accordingly. On a standard servo, this will set the angle of the shaft (in degrees), moving the shaft to that orientation. On a continuous rotation servo, this will set the speed of the servo (with 0 being full-speed in one direction, 180 being full speed in the other, and a value near 90 being no movement).

- Syntax

servo.write(angle)

- Parameters

servo: a variable of type Servo

angle: the value to write to the servo, from 0 to 180

4.4.2.3 pinMode()

- Description

Configures the specified pin to behave either as an input or an output. See the description of digital pins for details on the functionality of the pins.

As of Arduino 1.0.1, it is possible to enable the internal pullup resistors with the mode INPUT_PULLUP. Additionally, the INPUT mode explicitly disables the internal pullups.

- Syntax

pinMode(pin, mode)

- Parameters

pin: the number of the pin whose mode you wish to set

mode: INPUT, OUTPUT, or INPUT_PULLUP. (see the digital pins page for a more complete description of the functionality.)

- Returns

None

4.4.2.4 analogRead()

- Description

Reads the value from the specified analog pin. The Arduino board contains a 6 channel (8 channels on the Mini and Nano, 16 on the Mega), 10-bit analog to digital converter. This means that it will map input voltages between 0 and 5 volts into integer values between 0 and 1023. This yields a resolution between readings of: 5 volts / 1024 units or, .0049 volts (4.9 mV) per unit. The input range and resolution can be changed using analogReference().

It takes about 100 microseconds (0.0001 s) to read an analog input, so the maximum reading rate is about 10,000 times a second.

- Syntax

analogRead(pin)

- Parameters

pin: the number of the analog input pin to read from (0 to 5 on most boards, 0 to 7 on the Mini and Nano, 0 to 15 on the Mega)

- Returns

int (0 to 1023)

- Note

If the analog input pin is not connected to anything, the value returned by analogRead() will fluctuate based on a number of factors (e.g. the values of the other analog inputs, how close your hand is to the board, etc.

4.4.3 CODE FOR READING ANALOG INPUT AND CONTROL THE SERVO MOTOR

```
#include <Servo.h>// include the servo library
Servo myServo;  // create a servo object
int const potPin = A0; // analog pin used to connect the  circuit
int potVal;  // variable to read the value from the analog pin
//int angle;   // variable to hold the angle for the servo motor
int pos = 0;    // variable to store the servo position
void setup()
{
  pos = 0; /* Initialise pos */
 myServo.write(0);    /*When you create a new Servo object, its position
                        is automatically given a default of 90. By setting a position first,
                         Then attaching the servo, you can have it start at a
                          position other than 90.*/
 myServo.attach(9);   // attaches the servo on pin 9 to the servo object
```

```
  pinMode(potVal, INPUT);
}



void loop()
 {
  potVal = analogRead(potPin); // read the value of the potentiometer
  // scale the numbers from the pot
if(potVal>=204&& potVal <=446)// if analog voltage is between 0.5 v to
                                        2.18volts then move the motor clockwise.


for(pos; pos <= 170; pos += 1)  /* pos need not be at 0 for this to work.*
  {
    myServo.write(pos);              // tell servo to go to position  to variable 'pos'
    delay(15);                                 // waits 15ms for the servo to reach
                                      //the position.
 }
 }
  else
  {
for(pos; pos >= 0; pos -= 1) /* pos need not be at 170 for this to work.
                                      If potVal becomes < 204 rotate servo anticlockwise
{                                      in steps of 1 degree*/
    myServo.write(pos);              // tell servo to go to position in
                                       //  variable 'pos'
    delay(15);                    // waits 15ms for the servo to reach
```

```
                    //  the position

}
```

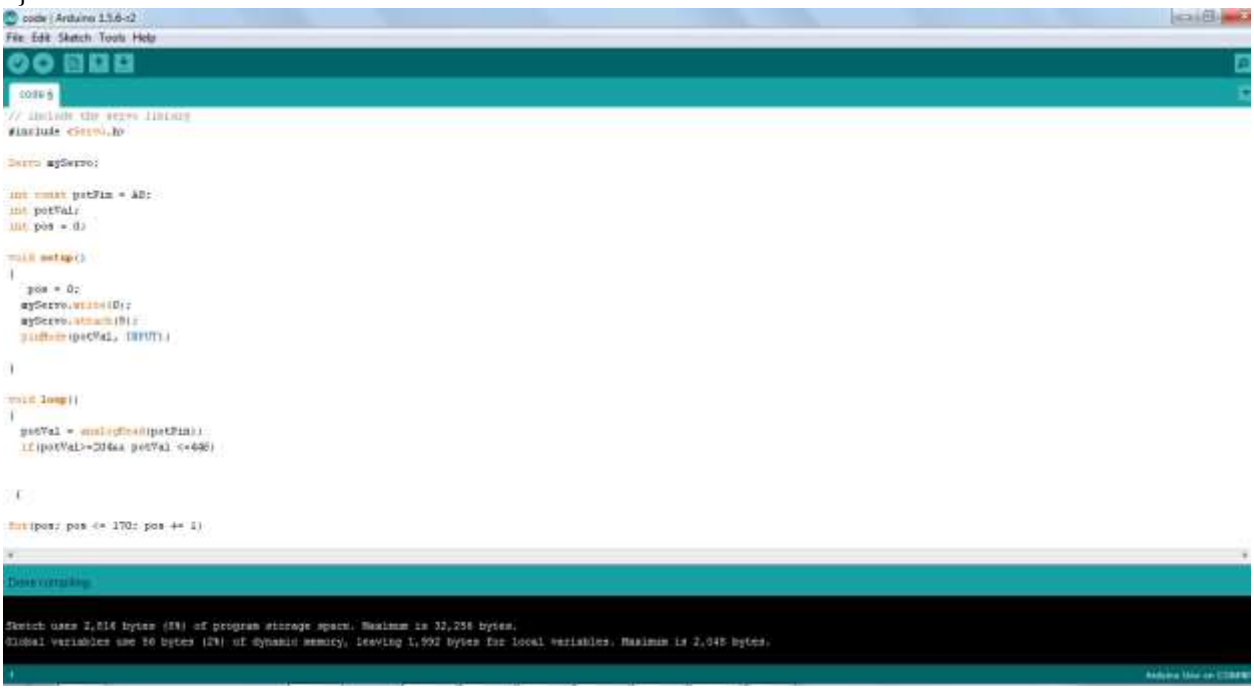

Fig :Screenshot of upper half of code

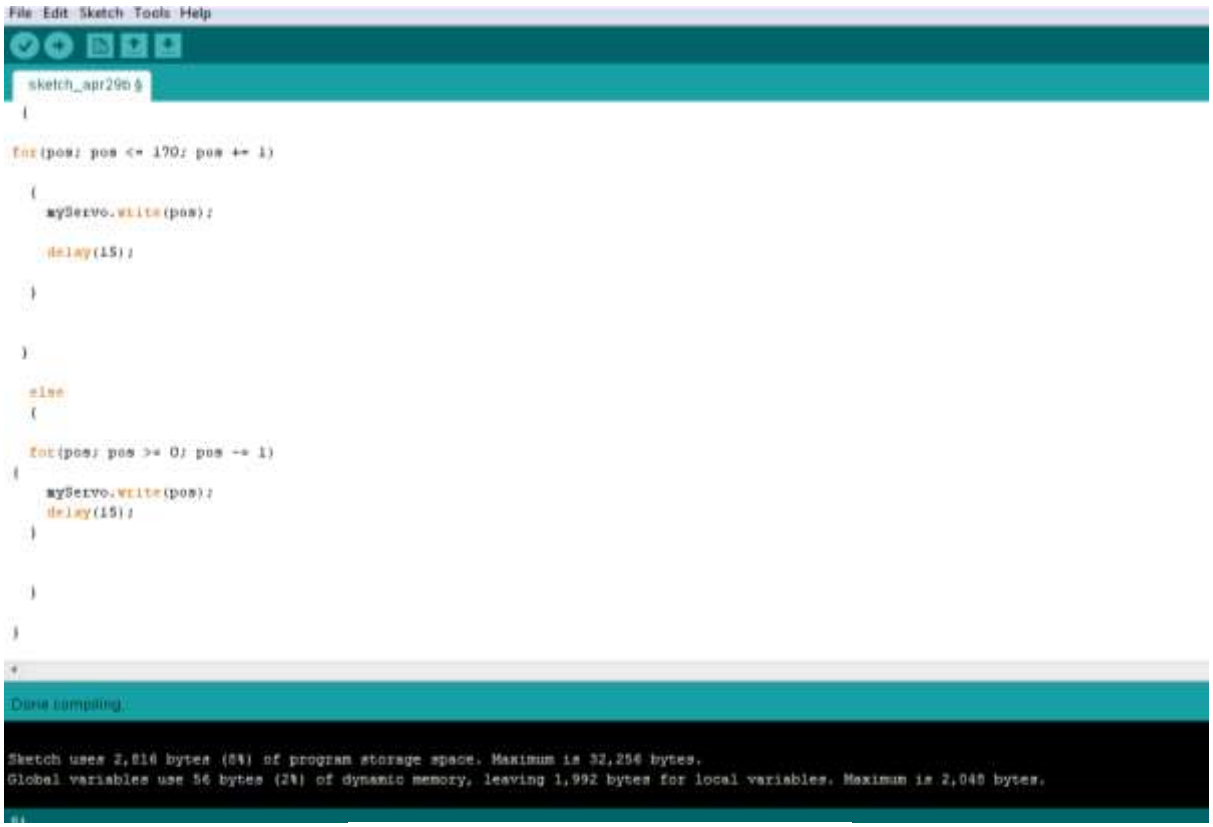

Fig: Screenshot of lower half of code

A rough estimate of the total cost of the prototype has been made in the table below:

Sr. No.	Component	Number of components	Cost per component(INR)	Total cost(INR)
1	DC Servo Motors	4	750	3000
2	Microcontroller (Arduino)	1	1500	1500
3	Integrated circuitry: Op amp LF-351	9	15	135
4	Integrated circuitry: INA 128p	3	450	1350
5	Surface electrodes	7	20	140
6	Mechanical components: Finger materials	3	-	-
			TOTAL	6125(approx)

REFERENCES:

PAPERS:

- Mechatronic Experiments Course Design: A Myoelectric Controlled Partial-Hand Prosthesis Project
- Design and Implementation of Prosthetic Arm Using Gear Motor Control Technique With Appropriate Testing

SITES:

- http://arxiv.org/ftp/arxiv/papers/1111/1111.2258.pdf
- http://www.scribd.com/doc/18651364/Myoelectric-Arm
- http://www.g9toengineering.com/MechatronicsStudio/MyoelectricProsthesis.htm
- http://i4d.mit.edu/prosthetic-arm/

International Journal of Engineering Research and General Science Volume 3, Issue 6, November-December, 2015
ISSN 2091-2730

Application of Soft Computing in Automatic Generation Control

Anupam Mourya[1], Rajesh kumar[2], Sanjeev Kumar[3]

[1] M.Tech Scholar, Electrical Engineering, Yamuna Institute of Eng. & Tech, Yamuna Nagar, Haryana, India
[2] Assistant Prof., Electronic and Communication Engineering, Shoolini University, Himachal Pradesh, India
[3] Assistant Prof, Electrical Engineering, Yamuna Institute of Eng. & Tech, Yamuna Nagar, Haryana, India
rajeshakela06@gmail.com,Anupam.mourya@gmail.com

Abstract— The objective of this paper is to study the load frequency control problem associated in two-area electrical power systems. In the present work some attention is given to single area power system, but the main emphasis is on the two area interconnected electrical power system. At first uncontrolled system is studied and then improvement of its response is learnt on the application of integral controller and PSO. All the study is done using MATLAB software both in SIMULINK and Workspace windows. By comparing the simulation of PSO based controller and workspace controller results obtained. By using matlab Software, a good agreement between these results is obtained. Thus the response of PSO controller is suitable than response of other controllers available

Keywords— PSO (based) Controller, Parameter calculations, Load frequency control, Integral Controller, SIMULINK and Workspace, MATLAB

1. INTRODUCTION

In actual power system operations, the load is changing continuously and randomly. As a result the real and reactive power demands on the power system are never steady, but continuously vary with the rising or falling trend. The real and reactive power generations must change accordingly to match the load perturbations. Load frequency control is essential for successful operation of power systems, especially interconnected power systems [13]. Without it the frequency of power supply may not be able to be controlled within the required limit band. To accomplish this, it becomes necessary to automatically regulate the operations of main steam valves or hydro gates in accordance with a suitable control strategy, which in turn controls the real power output of electric generators. The problem of controlling the output of electric generators in this way is termed as Automatic Generation Control (AGC) [14]. Automatic generation control is the regulation of power output of controllable generators within a prescribed area in response to change in system frequency, tie-line loading, or a relation of these to each other, so as to maintain the schedule system frequency and/or the established interchange with other areas within predetermined limits [13].Automatic Generation Control can be sub divided into fast (primary) and slow (secondary) control modes. The loop dynamics following immediately upon the onset of the load disturbance is decided by fast primary mode of AGC. This fast primary mode of AGC is also known as "Uncontrolled mode" since the speed changer position is unchanged. The secondary control acting through speed changer and initiated by suitable controller constitutes the slow secondary or the "Controlled modes" of AGC. The overall performance of AGC in any power system depends on the proper design of both primary and secondary control loops. So the overall performance of AGC in any power system depends on the proper design of both primary control loop (selection of R) and secondary control loops (selection of gain for supplementary controller).

Among the various types of load frequency controllers, the most widely employed are integral (I), proportional plus integral (PI), integral plus derivative (ID) and proportional plus integral plus derivative (PID) controllers. Their use is not only for their simplicity, but also due their success in large industrial applications

2. Block Diagram Representation of Load Frequency Control of an Isolated Area

A block diagram representation of an isolated power system by combining the block diagrams of turbine, generator, governor and load with feedback loop as shown in Fig. 2.1

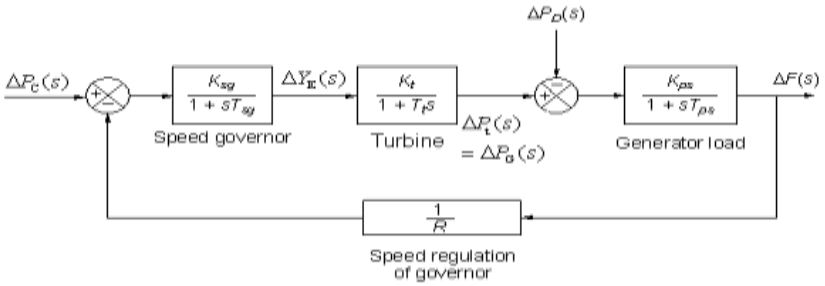

Fig. 2.1 Block Diagram Model of Load Frequency Control (isolated power system)

2.1 Steady State Analysis

The model of Fig. 2.1 shows that there are two important incremental inputs to the load frequency control system i.e. $-\Delta P_C$, the change in speed changer setting; and ΔP_D, the change in load demand. Let us consider the speed changer has a fixed setting (i.e. $\Delta P_C = 0$) and load demand changes. This is known as free governor operation. For such an operation the steady change in system frequency for a sudden change in load demand by an amount ΔP_D (i.e $\Delta P_D(s) = \Delta P_D/s$) is obtained as follows:

$$\Delta F(s)\,|_{\Delta P_C(s)=0} = -\frac{K_{ps}}{(1+T_{ps}s)+\dfrac{K_{sg}K_tK_{ps}/R}{(1+T_{sg}s)(1+T_ts)}} \times \frac{\Delta P_D(s)}{s} \tag{2.1}$$

$$\left|\begin{array}{l} \Delta f \textbf{ steady } \text{state} = \quad s\Delta F(s) \\ \\ \Delta P_C = 0 \qquad \Delta P_C(s) = 0 \end{array}\right| = -\left(\frac{K_{ps}}{1+(K_{sg}K_tK_{ps}/R)}\right)\Delta P_D \tag{2.2}$$

Let it be assumed for simplicity that K_{sg} is so adjusted that $K_{sg}K_t \approx 1$

It also recognized that $K_{ps} = 1/B$, where $B = (\partial P_D/\partial f) / P_r$ (in pu MW/unit change in frequency). Now

$$\Delta f = -\left(\frac{1}{B+\dfrac{1}{R}}\right)\Delta P_D \tag{2.3}$$

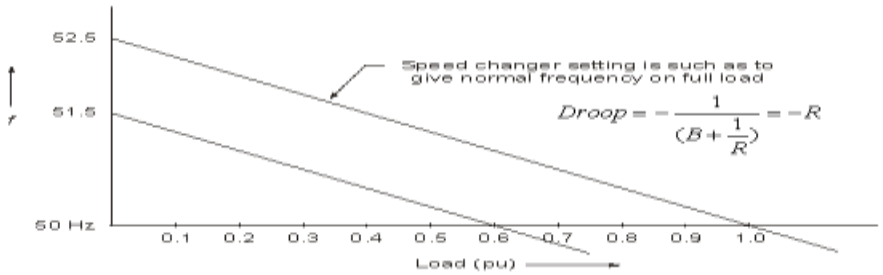

Fig. 2.2 Steady State LFC characteristics of a speed governor system

Fig. 2.2 shows the linear relationship between frequency and load for free governor operation with speed changer set to give a scheduled frequency of 100% at full load. It depicts two load frequency plots – one to give scheduled frequency at 100% rated load and the other to give the same frequency at 60% rated load.

The 'droop' or slope of this relationship is. $-\left(\dfrac{1}{B+\dfrac{1}{R}}\right)$

Consider now the steady effect of changing speed changer setting with load demand remaining fixed (i.e. $\Delta P_D = 0$). The steady state change in frequency is obtained as follows.

$$\Delta F(s)\Big|_{\Delta P_D(s)=0} = \frac{K_{sg}K_tK_{ps}}{(1+T_{sg}s)(1+T_ts)(1+T_{ps}s)+\dfrac{K_{sg}K_tK_{ps}}{R}} \times \frac{\Delta P_C}{s} \tag{2.4}$$

$$\Delta f\Big|_{\substack{steady\ state \\ \Delta P_D = 0}} = \left(\frac{K_{sg} K_t K_{ps}}{1 + \frac{K_{sg} K_t K_{ps}}{R}} \right) \Delta P_C$$

If, $K_{sg}K_t \approx 1$

$$\Delta f = \left(\frac{1}{B + \frac{1}{R}} \right) \Delta P_C \qquad (2.5)$$

If the speed changer setting is changed by ΔP_C while the load demand changes by ΔP_D the steady frequency change is obtained by superposition, i.e.

$$\Delta f = \left(\frac{1}{B + \frac{1}{R}} \right) (\Delta P_C - \Delta P_D) \qquad (2.6)$$

From Eq. (2.6) the frequency change caused by load demand can be compensated by changing the setting of the speed changer, i.e. $\Delta P_C = \Delta P_D$, for $\Delta f = 0$

2.2 Dynamic Response

To obtain the dynamic response giving the change in frequency as function of the time for a step change in load, we must obtain the Laplace inverse of Eq. (2.1). The characteristic equation can be approximated as first order by examining the relative magnitudes of the time constants involved. Typical values of the time constants of load frequency control system are related as

$$T_{sg} << T_t << T_{ps}$$

Consider T_{sg}=0.08 sec, T_t=0.3 sec., and T_{ps}=20 sec.

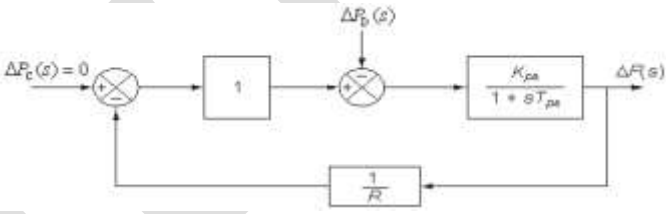

Fig. 2.3 first order approximate block diagram of load frequency control of an isolated area

Letting $T_{sg} = T_t = 0$, (and $K_{sg}K_t \approx 1$), the block diagram of Fig. 2.1 is reduced to that of Fig.2.3, from which we can write

$$\Delta F(s)\Big|_{\Delta P_c(s)=0} = -\left(\frac{K_{ps}}{1 + \frac{K_{ps}}{R} + T_{ps}s} \right) \times \frac{\Delta P_D}{s}$$

$$= -\frac{K_{ps}/T_{ps}}{s\left[s + \frac{R + K_{ps}}{RT_{ps}} \right]} \times \Delta P_D$$

$$\Delta f(t) = -\frac{RK_{ps}}{R + K_{ps}} \left\{ 1 - \exp\left[-\frac{t}{T_{ps}} \left(\frac{R + K_{ps}}{R} \right) \right] \right\} \Delta P_D \qquad (2.7)$$

Taking R=2.4, K_{ps}=120, T_{ps}=20 sec., ΔP_d =0.01 pu,

$$\Delta f\,(t) = -0.0235(1- e^{-2.55t}) \quad (2.8)$$

$\Delta st_{eady\ state}$ = - 0.0235 Hz

3. SIMULINK Model

3.1 Introduction

The large-scale power systems are normally composed of control areas (*i.e. multi-area*) or regions representing coherent groups of generators. The various areas are interconnected through tie-lines. The tie-lines are utilized for contractual energy exchange between areas and provide inter-area support in case of abnormal conditions. Without loss of generality we shall consider a two-area case connected by a single line as illustrated in Fig. 3.1. The concepts and theory of two-area power system is also applicable to other multi-area power systems i.e. three-area, four-area, five-area etc.

Fig. 3.1 Two interconnected control areas (single tie line)

Power transported out of area 1 is given by

$$P_{tie,\,1} = \frac{|V_1||V_2|}{X_{12}}\sin(\delta^0{}_1 - \delta^0{}_2) \quad (3.1)$$

Where

δ°_1, δ°_2 = power angles (angle between rotating magnetic flux & rotor) of equivalent machines of the two areas.

For incremental changes in δ_1 and δ_2, the incremental tie line power can be expressed as

$$\Delta P_{tie,\,1}(pu) = T_{12}\,(\Delta\delta_1 - \Delta\delta_2) \quad (3.2)$$

Where

$$T_{12} = \frac{|V_1||V_2|}{P_{r1}X_{12}}\cos(\delta^0{}_1 - \delta^0{}_2)$$ = *synchronizing coefficient*

Since incremental power angles are integrals of incremental frequencies, we can write above Eq. (3.2) as

$$\Delta P_{tie,\,1} = 2\pi T_{12}\left(\int \Delta f_1 dt - \int \Delta f_2 dt\right) \quad (3.3)$$

Where, Δf_1 and Δf_2 are incremental frequency change of areas 1 and 2 respectively.

Similarly the incremental tie line power out of area 2 is given by

$$\Delta P_{tie,\,2} = 2\pi T_{21}\left(\int \Delta f_2 dt - \int \Delta f_1 dt\right) \quad (3.4)$$

Where

$$T_{21} = \frac{|V_2||V_1|}{P_{r2}X_{21}}\cos(\delta^0{}_2 - \delta^0{}_1) = \left(\frac{P_{r1}}{P_{r2}}\right)T_{12} = a_{12}T_{12} \qquad (3.5)$$

With ref. to Eq. (1.9), the incremental power balance equation for area1 can be written as

$$\Delta P_{G1} - \Delta P_{D1} = \frac{2H_1}{f_1^0}\frac{d}{dt}(\Delta f_1) + B_1\Delta f_1 + \Delta Ptie,_1 \qquad (3.6)$$

It may be noted that all quantities other than frequency are in per unit in Eq. (3.6).

Taking the Laplace transform of Eq. (3.6) and reorganizing, we get and show the block diagram in fig 3.2

$$\Delta F_1(s) = [\Delta P_{G1}(s) - \Delta P_{D1}(s) - \Delta Ptie,_1(s)] \times \frac{Kps_1}{1 + Tps_1 S} \qquad (3.7)$$

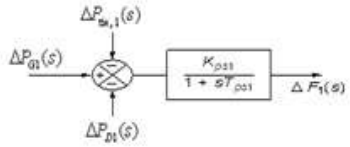

Fig. 3.2 Turbine-Load Model for Two-Area LFC

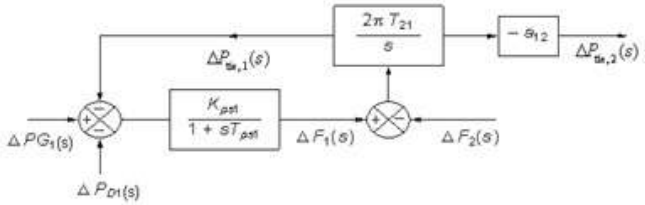

Fig. 3.3 Model Corresponding to Tie line Power Change

Taking the Laplace transform of Eq. (3.3), the signal $\Delta P_{tie,1}(s)$ is obtained as

$$\Delta P_{tie,1}(s) = \frac{2\pi T_{12}}{s}[\Delta F_1(s) - \Delta F_2(s)] \qquad (3.8)$$

The corresponding block diagram is shown in Fig. 3.3.

For the control area 2, $\Delta P_{tie,2}(s)$ is given as

$$\Delta P_{tie,2}(s) = \frac{-2\pi a_{12}T_{12}}{s}[\Delta F_1(s) - \Delta F_2(s)] \qquad (3.9)$$

This is also indicated by the block diagram of Fig. 3.3.

In the case of an isolated control area, ACE is the change in area frequency which when used in integral control loop forced the steady state frequency error to zero. In order that the steady state tie line power error in a two-area control be made zero another control loop (one for each area) must be introduced to integrate the incremental tie line power signal and feed it back to speed changer. This is accomplished by a single line-integrating block by redefining ACE as linear combination of incremental frequency and tie line power.

Thus, for control area 1

$$ACE_1 = \Delta P_{tie,1} + b_1\Delta f_1 \qquad (3.10)$$

Where,

constant b_1 is called *area frequency bias.*

Eq. (3.10) can be expressed in the Laplace transform as

$ACE_1(s) = \Delta P_{tie,\,1}(s) + b_1 \Delta F_1(s)$

Similarly, for the control area 2, ACE_2 is expressed as

$ACE_2(s) = \Delta P_{tie,\,2}(s) + b_2 \Delta F_2(s)$ (3.11)

3.2 Block Diagram of Uncontrolled Two-Area LFC

Block diagram of uncontrolled two-area power system is given in Fig. 3.4.

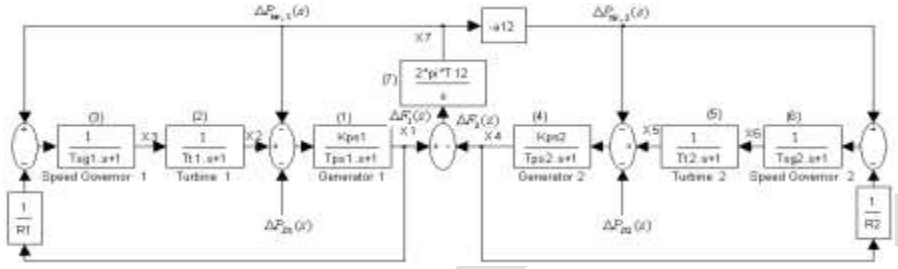

Fig. 3.4.Block diagram of two-area load frequency control without controller

3.2.1 SIMULINK Model for Uncontrolled Two-Area LFC

A SIMULINK model named **sm_A2_wc** is constructed as shown in Fig. 3.5.

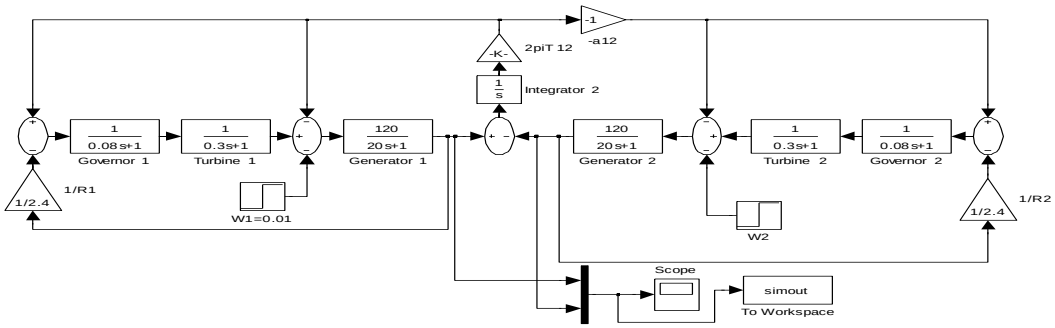

Fig. 3.5 SIMULINK model for two-area LFC without using controller

3.3 Block Diagram of Two-Area LFC with Integral Controller

Block diagram model and its corresponding diagram to derive state space model of two-area LFC with integral controller are given in Fig. 3.8 (a) and (b) respectively.

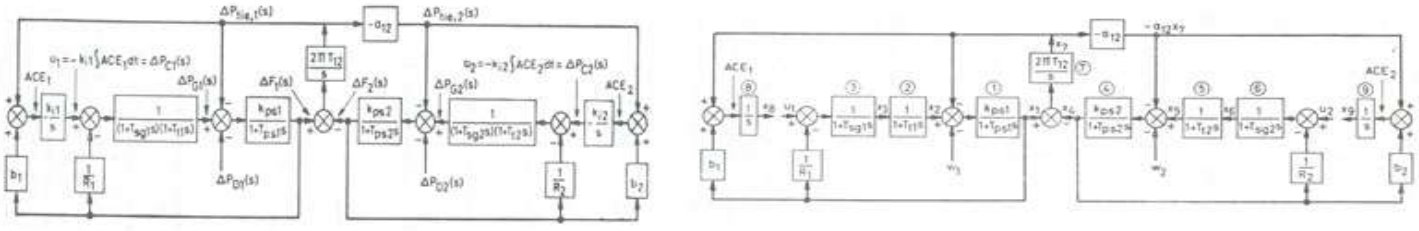

(a) (b)

Fig. 3.6 (a) Block diagram of two-area LFC with Integral controller (b) state space model of two-area LFC with integral controller

3.3.1 SIMULINK Model for Two-Area LFC with Integral Controller

A SIMULINK model named **sm_A2_I** is constructed as shown in Fig. 3.7

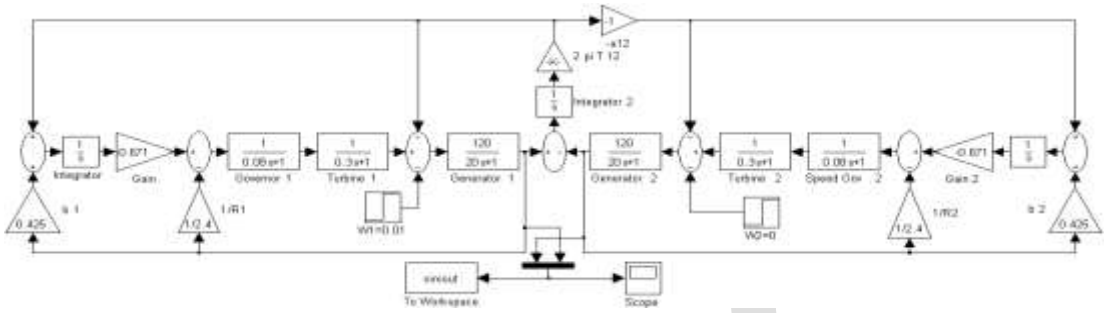

Fig. 3.7 SIMULINK model of two-area LFC with Integral controller

3.4 SIMULINK Model OF Two Area Power System with PSO

Two-Area Power System is controlled with using Particle Swarm Optimization Technique. PSO controller is applied to the Power System of Two area. PSO controller based. Two area Power System has good results than other controller. It has good dynamic response than other controllers.

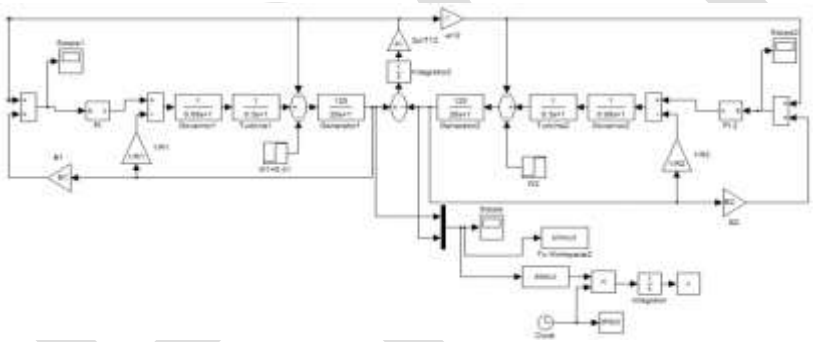

Fig.3.8. SIMULINK Model of Two area Power System with PSO

4. Results and Discussion

4. Two-Area Power System

Simulations Models were performed with no controller, with integral controller. PSO based controller is applied to two-area electrical power system by applying 0.01 p.u. MW step load disturbance to area 1. The Simulations were also performed with PSO based controller applied to two-area power system with Generation Rate Constraint as given in Fig. 3.8.

4.1 Two-Area Power System without Controller

From the Fig.3.4 and Fig. 3.5, we observe that both responses match with each other, also the steady-state frequency deviation, Δf (steady state) is -0.0178 Hz and frequency returns to its steady state value in 4.7 seconds. Results are shown in Table-1.

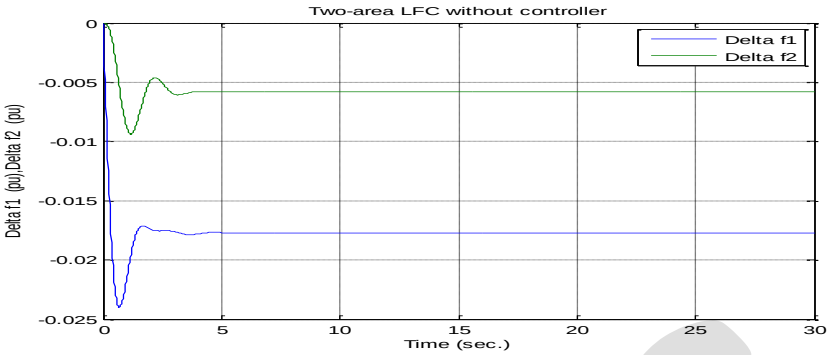

Fig.4.3.Result of Two Area LFC without Integral controller

This fig. shows Controlled Two Area power system without Integral controller, It shows the relationship between power unit and frequency(1/time) for two power system .The Power Unit is high at time zero second, oscillation will produce till time five second after that it damped out i.e. become study state, It mean frequency of load controlled

4.2 Two-Area Power System with Integral Controller

From the responses of the Figs. 3.6 and 3.7 we observe that both responses match with each other and steady state frequency deviation is zero, and the frequency returns to its nominal value in approximately 15 seconds. Results are shown in Table-1.

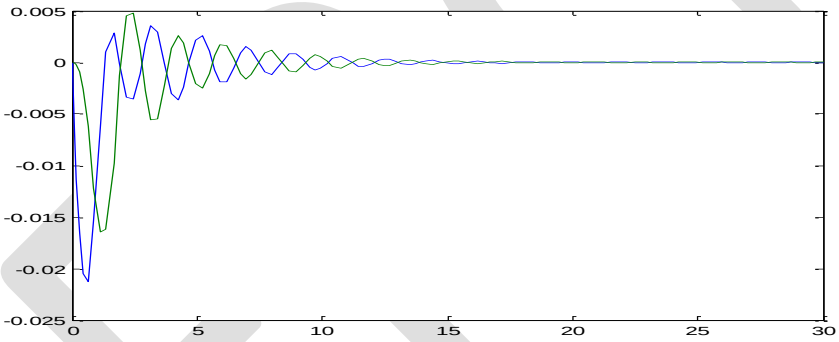

Fig.4.4.Result of Two area LFC with Integral controller

4.3 Two-Area Power System with Controller Based PSO

A MATLAB program is written in M-file for PSO based controller is run and the results so obtained are given in Fig. 4.5.

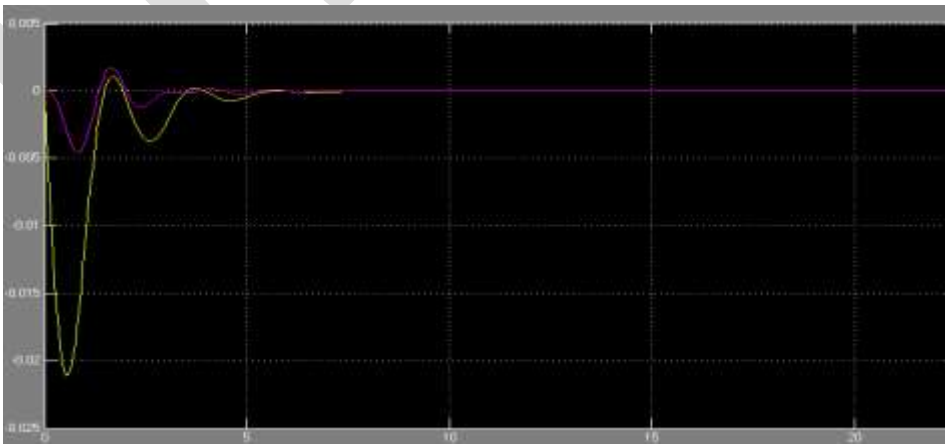

Fig. 4.5.Dynamic response of Two-Area PS with PSO based controller

The overall results without controller, with integral and with PSO based controllers applied to two-area power system are summarized in Table-1. Table-1 shows that the peak overshoot and settling time in case of optimal integral controller is better/less than the integral controller.

Table-1 Comparisons of settling time, peak overshoot & Frequency error of controller of two area Power System

For Δf_1 ↓	Without Controller		With Integral Controller		With PSO based Controller	
	Simulink	Workspace	Simulink	Workspace	Simulink	Workspace
Settling Time (s)	4.7	4.7	15.0	15.0	6.0	6.0
Peak overshoots (pu)	-0.0236	-0.0236	-0.0216	-0.0216	-0.020	-0.020
Freq. Error Δf_{ss} (pu)	-0.0178	-0.0178	0	0	0	0

ACKNOWLEDGMENT

The authors are grateful to Mr. Gagandeep Yadav, H.O.D, Electrical Engineering, Yamuna Institute of Engineering. & Technology, Yamuna Nagar, Haryana, India for providing necessary facilities, encouragement and motivation to carry out this work

CONCLUSION

In this paper LFC problem related to two-area power systems is studied for uncontrolled case and then with the application of the integral controller, PSO based controller using MATLAB SIMULINK/Workspace software.

In two-area power system, integral controller is used in both the areas to overcome system's steady state frequency errors and thereby enhancing system's dynamic performance. The integral controller is optimized using PSO based controller and is shown that the PSO based integral controller provides better dynamic performance than integral controller in terms of lesser settling time and peak overshoots. Then a PSO based PI controller is developed to control two-area power systems. In the case of PSO based controller applied to two Area power system, three (i.e. settling times, overshoots and integral absolute errors (IAE) of frequency deviation) performance criteria are utilized for the comparison. The simulation results given in Table-1 shows that proposed PSO based controller for load frequency control of two-area power system Power System is giving reduction in settling time and peak overshoots when compared with other controllers.

Table-1 shows that the PSO based controller developed better than the integral, optimal integral and other existing controllers with respect to the settling time, peak overshoots, integral absolute error and integral of time multiplied absolute error of the frequency deviation (Δf_1). The simulation results also show that proposed controller for load frequency control of Two-area system provide a reduction in settling time and peak overshoots when compared with other controllers.

REFERENCES:

1 Charls E. Fosha and Olle I. Elgerd, "The Meghawatt-Frequency Control Problem: A New Approach via Optimal Control Theory", *IEEE Trans. on PAS*, Vol. PAS-89, No. 4, April 1970.
2 CONCORDIA, C, KIRCHMAYER, L.K., and SZYMANSKI, E.A., "Effect of Speed Governor Deadband on Tie-line Power and Frequency Control Performance", *AIEEE Trans*., pp. 429-435, 1957, 76,
3 Elgerd. O. I., "Electric Energy Systems Theory: an introduction", *New York: McGraw-Hill*, 1982.
4 Olle I. Elgerd and Charles E. Fosha, "Optimum Megawatt-Frequency Control of Multiarea Electric Energy Systems", *IEEE Trans. on Power Apparatus and Systems*, Vol. PAS-89, NO. 4, pp. 556-563, April, 1970.
5 Nanda, J., and Kaul, B.L.,"Automatic Generation Control of an Interconnected Power System", *PROC. IEE, Vol. 125, No. 5, PP 385-390, MAY, 1978*
6 F.P. deMello, R.J.Mills and W.F. B'Rells, "Automatic Generation Control Part I - Process Modeling", *IEEE Trans. on Power Apparatus and Systems*, Vol. PAS- 92, pp 710-715, March/April 1973
7 O.P. Malik, A. Kumar and G.S. Hope, "A Load Frequency Control Algorithm based on Generalized Approach", *IEEE Trans. Power Systems*, vol. 3, no. 2, pp. 375-382, 1988
8 A. Kumar, O. P. Malik, and G. S. Hope, "Variable Structure-System Control Applied to AGC of an Interconnected Power System", *IEEE Proc*. 132, Part C, no. 1, pp. 23-29, 1985.

9 Bengiamin, N. N. and Chan, W. C. "Variable Structure Control of Electric Power Generation", *IEEE Trans. PAS* – 101, pp. 376 – 380, 1982

10 S.C.Tripathy, T.S.Bhatti, C.S.Jha, O.P.Malik and G.S.Hope, "Sampled Data Automatic Generation Control Analysis with Reheat Steam Turbine and Governor Deadband Effects", *MIEEE Transactions on Power Apparatus and Systems*, Vol.PAS-103, No.5: pp. 1045-1050, May 1984

11 S.C. Tripathi, R. Balasubramanian, P.S. Chandramohanan Nair, "Effect of Superconducting Magnetic Energy Storage on Automatic Generation Control considering governor deadband and boiler dynamics" *IEEE Trans. Power Syst*., vol. 7, no. 3, pp. 1266-1273, 1992

12 Ibraheem, Kumar, P. and Kothari, D. P., "Recent Philosophies of Automatic Generation Control Strategies in Power Systems", *IEEE Trans. Power System*, vol. 11, no. 3, pp. 346-357, February 2005

13 J. Kennedy and R. C. Eberhart, "Particle swarm optimization," in *Proc. IEEE Int. Conf. Neural Netw.*, Perth, Australia, 1995, vol. 4, pp. 1942–1948

14 H. Shayeghi, H. Shayanfar, A. Jalili, "Load Frequency Control Strategies: A Stateof-the-Art Survey for the Researcher", *Energy Conversion and Management*, 344–353, 2008

International Journal of Engineering Research and General Science Volume 3, Issue 6, November-December, 2015
ISSN 2091-2730

DTC BASED PMSM DRIVE FOR TORQUE RIPPLE REDUCTION - A SURVEY

K.Satheeshkumar[1], A.Vijayadevi[2], T.Senthilkumar[3]
[1,2]*Assistant Professor*,[3]*UG Student*
[1,2,3]*Department of EEE,*
[1,2,3]*Kalaignarkarunanidhi Institute of Technology, Coimbatore.*
Email id:[1]satheeshkumargceb@gmail.com
Email id: [2]vijayadevi.91@gmail.com
Email id: [3]senthiltsk304@gmail.com
Contact No: [1]9940965657

ABSTRACT- This paper presents a review of recently used Direct Torque control (DTC) techniques for Voltage Source Inverter (VSI) fed PMSM. A variety of techniques to reduce the torque ripples are described as follows space vector modulation (SVM), Multi rate control strategy, 12 sector based DTC, FDTC, ANN based DTC are presented.

Key words -PMSM, DTC, VSI, SVM, SVPWM

1. INTRODUCTION

The Permanent Magnet Synchronous Motor (PMSM) is becoming more and more attractive due to its high efficiency and high torque to current ratio. For a PMSM drive system, mechanical sensors are often required for correct communication of the inverters the use of mechanical sensors however reduces the reliability and increases the cost of the system. To overcome these disadvantages, sensor-less control scheme is much desired. Nowadays, the Direct Torque Control scheme is increasingly used in PMSM drive systems, because of its fast torque response and possibility of eliminating the mechanical sensor if the initial rotor position is known.

Variable speed drives are used in all industries to control precisely. The speed of electric motors driving loads ranging from pumps and fans to complex drive on paper machines, rolling mills, cranes and similar drives. In some places of the industries, it is required to maintain the torque constant with independent of the speed. Some examples for this are conveyors, mixers, screw feeders, positive displacement pump and majority of the electrical machine applications.

2. DTC SCHEME

DTC becomes more popular due to the advantages, such as elimination of current controller, elimination of the speed position sensor, lesser parameter dependence, no coordination transformation required. DTC is an optimized AC drive control principle, where the inverter switching directly controls the motor variables flux and torque. In higher speeds the method is not sensitive to any motor parameters, all calculations are done in stationary coordinate system.

For that, the knowledge about stator resistance, stator voltage and stator current alone required. In [1] this DTC scheme is established by I Takahashi et al., in mid 1980˝s from that onwards DTC scheme became more and more popular due to the above said its advantages.

A.BASIC PRINCIPLE

The basic block diagram of DTC scheme is given in the figure 2.1. The motor stator voltage, current, and stator resistance is measured, from that the actual flux and torque are estimated. That is compared with the reference flux and torque respectively in the comparator section as shown in the above figure 2.1. The error between the actual and reference is given to the hysteresis controller depending on the controller output, the voltage vector from the switching table is selected. The selected voltage vector is applied to the voltage source inverter through which the reference torque is achieved. The torque and flux are estimated by using the following equations.

$$Test = (3/2)\, p\, (\Psi_d \cdot i_q - \Psi_q \cdot i_d) \quad (1)$$
$$\Psi_d = L_d\, i_d + \Psi\, p \quad (2)$$
$$\Psi_q = L_q\, i_q \quad (3)$$

Where,
Test=Estimated Torque
p=No of poles
$\Psi_{d,q}$= d and q axis flux
L_d,L_q= d and q axis inductance

i_d,i_q=d and q axis current

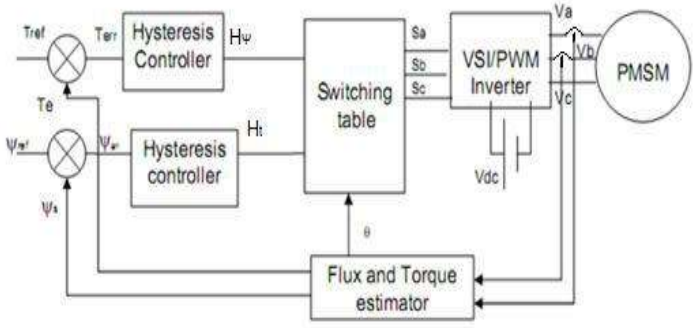

Figure 2.1 Basic Block Diagram

Torque ripples in this conventional DTC scheme are considerable. Many techniques are implemented to improve the performance of this conventional DTC scheme and some of them are discussed in this paper. The limitations of these methods are drift in the stator flux linkage estimation due to effect of the DC offset error in measurements and error in the estimation of stator flux linkage due to variation of stator flux linkage due to variation of stator resistance and requirement of a mechanical position sensor to detect the initial position. These three problems of DTC scheme for PMSM is analyzed and solutions are presented by Muhammad Fazlur Rahman et al., in [8].

B.SIX SECTOR CONCEPT

The entire section is divided into 6 sectors and each sector having 60°. Depending upon the actual and reference value, the corresponding switching vector is selected in the corresponding section. The switching table for the 6 sector based direct torque control is given in Table 1. It implemented the 3 level torque hysteresis and two level flux hysteresis controllers. Here 8 voltage vectors combinations for the 6 sector based switching table is implemented. The voltage vectors V0 and V7 are used as zero voltage vectors. If any one of these vector is selected, there is no change in the torque and flux. If any other voltage vector selected, the corresponding torque and flux deflection is obtained. The connection of power switches in a VSI with three-phase windings of a PMSM is shown in Figure 2.2, where the power switches of this voltage source inverter are 180° conducting mode, which means only three switching signal S_a, S_b and S_c are needed to uniquely determined the status of six switchers. If S = 1, the switches in upper leg of certain phase is on otherwise, S=0 represents the switches are connected with the lower leg of the three phase VSI.

H_ψ	H_T	S1	S2	S3	S4	S5	S6
1	1	V2	V3	V4	V5	V6	V1
	0	V0	V7	V0	V7	V0	V7
	-1	V6	V1	V2	V3	V4	V5
-1	1	V3	V4	V5	V6	V1	V2
	0	V7	V0	V7	V0	V7	V0
	-1	V5	V6	V1	V2	V3	V4

Table 1 Switching table for six sectors based direct torque control scheme

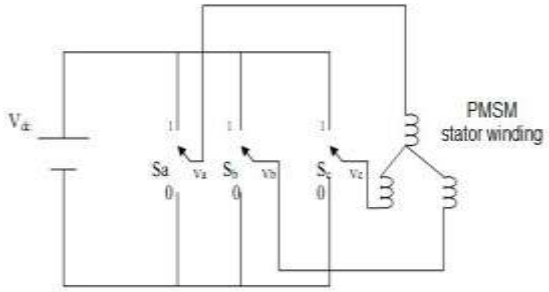

Figure2.2 Voltage Source Inverter Connections to PMSM

The inverter keeps the same state until the output of the hysteresis controllers changes their outputs at the sampling period. Therefore, the switching frequency is not fixed.

3. TYPICAL DTC SCHEMES TO REDUCE THE TORQUE RIPPLE

In the conventional DTC scheme the torque ripples are considerable in account. Many strategies were come to reduce this torque ripple for VSI fed PMSM drives on DTC based concept. However the torque ripple reduction was not impressive due to the transition between different sectors. In this paper some of the methods to reduce the ripples in the torque are analyzed and they are presented.

A.SPACE VECTOR MODULATION FOR DTC

Habetler introduced the concept of space vector modulation for DTC scheme in 1991[2]. The basic concept of this SVM is shown in the figure 3.1. One voltage space vector can be synthesized by two nearby basic voltage space vectors. During one switching period the most proper synthesized voltage space vector can be selected. The best way of selecting the proper voltage vector is select the vector which is having minimum switching activity required in the inverter when the sector changes. Then one zero vector and two non-zero vectors were used in every sector for reducing the torque ripple in [3]. To compensate the error between the reference and the actual torque and stator flux linkage. By selecting the proper synthesized voltage space vector the ripples in the torque gets reduces.

The problems of large torque and flux linkage pulsations and variable switching frequency can be solved effectively with the same hardware topology as that in the conventional DTC. The simulated and experimental results are compared by P.R. China et al, by using this SVM for DTC concept, and it is concluded with the following points. By using this SVM method the switching frequency of inverter can be fixed and the use of zero vectors in this SVM increases the performance of PMSM.

In recent years, some researchers tried to modify the SVM method based on power electronic techniques, to not only achieve better performance, but also improve the power efficiency of the system. Hybrid Space Vector Pulse Width Modulation (HSVPWM) techniques were implemented for reduction of stator current ripple, which indirectly leads to the reduction of the torque ripple and switching loss in [4]. In [5], DTC was developed based on the five zones HSVPWM to reduce the ripples in torque and flux. Brahmananda introduced a seven zones based HSVPWM method into DTC [13] in 2006. However, it requires relatively complex Calculation of the stator voltage equations.

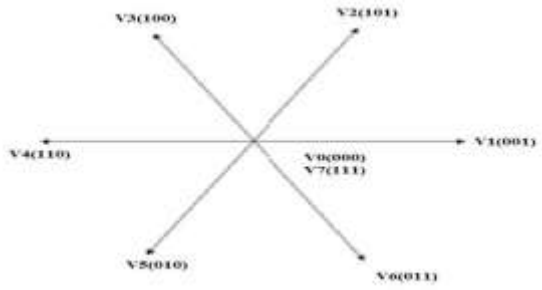

Figure 3.1 Selections of vectors by SVM

B.MULTI RATE CONTROL TRATEGY FOR DTC

N.Pandya et al., implemented the multi rate sampling interval time strategy with DTC for various control loops. The conventional DTC scheme is having single rate SVPWM. The performance of the PMSM drives gets increased by implementing the

proposed technique in [11]. This concept is explained by the figure 3.2 Accuracy of DTC depends upon the estimated value of torque, and flux. Which in turn depends upon the accuracy of the flux integrator, and its accuracy is depends upon its sampling time. Consider the fundamental sampling time; this sampling time is used to take the samples from the motor stator current, voltage, speed sensors. Those estimated values are used for flux and torque estimation. Due to multiple of fundamental sampling time in the torque, flux loop and in the speed loop, the number of samples gets increases, which leads to the accuracy of flux, and torque estimation. When the control system is complex, contains more than one control loop, to operate the whole system with a single sampling frequency is not acceptable, Time lag will occurs among the different loops presents in the system. This time lag is depends upon the loop parameters. Because of this time lag data loss is possible in discrete system. To avoid all these facts, in the present work multi rate sampling control system in Space Vector Modulation based DTC has been introduced. The performance of this proposed drive is examined and compared with single rate Space Vector Pulse Width Modulation based (SVPWM) DTC in [9].

The limitations of this sampling time selections are, the sampling time for flux and torque loop should be less than speed loop sampling time. Reason behind it is the change in speed of motor will take some time to settle down. So we need to consider this mechanical time lag. Until the settled value of speed is not obtained, the difference in the reference speed and estimated speed causes speed error and this will cause wrong torque reference selection which leads to misbehaviour of the system.

Figure 3.2 sampling time selection

This method is applicable only when the sampling time of speed loop and torque loop must be integer multiple, and we should assure that must be rational multiple of fundamental sampling time. By properly selecting the sampling time the accuracy of the motor drive gets increased, and the ripples in the torque decreased in DTC. By using the same digital signal processor the performance of 3-ph induction motor drive is improved using multi rate SVPWM DTC technique than single rate SVPWM DTC technique.

C.12 SECTOR BASED DTC

S.Pavithra et al., discussed this 12 sector concept to reduce the torque ripples in the basic DTC scheme. The conventional circular locus is divided, six sectors into 12 sectors circular locus, by each sector is having 30º. The switching table is constructed by 27 voltage vectors, the voltage vectors are shown in the figure 3.3, and they used 3 level diode clamped neutral point voltage source inverter. In those 27 voltage vectors 3 vectors are zero vectors, 6 vectors are large scale vectors, 12 vectors are small scale vectors and 6 are medium scale vectors. In this proposed work by this paper a 5 level hysteresis controller for torque, and three level hysteresis comparator for flux is implemented, which produce the better quantification of input variables and the 12 sector division causes the many voltage vectors with variable flux and torque variation. 12 voltage vectors are used to construct the switching table in [12], instead of using all the available 27 voltage vectors.

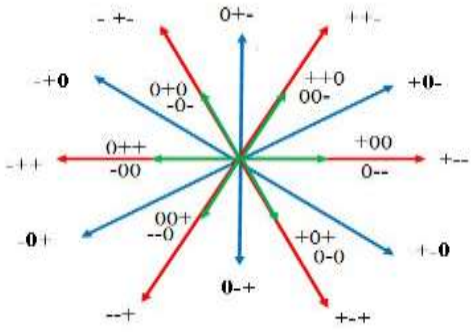

Figure 3.3 Switching State Vectors for 12 sectors

Zero vectors: V0, V25, and V26. Large vectors: VI, V3, V5, V7, V9, V11.
Medium vectors: V2, V4, V6, V8, V0, V12. Small vectors: V13,V14,V15,V16,V17,V18,

V19,V20,V21,V22,V23,V24.

This 12 voltage vectors consists of only zero, medium and large voltage vectors. By selecting the correct switching state, torque and the stator flux are regulated to their reference values. The basic DTC with a two level inverter finds no difference between small and large flux and torque errors. But in this proposed work for large and small error values, the corresponding large and small voltage vectors are selected to reduce the torque ripples.

D.DEAD-BEAT DTC-SVM SCHEMES

Habetler et al., in [2], proposed this technique. At first the changes in the torque and flux over one sampling period is predicted from the motor equations, and then to obtain the command value of stator voltage vector in stationary coordinates a quadratic equation is solved. This is a time-consuming algorithm and used in steady state. During transient state, an alternative algorithm is adopted and the appropriate voltage vector is selected prior from a switching table, which includes only active vectors. The main idea of the dead-beat DTC scheme is to force torque and stator flux magnitude to achieve their reference values in one sampling period, by simply synthesizing a suitable stator voltage vector applied by SVM method. Deadbeat control is not always possible, due to the limitation of inverter voltages and currents.

E. FUZZY BASED DTC

Modern control theories were used in power and dynamic control systems, in the past decades. Many new DTC controllers were realized by combining conventional DTC scheme with modern control computational methods like fuzzy logic, and artificial neural network (ANN). Mir introduced the FDTC in 1994[6]. FDTC controller was used to replace the switching table to select the space voltage vector in the conventional DTC system, and the two hysteresis controllers.

The errors of torque and flux and the angular position of the stator flux linkage are given as the inputs to the fuzzy logic controller. FDTC was applied for PMSM by Dan [7] in 2004. The errors in the torque, stator flux linkage and flux linkage angular position of the PMSM, are fuzzified into several fuzzy rules in order to select a suitable space voltage vector to obtain fast and smooth torque response. In a DTC controller, fuzzy logic method is used to obtain more available vectors to minimize the torque and flux ripples.

Based on DTC principle, the neural network controller is divided into the following five subnets, which are all individually trained:

- Optimum switching table subnet.
- Hysteresis comparator subnet
- Flux estimation subnet
- Torque calculation subnet
- Flux angle and magnitude calculation subnet

This ANN DTC scheme reduces the computation delay of every cycle. In 2006, an ANN based DTC controller was proposed for PMSM in [10]. Comparison between Back Propagation network and Radial Basis Function Network (RBFN) are done in that paper. The flexible neural network structures were used to implement the conventional DTC scheme for a voltage source inverter-fed PMSM drive. Based on the fundamental principle of DTC, an individual training strategy is employed for the neural network controller design. From the results obtained using the simulations concluded that the RFBN presents a good alternative to BP network. It was proved that ANN controller is possible to replace switching table of the DTC of PMSM, high and smooth torque response is obtained.

F. OTHER SIMPLE TECHNIQUES FOR DTC PERFORMANCE IMPROVEMENT

In [8], the basic problems of DTC like DC offset error, stator resistance variation, and the requirement of initial rotor position requirement are discussed by Muhammad Fazlur Rahman et al., and simple remedies are also presented in that paper. A programmable cascaded LPF can be used to compensate for the offset error, when the integrator is reset by the cascaded LPF. The flux locus remains centered and the ripple in speed has been significantly reduced. The stator flux vector is highly affected by the stator resistance variations at low speed. The stator resistance is continuously measured and updated during operation of the machine the error between the stator resistance of controller and the motor will causes the error in the estimated flux and torque so the resultant torque is also not an exact output. To avoid this PI stator resistance estimator is updated in the controller section the initial rotor position is detected by applying the high frequency sinusoidal voltage and considering the effects of the saliency on the amplitude of the corresponding stator current component. The magnetic pole is identified using the effect of magnetic saturation. This does not depends upon the load level (or) any motor parameters and suitable for DTC drive.

4. CONCLUSION

The main features of DTC can be summarized as follows.

- DTC needs only the stator parameters to flux and torque estimation and, therefore, it is not sensitive to rotor parameters.
- DTC is a motion-sensor less control method.
- DTC has a simple control structure

- The performance of DTC strongly depends on the quality of the estimation of the actual stator flux and torque.

In this paper the basic conventional DTC concept for PMSM motor is discussed and the Remedies to the DTC problems like DC offset, stator resistance variation, and initial rotor position requirement are discussed and the various techniques like SVM, Multi Rate sampling techniques, 12 sectors based DTC, FDTC, ANN based DTC are discussed to improve the performance of the DTC based system by reducing the torque ripples.

REFERENCES:

[1] IsaoTakahashiand Toshihiko Noguchi „ A New Quick-Response and High Efficiency Control Strategy of an Induction Motor "- IEEE Transactions on Industry Applications, vol.122.No.2. - 1986.

[2] T. G. Habetler, F. Profumo, and M.pastorelli "Direct torque control of induction machines over a wide speed range," in Conf. Rec. IEEE-IAS Annu. Meeting, pp. 600–606 - 1992.

[3] D. Sun, J. G. Zhu, and Y. K. He, "Continuous direct torque control of permanent magnet synchronous motor based on SVM," in Proc. 6th Int.Conf. On Electrical Machines and Systems, 9-11, Vol. 2, pp.596-599Nov. 2003.

[4] H. Krishnamurthy, G. Narayanan, V. T. Ranganathan, and R. Ayyar, "Design of space vector-based hybrid PWM techniques for reduced current ripple," in Proc. IEEE-APEC, Vol. 1, pp. 583-588 2003.

[5] U. Senthil, and B.G. Fernandes, "Hybrid space vector pulse width modulation based direct torque controlled induction motor drive," in Proc. IEEE Power Electronics Specialists Conf, Vol. 3, pp. 1112- 1117-2003.

[6] S. A. Mir, M. E. Elbuluk, and D. S. Zinger, "Fuzzy implementation of direct self-control of induction machines," IEEE Trans. Ind. Appl., Vol. 30, No. 3, pp. 729-735, May/Jun. 1994.

[7] D. Sun, Y. K. He, and J. G. Zhu, "Fuzzy logic direct torque control for permanent magnet synchronous motors," in Proc. 5th World Congress on Intelligent Control and Automation, Vol. 5, pp. 4401-4405,Jun. 2004.

[8] Muhammed Fazlur Rahman, Lixin Tang, and Limin Zhong, "problems associated with the direct torque control of an interior permanent-magnet synchronous motor drive and their remedies", 0278-0046-2004.

[9] T. B. Reddy, B. K. Reddy, J. Amarnath, D. S.Rayudu, and Md. H. Khan, "Sensorless direct torque control of induction motor based on hybrid space vector pulse width modulation to reduce ripples and switching losses-a variable structure controller approach," in Proc. IEEE Power India Conf.,10-12 Apr. 2006

[10] C. Zhang, B. Ma, H. Liu, and S. Chen, "Neural networks implementation of direct torque control of permanent magnet synchronous motor," in Proc. IMACS Multiconf. On Computational Engineering in Systems Appl.,Vol. 2, pp. 1839-1843, 4-6 Oct. 2006.

[11]Saurabh N. Pandya, and J. K. Chatterjee "Torque Ripple Minimization in Direct Torque Control based IM Drive Part-II: Multirate Control Strategy" 978-1- 244-1762-9-2008 [12]Pavithra.S, Sivaprakasam.A and T.Manikandan Performance Improvement of DTC for Induction Motor with 12-sector Methodology" IEEE- 978-1-61284-764-1 April 2011.

International Journal of Engineering Research and General Science Volume 3, Issue 6, November-December, 2015
ISSN 2091-2730

INCREASING THE POWER SYSTEM SWITCH GEAR CAPACITY BY USING SUPERCONDUCTING FAULT CURRENT LIMITER

Rajesh Velpula
Department of Electrical & Electronics Engineering
PSCMR College of Engineering & Technology

ABSTRACT- Superconducting fault-current limiters (SFCLs) have been the subject of research and development for many years and offer an attractive solution to the problem of rising fault levels in electrical distribution systems. SFCLs can greatly reduce fault currents and the damage at the point of fault, and help improve the stability of a power system. The resistance of an SFCL should be chosen to limit fault currents as much as possible. Not only does this benefit an electrical system through reduction in the potentially damaging effects of high fault currents, which is the primary purpose of the SFCL, but increasing the limitation of fault currents also has a consequence of shortening the recovery time of the SFCL by reducing the energy dissipated in the resistance of the SFCL. Superconducting fault-current limiters (SFCL) provide a new efficient approach to the reliable handling of such faults.(SCFLs) can be used for various nominal voltages and currents, and can be adapted to particular limiting characteristics in case of short circuits. Electrical equipment that controls high fault currents can increase the security of the network and allow power equipment to be designed more cost effectively. SFCL allows electrical interconnections of existing systems, which would not be possible without limiters .Finally, the SFCL is introduced in the higher capacity system. Thus, it is revealed that the outstanding current limiting performance of SFCL can be used to limit the fault to the level of the existing switchgear.

Key words: SFCL, Switch Gear, Stability, Fault Current, Circuit Breaker.

I. INTRODUCTION

Electric power systems are designed such that the impedances between generation sources and loads are relatively low. This configuration assists in maintenance of a stable, fixed system voltage in which the current fluctuates to accommodate system loads. The primary advantage of this arrangement is that loads are practically independent of each other, which allows the system to operate stably when loads change. However, significant drawback of the low interconnection impedance is that large fault currents (5 to 20 times nominal) can develop during power system disturbances. In addition, the maximum fault current in a system tends to increase over time for a variety of reasons, including:

- Electric power demand increases (load growth) and subsequent increase in generation.
- Parallel conducting paths are added to accommodate load growth.
- Interconnections within the grid increase.
- Sources of distributed generation are added to an already complex system.

In an effort to prevent damage to existing power-system equipment and to reduce customer downtime, protection engineers and utility planners have developed elaborate schemes to detect fault currents and activate isolation devices (circuit breakers) that interrupt the over-current sufficiently rapidly to avoid damage to parts of the power grid. While these traditional protection methods are effective, the ever-increasing levels of fault current will soon exceed the interruption capabilities of existing devices. Shunt reactors (inductors) are used in many cases to decrease fault current. These devices have fixed impedance so they introduce a continuous load, which reduces system efficiency and in some cases can impair system stability. Fault current limiters (FCLs) and fault current controllers (FCCs) with the capability of rapidly increasing their impedance, and thus limiting high fault currents are being developed. These devices have the promise of controlling fault currents to levels where conventional protection equipment can operate safely. A significant advantage of proposed FCL technologies is the ability to remain virtually invisible to the grid under nominal operation, introducing negligible impedance in the power system until a fault event occurs. Ideally, once the limiting action is no longer needed, an FCL quickly returns to its nominal low impedance state.

Superconducting fault current limiters (SFCLs) utilize superconducting materials to limit the current directly or to supply a DC bias current that affects the level of magnetization of a saturable iron core. While many FCL design concepts are being evaluated for commercial use, improvements in superconducting materials over the last 20 years have driven the technology to the forefront. Case in point, the discovery of high-temperature superconductivity (HTS) in 1986 drastically improved the potential for economic operation of many superconducting devices. This improvement is due to the ability of HTS materials to operate at temperatures around 70K instead of near 4K, which is required by conventional superconductors.

II. SUPERCONDUCTING FAULT CURRENT LIMITERS (SFCL)

2.1 FAULT-CURRENT PROBLEM

Electric power system designers often face fault-current problems when expanding existing buses. Larger transformers result in higher fault-duty levels, forcing the replacement of existing bus work and switchgear not rated for the new fault duty. Alternatively, the existing bus can be broken and served by two or more smaller transformers. Another alternative is use of a single, large, high-impedance transformer, resulting in degraded voltage regulation for all the customers on the bus. The classic tradeoff between fault control, bus capacity, and system stiffness has persisted for decades.

Other common system changes can result in a fault control problem:

i) In some areas, such as the United States, additional generation from co generators and independent power producers (IPPs) raises the fault duty throughout a system
ii) older but still operational equipment gradually becomes underrated through system growth; some equipment, such as transformers in underground vaults or cables, can be very expensive to replace
iii) Customers request parallel services that enhance the reliability of their supply but raise the fault duty.

2.2 BASICS OF SFCL

Superconducting fault current limiter is a promising technique to limit fault current in power system. Normally non-linear characteristic of superconductor is used in SFCL to limit fault current. In a normal operating condition SFCL has no influence on the system due to the virtually zero resistance below its critical current in superconductors. But when system goes to abnormal condition due to the occurrence of a fault, current exceeds the critical value of superconductors resulting in the SFCL to go resistive state. This capability of SFCL to go off a finite resistive value state from zero resistance can be used to limit fault current. Different types of SFCLs have been developed until now. Many models for SFCL have been designed as resistor-type, reactor-type, and transformer-type etc. In this project a resistive-type SFCL is modeled using simulink. Quench and recovery characteristics are designed. An impedance of SFCL according to time t is expressed by (3.1)

$$R_{SFCL} = \begin{cases} 0, & (t_0 > t) \\ R_m\left[1-\exp\left(-\frac{t-t_0}{T_{sc}}\right)\right]^{\frac{1}{2}}, & (t_0 \le t < t_1) \\ a_1(t-t_1)+b_1, & (t_1 \le t < t_2) \\ a_2(t-t_2)+b_2, & (t_2 \le t) \end{cases}$$

Where R_m is the maximum resistance of the SFCL in the quenching state, Tsc is the time constant of the SFCL during transition from the superconducting state to the normal state.

Furthermore, t0 is the time to start the quenching. Finally, $t_1$and $t_2$are the first and second recovery times, respectively. Quenching and recovery characteristics of the SFCL modelled by MATLAB using (3.1) are shown in Fig. 3.1. In normal condition impedance of SFCL is zero which is shown in Fig. 3.1. Quenching process of SFCL start at t=1s due to the occurrence of fault causing impedance rises to its maximum value. Impedance again becomes zero after the fault clears.

2.3 SUPERCONDUCTIVE FCL

Superconductors offer a way to break through system design constraints by presenting impedance to the electrical system that varies depending on operating conditions. Superconducting fault-current limiters normally operate with low impedance and are "invisible" components in the electrical system. In the event of a fault, the limiter inserts impedance into the circuit and limits the fault current. With current limiters, the utility can provide a low-impedance, stiff system with a low fault-current level, as Fig. 2.1 shows.

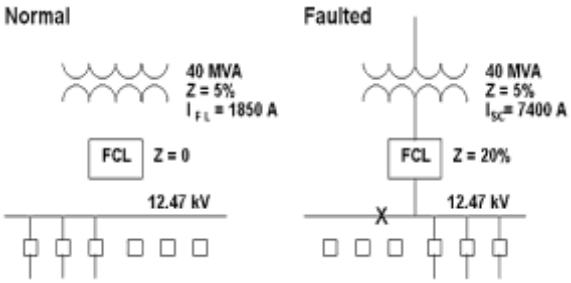

Fig. 2.1Fault control with a fault-current limiter.

In Fig. 2.1, a large, low-impedance transformer is used to feed a bus. Normally, the FCL does not affect the circuit. In the event of a fault, the limiter develops an impedance of 0.2 per unit (Z = 20%), and the fault current I_{SC} is reduced to 7,400 A. Without the limiter, the fault current would be 37,000 A.

The development of high temperature superconductors (HTS) enables the development of economical fault-current limiters. Superconducting fault-current limiters were first studied over twenty years ago. The earliest designs used low temperature superconductors (LTS), materials that lose all resistance at temperatures a few degrees above absolute zero. LTS materials are generally cooled with liquid helium, a substance both expensive and difficult to handle. The discovery in 1986 of high temperature superconductors, which operate at higher temperatures and can be cooled by relatively inexpensive liquid nitrogen, renewed interest in superconducting fault-current limiters.

2.4 STRUCTURE AND FUNCTIONAL PRINCIPLE OF THE FCL

The FCL, shown in Figure 2.2, is directly installed in the transformers neutral terminal. The FCL consists of a six-pulse thyristor rectifier (T1 to T6), a diode valve branch (V7 and V8), a freewheeling arm and an ohmic-inductive arm represented by R_d and L_d

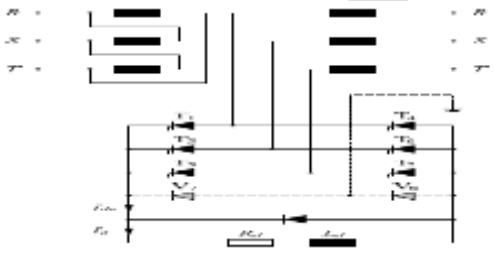

Fig 2.2 Fault Current Limiter (FCL) on a Diii-transformer

In case of no fault the thyristors are fired in their natural firing point and they behave like diodes in principle. Only in case of a fault the firing angle will be changed and the short circuit current will be limited actively. The inductance *Ld*will limit the rise of the short-circuit current. If the voltage across the choke falls under the threshold voltage of the diode, the freewheeling arm becomes active. In steady-state mode the currents in the FCL are not distorted. For controlling the short-circuit current only the behaviour in fault case will be discussed here. In fault case the currents will rise very fast, what directly induces the d.c current to rise very fast too? The whole d.c current has to flow through the coil and depending on its size it will convert to the steady state value with or without an overshoot. The task of the controller is to limit the possible overshoot on the one hand, as well as controlling the short-circuit current to a certain steady state value on the other hand. In fault case, the FCL operates in basically six operation modes.

These operation modes are commutation with a conducting freewheeling diode, commutation with a blocking freewheeling diode, two conducting thyristor valves at a blocking freewheeling diode, two conductive thyristors with a conducting freewheeling diode, intermittent d.c flow with a blocking freewheeling diode and intermittent d.c flow with a conducting freewheeling diode. For each state a mathematical description can be obtained by transforming the circuit into the state of the space phasor and solving the appropriate differential equations. For these mathematical transformations, in freewheeling case, the diode can be replaced by a voltage source in series with a resistor; whereby the voltage source is equivalent to the threshold voltage of the diode and the resistor describes the internal resistance of the diode. Once the freewheeling diode is blocking, it can be neglected..

2.5 Types of Superconducting Fault Current Limiters (SFCL) : The current limiting behaviour of SFCL depends on the nonlinear response of superconducting materials to temperature, current, and magnetic fields. Increasing any of these three parameters can cause a transition between superconducting and normal (resistive) conducting modes. SFCLs mainly have four categories.

a. Resistive type SFCL
b. Rectifier type SFCL
c. Shielded iron-core type SFCL
d. Saturated iron-core type SFCL

III. SIMULATION MODELS & RESULTS

3.1 SIMULATION MODEL OF SINGLE PHASE SYSTEM WITHOUT SFCL

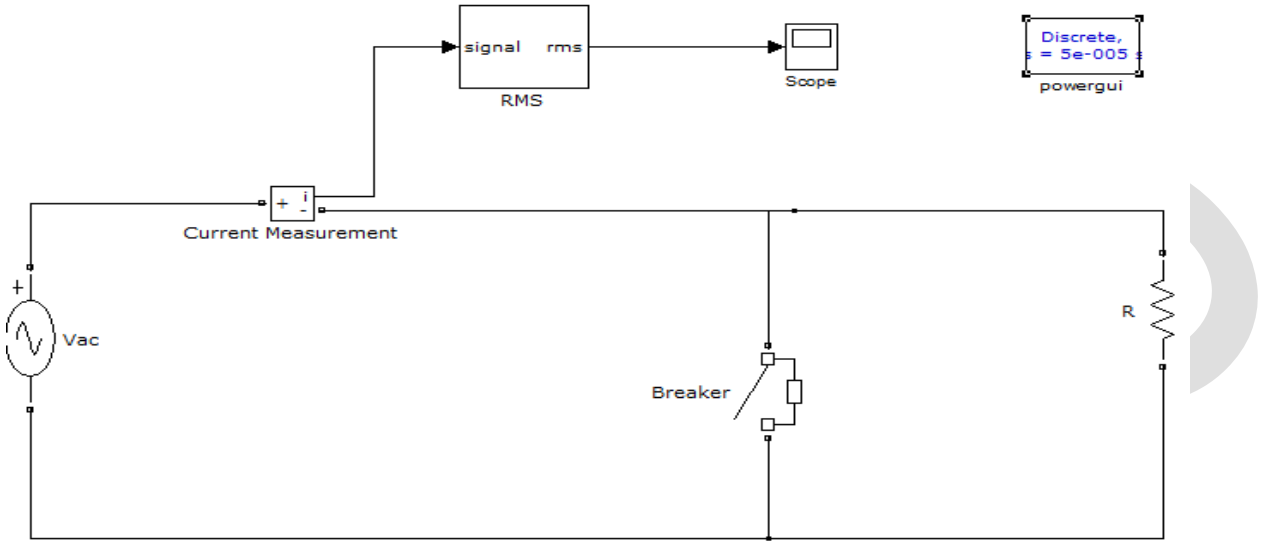

3.2 SIMULATION MODEL OF SINGLE PHASE SYSTEM WITH SFCL

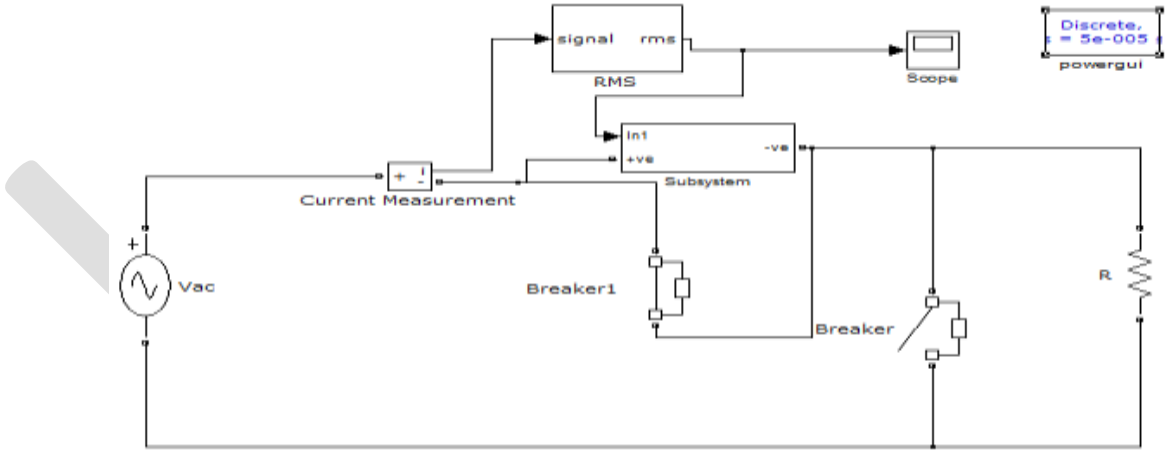

3.3 SIMULATION MODEL OF 110MW SYSTEM WITHOUT SFCL

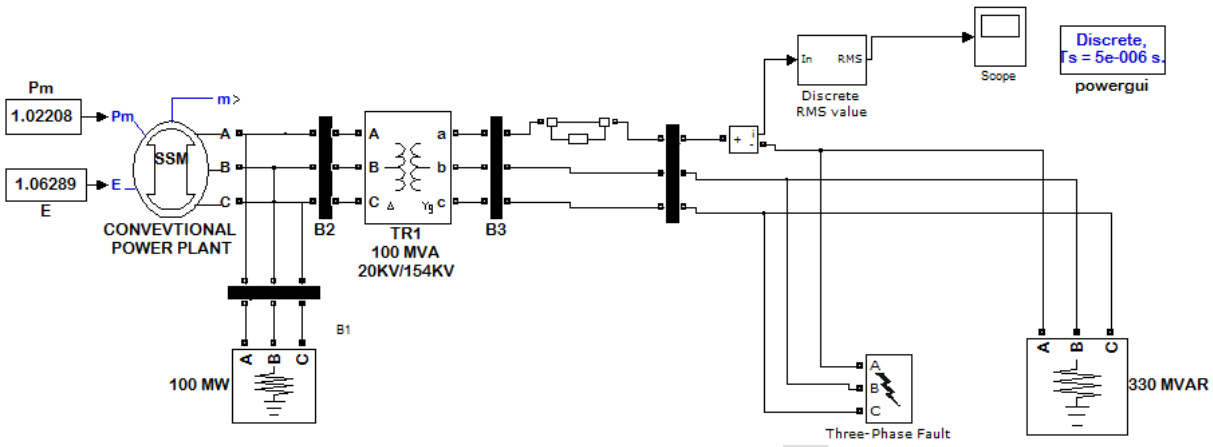

3.4 Simulated fault current waveforms with and without SFCL

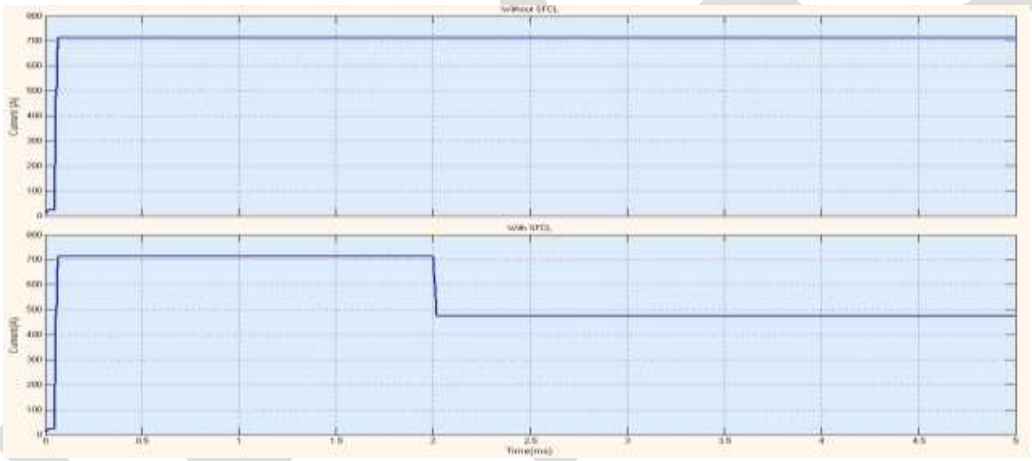

3.5 Simulated fault current waveforms for 110MW system in phase A

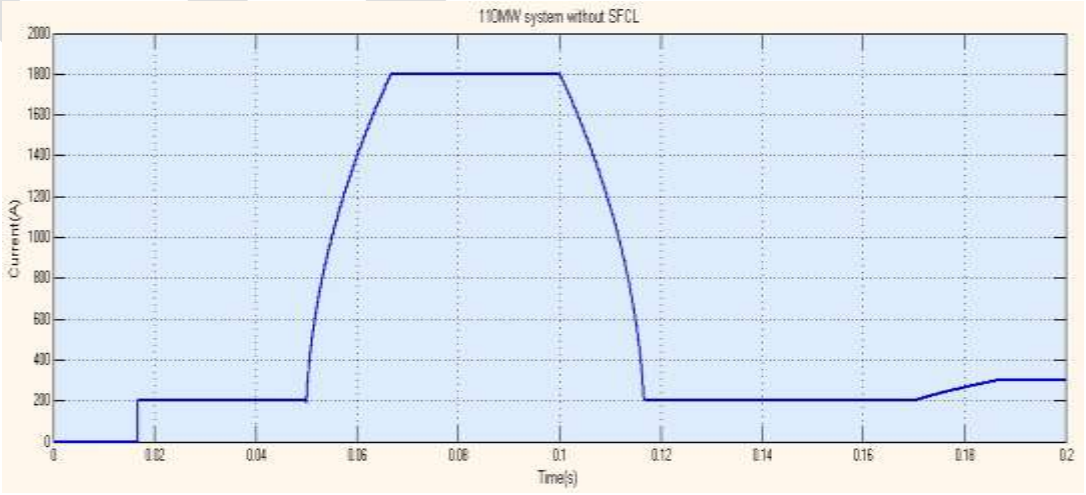

IV. CONCLUSION

This paper has proposed a study to increase the capacity of a power system by SFCL without changing the existing protective devices. The fault current 2700A of bigger system has been decreased to 1800A, in the range of smaller system, due to the use of SFCL. It is clear from the results that this inventive current limiting device is very efficient to decrease the fault current level significantly to the previous switchgear level. But coordination between the existing switchgear and SFCL is necessarily important for the practical application of this system. Otherwise it causes great hamper in the operation of protective devices which may results to get out of their original setting values. Thus, effective coordination between SFCL and existing protecting device will make it more successful in practical application issue. This coordination work may be the future issue.

REFERENCES:

[1] Hye-Rim Kim, Seong-Eun Yang, Seung-Duck Yu,Heesun Kim, WooSeok Kim, KijunPark, Ok-BaeHyun,Byeong-Mo Yang, JungwookSim, and Young-Geun Kim, "Installation and Testing of SFCLs," IEEE Trans. Appl. Supercond , vol. 22, no. 3, June 2012.

[2] M. Firouzi, G.B.Gharehpetian, and M. Pishvaie, "Proposed New Structure for Fault Current Limiting and Power Quality Improving Functions," International Conference on Renewable Energies and Power Quality (ICREPQ'10) Granada (Spain), 23rd to 25th March, 2010.

[3] M. T. Hagh and M. Abapour, "Non superconducting Fault Current Limiter With Controlling the Magnitudes of Fault Currents," IEEE Trans. Power Electronics, Vol.24, PP. 613–619, March 2009.

[4] Steven M. Blair, Campbell D. Booth, Nand K. Singh, and Graeme M. Burt, "Analysis of Energy Dissipation in Resistive Superconducting Fault-Current Limiters for Optimal Power System Performance," IEEE Trans. Appl. Supercond , vol. 21, no. 4, August 2011.

[5] A. S. Emhemed, R. M. Tumilty, N. K. Singh, G. M. Burt, andJ. R. McDonald, "Analysis of transient stability enhancement of LV connected induction micro generators by using resistive-type fault current limiters," IEEE Trans. Power Syst., vol. 25, no. 2, pp. 885–893, May 2010.

[6] Gum Tae Son, Hee-Jin Lee, Soo-Young Lee, and Jung-Wook Park, "A Study on the Direct Stability Analysis of Multi-Machine Power System With Resistive SFCL," IEEE Trans. Appl. Supercond , vol. 22, no. 3, June 2012.

[7] Jin-Seok Kim, Sung-Hun Lim, and Jae-Chul Kim, "Study on Application Method of Superconducting Fault Current Limiter for Protection Coordination of Protective Devices in a Power Distribution System," IEEE Trans. Appl. Supercond , vol. 22, no. 3, June 2012.

[8] B. C. Sung, D. K. Park, J.-W. Park, and T. K. Ko, "Study on optimal location of a resistive SFCL applied to an electric power grid, "IEEETrans. Appl. Supercond., vol. 19, no. 3, pp. 2048–2052, June 2009.

[9] S. M. Blair, C. D. Booth, I. M. Elders, N. K. Singh, G. M. Burt, and J. McCarthy, "Superconducting fault current limiter application in a power-dense marine electrical system," IET Elect. Syst. Transp., vol.1, no. 3, pp. 93–102, Sep. 2011.

[10] MathiasNoe, AchimHobl, Pascal Tixador, Luciano Martini, and Bertrand Dutoit, "Conceptual Design of a 24 kV, 1 kA ResistiveSuperconducting Fault Current Limiter," IEEE Trans. Appl. Supercond , vol. 22, no. 3, June 2012.

[11] Jin Bae Na, Young Jae Kim, Jae Young Jang, Kang SikRyu, Young Jin Hwang, Sukjin Choi, and Tae KukKo, "Design and Tests of PrototypHybridSuperconducting Fault Current Limiter With Fast Switch," IEEE Trans. Appl. Supercond , vol. 22, no. 3, June 2012.

International Journal of Engineering Research and General Science Volume 3, Issue 6, November-December, 2015
ISSN 2091-2730

Delineation of groundwater potential zones in Coimbatore district, Tamil Nadu, using Remote sensing and GIS techniques

Vasudevan S*, MUNGANYINKA Jeanne Pauline, Balamurugan P, Sumanta Kumar Sahoo and

Ashis Kumar Swain

Department of Earth sciences, Annamalai University, Annamalai Nagar-608 002

Corresponding author: devansiva@gmail.com

Abstract - Groundwater is one of the important natural resources which support the human health, economic development and ecological diversity. The main aim of this study is evaluation of ground water potential zones for Coimbatore District, Tamil Nadu. Remote sensing and GIS Technology contributes on efficient and effective result oriented methods for studying the occurrence and movement of ground water resources. Integration of various thematic layers influencing the ground water such as, geology, lineament density, geomorphology, drainage and land use have been used to classify the ground water potential zones. Based on this concept, weightage and ranking scores were assigned to each thematic layer with respect of influencing rate of water percolation. Finally weightage, multiplied by ranking and computed all the multiply values for quick assessment of ground water potential zones in the study area.

Keywords: Ground water Potential zone, weighted overlay analysis, RS and GIS.

1. INTRODUCTION

Ground water constitutes about two thirds of the freshwater resources of the world. In India it is a major source for all purposes of water requirements. It plays a vital role in the country's economic development and in ensuring its food security. More than 90% of rural and nearly 30% of urban population depend on ground water for drinking water. Water bearing formations of the earth's crust act as conduits for transmission and as reservoirs for storing water. The groundwater occurrence in a geological formation and the scope for its exploitation primarily depends on the formation of porosity. High relief and steep slopes impart higher runoff, while topographical depressions increase infiltration. An area of high drainage density also increases surface runoff compared to a low drainage density area. Surface water bodies like rivers, ponds, etc., can act as recharge zones [1].

Satellite imagery by virtue of providing synoptic view of the terrain at regular intervals offer immense potential in generating the information on parameters required for ground water exploration, exploitation and development. Remote sensing and GIS have been increasingly used for recharge estimation, draft estimation, mapping of prospective zones, identification of over exploited and under developed/ undeveloped areas and prioritization of areas for recharge structures which conjunctively facilitate systematic planning, development and management of ground water resources on a sustainable basis. This research paper is an effort to have

better understanding of the ground water occurrence and resources in the study area by using Remote Sensing and GIS techniques in combination with field/ existing data at Coimbatore district.

2 STUDY AREA

Coimbatore is an important district in western part of Tamil Nadu. The district has an area extent of 7466 sq. km. of which forest land covers an area of 1,558 sq. km. and which are only 5.74% of the state area. The study area Coimbatore district (Figure1) lies between north latitudes 10° 13' 00" to 11° 23' 30" and east longitudes 76° 39'00" to 77° 30' 00" and falls in the survey of India topographical maps numbers 58A, 58B, 58E, and 58F. The district is bounded on the northwest by the Nilgiris district, on the northeast by Erode district and to the southeast by Dindigual district and on the west and south by Kerala state.

3 MATERIALS AND METHODS

3.1 Methodology

The method of study broadly confined to field and laboratory interpretation and analysis, which includes ground truth and interpretation of remote sensing data and analysis of the same under GIS environment. A synoptic view of the methodology adopted is noted in the flow chart (Figure 2).

Geographic Information System (GIS) has become an increasingly powerful and important tool for hydrologist in the study and management of water resources. Remotely sensed data from satellite provides quick and useful base line information on the factor controlling the occurrence, potential and movement of groundwater such as lithology, geological structure, geomorphology, soils, land and land cover [2]. Present study following data types (Table 1);

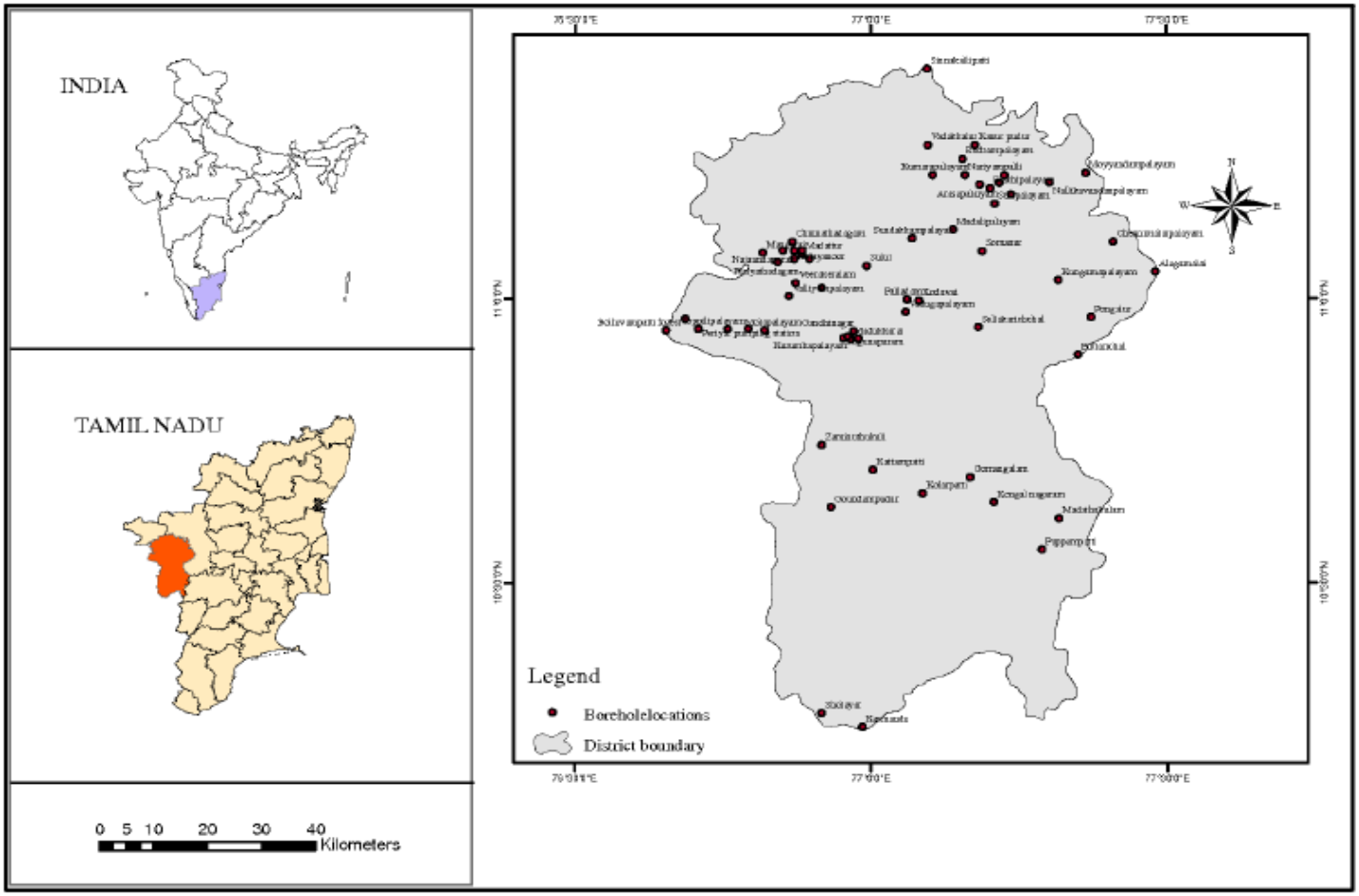

Figure 1: Study area and Location map of the Coimbatore district

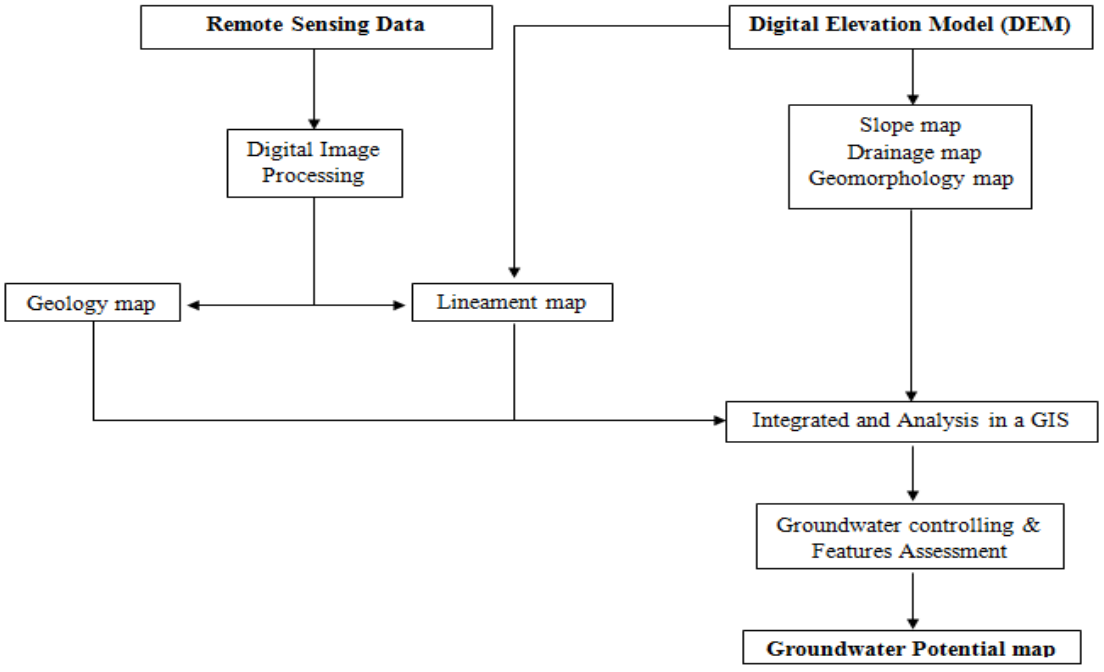

Figure 2: Flow chart showing methods employed for the study

Table 1. Details of various data sheets used

Types of Data	Details of Data	Source of Data
Toposheet	E 16 (1 : 50,000 scale)	Survey of India (SOI)
Thematic maps: Soil, Geology, Drainage, Gemorphology, Land use / Land cover, Lineament	Scale 1 : 50,000	National Bureau of Soil Survey and Land use planning (NBSS & LUP), Geological Survey of India (GSI), National Remote Sensing Centre (NRSC)
Slope		DEM
Satellite Sensor Resolution	IRS ID LISS III 23.5 meter	National Remote Sensing Centre (NRSC), Hyderabad

4 RESULTS AND DISCUSSION

Groundwater availability in Coimbatore district is mainly held by hard crystalline rocks which are devoid of primary openings. The occurrence and movement of groundwater in these rocks are controlled by the secondary openings like joints, fractures and fissures present in them. Due to heterogenous nature of crystalline rock, it requires careful planning and scientific approach to identify the groundwater potential zones. Remote sensing techniques using satellite imagery have proved to be an indispensable tool in morphometric analysis and groundwater studies [3].

As mentioned in the methodology the selected six parameters have been created using GIS techniques and it has been subjected to weightage analysis. The detailed discussion of each parameter is following;

4.1 Geology

Geology is one of the major factors which plays an important role in the distribution and occurrence of ground water. A detailed field investigation of the study area reveals an interesting igneous association set admits country rocks of Precambrian country rocks include Hornblende-Biotite-Gneisses, Garnet Sillimanite Gneiss, Granulites, Charnockites. Apart from these, older Ultrabasics occur as enclaves within Charnockites and gneisses. Granites and Quartz veins are also seen as intrusive bodies. The igneous association which are also Precambrian age consists of Magnesite bearing Ultrabasics and associated alkaline rocks (Figure 3). The weightage were assigned based on the rock's influence in the groundwater.

4.2 Lineament Density

Lineaments like joints, fractures and faults are hydrogeologically very important and may provide the pathways for groundwater movement [4].The Lineament map is generated from the satellite imagery by identifying the fault lines in the imagery using the ArcGIS. The density of the lineament is generated using the lineament map. The weights have been given by setting more threat levels to higher lineament density which is groundwater prone. The purpose of this is to analyze the spatial distribution of lineaments extracted from satellite images according to their density, intersection density, length and orientation in order to contribute to the understanding of the faults of the study area which is a important locations since they are weaker in nature and resulting in the percolation and storage of waves through these ruptured planes. Lineaments usually appear as straight lines or "edges" on the images which in all cases contributed by the tonal differences within the surface material. Lineament and Lineament density distribution for the district are as shown in figure 4.

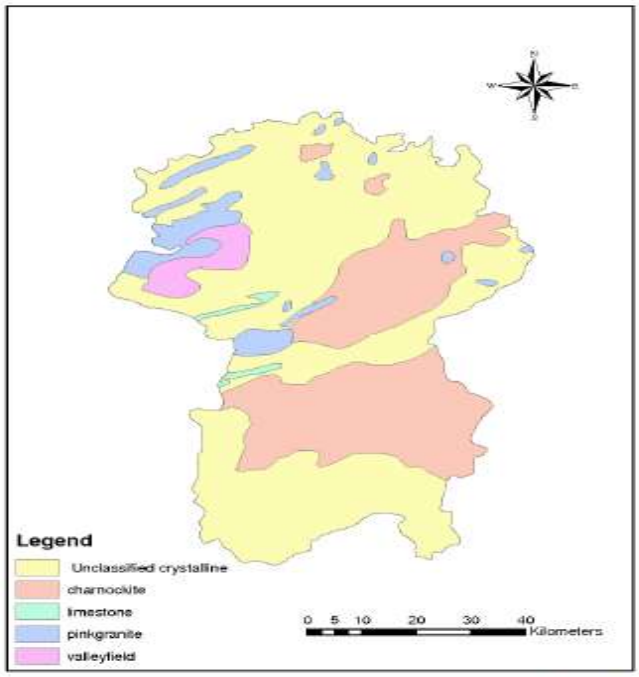

Figure 3: Geological Map of Coimbatore District

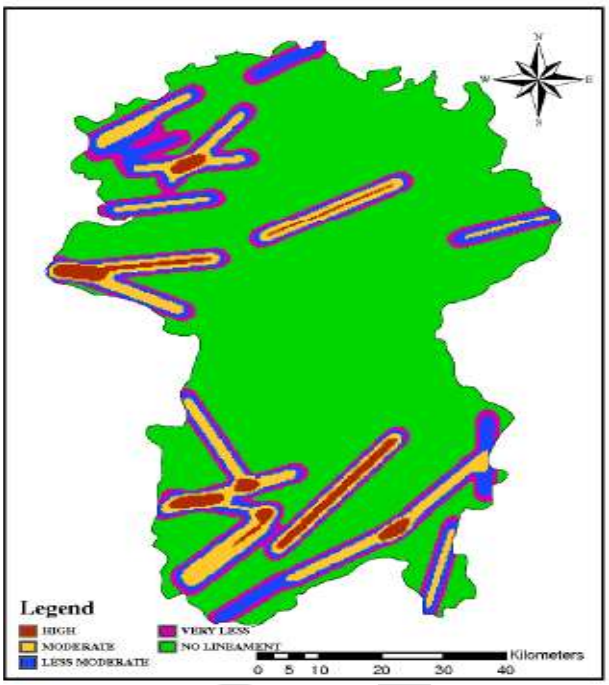

Figure 4: Lineament Density Map of the Study area

4.3 Geomorphology

Geomorphology is the study of earth structures and also helps in depict inherited process relating to the Groundwater potential zones also structural features. The area is marked by plateau landforms, structural, denudational and residual hills of Charnockites and Gneisses and linear ridges of basic Dykes. The gneisses and Ultra Basic hills have invariably generated a wide bazada zone. The various geomorphic units, as revealed from the studies are structural and residual hills, linear ridges, bazada zones, buried pediments, erosional plains, valley fills and uplands. A fractures and lineaments pattern are controling the geomorphology of the area and suggests that structural and denudational process predominate the fluvial process. The district has thick vegetation in hills and with agricultural activities in plains and valleys.

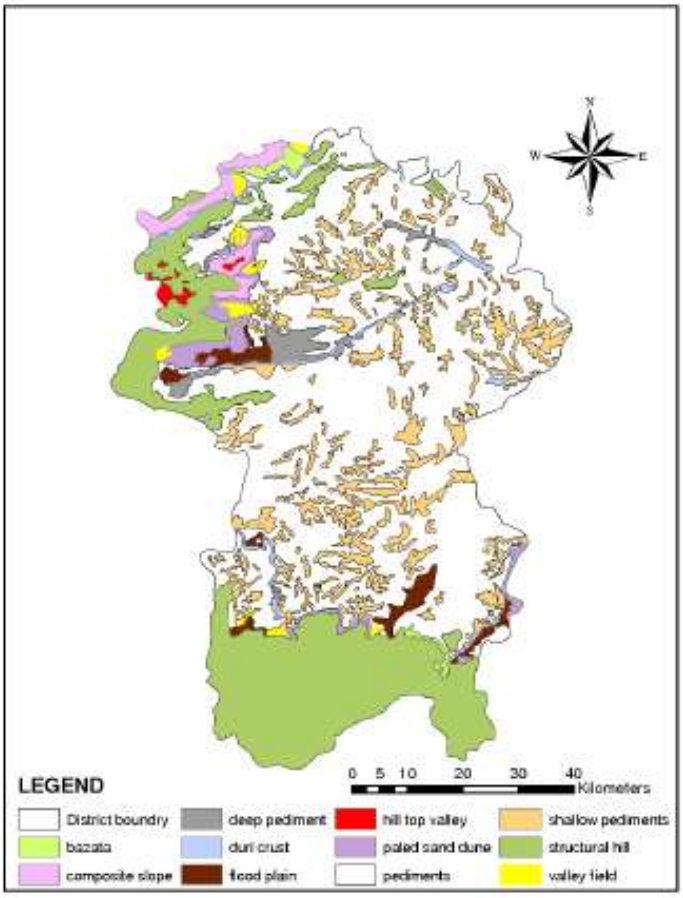

Figure 5: Geomorphology map of the study area

4.4 Drainage

The drainage is one of the factors which play the important role in groundwater occurrence. The scanty rainfall in the Coimbatore district leads to dependency of agricultural activities with respect to wells, irrigation project, tanks etc. The ephemeral rivers are Bhavani, Noyil, Palar, Aliyar and Amaravathi, which have been fully exploited by means of several anaicuts and dams built across them for irrigation purposes. There are number of masonary and earthen reservoirs and dams present here such as Amaravathi, Thirmurthi Parambikulam, Sholaiyar, Aliyar, etc.

The river drains an area of 1056 Sq.km with in this district. Five surface reservoirs are located on this river, which form part of the Parambikulam Aliyar project. The drainage pattern in the district (Figure 6) is mostly controlled by the structural features. Among the different drainage pattern and associated features recognized in this district, the following are noteworthy Radial, Parallel, Valley fills and Dendritic to Subdentritic. The drainage density map for the study area is shown in figure 6.

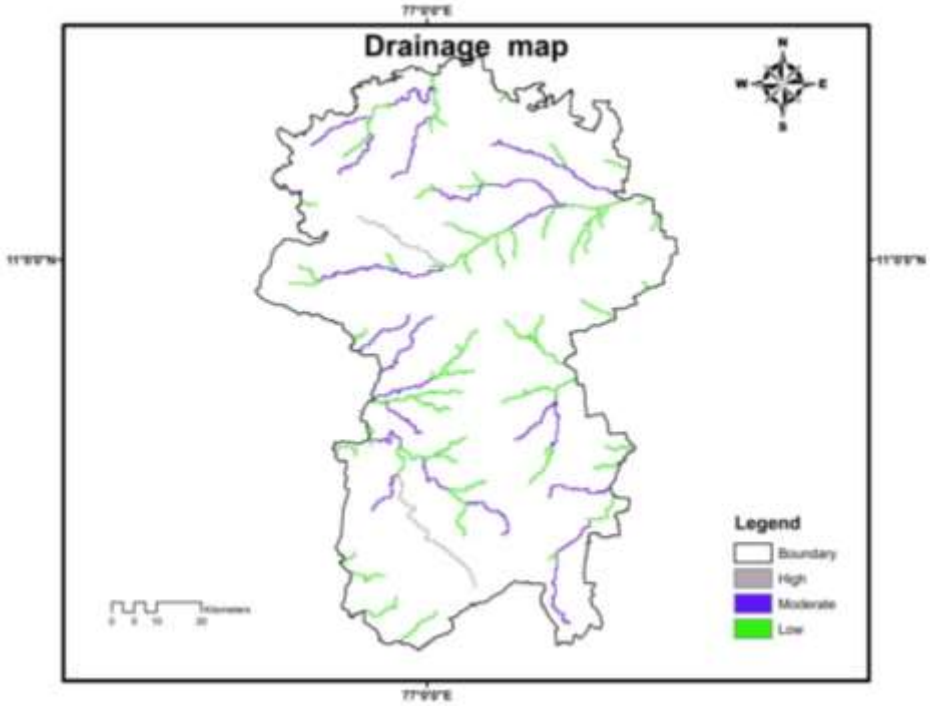

Figure 6: Drainage system and density of the Study area

4.5 Slope

The slope angle is considered as an important input as it has considerable influence in the study area for the identification of Groundwater potential zones. The slope of the study area was classified into six classes, such as less than 5 degree plain area, slope zone 5-15º, 15-25º, and 25-35º and above 45º and weightages of 5, 3, 2 and 1 was respectively assigned to them based on their groundwater prospects. In this case, higher weightage was given to shallow slopes and gradually lesser and lesser weightages were assigned steeper and steeper slopes because runoff is directly proportional to slope (Figure 7).

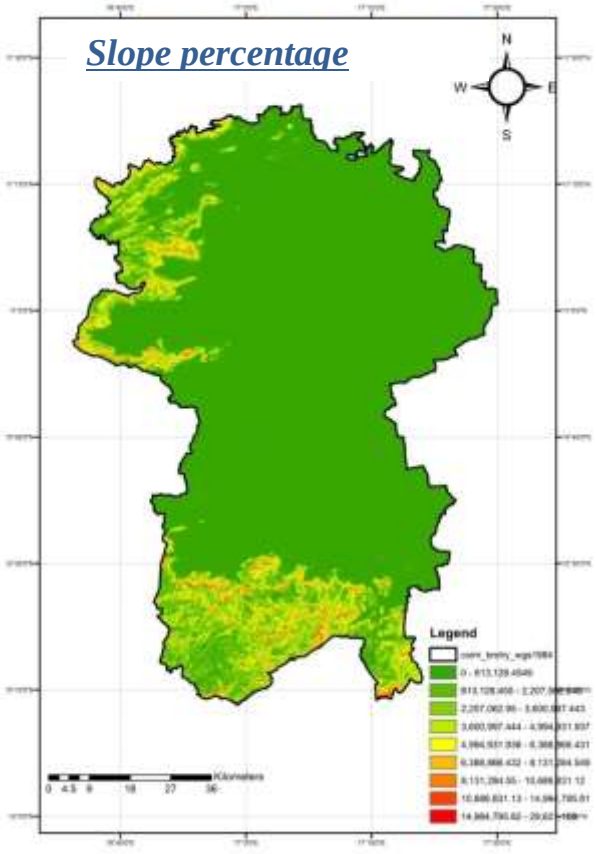

Figure 7: Slope Map of the study area

4.6 Land use and Land cover

Land use is clearly constrained by environmental factors such as soil characteristics, climate, topography, and vegetation. But it also reflects the importance of land as a key and finite resource for most human activities including agriculture, industry, forestry, energy production, settlement, recreation, and water catchments and storage.

The Land use/ Land cover map is generated from the satellite imagery and the area is classified in to Urban or Built up land, Residential, Commercial and Services, Industrial, Transportation, Communication and Utilities, Agricultural Land, Stony waste, Forest land, Water bodies and so on. The weights have been given based up on the threat levels. Land cover is the physical material at the surface of the earth includes grass, asphalt, trees, bare ground, water, etc. The Land cover map of the study area is shown in figure 8.

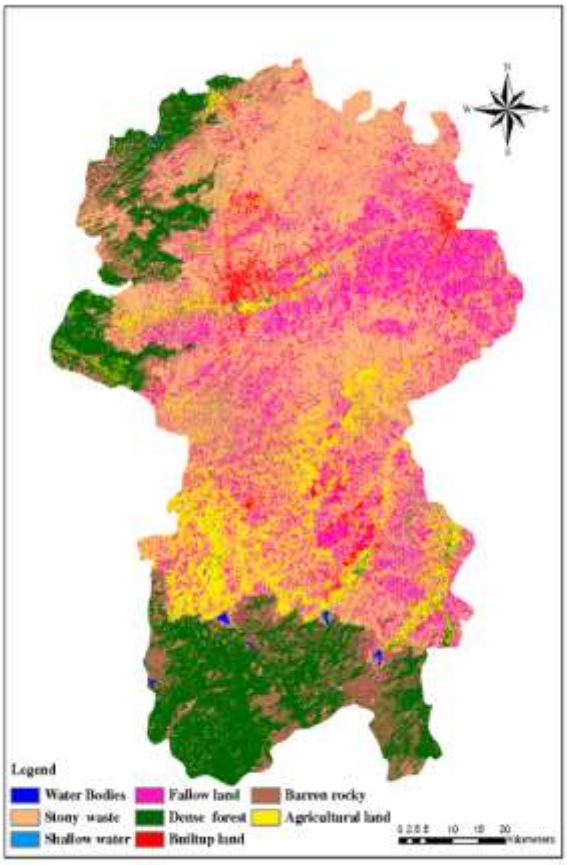

Figure 8: Land Cover Map of the study area

5. GIS INTEGRATION AND GROUNDWATER TARGETING

The above thematic vector layers were converted into to raster format. Using raster calculator in spatial analysis module of Arc GIS, all the raterised thematic layers were added one over the other and there from final integrated groundwater prospect map was derived (Figure 9). After generating the GIS layers on Geology, lineament density, geomorphology, slope, drainage, Landuse / Land cover, these six GIS layers were integrated one over the other using GIS Add function. Such GIS integration has resulted in to 2363 polygon classes and having weightage from 93 to 247. Such dynamic range of weightage of these 2363 polygon classes were grouped into three via: less than 93, 149-201 and more than 247. Accordingly, the polygon classes falling under these three weightage groups were dissolved and clubbed together and a GIS layer was prepared showing only the above three classes of polygons. Based on the weightages these were grouped into priority area I, II, and III for the groundwater potential zones. Such are weightages having more than 202 are favourable zones, if the weightages between 201 and 149 are moderately favourable zones and finally the weightages are less than 148 are grouped as low least favourable and are shown in figure 9.

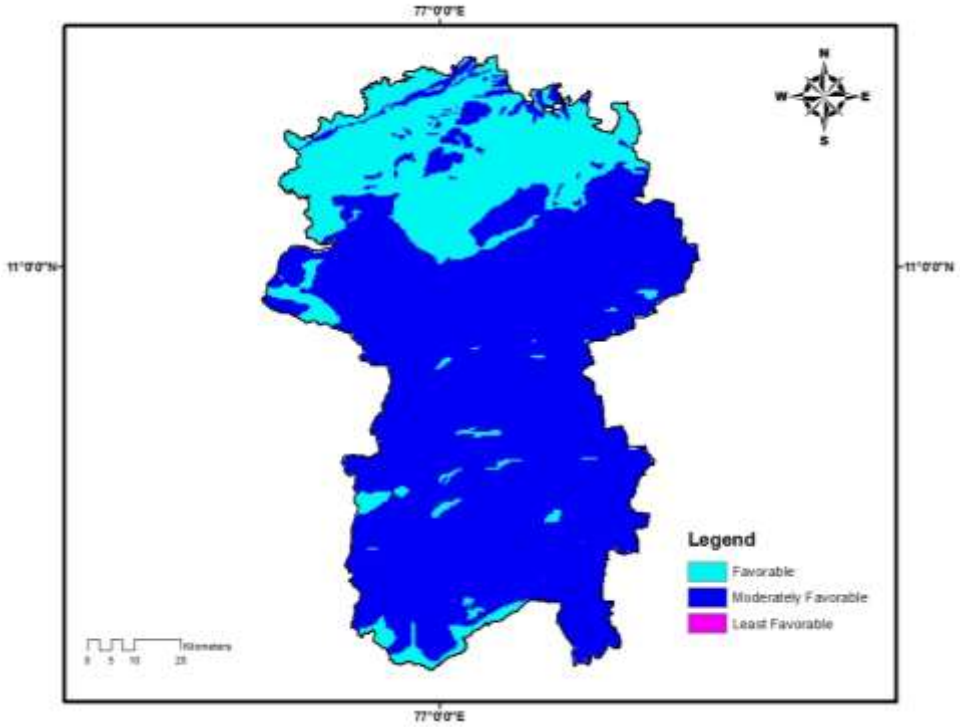

Figure 9: Integrated output and Groundwater potential zone

6. CONCLUSION

The study revealed that the usefulness of spatial data for assessment of groundwater for the study area and also demarcated the groundwater potential zones of Coimbatore district. From the analysis the weightages in the GIS layer was generated, for identifying the groundwater potential zones, different ranks and weightages of the thematic data sets was given and integrated using overlay functions of GIS analysis. Such weightages, the areas having more than 202 values buffered out as high groundwater potential zones. The areas having 149-201 are buffered out as moderately groundwater potential zones. And the area having less than 148 weightages are buffered out as low groundwater potential zones, the study area concern. For the study area, the high groundwater potential zones falling in major portions of Mettupalayam and Avinashi taluks and others are priority wise Coimabtore (north / south), Palladam, Pollachi and Velparai taluks.

REFERENCES:

[1] Murugesan B, Thirunavukkarasu R, Senapathi V and Balasubramanian G, "Application of remote sensing and GIS analysis for groundwater potential zone in kodaikanalTaluka, South India". Earth Science 7(1) 65-75 (2012).

[2] Thakur GS, and Raghuwanshi "RS Prospect and assessment of groundwater resources using remote sensing techniques in and around Choral River Basin, Indore and Khargone Districts, M P" Journal of the Indian Society of Remote Sensing 36(2):217–225(2008).

[3] Chakraborty, S and Paul, P. K " Identification of potential groundwater zones in the Baghmundi block of Purulia district,West Bengal using remote sensing and GIS". Jour. Geol. Soc. India, 64, 69-73(2004).

[4] Sankar, K "Evaluation of groundwater potential zones using remote sensing data in upper Vaigai river basin, Tamilnadu, India", J. Indian Soc. Remote Sensing 30(3), 119–130 (2002).

International Journal of Engineering Research and General Science Volume 3, Issue 6, November-December, 2015
ISSN 2091-2730

Survey On A Hybrid Approach For Web Usage Mining

Samira Nigrel[1], Asmita Patil[2], Pratiksha Bharmal[3], Jagruti Kadam[4], Jagruti Babaria[5]

Professor, Atharva College Of Engineering, Mumbai, Maharashtra[1], Student, Atharva College Of Engineering, Mumbai, Maharashtra.[2][3][4][5]

patilasmita94@gmail.com, +919028602465[2]

Abstract— With the large number of companies using the Internet to distribute and collect information, knowledge discovery on the web or web mining has become an important research area. Basically data mining techniques are used in web mining. Web mining is extended version of data mining. Data mining is work upon Off Line whereas Web mining is work upon On-Line. In data mining data is stored in (database) data warehouse and in web mining data is stored in server database & web log. The expansion of the World Wide Web (Web for short) has resulted in a large amount of data that is now in general freely available for user access. The different types of data have to be managed and organized in such a way that they can be accessed by different users efficiently. Therefore, the application of data mining techniques on the Web is now the focus of an increasing number of researchers. Several data mining methods are used to discover the hidden information in the Web. However, Web mining does not only mean applying data mining techniques to the data stored in the Web. The algorithms have to be modified such that they better suit the demands of the Web. Web mining can be divided into three areas, namely web content mining, web structure mining and web usage mining (also called web log mining).Web content mining focuses on discovery of information stored on the Internet, i.e., the various search engines. Web content mining is the process of extracting useful information from the contents of web documents. Content data is the collection of facts a web page is designed to contain. It may consist of text, images, audio, video, or structured records such as lists and tables. Application of text mining to web content has been the most widely researched. Issues addressed in text mining include topic discovery and tracking, extracting association patterns, clustering of web documents and classification of web pages. Research activities on this topic have drawn heavily on techniques developed in other disciplines such as Information Retrieval (IR) and Natural Language Processing (NLP). While there exists a significant body of work in extracting knowledge from images in the fields of image processing and computer vision, the application of these techniques to web content mining has been limited. Web structure mining can be used when improving the structural design of a website. The structure of a typical web graph consists of web pages as nodes, and hyperlinks as edges connecting related pages. Web structure mining is the process of discovering structure information from the web. This can be further divided into two kinds based on the kind of structure information used.

Keywords— Ant-based clustering, web usage mining, web mining, pre-processing, pattern discovery, pattern analysis, ant colony optimization.

INTRODUCTION

Web content mining is the process of extracting knowledge from web documents such as text and multimedia. Knowledge extraction from the structure of web and hyperlink references is called web structure mining. Web usage mining is the process of knowledge exploitation from the secondary data [1]. Web usage mining is a type of web mining, which exploits data mining techniques to discover valuable information from navigations of Web users. Web usage mining tries to make sense of the data generated by the Web surfer's sessions or behaviors. While the Web content and structure mining utilize the real or primary data on the Web, Web usage mining mines the secondary data derived from the interactions of the users while interacting with the Web. The Web usage includes the data from Web server access logs, proxy server logs, browser logs, user profiles, registration data, user sessions, transactions, cookies, user queries, bookmark data, mouse clicks and scrolls, and any other data as the results of the interactions. Web structure mining tries to discover the model underlying the link structures of the Web. The model is based on the topology of the hyperlinks with or without the description of the links. This model can be used to categorize Web pages and is useful to generate information such as the similarity and relationship between different Web sites. Web structure mining could be used to discover authority sites for the subjects (authorities) and overview sites for the subjects that point to many authorities (hubs) [4].

LITERATURE SURVEY

Web Mining – It is the application of data mining techniques to discover patterns from the Web. According to analysis targets, web mining can be divided into three different types, which are Web usage mining, Web content mining and Web structure mining.

Fig. 2: Web Mining

Web Content Mining (Analyse the content of web pages as well as results of web Searching) Web content mining is a process of extracting up information from texts, images and other contents. The technologies that are mainly used in web content mining are NLP (Natural language processing) and IR (Information retrieval). Web Structure Mining (Hyperlink Structure) Web structure mining is a process of extracting up information from linkages of web pages. Web structure mining is the process of using graph theory to analyse the node and connection structure of a web site. This graph structure can provide information about ranking and enhance search results of a page through filtering. Web Usage mining (analysing user web navigation) Web usage mining is a process of extracting information from user how to navigate web sites. Web usage mining also known as web log mining, aims to discover interesting and frequent user access patterns from web browsing data that are stored in web server logs, proxy server logs or browser logs.[14]

A. Pre Processing

Preprocessing consists of converting the usage, content, and structure information contained in the various available data sources into the data abstractions necessary for pattern discovery [5].As said in [12], pre-processing "consists of converting the usage, content, and structure information contained in the various available data sources into the data abstractions necessary for pattern discovery". This step can break into at least four sub steps: Data Cleaning, User Identification, Session Identification and Formatting. Unneeded data will be deleted from raw data in web log files in the data cleaning step. When a user requests a page, the request is added to the Log File; but if this page contains images, java scripts, flash animations, video, etc., they are added to the Log file as well. Most of the time, these are not needed for pattern discovery and should be omitted from log files [11].

B. Pattern Discovery

Pattern discovery is the discovery of frequently occurring ordered events or subsequences as patterns. An example of it is "Customers who buy a Canon digital camera are likely to buy an HP color printer within a month."There are several methods and techniques for pattern discovery. They are:

1. Clustering: A *cluster* is a collection of objects which are "similar" between them and are "dissimilar" to the objects belonging to other clusters.

2. Classification: Classification is the technique to map a data item into one of several predefined classes [2]. Classification can be done by using supervised inductive learning algorithms such as decision tree classifiers, naïve Bayesian classifiers, k-nearest neighbor classifiers, Support Vector Machines etc [5].

C. Pattern Analysis

Challenges of Pattern Analysis are to filter uninteresting information and to visualize and interpret the interesting patterns to the user. First delete the less significance rules or models from the Interested model storehouse; Next use technology of OLAP and so on to carry on the comprehensive mining and analysis; Once more, let discovered data or knowledge be visible; Finally, provide the characteristic service to the electronic commerce website[6].

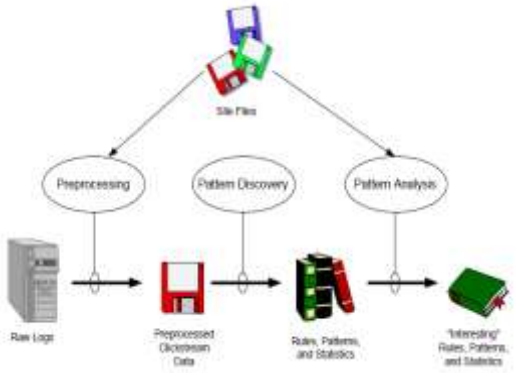

Fig. 2: Depicts three main tasks for Web Usage Mining process.

D. Ant colony optimization

The complex social behaviors of ants have been much studied by science, and computer scientists are now finding that these behavior patterns can provide models for solving difficult combinatorial optimization problems. The attempt to develop algorithms inspired by one aspect of ant behavior, the ability to find what computer scientists would call shortest paths, has become the field of ant colony optimization (ACO), the most successful and widely recognized algorithmic technique based on ant behavior[3].

E. Ant Based Clustering

Deneubourg et al. in [7] proposed ant-based clustering and sorting. In the case of ant-based clustering and sorting, two related types of natural ant behaviors are modeled. When clustering, ants gather items to form heaps. And when sorting, ants discriminate between different kinds of items and spatially arrange them according to their properties [8]. Lumer and Faieta[9]. in proposed ant-based data clustering algorithm, which resembles the ant behavior described in [7]. The agents (ants) and data are randomly initialized on a toroidal grid. By moving agents, data is sorted according to its neighbors. The picking and dropping probabilities, given a grid position and a particular data item *i*, are computed using the density functions. Handl & Meyer in [10] proposed an extension of this algorithm where the parameter _ is adaptively updated during the execution of the algorithm. We applied Handl & Meyer's Ant-based clustering algorithm for detecting user's patterns [11].

CONCLUSION

In this paper we survey the area on the web mining. From this survey we can say that A hybrid approach of ant based clustering algorithm with Lumer faieta can be used to remove the traffic from the weblogs.

REFERENCES:

[1] R. Cooley, Web Usage Mining: Discovery and Application of Interesting patterns from Web Data, Ph. D. Thesis, University of Minnesota, Department of Computer Science, 2000.
[2] Kobra Etminani, Mohammad-R. Akbarzadeh-T. 2, Noorali Raeeji Yanehsari, Web Usage Mining: users' navigational patterns extraction from web logs using Ant-based Clustering Method**,** IFSA-EUSFLAT, 2009.
[3] Marco Dorigo and Thomas Stützle, in "Ant colony Optimization," June 2009.

[4] Raymond Kosala, Hendrik Blockeel. Web Mining Research: A Survey**.** Volume 2, Issue 1-page 4, ACM SIGKDD, July 2000.
[5] Jaideep Srivastava , Robert Cooley, Mukund Deshpande, PangNing Tan, Web Usage Mining: Discovery and Applications of Usage Patterns from Web Data, Volume 1, Issue 2-page 5, ACM SIGKDD, Jan 2000.
[6] Rajni Pamnani, Pramila Chawan, Web Usage Mining: A Research Area in Web Mining.
[7] J. Deneubourg -L., S. Goss, N. Franks, A. Sendova-Franks, C. Detrain, L. Chrétien, The dynamics of collective sorting: robot-like ants and ant-like robots. Proceeding of the first international conference on simulation of adaptive behavior, pp. 356–365, MIT Press, 1991.
[8] J. Handl, B. Meyer, Ant-based and Swarm-based clustering, Swarm Intelligence, 1, pp. 95–113, 2007.
[9] E. Lumer, B. Faieta, Diversity and adaptation in populations of clustering ants. Proceeding of the third international conference on simulation of adaptive behavior, pp. 501–508, MIT Press, 1994.
[10] J. Handl, B. Meyer, Improved ant-based clustering and sorting in document retrieval interface. Proceeding of the Seventh International Conference on Parallel Problem Solving from Nature, Vol. 2439 of Lecture Notes in Computer Science, pp. 913-923, Germany: Springer-Verlag, 2002.
[11] Kobra Etminani , Mohammad-R. Akbarzadeh-T. 2, Noorali Raeeji Yanehsari, Web Usage Mining: users' navigational patterns extraction from web logs using Ant-based Clustering Method, ISBN: 978-989-95079-6-8, IFSA-EUSFLAT2009
[12] J. Srivastava, R. Cooley, M. Deshpande, and P.N. Tan, Web Usage Mining: Discovery and Applications of Usage Patterns from Web Data, SIGKDD Explorations, 1(2), pp. 12-23, 2000.
[13] Christian Blum, Ant colony optimization: Introduction and recent trends, Physics of Life Reviews 2 (2005) 353–373.
[14] Aparna N. Gupta , Prof. Arti Karndik ar, "A Review: Study of Various Clustering Techniques in Web Usage Mining", International Journal of Advanced Research in Computer and Communication EngineeringVol.3,Issue3,March2014

International Journal of Engineering Research and General Science Volume 3, Issue 6, November-December, 2015
ISSN 2091-2730

Analysis of hybrid PV/T air collector on the basis of carbon credit earned & energy matrices

Deepika Chauhan[1]*, Sanjay Agarwal [2] , YS Shishodia [3]

[1] Jaipur National University, Jaipur, India, 302025

[2] SOET, IGNOU, New Delhi, India 110068

[3] Jagannath University, Jaipur, India

* Corresponding author. Tel. +91-9252605292; email: deepika0501@gmail.com

Abstract-In this paper study has been carried out to evaluate overall thermal energy gain and exergy gain for the different Indian climatic condition of Jodhpur, Srinagar, Bangalore & New Delhi. This study involves the electrical and thermal output of opaque PV module having duct above the module. Further carbon credit & energy matrices analysis mainly in terms of energy payback period (EPBT), energy production factor (EPF) & life cycle conversion efficiency (LCCE) have been carried out which is based on overall thermal & exergy gain. The effect of different rate of interest of 8%, 10% & 12% on annualized uniform cost (AUC), EPF & LCCE has also been analyzed. It was found from envireoeconomic analysis that in terms of overall thermal & exergy gain, environmental cost is Rs 3261.97 /annum & Rs 699.99 /annum. It has been observed that annualized uniform cost (AUC) is higher for all cities in case of overall exergy gain as compare to overall thermal gain.

Key words: hybrid air collector, energy payback period, energy production factor, carbon credit earned, Solar cell, PV module, Life cycle conversion efficiency

1. INTRODUCTION

A lot of research work has been carried out in terms of the energy matrices of hybrid PVT air collector. Firstly energy payback period of about 40 years was reported by Slesser & Houman [15] but by doing the similar study energy payback period of about 12 years was reported by Hunt [8] which is in also support of the work done by kato et al.[11] for crystalline Si solar cell module. Furthermore an analysis has been done on the forecasting of EPBT for monocrystalline solar cell for the year 2020 by considering the various improved solar cell technology & efficiencies. Finally by doing forecasting Alsema & Nieuwlar [3] have reported that present EPBT of 5-6 years get reduced to 1.5-2 years. Taking into consideration annual cell production rate of .01 GW/y & cost in a range of 30,000-200,000 yen/t-c for reducing CO_2 emission, Yamada et al. [19] evaluated the EPBT to be around 6 years. Based on the survey, Gaiiddon and Jedliczaka [6] has done the comparative assessment and found that for a roof-mounted system EPBT of a complete PV system in the range of 1.6-3.3 years and for a PV façade it is 2.7 to 4.7 years. The value of energy relation factor by considering 30 year life period is found to be between 8 &18 for roof mounted system and between 5.4 & 10 for PV façade. They also give very useful result keeping in mind the environmental parameters which conclude that 40 ton of carbon dioxide is reduced by one single kWp of PV panel during its life cycle while carbon reduction of 23.5 ton is achieved per kWp for PV facades. Kalogirou [9] uses thermosiphon solar water heating system to study thermal performance, economics and environmental protection. His comparison shows the system to be financial with payback period of 4.5 years and with electricity back up found the life cycle saving of €2240 while with diesel back up he found payback period of 4.5 years and life cycle saving of €1056. When a system is in thermodynamic equilibrium with the environment, it is said to be in the dead state .At this state system possess no kinetic & potential energy and it has the temperature and pressure of its environment state. Considering the nine different dead state temperatures, Hakan et al. [7] analyzed the maisotsenko cycle based novel air collector on the basis of energy ,exergy, exergeoeconomic & enviroeconomic and found 58.85$/year to be the electrical energy consumption while from envireoeconomic point of view CO_2 emission cost was found to be 6.96$/year. In India about 60% of the electricity production is by means of coal which is the main cause behind CO_2 emission & that of acid rain. In present scenario whats so ever oil, gas and coal we have reserved, it will exhaust in about 22 years, 30 years and 80 years respectively. If India continues to grow at 8% Kalshion [10] the coal reserves will last in about less than 40 years. Raman & Tiwari [14] has done the analysis of hybrid PVT air collector, single & double pass for different Indian climatic condition of Jodhpur, New Delhi, Bangalore & Srinagar and found Jodhpur is most economical in terms of cost/kWh. After calculating carbon credit earned by PVT system at IIT, Delhi, Prabhakant & Tiwari [12] suggested that in order to reduce the emission of carbon dioxide & earned carbon credit, there should be more development of solar energy park.

By studying the potential of solar home system for diffusion and appropriate baseline, Chaurey & Kandpal [5] has made an attempt to estimate the CO_2 mitigation potential & concluded that if the carbon prices are taken as \$10/tCO_2 without transaction cost, carbon finance could reduce the effective burden of SHS to the user by 19%. An attempt was also made by Purohit [13] to estimate the CO_2 mitigation potential of solar home system under CDM in India. Overall performance of Opaque PV module having duct above the module has been analyzed by Deepika et al.[4] for Indian climatic condition of Jodhpur, New Delhi, Bangalore & Srinagar and concluded that the Bangalore city is having highest performance in terms of thermal energy, electrical energy, overall thermal energy, overall exergy gain, exergy efficiency.

2. PROPOSED MODULE DESCRIPTION

Proposed hypothetical module of hybrid PVT air collector with given dimension, design parameter, variation of climatic parameter have been used as in Deepika et al [4] as shown in figure 1(a) and its cross section view is shown in figure 1 (b).

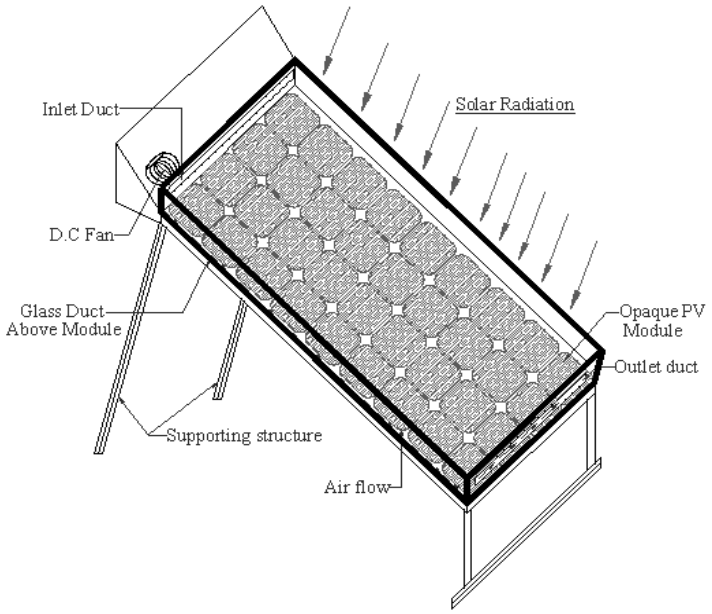

Figure 1 (a) Schematic diagram of opaque PV module having air duct on top of module

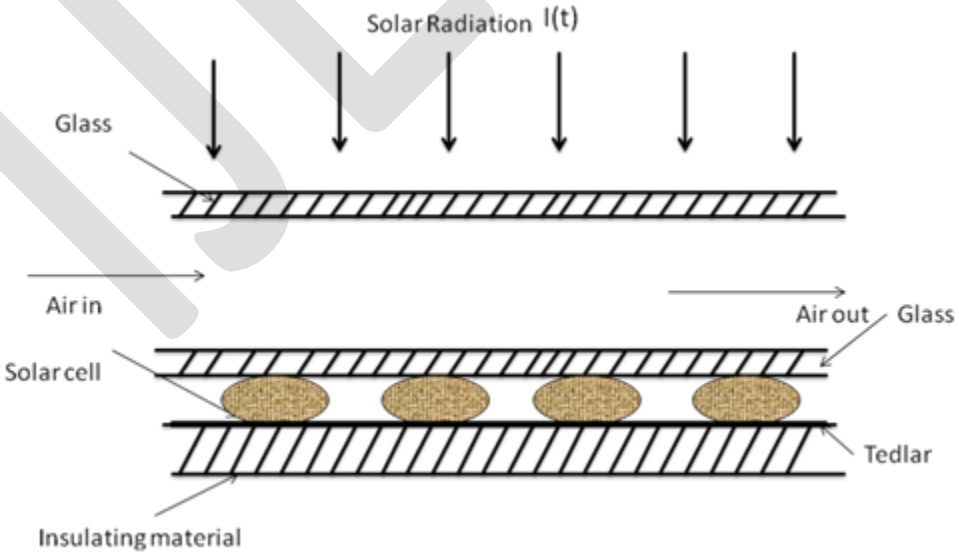

Figure 2(b): Cross-section view of opaque PV module having air duct on top of module

The value of overall thermal energy and exergy gain obtained from this has been used in this analysis. The hourly variation of monthly solar radiation, number of days falls under different climatic condition & hourly variation of ambient temperature are used as in Agarwal & Tiwari [1].

3. MATHEMATICAL FORMULATION OF VARIOUS FORMS OF ENERGY

The analysis which involved in life cycle cost analysis mainly covers the two forms of energy analysis. The first one is the embodied energy and other is energy matrices. Early researchers have carried out the study of life cycle conversion analysis (LCCA) without considering the effect of EPBT due to which actual life cycle cost was not obtained. In the present study an attempt has been made for investigation of life cycle cost of the PVT system by taking into account the effect of EPBT. The system has been analyzed based upon the overall exergy gain & thermal energy gain for climatic condition of New Delhi, Jodhpur, Srinagar and Bangalore, India. To calculate the quantity of energy use in generation of energy through PVT system LCCE analysis is to be done. This analysis mainly covers the field of embodied energy and energy matrices.

3.1 ANALYSIS OF EMBODIED ENERGY

Embodied energy can be defined by Treolar [18] as "the quantity of energy required by all of the activities associated with a production process, including the relative proportions consumed in all activities upstream to the acquisition of natural resources and the share of energy used in making equipments and in other supporting functions i.e direct energy plus indirect energy" .Thus embodied energy analysis is used to calculate the amount of required energy for manufacturing a material. After this analysis, there is also a need to know about the energy of different component. The breakup of embodied energy of each component of fabrication of PVT air collector is shown in Table 1.

Table 1. Breakup of embodied energy of different component of opaque PV module

Sr. No.	Component	Total embodied energy (kWh)
1	MS support structure	105.16
2	PV module (glass-Tedlar type) with duct above module	667.15
3	DC fan	26.82
Total		799.13

Table 2. Capital cost (Pc), Salvage value (Sv) & Maintenance cost (Mc) of hybrid PVT module air collector

Component	Quantity	PVT air collector	Salvage value (Sv) at the inflation rate of 4% (Present value of scrap for Iron @ Rs (15 kg)		
			After 20 year Iron scrap @Rs 33(kg)	After 30 year Iron scrap @Rs 49(kg	After 40 year Iron scrap @Rs 72(kg
Mild steel support structure @ Rs 50(kg)	10.7	535	353	524	770
PV module @ Rs 5000/ 75Wp	1no.	5000	100	100	100
DC fan(12 v &1.8 A)	1 no.	350	15	15	15
Paint @ Rs 80(kg)	0.4 kg	32	NA	NA	NA

Fabrication charges		500	NA	NA	NA
Capital cost		Rs 6417	Rs 468	Rs 639	Rs 885

Operational & maintenance cost=Rs 500/per year

Fan replacement cost & paint=Rs 600/-in every 10 year.

NA-no salvage value.

3.2 ENERGY MATRICES

Basically there are three energy matrices which are used to evaluated the performance of PVT system i.e energy payback period (EPBT), energy production factor (EPF) & LCCE (life cycle conversion efficiency).

3.2.1 ENERGY PAYBACK PERIOD (EPBT)

EPBT is defined as the ratio of total energy consumed in the production & installation of the system (Eenergyin) to the total energy available at the output.

$$EPBT = \frac{E_{energyin}(Kwh)}{E_{energyout}(kwh/year)} \quad (1)$$

3.2.2 ENERGY PRODUCTION FACTOR (EPF)

Overall performance of the PVT system can be evaluated by comparing the total energy supplied to the system and the total output energy available. The ratio of total energy output to the total energy input is defined as the energy production factor (EPF). The evaluation of EPF can be done on annual and life time basis as follows–:

i) On annual basis

$$\chi_{ann} = \frac{E_{energyout}}{E_{energyin}}$$

or $$\chi_{ann} = \frac{1}{EPBT} \quad (2)$$

If $\chi_{ann} \longrightarrow 1$ for EPBT=1, the system is worthwhile from energy point of view otherwise it is not.

ii) On Life time basis

$$\chi_{Life} = \frac{E_{energyout} \times T}{E_{energyin}} \quad (3)$$

Where T=Life time

$E_{energyout}$ = Total energy output

$E_{energyin}$ = Total energy input

3.2.3 LIFE CYCLE CONVERSION EFFICIENCY (LCCE)

This is defined as the net energy productivity of the system over the life time (T) years w.r.t input solar radiation

$$\phi_{Life}(t) = \frac{(E_{energyout} \times T) - E_{energyin}}{E_{solar} \times T} \quad (4)$$

4. ANNUALIZED UNIFORM COST

Present and future costs are also involved in order to calculate the life cycle cost analysis. There are various cost parameters that are to involved in the analysis like initial cost, operation & maintenance cost, replacement cost and salvage value. Let P is the initial cost which include support structure cost, DC fan cost, module cost etc,R_1,R_2-----Rn is the operation & maintenance cost which charged annually , $R_{10,1}$,$R_{10,2}$-----is the replacement cost of the fan & paint made in every ten year. By Raman & Tiwari [14] , the capital recovery factor over the life time can be expressed as-

$$CPRF = \frac{i(1+i)^n}{(1+i)^n - 1} \quad (5)$$

Where i = rate of interest per year

n = number of years

Then the net present value can be calculated based on different criterion-

i) Without considering the effect of EPBT

The computation of life cycle cost of the PVT system can be obtained by conventional cash flow diagram as shown in Figure (2)

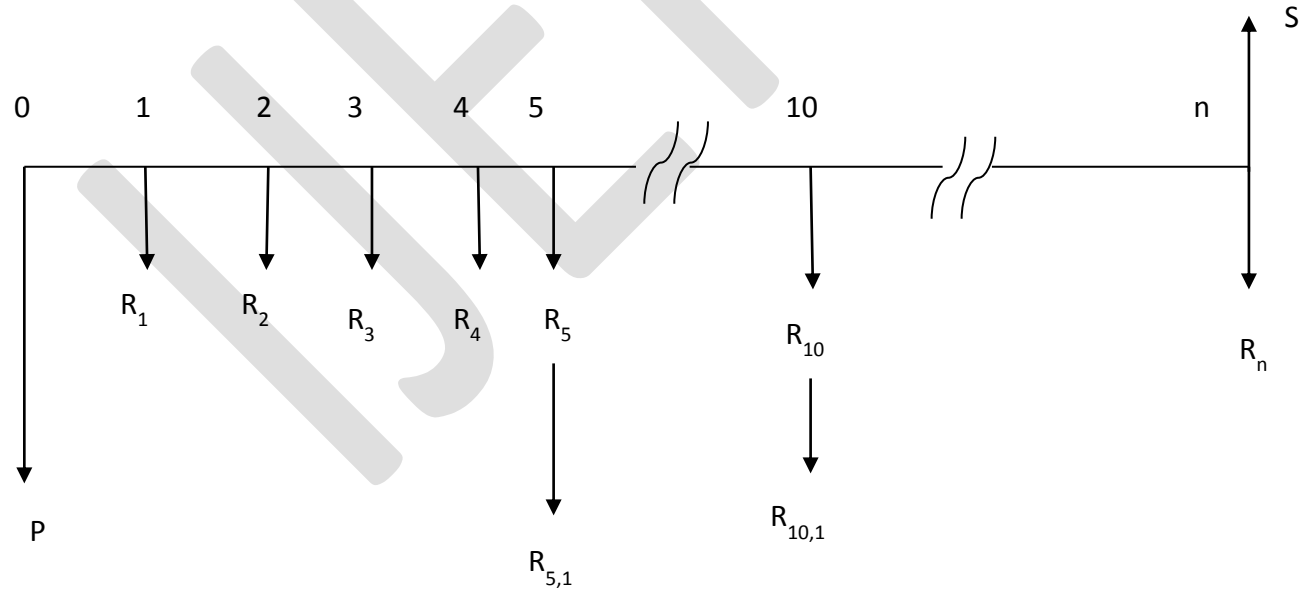

Figure. 2. Conventional cash flow diagram for life cycle cost of PVT system without considering effect of EPBT

Here NPVL can be calculated by the given formula-

$$NPVL = P_c + R_1 \times \left[\frac{(1+i)^n - 1}{i(1+i)^n}\right]_{i,n} + R_{10,2} \times \left[\frac{1}{(1+i)^n}\right]_{i,10} + \text{------} + R_{10,1} \times \left[\frac{1}{(1+i)^n}\right]_{i,10}$$

$$+ \text{--------} S_v \times \left[\frac{1}{(1+i)^n}\right]_{i,n} \qquad (6)$$

Where NPVL = Net Present Value of the PVT system

ii) Considering the effect of EPBT

Here the conventional cash flow diagram can be obtained as shown in figure (3)

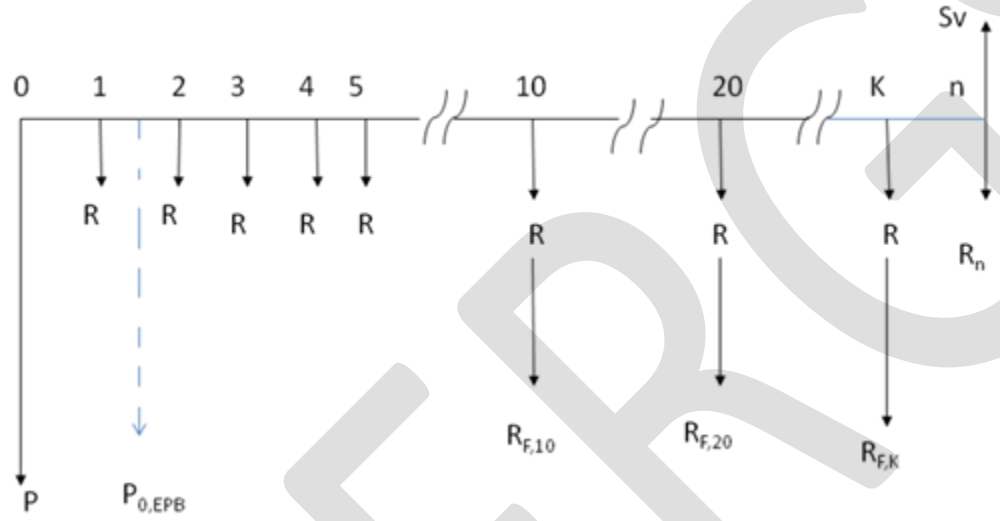

Figure. 3. Conventional cash flow diagram for life cycle cost of PVT system with considering effect of EPBT

$$\text{NPVL} = \text{P}_{\text{EPBT}} = \text{P}_c(1+\text{i})^{\text{EPBT}} + \text{R} \times (1+\text{i})^{\text{EPBT}-1} + \text{R} + \text{R} \times \left[\frac{(1+\text{i})^{\text{n}-\text{EPBT}} - 1}{\text{i}(1+\text{i})^{\text{n}-\text{EPP}}}\right] + \text{R}_{\text{F,10}} \times \left[\frac{1}{(1+\text{i})^{10-\text{EPBT}}}\right] + \text{R}_{\text{F,20}} \times \left[\frac{1}{(1+\text{i})^{20-\text{EPBT}}}\right]$$

$$+ \text{------} + \text{R}_{\text{F,K}} \times \left[\frac{1}{(1+\text{i})^{\text{K}-\text{EPBT}}}\right] + \text{--------} \text{S}_{\text{v}} \times \left[\frac{1}{(1+\text{i})^{\text{n}-\text{EPBT}}}\right] \qquad (7)$$

Therefore Annualized uniform cost (AUC) by Tiwari [17] is defined as the multiplication of the net present value of the PVT system and capital recovery factor is given by

$$AUC = NPVL \times CPRF \qquad (8)$$

The cost of per unit of electricity generated by the PVT system is defined as the ratio of annualized uniform cost and overall thermal energy or exergy produced by the PVT system.

5. CARBON CREDIT EARNED

The production of electricity from fossil fuel which result emission of CO_2 in the environment causes great hazard to human being. In order to avoid the CO_2 emission envireoeconomic analysis is very important mechanism to promote the development of renewable

energy technology which does not emit any carbon to the atmosphere. Total carbon credit earned on life time basis has been obtained on the basis of overall thermal energy gain & exergy gain.

5.1 Overall Thermal Energy Gain Basis

Overall thermal energy produced per annum for Bangalore is 1029.33 kWh

5.5 is taken as the unit cost of energy per annum then cost of energy produced per annum=1029.33x5.5=Rs 5661.31

The amount of CO2 emission for unit power consumption will be 2.08x0.982 = 2.04 kg/kWh

The carbon dioxide reduction per annum = 2.04x1029.33 = 2099.83kg

In ton = 2.099 t CO_2e

If carbon dioxide emission at present is being traded @€23/t CO_2e, then cost of carbon emission reduction per annum = 23x2.099 = € 48.296

This can be converted in rupees by multiplying current euro rupee conversion factor = 48.296x67.54 = Rs 3261.92

5.2 Overall Exergy Gain Basis

Overall exergy gain produced per annum for Bangalore is 220.89 kWh

5.5 is taken as the unit cost of energy per annum then cost of energy produced per annum=220.89 x5.5=Rs 1214.89

The amount of CO_2 emission for unit power consumption will be 2.08x0.982 = 2.04 kg/kWh

The carbon dioxide reduction per annum = 2.04x220.89 = 450.61 kg

In ton = 0.450 tCO_2e

If carbon dioxide emission at present is being traded @€23/t CO_2e, then cost of carbon emission reduction per annum=23x0.450= € 10.364

This can be converted in rupees by multiplying current euro rupee conversion factor = 10.364x67.54 = Rs 699.99

Similarly carbon credit analyzed can be done for New Delhi, Jodhpur, Srinagar and earned carbon credit as shown in Table 3.

TABLE 3.TOTAL CARBON CREDIT EARNED BY DIFFERENT CITIES FOR GIVEN PV MODULE

City	CO_2 mitigation per annum (tCO_2/annum)		Envireoeconomic (environmental cost) parameter Rs/annum	
	In terms of overall thermal energy gain	In terms of overall exergy gain	In terms of overall thermal energy gain	In terms of overall exergy gain
Bangalore	2.09	0.450	3261.97	699.99
New Delhi	1.90	0.406	2959.88	631.95
Jodhpur	2.05	0.446	3196.57	693.05
Srinagar	1.86	0.396	2889.37	615.97

6. RESULTS & DISCUSSION

THE OVERALL THERMAL ENERGY & EXERGY GAIN FOR THE OPAQUE PV MODULE HAVING DUCT ABOVE THE MODULE IS TAKEN AS IN DEEPIKA ET AL. [4] FOR DIFFERENT INDIAN CLIMATIC CONDITION. THE BREAKUP OF THE EMBODIED ENERGY OF DIFFERENT COMPONENT USED IN FABRICATION AND THE CAPITAL COST (PC) & SALVAGE VALUE (SV) OF THE GIVEN MODULE HAS BEEN SHOWN IN TABLE 1 & 2 RESPECTIVELY

TABLE 4.ENERGY PAYBACK PERIOD AND ENERGY PRODUCTION FACTOR ANNUALLY ON THE BASIS OF OVERALL THERMAL ENERGY & OVERALL EXERGY FOR
DIFFERENT CITIES

Basis	Energy Payback Period (EPBT)				Energy Production factor(EPF)			
	Bangalore	New Delhi	Jodhpur	Srinagar	Bangalore	New Delhi	Jodhpur	Srinagar
Overall Thermal Energy	0.77	0.85	0.79	0.87	1.29	1.17	1.26	1.14
Overall Exergy	3.61	4	3.65	4.11	0.27	0.25	0.27	0.24

TABLE 5 EPF & LCCE ON THE BASIS OF OVERALL THERMAL ENERGY & EXERGY FOR DIFFERENT VALUES OF LIFE TIME PERIOD (N=20, 30, 40 YEARS)

Life Time (Years)	City	EPF		LCCE	
		Energy basis	Exergy basis	Energy basis	Exergy basis
20	Bangalore	25.8	5.4	1.24	0.221
	New Delhi	23.4	5	1.12	0.2
	Jodhpur	25.2	5.4	1.21	0.220
	Srinagar	22.8	4.8	1.09	0.190
30	Bangalore	38.7	8.1	0.327	0.237
	New Delhi	35.1	7.5	0.297	0.216
	Jodhpur	37.8	8.1	0.318	0.237
	Srinagar	34.2	7.2	0.286	0.207
40	Bangalore	51.6	10.8	1.26	.2456
	New Delhi	46.8	10	1.14	0.225
	Jodhpur	50.4	10.8	1.235	.2453
	Srinagar	45.6	9.6	1.11	0.215

TABLE 6 VARIATION OF ANNUALIZED UNIFORM COST FOR DIFFERENT CITIES AT DIFFERENT RATE OF INTEREST & EXPECTED LIFE TIME PERIOD OF THE SYSTEM WITHOUT CONSIDERING THE EFFECT OF EPBT

Life Time (Years)	City	Annualized Uniform cost(AUC)					
		i=0.08		i=0.1		i=0.12	
		Energy basis	Exergy basis	Energy basis	Exergy basis	Energy basis	Exergy basis
20	Bangalore	1.15	5.39	1.25	5.84	1.34	6.25
	New Delhi	1.27	5.97	1.38	6.47	1.480	6.93
	Jodhpur	1.18	5.45	1.27	5.90	1.370	6.32
	Srinagar	1.30	6.13	1.41	6.64	1.51	7.11
30	Bangalore	1.07	4.98	1.18	5.51	1.291	6.01
	New Delhi	1.17	5.52	1.30	6.10	1.423	6.66
	Jodhpur	1.09	5.03	1.20	5.56	1.318	6.07
	Srinagar	1.20	5.66	1.33	6.26	1.45	6.84
40	Bangalore	1.06	4.94	1.18	5.50	1.295	6.03
	New Delhi	1.16	5.47	1.30	6.09	1.427	6.68
	Jodhpur	1.08	4.99	1.20	5.55	1.321	6.09
	Srinagar	1.19	5.62	1.33	6.25	1.46	6.86

Table 7 Variation of annualized Uniform Cost for different cities at different rate of interest & expected life time period of the system with considering the effect of EPBT

Life Time (Years)	City	Annualized Uniform cost(AUC)					
		i=0.08		i=0.1		i=0.12	
		Energy basis	Exergy basis	Energy basis	Exergy basis	Energy basis	Exergy basis
20	Bangalore	1.26	6.59	1.40	7.65	1.53	8.77
	New Delhi	1.40	7.42	1.55	8.67	1.69	10.01
	Jodhpur	1.29	6.67	1.43	7.74	1.56	8.88
	Srinagar	1.43	7.65	1.59	8.96	1.73	10.36
30	Bangalore	1.17	6.16	1.32	7.28	1.47	8.50

	New Delhi	1.30	6.94	1.46	8.26	1.63	9.71
	Jodhpur	1.20	6.23	1.35	7.38	1.50	8.61
	Srinagar	1.33	7.15	1.50	8.54	1.67	10.05
40	Bangalore	1.14	6.01	1.30	7.16	1.45	8.39
	New Delhi	1.26	6.78	1.44	8.12	1.61	9.59
	Jodhpur	1.16	6.08	1.32	7.25	1.48	8.50
	Srinagar	1.29	6.99	1.47	8.39	1.65	9.93

The energy payback period & energy production factor on the basis of overall thermal energy gain and exergy gain can be calculated from equation (1) & (2) respectively. The value of EPBT & EPF of given hybrid PV module have been shown in Table 4.It has been observed that the value of EPBT & EPF is more when analysis has been done on the basis of overall thermal energy gain basis and overall exergy gain respectively. The minimum value of EPBT for Jodhpur on the basis of overall thermal energy gain & exergy gain is 0.77 & 3.61 respectively while it is maximum for Srinagar is 0.87 & 4.11 respectively. The maximum value of EPF on the basis of overall thermal energy gain & exergy gain are 1.29 & 0.27 respectively. Life cycle conversion efficiency & annualized uniform cost for different life time period have been evaluated by equation (4) & (8) respectively while the net present value for different criterion has been evaluated by equation (6) & (7). It has been observed that value of EPF & LCCE increases from Srinagar to Bangalore and the same increasing trend follow while increasing the life time period of the system both on energy & exergy gain basis. The result of EPF & LCCE for the given PV module for the different Indian climatic condition have been shown in Table (5).

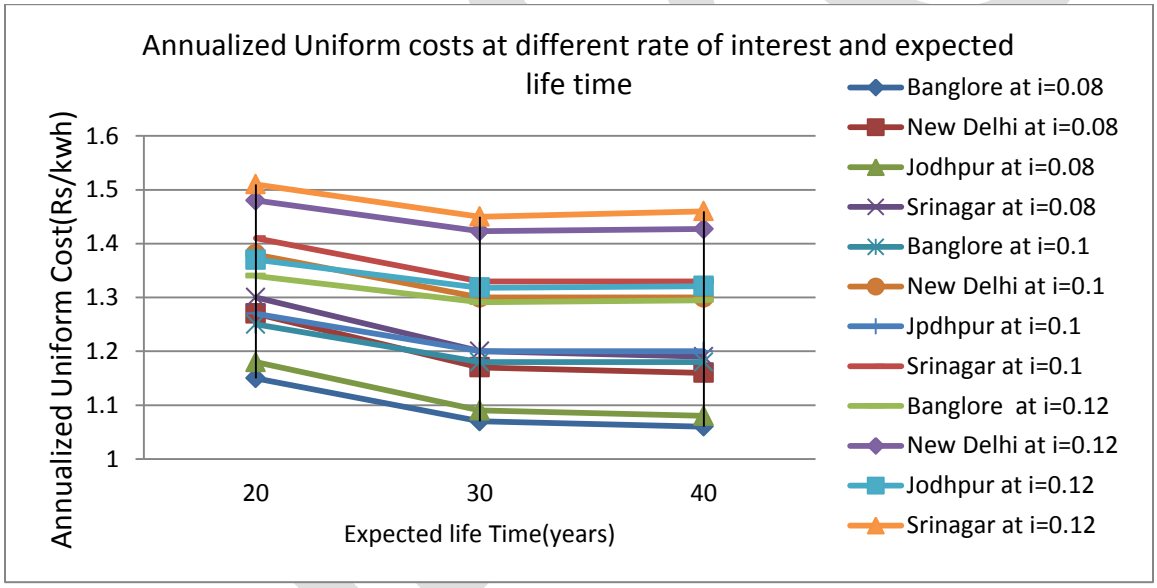

Figure 4 variation of annualized uniform cost at different rate of interest & expected life time period without considering the effect of EPBT

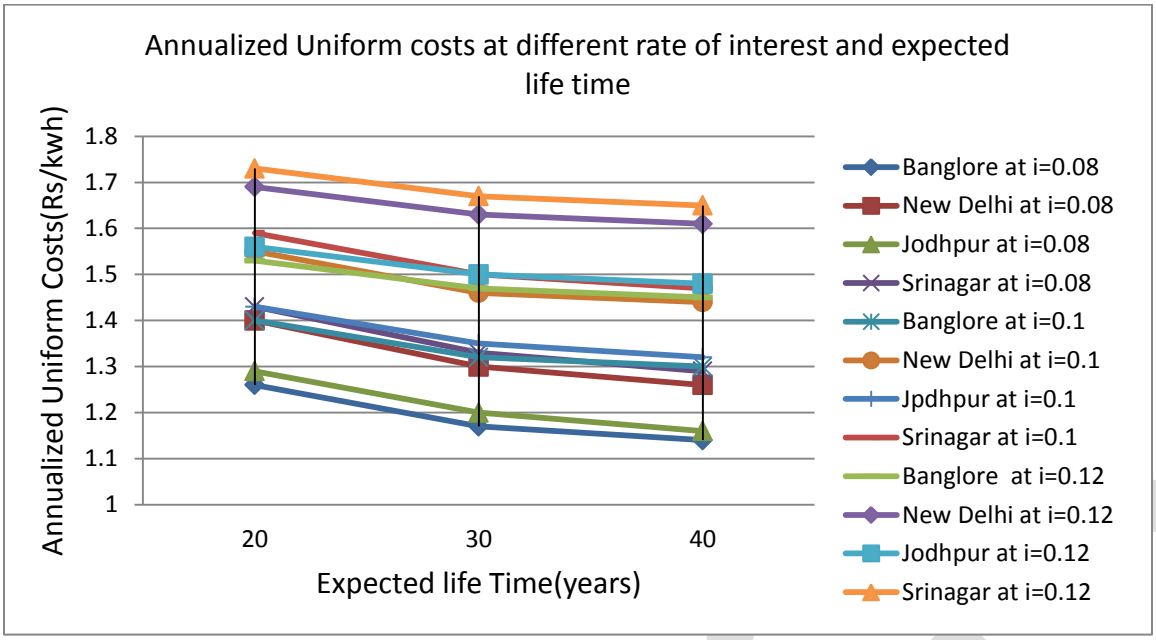

Figure 5 variation of annualized uniform cost at different rate of interest & expected life time period with considering the effect of EPBT

The effect of annualized uniform cost with different rate of interest & for different life time period without & with considering the effect of EPBT has been shown in Table (6) & (7) respectively. It has been found that with the increase in life time period of the system, the value of annualized uniform cost deceases while value of EPF & LCCE increases this result also proves the work done by Solanki et al.[16]. From Table 6 & 7, it has been observed that annualized uniform cost (Rs/kWh) is higher on the basis of overall exergy gain in comparison to overall thermal energy gain this is in accordance with result obtained by Agrawal & Tiwari [2].Here annualized uniform cost is an indication of energy incurred in the system and hence it can be concluded that system which is having lower value is a better system. It has also been that with considering the effect of EPBT annualized uniform cost has been increased by 7.5% for the minimum value & 45.7% for the maximum value. The plot of annualized uniform cost against various life time period & at different rate of interest with 8%,10% &12% is shown in the Figure (4) & (5) without & with considering the effect of EPBT. By comparing the figures (4) & (5), it has been found that Srinagar has got highest annualized uniform cost while Bangalore has got lowest one in both the cases.

6. CONCLUSION

From the present study various points have been concluded-

Highest payback period is 0.87 & 4.11 on the basis of overall thermal energy & exergy gain respectively.

Highest & lowest value of EPF & LCCE on the basis of overall thermal energy gain & exergy gain is for Bangalore & Srinagar respectively.

Bangalore has got the highest value of carbon credit earned on the basis of energy & exergy gain .

The value of annualized uniform cost without & with considering the effect of EPBT is highest for Srinagar for high rate of interest while Bangalore has got lower value at lower rate of interest.

REFERENCES:

[1]Agrawal, S., Tiwari, G.N., 2011a. Energy and exergy analysis of hybridmicro-channel photovoltaic thermal module. Solar Energy 85, 356–370

[2] Agrawal, S., Tiwari, G.N., 2013. Enviroeconomic analysis and energy matrices of glazed hybrid photovoltaic thermal module air collector Solar Energy 92, 139–146

[3] Alsema, E.A., Nieuwlaar, E., 2000. Energy viability of photovoltaic systems. Energy Policy 28, 999- 1010

[4] Chauhan D,shishodia S.,Agarwal S. Performance of Hybrid Air Collector under Different Condition, European Journal of Advances in Engineering and Technology, 2015, 2(3): 69-75

[5] Chaurey , A., Kandpal, T.C.,2009. Carbon abatement potential of solar home systems in India and their cost reduction due to carbon finance. Energy Policy 37, 115–125.

[6] Gaiddon, B., Jedliczka, M., 2006. Compared assessment of selected environmental indicators of photovoltaic electricity in OECD cities. International Energy Agency Photovoltaic Power Systems Programme. Report IEA-PVPS T10-01:2006.11, 363– 385

[7] Hakan, C., Ibrahim, D., Arif, H., 2012. Exergoeconomic, envireoeconomic and sustainability analyses of a novel air cooler. Energy and Buildings 55, 747–756.

[8] Hunt, L.P., 1977. Total Energy use in Production of Silicon Solar Cells from raw material to finish product. IEEE PV Specialists Conf., 347-352.

[9] Kalogirou, S., 2009. Thermal performance, economic and environmental life cycle analysis of thermosiphon solar water heaters. Solar Energy 83 (1), 39–48

[10] Kalshian, R., 2006. Energy versus emissions: the big challenge of the new millennium. By Info Change News and Features. <www.infochangeindia. org/agenda5_01.jsp

[11] Kato, K., Murata, A., Sakuta, K., 1998. Energy payback time and Life-cycle CO_2 emission of residential PV power system with silicon PV module. Progress in photovoltaics: Research and Applications 6, 105-115

[12] Prabhakant, Tiwari, G.N., 2008. Evaluation of carbon credits earned by a solar energy Park In Indian Conditions. The Open Fuels and Energy Science Journal 1, 57–66.

[13] Purohit P., 2009. CO2 emissions mitigation potential of solar home systems under clean develop ment mechanism in India. Energy 34, 1014–1023

[14] Raman, V., Tiwari, G.N., 2008. Life cycle cost analysis of HPVT air collector under different Indian climatic conditions. Energy Policy 36, 603–611

[15] Slesser, M., Hounam, I. , 1976. Solar energy breeders, Nature 262, 244.

[16] Solanki S.C, Gaur.M.K, Tiwari G.N Life cycle cost analysis & Earned carbon credit of photovoltaic Thermal(PV-T) Air collectors connected in series,proceeding of International conference on Energy Security,Global warming and sustainable climate(solaris-2012) 43-56

[17]Tiwari, G.N., 2002. Solar Energy: Fundamentals, Design. NarosaPublishing House, New Delhi, Modeling and Applications

[18]Treloar, G.J., 1994. Energy analysis of the construction of office buildings. Deakin University, Geelong, Master of Architecture thesis.

[19] Yamada, K., Komiyama, H., Kato,K., Inaba, A., 1995. Evaluation of photovoltaic energy systems in terms of economics, energy and CO2 emissions, Energy Conversion Management 36 (6-9), 819-822

International Journal of Engineering Research and General Science Volume 3, Issue 6, November-December, 2015
ISSN 2091-2730

ESSENTIAL BEST PRACTICES AND PROCESSES IN HIGHER EDUCATIONAL TECHNICAL INSTITUTIONS

[1]Dr.S.Mohan Kumar ME [CSE]., Ph.D[CSE]., [2]Prof. Karthikayini.T BE [CSE}., ME[CSE].,
[1] Associate Professor, Department of Computer Science and Engineering,
New Horizon College of Engineering,
Bangalore.
E-Mail:mohankumar.sugumar@gmail.com
[2] Assistant Professor, Department of Computer Science and Engineering,
New Horizon College of Engineering,
Bangalore.
E-Mail:karthikayini@outlook.com

Abstract— Best practices and processes in higher educational technical institutions are at most important and so much in demand. Enforcing the good practices and processes will lead and ensure the Quality assurance in Educational System. Establishing the Quality Assurance system is most expected practice and process in higher educational technical institutions. QAS should be formulated for monitoring the quality parameters in higher educational institutions. The National Assessment Accreditation Committee and National Board of Accreditation recommends for formulating various committees to effectively implement, monitor and control the Quality. The Medical checkup is essential for any person after certain age to self evaluate their own physical and mental performance and position, Likewise all the higher educational technical institutions should conduct academic audit to evaluate and identify their academic and administrative performances, and also strengths and weaknesses. The audit reports will express the status that where we are and finding solutions or initiating improvement activity will facilitate the Quality assurance for our higher educational institutions. Best practices and processes should be adopted and implemented properly to achieve the quality education. In this paper few best practices adopted and measurable results achieved are presented briefly.

Keywords— QAS (Quality Assurance service), BOS (Board of Studies), (HES) Higher education system, (ODF) Open Discussion Forums, paper less work, Document maintenance, attendance maintenance.

INTRODUCTION

Best Practices are very essential to make any process or system effective, let us see the best practices and processes which are proposed and not only these the institutions may choose and implement any activity which is meaningful and purposeful to improve the educational system especially the higher education system(HES).

#1: Effective Information passing:

In Today's Technological scenario passing all the messages/information's through the SMS and e-Mail will give first-rate results and response.

Academic Calendar, Syllabus, Attendance status, Test and Exam Notice, Time Table, Regulations, Results, Study materials, Model Questions and Model Answers, all the day to day activities, Programmes and etc sending to students through SMS and E-Mail will help us to make our students to actively participate in all over academic activities.

Academic Calendar, Test and Exam Time Table, Attendance Status, University and College regulation updates, Seminar, Conference, Symposium, workshop information's, College and department achievements, day to day activities, Programmes and etc sending to all parents through SMS and E-Mail will help us to make our students to actively participate in all over academic activities with the help of parents.

All the above mentioned details of students and parents should reach all the staff members (Teaching and Non-Teaching) to plan, organize, co-ordinate, monitor and control all the activities. Not only through the SMS and e-Mail, Through the Phone Call, College Notice Board, Department Notice Board, College Website, Department Website and as a circular/notice.

It is also responsibility of the Staff to communicate the information to student and Parents. It is the responsibility of the student to acknowledge for the information expected. It is a responsibility of the parents to make sure that their son or daughter responding/attending for the information received from the college. Any way it is our (HOD, Class Teacher, Exam in-charge) complete responsibility to ensure the information passing completed effectively.

All the information's/letters/message to parents should be in three languages English/Hindi/and regional Language.

 # 2: Weekly/Monthly/Yearly Progress Report:

Institutions must prepare the day to day progress report on weekly/monthly, yearly basis and it should be prepared well and also published and circulated to all, this will help the Management, Parents, Students, Staff members and general Public to understand our college strengths, values and merits.

 # 3: Active Guidance and Counseling:

Institution must facilitate the guidance and counseling facility to all the student, staff and parents to have clear mission ,vision and idea of all the activities, standards, requirements, achievements, overcome barriers and etc.

#4: Monthly Attendance Report:

Monthly attendance report of staff members and students should be reviewed or monitored. SMS/Email Alerts must be sent to the concerned person who has shortage.

 # 5: Forum Activities of Students and Staff:

Every institution will conduct forum activities / Association (Department/College Level) activities but active student and as well as staff (Teaching and Non-teaching) forum should be created and every week there should be a meaningful and purposeful activities. Activities may be technical or Non-technical. Eminent People and experienced people should be involved properly in all programmes.

 # 6: Open Discussion Forums(ODF):

College level open discussion forums should be organized for 1. Staff members, 2.Students, 3. Staff members with students, 4.Staff, Students and Parents, 5.Principal, HODs, Staff and Students. All type of standards, policies, procedures, academics and non-academics should be discussed in this forum and based on the finds and conclusions the policies should be framed and followed.

#7: Extra Classes/Research Oriented/Future Oriented Classes/Beyond the curriculum:

Colleges following the syllabus oriented teaching mostly, but it is not sufficient enough so extra classes related subjects with practical trainings and workshops should be conducted more and more, research oriented and future oriented classes should be preferred and conducted for the benefit of students and institutions.

 # 8: Staff, Students and Parents Induction Programme:

Organizing Induction programmes is very important, in the induction programme all the updated information's about department, college, university, systems, methods, approaches, standards and policies, mission and vision should be delivered properly. This will help us to effectively deal with all the academic activities.

 # 9: Promotion/Awards/Rewards/Appreciations:

Colleges should frame standards and policies to appreciate the students, staff and parents for their academic achievements through the promotion/awards/rewards/prizes/etc. , this will encourage all to involve in good and all activities and we can achieve measurable result of improvement.

#10: MOU with Core industries, Training Centers, Universities/Journal Publishers/Book Publishers inside and outside of our nation:

College and departments should sign more and enough memorandum of understanding with industries, training centers and institutes

 # 11: Staff Handbook / Student Handbook/Parent Handbook

Colleges should offer the handbook to students, staff and parents. The handbook must contain all the details about college policies and standards, University norms, Exam and Evaluation systems, Mission and Vision, About all the departments, staff members, achievements and etc. This will facilitate everyone to have better understanding about all academic activities and policies.

 # 12: Next Level of People/ Team and Hierarchy maintenance

College must have qualified, experienced and dynamic personality people in every level and in every departments, such people must get offer to lead the teams of members, but it is not sufficient enough in every team the next level of leads and heads should be identified and training them is must, this will help us to help us in future to create a new departments and to assign responsibilities. Each and every member should be treated equally and respected, recognized properly. Implementing the policies and procedures without deviation should be ensured at every time. Hierarchy maintenance also should be given equal importance.

#13: College website and Department Website

Websites of institution and department plays a major role in present scenario, all the information's about the college and department should be properly designed, developed and published. This will be a big communication and advertisement media.

College website should be updated with the following information's daily basis:

- College - day to day important news publication.
- Department important news publication.
- College calendar / Department Calendar Updates - publication.
- Seminar/Symposium/Conference/Workshops/Technical Events organized by every department – should be updated regularly in the website.

- Every department web pages should be updated with the following information's:

- About the Department
- Lab facilities: Detailed system and Lab Exercises, Photo's.
- Seminars Conducted
- Conferences Conducted
- Workshops Conducted
- Papers published by Faculty members
- Elective subjects offering
- Department Achievements
- Subjects offering(BOARD OF STUDIES (BOS) for framing the syllabus)
- Results and Placements offered
- Research, Consultancy and Extensions
- Faculty profiles with Photo and E-mail ID
- Industrial visits-offered
- Students Achievement
- Faculties Achievements
- Faculty Seminars offered
- Department Forum Activity Report

- Guest / Experts visit
- Class Toppers and University Rank Holders Report
- Students Projects
- MoU's Signed
- Proposal submission and Grants and Funds received
- Department Library
- General Library, Text Book and Reference Book Details
- National / International Journals available Report
- Department Academic calendar, Concern e-Library Department-Related Details
- Professional body membership
- Department wise / Class wise Time Table
- Canteen Facilities
- Mentoring and Grievances committee
- Feedback of Passed out Students, Present Students, Messages from eminent personalities
- Internet Centre

❖ Important Downloads – should be included.
❖ All events conducted Photo graph should be included properly.
❖ Alumni info
❖ Various Club activities for the student fraternity

 # 14: Student/Staff Grievances addressing within 24 Hours:

All the staff and students related grievances should be addressed within 24 Hours; Separate committees should be constituted to deal with the grievances issues. All the activities of the committee should be properly recorded and maintained. Due importance should be given to the recommendations given by the committees.

 # 15: Course wise and subject wise faculty experts:

Developing course wise and subject wise faculty expert members is most essential and so much in demand. Having expert members with course wise and subject wise will not only for teaching, they may be utilized to conduct short term training programmes, workshops, seminar, conferences, guest lectures, and creation of new labs. We are having the practice of collecting the feed-back from the immediate next batch students about the teachers and about their subject's expertise and based on this, we are fixing the subject and course wise expert faculty members.

 # 16: Paper-less Work Environment and Content Reuse:

Paper-less work environment and culture should be created for effective conduction of all the academic activities. Content reusability and all the advantages of re-usability concept should be utilized properly. Already we are started using Google-apps for the lesson plan management system, attendance maintenance, common forum for alumni details, etc.

 # 17: Documentation Maintenance:

Documentation maintenance is utmost important and so much in demand to identify, know, and understand and also to predict the present, past and future. Quality assurance, improvement, monitoring the documentation plays a major role. Applying for accreditation is possible only by maintaining the records, due importance and care should be given to these criteria.

 # 18: Exam and Evaluation:

The Internal and External test and exams should be well planned, designed and implemented in the colleges is most expected. Most importantly conduction of the same with zero malpractices is must. Already we are practicing that the question papers from outside institutions are utilized to conduct the internal exams, through this the self evaluation is achieved meaningfully.

19: Starting and ending of the Academic semester /year:

Every institution must start the academic semester and year with effective planning and also by addressing all the areas of academic.

#20: Quality Up-gradation Visits:

The Management / Head of the Institution should depute teams of staff members to various reputed colleges to study the laboratory facilities, infrastructure, placement techniques, teaching developments, library facilities, hostel facilities, etc. These teams after visiting the colleges should give a detailed report to the Principal, which should be discussed at the Management review meeting and necessary actions are to be taken/initiated.

ACKNOWLEDGMENT

I would like to thank Professor Karthikayini for her support and encouragement throughout this manuscript process.

CONCLUSION

All the above mentioned practices and processes are to be conducted properly with various teams and committees, it is not possible to the head of the institution alone to implement everything, it is the responsibility of every head of the departments, Staff members and students to support and to have every best practices in all the levels of activities of the Institution. Even after fixing all the policies and standards to maintain and achieve the Quality, various committees with special mission and vision should be constituted and all the activities of all the committees should be properly recorded and maintained. In a periodical interval, reviews and meetings should be conducted; all the findings, suggestions and recommendations should be forwarded to the college high committee for the effective implementations and approvals.

All the above mentioned few best practices are implemented and achieved a good and measurable result, actually so many best practices are still there, it is not possible to explain everything in this paper. The best practices varies from place to place, individual to individual and institution to institution, but all together achieving good result in the higher education and moving to the next level of excellence is expected. Best Practices and processes are possible through the effective implementation of meaningful and purposeful policies and standards. Every Higher Education Institution must create their own best practices and processes in the fields of teaching and learning, academic and administration to move to the next level of excellence.

REFERENCES:

1. R. Weaver and H. Cotrell, 'Using Interactive Images in the Lecture Hall.' Educational Horizons, 64:4, 180-185.
2. M. Hunter, Reinforcement (Tip Publications, El Segundo, California), 1983.
3. Weaver and Cotrell, 'Using Interactive Images in the Lecture Hall.' Educational Horizons, 64:4, 180-185.
4. Kenneth D. Moore, Classroom Teaching Skills: A Primer (Random House, New York) 1989.
5. Peter J. Frederick, 'Student Involvement: Active Learning in Large Classes.' In Teaching Large Classes Well. Edited by M.G. Weimer. New Directions for Teaching and Learning No. 32 (Jossey-Bass, San Francisco) 1987.
6. Brenda Wright Kelly and Janis Holmes, 'The Guided Lecture Procedure.' Journal of Reading 22:602-604.
7. Robert J. Menges, 'Research on Teaching and Learning: The Relevant and the Redundant.' Review of Higher Education 11: 259-268.
8. Joseph Campbell, The Power of Myth. (Doubleday, New York, 1988), p. 3-39.
9. Robin Fogarty, Designs for Cooperative Interactions (Skylight Publishing, Inc., 1990), p 42.
10. Gordon E. Greenwood & Forrest W. Parkay, Case Studies for Teacher Decision Making (Random House, NewYork), 1989.
11. M.B. Rowe, Teaching Science as Continuous Inquiry (McGraw Hill, New York), 1978.
12. Haim Ginott, Teacher and Child. (Macmillan, New York), 1971.
13. Rita Smilkstein, 'A Natural Teaching Method Based on Learning Theory' in Gamut: A Forum for Teachers and Learners (Seattle Community Colleges, Seattle, Washington), 1991.

14. K. Patricia Cross and Thomas A. Angelo, Classroom Assessment Techniques: A Handbook for Faculty, Second Edition. (Jossey-Bass Publishers, San Francisco, California), 1993.
15. Paul Cloke, 'Applied Rural Geography and Planning: A Simple Gaming Technique.' Journal of Geography in Higher Education 11(1): 35-45.
16. Charles C. Bonwell and James A. Eison, Active Learning: Creating Excitement in the Classroom. ASHE-ERIC Higher Education Report No.1. Washington, D.C.: The George Washington University, School of Education and Human Development. 1991.
17. Bonwell and Eison, Active Learning: Creating Excitement in the Classroom. ASHE-ERIC Higher Education Report No.1. Washington, D.C.: The George Washington University, School of Education and Human Development. 1991. p. 50-52.
18. David W. Johnson, Roger T. Johnson and Karl A. Smith, Cooperative Learning: Increasing College Faculty Instructional Productivity. ASHE-ERIC Higher Education Report No.4. Washington, D.C.: The George Washington University, School of Education and Human Development. 1991.
19. Robert E. Slavin, Cooperative Learning: Theory, Research, and Practice, Second Edition (Allyn & Bacon, Needham Heights, M.A. 02194-2310), 1995.
20. Jane Srygley Mouton and Robert R. Blake, Synergogy (Jossey-Bass Publishers, San Francisco, California), 1984, p. 22-54.
21. Robert E. Slavin, Cooperative Learning: Theory, Research, and Practice, Second Edition (Allyn & Bacon, Needham Heights, M.A. 02194-2310), 1995.
22. Mouton and Blake, Synergogy (Jossey-Bass Publishers, San Francisco, California), 1984, p. 74-91.
23. Mouton and Blake, Synergogy (Jossey-Bass Publishers, San Francisco, California), 1984, p. 92-111.
24. Robert F. Mager, Goal Analysis (David S. Lake Publishers, Belmont California), 1984.
25. James O. Hammons and Janice Barnsley, 'Everything You Need to Know About Developing a Grading Plan for Your Course (Well, Almost)' in Journal on Excellence in College Teaching, Vol.3, 1993, 51-68.
26. Carl R. Rogers, The Freedom to Learn (Charles E Merrill Publishing Company, Columbus, Ohio) 1969, p. 102-127.
27. Chris Argyris, Reasoning, Learning, and Action. (Jossey-Bass Publishers, San Francisco, California), 1982, p.181.
28. Malcolm S. Knowles and Associates, Androgogy in Action. (Jossey-Bass Publishers, San Francisco, California), 1984.
29. K. Patricia Cross and Thomas A. Angelo, Classroom Assessment Techniques: A Handbook for Faculty, Second Edition. (Jossey-Bass Publishers, San Francisco, California), 1993.

International Journal of Engineering Research and General Science Volume 3, Issue 6, November-December, 2015
ISSN 2091-2730

IMPLEMENTATION CONCEPT FOR ADVANCED CLIENT REPUDIATION DIVERGE AUDITOR IN PUBLIC CLOUD

[1]Ms.Nita R. Mhaske, [2]Prof. S.M.Rokade
[1]student , Master of Engineering, Dept. of Computer Engineering Sir Visvesvaraya Institute of Technology, Chincholi, Sinner
nita.mhaske90@gmail.com,9960530968
[2]Head Of Department of Computer Engineering, Sir Visvesvaraya Institute of Technology, Chincholi, Sinner ,
,smrokade@yahoo.com

Abstract— Cloud provides data storage and sharing services and people works together as a group. After creating the group, member of a group able to access, modify and shares latest updated data with the rest of the group members. To sure the integrity, group member need to upload the data with their sign. After modification user have to upload data with his own private key. If user is repudiated from group then data signed by repudiated user are signed by existing users. In this, proposed an auditing mechanism for integrity of shared data with efficient user repudiation. Existing user resign the data during user repudiation without downloading data .

Keywords—Diverge auditing , shared data, user repudiation, cloud computing.

INTRODUCTION

Cloud computing is a model for enabling ubiquitous, convenient, on-demand access to a shared pool of configurable computing resources. Cloud computing and storage solutions provide users and enterprises with various capabilities to store and process their data in third-party data centers. There are various essential characteristics of cloud such as on demand self service, broad network access , resource pooling ,rapid elasticity etc. There are three different service platform IaaS, PaaS, SaaS. Also there different deployment model like private cloud, public cloud, hybrid cloud. In this system we use IaaS platform with public cloud .Public cloud service provider like Amazon AWS. and operate the infrastructure at their data center and access is generally via the Internet. AWS offer direct connect services called "AWS Direct Connect".

As Cloud provides data storage and sharing services and people works together as a group. After creating the group ,member of a group able to access, modify and shares latest updated data with the rest of the group members. cloud providers provides secure and reliable environment to the users, still there may be problem with integrity of the data due to repudiation of user. Previously after repudiation of user any of the existing user download all the data , verity it and again upload all the data ,but it having communication overhead and time. In this system original user of the group resign the data with his private key due to this data in cloud remain safe. As a result, the efficiency of user repudiation can be significantly improved, and computation and communication resources of existing users can be easily saved.

RELATED WORK

Cong wang, Qian wang, Kui Pen, W. Lou proposed an distributed scheme for data with explicit dynamic operation .It also ensure users data securely stored in cloud. This system is efficient against Byzantine failure, malicious data attack etc. User can perform operation for checking storage correctness perform operation for checking and dynamic operation. Mostly focus on data checking and dynamic operation .

Cong wang, Qian Wang, Kui Ren, w. lou proposed system consist, as there are burden on user if we stored data locally. So that it uses the functionality of cloud data can stored remotely and user can access data as on demand. It uses TPA to audit the data on demand.In this , they utilized the public key based homomorphic authenticator with random mask technique to achieve privacy preserving auditing system for the data security purpose. In this most focus on security of data with public key..G.Ateniese ,R.Burns, R.curtmola proposed mechanism ,that allowed the client who stored the data at an untrusted server to verify that the server possesses the original data without retrieving it. They allow to verify data possession without having access to the actual data file.

C.Wang, Q.Wang, K.Ren proposed mechanism focusing on cloud data storage security which effect on quality of service, supports secure and efficient dynamics operations on data blocks including data update,delete and append. H.Shacham & B.Waters proposed two proofs for retrievability schemes for full proofs of security against arbitrary adversaries in the strongest scheme which is

Juels and Kaliski and secondly scheme with private verifiability. B.Wang, B.Li, H.Li, F.Li proposed first certificateless diverge auditing mechanism for verifying data integrity in the untrusted cloud is based on CDH assumption and DL assumption. .H.Wang proposed system for proxy provable data possession for the purpose when the client cannot perform the remote data possession checking. System was based on bilinear pairing technique.

SYSTEM DESIGN

In system design basic Block diagram includes three entities: the cloud, the public verifier, and two or many users (who share data as a group). The cloud offers data storage and sharing services to the group. The public verifier, such as a client who would like to utilize cloud data for particular purposes or a third-party auditor (TPA) who can provide verification services on data integrity, aims to check the integrity of shared data via a challenge-and response protocol with the cloud. In the group, there is one original user and a number of group users. The original user is the original owner of data. This original user creates and shares data with other users in the group through the cloud. Both the original user and group users are able to access, download and modify shared data. A user in the group can modify a block in shared data by performing an insert, delete or update operation on the block.

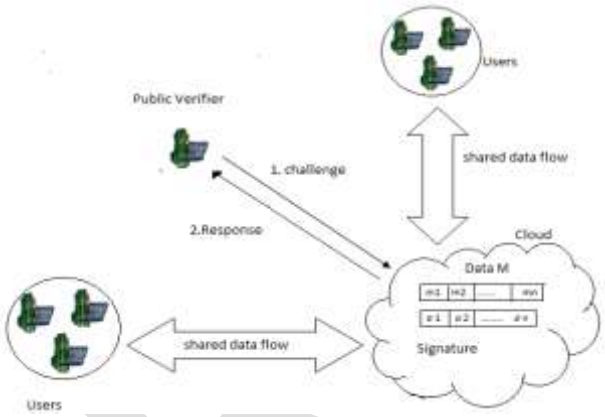

Figure 1: block diagram of proposed system

This system is divided into different modules as shown in figure 2. System consist of different moduls: controller, storage service, trusted third party auditor, security service, data re-signature service, most important entity is user. User get interface with system though web server and web application. Any web browser work on HTTP. User send and gain reply though HTTP. The component which handle this is called web server. Web application is intermediate between web server and controller.

All the services are executed though controller. Which operation executed first it is decided by controller (i.e. registration of user, upload, download). Storage service handle all database related operation (i.e. insertion, deletion, modification). Security to the data is provided through security service such as encryption and decryption of data If user want to check the data integrity periodically and whenever he want it done though third party auditor. Similarly not only user but also group admin and super admin can audit the data. Auditing done as challenge and email obtain from third party auditor taken as response. All members in the cloud and cloud computing environment should be trusted by each other and the members that have communication should be trusted by each other. Trust is major concern of the consumers and providers of service that participate in a cloud computing.

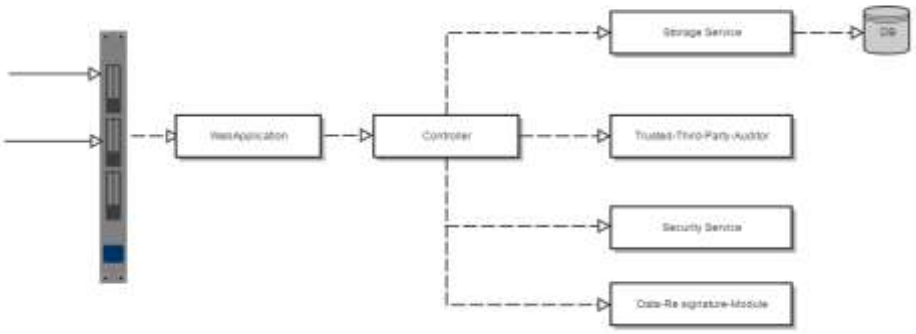

Figure 2:Modular system of proposed system

Design objective of the system are

- Integrity: The public verifier can be check the correctness i.e. integrity of shared data.
- secure user repudiation: after repudiating the user block signed by him are efficiently resigned by existing user.
- divergence: auditing the integrity of shared data without downloading all the data even if some data signed by cloud.
- Scalability: we add any number of user in the group as we can maintain our system properly.

For security purpose i.e. for encryption and decryption we used AES algorithm. Pseudo code for AES algorithm is as follows:

```
Cipher(byte in[4*Nb], byte out[4*Nb], word w[Nb*(Nr+1)])
    begin
        byte state[4,Nb]
        state = in
        AddRoundKey(state, w[0, Nb-1])
        for round = 1 step 1 to Nr-1
            SubBytes(state)
            ShiftRows(state)
            MixColumns(state)
            AddRoundKey(state,
        w[round*Nb, (round+1)*Nb-1])
        end for
        SubBytes(state)
        ShiftRows(state)
        AddRoundKey(state, w[Nr*Nb,
    (Nr+1)*Nb-1])
    End
```

Figure 3: AES algorithm

EXPERIMENTAL RESULT

Now we go for what exactly we done in the system is

1. User registration into the system

In this system we create number of group when user want to enter into the system he have to registered in to the system. At the time of registration he has to choice in which group he want to go and has to follow terms and condition.

2.User Task

After getting entry into the system user can perform various task with his private key such as upload data delete and modified the data .He give challenge as audit the system though perform audit tab provided to user by admin. Auditing report to the user as response to the user from TPA.

3.Admin task

As admin can perform all the operation user can perform with additional rights. He handle all group information, which user stay in the group. When user not follow terms and condition then admin has right to repudiate the user. All the file on account of repudiated user are get on admin account , due that integrity of that get maintain and this is done with reassignment report.

4.Auditing task

When user and admin asked for auditing then TPA will mail the report to the user who done the request. Auditing help us to maintain the integrity. In auditing report it consist server communication time and total time required for auditing.auditing time is nothing but time to response by TPA.server comunicationtime is input request comes what time and response in what time , the difference between this two .


Result :- Success

Audit Report

sendEmail

Go To Main Home Page

Number Of Record	Server Communication Time	Auditing Time
2	1010 (milisecond)	60 (milisecond)

Conclusions

In this system user can perform dynamic operation such as insert, delete, modify data. Admin of the group as rights to repudiate the user from the system. with this system we achieve efficient user repudiation so that integrity and security of data maintain

ACKNOWLEDGMENT

It is a great pleasure to acknowledge those who extended their support, and contributed time and psychic energy for this projectwork.At the outset, I would like to thank my Project guide Prof. S.M.Rokade, who served as sounding board for both contents and programming work. His valuable and skillful guidance, assessment and suggestions from time to time improved the quality of work in all respects. I am also thankful to Prof. S.M. Rokade, Head of Computer Engineering Department for his timely guidance, inspiration and administrative support without which my work would not have been completed. I am also thankful to the all staff members of Computer Engineering Department and Librarian, SVIT Chincholi, Nasik. Also I would like to thank my colleagues and friends who helped me directly and indirectly to complete this Project work. Lastly my special thanks to my family members for their support and co-operation during this Project work.

REFERENCES:

[1]. B. Wang, B. Li, Member, H. Li, "Panda: Public Auditing for Shared Data with Efficient User Revocation in the Cloud " in the Proceedings of IEEE INFOCOM 2014, 2014
[2]. B. Wang, B. Li, and H. Li, "Public Auditing for Shared Data with Efficient User Revoation in the Cloud," in the Proceedings of IEEE INFOCOM 2013, 2013, pp. 2904–2912.
[3]. M. Armbrust, A. Fox, R. Griffith, A. D. Joseph, R. H. Katz, A. Konwinski, G. Lee, D. A. Patterson, A. Rabkin, I. Stoica, an M. Zaharia, "A View of Cloud Computing," Communications of the ACM, vol. 53, no. 4, pp. 50–58, Apirl 2010.
[4]. G. Ateniese, R. Burns, R. Curtmola, J. Herring, L. Kissner, Z. Peterson, and D. Song, "Provable Data Possession at Untrusted Stores," in the Proceedings of ACM CCS 2007, 2007, pp. 598–610.
[5]. H. Shacham and B. Waters, "Compact Proofs of Retrievability," in the Proceedings of ASIACRYPT 2008. Springe Verlag,2008,pp. 90–107.
[6]. C. Wang, Q. Wang, K. Ren, and W. Lou, "Ensuring Data Storage Security in Cloud Computing," in the Proceedings of ACM/IEEEIWQoS 2009, 2009, pp. 1–9.
[7]. C. Wang, Q. Wang, K. Ren, and W. Lou, "Privacy-Preserving Public Auditing for Data Storage Security in Cloud Computing," in the Proceedings of IEEE INFOCOM 2010, 2010, pp. 525–533.
[8]. H. Wang, "Proxy Provable Data Possession in Public Clouds," IEEE Transactions on Services Computing, accepted.
[9]. B. Wang, B. Li, and H. Li, "Oruta: Privacy-Preserving Public Auditing for Shared Data in the Cloud," in the Proceedings of IEEE Cloud 2012, 2012, pp. 295–302.
[10]. B. Wang, S. S. Chow, M. Li, and H. Li, "Storing Shared Data on the Cloud via Security-Mediator," in Proceedings of IEEE ICDCS 2013, 2013.
[11]. B.Wang, B. Li, and H. Li, "Certificateless Public Auditing for Data Integrity in the Cloud," in Proceedings of IEEE CNS 2013, 2013, pp. 276–284.

International Journal of Engineering Research and General Science Volume 3, Issue 6, November-December, 2015
ISSN 2091-2730

Simulation of Quarter Car Model Using Matlab

Kuldeep.K.Jagtap[1], Dhananjay.R.Dolas[2]
PG Scholar, JNEC,Aurangabad[1], Associate Professor, JNEC, Aurangabad[2]
kdjagtap007@gmail.com[1],dhananjay_dolas@rediffmail.com[2]

Abstract-Vehicle suspension design includes a number of compromises to provide good leveling of stability and ride comfort. Suspension system has to perform complexity requirements, which includes road holding and equality, driving pleasure, riding comfort to occupant. Riding pleasure depends on vertical acceleration, with main objective to minimize vertical acceleration. In this work, the geometric parameters of suspension system are optimized using Matlab as an optimization tool. The values of tire deflection reduced from 0.023 to 0.021 m and Seat acceleration reduced from 34.19 to 31.86 m/s^2.

Keywords-Seat Acceleration, Tire Deflection, ride comfort, mathematical model.

I. INTRODUCTION

Traditionally automotive suspension designs have been a compromise between the three conflicting criteria of road holding, load carrying and passenger comfort. The suspension system must support the vehicle, provide directional control during handling maneuvers and provide effective isolation of passengers/payload from road disturbances. The parameters of Passive Suspension system are generally fixed, being chosen to achieve a certain level of compromise between road holding, load carrying and comfort.

The work presented here tries to analyze the effect of spring stiffness and Damping coefficient on the Seat Acceleration and Tire deflection and analysis by equation of motion using mathematical blocks available in Simulink.

S. J. Chikhale et al [1] analyzed that suspension model in Matlab-Simulink and MSc-Adams. Results for the analysis are compared for understanding the capability of the software to deal with the vibration problems.

P. Sathishkumar et al [2] discussed about the mathematical modeling and simulation of 2DOF quarter car model. The state space mathematical model is derived using Newton's second law of motion and free body diagram concept. The performance of the system is determined by Matlab/Simulink.

Nikos E. Mastorakis et al [3] have tested the performance of a suspension damper using a FFT with the simulation environment under MATLAB/Simulink. The Simulink results and experimental results are compared and are similar in nature.

K. S. Patil [4] obtained a mathematical model for the passive and active suspension systems for quarter car model in their research paper. Comparison between Passive and Active Suspension for Quarter Car Model is done. Dynamic model for linear quarter car suspensions systems has been formulated and derived.

S. Segla [5] has optimized the performance of the passive suspension system and compared with the performances of active and semi-active suspensions. Mat lab is used for the optimization of the suspension parameters.

2. Mathematical Model for Quarter Car

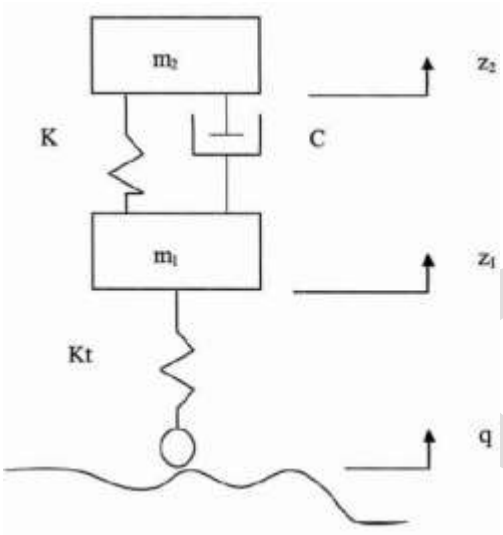

Fig 1.Quarter Car Model

The equation of motion for 2DOF system is given as:

$$M_2\ddot{Z}_2 + C(\dot{Z}_2 - \dot{Z}_1) + K(Z_2 - Z_1) = 0$$

$M_1\ddot{Z}_1 + C(\dot{Z}_1 - \dot{Z}_2) + K(Z_1 - Z_2) + K_t(Z1 - q) = 0$ Taking the Fourier transfer on both sides

$$Z_2(-\omega^2 m_2 + jwc + K) = Z_1(jwc + K)\ Z_1(-\omega^2 m_1 + jwc + K + K_t) = Z_2(jwc + K) + qK_t$$

For the purposes of design optimization, according to James' principle, the root mean square (RMS) of the sprung mass acceleration $\ddot{Z}_2$ can be expressed as follows,

Taking the amplitude ratio for amplitudes of sprung mass and road excitation

$$\frac{|Z_1|}{|q|} = \left[\frac{(1-\lambda^2)^2 + 4\xi^2\lambda^2}{\Delta}\right]^{1/2}$$

Where,

$$\Delta = \left[(1-(\omega/\omega_0)^2)(1+\gamma-\frac{1}{\mu}(\omega/\omega_0)^2 - 1\right]^2 + 4\xi^2(\omega/\omega_0)^2\left[\gamma - (\frac{1}{\mu}+1)(\omega/\omega_0)^2\right]$$

$$\gamma = \frac{K_t}{k}, \mu = \frac{m_2}{m_1}, \omega_0 = \sqrt{K/m_2}, \xi = \frac{C}{2\sqrt{m_2 K}}$$

The amplitude ratio between sprung mass displacement, Z_2, and the road excitation,q,is

$$\left|\frac{z_2}{q}\right| = \gamma\left[\frac{1+4\xi^2\lambda^2}{\Delta}\right]^{1/2}$$

The amplitude ratio between sprung mass acceleration, $\ddot{Z}_2$, and the road excitation, $\ddot{q}$, is

$$\left|\frac{\ddot{z}_2}{\dot{q}}\right| = \omega\gamma\left[\frac{1+4\xi^2\lambda^2}{\Delta}\right]^{1/2}$$

The suspension working space is the allowable maximum suspension displacement. The suspension working space in response to the road displacement input is:

$$\frac{f_d}{\dot{q}} = \frac{\gamma}{\omega}\lambda^2\left[\frac{1}{\Delta}\right]^{1/2}$$

The dynamic tire load is defined as $F_d = K_t(z_1 - q)$, and also the static tire load is $G = (m_1 + m_2)g = m_1(\mu+1)g$ where g is gravitational acceleration. Thus the amplitude ratio between the relative dynamic tyre load, $\left|\frac{F_d}{G}\right|$ and the road input, q, becomes

$$\frac{F_d}{G_q} = \frac{\gamma\omega}{g}\left[\frac{\left(\frac{\lambda^2}{1+\mu}-1\right)^2 + 4\xi^2\lambda^2}{\Delta}\right]$$

3. Simulink Model of Quarter Car

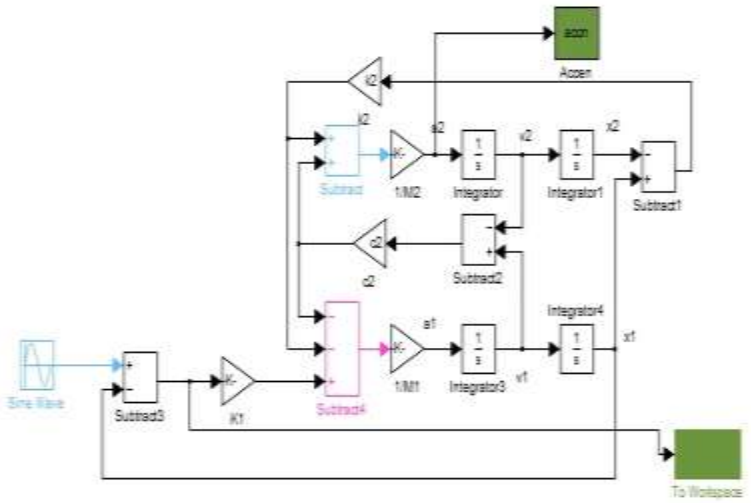

Fig no 2.Simulink Model of Quarter Car

The simulink results are obtained by suspension parameters as follows:

Table no1. Fix Parameters

Parameter	Value
M_1	40 Kg
M_2	60 Kg
K_t	100000 N/m

Table no 2. Variable Parameters

Parameter	Value
K_2	18760(N/m)
C2	900N-s/m)

a. Plot for Seat Acceleration

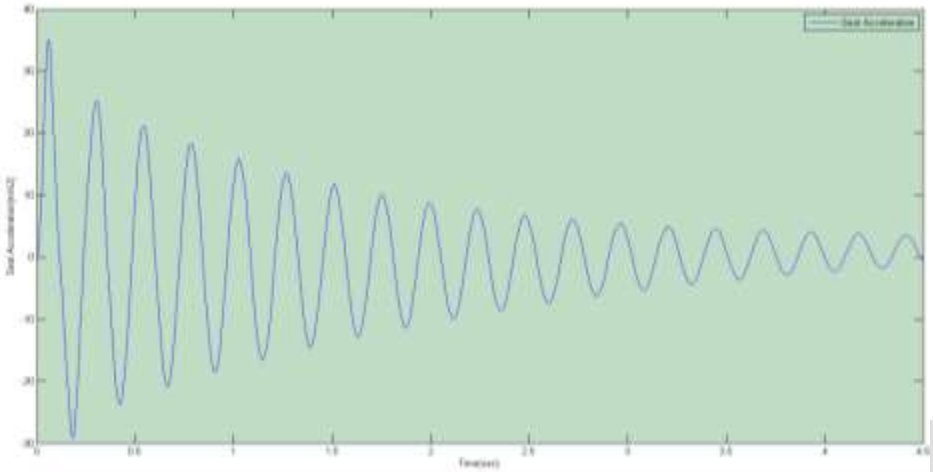

Graph no 1. Seat Acceleration

b. Plot for Tire Deflection

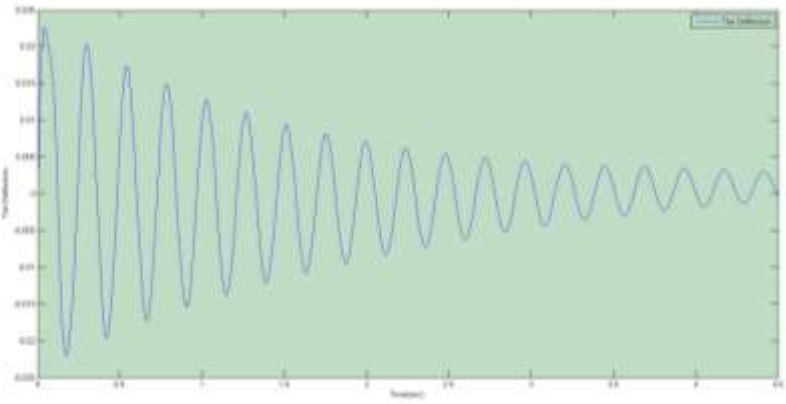

Graph no 2. Tire Deflection

From both the graphs, we get the maximum and minimum values of the seat acceleration and TD as follows:

Table no 3. Observed Values

Parameter	Maximum Value	Minimum Value
Seat Acceleration(M/s^2)	34.9176	-29.1136
Tire Deflection(m)	0.023	-0.0219

Now, optimization program was run using for the objective function:-

Min (TD) and min (Seat Acceleration)

The obtained values for the design variables K & C are:

Table no 4. Optimized Parameters

Parameter	Value
K_2	12265 (N/m)
C2	536 N-s/m)

c . Plot for Seat Acceleration

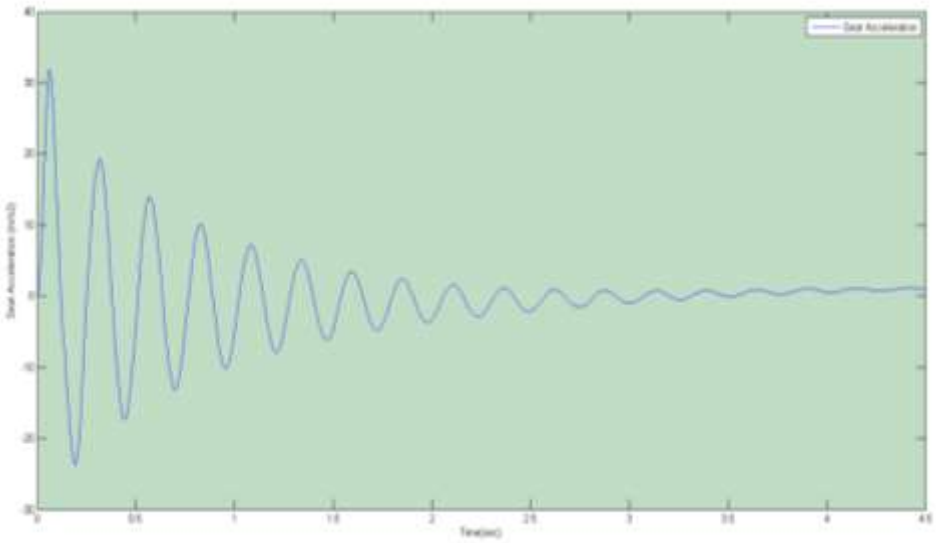

Graph no 4. Seat Acceleration vs. Time

d. Plot for Tire Deflection

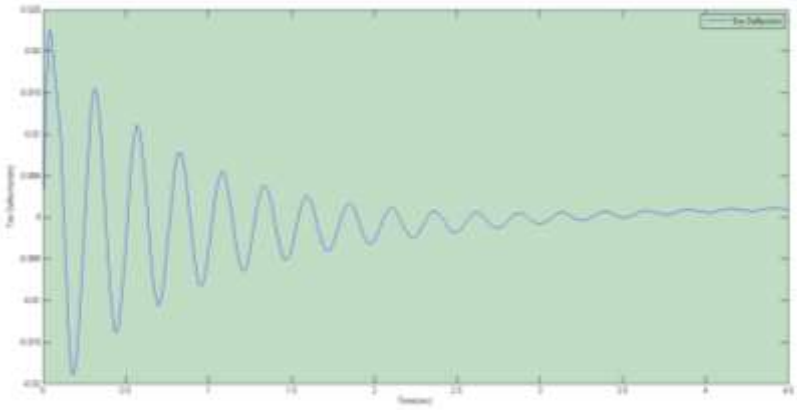

Graph no 5. Tire Deflection vs. Time

From both the graphs, we get the maximum and minimum values of the seat acceleration and TD as follows:

Table no 5. Maximum and Minimum values of the Seat Accl^n & TD

Parameter	Maximum Value	Minimum Value
Seat Acceleration(M/s^2)	31.8604	-23.7734
Tire Deflection(m)	0.022	-0.0189

4. Results and Discussion

Table no 6. Results comparison of Optimized Values

Parameter	**Classical Value**	**Optimized Value (Simulink Model)**
Seat Acceleration(m/s^2)	34.9176	31.8604
Tire Deflection(m)	0.023	0.022

From Table No 6 we can compare the classical and simulink values and can observe that the Seat Acceleration has been decreased by 3.0572 m/s^2 and Tire Deflection by 0.001 m.

Thus we can see that the seat acceleration values are reduced by optimization. The ride comfort will be increased with the minimization of the Seat acceleration and tire deflection**.**

Conclusion

The simulation result shows considerable difference in linear passive sprung mass. As the results of analysis of quarter car passive suspension are quite similar because experimental model contains inherent nonlinear properties of suspension parameters, so it is necessary to consider the nonlinearities in suspension system for analysis of tire dynamic force. Hence form above we conclude that the analysis of suspension system we can use only theoretical (MATLAB Simulink) models instead of difficult experimental setup.

5. ACKNOWLEDGEMENT

We would like to thank our mentor Dr. Sudhir Deshmukh, Principal MGM's JNEC for their valuable co-operation and support, also we wish to thanks Dr. M.S. Kadam, Head of Department and. All faculty members of Mechanical Engineering Department

REFERENCES:

[1] S.J.Chikhale, S.P. Deshmukh. "Comparative Analysis of Vehicle Suspension System in Matlab-Simulink and MSC-Adams with the help of Quarter Car Model". International Journal of Innovative Research in Science,Engineering and Technology.Vol 2,Issue 8,pp.4074-4081.

[2]P.Sathishkumar, J. Jancirani, Dennie John,S.Manikandan."Mathematical modelling and simulation quarter car vehicle suspension",International Journal of Innovative Research in Science,Engineering and Technology.Vol 3, pp.1280-1283.

[3] Nokos.E. Mastorakis. "Testing and Simulation of a Motor Vehicle Suspension".Vol 3, pp.74-83.

[4]K.S.Patil,Vaibhav Jagtap,Shrikant Jadhav,Amit Bhosale. "Performance Evaluation of Active Suspension for Passenger Cars Using MATLAB". Journal of Mechanical and Civil Engineering.pp.6-14.
[5] S.Segla, S.Reich. "Optimization and comparison of passive, active, semi-active vehicle suspension systems". IFToMM World Congress.2007
[6] Amol Kokare, Akshay Kamane,Vardhan Patil, Vikrant Pakhide. "Performance Evaluation of Shock Absorber Acting as a Single Degree of Freedom Spring-Mass-Damper System using MATLAB". International Journal of Engineering Research & Technology.Vol. 4 Issue 09, pp.730-734,2015
[7]Ranjeet Kumar S. Gupta, Vilas Sonawane, S. S. Sudhakar. "Optimization Of Vehicle Suspension System Using Genetic Algorithm". IJMET,Vol 6,Issue 2,pp.47-55.2015.
[8] R .Alkhatib, G.N.Jazar, and Golnaraghi. "Optimal Design of Passive Linear Suspension Using Genetic Algorithm". Journal of Sound and Vibration. Vol. 275, pp. 665-691,2004.

[9] A.E Baumal, J.J. McPhee, and Calamai."Application of Genetic Algorithms to the Design Optimization of an Active Vehicle Suspension System".Computer Methods in Applied Mechanics and Engineering.Vol. 163, pp. 87-94,1995.

[10]A. Bourmistrova, I.Storey and A. Subic. "Multiobjective Optimisation of Active and Semi-Active Suspension Systems with Application of Evolutionary Algorithm". International Conference on Modeling and Simulation. pp. 12-15 ,2005.

[11] M. Gobbi, and G. Mastinu."Analytical Description and Optimization of the Dynamic Behaviour of Passively Suspended Road Vehicles".Journal of Sound and Vibration. Vol. 245, No. 3, pp. 457-481, 2001.
[12]G.K.Grover, Text book of Mechanical Vibrations.
[13] Sadhu Singh, Mechanical Vibrations and Noise Control

International Journal of Engineering Research and General Science Volume 3, Issue 6, November-December, 2015
ISSN 2091-2730

Survey Paper For Real-Time Clustering for Big Data Streams

Bhavik Patel

GTU PG School Ahmedabad, pbhavik6518@gmail.com and +919429660402

Abstract — Big data is a recent term Appeared that has to define the vey large amount of data that surpass the traditional storage and processing requirements. Each and every growing volume of data generation is the reality. Today we are living in Social networks, smart cities, telephone networks, the internet are hand Reviews some of the data in the modern world and much of this information is discarded due to the high storage space. It Would require Relevant data can be extracted from this large amount of information and to be used to build better cities, offers better services, make predictive analysis, group similar information and many more applications. All of this is possible, due to machine learning and data mining can be found where patterns in the ocean of data generated every Second in order to cope with the volume, velocity and variety of data produced a streaming model has-been Studied. Were analysis of data has to uses low memory and process items only once.

Currently we are taking the advance of grid and cloud computing the missing component to help crunch this large amount of data is the power of distributed computing. Stream Processing Engines (SPE) have revealed to be a more flexible and powerful tool for dealing with Big Data.

This project merges the concepts of machine learning, streaming model and distributed computing to build a framework for developing, Testing and applying algorithms on large volume of data streams.

Keywords—

INTRODUCTION

The Internet is a worldwide platform for sharing information and making business. It has become a crucial medium for people and companies to connect and present themselves to the world. In this heterogeneous scenario data is represented in many forms and created by many sources. The large amount of information stored and produced is increasing every day and pushing the limits of storage and processing. Only in 2012 there was a rate of 2.5 quintillion bytes of data (1 followed by 18 zeros) created per day. Social networks, sensor networks, e-commerce and other data producing systems generate massive amounts of bytes per second. All of this information can and should be used for analyzing customer behavior, predicting trend and decision-making.

Map Reduce [2] is a programming model presented by Google for pro cessing large amounts of data in a distributed fashion that can be run on commodity resources, thus scaling the processing power to hundreds or thousands of machines. Map Reduce is and innovative way of parallelizing processing jobs where every problem has to be adapted into a two step process: a mapping phase and a reducing phase. The mappers takes an input key/value pair and produce a set of key/value pairs that are passed to the reducing job, which will merge the values into a smaller set. The open source \twin brother" of Google/Map Reduce and GFS are the Apache Hadoop1 and Hadoop Distributed File System (HDFS) projects [3] started at Yahoo!. A next level of the Map Reduce model are platforms for processing data in streaming where disk I/O operations are reduced for not using _les as its source and storage.

Patterns and relations can be extracted from data using methods from machine learning (ML) and data mining. Machine learning techniques for classifying information and clustering similar data are some of the main goals of these two areas of study. Such techniques are used in many ways and for different purposes. For example, machine learning algorithms can render very accurate predictive models that can be used to predict the price of housing depending on the size or location. Data mining algorithms on the other hand can deduce if a new piece of information is related to information. The literature is vast in machine learning and data mining algorithms and they have been developed in various programming languages. Tools and frameworks are also available as commercial and open source products. This variety of algorithms, tools and frameworks exists because there is no "one-size fits-all" solution, it depends on the problem scope, the volume of data and the complexity of the data. This works will focus on the volume and use some data mining techniques that use one common clustering algorithm - the k-means.

The scope of realtime big data analysis deals with using machine learning algorithms on unbounded streams of data. Data streams can be generated by many di_erent sources such as social networks, sensors, internet traffic, video and many others. To deal with this large volume of possibly unbounded flow of data some distributed stream processing platform has been implemented such as Apache S43 and Twitter Storm 4. These platforms can be considered an evolution of the batch, MapReduce, distributed file system model in the sense that they process owing data instead of always writing and reading from files.

Literature Review

The areas involved in this project are machine learning, data mining, streaming model and distributed systems. In these domains some interesting challenges appear in the present information society. The volume of data produced is enormous and much of the produced information is not used due to the lack of resources to store and process them. It would be too expensive to massively store all the information produced, thus inviable. The processing issue is starting to see a feasible horizon, but still has space to evolve. Therefore the important issue is not to store all the data, but to extract relevant statistics, summaries and models from the produced data.

Big Data

Big data is a recent term that has appeared to define the large amount of data that surpasses the traditional storage and processing requirements. Volume, Velocity and Variety, also called the three Vs, is commonly used to characterize big data. Looking at each of the three Vs independently brings challenges to big data analysis.

Volume

The volume of data implies in scaling the storage and being able to perform distributed querying for processing. Solutions for the volume problem are either by using datawarehousing techniques or using parallel processing architecture systems such as Apache Hadoop.

Velocity

The V for velocity deals with the rate in which data is generated and flows into a system. Everyday sensors devices and applications generate unbounded amount of information that can be used in many ways for predictive purposes and analysis. Velocity not only

deals with the rate of data generation but also with the speed in which an analysis can be returned from this generated data. Having realtime feedback is crucial when dealing with fast evolving information such as stock markets, social networks, sensor networks, mobile information and many others. Aiming to process these streams of unbounded ow of data some frameworks have emerged like the Apache! S4 and the Twitter Storm platforms.

Variety

One problem in big data is the variety of data representations. Data can have many di_erent formats depending of the source, therefore dealing with this variety of formats can be daunting. Distributed key-value stores, commonly referred as NoSQL databases, come in very handy for dealing with variety due to the unstructured way of storing data. This exibility provides and advantage when dealing with big data. Traditional relational databases would imply in restructuring the schemas and remodeling when new formats of data appear.

Algorithm

In the world of machine learning and data mining there are many algorithms in supervised, unsupervised and semi-supervised learning. They are used for different goals such as pattern recognition, prediction, classification, information retrieval and clustering. The practical applications of these algorithms are endless and can permeate any field of study.

A widely used algorithms for clustering is the k-means, which purpose is to split a dataset into k distinct groupings. The goal of k-means is to identify similarities between items in a dataset and group them together based on a similarity function. The most common used function is the euclidean distance function, but any other similarity function can be applied. K-means is an interesting option due to its simplicity and speed.

In essence it is an optimization problem where a local optimal clustering can be achieved, whereas a global optimal is not guaranteed. It is a heuristic algorithm in which the final result will be highly dependent on the initial settings, although a fairly good approximation is possible. For this reason choosing the exact solution for the k-means is an NP-hard problem. K- Means takes as input a number k of desired clusters and data set X 2 Rd.

The goal is to choose k centers to minimize the sum of squared Euclidean distance as presented in the following function.
Objective function,

$$\phi = \sum_{x \in X} (min \|x - c\|^2)$$

Historically k-means was discovered by some researchers from different disciplines. The most famous researcher to be coined the author is Lloyd(1957,1982) [6], along with Forgey(1965) [7], Friedman and Rubin(1967) [8], and McQueen(1967) [9]. Since then it has been widely studied and improved. The following Table 1 shows the pseudo-algorithm for k-means. The algorithm works in and iterative way and alternates between two major steps: reassigning the cluster ID of all points in dataset X and updating the cluster centroid based upon the data points in each cluster.

Algorithm 1 k - means algorithm

Require: Dataset X, number of clusters k

Randomly choose k data points from X

Use the k points as initial set of cluster representatives C

repeat

Reassign points in X to closest cluster mean

Update m such that mi is cluster ID of the ith point in X

Update C such that cj is mean of points in jth cluster

Check for convergence of objective function

until convergence of objective function F(x)

return Set of clusters representatives C, cluster membership vector m

Related Work

Data mining and machine learning have long since been studied and there is a vast literature on these subjects. A recent and more challenging approach for machine learning and data mining is to deal with the large amount of data produced everyday by the Internet and other systems. Finding patterns on data is very relevant for decision-making and having this information fast or on real-time is a bonus. Leaders and decision makers need to respond fast to evolving trends and behaviours.

Distributed Clustering Algorithms

In [20] some distributed clustering approaches are mentioned and they are separated into two categories; multiple communications round algorithms and centralized ensemble-based methods. The multiple communications methods require synchronization steps, which incurs in a large amount of message passing. The centralized approach use asynchronous communication and build local models that are transmitted to a centralized aggregator that build a global model.

Stream Clustering Algorithms

Stream clustering algorithms have been developed as an adaptation of traditional clustering algorithms to _t the streaming model and comply to its constraints. Different techniques were created to deal with evolving data such as one pass processing and summarization. Algorithms that can work on streams and still maintain good results as their batch processing relatives. Additionally to how data is processed, some data structures were developed to deal with the memory usage. Stream clustering can be characterized by two steps: data abstraction (also referred as the online component) and the data clustering (also referred as the offline component).

The online component deals with extracting only the relevant information in specific data structures to be used later on the offline component step. There are four commonly used data structures: feature vector, prototype array, coreset trees and grids

Following is a list of the 13 most relevant data stream clustering algorithms. Each one of them has improvements in performance, memory usage, computational complexity, clustering quality and scalability.

1. BIRCH [Zang et. al 1997]
2. Scalable k-means [Bradley et al. 1998]
3. Stream [Guha et al. 2000]
4. Single pass k-means [Farnstrom et al. 2000]
5. Stream LSearch [O'Callaghan et al. 2002]
6. CluStream [Aggarwal et a;. 2003]
7. DenStream [Cao et al. 2006]
8. D-Stream [Chen and Tu 2007]
9. ODAC [Rodrigues et al. 2006; 2008]
10. SWClustering [Zhou et al. 2008]
11. ClusTree [Kranen et al. 2011]
12. DGClust [Gama et al. 2011]
13. StreamKM++ [Ackermann et al. 2012]

All of these algorithms were designed for a single machine and did not take into account a distributed environment. This work focuses on using one of these algorithms - CluStream - in a distributed environment.

Stream Machine Learning Frameworks

Applying machine learning and data mining algorithms in streams of data has become very popular due to its appliances in various scenarios where streams of data are produced. For example, such algorithms can be used on sensor networks, monitoring of power consumption, telephone logs, internet traffic, social networks and many others. Many tools and frameworks are available as commercial and open source projects. The Massive Online Analysis (MOA) framework is a software environment that contains machine learning algorithms for learning on evolving data streams.

MOA is related to another project, the Waikato Environment for Knowledge Analysis (WEKA), which is a workbench for batch processing of ML algorithms [21]. Stream processing is different from batch in the sense that the dataset is potentially infinite. In order to process data that arrives in high speed some requirements have to be taken into account. Since data is arriving continuously the memory can easily be filled, thus a low memory approach has to be used. Each example has to be processed at a time and at most once; this is known as a one-pass approach. Another requirement is that the algorithms should be able to provide a prediction or summaries at any time, therefore the models have to be constantly updated.

CONCLUSION

Machine learning has become popular and has evolved to become an essential tool for predictive analysis and data mining. This popularity has resulted in the development of many tools for specific and generic uses.

This project presented some of the most important efforts in applying machine learning to clustering problems in different kinds of infrastructure, architecture and data models. The current state of machine learning tools taxonomy and points where SAMOA fits in this current scenario.

REFERENCES:

[1] P. Hunt, M. Konar, F. P. Junqueira, and B. Reed, “Zookeeper: wait free coordination for internet-scale systems," in Proceedings of the 2010 USENIX conference on USENIX annual technical conference, USENIXATC'10, (Berkeley, CA, USA), pp. 11{11, USENIX Association, 2010.

[2] J. Dean and S. Ghemawat, “Mapreduce: simpli_ed data processing on large clusters," Commun. ACM, vol. 51, pp. 107{113, Jan. 2008.

[3] K. Shvachko, H. Kuang, S. Radia, and R. Chansler, “The hadoop distributed _le system," in Proceedings of the 2010 IEEE 26th Symposium on Mass Storage Systems and T Technologies (MSST), MSST '10, (Washington, DC, USA), pp. 1{10, IEEE Computer Society, 2010.

[4] K. Tretyakov, “Machine learning techniques in spam filtering," tech. rep., Institute of Computer Science, University of Tartu, 2004.

[5] V. Estivill-Castro, “Why so many clustering algorithms: a position paper," SIGKDD Explor. Newsl., vol. 4, pp. 65{75, June 2002.

[6] S. Lloyd, “Least squares quantization in pcm," Information Theory, IEEE Transactions on, vol. 28, no. 2, pp. 129{137, 1982.

[7] E. Forgy, “Cluster analysis of multivariate data: Efficiency versus in terpretability of classification," Biometrics, vol. 21, no. 3, pp. 768{769, 1965.

[8] H. P. Friedman and J. Rubin, \On Some Invariant Criteria for Grouping Data," Journal of The American Statistical Association, vol. 62, pp. 1159{1178, 1967.

[9] J. MacQueen, “Some methods for classification and analysis of multi-variate observations," in Proc. Fifth Berkeley Symp. on Math. Statist. and Prob., vol. 1, pp. 281{297, Univ. of Calif. Press, 1967.

[10] T. Kanungo, D. M. Mount, N. S. Netanyahu, C. D. Piatko, R. Silverman, and A. Y. Wu, “A local search approximation algorithm for k-means clustering," in Proceedings of the eighteenth annual symposium on Computational geometry, SCG '02, (New York, NY, USA), pp. 10{18, ACM, 2002.

[11] D. Arthur and S. Vassilvitskii, “k-means++: The advantages of careful seeding," in Proceedings of the eighteenth annual ACM-SIAM symposium on Discrete algorithms, pp. 1027{1035, 2007.

[12] M. Mahajan, P. Nimbhorkar, and K. Varadarajan, “The planar k- means problem is np-hard," in WALCOM: Algorithms and Computation (S. Das and R. Uehara, eds.), vol. 5431 of Lecture Notes in Computer Science, pp. 274{285, Springer Berlin Heidelberg, 2009.

[13] M. Inaba, N. Katoh, and H. Imai, “Applications of weighted voronoi diagrams and randomization to variance-based k-clustering: (extended abstract)," in Proceedings of the tenth annual symposium on Computational geometry, SCG '94, (New York, NY, USA), pp. 332{339, ACM, 1994.

[14] D. J. Abadi, D. Carney, U. Cetintemel, M. Cherniack, C. Convey, S. Lee, M. Stonebraker, N. Tatbul, and S. Zdonik, “Aurora: a new model and architecture for data stream management," 2003.

[15] T. S. Group, “Stream: The stanford stream data manager," 2003.

[16] S. Chandrasekaran, O. Cooper, A. Deshpande, M. J. Franklin, J. M. Hellerstein, W. Hong, S. Krishnamurthy, S. Madden, V. Raman, F. Reiss, and M. Shah, “Telegraphcq: Continuous dataow processing for an uncertan world," 2003.

[17] D. J. Abadi, Y. Ahmad, M. Balazinska, U. Cetintemel, M. Cherniack, J.-H. Hwang, W. Lindner, A. S. Maskey, A. Rasin, E. Ryvkina, N. Tatbul, Y. Xing, and S. Zdonik, “The Design of the Borealis Stream Processing Engine," in Second Biennial Conference on Innovative Data Systems Research (CIDR 2005), (Asilomar, CA), January 2005.

[18] G. Agha, Actors: a model of concurrent computation in distributed systems. Cambridge, MA, USA: MIT Press, 1986.

[19] M. M. Gaber, A. Zaslavsky, and S. Krishnaswamy, “Mining data streams: a review," SIGMOD Rec., vol. 34, pp. 18{26, June 2005.

[20] S. Bandyopadhyay, C. Giannella, U. Maulik, H. Kargupta, K. Liu, and S. Datta, “Clustering distributed data streams in peer-to-peer environments," Information Sciences, vol. 176, no. 14, pp. 1952 { 1985, 2006. }Streaming Data Mining

[21] A. Bifet, G. Holmes, B. Pfahringer, J. Read, P. Kranen, H. Kremer, T. Jansen, and T. Seidl, “Moa: A real-time analytics open source framework," in Machine Learning and Knowledge Discovery in Databases (D. Gunopulos, T. Hofmann, D. Malerba, and M. Vazirgian nis, eds.), vol. 6913 of Lecture Notes in Computer Science, pp. 617-620, Springer Berlin Heidelberg, 2011.

International Journal of Engineering Research and General Science Volume 3, Issue 6, November-December, 2015
ISSN 2091-2730

A NOVEL RESOURCE COST PREDICTION AND COMPARISON SYSTEM FOR CLOUD CONSUMERS TO ACHIEVE COST EFFECTIVE USES

Udagandla Lokesh1 B.Krishna Sagar2

1PG Student,Department of Computer Science and Engineering, Madanapalle Institute of Technology & Science, India.
Mail id : loki.lokesh222@gmail.com

2Associate Professor,Department of Computer Science and Engineering, Madanapalle Institute of Technology & Science, India.
krishna.sagar521@gmail.com

ABSTRACT - With the spread of services related to cloud environment, it is tiresome and time consuming for users to look for the appropriate service that meet with their needs. Therefore, finding a valid and reliable service is essential. However, in case a single cloud service cannot fulfil every user requirements, a composition of cloud services is needed. In addition, the need to treat uncertainty in cloud service discovery and composition induces a lot of concerns in order to minimize the risk. Risk includes some sort of either loss or damage which is possible to be received by a target (i.e., the environment, cloud providers or customers). In this paper, we will focus on the uncertainty application for cloud service discovery and composition. A set of existing approaches in literature are reviewed and categorized according to the risk modeling.

KEYWORDS

Cloud Computing, Cloud Service Discovery, Cloud Service Composition, Risk, Uncertainty

1. INTRODUCTION

Cloud is a technology that represents networks and networking and computing is another technology that represents computer-related resources, applications and services. The combination of these two technologies is the concept of "Cloud computing" [1]. According to a cloud user, since the message entered a cloud and came out, so there was no need to know where it went. As soon as the web concept has been lead into the world, the user sent a Uniform Resource Locator (URL) to the internet and the request document could come back from any place. It was not necessary to know either the storage place or the owner. The utilization of cloud computing, nowadays, was compared to the electricity network from a century ago. Without installing any software or maintaining any hardware, users can use applications and conduct operations with internet access.

The essential characteristics of cloud model [2] are five as follows: on demand self-service, broad network access, resource pooling, rapid elasticity, and measured service. In addition, for the deployment models, there are three clouds that remains a unique entity, which are private cloud, community cloud and public cloud. Besides, hybrid cloud is another type of cloud models available in the market and it involves two or more clouds.

In cloud computing, there are three fundamental service models that will be described in details next section such as Infrastructure as a Service (IaaS), Software as a Service (SaaS), and Platform as a Service (PaaS).

Day after day, the number of cloud service providers increases and causes the competition in cloud market. The user can compare, evaluate and choose the cloud providers offering in the market which fulfil his requirements, but this task is a tedious and time consuming.

As cloud computing coming more popular, more and more organizations want to move to the cloud. Therefore, a risk assessment is needed to minimize the costs of implementing and maintaining controls and to help avoid surprises [3].

The terms risk and uncertainty are often used interchangeably. They are based on lack of certainty. When we talk about risk, we talk about unknown outcomes. It is the possibility of loss. Risk is quantifiable unlike uncertainty. The latter occurs when we have no idea about the outcome at the time when the decision is made [4].

On the one hand, the lack of knowledge and poor or imperfect information about all the inputs are the main causes of the uncertainty in decision making process. On the other hand, when the service provider try to describe the cloud service in a standard format, unpredictable future factors, like hacking leading to data breach or to data loss, are responsible for incomplete information, hence the need for uncertainty handling in cloud service discovery and composition. So, a good choice of cloud services conducts to a good result for the client, or a good composition between different cloud services.

In this paper, we will survey relevant contributions to the cloud service discovery and composition fields, which are inspired by the researches in cross-uncertainty. Particularly, specific interest is given to three known theories: probability theory, belief function theory and possibility theory. The remainder of this paper is organized as follows. Section 2 describes the cloud computing services. In section 3, we present the uncertainty theory and cloud risk modeling. Cloud Services Discovery and Composition are presented respectively in Section 4 and 5. Section 6 is the discusion.

2. CLOUD COMPUTING SERVICE

Cloud services [1] are wilfully presented within a narrow perspective of cloud applications. All the cloud services allow users to run applications and store data online. However, a different level of user control and flexibility is offered.

2.1. Type of Cloud Services

2.1.1. Infrastructure as a Service (IaaS)

IaaS is a way of delivering cloud computing infrastructure including hardware such as servers, networking hardware and software like operating system, middleware and applications [5]. The provider of the service is the one who owns the equipment and is in charge of its management. As long as there is internet and whenever the consumer needs, the resources are available and it can be used [2]. Two types of services distinguished in [6] that allow higher level services to automate setup: “Physical Resource Set” and “Virtual Resource Set”.

2.1.2. Software as a Service (SaaS)

The SaaS model helps the consumer to pay only the software/service he uses. This mode eliminates the need to install and run the application on the customer„s local computers. In SaaS layer [5], all the applications that give a direct service to the consumer are found. As shown in [6], the services of SaaS layer are: “Basic Application Services” and “Composite Application Services”. The Basic and Composite services are categorized into Application Services, which comprise the highest level building blocks for end-user applications running in the Cloud.

2.1.3. Platform as a Service (PaaS)

PaaS as the name suggests, provides computing platforms for building and running custom applications. It helps developers to speed the development of their applications and therefore save money [2]. The consumer does not manage or control the underlying cloud infrastructure including network, servers, operating systems, or storage, but has control over the deployed applications and possibly application hosting environment configurations. PaaS environment provide a complete operational environment for users to deploy and run their applications. The work in [6] categorizes the services of PaaS level into: “Programming Environments” and “Execution Environments”.

Cloud computing does not come without uncertainty. When the data of company is located on the cloud, it is threatened by hackers.

3. UNCERTAINTY THEORY AND CLOUD RISK MODELING

For most real-world problems, uncertainty and imprecision are both often inherent in modeling knowledge. Uncertainty can result from some errors and hence from non-reliability or from different background knowledge [7]. According to [8], uncertainty is associated with the measurement errors and resolution limits of measuring instruments, at the empirical level. At the cognitive level [8], it emerges from the vagueness and ambiguities in natural language. At the social level, uncertainty is both created and maintained for various objectives by people, for example privacy and secrecy purposes [8].

3.1. Theories of Uncertainty

3.1.1. Probability Theory

Probability theory studies the random phenomena behaviour. However, probability distribution [9] describes population probabilistic characteristics. Moreover, probability theory is a quantitative way of dealing with uncertainty which often affect several areas of life.

Given an event *A*, Probability of event *A*:

P(A)= Number of outcome favourable to A - 1
Total number ofo possible outcome

Probability theory has been developed based upon three known axioms:

i. **P(A) ≥0 (Probability is a nonnegative number)**
ii. **P(Ω) =1 (Probability of the whole set is unity)**
iii. **IF A∩B = ø, then P*(**
iv.

3.1.2. Belief Function Theory

Arthur P. Dempster is the first one who introduces the belief function theory [10] in the context of statistical inference. Then it was developed by Glenn Shafer and the theory was named after their names "Dempster-Shafer theory". The theory has another name „Evidence theory".

Belief function theory is based on two ideas as mentioned in [11]:

- The idea of achieving levels of belief for one issue from subjective probabilities for another related issue,

- Dempster's rule for relating such levels of belief when they depend on independent items of evidence.

In the first idea, the degree of belief, also referred to as a mass, is correspond to a belief function rather than a Bayesian probability distribution. The values of probability are assigned to sets of possibilities rather than single events.

As for the theory of Dempster-Shafer, its masses are assigned to the entire non-empty subsets of the entities that comprise a system. The framework proposed by Shafer allows propositions to be displayed as intervals which are bounded by two values. This will be explained bellow [12]:

- *belief* (denoted Bel): is constituted by the sum of the masses of all sets enclosed by an hypothesis. Belief measures the evidence strength in favour of a set of propositions. It ranges from 0 that indicate no evidence to 1 that denotes certainty.

- *plausibility* (denoted *Pl*): is an upper bound on the possibility of the truth of the hypothesis. It is defined to be *Pl(s)=1-Bel(~s)* with *belief* ≤ *plausibility*.

3.1.3. Possibility Theory

Because probability theory is not able to model uncertainty which result from lack or incomplete of knowledge, Zadeh [13] introduced possibility theory that differs from probability theory by the use of two sets functions respectively called possibility measure which is a maxitive set-functions and necessity measure that is a minitive set-functions [14]. In few words, for each event A from a subset S, the uncertainty may be evaluated through two levels: the possibility Π(A), denoting to what extent the occurrence of event A if possible, and the certainty N(A), denoting to what extend the occurrence of event A is certain, with:

$$\forall A \subseteq S, N(A) \leq \Pi(A) \quad (3)$$

and

$$\forall A \subseteq S, N(A) = 1 - \Pi(\overline{A}) \quad (4)$$

If the occurrence of *A* is certain $\Pi(A)=1$ and $N(A)=1$; if the occurrence of *A* is impossible:

$\Pi(A)=0$ and $N(A)=0$. If there is no knowledge available: $\Pi(A)=1$ and $N(A)=0$ (the event is possible and not necessary).

Dubois and Prade in [15] confirmed that possibility theory is a rough non-numerical probability version. For them, it is a simple methodology to reasoning since its probabilities are not precise.

3.2. Cloud Risk Modeling

When something happens and negatively affects the outcome, it is called risk [3]. Risks related to the use of cloud are cumulative according to the type of service to which they relate: IaaS presents a series of risks which are specific and are related to the management infrastructure; PaaS show the same risks with, in addition, those that are specific to this type and which are related to the management system software (i.e., it limits developers to provider languages and tools); Finally, the SaaS model has, in moreover, the specific risks related to data management and applications which not always suitable for business use.

The risk management has three general steps mentioned in [16]. First, the risk data is identified before it becomes problems. Then, it is analysed and converted to decision-making information.

Finally, the status of risk is controlled and some actions are taken into consideration to reduce the risk.

As many approaches based on probabilistic methods have been proposed to tackle the uncertainty in practical risk assessment and this is due by the Bayesian formulation for the treatment of rare events and poorly known processes. However, a number of theoretical and practical challenges seem to be still somewhat open [17]. This has sparked the emergence of a number of alternative approaches, which are:

- Use of interval probabilities due to the combination of probability analysis and interval analysis,
- Imprecise probability is considered to provide a more complicated representation of uncertainty,
- Random sets in the two forms proposed by Dempster and Shafer,
- Possibility theory that is formally a special case of the imprecise probability and random set theories.

4. CLOUD SERVICE DISCOVERY

With the growing number of various web services over the internet, the efficiency and the scalability of service discovery become a critical issue for cloud computing enabled applications. To discover a cloud service provider which is reliable is very vulnerable. A system is less trusted, if it provides us with information which is insufficient in relation to its abilities. By trust it is meant faith or confidence that a promised thing will for sure be realised [18,19]. Today, it is fundamental to have confidence between the service provider and the user [20]. It is not possible for the user to check whether the service is trustful and whether there is a risk linked to insider attacks. In cloud environment, service discovery is challenging among the available heterogeneous services and the large number of service providers. Moreover, security is an enormous challenge while searching for a suitable cloud service.

Raggad [21] proposes a decision support mechanism that applies Dempster and Shafer theory [22] to devise a risk driven cloud computing project solution. The decision support model consists of the following steps; the technical team collects evidence on available and relevant cloud computing providers and brokers. This belief structure consists of a basic probability assignment for every service, on the frame of discernment of cloud providers and brokers. After given the cloud computing power and the cloud brokerage power, the technical team contact relevant auditors to collect evidence on the capabilities of the defined cloud computing power (i.e., selected cloud providers) to establish all company‟s IT service requirements when executing the assigned IT services. This belief structure [21] is used to make sure that the cloud computing project solution adopted above can in fact establish all mandated IT service requirements. The last step is computing the total expected risk of acquiring cloud power based on which a decision can be made whether to acquire cloud computing or process candidate IT services internally.

Rajesh et al. [23] developed a new approach that uses the belief net to cleverly discover the appropriate and relevant web service relying on the available QoS parameters. They use ontology, as a semantic search engine, which helps the cloud customer to discover

the service that would fulfil a specific need. This ontology offers more precise and relevant results by using the semantic annotation that helps to bridge the ambiguity of the natural language.

In [24] a probabilistic flooding based method is proposed, which is easily to implement and not sensitive to the dynamic change in the network. This method combine Simple Additive Weighting (SAW) technique and skyline filtering, that is proposed to perform QoS-aware service discovery over a service registering-enabled P2P network, according to the user‟s functional requirements and QoS constraints. The Simple Additive Weighting is a technique that could be used to select a QoS-optimal service among a set of functionality equivalent services, taking into consideration of QoS properties of these services. There are still some limitations. Firstly, the time cost of service discovery for different service query under the same traffic situation, is not determined in a quantitative way. Moreover, simulation experiment is the only way to illustrate the performance of the method of service discovery. Finally, more uncertain factors could affect the performance of this method, such as node crush and traffic congestion.

In a novice research [20] trust mechanism is integrated into cloud service discovery process. As a solution for the specific risk problems, trust is used. Trust means the faith and the confidence that the service will surely be supplied as convenient. The Bayesian network was adopted for formulating this model. The probabilistic dependencies among the variables in the cloud service discovery field were captured as conditional probability [20]. Hence the model was illustrated as a series of connected Bayesian Network that is illustrated as an acyclic directed graph.

Relying on the state of the cloud infrastructure, cloud provider might not be the most reliable at a well precise moment. The limitation of the studies of efficiency of how to exploit a single cloud system let to the deployment of service composition phase.

5. CLOUD SERVICE COMPOSITION

Composition [25] is called static when it is done manually in customer„s requirement design step and the cloud service is automatically selected by the system. Nonetheless, in dynamic composition, the service selection and the process model are automatically done by programs. Service composition can scale Cloud computing in two dimensions: horizontal and vertical [26]. Horizontal service composition stands for the composition of services which are heterogeneous and which may be in several Clouds. Vertical service composition refers to the services which are homogenous in order to increase a given Cloud node capacity.

The failure of the composite service is engendered by the failure of individual cloud service. Composite service general reliability is the product of constituent cloud services reliability. Therefore, one unreliable cloud service can decrease the overall reliability to a very low level.

Many services are involved in an application and that can be available as a novice cloud service [27]. Any provider of this service will face a hard situation since it is essential to guarantee a particular level of QoS to end users. Simultaneously, the quality of the supplied service relies on agreements between both the partners and quality of services [28]. A composite service will be obliged to pay fines to its customers because it cannot meet the entire required request on time. In general, it is possible to speak about risk which quality of a composite web service can be affected because of problems with related services. In case the risk is important, it is a must to mitigate it.

In this part, we discuss several methods for service composition in the cloud using uncertainty. In [29] the approach uses Bayesian networks as well as probability mixtures to model service composition in order to access separately each quality of service. The consumer can then choose services according to its preferences from the varied qualities. The model illustrates the dynamism by developing the Bayesian network, which therefore positively affects the quality of the service in terms of trustfulness. Trust systems enable parties to determine the trustworthiness of participating parties [30]. The Bayesian approach illustrates the relationship of supplying a good quality of service among the composite and the constituent services. Moreover, it constantly updates trust to meet newly quality. Bayesian approach can first model the relations of the service

composition. Second, distinguish between any good or bad services in any partially noticeable setting. Third, deduct conditional probabilities from the relationships. However, the Bayesian approach didn‟t succeed to compute the constituent services and unconditional trustworthiness. Moreover, the Bayesian approach needs at least partial observability. In its model trust, it uses only the probability unlike modern approaches which use both probability and certainty.

Reference [31] focuses on Quality of Services. QoS satisfied prediction model which is relied on a hidden Markov model (HMM). HMM is a good technique to solve problems of prediction.

[32] presents algorithms as well as a framework that simplify cloud service composition for non talented users. The authors use a combination of fuzzy logic and algorithms for composition optimization to facilitate the user‟s task. Moreover a ranking system for

cloud service composition is provided to help users express their preferences in convenient way by using high-level linguistic rules. The main limitation in cloud service composition is the ability to find the appropriate combination which reduces the deployment cost and time, and increases the reliability.

6. DISCUSION

The real internet is more dynamic, and more uncertain factors could affect the performance of the method such as traffic congestion and the qualities offered by a service instance might vary over time, sometimes rapidly. But, the important hurdles to users adopting cloud services involve security, availability, and reliability.

The study allowed us to identify the main technical of cloud service discovery and composition under uncertainty that is an important nature of trust.

As a summary for detailed analysis of the related work (see Table 1 and 2), we have identified a set of characteristics as risk modeling namely: are:

Type of Service (TS): denotes the type of cloud services which are IaaS, PaaS and SaaS.

Type of uncertainty (TU): determines which theory or technique was used to model uncertainty.

Response Time (RT): refers to the interval between the sent request and the obtained reply.

Robustness of process (RP): it deals with error management during discovery.

Table 1. Summary of Cloud Service Discovery.

Contribution	***Risk Modeling***				
	Mechanism	***TS***	***TU***	***RT***	***RP***
Raggard [21]	Belief Function	IT service	Dempster & Shafer Theory	-	Expected Losses
Lin et al [22]	Service Registering	SaaS PaaS IaaS	Probability Theory	Small time to live	Node crush Traffic congestion
Rajesh et al. [23]	Bayesian Network	SaaS	Belief Network	Dynamic and Quick	Error handling is little hard
Akinwunmi et al. [20]	Trust mechanism	-	Probability Theory	Good	Less general risk users anxiety reduced

We can address the issues in the following tables 1 and 2 for the approaches that are discussed in the previous sections.

Literature in [21], [23] and [24] points out that there is only a few approaches in cloud service discovery which are under uncertainty. In fact, it is not possible for the user to be certain about the quality of the service and its trustworthiness. Also, in [24] a small Time To Live could avoid the traffic congestion, but this reduced the number of service information replicas, which may impair the service discovery efficiency. Moreover, we note that, the existing approaches use only the belief function or the probabilistic measures but not the possibilistic ones that have been successfully applied in decision making problems in conditions of uncertainty.

There are new challenges raised by service composition in cloud [32] which are caused by the diversity of users across different geographical locations with all their different legal constraints. An evaluation of techniques for service composition in the cloud is presented below in Table II.

Table 2. Summary of Cloud Service Composition.

Contribution	Risk Modeling				
	Mechanism	***TS***	***TU***	***RT***	***RP***
Hang et al. [29]	Bayesien Network	_	Probability Theory	_	Unconditional trustworthiness
Wu et al. [31]	Hidden Markov	SaaS PaaS IaaS	Prediction model	Small time to live	Expected larger error
dastjerdi et al. [32]	Defuzzification strategy [33]	IaaS	Fuzzy Preferences	Optimized	_

As shown in the above analysis, neither of the existing methods of cloud service composition is based on the possibility theory, which is very powerful to represent partial or incomplete knowledge [34].

These approaches have been proposed to tackle the problem of cloud service discovery and composition, but they were inadequate enough to handle the uncertainty associated with the cloud environment.

Possibility theory is distinct from probability theory, the theory of random sets, and Dempster-Shafer theory of belief and plausibility. Viewed in this prospect, the distinctness of possibility theory implies that it is in a complementary relation to probability theory and not an alternative to it. This involves that it addresses a class of issues in the management of uncertainty which are not addressed by probability theory [28].

7. CONCLUSIONS

Despite the cloud computing is the preeminent on-demand service system along with a “Pay-as-you-go”, the service provided does not respond to our needs with a total way (100%). In other words, the service provided is not in conformity with the request. This problem brings us to the uncertainty reasoning which is important to ensure the user's satisfaction.

The aim of this research is to give a general view of any new development in cloud service discovery and composition under uncertainty. The main objective is to emphasise the interest in the risk analysis by uncertainty handling, because, both risk and uncertainty research can help to make appropriate decisions about the necessary actions in case of shortage of knowledge about the system state.

Besides for researchers, this systematic review might have implications for practitioners. They can use this review as a source in searching for relevant approaches for Cloud Service Discovery and composition under uncertainty.

REFERENCES:

[1] Y Chang William, Abu-Amara Hosame & Feng Sanford Jessica, (2010) “Transforming Entreprise Cloud Service”, Springer Science Business Media, 525p.

[2] Palli George, (2010) “Cloud Computing: The New Frontier of Internet Computing”, IEEE Internet Computing, vol. 14, no. 5, pp. 70-73, MIC.113

[3] Samad Jeveria, W. Loke Sweng & Reed Karl, (2013), “Quantitative Risk Analysis for Mobile Cloud Computing: A Preliminary Approach and a Health Application Case Study”, In Proceedings of the 12th IEEE International Conference on Trust, Security and Privacy in Computing and Communications, Washington, DC, USA, pp. 1378-1385.

[4] French Nick & Gabrielli Laura, (2004), “The uncertainty of valuation”, Journal of Property Investment & Finance, Vol. 22 Iss: 6, pp.484 – 500.

[5] Zhu Yan, Wang Huaixi, Hu Zexing, Ahn Gail-Joon, Hu Hongxin & Yau Stephen S, (2011), "Dynamic audit services for integrity verification of outsourced storages in clouds", In Proceedings of the 2011 ACM Symposium on Applied Computing, New York, NY, USA, 1550-1557.

[6] Dimitrios Zissis & Dimitrios Lekkas, (March 2012) "Addressing cloud computing security issues", Future Gener.Comput. Syst. 28, 3,pp.583-592.

[7] Dastjerdi Amir Vahid, Tabatabaei Sayed G.H. & Buyya Rajkumar, (2010), "An Effective Architecture for Automated Appliance Management System Applying Ontology-Based Cloud Discovery",10th IEEE/ACM International Conference on Cluster, Cloud and Grid Computing, pp. 104-112.

[8] Dwlvedi Ashutosh, Mishra Deepak & Kalra Prem Kumar, (2006),"Handling Uncertainties-using Probability Theory to Possibility Theory", IIT Kanpur, pp.1-12.

[9] Aral Mustafa M., (2010), "Environmental Modeling and Health Risk Analysis (Acts/Risk)", springer, 470 pages.

[10] Denoeux Thierry, (2012) "Belief functions: theory and applications", in 2nd International Conference on Belief functions, springer, France9.

[11] Dempster A. P., (1968) "A generalization of Bayesian inference", Journal of the Royal Statistical Society, Series B, Vol. 30, pp. 205–247.

[12] Parmar S. Zarna & Shah Vrushank, (2013) "A Review on Strategies for Combining Conflicting Dogmatic Beliefs", journal of information, knowledge and research in electronics and communication engineering, vol. 02, issue: 02, pp.806-811.

[13] Zadeh Lotfi, (1965) "Fuzzy sets", Inform Control, 8, pp. 338-53.

[14] Dubois Didier, (2006) "Possibility Theory and Statistical Reasoning". Computational Statistics & Data Analysis, 51(1):pp.47-69.

[15] D. Dubois and H. Prade, (1992) "when upper probabilities are possibility measures",Fuzzy Sets and Systems Journal,49, 65-74.

[16] Kokash Natallia, & D'Andrea Vincenzo, (2007) "Evaluating Quality of Web Services: A Risk-Driven Approach", In W. Abramowicz (ed.), Springer, pp. 180-194.

[17] Aven Terje & Zio Enrico, (2011) "Some considerations on the treatment of uncertainties in risk assessment for practical decision making". Rel. Eng. & Sys. Safety, 96, pp.64-74.

[18] Costa Ana Cristina & Bijlsma-Frankema Katinka, (2007) "Trust and Control Interrelations," Group and Organization Management, 32(4): pp.392 – 406.

[19] Lund, M. and Solhaug, B. (2010). "Evolution in Relation to Risk and Trust Management," Computer, May 2010, pp. 49–55

[20] Akinwunmi A.O., Olajubu E.A., Aderoumu G.A., (2014) "A trustworhty model for reliable cloud service discovery", International Journal od Computer Applications, volume 87-number 16, New York, USA, pp.23-30.

[21] Raggad B. G., Ph.D., (2013) Seidenberg School of CS & IS, Pace University, New York.

[22] Shafer Glenn, (1976), "Mathematical Theory of Evidence", Princeton, N.J.: Princeton University Press, Business & economics, V42.

[23] Rajesh G., Gnanasekar A. & Suresh R.M., (2013) "Web Service Discovery Using Semantically Annotated Belief Network", IJREAT International Journal of Research in Engineering & Advanced Technology, Volume 1, Issue 1.

[24] Lin Wenmin, Dou Wanchun, Xu Zhanyang & Chen Jinjun, (2013) "A QoS-aware service discovery method for elastic cloud computing in an unstructured peer-to-peer network", Concurrency & Computation: Practice & Experience, 1843-1860.

[25] Lenk Alexander, Klems Markus, Nimis Jens, Tai Stefan & Sandholm Thomas, (2009) "What's inside the Cloud? An architectural map of the Cloud landscape." In Proceedings of the 2009 ICSE Workshop on Software Engineering Challenges of Cloud Computing, pp. 23-31.

[26] Charif Yasmine & Sabouret Nicolas, (2013) "Dynamic service composition enabled by introspective agent coordination", Auton Agent Multi-Agent Syst., pp. 54-85.

[27] Ylianttila Mika, Riekki Jukka, Zhou Jiehan, Athukorala Kumaripaba & Gilman Ekaterina, (2012), "Cloud Architecture for Dynamic Service Composition". Int. J. Grid High Perform. Comput. V4, issue 2, pp.17-31.

[28] Nikolaidis Efstratios, Chen Sophie, Cudney Harley, Haftka Raphael & Rosca Raluca, (2004) "Comparison of Probability and Possibility for Design Against Catastrophic Failure Under Uncertainty," ASME J. Mech. Des., 1263, pp. 386–394.

[29] Hang Chung-wei & Singh Munindar,(2011) "Trustworthy Service Selection and Composition", ACM Trans. Auton. Adapt. 17pages.

[30] Wenjuan Fan, Shanlin Yang, Harry Perros & Jun Pei, (2013), "A Multi-dimensional trust-aware cloud service selection mechanism based on Evidential Reasoning Approach", International Journal of Automation and Computing

[31] Wu Qingtao, Zhang Mingchuan, Zheng Ruijuan & Wei Wangyang, (2013)"A Qos-satisfied prediction model for cloud-service composition based on a hidden markov model", Mathematical Problems in Engineering, vol. 2013, Article ID 387083, 7 pages.

[32] Dastjerdi Amir Vahid & Buyya Rajkumar, (2014) " Compatibility-aware Cloud Service Composition Under Fuzzy Preferences", Cloud Computing, IEEE Transactions on Issue: 99 .

[33] Mamdani E.H. & Assilian S., (1975) "An experiment in linguistic synthesis with a fuzzy logic controller", International Journal of Man-Machine Studies, vol. 7, no. 1, pp. 1–13

[34] Benferhat Salem, Lagrue Sylvain & Papini Odile, (2004) "Reasoning with partially ordered information in a possibilistic logic framework", Fuzzy Sets and Systems 144(1), 25–41.

International Journal of Engineering Research and General Science Volume 3, Issue 6, November-December, 2015
ISSN 2091-2730

STUDY ON SECURITY CAPABILITIES IN CLOUD COMPUTING ENVIORNMENT

Shobha Elizabeth Rajan, Sreedevi P. , Ameena Beevi A.
Dept. of Computer Science & Engg., MG University, India
shobharajan90@gmail.com

Abstract - A move to use cloud computing, requires customer to have a clear understanding of potential security benefits and risks associated with cloud computing, and set realistic expectations with their cloud provider. Consideration must be given to the different models of service delivery: Infrastructure as a Service (IaaS), Platform as a Service (PaaS) and Software as a (SaaS) as each model brings Service different security requirements and responsibilities. The paper tries to study on the security features and capabilities currently prevailing in cloud computing field and the security provider by cloud service providers. Also the paper ties to review on the existing attempts to overcome the security pitfalls**.**

Keywords — Cloud service providers, Security, Artificial intelligence, Intrusion detection.

INTRODUCTION

Cloud computing security or cloud security is an growing sub-domain of computer security, network security, and, more broadly, information security. It refers to a broad set of policies, technologies, and controls deployed to protect data, applications, and the associated infrastructure of cloud computing. Organizations use the Cloud in a variety of different service models (SaaS, PaaS, and IaaS) and deployment models (Private, Public, Hybrid, and Community). [13] There are a number of security issues/concerns associated with cloud computing but these issues fall into two broad categories: security issues faced by cloud providers (organizations providing software-, platform-, or infrastructure-as-a-service via the cloud) and security issues faced by their customers (companies or organizations who host applications or store data on the cloud). The responsibility goes both ways, however: the cloud service provider must ensure that their infrastructure is secure and that their clients' data and applications are protected while the user must take measures to fortify their application and use strong passwords and authentication measures. When an organization elects to store data or host applications on the public cloud, it loses its ability to have physical access to the servers hosting its information. As a result, potentially business sensitive and confidential data is at risk from insider attacks. According to a recent Cloud Security Alliance Report [12], insider attacks are the third biggest threat in cloud computing. [14] Therefore, Cloud Service providers must ensure that thorough background checks are conducted for employees who have physical access to the servers in the data center. Additionally, data centers must be frequently monitored for suspicious activity. In order to conserve resources, cut costs, and maintain efficiency, Cloud Service Providers often store more than one customer's data on the same server. The result would be a chance that one user's private data can be viewed by other users. To manage such conditions the cloud service providers should provide with logical storage segregation and data isolation[13]. The immense use of virtualization in cloud infrastructure brings security concerns for customers or tenants of a public cloud service. [15] Virtualization alters the relationship between the OS and underlying hardware - be it computing, storage or even networking. This introduces an additional layer - virtualization - that itself must be properly configured, managed and secured. Specific concerns include the potential to compromise the virtualization software, or "hypervisor". While these concerns are largely theoretical, they do exist[16].

Since the era pushes for the growth of the data, the need for the storage space and the security issues with the storage spaces is of great importance. The extend of security features provided to the systems so far and the extend to upgrade the cloud system with security feature is to be considered with great importance. The paper intends to study on few existing cloud service providers and the security they offer. Also the works carried out so far in cloud computing field for enhancing security.

STUDY AND LITERATURE SURVEY

Even though the vulnerability of the existing cloud service are not much high, the growing technological world could make it a factor of concern. Let us consider a few providers glowing in the market based on 2015 review. [23] Dropbox is one the cloud service providers been rated well. It provides security features by; using encryption method for storage and transfer of data, uses SSL/TLS for file transfer, creating a secure tunnel protected by 128-bit or higher AES encryption, vulnerabitility checks are performed regularly on storage and infrastructures, two-way verification, file accessible only to

users with authorized links. In short it is designed with multi layer protection, secure data transfer, encryption, network configuration and application and user level controls that are distributed across a scalable and secure infrastructure.

[24]iCloud on the other hand has data encrypted both in transit (using SSL) and on the server. Rather than using AES-256 bit encryption, it uses a minimum of 128-bit AES which is less secure. But it uses 256-bit for the iCloud keychain (used to store and transmit passwords and credit card data, also employing elliptic curve asymmetric cryptography and key wrapping which is good).The iCloud keychain encryption keys, however, are created on your own devices and Apple can't access them. It cannot access any of the core material that could be used to decrypt that key data and only trusted devices that you have approved can access your iCloud keychain. Secure tokens are used for authentication when accessing iCloud and there is optional two-step verification.[25]There are several to keep user files safe in OneDrive. User files aren't shared with other people unless user save in public folder or choose to share them. To help protect OneDrive files from hardware failure, multiple copies of each file are saved on different drives and servers. Other things which help protect user files are: create a strong password, add security info to your Microsoft account, use two-step verification, back up OneDrive files. [26]Google Drive Sharing Policies**,** Change Google Docs Permissions in Bulk**,** View Publicly Shared Documents**,** Correct Public Document Sharing Policy**,** Google Drive Visibility**,**Google Drive Inventory are the security features provided by google drive. Inspite of all the security features provided by the providers reviews show that they have underwent many vulnerability issues[24]. The research field is constantly working on researches to handle the intrusion detection in various fields. Cloud computing field is also in it. [7] Multiple criteria linear programming and particle swarm optimization to enhance the accuracy of attacks detection is an attempt. Multiple criteria linear programming is a classification method based on mathematical programming which has been showed a potential ability to solve real-life data mining problems. However, tuning its parameters is an essential steps in training phase. Particle swarm optimization (PSO) is a robust and simple to implement optimization technique has been used in order to improve the performance of MCLP classifier. [6] proposes a self adaptive ids and a model. The major characteristics that a Hybrid Intrusion Detection System has to possess are Dynamic Nature, Self adaptive, Scalability and Efficiency. The Intrusion Detection System should have the capacity to change its nature of detection whenever it is necessary, which we call it as Dynamic Nature of a Hybrid Intrusion Detection System. The system is for private cloud, where the number of users in the private cloud will be limited in number. Hybrid Intrusion Detection would be the solution for the above problem statement. Hybrid Intrusion Detection System can be defined as a system that has the combination of both anomaly detection method and misuse detection method.

El-Sayed M. el at [8] explores a new countermeasure approach for anomaly based intrusion detection using a multicriterion fuzzy classification method combined with a greedy attribute selection. The proposed approach has the advantage of dealing with various types of attributes including network traffic basic TCP/IP packet headers, as well as content based, time-based and host-based attributes. At the same time, to reduce the dimensionality and increase the computational efficiency, the greedy attribute selection algorithm enables it to choose an optimal subset of attributes that is most relevant for detecting intrusive events. The simplicity of the constructed model allows it to be replicated at various network components in emerging open system infrastructures such as sensor networks, wireless ad hoc networks, cloud computing, and smart grids.

A four level framework for Intrusion detection is proposed[10] in which first procedure concerns to generate different training subsets by using k-means clustering, second procedure based on the training subsets different neuro-fuzzy models are trained, third procedure a vector for SVM classification and radial SVM classification is perform. Finally the decision tree is built using C4.5 decision tree algorithm . It works in a sequence by cascading different decision making algorithms based on their efficiency to handle different levels. SVMs classify data by determining a set of support vectors, which are members of the set of training inputs that outline a hyper plane in feature space. Computing the hyper plane to separate the data points leads to a quadratic optimization problem. There are two main reasons that for using SVMs for intrusion detection. The _rst reason is that its performance is in terms of execution speed, and the second reason is scalability. SVMs are relatively insensitive to the number of data points, and the classification complexity doesnot depend on the dimensionality of the feature space.The principle goal of em ploying the KMeans clustering scheme is to separate the collection of normal and attack data that behave similarly into several partitions which is known as K-th cluster centroids. In other words, K-Means estimates a fixed number of K, the best cluster centroid representing data with similar behavior. Work proposed in [18] is a hybrid system of SVM and hybrid C5.0 - SVM approach. The motivation for using the hybrid approach is to improve the accuracy of the intrusion detection system when compared to using individual approaches. The hybrid approach combines the best results from the different individual systems resulting in more accuracy.In a hierarchical hybrid intelligent system each layer provides some new information to the higher level. The overall functioning of the system depends on the correct functionality of all the layers. In the proposed system the data set is first passed through the C5.0 and node information is generated. Node information is determined according to the rules generated by the C5.0. All the data set records are assigned to one of the terminal nodes, which represent the particular class or subset. This node information (as an additional attribute) along with the original set of attributes is passed through the SVM to obtain the _nal output. The key idea here is to investigate whether the node information provided by the

C5.0 will improve the performance of the SVM. Thus the system enables automatic dataset generation according to the newly arriving attacks. Thus a data set with updated would be possible and as a result the system starts responding to any newly arriving attacks. But the work has only been designed to work in network environment and not in a cloud environment. It is very clearly understood that hybrid IDS give a better result since the data is processed more than once. In [12] hybrid (various decision making algorithm combinations)ids are analyzed and leads to conclude to the following table. Considering the advantage and disadvantages of all the algorithms we could consider a better combination for a better result.

CONCLUSION

The paper aims to study the existing security measures and the loop holes opening to the vulnerability. Solving the whole security issue is equivalent to catching a shadow. The maximum we could do is to get as much as close to the secure side. Attacks and security intrusions are evolving to be more stronger and breaking all the available defenses. In all defensive measures a automatically evolving defensive system is not possible. The existing system are been updated with timely patches to adjust with the evolving attacks. In situation a dynamically adjusting system is worth designing. Artificial intelligent agent could be employed for this. The rate of tolerance against attacks could be lessen and detection of attacks could be enhanced. The paper tries to conclude that a dynamically detecting system is required.

REFERENCE:

[1] Meghana Solanki and Mrs. Vidya Dhamdhere, "Intrusion Detection System by using K-Means clustering, C 4.5, FNN, SVM classifier", *Int. Journal of Emerging Trends & Technology in Computer Science*, Volume-3,Issue-06, Page no (1-23), Dec 2014.

[2] Sourya Joyee De and Asim K. Pal, "A Policy-based Security Framework for Storage and Computation on Enterprise Data in the Cloud", *International Conference on System Science, IEEE,* Page no (1-12), Jan 2014.

[3] Sheng-Wei Lee and Fang Yu, "Securing KVM-based Cloud Systems via Virtualization Introspection", *International Conference on System Science, IEEE*, Page no (1-10), Jan 2014.

[4] Dan Gonzales, *Member, IEEE*, Jeremy Kaplan, Evan Saltzman, Zev Winkelman, Dulani Woods, "Cloud-Trust - a Security Assessment Model for Infrastructure as a Service (IaaS) Clouds", *IEEE Transactions on Cloud Computing,* Page no (1-14), Jan 2015.

[5] Dawei Sun, Guiran Chang, Lina Sun and Xingwei Wang, "Surveying and Analyzing Security, Privacy and Trust Issues in Cloud Computing Environments", *Advanced in Control Engineering and Information Science, Elsevier,* Page no (1-5), Dec 2012.

[6] Praveen Kumar Rajendran, B.Muthukumar, G.Nagarajan, "Hybrid Intrusion Detection System for Private Cloud: A Systematic Approach*" International Conference on Intelligent Computing, Communication & Convergence, (ICCC-2014)*

[7] Seyed Mojtaba Hosseini Bamakan, Behnam Amiri, Mahboubeh Mirzabagheri, Yong Shia, "A New Intrusion Detection Approach using PSO based Multiple Criteria Linear Programming", *Information Technology and Quantitative Management , Elsevier,* Page no (1-5), Dec 2015.

[8] Srinavasin, Madhan (2012). "'State-of-the-art cloud computing security taxonomies: a classification of security challenges in the present cloud computing environment". *ACM ICACC.*

[9] "Top Threats to Cloud Computing v1.0" (PDF). Cloud Security Alliance. Retrieved 2014-10-20.

[10] Winkler, Vic. "Cloud Computing: Virtual Cloud Security Concerns". Technet Magazine, Microsoft. Retrieved 12 February 2012.

[11] Hickey, Kathleen. "Dark Cloud: Study finds security risks in virtualization". Government Security News. Retrieved 12 February 2012.

[12] Winkler,Vic (2011). *Securing the Cloud: Cloud Computer Security Techniques and Tactics*. Waltham, MA USA: Elsevier. p. 59 ISBN 978-1-59749-592-9.

International Journal of Engineering Research and General Science Volume 3, Issue 6, November-December, 2015
ISSN 2091-2730

COMPARISON OF PERTURB AND OBSERVE MPPT FOR PV SYSTEMS CONJUCTION WITH BUCK BUCK-BOOST CONVERTERS

P.shiva kumar 1, P.Balamurali2, Ch.Ravikumar3
1P.G.Student, Dept. of EEE, Aditya Institute of Technology And Management, Tekkali, Andhrapradesh

2Associate Professor, Dept. of EEE, Aditya Institute of Technology And Management ,Tekkali, Andhrapradesh

3Associate Professor, Dept. of EEE, Adity Institute of Technology And Management, Tekkali, Andhrapradesh

ABSTRACT :
To extract maximum energy from the photovoltaic(PV) systems maximum power point tracking (mppt)technique in conjunction with power electronic circuits is used .Because of low maintenance, suitable for all climates and wide power range photovoltaic power generation has become more important, main disadvantages in PV systems are high initial cost and low energy conversion efficiency .To improve energy efficiency it is required to run PV system always at maximum power point .so ,far different methods are proposed by researchers for extracting maximum power. This paper presents detail implementation of perturb and observe mppt using buck and buck –boost converters. Some results such as current voltage output power for each various combinations have been recorded. From the results it is observed that perturb and observe mppt conjunction with buck converter has less power loss from panel side to converter side out of all other converters . The simulation has been accomplished in software MATLAB math work

INDEX TERMS: *Maximum Power Point Tracking, Perturb and Observe, DC-DC Converters, Photovoltaic System*

1. Introduction

The use of advanced efficient photovoltaic solar cells (PVSCs) has featured as a better alternative of energy conservation, renewable power and demand-side management. Due to their initial high cost, PVSCs have not yet been an exactly a tempting alternative for electrical usage who are able to buy less expensive electrical energy from the utility grid. However ,they have been used widely for air conditioning in remote , water pumping and isolated or remote areas where utility power is not available or is high costly to transport. Although PVSC prices have decreased considerably during the last years due to new developments in the film technology and manufacturing process [1]. The harnessing of solar energy using PV modules comes with its own problems that arise from the change in insolation conditions. Those changes in insolation conditions strongly influence the efficiency and output power of the PV modules. A great research has been accomplished to improve the efficiency of the photovoltaic system. Different methods to track the maximum power point of a PV module have been suggested to solve the problem of efficiency and products using these methods have been made and now commercially available for consumers [2-3]

As the species of these MPPT flooded into the market that are intentional to improve the efficiency of PV modules under varying isolation conditions it is not known how many of these can actually provide on their promise under a diversity of field conditions. This research then seems at how a different kind of converter affects the output power of the module and also achieve if the MPPT that are said to be highly efficient and do track the true maximum power point under the different conditions. A maximum power point tracker is used for obtaining the maximum power from the solar PV module and conversion to the load. A non isolated DC-DC converter (step up/ step down) offers the purpose of conversion maximum power to the load. A DC-DC converter acts as an interface between the load and the module. By varying the ratio of duty cycle the impedance of load as it appears by the source is varied and matched at the peak power point with the source so as to conversion the maximum power [4-5].Therefore maximum power point tracker methods are required to maintain the PV module working at its MPP. Many MPPT methods have been suggested in the literature ; example are the Perturb and Observe (P&O) methods, Incremental Conductance (IC) methods and constant voltage methods.. etc. [6-12]. In this paper the most popular of MPPT technique (Perturb and Observe (P&O) method, Buck and Buck- Boost DC-DC converters will involve in Implementation study (Figure 1) [13].Some results such as current, voltage and output power for each various combination have been discussed. The MPPT technique will be implemented, by using Matlab tool Simulink, considering the variant of circuit combination.

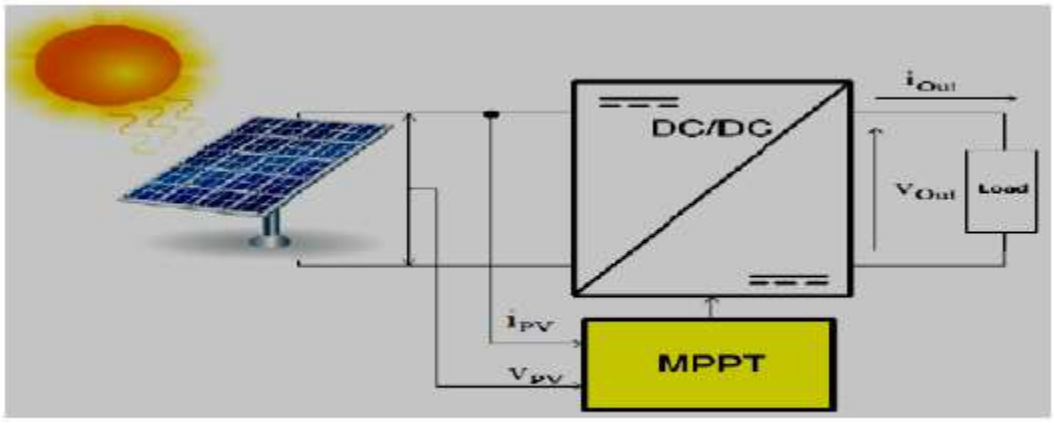

Figure 1. PV module and dc/ dc converter with MPPT

1 2. Photovoltaic Cell

Photovoltaic generators are neither fixed current sources nor voltage sources but can be approximated as current generators with dependant voltage sources. During darkness, the solar cell is not an active device. It produces neither a current nor a voltage. A solar panel cell essential is a p-n semiconductor junction. When exposed to the light, a current is generated (DC current).The generated current change linearly with the solar irradiance. Figure 2 show the equivalent electrical circuit of an ideal solar cell.

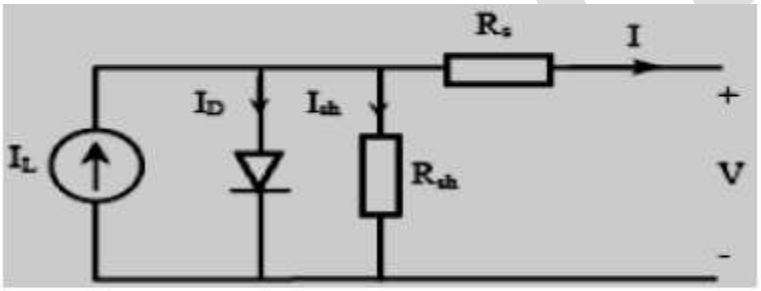

Figure 2. Equivalent circuit of a solar cell

The I-V characteristics of the solar cell circuit can be sets by the following equations . The current through diode is given by:

$$ID = IO [exp (q (V + I RS)/KT)) – 1] \quad (1)$$

While, the solar cell output current:

$$I = IL – ID – I sh \quad (2)$$

$$I = IL – IO [exp (q(V + I RS)/KT)) – 1] – (V + IRS)/ Rsh \quad (3)$$

Where,

I : Solar cell current (A)
IL : Light generated current (A)
IO : Diode saturation current (A)
q : Electron charge (1.6×10-19 C)
K : Boltzman constant (1.38×10-23 J/K)
T : Cell temperature in Kelvin (K)
V : solar cell output voltage (V)
Rs: Solar cell series resistance (Ω)
Rsh: Solar cell shunt resistance (Ω)

Electrical Characteristics	Ranges
Maximum Power (P_{max})	325W
Voltage at P_{max} (V_{mp})	34.5V
Current at P_{max} (I_{mp})	7.35A
Open-circuit voltage (V_{oc})	44.1V
Short-circuit current (I_{sc})	8.95A
Temperature coefficient of I_{sc}	1.33mv/ ^{o}C
Temperature coefficient of V_{oc}	-160 ± 20 mV/ ^{o}C
Temperature coefficient of power	-0.5 ± 0.05 %/ ^{o}C
NOCT	47 ± 2^{o}C

3.DC-DC Converter Analysis

3.1 Buck Converter

A buck converter or voltage regulator is also called a step down regulator since the output voltage is lower than the input voltage. In a simple example of a buck converter, a diode is connected in parallel with the input voltage source, a capacitor, and the load, which represents output voltage .A switch is connected between the input voltage source and the diode and an inductor is connected between the diode and the capacitor, shown in Figure 3

.

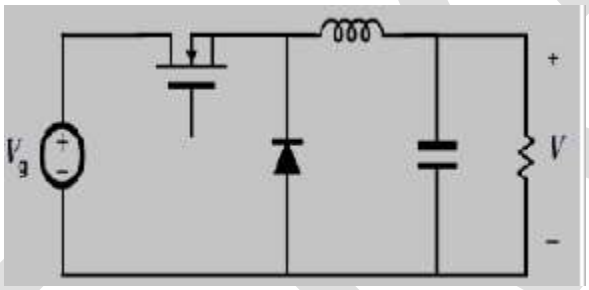

Figure 3. Basic buck converter

3.2 Buck-Boost Converter

The most important type of switching regulator is the buck-boost converter. In this converter, the buck and boost topologies covered earlier are combined into one. A buck-boost converter is also built using the same components used in the converters covered before. The inductor in this case is placed in parallel with the input voltage and the load capacitor. The switch or transistor is placed between the input and the inductor, while the diode is placed between the inductor and the load capacitor in a reverse direction, shown in Figure 4.The buck-Boost converter provides an output voltage that may be less than or greater than the input voltage .

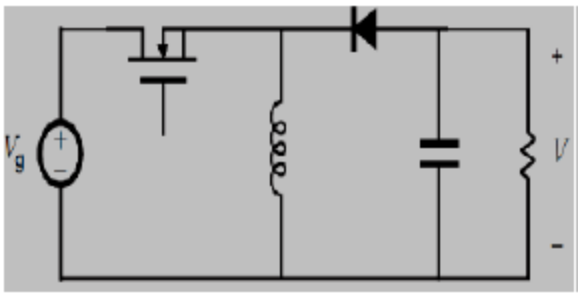

Figure 4. Basic buck-boost converter

4. Problem Overview

The MPPT method consider is to automatically find the current IMPP or voltage VMPP at which a PV module should work to extract the maximum output power PMPP under a given temperature and irradiance. Most of MPPT methods respond to variations in both irradiance and temperature, but some are precisely more useful if temperature is approximately constant. Most MPPT methods would

automatically respond to various in the module due to aging, though some are open-loop and would require periodic fine tuning. In our context, module will typically be connected to a power converter that can vary the current coming from the PV module to the load .

5. MPPT Control Algorithm The MPPT algorithm operates based on the truth that the derivative of the output power (P) with respect to the panel voltage (V) is equal to zero at the maximum power point. In the literature, various MPP algorithms are available in order to improve the performance of photovoltaic system by effectively tracking the MPP. However, most widely used MPPT algorithms are considered here, they are:

Perturb and Observe (P&O)
Incremental Conductance (In Cond)
Constant Voltage Method.

5.1 Perturb and Observe (P&O)

The most commonly used MPPT algorithm is P&O method. This algorithm uses simple feedback arrangement and little measured parameters. In this approach, the module voltage is periodically given a perturbation and the corresponding output power is compared with that at the previous perturbing cycle . In this algorithm a slight perturbation is introduce to the system. This perturbation causes the power of the solar module various. If the power increases due to the perturbation then the perturbation is continued in the same direction. After the peak power is reached the power at the MPP is zero and next instant decreases and hence after that the perturbation reverses as shown in Figures 6(a) and 6(b).When the stable condition is arrived the algorithm oscillates around the peak power point. In order to maintain the power variation small the perturbation size is remain very small. The technique is advanced in such a style that it sets a reference voltage of the module corresponding to the peak voltage of the module. A PI controller then acts to transfer the operating point of the module to that particular voltage level. It is observed some power loss due to this perturbation also the fails to track the maximum power under fast changing atmospheric conditions. But remain this technique is very popular and simple .[14]

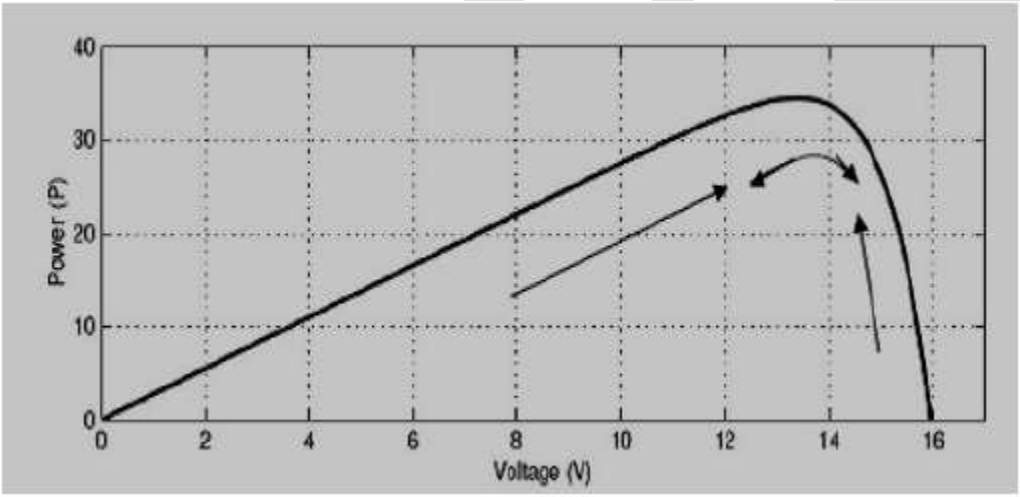

Figure 6(a). Graph Power versus Voltage for Perturb and Observe Algorithm

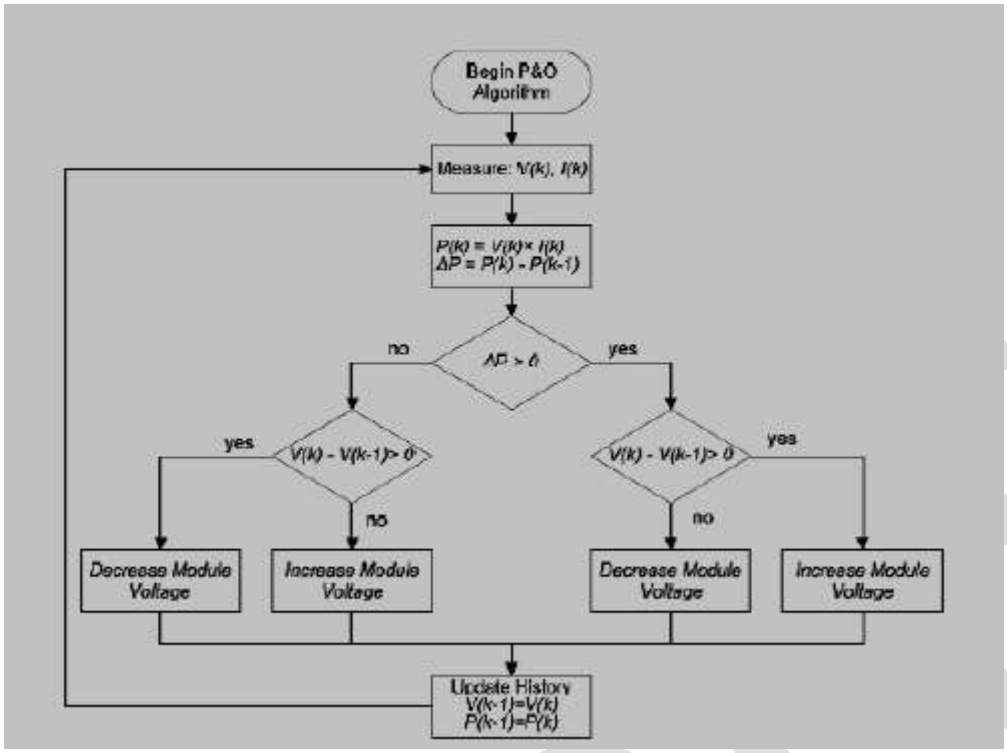

Figure 6(b). P&O Algorithm

6.MATLAB-SIMULINK Environment The model shown in Figure 7a 7b represents P-V and I –V curves of the pv panel

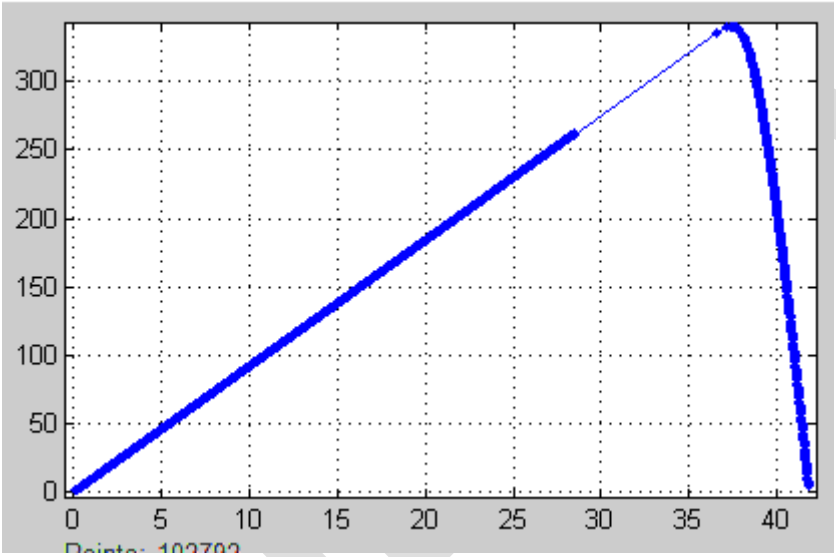

The P-V characteristics as shown in Figure7a. The point indicated as MPP is the point at which the panel power output is maximum

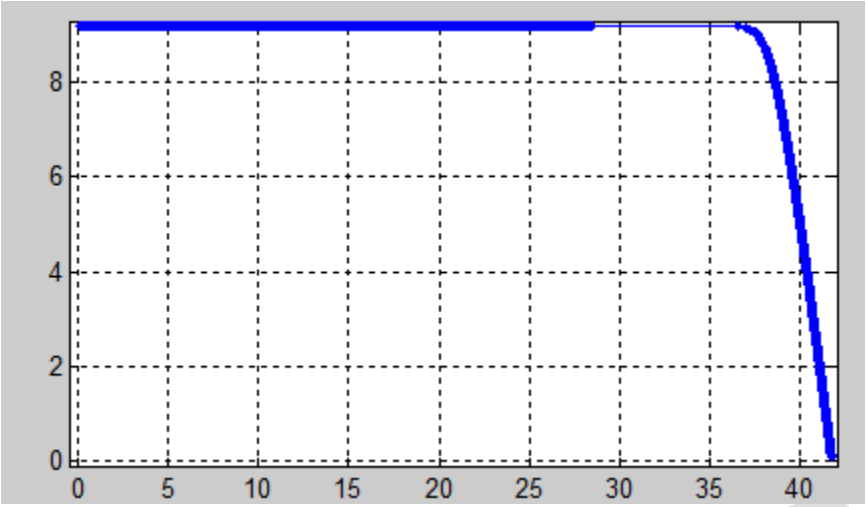

I -V characteristics of solar cell only for a certain insolation Ga and a certain cell temperature Tc are illustrated. Figure 7b

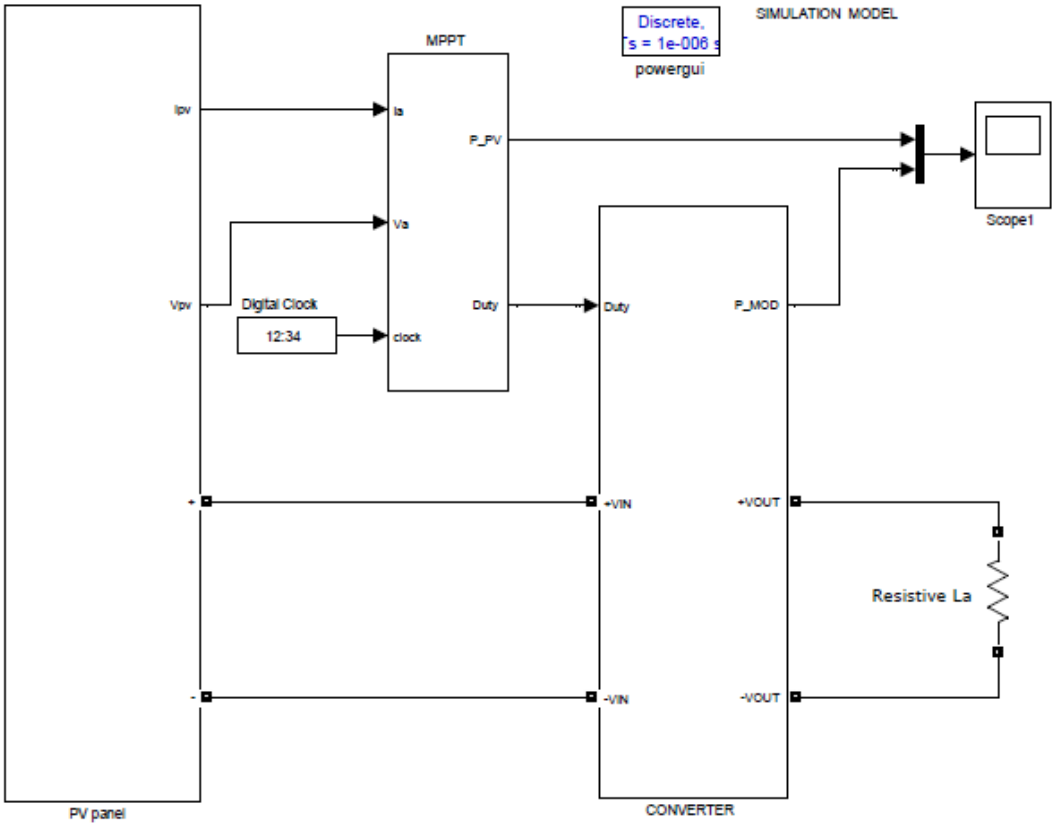

In Figure 8 show a mat lab SIMULINK® of complete diagram of a boost buck and buck-boost converters

while Figures 9 and 10 show a SIMULINK® of complete diagram of both

buck and buck-boost converters

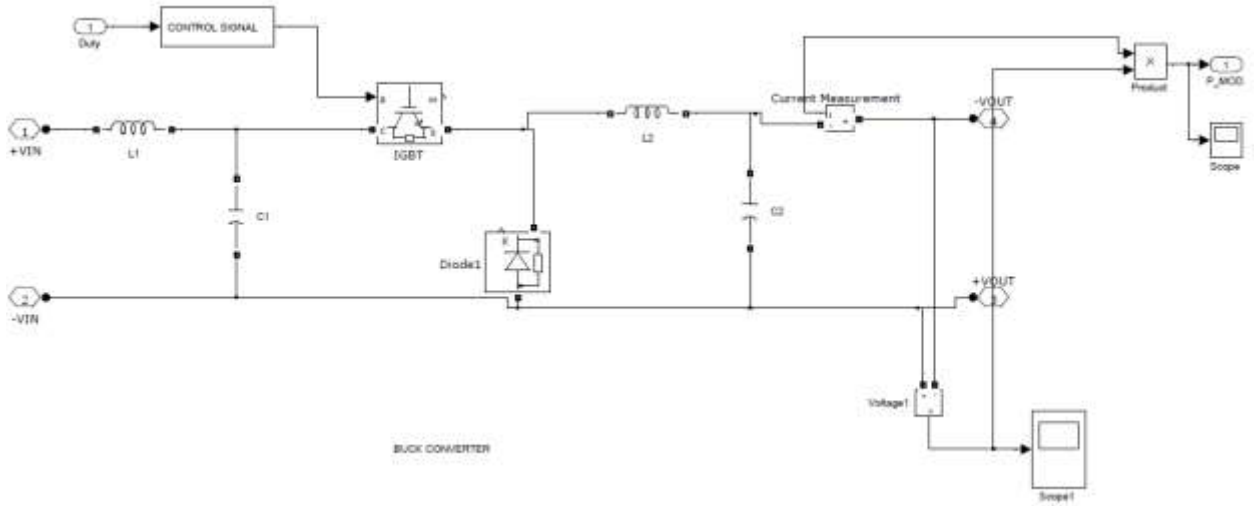

.
Figure 10 Buck converter design in matlab SIMULINK®

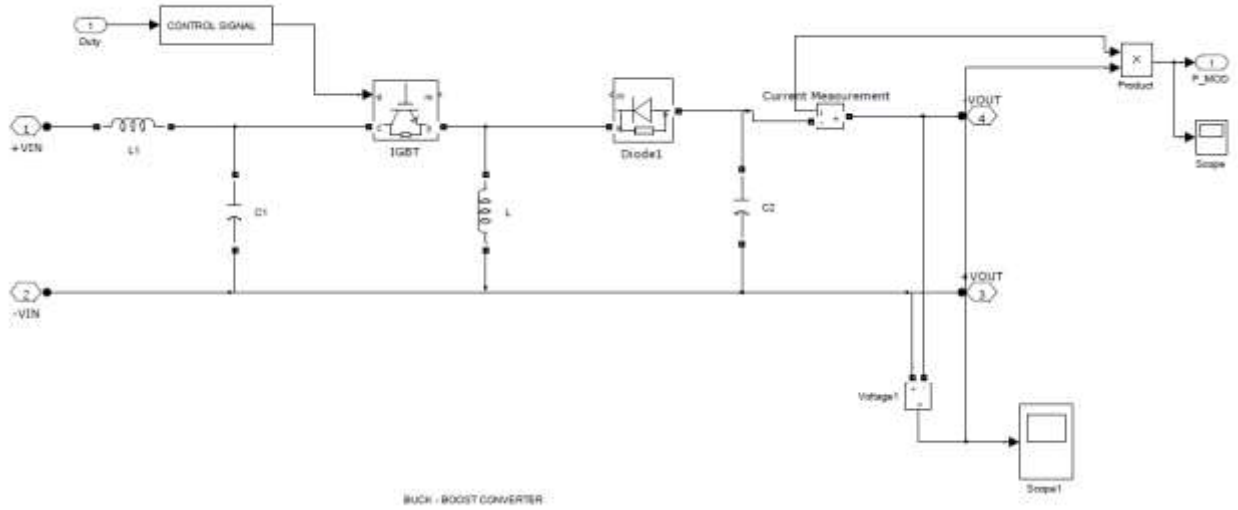

Figure 11 Buck-Boost converter design in matlab SIMULINK®

6.1.Results and Simulation

The models shown in the above figures were simulated using MATLAB® / SIMULINK® .Simulation and results for buck, boost and buck-boost converters have been recorded to make sure that comparison of the circuit can be obtained accurately. The voltage, current and output power is the main points of comparison to take into account. The complexity and simplicity of the circuit have been set based on the literature.

Buck-Boost Converter Simulation With Perturb and Observe Controller

The simulation result at constant temperature (T=50 degree) with changes in the isolation
(S=1000 to 850 w/m²)

It can be seen from Figures that the outputs of the PV panels and buck –boost converter clearly changes due to the change of the insolation as that variation of the converter affects the output of the PV panel the results below including current, voltage and power:

AT 1000w/ m²

At T=50 degree and S=1000w/ m²

I= 9.20Ampere, V=27.298 volt and P=250 watt

output of the buck- boost converter with P&O algorithm that results below including current, voltage and power

At T=50 degree and S=1000 w/ m^2

I=-4.087Ampere,V=-40.87voltandP=280w

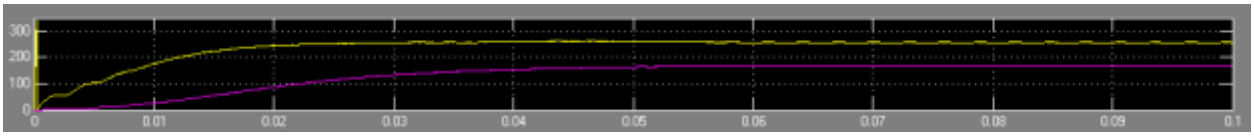

AT 850 w/ m²
From the Figure , the results below current, voltage, power of pv panel
At T=50 degree and S=850 w/ m²
I=7.82Ampere, V=24.15 volt and P= 180 watt,

the results below current, voltage, power of the buck- boost converter with P&O algorithm

At T=50 degree and S=850 w/ m²

I=-3.471Ampere,V=-34.71voltandP=120watt

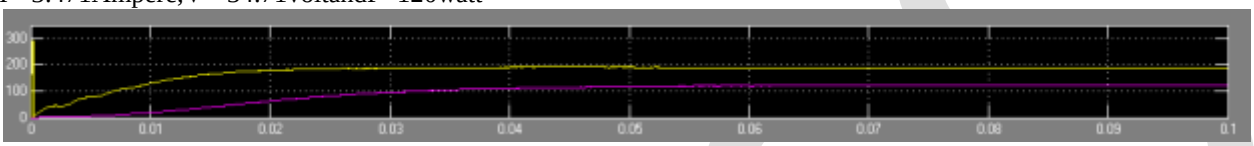

6.2. Buck Converter Simulation With Perturb and Observe Controller

The simulation result at constant temperature (T=50 degree) with changes in the insolation (S=1000 to 850 w/m²).
AT 1000w/ m²
Output current, voltage and power of PV panel
At T=50 degree and S=1000 w/ m²
I= 1.88 Ampere, V=41.1 volt and P=49 watt
Output current, voltage and power of buck converter with P&O algorithm
At T=50 degree and S=1000 w/ m²
I=1.93Ampere,V=19.73voltP=47watt

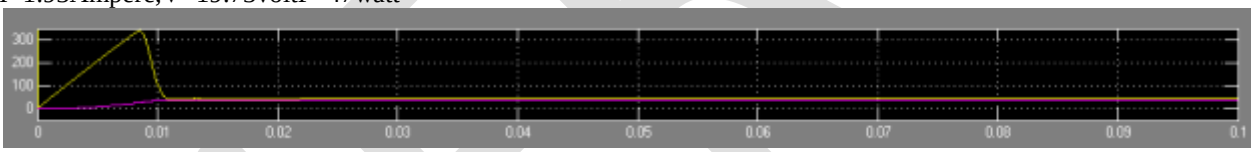

AT 850 w/ m²
The results below including current, voltage and power pv panel
At T=50 degree and S=850 w/ m²
I=1.076 Ampere, V=41.37 volt and P= 48 watt
Output current, voltage and power of buck converter with P&O algorithm
At T=50 degree and S=850 w/ m²
I=1.93Ampere,V=19.5voltP=46watt

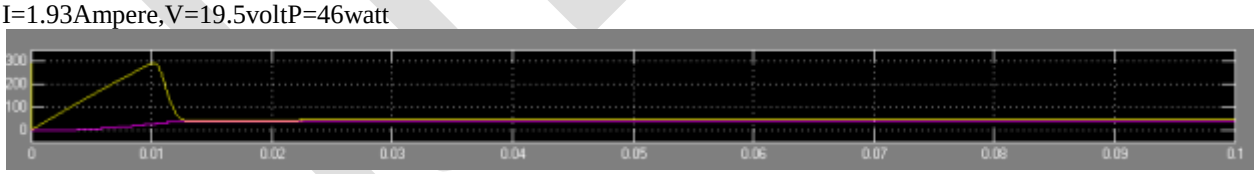

At T=50 degree and S=1000w/ m²

CONVERTER	I_{in}	V_{in}	P_{in}	I_{out}	V_{out}	P_{out}
BUCK	**1.088A**	**41.4V**	**49W**	**1.943A**	**39.43V**	**47W**
BUCK-BOOST	**9.20A**	**27.92V**	**250W**	**-4.087A**	**-40.87V**	**170W**

Table 1

At T=50 degree and S=850 w/ m²

CONVERTER	I_{in}	V_{in}	P_{in}	I_{out}	V_{out}	P_{out}

BUCK	1.076A	41.37V	48W	1.937A	38.5V	47W
BUCK-BOOST	7.82A	24.15V	180W	-3.471	-34.71V	120W

Table 2

From Tables 1&2, once the converters transfer the electrical power from the solar panel to the load and the controller start function, output value of the solar panel do not provide same input voltage value to controller (Vin). This is because the controller function that varies the value of duty cycle will change the input value that sense by the controller. The input voltages of this controller show a different each other. Input voltage of Buck that connected with P&O is 41.4 V(41.37V at 850 w/ m²) while input voltage of buck-boost that connected with P&O is 27.92V (24.15Vat 850 w/ m²). while input voltage of boost that connected with P&O is 38.38V (36.25Vat 850 w/ m²). The output value behaves as Buck, boost and buck-boost converters behave. The buck voltage will drop from 41.4V to 19.73V (41.37V to 19.5V at 850 w/ m²),
This system show that perturb and observe controller will work better with buck controller than buck-boost converter

7.CONCLUSION: P&O MPPT method is implemented with MATLAB-SIMULINK for simulation. Through simulation it is observed, that the system completes the maximum power point tracking successfully despite of fluctuations. Maximum power point changes with change in external environment quickly. Buck and buck-boost converters have succeeded to track the MPP but, buck converter is much effective because There is a small loss of power from the solar panel side to the buck converter output side compared with other converter.

REFERENCES:

[1] A.P. Yadav, S. Thirumaliah and G. Harith. "Comparison of MPPT Algorithms for DC-DC ConvertersBased PV Systems" International Journal of Advanced Research in Electrical, Electronics and Instrumentation Engineering Vol. 1, Issue 1, July 2012.
[2] Y.-H.Chang and C.-Y. Chang, "A Maximum Power Point Tracking of PV System by Scaling FuzzyControl," presented at International Multi Conference of Engineers and Computer Scientists, Hong Kong, 2010.
[3] S. Mekhilef, "Performance of grid connected inverter with maximum power point tracker and powerfactor control," International Journal of Power Electronics, vol.1, pp. 49-62.
[4] M.E.Ahmad and S.Mekhilef, "Design and Implementation of a Multi Level Three-Phase Inverter withLess Switches and Low Output Voltage Distortion," Journal of Power Electronics, vol. 9, pp. 594-604, 2009.
[5] H.N.Zainudin and S. Mekhilef, "Comparison Study of Maximum Power Point Tracker Techniques forPV Systems" Proceedings of the 14th International Middle East Power Systems ConferenceMEPCON'10), Cairo University, Egypt, December 19-21, 2010.
[6] R.Faranda and S. Leva, "Energy Comparison of MPPT techniques for PV Systems," WSEAS Transaction on Power Systems, vol. 3, pp. 446-455.
[7] Vikrant A. Chaudhari, "Automatic Peak Power Tracker for Solar PV Modules Using Dspace Software," in Maulana Azad National Institute of Technology. Master Thesis of Technology inEnergy. Bhopal: Deemed University, 2005.
[8] T.P.Nguyen, "Solar Panel Maximum Power Point Tracker," Ph. D. Thesis in Department of ComputerScience & Electrical Engineering: University of Queensland, 2001.
Emerging Trends in Electrical, Electronics & Instrumentation Engineering: An international Journal(EEIEJ), Vol. 1, No1, February 201444
[9] S.Balakrishna, N. A. Thansoe, G. Rajamohan, A. S. Kenneth and C. J. Ling, "The Study andEvaluation of Maximum Power Point Tracking Systems," International Conference on Energy andEnvironment 2006 (ICEE 2006), pp. 17-22, 2006.
[10] C.S.Lee, "A Residential DC Distribution System with Photovoltaic Array Integration," Degree of
Honors Baccalaureate of Science in Electrical and Electronics Engineering, Oregon State University,University Honors College 2008.
[11] T.Esram and P. L.Chapman, "Comparison of Photovoltaic Array Maximum Power Point TrackingTechniques," IEEE Transactions on Energy Conversion, Vol. 22, No. 2, 2007.
[12] E.I.O. Rivera, "Maximum Power Point Tracking using the Optimal Duty Ratio for DC-DC Convertersand Load Matching in Photovoltaic Applications," Twenty Third Annual IEEE Applied Power
Electronics Conference and Exposition, APEC 2008, pp. 987-991, 2008.
[13] D.Peftsis, G. Adamidis, P. Bakas and A. Balouktsis, "Photovoltaic System MPPT TrackerImplementation using DSP engine and buck–boost DC-DC converter", 13th Power Electronics and Motion Control Conference, 2008.
[14] M.Azab, "A New Maximum Power Point Tracking for Photovoltaic Systems," WASET, vol. 34,2008, pp. 571- 574.

International Journal of Engineering Research and General Science Volume 3, Issue 6, November-December, 2015
ISSN 2091-2730

VOLTAGE BALANCE CONTROL AND STABILITY OF A SYSTEM BY USING MODULAR CONVERTER WITH MULTIWINDING HIGH-FREQUENCY TRANSFORMER

1. Pradeep kumar satapathi, 2. B. Trinadha

1. P.G.Student, Dept. of EEE, Aditya Institute of Technology And Management, Tekkali, A.P.
pradeepsatapathi57@gmail.com, 08895951950
2. Assistant Professor, Dept. of EEE, Aditya Institute of Technology And Management, Tekkali, A.P.

ABSTRACT: A modular H bride rectifier or also called as cascaded H bride converter with multi winding high-frequency (MWHF) transformer is proposed for medium- or high-voltage applications. In the proposed converter, a step down transformer is no longer require in place of this we can use high frequency multi winding transformer while a cascaded *H*-bridge rectifier (CHBR) is connected directly with the input ac source. Then by composing a group of *H*-bridge converters an isolated dc-dc converter is made and a MWHF (multi winding high frequency) transformer with high power density is used to isolate the dc buses produced by the CHBR. The mathematical model and equivalent circuit of the MWHF transformer and the high frequency (HF) converter are obtained in this paper. Then, the naturally balance ability and the voltage stability under unbalanced loads is analyzed and is verified. To accelerate the dc bus voltage balancing process, a voltage balance control algorithm based on energy exchange between different transformer windings is proposed that is realized by accomplishing the phase shift adjustment of the terminal voltages on different windings. Experiments and simulations are done to verify the performance of the proposed modular converter.
INDEX TERMS: *H*-bridge, high-frequency (HF) transformer, multilevel converter, voltage balance control.

INTRODUCTION:

For medium- and high-voltage applications, MULTILEVEL converters gain increasing attention because of the voltage limitations on unit power electronic devices. Many kinds of multilevel topologies are proposed, to simplify the control and improve the reliability. The first kind is neutral-point-clamped (NPC) converters where a lot of capacitors or clamping diodes are needed to balance the neutral point voltage, and with the increase of voltage levels, the number of clamping diodes and capacitors will increase significantly. **A**nother kind is cascaded H-bridge converter that is modular type converter and the clamping devices are not necessary. An industrial-frequency multi winding isolated transformer is needed to produce the balanced voltage and isolated for the cascaded modules. The cost and volume of the whole converter is increased with respect to the transformer. Some novel converter topologies are studied to reduce the system cost and volume, to increase the power density, and also to increase the stability by modular design. The modular design can also simplify the converter structure and increase the fault operation capacity. In a transformer-less multilevel converter is proposed whose outputs in each module are not isolated. In this case, the output can only be connected with loads of multiphase motors or separate motors. The dc voltages are difficult to be balanced while the loads are unbalanced.

To realize isolation in the converters, the medium or high-frequency (HF) transformer is used. The transformer working on higher frequency is of high power density compared to the industrial-frequency transformer. The methods for the reducing switching loss and control and in the converter with high frequency transformer have been studied. It is difficult to be realized that the converter proposed needs a high-voltage ac–ac converter. The converter topology proposed by Akagi attracted a lot of researches, which is modular since the H-bridges are used for both the HF converters and high-voltage rectifier. In the topology proposed, the load unbalance will worsen the voltage balancing of the converters. So it can be cascaded again to feed one load only or it can feed balanced loads. Otherwise, the dc bus on the secondary side must be connected in parallel to keep voltage balance when feeding isolated unbalanced loads. The converters with high frequency transformer have also been studied for the applications such as in tractions that need higher power ratings. A lot of researches have been studied and implemented for the modulation methods for the HF converters and for the voltage balance control. The multi winding high frequency transformer is used for the energy balance and isolation. The windings linking the same flux can realize energy exchange, which can be used to balance the voltage and the load energy. So the voltage equalization can be realized easier.

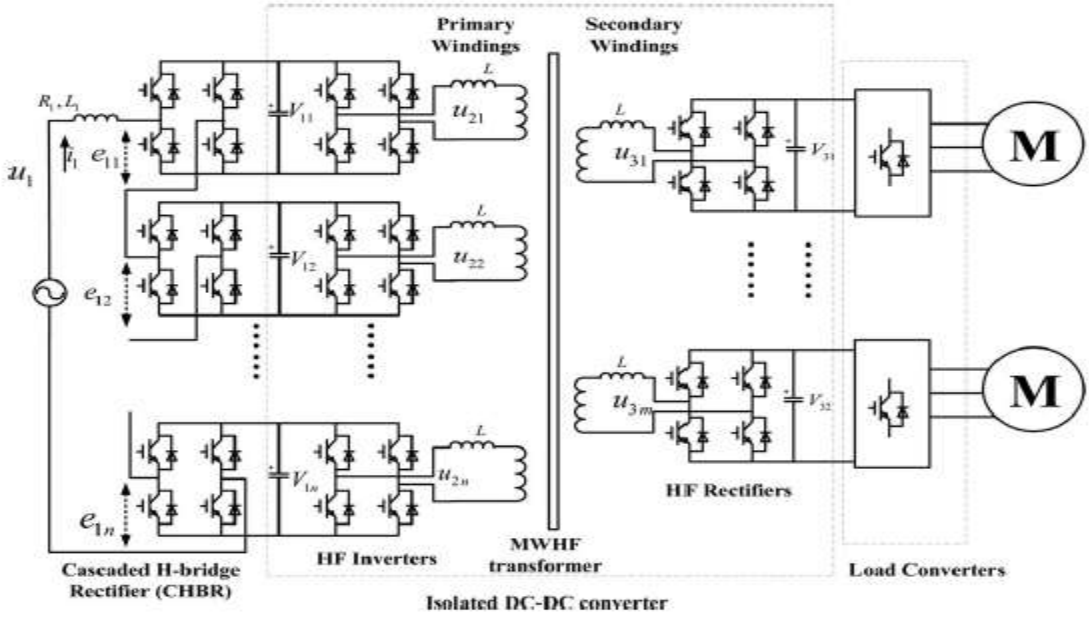

Fig. 1 General topology of proposed converter

In this paper, a novel modular multilevel converter is proposed where a multi-winding high-frequency (MWHF) transformer is used for the isolation and voltage balance. The cascaded H-bridge rectifier (CHBR) can be connected directly with the input ac voltage without need of the step-down transformer, this reduces the cost of extra step down transformer.

2. CASCADE H-BRIDGE MULTILEVEL CONVERTER

Cascaded H-bridge or also called CHB converters consist of H-bridge converters that are connected in series in each phase of the converter. From fig. 1 The AC-side output voltage of the single-phase leg of the converter *v*cA is the sum of the output voltages of both H-bridge converters *v*cA = *v*cA1+*v*cA2.One of the most commonly used pulse width modulation methods for CHB multilevel converters is the space vector pulse width modulation (SVPWM). The SVPWM method for the single-phase leg of the converter is illustrated in Fig. 2. In the PSPWM method the switching signals *s*1, *s*4, *s*5 and *s*8 are produced by comparing the modulating signal *S*M, which is characterised by the

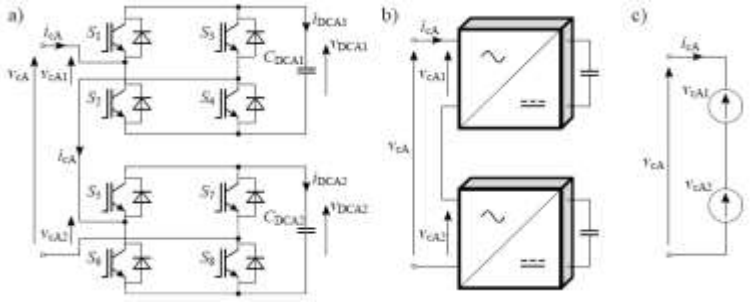

Fig. 2: Single-phase leg of the five-level cascaded H-bridge converter: a) the power part circuit, b) the block diagram, c) simplified circuit

amplitude *A*M and frequency *f*M, with uniformly phase-shifted triangular carrier signals *S*N1–*S*N4, which have the same peak values *A*N and the carrier frequency *f*N. The carrier frequency determines the switching frequency of transistors, thus *f*S = *f*N. Other switching signals (*s*2, *s*3, *s*6 and *s*7) are complementary to signals *s*1, *s*4, *s*5 and *s*8 respectively. Similarly to other PWM methods, two modulation indices can be defined for the PSPWM method. They are the amplitude modulation index *m*a = *A*M/*A*N and frequency

modulation index *m*f = *f*N/*f*M. One can see from Fig. 2 that switching signals affect the output voltages *v*cA1, *v*cA2 and DC - link currents *i*DCA1, *i*DCA2, which can be expressed by these two equations respectively.

$$v_{cA1} = v_{DCA1}\left(s_1 - \overline{s_4}\right),\ v_{cA2} = v_{DCA2}\left(s_5 - \overline{s_8}\right)$$
$$i_{DCA1} = i_{cA}\left(s_1 - \overline{s_4}\right),\ i_{DCA2} = i_{cA}\left(s_5 - \overline{s_8}\right)$$

The effective switching frequency in the H-bridge converter output voltage *v*c Ax is two times higher than the switching frequency *f*S (Fig. 2b) [1]. Since the output phase voltage *v*cA is the sum of voltages *v*cA1 and *v*cA2, *v*cA = *v*cA1+*v*cA2, the effective switching frequency observed in the output voltage of the five level CHB converter is four times higher than the switching frequency *f*S. This means that in each switching period *T*S there are four pulses which have the same width and are uniformly distributed. The effective switching frequency increase is one of the most important advantages of the CHB multilevel converter and allows using smaller reactive filters in the AC-side of the converter.

CONFIGURATION OF CASCADED H-BRIDGE RECTIFIER:

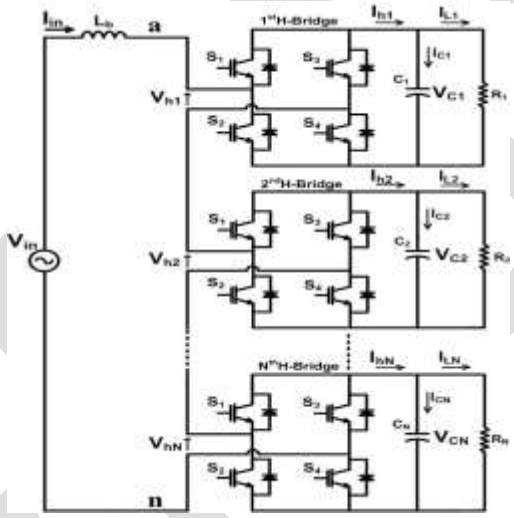

Fig. 3 Bidirectional CHB rectifier with N H-bridge cells.

A CHB converter is the best choice for working in high voltage and high-power applications due to its extreme modularity, simple physical layout and low losses

2.1 SELF-BALANCING ABILITY OF THE CONVERTER

In the proposed circuit, the multi winding high frequency transformer has the functions of isolation and energy balancing ability between each cell. The control of the high frequency or HF converters is the most important part of the control of the entire isolated dc/dc converter. In medium- or high-voltage applications, the switching frequency of the devices is limited while a high-frequency voltage is needed by the MWHF transformer. So square-wave modulation is usually used in this kind of converters. The square wave voltage input to the windings can be shown in Fig. 4. A 50% duty symmetrical square wave is used to approach the fundamental sinusoidal wave and to reduce harmonics. If the switching frequency is much higher than the output voltage frequency, such as in using high speed MOSFET or SiC devices, the sinusoidal modulation can also be adopted. To get larger flux and higher efficiency, all input voltages on the transformer windings are controlled to keep almost the same phase. The stability and voltage self-balance ability of the circuit will be analyzed in this section.

3. ISOLATED DC-DC CONVERTER

In DC-DC converter again it is devided into three main parts,

1. HF (high frequency) inverter.
2. MWHF (multi winding high frequency) transformer.
3. HF (high frequency) rectifier.

The proposed converter is shown in Fig. 1. There are three parts: the first is a cascaded *H*-bridge rectifier (CHBR) which is used to convert the input ac voltage to the cascaded dc buses. Because of the little limitation on cascaded levels, the CHBR can be connected with the grid voltage directly without using of step down transformer. The second part is an isolated dc–dc converter with an MWHF transformer, which is of higher power density than an industrial-frequency transformer. A group of *H*-bridge converters together with the transformer windings are used to convert the dc voltages to HF ac voltages, or convert the HF ac voltages to dc voltages. To be convenient, the HF converters connected with the primary windings of the transformer are named as the HF inverters while the ones connected with the secondary windings are named as the HF rectifiers. The third part is load converters to feed all kinds loads with different voltages and powers.

In the proposed converter, the unbalanced load may result voltage difference at the dc buses and will affect the stability of the converter. And the self-balancing speed is limited by changing the circuit parameters. So the voltage balance control method need to be studied to accelerate the voltage balancing and to eliminate the voltage difference caused by the power imbalance.

Supposing that the number of cascaded modules of the CHBR is *n*, which is the same as the number of the primary winding of the transformer. The number of the secondary winding is *m*. The total number of the transformer windings is $N = n + m$.

By energy balance principle, the state equation of one dc bus voltage is shown in (24)

$$\frac{d}{dt}\left(\frac{1}{2}CV^2\right) = P_i - P_o$$

Where *V* is the dc bus voltage, *C* is the value of capacitance, *P*i and *P*o are the instantaneous input and output powers on the dc bus. *P*o also equals the power input into the transformer windings if ignoring the converter losses. The filter inductance can be regarded as a part of the leak inductance of the transformer.

The average value of the dc bus voltage is affected by the active power input to the dc capacitor. And the fluctuation of the dc bus voltage is affected by the reactive power. It means that the dc bus voltage can be realized by adjusting the active power injected into the dc capacitor.

Since the carrier phase-shift PWM is used in CHBR, the active power input to each dc bus is fixed. The load power of the converter is determined by the loads. So the dc bus voltages can only be controlled by the active power flow from the dc buses to the transformer windings that can be controlled by the HF converters associated with the multi winding transformer.

In the multi winding transformer, all terminal voltages of the windings must have the same frequency to reduce the loss and harmonics. All windings are linked by the same flux if ignoring the leakage flux. The power can be transferred between the windings through the common flux, which can be used for the voltage balancing control. The energy exchange method will be studied in this section.

The state equation in each winding of the transformer is

$$u - e = Ri + L\frac{di}{dt}.$$

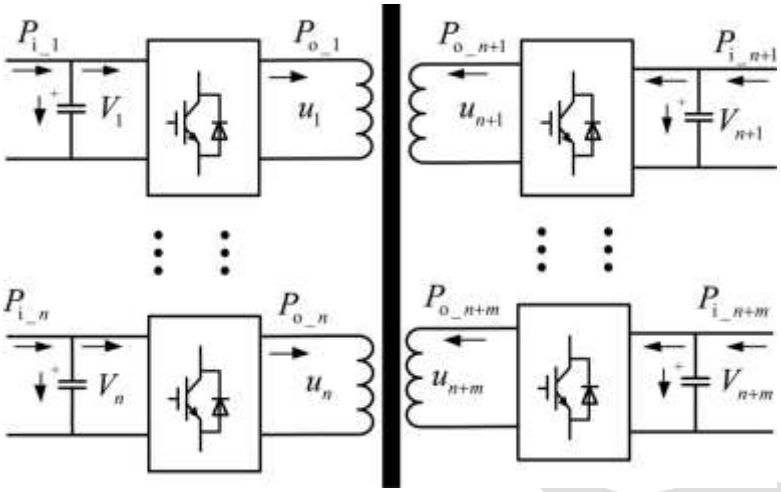

Fig. 4 Power flow between all windings.

Here *u* is the terminal voltage of the windings. Variable *e* is the back EMF produced by the flux. *R* and *L* are the resistance and inductance including the leak inductance of the winding and the filter inductance between the converter and the transformer. If ignoring the differences between the windings of the transformer, the back EMF and impedances are all the same. Then, the state equation of all windings can be shown as

$$\begin{cases} u_1 - e = Ri_1 + L\dfrac{di_1}{dt} \\ u_2 - e = Ri_2 + L\dfrac{di_2}{dt} \\ u_{n+m} - e = Ri_{n+m} + L\dfrac{di_{n+m}}{dt} \end{cases}$$

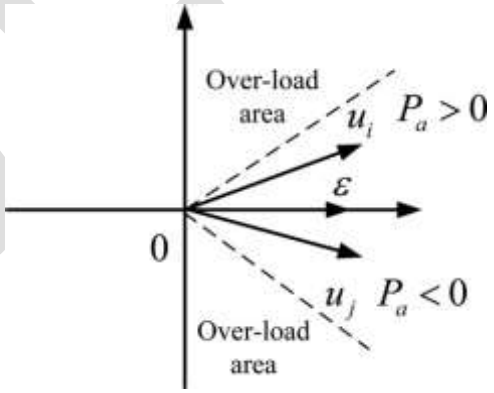

Fig. 5 Output power control by phase adjustment.

So the power flow between the windings is determined by the fundamental component whose phase is also the same with the symmetrical square wave. That means the active powers are also determined by the phase of the square wave voltage.

4. LOAD CONVERTERS

A load converter is a IGBT controlled inverter. Again the dc voltages are inverted to ac voltages at required level using inverter and connected to different loads to feed all kinds loads with different voltages and powers.

VOLTAGE BALANCE CONTROL:

We can see that if there is no phase difference between the terminal voltage and back EMF, the output active power of this winding will be zero even if there is an amplitude difference. It means that only phase of the terminal voltage can be used for active power control.

To be simple, the same modulation method is used for all HF inverters and HF rectifiers in the isolated dc–dc converter, except the difference of phase. So all the terminal voltages of the transformer windings have same amplitudes when the dc buses are balanced. As in the former analysis, the dc bus voltage can be adjusted by the re-distribution of the input and output power between the transformer windings, which can be realized by the adjustment of the phase angles of the terminal voltages.

Here *U*and *I* are the rated voltage and current of the windings. If the phase difference increases, the current and power passing the winding will increase quickly and overload will occur that will damage the transformer and converters. As the increase of the reactive power, the fluctuations of the dc bus voltages will increase, which will reduce the performance of the converter. So the phase difference is normally controlled to be little difference to avoid over-current and over-load, as shown in Fig.

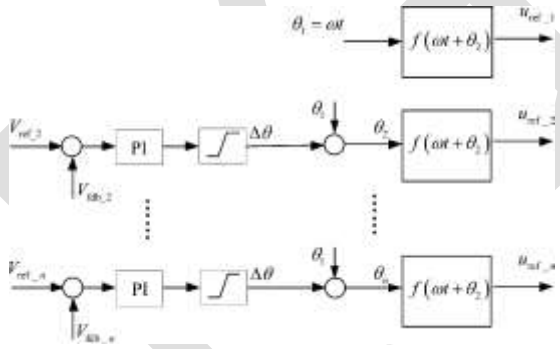

Fig. 6 PI regulators to get the control phase angles.

Because the summarized dc bus voltage connected with the CHBR is already controlled by the control scheme shown in Fig., only $n + m - 1$ dc buses are needed to be controlled directly by separate voltage balance controllers. These $n + m - 1$ dc buses are named directly-controlled dc buses. The last one can be balanced naturally if the summarized dc buses voltage and the $n + m - 1$ buses are all controlled well. So it can be named as indirectly-controlled dc bus.

The voltage difference is nonlinear with the phase difference angle, also the angle of the back EMF is difficult to be got directly, so a PI regulator for the dc voltage feedback is used where the phase difference with the back EMF is adaptively obtained. In practice, the output voltage phase on the first dc bus $\theta 1$ is used as a reference. Then, a group of PI regulators are used to get the phase angle of the terminal voltages on the other windings. The difference of the dc bus voltages and their reference values are used as the input of the PI regulators, as shown in above Fig. The output is the phase difference to the first cell.

By the adaptability of the PI regulator, the difference between the windings, such as the back EMF and impedance difference, can be compensated by the close-loop control.

SIMULATION IN MATLAB ENVIRONMENT:

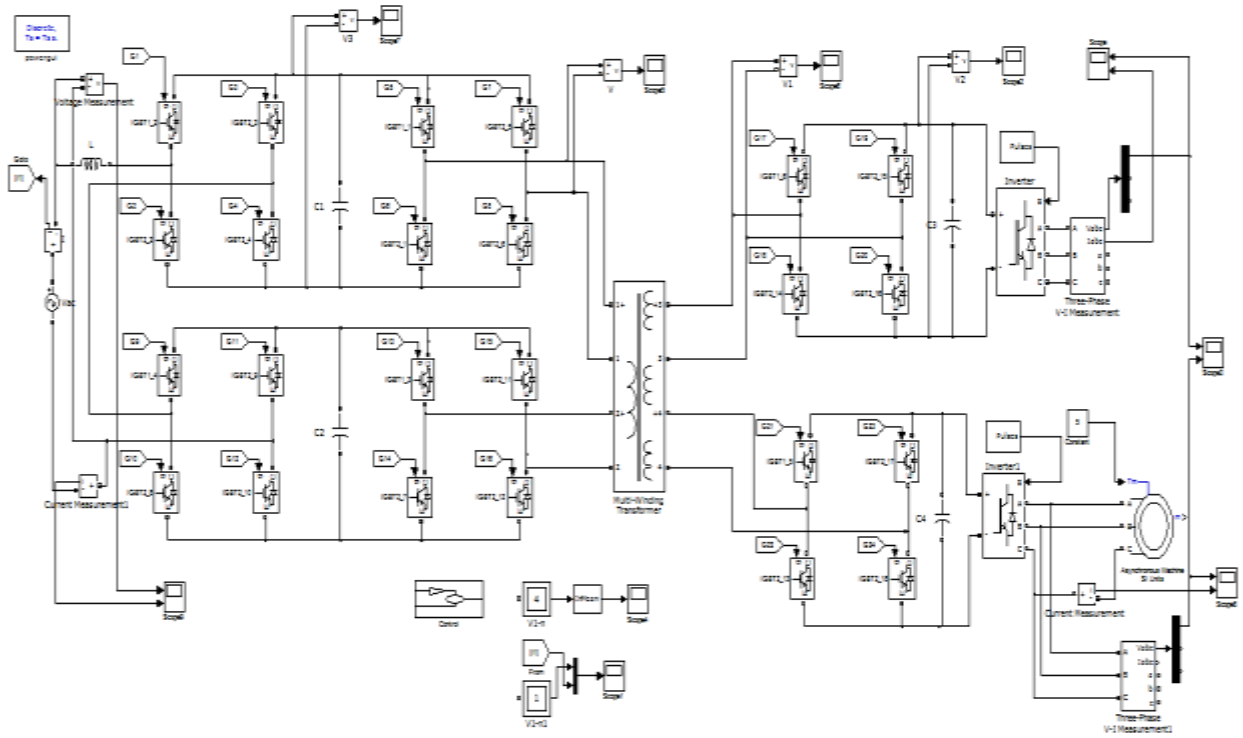

Fig.7 Simulating circuit diagram

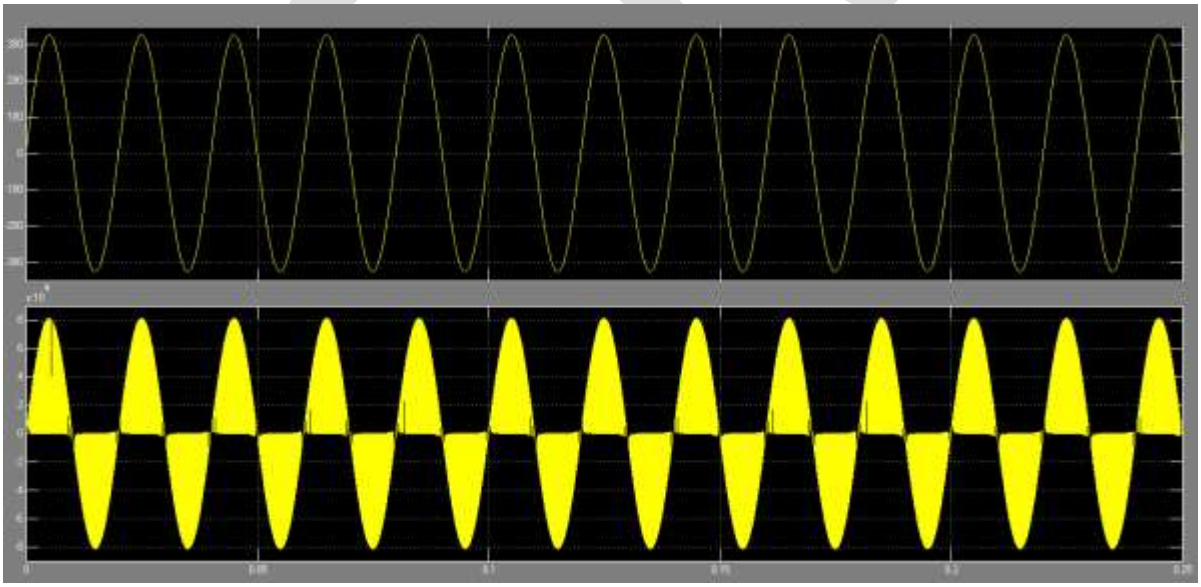

Fig.8 Input voltage and current

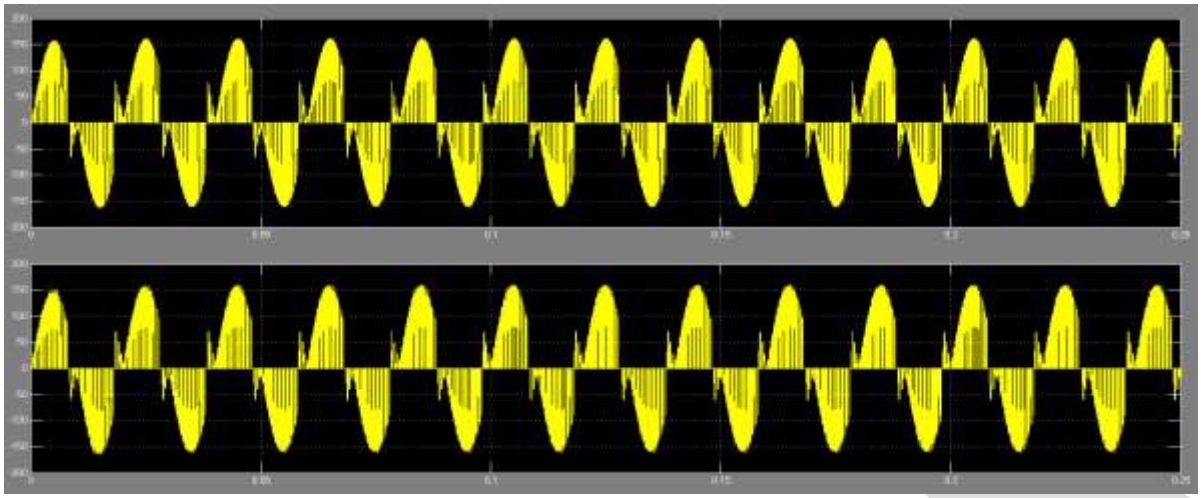

Fig.9 Output voltage at no load and full load

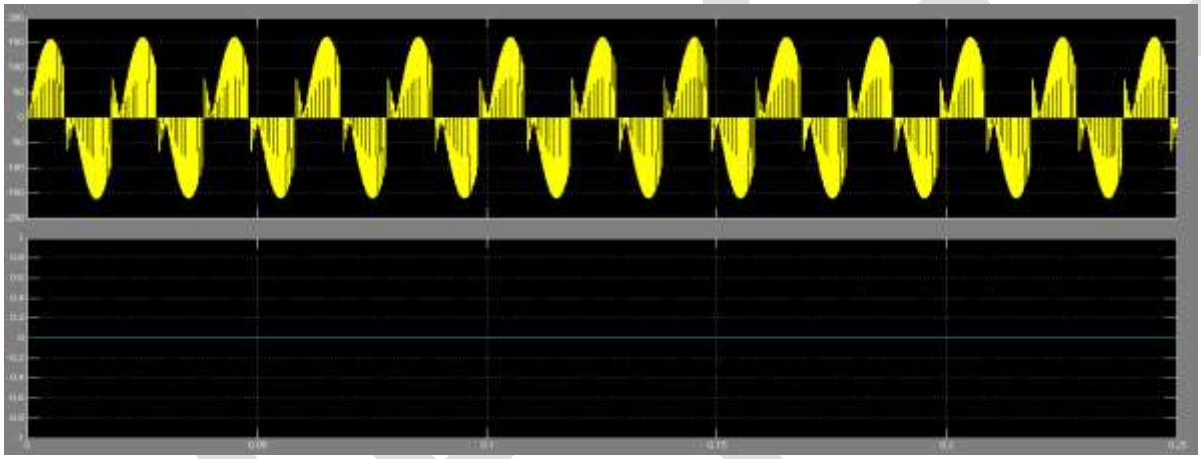

Fig.10 Output voltage and current at no load

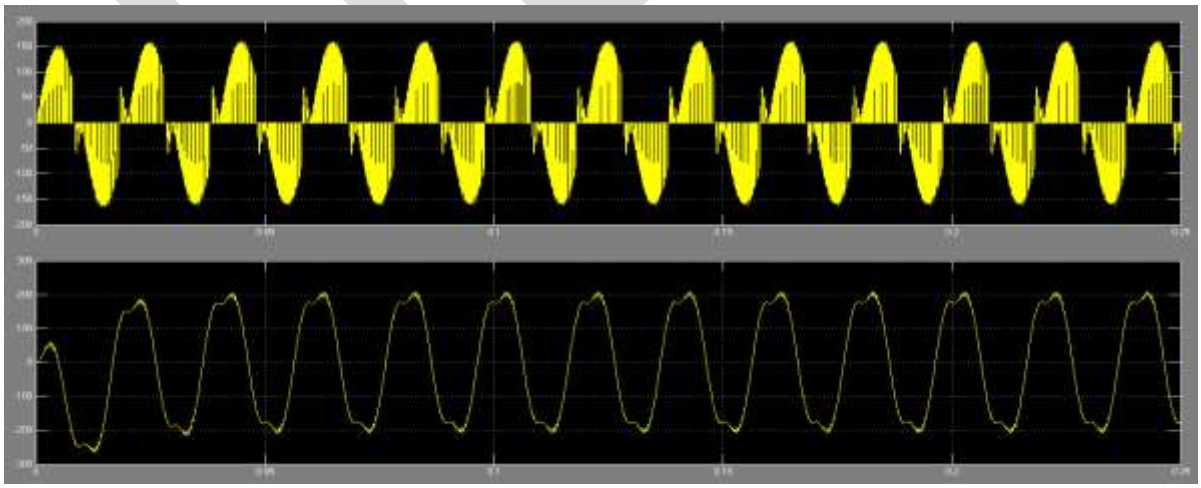

Fig.11 Output voltage and current at load (induction motor).

CONCLUSION:

The proposed modular type multilevel converter can be applied for medium or high-voltage applications. In this modular converter the high frequency transformer decreases the system weight and volume compared with the generally using industry-frequency transformer. The high frequency multi winding transformer can also realize the voltage balance control and the power redistribution but not effecting other connected load. It is modular and is of the characteristics of high reliability. A voltage balancing control method based on terminal voltage phase adjustment is studied in this paper. Simulations and experimental have been implemented and tested to verify the stability without control. It shows that the proposed experiment can be controlled stable and reliable under unbalanced (varying) loads and the proposed voltage balance control waveforms is also verified.

REFERENCES:

[1] P. Zhiguo, P. Fang Zheng, K. A. Corzine, V. R. Stefanovic, J. M. Leuthen,and S. Gataric, "Voltage balancing control of diode-clamped multilevelrectifier/inverter systems," *IEEE Trans. Ind. Appl.*, vol. 41, no. 6, pp. 1698–1706, Jun. 2005.

[2] M. D.Manjrekar, P. K. Steimer, and T. A. Lipo, "Hybrid multilevel powerconversion system: A competitive solution for high-power applications,"*IEEE Trans. Ind. Appl.*, vol. 36, no. 3, pp. 834–841, Mar. 2000.

[3] S. Kouro, M. Malinowski, K. Gopakumar, J. Pou, L. G. Franquelo, B.Wu,J. Rodriguez, M. A. Prez, and J. I. Leon, "Recent advances and industrialapplications of multilevel converters," *IEEE Trans. Ind. Electron.*, vol. 57, no. 8, pp. 2553–2580, Aug. 2010.

[4] A. Silke, H. Roman, andM. Rainer, "New transformerless scalable modularmultilevel converters for HVDC-transmission," in *Proc. PESC*, 2008,pp. 174–179.

[5] S. Qiang, L. Wenhua, L. Xiaoqian, R. Hong, X. Shukai, and L. Licheng,A steady-state analysismethod for a modular multilevel converter," *IEEETrans. Power Electron.*, vol. 28, no. 8, pp. 3702–3713, Aug. 2013.

[6] A. D. Aquila, M. Liserre, V. G. Monopoli, and P. Rotondo, "Overviewof PI-based solutions for the control of DC buses of a single-phase *H*-bridge multilevel active rectifier," *IEEE Trans. Ind. Appl.*, vol. 44, no. 3,pp. 857–866, Mar. 2008.

[7] T. Xinghua, L. Yongdong, and S.Min, "A PI-based control scheme for primarycascaded *H*-bridge rectifier in transformerless traction converters,"in *Proc. Int. Conf. Electrical Mach. Syst. (ICEMS)*, 2010, pp. 824–828.

[8] D. Sixing, L. Jinjun, L. Jiliang, and H. Yingjie, "A novel DC voltagecontrol method for STATCOM based on hybrid multilevel *H*-bridge converter,"*IEEE Trans. Power Electron.*, vol. 28, no. 1, pp. 101–111, Jan.2013.

[9] K. Sano and M. Takasaki, "A transformerless D-STATCOM based on amultivoltage cascade converter requiring no DC sources," *IEEE Trans.Power Electron.*, vol. 27, no. 6, pp. 2783–2795, Jun. 2012.

[10] G. Martin and R.Marquardt, "A new AC/AC multilevel converter family,"*IEEE Trans. Ind. Electron.*, vol. 52, no. 3, pp. 662–669, Mar. 2005.

[11] S. Falcones, X. Mao, and R. Ayyanar, "Topology comparison for solidstate transformer implementation," in *Proc. IEEE Power Energy Soc. Conf.*, 2010, pp. 1–8.

[12] J. Shi,W. Gou, H. Yuan, T. Zhao, and A. Q. Huang, "Research on voltageand power balance control for cascaded modular solid-state transformer,"*IEEE Trans. Power Electron.*, vol. 26, no. 4, pp. 1154–1166, Apr. 2011.

[13] S. Inoue and H. Akagi, "A bidirectional isolated DC–DC converter asa core circuit of the next-generation medium-voltage power conversion system," *IEEE Trans. Power Electron.*, vol. 22, no. 2, pp. 535–542,Feb. 2007.

[14] T. Zhao, G.Wang, S. Bhattacharya, and A. Q. Huang, "Voltage and powerbalance control for a cascaded *H*-bridge converter-based solid-state transformer,"*IEEE Trans. Power Electron.*, vol. 28, no. 4, pp. 1523–1532, Apr.2013.

[15] K. Florian, K. Johann, and Walter, "Accurate power loss model derivationof a high-current dual active bridge converter for an automotive application,"*IEEE Trans. Ind. Electron.*, vol. 57, no. 3, pp. 881–891, Mar.2010.

[16] M. Nymand and A. E. Michael, "High-efficiency isolated boost DC–DCconverter for high-power low-voltage fuel-cell applications," *IEEE Trans.Ind. Electron.*, vol. 57, no. 2, pp. 505–514, Feb. 2010.

[17] L. Xiaohu, L. Hui, and W. Zhan, "A start-up scheme for a three-stagesolid-state transformer with minimized transformer current response," *IEEE Trans. Power Electron.*, vol. 27, no. 12, pp. 4832–4836, Dec. 2012.

[18] H. Fan and H. Li, "High-frequency transformer isolated bidirectionalDC–DC converter modules with high efficiency over wide load range for20 kVA solid-state transformer," *IEEE Trans. Power Electron.*, vol. 26,no. 12, pp. 3599–3608, Dec. 2011.

[19] M. Glinka and R. Marquardt, "A new single phase AC/AC-multilevel converter for traction vehicles operating on ac line voltage," in *Proc. EPE*, 2003, pp. 1–10.

[20] P. Ladoux, M. Mermet, J. Casarin, and J. Fabre, "Outlook for SiC devices intraction converters," in *Proc. Elect. Syst. Aircraft, Railway Ship PropulsionESARS)*, 2012, pp. 1–6.

[21] Z. Chuanhong, M. Weiss, A. Mester, S. Lewdeni-Schmid, D. Dujic,
J. K. Steinke, and T. Chaudhuri, "Power electronic transformer (PET)converter: Design of a 1.2 MW demonstrator for traction applications,"
in *Proc. 2012 Int. Symp. Power Electron., Elect. Drives, Autom. Motion(SPEEDAM)*, 2012, pp. 855–860.
[22] D. Dujic, A. Mester,T.Chaudhuri, A. Coccia, F. Canales, and J. K. Steinke,"Laboratory scale prototype of a power electronic transformer for traction applications," in *Proc. 14th Eur. Conf. Power Electron. Appl. (EPE 2011)*,pp. 1–10.

International Journal of Engineering Research and General Science Volume 3, Issue 6, November-December, 2015
ISSN 2091-2730

SIMULATED DESIGN OF CHANNEL NOISE REDUCTION MODEL FOR EFFECTIVE COMMUNICATION

[1]B. O. Omijeh and [2] E. Vurebel

[1]Department of Electronic & Computer Engineering

[2]Centre for Information and Telecommunications Engineering

University of Port Harcourt, Nigeria

E-mail address: omijehb@yahoo.com;bourdillon.omijeh@uniport.edu.ng (B.O.Omijeh)

Abstract- In this paper, the Simulated Design of Channel Noise Reduction Model for effective Communication has been achieved. It is the comparative study of noise reduction technique using Simulink in Matlab work environment.The study is based on simulation of noise behavior in communications channel by varying the input parameters (Message Signal Amplitude, Noise Power, Input Power of Channel and Signal to Noise Ratio(SNR)); and the output:signal (strength and noise amplification) and measurements taken. The ODE3 (Bogacki-Shampine) solver with fixed step was used to model simple sine wave function for the message signal and Band-limited White Noise as the source. The signals were passed through the Additive White Gaussian Noise Channel and the parameters varied. The output signal was connected to a display block and scope for proper measurement. Again, Gaussian filter was introduced at the output of the channel for noise filtration and reduction; and a gain block added to improve the signal output. Transitional delay was also added to smooth out the final signal output. The results obtained from the measurement confirm that introducing the Gaussian filter offers significant improvement in signal strength over communication channel

Keywords: Noise, Channel, Reduction, Model, Gaussian Filter, Matlab/Simulink

Introduction

Noise is the major impairment to smooth transmission of message signal from one point to another in a communication system. Several studies have been carried out in the field of noise reduction technique in Communication.**[1]**refers to noise as disturbances due to environmental factor, thermal agitation, effect of temperature changes etc. These distortions superimpose itself on the message signal and introduce unwanted signals that impair signal quality [2-3]**.**As the signal is transmitted along the channel, the original signal is amplified along with the noise. For effective communication to be established between two points, noise in communication channel must be eliminated or reduced as low as possible [4].

In this study, key elements that are contributed to noise behavior in communication system were simulated. These are: 1. message signal, 2. noise source, 3. channel and 4. filter. In the model, thebehavior of additive white Gaussian noise (AWGN)channel was simulated using external band-limited noise, sinusoidal waveform (message signal) and the output of the channel characteristics passed through a Gaussian Filter to evaluate its effect in smoothening out the noise ripples that travels along with the message signal. An amplifier (Gain) circuit was placed at the output of the filter to improve on the signal quality; and a transition delay block added to provide some delay for the noise ripples.The overall output of the model was compared to the behavior of the noise model prior to introducing the filter.

For effective study of noise reduction technique in communication, it is important to evaluate the properties and characteristic of a channel. A communication channel can be defined as the medium used for transport of message signal which could be wire, optical fiber or free space. Channel is comprised of the source, transmitter, channel, receiver and the sink **[5-6].**

Channel properties could be definedby random variables:

Let Xand Ybe the random variables representing the input and output of the channel, respectively. Let $p_{Y|X}(y|x)$be the conditional distribution function of Ygiven$X$, which is an inherent fixed property of the communications channel. Then the choice of the marginal distribution$p_X(x)$completely determines the joint distribution$p_{X,Y}(x,y)$due to the identity

$$p_{X,Y}(x,y) = p_{Y|X}(y|x)\, p_X(x)$$

----------Equation 1

which, in turn, induces a mutual information$I(X;Y)$. The channel capacity is defined as

$$C = \sup_{p_X(x)} I(X;Y)$$ ----------Eqn. 1

where the supremum is taken over all possible choices of $p_X(x)$.

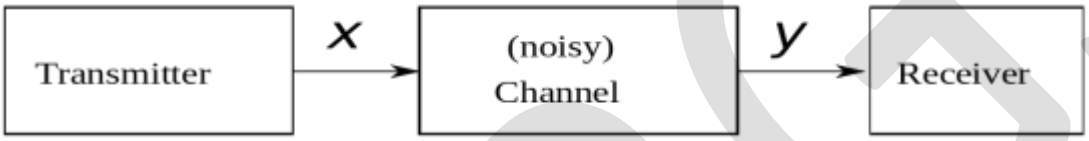

Fig.1: Simple Communications Channel

2.0 Noise in Communications Systems

Noise is broadly defined as unwanted or undesirable signal in a communication circuit **[5].**There are several types of noise such as Thermal Noise, Intermodulation Noise, Crosstalk, Impulse, Jitter, Echo etc.

This simulation was based on analysis of band-limited noise inter-modulated with inherent white noise in the additive Gaussian White noise and superimposed on the message signal of a continuous sine wave form [7].

Gaussian noise is statistical noise having a probability density function (PDF) equal to that of the normal distribution, which is also known as the Gaussian distribution [8].

The probability density function $p$of a Gaussian random variable z is given by eqn 2

$$p_G(z) = \frac{1}{\sigma\sqrt{2\pi}} e^{-\frac{(z-\mu)^2}{2\sigma^2}}$$ -----Eqn. 2

Where: z represents the grey level, μ the mean value and $\sigma$the standard deviation.

In this study, Gaussian noise was used as additive white noise for the channel and Band-limited Noise for the external noise source [9-10].

3.0 Noise Reduction Model

The design approach is based on the use of Simulink in Matlab work environment to analysis the impairment of noise on communication; and thereby developing a model to reduce its effect as low as possible.

The signal sources comprising of message signal and the band-limited noise source were passed through Additive Gaussian White Noise Channel to generate the effect of noise through a channel. The entire Model is shown in Fig.2

The combine noise and message signal were further passed through a Gaussian filter of ±3dB cutoff. A gain block and transport delay were further introduced to improve the signal output. The output was connected to a display block and scope for measurement of the parameters.

The amplitude of the message signal was varied and measurement taking. The process was repeated for the noise power, channel input power and the signal to noise ratio(SNR). Results from the output display block1 (after the AGWN) and block 2(after the filter) were recorded and tabulated for further analysis.

Some designed considerations were made to achieve the expected results.

3.1 Sine wave Block generating message signal of x(t)=Amp*sin[w(t)+θ].

In this study, a simple sine wave of varying amplitude, frequency and phase was used to represent the messaging signal. Amplitude of a sine wave is the maximum distance it ever reaches from zero.The amplitude was varied from 1 to 10 and measurement taken to verify the system behavior.

3.2 Band limited white noise with noise power of 0.1watt

The Band-Limited White Noise block generates normally distributed random numbers that are suitable for use in continuous or hybrid systems. Theoretically, continuous white noise has a correlation time of 0, a flat power spectral density (PSD), and a total energy of infinity. In practice, physical systems are never disturbed by white noise, although white noise is a useful theoretical approximation when the noise disturbance has a correlation time that is very small relative to the natural bandwidth of the system.

$tc \approx \frac{1}{1002\pi f max}$,

where f_{max} is the bandwidth of the system in rad/sec.

Additive Gaussian White Noise Channel signal to noise ratio of 10dB.

Additive White Gaussian Noise (AWGN) is a noise model used in Information theory to mimic the effect of many random processes that occur in nature. It is often used as a channel model in which impairment to communication is a linear addition of wideband or white noise with a constant spectral density (expressed as watts per hertz of bandwidth) and a Gaussian distribution of amplitude. The model does not account for fading, frequency selectivity, interference, nonlinearity or dispersion. However, it produces simple and tractable mathematical models which are useful for gaining insight into the underlying behavior of a system before these other phenomena are considered (**Anon,2015).**

The relative power of noise in an AWGN channel is typically described by quantities such as Signal-to-noise ratio (SNR) per sample and ratio of symbol energy to noise power spectral density (Es/N0) **(Anon, 2015).**

Mathematically, a Gaussian filter modifies the input signal by convolution with a Gaussian function; this transformation is also known as the Weierstrass transform.

Display output Block.

The output of the AWGN was connected to a display to measure the signal strength and noise amplification.

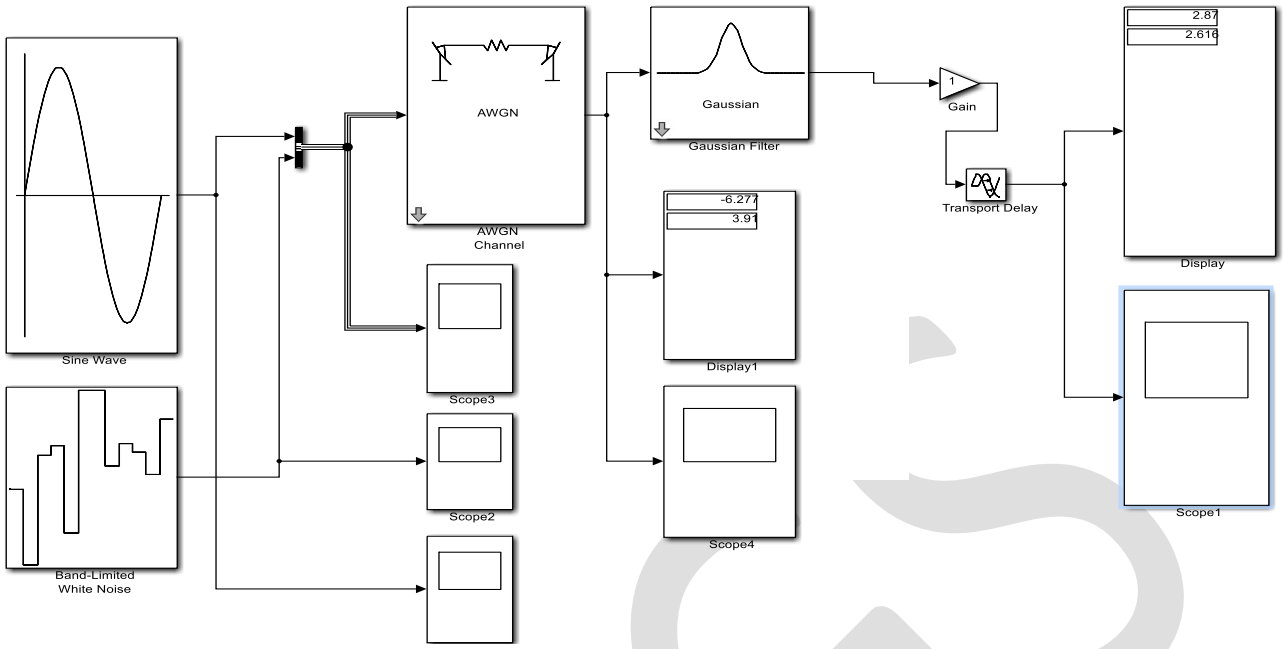

Fig.2: Simulated Design of Channel Noise Reduction Model

Results and Discussion

Test was carried out by varying the following parameters: (i) Amplitude of the Message Signal.

Input power of the Band-Limited Noise Source (iii) Signal to Noise Ratio(SNR) of the Additive Gaussian White Noise Channel (iv) Input Signal Power of the AWGN

And the following results obtained after simulation are shown in Fig. 3; 4; 5; 6;7

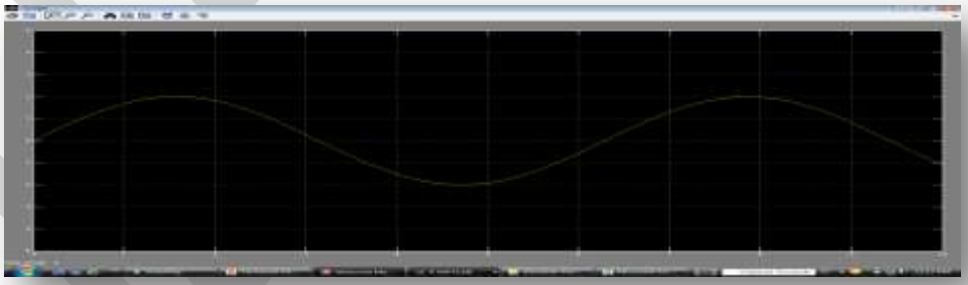

Fig.3: Output waveform of Message Signal without noise

Fig.4: Output waveform of Noise Signal

Fig.5: Output waveform of Noise and Message Signal without Channel

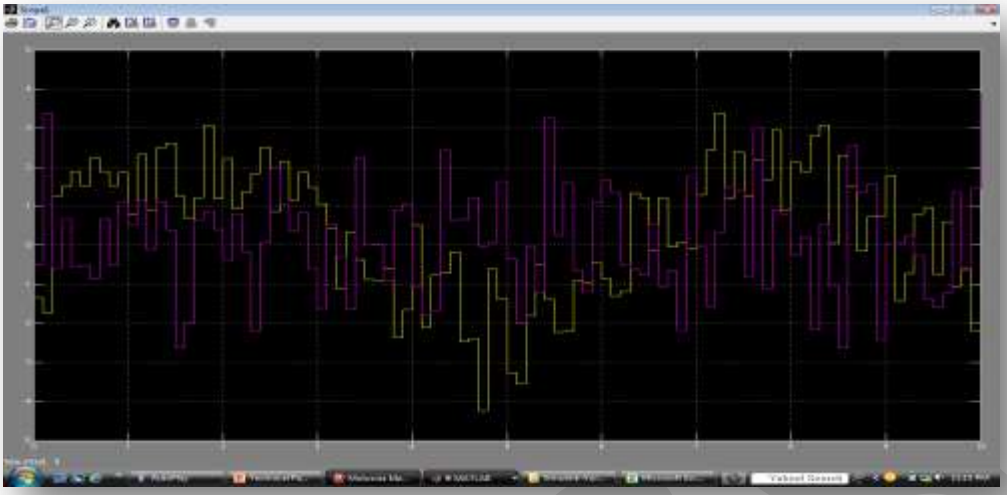

Fig.6: Output of AGWN Channel showing Message and Noise signal waveform

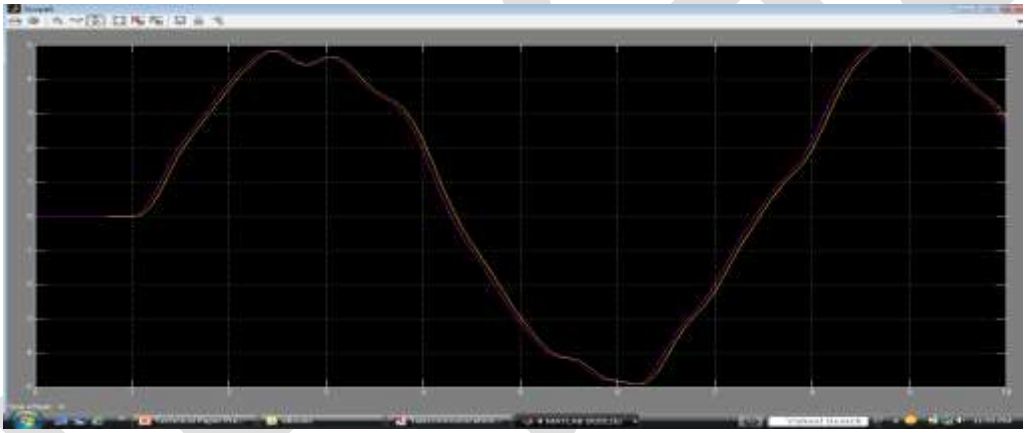

Fig.7: Output Waveform of Gaussian Filter

Table 1: Result of increasing amplitude of message signal

	Sine Wave	Display1		Display2	
S/N	Message Signal Amplitude	Signal Strength1	Noise Amplification1	Signal Strength2	Noise Amplification2
1	1	-1.38	3.91	2.786	2.071
2	2	-1.924	3.91	5.466	4.748
3	3	-2.468	3.91	8.545	7.424
4	4	-3.013	3.91	11.42	10.1
5	5	-3.557	3.91	14.3	12.78
6	6	-4.101	3.91	17.18	15.45
7	7	-4.645	3.91	20.06	18.13
8	8	-5.189	3.91	22.95	20.8
9	9	-5.733	3.91	25.82	23.48
10	10	-6.277	3.91	28.7	26.16

From Table 1, display 1 shows the signal strength and noise amplification after the AWGN, While Display 2 shows signal Strength and noise amplification after the Gaussian Filter

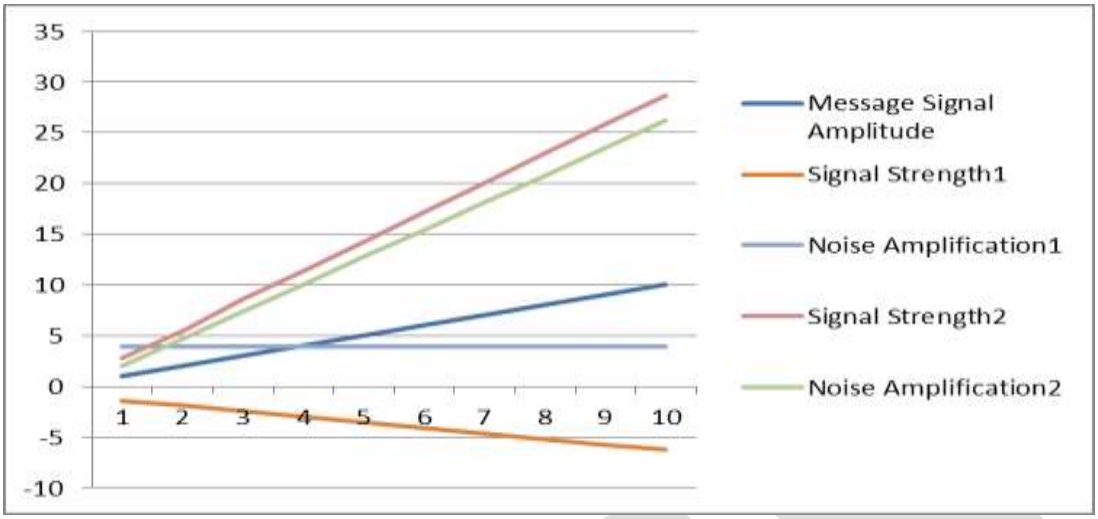

Fig.8: Graph Showing result of increasing Message Signal Amplitude

Table 2: Result of increasing Input Noise Power

	Band-Limted White Noise	Display1		Display2	
S/N	Input Noise Power	Signal Strength1	Noise Amplification1	Signal Strength2	Noise Amplification2
1	0.1	-1.38	3.91	2.786	2.071
2	0.2	-1.38	4.812	3.73	2.643
3	0.3	-1.38	5.504	4.455	3.082
4	0.4	-1.38	6.087	5.065	3.452
5	0.5	-1.38	6.601	5.603	3.778
6	0.6	-1.38	7.066	6.09	4.072
7	0.7	-1.38	7.794	6.537	4.343
8	0.8	-1.38	7.891	6.953	4.595
9	0.9	-1.38	8.265	7.344	4.832
10	1	-1.38	8.818	7.714	5.056

From table 2, Display 1 shows the signal strength and noise amplification after the AWGN while Display 2 shows the signal strength and noise amplification after the Gaussian Filter

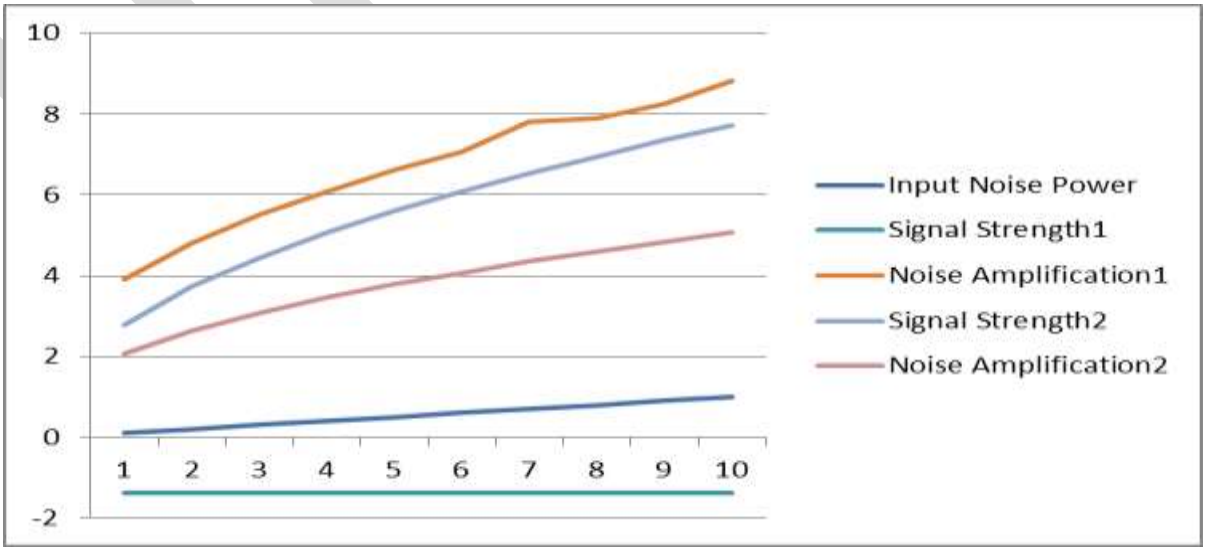

Fig.9: Graph showing increase in Input Noise Power

Table 3 Result of increasing Input Signal Power

		Display1		Display2	
S/N	Input Signal Power(watt)	Signal Strength1	Noise Amplification1	Signal Strength2	Noise Amplification2
1	1	-1.38	3.91	2.786	2.071
2	2	-1.727	4.627	1.804	1.249
3	3	-1.993	5.178	1.05	0.6182
4	4	-2.217	5.642	0.4143	0.08623
5	5	-2.414	6.05	-0.1456	-0.3824
6	6	-2.593	6.42	-0.6518	-0.8061
7	7	-2.757	6.76	-1.117	-1.196
8	8	-2.91	7.067	-1.551	-1.558
9	9	-3.053	7.374	-1.958	-1.899
10	10	-3.189	7.655	-2.343	-2.221

From table 3, Display 1 shows the signal strength and noise amplification after the AWGN, while Display 2 shows the Signal Strength and noise amplification after the Gaussian Filter.

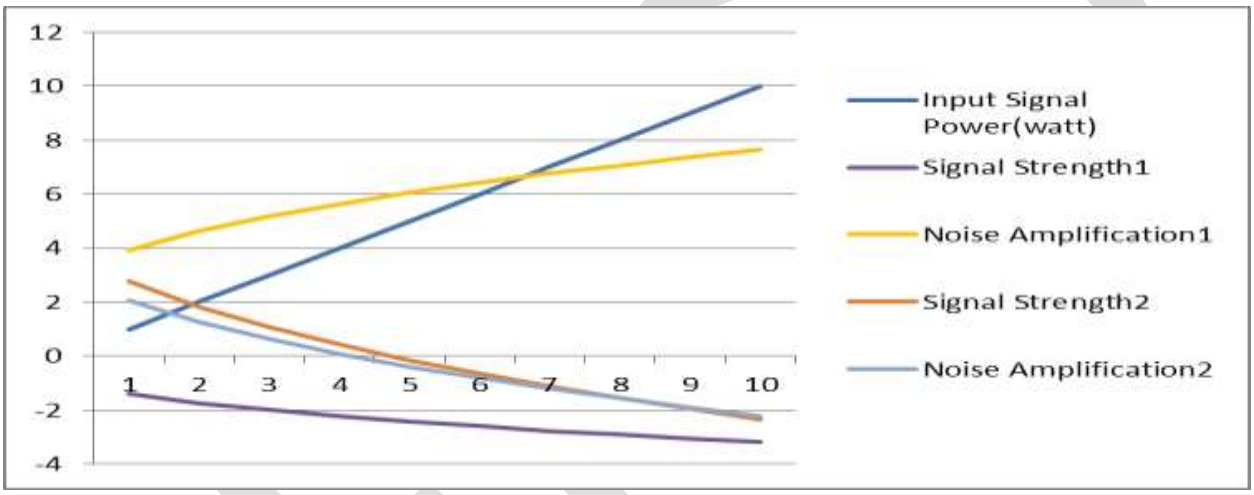

Fig.10: Graph showing effect of increasing Input Signal Power of Noise

Table 4: Test showing increase in Signal to Noise ratio

		Display1		Display2	
S/N	SNR(dB)	Signal Strength1	Noise Amplification1	Signal Strength2	Noise Amplification2
1	1	-1.38	3.91	2.786	2.071
2	2	-1.289	3.721	3.044	2.287
3	3	-1.208	3.553	3.274	2.48
4	4	-1.136	3.404	3.479	2.651
5	5	-1.072	3.27	3.662	2.804
6	6	-1.04	3.152	3.824	2.94
7	7	-0.9632	3.046	3.969	3.062
8	8	-0.9176	2.951	4.099	3.17
9	9	-0.877	2.867	4.214	3.266
10	10	-0.8408	2.792	4.317	3.352

From table 4, Display 1 shows the Signal Strength and Noise Amplification after the AWGN while Display 2 shows the signal strength and noise amplification after the Gaussian Filter

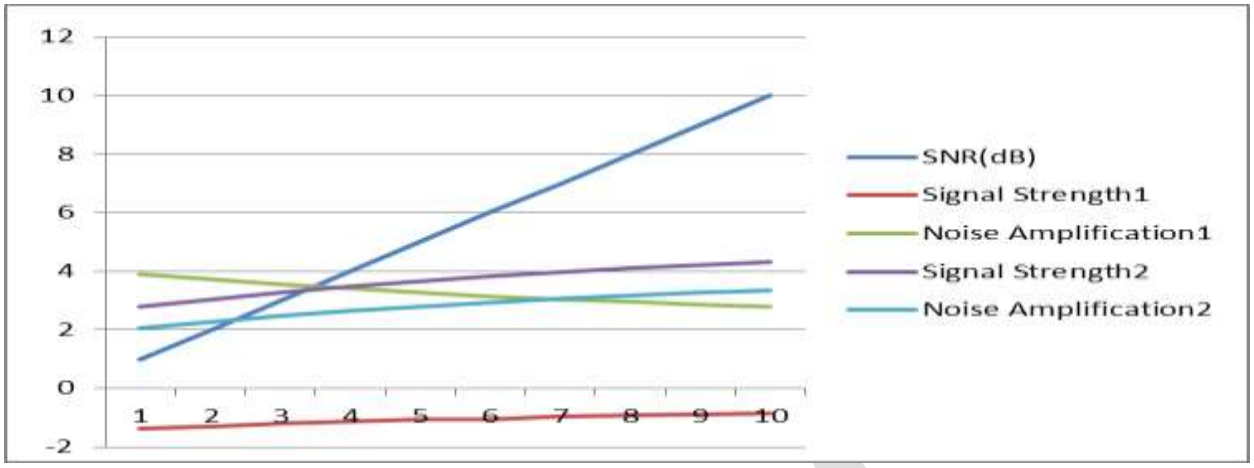

Fig 11: Graph showing effect of increasing Signal to Noise Ratio versus Signal Strength and Noise Amplification

Table 5: Test result of increase in all Parameters

Table 6.5 Test showing Proportional increase in all the parameters

		Display1		Display2	
S/N	SNR(dB)	Signal Strength1	Noise Amplication1	Signal Strength2	Noise Amplification2
1	1	-1.38	3.91	2.786	2.071
2	2	-2.142	5.263	5.992	4.802
3	3	-2.783	6.155	9.322	7.688
4	4	-3.36	6.808	12.72	10.65
5	5	-3.9	7.313	16.15	13.67
6	6	-4.416	7.72	19.59	16.7
7	7	-4.917	8.058	23.04	19.75
8	8	-5.049	8.348	26.48	22.81
9	9	-5.895	8.602	29.53	25.62
10	10	-6.379	8.83	33.34	28.9

From table 5, Display 1 shows the signal strength and noise amplification after the AWGN, while Display 2 shows the signal strength and noise amplification after the Gaussian Filter.

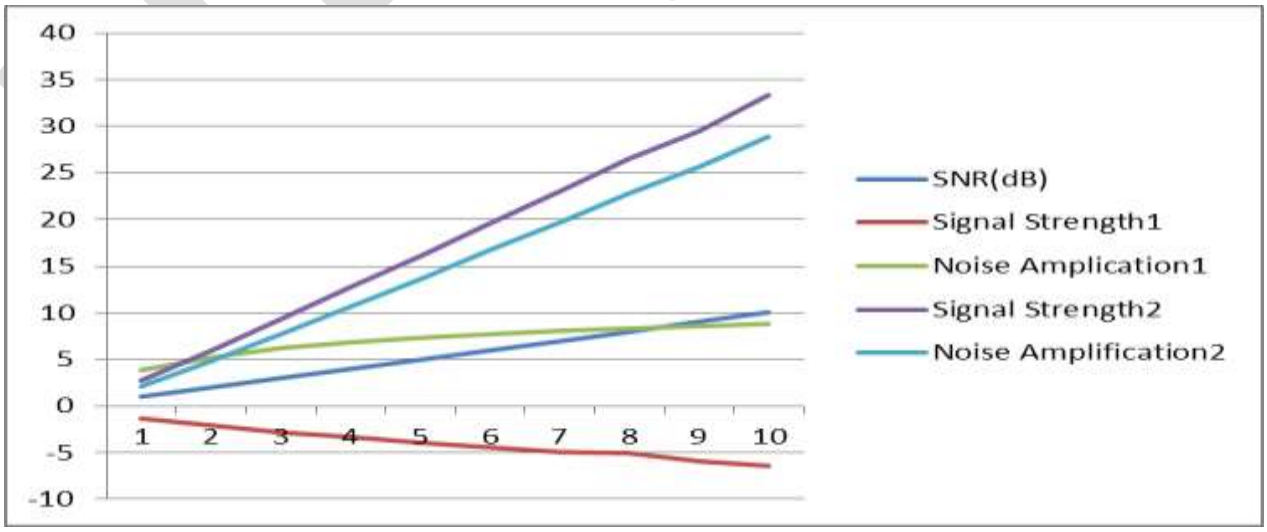

Fig.12Graph Showing effect of proportional increase in all Noise Parameter

Discussion

The noise and messaging signals do not interfere with each other without a channel. See Fig.5

There is significant improvement in signal strength after the Gaussian Filter compared to the degradation observed as you increase the amplitude of messaging signal in a noise channel. See Fig. 7 and Fig. 8

Increasing the input noise power shows proportional degradation in noise amplification and signal strength at the output of the Gaussian Filter as compared to the significant increase in noise amplification obtained at the output of the AWGN Channel. See Fig.9

Increasing the input signal power of the channel shows proportional decrease in signal.

Strength and noise amplification after the Gaussian Filter as compared to degradation in signal strength and increased noise amplification as obtained in the output of AWGN Channel. See Fig.10

Increase in the signal to noise ratio(SNR) improves the signal strength and noise amplification of the Gaussian Filter proportionally as compared to the increase o signal strength and decrease in the noise amplification as observed in the output of the AWGN Channel. See Fig.11

Increase in all the parameters shows proportional increase in signal strength and noise amplification. Never the less, it was observed that the signal strength shows significant improvement over the noise amplification. See Fig.12

Conclusion

The simulated design of a channel noise reduction model has been achieved. It was strongly observed that Increase in Signal to Noise Ratio (SNR) significantly improves signal strength and reduces noise amplification in channel but do not show significant improvement when applied to Gaussian Filter. The Gaussian Filter significantly improved signal strength and reduced noise in communication system

REFERENCES:

[1] Roger, L. F. (2007): Radio Systems Design for Telecommunications; A John Wiley &Sons, Inc., Publication.

[2] Carlos, J. and Borges, N. (2003): Intermodulation Distortion in Microwave and Wireless Circuit; Artech House, Microwave Library.

[3] Omijeh, B.O and Edeh, P.O (2008): "Path Loss Model for Microwave Radio Link in Southern Nigeria, International Research Journal in Engineering, Science and Technology, Vol. 5. No.1, pp 46-53.

[4] Roger, L. F. (2005): Fundamentals of Telecommunication; A John Wiley & Sons, Inc., Publication

[5] Omijeh, B. (2015): Fundamentals of Modern Digital Modulation Techniques; Lecture delivering, Centre for Information and Telecommunications Engineering, University of Port Harcourt.Unpublished

[6] Roger, L. F. (2004):Telecommunication System Engineering; A John Wiley & Sons, Inc., Publication.

[7] Paulo J., Borges N., Carlos J.: Intermodulation Distortion of Third-Order Non-Linear Systems with Memory Multisine Excitations, IEEE Transaction on Microwave Theory and Techniques, Vol. 55, No6. June 2007.

[8]Weizheng.W (1997). Noise in communication Systems, WWW.Mathworks.com

[9] Anon, 2015 https://en.wikipedia.org/wiki/Additive_white_Gaussian_noise

[10]Omijeh, B.O and Agoye, S.D(2015): Comparative Evaluation of Different Digital Modulation Schemes on AWGN, LOS and Non-LOS Fading Channel Based on BER Performance, International Journal of Scientific & Engineering Research, Volume 6, Issue 10, pp 371-377

International Journal of Engineering Research and General Science Volume 3, Issue 6, November-December, 2015
ISSN 2091-2730

Effect of Varying Surface Grinding Parameters on the Surface Roughness of Stainless Steel

Amandeep Singh Padda*, Satish Kumar**, Aishna Mahajan***

* M.Tech, Mechanical Engineering, CEC Landran (Mohali), Punjab, xeon.fast@yahoo.in

Abstract— Surface grinding is a very complex process to control yet it has very significant role in controlling the performance of the equipments and machine tools. Thus it is very important to analyse the process parameters by performing experiments. This is the purpose my research work in which I have tried to analyse the effect of varying surface grinding parameters on the surface roughness of Stainless Steel using white aluminium oxide grinding wheels. The main input parameters taken into consideration in this study are depth of cut, wheel speed and wheel grain size. Results are tabulated and plotted in form of comparison graphs for ease of analysis.

Keywords— Surface grinding, Surface roughness, Stainless steel, Grinding parameters, Grain size, Depth of cut, Wheel speed.

INTRODUCTION

Surface grinding is a material removal process that involves the interaction of abrasive grits with the workpiece at high cutting speeds and shallow penetration depths. The properties and grain size of these abrasive particles determine the performance of grinding operation. Each individual and irregularly shaped grain acts as a cutting element (single point cutting tool) in every grinding process. It is a mixture of cutting, plowing, and rubbing, with the percentage of each being highly dependent on the geometry of the grit. Surface grinding machines are used primarily to grind flat surfaces as in our analysis. It is a complex process to control because of a number of input parameters required to achieve the desired output of the operation. Most significant desired output parameter in surface grinding is the surface finish followed by other parameters like material removal rate, surface hardness, etc. Many input parameters like abrasive type, grain size, infeed, depth of cut, work speed, coolant used, etc control the surface finish of workpiece. Therefore a analysis is required to study the effect of input parameters on surface finish of various materials in surface grinding operation.

A number of studies have already been done to study the effects of input parameter in grinding process. Vishal Francis et. al. [1], stated that if feed and depth of cut were varied and spindle speed was kept constant to observe their effect on surface roughness then feed rate was found to be the most significant factor in case of cast iron and none of the factor was found be significant for mild steel and stainless steel. H. Adibi et. al. [2], stated that the amount of loading over the wheel surface increases sturdily with increasing depth of cut but is less affected by changes of table speed. Kirankumar R. Jagtap et. al. [3], Stated that the most influencing parameter to surface roughness for AISI 1040 is work speed (Nw) in rpm followed by depth of cut, grinding wheel speed and number of passes. Shih et. al. [6] proposed that, increasing the grinding wheel speed reduces the average chip thickness and increase the effective hardness of the wheel, resulting in more efficient workpiece material removal rates when the workpiece material is ceramic or steel. Hassui et. al. [8], proposed that, the wear of a grinding wheel has a direct effect on the workpiece vibration and both have effect on the workpiece quality. Nathan et al [9], proposed that, in the grinding process, a proper estimate of the life of the grinding wheel is very useful. When this life expires, redressing is necessary. Hardened C60 steel (Rc 40) specimens were ground with an A463–K5–V10 wheel in a cylindrical grinding machine. The results revealed that the surface quality and in service behaviour of a ground component is affected seriously by the occurrence of grinding burn.

METHODOLOGY

This research takes into account the effect of mainly three process parameters of Surface grinding process i.e. Wheel Speed (rpm), Wheel Grain size and Depth of cut on Surface Roughness with reference to Mild Steel, Die Steel and Stainless Steel as workpiece material. All other process parameters of surface grinding operation are kept constant. Stainless steel is widely used in industry machinery, precision tools, automobiles and household products and these applications require different part surface finish values in order to achieve maximum performance and working life period. Therefore this analysis is done to study the effect of input parameters on surface finish of stainless steel in surface grinding operation. A horizontal spindle and reciprocating table type Surface grinder, White Aluminium Oxide grinding wheels and an average table speed (up grinding) of 0.15 m/s is used throughout the experiment. Synthetic soluble oil (oil to water ratio of 1:25) is used as cutting oil. Material plates are cut into required number of small specimens using Power hacksaw and Chop saw. A Variable frequency drive is used to vary the rpm (wheel speed) of the grinding wheel to three different values. A total of 27 experiments are done on each material by varying wheel grain size, wheel speed (rpm) and depth of cut. Separate mild steel plates of thickness thinner than workpiece specimen are used to hold small workpiece specimen tightly, for stainless steel because of its non ferrous nature. Later surface roughness of each specimen is checked using Mitutoyo Surface roughness tester with cut-off length as 0.25cm. Stainless steel specimen approx. size taken for experiment is 30 x 20 x 6 mm (Length x

Width x Thickness) and material composition is given in Table 3. Process variables and their levels and number of experiments required is formed using N-factorial method as shown in Table 4.

Table 1: Machine Description

Sr. No.	Type	Specification
1.	Working area of grinder	225 x 400 mm
2.	Maximum height under wheel	250mm
3.	Vertical feed graduation	0.01 mm
4.	Cross feed graduation	0.05 mm
5.	Maximum spindle speed	2800 rpm
6.	Grinding wheel size (dia x bore x width) (mm)	178 x 31.75 x 13
7.	Electric Motor	1HP 3 Phase (2800rpm)
8.	Magnetic chuck	200 x 300 mm
9.	Dresser with holder	1 CR

Table 2: Wheel Parameters

Sr. No.	Type	Specification	Description
1.	Wheel Material	A	Aluminium Oxide (White)
2.	Grade	K	Medium
3.	Structure	5	Dense
4.	Binder	V8	Vitrified
5.	Shape	1	Straight
6.	Dimensions	Dia x Bore x Width (mm)	150 x 31.75 x 13

Table 3: Material Composition

Chemical Composition (%)	Stainless Steel T304
Carbon, C	0.08
Silicon, Si	1 Max.
Manganese, Mn	2 Max.
Phosphorus, P	0.045 Max.
Nickel, Ni	8 – 10.5
Sulphur, S	0.03 Max.
Chromium, Cr	18 – 20
Iron, Fe	Remaining

Table 4: Process variables and their Levels

Levels	Grinding Wheel Grain Size	Grinding Wheel Speed (rpm)	Depth Of Cut (mm)
1	46	1300	0.01
2	60	2000	0.02
3	120	2700	0.03

RESULTS AND CONCLUSION

3.1 Experimental results: Surface roughness of all 27 specimens is measured using the Mitutoyo Surface Roughness tester and given in Table 5 below.

Table 5: Experimental results for Stainless steel

Exp. No.	Material	Grain Size	Wheel Speed	Depth Of Cut	Surface Roughness, Ra
			rpm	mm	µm
1	Stainless Steel	46	1300	0.01	0.177
2	Stainless Steel	46	1300	0.02	0.185
3	Stainless Steel	46	1300	0.03	0.219
4	Stainless Steel	46	2000	0.01	0.140
5	Stainless Steel	46	2000	0.02	0.142
6	Stainless Steel	46	2000	0.03	0.155
7	Stainless Steel	46	2700	0.01	0.128
8	Stainless Steel	46	2700	0.02	0.134
9	Stainless Steel	46	2700	0.03	0.144
10	Stainless Steel	60	1300	0.01	0.138
11	Stainless Steel	60	1300	0.02	0.107
12	Stainless Steel	60	1300	0.03	0.109
13	Stainless Steel	60	2000	0.01	0.099
14	Stainless Steel	60	2000	0.02	0.096
15	Stainless Steel	60	2000	0.03	0.103
16	Stainless Steel	60	2700	0.01	0.111
17	Stainless Steel	60	2700	0.02	0.092
18	Stainless Steel	60	2700	0.03	0.095
19	Stainless Steel	120	1300	0.01	0.147
20	Stainless Steel	120	1300	0.02	0.134
21	Stainless Steel	120	1300	0.03	0.100
22	Stainless Steel	120	2000	0.01	0.185
23	Stainless Steel	120	2000	0.02	0.175
24	Stainless Steel	120	2000	0.03	0.169
25	Stainless Steel	120	2700	0.01	0.206
26	Stainless Steel	120	2700	0.02	0.202
27	Stainless Steel	120	2700	0.03	0.153

3.2 Graphs depicting the comparative results of effect of varying wheel grain size for a specific value of wheel speed on surface roughness of Stainless steel:

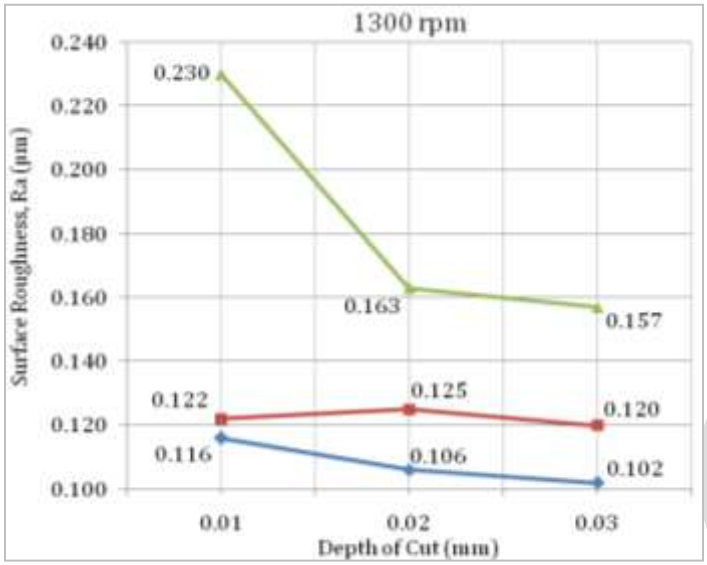

Fig 3.2(c)

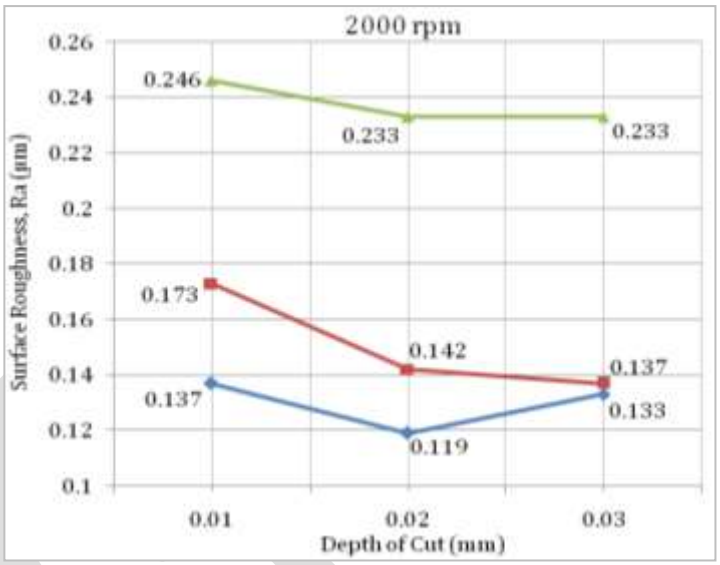

Fig 3.2(d)

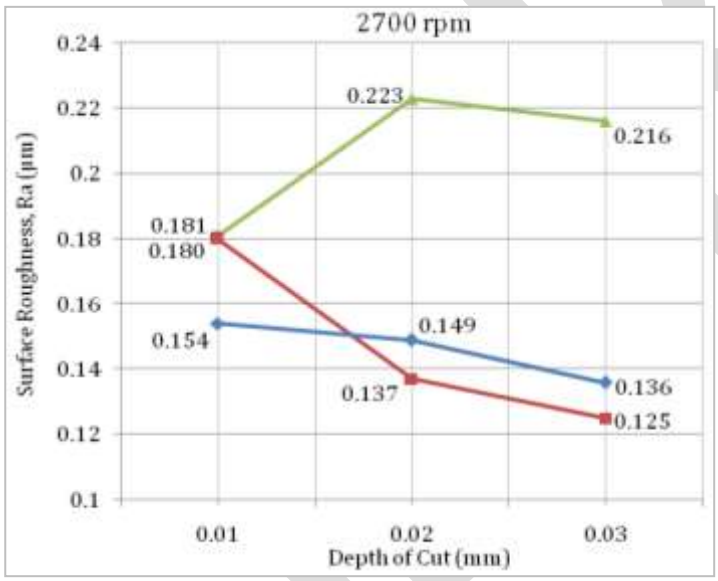

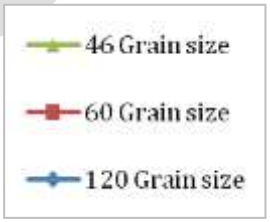

Surface finish comparison:

Wheel Speed(rpm)	***Grain size***
1300	120 > 60 > 46
2000	120 > 60 > 46
2700	60 > 120 > 46

Surface finish of stainless steel decreases with increase in speed of Al_2O_3 wheels. On an average at every speed better surface finish is shown by grain size 120. Only at 2700 rpm, grain size 60 shows better finish as compared to 120 grain size. Surface finish varies largely with small grain size but less with large grain size wheel. Fig. 3.1d shows comparative results for surface finish.

3.3 Graphs depicting the comparative results of effect of varying wheel speed (rpm) for a specific value of wheel grain size on surface roughness of Stainless steel:

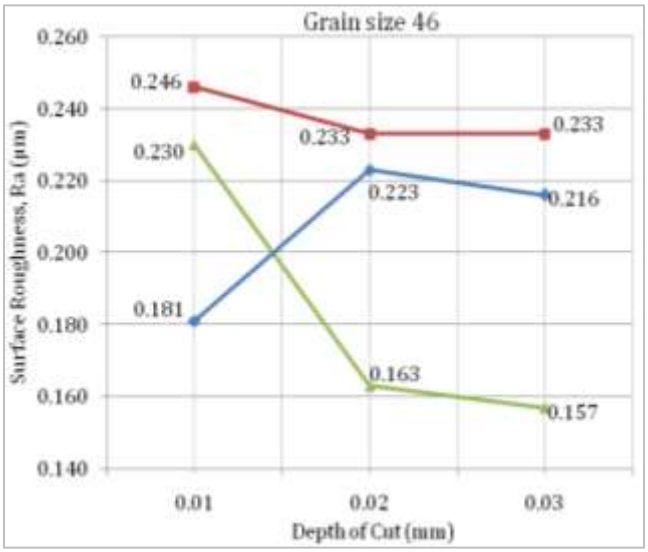

Fig. 3.3(c)

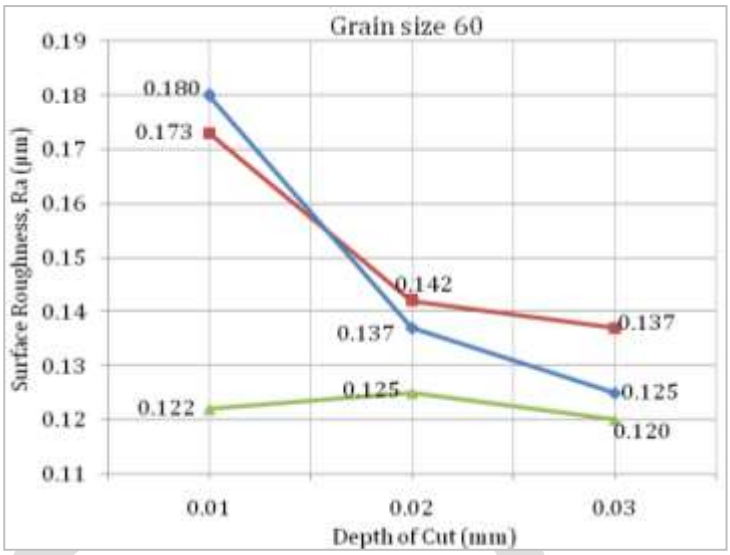

Fig. 3.3(d)

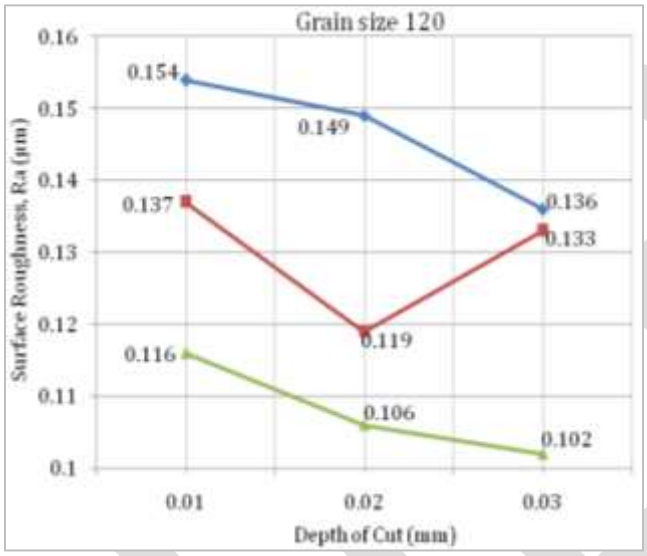

Surface finish comparison:

Grain size/ Depth of cut	***Wheel Speed(rpm)***
46 / 0.01	2700 > 1300 > 2000
46 / 0.02	1300 > 2700 > 2000
46 / 0.03	1300 > 2000 > 2700
60 / 0.01	1300 > 2000 > 2700
60 / 0.02	1300 > 2700 > 2000
60 / 0.03	1300 > 2700 > 2000
120/ 0.01	1300 > 2000 > 2700

Stainless Steel shows better surface finish at lower speeds of Al_2O_3 grinding wheels for almost every grain size at maximum depth of cut. The surface finish is increasing with increase in wheel grain size. Due to good surface toughness value of stainless steel, there is a lot of grain wear and fracture at high wheel speed. But at large depth of cut, the grains are able to shear the surface better thus allowing more cutting action. Fig. 3.1d shows comparative results for surface finish

CONCLUSION

Out of the three process parameters under study, most significant factor in surface grinding is wheel speed followed by grain size and depth of cut. Increasing wheel speed increases the tangential cutting force on material surface thus allowing more cutting and less of plowing and rubbing of grains. But this also increases stresses on Al_2O_3 wheel grains because of hardness and toughness of stainless steel, , thus leading to high grain wear and abnormal fracture. This reduces the cutting action and causes more of plowing and grain rubbing against the metal surface. As all grain size particles fail to provide better surface finish a high wheel speeds, it is clear that Al2O3 particles fail to grind stainless steel. Thus should not be used for grinding stainless steel.

With increase in depth of cut, there is a proportional increase in the normal pressure at the point of contact of wheel and workpiece. Very less depth of cut will lead to less cutting and more rubbing or plowing due to small shear pressure or good toughness value of material. Large depth of cut will also lead to less cutting and more rubbing or plowing due to more wear, abnormal fracture and completely break-off of wheel grains. Thus an optimum value needs to be determined depending upon material and machine/process

parameters.

Considering all the results we can say that in order to achieve minimum surface roughness with Al_2O_3 wheel, we need to choose an optimum value of grain size and depth of cut and a higher wheel speed or lower wheel speed for a certain material. Materials with good machining ability show better surface finish with higher wheel speed and materials with high toughness show poor surface finish with increasing grain sizes.

Studies like these can help to create a relation between independent and dependent variables in surface grinding process thus reducing the errors in design and improving the overall efficiency of the process which can lead to increase in productivity.

REFERENCES:

[1] Vishal Francis, Abhishek khalkho, Jagdeep Tirkey, Rohit Silas Tigga & Neelam Anmol Tirkey, "*Experimental Investigation And Prediction Of Surface Roughness In Surface Grinding Operation Using Factorial Method And Regression Analysis*", International Journal Of Mechanical Engineering And Technology (IJMET), ISSN 0976 – 6359 (Online), Volume 5, Issue 5, May (2014), pp. 108-114.

[2] H. Adibi, S. M. Rezaei & Ahmed A. D. Sarhan, "*Analytical modeling of grinding wheel loading phenomena* ", International Journal of Advance Manufacturing Technology, (2013) 68:473–485.

[3] Kirankumar Ramakantrao Jagtap, S.B.Ubale & Dr.M.S.Kadam, "*Optimization of cylindrical grinding process parameters for AISI 1040 steel using Taguchi method*" International Journal of Mechanical Engineering and Technology (IJMET), ISSN 0976 – 6359(Online) Volume 3, Issue 1, January- April (2012).

[4] Berend Denkena, Jens Kohler & Analia Moral, "*Grinding of Iron-Aluminides*", Procedia CIRP 9, 2 – 7 (2013).

[05] N. Alagumurthi, K. Palaniradja & V. Soundararajan, "*Heat generation and heat transfer in cylindrical grinding process - a numerical study*", International Journal of Advance Manufacturing Technology, (2007) 34:474–482.

[06] A.J.Shih, M.B.Grant, T.M.Yunushonis, T.O.Morris, S.B.mcspadden, "*Vitreous bond CBN wheel for high speed grinding of Zirconia and M2 Tool Steel*", Transactions of NAMRI/SME, Vol. 26, (1998).

[07] M.Janardhan, A.Gopala Krishna, "Determination and optimization of cylindrical grinding process parameters using taguchi method and regression analysis", ISSN 0975-5462, volume 3(2011), page 5659-5665.

[08] A. Hassui, A.E. Diniz, "Correlating surface roughness and vibration on plunge cylindrical grinding of steel", International Journal of Machine Tools & Manufacture, 43(2003) 855–862.

[09] R. Deiva Nathan, L. Vijayaraghavan, R. Krishnamurthy, *"In-process monitoring of grinding burn in the cylindrical grinding of steel"*, Journal of Materials Processing Technology 91 (1999) 37–42.

[10] Rodrigo Daun Monicia, Eduardo Carlos Bianchia,, Rodrigo Eduardo Cataib, Paulo Roberto de Aguiar, *"Analysis of the different forms of application and types of cutting fluid used in plunge cylindrical grinding using conventional and superabrasive CBN grinding wheels",* International Journal of Machine Tools & Manufacture 46 (2006), 122–131.

[11] Rogelio L. Hecker, Steven Y. Liang, *"Predictive modeling of surface roughness in grinding"*, International Journal of Machine Tools & Manufacture 43 (2003), 755–761.

[12] J. Kopac, P. Krajnik, "*High-performance grinding—A review*", Journal of Materials Processing Technology 175 (2006),278–284.

[13] K. Salonitis & T. Chondros & G. Chryssolouris, "*Grinding wheel effect in the grind-hardening process*", Intertanional Journal of Advanced Manufacturing Technology (2008), 38:48–58.

[14] Mikell P. Groover, "*Fundamentals of modern manufacturing: materials, processes and systems*", John Wiley & Sons Inc., 4th ed., ISBN 978-0470-467002, 2010, pg 604-621.

[15] J. T. Black Ronald A. Kohser, "*Materials and processes in manufacturing*", John Wiley & Sons, Inc, 10th edition, ISBN 13-978-0470-05512-0, 2008,pg 756-780.

International Journal of Engineering Research and General Science Volume 3, Issue 6, November-December, 2015
ISSN 2091-2730

MOS-2: A Two-Dimension Space for Positioning MAS Organizational Models

Hosny Abbas[1*], Samir Shaheen[2]

[1]Department of Electrical Engineering, Assiut University, Assiut, Egypt,

Email: hosnyabbas@aun.edu.eg

[2]Department of Computer Engineering, Cairo University, Giza, Egypt,

Email: sshaheen@eng.cu.edu.eg

Abstract- The increased complexity and dynamism of present and future Multi-Agent Systems (MAS) enforce the need for considering both of their static (design-time) and the dynamic (run-time) aspects. A type of balance between the two aspects can definitely give better results related to system stability and adaptivity. MAS organization is the research area that is concerned with these issues and it is currently a very active and interesting research area. Designing a MAS with an initial organization and giving it the ability to dynamically reorganize to adapt the dynamic changes of its unpredictable and uncertain environment, is the feasible way to survive and to run effectively. Normally, MAS organization is tackled by what is called, MAS organizational models, which are concerned with the description (formally or informally) of the structural and dynamical aspects of agent organizations. This paper proposes a two-dimension space, called MOS-2, for positioning and assessing MAS organizational models based on two dimensions: their adopted engineering viewpoint (agent-centered or organization-centered) as the vertical dimension and the agents awareness/unawareness of the existence of the organizational level as the horizontal dimension. The MOS-2 space is applied for positioning a number of familiar organizational models. Its future trends and possible improvements are highlighted. They include the following, (1) adding Time as a dimension, (2) increasing the considered dimensions, (3) providing a quantitative approach for positioning MAS organizational models.

Keywords - multi-agent systems (MAS), MAS organization, dynamic reorganization, organizational models, stability, adaptivity

1. INTRODUCTION

In contrast to initial MAS research, which concerned individual agents' aspects such as agents' architectures, agents' mental capabilities, behaviors, etc, the current research trend of MAS is actively interested in the adaptivity, environment, openness and the dynamics of these systems. In open environments, agents must be able to adapt towards the most appropriate organizations according to the state of the environment, which changes in an unpredictable manner. MAS organization [1] is currently considered as an emergent area of MAS research that relies on the notion of openness and heterogeneity of MAS and imposes new demands on traditional MAS models [2]. Considering MAS with no real structure isn't suitable for handling current software systems complexity, and higher order abstractions should be used and some way of structuring the society is typically needed to reduce system complexity, to increase system efficiency, and to more accurately model the problem being tackled [3].

Horling et al. [4] stated that our real world getting more complex and highly distributed and that should be reflected in new software engineering paradigms such as MAS. Therefore, the adoption of higher order abstract concepts like organizations, societies, communities, and groups of agents can reduce complexity, increase efficiency, and improve system scalability. Shehory [5] defined MAS organization as the way in which multiple agents are organized to form a multi-agent system. The relationships and interactions among the agents and specific roles of agents within the organizations are the focus of MAS organization. Dignum [26] pointed out that MAS organization can be understood from two perspectives, (1) organization as a process, and (2) organization as an entity. The first perspective considers agents organization as the process of organizing a set of individual agents, thus in this sense it is used to

refer to constraints (structures, norms and patterns) found in a social context that shape the actions and interactions of agents. On the other hand, the second perspective considers agents organization as an entity in itself, with its own requirements and objectives and is represented by (but not identical to) a group of agents. In fact, MAS organization demands the integration of both perspectives and relies for a great extent on the notion of openness and heterogeneity of MAS.

There are two familiar viewpoints of MAS engineering, the first one is the agent-centered MAS (ACMAS) in which the focus is given to individual agents. With this viewpoint, the designer concerns the local behaviors of agents and also their interactions without concerning the global structure of the system. The global required function of the system is supposed to emerge as a result of the lower level individual agents interactions. The agent-centered approach takes the agents as the "engine" for the system organization, and agent organizations implicitly exist as observable emergent phenomena, which states a unified bottom-up and objective global view of the pattern of cooperation between agents [6]. Ant colony [7] is a natural example of the ACMAS viewpoint, where there is no organizational behavior and constraints are explicitly and directly defined inside the ants. The main idea is that the organization is the result of the collective emergent behavior due to how agents act their individual behaviors and interact in a common shared and dynamic environment. In ACMAS, the MAS organization is actually a process not an entity; there is a consensus to call this process as *self-organization* [29][30][31].

The second viewpoint of MAS engineering is what is called organization-centered MAS (OCMAS) in which the structure of the system is given a bigger attention through the explicit abstraction of agent organizations. With that approach, the designer designs the entire organization and coordination patterns on the one hand, and the agents' local behaviors on the other hand. It is considered as a top-down approach because the organization abstraction imposes some rules or norms used by agents to coordinate their local behaviors and interactions with other agents. In OCMAS, the MAS organization is actually an explicit entity not a process and to distinguish it from the ACMAS approach, the change in system organization is often called *dynamic reorganization* [6][32], which is a more general name than self-organization.

When a researcher proposes an approach to dynamically reorganize a multi-agent system to adapt environments' changes, he actually proposes what the MAS community agreed to call it as an *organizational model* [19]. MAS organizational models will play a critical role in the development of future larger and more complex MAS. The main concern of organizational models is to describe the structural and dynamical aspects of organizations [8]. They have proven to be a useful tool for the analysis and design of multi-agent systems. Furthermore, they provide a framework to manage and engineer agent organizations, dynamic reorganization, self-organization, emergence, and autonomy within MAS.

Picard et al. [6] added the agents' awareness /unawareness of the existence of the organization structure as a dimension of the organization modification process and he identified four cases, (1) the agents don't represent the organization, although the observer can see an emergent organization. In some sense, they are unaware that they are part of an organization, (2) each agent has an internal and local representation of cooperation patterns which it follows when deciding what to do, this local representation is obtained either by perception, communication or explicit reasoning, (3) the organization exists as a specified and formalized schema, made by a designer but agents don't know anything about it and even do not reason about it. They simply comply with it as if the organizational constraints were hard-coded inside them, (4) agents have an explicit representation of the organization which has been defined, the agents are able to reason about it and to use it in order to initiate cooperation with other agents in the system.

In this paper, we propose a two-dimension space inspired from a previous work of Picard et al. [6], for positioning and comparing MAS organizational models. The proposed space is similar to a two-dimension Cartesian coordinate system, where the ACMAS/OCMAS are represented by the vertical axis and the agents' awareness/unawareness of the existence of the organizational level are represented by the horizontal axis as shown in Figure 1. A MAS organizational model is represented as a point (small circle) or an area (oval) as demonstrated in the figure and as will be explained later. A number of familiar organizational models are positioned and compared using the proposed MAS organization space; called MOS-2, where MOS stands for **M**AS **O**rganization **S**pace and the number 2 indicates that the space is a two dimension space.

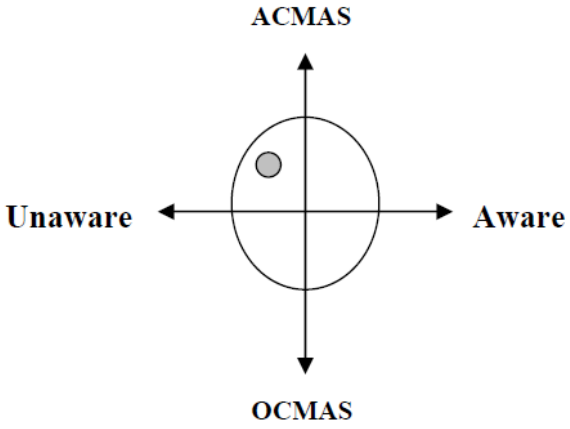

Figure 1: The MOS-2 MAS Organization Space

The central circle shown in the MOS-2 space can be seen as the unity circle (its radius is one). By this way it will be possible to precisely position an organizational model by determining the extent (i.e., percentage) to which it is an ACMAS or OCMAS approach and also the extent to which the individual agents are aware or unaware about the organizational aspects. In other words, the MOS-2 space can be used quantitatively not just qualitatively; this point is left as a future work but will be highlighted later in this paper. Furthermore, in the proposed space, the number of dimensions is two (Aware/Unaware, ACMAS/OCMAS), but it is also possible to increase the considered dimensions by adding new comparison aspects to address a fine-grained classes of MAS organizational models. In case the number of the considered comparison aspects (dimensions) is increased to be N, then the resultant space will be an N dimension space and can be called, MOS-N. Actually, this paper proposes only the two dimension case (MOS-2); other versions of higher dimensions are left as a future work.

The remaining of this paper is organized as follows: Section 2 explores the related work. Section 3 provides a background related to the two adopted comparison aspects. Section 4 presents the proposed MOS-2 space for positioning MAS organizational models. Section 5 demonstrates the applicability of MOS-2 on a number of familiar MAS organizational models and approaches. Section 6 discuss the results and provides a complete view based on these results. Section 7 highlights the possible future trends. Finally, Section 8 concludes this paper.

2. RELATED WORK

MAS organization was and still a very active and interesting research point in MAS. Concepts like organization, dynamic reorganization, self-organization, and emergence have attracted great attention in the last few years. The reason is related to the increasing complexity and highly distribution of modern real-life applications. This paper is not aimed to explain in details these concepts but interested readers can inspect their related references, for example [22][23][24][25][26][27][28]. The goal of this paper is to propose a visual semi-formal method for positioning and comparing a broad band of MAS organizational models. Organizational models are the tools to design methods, techniques, and approaches for managing the static and dynamic organization of MAS. Many researchers provided valuable narrative surveys and reviews contain informal analysis and evaluation of MAS organizational models. For instance, Picard et al. [6] aimed to study and propose a comprehensive view of how one could make multi-agent organizations adapted to dynamics, openness and large-scale environment. The authors proposed an analysis grid of different MAS organization approaches. The proposed grid has two dimensions: the vertical dimension identifies if the considered organization approach adopts the ACMAS, OCMAS, viewpoints. The second dimension is concerned with the awareness/unawareness of the individual agents of the organizational aspects. The authors claimed that the two dimensions of their grid are continuous, and it is completely possible to identify approaches that are at the boundary of two categories. Our propose work is inspired from Picard et al. work but in a more formal, visual and interesting way.

Alberola [18] provided, as a part of her PhD thesis, an analysis of how current reorganization approaches in MAS provide support to agent designers in order to develop adaptive agent societies. She described in detail some of the most relevant existing approaches, in order to show the advantages and limitations of each one. Alberola suggested that reorganization in agent societies can be represented as a loop process composed by different phases: Monitor, Design, Selection, and Evaluation phases. She also studied a number of familiar MAS organizational models by identifying the techniques adopted in each phase for each organizational model. Alberola study is valuable and it benefits us a lot but it is informal and contains intensive information and that makes it difficult to be captured by students and beginners.

V. Dignum [19] edited a handbook of research in MAS aimed to provide an overview of current work in agent organizations, from several perspectives, and focus on different aspects of the organizational spectrum. The handbook explored a number of familiar MAS organizational models and what makes it interesting is that the authors of the selected models wrote themselves the chapter that tackled their model. From the other hand, the handbook did not provide a general comparison or any type of positioning of the considered models.

Jensen et al. [20] investigated the agent-centered and organization-centered approaches to designing and implementing multi-agent systems. The authors have developed and evaluated two teams of agents for a variant of the well-known Bomberman computer game. One team is based on the basic Jason system, which is an implementation in Java of an extension of the logic-based agent-oriented programming language AgentSpeak. The other team is based on the organizational model Moise+, which is combined with Jason in the middleware called J-Moise+. They concluded that the agent-criented approach has a number of advantages when it comes to game-like scenarios with just a few different character types.

Horling and Lesser [21] also stated that organizational design employed by an agent system can have a significant, quantitative effect on its performance characteristics, and they surveyed the major organizational paradigms used in multi-agent systems. These include hierarchies, holarchies, coalitions, teams, congregations, societies, federations, markets, and matrix organizations. Also, they provided a description of each paradigm, and discuss its advantages and disadvantages, further, they provided examples of how each organization paradigm may be instantiated and maintained. But their work was not targeted to organizational models, which concerns both of static and dynamic aspects; they just concerned how to structure MAS with different paradigms.

In nutshell, the related work was valuable for us in designing the MOS-2 space for positioning MAS organizational models and approaches in a visual, semi-formal, easy to understand way. Providing a 2-dimension space for identifying an organizational model features and limitations in the scope of two or more dimensions is a good idea. It provides an effective tool to compare visually an organizational model with other models. This way enables designers and beginners to quickly capture a certain model in their minds and allows them to remember easily the considered model and its features or limitations relative to other models.

3. BACKGROUND

This paper is not concerned with the promotion of one MAS engineering viewpoint (ACMAS or OCMAS) relative to the other one, but the main concern is to position MAS organizational models and show the extent to which a certain model benefits from the adoption of each of these viewpoints. We have to emphasize here that both of the MAS engineering viewpoints (ACMAS/OCMAS) are generally not mutually exclusive and have led to different approaches in the domain [6]. In other words, it is possible to mix both viewpoints in one organizational model to take benefit of their pros and avoid their cons. Table 2 provides a comparison between the two viewpoints by presenting the characteristics and the shortcomings of each one. Also, Figure 2 provides the advantages and disadvantages of the adoption of each viewpoint relative to the individual agents' awareness or unawareness of the higher level organizational aspects.

Figure 2 represents the basis of the proposed two-dimension space as it orthogonally aligns the two comparison aspects into a vertical (ACMAS/OCMAS) and a horizontal (Awareness/Unawareness) axes. As demonstrated in the figure, four quadrants are resulted: ACMAS-Awareness, ACMAS-Unawareness, OCMAS-Unawareness, and OCMAS-Awareness. Therefore, a MAS organizational model that is positioned in one of these quadrants will simultaneously benefit and suffer from the advantages and disadvantages of this quadrant respectively. Note also that, an organizational model can be positioned into more than one quadrant.

Table 1: Comparison between the ACMAS and OCMAS viewpoints

	Characteristics	Shortcomings
ACMAS	• Organization is a process (self-organization) • Informal/Bottom-up/Emergent/Endogenous • The focus is given to individual agents • Agents are the "engine" for the system organization • An agent may communicate with any other agent • An agent is responsible to define its relations with other agents • An agent is responsible to constrain its accessibility from other agents • Agents are autonomous and no constraint is placed on the way they interact • An agent provides a set of services available to other agents	• Unpredictability and Uncertainty: lead to unreliability • Lack of Modularity: all agents are accessible from everywhere • Undesirable Emergent Behavior: can impact system performance • Dual Responsibility: agents have to manage simultaneously both the functional an the organizational aspects
OCMAS	• Organization is often an explicit entity • Support dynamic reorganization • Formal/ To-down/ Pre-exist organization • Reduce system complexity • Increase system efficiency • Improve system scalability • Provide Effective coordination • Limit the scope of interactions • Tuning of the agents autonomy • Structuring of agents interactions • Separation of concerns • Modularity/Reliability	• Computational / Communication overhead • Reduce overall flexibility or reactivity • Add additional layer of complexity

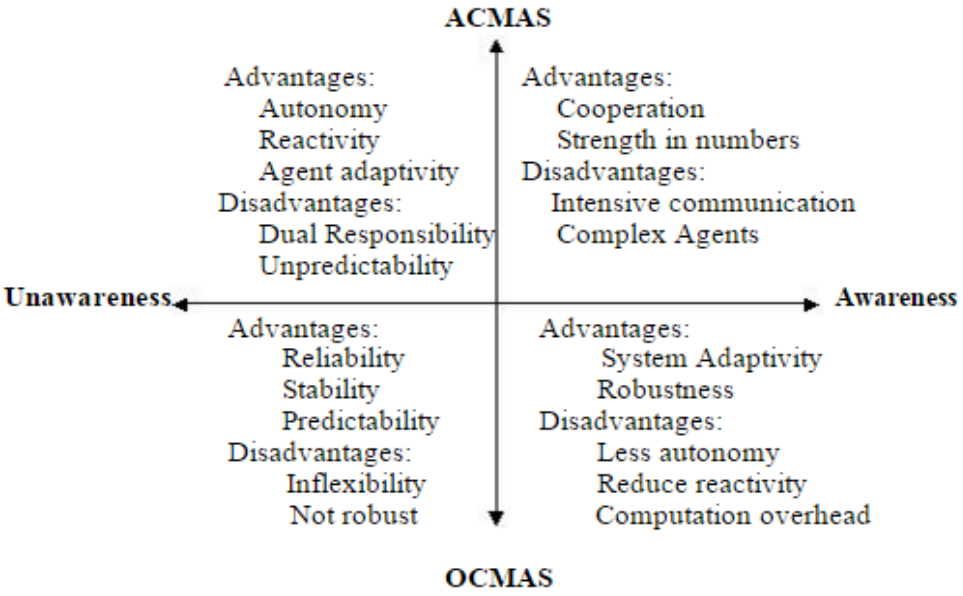

Figure 2: Advantages and Disadvantages of MOS-2 Quadrants

4. THE PROPOSED MOS-2 SPACE

Figure 3 presents the proposed MOS-2 space. As shown in the figure, the axes of a two-dimensional Cartesian system divide the space into four infinite regions, called quadrants, each bounded by two half-axes. In mathematics, these are often numbered from 1st to 4th and denoted by Roman numerals, lets take the same naming conversion, and thus the four quadrants can be identified as follows:

1. The I symbol identifies the ACMAS-Aware space quadrant
2. The II symbol identifies the ACMAS-Unaware space quadrant
3. The III symbol identifies the OCMAS-Unaware space quadrant
4. The IV symbol identifies the OCMAS-Aware space quadrant

Therefore, to position a MAS organizational model it should be studied and explored to see to which quadrant in the MOS-2 space it is best fit according to its characteristics and properties. If the considered model fits one of MOS-2 quadrants, then its position will be represented by a small circle as shown in Figure 4-a. But, if the model fits two quadrants, then its position is represented by a small oval shape expanded along the two space quadrants as demonstrated in Figure 4-b. Note that the oval part appeared in each quadrant should be relative to the extent to which the model realizes the characterizes of the MAS organization class represented by that quadrant. If the considered model realizes (partially or fully) the characteristics of three space quadrants then the position of this model can be represented as a half-circle expanded along the three space quadrants as shown in Figure 4-c. Finally, in case the considered model fits the whole space (it is rare but possible) then a circle expanded along the four space quadrants can be used to represent that perfect organizational model!, this case is demonstrated in Figure 4-d. Note also that the MOS-2 space can be enlarged to position simultaneously many organizational models. The next section applies the proposed space for positioning a number of familiar MAS organizational models.

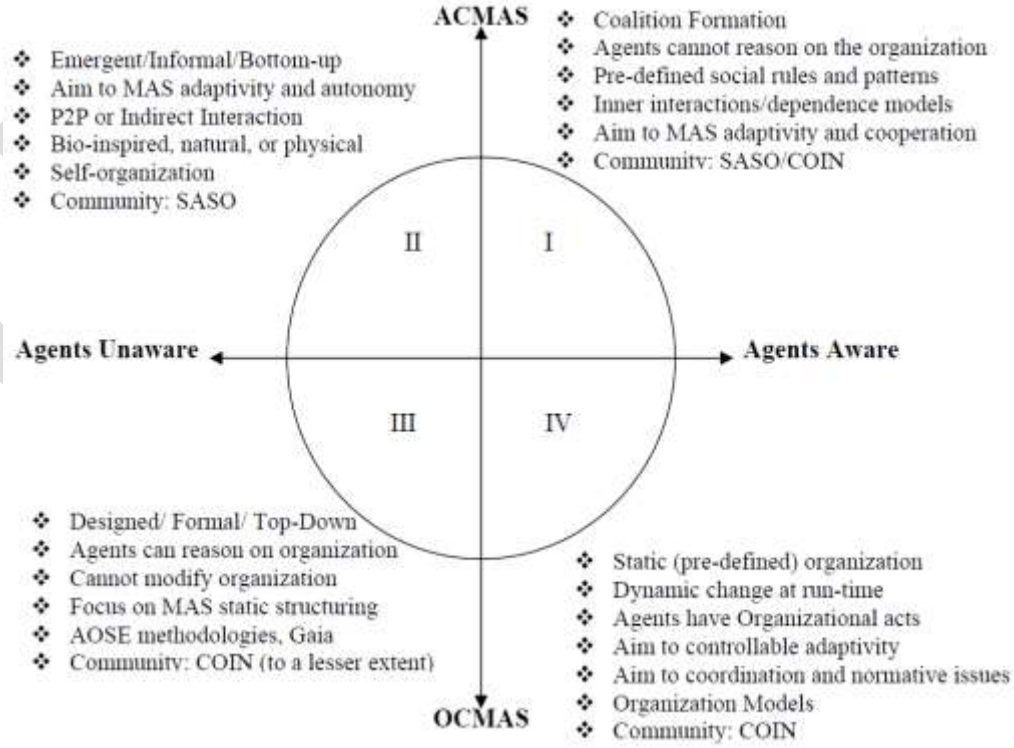

Figure 3: The MOS-2 space with the characteristics of each organization class

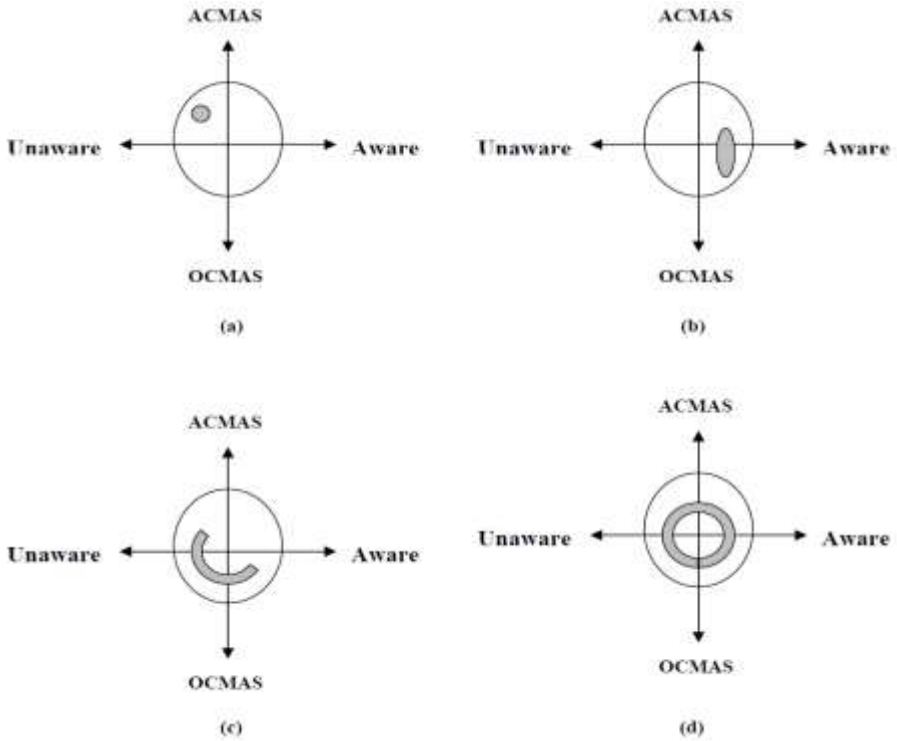

Figure 4: positioning of different types of organizational models

5. THE APPLICABILITY OF MOS-2 SPACE: CASE STUDIES

This section applies the MOS-2 space to position and compare a number of familiar MAS organizational models. The selected models are: AGR, MACODO, MOISE, Swarm-based approaches, Contract Net coordination model, and Gaia development methodology. Actually, there are a large number of MAS organizational models and approaches but we found that the selected ones are enough to demonstrate the usage of the proposed space and we leave to the reader the mission of trying to position any other model found in the literature or proposed by him.

AGR

The AGR [8][9] is a MAS organizational model that adopts the OCMAS viewpoint. This model is influenced by both AOSE and social reasoning, in the sense that organization is used by designer to specify the system-to-be and by the agents that can dynamically perform organizational acts and possibly modify the organization. The designer uses abstract concepts such as Group Structure and Organizational Structure to specify application in design-time. The group structure is an abstract representation of the roles required in this group and their interaction relationships and protocols. The organization structure is the set of group structures expressing the design of a multi-agent organizational scheme. In run-time, the agents can reason on the organizational aspects and can modify the application structure by the dynamic creation of agents groups (agents partitioning) and dynamic forming of hierarchies of groups. Therefore, the AGR model fits well with the III and IV quadrants of MOS-2 space and can be positioned as shown in Figure 5-a.

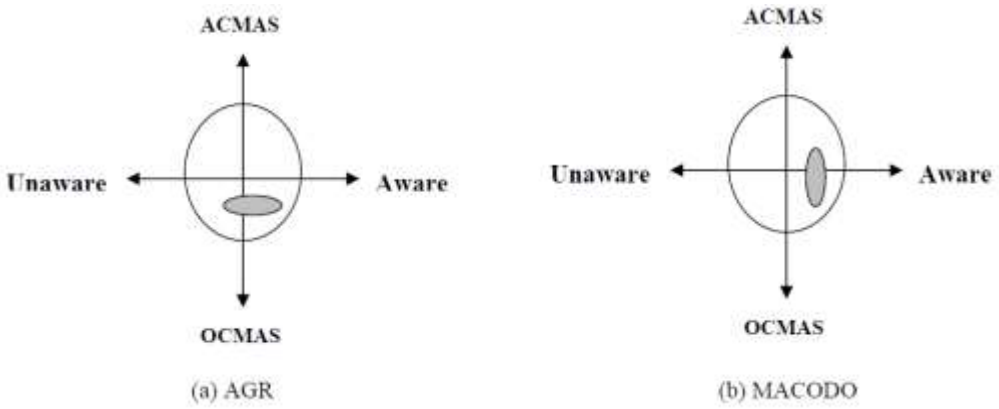

Figure 5: Positioning of AGR and MACODO organizational models

MACODO

The MACODO [10][11] is a MAS organizational model that is really an interesting model because it tries to realize (although partially) both of the MAS engineering viewpoints: ACMAS and OCMAS. It, to a large extent, belongs to the OCMAS philosophy, which provides an explicit representation of agent organizations. Although it provides a formal predefined specification for system dynamic reorganization, it allows the agents to (according to the environment context) form a type of short-lived coalitions by presenting a cooperative behavior with each other. The agents' cooperative behavior is supervised and controlled by the organization controllers. The organizational model is part of an integrated approach, called MACODO (Middleware Architecture for COntext-driven Dynamic agent Organizations); in this model, the life-cycle management of dynamic organizations is separated from the agents, organizations are first-class citizens, and their dynamics are governed by laws. We see that, the MACODO organizational model is best fit with two space quadrants, IV and I of the MOS-2 space, as presented in Figure 5-b.

MOISE

Hannoun et al. [12] proposed MOISE (Model of Organization for multI-agent SystEms); for modeling organizational aspects of MAS. The MOISE model is aimed at providing support in order to adapt an agent organization to its environment and to help it to efficiently achieve its goals. This model defines an organization which is composed by agents, roles, missions, and the deontic dimension. Each role represents a set of constraints that an agent follows when it plays this role. These constraints represent the structure dimension (relations between roles) and the functional dimension (missions, deontic dimension). A mission is a set of coherent goals that an agent can commit to. The deontic dimension specifies the permissions and obligations of a role in a mission. MOISE adopts a proactive reorganization carried out in a distributed way by monitor agents. The logic for reorganization is implemented at design time and cannot be changed during runtime. But the agents can modify the MAS organization according to the predefined logic. For example, the agents can change their roles or give a new obligation; a new role can be added to the system, etc. We see the MOISE model similar to the AGR model and can be positioned in the same way through quadrants III and IV of the MOS-2 space, as shown in Figure 6-a.

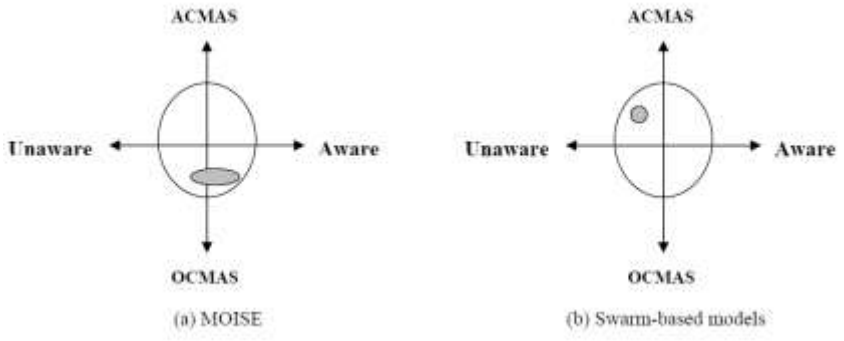

Figure 6: Positioning of MOISE and Swarm-based organizational models

Swarm-Based Approaches

The swarm-based approaches adopt the ACMAS viewpoint where the agents are unaware of any higher level structure. The system organization is dynamic and informal, it is an emergent phenomena appears to the observer in the higher level as a result of the individual agents lower level interactions directly (in a peer to peer fashion) or indirectly (through environment). In this type of agent systems, the designer concerns only the individuals and the environments, and he doesn't give any attention to the global organizational level. When the designer develops an individual agent he put in his mind the application domain and its environment only. In these systems, the individuals are purely reactive that simply react to environment changes. The ant colony [13] represents a realistic natural example of these systems. In the ant colony there is no organizational behavior and constraints are explicitly and directly defined inside the ants. The main idea is that the organization is the result of the collective emergent behavior due to how agents act their individual behaviors and interact in a common shared and dynamic environment. This class of systems represents the pure ACMAS viewpoint, which is located in the II quadrant in the MOS-2 space, as shown in Figure 6-b.

Contract Net

Contract Net Protocol (CNP) [14] is a task-sharing protocol in multi-agent systems, consisting of a collection of nodes or software agents that form a purposeful coalition. The agents are pre-augmented by the designer with some social rules, interaction models, and dependency models to be able to participate in purposeful coalitions. The organization is implicit and depends on the situation faced by the agents. The agents may be not able to reason about the global system organization, but they just follow the predefined social rules. The CNP model is best fit with the I-quadrant in the MOS-2 space, and can be represented by a small circle as shown in Figure 7-a.

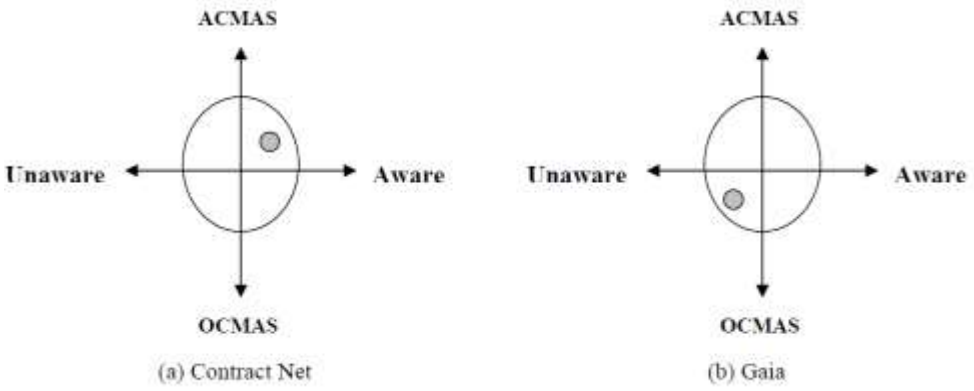

Figure 7: Positioning of Contract Net and Gaia organizational models

GAIA

The Gaia [15] is an agent-oriented software engineering methodology (AOSE) [16]; it considers the system organization at the design-time. Organizations are specified before encoding the agents. Agents can reason on the organization at run-time but cannot be able of modifying it. In other words, In MAS that are modeled by the Gaia methodology, the system structure is defined in design-time and doesn't change in run-time (fixed structure). The Gaia-based MAS can be positioned in the III quadrant in the MOS-2 space, which represents the AOSE engineering approaches, as shown in Figure 7-b.

NOSHAPE

The NOSHAPE MAS organizational model [17] is a recent model, although it is not matured yet, but it provides a novel approach for engineering complex and highly distributed MAS. Like the MACODO model, the NOSHAPE model tries to adopt the two MAS engineering viewpoints: the ACMAS and the OCMAS. The NOSHAPE model allows individual agents to loosely reshape the higher level system organization by emitting triggers (triggers can be seen as the pheromones released in the environment by ants in the ant colony as a type of indirect interaction). According to these triggers, the organizational level changes the system organization by establishing overlap relationships among higher order entities (agents' organizations, organizations' worlds, and worlds' universes). There are no any constraints imposed on the individual agents (except for mobility). The relationship between the individual agents' level and the organizational level is loose and depends only on the agents triggers. The organizational level can be seen as a helper or a guide to the agents. So, in the NOSHAPE model, the system structure emerges as a result of the agents triggers which are managed in a service-oriented manner, it is not possible to predict the next shape (structure) of the system, there are a pre-defined specification, and agents can modify indirectly the whole system structure by just emitting triggers. The NOSHAPE model aims to provide generality (relative to systems scale) and also aim to make the relation between the level of individual agents and the organizational level loosely coupled, so the agents can behave according to the ACMAS viewpoint (where agents are unaware of the organizational aspects) and the organizational level behaves according to the OCMAS viewpoint independently. Therefore, the NOSHAPE model can be positioned along the quadrants II, III, IV of MOS-2 space, as shown in Figure 8.

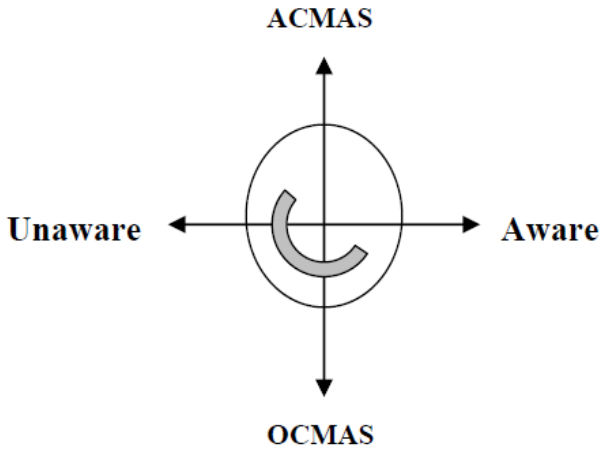

Figure 8: Positioning of the NOSHAPE MAS organizational model

COMPLETE VIEW

All of the selected MAS organization models can be positioned and represented on one space diagram as shown in Figure 9. Based on the complete view shown in Figure 9, we can claim that the more space quadrants an organizational model visits, the more it has of features. In other words, it will possess the advantages of each space quadrants. Not only this, but also it will have the chance to match the disadvantages of one space quadrants to the advantages of another one. According to these results, we claim that the NOSHAPE model is a promising one because it visits three space quadrants.

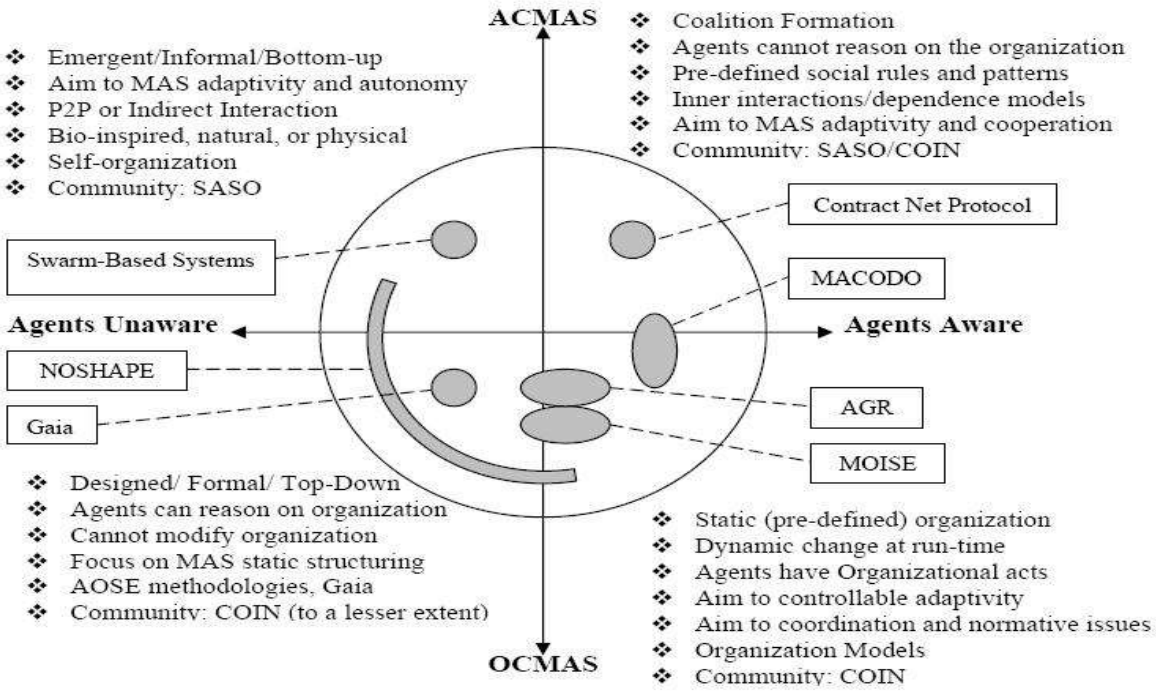

Figure 9: Complete view of positioning MAS organizational models

6. FUTURE TRENDS

The proposed MOS-2 space can be evolved to precisely position and compare MAS organizational models and approaches by considering the following issues:

1. Adding Time as a Dimension
2. Increasing the considered dimensions
3. The quantitative Approach

In the following subsections, these issues will be highlighted and some suggestions and ideas will be proposed to be addressed in future.

Adding Time as a Dimension

Based on the proposed MOS-2 space for MAS organization classification, is it possible to ask this question "can an organizational model evolves dynamically and changes to a novel emergent model"? May be it seems like a pure fantastical idea but as we all know "science is not about why? It's about why not?" What this question means is to add a third dimension to the proposed space, it is Time, so it may seem logical to call it MOS-2T, let's illustrate this amazing idea! Consider the organization space shown in Figure 10-a, as shown there is a model M_0 positioned in the III quadrant (the AOSE quadrant), with the addition of time as a third dimension, lets denote the absolute position of a model as a tuple <P, T> where P is the observed position of the considered model on the space and T is the time where we observed the position, then:

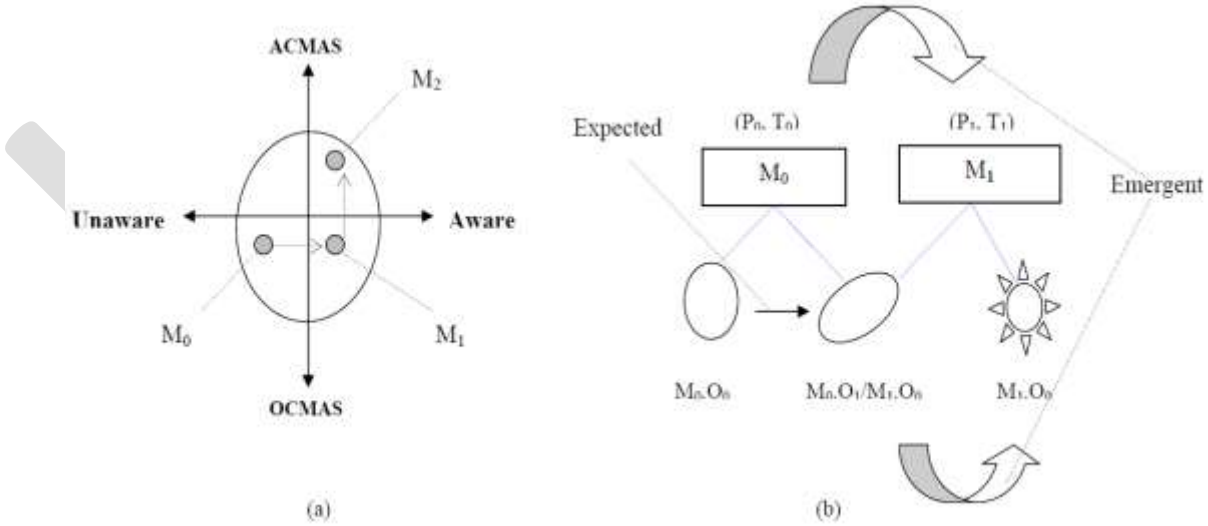

Figure 10: Dynamic evolution of organizational models

At T_0 the position of model M_0 is $<P_0, T_0>$, we may write it like:

$P(M_0)= <P_0, T_0>$ where P: M ⇨ P x T where $P = \{P_0, P_1, P_2, \ldots P_k\}$ or the set of possible positions. And $M=\{M_0, M_1, M_2, \ldots M_n\}$ is the set of possible models (assume it is a finite set).

If at time T_1 the model M_0 changed to a new emergent model M_1 (we can say that it is evolved, ignore questions like why? When? How? At least for now) then:

$P(M_1)= <P_1, T_1>$

And at time T_2 also M_1 evolved to M_2 as follows

$P(M_2)=<P_2,T_2>$ As demonstrated in Figure 10-a.

Also let's denote the organization of a MAS when the organization model M_0 is active at T_0 by

$O(M_0, T_0)= M_0.O_0$ where O: M x T ⇨ M.O where $M.O=\{M.O_0, M.O_1, \ldots, M.O_m\}$ or the set of possible organizations under the umbrella of a certain organizational model M.

So with M_0 is active, a dynamic organization change can happen as follows:

$M_0.O_0 \rightarrow M_0.O_1$

That is normal and expected according to the specification of the organization model M_0. But what is not normal is when the model M_0 is no longer active because it evolved to a novel emergent model:

$M_0 \rightarrow M_1$

As demonstrated in Figure 10-b, then it is expected to see a new organization of the system that is not planned by the designer and may violate the designer specifications, that can only happen if the agents are intelligent and have learning capabilities, so they may cause this amazing change in the organizational model as an emergent phenomena. As we see in Figure 10-b, after the dynamic emergent change of the organizational model takes place, the system organization $M_0.O_1$ relative to M_0 becomes $M_1.O_0$ relative the

emergent model M_1, in other words $M_0.O_1$ becomes the initial organization of M_1, and the new model (M_1) will cause the system organization to change to a novel organization that is not planned by the designer. Dynamic evolution of pre-defined organizational models because of agents' intelligence and their ability to learn is expected to be the next mainstream research area in MAS discipline.

Increasing the Considered Dimensions

The dimension of the proposed MOS-2 MAS organization space can be increased by adding other characteristics or properties of MAS organizational models. For example, a new dimension to represent the extent to which the model tackles the inter-reorganization and intra-reorganization can be added. The inter-reorganization is concerned with the organizational level interactions (i.e., interactions between groups of agents), and the intra-reorganization is concerned with individual agents interactions inside one group of agents. In this case the organization space will be a 3-dimension space as shown in Figure 11. Also in this case the name of space will be MOS-3 and if the time dimension is added, its name will be MOS-3T. The space shown in Figure 11 demonstrates how a model can be positioned in MOS-3 by considering three defined dimensions (x, y, z) correspond to classification criteria of MAS organizational models.

More dimensions can be added and the more dimensions added, the more fine-grained classification of MAS organizational models can be achieved. Therefore, the general name of the proposed space can be written as MOS-NT, where N is the number of used dimensions and T is the time dimension (the T should be removed if the time dimension is not considered).

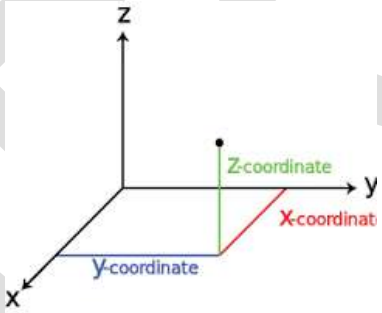

Figure 11: A 3-dimension space for MAS organization

The Quantitative Approach

In the previous sections, we tackled MAS organizational models in a qualitative way. In fact, the qualitative positioning of MAS organizational models is largely limited by the imagination of the researcher. In the qualitative approach, the researcher depends on descriptions and observations, but sometimes it is better to provide a quantitative data based on rigorous measurements and calculations. So, it is possible to quantify the position of a MAS organizational model by finding numerically the extent to which the model realizes a certain dimension (i.e., ACMAS). Consider the MOS-2 space shown in Figure 12, what if we considered the central circle shown in the space as the unity circle, so the maximum value of a dimension is 1 and the minimum value is -1 (i.e., - ACMAS= OCMAS). Thus, when positioning a model, we should find a way to accurately calculate the extent to which the model can be considered to realize a certain dimension.

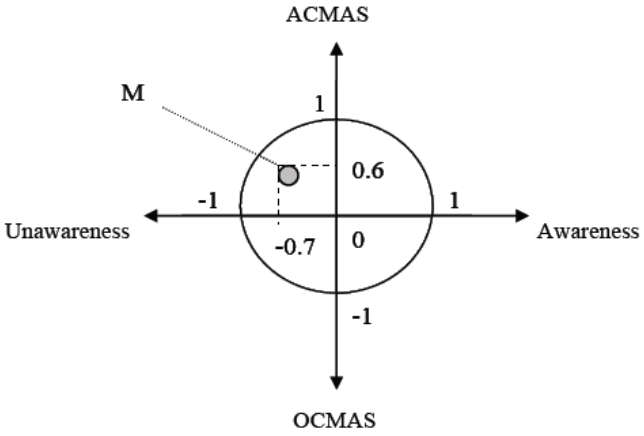

Figure 12: MOS-2 with a quantitative approach

Assume that there is a function V that is designed to calculate numerically the extent to which a model M is ACMAS/OCMAS. The function V can have the following signature:

V: M ⇨ [-1,1]

Similarly assume that there is a function W that is designed to calculate numerically the extent to which the agents in a model M are Aware/Unaware. The function W can have the following signature:

W:M ⇨ [-1,1]

Therefore the quantitative position of the model M in MOS-2 space can be determined as follows:

P(M)=(V(M), W(M))

The example in Figure 12 shows that:

V(M)= -0.7 and W(M)= 0.6

So the position of the model M can be written as follows:

P(M) = (V(M), W(M)) = (-0.7, 0.6)

The problem now is how to implement the functions V and W. The complexity of these functions will increase as the number of considered dimensions increases. Not only this but also the number of this functions will increase because each considered dimension will need a function to quantify the extent to which this dimension is realized by the MAS organizational model. Moreover, their implementation will be more complex if the time dimension is considered. This research trend is highlighted as future work.

7. CONCLUSIONS

This paper proposes a new method for positioning and comparing of MAS organizational models based on a two dimension space, called MOS-2. MOS-2 uses two comparison aspects: the MAS engineering viewpoint (ACMAS/OCMAS) and the agents' awareness/unawareness of the existence of a higher organizational level. The proposed space provides a feasible, effective, visual, and semi-formal positioning method for comparing MAS organizational methods using an orthogonal coordinate system similar to the familiar Cartesian coordinate system. The applicability of the proposed MAS organization space have been demonstrated by using it to position and compare a number of familiar and recent MAS organizational models, other models can be positioned similarly. Future trends are highlighted and discussed in Section 7.

REFERENCES:

[1] Hosny Ahmed Abbas, Samir Ibrahim Shaheen, Mohammed Hussein Amin. Organization of Multi-Agent Systems: An Overview. International Journal of Intelligent Information Systems. Vol. 4, No. 3, 2015, pp. 46-57. doi: 10.11648/j.ijiis.20150403.11
[2] Sichman, J. S., Dignum, V., & Castelfranchi, C. (2005). Agents' organizations: a concise overview. Journal of the Brazilian Computer Society, 11(1), 3-8.
[3] Jennings, N. R., & Wooldridge, M. Agent-Oriented Software Engineering. in Bradshaw, J. ed. Handbook of Agent Technology, AAAI/MIT Press, 2000.
[4] Horling, B., & Lesser, V. (2004). A survey of multi-agent organizational paradigms. The Knowledge Engineering Review, 19(4), 281–316.doi:10.1017/ S0269888905000317.
[5] Shehory, O. Architectural properties of multi-agent systems. Technical Report CMU-RI-TR-98-28, The Robotics Institute, Carnegie Mellon University, Pittsburgh, Pennsylvania 15213, 1998.
[6] Picard, G., Hübner, J. F., Boissier, O., & Gleizes, M. P. (2009, June). Reorganisation and self-organisation in multi-agent systems. In 1st International Workshop on Organizational Modeling, ORGMOD (pp. 66-80).
[7] A. Drogoul, B. Corbara, and S. Lalande. MANTA: New experimental results on the emergence of (artificial) ant societies. In Nigel Gilbert and Rosaria Conte, editors, Artificial Societies: the Computer Simulation of Social Life, pages 119–221. UCL Press, London, 1995.
[8] Ferber, J., Michel, F., & Báez, J. (2005). AGRE: Integrating environments with organizations. In Environments for multi-agent systems (pp. 48-56). Springer Berlin Heidelberg.
[9] Ferber, J., & Gutknecht, O. (1998, July). A meta-model for the analysis and design of organizations in multi-agent systems. In Multi Agent Systems, 1998. Proceedings. International Conference on (pp. 128-135). IEEE.
[10] Weyns, D., Haesevoets, R., & Helleboogh, A. (2010). The MACODO organization model for context-driven dynamic agent organizations. ACM Transactions on Autonomous and Adaptive Systems (TAAS), 5(4), 16.
[11] Weyns, D., Haesevoets, R., Helleboogh, A., Holvoet, T., & Joosen, W. (2010). The MACODO middleware for context-driven dynamic agent organizations.ACM Transactions on Autonomous and Adaptive Systems (TAAS), 5(1), 3.
[12] Hannoun, M., Boissier, O., Sichman, J. S., & Sayettat, C. (2000). MOISE: An organizational model for multi-agent systems. In Advances in Artificial Intelligence (pp. 156-165). Springer Berlin Heidelberg.
[13] A. Drogoul, B. Corbara, and S. Lalande. MANTA: New experimental results on the emergence of (artificial) ant societies. In Nigel Gilbert and Rosaria Conte, editors, Artificial Societies: the Computer Simulation of Social Life, pages 119–221. UCL Press, London, 1995.
[14] Smith, R. G. (1980). The contract net protocol: High-level communication and control in a distributed problem solver. IEEE Transactions on computers, (12), 1104-1113.
[15] Wooldridge, M., Jennings, N. R., & Kinny, D. (2000). The Gaia methodology for agent-oriented analysis and design. Autonomous Agents and Multi-Agent Systems, 3(3), 285-312.
[16] Giorgini, P., & Henderson-Sellers, B. (2005). Agent-oriented methodologies: an introduction. Agent-oriented Methodologies, 1-19.

[17] Abbas, H. A. (2014). Exploiting the Overlapping of Higher Order Entities within Multi-Agent Systems. International Journal of Agent Technologies and Systems (IJATS), 6(3), 32-57. doi:10.4018/ijats.2014070102.
[18] Alberola Oltra, J. M. (2013). Reorganization in Dynamic Agent Societies (Doctoral dissertation), CH 2.
[19] Dignum, V. (Ed.). (2009). Handbook of Research on Multi-Agent Systems: Semantics and Dynamics of Organizational Models: Semantics and Dynamics of Organizational Models. IGI Global.
[20] Jensen, A. S., & Villadsen, J. (2013). A comparison of organization-centered and agent-centered multi-agent systems. Artificial Intelligence Research, 2(3), p59.
[21] Horling, B., & Lesser, V. (2004). A survey of multi-agent organizational paradigms. The Knowledge Engineering Review, 19(4), 281–316.doi:10.1017/ S0269888905000317.
[22] Giovanna Di Marzo Serugendo et al (2011), "Self-organizing Software, From Natural to Artificial Adaptation", Springer.
[23] Giovanna di Marzoserugendo et al, "Self-organization in multi-agent systems", The Knowledge Engineering Review, Vol. 20:2, 165–189., 2005, Cambridge University Press.
[24] Dignum, V., Dignum, F., & Sonenberg, L. (2004, September). Towards dynamic reorganization of agent societies. In Proceedings of Workshop on Coordination in Emergent Agent Societies at ECAI (pp. 22-27).
[25] Sichman, J. S., Dignum, V., & Castelfranchi, C. (2005). Agents' organizations: a concise overview. Journal of the Brazilian Computer Society, 11(1), 3-8.
[26] Dignum, V. (2009). The role of organization in agent systems. Handbook of Research on Multi-Agent Systems: Semantics and Dynamics of Organizational Models, 1-16.
[27] A. Drogoul, B. Corbara, and S. Lalande. MANTA: New experimental results on the emergence of (artificial) ant societies. In Nigel Gilbert and Rosaria Conte, editors, Artificial Societies: the Computer Simulation of Social Life, pages 119–221. UCL Press, London, 1995.
[28] Hosny Ahmed Abbas, Samir Ibrahim Shaheen, Mohammed Hussein Amin. Organization of Multi-Agent Systems: An Overview. International Journal of Intelligent Information Systems. Vol. 4, No. 3, 2015, pp. 46-57. doi: 10.11648/j.ijiis.20150403.11
[29] De Wolf, T., & Holvoet, T. (2005). Emergence versus self-organisation: Different concepts but promising when combined. In Engineering self-organising systems (pp. 1-15). Springer Berlin Heidelberg.
[30] Serugendo, G. D. M., Irit, M. P., & Karageorgos, A. (2006). Self-organisation and emergence in MAS: An overview. Informatica, 30(1).
[31] Schillo, M., Fley, B., Florian, M., Hillebrandt, F., & Hinck, D. (2002, August). Self-organization in multiagent systems: from agent interaction to agent organization. In Third International Workshop on Modelling Artificial Societies and Hybrid Organisations (MASHO) (pp. 37-46).
[32] Dignum, V., Dignum, F., & Sonenberg, L. (2004, September). Towards dynamic reorganization of agent societies. In Proceedings of workshop on coordination in emergent agent societies (pp. 22-27).

International Journal of Engineering Research and General Science Volume 3, Issue 6, November-December, 2015
ISSN 2091-2730

EVALUATING THE INTEGRATED MANAGEMENT SYSTEMS INTO BITOLA'S REGION WITH A SPECIAL ACCENT ON INJURIES SPOTTED IN LARGER INDUSTRIAL CAPACITIES

Ivo Kuzmanov[1], Roberto Pasic[2]

[1,2] Assistant Professor's, Faculty of Technical Science, University St. Kliment Ohridski Bitola

[1]ivo.kuzmanov@tfb.uklo.edu.mk, [2]roberto.pasic@uklo.edu.mk

Abstract - The main object of the paper is to represent a complete research conducted into larger industrial entities from Bitola, which is conducted in the time frame January 2014 - February 2015, with a starting aim to research the implemented [1] Integrated Management Systems in the companies. To be more precise the main aim of the research was to see how the implemented [10], [11], [12], [13], [9] ISO 9001, ISO 14001 and OSHAS 18001 systems were used in larger companies in Bitola's region, R. Macedonia, and to see are there any injuries in the companies that were under research. Actually the paper represents only a small segment from the conducted research in which a detail analyzes considering the spotted injuries in Bitola's region is done. For that purpose three relevant sources of information were used, such as: the companies where the injury was spotted, the local inspectors for health and safety and the local health fund (the last two as relevant government institutions). At the end of the paper a detail review of the spotted injuries in two larger industrial capacities is presented, considering the time frame for monitoring since January 2014 till January 2015. The companies represented into the paper are chosen because both are the largest ones from the companies in Bitola's region and also among the largest in R. Macedonia, considering the number of employees and considering the annual productions and profits (the first one from the tobacco industry and the second from the electricity production sector). Considering the analyses [6] several key criteria were used, such as: the gender of the injured employee, total numbers of injured people, the age of the injured persons, qualifications, the day of the week when the injury is spotted, the time frame, number of lost work days as a result of the injury etc.

Key words - QMS, Integrated Management Systems, ISO9001, ISO14001, OSHAS 18001, injury, Bitola's region.

INTRODUCTION

Speaking about the research that will be presented the same one was conducted in the period January 2014 – February 2015 in which all of the industrial systems that are working in Bitola's region and government institutions were a main subject of the research. The research was separated into three different parts: gathering the data, putting the data into a special computer program and analyzing the data considering the spotted injuries, than analyzing the implemented integrated management system into companies that has the same one (considering the practical usage of the same one and the benefits from it), as well as considering the potentials for future improvements and also practical usage of problem solving techniques that will give better results from the practical usage of the integrated management systems. With the research a larger specter of industrial capacities were considered with a special accent on industrials entities from the milk production industry, tobacco industry, power plants, automotive industry, production of electricity cables, as companies with larger number of employees and financial profits that are one of the largest ones in R. Macedonia.

In addition, only small part of the results from the conducted research is represented considering the spotted injuries into Bitola's region into the year 2014 and the same ones are analyzed having in mind several key criteria such as: the gender of the injured person, total numbers of injured people, the age of the injured persons, qualifications and work experience, the day of the week when the injury is spotted, the time frame and also the total lost working days as a result of the injury. On the other hand, two of the largest companies from Bitola's region are represented considering the injuries and the previous mentioned criteria. Those are A.D. ELEM – REK Bitola (the largest company from the electricity production business) and SOCOTAB Bitola (one of the largest companies from the tobacco business in Macedonia). Both of the companies are also the largest ones considering the total number of employees in Bitola.

PRESENTING THE INJURIES INTO BITOLA'S REGION

Considering the results from the research, this part of the papers represents the spotted and analyzed injuries into industrial capacities that gravitates Bitola region. In this point it is more than important to say that all of the data represented in addition are official data from three different sources (the companies, the local health and safety branch office as a government institution and the health fund). Considering the way of gathering the data almost all of the injuries that happened in industrial entities were spotted and took a part in the analyzes that are represented in addition. This corresponds to the starting hypothesis, which says that not every injury that happened is spotted by the companies itself and the local health and safety inspectors, although it is a legal obligation for the companies and the employees according to Macedonian laws. Seeing the results, considering the information from previous years, communicating with employees and inspectors, there are some injuries that aren't spotted such as small cuttings and other small injuries, which aren't spotted from the employees, and that is the main reason why these injuries aren't a part of the researched and presented injuries from the industrial systems. In a non formal communication with the employees, there are more the 300 such injuries in only one year, so this could be a starting point for further research and a point of view for future education and training with an aim all of the injuries to be spotted and to avoid such injuries in future. From the communication there were such employees which said that these kinds of injuries were reasons for more serious injuries in the near future.

From the analyzed data, there were total 323 spotted injuries in companies into Bitola's region in 2014, from which one injury is fatal. Considering the fact that similar research was conducted also in the year 2014 considering the injuries into Bitola's region in 2013 (from which 351 were spotted in the year 2013), we could say that a small reducing of the spotted injuries is present. To be more precise there are 8.49% less injuries in the year 2014 than the ones from 2013. On the other hand considering the law regulations, the larger education for the employees and the management into the companies considering health and safety issues, but also the larger safety measures and usage of PPE (Personal Protective Equipment) equipment into direct work places, these results were more than expected.

In addition of the paper several tabular views are presented considering the analyzes with usage of the previous mentioned criteria: the gender of the injured persons, total numbers of injured people, the age of the injured employee, the day of the week when the injury was spotted, time frame and also the number of the lost days as a result of the injury.

Tabular view 1: Analyzing the injuries using the criteria – Gender of the injured person

Criteria – The gender of the injured person			
Professional disease	**Male**	**Female**	**Total**
0	249	74	323
In percents	77%	23%	100%

Tabular view 2: Analyzing the injuries using the criteria – What kind of a injury

Criteria – What kind of a injury			
Light	**Heavy**	**Death**	**Total**
281	41	1	323
87%	12.7%	0.3%	100%

Tabular view 3: Analyzing the injuries considering the criteria – Age of the injured person

Criteria – Age of the injured person			
18-25	**25-35**	**35-45**	**45-65**
7	64	95	157

2.1%	19.8%	29.4%	48.7%

Tabular view 4: Analyzing the injuries considering the criteria – Day in the week

Criteria – Day in the week when the injury is spotted		
Day	**Spotted injuries**	**In percents**
Monday	52	16.1 %
Tuesday	53	16.4 %
Wednesday	48	14.86 %
Thursday	58	17.95 %
Friday	54	16.7 %
Saturday	39	12.07 %
Sunday	17	5.26 %
There wasn't an exact day when the injury was spotted	2	0.66 %
TOTAL	**323**	**100%**

Tabular view 5: Analyzing the injuries considering key criteria – Time frame

Criteria – Time frame		
Time frame	**Spotted injuries**	**In percents**
00-04	12	3.70 %
04-08	42	13.00 %
08-12	109	33.75 %
12-16	93	28.79 %
16-20	44	13.60 %
20-24	19	5.88 %
There wasn't a time frame into the data for the spotted injuries	4	1.28 %
TOTAL	**323**	**100%**

Seeing the data presented into the tabular views above, we could say that the tabular views number 4 and 5 are the most interesting. Seeing from this perspective I could say that although there was an excellent cooperation with the industrial entities and a special reports were given to the companies in which they could spot every injury, some of the injuries were spotted without any additional data (such as the day when the injury was spotted and also the time frame). Seeing these mistakes, an effort was made for the spotted injuries to get an additional data from the branch office for health and safety in Bitola and also from the health fund but also there wasn't any kind of data (only the injuries were spotted without any further information). These conclusions were a starting point for software which could be used to evidence the injuries, that was specially made and could be used in the following period and for further research. The software that was made could be modified according to the legal requirements and according to the research, but the same one could avoid this kind of mistakes and could reduce the time needed for analyzing the data.

In addition of the paper also a detail representation of the spotted injuries using the previous mentioned criteria is presented, using the information from the largest industrial entities considering number of employees and financial profits in the past few years. The same ones are from the electricity production sector (A.D. ELEM REK Bitola) and from the tobacco industry (SOCOTAB Bitola).

PRESENTING THE RESULTS FROM TWO REPRESENTATIVE INDUSTRIAL ENTITIES FROM BITOLA'S REGION

In this part of the paper, and as a part of the previous mentioned research conducted into Bitola's region, a detail review of the results from two largest industrial entities from the region is presented. Both companies are one of the largest entities in Republic Macedonia considering number of employees and also at the same time the largest ones in Bitola's region. Considering the number of employees we could say that SOCOTAB as a company from the tobacco industry has more than 1200 employees and A.D. ELEM REK Bitola as

an entity that works in the electricity production sector has more than 3600 employees. Both of the companies have also one of the largest financial profits among the industrial entities in Republic Macedonia.

On the other hand considering the injuries we could say that A.D. ELEM REK Bitola is also the most representative industrial system among Bitola's industrial entities with totally 127 spotted injuries, which considered the total number of spotted injuries into Bitola's region (323) is more than noticeable 39.32%.

In addition of the paper, several tabular views are given from which we could see the situation about the injuries in these industrial capacities considering the time frame January 2014 – January 2015.

Tabular view 6: Analyzing the spotted injuries considering the criteria gender of the injured person

Criteria – Gender of the injured person			
Industrial entity	**Male**	**Female**	**Total**
A.D. ELEM REK Bitola	115	12	127
SOCOTAB Bitola	3	4	7

Tabular view 7: Analyzing the spotted injuries considering the criteria difficulty of the spotted injury

Criteria – Difficulty of the spotted injury			
Industrial entity	**Light**	**Heavy**	**Death**
A.D. ELEM REK Bitola	118	9	0
SOCOTAB Bitola	5	2	0

Tabular view 8: Analyzing the spotted injuries into the chosen industrial entities considering the criteria lost work days as a result of the injury

Criteria – Lost work days			
Industrial entity	**Less than a month (30 days)**	**More than a month (more than 30 days)**	**Total**
A.D. ELEM REK Bitola	1607	521	2128
SOCOTAB Bitola	112	16	128

Seeing the presented results for the companies, we could conclude that exactly 11 injuries were with multiple injured body parts (heavy injuries) and all of the spotted injuries resulted with a total number of 2256 lost work days. Considering the fact that in one year there are approximately 260 work days (without holidays and weekend days) we could correspond this numbers to exactly 9 workers who will lose all of the working days in a period of a year. That is a fact that should be analyzed in an additional research.

Seeing the presented results we could conclude at this point that this is only a small part of the detailed research considering several key criteria, after which all of the results are presented to the management teams into the industrial capacities and several key steps for reducing the numbers of injured people are proposed to the same ones.

CONCLUSION

The paper represents only a small part from a larger research conducted on business entities in Bitola's region, considering the integrated management systems and the spotted injuries in the same ones. Considering the spotted injuries in Bitola's region which is totally 323 persons (and having in mind the total number of employed people in Bitola which is something above 14.000), we could say that the numbers aren't such bad, but on the other hand considering the Macedonian laws regarding the health and safety issues we could conclude that this is a significant number. From the results presented into the paper we could say that something more than 1/3 of the total injured people are spotted in the both largest companies which are presented.

Also at this point we could say that starting points for future analyzes and a detail strategic plan for future reduce of the injuries are made and presented to the companies. On the other hand from the presented results for the chosen industrial entities, we could

consider future steps for avoiding the injuries, monitoring on direct work places with higher risks, additional research and finally presenting the gathered data in a completely new paper.

REFERENCES:

[1] Wayne Pardy, and Terri Andrews "Integrated Management Systems" Published by Government Institutes, An imprint of the Scarecrow Press Inc., ISBN 978-1-60590-658-4, 2010

[2] E.Scott Geller "Behavior-based Safety: A Solution to Injury Prevention" Risk and Insurance 15, no.12, October 1, 2004:66

[3] Thomas R. Krause, John H. Hidley, and Stanley J. Hodson "The Behavior-based Safety Process: Managing Involvement for an Injury-free Culture" New York: Van Nostrand Reinhold, 1990

[4] E. S. Geller "The Psychology of Safety: How to Improve Behaviors and Attitudes on the Job" Randor, PA: Chilton Book Company, 1996

[5] Glendon A. Ian, Sharon Clarke, and Eugene F. McKenna "Human Safety and Risk Management" Manchester, UK: UMIST, 2006

[6] National Safety Council "The Comparative Analysis Model: Mapping and Analyzing Safety and Health Management Systems" www.nsc.org/resources/dod-matrix.aspx

[7] Government of Australia "Health and Safety Report on Health and Safety Management Systems" www.ascc,gov.au

[8] OHSAS 18001 blog. Ohsas18001expert.com/

[9] Munro R.A., and W. J. Luka "OSHAS 18001 Puts Safety First" Quality Digest, www.qualitydigest.com/june05/articles/02_article.shtml

[10] www.scribd.com/doc/1035015/OHSAS-18001-2007

[11] www.scribd.com/doc/2563663/iso-9001-2000-why

[12] www.scribd.com/doc/2910021/ISO-9001-by-kashif

[13] Total Logical Concepts.com www.tlcnh.com/download/ISO14001ChecklistSample.pdf

International Journal of Engineering Research and General Science Volume 3, Issue 6, November-December, 2015
ISSN 2091-2730

SYNTHESIS, REACTION MECHANISM AND KINETIC STUDY OF 5-CHLORO, 2-METHYL ANILINE PHOSPHATE DI-ESTER IN ACID MEDIA

Dr. Amit chaudhary Chem. Dept., D.S. College, Aligarh

Email- amitchaudhary111114@gmail.com

ABSTRACT- Kinetic measurement of the hydrolysis of di–5-chloro, 2-methyl aniline phosphate ester has been carried out in the acid range 0.1 to 6.0 mol. dm^{-3} HCl at 80 $\pm$ 0.5 °C in 20% aqueous dioxane mixture. The inorganic phosphate obtained in overall hydrolysis has been estimated colorimetrically by Allen's modified method [1]. The overall systematic ionic data proves the presence of acid catalysed hydrolysis. In the hydrolysis of diester conjugate acid, neutral and mononegative species have been found to be reactive, but in this discussion only conjugate acid species have been given. The first order rate coefficients have been calculated using integrated form of the corresponding rate equation.

$$K_e = K_{H^+}.C_{H^+}.\exp.\mu$$

The rate coefficients estimated by the above equation are fairly in good agreement with experimentally observed rate. Arrhenius parameters, Linear free energy relationship etc. have been used to propose probable machanism. Temperature, solvent, substrate concentration effects etc. have been studied to find out the participation of water molecule, bond-fission and molecularity of the reaction.

INTRODUCTION: The recent intrest in biochemistry of di-ester [2, 3] having C-N-P linkage [4 - 21], reflects the current emphasis on acid hydrolysis of 5-chloro, 2-methyl aniline phosphate di-ester. In this field chemical research has entered into a new dimension leading to the synthesis of organophosphate pesticides [22 - 24], insecticides [25 - 26] and plant harmones [27] etc. Bunton and co-workers [28] found that acid calatysed hydrolysis occurs only when an electron attracting substituent is present in aryl part.

EXPERIMENTATION : The method of preparation of the phosphate di-ester of 5-chloro, 2-methyl aniline has been done by general methods [29 - 30] which involves the direct reaction of $POCl_3$ with respective amine. The residue left after removing 5-chloro, 2-methyl aniline phosphate mono-ester was washed with hot distilled water and 0.5 mol. dm^{-3} NaOH solution was added to remove 5-chlolo, 2 methyl aniline phosplate monoester and unreacted $POCl_3$. The aryl amine finally digested in 5.0 mol dm^{-3} NaoH to separate di-ester from tri-ester. It was filtered off and the filterate was acidified with dilute HCl using phenolphthalein as an indicator. The white precipitate so obtained was separated by filteration and made free from hydroxyl ions with repeated washings with hot distilled water. It was then dried at room temperature and recrystallised with absolute ethyl alcohol to give a white crystalline solid, which was indentified as 5-chloro, 2-methyl aniline phosphate diester with following physical properties:

1. Melting point (observed) = 266°C

2. Theoretical Percentage of 'P' = 8.93

Observed percentage of 'P' = 8.72

3. Infra Red spectrum (fig.1) of diester showed the appearance of absorption bands characterstics of

adjacent H = 820,800 cm^{-1}.

aromatic ring = 940 cm^{-1}.

O
‖
P — OH = 988 cm^{-1}.

P — OH = 1122 cm^{-1}.

Secondary amine = 1230 cm^{-1}

P = N = 1422 cm^{-1}.

tri substituted = 1500 cm^{-1}.

Aromatic ester = 1738 cm^{-1}.

All the above properties confirm the structure of di- 5-chloro, 2-methyl aniline phoshate ester.

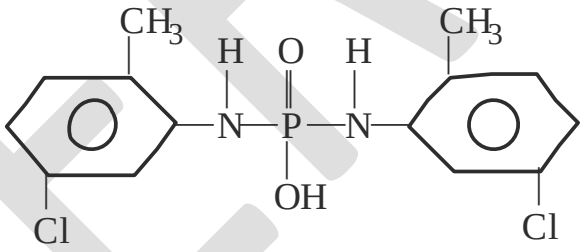

FIG. 1. IR SPECTRUM FOR 5-CHLORO, 2-METHYL ANILINE PHOSPHATE DIESTER.

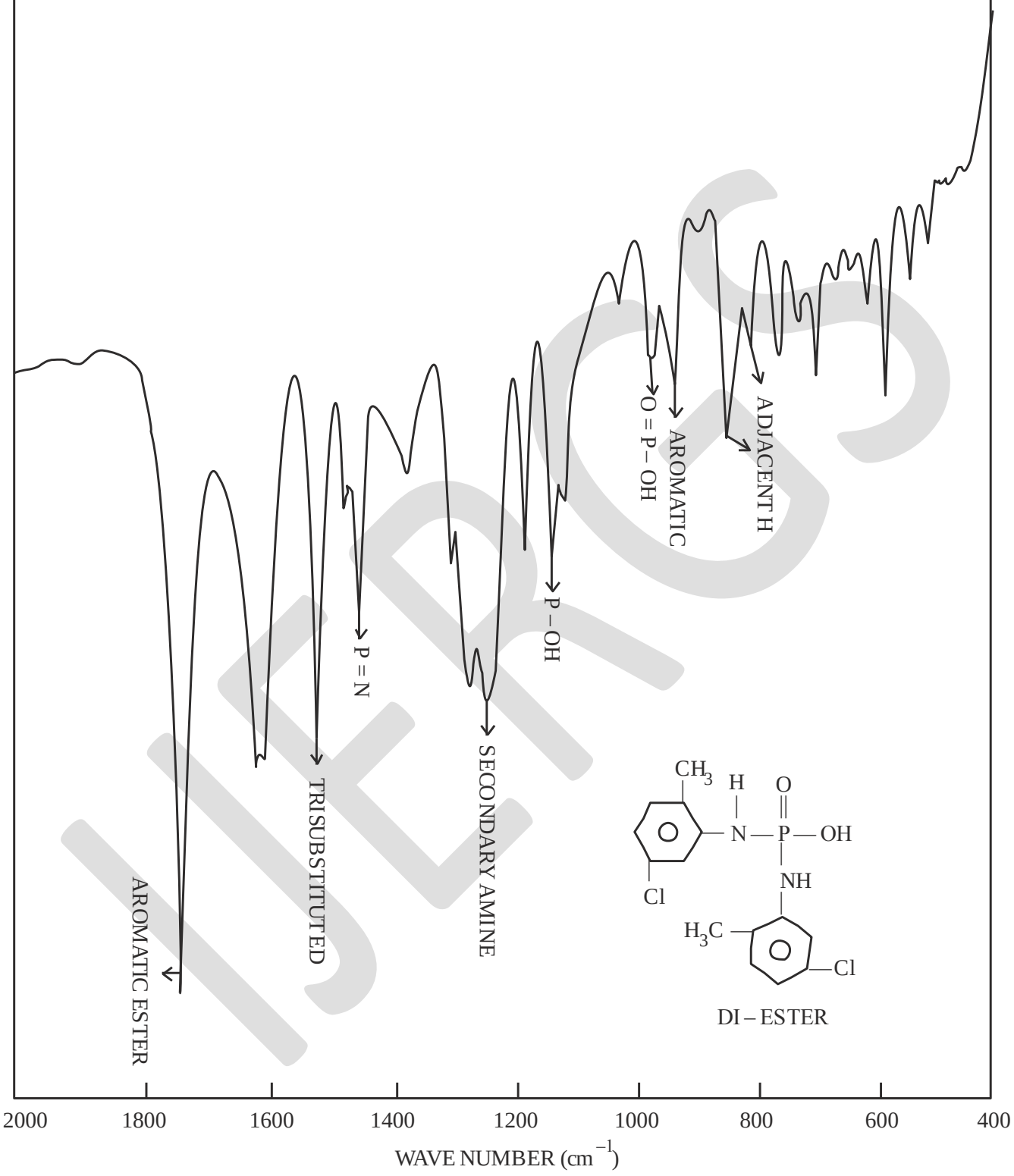

RESULT AND DISCUSSION :

HYDROLYSIS VIA CONJUGATE ACID SPECIES : The investigation of the hydrolysis of di- 5-chloro, 2-methyl aniline phosphate ester shows that it is reacitve via neutral, mono-negative and conjugate acid species. The kinetic study of the hydrolysis of above diester have been carried in acid and buffer media in the region 0.1 to 6.0 mol dm^{-3} and pH 1.24 to 7.46 at a temperature 80 $\pm$ 0.5°C. Kinetic runs were made in 20% aqueous dixon due to its solubility reasons. Table I and Fig II summarises the pseudo first order rate coefficient of the hydrolysis of 5-chloro, 2-methyl aniline phosphate diester.

TABLE 1. pH log RATE PROFILE OF DI-5-CHLORO, 2-METHYL ANILINE PHOSPHATE AT 80 $\pm$ 0.5°C

HCl (mol dm^{-3})	pH	10^5 ke.(mol dm^{-3} min^{-1}) (obsd.)	5 + log ke.
6.0	–0.778	58.24	1.74
5.0	–0.699	112.60	2.05
4.0	–0.602	197.66	2.29
3.0	–0.477	165.31	2.21
2.5	–0.400	146.29	2.16
2.0	–0.300	126.44	2.10
1.0	0.000	80.32	1.90
0.5	0.301	56.30	1.75
0.2	0.700	43.12	1.63
0.1	1.000	35.78	1.55
Buffers–			
Composition of buffers have been given in experimental section	1.24	29.16	1.46
	2.20	21.85	1.34
	3.30	17.37	1.24
	4.17	13.48	1.13
	5.60	9.77	0.99
	6.43	7.94	0.90
	7.46	6.76	0.83

FIG.II pH – log RATE PROFILE OF DI – 5 – CHLORO, 2 – METHYL ANILINE PHOSPHATE AT 80°C

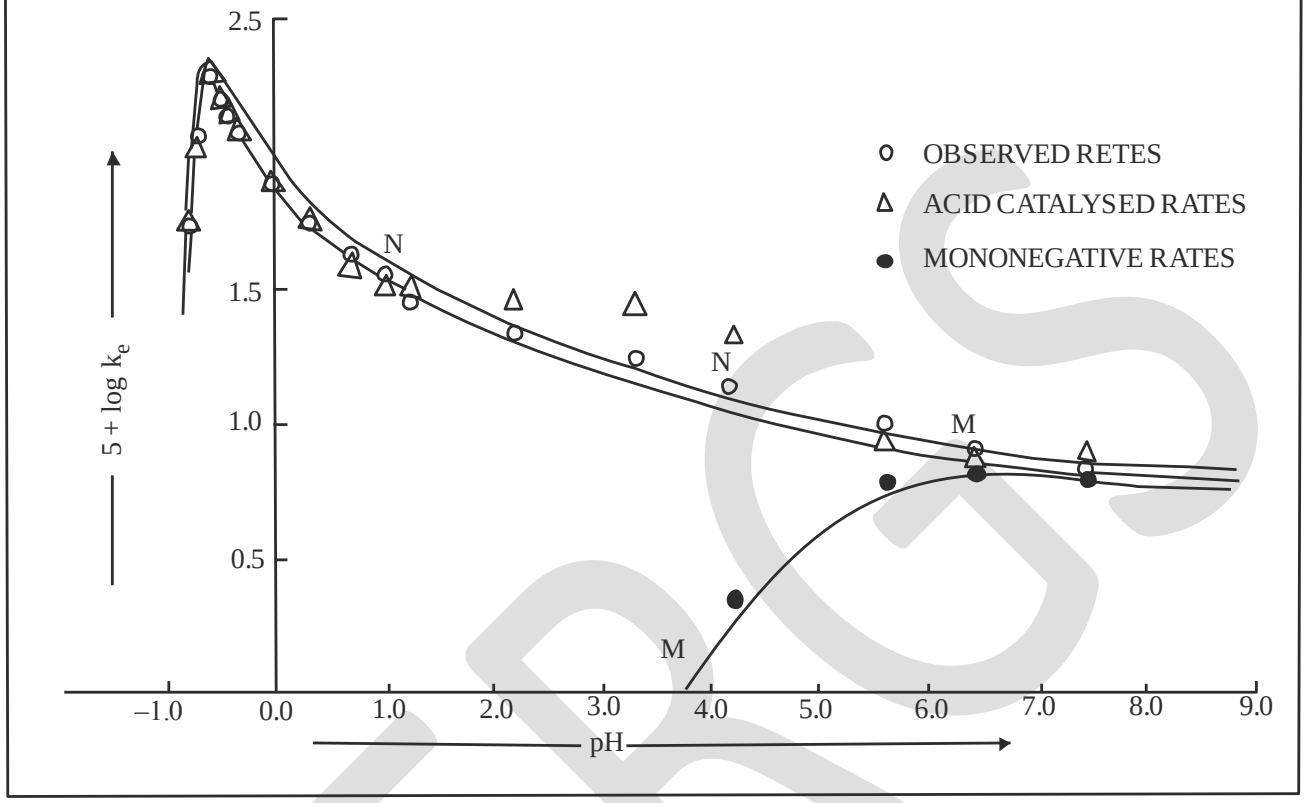

Result shows that the rate increases with the increase in acid medium upto 4.0 mol dm^{-3} HCl. Further rise in acidity bring about lowering in rates. This bend in pH log rate profile could be determined by carrying out kinetic runs at constant ionic strength. The cause of bend may be due to water activity effect or ionic strength effect or due to simultaneous action of both.

EFFECT OF IONIC STRENGH :

The ionic strength effect on the rate of hydrolysis of 5-chloro, 2-methyl aniline phosphate diester was examined by carrying out kinetic runs at different ionic strength by using appropriate mixture of KCl and HCl acid. Table-2 summarises the rate coefficient and Fig III describes a plot of log rate Vs acid molarities, which gives three linear curves indicating the presence of acid catalysis. Different intercepts on the rate axis are the neutral rate at corresponding ionic strength.

TABLE 2. HYDROLYSIS OF DL-5-CHLORO, 2-METHYL ANILINE PHOSPHATE AT CONSTANT IONIC STRENGTH AT 80°C

Ionic Strength (μ)	Composition		10^5 ke. (mol dm^{-3} min^{-1}) (obsd.)
	HCl (mol dm^{-3})	KCl (mol dm^{-3})	
1.0	0.2	0.8	34.01
1.0	0.4	0.6	44.72
1.0	0.6	0.4	55.00
1.0	0.8	0.2	63.04
1.0	1.0	0.0	77.56
2.0	0.2	1.8	27.20
2.0	0.5	1.5	43.13
2.0	1.0	1.0	61.72
2.0	1.5	0.5	88.43
2.0	1.8	0.2	98.63
2.0	2.0	0.0	108.10
3.0	0.5	2.5	36.11
3.0	1.5	1.5	70.10
3.0	2.0	1.0	87.63
3.0	2.5	0.5	106.72
3.0	3.0	0.0	129.00

FIG. III

HYDROLYSIS OF DI – 5 – CHLORO, 2 – METHYL ANILINE PHOSPHATE ESTER AT CONSTANT IONIC STRENGTH AT 80° C

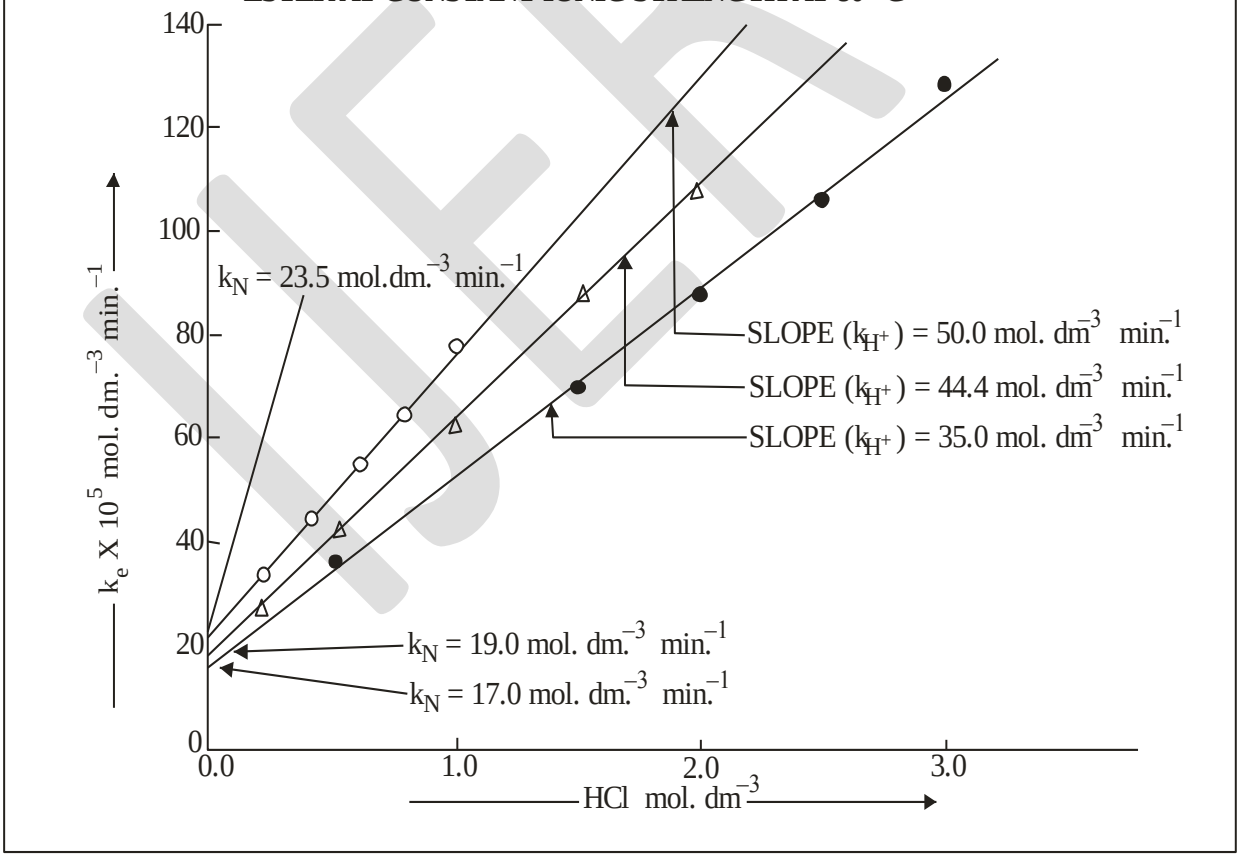

Variation of the neutral rates with ionic strength is governed by the following rate expressions.

$$K_H^+ = K_{H_0}^+ \exp b_H^+ . \mu \quad (1)$$

or, $$K_H^+ . C_H^+ = K_{H_0}^+ . C_H^+ \exp . b_H^+ . \mu \quad (2)$$

or, $$5 + \log K_H^+ . C_H^+ = 5 + \log K_{H_0}^+ + \log C_H^+ + b'_H^+ . \mu \quad (3)$$

where K_H^+, $K_{H_0}^+$, b'_H^+ and μ are specified acid catalysed rates at that ionic strength, at zero ionic strength and ion strength respectively

Similarly, the specific neutral rates may be represented as follows :

$$K_N = K_{No} \exp b_N . \mu \quad (4)$$

or, $$5 + \log K_N = 5 + \log K_{N_0} + b'_N . \mu \quad (5)$$

where K_N, K_{N_0}, b'_N and μ are specific neutral rates at that ionic strength, at zero ionic strength, a constant and ionic strength respectively where and b'_H and $b'_N = \frac{b}{2.303}$.

The equation (3) and (5) may be used to compute the acid catalysed and neutral rates at each experimental molarity. Thus both acid catalysed and neutral rates may be represented as :

$$K_e = k_H^+ . C_H^+ + K_N . (6)$$

The specific acid catalysed and specific neutral rates for the hydrolysis of dister which have been calculated from the above equations have summaruised in table 3.

TABLE 3. SPECIFIC ACID CATALYSED [K_H^+]AND SPECIFIC NEUTRAL [K_N] RATES FOR THE HYDROLYSIS OF 5-CHLORO, 2-METHYL PHOSPHATE DIESTER AT DIFFERENT IONIC STRENGTH AT 80°C.

Ionic Strength (μ)	**$10^5 K_H^+$ (mol dm^{-3} min^{-1})**	**5 + log K_H^+**	**$10^5 K_N$ (mol dm^{-3} min^{-1})**	**5 + log K_N**
1.0	50.0	1.69	23.5	1.37
2.0	44.4	1.64	19.0	1.27
3.0	35.0	1.54	17.0	1.23

With the help of above equations, theoretical rates can be calculated which are then compared with the experimental rates and there is a remarkable similarities between the two rates upto 4.0 mol. dm^{-3} HCl. The value of acid catalysed (5 + log $K_{H_0}^+$ = 1.77) and specific neutral rate (5 + log K_{N_0} = 1.46) can be otained from the intercepts on the rate axis while b'_H^+ = –0.031 and b'_N = – 0.033 can be obtained from the slopes of fig. IV

FIG. IV **HYDROLYSIS OF DI – 5 – CHILORO, 2 – METHYL ANILINE PHOSPHATE AT 80° C (log SPECIFIC RATE Vs IONIC STRENGTH)**

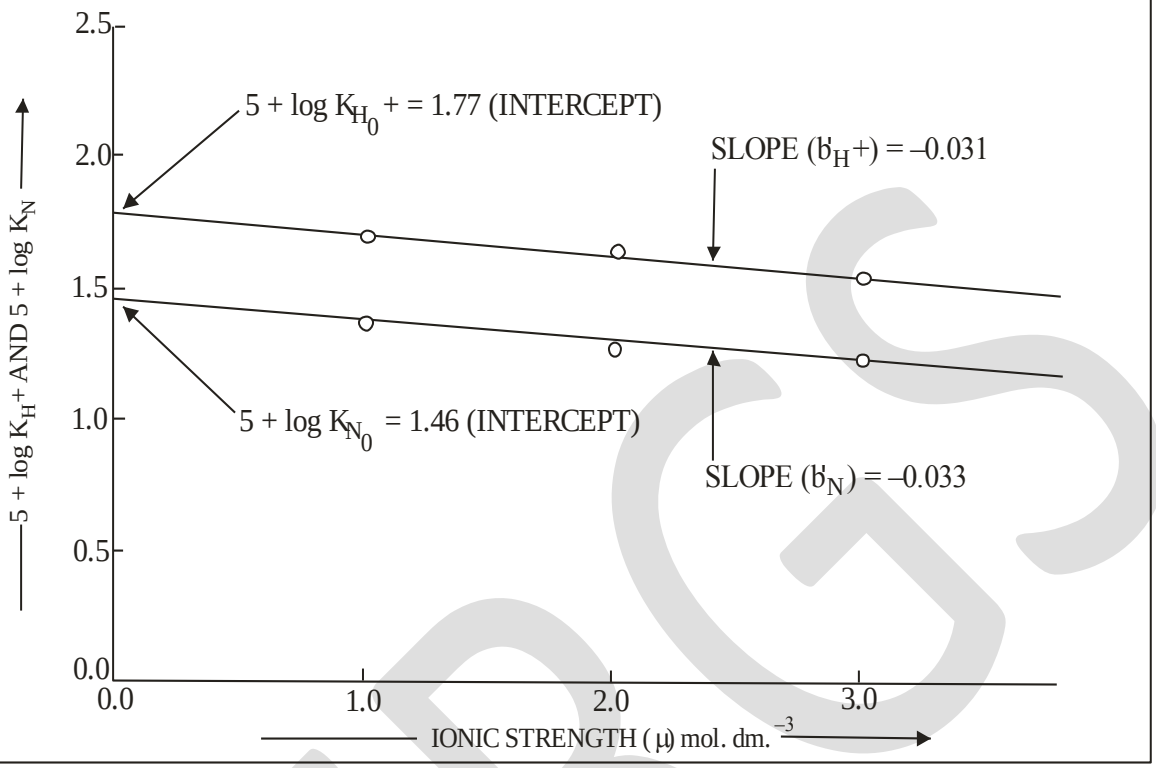

Table 4 summarises both the observed and calculated rates of hydrolysis of di-5-chloro, 2-methyl aniline phosphate at 80°Cin the acid region from 1.0 to 6.0 mol dm^{-3} HCl. It is clear from the results that there is fairly good agreement between calculated and experimentally observed rates upto 4.0 mod dm^{-3} HCl. There is steep fall in the rates, beyond 4.0 mol dm^{-3} HCl which has been presumed due to participation of water molecule as a second reaction partner in the nucleophilic substitution reaction. Thus acid catalysed and neutral rates have been calculated by the modified form suggested by Bronsted-Bjerrum [31, 32]

$$K_H^+ . C_H^+ = K_H^+ . \exp. b_H^+ . \mu \, (a_{H_2O})^n \qquad (7)$$

and its logrithmic form can be showed as :

$$5 + \log K_H^+ . C_H^+ = 5 + \log K_{H_0}^+ + \log C_H^+ + b'^+_H . \mu + n \log a_{H_2O} . \qquad (8)$$

and neutral rates at higher concentration are as follows.

$$K_N = K_{N_0} \exp. b_N . \mu \, (a_{H_2O})^n \qquad (9)$$

and its lognrithmic form can be showed as

$$5 + \log K_N = 5 + \log K_{N_0} + b'_N . \mu + n \log a_{H_2O} \qquad (10)$$

Where (a_{H_2O}) is water activity and n is an integer value.

TABLE 4 : CALCULATED AND OBSERVED RATES FOR THE HYDROLYSIS OF DI- 5-CHLORO, 2-METHYL ANILINE PHOSPHATE AT 80°C

HCl (mol. dm^{-3})	$10^5.K_N$ (mol.$dm.^{-3}$ min^{-1}) from. eq. (5)	$10^5. K_H. + C_H+$ (mol. dm. $min.^{-1}$) from eq. (3)	$10^5. K_H^+. C_H^+$ (mol.dm^{-1}) from eq. (8)	$10^5. KN$ (mol.dm^{-3}. $Min.^{-1}$) from eq. (10)	Ke. 10^5 (mol. $dm.^{-3}$ $min.^{-1}$) (calcd.) from eq. (6)	5+log Ke (calcd.)	10^5. Ke (mol. dm^{-3} $min.^{-1}$) (obsd.)
0.1	28.62	5.84	–	–	34.46	1.53	35.78
0.2	28.40	11.58	–	–	39.98	1.60	43.12
0.5	27.76	28.47	–	–	56.23	1.75	56.30
1.0	26.73	54.82	–	–	81.55	1.91	80.32
2.0	24.77	101.85	–	–	126.62	2.10	126.44
2.5	23.85	123.73	–	–	147.58	2.16	146.29
3.0	22.96	142.56	–	–	165.52	2.21	165.31
4.0	21.28	177.01	–	–	198.29	2.29	197.60
5.0	19.72	206.06	100.92*	9.66*	110.58	2.04	112.60
6.0	18.28	258.22	53.57*	4.25*	57.82	1.76	58.24

Where, n = 0 for 0.1 to 4.0 mol dm^{-3} HCl and n* = 2, 3 respectively for 5.0 and 6.0 mol dm^{-3} HCl for acid and neutral rates

Table 5 summarises Arrhenius parameters [33] of di-ester at 3.0 and 5.0 mol. dm^{-3} HCl. The magnitude of Arrhenius parameters fall is the range at bimolecular nature of hydrolysis. The value of activation enrgy (E) is very low i.e. < 25 kcal mol^{-1}, the value of entropy of activation ($\Delta S^{\neq}$) is negative and frequency factor (□) has power less than 12. Hence, the reaction proceeds bimolecularly via conjugate acid species.

TABLE 5 ARRHENIUS PARAMETER FOR THE RATE OF HYDROLYSIS OF DI-5- CHLORO, 2-METHYL ANILINE PHOSPHATE VIA CONJUGATE ACID SPECIES AT 80°C.

HCl (mol dm^{-3})	Parameters		Entropy – □$S^{\neq}$ (e.u)
	Energy of activation (E) Kcal. $mole^{-1}$)	Frequency factor (λ) (sec^{-1})	
3.0	21.50	5.56×10^7	20.80
5.0	21.96	7.30×10^8	20.30

Table 6 describes the comparative isokinetic rate data of some other similar substituted phosphate diesters (the bond-fission and molecularity of which are known). Fig V shows isokinetic relationship of 5-chloro, 2-methyl aniline phosphate diester with some other phosphate dieters. The linearity of the curve shows similarity of mechanism of present diester with other diesters of known mechanism, since the point at 5-choloro, 2-methyl aniline phosphate diester lies on the same line of other phosphate diester. Thus, 5-chloro, 2-methyl aniline phosphate diester undergo bimolecular hydrolysis with P–N bond fission.

TABLE 6: COMPARATIVE ISOKEINETIC DATA RATE DATA FOR THE HYDROLYSIS OF SOME PHOSPHATE DIESTER VIA THEIR CONJUGATE ACID SPECIES

S. No.	Phospate di-ester	Temp °C	Medium	E.K. (cals/ mole.)	-□ S ≠ (e.u)	Bond fission	Molecularity	Reference
1.	2,6-di-methoxy phenyl	98	–	31.56	2.57	P–O	–	34
2.	□-naphthyl amine	98	2.5	23.57	12.71	P–N	2	35
3.	p-phenatidine	98	3.0	20.55	31.84	P–N	2	36
4.	m-nitroaniline	98	3.0	16.61	31.90	P–N	2	35
5.	p-bromoaniline	50	3.0	9.15	55.98	P–N	2	37
6.	p-chloroaniline	90	3.0	9.15	56.78	P–N	2	37
7.	2, 4-dinitrodi phenylamine	25	3.0	7.59	52.5	P–N	2	38
8.	4-chloro, 3,5, di-methylphenyl	98	–	29.75	22.02	P–O	–	39
9.	o-toluidine	50	1.0	11.49	38.66	P–N	2	40
10.	Cylohexyl amine	50	5.0	12.09	37.11	P–N	2	41
11.	p-propoxyaniline	97	3.0	23.79	17.98	P–N	2	42
12.	5-chloro, 2-methyl-aniline	80	3.0	21.50	20.80	P–N*	2	This work
		80	5.0	21.96	20.30	P–N*	2	This work

* Bond fission assumed

FIG.V **COMPARATIVE KINETIC RATE DATA FOR THE HYDROLYSIS OF SOME PHOSPHATE DI – ESTERS VIA THEIR CONJUGATE ACID SPECIES**

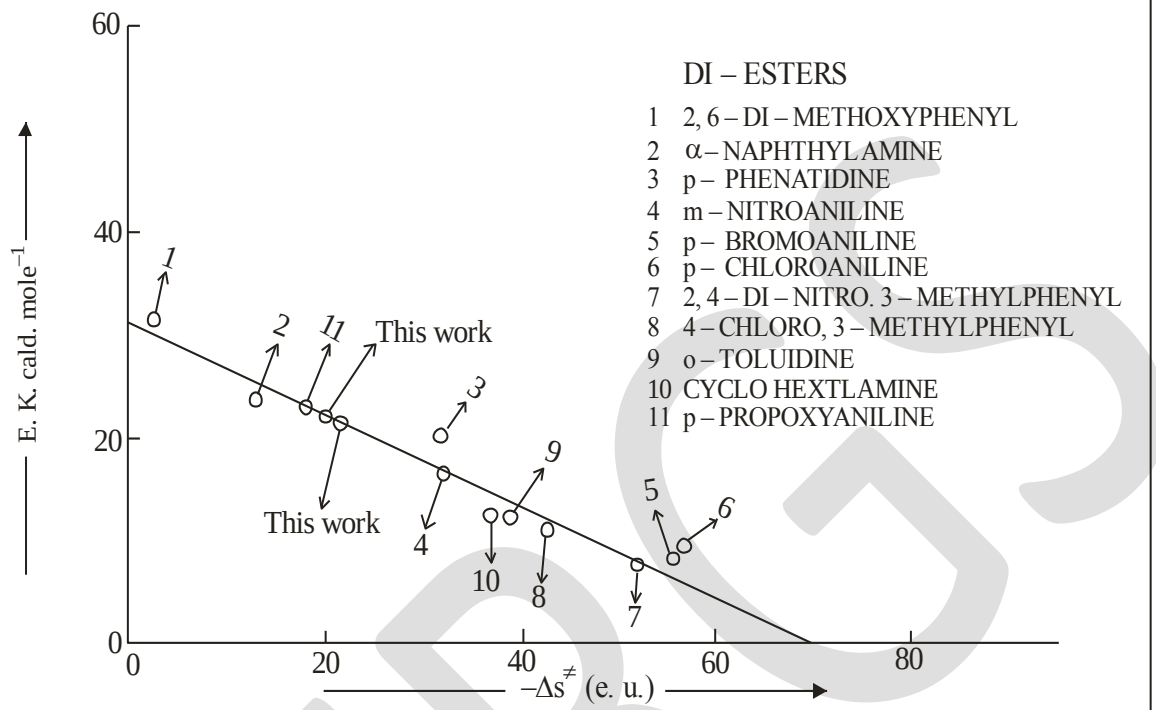

Bimoleular mechanism of 5-chloro, 2-methyl aniline phosphate diester is also supported by Hammett relationship [43–45] (Slope value = 0.31), Zucker- Hammet plot [46] (Slope value = 0.66), Bunnett plot [47,48] (slope value □ = 10.0 and □* = 5.0) and Bunnett-olsen plot [49] (□ = 1.63) (Figs.not shown)

MECHANISM : Taking into account all the above consideration, the most probable reaction path via conjugate acid species of di-5chloro, 2-methyl aniline phosphate ester may be formulated as

(I) Formation of conjugate acid species by fast pre equilibrium Proton transfer :

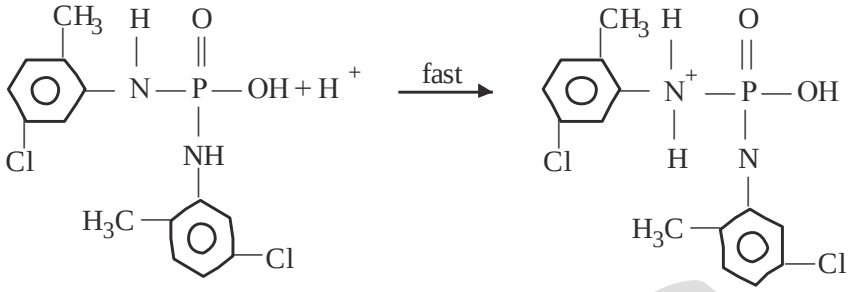

(Neutral species) (Conjugate acid species)

(II) Bimolecular heterolysis of conjugate acid species involving P–N bond fission $S_{N}2$ (P) :

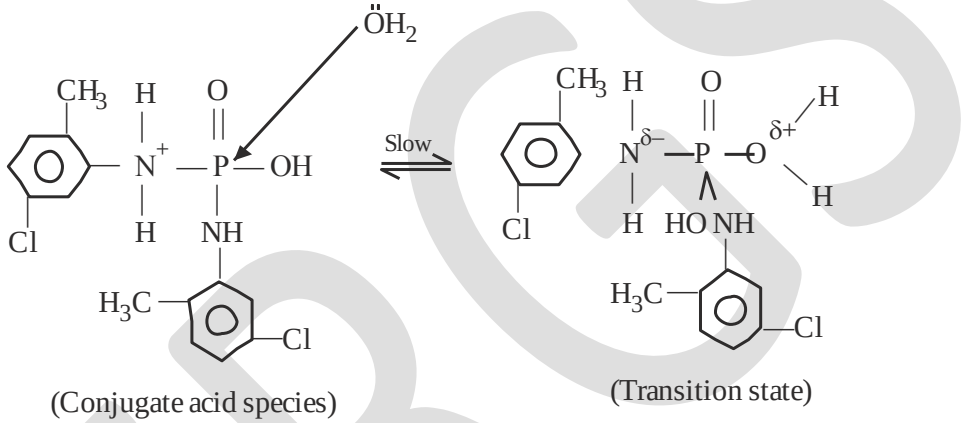

(Conjugate acid species) (Transition state)

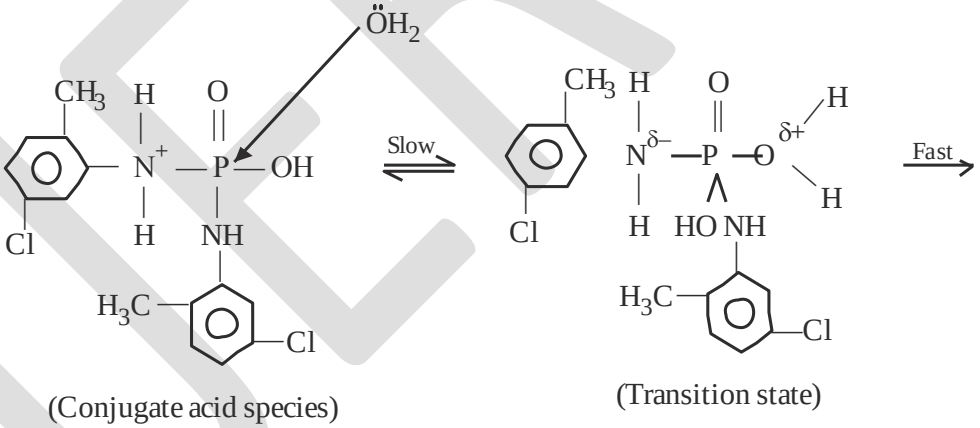

(Conjugate acid species) (Transition state)

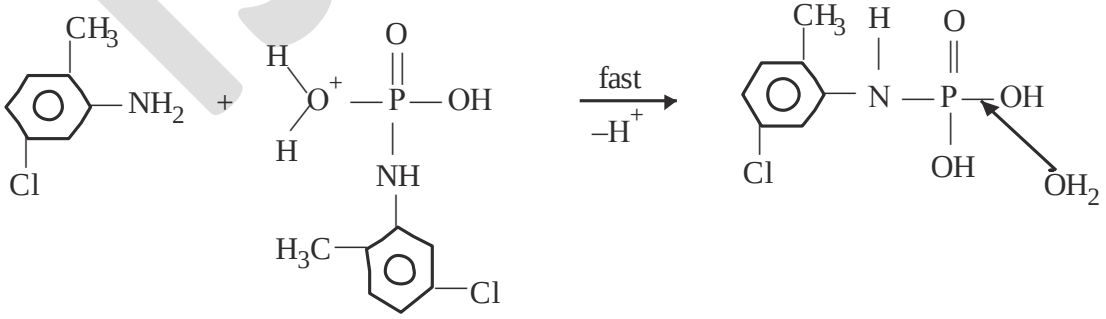

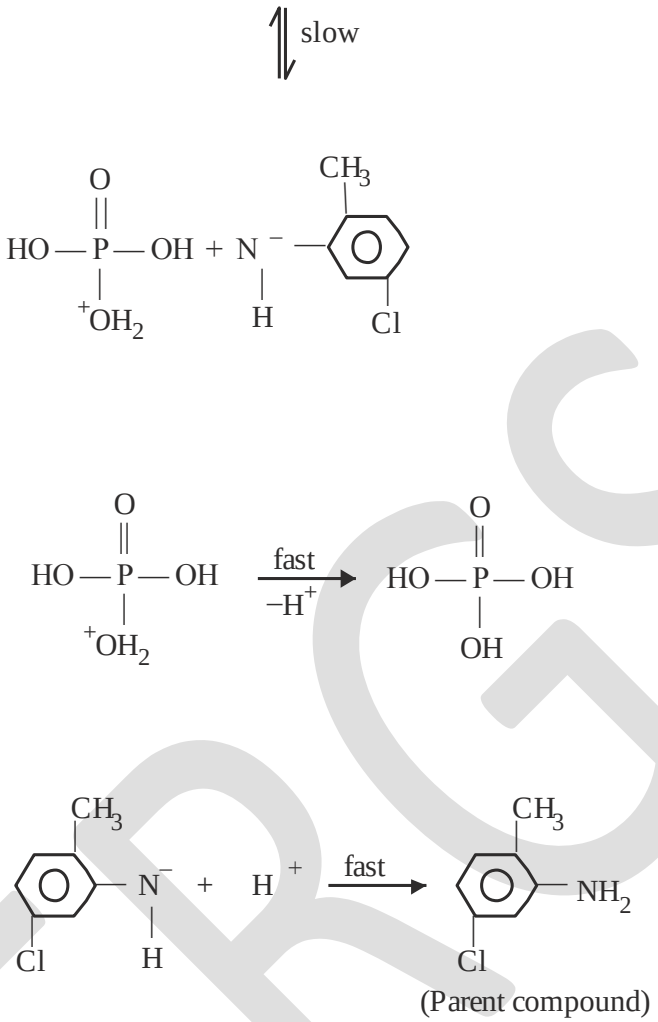
slow
fast
fast
(Parent compound)

REFERENCES:

1. Allen, R.J.L., *Biochem J.* (34), (1940)

2. Cox, J.R. and Ramsay, O. B., *chem.. Rev.* (64) No.4, 317-352 (1964).

3. Mejia–Radillo, Yamilet–Yastsimissky. Anatoly, K., *Inorganic Chemica. Acta, Vol.* (328), 241–246 (2002).

4. Tiwari, B.K, Chaudhary, A. and Dixit, D.K., *Acta Ciencia Indica*, *vol* (XXIVC) *No* 1, 015 (1998)

5. Tewari, B.K., Ph.D. Thesis, Agra Univ., Agra (1985).

6. Kumar, Abanish, Ph.D. Thesis, Dr. B.R.A. Univ., Agra (2013)

7. Kumar, Raman, Ph.D. Thesis, Dr. B.R.A., Univ. Agra (2013).

8. Verma, Devdutt, Ph.D. Thesis, Dr. B.R.A., Univ. Agra (2013)

9. Shindhe, C.P., Nikam, A.R. and Mhala, M.M., *Acta Ciencia Indica, Vol.* (XIIC), No. 1, 46 (1986).

10. Kushwaha, R.S., Tiwari, B.K., Singh, P., Upadhayaya, S and Sharma Indu Shekhar, *Journal of Indian Council of Chemists*, Vol. (IV), No. 3 (1988).

11. Singh Archana and Prabha, Shashi, *Asian J. of Chem*. Vol (8) No. 1, 129–133 (1996).

12. Saxena, Amrita, Ph.D. Thesis, Dr. B.R.A. Univ., Agra (2014).

13. Singh, Sanchita, Ph. D. Thesis, Dr. B.R.A. Univ., Agra (2014).

14. Singh, Pratap and Kumar, Abanish, *J. of Indian council of Chemists*, Vol (28) No. 1 P– 56–69 (2011).

15. Chaudhary, Gaurav, Ph.D. Thesis, Dr. B.R.A. Univ., Agra (2013).

16. Patel, Anil, Ph.D. Thesis, Dr. B.R.A. Univ., Agra (2012).

17. Tiwari, B.K., Agarwal (Miss) Anupam, Parihar, P.S., Dixit, V.K., Kadam (Miss) Rishika, Singh, R. and Singh, P., *Asian Journal of Chem.*, Vol. (18), No. 4 (2006).

18. Tiwari, B.K., Chaturvedi, K. and Chaudhary, A., *Acta Ciencia. Indica*, Vol (XXVIC), No.2, 053 (2000).

19. Singh, R.K. and Gupta, Ruchi, *Acta Ciencia Indica*, Vol. (XXIVC), No. 1, 055 (2003).

20. Tiwari, B.K., (Miss) Kanta, Solanki, (Miss) Ashita, David (Miss) Shweta, Rajput, R.P. *Acta Ciencia Indica*, Vol (XXVIIC), No. 3, 113–124 (2001).

21. Tiwari, B.K., solanki (Miss) Ashita, David (Miss) Shweta, (Miss) Kanta, Sharma, Ajay, *Acta Ciencia Indica*, Vol. (XXVIIC). No. 3, 129–141 (2001).

22. *The Chemistry of organophosphorous Pesticides Fert.*, K.J. Schimidt, Springer Verlog Berlin Heideiberd, New York (1973).

23. Metcalf, R.L., *Organic pesticides*, Interscience publicshers, New York, Chapter (XI), 255–261 (1955).

24. *Chemical Abstrat*, No. (154), 1993 : (1960).

25. Schrader, G., Entwicklung newer, *"Insecticide of Grudlaye Organischerflour and Phophoverbi no dungen."* Verlag Chemic, Winheim, Bergster (1952).

26. Schlesinger, A.H., C.A., (49) 5517^{e} (1955).

27. Maquire, M.H. and shaw, *G.J., Cheam. Soc.*, 1979–82 (1953).

28. Barnard, P. W.C., Bunton, C.A., Killerman, D., Mhala, M.M. Silver, B., Vernon, C.A. and Welch, V.A., *J. Chem. Soc.*, Sec (B), 227–235 (1966).

29. Paul Otto. Ber., (28), 816 (1895).

30. Rudert, P., Ber., (26), 565 (1893).

31. Bronsted, J., *Z. Physik, Z. Chem.,* (102), 169 (1992); (115), 237 (1925).

32. Bjerrum, N., Z. *Physik, Z. Chem.,* 108, 82 (1924) ; 118, 251 (1925).

33. Arrhenius, S., Z. Physik chem., 4 226 (1989).

34. Prabha (Miss.), Shashi, Ph. D. Thesis, Jiwaji Univ. Gwalior (1971).

35. Bhoite, A.K., *"Kinetic study of hydrolysis of compds.containing C,N and P* (C-N-P) *Linkage"* Ph.D. Thesis, Jiwaj Univ., Gwalior (1977).

36. Kulshrestha, K., Ph. D. Thesis, Jiwaji Univ., Gwalior (1982).

37. Bhadoria, Singh, K.A., Ph. D Thesis, Jiwaji Univ., Gwalior (1982).

38. Dubey, R., Ph. D. Thesis, Jiwaji Univ., Gwalior (1993).

39. Kushwaha, R.S., Ph.D. Thesis, Jiwaji Univ., Gwalior (1980).

40. Sagne, A.N., Ph. D. Thesis, Jiwaji Univ., Gwalior (1972).

41. Chauhan, K.P.S., Ph. D. Thesis, Jivaji Univ., Gwalior (1977).

42. Chaudhary, Amit., Ph.D. Thesis, Dr. B.R.A. Univ., Agra (1998).

43. Hammett, L.P., *"Physical Organic Chemistry",* McGraw-Hill Book Co. Ltd., London, 273 (1940).

44. Hammett, L.P. and Dyrup, A.J., *J. Am. Chem. Soc.*, (54), 2721 (1933).

45. Long, F.A. and Paul, M.A., *Chem. Revs.*, (57) (1957).

46. *Zucker, L. and Hammett, L.P., J. Am. Chem. Soc.*, (61) 2779–2785 (1939).

47. Bunnett, J.F. *J. Am. Chem. Soc.*, (83). 4956, 4968, 4973, 4978 (1967).

48. Bunnett J.F. *"Technique of Organic Chemistry",* Vol III ed. A weisaberger, *"Rates and mechanism of reactions"* Part (I), Ch VI., Pg. 177 (1961).

49. Bunnett J.F. and Olsen F.P., *Canada. J. Chem.*, (44) 1971 (1966).

International Journal of Engineering Research and General Science Volume 3, Issue 6, November-December, 2015
ISSN 2091-2730

Li-Fi – A CHANGE TOWARDS FUTURE

Naman Jain, Ved Sharma
Department of Electronics and Telecommunication, TCET,
Email id: namannrj@gmail.com Contact no: 8080012317
Email id: vslethal@gmail.com Contact no: 8898498776

ABSTRACT: As the number of electronic gadget is constantly increasing day-by-day, the demand for wireless data transmission i.e. internet is also increasing rapdily. The slow speed in transmission of data, stealing data from neighbour or competing for bandwidth wherever free internet is available are some of the common traits that are observed these days. Whenever many device access wireless internet, the transmission speed of data reduces considerably. To oversome these problems the solution available is "Data through illumination" or "Visible Light Communication" and the technology is known as "Li-Fi"

Li-Fi can be used as a complementary technology to Wi-Fi as it uses LED light for the transmission of data. Light being the fastest travelling 'thing' in the universe ensures the faster transmission of data than Wi-Fi and also light is almost present everywhere ensures uninterrupted communication. The bit-rate achieved by Li-Fi can never be matched bt Wi-Fi.
Li-Fi is the transfer of data through light by taking fiber out of fiber optics and sending data through LED light. In this paper we are going to emphasize on various aspects of Li-Fi technology such as its working, its advantages over Wi-Fi, features and applications.

KEYWORD: Li-Fi, Wi-Fi, LED, VLC, Radio Frequency waves, light, speed, transmission of data.

I. INTRODUCTION

Li-Fi stands for "Light Fidility". Li-Fi is a Visible Light Communication (VLC) technology developed by a team of scientists including Dr Gordon Povey, Prof. Harald Haas and Dr Mostafa Afgani at the University of Edinburgh. Li-Fi is similar to Wi-Fi as it is bi-directional, high speed and fully networked wireless communication technology. In simple terms Li-Fi can be considered as a light based Wi-Fi as it uses light instead of radio waves for transmission of data. Li-Fi would use transceiver-fitted LED lamps that can light a room as well as transmit and receive information in the form of data. Since simple light bulbs are used, there can technically be any number of access points.

This technology makes use of a segment of electromagnetic spectrum that is not utilised efficiently even today- The Visible Spectrum. Over the years light has played a major role in our life and light doesn't have any significant ill-effects. Moreover a huge amount of space is unoccupied in this spectrum.

The basic ideology behind this technology is that LED light whose intensity varies quicker than the human eye can be used for transmission of data way quicker than the technology available that is Wi-Fi. Encoding of data in the light can be done by varying the rate at which LED flickers ON and OFF,giving strings of 0's and 1's.

The testing of Lifi technology in the labs have achieved a blistering high speeds. Researchers at the Heinrich Hertz Institute in Berlin, Germany, have reached data rates of over 500 Megabytes/seconds by just using a standard white-light LED.The maximum speed that can be obtained in transmission of data for Li-Fi technology is 10 Gbit/s whereas for Wi-Fi it is only about 54Mbit/s.

II. WORKING OF LIFI TECHNOLOGY

Dull performance of Wi-Fi technology can be overcome with the use of Li-Fi technology. Li-Fi technology typically makes use of white LED bulbs at the downlink transmitter.

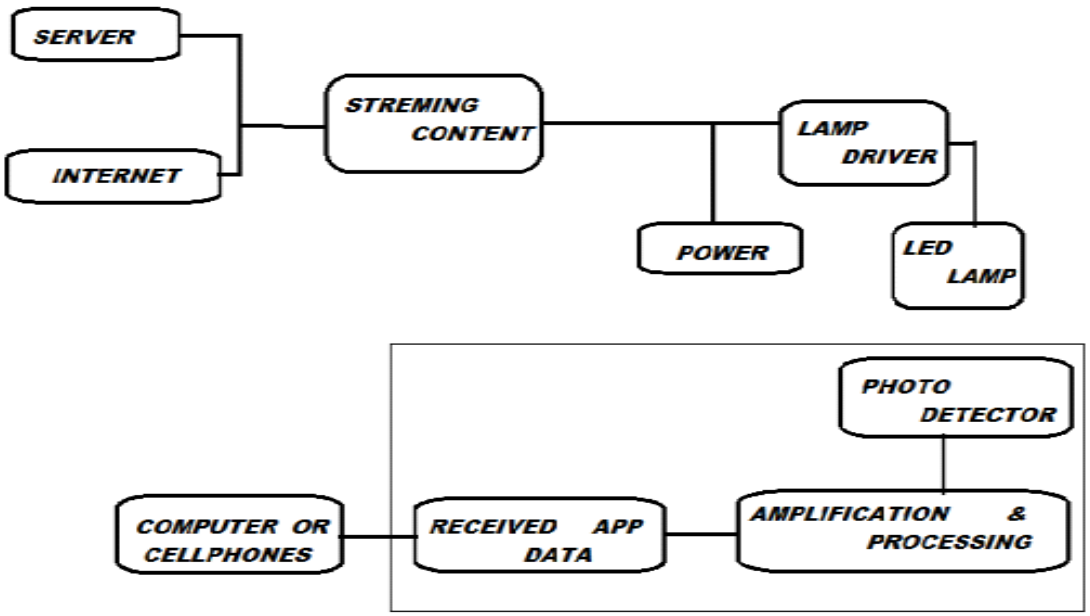

Fig. 1 WORKING OF Li-Fi

A constant current is applied to the LED bulb resulting in emission of photons which is observed as visible light. However, by varying the current, the optical output of very high speed can be achieved. LED being a semi-conductor device, the current and output can be modulated at very high speeds and can be detected using photo-detector device.

The Li-Fi setup is based on this property of optical current. The operational methodology is very simple- inorder to transmit a 1, LED bulb has to be switched ON and inorder to transmit a 0, LED bulb has to be switched OFF. The LED can be switched ON and OFF at a very speed resulting in formation of array of information that is to be transmitted at a very high speed. Hence, only variation in the rate of LED's flicker has to be done according to the data that we want to encode.

Further enhancements can be made by using lights of different colors to change the frequency of light with each frequency encoding a different data channel.

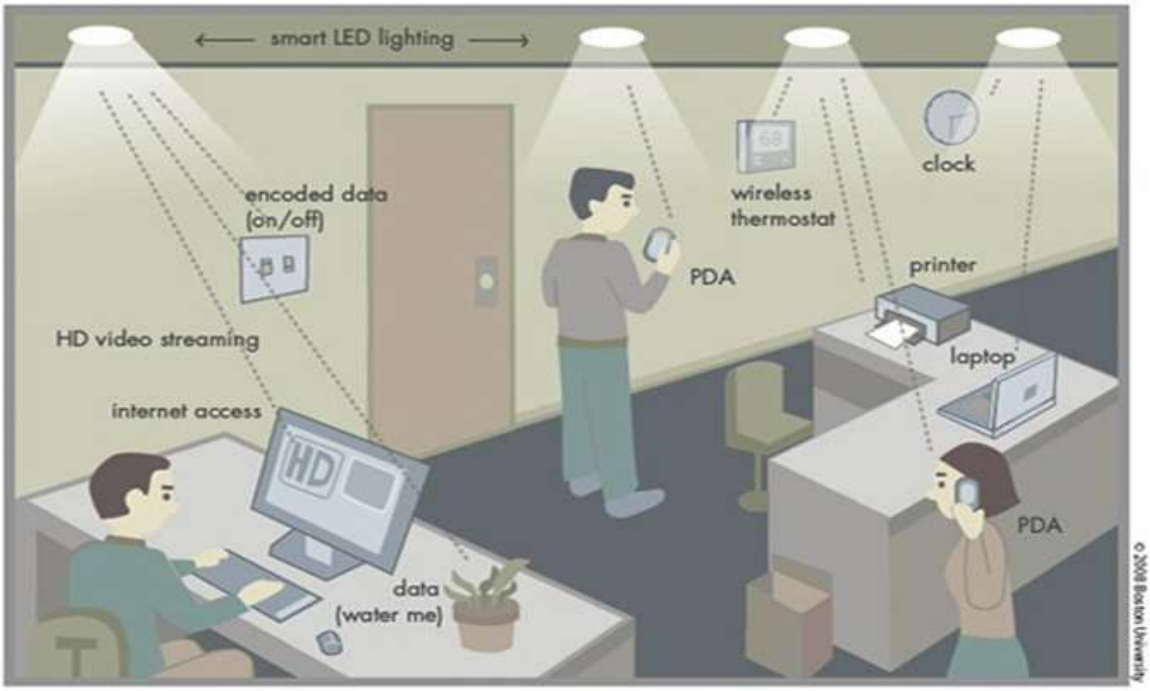

Fig. 2 Li-Fi system connecting devices in a room.

Li-Fi technology makes use of direct modulation techniques similar to those used in low-cost infra-red communications devices such as remote control units whereas Wi-Fi makes use of radio frequency communication which requires radio circuits, antennas and complex receivers.

III. STANDARDS

Like Wi-Fi, Li-Fi technology also makes use of 802.11 protocols but instead of using radio frequency waves for transmission of data it makes use of Visible Light Communication (VLC) which has a much wider bandwidth. IEEE 802.11 is a set of specifications of Media Access Control (MAC) and Physical Layer (PHY) for setting a Wireless Local Area Network in different frequency bands which includes 2.4, 3.6, 5, and 60 GHz. The MAC layer allows using the link with different layers as with TCP protocol. This standard is capable to transmit data in the form of audio, video and multimedia services at very high speed. It considers various parameters such as optical transmission mobility, its compatibility with artificial lighting present in infrastructures, and the interference which may be generated by ambient lighting.

IV. COMPARISON BETWEEN Li-FI AND Wi-Fi

Li-Fi and Wi-Fi can be compared on various parameters which are as follows:

Parameter	Li-Fi	Wi-Fi
Speed	***	***
Range	*	**
Security	***	**
Data Density	***	*
Reliability	**	**
Power Available	***	*
Ecological Impact	*	**
Transmit/Receive power	***	**
Device-to-device connectivity	***	***
Obstacle interference	***	*
Bill of Materials	***	**
Market maturity	*	***

Table 1: Wifi v/s Lifi based on parameters

Comparison based on features:

SR. NO	Li -Fi	Wi-Fi
1	Data transmission takes place using bits.	Data transmission takes place using radio waves.
2	Fast speed internet (1- 3.5Gbp0073)	Comparatively slow speed (54-250 Mbps)
3	Range is limited (10 Meters)	Extended range (20-100 meters)
4	The Spectrum range is 10000times than Wi-Fi	It has radio spectrum range
5	It uses Point-To-Point network topology	It uses Point-To-Multi network topology.
6	It uses light as its data transfer medium	It uses radio spectrum as data transfer medium.
7	It is cheaper because free band doesn't need license and it uses light	Expensive because it uses radio spectrum.
8	The frequency band is 100 times of Tera Hz	The frequency band is 2.4GHz.
9	Data density is high	Data Density is comparatively low
10	Lifi is more secured	Comparatively less secured

Table 2: Wifi v/s Lifi based on features

V. APPLICATIONS

With the growing number in the use of LED light, the number of applications increases. Some of the applications are as follows:

- **Medical applications:** Unlike the Wi-Fi technology, Li-Fi technology makes use of LED light, which is not hazardous to the patient in the hospital.
- **Education System:** As the speed for internet access of Li-Fi is greater than Wi-Fi, it can replace it in the educational institutes and companies.
- **Aviation:** Wi-Fi can't be used in aircraft industry as the radio waves could interfere with the navigation system of the aircraft but Li-Fi makes use of light. Therefore, Li-Fi can be used for internet access by the passengers from every light source available such as overhead lights.
- **Underwater communication:** The signal absorption rate is stronger in water making RF use impossible. Also RF waves disturb marine life making use of Wi-Fi difficult but these problems can be overcome by using Li-Fi technology.
- **Toys:** Many toys have LED and these can be used as a mode of communication without any hazardous effect.
- **Applications in Hazardous environments:** Safer alternative is provided by VLC technology in the form of Li-Fi in sensitive areas such as mines, power plants, etc.
- **Smart Lighting:** Any public or private lighting such as street lights can be used for both lighting purpose and as a Li-Fi hotspot for transmission of data.

VI. ADVANTAGES

Li-Fi technology makes use of light for transmission of data unlike Wi-Fi which uses Radio Frequency waves. So, due to this there are many advantages of Li-FI over Wi-Fi:

- **Capacity:** The transmission of data is effectively possible as the bandwidth of light is 10000 times greater than the bandwidth of radio waves. Therefore, the capacity of Li-FI is greater than that of Wi-Fi.
- **Availability:** Light is omni-present, hence, Li-Fi is also present everywhere but for better transmission LED light is necessary.
- **Bandwidth:** The bandwidth of light is 10000 times greater than that of radio waves and unlicensed.
- **Low Cost:** Light is unlicensed and free to use, also a very few components are required making it cheap.
- **Data Density:** One of the drawback of RF waves is that it tends to spread out and cause interference. About 1000 times the data density can be obtained by Li-Fi as light can be contained in a tight illumination area.
- **Security:** Stealing data form neighbour is a common trait observed these days but this problem can be solved using Li-Fi technology as light cannot penetrate through walls.
- **Eco-friendly:** RF waves are hazardous to both human life as well as marine life but light is non-hazardous making the technology eco-friendly.
- **Efficiency:** LED light consumes less energy making it more efficient.

VII. LIMITATIONS

- If anything comes in the way of propagating light towards reciever, the transmission of data is cut then and there itself.
- The light waves cannot penetrate through walls making the range for transmission smaller.

VIII. CONCLUSION

With the number of electonic devices increasing every minute, there is a possibility that Li-Fi technology soon becomes reality. On implementation of this technology, every bulb could be then used a Li-Fi hotspot with better transmission rate of data.

Implementing this technology will have a direct impact on environment making it cleaner and greener as this technology uses light for transmission of data and light does not have any ill-effects on environments unlike Wi-Fi which makes use of RF waves which are hazardous in nature.

Medical applications is one of the brighter side to this technology as Wi-Fi could not be used for such applications.Also with the increase in number of Wi-Fi users the speed for transmission od data has reduced and price for the service has increases. Thus, Li-Fi can overcome all these problems and can be used cheaply and readily.

REFERENCES:

[1] http://en.wikipedia.org/wiki/Li-Fi

[2] http://www.lifi.com/pdfs/techbriefhowlifiworks.pdf

[3] Haas, Harald (July 2011). "Wireless data from every light bulb", TED Global. Edinburgh, Scotland.

[4] PoojashreeN.S, P. Haripriya, Muneshwara M.S , Anil G.N, International Journal on Recent and Innovation Trends in Computing and Communication, ISSN: 2321-8169 288 – 291, Volume: 2 Issue: 2, February 2014.

[5] Sinku U. Gupta, Research on Li-Fi Technology & Comparison of Li-Fi/Wi-Fi, International Journal of Advanced Research in Computer Science and Software Engineering, ISSN: 2277 128X , Volume 5, Issue 6, June 2015.

[6] http://studymafia.org/wp-content/uploads/2015/02/ECE-Li-Fi-Technology-report.pdf

[7]http://www.ispreview.co.uk/index.php/2013/01/tiny-led-lights-set-to-deliver-wifi-style-internet-communications.html

[8] http://groupivsemi.com/working-lifi-could-be-available-soon

[9] Richard Gilliard, Luxim Corporation, ―The lifi® lamp high efficiency high brightness light emitting plasma with long life and excellent color quality.

[10] Visilink, ―Visible Light Communication Technology for Near-Ubiquitous Networking‖ White Paper, January 2012.

[11] Jyoti Rani, PrernaChauhan, RitikaTripathi, ―Li-Fi (Light Fidelity)-The future technology In Wireless communication‖, International Journal of Applied Engineering Research, ISSN 0973-4562 Vol.7 No.11 (2012).

[12] Tony Smith (24 May 2012)."WTF is... Li-Fi? Optical data transfer's new leading light?".The Register. Retrieved 22 October 2013.

International Journal of Engineering Research and General Science Volume 3, Issue 6, November-December, 2015
ISSN 2091-2730

MECHANICAL AND DURABILITY PROPERTIES OF HSC USING RHA, QUARRY DUST AND POLYPROPYLENE FIBER

N.Rishinath, S.P.Kanniyappan, A.Krishnamoorthi

Assistant Professor, Adhiparasakthi College of Engineering, Kalavai, Tamilnadu, India
rishinathnehru@gmail.com, +91 7200272439

Abstract- In the past two decades, construction sector has made a tremendous change in the dimensions of its boundaries. Because of mankind's unpredictable innovation added along with the technological advancements, unimaginable architectural designs have been made into existence only because of the advanced building materials which helped to get the required physique for the structure without adjusting any collapse and serviceability criteria. As concrete is considered as important building material, lots of variations has been made in the type of cement to be used as well concrete making technology in order to make the structure adaptable in any environmental condition as well fulfill the conditions for which it has been constructed. The most recent innovation in concrete technology is the "High Strength Concrete". As the name suggests, this type of concrete are very strong and makes the concrete structure to be highly resistant to environmental hazards.

The waste products from different sectors are considered to be harmful for disposal and hence turned to be an issue. With the innovation of using these waste by-products as a replacement of basic ingredient in concrete, an effective and efficient way of disposing them has come into act. This study examines the properties of High Strength Concrete (HSC) having Quarry dust by completely replacing natural river sand and partial replacement of cement with 5%, 10%, and 15%, of Rice Husk Ash (RHA), and 0.3% of polypropylene fiber.

Keywords

Cement, Coarse aggregate, Quarry dust, Rice Husk Ash, Polypropylene fiber, super plasticizers, High strength concrete, Fiber reinforced concrete, compression test, Split tensile test, Flexural test, Beam test, Acid attack, Sulphate attack, Alkaline attack.

INTRODUCTION

The world at the end of the 20th Century that has just been left behind was very different to the world that its people inherited at the beginning of that Century. The latter half of the last century saw unprecedented technological changes and innovations in science and technology in the fields of communications, medicine, transportation and information technology, and in the wide range and use of materials. The construction industry has been no exception to these changes when one looks at the exciting achievements in the design and construction of buildings, bridges, offshore structures, dams, and monuments, such as the channel tunnel and the millennium wheel. There is no doubt that these dramatic changes to the scientific, engineering and industrial face of the world have brought about great social benefits in terms of wealth, good living and leisure, at least to those living in the industrialized nations of the world.

Extensive research has now established, beyond a shadow of doubt that the most direct, sound and economically attractive solution to the problems of reinforced concrete durability lies in the incorporation of finely divided siliceous materials in concrete. The fact that these replacement materials, or supplementary cementing materials as they are often known and , such as Pulverized Fuel Ash (PFA), Ground Granulated Blast Furnace Slag (GGBS), Silica Fume (SF), Rice Husk Ash, Natural Pozzolana, and Volcanic Ash are all either pozzolanic or cementitious make them ideal companions to Portland Cement (PC).

CONCRETE AND ENVIRONMENT

Concrete as a construction material is still rightly perceived and identified as the provider of a nation's infrastructure and indirectly, to its economic progress and stability, and indeed, the quality of life. It is so easily and readily prepared and fabricated into all sorts of conceivable shapes and structural systems in the realms of infrastructure, habitation, transportation, work and play. Its great simplicity lies in that its constituents are most readily available anywhere in the world; the great beauty of concrete, and probably the major cause of its poor performance, on the other hand, is the fact that both the choice of the constituents, and the proportioning of its constituents are entirely in the hands of the engineer and the technologist.

The most outstanding quality of the material is its inherent alkalinity, providing a passivating mechanism and a safe, non-corroding environment for the steel reinforcement embedded in it. Long experience and a good understanding of its material properties have confirmed this view, and shown us that concrete can be a reliable and durable construction material, and plays a rightful role and large quantum of concrete is being utilized. River sand, which is one of the constituents used in the production of conventional concrete, has become highly expensive and also scarce. In the backdrop of such a bleak atmosphere, there is large demand for alternative materials from industrial waste.

ENHANCED PROPERTIES OF RHA CEMENT

Portland cement produces an excess of lime. Adding a Pozzolana, such as RHA this combines with lime in the presence of water, results in a stable and more amorphous hydrate calcium silicate. Laboratory research and field experience has shown that careful use of pozzolana is useful in countering all of these problems. The RHA is not just a "filler", but a strength and performance enhancing additive, its chemical properties are listed in the table 1.

This project present the usage of Rice Husk Ash (RHA) as a replacement along with cement, feasibility of the usage of quarry dust as hundred percent substitutes for river sand and with polypropylene fiber as admixture. Tests were conducted to ensure there mechanical strength and durability studies were done for concrete with RHA, quarry dust and polypropylene fiber and compared with conventional concrete.

Table 1 Chemical Composition of RHA

Sl.No	Parameters	Values
1	Silicon dioxide (SiO_2)	87.20%
2	Aluminum oxide (Al_2O_3)	0.15%
3	Ferric oxide (Fe_2O_3)	0.16%
4	Calcium oxide (CaO)	0.55%
5	Magnesium oxide (MgO)	0.35%
6	Sulphur trioxide (SO_3)	0.24%
7	Carbon (C)	5.91%
8	Loss on Ignition	4.94%

FIBER REINFORCED CONCRETE

Concrete is by nature a brittle material that performs well in compression, but is considerably less effective when in tension. Reinforcement is used to absorb these tensile forces so that the cracking which is inevitable in all high-strength concretes does not weaken the structure.Latest developments in concrete technology now include reinforcement in the form of fibers, notably polymeric fibers, as well as steel or glass fibers.

Fiber-reinforcement is predominantly used for crack control and not structural strengthening. Although the concept of reinforcing brittle materials with fibers is quite old, the recent interest in reinforcing cement-based materials with randomly distributed fibers is quite old; the recent interest in reinforcing cement based materials with randomly distributed fibers is based on research starting in the 1960's. Since then, there have been substantial research and development activities throughout the world. It has been established that the addition of randomly distributed polypropylene fibers to brittle cement based materials can increase their fracture toughness, ductility and impact resistance. Since fibers can be premixed in a conventional manner, the concept of polypropylene fiber concrete has added an extra dimension to concrete construction.

HIGH STRENGTH CONCRETE

Concrete is generally classified as Normal Strength Concrete (NSC), High Strength Concrete (HSC) and Ultra High Strength Concrete (UHSC). There are no Clear cut boundaries for the above classification. In the world scenario, however, in the last 15 years, concrete of very high strength entered the field of construction, in particular construction of high –rise buildings and long span bridges. Concrete strengths of 90 to 120 MPa are occasionally used.

The advent of prestressed Concrete Technology Techniques has given impetus for making concrete of higher strength. In India there are cases of using high strength concrete for prestressed concrete bridges. But strength of concrete more than 35 Mpa was not commonly used in general construction practices.

MATERIALS USED AND THEIR SPECIFICATIONS

Materials play an important role in Concrete. The materials used for preparing HSC concrete are Cement, Fine Aggregate, Coarse Aggregate, Water, RHA, polypropylene fiber and Super plasticizers which are confirming to the requirements of the Indian Standard (IS) specifications are given in table 2.

Table 2 Materials used and their specifications

Sl. No.	Material	Type	IS Specification
1	CEMENT	Ordinary Portland Cement (OPC)53 Grade	IS 12269-2013
2	COARSE AGGREGATE	Crushed Angular Aggregate(Size = 20 Mm)	IS 2386(Part I &III)-1963
3	FINE AGGREGATE	Natural Sand(Size ≤ 4.75 Mm)	IS 2386(Part I &III)-1963
		Quarry Dust(Size ≤ 4.75 Mm)	
4	WATER	Clean Potable Water(PH Value=7.0)	IS 456 – 2000
5	POZZOLANIC MATERIAL	Rice Husk Ash	IS 12269 : 2013
6	FIBER	Polypropylene	IRC:44-2008
7	SUPERPLASTICIZERS	Poly Carboxylate Ether (PCE) (Dosage=0.3% Of Total Cementitious Materials)	IS 9103

EXPERIMENTAL INVESTIGATION

The materials used for this study were initially investigated and tested. The test was carried out for different materials such as Cement, RHA, Fine aggregate, Coarse aggregates and their results were listed in tables.

Cement and RHA

Ordinary Portland cement of 53 grade confirming to 12269-2013was used in the present study. The properties of cement and RHA are shown in Table 3.

Table 3 Testing of Cement and RHA

Sl.No.	Type of Test	Values obtained for Cement	Values obtained for RHA
1	Fineness Test by Sieving	4%	1%
2	Standard Consistency Test	26%	30%
3	Initial Setting Time	35 Minutes	40 Minutes
4	Final Setting Time	9 Hours	10
5	Specific Gravity Test	3.15	2.08

Fine aggregate and Quarry Dust

Natural sand and Quarry Dust with fraction passing through 4.75mm and retained on 600 micron sieve is used and will be tested as per IS 2386(Part I& III)-1963. The properties of the fine aggregate and quarry dust are shown in Table 4.

Table 4 Testing of Fine Aggregate and Quarry Dust

Sl. No.	Type of Test	Values obtained for Sand	Values obtainedQuarry Dust
1	Fineness Modulus Test	2.541	2.529
2	Bulkiness Of Sand	6.66%	5.26%
3	Specific Gravity Test	2.59	2.57
4	Water Absorption Test	0.53%	0.91%

Coarse aggregate

Crushed aggregate confirming to IS 2386(Part I& III)-1963 was used. Aggregates of size 20mm has been selected for the study. The properties of the coarse aggregate are shown in Table 5.

Table 5 Testing of Coarse Aggregate

Sl. No.	Type of test	Values obtained
1	Fineness Modulus Test	2.28
2	Specific Gravity Test	2.27
3	Water Absorption Test	0.4%
4	Aggregate Crushing Value	12.85%
5	Aggregate Impact Value	12.18%
6	Aggregate Abrasion Value	36.55%
7	Flakiness Index	36.30%
8	Elongation Index	45.55%

MIX DESIGN

Mix design can be defined as the process of selecting suitable ingredients of concrete and determining their relative proportions with the object of producing concrete of certain minimum strength and durability as economically as possible. Mix design for each set having different combinations are carried out by using **ACI 211.4R-93** method. The mix proportion obtained for normal M60 grade concrete is **1:0.9:2.1** with a water-cement ratio of **0.31.**

FRESH CONCRETE

The fresh concrete is made with the mix ratio as per design standards for M60 grade concrete and the workability of the concrete was tested. The properties of fresh concrete are given in table 6.

Table 6 Properties of Fresh concrete

Sl.No.	Property	Result
1	Slump value	50 mm
2	Flow value	50%
3	Compaction factor value	94.70%
4	Vee-Bee Consistency value	8 seconds

EXPERIMENTAL PROCEDURE

STRENGTH TEST

The specimen of standard cube of size 15cmx15cmx15cm, standard cylinder of size 30cm height and 15cm diameter, prismof size 10cmx10cmx50cm and beam of size 2m x 15cm x 20 cm were used to determine the compressive strength, split tensile strength, flexural strength and structural strength of the concrete. These specimens were tested on 7^{th}, 14^{th}& 28^{th}day'sstrength.

Experiments Conducted

The following experiments were conducted on the specimens casted.

- Compression test
- Split tensile test
- Flexural test
- Beam test

Compression Test

Compression test is the most common test conducted on hardened concrete, partly because it is an easy test to perform, and partly because most of the desirable characteristic properties of concrete are qualitatively related to its compressive strength. The cube specimen is of the size 15 x 15 x 15 cm were tested for compressive strength as per IS 516-1959 using a calibrated compression testing machine.

Split Tensile test

Split tensile strength of concrete is usually found by testing concrete cylinder of size 30cm height and 15cm diameter. The specimens were tested for its tensile strength as per IS: 516-1959 using a calibrated compression testing machine.

Flexural Strength Test

Flexural strength is the one of the measure of tensile strength of concrete. It is the ability of a prism to resist failure in bending. It is measured by loading un-reinforced slab or prism of size 10cm x 10cm x 50cm. The specimens were tested for its flexural strength as per IS: 516-1959 using a calibrated flexural testing machine.

Beam Test

The beams of size 2m x 15cm x 20 cm were tested under monotonic loading.The load was applied gradually to the beam till its failure. Dial gauge was fixed beneath the beam at its mid span. For each increment of loading dial gauge reading were recorded. First crack load was observed and recorded. And for each increment of load crack growth was observed and marked.

DURABILITY TEST

Durabilitytests is planned to evaluate chemical attack which results in volume change, cracking of concrete and the consequent deterioration of concrete becomes an important part of discussion.

Under chemical attack we shall discuss about the following tests:

1. Acid Attack
2. Sulphate Attack
3. Alkaline Attack

Acid Attack

In order to assess the weight loss, concrete cubes is exposed to chemical media. For acid test, hydrochloric acid (HCL) solution was prepared by mixing 5% of Conc.Hcl with one liter of distilled water as per ASTM G20-8 or make an Acidic solution with 1N (Normality) as per laboratory standards. After normal curing (28 days) cubes were taken out and weight of cube was noted. Than weighted cubes was immersed in the prepared hydrochloric acid for 30 and 60 days. After curing the cubes were taken out from acid and weight of cubes was noted. From this weight loss of cubes is calculated. And then compression test is done to find its compression strength.

Sulphate Attack

To assess the weight loss concrete cubes is exposed to chemical media. For Sulphate test, Magnesium Sulphate ($MgSO_4$) solution was prepared by mixing 5% of Magnesium Sulphate salt with one liter of distilled water as per ASTM G20-8 or make a solution with N/2 (Normality) as per laboratory standards. After normal curing (28 days) cubes were taken out and weight was noted. Than weighted cubes was immersed in the prepared Magnesium Sulphate solution for 30 and 60 days. After curing the cubes were taken out and weighted. From this weight loss is calculated. And then compression test is done to find its compression strength.

Alkaline Attack

To assess the weight loss concrete cubes is exposed to chemical media. For alkaline test, Sodium hydroxide (NaOH) solution was prepared by mixing 5% of sodium hydroxide pellets with one liter of distilled water as per ASTM G20-8 or make an Alkali solution with 1N (Normality) as per laboratory standards. After normal curing (28 days) cubes were taken out and weight was noted. Than weighted cubes was immersed in the prepared sodium hydroxide solution for 30 and 60 days. After curing the cubes were taken out and weighed. From this weight loss is calculated. And then compression test is done to find its compression strength.

EXPERIMENTAL RESULTS

STRENGTH TEST

Compression Test

The Compressive strength test results of the hardened concrete cubes for standard, 5%, 10% & 15% RHA replaced concrete for 7, 14 and 28 days were given in table 7 with its graphical representation

Table 7 Compressive Strength for Cubes

% of RHA (Replacement for Cement)	Compressive Strength (N/mm^2)		
	7th day	14th day	28th day
0	21.63	54.42	65.30
5	19.24	52.11	61.52
10	18.00	50.63	60.13
15	18.37	47.71	56.20

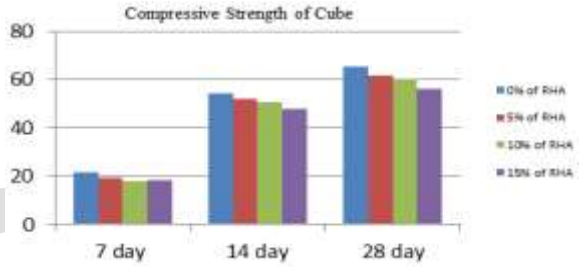

Split Tensile test

The Split tensile strength test results of the hardened concrete Cylinders for standard, 5%, 10% & 15% RHA replaced concrete for 7, 14 and 28 days were given in table 8with its graphical representation.

Table 8 Split tensile strength for Cylinders

% of RHA (Replacement for Cement)	Split tensile strength (N/mm^2)		
	7th day	14th day	28th day
0	6.98	8.30	9.90
5	7.50	9.20	10.30
10	8.70	9.90	11.20
15	7.20	8.80	10.00

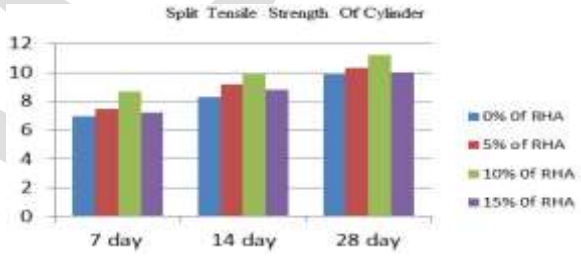

Flexural Strength Test

The Flexural strength test results of the hardened concrete Prisms for standard, 5%, 10% & 15% RHA replaced concrete for 7, 14 and 28 days were given in table 9 with its graphical representation

Table 9 Flexural strength for Cylinders

% of RHA (Replacement for Cement)	Flexural strength (N/mm^2)		
	7th day	14th day	28th day
0	8.90	9.70	11.20
5	9.80	10.70	12.90
10	10.30	11.70	13.65
15	9.75	10.10	11.90

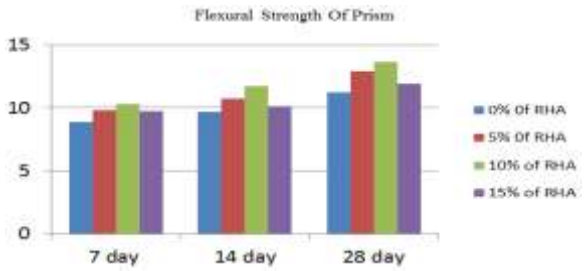

Beam Test

The table 10 gives the loads taken by conventional concrete beam and 10% RHA replaced concrete beam for two samples. From the results it was observed that 10% RHA replaced concrete beam is higher than that of normal conventional concrete beam and the graph was plotted between load and samples.

Table 10 Comparison of First and Ultimate crack Load of CC and RHA10%

Sl.No.	Beam ID	First Crack Load in (Ton)	Ultimate Load in (Ton)	Ultimate Load/ First Crack Load
1	CC 1	1.4	7	5
2	CC 2	2.8	7	2.5
3	RHA 10% 1	2.8	9.8	3.5
4	RHA 10% 2	2.8	9.8	3.5

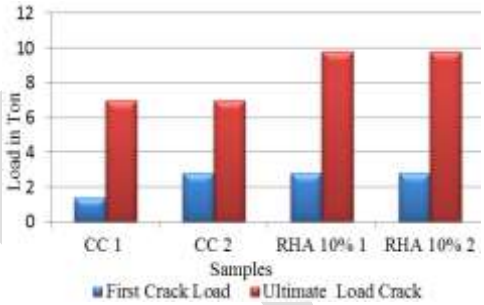

DURABILITY TEST

Acid Test

Acid Test is carried out to obtain weight loss of different type of concrete. Acid test results are shown in table 11 & 12. From the result it will be observed that weight loss is nearly equal for conventional HSC and quarry dust HSC. Quarry dust and Rice Husk Ash has good void filling ability. So that acid test on quarry dust HSC will show the good result. From the result we can found that acid attack in quarry dust concrete will be very less after long duration.

Table 11 Percentage Loss in weight due to Acid Attack

Sl. No	Type of concrete	Percentage Loss in weight (kg)	
		30 days	60 days
1	NormalConventional concrete	1.1	1.6
2	RHA Concrete(5% Replacement)	1.05	1.58
3	RHA Concrete(10% Replacement)	1.0	1.50
4	RHA Concrete(15% Replacement)	1.18	1.8

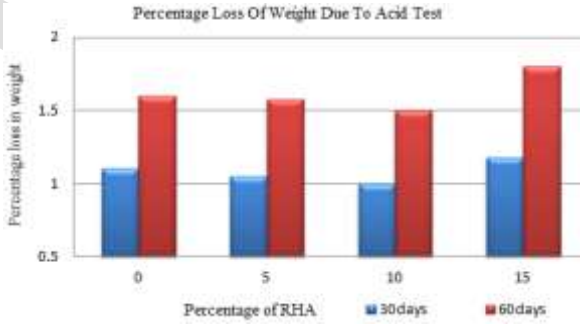

Table 12 Compressive Strength after Acid Test

% of RHA (Replacement for Cement)	Compressive strength in (N/mm^2)	
	30 days	60 days
0	59	56
5	57	54
10	60	57
15	54	53

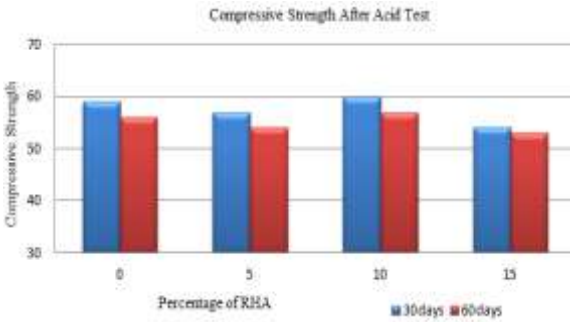

Sulphate Test

Sulphate Resistance test was carried out to obtain weight loss of different type of concrete. Sulphate attack test results are shown in table 13 & 14. From the result it will be observed that 30 & 60 days Magnesium Sulphate attack to the RHA concrete is less when compared to normal conventional concrete.

Table 13 Percentage Loss in weight due to Sulphate Attack

Sl. No	Type of concrete	Percentage Loss in weight (kg)	
		30 days	60 days
1	Normal Conventional concrete	0.5	0.97
2	RHA Concrete (5% Replacement)	0.6	0.9
3	RHA Concrete (10% Replacement)	0.4	0.8
4	RHA Concrete (15% Replacement)	0.9	1.1

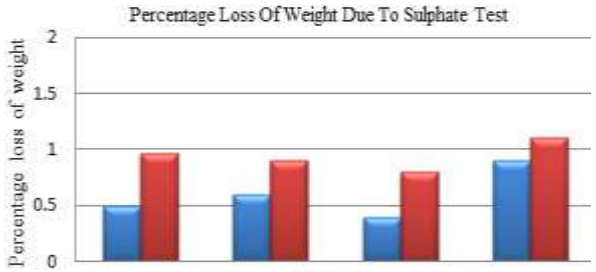

Table 14 Compressive Strength after Sulphate Test

% of RHA (Replacement for Cement)	Compressive strength in (N/mm^2)	
	30 days	60 days
0	59	55
5	56	54
10	60	57
15	58	52

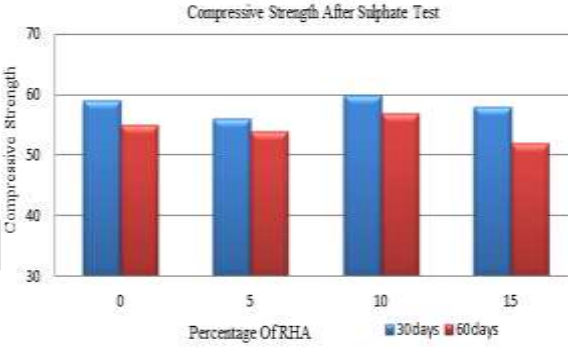

Alkaline Test

Alkaline test was carried out to obtain weight loss of different type of concrete. Alkaline test results are shown in table 15 & 16. From the result it will be observed that weight loss is nearly equal for conventional HSC and quarry dust HSC. Quarry dust and RHA are the substance which has good resistance to alkaline. So that alkaline test on quarry dust HSC will show the good result. From the result we can found that alkaline attack in quarry dust concrete will be very less after long duration.

Table 15 Percentage Loss in weight due to Alkali Attack

Sl. No	Type of concrete	Percentage Loss in weight (kg)	
		30 days	60 days
1	NormalConventional concrete	0.45	0.56
2	RHA Concrete(5% Replacement)	0.53	0.6
3	RHA Concrete(10% Replacement)	0.4	0.53
4	RHA Concrete(15% Replacement)	0.7	0.81

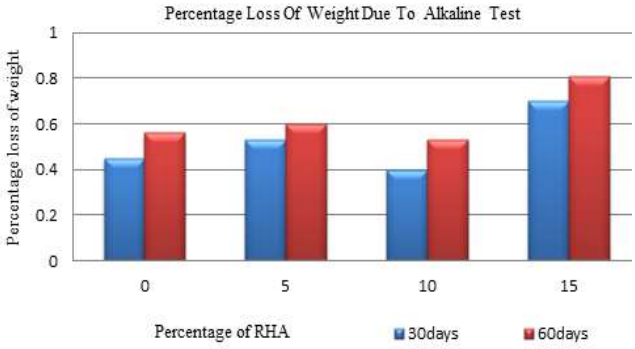

Table 11.19 Compressive Strength after Alkaline Test

% of RHA (Replacement for Cement)	Compressive strength in (N/mm^2)	
	30 days	60 days
0	58	50
5	55	49
10	61	56
15	59	55

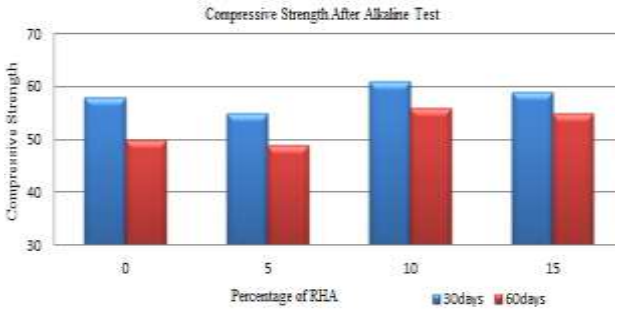

CONCLUSION

This project work is based on the usage of the rice husk ash, an agricultural waste material used as partial replacement of cement, Quarry dust a cheap material used as complete replacement for sand and addition to that polypropylene fiber are used in the concrete mixtures. The partial substitution of cement with RHA presents better results in the improvement of compressive strength at different ages and, at the same time the reduction of cracks has been achieved due to presence of polypropylene fiber.

The experimental investigation was conducted for high strength concrete with quarry dust as fine aggregate with partial replacement of cement with rice husk ash and also with addition of polypropylenefiber. To improve the workability of the concrete mix, super plasticizer is also used. Properties of materials used in concrete were listed out. Workability, strength and durability characteristics of the of high strength concrete were compared with conventional concrete.

Quarry dust has lots of finer dust particle than sand, which reduce the workability of concrete. To compensate this problem super plasticizer was used. When quarry dust was used with super plasticizer it will show better workability and flow ability. Combination of quarry dust and rice husk ash exhibiting good performance due to efficient micro filling ability and pozzolanic action of rice husk ash. From this can conclude that 100% replacement of sand with quarry dust shows good strength and durability. From this study it was conclude quarry dust is the better alternative for natural sand.

Compressive strength of conventional concrete is higher than the quarry dust concrete, cement was partially replaced by 5%, 10% and 15% rice husk ash. When it was added with 0.3% of polypropylenefiber their flexural strength was increasing.And beam test result also show the fibrous nature of RHA and polypropylenefiber increased the load carrying capacity and reduced the micro cracks. And increase the ductility of the beam.

When adding 5%, and 10% of rice husk ash content compressive strength and tensile strength of the mix will increase. When 15% of rice husk ash was added strength will decrease because it will decrease the bonding between the materials. From the experimental investigation it was found that the optimum RHA content is 10%.

REFERENCES:

[1] AlirezaNajiGiviSuraya, Abdul Rashid, Farah Nora A. Aziz and MohamadAmranMohdSalleh"Assessment of the effects of rice husk ash particle size on strength, water permeability and workability of binary blended concrete" construction and Building Materials 24 (2010) 2145–2150.

[2] Godwin A. Akeke, Maurice E. Ephraim, Akobo, I.Z.S and Joseph O. Ukpata., "Structural Properties Of Rice Husk Ash Concrete" International Journal of Engineering and Applied Sciences, Vol. 3, Issue 3, ISSN 2305-8269, May 2013.

[3] Anithaselvasofia S.D, Gayathri R, SwathiG and Prince arulraj G, "Experimental Investigation On Quarry Dust Concrete With Chemical Admixture" International Journal of Latest Research in Science and Technology, ISSN (Online):2278-5299, Volume 2,Issue 2: Page No.91-94, March - April 2013.

[4] M. Devi, V. Rajkumar and K. Kannan 'Inhibitive Effect of Organic Inhibitors in Concrete Containing Quarry Dust As Fine Aggregate" International Journal of Advances in Engineering Sciences, Vol.2, Issue 1, Jan 2012.

[5] V.Priyadharshini and A.Krishnamoorthi, "High Performance Concrete using Quarry dust as Fine aggregate", International Science and Research Journal, Vol. 2, Issue 2, Jun 2014.

[6] G.Balamurugan and P.Perumal "Use of Quarry Dust to Replace Sand in Concrete –An Experimental Study", International Journal of Scientific and Research Publications, Vol. 3, Issue 12, December 2013.

[7] K.S. Johnsirani, A. Jagannathan and R. Dinesh Kumar "Experimental Investigation on Self Compacting Concrete Using Quarry Dust" International Journal of Scientific and Research Publications, Vol. 3, Issue 6, June 2013.

[8] Hardikkalpeshbhai Patel and Jayesh Kumar Pitroda, "A Study of Utilization Aspect of Quarry Dust" Journal of International, Vol. 1, Issue 9, October 2013.

[9] Mehul J, Patel, and M. Kulkarni, "Effect of polypropylene fiber on the high strength concrete" Journal of Information, Knowledge and Research in Civil Engineering, Vol. 2, Issue 2, Page 125, November 2012 .

[10] M. Tamil Selvi and T.S. Thandavamoorthy, "Studies on the Properties of Steel and Polypropylene Fiber Reinforced Concrete without any Admixture", International Journal of Engineering and Innovative Technology, Vol. 3, Issue 1, July 2013.

[11] IS 12269: 2013, Ordinary Portland cement 53 Grade — Specification.

[12] IS: 2386 (Part I) – 1963, Methods of Test for Aggregates for Concrete, Part I Particle Size and Shape.

[13] IS: 2386 (Part II)-1963, Methods of Test for Aggregates for Concrete, Part II Estimation of Deleterious Materials and Organic Impurities.

[14] IS:2386 (Part IV)-1963, Methods Of Test For Aggregates For Concrete, Part IV Mechanical Properties

[15] IS: 2386 (Part III) – 1963, Methods of Test for Aggregates for Concrete, Part III Specific Gravity, Density, Voids, Absorption and Bulking.

[16] IS. 456: 2000, Plain and Reinforced Concrete Code of Practice.

[17] IS 12269 : 2013, Ordinary Portland Cement, 53 Grade — Specification

[18] IS 9103: 1999, Concrete Admixtures – Specifications.

[19] IRC:44-2008, Guidelines For Cement Concrete Mix Design For Pavements (Second Revision)

[20] ACI 211.4R-93, Guide for Selecting Proportions for High-Strength Concrete with Portland Cement and Fly Ash

[21] M.S.Shetty, Concrete Technology Theory and practice, S.Chand& Company Ltd., Ram Nagar, New Delhi-110 055

[22] G.L.Ghambir, "Concrete Technology", Tata McGraw-hill Publishing company Limited, New Delhi

International Journal of Engineering Research and General Science Volume 3, Issue 6, November-December, 2015
ISSN 2091-2730

G_m/I_D based Three stage Operational Amplifier Design

Rishabh Shukla
SVNIT, Surat
shuklarishabh31081988@gmail.com

Abstract— A nested Gm-C compensated three stage Operational Amplifier is reviewed using g_m/I_D based approach. With the given specifications such as Gain, Phase Margin, Input common mode range and Unity gain frequency, operational amplifier has been designed in such a way that all the transistors are biased in moderate inversion. Spice simulations are carried out using TSMC 180 nm technology. The simulated results show agreement with the specification for 1.8 V supply.

Keywords— CMOS Integrated Circuit, Low power, Stability, Compensation, Nested G_m-C compensation, Gain margin, Phase margin, Pole, Zero.

INTRODUCTION

The operational amplifiers (Op-amp) are most important building block of many analog and mixed signal circuits like amplifiers, filters, comparators etc. With the scaling of transistors and supply, now a day's multistage amplifiers are often used. In low voltage designing cascoding can't be used because of headroom limitations. Hence designer has been moved towards cascading, because it avoids vertical stacking of transistors hence removes the headroom problem. In order to achieve a high voltage gain, it is advantageous to used more than two stages. But to design such a multistage operational amplifier is a challenging task since high impedance nodes lead instability issues. To stabilize the op-amp several compensation techniques has been proposed [1]. The Nested miller compensation (NMC) technique suffers from bandwidth reduction, issue while NMC with nulling resistor suffers from right half plane zero problems [2,3]. The multipath NMC (MNMC) increases the bandwidth by cancelling the non-dominant pole with zero. Major drawback of this technique is that slight variation in temperature or any other parameter may change the location of zero, which leads improper cancellation [4]. The reversed NMC (RNMC) introduces the right half plane zero, hence decreases the bandwidth and phase margin [5]. The nested G_m-C compensation technique is much easier to analyze as compare to MNMC. The power consumption by feed-forward stages can be controlled by proper implementations [6,7]. In this paper nested G_m-C compensation technique has been adopted for three stage op-amp designing.

DESIGN APPROACH

The G_m/I_D based technique has been adopted to bias all the transistors in moderate inversion in order to achieve best trade-off among gain, bandwidth and power. In this methodology transistors are characterized under same environment to plot the intrinsic gain and $I_D/(W/L)$ as a function of G_m/I_D. G_m/I_D is a ratio which measures the efficiency to translate current into transconductance, i.e. large transconductance can be achieved by making the ration large [8,9]. Since the above plots are independent to size hence it becomes quite easy to size each transistor for a given current. The required current can be obtained from specifications. The transfer function of three stage op-amp can be written as,

$$A(s) = -\frac{A_o}{\left[\left(1+\frac{A_O s}{\omega_1}\right)\left(1+\frac{s}{\omega_2}+\frac{s}{\omega_2\omega_3}\right)\right]}$$

In this expression A_o is open loop gain and ω_1 is unity gain frequency. In order to make op-amp as single pole system it is necessary that both second and third pole must be far from UGB. Hence in this way op-amp can be stabilize but it consumes large power [7].

[1] SPECIFICATIONS

In order to design three stage op-amp following specification has been used,

1. Supply, V_{DD} = 1.8V and V_{SS} = 0V.
2. Gain > 80 dB
3. GBW > 20 MHz
4. ICMR = 0 to 1.5V
5. Phase Margin = 50^o to 60^0

[2] DESIGN EQUATIONS

Following relations has been adopted,

1. $\mathrm{UGB} = \frac{G_{m1}}{2\pi C_{m1}}$

2. $P_1 = \frac{G_{m2}}{2\pi C_{m2}}$, $P_2 = \frac{G_{m3}}{2\pi C_L}$

3. $G_{mfi} = G_{mi}$ for i = 1 to 3

4. $V_{cm}(+) = -|V_{Tpmax}| - V_{SDsat1} + V_{DD}$

5. $V_{cm}(-) = -|V_{Tpmax}| + V_{SDsat2} + V_{DSsat4}$

6. $\mathrm{PM} = 90^{\circ} - \tan^{-1}\{\frac{\frac{\omega_1}{\omega_2}}{1-\frac{\omega_1^2}{\omega_2\omega_3}}\}$

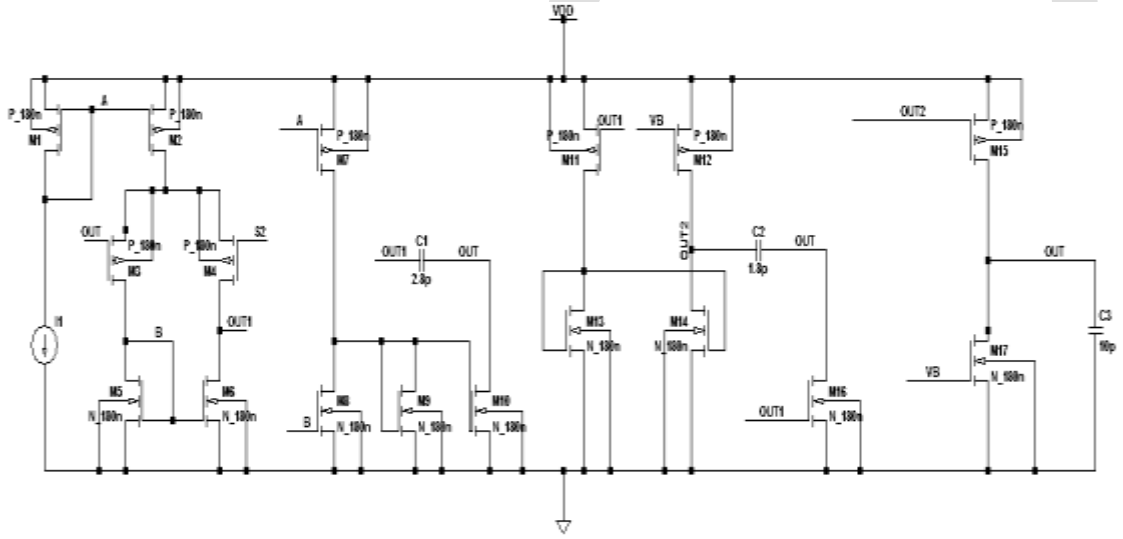

Figure 1: Three stage NGCC Op-amp [7]

[3] DESIGN PARAMETERS AND TRANSISTORS SIZE

With the help of above specifications, design equations and G_m/I_D plots aspect ratios of all the transistors has been calculated and simulated results for size of transistors belong to core block has been summarized in Table 1.

Table1: Summary of size of transistors after simulation

Transistors	W/L ratio (Simulated value)
M_3,M_4	31.66/0.5
M_5,M_6	7/0.5
M_{11},M_{12}	22/0.5
M_{13},M_{14}	7/0.5
M_{15}	58/0.36
M_{17}	30/0.5

The bias current for first stage current mirror has been chosen as 10 µA.

SIMULATION RESULTS

The SPICE simulation has been carried out using TSMC 180nm technology. The supply has been chosen as 1.8V and the simulated results have been summarized in Table 2.

1. FREQUENCY RESPONSE

The simulated result shows that op-amp has an open loop gain of 94.23 dB, UGB is 27 MHz and phase margin is 60^{o} for 10 pF capacitive load.

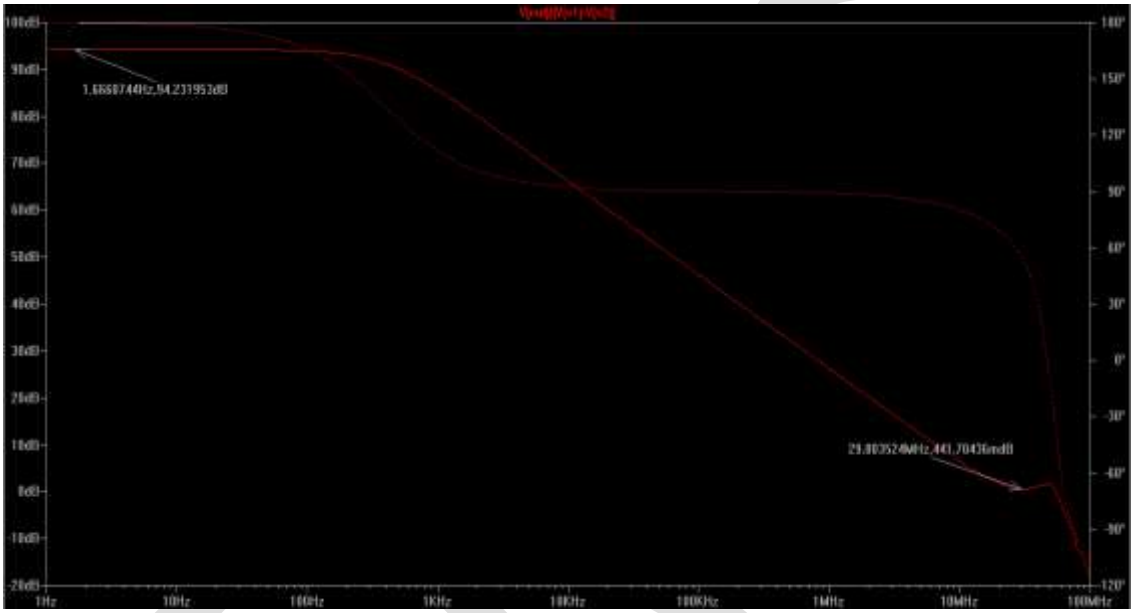

Figure 2: Frequency Response of Three stage Op-amp for a 10 pF capacitive load

2. Input Common mode range

The simulated result shows that designed op-amp has ICMR in the range of 64 mV to 1.78 mV.

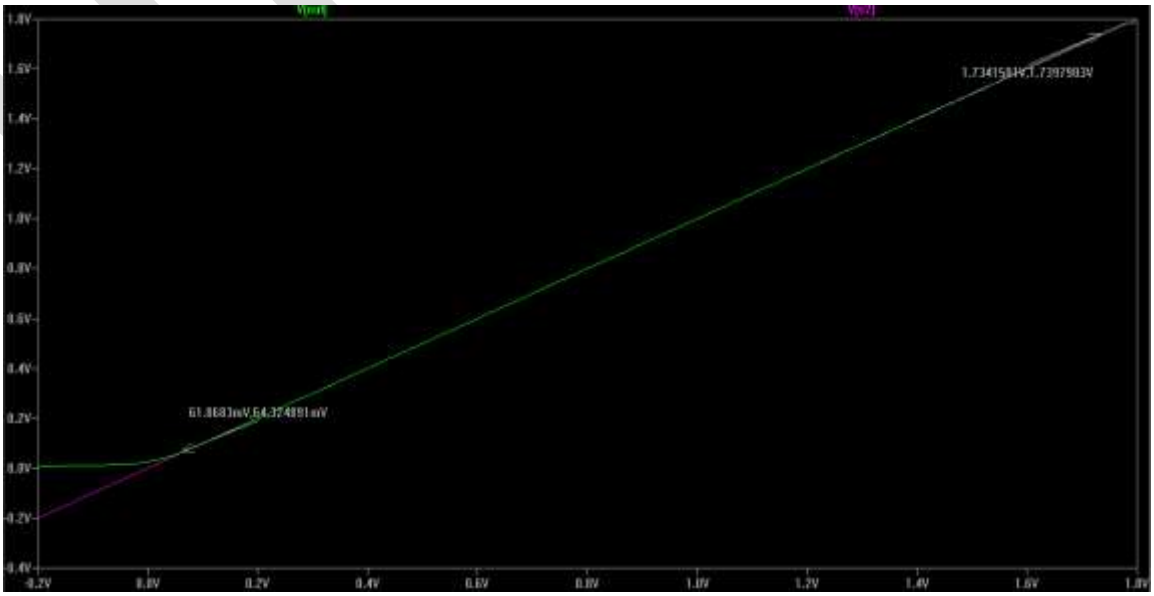

Figure 3: Frequency Response of Three stage Op-amp for a 10 pF capacitive load

3. Step Response: An step of 0V to 1.2V is applied across unity gain opamp and output has been plotted as sjown in Figure 3.

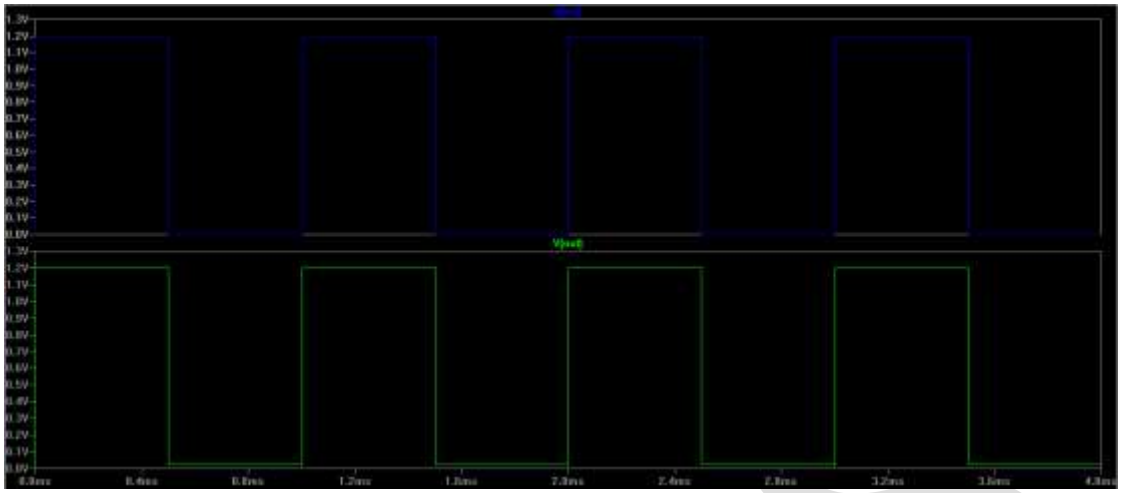

Figure 4: Step Response of unity gain op-amp

4. Slew Rate and offset voltage of Op-amp

Slew rate of simulated op-amp has been found as 15 V/µs and off-set voltage is almost 26 mV.

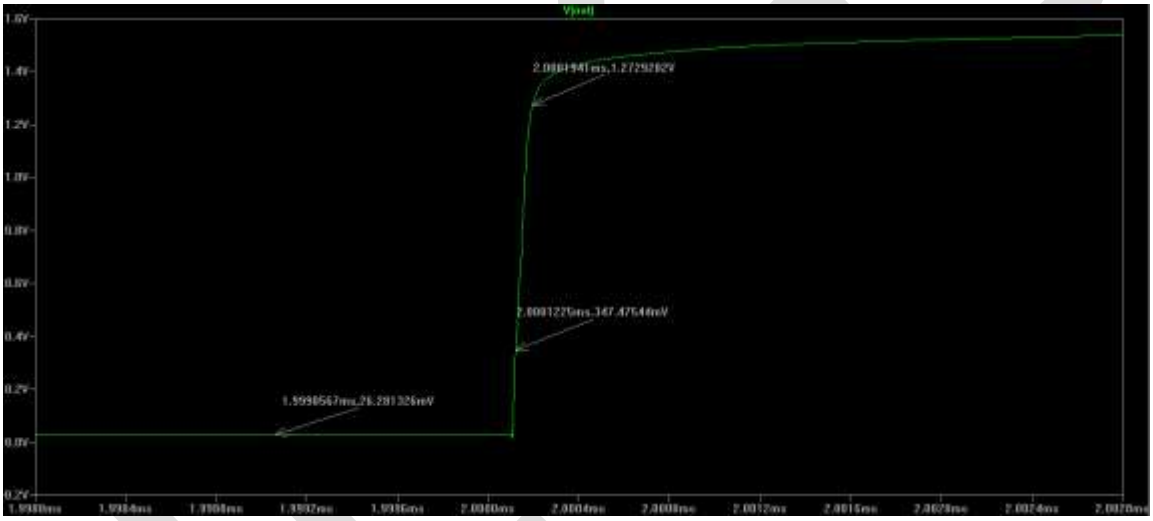

Figure 5: Large signal step response of unity gain opamp for offset voltage and slew rate calculation

The simulated results have been summarized in Table 2.

Table 2: Comparison of parameters for 5pF and 10pF load

Parameter	Simulated Value	
	C_L = 5 pF	C_L = 10 pF
Gain	94.23 dB	94.23 dB
UGB	23.94 MHz	29.8 MHz
Phase Margin	69^o	52.55^o
Slew Rate	15.6 V/µs	14.5 V/µs
ICMR	64 mV- 1.73mV	64 mV - 1.74mV
Offset Voltage	26 mV	26 mV
Settling Time	80 ns	85 ns
Power Consumed (I_{VDD}x V_{DD})	2.86 mW	2.86 mW

CONCLUSION

In this paper a three stage nested G_m-C compensated operational amplifier has been designed using G_m/I_D methodology and 180 nm technology. All the transistors are biased in moderate inversion region in order to achieve best tradeoff among gain, area, and bandwidth. The simulated results show that op-amp is capable to give an open loop gain of 94.23 dB at a phase margin of 69^0 and UGB of 23.94 MHz for 5 pF load and 52.55^0, 29.8 MHz for 10 pF capacitive loads. Hence simulated result shows excellent agreement

with specifications.

REFERENCES:

[1] A. Garimella and P. M. Furth, "Frequency compensation techniques for op-amps and LDOs: A tutorial overview," 2011 IEEE 54th International Midwest Symposium on Circuits and Systems (MWSCAS).

[2] K. N. Leung and P. Mok, "Nested Miller compensation in low-power CMOS design," IEEE Transactions on Circuits and Systems II: Analog and Digital Signal Processing IEEE Trans. Circuits Syst. II, pp. 388–394.

[3] G. Palumbo and S. Pennisi, "Design methodology and advances in nested-Miller compensation," IEEE Trans. Circuits Syst. I IEEE Transactions on Circuits and Systems I: Fundamental Theory and Applications, pp. 893–903.

[4] R. Eschauzier, L. Kerklaan, and J. Huijsing, "A 100 MHz 100 dB operational amplifier with multipath nested Miller compensation structure," 1992 IEEE International Solid-State Circuits Conference Digest of Technical Papers.

[5] A. D. Grasso, G. Palumbo, and S. Pennisi, "Advances in Reversed Nested Miller Compensation," IEEE Trans. Circuits Syst. I IEEE Transactions on Circuits and Systems I: Regular Papers, pp. 1459–1470.

[6] F. You, S. Embabi, and E. Sanchez-Sinencio, "A multistage amplifier topology with nested Gm-C compensation for low-voltage application," 1997 IEEE International Solids-State Circuits Conference. Digest of Technical Papers.

[7] J. S. Lee, J. Y. Sim, and H. J. Park, "A design guide for 3-stage CMOS nested Gm-C operational amplifier with area or current minimization," 2008 International SoC Design Conference.

[8] P. Jespers, "The gm/ID Methodology, A Sizing Tool for Low-voltage Analog CMOS Circuits."

[9] F. Silveira, D. Flandre, and P. Jespers, "A gm/ID based methodology for the design of CMOS analog circuits and its application to the synthesis of a silicon-on-insulator micropower OTA," IEEE J. Solid-State Circuits IEEE Journal of Solid-State Circuits, pp. 1314–1319.

International Journal of Engineering Research and General Science Volume 3, Issue 6, November-December, 2015
ISSN 2091-2730

The Use of Periwinkle Shell Ash as Filtration Loss Control Agent in Water-Based Drilling Mud

Ikechi Igwe, Bright Bariakpoa Kinate

Petroleum Engineering Department, Faculty of Engineering, Rivers State University of Science and Technology, Port Harcourt, Nigeria

igwe.ikechi@ust.edu.ng

Abstract— Experimental assessment of the suitability of Periwinkle Shell Ash (PSA) for use as filtration loss control additive in water-based drilling mud has been presented. Locally sourced periwinkle shells were soaked overnight in warm water treated with Sodium Chloride (NaCl) to remove dirt and any contaminant. Thereafter, the periwinkle shells were washed and air dried, and then heated in an electric muffle furnace at 995 ^{o}C. The calcined shells were then crushed with the aid of a jaw crusher and grinded to fine particles. The ensuing ash was then sieved through BS sieve (75microns) to obtain a fine ash (nanoparticles). This fine ash particles is the PSA used for the formulation of the mud sample of interest. The filtration characteristics of the formulated mud samples were tested using American Petroleum Institute (API) filter press and in accordance to API recommended practice for field testing water based drilling fluids (API RP 13B-1). Filtration control characteristics of the mud samples were demonstrated by the filtrate volume and the thickness and consistency of the mud filter cake deposited on the filter paper after 30 minutes of filtration. Physical examination of the filter cakes indicates that filter cake formed by sample C, prepare with 2.0 g of PSA, was thinner (0.75 mm thick) and more consistent than the rest. After 30 minutes of filtration, mud samples A, B, C, and D produced 7.7 ml, 7.2 ml, 6.7 ml, and 7.0 ml filtrate volumes, respectively. This imply that sample C formulated with 2.0 g of PSA, which produced the least filtrate volume (6.7 ml) after 30 minutes of filtration, demonstrated better filtration control characteristics than samples A, B, and D. Addition of PSA to the various mud samples improved the filtration characteristics of the formulated water-based drilling mud with respect to reduced filtrate volume and thinner and consistent mud filter cakes. PSA has proved to possess good filtration (fluid loss) control properties.

Keywords— API Filter Press, Drilling Fluid, Filter Cake, Filtration Control, Filter Cake Thickness, Filtrate Volume, Periwinkle Shell Ash, Water-based Mud, Waste to Wealth.

INTRODUCTION

Rotary drilling process, the most widely used drilling method in the oil and gas industry, involve the circulation of drilling fluids. These fluids in its liquid form are called water-based drilling mud (if water is the continuous phase) or oil-based drilling mud (if oil is the continuous phase). Rapid filtration of drilling fluid into surrounding permeable formation occurs during drilling operations, resulting to loss circulation problems. Fluid loss is minimized by the creation of low permeable filter cake at the surface of the wellbore, which prevents solid particles from flowing into the pores of the formation together with the continuous phase [1]. These solid particles tend to plug the pore spaces of the formation either by physical or chemical processes, thereby reducing the permeability and porosity of the formation and by so doing, hamper the flow of fluids through such formations to the wellbore [1]. This is generally referred to as formation damage. Formation damage associated with drilling mud occurs when particles (such as drill solids, weighting agents and/or soft particles like polymers) invade the reservoir rock, thus plugging pores and forming internal filter cake [1].

Most Particulate materials contained in water-base mud (clays, cuttings, and weighting agents) are potentially damaging, and if forced into the pay zone, they can progressively fill the pores of the reservoir rock. Any subsequent production of hydrocarbon or injection of fluids at moderate or high flow rates will cause these materials to bridge over pore throat entries and severely decrease permeability near the wellbore region [2]. Such damaging process is limited to the first few inches around the wellbore (an average value of 3 in. (7.5 cm) is commonly used), but the resultant permeability reduction can be as high as 90% [2]. Invasion of formation rock by drilling fluid solids is favored by large pore size of the formation rock, presence of fissures and natural fractures in the reservoir, small particle size of the solid components of the drilling fluid (weighting agents and lost-circulation preventers whose initial particles are usually coarse and can be fragmented by the drilling bit), low drilling rate resulting in mud cake destruction (mud loss increase) and long

mud-to-formation contact time, high drilling fluid circulation rate (mud cake erosion), high drilling fluid density causing large overbalance pressure, and scrapping mud cake which provokes pressure surges and increase formation-to-mud contact time during bit trips [2].

Water-based mud filtrates may have a low salinity and a high pH and may contain dispersants and polymers. Polymers are stable at circulating temperatures, but can decompose and form residues when subjected to static reservoir temperatures for long periods of time. High salinity water-base mud generates filtrates that can react with formation brines and precipitate various types of scale. Formations drilled at high circulation rates are invaded by filtrates with temperatures well below the reservoir temperature. The cooling they cause may provoke the deposition of paraffin and/or asphaltenes [3]. These numerous drawbacks of water-base drilling fluid led to the development of oil-based mud for drilling through clayey sandstone [4]. The initial conclusion was that this new mud was a safe, all-purpose drilling fluid. It is now recognized, however, that although the problems of oil-base mud are less numerous than those of water base mud, they are often much more severe [5]. Oil based mud contain more solids than water-based mud. Consequently, particle invasion is more pronounced. Several types of materials are used to reduce particle invasion (filtration rate) and improve mud cake characteristics. Since filtration problems usually are related to flocculation of the active clay particles, deflocculants also aid filtration control. When clays cannot be used effectively as deflocculating agents, water-soluble polymers are substituted. The common water soluble polymers used for filtration control are Starch, Sodium carboxy methyl cellulose (CMC), and sodium polyacrylate. Polymers reduce water loss by increasing the effective water viscosity [6].

Particulate invasion of the region around the wellbore, and subsequent solid entrainment, as well as loss circulation are the major formation damage mechanisms associated with water-base drilling mud. These mechanisms usually lead to the formation of zone of altered permeability around the wellbore (skin effect), which adversely affects the productivity of such well [1]. During hydrocarbon production, backflow with hydrocarbons may partially clean up the internal filter cakes, but in general, the permeability of the invaded region is seriously impaired such that hydrocarbon production is reduced. For this reason, several experimental works have been done to control solid entrainment in porous media due to drilling operation [1].

Various research works have been done on the formulation of drilling mud using locally available materials as additives. These research ranges from the use of locally available clay as a substitute for bentonite to the use of local starch as a fluid loss control additive. Olatude *et al.* [7] formulated water based drilling fluid using bentonite, guar gum, polyanionic cellulose (PAC) and gum Arabic. The rheological behavior and the filtration loss property of each drilling fluid developed were measured using API recommended standard procedures. They noticed that Guar gum shows the highest gel strength and the most stable rheological properties with poor filtration loss property while gum Arabic had unstable rheological properties with stable gel strength and good filtration loss property [7]. However, gum Arabic is only found in the northern part of Nigeria and not in the southern part (Niger Delta region) where major drilling operations take place. This makes Periwinkle shells, waste product found in abundance in the Niger Delta region of Nigeria, more economical than the gum Arabic.

Omotioma *et al.* [8] used locally sourced cassava starch to improve the rheological properties of water based mud. Their results show that the rheological properties of water based mud were improved with the addition of 4% locally sourced cassava starch addictive to it. Samavati *et al.* [9] investigated the rheological and fluid loss properties of water based drilling mud containing acid modified *fufu* starch (cassava derivative)**.** Their result show that the rheological properties, which (viscosity, plastic viscosity, yield point and gel strength) for the modified *fufu* showed significant improvement when 16% acid was employed. A significant amount of fluid loss reduction was also obtained within light and average mud weights formulation (75 pcf and 100 pcf). However, none of the samples (modified and unmodified) meet the fluid loss standard requirement for the applied temperature [9]. Also, Ademiluyi *et al.,* [10] compared local polymer (cassava starch) with an imported type in controlling viscosity and fluid loss in water-based mud. Five different cassava starches were tested as viscosifiers and fluid loss control additives in water based mud and compared with Barazan D, an imported sample. Their experimental results indicated that at same concentration, the imported sample had higher rheological properties compared with the local samples. They also discovered that some of the newly developed local starch products (with high amylose content and high water absorption capacity) have similar or better filtration control properties than the imported sample. However, the viscosity of the drilling fluid produced from the local starches was lower than that of the imported type [10]. Amanullah and Yu [11] investigated the use of corn-based starches for oil field application in terms of suitability as drilling fluid additives. Their experimental results showed that some of the newly developed starch products had similar filtration control properties than that of a widely modified starch. Cassava and corn are major food items, and in high demand, in most part of Nigeria. It should be more economical and environmentally profitable to used non-food resources such as periwinkle shells (waste product) for drilling mud formulation (filtration control agent). Hence, the needs for this research work.

Periwinkle or winkle (*Littorina littorea*) is a species of small edible sea snail, a marine gastropod mollusc that has gills and an operculum, and is classified within the family Littorinidae, the periwinkles [12]. This is a robust intertidal species with a dark and sometimes banded shell. It is native to the rocky shores of the northeastern, and introduced to the northwestern, Atlantic Ocean. The shell is broadly ovate, thick, and sharply pointed except when eroded [12]. The shell contains six to seven whorls with some fine threads and wrinkles. The color is variable from grayish to gray-brown, often with dark spiral bands [12]. The width of the shell

ranges from 10 to 12 mm at maturity, with an average length of 16–38 mm. Shell height can reach up to 30 mm, 43 mm or 52 mm [12]. They are found in the lagoons and mudflats of the Niger Delta region, between Calabar in the South and Badagry in the West of Nigeria [13]. The people in these areas consume the edible part as sea food and dispose the shells as waste [13]. Few people utilize the shells as coarse aggregate in concrete works in areas where there are neither stones nor granite. However, a large amount of these shells are still disposed as waste and with disposal already constituting a problem in areas where they cannot find any use for it, and large deposits have accumulated in many places over the years [13].

Most technical application of Periwinkle Shell Ash (PSA) in Nigeria have been in the area of Civil Engineering, using PSA as partial replacement for ordinary Portland cement in concrete [13, 14, 15, 16, 17]. There is no known application of PSA in the formulation of drilling mud. The successful application of PSA in concrete should encourage research on its applicability in other area of engineering. This work intends to use PSA as filtration control addictive in the formulation of water-based drilling mud. Thereby, converting waste to wealth, creating wealth and job opportunities. This will impact positively on the Nigeria economy and the environment, considering the local content policy of the Nigerian National Petroleum Corporation (NNPC), which encourages the development and use of local contents in the oil and gas sector.

MATERIALS AND METHODS

A. Apparatus and Materials

The following apparatus were used for the experiments: conical flask, beakers, pH meter, baroid mud balance, jaw crushers, BS sieve, wire mesh, furnace, thermometer, stopwatch, graduated cylinder, and API filter press. The raw materials (addictives) used for the experiments and their functions are presented in table 1.

Table 1: Raw Material/Addictives and their Functions

Raw Material/Addictive	Function
Water	Continuous phase
Caustic Soda	pH modifier (to add alkalinity to the mud)
Soda Ash	pH modifier (to add alkalinity to the mud)
Xanthium Gum	Viscosifier and fluid loss control agent
Polyanionic Cellulose (PAC)	Viscosifier and fluid loss control agent
Potassium Chloride (PCl)	Shale Hydration Inhibitor
Barite	Weighting agent
Periwinkle Shell Ash (PSA)	Filtration control agent

B. Preparation of Periwinkle Shell Ash (PSA)

The periwinkle shells used for this work were sourced from Soku community, in Akuku-Toru Local Government Area of Rivers State, Nigeria. The periwinkle shells were soaked overnight in warm water treated with Sodium Chloride (NaCl) to remove dirt and any contaminant as shown in fig.1. Thereafter, the periwinkle shells were washed and air dried, and then heated in an electric muffle furnace at 995 ^{o}C. The calcined shells were then crushed with the aid of a jaw crusher and grinded to fine particles. The ensuing ash was then sieved through BS sieve (75microns) to obtain a fine ash (nanoparticles). This fine ash particles shown in fig.2 is the PSA used for the formulation of the mud sample of interest.

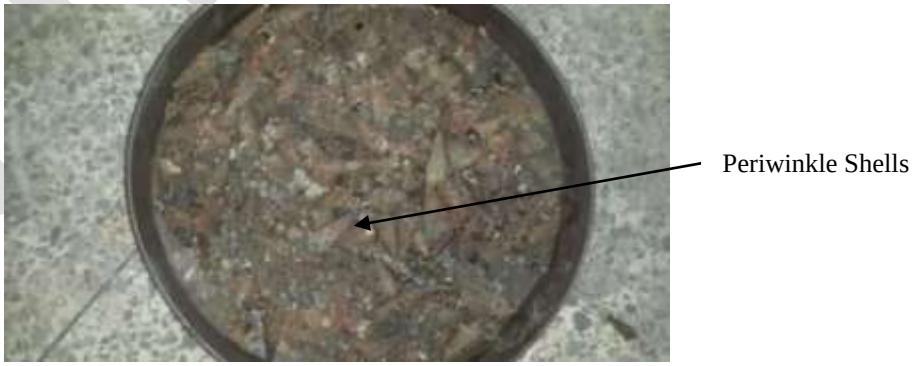

Fig.1: Soaked Periwinkle Shells

Fig.2: Grinded Periwinkle Shells

C. Formulation of Mud Samples

Four (4) different mud samples (A, B, C, and D) were formulated with varying amount of the various addictives. The composition of the various mud samples are presented in table 2.

Table 2: Composition of Mud Samples

Addictive	Sample A	Sample B	Sample C	Sample D
Water (ml)	350	350	350	350
Caustic Soda (g)	0.2	0.2	0.2	0.2
Soda Ash (g)	0.2	0.2	0.2	0.2
Xanthan Gum (g)	1.5	1.5	1.5	1.5
Bentonite (g)	20	20	20	20
Polyanionic Cellulose (PAC) (g)	0.8	0.8	0.8	0.8
Potassium Chloride (KCl) (g)	25	25	25	25
Barite (g)	30	30	30	30
PSA (g)	-	3.0	2.0	2.5

D. Filtration Test Experiment

Static filtration test was carried out on samples A, B, C, and D using API filter press. API recommended practice for field testing water based drilling fluids, API RP 13B-1 [18], was strictly followed during the experiment. The filtration test was conducted for thirty (30) minutes of filtration. Filtration control characteristics of the mud samples were demonstrated by the filtrate volume and the thickness and consistency of the filter cake (the residue) deposited on the filter paper after 30 minutes of filtration. The filtrate volume and filter cake characteristics for each of the samples tested were measured and recorded accordingly. The mud filter cake thickness is measured to the nearest millimeter.

RESULTS AND DISCUSSIONS

The results of the filtration experiment are presented in tables 3 and 4. The filtrate volumes after 30 minutes of filtration are presented in table 3 while the filter cake thickness of each mud sample after 30 minutes of filtration are presented in table 4 and shown graphically in fig.3. Physical examination of the filter cakes indicates that filter cake from sample C, prepare with PSA was thinner (0.75 mm thick) and more consistent than the rest. Table 3 shows that after 30 minutes of filtration, sample A, B, C, and D produced 7.7 ml, 7.2 ml, 6.7 ml, and 7.0 ml filtrate volumes, respectively. This imply that sample C formulated with 2.0 g of PSA, which produced the least filtrate volume (6.7 ml) after 30 minutes of filtration, demonstrated better filtration control characteristics than samples A, B, and D. Hence, PSA have proved to possess good filtration control properties which were majorly responsible for the thinner filter cake and minimal filtrate volume produced from sample C. However, increasing the quantity of PSA to 2.5 and 3.0 g in samples D and B, respectively, did not result to better filtration characteristics. The results show that increased filtrate volume indicates poor filtration control characteristics of mud (filter cake). The relationship between mud filter cake thickness and filtration volume is somewhat linear as shown in fig.4. Therefore, periwinkle shells, waste products found in abundance in the Niger Delta region of Nigeria, can be converted to wealth, to create wealth and business venture for the people of the region.

Table 3: Filtrate Volume from the Various Mud Samples

Time (min)	Filtrate Volume (ml)			
	Sample A	Sample B	Sample C	Sample D
5	3.2	3.0	2.6	2.8
10	4.7	4.5	4.4	4.5
15	6.1	5.4	5.1	5.2
20	6.6	5.9	5.4	5.7
25	7.0	6.5	6.0	6.2
30	7.7	7.2	6.7	7.0

Table 4: Filter Cake Thickness after 30 minutes of Filtration

Mud Sample	Sample A	Sample B	Sample C	Sample D
Filter Cake Thickness (mm)	1.0	0.9	0.75	0.8

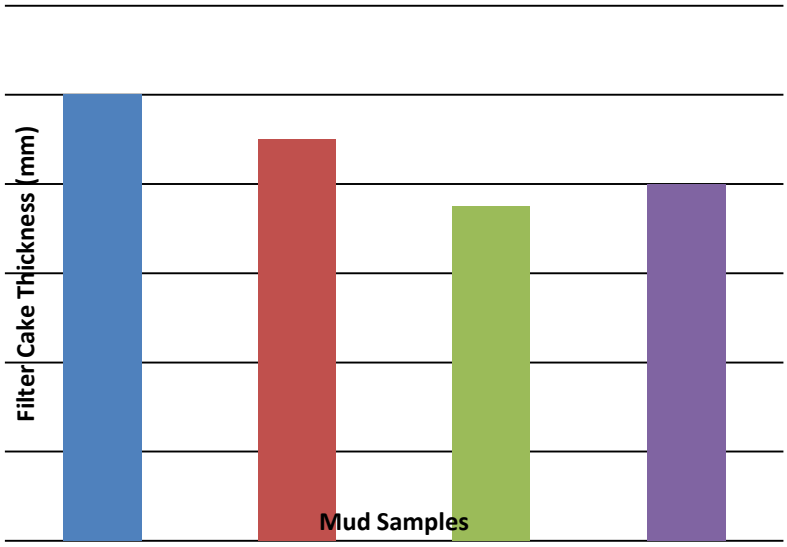

Fig.3: Mud Filter Cake Thickness

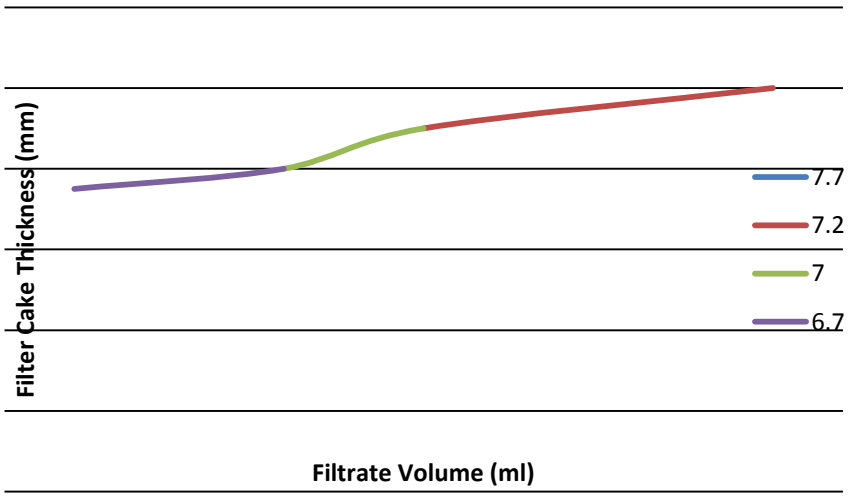

Fig.4: Relationship between Mud Filter Cake Thickness and Filtration Volume

CONCLUSIONS

This research has shown that PSA has good filtration (fluid loss) control properties. Addition of PSA to the various mud samples improved the filtration characteristics of the formulated water-based drilling mud with respect to reduced filtrate volume and thinner and consistent mud filter cakes. Mud sample C formulated with 2.0 g of PSA exhibited the best filtration control characteristics with minimal filtrate volume of 6.7 ml after 30 minutes of filtration. Physical examination of the mud filter cakes formed after 30 minutes of filtration show that sample C produced the best filter cake with minimum thickness of 0.75 mm. However, increasing the quantity of PSA to 2.5 and 3.0 g in samples D and B, respectively, did not result to better filtration characteristics. The relationship between mud filter cake thickness and filtration volume is somewhat linear. Therefore, periwinkle shells, waste products found in abundance in the Niger Delta region of Nigeria, can be converted to wealth, to create wealth and business venture for the people of the region.

REFERENCES:

[1] Boek, E. S., Hall, C.,and Tardy, P. M. J. "Deep Bed Filtration Modelling of Formation Damage Due To Particulate Invasion For Drilling Fluids," Jan 2012 *In: Transport in Porous Media.* Vol. 91, no. 2, Jan 2012, pp. 479-508.

[2] Micheal, J. E., and Kenneth, G. N. "Reservoir Stimulation." Schlumberger Educational Services, Texas, 1989, pp. 565-580.

[3] Peden, J. M., Avalo, M. R., and Arthur, K. G. "The Analysis of Dynamic Filtration and Permeability Impairment Characteristics of Inhibited water based mud." *SPE Fornation Damage Control Symposium*, Lafayette, Louisiana, SPE-10655-MS, 24-25 March, 1982.

[4] Methven, N. E., and Kemick, J. G. "Drilling and Gravel Packing with an oil base fluid system." *Journal of Petroleum Technology*, vol. 21, iss. 06, pp. 671-679, June 1969.

[5] Goode, D. L., Berry, S. D., and Stacy, A. L. "Aqueous-Based Remedial Treatments for Reservoirs Damaged by Oil-Phase Drilling muds." *SPE Fornation Damage Control Symposium*, Bakersfield, California, SPE-12501-MS, 13-14 February, 1984.

[6] "Specifications for Oil Well Drilling Fluid Materials." *API*, Dallas, pp.39, 40-45, 2001

[7] Olatunde, A. O., Usman, M. A., Olafadehan, O.A., Adeosun, T. A., and Ufot, O. E. "Improving the Rheological Properties of Drilling Fliud Using Locally Based Materials," *Petroleum & Coal*, vol. 54, no. 1, pp. 65-75, 2012.

[8] Omotioma, M., Ejikeme, P. C. N., and Ume, J. I. "Improving the Rheological Properties of Water Based Mud with the Addition of Cassava Starch," *IOSR Journal of Applied Chemistry (IOSR-JAC)*, e-ISSN: 2278-5736. vol 8, iss. 8, ver. I, PP 70-73, August 2015.

[9] Samavati R., Abdullah N., Tahmasbi Nowtarki K., Hussain S. A., and Awang Biak D. R. "Rheological and Fluid Loss Properties of Water Based Drilling Mud Containing HCl-Modified *Fufu* as a Fluid Loss Control Agent," *International Journal of Chemical Engineering and Applications*, vol. 5, no. 6, pp. 446-450, December 2014.

[10] Ademiluyi T., Joel, O. F., and Amuda A. K. "Investigation of Local Polymer (Cassava Starches) as a Substitute for Imported Sample in Viscosity and FluidLoss Control of Water Based Drilling Mud," *ARPN Journal of Engineering and Applied Sciences*, vol. 6, no. 12, pp. 43-48, December 2011.

[11] Amanullah, M.D. and Yu, L. Superior Corn-Based Starches for Oil Field Application. *CSIRO petroleum, Australian Resources Research Centre*, 2004, http://www.cropscience.org.au/icsc2004/poster /3/5/1010_amanullahm.htm.

[12] Wikipedia, "Common Periwinkle," https://en.wikipedia.org/wiki/Common_periwinkle, accessed on 22nd September, 2015.

[13] Festus A. Olutoge, Oriyomi M. Okeyinka and Olatunji S. Olaniyan, "Assessment Of The Suitability Of Periwinkle Shell Ash (PSA) As Partial Replacement For Ordinary Portland Cement (Opc) In Concrete," *IJRRAS*, vol.10 iss. 3, pp. 428-434, March 2012. www.arpapress.com/Volumes/Vol10Issue3/IJRRAS_10_3_08.pdf.

[14] Umoh, A.A. And Femi, O.O., "Comparative Evaluation of Concrete Properties with Varying Proportions of Periwinkle Shell and Bamboo Leaf Ashes Replacing Cement," *Ethiopian Journal of Environmental Studies and Management*, vol. 6, no.5, pp. 570-580, 2013. http://dx.doi.org/10.4314/ejesm.v6i5.15.

[15] Olufemi, I. A. and Joel, M. "Suitability of Periwinkle Shell as Partial Replacement for River Gravel in Concrete," *Leonardo Electronic Journal of Practices and Technologies*, Issue 15, pp. 59-66. July-December 2009. http://lejpt.academicdirect.org.

[16] Dahunsi, B. I. O. "Properties of Periwinkle-Granite Concrete," *Journal of Civil Engineering, JKUAT*, vol. 8, issue 1. Pp. 27-36, ISSN: 1562-6121, 2002. http://dx.doi.org/10.4314/jce.v8i1.18993.

[17] Olusola, K. O. and Umoh, A. A. "Strength Characteristics of Periwinkle Shell Ash Blended Cement Concrete**,"** *International Journal of Architecture, Engineering and Construction*, Vol. 1, No. 4, pp. 213-220, December 2012.

[18] Fann. "LPLT Filter Press Instruction Manual," October 2014. http://hamdon.net/products/filter-press-api-lplt/.

International Journal of Engineering Research and General Science Volume 3, Issue 6, November-December, 2015
ISSN 2091-2730

Bio-Computational Characterization of *Wolbachia* surface protein in different species of Drosophila

Amrutha.K.M, Dr. Mahesh Pattabhiramaiah and Anusha.P.K

Centre for Applied Genetics, Department of Zoology, Jnanabharathi, Bangalore University,

Bangalore - 560056

Email:reply2mahesh@gmail.com

Ph no: 91-9916130942

Abstract - *Wolbachia* surface protein (WSP) is an eight beta-barrel, trans-membrane structure, which participates in host immune response, cell proliferation, pathogenicity and controlled cell death program. The current study employs the bio-informatics tool to unravel the structural and functional properties of the WSP infecting drosophila. The present study was focused on sequence analysis, insilico prediction of the secondary and tertiary structure of wsp sequence. Sequence analysis and physiochemical properties revealed that this protein is highly stable, negatively charged and having more hydrophobic regions. SOPMA was used to predict secondary structure of wsp, which revealed that the protein contains more of random coils and extended strands than alpha helix and beta sheets. SVM prot analysis revealed the functionality of protein including the details of metal binding sites. Multiple sequence alignment was performed using MUSCLE server which revealed highly conserved regions. The RNA structure was predicted by using Genebee service software, a set of homologous sequences as the stems with their free energy. The protein orientation and trans-membrane region was predicted using TMpred, which will be useful for drug designing. The predicted 3D model was analyzed using Swiss Model which will be helpful for further structure based studies.

Keywords - *Wolbachia* Surface Protein, Drosophila, SOPMA, SVM prot, ProtParam, MUSCLE, TMpred and Swiss Model.

INTRODUCTION

The genus *Wolbachia* (Rickettsiaceae) is a group of intracellular, gram-negative and endosymbiontic bacteria that belong to the order Rickettsiales in the α-subdivision of the class Proteobacteria [35]. The genus *Wolbachia* comprises a group of maternally inherited intracellular bacteria that have been identified in a wide range of arthropod hosts. They are parasitic bacteria of invertebrates including insects, chelicerates, crustaceans, nematodes and dipterans.

Although, *Wolbachia* usually is vertically transmitted, there are cases of horizontal transmission even across host species [36 & 19]. *Wolbachia* infection commonly causes reproductive disorders such as feminization, parthenogenesis and cytoplasmic incompatibility, but also direct morbidity such as neural tissue invasion and destruction [21].

The fruit fly *Drosophila melanogaster*, offers the ideal opportunity to investigate the host-parasite interaction. Not only is it an extremely powerful model host for investigating all aspects of infection and immunity [6 & 23], it is also one of the best-developed model systems for behavioral ecology and genetics [30 & 24]. *Wolbachia* is present in most natural population of *D.melanogaster*, although with variable frequencies of infection [25].

Wolbachia surface protein (WSP), an abundantly expressed protein of Wolbachia, was identified in the endobacteria of Drosophila spp, and has been characterized for *Wolbachia* residing in *D. immitis* [5 & 3]. WSP is a low-molecular-weight protein of 22 kDa. WSP belongs to pfam0617, primarily defined by antibody recognition.

Wolbachia surface protein (WSP) is an eight beta-barrel transmembrane structure which participates in host immune response, cell proliferation, pathogenicity and controlled cell death program. Recombination has a large impact on diversity of this protein including positive selection, which is major constraint on protein evolution. In *Wolbachia*, increased recombination is observed in ankyrin proteins, surface proteins and in some hypothetical proteins.

The wealth of *Wolbachia* surface protein sequence information that has been made publicly available in recent years requires the development of high-throughput proteomics approaches for its analysis. Characterization of proteins of interest from a particular biological study requires the application of suitable bioinformatics tools to process, annotate and prioritise the data in order to gain maximum benefit from the results generated.

From a protein function standpoint, transfer of annotation from known proteins to a novel target is currently the only practical way to convert vast quantities of raw sequence data into meaningful information. New bioinformatics tools now provide more sophisticated methods to transfer functional annotation, integrating sequence, family profile and structural search methodology.

Present study explored the physicochemical nature, three dimensional structure and detail of interactions and functions of the wsp structure. The structural characterization of WSP would provide the clues to its biological function, physiological role and is a prerequisite for the development of new drug targets. The physicochemical and the structural properties of the proteins are well understood with the use of computational tools by through insilico analysis. The statistics about a protein sequence such as number of amino acid, frequency is predicted by CLC work bench. Simple Modular Architecture Research Tool (SMART) is a biological database that is used in the identification and analysis of protein domains within protein sequences [29 & 17]. Sequence length, and

the physico-chemical properties of proteins such as molecular weight, extinction coefficient, GRAVY, aliphatic index, instability index, etc., can be computed by ProtParam. The TMpred program makes a prediction of membrane-spanning regions and their orientation. The algorithm is based on the statistical analysis of TMbase, a database of naturally occurring transmembrane proteins. The prediction is made using a combination of several weight-matrices for scoring [15]. MUSCLE stands for Multiple **S**equence **C**omparison by **L**og- **E**xpectation. The protein 3D model and its characteristics can be predicted by Swiss model server [32]. Protein homology modeling and analogy recognition is made through Phyre2 online server. Further Computer-aided techniques for the efficient identification and optimization of novel molecules with a desired biological activity have become a part of the drug discovery process.

Bioinformatics has revolutionized in the field of molecular biology. The raw sequence information of proteins and nucleic acid can convert to analytical and relative information with the help of soft computing tools. Prediction of protein function is important application of bioinformatics. The amino acid sequence provides most of the information required for determining and characterizing the molecule‘s function, physical and chemical properties. Sequence analysis and physicochemical characterization of proteins using biocomputation tools have been done by many researchers and reported [2, 18, 26, 20, & 34].

The extensive knowledge available on Drosophila provides a solid base on which to test new hypothesis on host–*Wolbachia* interactions. The main objective of this study was to perform physiochemical characterization of the wsp in Drosophila, which are very much necessary in understanding the *Wolbachia* -host interactions with special reference to parasitic *Wolbachia*, which causes different reproductive anomalies in arthropod hosts. The structural characterization would provide the clues to its biological function, physiological role and is a prerequisite for the development of integrated pest managements.

Materials and Methods:

Protein sequence retrieval : The Protein Sequences of *wolbachia* surface protein(15 sequences) were retrieved in FASTA format from NCBI database (Table1) .

Amino acid Composition: The amino acid composition of selected proteins were computed using the tool CLC free workbench (www.clc.bio.com/..../clc-main-workbench), tabulated in (Table-2).

Primary structure analysis: Counts of hydrophobic and hydrophilic residues were calculated from the primary structure analysis by CLC workbench (Table-3).

Physiochemical parameters: The physiochemical parameters such as theoretical isoelectric point (Ip), molecular weight, total number of positive and negative residues, extinction coefficient, instability index [8] aliphatic index [7] and grand average hydropathy (GRAVY) [16] were computed using the Expasy‘s ProtParam server (http://web.expasy.org/protparam/) [22], and tabulated in (Table-4).

Secondary structure prediction: The secondary structure was predicted by self-optimized prediction method with alignment by SOPMA server **(**https://npsa-prabi.ibcp.fr/cgi-bin/npsa_automat.plpage=npsa_sopma.html) [2] (Table-5).

Domain architecture analysis: Domain organization and domain composition was analyzed using Simple Modular Architecture Research Tool (SMART) (http://smart.embl-heidelberg.de) (Table-6).

SVM prot analysis: The protein function prediction and classification of proteins were analyzed using SVM Prot (http://jing.cz3.nus.edu.sg/cgi-bin/svmprot.cgi.) (Table-7).

Transmembrane region prediction: Transmembrane helices were predicted by the TMpred software. (http://www.ch.embnet.org/software/TMPRED_form.html) (Fig-1) (Table-8).

Sequence Homology Analysis: The sequence homology was analyzed by MUSCLE (http://www.ebi.ac.uk/Tools/msa/muscle/) (Fig-2).

Tertiary structure Prediction: Tertiary structure prediction (Fig-3) of *wolbachia* surface protein was performed using bioinformatics tool Phyre2 (www.sbg.bio.ic.ac.uk/phyre2/index.cgi).

RNA structure prediction: The protein sequences were reverse transcribed to DNA using Sequence manipulation suite (SMS) (http://www.bioinformatics.org/sms2/rev_trans.html). The reverse transcribed DNA was converted to RNA using transcriptional and translational tool (http://www.attotron.com/cybertory/analysis/trans.html). RNA structure was predicted using (http://www.genebee.msu.su/services/rna2_reduced.html) (Fig-4).

Swiss model: SWISS-MODEL is a fully automated protein structure homology-modeling server, accessible via the ExPASy web server or from the program Deep View (Swiss Pdb-Viewer) (http://swissmodel.expasy.org/). The purpose of this server is to make Protein Modeling accessible to all biochemists and molecular biologists worldwide. (Fig-5)

(Table 1) - *Wolbachia* Surface Protein Sequences Retrieved from NCBI

Sl No	Species	ID	Length	Protein Sequence
1	*Drosophila sechellia*	ABD75492.1	189	VRLQYNGEILPLFTKVDGATGAKKKTADTDTTTDLYKASFMAGGGAFGYK DDIRVDVEGLYSQLSKDTLDVAPTPAIADSLTAFSGLVNVYYYDIAIEDMPITP YVGVGVGAAYISTPLATAVSSQNGKFAFAGQARAGVSYDITPEIKLYAGAR YFGSFCAHFDKDTAAASKDKGELKVLYSTVGAEA
2	*Drosophila sturtevanti*	ABD75491.1	186	VRLQYNGEILPLFTKIDGIQKTKGKEKDSPLKASFVAGGGAFGYKMDDIRVD VEGLYSWLNKDADVVGDTVADNLTAISGLVNVYYYDVAIEDMPITPYIGVGI GAAYISTPLKTAVNEQNSKFGFAGQVKAGVSYDVTPEIKLYAGARYFGSYG AHFDKSEEVDKAVGGKETKVTKDAYKVLYSTV
3	*Drosophila nikananu*	ABD75490.1	189	VRLQYNGEFLPLFTKIDGITNATGKEKDSPLKASFIAGGGAFGYKMDDIRVD VEGLYSQLSKDTTIINTSEENVADSLTAFSGLVNVYYYDIAIEDMPITPYVGVG VGAAYISTPLKPAINEQNSKFGFAGQVKAGVSYDVTPEIKLYAGARYFGSYG AHFDKSEEVDKAGGGKETKVTKDAYKVLYSTV
4	*Drosophila mauritiana*	ABD75488.1	183	VRLQYNGEVLPFKTRIDGIEYKKGTEVHDPLKASFMAGGAAFGYKMDDIRV DVEGLYSQLNKNDVSGATFTPTTVANSVAAFSGLVNVYYDIAIEDMPITPYV GVGVGAAYISNPSEASAVKDQKEFGFAYQAKAGVSYDVTPEIKLYAGARYF GSYGASFNKEAVSATKEINVLYSAVGAEA
5	*Drosophila ananassae*	ABD75484.1	189	VRLQYNGEFLPLFTKVDGITYKKDKSDYSPLKPSFIAGGGAFGYKMDDIRVD VEGVYSYLNKNDVKDVTFDPANTIADSVTAISGLVNVYYDIAIEDMPITPYIG VGVGAAYISTPLEPAVNDQKSKFGFAGQVKAGVSYDVTPEVKLYAGARYF GSYGANFDGKKTDPKDSTRQVTDAGAYKVLYSTV
6	*Drosophila arawakana*	ABD75483.1	189	VRLQYNGEFLPLFTKVDGITYKKDKSDYSPLKPSFIAGGGAFGYKMDDIRVD VEGVYSYLNKNDVKDVTFDPANTIADSVTAISGLVNVYYDIAIEDMPITPYIG VGVGAAYISTPLEPAVNDQKSKFGFAGQVKAGVSYDVTPEVKLYAGARYF GSYGANFDGKKTDPKDSTRQVTDAGAYKVLYSTV
7	*Drosophila simulans*	ABD75482.1	189	VRLQYNGEFLPLFTKVDGITYKKDKSDYSPLKPSFIAGGGAFGYKMDDIRVD VEGVYSYLNKNDVKDVTFDPANTIADSVTAISGLVNVYYDIAIEDMPITPYIG VGVGAAYISTPLEPAVNDQKSKFGFAGQVKAGVSYDVTPEVKLYAGARYF GSYGANFDGKKTDPKNSTGQAADAGAYKVLYSTV
8	*Drosophila melanogaster*	ABD75481.1	189	VRLQYNGEFLPLFTKVDGITYKKDKSDYSPLKPSFIAGGGAFGYKMDDIRVD VEGVYSYLNKNDVKDVTFDPANTIADSVTAISGLVNVYYDIAIEDMPITPYIG VGVGAAYISTPLEPAVNDQKSKFGFAGQVKAGVSYDVTPEVKLYAGARYF GSYGANFDGKKTDPKNSTGQAADAGAYKVLYSTV
9	*Drosophila tropicalis*	ABD75479.1	189	VRLQYNGEFLPLFTKVDGITYKKDKSDYSPLKPSFIAGGGAFGYKMDDIRVD VEGVYSYLNKNDVKDVTFDPANTIADSVTAISGLVNVYYDIAIEDMPITPYIG VGVGATYISTPLEPAVNDQKSKFGFAGQVKAGVSYDVTPEVKLYAGARYFG SYGANFDGKKTDPKDSTRQVTDAGAYKVLYSTV
10	*Drosophila willistoni*	ABD75478.1	189	VRLQYNGEFLPLFTKVDGITYKKDKSDYSPLKPSFIAGGGAFGYKMDDIRVD VEGVYSYLNKNDVKDVTFDPANTIADSVTAISGLVNVYYDIAIEDMPITPYIG VGVGATYISTPLEPAVNDQKSKFGFAGQVKAGVSYDVTPEVKLYAGARYFG SYGANFDGKKTDPKDSTRQVTDAGAYKVLYSTV
11	*Drosophila pseudotakahashii*	ABD75474.1	181	VRLQYNGEILPLFTKVDGITYKKDNSDYSPLKASFIAGGGAFGYKMDDIRVD VEGVYSYLNKNDVTDAKFTPDTIADSLTAISGLVNVYYDIAIEDMPITPYIGV GVGAAYISTPLKDAVNDQKSKFSFAGQVKAGVSYDVTPEVKLYAGARYFGS FGAHFDKDAAAGKDKGELKVLYSTV
12	*Drosophila bicornuta*	ABD75473.1	187	VRLQYNGEVLPLFTKVDNMKIKKGTDDVDPFKASFIGGGAAFGYKMDDIRV DIEGLYSQLNKNVNNDEVLTPDTVAGSLTAISGLVNVYYDIAIEDMPITPYVG VGVGAAYISTPLKDAVNDQKSKFGFAGQVKAGVSYDVAPEVKLYAGARYF GSYGANFDKSGGEKDKGGHTVLYSTVGAEAGVA
13	*Drosophila fumipennis*	AAU95644.1	187	SYYVRLQYNGEVLPLFTKVDNMKIKKGTDDVDPFKASFIGGDAAFGYKMD DIRVDIEGLYSQLNKNVNNGEALTPDIVAGSLTAISGLVNVYYDIAIEDMSITP YVGVGVGAAYISAPLNDAVNGQKSKFGFAGQVKAGVSYDVTPEVKLYAGA RYFGSYGANFDKSSGEKNKGGHTVLYSTVGAEA

14	*Drosophila suzukii*	AFP86012.1	182	VRLQYNGEILPLFTKIEGIEYKKATDIHNPLKASFIAGGGAFGYKMDDIRVDV EGLYSQLNKNDVTGAAFNPDTVADSLTAISGLVNVYYYDIAIEDMPITPYVGV GVGAAYISTPLKDAVNDQKSKFGFAGQVKAGVSYDVTPEVKLYAGARYFG SFGAHFDKDTAAASKDKGELKVLYSTV
15	*Drosophila nigrocirrus*	AFP85988.1	184	VRLQYNGEFLPLFTKVDGITNATGKEKDSPLKASFIAGGGAFGYKMDDIRVD VEGLYSWLNKDADVVGDTVADNLTAISGLVNVYYYDVAIEDMPITPYIGVGV GAAYISTPLKTPINDQKSKFGFAGQVKAGVSYDVTPEIKLYAGARYFGSYGA NFDGKKTDPKDSTKQVTDAGAYKVLYSTV

(Table 2)- REPRESENTATION OF FREQUENCY OF AMINO ACIDS of WSP

Sl No	Amino acid	ABD75492.1	ABD75491.1	ABD75490.1	ABD75488.1	ABD75484.1	ABD75483.1	ABD75482.1	ABD75481.1	ABD75479.1	ABD75478.1	ABD75474.1	ABD75473.1	AAU95644.1	AFP860112.1	AFP85988.1
1	Alanine (A)	0.143	0.091	0.09	0.131	0.085	0.085	0.095	0.095	0.079	0.079	0.099	0.096	0.096	0.11	0.092
2	Cysteine (C)	0.005	0	0	0	0	0	0	0	0	0	0	0	0	0	0
3	Aspartic Acid (D)	0.085	0.081	0.069	0.055	0.095	0.095	0.09	0.09	0.095	0.095	0.099	0.086	0.075	0.082	0.092
4	Glutamic Acid (E)	0.032	0.048	0.058	0.06	0.026	0.026	0.026	0.026	0.026	0.026	0.028	0.037	0.037	0.038	0.027
5	Phenylalanine (F)	0.048	0.038	0.048	0.049	0.048	0.048	0.048	0.048	0.048	0.048	0.05	0.043	0.043	0.049	0.043
6	Glycine (G)	0.101	0.113	0.111	0.098	0.101	0.101	0.106	0.106	0.101	0.101	0.099	0.128	0.123	0.104	0.114
7	Histidine (H)	0.005	0.005	0.005	0.005	0	0	0	0	0	0	0.006	0.005	0.005	0.011	0
8	Isoleucine (I)	0.048	0.059	0.063	0.049	0.053	0.053	0.053	0.053	0.053	0.053	0.061	0.048	0.053	0.06	0.054
9	Lysine (K)	0.069	0.097	0.085	0.066	0.085	0.085	0.085	0.085	0.085	0.085	0.088	0.08	0.075	0.082	0.087
10	Leucine (L)	0.069	0.059	0.058	0.044	0.048	0.048	0.048	0.048	0.048	0.048	0.061	0.059	0.059	0.066	0.06
11	Methionine (M)	0.016	0.011	0.011	0.016	0.011	0.011	0.011	0.011	0.011	0.011	0.011	0.016	0.016	0.011	0.011

12	Asparagine (N)	0.016	0.032	0.037	0.044	0.037	0.037	0.042	0.042	0.037	0.037	0.033	0.048	0.059	0.038	0.038
13	Proline (P)	0.037	0.032	0.037	0.038	0.053	0.053	0.053	0.053	0.053	0.053	0.039	0.037	0.032	0.038	0.043
14	Glutamine (Q)	0.021	0.022	0.021	0.022	0.021	0.021	0.021	0.021	0.021	0.021	0.017	0.021	0.021	0.022	0.022
15	Arginine (R)	0.021	0.016	0.016	0.022	0.021	0.021	0.016	0.016	0.021	0.021	0.017	0.016	0.016	0.016	0.016
16	Serine (S)	0.063	0.054	0.069	0.071	0.063	0.063	0.063	0.063	0.063	0.063	0.066	0.053	0.07	0.055	0.054
17	Threonine (T)	0.085	0.059	0.069	0.049	0.063	0.063	0.058	0.058	0.069	0.069	0.055	0.048	0.043	0.055	0.071
18	Valine (V)	0.074	0.108	0.085	0.104	0.106	0.106	0.101	0.101	0.106	0.106	0.094	0.112	0.102	0.093	0.098
19	Tryptophan (W)	0	0.005	0	0	0	0	0	0	0	0	0	0	0	0	0.005
20	Tyrosine (Y)	0.063	0.07	0.069	0.077	0.085	0.085	0.085	0.085	0.085	0.085	0.077	0.064	0.075	0.066	0.071

(Table 3)-Hydrophilic and hydrophobic residues computed by CLC WORK BENCH

Accession Number	Counts of hydrophilic residues	Counts of hydrophobic residues
ABD75492.1	48	101
ABD75491.1	44	96
ABD75490.1	50	95
ABD75488.1	48	97
ABD75484.1	51	95
ABD75483.1	51	95
ABD75482.1	51	97
ABD75481.1	51	97
ABD75479.1	52	94
ABD75478.1	52	94
ABD75474.1	45	93
ABD75473.1	44	101
AAU95644.1	50	98
AFP86012.1	43	97
AFP85988.1	47	96

(TABLE 4) – Physiochemical Parameters Computated by Expasy ProtParam

Accession Number	PI	Mol.Wt	-R	+R	EC	II	AI	Gravy
ABD75492.1	4.83	19919.4	22	17	17880	17.51	81.16	0.011
ABD75491.1	5.25	20060.7	24	21	24870	21.83	86.45	-0.151
ABD75490.1	4.96	20331.8	24	19	19370	23.41	81.01	-0.185
ABD75488.1	4.91	19578.9	21	16	20860	27.06	79.45	-0.066
ABD75484.1	4.99	20503.0	23	20	23840	22.68	78.36	-0.216
ABD75483.1	4.99	20503.0	23	20	23840	22.68	78.36	-0.216
ABD75482.1	4.97	20344.8	22	19	23840	20.59	77.88	-0.194
ABD75481.1	4.97	20344.8	22	19	23840	20.59	77.88	-0.194
ABD75479.1	4.99	20533.0	23	20	23840	22.68	77.83	-0.229
ABD75478.1	4.99	20533.0	23	20	23840	22.68	77.83	-0.229
ABD75474.1	4.98	19549.0	23	19	20860	17.21	84.59	-0.112
ABD75473.1	4.87	19814.3	23	18	17880	16.89	83.90	-0.112
AAU95644.1	4.98	19931.3	21	17	20860	17.78	82.89	-0.124
AFP86012.1	5.16	19525.0	22	18	17880	21.78	87.36	-0.065
AFP85988.1	4.97	19727.2	22	19	24870	18.03	82.12	-0.154

(TABLE 5)- Representation Of helix, sheets, turns, coils by Garnier peptide Analysis through online tool by SOPMA

Accession Number	Helix(H) Residue Totals	Percentage (%)	Sheet(E) Residue Totals	Percentage (%)	Turns (T) Residue Totals	Percentage (%)	Coils Residue Totals	Percentage (%)
ABD75492.1	45	23.81	59	31.22	23	12.17	62	32.80
ABD75491.1	52	27.96	58	31.18	22	11.83	54	29.03
ABD75490.1	39	20.63	60	31.75	22	11.64	68	35.98
ABD75488.1	61	33.33	49	26.78	24	13.11	49	26.78
ABD75484.1	26	13.76	68	35.98	23	12.17	72	38.10
ABD75483.1	26	13.76	68	35.98	23	12.17	72	38.10
ABD75482.1	31	16.40	65	34.39	21	11.11	72	38.10
ABD75481.1	31	16.40	65	34.39	21	11.11	72	38.10
ABD75479.1	24	12.70	68	35.98	23	12.17	74	39.15
ABD75478.1	24	12.70	68	35.98	23	12.17	74	39.15
ABD75474.1	32	17.68	61	33.70	27	14.92	61	33.70
ABD75473.1	38	20.32	59	31.55	24	12.83	66	35.29
AAU95644.1	36	19.25	58	31.02	24	12.83	69	36.90
AFP86012.1	45	24.73	60	32.97	25	13.74	52	28.57

AFP85988.1	32	17.39	71	38.59	19	10.33	62	33.70

(TABLE 6) - SMART ANALYSIS

NAME	START	END	E-VALUE
ABD75492.1	14	34	N/A
ABD75491.1	103	166	536
ABD75490.1	No domain	No domain	No domain
ABD75488.1	4	86	1640
ABD75484.1	No domain	No domain	No domain
ABD75483.1	No domain	No domain	No domain
ABD75482.1	No domain	No domain	No domain
ABD75481.1	No domain	No domain	No domain
ABD75479.1	No domain	No domain	No domain
ABD75478.1	No domain	No domain	No domain
ABD75474.1	No domain	No domain	No domain
ABD75473.1	No domain	No domain	No domain
AAU95644.1	No domain	No domain	No domain
AFP86012.1	53	89	2260
AFP85988.1	No domain	No domain	No domain

(TABLE 7)- SVMPROT ANALYSIS

Accession Number	Protein Family							
	Metal Binding		Zinc Binding		All Lipid Protein		Outer Membrane	
	R	P	R	P	R	P	R	P
ABD75492.1	1.0	58.6	1.4	71.3	-	-	-	-
ABD75491.1	1.0	58.6	-	-	1.3	68.5	1.0	58.6
ABD75490.1	1.1	62.2	3.7	97.0	-	-	1.0	58.6
ABD75488.1	1.0	58.6	3.2	95.2	-	-	-	-
ABD75484.1	1.0	58.6	-	-	1.5	73.8	-	-
ABD75483.1	1.0	58.6	-	-	1.5	73.8	-	-
ABD75482.1	1.0	58.6	1.3	68.5	1.5	73.8	-	-
ABD75481.1	1.0	58.6	1.3	68.5	1.5	73.8	-	-
ABD75479.1	1.0	58.6	-	-	1.6	76.2	-	-
ABD75478.1	1.0	58.6	-	-	1.6	76.2	-	-
ABD75474.1	1.0	58.6	1.2	65.4	1.2	65.4	-	-
ABD75473.1	1.0	58.6	1.6	76.2	-	-	-	-
AAU95644.1	1.0	58.6	1.4	71.3	-	-	-	-
AFP86012.1	-	-	1.7	78.4	2.0	83.9	1.0	58.6
AFP85988.1	1.0	58.6	2.0	83.9	1.0	62.2	1.0	58.6

(TABLE 8)- Transmembrane region scoring showing helices (ABD75481.1)

	Inside-Outside	Outside-Inside
Helices	(73- 91 (19) 466)	(76- 94 (19) 538)
	(103- 121 (19) 303)	(98- 115 (18) 427 +)

(TABLE 9)- RNA structure stems with free energy (ABD75481)

Stem no	1	2	3	4	5	6	7	8	9	10	11	12	13	14	15	16	17	18	19
Free energy(Kkal/mol)	-16.500000 Kkal/mol	-14.600000 Kkal/mol	-13.500000 Kkal/mol	-13.200000 Kkal/mol	-13.200000 Kkal/mol	-12.700000 Kkal/mol	-11.400000 Kkal/mol	-11.300000 Kkal/mol	-10.000000 Kkal/mol	-9.400000 Kkal/mol	-8.900000 Kkal/mol	-8.900000 Kkal/mol	-8.400000 Kkal/mol	-8.300000 Kkal/mol	-7.300000 Kkal/mol	-7.000000 Kkal/mol	-6.700000 Kkal/mol	-6.600000 Kkal/mol	-6.100000 Kkal/mol

(Fig-1) Transmembrane region prediction (ABD75481.1)

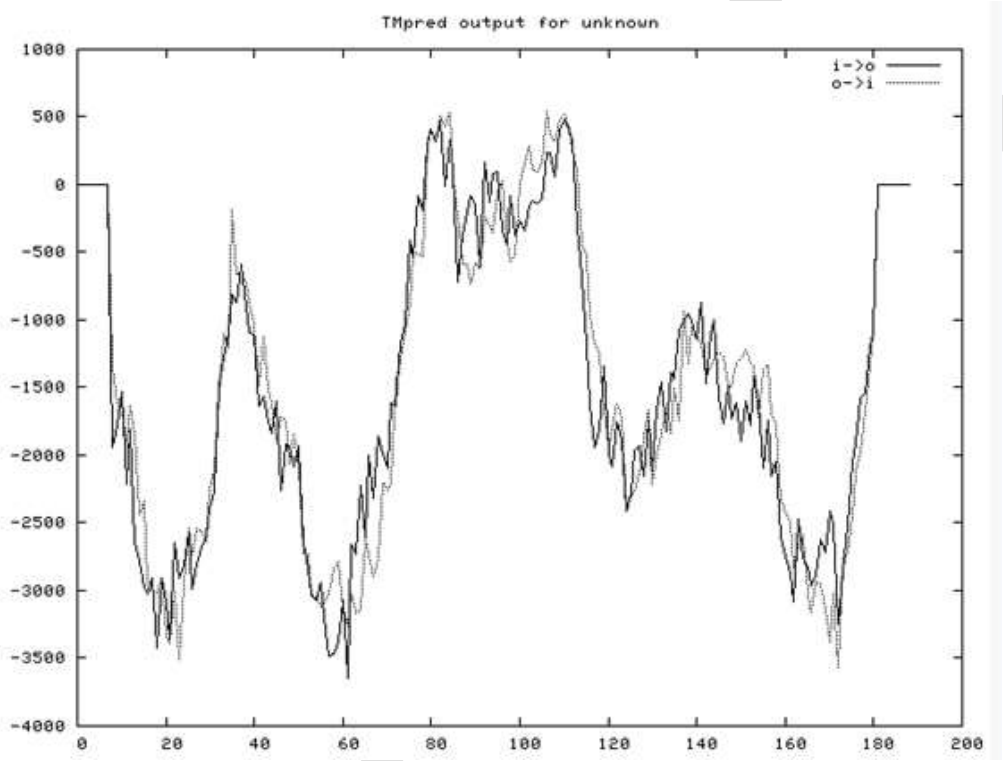

(Fig-2) MUSCLE-Multiple sequence alignment of wsp drosophila

Conserved sequences for hierarchical clustering, primary constructions, identity percentage strong and weakly similar sequences is predicted.

```
gi|89515329|gb|ABD75488.1|      YISNPSEASAVKDQKEFGFAYQAKAGVSYDVTPEIKLYAGARYFGSYGASFN------KE
gi|89515337|gb|ABD75492.1|      YISTPLATAVSSQNGKFAFAGQARAGVSYDITPEIKLYAGARYFGSFCAHFD------KD
gi|89515299|gb|ABD75473.1|      YISTPLKDAVNDQKSKFGFAGQVKAGVSYDVAPEVKLYAGARYFGSYGANFD--------
gi|53854523|gb|AAU95644.1|      YISAPLNDAVNGQKSKFGFAGQVKAGVSYDVTPEVKLYAGARYFGSYGANFD--------
gi|89515335|gb|ABD75491.1|      YISTPLKTAVNEQNSKFGFAGQVKAGVSYDVTPEIKLYAGARYFGSYGAHFD--KSEEVD
gi|89515333|gb|ABD75490.1|      YISTPLKPAINEQNSKFGFAGQVKAGVSYDVTPEIKLYAGARYFGSYGAHFD--KSEEVD
gi|400365113|gb|AFP85988.1|     YISTPLKTPINDQKSKFGFAGQVKAGVSYDVTPEIKLYAGARYFGSYGANFDGKKTDPKD
gi|89515317|gb|ABD75482.1|      YISTPLEPAVNDQKSKFGFAGQVKAGVSYDVTPEVKLYAGARYFGSYGANFDGKKTDPKN
gi|89515315|gb|ABD75481.1|      YISTPLEPAVNDQKSKFGFAGQVKAGVSYDVTPEVKLYAGARYFGSYGANFDGKKTDPKN
gi|89515321|gb|ABD75484.1|      YISTPLEPAVNDQKSKFGFAGQVKAGVSYDVTPEVKLYAGARYFGSYGANFDGKKTDPKD
gi|89515319|gb|ABD75483.1|      YISTPLEPAVNDQKSKFGFAGQVKAGVSYDVTPEVKLYAGARYFGSYGANFDGKKTDPKD
gi|89515311|gb|ABD75479.1|      YISTPLEPAVNDQKSKFGFAGQVKAGVSYDVTPEVKLYAGARYFGSYGANFDGKKTDPKD
gi|89515309|gb|ABD75478.1|      YISTPLEPAVNDQKSKFGFAGQVKAGVSYDVTPEVKLYAGARYFGSYGANFDGKKTDPKD
gi|89515301|gb|ABD75474.1|      YISTPLKDAVNDQKSKFSFAGQVKAGVSYDVTPEVKLYAGARYFGSFGAHFD------KD
gi|400365161|gb|AFP86012.1|     YISTPLKDAVNDQKSKFGFAGQVKAGVSYDVTPEVKLYAGARYFGSFGAHFD------KD
                                *** *   .   :: :*.** *..******::**:***********: * *:
```

Alignment data;

Primary Construction. KKYMFYPDFLCKQPSE2C, Alignment length:

Identity (*): Strongly similar (:): Weakly similar (.)

(Fig- 3) RNA Structure prediction (ABD75481.1)

Free Energy of Structure = -107.4 kkal/mol

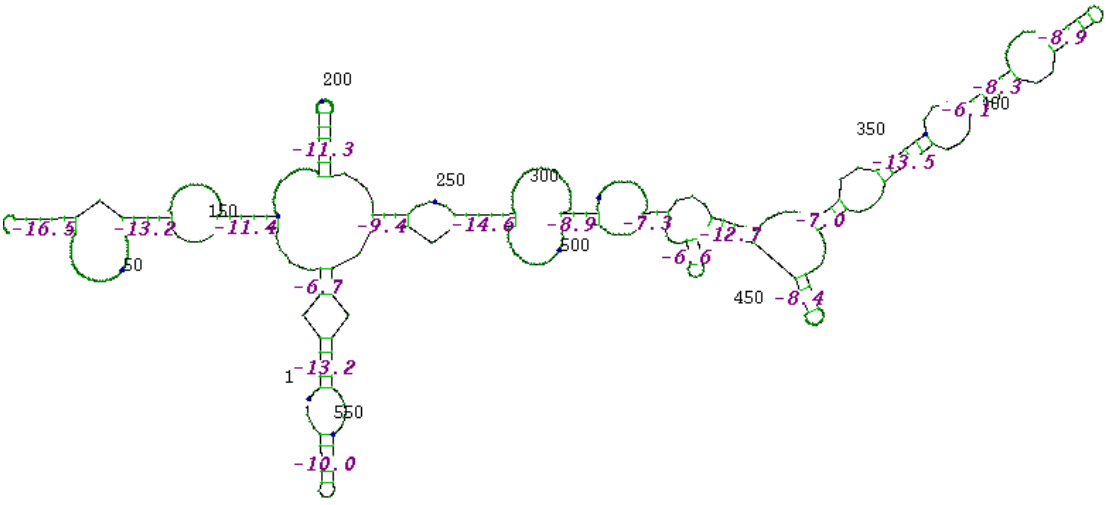

(Fig- 4) Protein Homology/analogy recognition by Swiss model (ABD75481.1)

Model 1 **Model 2** **Model 3**

(Fig-5) Model building using SWISS model of (ABD75481.1)

Model #01	File	Built with	Oligo-State	Ligands	GMQE	QMEAN4
	PDB	ProMod Version 3.70	MONOMER	None	0.44	-5.94

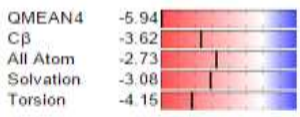

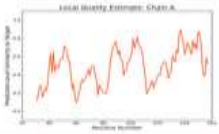

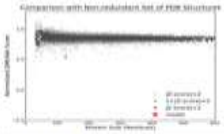

Template	Seq Identity	Oligo-state	Found by	Method	Resolution	Seq Similarity	Range	Coverage	Description
2maf.1.A	26.19	monomer	HHblits	NMR	NA	0.33	31 - 157	0.67	Opacity protein opA60

The template contained no ligands.

```
Target    VRLQYNGEFLPLFTKVDGITYKKDKSDYSPLKPSFIAGGGAFGYKMDDIRVDVEGV-YSYLNKNDVK----DVTF-----
2maf.1.A  ------------------------------IRTRSVHPRVSVGYDFGGWRIAADYARYRKWNNNKYSVNIENVRIRKENG

Target    ---DP--ANTIADSVTAI-SGLVNVYYDIAIEDMPITPYIGVGVGAAYISTPLEPA------------------------
2maf.1.A  IRIDRKTENQENGTFHAVSSLGLSAIYDFQIND-KFKPYIGARVAYGHVRHSIDSTKKTIEVTTVPSNAPNGAVTTYNTD

Target    -----VNDQKSKFGFAGQVKAGVSYDVTPEVKLYAGARYFGSYGANFDGKKTDPKNSTGQAADAGAYKVLYSTV
2maf.1.A  PKTQNDYQSNSIRRVGLGVIAGVGFDITPKLTLDAGYRYHNW--------------------------------
```

(Fig - 6) 3D View Of The Structure With Ligand Binding: (ABD75481.1)

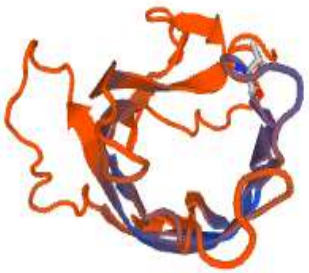

DISCUSSION:

Annotation of protein function is one of the key problems in post genomic era. This demands bioinformatics and computational biology to predict the function of unannoated hypothetical proteins by using various efficient tools and web servers. In our study, the analysis of *Wolbachia* surface protein was done using various bio-informatics tools and servers. The sequence and structural features of wsp and its complexities was annotated. The results of which allows for the designing of desired drugs. The results are discussed under following heads;

Amino acid composition:

The physiochemical analysis of amino acids of wsp in drosophila was analyzed by CLC workbench, which revealed the sequence length of all amino acids which is found to be 180-189 amino acids, tabulated in (Table 1). The most abundant amino acids present in this protein were Glycine, Alanine and Valine which are tabulated (Table 2).This abundancy of these amino acids in the protein reveals that the protein is hydrophobic in nature since these amino acids has side chains and has small dipole moments.

Residues of cysteine and tryptophan are absent which predicts the absence of Sulphide Bridge in the protein.

Primary sequence analysis:

The primary sequence analysis predicted by CLC work bench revealed that the *Wolbachia* surface protein are hydrophobic in nature as its percentage is more which ranges between 93-101 (Table 3).

Physiochemical Analysis:

Physiochemical properties of WSP by ProtParam tools are presented in (Table 4)**.** Results show that wsp has a molecular weight of 20533 Daltons, which has highest sequence length of 186 aa (ABD75479.1) and least was found to be 19525 Daltons with its sequence length of 182 aa (AFP86012.1).

Isoelectric point is the pH at which the surface of a protein is covered with charge but net charge of protein is zero. The computed PI value reveals that the protein is basic in nature, due to its least soluble property. Computed isoelectric point of proteins > 7 soluble is acidic buffers. Isoelectric point is predicted which ranges from 4.25 - 5.25 (Table 4).Useful for developing buffer system for purification of proteins and separating the protein on a polyacrylamide gel by isoelectric focusing.

Extinction co-efficient of wsp at 280nm is ranging from 17880-24870M^{-1} Cm^{-}. This infers that the protein can absorb the light at 280nm.The extinction co-efficient can be used to calculate the concentration of a protein in solution.

Stability of wsp was studied by analyzing the values for instability index, aliphatic index and Grand average of hydropathicity (GRAVY) index.

A protein whose instability index is below 40 is predicted as stable, and a value above 40 leads to structural instability. Here the instability index ranges from 16.89 to 27.06 thereby classifying the protein as stable. The aliphatic index refers to the relative volume of a protein that is occupied by aliphatic side chains and contributes to the increased thermo stability of protein. Aliphatic index of wsp was 77.83-87.36 which indicates that the proteins are thermo stable. GRAVY index indicates the solubility of proteins, GRAVY index of wsp was -0.011 to -0.229. A negative GRAVY value for wsp describes it to be hydrophobic in nature. This indicates interaction with water. Though it can play a role in substrate recognition. Here the protein sequences showing negative value indicate the stability of protein. In particular, hydrophobic amino acids can be involved in binding/recognition of ligands.

Secondary Structure Prediction:

SOPMA was employed for calculating the secondary structural features of the selected protein sequences considered in this study. This method calculates the content of α-helix, β-sheets, turns, random coils and extended strands. SOPMA is a neural network based methods; global sequence prediction may be done by this sequence method [22].

High percentage of helices in the structure makes the protein more flexible for folding, which might increase protein interactions. Moreover the predicted secondary structural information of wsp was considered to improve the target-template alignment and for building 3D model of the wsp.

The secondary analysis showed that wsp contain more of random coils and extended strands (range: 20-40%) than alpha sheets and beta sheets. High percentage of random coils and extended strands in the structure makes the protein more flexible and which might increase protein interactions.

Being hydrophobic, glycine prefers to be buried in protein hydrophobic cores. It also shows a preference for being within extended strand more so than in beta strands. The very high coil structural content of wsp is due to the rich content of more flexible glycine and hydrophobic. Proline has a special property of creating links in polypeptide chains and disrupting ordered secondary structure. The consequence in which most of the amino acid side chains of trans membrane segments is non-polar (*e.g. Gly*, Ala, Val ,Asp, Serinr, leu, Phe) and the very polar CO-NH groups (peptide bonds) of the polypeptide backbone of trans membrane segments which participates in hydrogen bonding (H-bonds) in order to lower the cost of transferring them into the hydrocarbon interior. This H-bonding is most easily accomplished with alpha-helices for which all peptide bonds are H-bonded internally. The distribution of amino acids in WSP complex protein (Table 5) shows random distribution of alpha helix, beta turns, extended strands and more distribution of random coils from all these organisms.

Domain Analysis:

SMART Analysis-

Many proteins are multidomain in character and possess multiple functions that often are performed by one or more component domains. A Web-based tool (SMART) has been designed that makes use of mainly public domain information to allow easy and rapid annotation of signaling multidomain proteins. The tool contains several unique aspects, including automatic seed alignment generation, automatic detection of repeated motifs or domains, and a protocol for combining domain predictions from homologous subfamilies. The ability of SMART to annotate single sequences or large datasets is exemplified by the cases described in wsp. Expect value (E) a parameter that counts the number of hits one can "expect" to see by chance for a database of a particular size. It decreases exponentially as the Score (S) of the match increases. Here it is in the range 536, 1640, 2260 (ABD75491.1, ABD75488.1, and AFP86012.1) respectively (Table 6).

SVM prot Analysis-

Support vector machines method for the classification of proteins with diverse sequence distribution. SVMProt shows a certain degree of capability for the classification of distantly related proteins and homologous proteins of different function and thus may be used as a protein function prediction tool that complements sequence alignment methods. It has been employed in protein studies including protein–protein interaction prediction, fold recognition, solvent accessibility and structure prediction. The prediction accuracy ranges from 1.1 to 99% in this study. Thus SVM classification of protein functional family, a potentially developed into a protein function prediction tool to complement methods based on sequence similarity and clustering. In wsp metal binding sites, revealed through this server was Zinc Binding, All Lipid protein and outer membrane protein family was found in only four species of drosophila which was 1.0 is the R value and 58.6 is the P value.(ABD75491.1, ABD75490.1, AFP86012.1 and AFP85988.1) (Table 7).

Based on the Classification of proteins of our interest and its values, we predict that , these proteins may act as drug targets , Metal binding sites, bonding involved ligation and integrated pest management is concerned.

Transmembrane region prediction

The difference between the value of sequence scored and the threshold indicates the possibility of the protein being an outer membrane protein. TMbase is a database of transmembrane proteins and their helical membrane- spanning domains. Possible transmembrane helices, of the accession number (ABD75481.1), the sequence positions inside to outside 2 helices is found and outside to inside 2 helices is found. Transmembrane topology suggestions are purely speculative and should be used with extreme caution since they are based on the assumption that all transmembrane helices have been found. In most cases, the prediction plot (Fig 1) that is created should be used for the topology assignment of unknown proteins.

The sequence positions in brackets dominate the core region. Only scores above 500 are considered significant (Table 8). So, looking at these values we can interpret that they are insignificant because the score is below 500.

These results showed that *wolbachia* surface protein has two trans-membrane domains and it is a cytoplasmic protein having two transmembrane regions (Table 8). This shows that wsp has membrane binding properties and can be involved in transport of materials across the cell membrane.

Sequence Homology Analysis-

The identification of catalytic residues is a key to understanding the function of enzymes. MUSCLE server was used for multiple sequence alignment of WSP of various drosophila species (Fig 2).With the information from other functionally similar sequences with known crystallographic structures, we can identify the key catalytic residues. The compared sequences varied in length but essentially conserved the key catalytic residues which have been highlighted with an asterisk (*) symbol.

Multiple sequence alignment of wsp sequences revealed significant conserved (glutamine, threonine and aspartic acid) and semi conserved regions (valine, alanine and aspartic acid) are represented as strongly similar (:): Weakly similar (.) as shown in (Fig 2). Multiple Sequence alignment is widely accepted method which provides the researchers for strain typing [10].

RNA Structure Prediction

RNA is now appreciated to serve numerous cellular roles, and understanding RNA structure is important for understanding a mechanism of action. This contribution discusses the methods available for predicting RNA structure (Fig 3). Secondary structure is the set of the canonical base pairs, and secondary structure can be accurately determined by comparative sequence analysis. Secondary structure can also be predicted. The most commonly used method is free energy minimization. The free energy of 19 stems are tabulated (Table 9).The accuracy of structure prediction is improved either by using experimental mapping data or by predicting a structure conserved in a set of homologous sequences. Additionally, tertiary structure, the three-dimensional arrangement of atoms, can be modeled with guidance from comparative analysis and experimental techniques. New approaches are also available for predicting tertiary structure.

Tertiary Structure Analysis:

The tertiary structure of the wsp was annotated using Swiss Modell server. The predicted complex structure was observed in Swiss Model which shows steriochemical rotation of torsion angles. The identification of active site amino acids present in WSP complex structure was predicted using Swiss Model. A greater number of variable active sites are present in these organisms and these protein structures can be used for drug binding sites.

SWISS MODELL RESULTS: The 3D structure analysis of wsp were done by using SWISS-MODEL automated modeling server, the three models are shown (Fig 4 & 5). Template selection, alignment and model building are done completely automated by the server of the ID number**.** Predicting the protein 3D structures by this method are used which implements the four steps of the homology modeling approach.

A. Template searching to identify the structure homology: Template search with Blast and HHBlits has been performed against the SWISS-MODEL template library (SMTL, last update: 2015-09-23, last included PDB release: 2015-09-18).

The target sequence was searched with BLAST [1] against the primary amino acid sequence contained in the SMTL. A total of 10 templates were found.

An initial HHblits profile has been built using the procedure outlined in [27], followed by 1 iteration of HHblits against NR20. The obtained profile has then been searched against all profiles of the SMTL. A total of 126 templates were found.

B. Template selection: For each identified template, the template's quality has been predicted from features of the target-template alignment. The templates with the highest quality have then been selected for model building.

C. Model building: Models are built based on the target-template alignment using Promod-II. Coordinates which are conserved between the target and the template are copied from the template to the model. Insertions and deletions are remodeled using a fragment library. Side chains are then rebuilt. Finally, the geometry of the resulting model is regularized by using a force field. In case loop modeling with ProMod-II [9] does not give satisfactory results, an alternative model is built with MODELLER [28].

D. Model quality estimation: The global and per-residue model quality has been assessed using the QMEAN scoring function [4]. For improved performance, weights of the individual QMEAN terms have been trained specifically for SWISS-MODEL.

E. Ligand Modeling

Ligands present in the template structure are transferred by homology to the model when the following criteria are met (Gallo - Casserino, to be published):

(a) The ligands are annotated as biologically relevant in the template library.

(b) The ligand is in contact with the model.

(c) The ligand is not clashing with the protein.

(d) The residues in contact with the ligand are conserved between the target and the template.

If any of these four criteria is not satisfied, a certain ligand will not be included in the model. The model summary includes information on why and which ligand has not been included.

It provides the details of ligand binding sites of wsp in drosophila. The results which were annotated by Swiss model server make the protein modeling accessible to all biochemists and molecular biologists worldwide. A greater number of variable active sites are present in these organisms and these protein structures can be used for drug binding sites.

Conclusion: *Wolbachia* are a diverse group of intracellular bacteria, that show impressive adaptations within invertebrate cells and in manipulating the biology of drosophila. The mechanisms of *Wolbachia*-host interaction are important in understanding of the bacterial life and their pathogenicity as well as generation of new drug targets. In the vinegar fly, genus drosophila, *Wolbachia* causes an egg mortality phenotype known as cytoplasmic incompatibility (CI). CI has been studied in several taxa including *D. simulans* [13, 14, & 12] and *D. melanogaster* [11 & 31]. CI is manifest as severe egg mortality (up to 95%) when an infected male mates with an uninfected female [35]. This property of the drosophila and *Wolbachia* relationship attributes for the researchers to study the parasitic and mutualistic interactions.

Using the Drosophila model system, it should be possible to examine the cues affecting male killing. Annotation of the wsp in drosophila allows the comparative studies into the mechanism of male killing. Beyond this, comparison of the mechanism of *Wolbachia* male killing to that cytoplasmic incompatibility and parthenogenesis induction can be undertaken.

Present interpretation of the sequence and structural analysis of *Wolbachia* surface protein explored the physicochemical nature, three dimensional structure and detail of interactions with wsp and drosophila. Insilico analysis of the wsp in drosophila species provides the information of the mutualistic behavior which allows for further studies and in management of pests. Based on the findings, it could be concluded that further characterization of *wolbachia* in drosophila is novel and will be important for evaluating the functionality of the wsp protein which paves the path in strain typing.

The Biophysical characterization of the protein would provide the clues to its biological functions and physiological role. The conformation of these requires crystal structure and complete functional description to elucidate the effects of non-synonymous substitutions on protein structure and functionality. The comparative analysis will highlight the multiple roles of *Wolbachia* proteins which extend to cytoplasmic incompatibility, feminization of genetic males, parthenogenesis induction and male killing. Further, Structural characterization of WSP will be a break through towards gaining information on *Wolbachia* induced different phenotypes and further this would be used for applied research such as i) Management of (Arthropod) pest that cause major damage in agriculture industry. ii) Control of important vectors that cause the major diseases. iii) Enhancing the fitness and efficacy of Bio control agents. IV) Development of new drug targets [33].

Insilico analysis of wsp in various drosophila species provides the details of the protein's functionality and structural elucidation details which help in the structural based studies. Further, the Insilco predictions of *wolbachia* surface protein complexes will help in revealing the interactions with the host which greatly enhances the hypothesis and experimental investigations.

ACKNOWLEDGEMENT:
My heartful thanks to our Co-ordinator, Prof. Dr. M. S. Reddy, for the support and encouragement.

REFERENCES:

[1] Altschul S.F, Madden T.L, Schaffer A.A, Zhang J, Zhang Z, Miller W, and Lipman D.J. "Gapped BLAST and PSI-BLAST: a new generation of protein database search programs". Nucleic Acids Res, 25, 3389-3402, 1997
[2] Ashokan K.V, Mundaganur D.S, and Mundaganur, Y.D. "Catalase: Phylogenetic characterization to explore protein cluster". Journal of research in Bioinformatics. 1:001-008, 2011
[3] Bazzocchi C, Jamnongluk W, O'Neill S.L, Anderson T.J, Genchi C, and Bandi C. "WSP gene sequences from the Wolbachia of filarial nematodes". Curr. Microbiol. 41:96, 2000
[4] Benkert P, Biasini M, and Schwede T. "Toward the estimation of the absolute quality of individual protein structure models". Bioinformatics, 27, 343-350, 2011
[5] Braig H.R, Zhou W, Dobson S.L, and O'Neill S.L. "Cloning and characterization of a gene encoding the major surface protein of the bacterial endosymbiont Wolbachia pipientis". J. Bacteriol. 180:2373, 1998
[6] Buchon N, Silverman N, and Cherry S. "Immunity in Drosophila melanogaster — from microbial recognition to whole-organism physiology". Nature Reviews Immunology, 14:796–810, 2014
[7] Eisenhaber F, Imperiale F, Argos P and Froemmel C. "Prediction of secondary structural content of proteins from their amino acid composition alone. I. New analytic vector decomposition methods". Proteins: Struct. Funct. Design.25:157-168, 1996
[8] Gill S.C. and Von Hippel P.H. "Calculation of protein extinction coefficients from amino acid sequence data". Anal. Biochem.182: 319-326, 1989
[9] Guex N and Peitsch M.C. "SWISS-MODEL and the Swiss-PdbViewer: an environment for comparative protein modeling". Electrophoresis, 18, 2714-2723, 1997

[10] Guruprasad N. M, Harish B.M, Jalali S.K, and Puttaraju H.P. "Characterization of Wolbachia cell division protein (ftsz) gene for potential management of Uzifly Exorista sorbillans (Diptera: Tachinidae)". Journal of Entomology and Zoology Studies; 3 (2): 57-61, 2015
[11] Hoffmann A.A.A, Clancy D.J, and Merton E. "Cytoplasmic incompatibility in Australian populations of Drosophila melanogaster". Genetics 136: 993–999, 1994
[12] Hoffmann, A, A., and M, Turelli. 1988. Unidirectional incompatibility in Drosophila simulans: inheritance, geographic variation and fitness effects. Genetics 119: 435–444.
[13] Hoffmann A.A, Turelli M, Simmons G.M. "Unidirectional incompatibility between populations of Drosophila simulans". Evolution, 40, 692–701, 1986
[14] Hoffmann A.A, Turelli M, Harshman L.G. "Factors affecting the distribution of cytoplasmic incompatibility in Drosophila simulans". Genetics 126: 933–948, 1990
[15] Hofmann K and Stoffel W. "TM base - A database of membrane spanning proteins segments" Biol. Chem. Hoppe-Seyler **374,**166, 1993
[16] Kitchen D.B, Decornez H, Furr J.R, and Bajorath J. "Docking and scoring in virtual screening for drug discovery: methods and applications". Nature reviews Drug discovery. 3(11):935-949, 2007
[17] Letunic.I, Doerks.T and Bork.P "SMART 6: recent updates and new developments". Nucleic Acids Res. 37: 229/32, 2009
[18] Madhu S and Mahesh P. "Sequence analysis of Semaphorin in tumor progression: An Insilico approach". International Journal of Asian Academic Research of Multidisciplinary .1(29): 407-423, 2015
[19] Mahesh P, Brueckner D, and Reddy M.S. "Horizontal transmission of Wolbachia in the honeybee subspecies Apis mellifera carnica and its ectoparasite Varroa destructor". International journal of environmental sciences. Volume 2, No 2,526-535, 2011
[20] Mahesh P, Divya P, Akshatha M, Prathima R and Lava Kumar C. "Insilico characterization and phylogenetic analysis of novel probiotic bacteria in honey bees". International Journal of Asian Academic Research of Multidisciplinary .1(32): 337-357, 2015
[21] McGraw E.A, and O'Neill S.L. "Wolbachia pipientis: intracellular infection and pathogenesis in Drosophila". Curr Opin Microbiol 7:67–70.3, 2004
[22] Mugilan A, Ajitha M. C, Devi and Thinagar. "In silico Secondary Structure Prediction Method (Kalasalingam University Structure Prediction Method) using Comparative Analysis". Trends in Bioinformatics. 3(1):11-19, 2010
[23] Neyen C, Bretscher A.J, Binggeli O, and Lemaitre B. "Methods to study Drosophila immunity". Methods (San Diego, Calif.) 68:116–128, 2014
[24] Nichols C.D, Becnel J, and Pandey U.B. "Methods to Assay Drosophila Behavior". Journal of Visualized Experiments, 2012
[25] Nunes M.D.S, Nolte V, Schlötterer C. "Nonrandom Wolbachia infection status of Drosophila melanogaster strains with different mtDNA haplotypes". Mol Biol Evol 25: 2493–2498, 2008
[26] Praveen Kumar K.S and Mahesh Pattabhiramaiah "Sequence analysis of basic phospholipase A2 (neurotoxin) as a potential drug target: an in silico approach". International Journal of Engineering Research and General Science Volume 3, Issue. 1057-1067, 2015
[27] Remmert M, Biegert A, Hauser A. and Soding J. "HHBlits: lightning-fast iterative protein sequence searching by HMM-HMM alignment". Nat Methods, 9, 173-175, 2012
[28] Sali A and Blundell T.L. "Comparative protein modeling by satisfaction of spatial restraints". J Mol Biol, 234, 779-815, 1993
[29] Schultz J, Milpetz F, Bork P and Ponting CP. "SMART, a simple modular architecture research tool: identification of signaling domains". Proc. Natl. Acad. Sci. *U.S.A.* 95 (11): 5857/64, 1998
[30] Sokolowski M.B. "Drosophila: Genetics meets behavior". Nature Reviews Genetics 2:879–890, 2001
[31] Solignac M, Vautrin D, Rousset F. "Widespread occurrence of the proteobacteria Wolbachia and partial cytoplasmic incompatibility in Drosophila Melanogaster". Cr Acad Sci Iii-Vie 317: 461–470, 1994
[32] Tsetlin V.I and Hucho F. Snake and snail toxins acting on nicotinic acetylcholine receptors. Fundamental aspects and sciences, Bioinformatics. 4: 53-62, 2004
[33] Uday J, SampathKumar S, Huchesh C.H, Chethana V.C, Puttaraju H.P. "Insilco Analysis of Wolbachia Surface Protein in Wolbachia Endosymbiont of D. Melenogaster". B I O M I R R O R an Open Access Journal. Vol.5: 24-29, 2014
[34] Vishwanath K.V, Mahesh P, and Keerthi R. "Bio computational analysis of protein sequence of sickle cell anemia". International Journal of Engineering Research And Generic Science. Vol 1: Issue 1: 63-73, 2015
[35] Werren J.H. "Biology of Wolbachia". Ann Rev Ent 42: 587–609, 1997
[36] **Werren J. H, Windsor D, and Guo L.R**. "Distribution of Wolbachia among neotropica arthropods". Proc. R. Soc. Lond. B Biol. Sci. 262**:**197-204, 1995

International Journal of Engineering Research and General Science Volume 3, Issue 6, November-December, 2015
ISSN 2091-2730

Survey on Decision Support System for Medical Diagnosis Using Data Mining

Huzaifa Shabbir Dhorajiwala[1], Er. Asadullah Shaikh[2]

[1]Department of Computer Engineering, M.H. Saboo Siddik College of Engineering, Mumbai, Maharashtra, India
dhorajiwalahuzaifa@gmail.com Mob: 9820047237

Abstract— Industries in healthcare gathers a large amount of data that has not been appropriately mined and which is not feasible. Research of these covered patterns and relationships among them have not been put into use. The main motto of our project based on Medical diagnosis is to prepare knowledge based aspects with the help of collecting data regarding various kinds of diseases such as heart disease and diabetes. Another aspect of our research is to develop decision support systems in medical field to ease the workload of the physicians. In our proposed system, we make use of different algorithms such as ID3 algorithm, CART algorithm, Genetic algorithm and LS-SVM algorithm which classifies the above mentioned diseases to compare the usefulness and how effective it is.

Keywords— Healthcare, Medical Diagnosis, ID3 algorithm, CART, Genetic and LS-VSM, Decision Support.

INTRODUCTION

The Healthcare Industry gathers data in bulk that is not well mined and not put into use which is feasible. Analysis of the hidden patterns and the relationships among them often goes undetected. We can overcome these shortcomings by using advanced data mining techniques. With the help of these data mining techniques and decision support techniques we can improve the management of heart disease.

Providing quality services at minimal costs is the major challenge faced by the Healthcare Industries.

Quality services means treating patients correctly, taking care of the financial conditions of each and every individual. Substandard decisions can lead to worse results. Even the highly rated hospitals and clinics in India do not have software that checks and predicts a disease through data mining techniques.

There is a large amount of data which goes undetected and this data can be turned into information which could prove useful in various Healthcare centres. Medical diagnosis is said to be instinctive. It is totally dependent on the physician who examines the patients. It becomes very difficult for the physician to make good decisions if the data is too large. The data often becomes impossible to manage.

In such cases, the doctor or the physician uses machine learning techniques to derive past rules, patients who were treated successfully and this helps the physician to make the examination process more trustworthy.

The concept of Decision Support System [DSS] is very large because of many different approaches and a vast range of domains which prove helpful in making decisions. DSS phraseology implies to a class of computer information systems which includes knowledge based systems that help us in making decisions

LITERATURE SURVEY

Algorithms such as ID3 and C4.5 were proposed by Quinlan for promoting classification models which was extracted from data known as decision tress. Set of information are known to us. Per capita of information has the same format consisting of number of element pairs. An element represents the group of the information. The dilemma is to find a decision tree that on the base of solution to problems about the non-listing elements forecast properly the value of the listing elements. Normally the listing element takes only the values i.e. {right, wrong} or {pass, fail} or something identical. In any instance one of its points will mean fail.

A. ID3 Algorithm

Itemized Dichotomize 3 algorithm also known as ID3 algorithm was put forward by J.R Quinlan in the year 1970. It is a materialistic algorithm that will pick up the next element based on the data that been collected related to the element. The data obtain is calculated by entropy, ID3 algorithm tender that the initiate tree is minuscule with lower elements that are put closer to the tree. ID3 algorithm is a sample of symbolic learning and rule induction. It is also an administer learner which means it's an example like a training data set which makes the decisions. J. Ross Quinlan introduced it late back in 1979. It is like a decision tree on numerical evaluation.

Fig.1 Decision Tree

A decision tree classifies data using its elements. It is upturned process. Decision nodes and leaf nodes are included in the tree. In Fig 1, "link From Academia" element is a decision node and the "author" attribute is the leaf node. The leaf node has equivalent data which means additional classification is not required. ID3 algorithm constructs same decision trees until all the leaf nodes are equivalent.

B. CART Algorithm

Classification and regression trees is a non- parametric technique that produces either classification or regression trees, built upon on whether the subordinate variable is absolute or numeric, respectively. Trees are formed by a collection of rules based on values of certain variables in the modelling data set. Rules are selected based on how well splits based on variables' values can differentiate observations based on the dependent variable once a rule is selected and splits a node into two, the same logic is applied to each "child" node (i.e. it is a looping procedure). Splitting stops when CART encounter no further gain can be made, or some pre-set stopping conditions are met. The basic idea of tree growing is to choose a split among all the possible splits at each node so that the resulting child nodes are the "purest". In this algorithm, only unilabiate splits are considered. That is, each split built upon on the value of only one predictor variable.

SURVEY

The purpose of the current study is the growth and examination of a clinical decision support system for the treatment of patients with heart disease and diabetes. One of the study shows, heart disease is the major cause of death in the universe every year. In the United States, almost 930,000 people die and its price is about 393.5 billion dollars. Heart disease also knows as coronary artery disease (CAD), is a major term that can refer to any state that affects the heart. Diabetes mellitus is a chronic disease and a broad public health challenge altogether. According to the international diabetes federation, there are about 246 million diabetic people worldwide, and this number is predicted to increase to 380 million by 2025.

A. Experimental Data

Table 1: Description of the features in the heart disease dataset

No	Name	Description
1	Age	age in years
2	Sex	1 = male ; 0 = female
3	Cp	chest pain type (1 = typical angina; 2 = atypical angina ; 3 = non-anginal pain; 4 = asymptomatic)
4	Trestbps	resting blood pressure(in mm Hg on admission to the hospital)
5	Chol	serum cholestoral in mg/dl
6	Fbs	(fasting blood sugar > 120 mg/dl) (1 = true; 0 = false)
7	Restecg	resting electrocardiographic results (0 = normal; 1 = having ST-T wave abnormality; 2 = showing probable or define left ventricular hypertrophy by Estes' criteria)
8	Thalach	maximum heart rate achieved
9	Exang	exercise induced angina (1 = yes; 0 = no)
10	Oldpeak	ST depression induced by exercise relative to rest
11	Slope	the slope of the peak exercise ST segment (1 = upsloping; 2 = flat ; 3= downsloping)
12	Ca	number of major vessels (0-3) colored by flourosopy
13	Thal	(3 = normal; 6 = fixed defect; 7 = reversible defect)
14	Num	Diagnosis classes (0 = healthy; 1 = patient who is subject to possible heart disease)

Table 2: description of the features in the diabetes dataset

No	Attribute Name	Description
1	Number of times pregnant	Numerical values
2	Plasma glucose concentration	glucose concentration in a 2 hours in an oral glucose tolerance test
3	Diastolic blood pressure	In mm Hg
4	Triceps skin fold thickness	Thickness of skin in mm
5	2-Hour serum insulin	Insulin (mu U/ml)
6	Body mass index	(weight in kg/(height in m)^2)
7	Diabetes pedigree function	A function – to analyse the presence of diabetes
8	Age	Age in years
9	Class	1 is interpreted as "tested positive for diabetes and 0 as negative

B. ID3 Algorithm

Itemized Dichotomize 3 algorithm also known as ID3 algorithm was put forward by J.R Quinlan in the year 1970. It is a materialistic algorithm that will pick up the next element based on the data that been collected related to the element. The data obtain is calculated by entropy ID3 algorithm tender that the initiate tree is minuscule with lower elements that are put closer to the tree. ID3 algorithm is a sample of symbolic learning and rule induction. It is also an administer learner.

1) Training Data and Set: ID3 algorithm is an administer learner. It requires training data sets to make settlement. The training set lists the elements and their feasible values. ID3 doesn't deal with constant, numeric information which means we have to approximate them. Elements such as age which can have values like 1 to 100 are listed like old or young.

TABLE I
TRANING SET

Attributes	**Values**
Age	Young, Middle aged, Old
Height	Tall, Short, Medium
Employed	Yes, No

The training data is the list of data containing actual values

TABLE II
TRANING DATA

Age	**Height**	**Employed**
Young	Tall	Yes
Old	Short	No
Old	Medium	No
Young	Medium	Yes

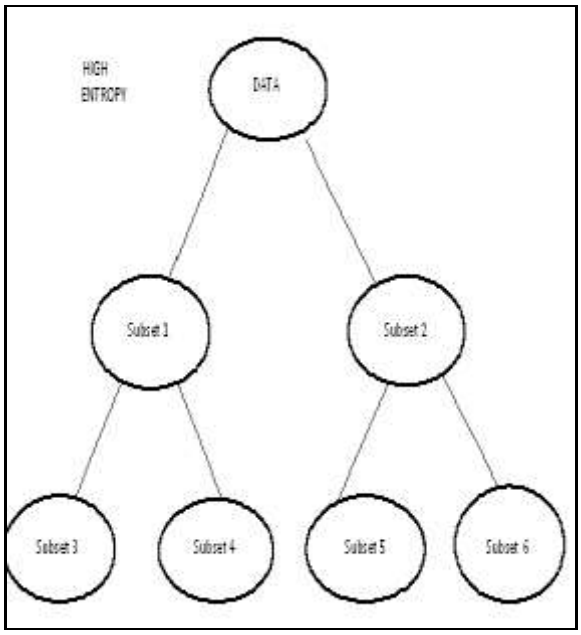

Fig. 1 Entropy

2) Entropy:

Entropy introduce to the non-coherence of the information. It ranges from 0-1. Data sets with entropy 1 means it is as non-coherence which is of similar kind. In Fig [2], the root of the tree has a collection of Data. It has big entropy which means the data is coherent. The set of data is properly divided into subsets 3, 4, 5 and 6 where it is now of same kind and the entropy is 0 or close to 0.

Entropy is calculated by the formula:

E(S) = - (p+)*log2(p+) - (p-)*log2(p-)

"S" represents the set and "p+" are the number of data in the set "S" with right values and "p –"are the numbers of elements with wrong values.

The aim of ID3 algorithm is to divide data using decision trees, such that the concluding leaf nodes are all similar with 0 entropy.

3) Steps for ID3 algorithm : ID3 algorithm works in the following steps :-

• Create a root node for the tree
•If all examples are positive, Return the single-node tree Root, with label = +.
• If all examples are negative, Return the single-node tree Root, with label = -.
• If number of predicting attributes is null, then Return the single node tree Root, with label = most common value of the target attribute in the examples.

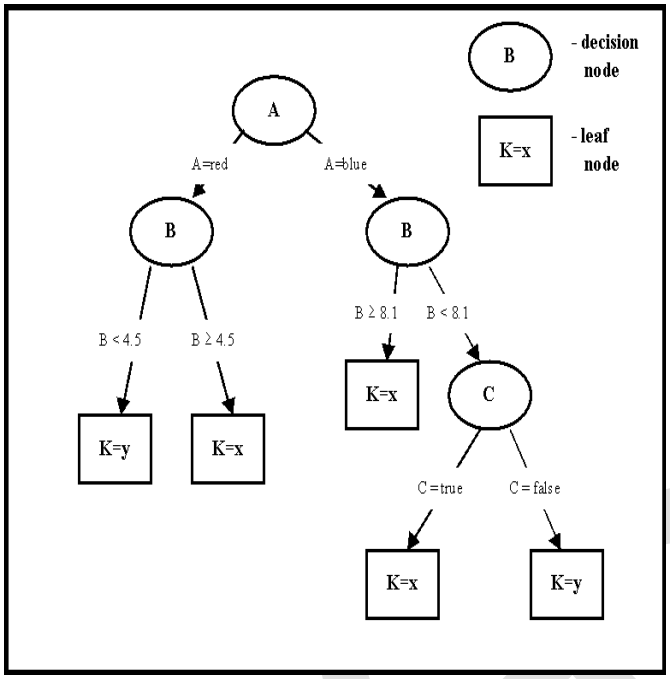

Fig. 2Solving example using ID3 algorithm

C. CART Algorithm

Classification and regression trees is a non- parametric technique that produces either classification or regression trees, built upon on whether the subordinate variable is absolute or numeric, respectively. Trees are formed by a collection of rules based on values of certain variables in the modelling data set. Rules are selected based on how well splits based on variables' values can differentiate observations based on the dependent variable once a rule is selected and splits a node into two, the same logic is applied to each "child" node (i.e. it is a looping procedure). Splitting stops when CART encounters no further gain can be made, or some pre-set stopping condition is met. The basic idea of tree growing is to choose a split among all the possible splits at each node so that the resulting child nodes are the "purest". In this algorithm, only unilabiate splits are considered. That is, each split built upon on the value of only one predictor variable.

The construction of CARTs (classification and regression trees) is best described in breiman84 and has become a common basic method for building statistical models from simple feature data. CART is dominant because it can compromise within complete data; multiple types of features (floats, enumerated sets) both in input features and predicted appearance, and the trees it generates often contain rules which are humanly readable

Decision trees contain a binary question (yes/no answer) about some feature at each node in the tree. The leaves of the tree contain the prime prediction based on the training data. Decision lists are a compressed form of this where one answer to each question leads precisely to a leaf node. A tree's leaf node may be a part of some class as a single member, a probability density function (over some discrete class), a predicted mean value for a stable feature or a Gaussian (mean and standard deviation for a continuous value).

All possible splits consist of possible splits of each predictor. CART innovations include:

• Solving the "how big to grow the tree"- problem;
• Using closely two-way (binary) splitting;
• Incorporating automatic testing and tree verification and
• Giving a completely new approach for handling missing values.

D. Genetic Algorithm:

Genetic Algorithm is an evolutionary algorithm which offers multi criterion optimization for higher dimensional space problems [11].It's a popular stochastic search method used for feature selection. It is based on Darwin's theory of natural selection and 'survival

of the fittest' [11]. Genetic algorithm search initially starts with the least number of attributes. Every set of individuals are called population and each individuals are called as chromosomes. These chromosomes are constituted of many genes which are most binary value indicating the presence of the element in the set. The search of the best result is based on the objective function called as Fitness Function [11].

$$\text{Fitness} = \frac{\text{Total No of Correctly classified Instances}}{\text{Total No of Training Samples}}$$

The selected solutions with highest fitness value have more influence than that of the new solutions with less fitness value. This function plays a key role in the selection of the best solution of the problem. In Genetic algorithm, each iteration is known as generation [11]. Fittest individuals are selected from eachgeneration and pooled out to form base for new populations. A new population is created based on the compliance to the fitness function. Off springs are generated based on the genetic operator's cross over and mutation. Threshold for fitness function will be the maximum accuracy at which the system converges. This process continues till the Fitness threshold is met.

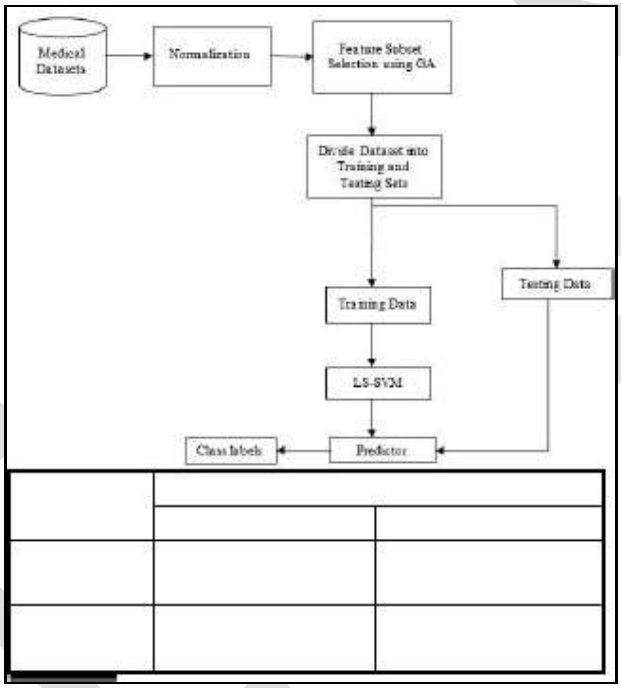

Fig 3. Proposed System.

E. LS-SVM Algorithm.

Least Square Support Vector machine (LS-SVM) is a kind of Support vector machine based on the structural risk minimization principle of statistic all earning theory [12]. Support vector machine (SVM) was introduced by Fisher [13] and has been used successfully in most regression and classification problems. The key role of SVM in Classification problem is to divide the data into two distinct classes with maximum margin and minimum classification error rate. In order to solve constrained quadratic programming problems, SVM requires higher computational load, which is a major drawback in using in high dimensional problems. In order to overcome this problem, LS-SVM was introduced by Suykens and Vandewalle [12], which uses linear equations to solve the problems.LS-SVM are used for classification problems to find a hyper plane, which could separate various classes with higher margin. An optimal hyper plane is obtained using maximum Euclidean distance to the nearest point. It maps the input vector into higher dimensional space for non-separable data. Then the optimal separating hyper plane is found. X IЄR p and YIЄ {0, 1} where XI is 'p' dimensional input vector and YI is the corresponding class label.

$$F(X) = \text{sign}\left(\sum_{i-1}^{N} Y_i \alpha_i K(X, X') + b\right)$$

Where f(X) is the output of new input vector XIЄ R p(Equation 3).XIis the support vectors belongs to training set. The dataset used for training the classifier are training set.Iα

is the Lagrange multipliers and b be the realconstant.LS-SVM performance depends mainly on two key parameters. Choosing best value for these parameters is important to maintain the classifiercharacteristic. The two kernel parameters are C and Gamma(γ) . C be the box constraint and Gamma be the regularization factor[12].Input data sets are distributed in nonlinear dimensional space. These are converted into high dimensional linear feature space by using kernels. Radial Basis Kernel is used for such mapping for our medical datasets, which is given in (4).

RBF Kernels:

$$K(x, x') = \exp(-(x-x)^2/\sigma^2).$$

Performance Evaluation:

The proposed System is examined by 10 fold cross validation methodology. The performance of the system is evaluated using four measures: Confusion Matrix, Sensitivity, Specificity and Classification Accuracy.

Confusion Matrix:

Confusion matrix [13] (COM) is a 2×2 matrix which shows the predicted and actual classification given in Table 1.

Table 1
Confusion Matrix

Predicted	Actual
Positive	
Negative	Positive
TP (true positive)	FP (false positive)
Negative	
FN (false negative)	TN (true negative)

-TN is the correct predictions of an instance as negative
.
-FN is the incorrect predictions of an instance as positive
.
-FP is the incorrect of predictions of an instance as negative
.
-TP is the correct predictions of an instance as Positive

Classification Accuracy:

Performance of classifier is commonly measured using classification accuracy (CA). It provides the rate of correctly predicted instances to the overall instances in the dataset. CA can be calculated from Confusion Matrix [13] using the equation (5).

$$\text{Accuracy} = \frac{TN + TP}{TP + TN + FP + FN}$$

$$\text{Sensitivity} = \frac{TP}{TP + TN}$$

$$\text{Specificity} = TN$$

TN + FP.

IV. EXISTING SYSTEM

A vital question faced by the healthcare organizations (hospitals, medical centers) is the provision of standard services at inexpensive price. Value services suggest diagnosing patients properly and examining treatments that are fruitful. Deprived clinical decisions leads to disastrous results that cannot be accepted. Hospitals should also decrease the price of clinical test. They can attain this upshot by assigning appropriate computer-based data and decision support systems.

In today's world many hospitals manage details and data related to patients. Numbers, text, charts and images are generated by the decision support system. Woefully, these data are not used to support clinical decision making. There is a opulence of unseen information in these data that is largely not utilized. This objects an important question: "How the useful information can be extracted from the untapped data?" This is the main purpose for this paper.

Diabetes	Classification Accuracy
SVM [15]	77.73
Grid Algorithm [9]	76.47
ACO –SVM [16]	67.11
DSS [17]	75.73
GA-LSSVM (Proposed)	81.33

Fig 4.Accuracy Comparison

V. SCOPE

Data mining utilization in healthcare can have tremendous potential and usefulness. Nevertheless, the success of healthcare data mining depends on the availability of clean healthcare statistics. In this respect, it is fault-finding that the healthcare industry explores how data can be better captured, stored, planned and mined. Practicable guidance includes the standardization of clinical vocabulary and the sharing of data across organizations to enhance the benefits of healthcare data mining utilization.

Future Directions of Health care system through Data Mining Tools

As healthcare data are not finite to just quantitative data (e.g., doctor's notes or clinical records), it is required to also explore the use of content mining to expand the scope and nature of what healthcare data mining can directly do. This is specially used to blended all the data and then mining the content. It is also useful to look into how images (e.g., MRI scans) can be import into healthcare data mining utilization. It is noted that progress has been made in these areas.

B. UNIQUENESS

Human medical data are most profitable and challenging of all biological data to mine and study. Most closely watched category on the earth. Human subjects can provide information that cannot be gained easily from animal examination, such as optical and audible sensitivity, the recognition of pain, soreness, illusion and exposures. Most animal knowledge are limited, and therefore cannot record longstanding disease processes of medical concern, such as preneoplasia. With human statistics, there is no issue of having to deduce animal analyse to the human species.

1) Intermixture of medical statistics: Intermixture of medical statistics the major areas of intermixture of medical statistics are Volume and complication of medical statistics (crude medical data are colossal, voluminous and composite. These are gathered via interviews with the patients, various images from diagnostic approach and clinical response, analysis), Importance of physician's interpretation (the physician's perception of diagnostic decisions, even specialists from similar practice vary in describing a patient's condition hence it becomes problematic to mine). Awareness and particularity analysis (precision in nearly all interpretation and medications in medicine is subject to flaws, there is need to differentiate between a test and diagnosis in medicine. The medical condition of the patient is described by various inspection and based on these inspection disease is diagnosed. Both inspection and diagnosis are subject to awareness and particularity analysis.), Poor mathematical simulating (medical data cannot be put into formulas equations and figure because the theoretical structure of medicine consists of word characterization and images).

2) High-principled, legal and social problems: Since the medical statistics are gathered on human beings, it involves high-principled, legal and social problems that are constructed to avoid the wrongdoing of patients and squandering of their data. These issues may refer to data hold, fear of law threads, isolation and preservation of human data, expected benefits and administrative problems.

3) Analytical ideology: Analytical ideology of medical data is contrast from non-medical data. Medical data is collected to provide gain to the respective patients. Sometimes the patient who has permission to be involved in the research projects may not get any gain but the data collected from such patients is narrowly observed and is regulated by legal and high-principled attention.

4) Appropriate status of medicine Medical science: Appropriate status of medicine Medical science like special status in everyday life. Medical care is a vital part; it gives life to the patient and ambition for a beneficial life. Every patient await recovery after going to the medicine person and demands belief, understanding and care but no one recognize the uncertainty which medicine person face. Everybody wants to enjoy the benefits of research but no one is ready to contribute into it. The collected medical data when published is used for social causes without harming the dignity of the patients. Though medical science enjoys special status yet it has to face many barriers. It is still doubtful as to what questions to be request from patients, what attempt to be performed on the patients and what conclusions may not be drawn. That is why experiments on animals are conducted and results from these experiments are considered reliable.

VI. CONCLUSION

The decision-tree algorithm is one of the popular productive classification methods. The data will determine the algorithm in terms of its efficiency and correction rate. We used 10-fold cross authentication to figure out confusion matrix of each model and then check out the performance by using precision, recall, F measure and ROC space. As conventional, bagging algorithms, especially CART, showed the best performance among the tested algorithms. The results showed here make clinical application more practicable, which will provide strong leading in curing CAD, hepatitis and diabetes. The analysis is made on the decision tree algorithms ID3 and CART towards their steps of refining data and complexity of ongoing data. Finally it can be declare that between the two algorithms, the CART algorithm is the best in performance of rules generated and accuracy. This showed that the CART algorithm is better in induction and rules generalization than the ID3 algorithm. Finally, the results are reserved in the decision support depository. Since, the knowledge base is currently concentrated on a narrow set of diseases. The approach has been authenticated through the case study; it is feasible to widen the scope of formed medical knowledge. Additionally, decision support can be more enhance by considering interactions between the different medicaments that the patient is on.

In this paper, a decision support system based on GA-LSSVM is proposed for the diagnosis of the diabetes disease. A Gaussian radial basis function issued as a kernel of LS-SVM [14].

The robustness of the proposed system were analyzed with metrics like classification accuracy, using 10-fold cross-validation and confusion matrix. The accuracy of the system for the PID dataset was found to be 81.33% with GA as a feature selection method. In future, this system can be used for the diagnosis of real life medical data of patients [14].

The LSVM Algorithm is not a very feasible solution to decision making in medical field. The algorithm is difficult to implement and the time and space complexity is also high.

The genetic Algorithm is a very optimal solution to the medical field for its Diagnosis. Genetic algorithm due to its fitness function can give accurate results and provides optimal solution.

REFERENCES:

[1] UCI Machine Learning Repository http://www.ics.uci.edu/~mlearn/MLRepository.html.

[2] American Diabetes Association, "Standards of medical care in diabetes—2007," Diabetes Care, vol. 30, no. 1, pp. S4 S41, 2007.

[3] J. Du and C.X. Ling, "Active Learning with Generalized Queries," Proc. Ninth IEEE Int'l Conf. Data Mining, pp. 120-128, 2009

[4] Jiawei Han and Micheline Kamber, "Data Mining Concepts and techniques", 2nd ed., Morgan Kaufmann Publishers, San Francisco, CA, 2007.

[5] H.W. Ian, E.F., "Data mining: Practical machine learning Tools and techniques," 2005: Morgan Kaufmann.

[6] R. Detrano, A.J., W. Steinbrunn, M. Pfisterer, J.J. Schmid, S.Sandhu, K.H.Guppy, S. Lee, and V. Froelicher, "International application of a new probability algorithm for The diagnosis of coronary artery disease," American Journal Of Cardiology, 1989. 64: p. 304-310.

[7] G. John, "Models if incremental concept formation," Journal Of Artificial Intelligence, 1989: p. 11-61.

[8] A. L. Gamboa, M.G.M., J. M. Vargas, N. H. Grass, and R. E. Orozco, "Hybrid Fuzzy-SV Clustering for Heart Disease Identification," in Proceedings of CIMCA-IAWTIC'06. 2006.

[9] D. Resul, T.I., S. Abdulkadir, "Effective diagnosis of heart Disease through neural networks ensembles," Elsevier, 2008.

[10] Z. Yao, P.L., L. Lei, and J. Yin, "R-C4.5 Decision tree Model and its applications to health care dataset, in Proceedings of the 2005 International Conference on Services Systems and Services Management," 2005. p. 1099-1103

[11] R.Yuan, B.Guangchen,"Determination Of Optimal SVM Parameters by Using Genetic Algorithm/Particle Swarm Optimization", Journal of Computers, No.5, pp.1160-116, 2010

[12] *Ersen*, Y, An Expert System Based on Fisher Score and LS-SVM for Cardiac Arrhythmia Diagnosis" Computational and Mathematical Methods in Medicine, pp.1-6, 2013.

[13] Duygu, C. and Esin, a New Intelligent Hepatitis Diagnosis System: PCA LSSVM Expert Systems with Applications, 2011.

[14] Reference Paper of IJESRT for Medical Diagnosis for Decision Support System.

International Journal of Engineering Research and General Science Volume 3, Issue 6, November-December, 2015
ISSN 2091-2730

A NOVEL MULTILEVEL INVERTER BASED ON SWITCHED-CAPACITOR FOR HIGH-FREQUENCY POWER DISTRIBUTION APPLICATIONS

[1]V. Harikrishna, [2] K. Sathish Kumar

Brahmaiah College of Engineering, affiliated JNTU-Anantapur[1, 2]

Northraju palem, SPSR Nellore, Andhra Pradesh.

Abstract—A novel switched-capacitor-based cascaded multilevel inverter is proposed in this paper, which is constructed by a switched-capacitor frontend and H-Bridge backend. Through the conversion of series and parallel connections, the switched capacitor frontend increases the number of voltage levels. The output harmonics and the component counter can be significantly reduced by the increasing number of voltage levels. Phase opposition disposition technique is used as multicarrier modulation. The circuit topology with intended control strategy is examined for voltages, currents and THD of the system. The proposed system with POD PWM technique is implemented on MATLAB/SIMULINK model design for analysis that confirms the feasibility of proposed multilevel inverter.

Keywords— cascaded multi-level inverter, multi-carrier pulse width modulation, POD, THD.

I. INTRODUCTION

High-frequency ac power distribution system potentially becomes an alternative to traditional dc distribution due to the fewer components and lower cost. The existing applications can be found in computer [1], telecom [2], electric vehicle [3], and renewable energy micro grid [4], [5]. However, HFACPDS has to confront the challenges from large power capacity, high electromagnetic interference (EMI), and severe power losses [6]. A traditional HFAC PDS is made up of a high-frequency (HF) inverter, an HF transmission track, and numerous voltage-regulation modules. HF inverter accomplishes the power conversion to accommodate the requirement of point of load. In order to increase the power capacity, the most popular method is to connect the inverter output in series or in parallel. However, it is impractical for HF inverter, because it is complicated to simultaneously synchronize both amplitude and phase with HF dynamics. Multilevel inverter is an effective solution to increase power capacity without synchronization consideration, so the higher power capacity is easy to be achieved by multilevel inverter with lower switch stress. Non polluted sinusoidal waveform with the lower total harmonic distortion (THD) is critically caused by long track distribution in HFAC PDS. The higher number of voltage levels can effectively decrease total harmonics content of staircase output, thus significantly simplifying the filter design [7].

HF power distribution is applicable for small-scale and internal closed electrical network in electric vehicle (EV) due to moderate size of distribution network and effective weight reduction [8]. The consideration of operation frequency has to make compromise between the ac inductance and resistance [9], so multilevel inverter with the output frequency of about 20 kHz is a feasible trial to serve as power source for HF EV application. The traditional topologies of multilevel inverter mainly are diode-clamped and capacitor-clamped type [10], [11]. The former uses diodes to clamp the voltage level, and the latter uses additional capacitors to clamp the voltage. The higher number of voltage levels can then be obtained; however, the circuit becomes extremely complex in these two topologies. Another kind of multilevel inverter is cascaded H-Bridge constructed by the series connection of H-Bridges [12], [13]. The basic circuit is similar to the classical H-bridge DC–DC converter. The cascaded structure increases the system reliability because of the same circuit cell, control structure and modulation. However, the disadvantages confronted by cascaded structure are more switches and a number of inputs. In order to increase two voltage levels in staircase output, an H-Bridge constructed by four power switches and an individual input are needed. Theoretically, cascaded H-Bridge can obtain staircase output with any number of voltage levels, but it is inappropriate to the applications of cost saving and input limitation A number of studies have been performed to increase the number of voltage levels. A switched-capacitor (SC) based multilevel circuit can effectively increase the number of voltage levels. However, the control strategy is complex, and EMI issue becomes worse due to the discontinuous input current single-phase five-level pulse width-modulated (PWM) inverter is constituted by a full bridge of diodes, two capacitors and a switch. However, it only provides output with five voltage levels, and higher number of voltage levels is limited by circuit structure. An SC-based cascaded inverter was presented with SC frontend and full bridge backend. However, both complicated control and increased components limit its application. The further study was presented using series/parallel conversion of SC. However, it is inappropriate

to the applications with HF output because of multicarrier PWM (MPWM). If output frequency is around 20 kHz, the carrier frequency reaches a couple of megahertz. Namely, the carrier frequency in MPWM is dozen times of the output frequency. Since the carrier frequency determines the switching frequency, a high switching loss is inevitable for the sake of high-frequency output. A boost multilevel inverter based in partial charging of SC can increase the number of voltage levels theoretically. However, the control strategy is complicated to implement partial charging.

Therefore, it is a challenging task to present an SC-based multilevel inverter with high-frequency output, low-output harmonics, and high conversion efficiency. Based on the study situation aforementioned, a novel multilevel inverter and simple modulation strategy are presented to serve as HF power source.

The rest of this paper is organized as follows. The discussions of nine-level inverter are presented in Section II, including circuit topology, modulation strategy. The matlab implementation of the topology is discussed in Section III. The voltage, current band THD analysis is discussed in Section IV. The performance evaluation accomplished by simulation and experiment is described.

SWITCHED CAPACITOR BASED CASCADED INVERTER

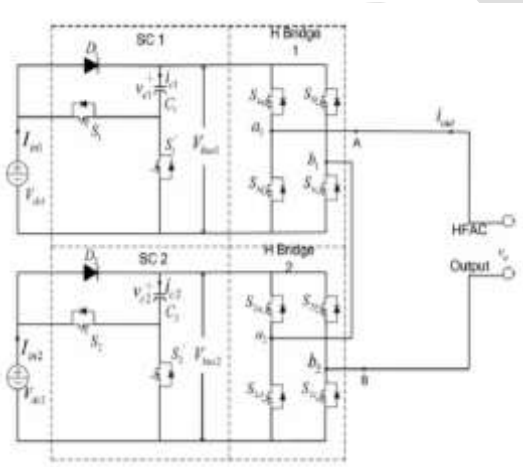

switched capacitor multi-level inverter using POD technique

The proposed circuit is made up of the Switched Capacitor frontend and cascaded H-Bridge at the backend. If the numbers of voltage levels obtained by switched capacitor frontend and cascaded H-Bridge backend are $m1$ and $m2$, respectively, the number of voltage levels is $2 \times m1 \times m2+1$ in the entire operation cycle.

A. Circuit Topology

Fig.1 shows the circuit topology of nine-level inverter for m1 = 2 and m2 = 2 where S1, S2, S_1, S_2 as the switching devices of Switched capacitor circuits SC1 and SC2 are used to convert the series or parallel connection of C1 and C2 . S1a, S1b, S1c, S1d, S2a, S2b, S2c, S2d are the switching devices of cascaded H-Bridge. Vdc1 and Vdc2 are input voltage. D1 and D2 are diodes to restrict the current direction. i_{out} and v_o are the output current and the output voltage, respectively.

It is worth noting that the backend circuit of the proposed inverter is cascaded H-Bridges in series connection. It is significant for H-Bridge to ensure the circuit conducting regardless of the directions of output voltage and current. In other words, H-Bridge has four conducting modes in the conditions of inductive and resistive load, i.e., forward conducting, reverse conducting, forward freewheeling, and reverse freewheeling.

I. MATLAB IMPLEMENTATION OF PROPOSED SYSTEM

The Proposed system is implemented by using MATLAB/SIMULINK model design software as shown in fig.2. Each h-bridge block is associated with small buck/boost circuit which is controlled by PWM control. The input from either solar or battery or fuel cell is not enough to meet the load demand or change in load instantly so in order to have the steady state an extra arrangement of switch before to the each H-bridge converter is used as shown in fig.3

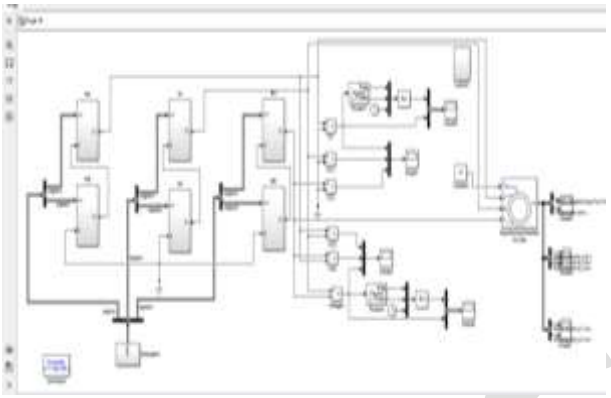

Matlab design of proposed system

As shown in fig.2 the three phase system of proposed converter with switched capacitor nine-level converter is controlled here by Phase opposition disposition technique. In this technique there will be one reference wave and two carrier waves for each asymmetric H-bridge structure so as have required PWM.

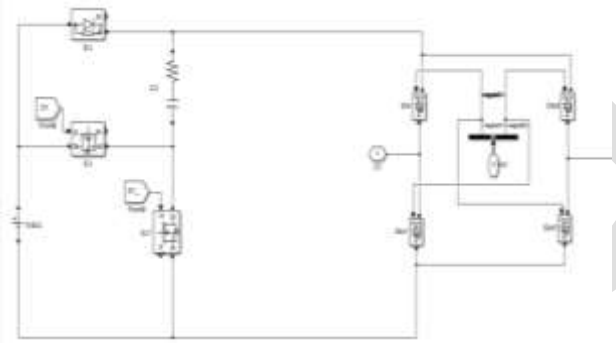

Modified H-bridge cell of single phase

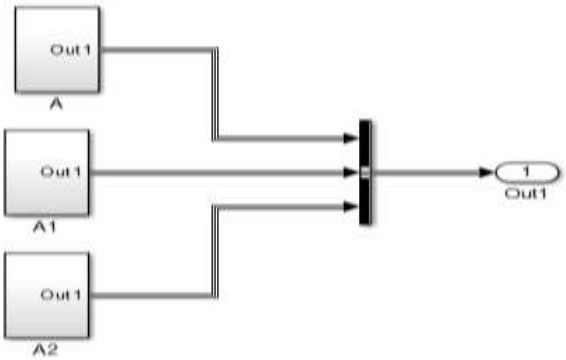

control system of proposed converter

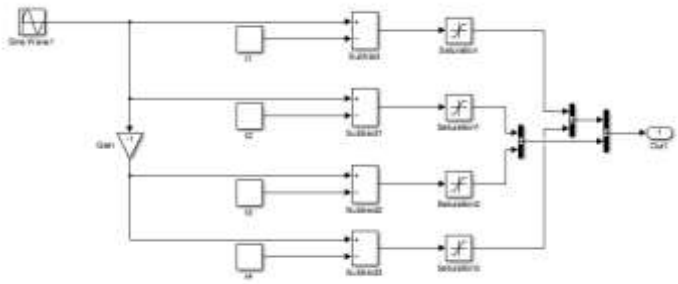

III. POD scheme of multi-carrier modulation using Matlab

IV. RESULTS AND ANALYSIS

The novel design of three phase switched capacitor Multi-level Inverter using Phase of disposition as control strategy has fruitful results. The phase output voltage of the proposed converter feeding the power to Induction motor is as shown in the following figs. The Fig.5 represents the line voltage waveform of the multi-level inverter. Using the asymmetric design of the proposed H-bridge converter the level has improved to nine-level instead of five-level.

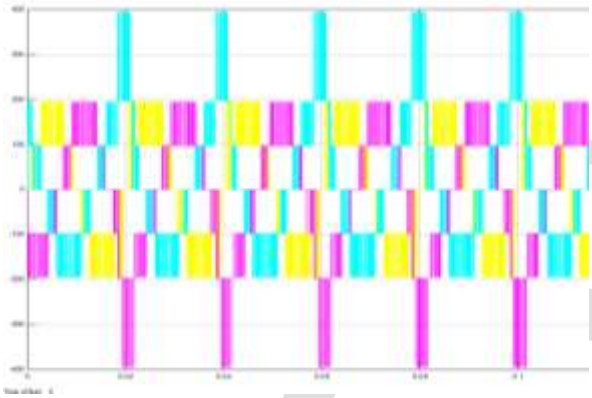

The line voltage waveform of the proposed converter

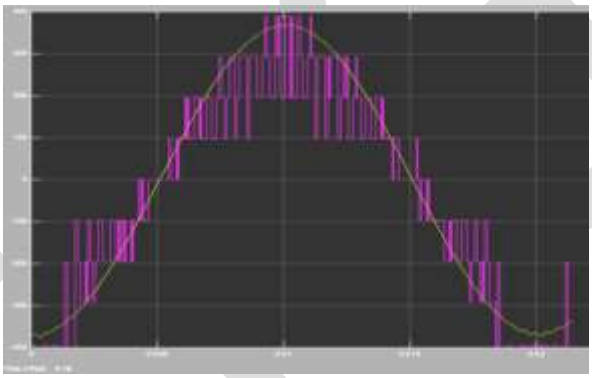

The line voltage and grid connected voltages of the proposed converter

The fig.7 clearly shows the comparison of the grid connected voltage and line voltage waveform of proposed converter. The nature of the nine-level waveform is almost like sinusoidal with small THD

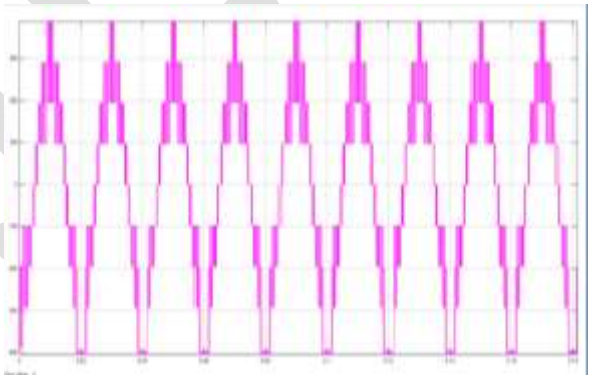

The none-level phase voltage waveform of the switched capacitor multi-level converter

The fig.8 shows the seven-level waveform of the proposed converter output voltage waveform when using POD modulation technique.

V. CONCLUSION

In this paper a novel Switched Capacitor based cascaded multilevel inverter has proposed. A 9-level circuit topology is examined in depth. Compared with conventional cascaded multilevel inverter, the proposed inverter can greatly decrease the number of switching devices. A phase opposition disposition modulation is used as control technique with the low switching frequency and simple implementation. The accordant results of simulation confirm the feasibility of proposed circuit and modulation method

REFERENCES:

[1] P. Jain and H. Pinheiro, "Hybrid high frequency AC power distribution architecture for telecommunication systems," IEEE Trans. Aerospace Electron Syst., vol. 35, no. 1, pp. 138–147, Jan. 1999.

[2] J. Drobnik, "High frequency alternating current power distribution," in Proc. 16th Int.Telecommun. Energy Conf., (INTELEC '94), Oct. 30–Nov. 3, pp. 292–296.

C.K. Bose, M.-H. Kin, and M. D. Kankam, "High frequency AC vs. DC distribution system for next generation hybrid electric vehicle," in Proc.IEEE Int. Conf. Ind. Electron., Control, Instrum. (IECON), Aug. 5–10, 1996, vol. 2, pp. 706–712.

[3] S. Chakraborty and M. G. Simoes, "Experimental evaluation of active filtering in a single-phase high-frequency AC microgrid," IEEE Trans.Energy Convers., vol. 24, no. 3, pp. 673–682, Sep. 2009.

[4] R. Strzelecki and G. Benysek, Power Electronics in Smart Electrical Energy Networks. London, U.K.: Springer-Verlag, 2008.

[5] Z.Ye, P. K. Jain, and P. C. Sen, "A two-stage resonant inverter with control of the phase angle and magnitude of the output voltage," IEEE Trans. Ind. Electron., vol. 54, no. 5, pp. 2797–2812, Oct. 2007.

[6] L. M. Tolbert, F. Z. Peng, and T. G. Habetler, "Multilevel PWM methods at low modulation indices," IEEE Trans. Power Electron., vol. 15, no. 4, pp. 719–725, Jul. 2000.

D.C. Antaloae, J. Marco, and N. D. Vaughan, "Feasibility of high frequency alternating current power for motor auxiliary loads in vehicles,"IEEE Trans. Veh. Technol., vol. 60, no. 2, pp. 390–405, Feb. 2011.

[7] K. W. E. Cheng, "Computation of the AC resistance of multi stranded conductor inductors with multi layers for high frequency switching converters," IEEE Trans. Magn., vol. 36, no. 4, pp. 831–834, Jul. 2000.

[8] P. P. Rodriguez, M. M. D. Bellar, R. R. S.Mu˜noz-Aguilar, S. S. Busquets-Monge, and F. F. Blaabjerg, "Multilevel clamped multilevel converters(MLC)," IEEE Trans. Power Electron., vol. 27, no. 3, pp. 1055–1060,Mar. 2012.

[9] K. Ilves, A. Antonopoulos, S. Norrga, and H.-P. Nee, "A new modulation method for the modular multilevel converter allowing fundamental switching frequency," IEEE Trans. Power Electron., vol. 27, no. 8, pp. 3482–3494, Aug. 2012.

[10] H. Akagi, "Classification, terminology, and application of the modular multilevel cascade converter (MMCC)," IEEE Trans. Power Electron., vol. 26, no. 11, pp. 3119–3130, Nov. 2011.

[11] M. F. Kangarlu and E. Babaei, "A generalized cascaded multilevel inverter using series connection of sub multilevel inverters

International Journal of Engineering Research and General Science Volume 3, Issue 6, November-December, 2015
ISSN 2091-2730

IDENTIFITION OF SQUATS IN RAILWAY INFRASTRUCTURE

Rubina Sultana[1]

Asma Mehdia [2]

[1] Rubina Sultana has completed M.TECH in Embedded Systems

[2] Asma Mehdia has completed M.TECH in Computer Science

ABSTRACT:
Squats have become a major tricky problem in the track of many railways. In the quest for the root causes of squats, it is observed that they are occasionally found at locations of track stiffness changes such as at fish-plated insulated joints and at switches and crossings. Obviously, there should be other factors in the track, which, together with the stiffness change, have played important roles otherwise there will be squats at all such locations. A validated hybrid multibody-finite element model of vehicle–track vertical interaction is extended to simulate the frictional dynamic rolling contact at a fish-plated insulated joint in order to identify such factors. Elastic–plastic rail material property is taken into account. It is found that it is track short defect in the preload condition of the bolts and the contact between the fishplates and the rail head, which together with the stiffness change, causes large normal and longitudinal contact force variation at the fishplate end so that differential wear and differential plastic deformation may accumulate at a fixed location. With proper wavelength, the accumulated rail top geometry deviation may grow into a squat. The significance of the present work lies in that other track short defects such as damaged and improper railpads and fastening, and ballast voids may also have such effects, which may be responsible for a large portion of the many squats in the tracks. This gives the direction for further work.

KEYWORDS: Squats, Rail pads, Wavelength, Switches, Crossings.

INTRODUCTION

The Embedded Technology is now in its prime and the wealth of Knowledge available is mind-blowing. Embedded System is a combination of hardware and software. Embedded technology plays a major role in integrating the various functions associated with it. This needs to tie up the various sources of the Department in a closed loop system. This proposal greatly reduces the manpower, saves time and operates efficiently without human interference. This project puts forth the first step in achieving the desired target. With the advent in technology, the existing systems are developed to have in built intelligence.

LITERATURE SURVEY

Three factors compose the basis of a forest fire: the fire source, environmental elements and combustible material. A forest fire usually occurs as the result of their combined effects (Song et al., 2006). According to the Canada Fire Weather Index Forecast Model, the moisture content of the combustible material plays an important role in forest fires, which means the probability of forest fires depends on the moisture content (Tian et al., 2006). Therefore, the moisture content of combustible materials is a major point of assessment and predicts whether a fire will take place. The moisture content has much to do with relative humidity in the atmosphere, air temperature,wind and similar factors (Shu et al., 2003; Zhang, 2004). Water evaporation can be directly affected by relative humidity. At the same time, the physical properties of combustible materials can be changed indirectly by air temperature. Thus, relative humidity and air temperature are regarded as the two main factors which affect the moisture content of the fuel. Therefore, to reflect the moisture content indirectly, these two parameters are the main objects of our investigation, which should provide an

important basis for the prediction and monitoring of forest fires. Certainly, forest fires are also caused by other factors, such as the active degree of thunder and lightning above the forest, human factors, wind speed, and condition of area vegetation. However, these factors will be ignored in our discussion.

METHODOLOGIES

1) Power Supply

The power supply section is the section which provide +5V for the components to work. IC LM7805 is used for providing a constant power of +5V. The ac voltage, typically 220V, is connected to a transformer, which steps down that ac voltage down to the level of the desired dc output. A diode rectifier then provides a full-wave rectified voltage that is initially filtered by a simple capacitor filter to produce a dc voltage. This resulting dc voltage usually has some ripple or ac voltage variation. A regulator circuit removes the ripples and also retains the same dc value even if the input dc voltage varies, or the load connected to the output dc voltage changes. This voltage regulation is usually obtained using one of the popular voltage regulator IC units.

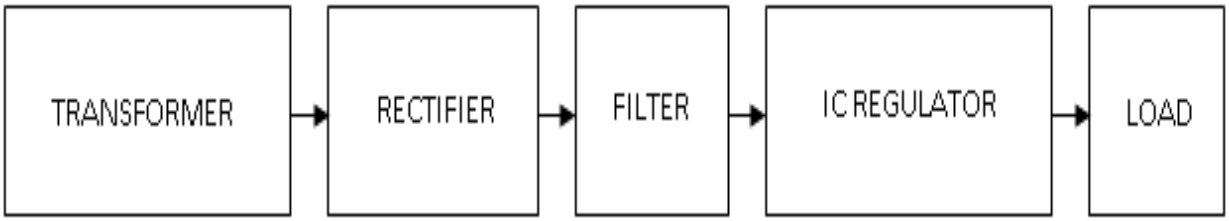

Figure 1. Block Diagram of Power Supply

2) Transformer

Transformers convert AC electricity from one voltage to another with little loss of power. Transformers work only with AC and this is one of the reasons why mains electricity is AC. Step-up transformers increase voltage, step-down transformers reduce voltage. Most power supplies use a step-down transformer to reduce the dangerously high mains voltage (230V in India) to a safer low voltage. The input coil is called the primary and the output coil is called the secondary. There is no electrical connection between the two coils; instead they are linked by an alternating magnetic field created in the soft-iron core of the transformer. Transformers waste very little power so the power out is (almost) equal to the power in. Note that as voltage is stepped down current is stepped up. The transformer will step down the power supply voltage (0-230V) to (0- 6V) level. Then the secondary of the potential transformer will be connected to the bridge rectifier, which is constructed with the help of PN junction diodes. The advantages of using bridge rectifier are it will give peak voltage output as DC.

3) Rectifier

There are several ways of connecting diodes to make a rectifier to convert AC to DC. The bridge rectifier is the most important and it produces full-wave varying DC. A full-wave rectifier can also be made from just two diodes if a centre-tap transformer is used, but this method is rarely used now that diodes are cheaper. A single diode can be used as a rectifier but it only uses the positive (+) parts of the AC wave to produce half-wave varying DC

4) Bridge Rectifier

When four diodes are connected as shown in figure, the circuit is called as bridge rectifier. The input to the circuit is applied to the diagonally opposite corners of the network, and the output is taken from the remaining two corners. Let us assume that the transformer is working properly and there is a positive potential, at point A and a negative potential at point B. the positive potential at point A will forward bias D3 and reverse bias D4.

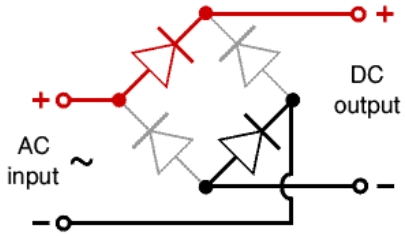

Figure 2. Bridge Rectifier

The negative potential at point B will forward bias D1 and reverse D2. At this time D3 and D1 are forward biased and will allow current flow to pass through them; D4 and D2 are reverse biased and will block current flow.

One advantage of a bridge rectifier over a conventional full-wave rectifier is that with a given transformer the bridge rectifier produces a voltage output that is nearly twice that of the conventional full-wave circuit.

i. The main advantage of this bridge circuit is that it does not require a special centre tapped transformer, thereby reducing its size and cost.

ii. The single secondary winding is connected to one side of the diode bridge network and the load to the other side as shown below.

iii. The result is still a pulsating direct current but with double the frequency.

PROBLEM DEFINITION:

ZigBee is used in applications that require a low data rate, long battery life, and secure networking. ZigBee has a defined rate of 250 kbit/s, best suited for periodic or intermittent data or a single signal transmission from a sensor or input device. Applications include wireless light switches, electrical meters with in-home-displays, traffic management systems, and other consumer and industrial equipment that requires short-range wireless transfer of data at relatively low rates. The technology defined by the ZigBee specification is intended to be simpler and less expensive than other WPANs, such as Bluetooth or Wi-Fi. Since ZigBee can be used almost anywhere, is easy to implement and needs little power to operate, the opportunity for growth into new markets, as well as innovation in existing markets, is limitless. Here are some facts about ZigBee:

- With hundreds of members around the globe, ZigBee uses the 2.4 GHz radio frequency to deliver a variety of reliable and easy-to-use standards anywhere in the world.
- Consumer, business, government and industrial users rely on a variety of smart and easy-to-use ZigBee standards to gain greater control of everyday activities.
- With reliable wireless performance and battery operation, ZigBee gives you the freedom and flexibility to do more.
- ZigBee offers a variety of innovative standards smartly designed to help you be green and save money.

ZigBee is a wireless technology developed as an open global standard to address the unique needs of low-cost, low-power, wireless sensor networks. The standard takes full advantage of the IEEE 802.15.4 physical radio specification and operates in unlicensed bands worldwide at the following frequencies: 2.400–2.484 GHz, 902-928 MHz and 868.0–868.6 MHz.

1. The power levels (down from 5v to 3.3v) to power the zigbee module.
2. The communication lines (TX, RX, DIN and DOUT) to the appropriate voltages.

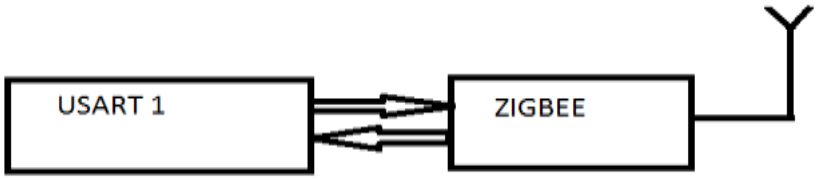

Figure 3.Communications between USART and ZIGBEE

The Zigbee module acts as both transmitter and receiver. The Rx and Tx pins of ZIGBEE are connected to Tx and Rx of 8051 microcontroller respectively. The data's from microcontroller is serially transmitted to Zigbee module via UART port. Then Zigbee transmits the data to another Zigbee. The data's from Zigbee transmitted from Dout pin. The Zigbee from other side receives the data via Din pin. ZigBee module. The €1 coin, shown for size reference, is about 23 mm in diameter. **ZigBee** is a specification for a suite of high level communication protocols using small, low-power digital radios based on the IEEE 802.15.4-2003 standard for Wireless Personal Area Networks (WPANs), such as wireless headphones connecting with cell phones via short-range radio. The technology defined by the ZigBee specification is intended to be simpler and less expensive than other WPANs, such as Bluetooth. ZigBee is targeted at Radio-Frequency (RF) applications that require a low data rate, long battery life, and secure networking.

Overview

ZigBee is a low-cost, low-power, wireless mesh networking proprietary standard. The low cost allows the technology to be widely deployed in wireless control and monitoring applications, the low power-usage allows longer life with smaller batteries, and the mesh networking provides high reliability and larger range.

The ZigBee Alliance, the standards body that defines ZigBee, also publishes application profiles that allow multiple OEM vendors to create interoperable products. The current list of application profiles either published or in the works are:

- Home Automation
- ZigBee Smart Energy
- Commercial Building Automation
- Telecommunication Applications
- Personal, Home, and Hospital Care
- Toys

The relationship between IEEE 802.15.4 and ZigBee is similar to that between IEEE 802.11 and the Wi-Fi Alliance. The ZigBee 1.0 specification was ratified on 14 December 2004 and is available to members of the ZigBee Alliance. Most recently, the ZigBee 2007 specification was posted on 30 October 2007. The first ZigBee Application Profile, Home Automation, was announced 2 November 2007.

ZigBee operates in the Industrial, Scientific and Medical (ISM) radio bands; 868 MHz in Europe, 915 MHz in the USA and Australia, and 2.4 GHz in most jurisdictions worldwide. The technology is intended to be simpler and less expensive than other WPANs such as Bluetooth. ZigBee chip vendors typically sell integrated radios and microcontrollers with between 60K and 128K flash memory, such as the Jennic JN5148, the Free scale MC13213, the Ember EM250 and the Texas Instruments CC2430. Radios are also available stand-alone to be used with any processor or microcontroller. The first stack release is now called Zigbee 2004. The second stack release is called Zigbee 2006, and mainly replaces the MSG/KVP structure used in 2004 with a "cluster library". The 2004 stack is now more or less obsolete. Zigbee 2007, now the current stack release, contains two stack profiles, stack profile 1 (simply called

ZigBee), for home and light commercial use, and stack profile 2 (called ZigBee Pro). ZigBee Pro offers more features, such as multi-casting, many-to-one routing and high security with Symmetric-Key Key Exchange (SKKE), while ZigBee (stack profile 1) offers a smaller footprint in RAM and flash. Both offer full mesh networking and work with all ZigBee application profiles. ZigBee 2007 is fully backward compatible with ZigBee 2006 devices: A ZigBee 2007 device may join and operate on a ZigBee 2006 network and vice versa. Due to differences in routing options, ZigBee Pro devices must become non-routing ZigBee End-Devices (ZEDs) on a ZigBee 2006 or ZigBee 2007 network, the same as ZigBee 2006 or ZigBee 2007 devices must become ZEDs on a ZigBee Pro network. The applications running on those devices work the same, regardless of the stack profile beneath them.

IMPLEMENTATION

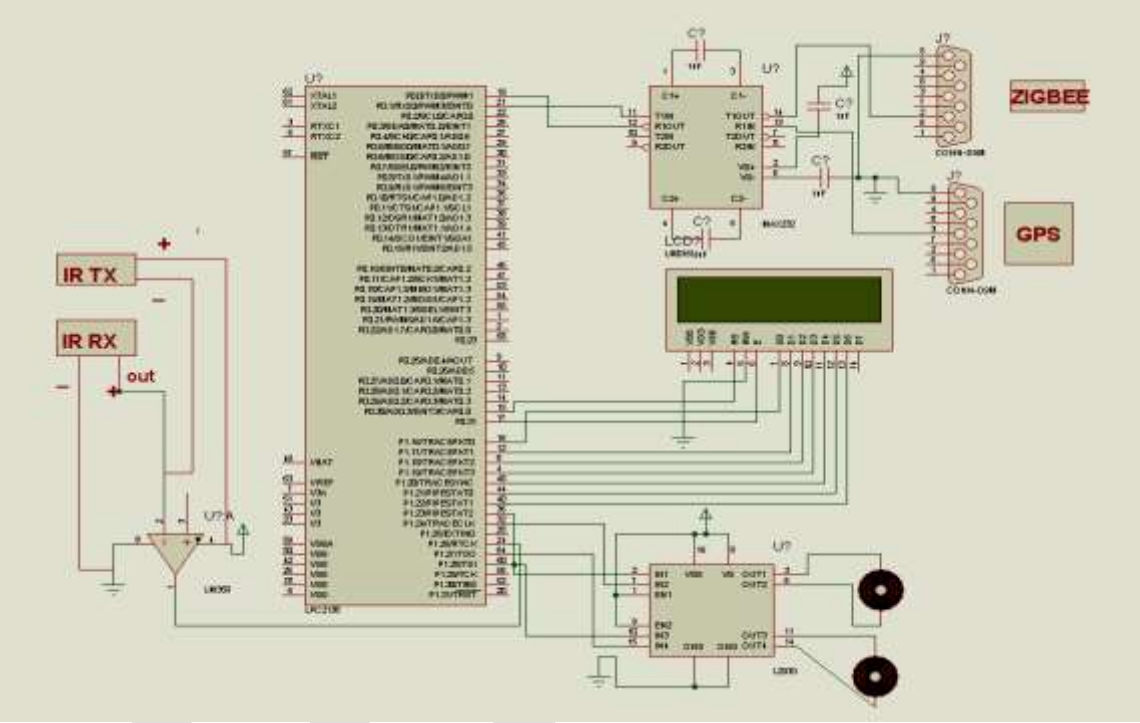

Figure 4.1 SCHEMATIC DAIGRAM

WORKING PRINCIPLE:

This system involves the design of crack finding robot for finding cracks in railway tracks. Here the microcontroller is interfaced with Robot, Zigbee, and GPS, LCD and crack sensor. The IR sensor senses the voltage variations from the crack sensor and then it gives the signal to the microcontroller. The microcontroller checks the voltage variations of the measured value with the threshold value. If the microcontroller detects the crack, it immediately gets the location information using GPS and sends that location and crack information to the control section. The control section displays the location in map. The LCD is used to display the current status of this system.

- Working of IR sensor is very simple and working principle is totally based on change in resistance of IR receiver. Here in this sensor we connect IR receiver in reverse bias so it give very high resistance if it is not exposed to IR light. The resistance in this case is in range of Mega ohms, but when IR light reflected back and falls on IR receiver. The resistance of IR receiver it comes in range between Kilo ohms to hundred of ohms. We convert this change in resistance to change in voltage. Then

this voltage is applied to a comparator IC which compares it with a threshold level. If voltage of sensor is more than threshold then output is high else it is low which can be used directly for microcontroller. The voltage variations from the crack sensor and connected to LM358 which is operational amplifier for uniform signal and then it give the signal to the microcontroller P1.26.The microcontroller checks the voltage variations of the measured value with the threshold value. If the microcontroller detects the crack, it immediately gets the location information using GPS and sends that location and crack information to the control section.

- The basis of the GPS is a constellation of satellites that are continuously orbiting the earth. These satellites, which are equipped with atomic clocks, transmit radio signals that contain their exact location, time, and other information. The radio signals from the satellites, which are monitored and corrected by control stations, are picked up by the GPS receiver.

- A GPS receiver needs only three satellites to plot a rough, 2D position, which will not be very accurate. Ideally, four or more satellites are needed to plot a 3D position, which is much more accurate.GPS is communicated through serial communication and connected to UART0, and updated to control section through Zigbee via serial communication.
- The Zigbee module acts as both transmitter and receiver. The Rx and Tx pins of ZIGBEE are connected to Tx and Rx of ARM7 respectively. The data's from ARM 7 is serially transmitted to Zigbee module via UART1 port.
- Then Zigbee transmits the data to another Zigbee. The data's from Zigbee transmitted from Dout pin. The Zigbee from other side receives the data via Din pin.
- The LCD is used to display the current status of this system here it is 16X2, **a 16x2 LCD** means it can display 16 characters per line and there are 2 such lines. In this LCD each character is displayed in 5x7 pixel matrix.LCD standard requires 3 control lines and 8 I/O lines for the data bus. **8 data pins D7:D0** Bi-directional data/command pins. Alphanumeric characters are sent in ASCII format. **RS: Register Select** RS = 0, Command Register is selected RS = 1, Data Register is selected **R/W: Read or Write**0 Write, 1-> Read E**: Enable (Latch data)** Used to latch the data present on the data pins. A high-to-low edge is needed to latch the data. So the data and Control pins are connected for P0.30, P0.31& P1.16-P1.22.
- For Robot to move using DC Motor which will drive by motor driver IC here four operational pin are connect to ARM 7 P1.23-P1.26 of L293D IC and output pins are connected to M1 and M2 Respectively.

CONCLUSION

This paper presents an automatic method for detecting railway surface defects called "squats" using IR measurements on trains. The method is based on a series of research results from our group in the field of railway engineering that includes numerical simulations. We enhance the IR signal by identifying the voltage variations, using improved IR modules interfaced to the microcontroller for making measurements. The automatic detection algorithm for squats is based on the voltage variations from the IR receiver and determines the squat locations by using GPS. The methodology is also sensitive to small rail surface defects and enables the detection of squats at their earliest stage. The hit rate for small rail surface defects was 78%.

REFERENCES:

[1] Z. Li, R. Dollevoet, M. Molodova, and X. Zhao, "Squat growth—some observations and the validation of numerical predictions," *Wear*, vol. 271, no. 1, pp. 148–157, May 2011.

[2] *UIC Code, Rail Defects, 4th ed.*, International Union of Railways, Paris, France, 2002.

[3] J. Smulders, "Management and research tackle rolling contact fatigue," *Railway Gazette Int.158*, no. 7, pp. 439–442, Jul. 2003.

[4] P. Clayton and M. Allery, "Metallurgical aspects of surface damage problems in rails," *Can. Metall. Q.*, vol. 21, no. 1, pp. 31–46, Jan. 1982.

[5] Rail Damages, the Blue Book of Rail Track, U.K., 2001.

[6] A. Zoeteman, "Life cycle cost analysis for managing rail infrastructure: Concept of a decision support system for railway design and maintenance," *Eur. J. Transport Infrastructure. Res.*, vol. 1, no. 4, pp. 391–413, 2001.

International Journal of Engineering Research and General Science Volume 3, Issue 6, November-December, 2015
ISSN 2091-2730

NUMERICAL SIMULATION OF SCRAMJET ENGINE

A Animhons[1*], D. Nirmalkumar[2], A. Johnsree[3]

[1]Department of Aeronautical Engineering, Hindustan Institute of Technology, Coimbatore.

[2]Department of Aeronautical Engineering, Hindustan Institute of Technology and Science, Chennai.

[3]Department of Aeronautical Engineering, karpagam Institute of Technology, Coimbatore.

[*]Corresponding author: A. Animhons; Email-animhonsasokan@yahoo.com,

Abstract - The analysis of scramjet engine is a well-known problem when compared to other engine simulations. I intend to analyze the scramjet engine using the software package Fluent – Gambit. This analysis describes the flow field through the scramjet engine. The engine is modeled using Gambit and imported to Fluent. The boundary conditions are specified accordingly to simulate cold flow conditions. In this context, an attempt has been made to investigate the flow field and analyze the graphical results obtained using Fluent. Here, the computation has been carried out at supersonic speed to solve the flow field variable. The results are obtaining in graphical format for temperature, velocity, pressure and Mach number variation along length of the engine. The analysis is intended for various inlet Mach no (2, 3 and 4) conditions. The results will be further sharpened by refining grid and by using various viscous models. Fluent is a computational fluid dynamics (CFD) software package to simulate fluid problems. It uses the finite-volume method to solve the governing equations for a fluid. It provides the capability to use different physical models such as incompressible or compressible, in viscid or viscous, laminar or turbulent, etc. Geometry and grid generation is done by using Gambit which is the preprocessor bundled with Fluent. Modeling, meshing and solutions of flow variable around the complex geometry have been solved using this software. The various features of the preprocessor, solver and postprocessor of the software are being highlighted in below analysis.

Keywords - scramjet inlet, contraction ratio, ramp, cowl lip, normal shock, oblique shock, shock train

INTRODUCTION

Definition of a Scramjet Engine

In order to provide the definition of a scramjet engine, the definition of a ramjet engine is first necessary, as a scramjet engine is a direct descendant of a ramjet engine. Ramjet engines have no moving parts, instead operating on compression to slow free stream supersonic air to subsonic speeds, thereby increasing temperature and pressure, and then combusting the compressed air with fuel. Lastly, a nozzle accelerates the exhaust to supersonic speeds, resulting in thrust. Figure 1 shows a two- dimensional schematic of a ramjet engine

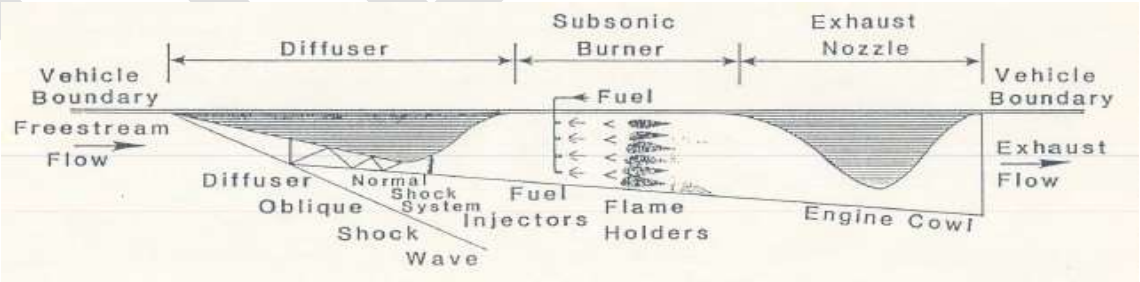

Fig. 1: Two-dimensional Schematic of a Ramjet Engine

Due to the deceleration of the free stream air, the pressure, temperature and density of the flow entering the burner are "considerably higher than in the free stream". At flight Mach numbers of around Mach 6, these increases make it inefficient to continue to slow the flow to subsonic speeds. Thus, if the flow is no longer slowed to subsonic speeds, but rather only slowed to

acceptable supersonic speeds, the ramjet is then termed a 'supersonic combustion ramjet,' resulting in the acronym scramjet. Figure 2 shows a two-dimensional schematic of a scramjet engine.

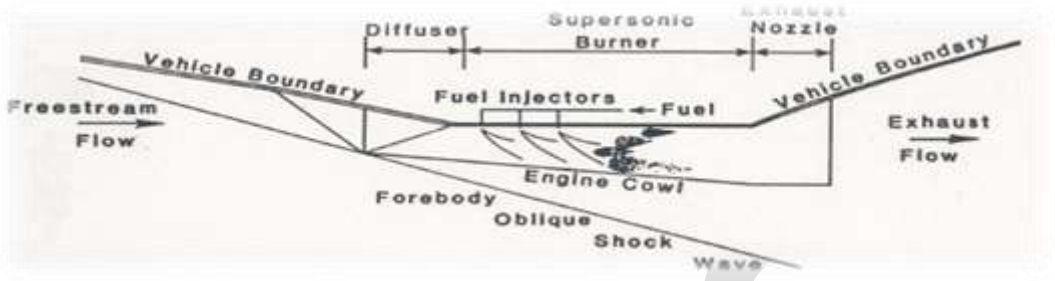

Fig. 2: Two-dimensional Schematic of a Scramjet Engine

Though the concept of ramjet and scramjet engines may sound like something out of science fiction, scramjet engines have been under development for at least forty years. The following subsection will give a brief chronological history of the scramjet engine.

NUMERICAL ANALYSIS

LAWS GOVERNING FLUID MOTION

The laws governing fluid motion are (i) Conservation of Mass (ii) Newton's Laws of Motion (iii) Conservation of Energy.

Continuity Equation

The law of Conservation of Mass expressed in the form of a differential equation is called the continuity equation. If we consider a control volume; then the conservation of mass can be interpreted as the rate of mass leaving an elemental volume minus the mass entering the same volume is equal to the rate of change of mass in the control volume which is equal to the rate of change of density multiplied by the volume of the element.

For Unsteady flow, the continuity Equation can be written as

$$\frac{\partial \rho}{\partial t} + \nabla.(\rho \mathbf{V}) = 0$$

For Steady Flow, the above equation Reduces to:

$$\nabla.(\rho \mathbf{V}) = 0$$

Where, V is the Velocity and ρ is the Density.

Momentum Equation

The physical principle involved in the Momentum Equation is the Newton' Second Law of Motion according to which rate of change of Momentum= force.

The total rate of change of Momentum is made of:

- Rate of change of momentum inside the control volume
- The difference between momentum flux leaving and entering (i.e. net flux)

Therefore in differential form momentum equation can be written as

$$\frac{\partial(\rho u)}{\partial t} + \nabla.(\rho u\mathbf{V}) = -\frac{\partial p}{\partial x} + \rho f_x + (F_x)_{Viscous}$$

$$\frac{\partial(\rho v)}{\partial t} + \nabla.(\rho v\mathbf{V}) = -\frac{\partial p}{\partial y} + \rho f_y + (F_y)_{Viscous}$$

$$\frac{\partial(\rho w}{\partial t} + \nabla.(\rho w\mathbf{V}) = -\frac{\partial p}{\partial z} + \rho f_z + (F_z)_{Viscous}$$

Where, □ is the density, P is the pressure acting, V is the Velocity, u,v, w is the velocity vectors, F_x,F_y,F_z is the viscous force and f_x,f_y,f_z is the body force acting in the X-, Y- and Z- axis respectively.

These equations show a viscous flow and are also known as the Navier-Stokes Equation.

For an in-viscid flow, the equations become,

$$\nabla.(\rho u\mathbf{V}) = -\frac{\partial p}{\partial x}$$

$$\nabla.(\rho v\mathbf{V}) = -\frac{\partial p}{\partial y}$$

$$\nabla.(\rho w\mathbf{V}) = -\frac{\partial p}{\partial z}$$

Where, □ is the density, P is the pressure acting, V is the Velocity, u, v, w is the velocity vectors acting in the X-, Y- and Z- axis respectively.

These equations are known as the Euler's Equations.

Energy Equation

The physical principle involved in the energy equation is that; Energy can neither be created nor be destroyed.

Therefore,

Energy equation is given as

$$\frac{\partial}{\partial t}\left[\rho\left(e+\frac{V^2}{2}\right)\right] + \nabla.\left[\rho\left(e+\frac{V^2}{2}\right)\mathbf{V}\right] = p\dot{q} - \nabla.(p\mathbf{V}) + \rho(\mathbf{f}.\mathbf{V}) + \dot{Q}'_{Viscous} + \dot{W}'_{Viscous}$$

Where, □ is the density, P is the pressure acting, V is the Velocity, e is the internal energy of the system, Q is the viscous heat source or sink, W is the viscous work done and f is the body force acting on the system. The above equation is a partial differential equation which relates the flow field variables at a given point in space.

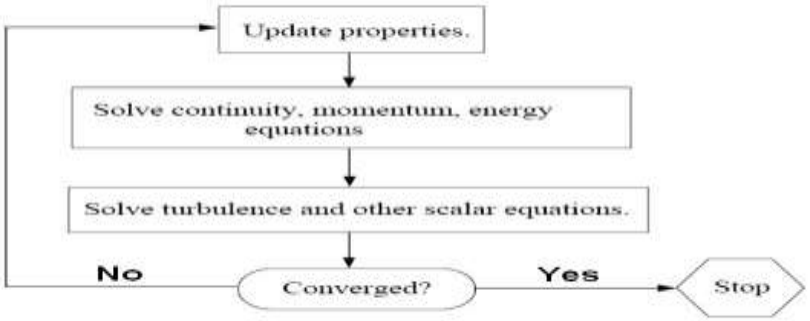

Fig. 3. Overview of the Coupled Solution Method

THEORITICAL CALCULATIONS

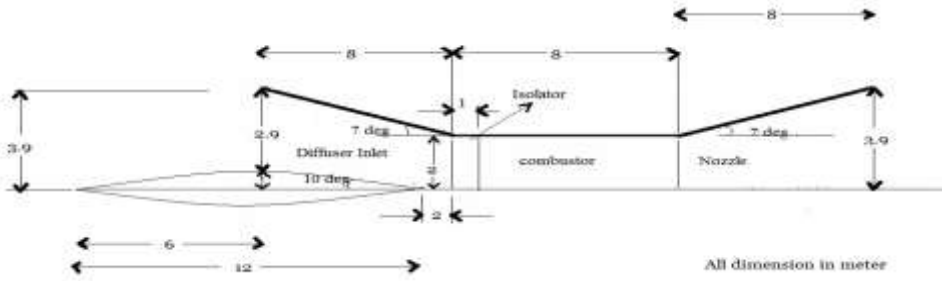

Fig. 4: Scramjet engine theoretical parameter

THEORY DESCRIPTION

The starting mach number of this engine is 5; at the corner cone section creates the oblique shock in front the engine. According to the shock, the mach value is reducing to 4 at the diffuser inlet. Using the area-mach number relation the mach value is decreasing to the diffuser section because of the decreasing the area, at the diffuser exit the mach value is 3.1. The step of the decreasing mach value is shown in below diagram and theoretical calculations are given in below. Area ratio, pressure and temperature values are finding to the respective Mach number in using gas tables. In the isolator and combustion chamber mach value is same 3.1, because of constant area value. At the nozzle inlet the Mach number is 3.1, it also increasing for increasing the divergent area section. In the divergent exit or nozzle exit Mach number value is increasing to 4.7 for according to the theoretical calculation. Pressure and temperature values are finding to the same gas tables.

EFFECT OF OBLIGUE SHOCK FORMATION IN CORNER OF THE CONE SECTION

The effect of shock in cone section will reducing the Mach number value 5 to 4 in the engine using oblique shock in perfect gas table.

TABLE 1: EFFECT OF AN OBLIQUE SHOCK IN CONE SECTION

M_1	Θ	β	$\frac{P_2}{P_1}$	M_2
5	10	19.38	3.043	3.999

TABLE 2: PHYSICAL PARAMETER

RADIUS (m)	AREA (m^2)	$\frac{A}{A^*}$	M	$\frac{P}{P_\circ}$	$\frac{T}{T_\circ}$	P (pa)	T (k)
2.90	26.40	10.71	4.0	0.0066	0.2381	668.74	71.43
2.65	22.00	8.96	3.8	0.0086	0.2572	871.39	77.16
2.47	19.21	7.81	3.6	0.0106	0.2729	1074.04	81.87
2.25	15.89	6.46	3.4	0.0141	0.2958	1428.68	88.74
2.00	12.56	5.10	3.1	0.0208	0.3309	2107.56	99.27
2.25	15.89	6.46	3.4	0.0141	0.2958	1428.68	88.74
2.80	24.61	10.00	3.9	0.0072	0.2446	729.54	73.38
3.40	36.29	14.75	4.4	0.0041	0.2083	415.43	62.49
3.90	47.75	19.41	4.7	0.0027	0.1846	273.57	55.38

SCRAMJET ENGINE SECTIONAL PARAMETER

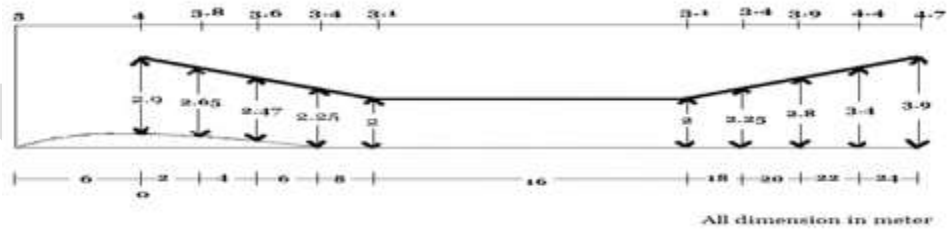

Fig. 5. Scramjet engine sectional parameter.

NUMERICAL ANALYSIS OF COLD FLOW IN 2 - D SECTION

SIMPLE PROBLEM DESCRIPTION

Initially, it is to analyze the simple 2-D section of scramjet engine is without front and back domain and cone. This scramjet engine consists of a convergent diffuser section, combustion chamber and divergent nozzle section. The engine has been designed using gambit software. Boundary conditions are applied in each section of the engine using gambit. Next this model meshed by appropriate mesh size and the mesh model is exported to the mesh option. This mesh model can be solved using fluent software in appropriate solving condition, until the results are converged. The convergent results are showed in the graphical formats according to the pressure, velocity and temperature along the position of the length of an engine. Here three types of convergent results can be analyzed in fluent convergent criteria according to the Mach number. That Mach numbers are 2, 3, 4 respectively. Above all the Mach number convergent results are given below. Changes occur as per the mesh size of the model.

SIMPLE GEOMETRY OF 2-D SCRAMJET ENGINE

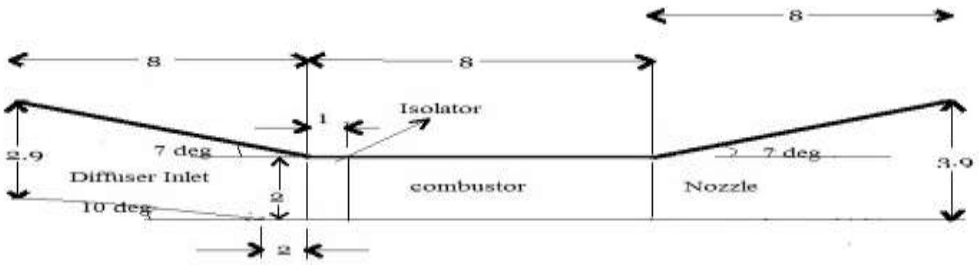

DESIGN OF THE SIMPLE SCRAMJET

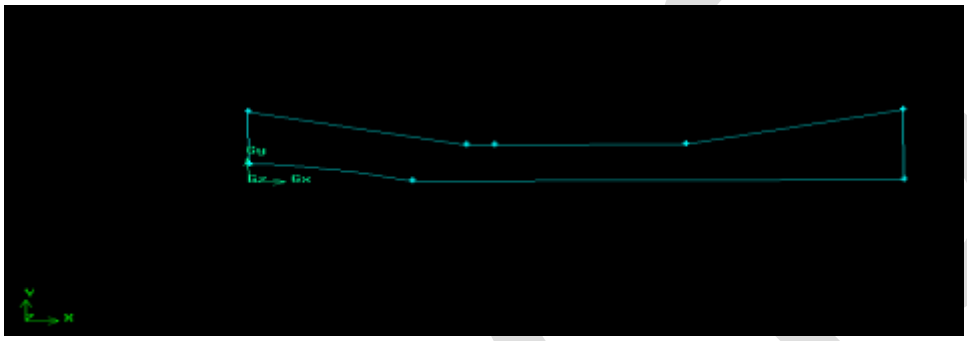

Fig. 6. Simple 2-D scramjet engine

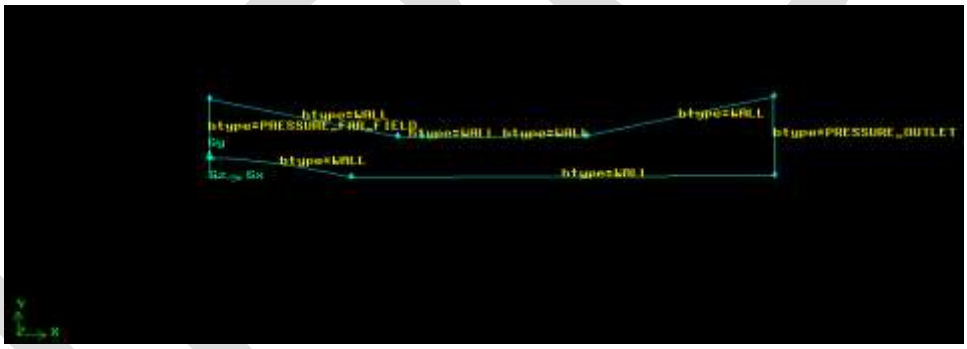

Fig. 7. Simple scramjet engines boundary condition

MESH MODEL OF SCRAMJET ENGINE WITHOUT CONE

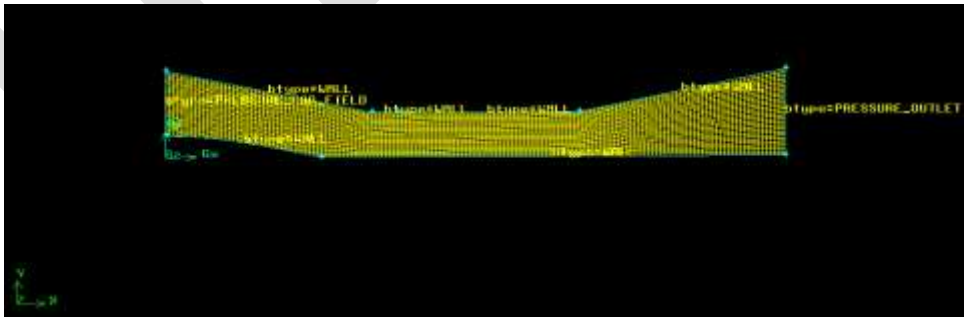

Fig. 8. Mesh size of 2-D section is 0.2.

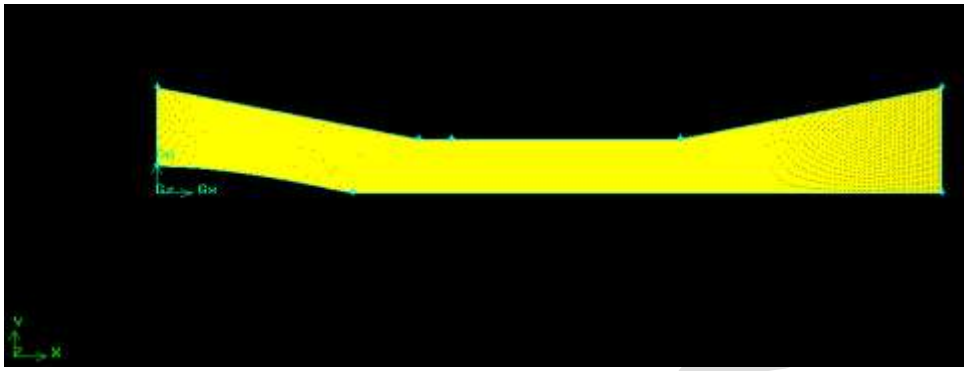

Fig. 9. Mesh size of 2-D section is 0.05

ANALYSIS IN FLUENT

PROCEDURE: (2D VERSION OF FLUENT)

- **FILE READ CASE**

The file channel mesh is selected by clicking on it under files and grid is checked.

- **GRID CHECK**

The grid was scaled to 1 in all x, y and z directions.

- **GRID SCALE**

The grid was displayed.

- **DISPLAY GRID**

Grid is copied in ms-word file.

- **DEFINE**

- **MODELS** **SOLVER**

Solver is segregated

Density based solver

Implicit formulation

Space 2-D

Time steady

ENERGY

Energy equation

VISCOUS MODEL

K-epsilon

- **MATERIALS** **TYPE**

Fluid

FLUENT FLUID MATERIAL

Air

CONDITIONS

Dynamic Viscosity, $\mu = 1.7894 \times 10\text{-}5$ kg/m-s

Density, ρ = ideal gas

Thermal Conductivity, K= 0.0242 W/m-K

Specific heat, Cp= 1006.43 J/kg- K

- **OPERATING CONDITIONS**

  Operating pressure= 101325 Pa

- **BOUNDARY CONDITIONS**

PARTS	CONDITION
Inlet	Pressure far field
Body	Wall
Outlet	Pressure outlet

➢ **SOLVE**

- **CONTROLS** **SOLUTIONS**

  All energy equations are used.

  Under relaxation factors

  Pressure = 0.3

  Density = 1

  Body Force = 1

  Momentum = 0 .7

- **INTIALIZE**

  Compute form inlet

  Temperature = 300 k

- **MONITOR**

  Residual

- **ITERATE**

  Convergence was checked.

➢ **PLOT XY PLOT**

Y AXIS - pressure, velocity and temperature

X AXIS - grid

1. X AXIS = X CO-ORDINATE
2. Y AXIS = Y CO-ORDINATE

Find the pressure, velocity, temperature and Mach number on line varying y co-ordinates with respect to x co-ordinates as length of an engine.

RESULTS AND DISCUSSIONS

MACH 2 INLET CONDITION RESULTS

CONTOUR RESULTS FOR MACH 2

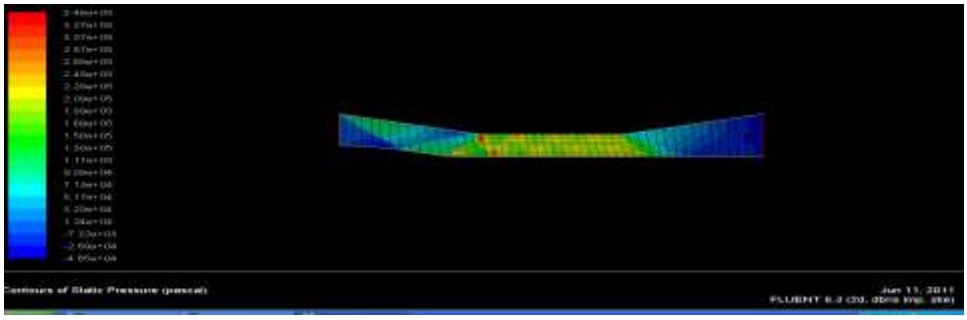

Fig. 10. Contours of pressure in Mach 2

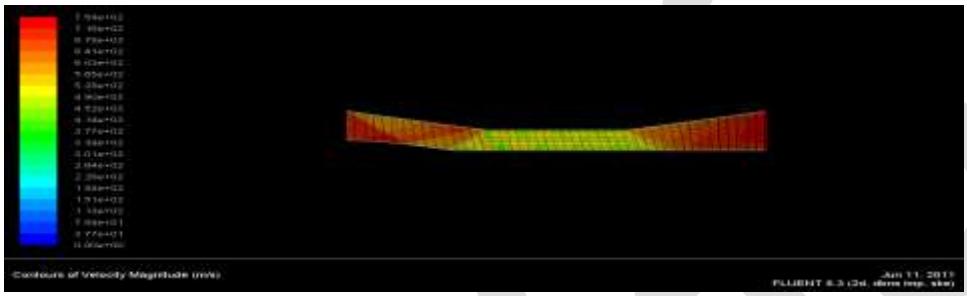

Fig. 11. Contours of velocity in Mach 2

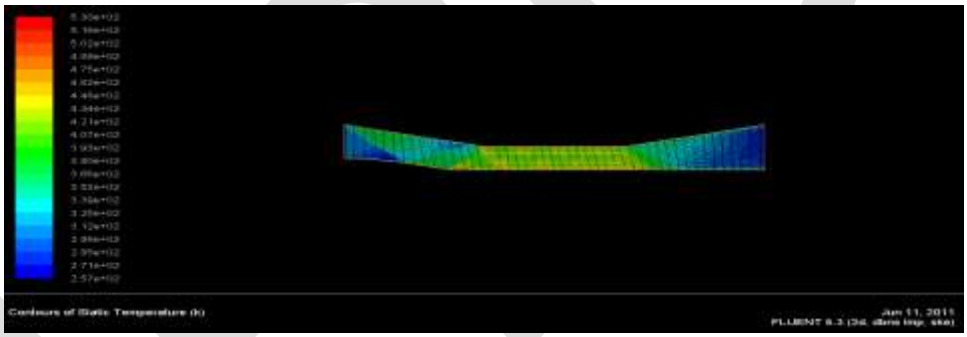

Fig. 12. Contours of Temperature in Mach 2

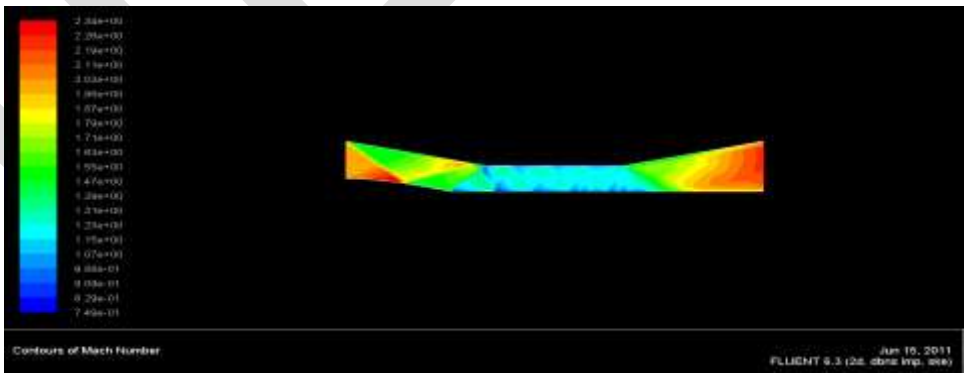

Fig. 13. Contours of Mach number in Mach 2.

Figure 10. The initial pressure value is assumed to be sea level condition. According to the contour, in the diffuser section due to the area convergence the pressure is raised. At the combustion chamber, the pressure values remains constant because of the constant area. As the area is diverged at the final in nozzle section, the pressure values are dropped.

Figure 11 The initial velocity is assumed to be 600 m/s. According to the contour, in the diffuser section due to the area convergence the velocity is dropped. At the combustion chamber, the velocity remains constant because of the constant area. As the area is diverged at the final in nozzle section, the velocities are raised.

Figure 12. The initial temperature value is assumed to be sea level condition. According to the contour, in the diffuser section due to the pressure raised, temperature value also raised. At the combustion chamber, temperature values remains constant because of the constant pressure. As the final in nozzle section, the temperature values are decreases to decrease the pressure value.

Figure 13 .The initial Mach number is assumed to be 2. According to the contour, in the diffuser section due to the area convergence the Mach number is raised. At the combustion chamber, Mach number remains constant because of the constant area. As the area is diverged at the final in nozzle section, the Mach number is dropped.

GRAPH FOR MACH 2

PRESSURE GRAPH FOR MACH 2

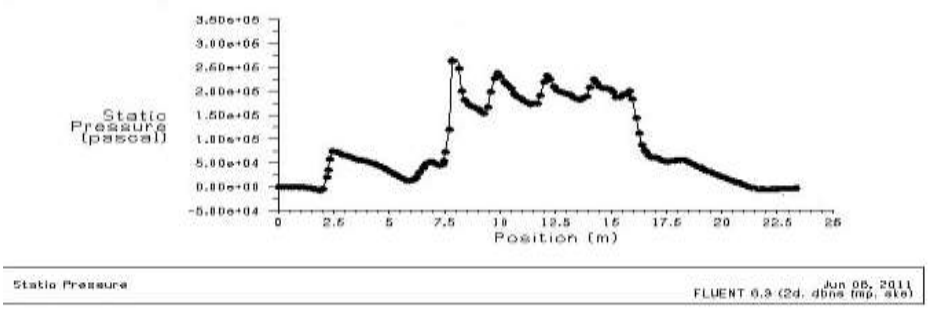

The initial pressure value is assumed to be sea level condition. According to the graph, in the diffuser section due to the area convergence the pressure is raised. At the combustion chamber, the pressure values remains constant because of the constant area. As the area is diverged at the final in nozzle section, the pressure values are dropped. Because of the oscillations, Pressure raising and dropping are not in expected format. Since, it is due to an unsatisfied condition.

VELOCITY GRAPH FOR MACH 2

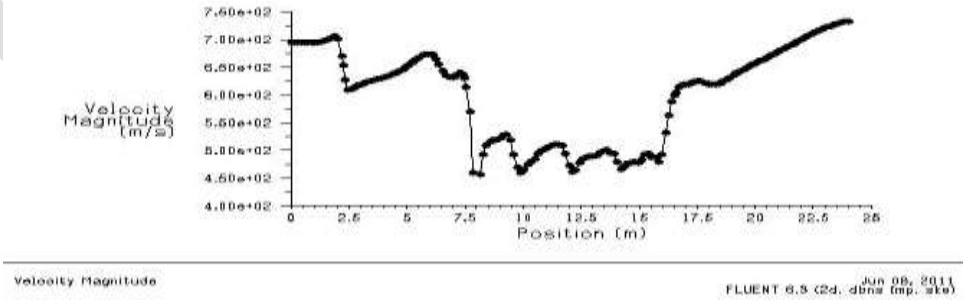

The initial velocity is assumed to be 600 m/s. According to the contour, in the diffuser section due to the area convergence the velocity is dropped. At the combustion chamber, the velocity remains constant because of the constant area. As the area is diverged at the final in nozzle section, the velocities are raised. Because of the oscillations, velocity raising and dropping are not in expected format. Since, it is due to an unsatisfied condition.

TEMPERATURE GRAPH FOR MACH 2

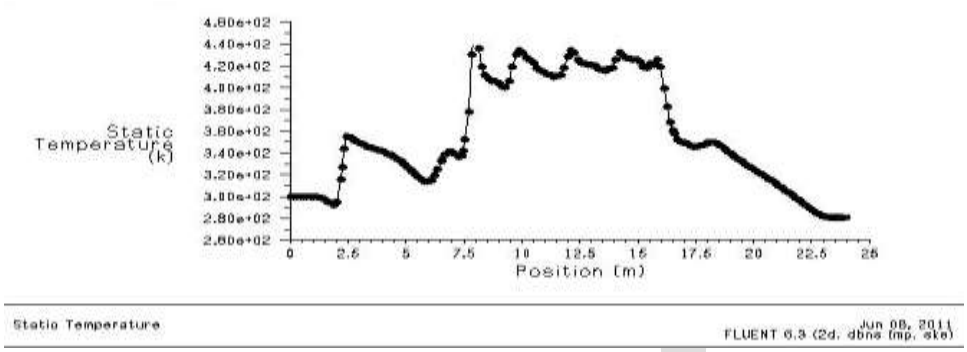

The initial temperature value is assumed to be sea level condition. According to the contour, in the diffuser section due to the pressure raised, temperature value also raised. At the combustion chamber, temperature values remains constant because of the constant pressure. As the final in nozzle section, the temperature values are decreases to decrease the pressure value.

MACH NUMBER GRAPH FOR MACH 2

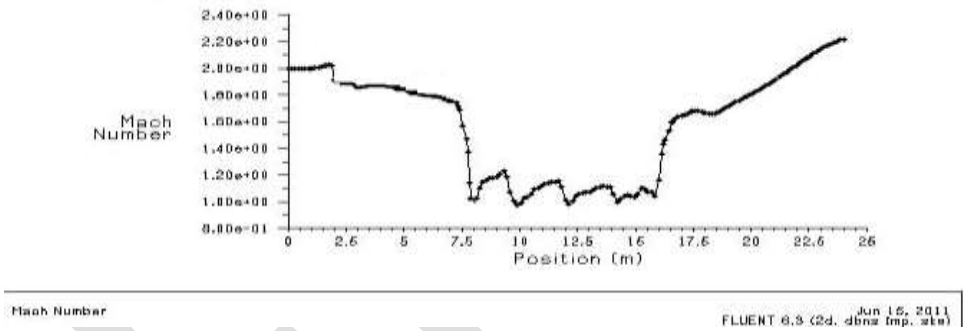

The initial Mach number is assumed to be 2. According to the contour, in the diffuser section due to the area convergence the Mach number is raised. At the combustion chamber, Mach number remains constant because of the constant area. As the area is diverged at the final in nozzle section, the Mach number is dropped.

MACH 3 INLET CONDITION RESULTS

CONTOUR RESULTS FOR MACH 3

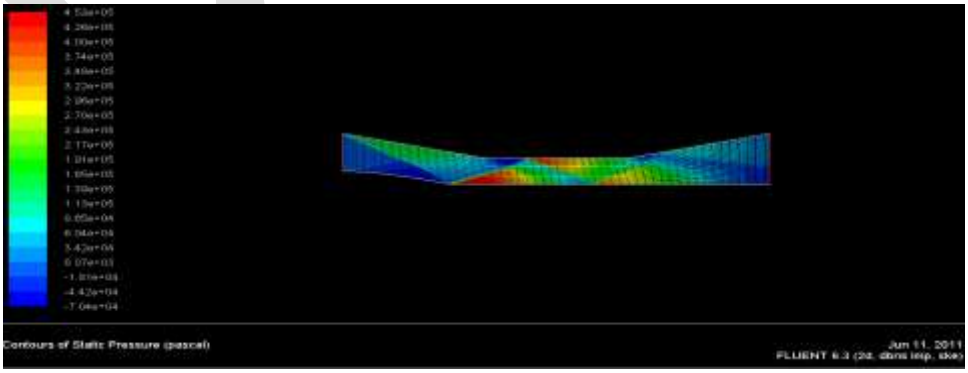

Fig. 14. Contours of pressure in Mach 3

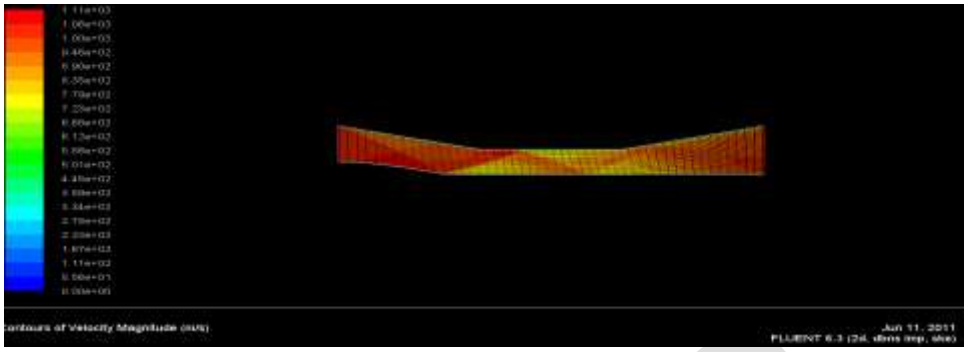

Fig. 15. Contours of velocity in Mach 3

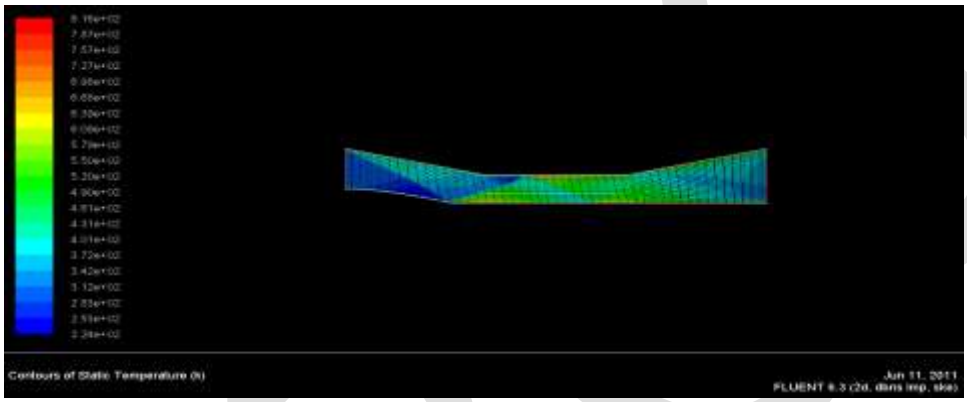

Fig. 16 Contours of Temperature in Mach 3

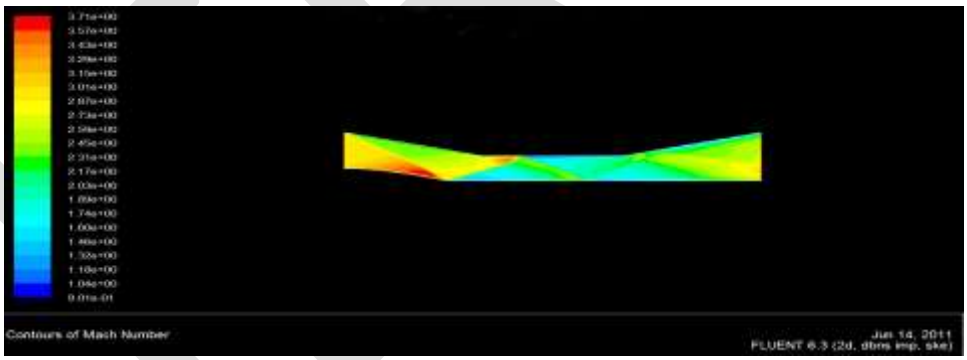

Fig. 17 Contours of Mach number in Mach 3

Figure 14. The initial pressure value is assumed to be sea level condition. According to the contour, in the diffuser section due to the area convergence the pressure is raised. At the combustion chamber, the pressure values remains constant because of the constant area. As the area is diverged at the final in nozzle section, the pressure values are dropped.

Figure 15. The initial velocity is assumed to be 912 m/s. According to the contour, in the diffuser section due to the area convergence the velocity is dropped. At the combustion chamber, the velocity remains constant because of the constant area. As the area is diverged at the final in nozzle section, the velocities are raised.

Figure 16. The initial temperature value is assumed to be sea level condition. According to the contour, in the diffuser section due to the pressure raised, temperature value also raised. At the combustion chamber, temperature values remains constant because of the constant pressure. As the final in nozzle section, the temperature values are decreases to decrease the pressure value.

Figure 17.The initial Mach number is assumed to be 3. According to the contour, in the diffuser section due to the area convergence the Mach number is raised. At the combustion chamber, Mach number remains constant because of the constant area. As the area is diverged at the final in nozzle section, the Mach number is dropped.

GRAPH FOR MACH 3

PRESSURE GRAPH FOR MACH 3

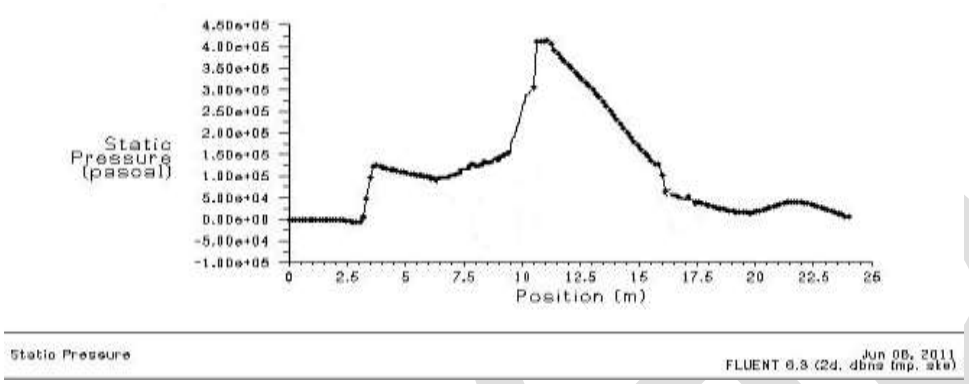

The initial pressure value is assumed to be sea level condition. According to the graph, in the diffuser section due to the area convergence the pressure is raised. At the combustion chamber, the pressure values remains constant because of the constant area. As the area is diverged at the final in nozzle section, the pressure values are dropped. Because of the oscillations, Pressure raising and dropping are not in expected format. Since, it is due to an unsatisfied condition.

VELOCITY GRAPH FOR MACH 3

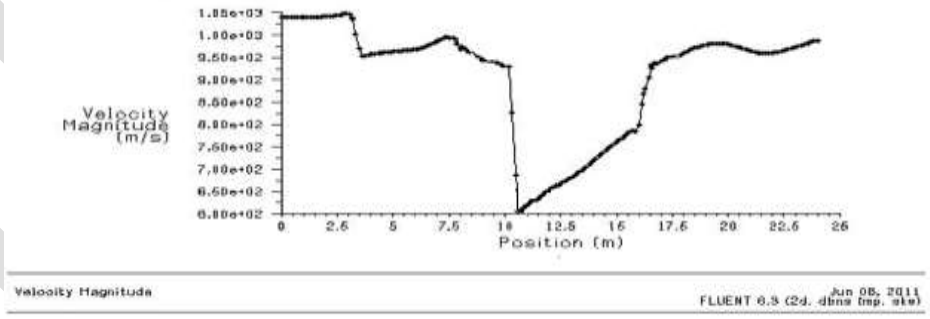

The initial velocity is assumed to be 1050 m/s. According to the contour, in the diffuser section due to the area convergence the velocity is dropped. At the combustion chamber, the velocity remains constant because of the constant area. As the area is diverged at the final in nozzle section, the velocities are raised. Because of the oscillations, velocity raising and dropping are not in expected format. Since, it is due to an unsatisfied condition.

TEMPERATURE GRAPH FOR MACH 3

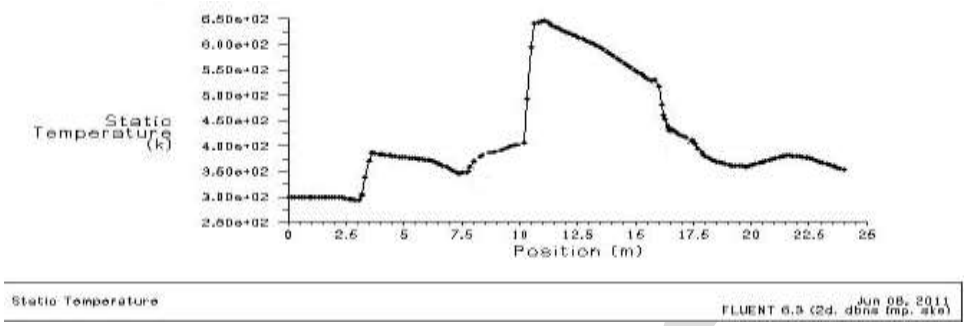

The initial temperature value is assumed to be sea level condition. According to the contour, in the diffuser section due to the pressure raised, temperature value also raised. At the combustion chamber, temperature values remains constant because of the constant pressure. As the final in nozzle section, the temperature values are decreases to decrease the pressure value.

MACH NUBER GRAPH FOR MACH 3

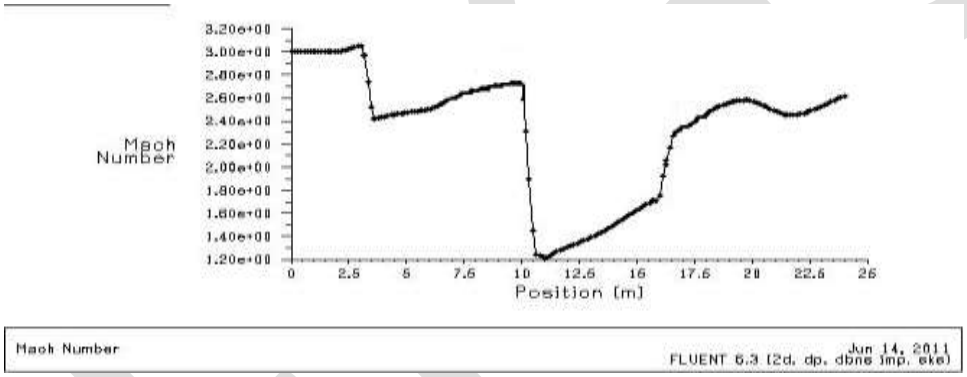

The initial Mach number is assumed to be 3. According to the contour, in the diffuser section due to the area convergence the Mach number is raised. At the combustion chamber, Mach number remains constant because of the constant area. As the area is diverged at the final in nozzle section, the Mach number is dropped.

7.3. MACH 4 INLET CONDITION RESULTS

7.3.1. CONTOURS FOR MACH 4

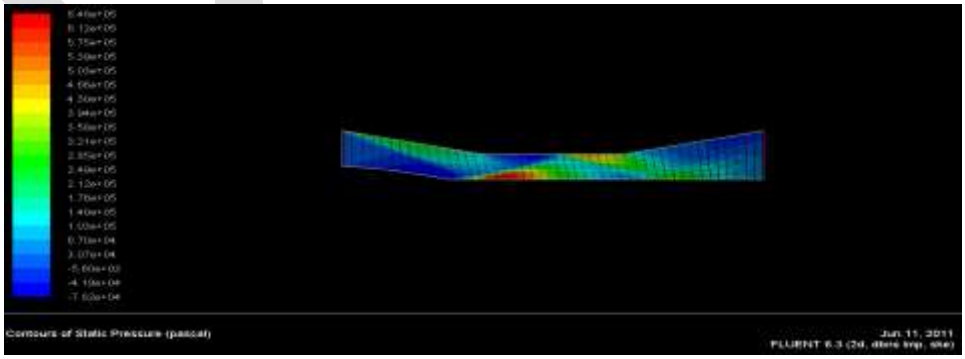

Fig. 18. Contours of pressure in Mach 4

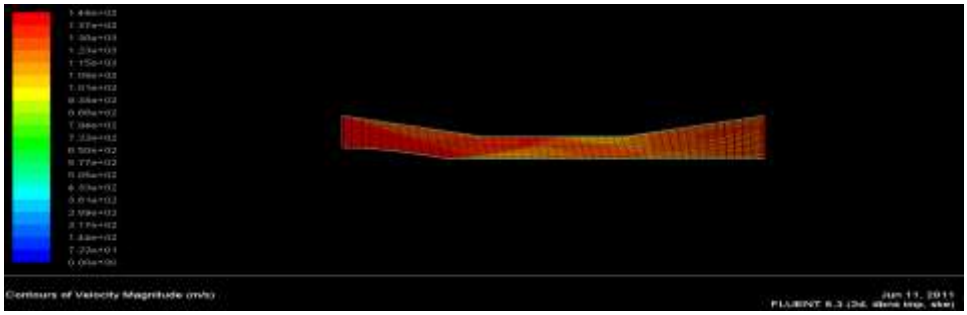

Fig. 19 Contours of Velocity in Mach 4

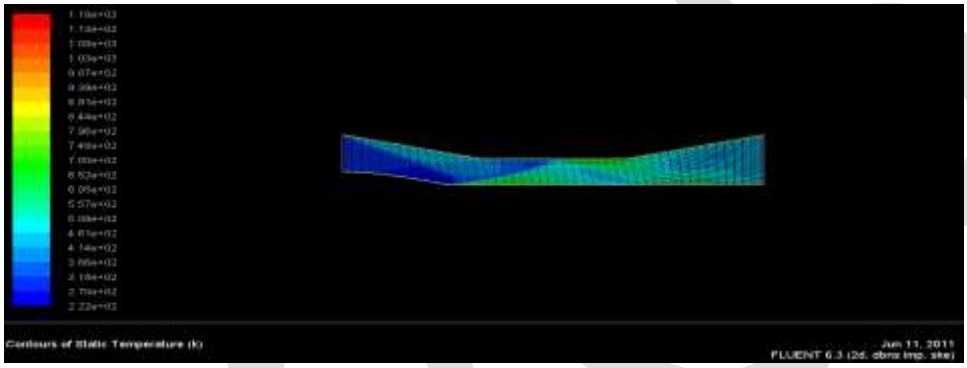

Fig. 20 Contours of Temperature in Mach 4

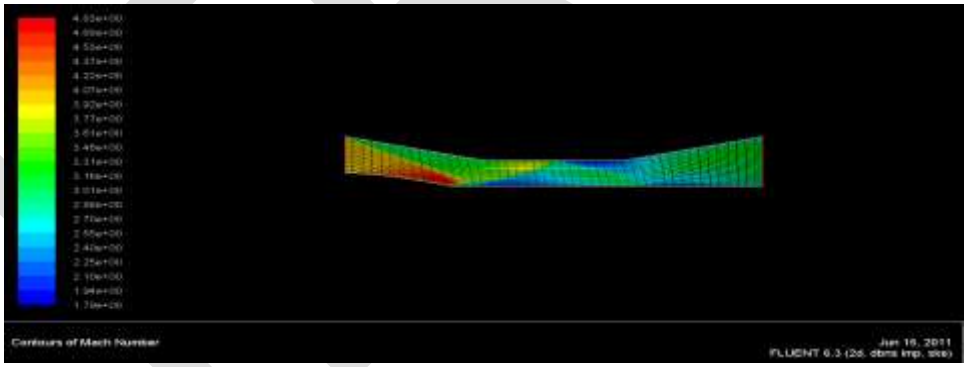

Fig. 21. Contours of Mach number in Mach 4

Figure 18. The initial pressure value is assumed to be sea level condition. According to the contour, in the diffuser section due to the area convergence the pressure is raised. At the combustion chamber, the pressure values remains constant because of the constant area. As the area is diverged at the final in nozzle section, the pressure values are dropped.

Figure 19 The initial velocity is assumed to be 1340 m/s. According to the contour, in the diffuser section due to the area convergence the velocity is dropped. At the combustion chamber, the velocity remains constant because of the constant area. As the area is diverged at the final in nozzle section, the velocities are raised.

Figure 20. The initial temperature value is assumed to be sea level condition. According to the contour, in the diffuser section due to the pressure raised, temperature value also raised. At the combustion chamber, temperature values remains constant because of the constant pressure. As the final in nozzle section, the temperature values are decreases to decrease the pressure value.

Figure 21.The initial Mach number is assumed to be 4. According to the contour, in the diffuser section due to the area convergence the Mach number is raised. At the combustion chamber, Mach number remains constant because of the constant area. As the area is diverged at the final in nozzle section, the Mach number is dropped.

GRAPH FOR MACH 4

PRESSURE GRAPH FOR MACH 4

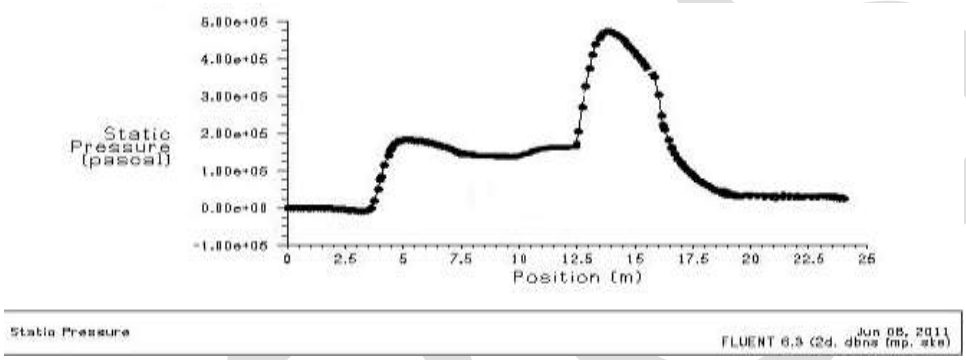

The initial pressure value is assumed to be sea level condition. According to the contour, in the diffuser section due to the area convergence the pressure is raised. At the combustion chamber, the pressure values remains constant because of the constant area. As the area is diverged at the final in nozzle section, the pressure values are dropped.

VELOCITY GRAPH FOR MACH 4

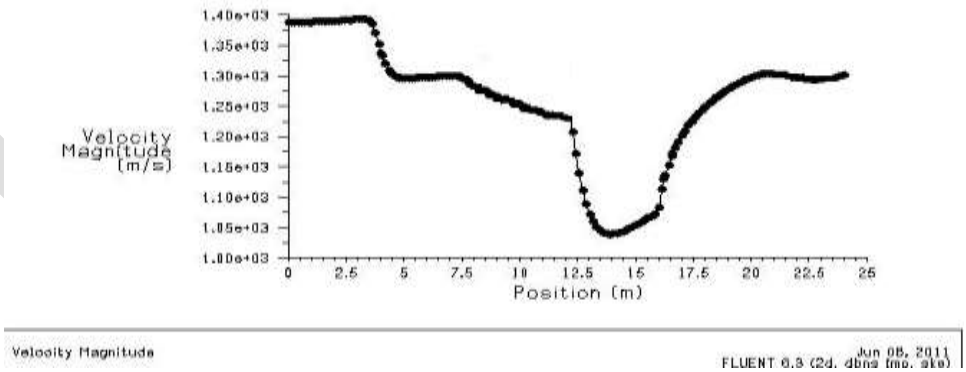

The initial temperature value is assumed to be sea level condition. According to the contour, in the diffuser section due to the pressure raised, temperature value also raised. At the combustion chamber, temperature values remains constant because of the constant pressure. As the final in nozzle section, the temperature values are decreases to decrease the pressure value.

TEMPERATURE GRAPH FOR MACH 4

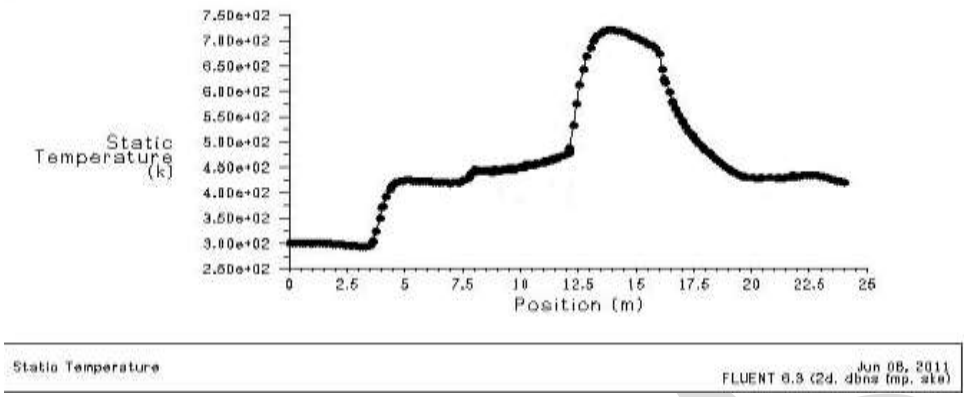

The initial temperature value is assumed to be sea level condition. According to the contour, in the diffuser section due to the pressure raised, temperature value also raised. At the combustion chamber, temperature values remains constant because of the constant pressure. As the final in nozzle section, the temperature values are decreases to decrease the pressure value.

7.3.2.4. MACH NUMBER GRAPH FOR MACH 4

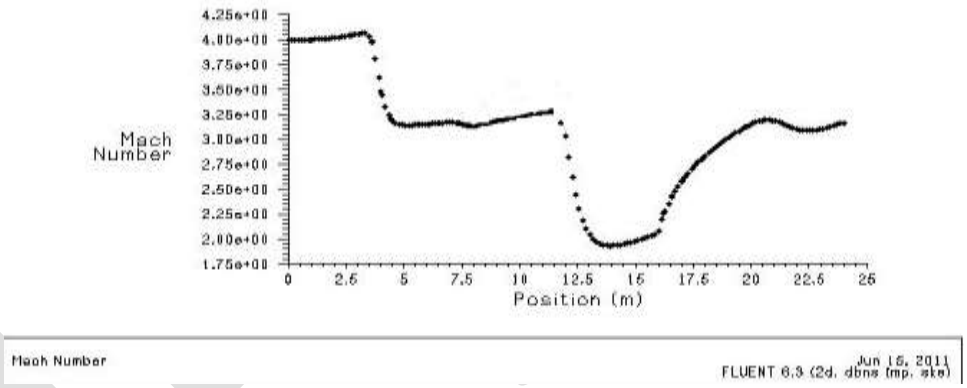

The initial Mach number is assumed to be 4. According to the contour, in the diffuser section due to the area convergence the Mach number is raised. At the combustion chamber, Mach number remains constant because of the constant area. As the area is diverged at the final in nozzle section, the Mach number is dropped.

MODIFICATION RESULTS IN MACH 4

PROBLEM DESCRIPTION

The results that have been found in above are not in expected form. This is due to an unsatisfied condition respectively. Their by, this drawback undergoes another check for an expected result. The parameter like boundary condition and viscous model has been changed. And again iterate this problem continuously, until the results are converged. Then convergent results are showed to the contour and graph format. This modification results are shown in below.

Changes made in viscous model- Spalart-Allamaras model.

Changes made by boundary condition

PARTS	CONDITION
Inlet	Pressure far field
Body	Wall
Outlet	Pressure outlet
Symmetry	Axis

Here boundary conditions are different from above the section. Solver has been run in to the axi-symmetric condition.

Inlet condition:

Starting Mach number = 4

Temperature = 229 k

Gauge pressure = 100659 pa

Space = axi-symmetric

Density = ideal gas

MODIFICATION OF CONTOUR RESULTS FOR MACH 4

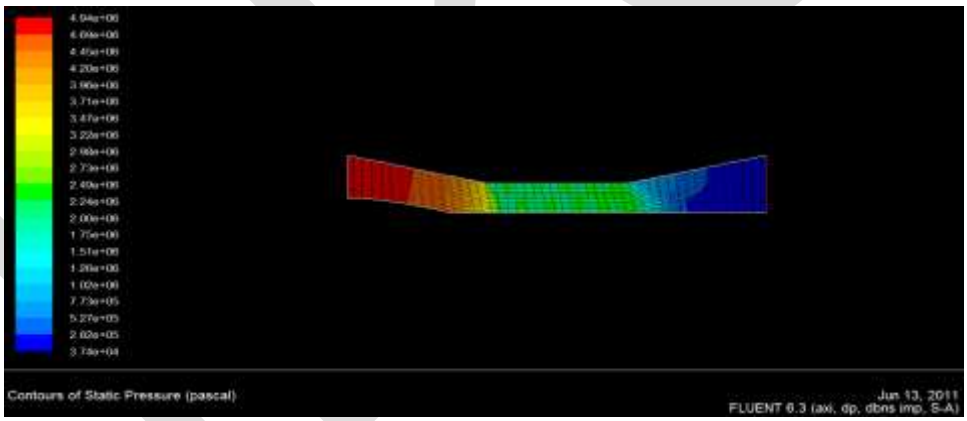

Fig.22. Modify Contours of pressure in Mach 4

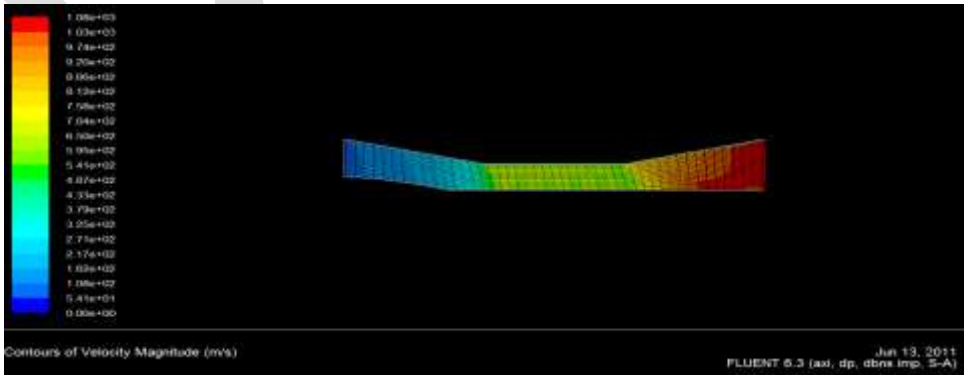

Fig.23. Modify Contours of Velocity in Mach 4

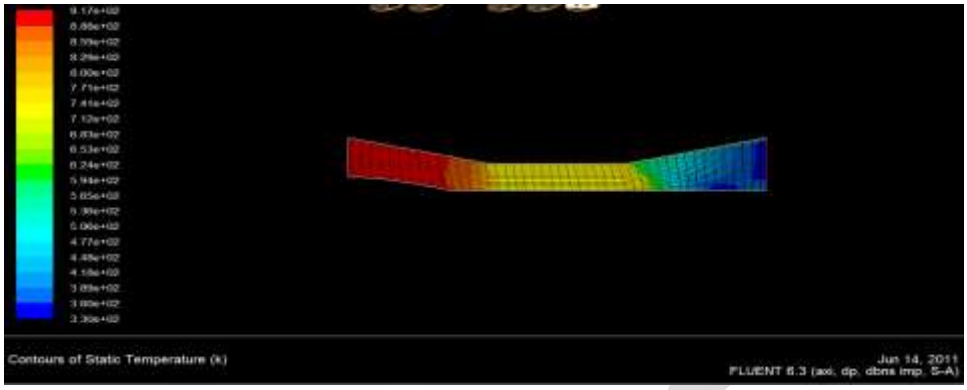

Fig.24. Modify Contours of Temperature in Mach 4

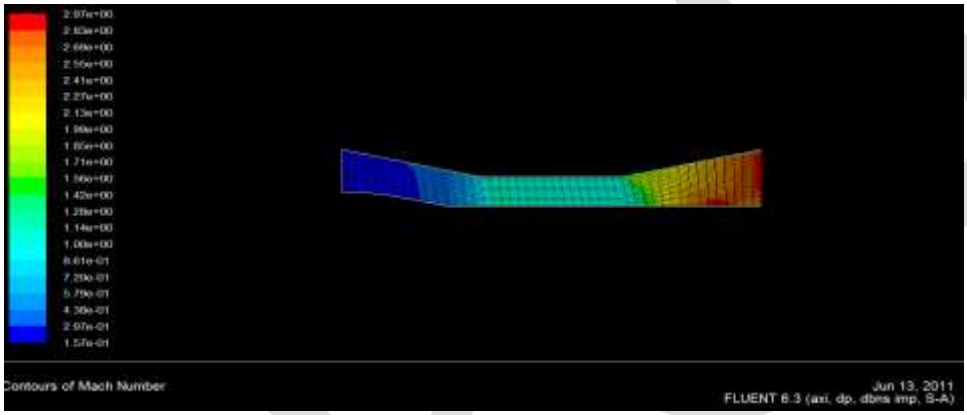

Fig.25. Modify Contours of Mach number in Mach 4

Fig.22. The air is passed through the scramjet engine without cone section. The initial pressure is assumed to be gauge pressure value; the pressure value is increased, when the air is passed out through the diffuser due to the convergent of area section. At combustion chamber the pressure value is remains constant, at the constant area section. Again the value gets decreased as the area gets diverged.

Fig. 23 Initially, the velocity is assumed to be 1340 m/s, the velocity is converged when the air is passed out through the diffuser section. The velocity is decreases as the area gets converged. At combustion chamber velocity becomes constant at the constant area section. Again the value gets increased as the area gets diverged.

Fig. 24 The air is passed through the scramjet engine without cone section. The initial temperature is assumed to be 229 K, Here temperature must be increased, when the air is passed out through the diffuser due to the increase in pressure. At combustion chamber the temperature value is remains constant, at the constant pressure. Again this value gets decreased as the pressure gets decreased.

Fig. 25The air is passed through the 2-D scramjet engine without cone section. The initial condition of the Mach number is assumed to be value 4; the Mach number is converged when the air is passed out through the diffuser section. The Mach number decreases as the area gets converged. At combustion chamber the Mach number becomes constant at the constant area section. Again the value gets increased as the area gets diverged.

GRAPH RESULTS

PRESSURE GRAPH

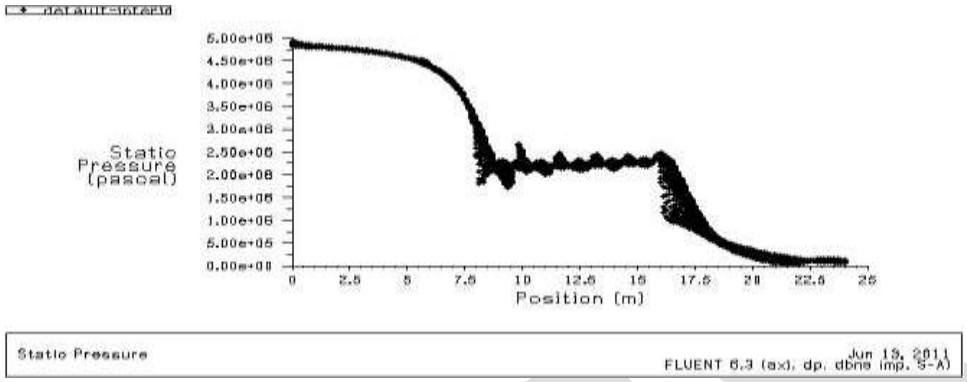

The air is passed through the scramjet engine without cone section. The initial pressure is assumed to be gauge pressure value; the pressure value is increased, when the air is passed out through the diffuser due to the convergent of area section. At combustion chamber the pressure value is remains constant, at the constant area section. Again the value gets decreased as the area gets diverged. The draw back specified here is that the assumed pressure value is gauge pressure, but the value considered by the software is different and occurs in higher value. This non convergence result of the diffuser section is alone showed in the above graph and this is considered to be main draw back of the proposed system.

VELOCITY GRAPH

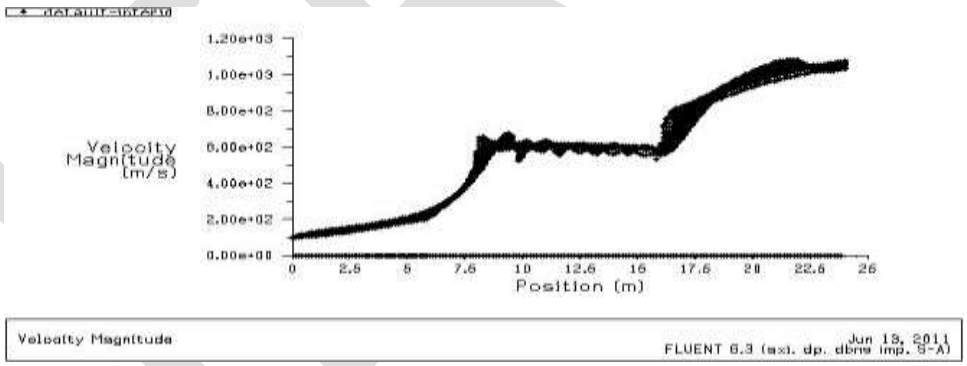

Initially, the velocity is assumed to be 1340 m/s, the velocity is converged when the air is passed out through the diffuser section. The velocity is decreases as the area gets converged. At combustion chamber velocity becomes constant at the constant area section. Again the value gets increased as the area gets diverged. . The draw back specified here is that the assumed velocity is 1340 m/s, but the value considered by the software is different and occurs in low value. This non convergence result of the diffuser section is alone showed in the above graph and this is considered to be main draw back of the proposed system.

TEMPERATURE GRAPH

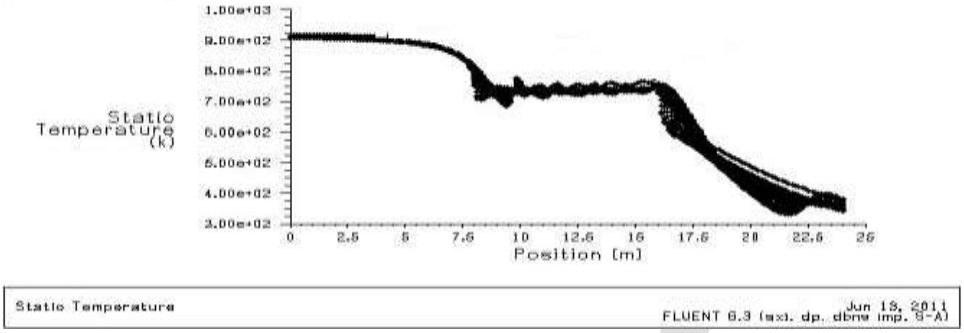

The air is passed through the scramjet engine without cone section. The initial temperature is assumed to be 229 K; Here, temperature must be increased, when the air is passed out through the diffuser due to the increase in pressure. At combustion chamber the temperature value remains constant, at the constant pressure. Again this value gets decreased as the pressure gets decreased. The draw back specified here is that the assumed temperature is229 K, but the value considered by the software is different and occurs in higher value. This non convergence result of the diffuser section is alone showed in the above graph and this is considered to be main draw back of the proposed system.

MACH NUMBER GRAPH:

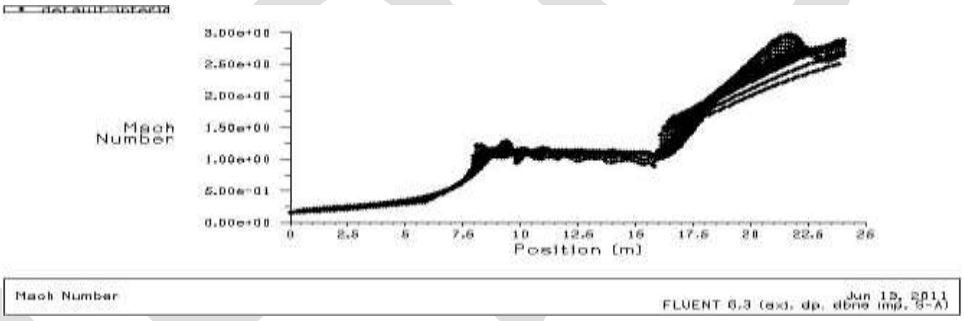

The air is passed through the 2d scramjet engine without cone section. The initial condition of the Mach number is assumed to be value 4, the mach number is converged when the air is passed out through the diffuser section. The Mach number decreases as the area gets converged. At combustion chamber the Mach number becomes constant at the constant area section. Again the value gets increased as the area gets diverged. The draw back specified here is that the assumed Mach number is 4, but the value considered by the software is different and occurs in negative value. This non convergence result of the diffuser section is alone showed in the above graph and this is considered to be main draw back of the proposed system.

CONCLUSION

The project has been successfully accomplished, where as partial results are produced. Despite of variation made in Mach number and mesh size of model. The results where found to be unexpected form**,** Because of an unsatisfied condition. So again further changes made in boundary condition and viscous model. Compare to the previous analysis, the project was found to better results. But these results are not in an expected form. Some few draw back is there. The draw back specified here is that the assumed Mach number is 4, but the value considered by the software is different and gets in negative value. The diffuser section is alone showed non Convergence results. This is considered to be main draw back of the proposed system.

REFERENCES:

1. Charles E Cockrell Jr and Walter C Engelund. (2001). "Integrated Aeropropulsive Computational Fluid Dynamics Methodology for the Hyper-X flight Experiment." The American Institute of aeronautics and astronautics, Inc. PP 836-843.

2. Christopher J Steffen , Jr. National Aeronautics and Space Administration Glenn Research Center Cleveland, Ohio 44135.

3. Dean Andredis., E. T. Curran and, S. N. B. Murthy. (2004). "Scramjet integrate air and space." American Institute of physics. Progress in Astronautics and Aeronautics. pp 26-29.

4. E. L. Houghton and P. W. Carpenter. "Aerodynamics for Engineering Students." A division of Reed Elsevier India Private Ltd.

5. Rathakrishnan. E. (2008) . "Gas Dynamics." Prentice-Hall of India Private Ltd.

6. Eunju Jeong , In-Seuck Jeung and Jeong-Yeol Choi. (2002). "Numerical Study On Combustion Process Of Model Scramjet Engine With a Backward step." American Institute of aeronautics and astronautics, Inc. pp 1-5.

7. Versteeg, H. K. and W. Malalasekera. (1995). "An Introduction to Computational Fluid Dynamics." Finite Volume Method. Pearson education Ltd.

8. Herrmann Schlichting and Klaus Gersten. "Boundary-layer theory." Springer (India) Private Ltd.

9. In-Seuck Jeung and Jeong-Yeol Choi. "Numerical Simulation of Supersonic Combustion for Hypersonic Propulsion." National Research Laboratory Program (M10500000072-05J000007210). pp 475-482.

10. Jeong-Yeol Choi. "Detached Eddy Simulation of Combustion Dynamics in Scramjet Combustors." Pusan National University, Busan 609-735.

11. John D. Anderson., Jr. (1989). "Hypersonic and High temperature gas dynamics." McGraw-Hill.Inc.

12. Leo C. Franciscus and John L. Allen. (1972). "Upper-Stage Space-Shuttle Propulsion by means of Separate Scramjet and Rocket Engines." National Aeronautics and space Administration Washingdon, D.C. pp 1-27.

13. M. Deepu., S.S.Gokhale., S.Jayaraj. (2007). "Recent Advances in Experimental and Numerical Analysis of Scramjet Combustor Flow Fields." Vol 88, pp 13-21.

14. Magnus Brglund., Nikas Wikstrom and Christer Fureby. (2005). "Numerical Simulation of Scramjet Combustion." Swedish Defence Research Agency.

15. N. R. Mudforda., P. J .Mulreanya ., J. R. McGuirea. (2003). "Computational Fluid Dynamics for intake-injection Shock Induced Combustion." Australian Defence Force Academy. pp 17-37.

16. Paul G. Ferlemann., ATK Hampton, Virgina. "Forebody and Inlet Design for the HiFire 2 Flight Test." NASA Langley Research Center. pp 1-27.

Takeshi Kanda., "Study of Scramjet Engine System". Ramjet Propulsion Research Division, Kakuda Research Center. pp 1-2

International Journal of Engineering Research and General Science Volume 3, Issue 6, November-December, 2015
ISSN 2091-2730

High Speed Peak Detection

Sarita Bhagat[1], Mr.Gopalakrishnan[2]
ME student[1], Assistant Professor[2], Department of Instrumentation,
Vivekanand Education Society's Institute of Technology (VESIT) Mumbai University, Mumbai,
sarita.bhagat@ves.ac.in, Mob: +91-9664708147

Abstract— peak-detector circuits are used in many applications such as amplitude measurement, automatic gain control, and data regeneration in Electronics. We can build a simple and fast peak detector from a serial diode and a shunt capacitor, but it suffers from serious inaccuracy due to the diode's forward-voltage drop. The peak detector monitors a voltage of interest and retains its peak value as its output. The circuit gives a DC output voltage that is the peak input voltage over a wide frequency range, with a very low ripple voltage and low harmonic distortion. In this paper peak detector is used to detect the maximum magnitude of a signal over a period of time.

For high frequency circuits we require to know the peak value of an input voltage waveform to compare it with reference value to improve the accuracy of the circuit. Simple peak detector circuits can miss the peak of sharp-peaked signals, which gives inaccurate value of the peak. These limitations are removed in the high speed peak detection circuit. The proposed solution improves both linearity and accuracy without compromising speed. This is accomplished by properly combining the output signal of simple peak detector and comparator. Results show the improvement in detection accuracy.

Keywords—Peak Detection, voltage drop, Analog switch, Reverse capacitance, depletion region, negative saturation, feedback

INTRODUCTION

High speed peak detection function is one of the important requirements in many applications, such as instrumentation and measurement. Peak detection circuits are mostly used in nuclear instrumentation. Peak detectors can be used to improve the effective conversion time of a high resolution spectroscopy ADC without compromising any other performance. Peak detectors also used to hold the value of the detected peak long enough for the quantization process [10]. The Multichannel Pulse-Height Analyser is the primary tool used in nuclear science to record the energy or time spectra available from nuclear radiation detectors. For pulse height analysis of various signals, no assumption can be made on the shape or on the timing of the pulses and therefore there is a requirement to detect and store the true amplitude of the peak. Peak detector circuits are also used in biomedical applications such as X-ray imaging where X-ray photon energy is determined by the detected peak amplitude. Peak detectors are used to obtain the peak voltage of the rapidly changing AC input signals.
Fast peak detectors requires amplifiers with high slew rate. This condition causes either a long overload, or DC accuracy errors. To support the high slew rate at the output, the amplifier must deliver large currents into the capacitive load of the detector which can results in amplifier instability with a large capacitive load, as well as change in the accuracy of the output voltage.

Peak Detector Circuit

1. Theoretical Peak Detector

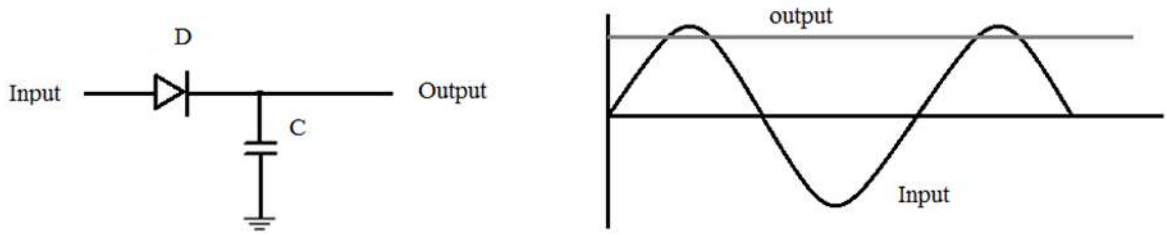

Fig 1. Typical peak detector circuit with input and output waveforms

Typical peak detector circuit is a series connection of a diode and a capacitor which gives a DC voltage equal to the peak value of the applied AC signal. An AC voltage source applied to the peak detector, charges the capacitor to the peak of the input. The diode conducts in positive half cycles, charging the capacitor to the waveform peak. When the input waveform falls below the DC "peak" stored on the capacitor, the diode is reverse biased, blocking current flow from capacitor back to the source. Thus, the capacitor retains the peak value even as the waveform drops to zero. Fig 1 graph shows that the output peak voltage is lower than the input peak voltage by approximately 0.7V. This represents the voltage drop across the diode

2. Practical peak detector circuit

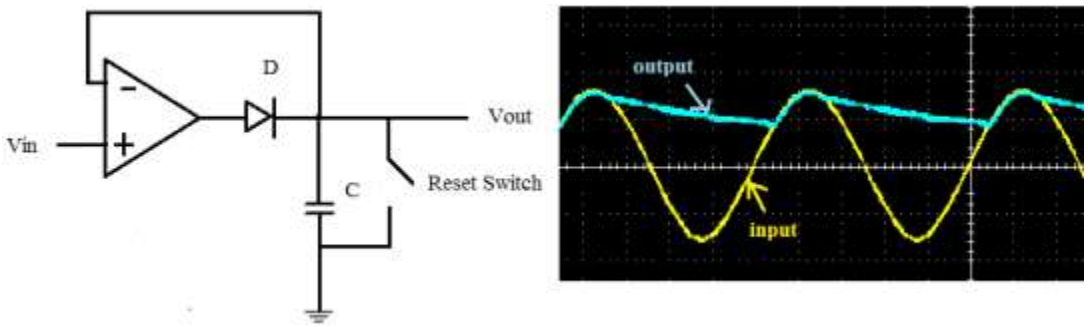

Fig 2.Practical peak detector circuit with input-output waveforms

Fig2 shows more advanced version of a peak detector that eliminates the voltage drop across the diode discussed above. In this circuit op-amp is used with peak detect diode in the feedback loop of op-amp. Fig 2 graph shows that we eliminate the voltage drop across diode. This circuit will work well for slow signals. However, it does not work well for fast signals.

Working of the practical peak detector circuit:

The diode conducts in the positive half cycles, charging the capacitor to the waveform peak. When the input waveform falls below the peak stored on the capacitor, the diode is reverse biased, blocking current flow from capacitor back to the source. Thus, the capacitor retains the peak value even as the waveform drops to zero. Therefore we require the reset switch to discharge the capacitor. When switch is closed capacitor can discharge through this path. The switch can be operated such that, the peak is held for some time before it discharges, so as to make sure that the system does not miss out any peak and detects its amplitude with greater accuracy.

There is, however, a fundamental problem with this simple circuit is that when the input signal is less (more negative) than the voltage being held on the capacitor, the diode will be reverse biased and the output of the op amp will be disconnected from the inverting input terminal. The op-amp in this case have no negative feedback and causes its output to saturate at the negative supply rail. When the input voltage again becomes more positive than the voltage held on the capacitor, the output moves out of saturation to detect next peak so the response time of the amplifier will be affected. The circuit may not respond properly to fast, for short duration positive peaks in the input signal.

This limitation comes from the op-amp going into saturation during negative cycles of the signal. This can be overcome by tracing the input voltage while the op-amp remains in the active region, without going into saturation during negative cycles of the signal.

Modified peak detector circuit

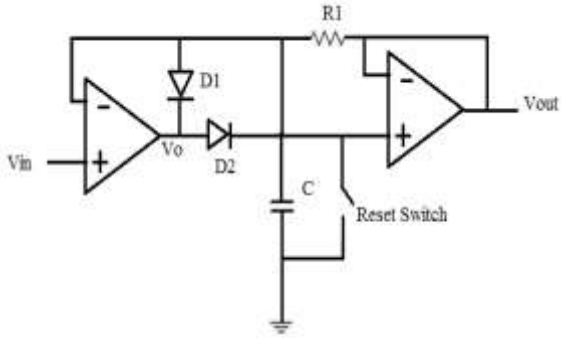

Fig3: Modified peak detector

The limitation of the practical peak detector can be removed by the modified peak detector. The operation of Diode D1 and Buffer Op-amp prevents First Op-amp from going into negative saturation and allows Op-amp to always operate in the active region, which allows peak detection of fast signals.

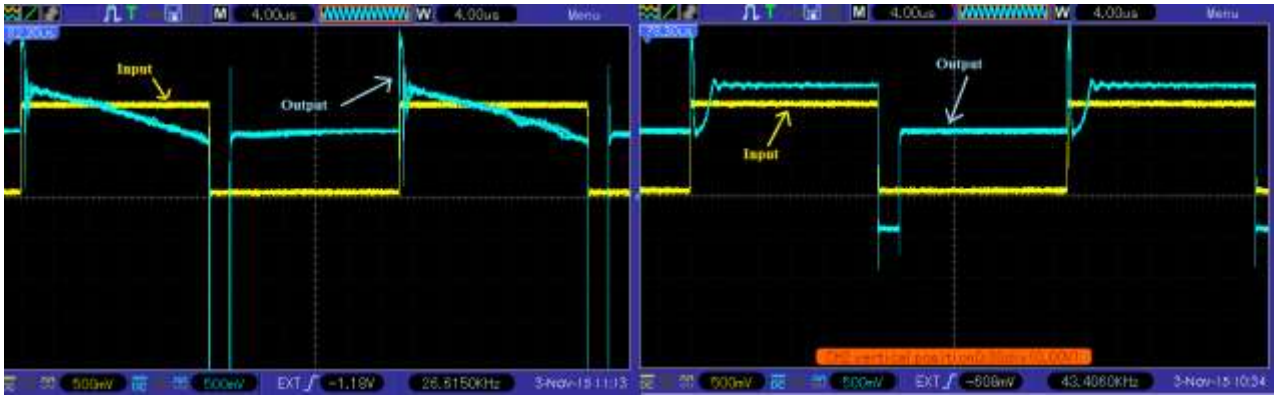

Fig4: Negative saturation of the Practical peak detector and Modified peak detector

Working of modified peak detector:

The diode D2 conducts in the positive half cycles and D1 becomes reverse biased, charging the capacitor to the waveform peak. When the input waveform falls below the peak stored on the capacitor, the diode D2 becomes reverse biased and D1 becomes forward biased, here diode D1 prevents the op-amp going into negative saturation by feedback path and diode D2 prevents the capacitor from discharging.

When switch is closed the capacitor start discharging through the closed path of switch and diode D2. This leads to diode D2 acts as a capacitor (reverse capacitance), due to the presence of reverse biased voltage. The reverse capacitance of the diode arises when the D2 is in reverse biased condition causes the majority charge carriers to move away from the junction, so the thickness of the depletion region increases with the increase in reverse bias voltage. Increase in reverse biased voltage causes increase in reverse capacitance. To solve this problem we need to reduce the reverse biased voltage across the diode D2.

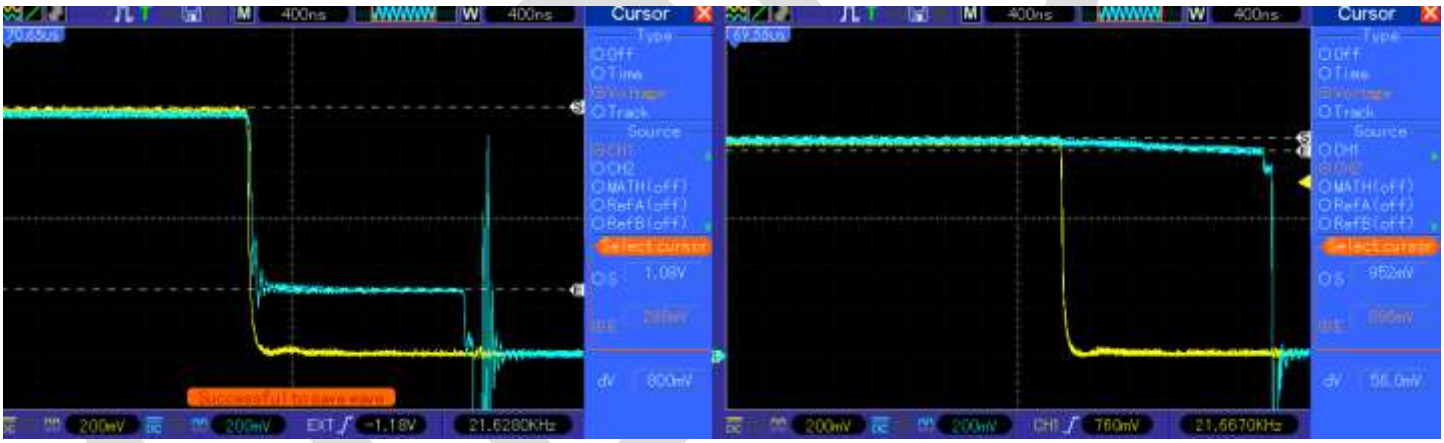

Fig5: Output of the Practical peak detector and Output of the Modified peak detector

On comparison of these outputs we can see the modified peak detector gives more precise output.

Block Diagram of High Speed Peak Detector

Occurrence of the pulse is detected by the comparator. Comparator compares input signal with reference voltage and its output drives monostable multivibrator. Using monostable multivibrator switch is operated. When pulse is detected switch will be open, diode will be in the forward bias and capacitor starts charging until its peak value. The diode conducts in the positive half cycles, charging the capacitor to the waveform peak. When the input waveform falls below the peak stored on the capacitor, the diode is reverse biased, blocking current flow from capacitor back to the source. Thus, the capacitor retains the peak value even as the waveform drops to zero. Therefore it is required to reset switch to discharge the capacitor. When switch is closed capacitor can discharge through this path. Another view of the peak detector is that it is the same as a half-wave rectifier with a filter capacitor added to the output.

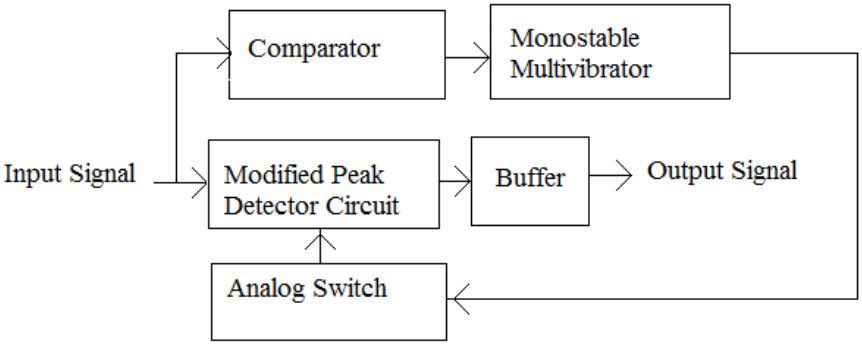

Block diagram of high speed peak detector

EXPERIMENTAL SETUP

The designed peak detector has been experimentally characterized and the performance has been evaluated. The Fig shows experimental setup of the Peak detector circuit.

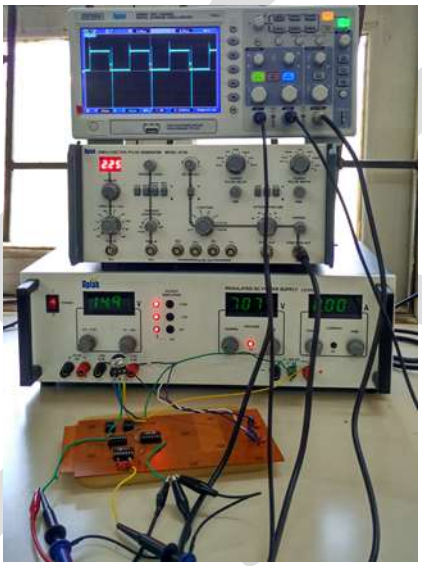

Fig.6 Experimental setup

ACKNOWLEDGEMENT

We the authors would like to express our gratitude to HOD of Instrumentation Department Dr. P. P. Vaidya for sharing his pearls of knowledge and wisdom and giving us a golden opportunity to do this wonderful project, as well as our principal Dr. Mrs. J. M Nair for her encouragement. We would also like to thank our family and friends for extending their generous support in the course of work.

CONCLUSION

Peak detector circuits are important to obtain the peak value of the rapidly changing AC input signal. In this paper a comprehensive and systematic overview of the basic peak detector circuit is presented. By using the basic peak detector circuit design different setups are designed and their outputs are observed. Experimental setups are made on general purpose PCB and the outputs are observed on digital storage oscilloscope.
In this paper, the main limitations of traditional peak detectors have been theoretically analyzed and discussed. The reduction of negative saturation voltage gives a beneficial effect on its accuracy. This is accomplished by properly combining the output signal of simple peak detector and comparator. Results showed significant improvement in detection accuracy and linearity, for a wide class of input waveforms.

REFERENCE

[1] Werner Haas And Peter Dullenkopf, "A Novel Peak Amplitude And Time Detector For Narrow Pulse Signals", *IEEE Transactions On*

Instrumentation And Measurement, Vol.M-35, No. 4, December 1986

[2] Pierre F. Buckens and Michel S. Veatch , "A High Performance Peak-Detect and Hold Circuit for Pulse Height Analysis", *IEEE Transactions On Nuclear Science*,Vol.-39, No. 4, 1992

[3] M. W. Kruiskamp and D. M. W. Leenaerts, "A CMOS Peak Detect Sample and Hold Circuit", *IEEE Transactions On Nuclear Science*, Vol.-41, No. 1, February 1994

[4] Robert G. Meyer, "Low-Power Monolithic RF Peak Detector Analysis", *IEEE Journal Of Solid-State Circuits*, Vol.-30, No. 1, January 1995

[5] Dan Costin, Pompiliu Opris, "High Speed Peak Detector For Glitchcbtchihg Used In Digital Storage Scopes", *IEEE*, 1995

[6] Calogero D. Presti, Francesco Carrara, Antonino Scuderi, and Giuseppe Palmisano, "Fast Peak Detector with Improved Accuracy and Linearity for High-Frequency Waveform Processing", STMicroelectronics.

[7] Wang Pengtian,Wang Zibin, "Improvement of Peak Detection for Digital Storage Oscilloscope",*ICEMI*, 2011

[8] John Wright, "Peak Detectors Gain in Speed and Performance", Design Notes, Design Note 61

[9] Dan Costin, "High Speed Peak Detector for Glitch Catching used in Digital Storage Scopes"

[10] P. Y. Chang and H.P. Chou "A High Precision Peak Detect Sample and Hold Circuit."

International Journal of Engineering Research and General Science Volume 3, Issue 6, November-December, 2015
ISSN 2091-2730

Analysis of Analytical and Numerical Methods of Epidemic Models

Poonam Kumari
Assistant Professor, Department of Mathematics
Magadh Mahila College, Patna University
Email : poonamkumari1865@gmail.com

Abstract— In this paper, we study SIR epidemic models for a given constant population. These mathematical models are described by nonlinear first order differential equations. First, we find the analytical solution by using the Differential Transformation Method. We then compute the numerical solution by using fourth-order Runge-Kutta Method and compare the analytical solution with the numerical. The profiles of the solutions are provided, from which we infer that the analytical and numerical solutions agreed very well.

Keywords— SIR epidemic model, Susceptible class, Infective class. Recovered class, Nonlinear Ordinary Differential Equations, Differential Transformation Method, Runge-Kutta Method

Introduction

Epidemic models are tools to analyse the spread and control of infectious diseases. The models that describe what happens on the average at the population scale are called deterministic or compartmental models. They fit well large populations.

In this paper, we study the SIR epidemic model, which is a standard compartmental model used to describe many epidemiological diseases [1]. This model was formulated by A. G. McKendrick and W. O. Kermack in 1927 [2]. We solve the resulting differential equations of the model by analytical as well as numerical methods. To find the analytical solution, we use Differential Transformation Method, which expresses the dependent variable explicitly as function of independent variable in the form of a convergent series with easily computable components.

Objective

The purpose of this article is to translate the real world problem of the spread of infectious diseases into mathematical vocabulary and to find the solution of it with the help of Mathematics. Simply formation of mathematical model of infectious diseases is not enough for a disease control. Unless we know an efficient method to solve the mathematical model, we cannot help in any detection or therapy program.

This work is an effort to help in various infectious disease control programs by providing a practical, efficient and accurate method to solve a mathematical model.

Formulation of SIR Epidemic Model

In this model, a fixed population with only the following three compartments is considered :

1. **s (t)** : It represents the number of susceptible at time t, i.e., the number of individuals who do not have the disease at time t but could get it.
2. ***i* (t)** : It represents the number of infective at time t, i.e., the number of individuals who have the disease at time t and can transmit it to others.
3. ***r* (t)** : It represents the number of individuals who have been infected but recovered from the disease at time t. The individuals in this category are not able to be infected again or transmit the infection to others, i.e., they acquire permanent immunity or they have been placed in isolation or they have died.

If *n* be the size of the population at any time t, then the differential equations for the SIR model are:

$$\frac{d\,s(t)}{d\,t} = -\frac{\beta\, s(t) i(t)}{n} \qquad \text{.....(1)}$$

$$\frac{d\,i(t)}{d\,t} = \frac{\beta\, s(t) i(t)}{n} - \gamma\, i(t) \qquad \text{.....(2)}$$

$$\frac{d\,r(t)}{d\,t} = -\gamma\, i(t) \qquad \text{.....(3)}$$

with the initial conditions

$$\left.\begin{aligned} s(0) &= s_0 > 0 \\ i(0) &= i_0 > 0 \\ r(0) &= r_0 = 0 \end{aligned}\right\} \qquad \text{.....(4)}$$

It can be seen that $\frac{d}{d\,t}\left[s(t) + i(t) + r(t)\right] = 0$, therefore it is true that the population size is constant, i.e., s(t) + i(t) + r(t) = *n*.

Analytical Solution of SIR Epidemic Model

To find the analytical solution, we use Differential Transformation Method, which was first introduced by Zhou [3] for solving linear and nonlinear initial value problems in electrical circuit analysis. But, now a days, the method has been applied to solve a variety of problems that are modelled with differential equations.

The concept of differential transformation is derived from the Taylor series expansion. In this method, given system of differential equations and related initial conditions are transformed into a system of recurrence equations that finally leads to a system of algebraic equations whose solutions are the coefficients of a power series solution.

Taylor series expansion of a function $f(x)$ about the point $x = 0$ is as follows :

$$f(x) = \sum_{k=0}^{\infty} \frac{x^k}{k!}\left[\frac{d^k f}{dx^k}\right]_{x=0} \qquad \text{.....(5)}$$

Definition 1. The differential transformation F(k) of a function $f(x)$ is defined as follows :

$$F(k) = \frac{1}{k!}\left[\frac{d^k f}{dx^k}\right]_{x=0} \qquad \text{.....(6)}$$

Definition 2. It follows from equations (5) and (6) that the differential inverse transformation $f(x)$ of F (k) is given by :

$$f(x) = \sum_{k=0}^{\infty} x^k F(k) \qquad \text{.....(7)}$$

Using equations (6) and (7), the following mathematical operations can be obtained :

1. If $f(x) = g(x) \pm h(x)$, then $F(k) = G(k) \pm H(k)$
2. If $f(x) = \text{c}\, g(x)$, then $F(k) = \text{c}\, G(k)$, where c is a constant
3. If $f(x) = \frac{dg(x)}{dx}$, then $F(k) = (k+1)G(k+1)$
4. If $f(x) = \frac{d^m g(x)}{dx^m}$, then $Y(k) = (k+1)(k+2).....(k+m)G(k+m)$
5. If $f(x) = 1$, then $F(k) = \delta(k)$
6. If $f(x) = x$, then $F(k) = \delta(k-1)$
7. If $f(x) = x^m$, then $F(k) = \delta(k\text{-}m) = \begin{cases} 1, & \text{if } k = m \\ 0, & \text{if } k \neq m \end{cases}$
8. If $f(x) = g(x)\, h(x)$, then $F(k) = \sum_{m=0}^{k} H(m)G(k-m)$

9. If $f(x)=e^{mx}$, then $F(k)=\frac{m^k}{k!}$

10. If $f(x)=(1+x)^m$, then $F(k)=\frac{m(m-1)(m-2).....(m-k+1)}{k!}$

Now, we consider the SIR Model given by equations (1), (2) and (3) with the initial conditions

s(0) = 100, $i(0)$ = 30, (0) = 20, n = 150, β = 0.1 and γ = 0.2 …..(8)

If S(k), I(k) and R(k) denote the differential transformation of s(t), i(t) and r(t) respectively, then the following recurrence relations of equations (1), (2) and (3) can be obtained :

$$S(k+1)=\frac{1}{k+1}\left[-\frac{\beta}{n}\sum_{m=0}^{k}S(m)I(k-m)\right] \quad .....(9)$$

$$I(k+1)=\frac{1}{k+1}\left[\frac{\beta}{n}\sum_{m=0}^{k}S(m)I(k-m)-\gamma I(k)\right] \quad .....(10)$$

$$R(k+1)=\frac{1}{k+1}\left[\gamma I(k)\right] \quad .....(11)$$

with the initial conditions

S(0) = 100, $I(0)$ = 30, $R(0)$ = 20, n = 150, β = 0.1 and γ = 0.2 …..(12)

$$\therefore\ S(1)=-\frac{0.1}{150}S(0)I(0)=-\frac{0.1}{150}\times 100\times 30=-2$$

$$I(1)=\frac{0.1}{150}S(0)I(0)-0.2(I(0))=\frac{0.1}{150}\times 100\times 30-0.2(30)=2-6=-4$$

$$R(1)=0.2(I(0))=0.2(30)=6$$

$$S(2)=\frac{1}{2}\left[-\frac{0.1}{150}\{S(0)I(1)+S(1)I(0)\}\right]=\frac{1}{2}\left[-\frac{0.1}{150}\{100(-4)+(-2)30\}\right]=0.153333$$

$$I(2)=\frac{1}{2}\left[\frac{0.1}{150}\{S(0)I(1)+S(1)I(0)\}-0.2I(1)\right]=\frac{1}{2}\left[\frac{0.1}{150}\{100(-4)+(-2)30\}-0.2(-4)\right]=0.246667$$

$$R(2)=\frac{1}{2}0.2\,I(1)=\frac{1}{2}0.2(-4)=-0.4$$

$$S(3)=\frac{1}{3}\left[-\frac{0.1}{150}\{S(0)I(2)+S(1)I(1)+S(2)I(0)\}\right]$$

$$=\frac{1}{3}\left[-\frac{0.1}{150}\{100(0.246667)+(-2)(-4)+0.153333(30)\}\right]$$

$$=-0.00828148666$$

$$I(3)=\frac{1}{3}\left[\frac{0.1}{150}\{S(0)I(2)+S(1)I(1)+S(2)I(0)\}-0.2\,I(2)\right]$$

$$=\frac{1}{3}\left[\frac{0.1}{150}\{100(0.246667)+(-2)(-4)+0.153333(30)\}-0.2(0.246667)\right]$$

$$=-0.00816298$$

$$R(3)=\frac{1}{3}0.2\,I(2)=\frac{1}{3}0.2\,(0.24667)=0.0164444666$$

Therefore, using the equations

$$s(t)=\sum_{k=0}^{\infty}t^k S(k)=S(0)+t\,S(1)+t^2S(2)+t^3S(3)+.....$$

$$i(t)=\sum_{k=0}^{\infty}t^k I(k)=I(0)+t\,I(1)+t^2I(2)+t^3I(3)+.....$$

$$r(t)=\sum_{k=0}^{\infty}t^k R(k)=R(0)+t\,R(1)+t^2R(2)+t^3R(3)+.....$$

the closed form of the solution when k = 3 can be written as follows :

$$s(t)=100-2t+0.153333t^2-0.0082814866t^3+.....$$

$$i(t)=30-4t+0.246667t^2-0.00816298t^3+.....$$

$$r(t)=20+6t-0.4t^2+0.0164444666t^3+.....$$

Numerical Solution of SIR Epidemic Model

Using equations (1), (2), (3) and the initial conditions (8), the values of s(t), *i*(t) and *r*(t) are calculated by fourth-order Runge-Kutta Method at t = 0.2, 0.4, 0.6, 0.8 and 1.0, taking the interval of differencing h = 0.2.The numerical results are compared with the results obtained by DTM.

To evaluate s(t) at t = 0.2, we have

$$k_1=h\left[-\frac{\beta\,s(0)i(0)}{n}\right]=0.2\left[-\frac{0.1\times100\times30}{150}\right]=-0.4$$

$$k_2=-\frac{h\beta}{n}\left[\left\{s(0)+\frac{k_1}{2}\right\}\left\{i(0)+\frac{h}{2}\right\}\right]=-\frac{0.2\times0.1}{150}\left[99.8\times30.1\right]=-0.40053066$$

$$k_3=-\frac{h\beta}{n}\left[\left\{s(0)+\frac{k_2}{2}\right\}\left\{i(0)+\frac{h}{2}\right\}\right]=-\frac{0.2\times0.1}{150}\left[99.79973467\times30.1\right]=-0.4005296018$$

$$k_4=-\frac{h\beta}{n}\left[\{s(0)+k_3\}\{i(0)+h\}\right]=-\frac{0.2\times0.1}{150}\left[99.5994704\times30.2\right]=-0.4010538675$$

$$\therefore\Delta s=\frac{1}{6}(k_1+2k_2+2k_3+k_4)$$

$$=\frac{1}{6}(-0.4-0.80106132-0.8010592036-0.4010538675)$$

$$=-0.4005290652$$

and $s(0.2)=s(0)+\Delta s=100-0.4005290652=99.5994709348\approx99.59947093$

Similarly, to evaluate *i* (t) at t = 0.2, we have

$$k_1=h\left[\frac{\beta\,s(0)i(0)}{n}-\gamma\,i(0)\right]=0.2\left[\frac{0.1\times100\times30}{150}-0.2\,(30)\right]=-0.8$$

$$k_2 = h\left[\frac{\beta}{n}\left\{s(0)+\frac{h}{2}\right\}\left\{i(0)+\frac{k_1}{2}\right\}-\gamma\left\{i(0)+\frac{k_1}{2}\right\}\right]$$

$$= 0.2\left[\frac{0.1}{150}\times 100.1\times 29.6 - 0.2(29.6)\right]$$

$$= -0.78893866668$$

$$k_3 = h\left[\frac{\beta}{n}\left\{s(0)+\frac{h}{2}\right\}\left\{i(0)+\frac{k_2}{2}\right\}-\gamma\left\{i(0)+\frac{k_2}{2}\right\}\right]$$

$$= 0.2\left[\frac{0.1}{150}\times 100.1\times 29.6055306666 - 0.2(29.6055306666)\right]$$

$$= -0.789086077368$$

$$k_4 = h\left[\frac{\beta}{n}\{s(0)+h\}\{i(0)+k_3\}-\gamma\{i(0)+k_3\}\right]$$

$$= 0.2\left[\frac{0.1}{150}\times 100.2\times 29.2109139226 - 0.2(29.2109139226)\right]$$

$$= -0.7781787469$$

$$\therefore \Delta i = \frac{1}{6}(k_1 + 2k_2 + 2k_3 + k_4)$$

$$= \frac{1}{6}(-0.8 - 1.57787733336 - 1.578172154736 - 0.7781787469)$$

$$= -0.789038039166$$

and $\mathrm{i}(0.2) = i(0) + \Delta i = 30 - 0.789038039166 = 29.210961960834 \approx 29.21096196$

Similarly, to evaluate r (t) at t = 0.2, we have

$$k_1 = h\gamma\, i(0) = 0.2\times 0.2\times 30 = 1.2$$

$$k_2 = h\gamma\left\{i(0)+\frac{h}{2}\right\} = 0.2\times 0.2(30+0.1) = 1.204$$

$$k_3 = h\gamma\left\{i(0)+\frac{h}{2}\right\} = 0.2\times 0.2(30+0.1) = 1.204$$

$$k_4 = h\gamma\{i(0)+h\} = 0.2\times 0.2(30+0.2) = 1.208$$

$$\therefore \Delta r = \frac{1}{6}(k_1 + 2k_2 + 2k_3 + k_4) = \frac{1}{6}(1.2 + 2.408 + 2.408 + 1.208) = 1.204$$

and $\mathrm{r}(0.2) = r(0) + \Delta r = 20 + 1.204 = 21.204$

Using the above formulae, the values of s(t), i(t) and r(t) are calculated for other values of t.

Comparison of Analytical Solution with the Numerical Solution

The numerical results are compared with the results obtained by DTM and displayed below.

t	s(t) by DTM (4 iterate)	s(t) by fourth-order Runge -Kutta Method	Difference

0.2	99.60606707	99.59947093	0.00659614
0.4	99.22400326	99.21098305	0.01302021
0.6	98.85341108	98.83415434	0.01925674
0.8	98.4938930	98.46861578	0.02527722
1.0	98.14505151	98.11400069	0.03105082

Table 1 : Numerical Comparison of s(t)

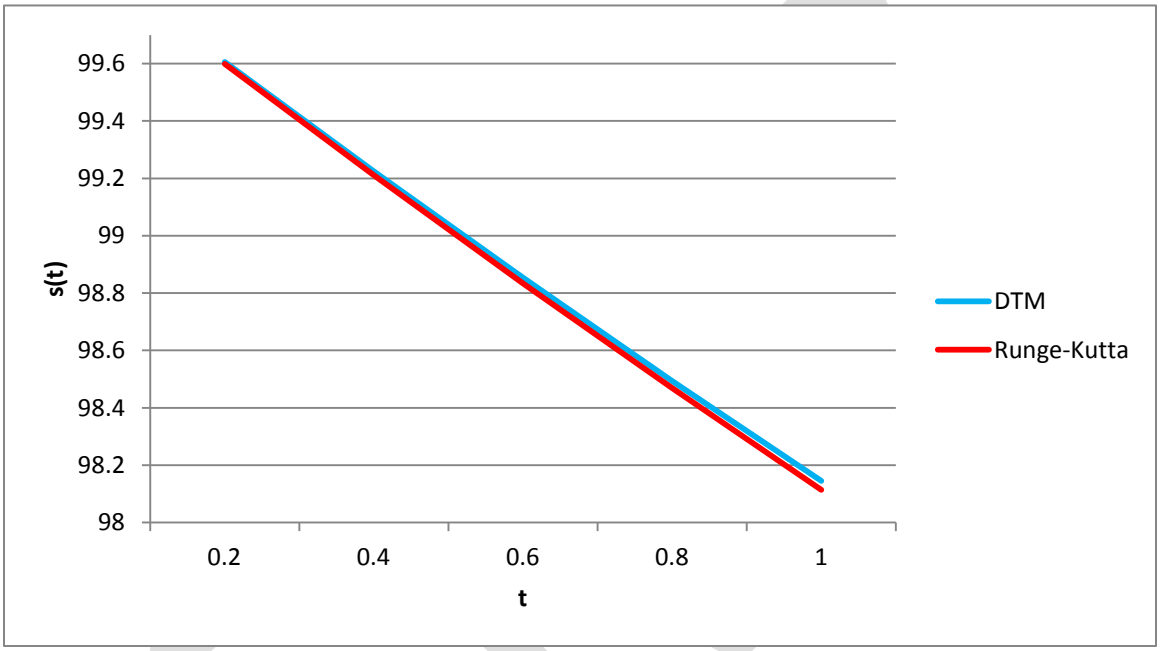

Figure 1 : Plot of s(t) versus time t

t	*i*(t) by DTM (4 iterate)	*i*(t) by fourth-order Runge -Kutta Method	Difference
0.2	29.20980138	29.21096196	0.00116058
0.4	28.43894429	28.44115771	0.00221342
0.6	27.68703692	27.69020597	0.00316905
0.8	26.95368743	26.95772764	0.00404021
1.0	26.23850402	26.24334619	0.00484217

Table 2 : Numerical Comparison of i(t)

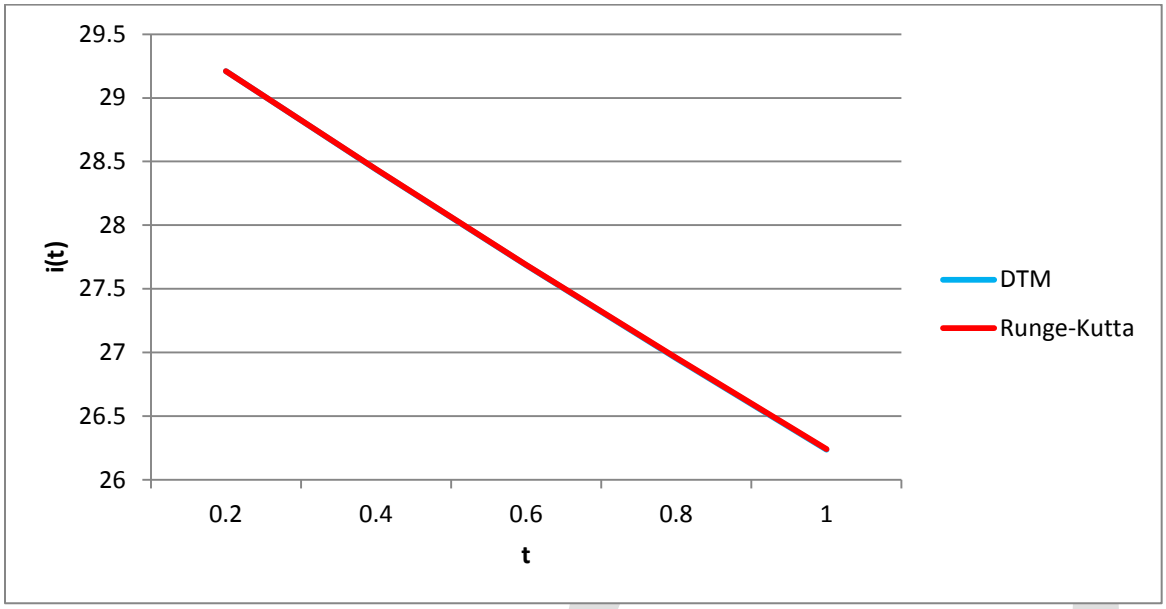

Figure 2 : Plot of *i*(t) versus time t

t	*r*(t) by DTM (4 iterate)	*r*(t) by fourth-order Runge -Kutta Method	Difference
0.2	21.18413156	21.20400000	0.01986844
0.4	22.33705245	22.37643853	0.03938608
0.6	23.45955200	23.51808484	0.05853284
0.8	24.55241957	24.62969308	0.07727351
1.0	25.61644447	25.71200219	0.09555772

Table 3 : Numerical Comparison of r(t)

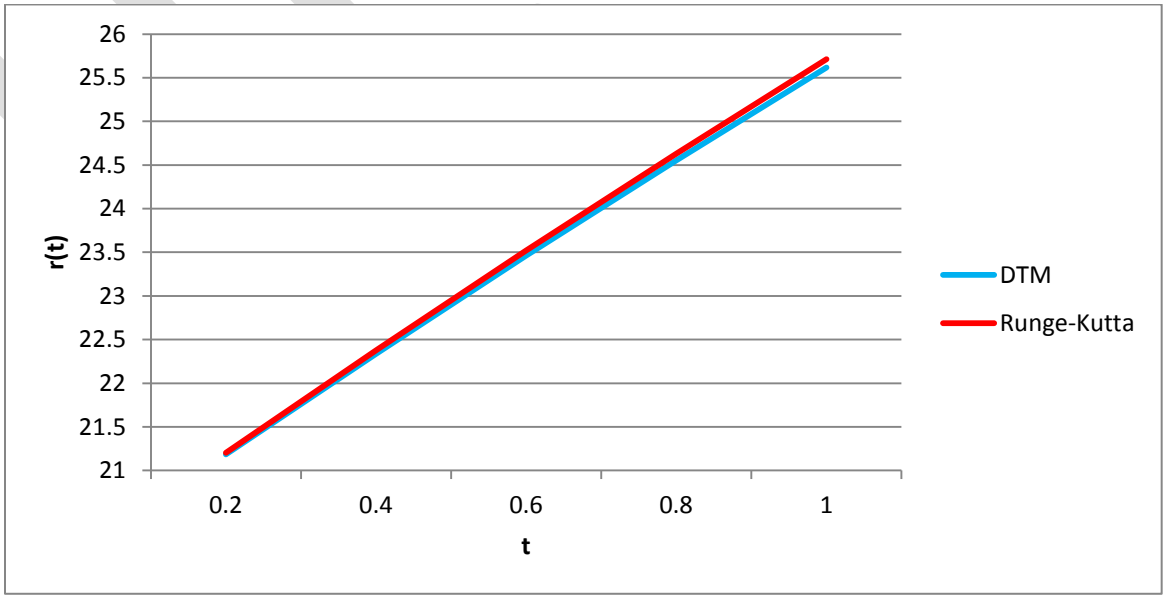

Figure 3 : Plot of *r*(t) versus time t

It can be seen that the value of s(t) + i(t) + r(t) calculated by DTM is exactly equal to n for every t, whereas the value of s(t) + i(t) + r(t) calculated by fourth-order Runge -Kutta Method differs slightly from n for various values of t.This confirms the ability of DTM as a powerful tool for solving non linear equations.

Conclusion

In this paper, Differential Transformation Method (DTM) has been used to solve SIR Epidemic Model with given initial conditions. As this method provides an explicit solution of the model, it is very useful in understanding and analysing an epidemic. The numerical comparison of this method with the fourth-order Runge -Kutta Method proves the efficiency and accuracy of the method. Moreover, this method provides a direct scheme for solving differential equations without the need for linearization, perturbation or any transformation. It may, therefore, be concluded that it is a powerful mathematical tool for solving epidemic models.

REFERENCES :

[1] Hethcote H.W. "The Mathematics of Infectious Diseases", SIAM Review 42(4), 599-653 (2000).
[2] W. O. Kermack and A. G. McKendrick, "Contribution to the Mathematical Theory of Epidemics", Proc. Roy. Soc. Lond. A 115, 700-721 (1927).
[3] J.K.Zhou, "Differential Transformation and its Application for Electrical Circuits", Huazhong University Press, China (1986).
[4] G. Adomian, "A Review of the Decomposition Method in Applied Mathematics", J. Math. Anal. Appl., 135, 501-544 (1988).

International Journal of Engineering Research and General Science Volume 3, Issue 6, November-December, 2015
ISSN 2091-2730

COMPARISON OF ECG SIGNAL DENOISING ALGORITHMS IN FIR AND WAVELET DOMAINS

Dipti Thakur, Sagar Singh Rathore

E&TC, SSGI Bhilai, (India), diptitahkur0907@gmail.com

Abstract- In the transmission of any signal it is often contaminated with different noises. ECG (electrocardiograph) is the measure of electrical activity of heart and it is used for the diagnosing cardiac diseases, but before the analysis of this ECG signal we have to denoise these signals properly. since ECG is non-stationary signal, wavelet based denoising of ECG signal is considered along with it for simplicity of filters, FIR filters are used and performance of both is compared in terms of signal to noise ratio, time elapsing.

Keywords- ECG, SNR, Window, Thresholding, Wavelet, BLW, PLI, HFN

INTRODUCTION

The ECG signals are analyzed widely for the diagnosis of many cardiac diseases. The electrical signals are traced using non invasive electrodes which are placed on the chest and limbs of the body part. The heart muscle cells which are located in atria and ventricles contract generating electric pulses by self excitable, some cells in the human body are self-excitable, in cardiac system there is also a group of node present which is self-excitable contracting without any signal from the nervous system which are then traced by the ECG. The ECG signals of a normal heart beat consist of three parts: P wave, QRS complex and T wave. The P wave represents the atrial contractions & QRS complex denote ventricle contractions as shown in figure—1 [1. The third wave in an ECG is the T wave. This is produced when the ventricles are repolarising. These waves show sample range of deformities in the ECG signal they are generally contaminated by several types of noises. These include Power Line interference (PLI), Base line wander, muscle contraction and motion artifacts. PLI includes the main part of the distortions at 50-60 Hz. Motion artifacts are the transient baseline changes caused by mismatching of impedance between the electrodes and the skin. [2] Baseline wander is the continuous drifting of the ECG Signal from the baseline. It is mainly caused by respiration and increased body movements [3].

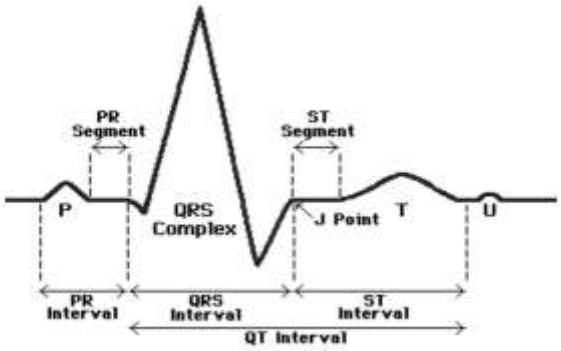

Figure 1 Standard ECG Waveform

Numerous methods have been reported to denoise ECG signals based on filter banks, principal component analysis (PCA), independent component analysis (ICA), neural networks (NNs), adaptive filtering, empirical mode decomposition (EMD), and wavelet transform. The filter bank based denoising process smoothes the P and R amplitude of the ECG signal, and it is more sensitive to different levels of noise [4] Comparatively, the denoising methods based on filter bank and that based on wavelet are compared in reducing noise from the ECG signals. Since, ECG signals are relatively weak and may have strong background noises, the thresholding performed in either FIR or wavelet domain alone will result in an inadequate denoising as far as reliable clinical applications are concerned [5].

DISCRETE WAVELET TRANSFORM

The biomedical signals such as ECG signal, noise reduction is only possible if we using more advanced signal processing method as wavelet denoising technique.

The wavelet transform is similar to the Fourier transform. For the FFT, the basis functions are sine and cosines. For the wavelet transform, the basis functions are more complicated called wavelets, mother wavelets or analyzing wavelets and scaling function. In wavelet analysis, the signal is broken into shifted and scaled versions of the original (or mother) wavelet**.[6]** The fact that wavelet transform is a multiresolution analysis makes it very suitable for analysis of non-stationary signals such as the ECG signal [7].

$$x(t) = \sum_{k} a_{j0,k}\, \varphi_{j0,k}(t) + \sum_{j=j0}^{\infty} \sum_{k} b_{j,k}\, \psi_{j,k}(t) \quad (1)$$

Where a, b are the coefficients associated with φj,k(t) and ψj,k(t) respectively.

The discrete wavelet transform (DWT) is an implementation of the wavelet transform using a discrete set of the wavelet scales and translations obeying some defined rules. In other words, this transform decomposes the signal into mutually orthogonal set of wavelets. The scaling function φj,k(n) and the mother wavelet function ψj,k(n) in discrete domain are: The DWT of an discrete signal x(n) . It is quite similar to the Eq. (1)

$$x(n) = \sum_{k} w\,\varphi(j0,k)\varphi_{j0,k}(n) + \sum_{j=j0}^{\infty} \sum_{k} w_{\psi}\,(j_0,k)\psi_{j,k}(n) \quad (2)$$

Here Wφ(j0,k) and Wψ(j0,k) are called the wavelet coefficients. φj,k(n) and ψj,k(n) are orthogonal to each other. Hence we can simply take the inner product to obtain the wavelet coefficients.

FIR FILTER

FIR filters are digital filters with finite impulse response. They are also known as non-recursive digital filters and they do not have the feedback, even though recursive algorithms can be used for FIR filter realization. FIR filters can be designed using different methods, but most of them are based on ideal filter approximation. The objective is not to achieve ideal characteristics, as it is impossible anyway, but to achieve sufficiently good characteristics of a filter. The transfer function of FIR filter approaches the ideal as the filter order increases, thus increasing the complexity and amount of time needed for processing input samples of a signal being filtered.[8]

METHODOLOGY

1. DENOISING METHODS IN WAVELET DOMAIN

By applying the wavelet transform, ECG signals were decomposed to the approximate (low frequency component) and detailed (high frequency component) information. Each stage consists of two digital filters and two down samplers by 2.The first filter, g [n] is the high pass filter and h[n] is the low pass filter. The down sampled output of first high pass filter is called detail coefficients (D1) and output of low pass filter is the approximation coefficients (A1).The first approximation (A1) is further decomposed and this process is continued. . The reverse process of combining the coarser approximation and detail coefficients to yield the approximation coefficients at a finer resolution is referred as reconstruction or synthesis [9].

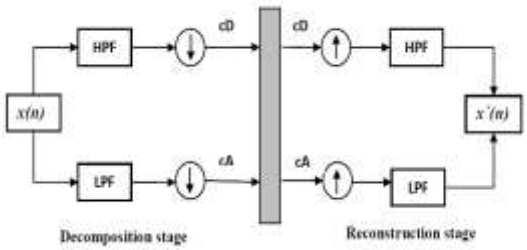

Figure-2 Decomposition and Reconstruction

The general wavelet based method for denoising estimation is to transform the data into wavelet domain, threshold the wavelet coefficients and invert the transform [10].It follows three steps:

1. **Decomposition:** Choose a wavelet, and Compute the wavelet decomposition at level N.
2. **Thresholding**: For each level from 1 to N, select a threshold and apply different thresholding to the detailed coefficients In this step thresholding is used which is major part of wavelet, the selection of right thresholding method will provide better noiseless output .In this paper 4 types of thresholding are used

- 'Rigrsure' uses for the soft threshold estimator.
- 'sqwrlog' uses a fixed-form threshold
- 'Heursure' is a mixture of the two previous options.
- 'Minimaxi' uses a fixed threshold chosen to yield minimax performance for mean square error against an ideal procedure [11] and also applied filters like (haar, db2, db6, db10, bior2.2, bior3.3, coieflet3, coieflet4, symlet4, symlet8).

3. **Reconstruction** after decomposition thresholding is applied to detail coefficients and after that signal is reconstructed by using original approximate coefficients and modified detail coefficients.

2. DENOISING METHODS IN FIR DOMAIN WINDOW METHODS

(1) **Blackman window-** The periodic Blackman window is constructed by extending the desired window length by one sample to N+1, constructing a symmetric window, and removing the last sample. The periodic version is the preferred method when using a Blackman window in spectral analysis because the discrete Fourier transform assumes periodic extension of the input vector. In the symmetric case, the second half of the Blackman window $M \leq n \leq N-1$ is obtained by flipping the first half around the midpoint. The symmetric option is the preferred method when using a Blackman window in FIR filter design The following equation defines the Blackman window of length N.

$$W(n)= 0.42-0.5\cos\left(\frac{2*pie*n}{N-1}\right)+0.08\cos\left(\frac{4*pie*n}{N-1}\right), \quad \text{for } 0<=n<=M-1 \qquad (3)$$

(2) **Hamming window-** an L-point Hamming window using the window sampling specified by 's flag', which can be either 'periodic' or 'symmetric' (the default). The 'periodic' flag is useful for DFT/FFT purposes, such as in spectral analysis. The DFT/FFT contains an implicit periodic extension and the periodic flag enables a signal windowed with a periodic window to have perfect periodic extension. When 'periodic' is specified, hamming computes a length L+1 window and returns the first L points. When using windows for filter design, the 'symmetric' flag should be used. The coefficients of a Hamming window are computed from the following equation.

$$W(n)= 0.54 -0.46\cos\left(2 * pie * \frac{n}{N}\right), \quad 0<=n<=N. \qquad (4)$$

The window length is L=N+1

The width of main lobe is approximately 8π /M and the peaks of first lobe are at – 43dB.

(3) **Hanning window-**
The coefficient of a Han window is calculated from the following equation.

$$W(n)= 0.54 \ -0.5\cos(2 * pie * \frac{n}{N}), \quad 0<=n<=N. \tag{5}$$

The width of main lobe is approximately 8π/M and peak of first side lobe is at – 32dB [12].

ANALYSIS METHOD

The first step is to obtain ECG signal form a data base. The data base used for the experiments is MIT-BIH Arrhythmia database, available online [13].All the 48 signals from database has been used for experiment. Wavelet toolbox is used in mat lab. Four different types of thresholding and ten different filters are analyzed for comparison of different techniques and to get the best combination of thresholding and filter. In FIR part all 48 signal is tested against all 3 windows The performance is evaluated in terms of the SNR**,** time elapse **[**14]

(1) $$\text{SNR (DB)} = \ 10 \ \log_{10}\left(\frac{A^2 signal}{A^2 noise}\right) \tag{6}$$

RESULT AND DICUSSION

(A)**The original ECG signal of 100m**

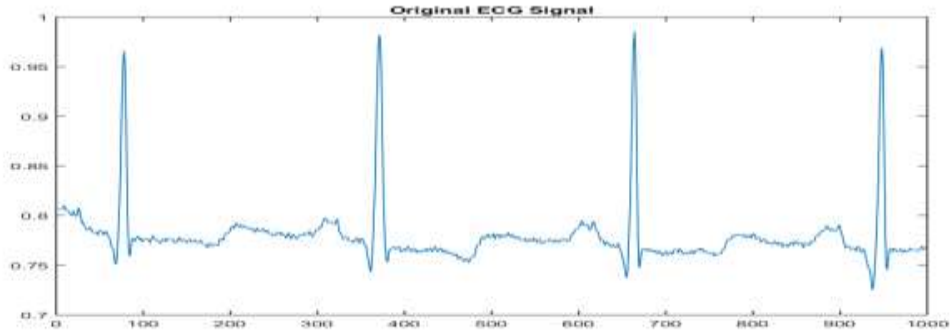

Figure 3 Original 100m.mat signal.

(B)**Generation of Noises**

1. HFN: High frequency noise is generated by multiplying sine wave of 150 Hz frequency with a random signal.

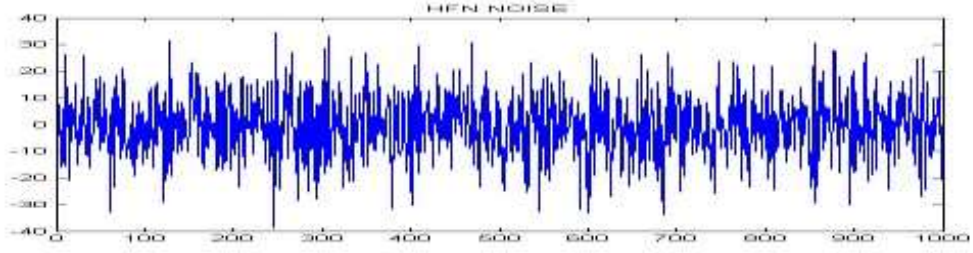

Figure 4 HFN

2. BLW-We generated the baseline drift by adding two sine waves of frequency 0.2 Hz and 0.06 Hz and triangular wave

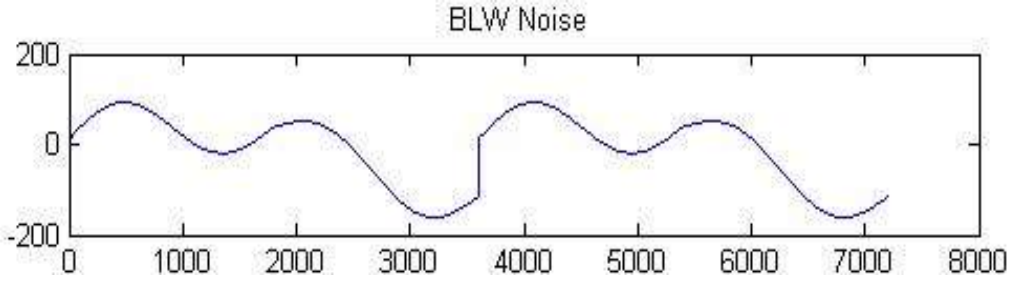

Figure 5 BLW

3. Power line interference: Here the 50 Hz power supply is considered. So, a sine wave of 50 Hz amplitude was taken to represent the power line interference.

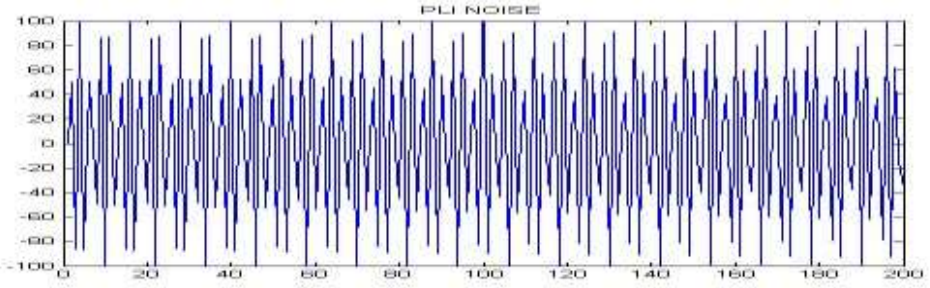

Figure 6 :PLI

(C) Signal Added with Noises.

1. HFN added signal

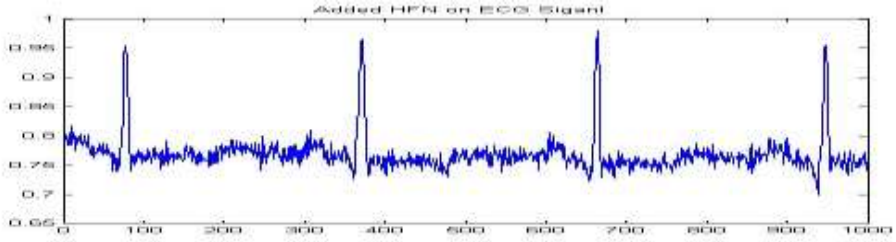

Figure7: noisy ECG signal with HFN

(2)BLW added signal

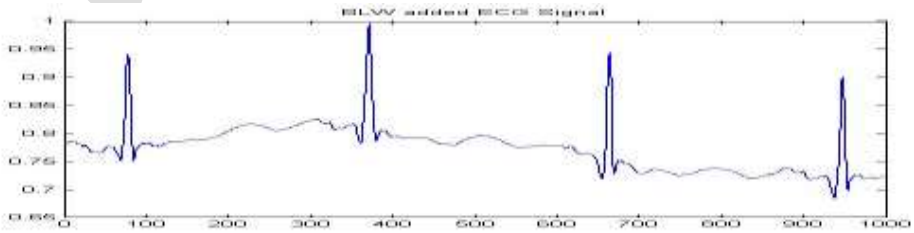

Figure8: Noisy ECG signal with BLW

(3)PLI added signal

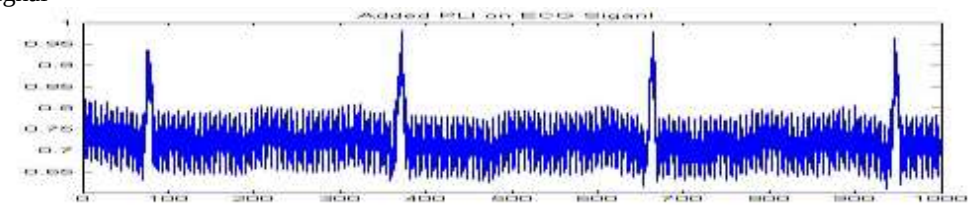

Figure 9 :Noisy ECG is signal with PLI

(D) Wavelet Domain

All the 48 ECG signal from the MIT-BIH database are taken and added with high frequency noise, Power line interference and baseline wonder. The proposed method is applied for all 4 thresholding and different filter (haar, db2, db6, db10, bior2.2, bior3.3, coieflet3, coieflet4, symlet4, symlet8). in wavelet domain. After analyzing 48 signals the noises sym4 and rigrsure thresholding is giving best result so we have shown the result in terms of average of all 48signals SNR. Figure-10, 11, 12 shows the filtered ECG signal.

Table I Average SNR values of 10 filters for high frequency noise

SIGNAL	AVG OF 48
HAAR	**38.13648**
DB2	**39.09739**
DB6	**39.42064**
DB10	**39.40012**
SYMLET4	**39.3974**
SYMLET20	***39.45396***
BIOR2.2	**38.13648**
BIOR3.3	**39.18837**
COIEF3	**39.12079**
COIEF4	**39.41658**

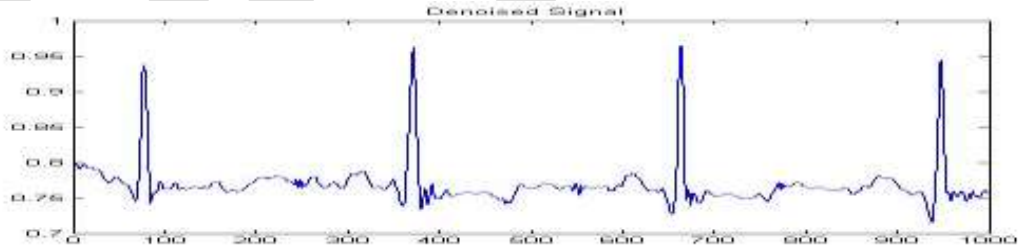

Figure 10: Filtered ECG signal for HFN for sym20.

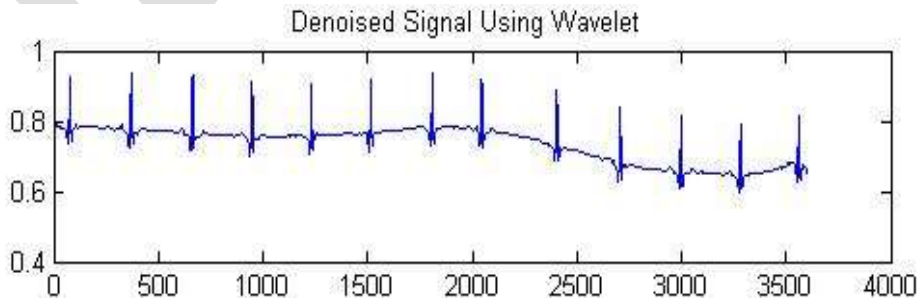

Figure 11: Filtered ECG signal for BLW for sym4.

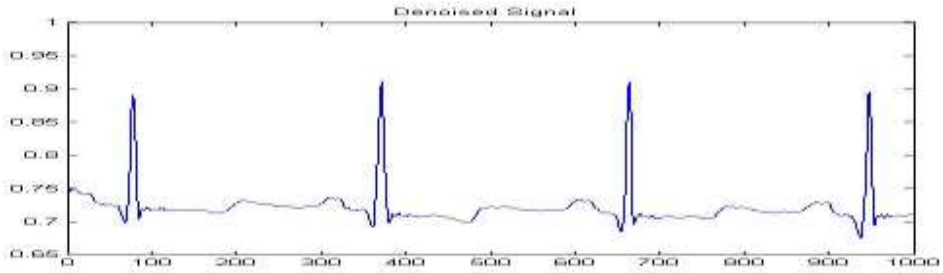

Figure 12 : Filtered ECG signal for PLI for sym20.

(E) FIR domain:

All 48 signals are applied to 3 window techniques Blackman, hamming and hanning. Among which Blackman window is giving best result.

Table II Average SNR values of 3 window for high frequency noise

Window	**SNR**
HAMMING	**37.04833**
HANNING	**37.05351**
BLACKMAN	***37.07339***

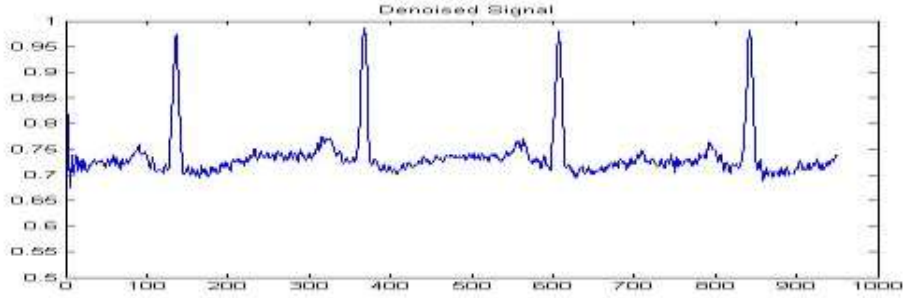

Figure 13:filtered ECG signal in HFN for Blackman window.

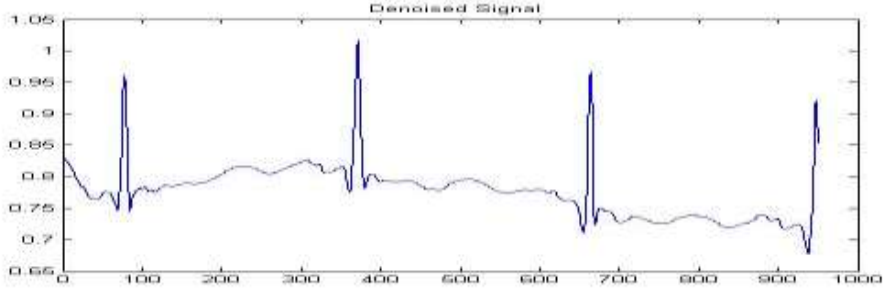

Figure 14: filtered ECG signal in BLW for Blackman window.

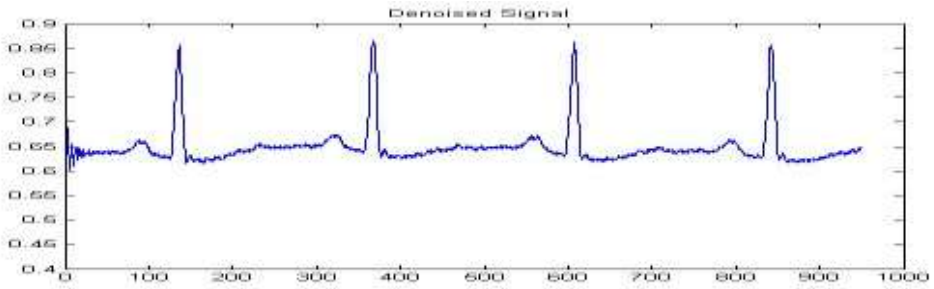

Figure 15: filtered ECG signal in PLI for hanning window.

COMPARISON OF WAVELET AND FIR

From the above table we can easily compare the performance of wavelet and FIR filter on the basis of SNR, TIME ELAPSING. Here we took the best methods of both the filtering.

(1) SIGNAL TO NOISE RATIO

Table III comparison of sym4 and Blackman on the basis of SNR

NOISES	AVG OF 48 SIGNALS (WAVELET)	AVG OF 48 SIGNALS BLACKMAN(FIR)
HFN	*39.45396*	33.55802
PLI	*18.26185*	17.00761
BLW	*21.7968*	20.05052

(2)TIME ELAPSING

Table IV comparison of sym4 and Blackman on the basis of time elapsing

NOISES	AVG OF 48 SIGNALS SYM4(WAVELET)	AVG OF 48 SIGNALS BLACKMAN(FIR)
HFN	*0.421366*	0.001746
PLI	*0.399985*	0.001755
BLW	*0.12686*	0.001709

CONCLUSION-

ECG signals are affected by different noise sources like high frequency noise, power interference and baseline wandering. In this paper we propose a denoising technique based on discrete wavelet transform and FIR filter and answer is compared in terms of SNR. From the filtered figure it can be easily concluded that wavelet filter is giving better ECG graph. In the table-III SNR is compared of Wavelet and FIR, wavelet is again giving better result for all of the three noises. In the table IV time requirement for execution of process is compared here result is opposite of previous. For FIR time elapsing is less.

REFERENCES:

[1] Köhler, Bert-Uwe, Carsten Hennig, and Reinhold Orglmeister. "The principles of software QRS detection." *Engineering in Medicine and Biology Magazine, IEEE*21.1 (2002): 42-57.

[2] Joshi, Sarang L., Rambabu A. Vatti, and Rupali V. Tornekar. "A Survey on ECG Signal denoising techniques." *Communication Systems and Network Technologies (CSNT), 2013 International Conference on*. IEEE, 2013.

[3] Liu, Xin, et al. "Multiple functional ECG signal is processing for wearable applications of long-term cardiac monitoring." *Biomedical Engineering, IEEE Transactions on* 58.2 (2011): 380-389.

[4] Sharma, L. N., S. Dandapat, and A. Mahanta. "Multiscale wavelet energies and relative energy based denoising of ecg signal." *Communication Control and Computing Technologies (ICCCCT), 2010 IEEE International Conference on*. IEEE, 2010.

[5] Li, Nianqiang, and Ping Li. "An improved algorithm based on EMD-wavelet for ECG signal de-noising." *Computational Sciences and Optimization, 2009. CSO 2009. International Joint Conference on*. Vol. 1. IEEE, 2009.

[6] Aouinet, Akram, and Cherif Adnane. "Electrocardiogram Denoised Signal by Discrete Wavelet Transform and Continuous Wavelet Transform." *Signal Processing: An International Journal (SPIJ)* 8.1 (2014): 1.

[7] Mallat, Stephane G. "A theory for multiresolution signal decomposition: the wavelet representation." *Pattern Analysis and Machine Intelligence, IEEE Transactions on* 11.7 (1989): 674-693.

[8] Kauav.S, Markam K. (2014) "Removal of artifacts from electrocardiogram using different fir window techniques" ISSN: 2321-2667 Volume 3, Issue 3, May 2014.

[9] Raghuveer.M.Rao,Ajit.S.Bopardikar," Wavelet transform Introduction to Theory and applications", Proc.of the.

[10] Patil, Preeti B., and Mahesh S. Chavan. "A wavelet based method for denoising of biomedical signal." *Pattern Recognition, Informatics and Medical Engineering (PRIME), 2012 International Conference on*. IEEE, 2012.

[11] Garcia, Tomas B. *12-lead ECG: The art of interpretation*. Jones & Bartlett Publishers, 2013.

[12] Gomes, Pedro R., Filomena O. Soares, and J. H. Correia. "ECG Self-diagnosis System at PR interval." *Proceedings of VIPIMAGE* (2007): 287-290.

[13] ww.physionet.org/physiobank/database/mitdb/ MIT-BIH Database distribution, Massachusetts Institute of Technology, 77 Massachusetts Avenue, Cambridge

[14] Georgieva-Tsaneva g. & Tcheshmedjiev k.,2013" Denoising of Electrocardiogram Data with Methods of Wavelet Transform" International Conference on Computer Systems and Technologies - CompSysTech'13

International Journal of Engineering Research and General Science Volume 3, Issue 6, November-December, 2015
ISSN 2091-2730

An Embedded Web Server Based Control and Data Logging System

Anoop T R

Mar Athanasius College of Engineering Kothamangalam, anooptr267@gmail.com, 9497171779

Abstract— An embedded system is designed for specific control functions within a larger system, often with real-time computing constraints But when networking technology is combined with it, the scope of embedded systems would be further more. Here design and implementation of embedded web server in LPC1769 is presented. That can be used as a control and data logging system in any embedded systems. Here in this design, a FAT file system is implemented first, then that file system is used for saving and accessing files to and from an SD card. By combining the web server and FAT file system operations the system can save processed data as files, access and manage these files from LAN or internet through web browsers, monitor embedded system status and control embedded system operations.

Keywords— Data Logging System, Embedded Web Server, Secure Digital (SD) Card, LPC1769, SPI (Serial Peripheral Interface), FAT file system, FatFs.

INTRODUCTION

The arrival of internet reduced the whole world communication boundary to that of a single village. After the "everybody in internet wave" now obliviously follows the "everything in the internet wave" .When the embedded device are provided with internet access, it is of no doubt that demand will rise due to the remote accessing capability of the devices[2].

The paper includes complete implementation of an embedded HTTP Web Server and a FAT file system in a LPC1769, which are work together for work as a control and data logging system.The Secure Digital (SD) Card is a non-volatile memory card format developed by the SD Card Association for use in portable devices. It is based on flash memory technology and widely used in digital cameras, cell phones, e-book readers, tablet computers, notebook computers, media players, GPS receivers, and video game consoles. Ever since its adoption in the year 2000, the format has proven very popular and is considered the de-facto industry standard.

SECURE DIGITAL MEMORY CARD

The Secure Digital Memory Card (SDC below) is the de facto standard memory card for mobile equipments. The SDC was developped as upper-compatible to Multi Media Card (MMC below). SDC compliant equipments can also use MMCs in most case. There are also reduced size versions, such as RS-MMC, miniSD and microSD, with the same function. The MMC/SDC has a microcontroller in it. The flash memory controls (block size conversion, error correction and wearleveling - known as FTL) are completed inside of the memory card. The data is transferred between the memory card and the host controller as data blocks in unit of 512 bytes, so that it can be seen as a block device like a generic harddisk drive from view point of upper level layers[3].

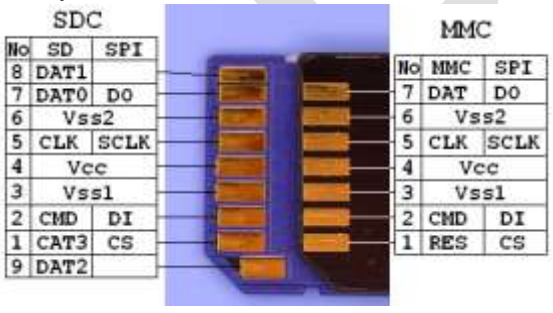

SDC/MMC contact surface

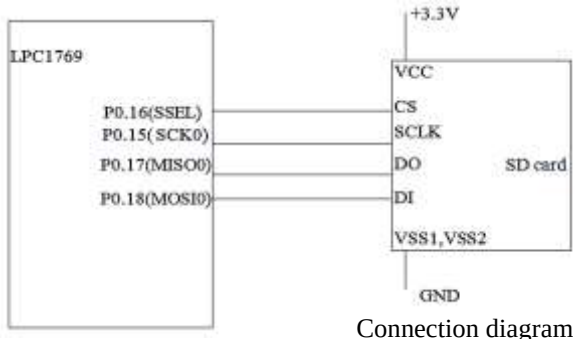

Connection diagram

COMMAND AND RESPONSE

In SPI mode, the data direction on the signal lines are fixed and the data is transferred in byte oriented serial communication. The

command frame from host to card is a fixed length packet that shown below. The card is ready to receive a command frame when it drives DO high. After a command frame is sent to the card, a response to the command (R1, R2, R3 or R7) is sent back from the card. Because the data transfer is driven by serial clock generated by host controller, the host controller must continue to read data, send a 0xFF and get received byte, until a valid response is detected. The DI signal must be kept high during read transfer (send a 0xFF and get the received data). The response is sent back within command response time (NCR), 0 to 8 bytes for SDC, 1 to 8 bytes for MMC. The CS signal must be driven high to low prior to send a command frame and held it low during the transaction (command, response and data transfer if exist). The CRC feature is optional in SPI mode. CRC field in the command frame is not checked by the card.

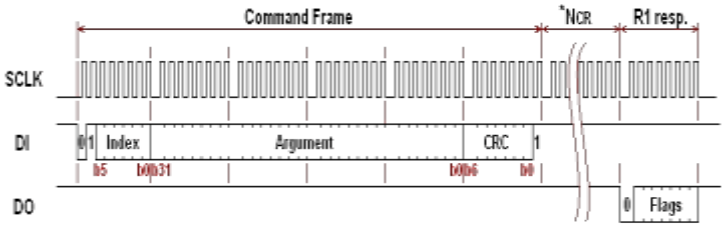

SPI COMMAND SET

Each command is expressed in abbreviation like GO_IDLE_STATE or CMD<n>, <n> is the number of the command index and the value can be 0 to 63. Following table describes only commands that to be usually used for generic read/write and card initialization. For details on all commands, please refer to spec sheets from MMCA and SDCA.

Command Index	Argument	Response	Data	Abbreviation	Description
CMD0	None(0)	R1	No	GO_IDLE_STATE	Software reset.
CMD1	None(0)	R1	No	SEND_OP_COND	Initiate initialization process.
ACMD41(*1)	*2	R1	No	APP_SEND_OP_COND	For only SDC. Initiate initialization process.
CMD8	*3	R7	No	SEND_IF_COND	For only SDC V2. Check voltage range.
CMD9	None(0)	R1	Yes	SEND_CSD	Read CSD register.
CMD10	None(0)	R1	Yes	SEND_CID	Read CID register.
CMD12	None(0)	R1b	No	STOP_TRANSMISSION	Stop to read data.
CMD16	Block length[31:0]	R1	No	SET_BLOCKLEN	Change R/W block size.
CMD17	Address[31:0]	R1	Yes	READ_SINGLE_BLOCK	Read a block.
CMD18	Address[31:0]	R1	Yes	READ_MULTIPLE_BLOCK	Read multiple blocks.
CMD23	Number of blocks[15:0]	R1	No	SET_BLOCK_COUNT	For only MMC. Define number of blocks to transfer with next multi-block read/write command.
ACMD23(*1)	Number of blocks[22:0]	R1	No	SET_WR_BLOCK_ERASE_COUNT	For only SDC. Define number of blocks to pre-erase with next multi-block write command.
CMD24	Address[31:0]	R1	Yes	WRITE_BLOCK	Write a block.
CMD25	Address[31:0]	R1	Yes	WRITE_MULTIPLE_BLOCK	Write multiple blocks.
CMD55(*1)	None(0)	R1	No	APP_CMD	Leading command of ACMD<n> command.
CMD58	None(0)	R3	No	READ_OCR	Read OCR.
*1:ACMD<n> means a command sequense of CMD55-CMD<n>.					
*2: Rsv(0)[31], HCS[30], Rsv(0)[29:0]					
*3: Rsv(0)[31:12], Supply Voltage(1)[11:8], Check Pattern(0xAA)[7:0]					

SPI RESPONSE

There are some command response formats, R1, R2, R3 and R7, depends on the command index. A byte of response, R1, is returned for most commands. The bit field of the R1 response is shown in right image, the value 0x00 means successful. When any error occured, corresponding status bit in the response will be set. The R3/R7 response (R1 + trailing 32-bit data) is for only CMD58 and CMD8.Some commands take a time longer than NCR and it responds R1b. It is an R1 response followed by busy flag (DO is driven to low as long as internal process is in progress). The host controller should wait for end of the process until DO goes high (a 0xFF is received).

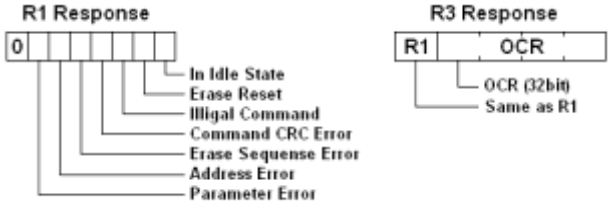

INITIALIZATION PROCEDURE FOR SPI MODE

After power on reset, MMC/SDC enters its native operating mode. To put it SPI mode, follwing procedure must be performed

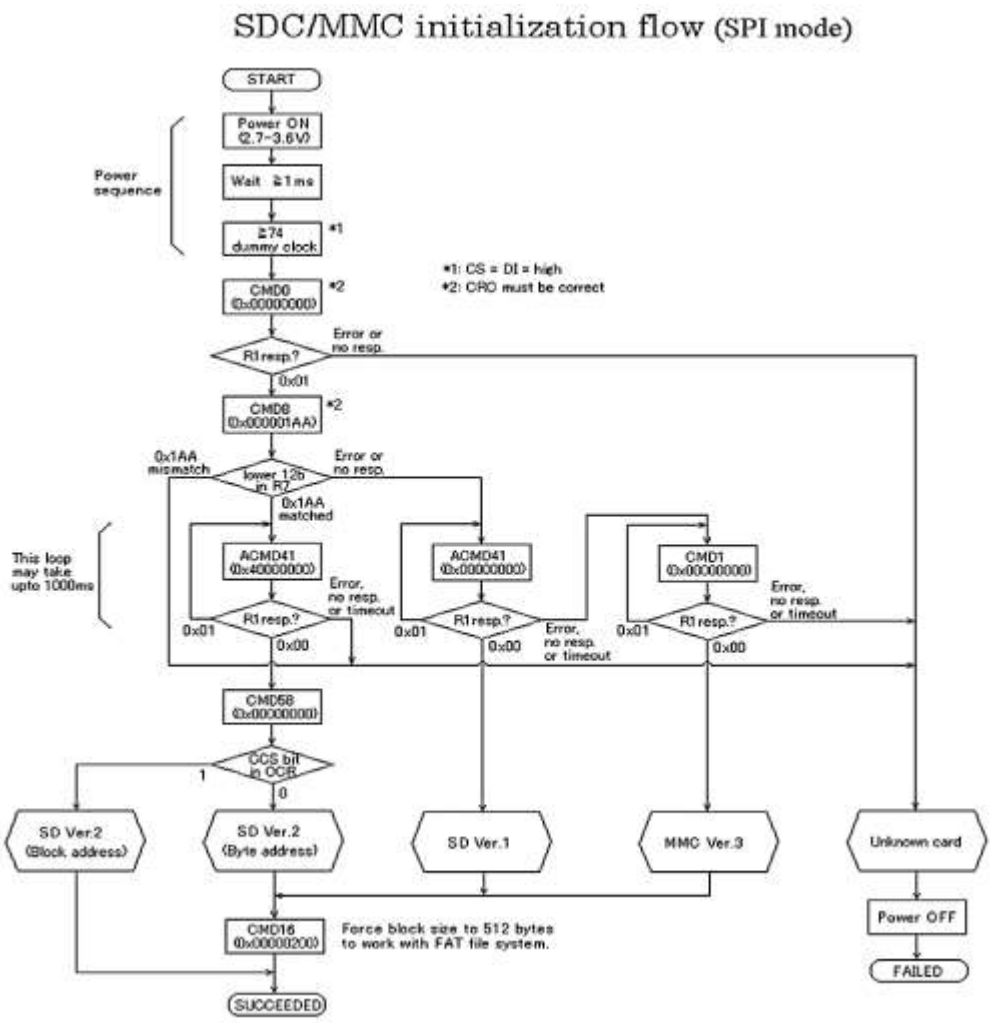

DATA PACKET AND DATA RESPONSE

In a transaction with data transfer, one or more data blocks will be sent/received after command response. The data block is transferred as a data packet that consist of Token, Data Block and CRC. The format of the data packet is showin in right image and there are three data tokens. Stop Tran token is to terminate a multiple block write transaction, it is used as single byte packet without data block and CRC.

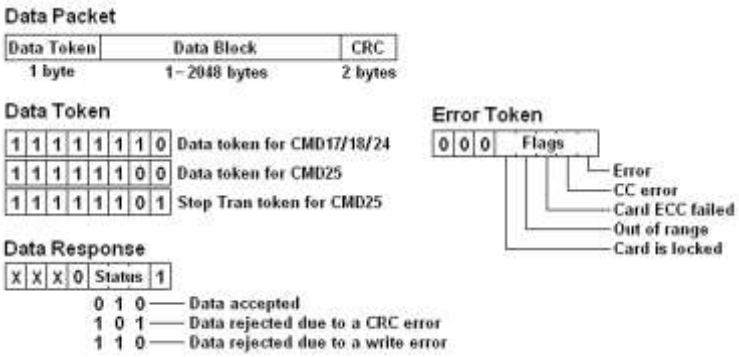

FAT FILE SYSTEM

- FAT stands for File Allocation Table
- The disk is divided into clusters, the unit used by the file allocation, and the FAT describes which clusters are used by which files.
- A FAT file system volume is composed of four basic regions,
    1. Reserved Region
    2. FAT Region

3. Root Directory Region (doesn't exist on FAT32 volumes)
4. File and Directory Data Region

Contents	Boot Sector	FS Information Sector (FAT32 only)	More reserved sectors (optional)	File Allocation Table #1	File Allocation Table #2 ... (conditional)	Root Directory (FAT12/FAT16 only)	Data Region (for files and directories) ... (to end of partition or disk)
Size in sectors	(number of reserved sectors)			(number of FATs) * (sectors per FAT)		(number of root entries*32) / (bytes per sector)	(number of clusters) * (sectors per cluster)

FATFS - GENERIC FAT FILE SYSTEM MODULE

FatFs is a generic FAT file system module for small embedded systems. The FatFs module is written in compliance with ANSI C (C89) and completely separated from the disk I/O layer. Therefore it is independent of the platform. It can be incorporated into small microcontrollers with limited resource[4].

Features:

- Windows compatible FAT file system.
- Platform independent. Easy to port.
- Very small footprint for code and work area.
- Various configuration options:
- Multiple volumes (physical drives and partitions).
- Multiple ANSI/OEM code pages including DBCS.
- Long file name support in ANSI/OEM or Unicode.
- RTOS support for multi-task operation.
- Multiple sector size support upto 4KB.
- Read-only, minimized API, I/O buffer and etc...

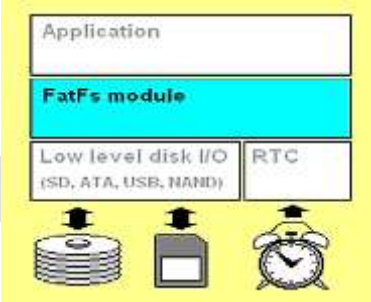

FATFS MODULE APPLICATION INTERFACE

FatFs module provides following functions to the applications. In other words, this list describes what FatFs can do to access the FAT volumes.

- f_mount - Register/Unregister a work area
- f_open - Open/Create a file
- f_close - Close an open file
- f_read - Read file
- f_write - Write file
- f_lseek - Move read/write pointer, Expand file size
- f_truncate - Truncate file size
- f_sync - Flush cached data
- f_forward - Forward file data to the stream
- f_stat - Check existance of a file or sub-directory
- f_opendir - Open a directory
- f_closedir - Close an open directory
- f_readdir - Read a directory item
- f_mkdir - Create a sub-directory
- f_unlink - Remove a file or sub-directory
- f_chmod - Change attribute
- f_utime - Change timestamp
- f_rename - Rename/Move a file or sub-directory
- f_chdir - Change current directory
- f_chdrive - Change current drive
- f_getcwd - Retrieve the current directory
- f_getfree - Get free space on the volume
- f_getlabel - Get volume label
- f_setlabel - Set volume label
- f_mkfs - Create a file system on the drive
- f_fdisk - Divide a physical drive
- f_gets - Read a string
- f_putc - Write a character

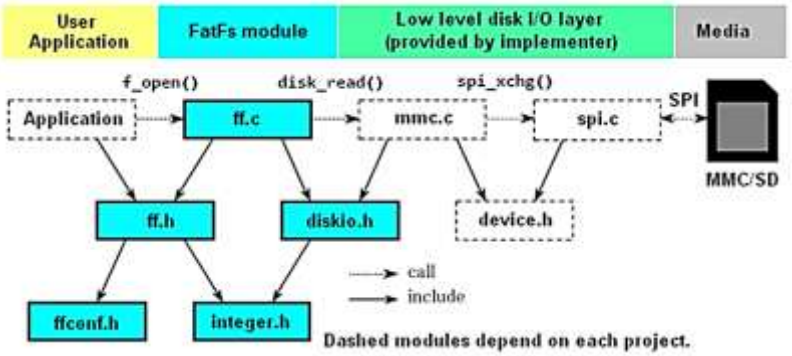

- f_puts - Write a string
- f_printf - Write a formatted string
- f_tell - Get current read/write pointer
- f_eof - Test for end-of-file on a file
- f_size - Get size of a file
- f_error - Test for an error on a file

EMBEDDED WEBSERVER

The implementation of embedded Internet technology is achieved by means of the embedded web server. It runs on embedded system with limiting computing resources to serve web documents including static and dynamic information about embedded system to web browser. We can connect any electronic device/equipment to web server and can obtain the real-time status information and control remote equipments without time and space restriction through web page released by embedded web server. Embedded server is a single chip implementation of the Ethernet networking standard. It consists of two primary elements communicating with each other: i) a server consisting of an ARM processor with an Ethernet controller and ii) a client computer which is connected to controller through this RJ45 interface. The client computer sends/receives data to/from the arm microcontroller using TCP packets. The client has to enter IP address to access this server. This request is taken by the operating system of the client and given to the LAN controller of the client system. The LAN controller sends the request to the router that processes and checks for the system connected to the network with the particular IP address. If the IP address entered is correct and matches to that of the server, a request is sent to the LAN controller of the server and a session is established and a TCP/IP connection is establishes and the server starts sending the web pages to the client through which we can remotely monitor and control the sensors and SD card content.

In this paper embedded systems and Internet technology are combined to form a new technology - the Embedded Internet Technology, which developed with the popularization of computer network technology in recent years. The heart of communication is TCP/IP protocol. Network communication is performed by the IEEE 802.3 Ethernet standard. It is the most modern technology of embedded systems. Since ARM processor has fast execution capability and Ethernet standard can provide internet access with reasonable speed, this system is suitable for enhancing security in industrial conditions by remotely monitoring and controlling various industrial appliances.

HTTP REQUEST METHODS

Two commonly used methods for a request-response between a client and server are:

1. GET - Requests data from a specified resource
2. POST- Submits data to be processed to a specified resource

post method is used in this work for sending http requests as follows

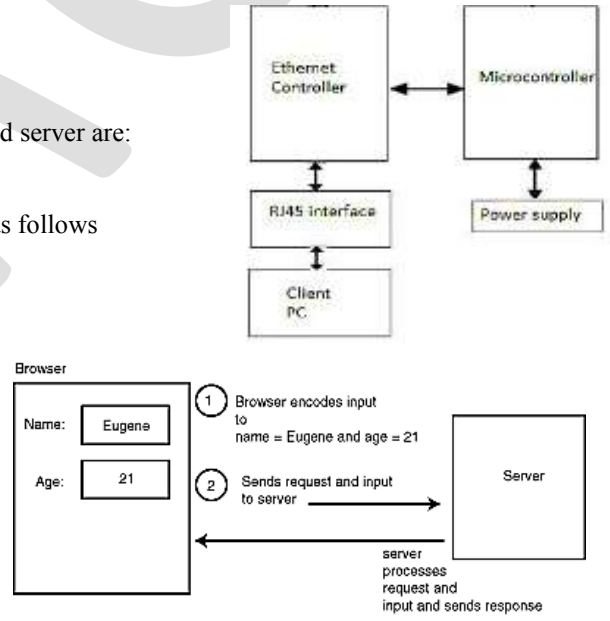

POST METHOD

PROPOSED SYSTEM

The objective of the project was to develop an embedded web server based control and data logging system using LPC1769

The main features are listed below:

- For saving processed data as files using FAT file system
- Access and manage these files from LAN or internet through web browsers
- Monitor embedded system status by monitoring sensor outputs

- Control embedded system operations by commands from user through web browsers

The main highlights of proposed system are:

- HTML web page based user interface
- User name and password authentication
- Security levels like system log file, emergency shutdown etc.
- Direct file opening and file downloading in browser
- Files & folder list
- Embedded s/m operations and modules control
- Status monitoring through sensor data

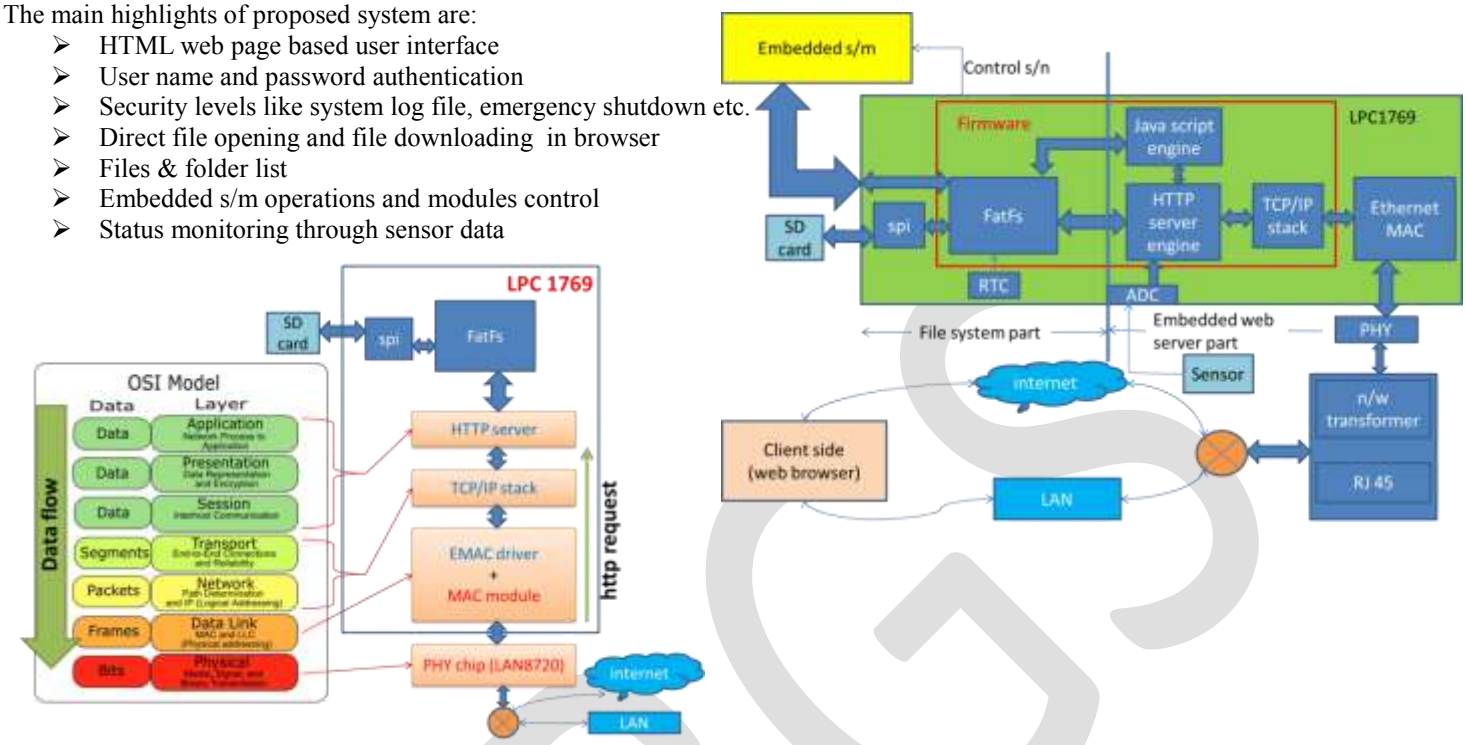

For saving processed data as files, processed raw data is given to the FatFs and it will save the data as files in SD card.For access and manage files in the SD card from LAN or internet through web browsers file system module and embedded web server act together.For monitoring embedded system status, sensor output data is transferred through HTML web pages in real time.According to the control commands from the user through the web browser appropriate control signals will generated by the system for controlling the embedded system operations.

ACKNOWLEDGMENT

I am greatly indebted to my academic mentors, whose support has given me the confidence to make a study on the topic and present the Thesis work. I hereby express my heart full gratitude to Prof. Sunny Joseph, Head of the Department of Electronics and communication, for being a great source of inspiration. I will remain indebted to my guide, Dr. Mathew K, Asst. Professor in Electronics and communication Department, for his valuable guidance and help extended to me. His guidance enabled me to complete study of the topic in time and present it well. My deep sense of gratitude goes to all teachers of Electronics and communication department who gave valuable support and guidance. I express my gratitude to the college management and our principal Prof. Geetha B for providing us good library facilities and internet facilities that helped me a lot for the study of topic in detail.

CONCLUSION

An embedded system is designed for specific control functions within a larger system, often with real-time computing constraints But when networking technology is combined with it, the scope of embedded systems would be further more. Here design and implementation of embedded web server in LPC1769 is presented. That can be used as a control and data logging system in any embedded systems. Here in this design, a FAT file system is implemented first, then that file system is used for saving and accessing files to and from an SD card. By combining the web server and FAT file system operations the system can save processed data as files, access and manage these files from LAN or internet through web browsers, monitor embedded system status and control embedded system operations.

Proposed systems future scopes are:

- Can be used with any embedded systems
- Std. file system FAT is used
- Remote data monitoring

- Remote system status check
- Remote system control
- Small size
- Large storage area at cheap cost

REFERENCES:

[1] Design and Development of Air Temperature and Relative Humidity Monitoring System With AVR Processor Based Web Server,Mitar Simić ,NORTH Point Ltd, Member of the NORTH Group
[2] Design of ARM Based Data Acquisition & Control Using GSM & TCP/IP Network,Suraj Patinge,Yogesh Suryawanshi, Sandeep Kakde,Dept. of Electronics Engineering,Y. C. College of Engineering
[3] www.nxp.com
[4] elm-chan.org
[5] ISO 7730, 1984.
[6] K. Samalekas, E. Logaras, E. S. Manolakos, "Embedded Web Server for the AVR Butterfly Enabling Immediate Access to Wireless Sensor Node Readings", SENSAPPEAL 2009, LNICST 29, pp. 145–158, 2010.
[7] T.Tan, "Embedded ATMEL HTTP Server", Master thesis, Cornell University, 2004.
[8] S. Sunny, M. Roopa, "Data Acquisition and Control System Using Embedded Web Server", International Journal of Engineering Trends and Technology- Volume 3 Issue 3, 2012.
[9] I. Hariyale, V. Gulhane, "Development of an Embedded Web Server System for Controlling and Monitoring of Remote Devices Based on ARM and Win CE", International Journal of Recent Technology and Engineering (IJRTE), Volume 1, Issue 2, June 2012.
[10] V. Mishra, "AVR microcontroller based web server", Master thesis, Cochin University of Science and Technology, 2009.
[11] www.embeddedmarket.com
[12] V. B. R. Roy, S. Dessai, S. G. S. P. Yadav, "Design and Development of ARM Processor Based Web Server", International Journal of Recent Trends in Engineering, Vol. 1, No. 4, May 2009.
[13] I. Hariyale, V. A. Gulhane, "Development of an Embedded Web Server System for Controlling and Monitoring of Remote Devices", 2nd National Conference on Information and Communication Technology (NCICT), 2011

International Journal of Engineering Research and General Science Volume 3, Issue 6, November-December, 2015
ISSN 2091-2730

A STUDY ON SEDIMENTS DEPOSITIONAL MECHANISM AT NAYAKANKUPPAM COAST, TAMILNADU, INDIA

NYIRABUHORO Pascaline, MUGERWA Theophile*, NDIKUMANA Jean de Dieu, MUNGANYINKA Jeanne Pauline, NDAYISHIMIYE Jean Claude, UWAMUNGU Placide

Department of Earth Sciences, Annamalai University, Tamil Nadu, India.

*Corresponding Author:luanmugerwa@gmail.com

Abstract— Textural analysis carried out for the sediments of the Nayakkankuppam coast revealed that inlet part is dominated by fine sand, central part is dominated by medium sand and outlet part is dominated by coarse sand. The grain size parameters namely Mean size (MZ), standard deviation (σ1), skewness(Ski), and kurtosis (KG) of percentile values derived from the cumulative curves following Folk and Ward and the moment technique based upon grouped data are most widely used. It is observed that in Nayakkankuppam, most of the samples were fallen in the moderately well sorted to well sorted nature. Skewness measures asymmetry of frequency distribution and marks the position of mean with respect to median. The fine skewed nature of the sediments clearly exhibits sediment input from various sources of tributaries. The finely skewed nature is also implies a low velocity than normal, this skewness data indicated that the sediments are nearly symmetrical to fine skewed, the median class of the sediments dominate almost throughout their distribution. The kurtosis data indicated Mesokurtic to platykurtic. The CM pattern divulged that the sediments were transported bottom suspension and rolling as well as graded suspension. The comparison with the tractive current diagram, the berm samples fall in beach environment, the remaining samples fall in beach and tractive current environment.

Keywords— Sediments, depositional mechanism, sand**,** coastal environment**.**

1. INTRODUCTION

At present, few research works are available to understand processes involving in a wide variety of environmental formation and long-term interaction among environmental components. A beach which is the zone of unconsolidated materials is a dynamic environment constantly acted upon by waves; currents and tide. Depending upon the intensity, nature and duration of the coastal processes, the beaches constantly undergo physical changes that in turn result in different types of sediments. These often reflect the dynamic conditions that were prevalent at the time of deposition with the study of seasonal fluctuations of the beach profiles where beach changes were mentioned [1].

Heavy minerals studies were used mainly to understand the provenance history, diagenetic changes, sediment source and sediment transport [2]. Since few decades, important contributions were made by sedimentologists on the study of the nature of sediments in modern environments. Present day littoral sediments were studied not only to understand their mode of deposition, but also to recognize ancient beach sediments in the geologic history. Specific studies on statistical properties of the grain size distribution, grain size variation across the beach, degree of roundness, shape of the sediment grains and sedimentary structure etc., were also attempted [3].

For an effective conservation of the coastal zone, knowledge of the basic processes in modern as well as palaeo-environments is imperative. With this broader perspective in mind, a detailed programme has been worked out to decipher the interrelationship of the strand plain, beach and inner shelf sediments based on the granulometry, surface textures and mineralogy. Thus, the main objectives of the investigation were (i) to study the textural characteristics of the sediments in the foreshore and breaker zone of Nayakkankuppam coast, (ii) to determine the grain size distribution of the sediments in the light of wave energy and morphological changes of the beach during different seasons, (iii) to derive a depositional mechanism–controlling the variability in the sand mineralogy.

2. STUDY AREA

The study area forms (fig-1) part of Nayakankuppam, Nagapattinam District, Tamil Nadu, India. It falls between the latitude 11°11’ 46.49”N and 79° 50’ 28.85”E in survey of India toposheet 58 M/15. Major rivers flowing in the study area includes Cauvery, Arasalar, Tirumalairajanar, Vellar, Adappar, Vettar and Vedaranyam canal. The study area is surrounded by Tanjore District in the west, Cuddalore District in the North, Palk Strait in the south and Bay of Bengal in the East.

It is a part of Cauvery delta where the distributaries of Cauvery bring in considerable amount of sediment load to the Bay of Bengal. The area is composed of soft unconsolidated sediments of Pleistocene, Holocene and Quaternary age. The deltaic plain/coastal sediment is mainly constituted by unconsolidated sand with or without clay silt with considerable permeability. The area is gently dipping towards Bay of Bengal. The area is packed with various land forms of Aeolian and marine origin. The presence of geomorphic land forms like beach, beach ridges, sand dunes, mud flats, alluvial plain, flood plain and palaeochannels indicate that the area underwent rhythmic processes dominated by Aeolian over beach process and vice versa.

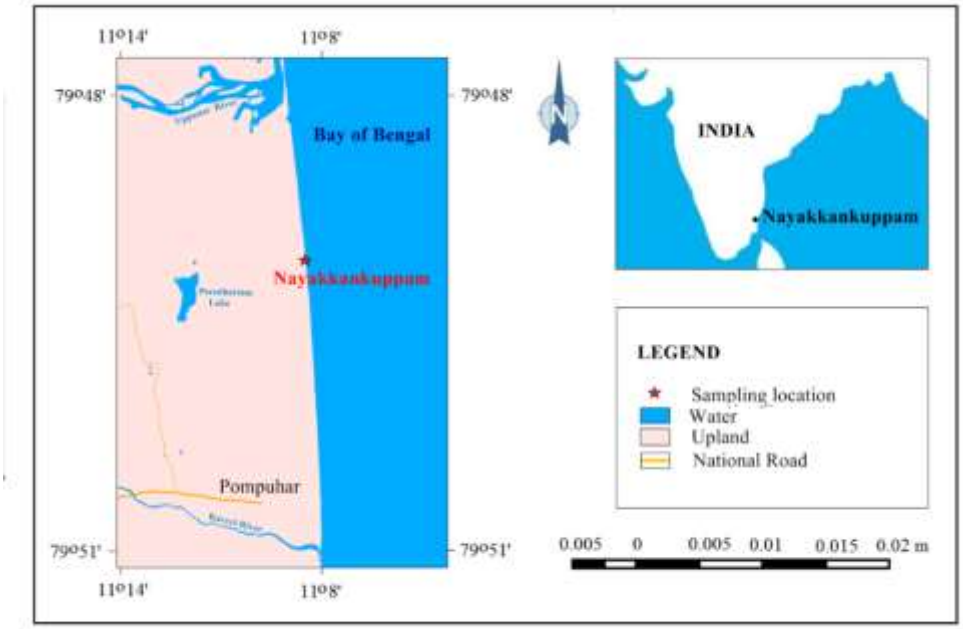

Fig-1: Study area map and sampling location

3. MATERIALS AND METHODS

Sampling of sediments was carried out by pit sampling method. The pit of 1m deep had been dug out from sampling site and one sample was collected to a depth of 100cm from each surface at 2 cm interval from the surface downward the bottom using appropriate spoon. In other words, in situ, 50 samples in total were directly packed in different polythene bags and carried to the laboratory. In lab, each sample was dried and mixed by following coning and quartering method and 100gm of the sample was taken for sieving. Sieving of dried sediments sample was carried out by using a series of standard ASTM test sieves of ¼ Φ interval to get known size fractions in Ro tap sieve shaker for 15 minutes.

The weight percentage and cumulative weight percentage were manually recorded. The log-probability graph was used to draw segments from the calculated values. From the graphs, statistical parameters like mean (M_z), standard deviation (σ_I), skewness (SK_I) and kurtosis (K_G) were calculated and processed in the spreadsheet for statistical analysis. [4]

4. RESULTS AND DISCUSION

4.1 Vertical size distribution of sediments

Grain size distribution has been used for the determination of sedimentary environment with the help of log-probability studies. The entire grain size distribution is believed to be considered of several normal subpopulations representing the sediments transported by the process of rolling, suspension and siltation [5]. The combination of two or more of these processes produces characteristics log

probability curve shapes. Thus, the mentioned characteristics of the sediments and the mechanisms were utilized to study the size analysis. Textural attributes of sediments and sedimentary rocks viz. mean (Mz), Standard deviation (σ_1), Skewness (Sk_I) and Kurtosis (K_G) are widely used to reconstruct the depositional environments of sediments and sedimentary rocks. Correlation between size parameters and transport processes/depositional mechanisms of sediments has been established by exhaustive studies from many modern and ancient sedimentary environments [6]. The size analyses of the sediments from various locations show one surface creep, either one or two siltation and one suspension. About 95% of the samples exhibit the fine truncation at less than 95% and coarse truncation at about 5% and others exhibit the fine truncation more than 90% and coarse truncation below 10%. The steepness and truncation points of the sediments exhibit that they were deposited mostly by the back and forth motion of water. On the basis of probability curves the samples indicate that the coarser grains are lacking and indicate a moderately high energy condition. The steepness of the curves of samples indicates that they were well sorted to very well sorted. The bottom sets of sediments clearly gives two well-defined saltated populations and having sharp contacts of curves in the fine and coarse truncation. This indicates that the sediments were deposited by the seasonal cyclic tidal waves by back and forth action. The histogram of size frequency distribution shows a bimodal or polymodal distribution (Fig-2) which in turn indicates a wide range of size distribution and asymmetrical nature of sediments. Some of the samples exhibit unimodal distribution also indicating good sorting i.e. dominant of one fraction over the others. This also infers that the samples have received the sediments from different sources during seasonal and tidal variations.

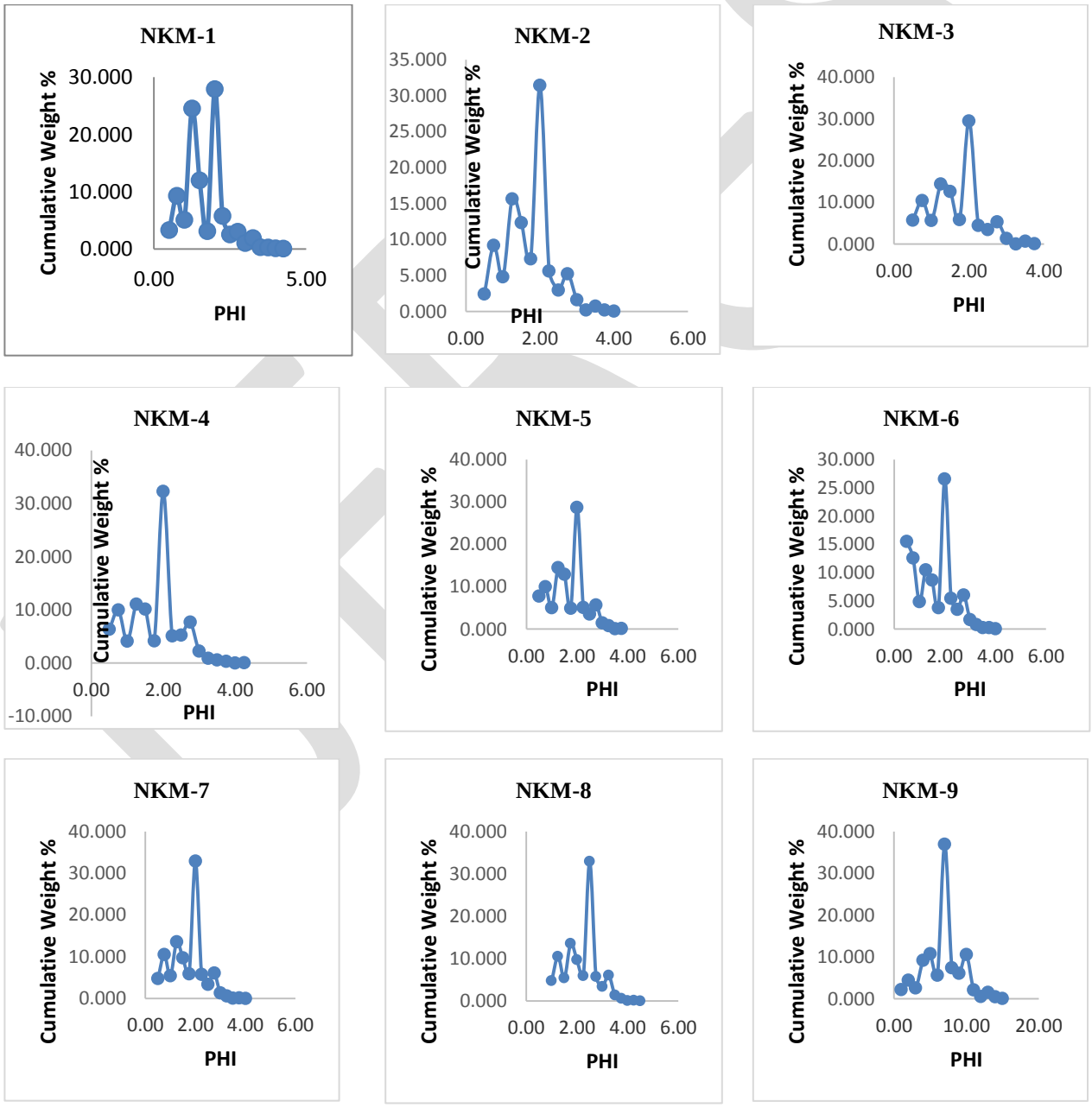

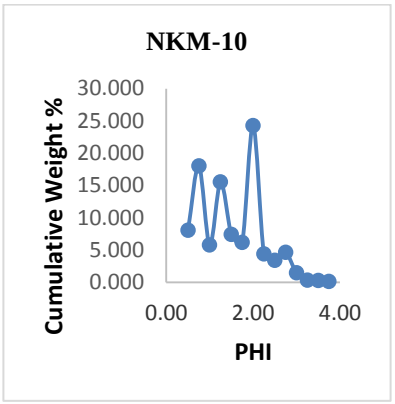
NKM-10
Cumulative Weight %
30.000
25.000
20.000
15.000
10.000
5.000
0.000
0.00
2.00
4.00
PHI

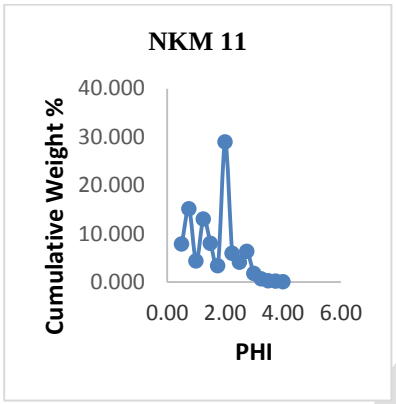
NKM 11
Cumulative Weight %
40.000
30.000
20.000
10.000
0.000
0.00
2.00
4.00
6.00
PHI

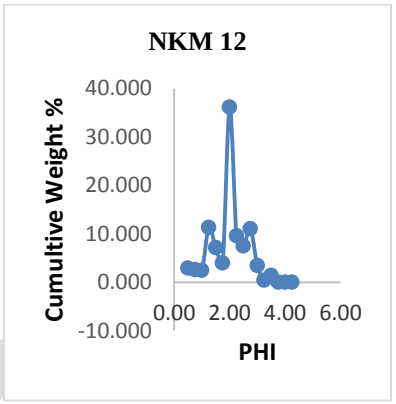
NKM 12
Cumultive Weight %
40.000
30.000
20.000
10.000
0.000
-10.000
0.00
2.00
4.00
6.00
PHI

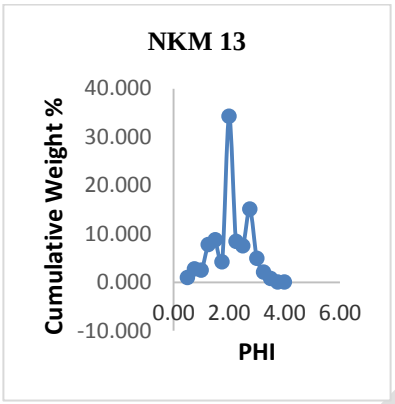
NKM 13
Cumulative Weight %
40.000
30.000
20.000
10.000
0.000
-10.000
0.00
2.00
4.00
6.00
PHI

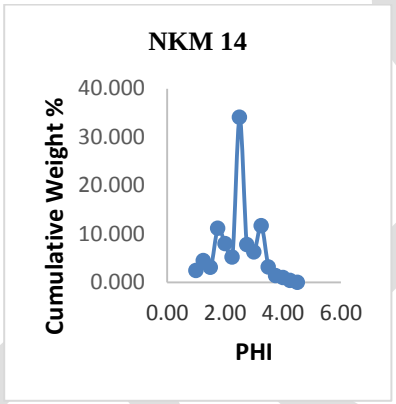
NKM 14
Cumulative Weight %
40.000
30.000
20.000
10.000
0.000
0.00
2.00
4.00
6.00
PHI

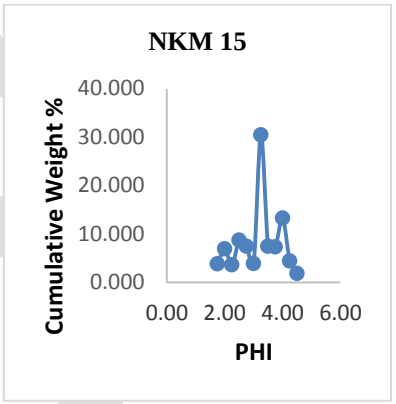
NKM 15
Cumulative Weight %
40.000
30.000
20.000
10.000
0.000
0.00
2.00
4.00
6.00
PHI

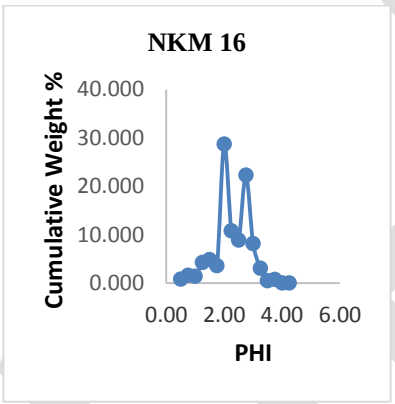
NKM 16
Cumulative Weight %
40.000
30.000
20.000
10.000
0.000
0.00
2.00
4.00
6.00
PHI

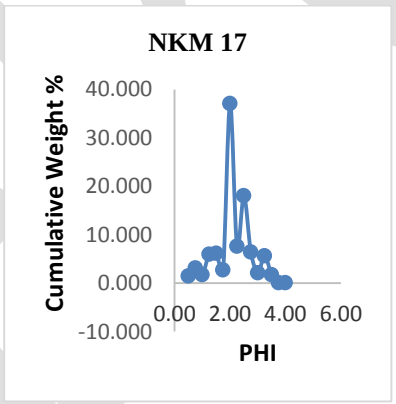
NKM 17
Cumulative Weight %
40.000
30.000
20.000
10.000
0.000
-10.000
0.00
2.00
4.00
6.00
PHI

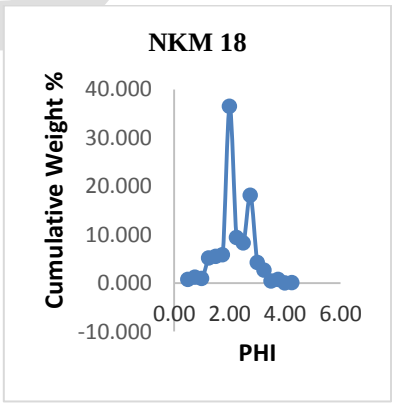
NKM 18
Cumulative Weight %
40.000
30.000
20.000
10.000
0.000
-10.000
0.00
2.00
4.00
6.00
PHI

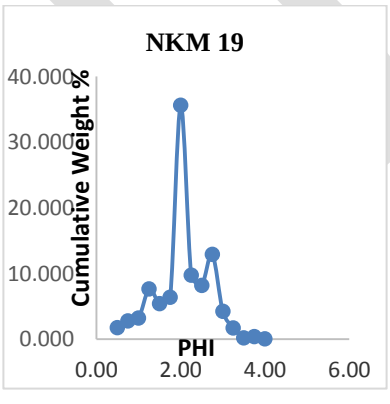
NKM 19
Cumulative Weight %
40.000
30.000
20.000
10.000
0.000
0.00
2.00
4.00
6.00
PHI

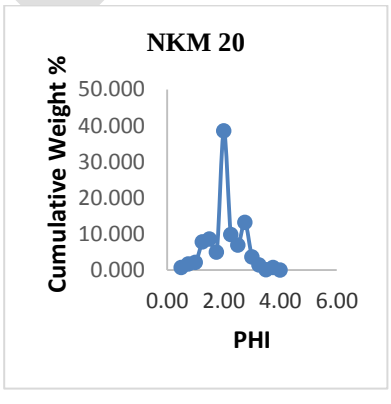
NKM 20
Cumulative Weight %
50.000
40.000
30.000
20.000
10.000
0.000
0.00
2.00
4.00
6.00
PHI

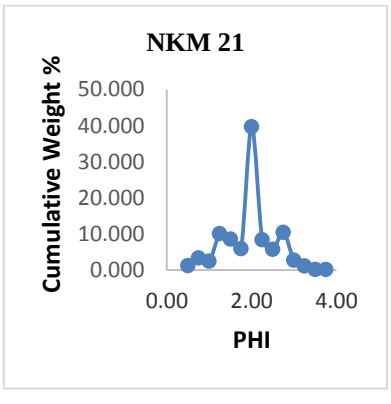
NKM 21
Cumulative Weight %
50.000
40.000
30.000
20.000
10.000
0.000
0.00
2.00
4.00
PHI

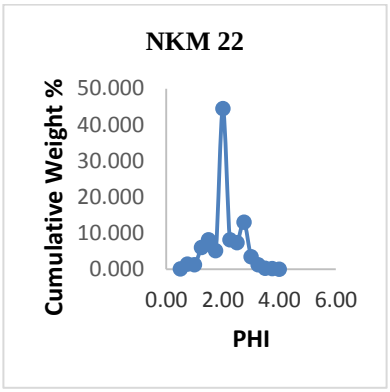
NKM 22
Cumulative Weight %
50.000
40.000
30.000
20.000
10.000
0.000
0.00 2.00 4.00 6.00
PHI

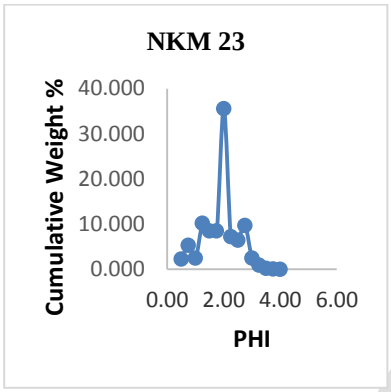
NKM 23
Cumulative Weight %
40.000
30.000
20.000
10.000
0.000
0.00 2.00 4.00 6.00
PHI

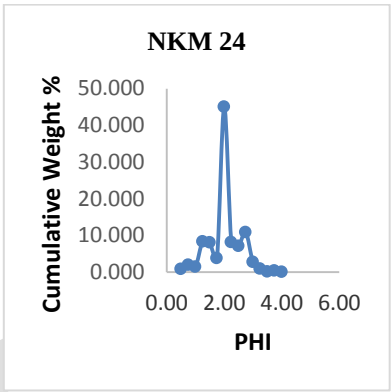
NKM 24
Cumulative Weight %
50.000
40.000
30.000
20.000
10.000
0.000
0.00 2.00 4.00 6.00
PHI

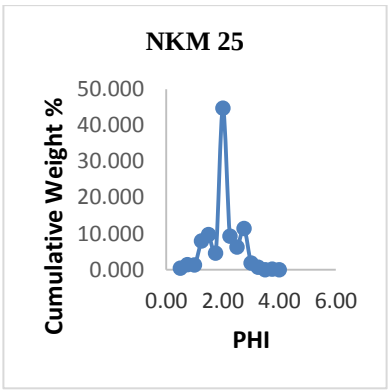
NKM 25
Cumulative Weight %
50.000
40.000
30.000
20.000
10.000
0.000
0.00 2.00 4.00 6.00
PHI

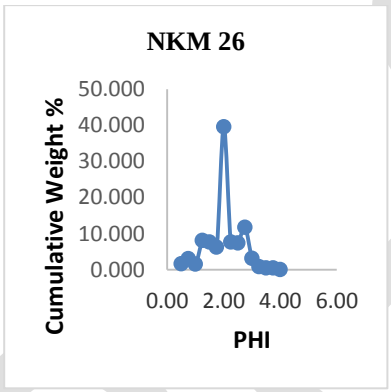
NKM 26
Cumulative Weight %
50.000
40.000
30.000
20.000
10.000
0.000
0.00 2.00 4.00 6.00
PHI

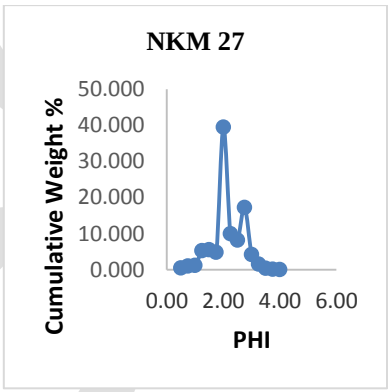
NKM 27
Cumulative Weight %
50.000
40.000
30.000
20.000
10.000
0.000
0.00 2.00 4.00 6.00
PHI

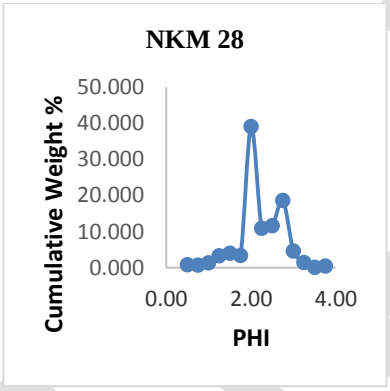
NKM 28
Cumulative Weight %
50.000
40.000
30.000
20.000
10.000
0.000
0.00 2.00 4.00
PHI

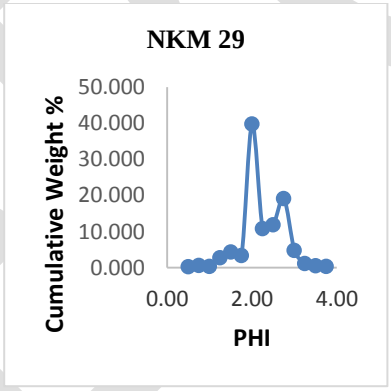
NKM 29
Cumulative Weight %
50.000
40.000
30.000
20.000
10.000
0.000
0.00 2.00 4.00
PHI

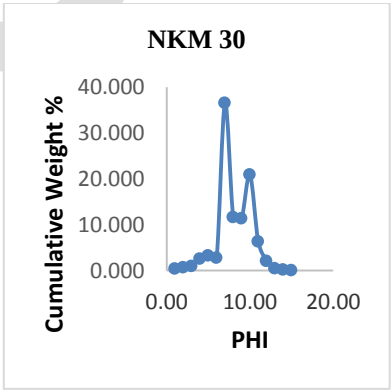
NKM 30
Cumulative Weight %
40.000
30.000
20.000
10.000
0.000
0.00 10.00 20.00
PHI

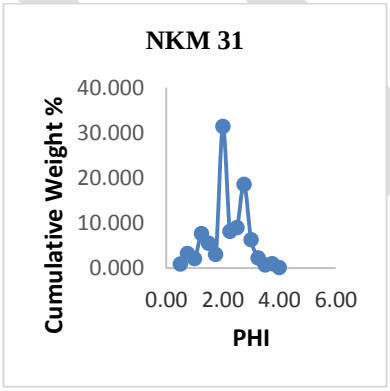
NKM 31
Cumulative Weight %
40.000
30.000
20.000
10.000
0.000
0.00 2.00 4.00 6.00
PHI

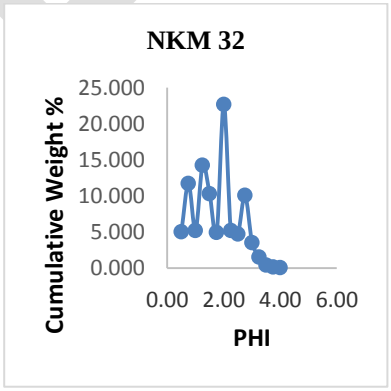
NKM 32
Cumulative Weight %
25.000
20.000
15.000
10.000
5.000
0.000
0.00 2.00 4.00 6.00
PHI

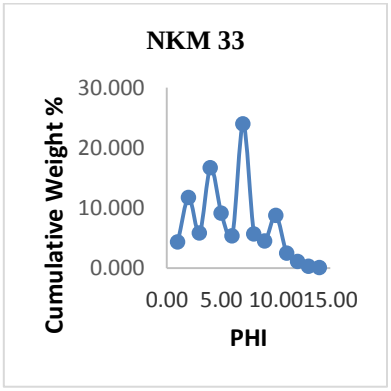
NKM 33
Cumulative Weight %
30.000
20.000
10.000
0.000
0.00 5.00 10.00 15.00
PHI

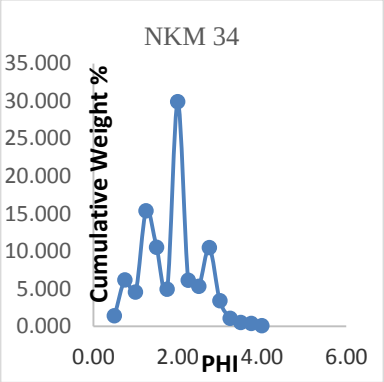
NKM 34
Cumulative Weight %
35.000
30.000
25.000
20.000
15.000
10.000
5.000
0.000
0.00
2.00
4.00
6.00
PHI

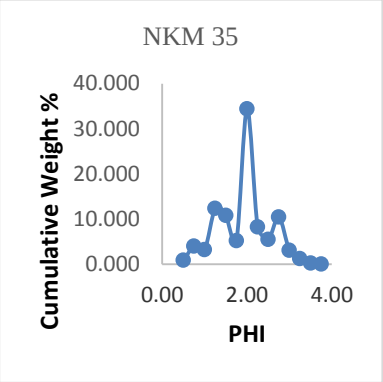
NKM 35
Cumulative Weight %
40.000
30.000
20.000
10.000
0.000
0.00
2.00
4.00
PHI

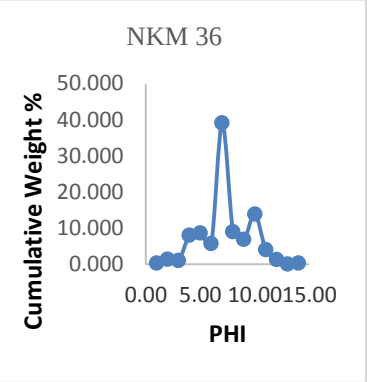
NKM 36
Cumulative Weight %
50.000
40.000
30.000
20.000
10.000
0.000
0.00
5.00
10.00
15.00
PHI

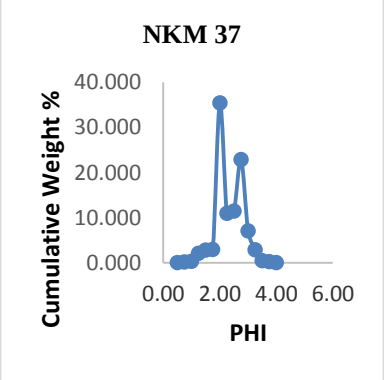
NKM 37
Cumulative Weight %
40.000
30.000
20.000
10.000
0.000
0.00
2.00
4.00
6.00
PHI

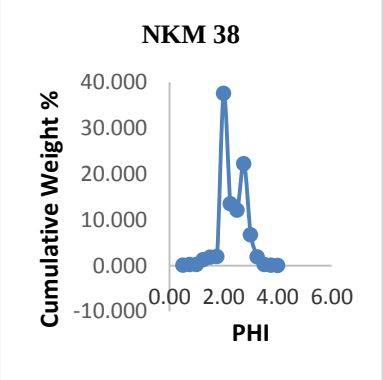
NKM 38
Cumulative Weight %
40.000
30.000
20.000
10.000
0.000
-10.000
0.00
2.00
4.00
6.00
PHI

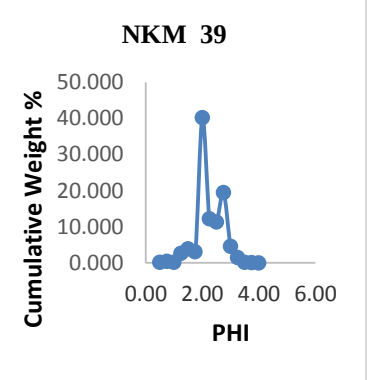
NKM 39
Cumulative Weight %
50.000
40.000
30.000
20.000
10.000
0.000
0.00
2.00
4.00
6.00
PHI

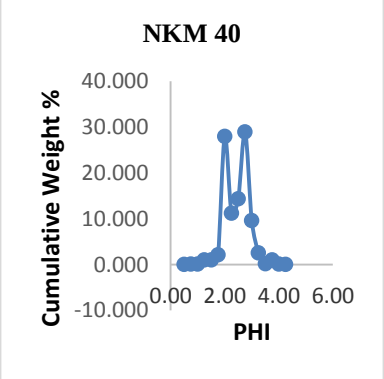
NKM 40
Cumulative Weight %
40.000
30.000
20.000
10.000
0.000
-10.000
0.00
2.00
4.00
6.00
PHI

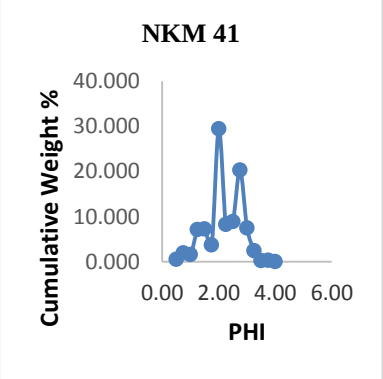
NKM 41
Cumulative Weight %
40.000
30.000
20.000
10.000
0.000
0.00
2.00
4.00
6.00
PHI

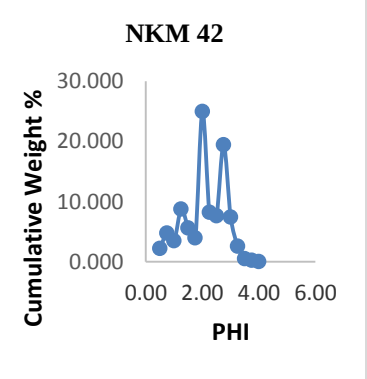
NKM 42
Cumulative Weight %
30.000
20.000
10.000
0.000
0.00
2.00
4.00
6.00
PHI

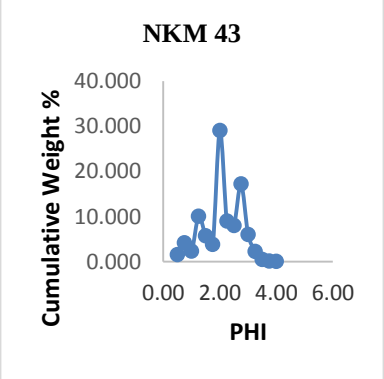
NKM 43
Cumulative Weight %
40.000
30.000
20.000
10.000
0.000
0.00
2.00
4.00
6.00
PHI

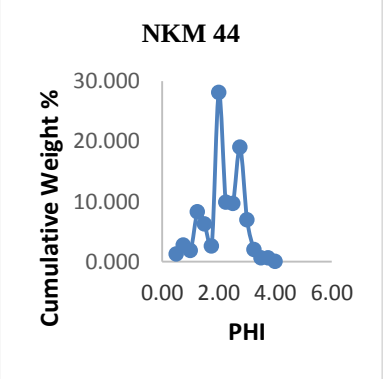
NKM 44
Cumulative Weight %
30.000
20.000
10.000
0.000
0.00
2.00
4.00
6.00
PHI

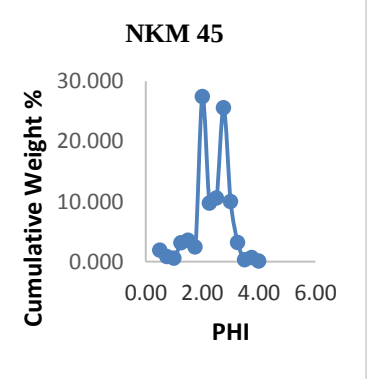
NKM 45
Cumulative Weight %
30.000
20.000
10.000
0.000
0.00
2.00
4.00
6.00
PHI

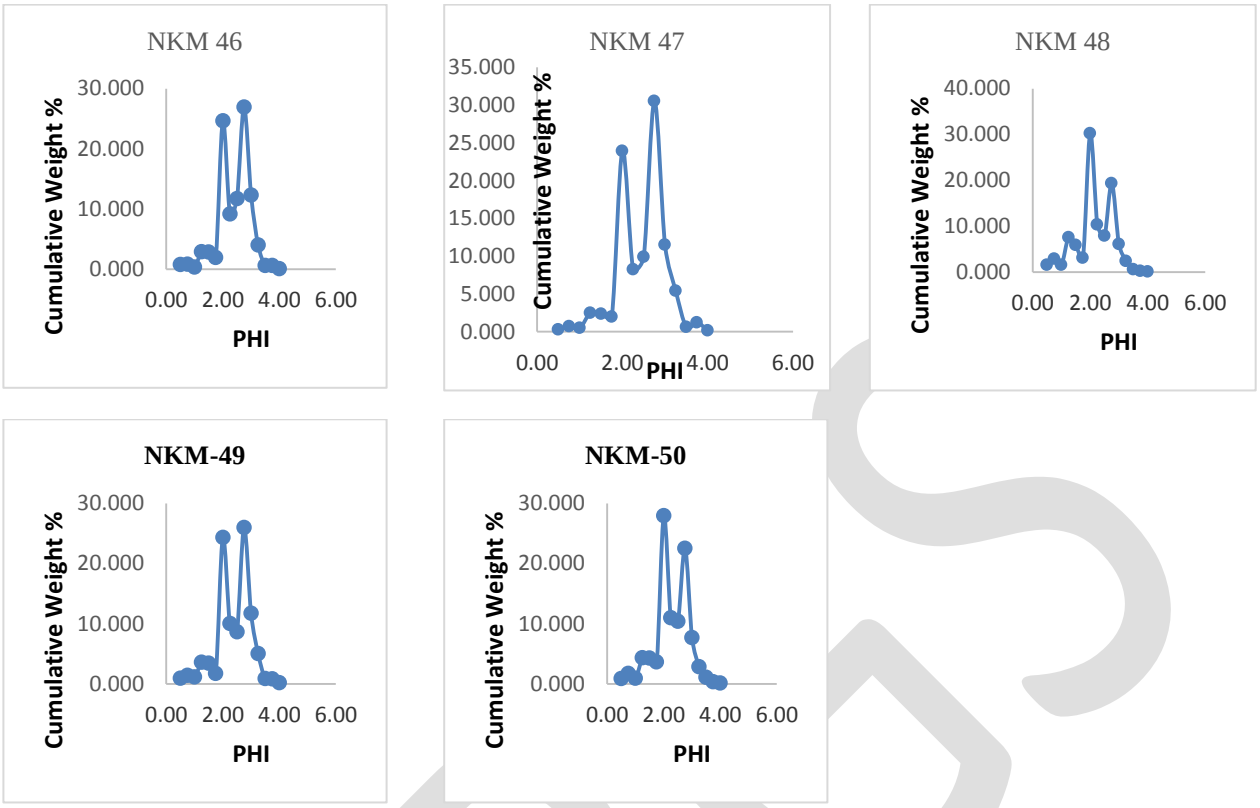

Fig-2: vertical size distribution of sediments

4.2 Statistical Analysis

Textural attributes of sediments and sedimentary rocks viz. mean (Mz), Standard deviation (σ_1), Skewness (Sk_I) and Kurtosis (K_G) are widely used to reconstruct the depositional environments of sediments and sedimentary rocks. Correlation between size parameters and transport processes or depositional mechanisms of sediments has been established by exhaustive studies from many modern and ancient sedimentary environments [6]. The table 1 displays all statistical parameters that were used to interpret our results.

Table-1: Statistical parameters and their corresponding remarks

Depth	Mean	Standard deviation	Skewness	Kurtosis	Remarks			
2	1.483	0.544	0.059	1.293	MS	MWS	NS	LK
4	1.533	0.537	-0.087	1.105	MS	MWS	NS	LK,
6	1.443	0.623	0.078	1.257	MS,	MWS	NS	LK
8	1.593	0.661	0.148	1.110	MS,	MWS	FS	LK
10	1.430	0.641	0.002	1.123	MS,	MWS	NS	LK
12	1.387	0.801	-0.168	0.978	MS,	MS	NS	MK
14	1.473	0.588	0.068	1.095	MS,	MWS	NS	MK
16	1.837	0.641	0.066	1.132	MS,	MWS	NS	LK
18	1.577	0.640	-0.044	1.052	MS,	MWS,	NS	MK
20	1.643	0.893	0.352	1.193	MS,	MWS,	VFSK	LK

22	1.467	0.697	0.135	0.948	MS,	MWS,	FSK	MK
24	1.853	0.702	0.046	1.138	MS,	MWS,	NS	LK
26	1.983	0.608	-0.058	0.888	MS,	MWS,	NS	PK
28	1.823	0.653	0.013	0.977	MS,	MWS,	NS	MK
30	1.823	0.722	0.021	0.932	MS,	MS,	NS	MK
32	2.073	0.525	-0.081	1.166	FS,	MWS,	NS	LK
34	2.017	0.586	-0.106	1.218	FS,	MWS	CSK	LK
36	2.080	0.543	0.147	1.011	FS,	MWS	FSK,	MK
38	1.933	0.588	0.010	1.153	MS,	MWS,	NS,	LK
40	1.980	0.536	0.113	1.371	MS,	MWS,	FSK,	LK
42	1.903	0.577	-0.066	1.154	MS,	MWS,	NS,	LK
44	1.993	0.415	0.464	0.883	MS,	WS,	VFSK,	PK
46	1.337	0.603	-0.063	1.332	MS,	MWS,	NS,	LK
48	1.967	0.523	0.072	1.639	MS,	MWS	NS,	VLK
50	1.850	0.517	0.095	1.148	MS,	MWS,	NS,	LK
52	1.910	0.624	-0.033	1.318	MS,	MWS,	NS,	LK
54	2.010	0.515	0.190	0.929	FS,	MWS	FSK,	MK
56	2.110	0.455	0.308	1.040	FS,	WS,	VFSK	MK
58	2.133	0.421	0.332	0.893	FS,	WS,	VFSK	PK
60	2.117	0.492	0.131	0.863	FS,	WS,	FS	PK
62	2.003	0.643	-0.001	1.293	FS,	MWS	VCSK	LK
64	1.663	0.746	0.179	1.025	MS,	MS,	FSK	MK
66	1.597	0.664	-0.073	0.974	MS,	MWS,	NS	MK
68	1.750	0.653	0.182	1.025	MS,	MWS,	FSK	MK
70	1.807	0.599	0.141	2.967	MS,	MWS,	FSK	VLK
72	1.933	0.569	0.131	1.054	MS,	MWS,	FSK	MK
74	2.200	0.437	0.286	0.849	FS,	WS	FSK	PK
76	2.167	0.430	0.204	0.790	FS,	WS	FSK	PK
78	2.133	0.412	0.321	0.869	FS,	WS	VFSK	PK
80	2.320	0.414	-0.090	0.761	FS,	WS,	VCSK	PK
82	2.013	0.615	0.081	0.879	FS,	MWS	NS	PK
84	1.927	0.720	-0.074	0.914	MS,	MS,	NS	MK
86	1.897	0.699	-0.049	0.945	MS,	MWS,	NS	MK
88	2.043	0.583	0.080	1.066	FS,	MWS,	NS	MK
90	2.273	0.525	-0.137	1.067	FS,	MWS,	CSK	MK
92	2.243	0.501	0.267	0.926	FS,	MWS,	FSK	MK
94	2.357	0.519	-0.370	0.840	FS,	MWS	VCSK	PK
96	1.983	0.643	0.015	0.906	MS,	MWS,	NS,	PK
98	2.267	0.569	-0.023	0.876	FS,	MWS,	NS,	PK
100	2.203	0.523	0.059	1.097	FS,	MWS,	NS,	MK
Maximum	**2.357**	**0.893**	**0.464**	**2.967**				
Minimum	**1.337**	**0.412**	**-0.370**	**0.761**				
Average	**1.889**	**0.593**	**0.065**	**1.089**				

MS-Medium Sand, FS-Fine Sand, MWS-Moderately well sorted, MS-Moderately Sorted

WS-Well Sorted, NS-Near Symetrical, FSK-Fine Skewed, VFSK-Very fine skewed

VCSK-Very coarse skewed, PK-Platy kurtic, MK-Mesokurtic, VLK-Very leptokurtic

LK-Leptokurtic

4.2.1 Mean (Mz)

It is the average size of the sediments and is influenced by the source of supply, transporting medium and the energy conditions of the depositing environment. Mean size indicates the central tendency or the average size of the sediment in terms of energy; it indicates the average kinetic energy / velocity of depositing agent. [9] The vertical mean size (Fig-3) ranges between 1.337Φ (44-46 cm) to 2.357 Φ (92-94 cm) in the Nayakkankuppam. The average mean size is 1.889. Predominantly 62% of the samples fall in medium sand category and remaining 38% samples are falls in fine sand category. The fine grain nature indicates the moderately low energy condition in the basin of deposition. The mean size indicates that the medium sand was deposited at a moderate energy conditions whereas the fine sand was deposited at a moderately low energy conditions. The variation in phi mean size, therefore, reveals the differential energy conditions leads to the deposition of these kinds of sediments in different locations [7].

Sands deposited by rivers almost invariably contain fine particles from suspended load. Sands deposited on the parts of beaches where the breaking waves continuously wash thin sheets of back and forth invariably lack admixtures of fine grained sediments [8]. Fine grained nature of sediments in the study region shows that they were deposited by river processes. But when the shelf was emergent during the last ice age, streams deposited sands there. The analysis of vertical sediments generally reveals a fine grained nature in the top and medium sand at the bottom indicating the general fining up of sediments.

4.2.2 Standard Deviation

It is expressed by inclusive graphic standard deviation (σ_1) as it covers both the tails of the distribution. Standard deviation is a poorly understood measure that depends on the size range of the available sediments, rate of depositing agent and the time available for sorting. The sorting variations observed attribute ~~to~~ the difference ~~in~~ from water turbulence and variability in the velocity of depositing current. The moderately well sorted character of the sediments indicates the influence of stronger energy conditions of the depositing agents or prevalence of strong energy conditions in the basin.

In the Nayakkankuppam coast the mean size varies ranges 0.893ϕ (20-22cm) to 0.412ϕ (78-80cm) with an average of 0.593ϕ. About 76% of all samples were moderately well sorted whereas 16% and 8% were respectively well sorted and moderately sorted in their natures. This indicates the influences of stronger energy condition of depositing agents or prevalence of strong energy condition in the basin. The variation in mean size reveals the differential energy conditions, resulting in their deposition.

4.2.3 Skewness

It is used to determine the symmetry of the central part of the distribution. It reflects the symmetry or asymmetry of the frequency distribution of the sediments. It is the measure of particle size sizes as it indicates that particles in excess of the normal distribution are present in coarser fraction or finer fraction, extremes of the distribution. If the skewness is negative, the sample is coarsely skewed, that is the mean is towards the coarser side of the median. When the skewness value is positive the sample is described as finely skewed. Coarsely skewed sample implies that the velocity of the depositing agent operated at a higher value than the average velocity for a greater length of time than normal and / or the velocity fluctuations towards the higher values occurred more often than normal [9].

In the present study, the minimum and maximum skewness values are –0.370 ϕ (94-96 cm) to 0.464 ϕ(44-46 cm) respectively with an average value of 0.065 ϕ with representation of 36% near symmetrical, 30% of the sample fine skewed and 14% very fine skewed and 10% very coarse skewed and the rest of them are coarse skewed. From the analysis it was inferred that the middle and some bottom set of the sediments show slightly negative skewness values. The top sets show positive skewness. Thus it reflects the fluctuation of the energy conditions in the depositional environment. The positive skewness of sediments points to unidirectional transport (channel flow) or the deposition of sediments in sheltered low energy environment. Majority of negative values indicating near symmetrical multi direction of transport are deposition of sediments in agitated moderately energy environment.

4.2.4. Kurtosis

Kurtosis is a quantitative measure used to describe the departure from normality of distribution. Many curves designated as 'normal' by the skewness measure turns out to markedly non-normal when the kurtosis is computed. It is the ratio between the sorting in 'tails' of the curve to that of the central portion. Values of the fourth moment Kurtosis ranges between 0.761ϕ (80-82cm) to 2.961ϕ (70-72cm) with an average 1.089ϕ. 38% of the samples falls under mesokurtic, 34% are leptokurtic and 24% of the sample indicating platykurtic and rest of the samples very leptokurtic in nature of distribution. Characters infer that this part of the sediments is keeping the original character of sediments existed during deposition without any mixing of population or otherwise a single supply is maintained in this period of deposition. The mesokurtic to leptokurtic nature of sediments refers to the continuous addition of finer or coarser materials after the winnowing action and retention of their original characters during deposition.

According to Cadigan's verbal scale most of the sediments are moderately peaked. The leptokurtic nature of the sediments indicates the higher kurtosis values and the mixing of a predominant population with very minor amounts of coarser and finer materials [10]. The leptokurtic behavior of the sediments also indicates the variations of the energy conditions of the environmental setup of depositions of the sediments. The leptokurtic character reflects the extreme skewness values, either positive or negative, indicating concentration of coarser and finer grained materials finally showing the impact of fluctuation of energy condition in the deposition of the sediments from most of the formations. The accumulation of finer materials was by the influence of moderate to low energy conditions in the environmental setup showing the leptokurtic character of the sediments.

The mesokurtic character of the sediments indicates moderate winnowing action of the depositing agent. The mesokurtic nature of the sediments in the study area suggests that the sediments achieved good sorting in the high energy environment. The dominance of mesokurtic and leptokurtic characters of sediments in the study area revealed that the better sorted sediments were deposited by unidirectional flow of current and allows the sediments to settle in high energy environment.

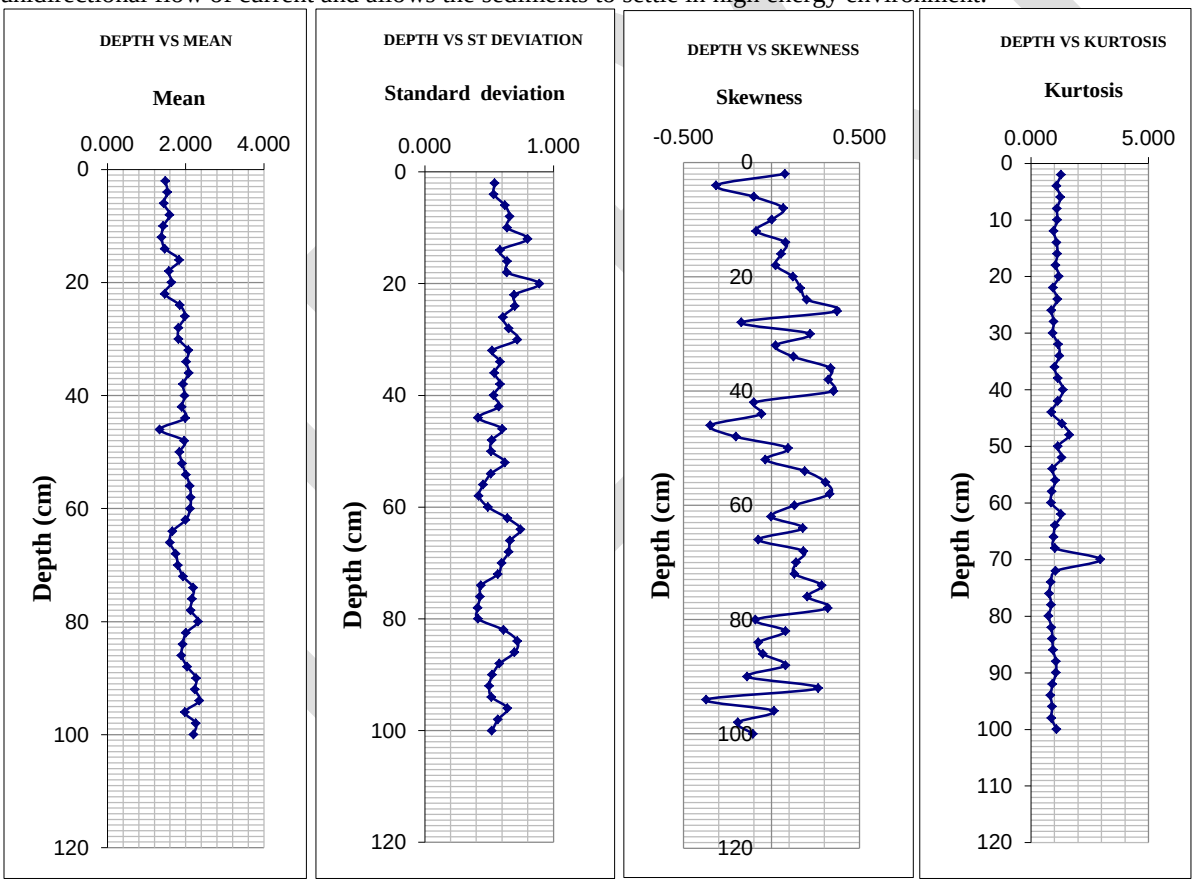

Fig-3. Vertical variation of Mean, Std. dev, Skewness and Kurtosis

The size analyses of the sediments from various locations show one surface creep, either one or two siltation and one suspension. About 95% of the samples exhibit the fine truncation at less than 95% and coarse truncation at about 5% and others exhibit the fine truncation more than 90% and coarse truncation below 10%. The steepness and truncation points of the sediments exhibit that they were deposited mostly by the back and forth motion of water. On the basis of probability curves the samples indicate that the coarser

grains are lacking and indicate a moderately high energy condition. The steepness of the curves of samples indicates that they were well sorted to very well sorted. The bottom sets of sediments clearly gives two well-defined saltated populations and having sharp contacts of curves in the fine and coarse truncation. This indicates that the sediments were deposited by the seasonal cyclic tidal waves by back and forth action. The histogram of size frequency distribution shows a bimodal or polymodal distribution (Fig-2) which in turn indicates a wide range of size distribution and asymmetrical nature of sediments. Some of the samples exhibit unimodal distribution also indicating good sorting, it means dominant of one fraction over the others. This also infers that the samples have received the sediments from different sources during seasonal and tidal variations.

4.3. Depositional Environment

Depositional sedimentary environment has been variously defined. A depositional environment can be defined in terms of physical, biological, chemical or geomorphic variables. Thus, a depositional sedimentary environment is a geomorphic unit in which deposition takes place. This is characterized by an unset of physical, biological and chemical processes operating at a specified rate and intensity which imparts sufficient imprint on the sediment. The character of a sediment so produced is determined both by the intensity of the formative processes operating on it and by the duration through which such action is continued .The study of physical factors (hydrodynamic condition), if combined with the study of biological and chemical factors provides a more complete picture of the sedimentary depositional environment [11].

A broad depositional environment may be subdivided into smaller, essentially uniform sub environment or sedimentation units, where sediments with their own characteristic features are deposited. These units in ancient sediments are lithosomes. As sedimentation proceeds, with time facial boundaries migrate laterally under the influence of transgression and regression, and different facies are arranged in an orderly sequence. Scientist Curray gives a thorough discussion on transgression-regression processes and their effect on coastal sediments. The products of transgression and regression depends upon various factors, such as rate and supply of sediments, intensity of hydrodynamic processes, configuration of basin of sedimentation, local tectonics and rate and direction of relative sea level changes. All these factors can be grouped into two parameters-(a) rate of deposition, and (b) rate and direction of relative sea level change. Curray constructed a diagram, that clearly shows that deposition and erosion can control the trangression-regression processes (Fig-3). In general rising of relative sea level results in transgression; falling relative sea level, in regression. Rapid rate of sedimentation as in the deltaic regime can forced regression or delta progradation.

The variation in the energy and the fluidity factors seems to have excellent correlation with different processes and the environments of deposition. In littoral (beach) zone there is constant pounding of waves making the beach deposits better sorted and more uniformly distributed than the shallow marine deposits where the wave action is less prominent and more variable. [9] introduced the linear discriminant functions for environmental interpretation and the method was the combination of all the grain size parameters into a single linear equation. Results of the functions were tabulated in Grain size parameters of all the sediments were substituted into the following equations.

Table- 2: Linear Discriminant Function Values according to Sahu

Sl. No	Depth	Y1	Remarks-Y1	Y2	Remarks-Y2	Y3	Remarks-Y3	Y4	Remarks-Y4
1	2	-4.197	Aeolian	42.660	Beach	-2.170	Shallow Marine	0.951	turbidity
2	4	-4.404	Aeolian	42.945	Beach	-2.089	Shallow Marine	0.990	Turbidity
3	6	-3.713	Aeolian	48.091	Beach	-2.989	Shallow Marine	0.885	Turbidity
4	8	-4.068	Aeolian	53.646	Beach	-3.373	Shallow Marine	0.973	Turbidity
5	10	-3.582	Aeolian	49.383	Beach	-3.192	Shallow Marine	0.866	Turbidity
6	12	-2.575	Beach	63.870	Beach	-5.225	Shallow Marine	0.742	Turbidity

7	14	-3.977	Aeolian	45.776	Beach	-2.609	Shallow Marine	0.923	turbidity
8	16	-5.035	Aeolian	55.754	Beach	-3.076	Shallow Marine	1.160	turbidity
9	18	-4.112	Aeolian	51.600	Beach	-3.138	Shallow Marine	0.973	turbidity
10	20	-2.912	Aeolian	78.118	Sh. Agitated water	-6.517	Shallow Marine	0.864	turbidity
11	22	-3.437	Aeolian	54.886	Beach	-3.837	Shallow Marine	0.863	turbidity
12	24	-4.789	Aeolian	61.387	Beach	-3.789	Shallow Marine	1.138	turbidity
13	26	-5.709	Aeolian	55.331	Beach	-2.673	Shallow Marine	1.282	turbidity
14	28	-4.928	Aeolian	56.555	Beach	-3.216	Shallow Marine	1.143	turbidity
15	30	-4.576	Aeolian	62.789	Beach	-4.047	Shallow Marine	1.105	turbidity
16	32	-6.378	Aeolian	50.561	Beach	-1.823	Shallow Marine	1.385	turbidity
17	34	-5.927	Aeolian	54.137	Beach	-2.433	Shallow Marine	1.317	turbidity
18	36	-6.332	Aeolian	51.933	Beach	-1.990	Shallow Marine	1.382	turbidity
19	38	-5.619	Aeolian	52.977	Beach	-2.478	Shallow Marine	1.255	turbidity
20	40	-6.003	Aeolian	49.872	Beach	-1.952	Shallow Marine	1.313	turbidity
21	42	-5.559	Aeolian	51.665	Beach	-2.374	Shallow Marine	1.239	turbidity
22	44	-6.475	Aeolian	42.514	Beach	-0.940	Shallow Marine	1.369	turbidity
23	46	-3.426	Aeolian	44.821	Beach	-2.804	Shallow Marine	0.818	turbidity
24	48	-6.007	Aeolian	48.764	Beach	-1.835	Shallow Marine	1.309	turbidity
25	50	-5.613	Aeolian	46.525	Beach	-1.814	Shallow Marine	1.227	turbidity
26	52	-5.374	Aeolian	55.497	Beach	-2.868	Shallow Marine	1.221	turbidity
27	54	-6.191	Aeolian	48.896	Beach	-1.751	Shallow Marine	1.343	turbidity
28	56	-6.764	Aeolian	46.632	Beach	-1.212	Shallow Marine	1.439	turbidity
29	58	-6.957	Aeolian	45.052	Beach	-0.946	Shallow Marine	1.468	turbidity
30	60	-6.656	Aeolian	49.066	Beach	-1.521	Shallow Marine	1.429	turbidity
31	62	-5.619	Aeolian	58.535	Beach	-3.052	Shallow Marine	1.279	turbidity
32	64	-3.875	Aeolian	62.600	Beach	-4.401	Shallow Marine	0.976	turbidity
33	66	-4.067	Aeolian	53.969	Beach	-3.407	Shallow Marine	0.975	turbidity
34	68	-4.667	Aeolian	55.412	Beach	-3.236	Shallow Marine	1.091	turbidity
35	70	-5.121	Aeolian	51.862	Beach	-2.628	Shallow Marine	1.159	turbidity
36	72	-5.700	Aeolian	51.532	Beach	-2.285	Shallow Marine	1.264	turbidity

37	74	-7.144	Aeolian	46.986	Beach	-1.046	Shallow Marine	1.510	turbidity
38	76	-7.049	Aeolian	46.071	Beach	-1.002	Shallow Marine	1.489	turbidity
39	78	-6.984	Aeolian	44.542	Beach	-0.879	Shallow Marine	1.471	turbidity
40	80	-7.645	Aeolian	47.578	Beach	-0.840	Shallow Marine	1.605	turbidity
41	82	-5.784	Aeolian	56.363	Beach	-2.739	Shallow Marine	1.300	turbidity
42	84	-4.958	Aeolian	64.228	Beach	-3.992	Shallow Marine	1.181	turbidity
43	86	-4.961	Aeolian	61.800	Beach	-3.739	Shallow Marine	1.172	turbidity
44	88	-6.033	Aeolian	54.314	Beach	-2.395	Shallow Marine	1.337	turbidity
45	90	-7.092	Aeolian	53.691	Beach	-1.766	Shallow Marine	1.529	turbidity
46	92	-7.076	Aeolian	51.604	Beach	-1.559	Shallow Marine	1.517	turbidity
47	94	-7.415	Aeolian	54.595	Beach	-1.687	Shallow Marine	1.592	turbidity
48	96	-5.547	Aeolian	58.208	Beach	-3.056	Shallow Marine	1.264	turbidity
49	98	-6.892	Aeolian	56.760	Beach	-2.190	Shallow Marine	1.505	turbidity
50	100	-6.850	Aeolian	52.458	Beach	-1.768	Shallow Marine	1.479	Turbidity

a. Y_1 (Aeolian; Beach): $-3.5688Mz+3.7016\sigma_1^2-2.0766Ski+3.1135K_G$

b. Y_2 (Beach; Sh.Marine): $15.6534Mz+65.7091\sigma_1^2+18.1071Ski+18.5043K_G$

c. Y_3 (sh.marine; fluvial): $0.2852\ M_Z - 8.7604\ \sigma_1^2 - 4.8932\ Sk_i + 0.0482\ K_G$

d. Y4 (Fluvial; turbidity): $0.7215\ M_Z - 0.4030\ \sigma_1^2 + 6.7322\ Sk_i + 5.2927\ K_G$

According to [9] the variations in the energy and fluidity factors seem to have excellent correlation with the different processes and the environment of deposition. Sahu's linear discriminant functions of Y1 (Aeolian, beach), Y2 (Beach, Shallow agitated water), Y3 (Shallow Marine, Fluvial) and Y4 (Turbidity, Fluvial) were used to decipher the process and environment of deposition. With reference to the Y1 values, 98% fall in Aeolian process and 2% fall in beach process. Y2 values 98% of the sample fall in Beach process and rest of the (2%) sample shallow agitated water. Further the samples (100%) Y3 indicate that they were the combination of shallow marine. Then Y4 values show that about 100% of the sample in Turbidity action. The results indicate that most of the sediments were deposited under shallow marine environment by beach and fluvial processes by a near shore whirlpool agitating turbidity action of water.

4.4. CM Pattern

[12] established the relation between texture of sediments and process of deposition using C – the coarsest 1 percentile grain size and M- the median. The C and M plotter in logarithmic paper enabled to distinguish the mode of transportation by means of sub population such as rolling, saltation and suspension. The time gap in the mode of transportation and the agent of deposition which also inferred. Passega divided the CM pattern into different sector namely NO, OP, PQ, QR and RS for different mode of transportation [12].

The plotted result of Nayakkankuppam coast sediments (Fig-4) shows that most of the samples fall in bottom suspension and rolling to rolling condition except in low tideline samples where it falls in rolling to bottom suspension condition. The comparison with the tractive current diagram, the berm samples fall in beach environment, the remaining samples fall in beach and tractive current environment, that is by interaction with wave actions.

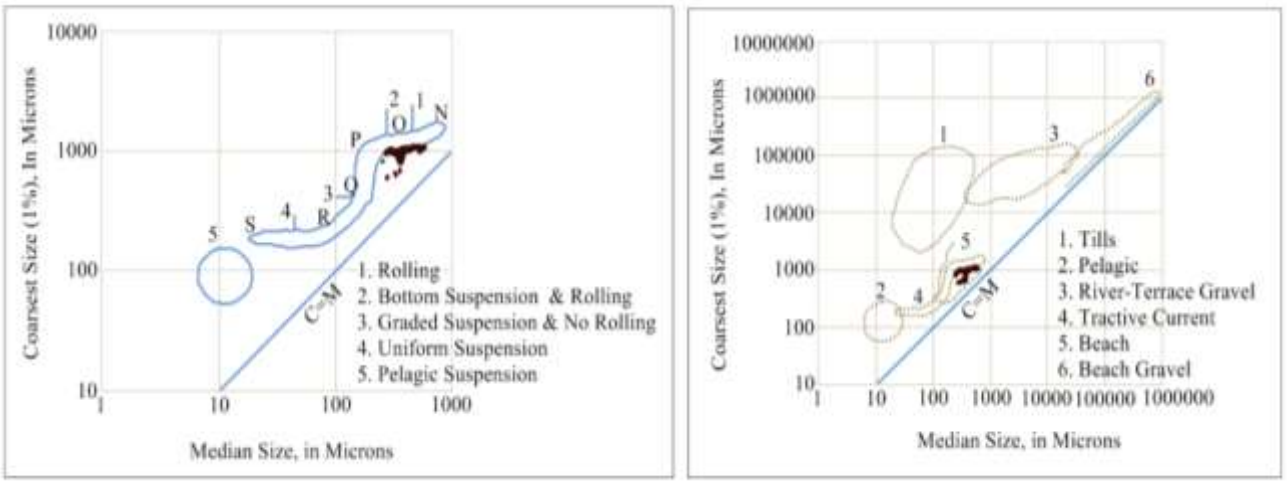

Fig-4: CM diagram (Passega, 1964) and tractive currents deposit plot for Nayakkankuppam coast Samples

5. CONCLUSION

The coastal zone of Tamilnadu is endowed with varied landscapes such as sandy beaches, backwaters, deltas, lagoons, mangrove forests and coral reef ecosystems. The coast has been constantly undergoing physical changes in the geological past and the present. The Tamilnadu coast is nearly 850 km long and has many major rivers draining into the Bay of Bengal and these rivers bringing in considerable sediments, both natural and anthropogenic in nature affecting the shore processes significantly. Thus the land-ocean interaction in the coastal zone is important in determining the sedimentation and erosion pattern of the coastline. With a view to observe the past sharp changes taken place in the coastal sediment characteristics, the sediments were analyzed by taking vertical pits at Nayakkankuppam coast. Granulometric analyses were carried out for the sediments collected at a vertical interval of 2 cm in each pit.

Textural analysis carried out for the sediments of the Nayakkankuppam coast reveals that inlet part is dominated by fine sand, central part is dominated by medium sand and outlet part is dominated by coarse sand. The grain size diagram to spatially highly distribute in the medium sand to fine sand. The standard deviation is the measure of sorting sediments and indicates the fluctuations in kinetic energy of the depositing agent about its average velocity. The Nayakkankuppam coast it is observed that most of the samples were falls in the moderately well sorted to well sorted nature. Skewness measures asymmetry of frequency distribution and marks the position of mean with respect to median. The fine skewed nature of the sediments clearly exhibits sediment input from various sources of tributaries. The finely skewed nature is also implies a low velocity than normal. This skewness data indicate that in the sediments nearly symmetrical to fine skewed the median class of the sediments dominate almost throughout their distribution. The kurtosis data indicate Mesokurtic to platykurtic. The CM pattern divulges that the sediments are transported bottom suspension and rolling as well as graded suspension. The comparison with the tractive current diagram, the berm samples fall in beach environment, the remaining samples fall in beach and tractive current environment.

REFERENCES:

[1] Armen, J.W. and Mc Cannel, B., 1977.Longshore sediment transport and sediment budget for the Malpleque barrier system, southern Gulf of St. Lawrence. Canadian Jour. *Earth Sci.*, 14: 2429-2439.

[2] Leupke, G., 1980. Opaque minerals an aid in distinguishing between source and sorting effect of beach sand mineralogy in south western Oregon. *Jour. Sed. Petrol.*, 50: 489-496.

[3] Mazullo, J., Ehrlich, R. and Hemming, M.A., 1984. Provenance and areal distribution of Late Pleistocene and Holocene quartz sand on the southern New England continental shelf. *Jour. Sed. petrol.*, 54: 1335-1348.

[4] McHendrie, 1988.US Geological Survey: marine geology grain -size program

[5] Inman DL, 1949.Sorting of sediments in light of fluid mechanics. Journal of Sedimentary Petrology 19:51-70

[6] Folk RL, Ward WC, 1957. Brazo river bar: A study in the significance of grain size parameters. Journal of Sedimentary Petrology 27:3-26.

[7] Rajmohan S. Singarasubramanian S.R., Suganraj K., Sundararajan M. and Rajganapathi. V.C. 2012.Textural characterization of vellar river along the east coast of India. International journal of current research. Vol.4, Issue, 07, pp.169-173, July, 2012.

[8] Friedman GM and Sanders JE, 1978.Principles of sedimentology. Wiley: New York.

[9] Sahu, B.K, 1964. Depositional mechanism from the size analysis of clastic sediments. Jour.Sedi. Petro., (34), 73-83.

[10] Mason C.C and Folk R.L, 1958. Differentiation of beach, dune and Aeolian flat environment by size analysis, Mustang Island, Texas. Jour. Sedi. Petrol., (28) 211-226.

[11] Reinick, H.E and Singh, I.B, 1980.Depositional sedimentary environment: With reference to terrigenous clastic. Springer, 549.

[12] Passega, R., 1964. Grain size representation by CM patterns as geological tool.Journal os Sedimentary Research. Vol.34 no.4 pp. 830-847.

[13] Erattupuzha, J.J and George V, 1980. Shoreline Changes on the Kerala coast: in geology and geomorphology of kerala.GSI.

[14] Christiansen .C. and Miller, J.T, 1980. Beach erosion at Klim, Den-mark-a ten year record, coastal Engineering.

[15] Erol, D, 1983. Historical changes on the coastline of turkey: in coastal problems of Mediterranean sea. Balagria, Italy,

[16] J.Neale and J Flenley, Pringle, A, 1981. Beach development and coastal erosion in Holderness, North Pimber side: Quaternary in Britain.

[17] Raj, J.K, 1982. Net directions and rates of present day beach transport by drift along the east coast of peninsular Malaysia,

[18] Bird, E.C.F and Schwartz,M.L, 1985. Worlds coastline, vannostrand Reinhold company,

[19] Peterson, C., Komar, P.D. and Scheidegger, K.F., 1986. Distribution, geometry and origin of heavy mineral placer deposits on Oregon beaches. *Jour. Sed. Petrol.*, 56: 67-77.

[20] Harold G. Reading, 1996. Sedimentary Environments: processes, facies and Stratigraphy. Blackwell Publishing Limited

International Journal of Engineering Research and General Science Volume 3, Issue 6, November-December, 2015
ISSN 2091-2730

IoT: The Age of Machine

Dharam J. Gami

Atmiya Institute of Technology and Science,

Gujarat Technological University, Gujarat

Email: dharam_gami@rediffmail.com

Abstract— IoT is not just a technology but it is an ideology or a concept which leads to a new age that is age of machine. IoT is the key to fully digitalize the world. Move towards IoT will revolutionise human life where machine-to-machine communication is emphasized and human interaction is minimized. IoT demands everything on internet and be controlled and managed by machine itself. The goal of this paper is to give an imagination and a Skelton of IoT. This paper also highlights the challenges in IoT implementation and other critical issues.

Keywords— IoT, age of machine, smart objects, IoT challenges, automation, architecture, open loop, RFID.

INTRODUCTION

The term IoT was first coined by Kevin Ashton in 1992 [7]. IoT don't have any exact or wildly accepted definition. We can explain IoT by saying that "IoT is a network of things, where thing refers to a smart object. Objects are embedded with electronics, software, sensors, and network connectivity, which enable these objects to collect and exchange data [7]. The idea is to connect every object via Internet and make them communicate. IoT is expected to offer advanced connectivity of devices, systems, and services that goes beyond machine-to-machine communications (M2M) and covers a variety of protocols, domains, and applications [12]. To do so, creating a new framework, infrastructure or technology is not feasible. So, IoT implementation needs to use existing infrastructure as well as existing technologies. IoT architecture has not been standardized yet as it will depend on involved technologies and scope of application.

Evolution Towards IoT

Internet started its journey by connecting computers where WWW was the top level service. Introducing social networking made revolution and connect people via internet [6]. Future internet will connect smart things which will be "internet of things". Moving towards "internet of computer" to "internet of things" involves many other technologies. IoT will require two main functions: Identification and networking. For identification purpose, RFID, NFC, barcodes and QRCode plays an important role [9]. RFID is considered as a batter candidate for object identification [1]. Evolution in network technologies like GPRS, GSM, UMTS, Wifi, WiMax, 3G and 4G change the human life style. IoT may use these technologies to connect things [5].
In a 2005 report the International Telecommunications Union (ITU) suggested that the "Internet of Things will connect the world's objects in both a sensory and intelligent manner" [8]. By combining various technological developments, the ITU has described four dimensions in IoT: item identification ("tagging things"), sensors and wireless sensor networks ("feeling things"), embedded systems ("thinking things") and nano-technology ("shrinking things").

IoT and Artificial Intelligence

It should be noted that, IoT does not possess any kind of decision making algorithm unlike AI. Ambient intelligence and autonomous control are not part of the original concept of the Internet of Things [7]. But IoT can be considered as the first step to AI. Protocols in IoT should have rigid boundary for decision making based on predefined algorithms and so it do not possess any intelligence.

Architecture of IoT

IoT architecture has not been standardized yet. But it should be event-driven and follow bottom-up approach (based on the context of processes and operations, in real-time)[7]. Basic and architecture of IoT is considered of three layers: (1)Perception layer (2)Network layer (3)Application layer [4]

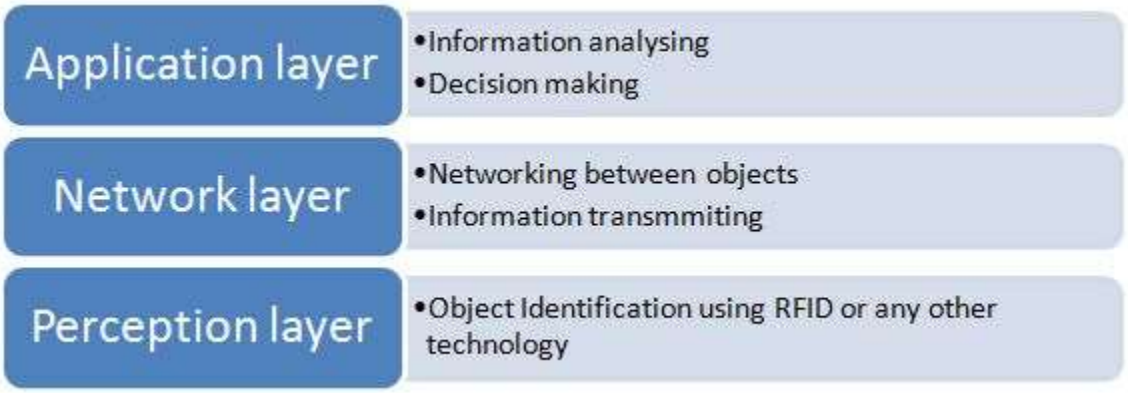

Figure 1: IoT Architecture

(1) **Perception layer:** Do object identification and information gathering using edge technology like RFID, Barcodes, NFC and sensor networks
(2) **Network layer:** The main function is to transmitting and processing information
(3) **Application layer:** This layer is combination of IoT's social division and industry demand to realize the extensive intellectualization. Processed information is analyzed and decisions are made

IoT architecture should possess the characteristics of SOA. However, some Basic requirements of Architecture of IoT are as follows:

(1) **Open loop:** closed loop architecture is design for particular application or particular technology and has boundary in its acceptance. For example traditional RFID architecture is closed loop where set of tags can only be read by set of readers [1]. One should relax this boundary by making the elements of architecture generally acceptable and by widen the scope of application.
(2) **Scalable:** in very near future there are millions of object will be deployed over internet and the growth rate is exponential. So the architecture must be enough scalable to accommodate all the objects without affecting the performance and efficiency of network.
(3) **Adaptable:** IoT need to accommodate and adapt existing technology as well upcoming technologies to achieve the goal. All applications do not of same types and so, based on demands and requirements IoT should adapt change in its architecture also.
(4) **Flexible:** To deal with different objects and process their information is very essential. Architecture should be flexible enough to deal with heterogeneous objects.
(5) **Reliable:** In IoT everything is on internet and communication is also through internet. Architecture should be reliable enough for object identification and message delivery

Challenges:

IoT demands open loop architecture which leads to expose everything to public. As well attacker may get more area to exploit.

(1) **Authentication:** object identification is the main function in IoT where authentication is critically important. Traditional cryptographic schemes are not appropriate for IoT [1][2]. Technology like RFID need very secure and lightweight authentication. In case of machine-to-machine communication, failure of authentication raises many problems and makes the architecture vulnerable to many kinds of attacks. Authentication is must for reliable communication.
(2) **Identity and privacy preservation:** open loop architecture exposes the identity to public which need to be preserved from misuse. Also, privacy must not be compromised. The question "who can access what" has a significant role in IoT[6]. Here who relates with identity and what relates with privacy.
(3) **Standardization:** IoT will deal with heterogeneous systems and networks. So, the role of each and every entity as well as the rules related to them should be defined and standardized [6]. Malfunction, anonymous and inefficient activity must be regulated by standardizing them.
(4) **Data flow:** IoT will consist billions of object. Information exchange between them produces tremendous traffic over internet. Regulate and analyse this traffic is very difficult but essential also.
(5) **Power consumption:** IoT will work on 6LoWPAN [7]. So, existing cryptographic scheme will solve many security issues but they are power consumptive which are not accepted in IoT. So, we cannot use them directly as they are. It is expected that IoT devices will be integrated into all forms of energy consuming devices [7]. Among cryptographic schemes, asymmetric key cryptography is more power consumptive than symmetric key cryptography [3]. Hash

functions are faster and will be the good choice for message authentication purpose rather than other cryptographic techniques [10].

The age of machine: criticism

In spite of the challenges discussed above, world move towards IoT rapidly. South Korea, Denmark and Switzerland have 37.9, 32.7 and 29 IoT devices online per 100 inhabitants respectively where as India have 0.6 devices online per 100 inhabitants [7]. IoT have billions of objects connected via internet. As well those are controlled and managed by the machine itself. Today also, people are machine dependent. They need machine in each and every step of life from day start to day end. One step ahead, IoT will make all these machines communicate with each other. In Today's life, machine is necessary but tomorrow, it will be the habit and the day after it, machine will be the synonym of life. In a different meaning, it will be the raise of machine age where machine will control the world. In a January 2014 article in Forbes, cybersecurity columnist Joseph Steinberg said that internet connected application can spy you in your own home [11] and IoT will play significant role in this if IoT will be implemented in its true meaning. Working principles of machine are different from human being as machine's decisions are rigid and lacking in intelligence. If our routine decisions will be made by machines then it will make human life more complex and complicated. Machine's decision is irrespective of human desire and may lead to unwanted and unnecessary events. This can be solved if we bring IoT and Artificial Intelligence together but this solution will raise many questions.

CONCLUSION

IoT is coming with lots of challenges, controversies and criticisms. It will save time and human effort but also makes human life machine dependent. RFID is a pivotal technology for object identification. To enable IoT, architecture should be made open loop and adaptive.

REFERENCES:

[1] Imran Erguler "A potential weakness in RFID-based Internet-of-things systems" Pervasive and Mobile Computing 20 (2015) 115–126, Elsevier.
[2] Gope P, Hwang T "lightweight authentication protocol preserving strong anonymity for securing RFID system" Computers and Security (2015), Elsevier .
[3] Sadaqat Ur Rehman, Muhammad Bilal, Basharat Ahmad, Khawaja Muhammad Yahya, Anees Ullah, Obaid Ur Rehman "Comparison Based Analysis of Different Cryptographic and Encryptions Techniques Using Message Authentication code (MAC) in Wireless Sensing Network(WSN)" IJCSI International Journal of Computer Science Issues, Vol. 9, Issue 1, No 2, January 2012.
[4] Miao Wu, Ting-lie Lu, Fei-Yang Ling, ling Sun, Hui-Ying Du "Research on the architecture of Internet of things" 2010 3rd International Conference on Advanced Computer Theory and Engineering(ICACTE).
[5] Lu Tan, Neng Wang "Future Internet: The Internet of Things" 2010 3rd International Conference on Advanced Computer Theory and Engineering(ICACTE).
[6] Louis COETZEE, Johan EKSTEEN "The Internet of Things – Promise for the Future? An Introduction" IST-Africa 2011 Conference Proceedings.
[7] https://en.wikipedia.org/wiki/Internet_of_Things .
[8] International Telecommunications Union, ITU Internet Reports 2005: "The Internet of Things", Executive Summary, Geneva: ITU, 2005.
[9] Techvibes From M2M to The Internet of Things: Viewpoints From Europe 7 July 2011.
[10] Helena Rifa-Pous, Jordi Herrera-Joancomartı "Computational and Energy Costs of Cryptographic Algorithms on Handheld Devices" Future Internet 2011, 3, 31-48; doi:10.3390/fi3010031.
[11] Joseph Steinberg (27 January 2014) "These Devices May Be Spying On You (Even In Your Own Home)", Forbes.
[12] J. Höller, V. Tsiatsis, C. Mulligan, S. Karnouskos, S. Avesand, D. Boyle: From Machine-to-Machine to the Internet of Things: Introduction to a New Age of Intelligence. Elsevier, 2014, ISBN 978-0-12-407684-6.

International Journal of Engineering Research and General Science Volume 3, Issue 6, November-December, 2015
ISSN 2091-2730

Flux of tissue substrates in *Danio rerio* exposed to raw tannery effluent

Sivakumar P.[1], Kanagappan M.[2] and Sam Manohar Das S.[3]

[1]Research Scholar, Department of Zoology, Scott Christian College (Autonomous), Nagercoil, India.
[2]Associate Professor, Department of Zoology, Scott Christian College (Autonomous), Nagercoil, India.
[3]Associate Professor, Department of Zoology,Scott Christian College (Autonomous), Nagercoil, India.

Corresponding author: capeparam@rediffmail.com

Abstract -The present study in raw tannery effluent is to investigate the biochemical parameters in the gill, muscle and liver of *Danio rerio*. The study is conducted to determine the carbohydrate, protein and lipid content in the muscle, liver and gills of *Danio rerio* exposed to sublethal concentration of tannery effluent for 45 and 90 days. The results showed significant decrease in the carbohydrate, protein and lipid content levels in exposed fish, *Danio rerio* after 45 and 90 days exposure when compared with control, it was concluded that the effect of the presence of toxic substance in the tannery effluent on different organs act differently depending on the duration of exposure time.

Key Words: Tannery effluent, Muscle, Gill, Liver, Protein, Lipid, Carbohydrate, *Danio rerio.*

1. INTRODUCTION

Industrial effluent or waste is a great menace not only to the health of human race but also to the entire living organism all over the world. Industrial effluent mainly contributes to aquatic pollution containing a vast array of toxic substances including heavy metals [1, 2]. It leads to alteration in physical, chemical and biochemical properties of water bodies as well as environment.

The industrial wastes generally contain high quantities of dissolved and suspended solids, organic and inorganic chemicals, high BOD and COD, oil and grease, besides toxic metals which cause deleterious effects on the freshwater fish when discharged in to water bodies. The problem of environmental pollution and its deleterious effects on aquatic biota, including fish is receiving focus during the last few decades [3, 4].

Tannery effluent is one of the hazardous pollutants of the industry and the effluents are ranked as the highest pollutants among all industrial wastes [5, 6].Through the excessive organic load present in tannery waste the oxygen content of the waters is depleted and leads to the death of fish and other aquatic animals. These effluents contain toxic chemicals such as sulfides, chromium salts and other substances, including heavy toxic trace metals that turn tannery effluents into noxious wastewaters [7, 8].

The untreated effluent containing chromium from the tanneries are discharged into fresh water bodies affected the aquatic organisms. Chromium is one of the highly toxic heavy metal to aquatic fauna. Heavy metals concentration in the tissues of fish enters into human beings through food chain and causes potential health hazards sometimes lethal [9].

Fish population is generally considered to be very sensitive to all kinds of environmental stressors to which they are exposed. Gills, liver and muscle are the primary target organs. Effects of tannery effluents on the muscle and liver glycogen in fish *Sarotherodon mossambicus* [10]. The biochemical changes occurring in the body give early indication of stress [11]. During the stress an organism needs sufficient energy which is supplied from reserve materials like, protein, lipid and glycogen. If the stress is mild, then only stored glycogen is used as a source of energy, but when the stress is strong, then the energy stored in lipid and protein will be used. Proteins are highly sensitive to heavy metals and are one of the earliest indicators of heavy metals poisoning. The impairment in protein synthesis due to heavy metal stress was reported by many investigators [12, 13]. Measurement of total protein provides an insight on the biochemical mechanism of metabolism under stressful conditions [14].

Considering the above facts, the present study is aimed to assess the effect of industrial effluents on the biochemical composition of gill, liver and muscle of the fish *Danio rerio.*

2. MATERIALS AND METHODS

2.1 Collection of Sample

The test fish *Danio rerio* (*D.rerio*) of length 4.7 ± 1.0 cm and 3.9 ± 1gm of body weight were collected from Nagercoil J.J. aqua farm in Kanyakumari district and acclimated to the laboratory conditions for 30 days. The medium was changed once in two days and no mortality of fishes was recorded during the period of investigation.

2.2 Collection of Effluent

The tannery effluent was collected from a tannery at Ambur, Vellore District in Tamil Nadu. Only the raw effluent was used for the study. Various parameters of the tannery effluent and the water sample from the laboratory were also analyzed.

2.3 Bio-chemical Analysis

2.3.1 Estimation of total proteins

About 50mg of muscle, liver and gill were dissected out from the fish were homogenized in 5ml of 25% of trichloroacetic acid buffer, precipitated with 10ml of 80% ethanol and centrifuge at 1000rpm for 15 min. The tissue sample was homogenized and was treated with ethanol. The precipitate was dissolved in 10ml of 1N NaOH solution and was used for total protein estimation. The results were expressed as mg protein/g wet tissue. Total protein content of the selected tissues was estimated by the method of Lowry using bovine serum albumin as standard [15].

2.3.2 Estimation of carbohydrates

Sulphuric acid (66% [v/v]) containing 50mg of anthrone and 1gm of thiourea were prepared fresh for every experiment to determine the total carbohydrates present in the sample. Standard stock glucose solution was prepared by dissolving 100mg of glucose in 100mg of standard benzoic acid. The samples were de proteinzed with 80% ethanol and centrifuged at 1000g for 10min. The clear supernatant was used for the carbohydrate estimation following the method of Roe using anthrone reagent [16].

2.3.3Estimation of Lipids

50mg of wet tissue was homogenated with 1 to 5 ml of chloroform with tissue homogenizer. It was centrifuged at 1000rpm for 10 min. The supernatant was collected and evaporated to dryness. To this, 3ml of potassium dichromate was added and read at 620nm. The dichromate reagent was prepared by dissolving 2gms of potassium dichromate in 100ml of concentrated sulphuric acid [17].

3. RESULT

3.1 Total Protein content

The protein levels in Muscle, gill and liver of *D. rerio* exposed to sub-lethal concentration of tannery effluent showed significant decrease when compared to control fish. The decrease in muscle, gill and liver *D. rerio* protein levels were more pronounced at 90 days of exposure periods (Table :1). The total protein concentration of muscle, gill and liver was 38,18 and 23 mg/100mg wet tissue for 45 days and it decrease from control fishes and 33, 15 and 20 mg/100mg wet tissues showing a significant decrease from control at the end of 90 days exposure respectively. The mean difference were statistically significant at $P \leq 0.05$ level. (Fig. 1).

3.2 Total Lipid content

During sublethal exposure of tannery effluent, total lipid level in serum significantly decreased in experimental fish than the control (Table:2). The total lipid concentration of Muscle, gill and liver was 45,34 and 27 mg/100mg wet tissues and it decrease from control fishes exposed for 45 days and 38, 23 and 22 mg/100mg wet tissue showing a significant decrease from control at the end of 90 days exposure respectively. The mean difference between control and experimental groups were statistically significant at $P \leq 0.05$ level. (Fig. 2).

3.3 Total Carbohydrate content

The total carbohydrate concentration of Muscle, gill and liver of the exposed fishes was 29, 24 and 26 mg/100mg wet tissues and it decrease from control in fishes exposed for 45 days and 27, 20 and 23 mg/100mg wet tissues showing a significant decrease from control at the end of 90 days exposure respectively (Table:3). The mean difference between control and experimental groups were statistically significant at $P \leq 0.05$ level. (Fig.3).

Table -1 : Protein level in selected tissues of *D. rerio* exposed to untreated tannery effluent (mg/100mg wet weight of tissue)

Days in Exposure / Different Tissues	Muscle	Gill	Liver
Control	41 ± 1.4	20 ± 1.5	25 ± 2.0
45 days	38 ± 1.6 (-7.3%)*	18 ± 2.0 (-10%)	23 ± 2.0 (-8%)
90 days	33 ± 2.2 (-19.5%)*	15 ± 3.2 (-25%)*	20 ± 2.9 (-20%)*

* Significant difference ($p \leq 0.05$)

[Each value indicate the mean (x±SD) of five estimations]

Table - 2 : Lipid content in selected tissues of *D. rerio* exposed to untreated tannery effluent (mg/100mg wet weight of tissue)

Days in Exposure / Different Tissues	Muscle	Gill	Liver
Control	49 ± 2.5	40 ± 2.2	30 ± 2.5
45 days	45 ± 1.9 (-8.2%)	34 ± 1.5 (-15%)*	27 ± 1.6 (-10%)*
90 days	38 ± 1.5 (-22.5%)*	23 ± 1.8 (-42.5%)*	22 ± 1.4 (-26.6%)*

* Significant difference ($p \leq 0.05$)
[Each value indicate the mean (x±SD) of five estimations]

Table -3 : Carbohydrate content in selected tissues of *D. rerio* exposed to untreated tannery effluent (mg/100mg wet weight of tissue)

Days in Exposure / Different Tissues	Muscle	Gill	Liver
Control	30 ± 1.9	30 ± 1.0	30 ± 1.0
45 days	29 ± 1.6 (-3.3%)	24 ± 1.6 (-20%)*	26 ± 1.4 (-13.3%)*
90 days	27 ± 3.5 (-10%)*	20 ± 1.5 (-33.3%)*	23 ± 1.8 (-23.3%)*

* Significant difference ($p \leq 0.05$)
[Each value indicate the mean (x±SD) of five estimations]

Figure 1: Changes in the protein level in selected tissues of *D. rerio* exposed to untreated tannery effluent (mg/100mg wet weight of tissue)

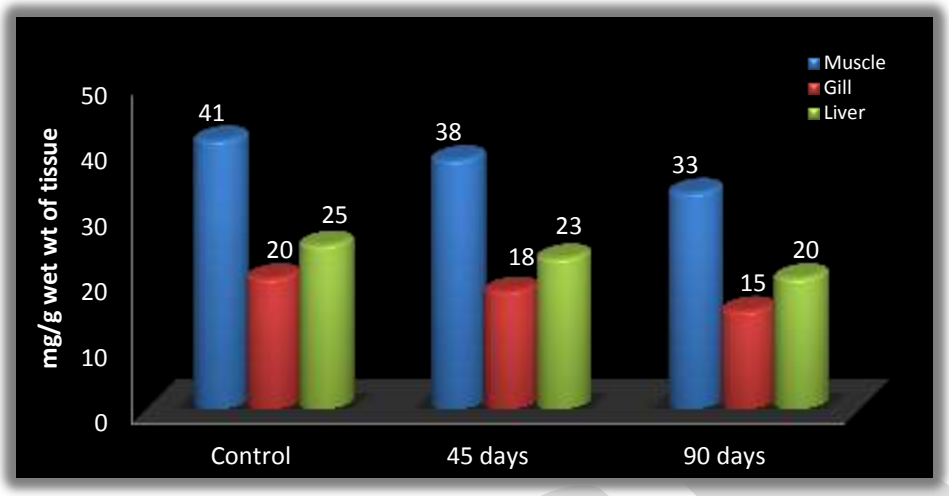

Figure 2: Changes in the lipid content in selected tissues of *D. rerio* exposed to untreated tannery effluent (mg/100mg wet weight of tissue)

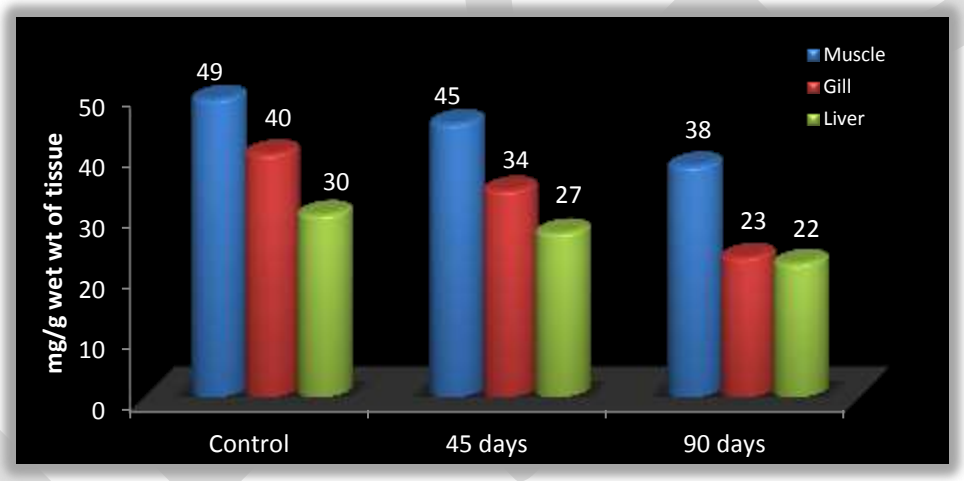

Figure 3: Changes in the carbohydrate content in selected tissues of *D. rerio* exposed to untreated tannery effluent (mg/100mg wet weight of tissue)

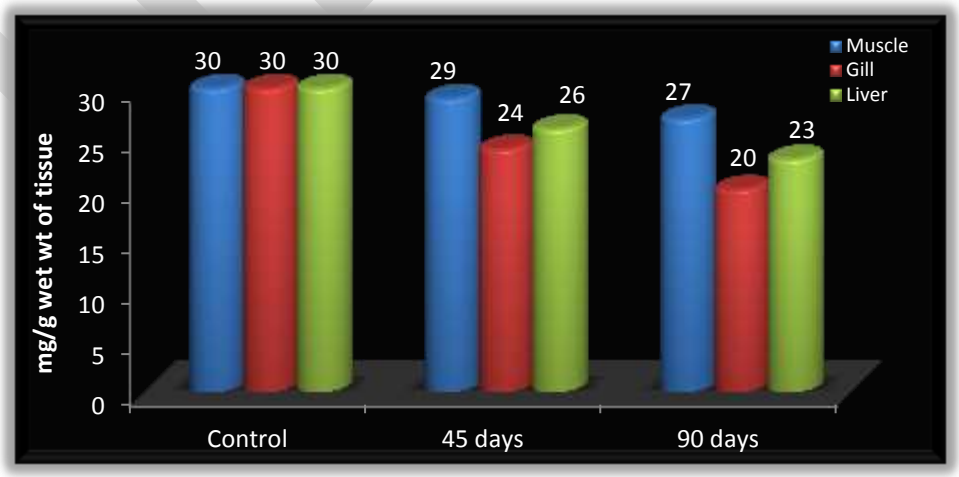

4. DISCUSSION

The observations from the present study showed that, the tannery effluent at sublethal concentrations altered the biochemical composition (Carbohydrate, Protein and Lipid) of the various organs of test fish, due to utilization of biochemical energy to counteract the toxic stress caused due to heavy metals present in effluents.

Heavy metal poisoning induced physiological and biochemical changes in the liver of an animal can be regarded as an index for the identification of pollutant stress [18]. The depletion of protein level induces diversification of energy to meet the impending energy demands during the toxic stress. The reduction in tissue proteins reflects a prior increased energy cost of homeostasis, tissue repair and detoxification under toxic stress. It is also possible that when an animal is under toxic stress, diversification of energy occurs to accomplish the impending energy demands. Hence depletion in protein level is observed [19].

The decrease in total protein level in liver and muscle of *Channa punctatus* exposed to monocrotophos for 15, 30 and 60 days [20]. A significant decrease was reported in the protein content in almost all tissues in *Channa punctatus* when exposed to sublethal and lethal concentration of fenvalerate [21]. The decrease in protein content in rainbow trout (*Oncarhynchus mykiss) was* due to contaminated environment condition [22].

The reduction in the glycogen levels in the tissues of fry of common carp, *Cyprinus carpio* (Linn) was reported [23]. This may be due to generalized disturbances in carbohydrate consumption [24]. The reduction in protein, glycogen and lipid in tissues of freshwater fish *Labeo rohita* induced by heavy metals from electroplating industry [25]. Decrease in the level of tissue protein may be due to excessive proteolysis to overcome the metabolic stress, as deposited protein in the cytoplasm can easily be used to replace the loss of proteins that occur during physiological stress [26].

Biochemical changes occurred in *Cyprinus carpio* in response to nickel and lead [27]. Effects of mercury and cadmium on proteins and enzymes in *Oreochromis mossambicus* [28]. Effects of copper and mercury on the glycogen and protein contents of liver and muscle of the fish *Macrones gulio* [29].

Decreased content of the carbohydrate was probably due to glycogenolysis and utilization of glucose to meet increased metabolic cost [30]. Decreased in carbohydrate content might indicate an immediate utilization to meet the excess demand of energy under toxic stress of tannery effluent. This condition happened by rapid glycogenolysis and inhibitions of glycogenesis through activation of glycogen phosphorylase and depletion of glycogen transferase respectively or through stress induced increase in catacholamines.

Carbohydrate depletion is more prevalent under hypoxic conditions due to toxic stress [31,32]. The decline in protein showed, an intensive proteolysis which in turn could contribute to increase of free amino acids to enter into TCA cycle as keto acids thus supporting the view of Jha [33]. The level of protein, carbohydrates and lipid contents were gradually decreased in the fish *Oreochromis mossambicus* reared at the sublethal concentration of textile dye effluent [34].

Decrease in total lipid content might be due to utilization of lipids during the toxic stress[35] and Insecticides are found to reduce the concentration of lipids in the tissues of fishes [36,37]. The endogenous fat in animal is found to be the only source of energy during prolonged stress. Thus, the reduced level of total lipids in the blood of the species under study is the indicative of the utilization of the same to meet the energy demand during the stress caused by the tannery effluent.

Decrease in protein might be due to inhibition of protein synthesis or increase in the rate of degradation of amino acids [38,39] which may be entered into tricarboxylic acid (TCA) cycle through aminotransferases, probably to cope up with high energy demands in order to meet the stress condition. The fall in protein level during exposure might be due to increased catabolism and decreased anabolism of proteins.

The biochemical substances, such as proteins, carbohydrate and lipid play a role in the tissue construction and energy production. In the present investigation protein, carbohydrate and lipid contents in different tissues of *D.rerio*, which were exposed to sublethal (4.5ppm) concentration of raw tannery effluent showed decrease protein, carbohydrate and lipid contents in muscle, gill, and liver at 45 and 90 days of exposure. The present observations revealed that the decline in the protein, lipid and carbohydrate level in different tissues was directly proportional to the exposure days.

5. CONCLUSION

In the present study, it was observed when the muscle, gill and liver of *D.rerio* were kept in sublethal concentration of raw tannery effluent showed decrease in protein, carbohydrates and lipid contents under different period of exposure.

REFERENCES:

[1] Ghem, T, T. Balogun, J.K.,Lawaland F,Aand Annune P A. "Trace metal accumulation in *Clarias garipinu*s exposed to sublethal level of tannary effluent", Sci. Total. Environ., 271,1-9(2001).

[2] Woodlings, J.D., Brinkman SF and Horn BJ. "Non uniform accumulation of Cd and Cu in kidneys of wild brown trout *Salmo trutta* populations", Arch. Environ. Contam. Toxicol. 40, 318-385(2001).

[3] Jagadeesan g., Jebanesan,A.,Mathivanan,A. "In vivo recovery of organic constituents in gill tissue of *Labeo rohita* after exposure to sub lethal concentrations of mercury", J.Exp.Indelleriia.,3, 22-29 (2001).

[4] Zikic R.V and Stajn S. "Activities of superoxide dismutase and catalase in eryththrocyte and plasma transaminases of gold fish (*Carrasius auratus*) exposed to Cadmium", Physiol. res.,50, 105-111 (2001).

[5] Deepali, K. Gangwar, K. and Joshi, B. D. "Comparative Study of Physico-Chemical Properties of Effluent from Tannery Industries", Indian Journal of Environmental Sciences, 3(2) 49-152 (2009).

[6] Belay, A.A. "Impacts of Chromium from Tannery Effluent and Evaluation of Alternative Treatment Options", Journal of Environmental Protection, 1, 53-58(2010).
[7] Ates, E., Orhon, D., Tunay, O. "Characterization of tannery wastewater for retreatment-Selected Case Studies", Water Science and Technology, 36, 217–223(1997).
[8] Cooman, K. Gajardo, M., Nieto, J. "Tannery waste water Characterization and toxicity effect on Daphnia sp.", Environmental Toxicology, 18, 45 -51 (2003).
[9] El-Shehawi A M., Ali F K and Seehy M A. " Estimation of water pollution by genetic biomakers in tilopia and cat fish species shows species site interaction", Afr. J. Biotech., 6,840-846 (2007).
[10] Natarajan, A.V. "Effects of tannery effluents on the muscle and liver glycogen in a fish *Sarotherodon mossambicus*", The Indian Zoologists, 13(1,3), 147-151(1989).
[11] Mayer, F. L., Versteeg, D. J., Mckee, M. J., Folmar, L. C., Graney, R. L., McCume, D. C. and Rattner, B. A. Physiological and nonspecific biomarkers. In: Huggett, R. J., Kimerle, R. A., Mehrle, Jr. P. M. Bergman, H. L. (Eds.). Biomarkers; Biochmeical, Physiological, and Histological Markers of Anthropogenic Stress. *Lewis publishers*, Chelsea, USA,5-85 (1992).
[12] Jacobs JM, Carmichael N, Cavanagh JB. "Ultrastructural changes in nervous system of rabbits poisoned with methyl mercury", Toxicol Appl Pharmacol,39, 249–61 (1977).
[13] Syversen TL. "Effects of methyl mercury on protein synthesis in vitro", Acta Pharmacol Toxicol (Copenh), 49, 422–426 (1981).
[14] Keiltey, T. 1. and Stehly, G. R. "Preliminary investigation of protein utilization by an aquatic earthworm in response to sublethal stress", Bull. Environ.Contam Toxicol.,43, 350-354(1989).
[15] Lowry, O. H., Rosenbrough, N. J., Farr, W. L. and Randall, R. J. "Protein measurements with the folin-phenol reagent", J. Biol., Chem.,193, 265–275(1951).
[16] Roe, J. R. , "The determination of sugar in blood and spinal fluid with anthrone reagent", J . Biol. Chem., 20,335-343(1955).
[17] Bragdon, J. H., "Colorimetric determination of blood lipids", J. Biol. Chem. 190, 513(1951).
[18] Bose, S, Mukhopadhyay, B, Shibani Chaudhury and Bhattacharya "Correlation of metal distribution, reduced glutathione and metalothionein level in liver and kidney of rat", Ind. J. Exp. Biol, 32, 679-681(1994).
[19] Neff, J.M. "Use of biochemical measurements to detect pollutant – mediated damage to fish" In : Cardwell, R.D., Purdy, R., Bahner, R.C., Eds. Aquatic toxicology and hazard assessment. Philadelphia, American Society for testing Materials, 155-181(1985).
[20] Sastry, K.V. and Dasgupta, A. "Effect of Nuvacron on the Kidney of a fresh water teleost, *Channa punctatus*", J. Environ. Biol., 12(13), 243-248(1991).
[21] Tilak, K.S.; K. Satyaradhan and P.B. Thathaji "Biochemical changes induced by fenavalerate in the freshwater fish, *Channa punctatus.*", J. Ecotoxico. Environ. Moni., 13(4), 261-270(2003).
[22] Atamanlp, M, Keles, M.S., Haliloglu, H.I and Aras, M.S. "The effect of cypermethrin (asynthetic pyrethroids) on some biochemical parameters(Ca,P,N and TP) of rainbow trout (*Oncorhynchus mykiss*)", Turk J.Vet Anim Sci., 26,1157-1160(2002).
[23] Reddy, S.A., Reddy, V.M. and Radhakrishnaiah, K. "Impact of Cu on oxidative metabolism of fry of Common Carp, *Cyprinus carpio* (linn.) at different pH", J Environ. Biol.,29(5) 721-724 (2008).
[24] Simon L.M., Nemcsok J. and Boross, L. "Studies on the effect of paraquate on glycogen mobilaztion in liver of Common carp *Cyprinus carpio* L", Comp Biochem Physiol 75C(1),167-169 (1983).
[25] Muley DV.,Karanjkar DM., Maske SV. "Impact of industrial effluents65Muley on the biochemical composition of Fresh water fish *Labeo rohita*", J. Environ. Biol., 28(2) 245-249 (2007).
[26] Patil, A .G. "Protein changes in different tissues of freshwater bivalve Parreysia cylindrical after exposure to indoxacarb", Recent Research in Science and Technology",3(3),140-142 (2011).
[27] Cyril Arun Kumar, L. Anusha Amali, A. Selvanayagam, M. "Biochemical dynamics in *Cyprinus carpio* communis (Linn) in response to heavy metals nickel and lead", Indian.J. Environ. Toxicol.,3(1&2),35-38 (l993).
[28] Rema, L. "Biochemical responses to heavy metals in *Oreochromis mossambicus* (Peters) with special reference to metal and detoxifying mechanism", Ph.D thesis, Division of marine biology, Cochin University of Science and Technology, l-200 (1995).
[29] Asha. "*Effects of Mercury and copper on fish Macrones gulio*", Ph.D Thesis, Cochin University of Science and Technology, Kochi-16, Kerala. l-150 (2001).
[30] Viswarajan S, Beena S and Palaveesam S. "Effect of tannic acid on the protein, carbohydrate and lipid levels in the tissues of the fish *Oreochromis mossambicus*", Environ. and Ecol. 6 (2), 289-292 (1988).
[31] Dezwaan A and Zandee DT. "The utilization of glycogen accumulation of some intermediates during anaerobios in *Mytilus edulis* L.", Comp. Biochem. Physiol. 43B,47-54 (1972).
[32] Chandrawathy M and Reddy S.L.N, "In vivo effects of lead acetae on dehydrogenase activities and metabolites in the freshwater fish, *Anabuss candens*", J. Ecotoxicol. Environ. Monit. 5(2), 107-111 (1995).
[33] Jha, B.S. "Alteration in the protein and lipid content of intestine, liver and gonads in the lead exposed freshwater fish *Channa punctatus* (Bloch)", J. Environ. Ecoplan., 2(3), 281-284 (1991).
[34] Baskaran, P. and Palanichamy, S. "Impact of agricultural (ammonium chloride) fertilizer on physiology and biochemistry of freshwater teleost fish, *Oreochromis mossambicus*", *J.Ecobiol*., 2, 97-106 (1990).

[35] Tantorpole, T.V., Pawar, A.H. and Kulkami, K.M. "Influence of cythion on total lipids in liver of the frog,*Ranacyano phlyctis*". J. Aquat. Biol., l8(l), 95-96 (2003).

[36] Jebakumar, S.R.D., S.D.J. Flora., R.M. Ganesan., G. Jagathesan and J. Jayaraman "Effect of short term sublethal exposure of cypermethrin on the organic constituents of the fresh water fish *Lepidocephalichthys thermalis*". J. Environ. Biol.,11(2):203-209 (1990).

[37] Govindan, V.S., L. Jacon and R. Devika, "Toxicity and metabolic changes in *Gambusia affinis* exposed to phosphomidon". J. Ecotoxicol. Environ.Monit.4(1),1-6(1994).

[38] Ganeshwade, R. M. "Biochemical Changes Induced by Dimethoate in the Liver of Fresh Water Fish *Puntius Ticto* (HAM)", Biological Forum. An International Journal, 3(2),65-68(2011).

[39] Binukumari, S. and J. Vasanthi, "Changes in cholesterol content of the freshwater fish, *Labeo rohita* due to the effect of an insecticide 'encounter' (herbal plant extract)",*IJPSR*, 5,397-399 (2014).

International Journal of Engineering Research and General Science Volume 3, Issue 6, November-December, 2015
ISSN 2091-2730

Time-Dependent Key Generation Method Based on Secure Wireless Communication

Remya M Nair

Assistant Professor, Dept. of ECE, SHM Engineering college Kollam, India

remyamn27@gmail.com

Abstract— Security is an important issue in wireless communication systems as the wireless channel is unguided. Cryptographic techniques in the wired communication may be used to secure the wireless communication, but the characteristics of radio channel are not exploited efficiently. This project presents a synchronized random key generation for each node which depends on the clock time. So there is no need any key transfer. Key generation protocol is used here. Key generation protocol depends on the global timing method. Here we use base station time as a global time. Pseudo random number creation depends upon the time and the initial value of linear feedback shift register. So each and every second create a new key. So the level security is too high and power consumption is very low.

Keywords— cryptography, wireless communication, Encrypt, decrypt, network security, shift register, GPS, MATLAB

INTRODUCTION

The development of wireless communications and wireless networks is very rapid in recent years, varieties of wireless applications continue to emerge. However, it is more difficult to secure wireless communications than wired communications as the wireless channel is unlimited. Securing the wireless communication is an extremely important aspect almost in every wireless communications system.

The classical cryptography is used to secure the wired communication. Two types of cryptographic techniques are used: public key cryptography and secret key cryptography. The transmitter converts the plaintext to encrypted message using public or private keys in the application layer. However, distributed parallel computing makes the public key cryptography become unsafe. Hence, the security of private keys determines the security of the systems for the secret key cryptography.

The basic idea is that the node receives a random vector and a master key before deployment. Any two nodes are able to establish their pair wise key by combining their vectors with the master key. In this way, the proposed scheme solves three problems: the node establishes its pair wise keys independently, rather than search for it passively; as a result, any two nodes could establish a pair wise key, and the problem on connectivity is solved. By using a random vectors and a master key to establish the pair wise keys, the node needn't store a lot of keys. Therefore, the memory overhead has been reduced. As the probability that any two nodes receive the same vector in network is quite low, it can be make sure that all the pair wise keys are different with each other, so the network's resilience to the capture attack has been enhanced.

LITERATURE SURVEY

Wireless Communication

Wireless communication is, by any measure, the fastest growing segment of the communication industry. As such, it has captured the attention of the media and the imagination of the public. Cellular phones have experienced exponential growth over the last decade, and this growth continues unabated worldwide, with more than a billion worldwide cell phone users projected in the near future. Indeed, cellular phones have become a critical business tool and part of everyday life in most developed countries, and are rapidly supplanting antiquated wire line systems in many developing countries.

In addition, wireless local area networks are currently poised to suppliment or replace wired networks in many businesses and campuses. Many new applications, including wireless sensor networks, automated highways and factories, smart homes and appliances, and remote telemedicine, are emerging from research ideas to concrete systems. The explosive growth of wireless systems coupled with the proliferation of laptop and palmtop computers indicate a bright future for wireless networks, both as stand-alone systems and as part of the larger networking infrastructure. However, many technical challenges remain in designing robust wireless networks that deliver the performance necessary to support emerging applications.

Network Security

In the field of networking, the special area of network security consists of the provisions and policies adopted by the network administrator to prevent and monitor unauthorized access, misuse, modification, or denial of the computer network and network-accessible resources .The terms network security and information security are often used interchangeably. Network security is generally taken as providing protection at the boundaries of an organization by keeping out intruders (hackers). Information security, however, explicitly focuses on protecting data resources from malware attack or simple mistakes by people within an organization by use of data loss prevention (DLP) techniques. One of these techniques is to compartmentalize large networks with internal boundaries.

The terms network security and information security are often used interchangeably. Network security is generally taken as providing protection at the boundaries of an organization by keeping out intruders (hackers). Information security, however, explicitly focuses on protecting data resources from malware attack or simple mistakes by people within an organization by use of data loss prevention (DLP) techniques. One of these techniques is to compartmentalize large networks with internal boundaries.

Network security starts from authenticating the user, commonly with a username and a password. Since this requires just one thing besides the user name, i.e. the password which is something you 'know', this is sometimes termed one factor authentication. With two factor authentication something you 'have' is also used (e.g. a security token or 'dongle', an ATM card, or your mobile phone), or with three factor authentication something you 'are' is also used (e.g. a fingerprint or retinal scan).

Cryptography

Cryptography is the practice and study of techniques for secure communication in the presence of third parties . More generally, it is about constructing and analyzing protocols that overcome the influence of adversaries and which are related to various aspects in information security such as data confidentiality, data integrity, and authentication. Modern cryptography intersects the

disciplines of mathematics, computer science, and electrical engineering. Applications of cryptography include ATM cards, computer passwords, and electronic commerce.

Cryptology prior to the modern age was almost synonymous with encryption, the conversion of information from a readable state to apparent nonsense. The sender retained the ability to decrypt the information and therefore avoid unwanted persons being able to read it. Since World War I and the advent of the computer, the methods used to carry out cryptology have become increasing complex and its application more widespread.

Secret key Cryptography:

With secret key cryptography, a single key is used for both encryption and decryption. As shown in Figure 1A, the sender uses the key (or some set of rules) to encrypt the plaintext and sends the cipher text to the receiver. The receiver applies the same key (or rule set) to decrypt the message and recover the plaintext. Because a single key is used for both functions, secret key cryptography is also called symmetric encryption.

With this form of cryptography, it is obvious that the key must be known to both the sender and the receiver; that, in fact, is the secret. The biggest difficulty with this approach, of course, is the distribution of the key .Secret key cryptography schemes are generally categorized as being either stream ciphers or block ciphers. Stream ciphers operate on a single bit (byte or computer word) at a time and implement some form of feedback mechanism so that the key is constantly changing. A block cipher is so-called because the scheme encrypts one block of data at a time using the same key on each block. In general, the same plaintext block will always encrypt to the same cipher text when using the same key in a block cipher whereas the same plaintext will encrypt to different cipher text in a stream cipher.

Random Key Generation

Key generation is the process of generating keys for cryptography. A key is used to encrypt and decrypt whatever data is being encrypted/ decrypted. Modern cryptographic systems include symmetric-key algorithms (such as DES and AES) and public-key algorithms (such as RSA). Symmetric-key algorithms use a single shared key; keeping data secret requires keeping this key secret. Public-key algorithms use a public key and a private key. The public key is made available to anyone (often by means of a digital certificate). A sender encrypts data with the public key; only the holder of the private key can decrypt this data.

Since public-key algorithm tend to be much slower than symmetric-key algorithms, modern systems such as TLS and SSH use a combination of the two: one party receives the other's public key, and encrypts a small piece of data (either a symmetric key or some data used to generate it). The remainder of the conversation uses a (typically faster) symmetric-key algorithm for encryption.

SYSTEM DESIGN

Establishment of Keys

The establishment of keys consists of four phases; including initialization, pair wise key establishment, cluster key establishment and station key establishment. The meanings of each phase are as follows:

Initialization

Before deployment, the node receives a master key K, a node identifier Id and a random vector 'a'. Firstly, generate a k-dimensional vector group A,

$$A= (\ \mathbf{a1} \quad \mathbf{a2} \quad \mathbf{\ldots\ an}\ )$$

where, **a1, a2, an** represents the vectors in a vector group which is represented as a string.

Each vector of A is generated by the random number generator, ai(0, 1). Every node receives a vector ai from vector group A at random without replacement. In addition, the node should also receive other information, including the master key and a random number generator.

Pairwise Key Establishment

The pair wise key is generated between two nodes which are obtained by the grouping of vectors from each node with the master key. The key is generated by combining the diagonally available strings. The matrix is a symmetric matrix and it is said to contain two bit strings as its elements.

Generally the matrix for key generation is given as

$$K= \begin{pmatrix} aii & aij & aik \\ aji & ajj & ajk \\ aki & akj & akk \end{pmatrix}$$

i.e., K is the concatenation of aii, ajj, akk

The first row denotes the Master key, the second row denotes the transmitting node's vector and the third row denotes the receiving node's vector.

Cluster Key Establishment

The cluster key is generated between the cluster-head and a node which is obtained by the grouping of the vectors from the node and cluster-head with that of the master key.The cluster-head is selected by means of the estimation of energy consumption by nodes.

Mathematical Expression

The general mathematical expression for the generation of the key can be given as

$$T(K)=aii+ajj+akk$$

Here T(K) represents the trace of a matrix. Trace of a matrix is nothing but combining the diagonal strings of a matrix.The key is generally formed by combining the first two bits of the Master key, the next two bits of the transmitter node and the last two bits of the receiving node.

Block Diagram

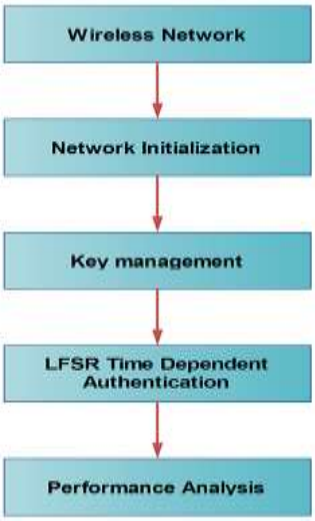

Fig. 1. Block Diagram of Time-Dependent Key Generation Method .

4.5 Authenticate Data Update

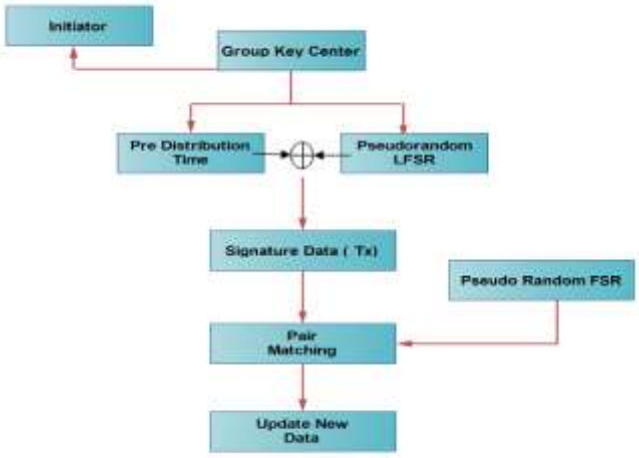

Fig. 2. Authenticate Data Update

In the case of the pair wise key establishment, both the transmitter and the receiver are nodes while in the case of the cluster key establishment, the transmitter is a node and the receiver is the cluster-head and in the case of the station key the cluster-head is the

transmitter and the receiver is the Base station.Our proposed scheme is based on Level architectural routing which mainly reduces the memory overhead and provides security.

System Model

This paper compare the simple location dependend key generation method using multiple antenna and time dependend key generation for secure wireless communication.

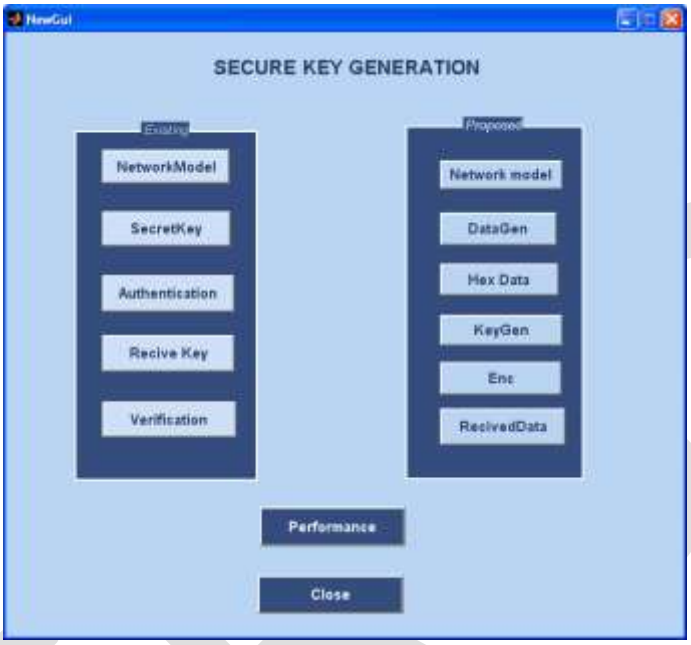

Fig. 3. System Model

In the existing system we are using multiple antennas for measuring the distance between the nodes. If the distances are same, they will start data transfer. In the existing work, there will be a key generating center that will send key updating request to the base station.

Result And Discussion

The base station will send that request to the nodes that are included in the communication.

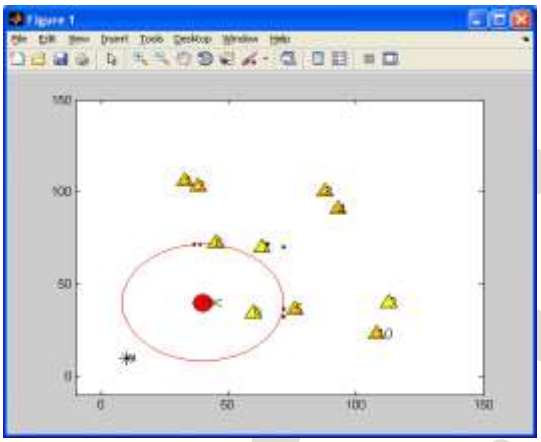

Fig.4. Key Generating Center asking for key updation

Then the nodes will send the acknowledgement to the base station. Then the secret data will be generated and send to the nodes

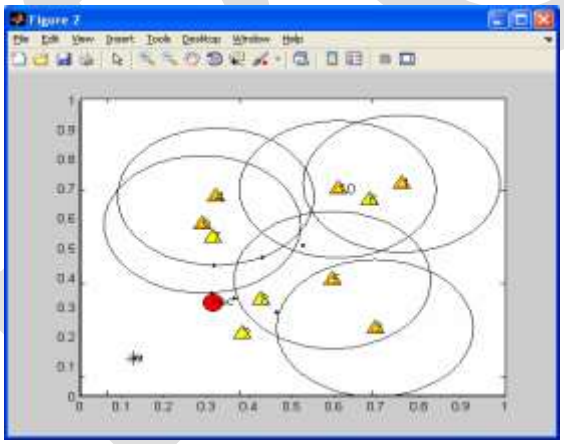

Fig.5. Acknowledgement send by the nodes

The secret data will send into the nodes. Secret data will be encrypted and then send to the nodes.

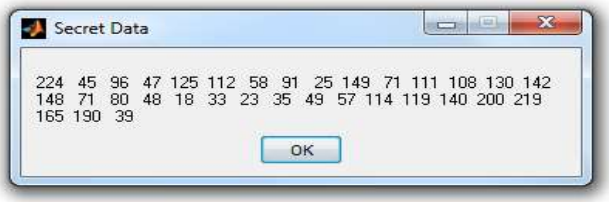

Fig.6.Secret Data

The authenticate data will received by the nodes.

Fig.7. Authenticate Data at the transmitter side.

At the receiving side, the received data is decrypted and the data will be the same

Fig.8. Authenticate Data at the receiver side

Thus the data is authenticated without any change.

Fig.9.Data Authentication

In the proposed work, there will be no key transfer. Some binary data will be generated and we will convert it into hexadecimal number.

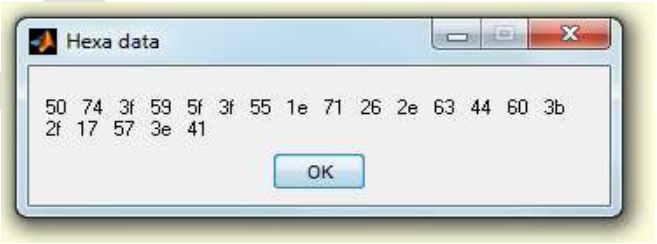

Fig. 10. Hexadecimal equivalent for data generated

Then a key is generated using LFSR. Then we will convert the key into hexadecimal number.

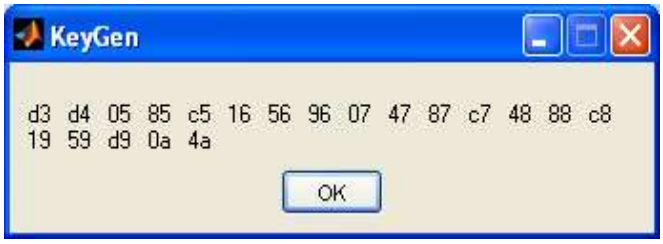

Fig. 11. Key generated by the LFSR

Secret data is encrypted using the key generated

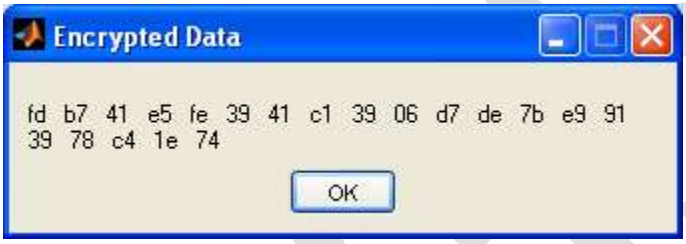

Fig. 12. Encrypted data

At the receiving side the data will be decrypted and we will get the same data.

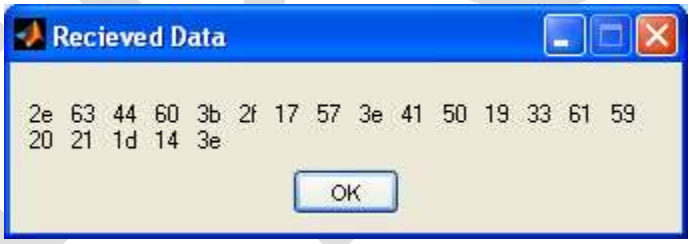

Fig.13. The data that is decrypted by the receiver

Performance Chart

Compare the performance of the proposed work with the existing work, delay in the network will be less in the proposed work as the nodes communicate directly.

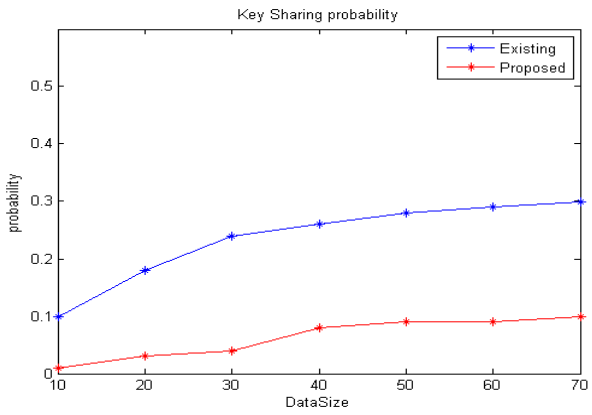

Fig.14. Key Sharing Probability

Compare the delay and data size of proposed and existing work. Delay in the proposed network will be less, because the nodes communicate with each other directly.

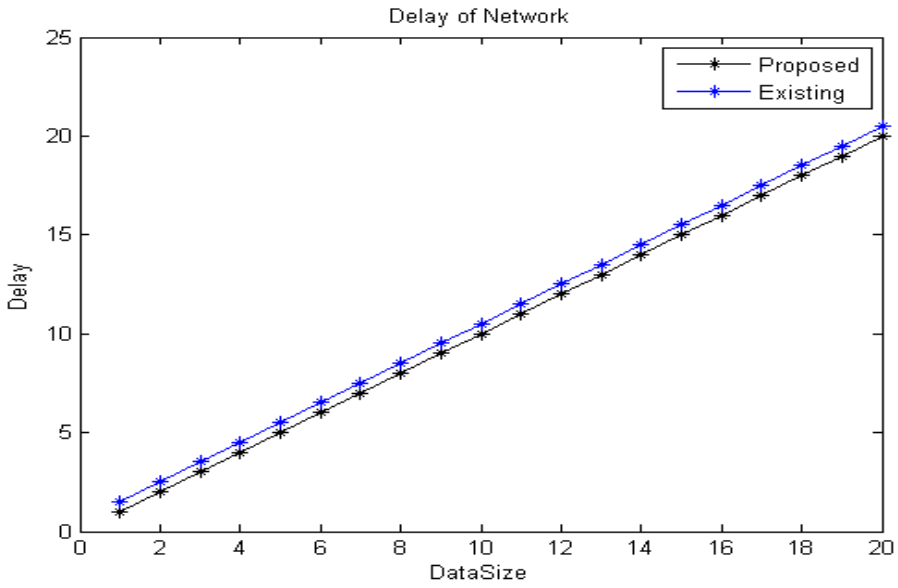

Fig.15. Delay of Network

CONCLUSION

In the key pre-distribution schemes a large quantity of keys are needed to establish the shared key, that causes great memory overhead; an attacker could capture a node and attack the network using the subset of keys. These problems have been rectified in the proposed key management scheme that is based on vector group, which is able to establish the pair wise keys independently. It provides a better security performance with a low memory overhead.

Simulation results show that the proposed scheme could establish all the keys by one- broadcast, and reduce the communication overhead , the energy consumption has been effectively reduced; the probability that any two pair of nodes establish the same pair wise key has been decreased to 0, accordingly, the threat of node capture has also been reduced, and the security of the network has been improved; the perfect memory overhead of nodes in WSN is only to store the pair wise keys related to its neighbors. In the proposed scheme, the memory overhead approximately equals to the node degree, therefore, it has a lower memory overhead than typical key pre-distribution schemes. Moreover in the proposed scheme, we only use binary arithmetic to generate keys and hence it is easy to calculate and cause less energy consumption.

REFERENCES:

[1]Jianguo Zhang, Qinye Yin, Pengcheng MU" A Simple Location-dependent Key GenerationMethod Based on Multiple Antennas for SecuringWireless Communication" in proc. ICACT2011 .p.992

[2] R. Wilson, D. Tse and R. A. Scholtz,, "Channel identification: secret sharing using reciprocity in ultrawideband channels," IEEE Transactions on Information Forensics and Security, vol. 2, no. 3, pp. 364 -375, Sep. 2007.

[3] M Shin, J Ma, A Mishra, et al., "Wireless network security and interworking," Proceeding of the IEEE, vol. 94, no. 2, pp. 455-466, Feb. 2006.

[4] B. Azimi-Sadjadi, A. Kiayias, A. Mercado, et al., "Robust key generation from signal envelopes in wireless networks," in Proc. ACM CCS '07, 2007, p 401.

[5] X. Li, J. Hwu, E. P. Ratazzi, "Using antenna array redundancy and channel diversity for secure wireless transmissions," Journal of Communications, vol. 2, no. 3, pp. 24-32, Mar. 2007

[6] . J. W. Wallace, C. Chen, and M. A. Jessen, "Key generation exploiting MIMO channel evolution: algorithms and theoretical limits," in Proc. EuCAP'09, 2009, p. 1499.

[7] N. Vereshchagin, "A new proof Ahlswede - Gacs - Korner theorem on common information," Tech. Rep., September 2002, ´ http://lpcs.math.msu.su/˜ver/papers/gka.ps.

[8] A. A. Hassan, W. E. Stark, J. E. Hershey, and S. Chennakeshu, "Cryptographic key agreement for mobile radio," Digital Signal Processing, vol. 6, pp. 207–212, Oct. 1996.

[9] J. E. Hershey, A. A. Hassan, and R. Yarlagadda, "Unconventional cryptographic keying variable management," Trans. on Communications, vol. 43, pp. 3–6, Jan. 1995.

[10] M. A. Tope and J. C. McEachen, "Unconditionally secure communications over fading channels," in Proc. MILCOM. IEEE, 2001, pp. 54–58.

[11] A. F. Molisch, J. R. Foerster, and M. Pendergrass, "Channel models for ultrawideband personal area networks," Wireless Communications, pp. 14–21, Dec. 2003.

[12] J. G. Proakis, Digital Communications, 4th ed. New York, NY: McGraw-Hill, 2001.

International Journal of Engineering Research and General Science Volume 3, Issue 6, November-December, 2015
ISSN 2091-2730

Feasibility of using Cocoa Pod Husk Ash (CPHA) as a stabilizer in the production of Compressed Earth bricks

Manu Isaac Yaw[1], Asiedu Emmanuel[2], Yalley Peter P. K.[3], Denutsui K. Senyo[2]

[1]Takoradi Technical Institute, Takoradi

[2]Department of Building Technology, Takoradi Polytechnic, Takoradi

[3]Department of Design and Technology Education, University of Education, Kumasi

Email: easiedu47@yahoo.com

Contact: +233 206601092

Abstract—Indiscriminate disposal of cocoa pod husks has been a threat to the environment especially in cocoa growing communities thus the need to explore alternative ways of utilizing this waste product. This paper examined the suitability of CPHA as a stabilizer in the production of stabilized earth bricks. Laboratory experiments were conducted on compressed earth bricks to investigate the effects of the CPHA on their compressive strength, dry density, abrasion resistance and water absorption characteristics. The earth bricks were moulded with different percentages of Cocoa Pod Husk Ash consisting of 0%, 5%, 10%, 15%, 20% and 25%. Using a mould dimension of 200mm x 100mm x 75mm, earth bricks were manually casted and cured for 28 days. Data results showed remarkable improvement in all the properties studied on the earth bricks but varied depending on the ash content. The study also revealed that cocoa pod husk ash can be used as a stabilizer in the production of earth bricks especially when the Cocoa pod husk ash content is 10% by weight as higher ash contents slightly decline the engineering properties.

Keywords— Cocoa Pod Husk Ash (CPHA), Stabilization, Earth bricks, Water Absorption, Abrasion resistance, Compressive strength, Cocoa

INTRODUCTION

Earth has been used as a building material for various types of houses with notable advantages in the tropics. These houses which include adobe, wattle and daub and others act as heat and cold absorbers thus making them more comfortable to live in. Even though, it is the most abundant construction material globally, its use has been limited due to its poor mechanical and durability properties when used as masonry blocks. These challenges associated with the use of earth blocks have over the years been minimized by stabilizing. Stabilization entails modifying any property of earth in order to improve its engineering performance. The art of stabilization is not new as Indians have stabilized earth from pre-historic times up to 600 BC although in recent times, the process has been conducted popularly with cement and lime [14]. Studies conducted on stabilized earth have shown remarkable improvement which includes increase in strength, water repellant and cohesion with reduced permeability, shrinkage and expansion [22].

With the skyrocketing prices of these stabilizing agents, studies have been tilted to the area of using agricultural and industrial byproducts and wastes which possess cementitious properties. Some of the notable byproducts with such properties include the ashes of rice husk, groundnut and coconut shells, corn cob and husks, wheat husk among others [26]. Aside, the enormous benefits derived from these agricultural byproducts, the process of utilizing them as stabilizing agents also minimizes the negative effects on the environment due to improper disposal mechanisms. One abundant agricultural byproduct indiscriminately disposed on most Ghanaian farms for decades is cocoa pod husks.

Regarded as the Food of the Gods or *Threobroma* cacao L., cocoa has been an indispensable part of our lives through its use for a wide variety of edible products. The fat from cocoa (cocoa butter) is used in the cosmetics and pharmaceutical industries [9]. Aside these benefits, local indigenes have substantial benefits such as the use of the cocoa pod husk in the production of soaps, fertilizer [19] and as poultry feed whiles the juice is used for vinegar and other alcoholic beverage production [17]. Others benefits attached to cocoa include the use of the shells of the Cocoa beans, a by-product of chocolate production are commonly sold as mulch for landscaping [11] whiles cocoa pulp can also be used in soft drink, alcohol and pectin (for jelly, marmalade and jam) production. It is stunning to know that the numerous benefits associated with cocoa plant could be attributed to the cocoa beans which constitute only 10% by weight of the cocoa fruit [2] whiles the remaining 90% predominately the cocoa pulp and cocoa pod husk are regarded as wastes with minimal commercial values in Ghana.

Even though, cocoa has been cultivated in Ghana for long, adequate information on the use of Cocoa Pod Husk Ash in stabilizing earth blocks is rare. This study seeks to determine the feasibility of utilizing the ash of cocoa pod husk as a stabilizing agent in the production of compressed earth bricks for masonry purposes.

MATERIALS AND EXPERIMENTAL STUDIES

The materials used in the investigation consisted of:
Earth: The earth was sourced from Nchaban - Nkwanta, a suburb of Sekondi-Takoradi. The samples were dried in the open before sieving through a 5mm mesh sieve whiles lumps present were pulverized (depicted in Fig. 1). This was done to eliminate outsized particles including gravels and stones could negatively impede on the bricks properties [27]. The physical properties of the earth as presented in Table 1 were obtained in accordance with [7].

Figure 3 Before and after pulverizing the earth sample

Water: The water was potable as supplied by Ghana Water Company.

Cocoa Pod Husk Ash: Dried Cocoa Pod Husks were obtained from Wassa - Mampong in the Western Region. They were gathered in the open and burned into ashes (as shown in Fig. 2). The ashes obtained were allowed to cool before sieving using a 300μm mesh sieve. This was aimed at removing all partially burnt carbon particles so as to obtain the reactive form of the ashes which are mostly in very fine forms.

Figure 4 Dried Cocoa Pod Husks before and after combustion

CHEMICAL COMPOSITION OF THE COCOA POD HUSK ASH

The chemical composition of the Cocoa Pod Husk Ash (CPHA) was determined by the X-ray Fluorescence technique. This was done by mixing 4.0g of the ash sample homogenously with 0.9 grams of Hoechst wax in a mill before pressing with a hydraulic press at 15

tons to a 32mm pellet. Multi-element determinations from the prepared pellet were carried out using an energy-dispersive polarizing X-ray Fluorescence Spectrometer (SPECTOR X-LAB 2000). The compositions of the ash have been presented in Table 1.

PREPARATION OF BRICK SPECIMEN

The production process of the bricks involved batching, mixing and casting of bricks using a manually operated moulding machine having a mould dimension of 200mm x 100mm x 75mm. The earth samples and the Cocoa Pod Husk Ash (CPHA) were batched by weight. Bricks specimen were categorized into batches. The batches consisted of earth sample with varying percentages of Cocoa Pod Husk Ash in steps of 5% which ranged from 0% to a maximum of 25%. This was done to determine the effects of the CPHA on the properties of compressed earth bricks and to aid in possible predictions of higher percentages of the ash.
The batched materials (earth and CPHA) were manually mixed in a tray to prevent harmful materials that could alter and affect the properties of the produced specimen. After a thorough mix, water was added in piecemeal until the optimum water content of the batch was attained using the ball test as explained by [21]. The wet homogenously mixed material was placed in the mould box and tamped to ensure maximum compaction before inscribing reference marks on them for easy identification. In total, 18 compressed earth bricks stabilized with Cocoa Pod Husk Ash were produced for each batch which were 0% representing the control batch and 5%, 10%, 15%, 20% and 25% representing bricks specimen with the corresponding ash content.
After casting, bricks were air dried under a shade and covered with polyethylene sheets. This was done with the aim of preventing dry shrinkage and rapid evaporation of water which would cause cracks and affect the dried bricks. The bricks were then transferred into the laboratory where they were cured for the remaining 21 days before investigations were conducted on them.

TESTING OF EARTH BRICKS SPECIMEN

The study sorts to determine the suitability of CPHA as a stabilizer in the production of compressed earth bricks. Investigations carried out on the dried earth bricks properties were the dry density, compressive strength and some durability properties. For each investigation, randomly selected bricks were used after curing for 28 days.
Density: The selected bricks were cleaned with a non-absorbent cloth to remove all loose matter stuck on them. Their weights and dimensions (i.e. length, breadth and thickness) were deduced before calculating the density using the formula outlined in Eqn. 1 before deducing the average for the batch.

$$Density = \frac{\text{Dry Mass}}{\text{Volume}} \quad \text{..... Eq. 1}$$

Compressive Test: Earth bricks specimen from each batch were tested for their compressive strengths using an ADR 2000 Compression Testing machine after 28 days curing age.
The durability properties of the bricks specimen focused on the water absorption and resistance to abrasion characteristics of the compressed earth bricks. They were deduced using African Regional Standards for Compressed Earth Blocks as recommended and described in [1]. The water absorption test focused on the change in weight of the bricks after immersing in water for 10 minutes. Literally, earth bricks with higher absorption values tend to be more porous and unsuitable as a masonry unit. The abrasion result on the other hand centered on the ability of the bricks specimen to resist tear and wear arising from brushing with a metal brush at a constant pressure. Earth bricks with higher resistance values shows bricks specimen with better bonds between soil particles whiles those with lower resistance values tends to be poorly bonded thus unsuitable as a masonry unit.

EXPERIMENTAL RESULTS AND DISCUSSION

The results of the experimental study on the earth sample, cocoa pod husk ash and the stabilized earth bricks have been outlined below.

CHEMICAL COMPOSITION OF THE COCOA POD HUSK ASH

Studies on the chemical composition of the Cocoa Pod Husk Ash (CPHA) were conducted using the X-ray Fluorescence technique with focus on its Pozzolanic properties has been presented in Table 1 below. According to [6], materials regarded as Pozzolanic in nature should have compounds such silica (SiO_2), Alumina (Al_2O_3) and Iron Oxide (Fe_2O_3) exceeding 50% by composition. Data results showed a combined sum of 13.618% for the SiO_2, Al_2O_3 and Fe_2O_3 which were far below the minimum quantum of 50% indicating the CPHA does not have adequate amount of siliceous or aluminous compounds to exhibit Pozzolanic characteristics. It is also evident that the quantum of K_2O was relatively high which is likely to result in a weaken bonds between the particles in the soil matrix due to alkali reaction in higher variations. This undesirable amount of K_2O present in the CPHA makes it an ideal natural source of alkaline for soap production as seen in most rural communities in Ghana.

Table 1 Oxides Composition of Cocoa Pod Husk Ash (CPHA)

Oxides	**Mass (%)**
SiO_2	9.727
Fe_2O_3	0.447
Al_2O_3	3.444
CaO	0.000
MgO	4.299
SO_3	2.171
P_2O_5	0.276
Cl	0.155
K_2O	25.61
MnO	0.09

CHARACTERISTICS OF THE EARTH SAMPLE

A number of tests were performed on the earth sample to determine its basic characteristics as presented in Table 2. The varying nature and their quantity in ideal amount of the particle sizes influence the engineering properties of earth bricks. The earth sample was described as well graded with uniformity coefficient (Cu) and coefficient of curvature (Cc) of 23.1 and 0.92 respectively [24]. The specific gravity of the earth sample was 3.75 which fell within the recommended range of 2.55 and 4.00 for lateritic soils [15].

Table 2 Characteristics of the Earth sample

Properties	**Results**
Shrinkage limit	8.3%
Liquid limit	46.4%
Plastic limit	29.6%
Plasticity index	16.8%
Natural moisture content	4.8%
Maximum dry density	1860kg/m^3
Optimum moisture content	8.6%
Sand/Gravel content	54.55%
Silt content	32.72%
Clay content	12.73%
Specify gravity	3.75
Soil description	Lean clayey soil
Particle size	Cu = 23.1; Cc = 0.92

The sedimentation test is among standardized field test used to determine the approximate volume percentages of constituents of soil. The result showed silt content of 32.72%, clay content of 12.73% and sand/gravel content of 54.55%. It is important to indicate that for an effective stabilization of soil, the clay fraction is essentially responsible due to its ability to provide cohesion within a soil matrix. Although, the clay fraction was within the limit of 8% - 30%, its silt content exceeded the range of 10% - 25%, which is likely to inhibit an effective bond between the various particles within the soil matrix [23]. Such soils are referred as lean clayey soil [16].

The Atterberg consistency limit test conducted on the soil sample revealed a liquid limit of 46.4%, plastic limit of 29.6% and a plasticity index of 16.8%. The shrinkage limit was also 8.3% within the recommended range of 8% - 18% suitable for engineering applications. The plots of plastic index against liquid limit on the plasticity chart (as depicted in Fig. 3 below) shows the earth (soil) falling beneath the A-line but within the intermediate plasticity zone making it ideal for construction and other engineering works [12].

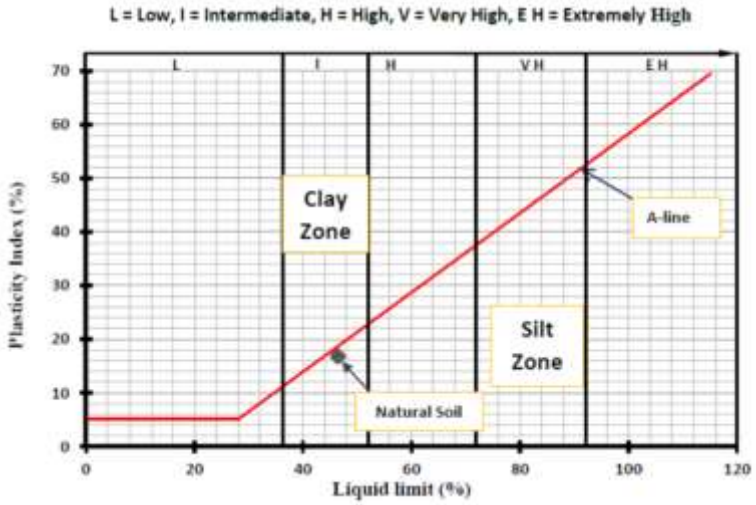

Figure 5 Earth (Natural soil) shown on the Plasticity chart

PROPERTIES OF THE EARTH BRICKS

The properties studied were; compressive strength, density, abrasion coefficient and water absorption rise of each variation level after 28-days curing age.

COMPRESSIVE STRENGTH

The mean compressive strengths of the various earth bricks ranged between 2.4148N/mm^2 and 4.2234N/mm^2 (as shown in Table 2). Earth bricks with 5% CPHA showed some improvement over the control group (earth bricks with no stabilizer) as much as 49% as the mean compressive strength increased from 2.4148N/mm^2 to 3.5964N/mm^2. As the CPHA content increased to 10% the earth bricks recorded the highest average compressive strength of 4.2234N/mm^2 which was almost 75% better than the control specimen. Earth bricks with 15% CPHA caused a slight dip as the compressive strength of 3.731N/mm^2 but this was found to be 54.5% better than bricks without stabilizer. Furthermore, bricks with 20% and 25% CPHA content had compressive strengths of 3.572N/mm^2 and 3.538N/mm^2 respectively which were found to be 47.9% and 46.5% higher than the compressive strength of the control batch group.
The ANOVA result shown in Table 2 displays the F-ratio, which in this case equals 248.888, indicating a statistically significant difference between the mean compressive strengths from one level of CPHA to another at the 95% confidence level. Analysis of the relationship between the mean compressive strengths and varying CPHA contents gave a Pearson's correlation coefficient of 0.449 indicating a slightly weak positive correlation between the mean compressive strengths and the CPHA. This relationship was best described by the regression model which had an R-Squared adjusted of 0.174, indicating that the CPHA explains 17.4% of the variability in the compressive strengths of the earth bricks.

$$\text{Compressive strength} = 3.152 + 0.029*\text{CPHA} \quad \ldots\ldots\ldots\ldots\ldots\ldots \quad \text{Eq. 2}$$

The model expressed by Eq. 2 further indicated that a unit percentage change in the CPHA causes a corresponding increase in the compressive strength of the bricks by 0.029N/mm^2 whiles the rest may also be attributed to method of compaction, curing process, water content and other factors.

Table 3 Summary of the compressive strength results of Earth bricks with varying CPHA

CPHA Content	Mean Stress	SD	R-Squared	R^2 –Adjusted	F-ratio	P-value
Soil + 0% CPHA	2.4148	0.03095	0.2020	17.4	248.888	0.000
Soil + 5% CPHA	3.5964	0.05737				
Soil + 10% CPHA	4.2234	0.13832				
Soil + 15% CPHA	3.7310	0.11149				
Soil + 20% CPHA	3.5720	0.06221				
Soil + 25% CPHA	3.5380	0.05450				

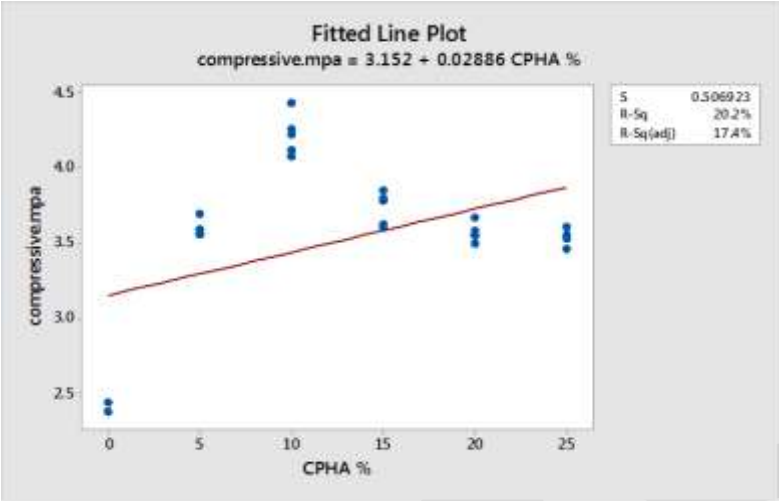

Figure 6 Compressive strength results of earth bricks with varying CPHA

Earth bricks stabilized with CPHA varied in their acceptability to the minimum requirement for masonry purposes. It was evident that the control batch did not meet the minimum requirement as recommended by [10]. Bricks with 5%, 15%, 20% and 25% CPHA contents were able to meet the minimum compressive strength of 3.00N/mm^2 for Class B masonry units. Finally, earth bricks with 10% CPHA content qualified as a Class A masonry unit which required a minimum 4.00N/mm^2.

Generally, all earth bricks had significant improvements as the CPHA content was introduced portraying a trait exhibited by some agricultural and industrial wastes ashes such as rice husk ash [20], sugar cane bagasse ash among others [18]. Earth bricks gradually increased from 2.4148N/mm^2 to 4.2234N/mm^2 a as the CPHA content increased from 0% to 10%. The increase could be attributed to the presence of compounds (K_2O, Fe_2O_3, Al_2O_3, SiO_2) which tend to react with the clays to form cementitious matrix in small quantities [4].

Quite surprisingly, as the CPHA content exceeded 10%, there was a slight decline from 4.1964N/mm^2 to 2.832N/mm^2 as the CPHA increased from 10% to 25%. This dip in compressive strengths was attributed to the high content of the Potassium ions (K+). This phenomenon could be attributed to the replacement of strong cautions in the clay minerals with substantial amount of K+ which tend to weaken the bonds among clay minerals invariably, reducing the compressive strengths of the earth bricks.

DENSITY

The dry density of a masonry unit is largely a function of the constituent material's characteristics, moisture content during pressing and the degree of compaction load applied. Deducing from the data, bricks without CPHA (control batch) had the least average density of 1592.94kg/m^3 which increased to 1654.498kg/m^3 when CPHA content increased to 5%. An extra 5% addition of CPHA (making 10% CPHA) resulted in bricks with the highest mean dry density of 1809.048kg/m^3. However, specimens with 15%, 20% and 25% CPHA declined as they recorded mean dry densities of 1742.294kg/m^3, 1711.528kg/m^3 and 1716.68kg/m^3 respectively. The increase in the dry densities of the earth bricks associated with the increasing CPHA content was attributed to the fact that the pores in the earth bricks were filled by the ash and subsequently increase the weight of the bricks. After attaining, the optimum quantity (most pores filled), the CPHA tend to displace the soil particles instead, thereby causing a reduction in the densities of the earth bricks as seen with bricks with higher CPHA content (> 10%).

Table 4 Summary of the dry density results of Earth bricks with varying CPHA

CPHA Content	Mean Density	SD	R-Squared	R^2 –Adjusted	F-ratio	P-value
Soil + 0% CPHA	1592.9420	38.45751	0.2200	19.3	20.657	0.000
Soil + 5% CPHA	1654.4980	20.96443				
Soil + 10% CPHA	1809.0480	34.10533				
Soil + 15% CPHA	1742.2940	19.02670				
Soil + 20% CPHA	1711.5280	27.49890				
Soil + 25% CPHA	1716.6800	61.54743				

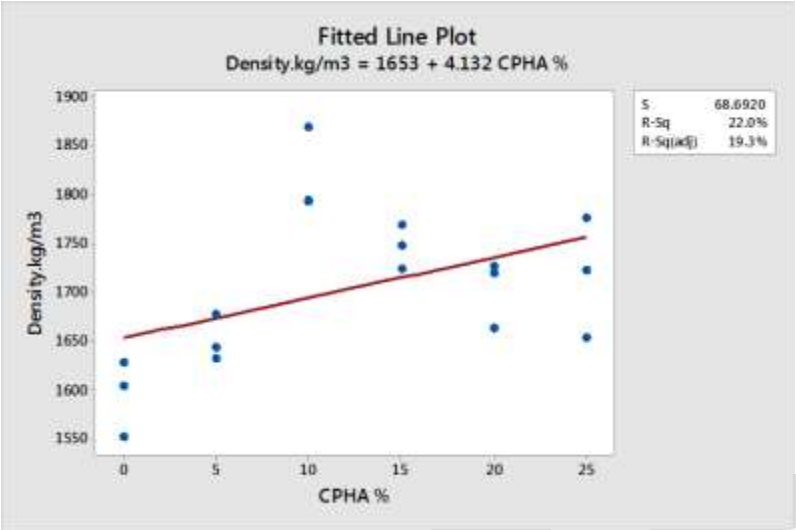

Figure 7 Dry densities of earth bricks with varying CPHA

A one-way analysis of variance shows F-value of 20.657 indicating that the stabilizer (CPHA) had an effect on the dry densities statistically. Further analysis on the relationship between CPHA content and the earth bricks was conducted using a regression model (as depicted in Eq. 3). The result of a linear regression model to describe the relationship between Density and CPHA is given as:

$$\text{Density} = 1653 + 4.132*\text{CPHA}\ (\%) \quad \ldots\ldots\ldots\ldots\ldots\ldots\ldots \quad \text{Eq. 3}$$

The Adjusted R-Squared of 0.193 of Eq. 3 as presented in Fig. 5 indicates 19.3% of the variability in Density was explained by the CPHA. The Pearson's correlation coefficient equals 0.469, indicating a slightly weak but positive relationship between the CPHA content and the densities of the bricks. The equation also depicts that an increase of 4.132kg/m^3 in the density of the bricks as the level of CPHA was increased by a percentage unit.

DURABILITY PROPERTIES

The durability properties of the specimens studied in this research consisted of the abrasion test and the water absorption by capillarity.

ABRASION COEFFICIENT OF THE EARTH BRICKS

The abrasion resistance coefficients of the stabilized earth bricks was determined using the procedures proposed by African Regional Standards for Compressed Earth Blocks. It measures the resistance of the specimen to abrasion or wear. Literally, specimen with higher abrasion resistance coefficients, have better resistance to wear and the vice versa. The abrasion coefficients were deduced using Eq. 4.

$$Ca = \frac{S}{M1-M2} \quad \ldots\ldots\ldots\ldots\ldots\ldots\ldots\ldots\ldots\ldots\ldots\ldots\ldots\ldots \quad \text{Eq. 4}$$

Earth bricks specimen showed an improvement in the abrasion resistance as the content of the CPHA increased from 0% to 10% before declining as presented in Table 5 and depicted in Fig. 6. Earth bricks with 10% CPHA content gave the highest resistance to abrasion while the control batch (earth bricks with no CPHA) had the least resistance to abrasion.
Generally, the CPHA influenced the ability of the bricks to resist wear as the F-ratio from a one-way ANOVA equaled 108.337. Further analysis on the relationship between the abrasion coefficients and the CPHA was explored using a Pearson's correlation coefficient gave 0.351, indicating a weak positive relationship between the abrasion coefficients and the CPHA contents.

Table 5 Summary of the Abrasion results of Earth bricks with varying CPHA content

CPHA Content	Mean Abrasion	SD	R-Squared	R^2 –Adjusted	F-ratio	P-value
Soil + 0% CPHA	0.3546	0.03993	0.2312	9.2	240.288	0.000
Soil + 5% CPHA	0.5024	0.04241				
Soil + 10% CPHA	1.2088	0.06457				
Soil + 15% CPHA	0.8494	0.03172				
Soil + 20% CPHA	0.7248	0.04011				
Soil + 25% CPHA	0.6858	0.02744				

Earth bricks showed an improvement in their resistance to tear and wear (abrasion) as the content of the CPHA increased from 0% to 10% before declining, similar to the trends exhibited by other properties studied. Generally, this pattern was in agreement with other studies conducted on most agricultural-based stabilizing agents [26], [3], [25].

Literally, bricks with higher abrasion resistance coefficients showed higher resistance to disintegration than bricks with lower abrasion coefficients. Increasing abrasion coefficients of the stabilized bricks associated with increasing CPHA content was attributed to the improved bonding between the soil particles facilitated by both the low K+ ions and the clay particles. As the K+ ions increased, clay particles necessary for effective bonds between all the particles were weakened resulting in weak bonding between particles which were easily displaced by wear (abrasion).

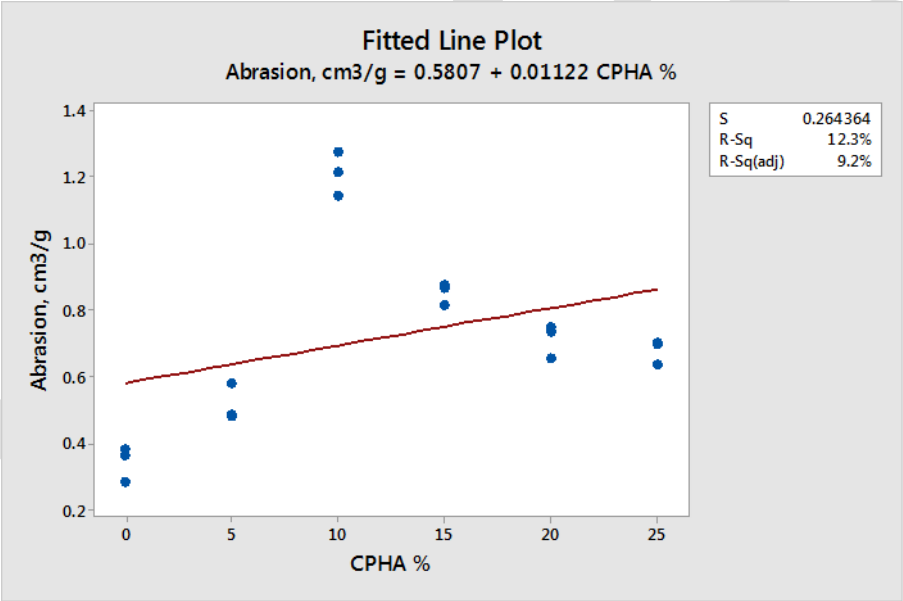

Figure 8 Abrasion coefficients of earth bricks with varying CPHA

This relationship was best predicted by the equation of the fitted model in Fig. 6.

$$\text{Abrasion} = 0.581 + 0.011*\text{CPHA} \quad \ldots\ldots\ldots\ldots\ldots\ldots\ldots\ldots\ldots\ldots \quad \text{Eq. 5}$$

With an Adjusted-R squared of 0.92, it can be observed that the CPHA explains 9.2% of the variability in the abrasion coefficients.

WATER ABSORPTION COEFFICIENTS OF THE EARTH BRICKS

Literally, stabilized bricks with low absorption coefficients (low initial rate of absorption) absorbs minimal amount of water which enhances better bonding between masonry units as some water is retained for proper hydration. Bricks without physical cracks were selected for this test per the procedures outlined by the African Regional Standards for Compressed Earth Blocks and deduced using the formula indicated in Eq. 6.

$$Cb = \frac{100 \times (M1 - M2)}{s\sqrt{10}} \quad \text{..... Eq. 6}$$

Generally, the use of CPHA as a stabilizer reduced the water absorption capacity of the bricks (as presented in Table 6 and Fig. 7). This was evident as earth bricks with no stabilizer (control batch) recorded the highest water absorption coefficient of 22.1856g/cm^{2}min. As the CPHA content increased to 5% the absorption coefficient of the earth bricks reduced to 19.067g/cm^{2}min (representing almost 16%) whiles those made with 10% CPHA an absorption coefficient of 4.6866g/cm^{2}min indicating about 373% reduction in their capability to absorb water when compared to the controlled specimen. Furthermore, as the percentage of CPHA content increased to 15%, the absorption coefficient of the earth bricks increased slightly to 8.4464g/cm^{2}min indicating about 163% reduction in water absorption whiles earth bricks with 20% CPHA content recorded an average absorption coefficient of 12.288g/cm^{2}min (80.5% reduction in absorption when compared with controlled group's average) whilst those made from 25% CPHA had absorption coefficients of 13.324g/cm2min (66.5% reduction in absorption when compared with controlled group's average).

Analysis of the results using a one-factor ANOVA showed F-ratio of 57.507 which was statistically significant at 95% confidence level indicating that the water absorption coefficients of the earth bricks were influenced significantly by the different percentages of the ash.

Table 6 Summary of absorption results of Earth bricks with varying CPHA content

CPHA Content	Mean Absorption	SD	R-Squared	R^2 –Adjusted	F-ratio	P-value
Soil + 0% CPHA	0.3546	0.03993	0.2312	0.1234	57.507	0.000
Soil + 5% CPHA	0.5024	0.04241				
Soil + 10% CPHA	1.2088	0.06457				
Soil + 15% CPHA	0.8494	0.03172				
Soil + 20% CPHA	0.7248	0.04011				
Soil + 25% CPHA	0.6858	0.02744				

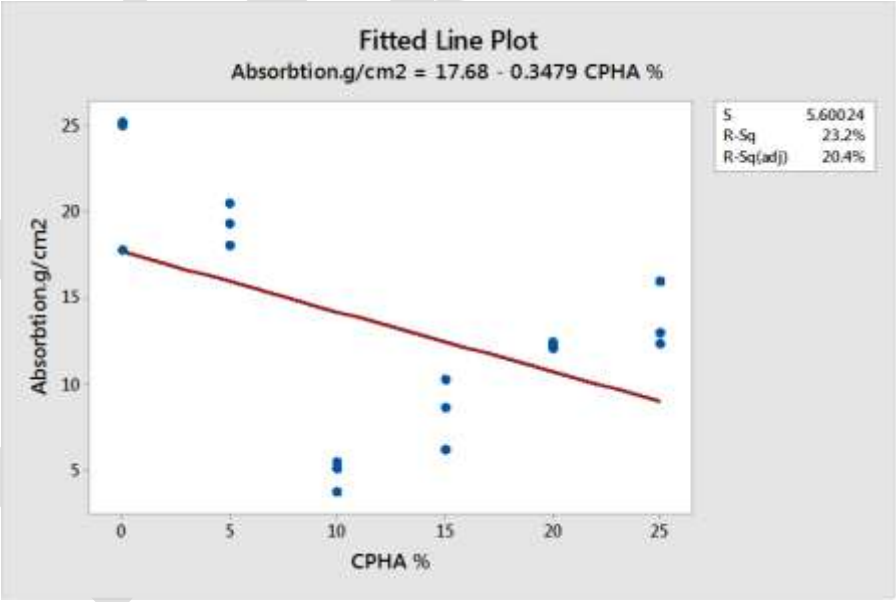

Figure 9 Abrasion coefficients of earth bricks with varying CPHA

The relationship between the CPHA content and the water absorption coefficients of the earth bricks was proved by a correlation coefficient of - 0.481, indicating a slightly strong negative relationship between them. This relationship indicated that as the percentage of CPHA increases, the water absorption capabilities of the bricks reduces which is best described by the equation.

Absorption = 17.68 - 0.348*CPHA …… Eq. 7

To this end, the model (Eq. 7) reveals that a unit percentage change in CPHA results in 0.348g/cm2min decrease in absorption

capabilities of the bricks. This decrease in the absorption coefficients associated with increasing CPHA could be attributed to the decreasing volume of voids which have been filled with the fine particles of the CPHA therefore minimizing the permeability of the earth bricks. Further increase in the CPHA content after 10% addition resulted in a divergence by increasing the water absorption coefficients as seen earlier with the previous properties studied. Such sudden change in pattern according to [13] might be attributed to the declining bond strength between the soil particles caused by the substantial amount of K+ ions present as the CPHA content increase resulting in a porous material.

CONCLUSION

The contents of the CPHA did not satisfy the recommendations of ASTM C 618 for Pozzolanic materials as the SiO_2, Fe_2O_3, Al_2O_3 contents totaled only 13.618%. It was evident that Potassium (K_2O) was relatively the highest constituting 25.61% by weight making the ash a natural source of alkaline. Data showed a gradual increase in in the engineering properties of the stabilized earth bricks as the CPHA content increased from 0% to 10% before declining slightly after subsequent additions. Data showed that the optimum amount of ash required for stabilizing the earth is 10% by weight.

Based on the study, effective stabilization of earth with similar characteristics for bricks production requires lower CPHA contents as higher content reduces the engineering properties.

REFERENCES:

[1] Adam, E. A., and Agip, A. R. A. (2001). "Compressed stabilized earth blocks manufactured in Sudan". United Nations Education Scientific and Cultural Organization (UNESCO). 7 Place de fontenoy, 75352 Paris 07 SP, France. pp 4-27.

[2] ADM Cocoa (2009). "The deZaan: Chocolate and Cocoa Manual". 40th Anniversary Edition. ADM Cocoa.

[3] Agbede, I. O. and Joel, M. (2011). "Effect of Rice Husk Ash on the Properties of Ibaji Burnt Clay Bricks". American Journal of Scientific and Industrial Research. Pp. 674 - 677. 2011.

[4] Amoanyi, R., (2012). "The study of alternative chemical stabilization of clays with agricultural waste materials for rural housing". An unpublished thesis submitted to the Department of Materials Engineering in partial fulfillment of the requirements for the degree of Doctor of Philosophy in Materials Engineering.

[5] Amu, O. O., Ogunniyi, S. A. and Oladeji, O. O. (2011). "Geotechnical properties of lateritic soil stabilized with sugarcane straw ash". American Journal of Scientific and Industrial Research. Vol. 2 (2): 323-331.

[6] ASTM C 618-78. (2012). "Standard Specification for Coal Fly Ash and Raw or calcined Natural Pozzolan for use in concrete".

[7] British Standard Institution. (1990). "Methods of Test for Soils for Civil Engineering Properties". British Standard Institution: (BS 1377). London, UK.

[8] Das, B. M. (2000). "Fundamentals of Geotechnical Engineering". 4th edn. Thomson Learning, USA.

[9] Fapohunda S. O. and Afolayan A. (2012). "Fermentation of Cocoa Beans and Antimicrobial Potentials of the pod Husk Phytochemicals". Journal of Physiology and Pharmacology Advances. Vol. 2(3): 158-164.

[10] Ghana Standard Authority. (2010). "Building and construction materials-specification for blocks". Part 1: Precast sandcrete blocks: GS 297-1: 2010.

[11] Hansen, S., Trammel, H., Dunayer, E., Gwaltney, S., Farbman, D. and Khan, S. (2003). "Cocoa bean mulch as a cause of methylxanthine toxicosis in dogs". ASPCA Animal Poison Control Center, Urbana, IL Reterived from http//www.apcc.aspca.org

[12] Houben, H., and Guillaud, H. (1994). "Earth construction: A comprehensive guide. CRATerre-EAG". Intermediate Technology Publications. London, England.

[13] Kabiraj. K. and Mandal, U. K. (2012). "Experimental investigation and feasibility study on stabilized compacted earth block using local resources". International Journal of Civil and Structural Engineering Volume 2, No 3. ISSN 0976 – 4399.

[14] Kulkarmi, R. P. (1973). "Soil Stabilization by Early Indian Methods". Maharashtra Engineering Research Institute, Nasik, Maharashtra. Pp 53, 8.

[15] Magnien, R., (1966). "Laterite and Lateritic soils and other problem soils in Africa. An Engineering Study for Agency for International Development. AID/csd-2164. Lyon Associates, Inc. Baltimore, MaryIand, U. S.A

[16] Minke, G. (2006). "Building with earth: design and technology of a sustainable architecture". Birkhauser Publishers for Architecture. Boston.

[17] Nfor, B. K. Forton, O. T., Thomas A. Bemu, T. A. and Verhaert, P. D. E. M. (2012). "Valorization of the byproducts of cocoa production – Towards a more sustainable cocoa value chain in Cameroon".

[18] Ogunbode, E. B. and Apeh, J. A. (2012). "Waste to wealth: A study of laterite bricks produced using blended incinerated corn-cob ash cement". West Africa Built Environment Research (WABER) Conference, 4.1023-1031.

[19] Oladokun, M. A. O. (1986). "Use of cocoa pod husk as fertilizer for maize production". Nigerian Journal of Agronomy, 1 (1986) 103.

[20] Olaoye, G. S. and Anigbogu, N. A. (2000). "Properties of compressed earth bricks stabilized with termite mound materials". Nigerian Journal of Construction Technology and Management. Vol. 3:1

[21] Raheem, A. A., Bello, O. A. and Makinde, O. A. (2010). "A comparative study of cement and lime stabilized lateritic interlocking

blocks". Pacific Journal of Science and Technology. Vol. 11 (2): 27-34.
[22] Reddy, K. (2008). Engineering properties of soils based on laboratory testing. UIC
[23] Rigassi, V. (1985). "Compressed Earth Blocks: Manual of Production". Volume 1. Manual of Production. Deutsches Zentrum fur Entwicklungstechnologien GATE in: Deutsche Gesellschaft fur Tecchnische Zusammenarbeit (GTZ) GmbH in coordination with BASIN. Reterieved from: http://www.gtz.de/basin/publications/books/cebvol1.pdf
[24] Viswanadham, B. V. S. (2003). "Soil Mechanics". Department of Civil Engineering Indian Institute of Technology, Bombay. Lecture – 7. Retrieved from: http//www.textofvideo.nptel.litm.ac.in
[25] Walker, P. (1995). "Strength, durability and shrinkage characteristics of cement stabilized soil blocks". Cement and Concrete Composites. Vol. 17: 301-310.
[26] Yalley, P. P. K. and Asiedu, E. (2013). "Enhancing properties of earth brick by stabilizing with corn husk ash". Civil and Environmental Research. Vol. 3(11): 43-52. Retrieve from http://www.iiste.org
[27] Oshodi, O. R. (2004). "Techniques of producing and dry stacking interlocking blocks". Nigerian Building and Road Research Institute Workshop on local Building Materials. Ota, Ogun State Nigeria.

International Journal of Engineering Research and General Science Volume 3, Issue 6, November-December, 2015
ISSN 2091-2730

AN OVERVIEW OF SIMULATION OF PRIVATECLOUD ENHANCING MOBILE DEVICE PERFORMANCE

Chanky Swami, Nishant Anand
M.tech. Student, CBS Group of Institutions, Jhajjar, Haryana;c.innovator@gmail.com@gmail.com;9582593790

Abstract: This research implements and develops cross-platform architecture for connecting mobile devices to the WS. The architecture includes a platform independent design of mobile service client and a middleware for enhancing the interaction between mobile clients and WS. The middleware also provides a personal service mashup platform for the mobile client. Finally, the middleware can be deployed on Cloud Platforms, like Google App Engine and Amazon EC2, to enhance the scalability and reliability.

Keywords: Cloud, web services, MCC (Mobile cloud computing), search engine, middleware.

I. INTRODUCTION

Today, mobile devices like iPhone, Blackberry, Android, have included applications that consume WS from popular websites, such as Google, Facebook, and Twitter. However, there are problems in connecting mobile devices to existing WS. Firstly, WS need to provide optimization for mobile clients. For example, the size of the WS messages needs to be reduced to fit the bandwidth of mobile clients. Secondly, mobile clients have to adapt to different kinds of WS, for example, SOAP and RESTful WS. The growing number of mobile clients and availability of WS also drives the needs of customizing and personalize service mashups. This thesis investigates how we can stimulate Cloud which can help mobile clients connect to existing WS.

II. CLOUD AND CLOUD COMPUTING

What is cloud computing?Cloud computing as a paradigm, which shifts the location of computing infrastructure to the network in order to reduce the costs associated with the management of hardware and software resources.

Cloud Platforms usually refer to application hosts that offer computational power, storage and Web access. Two well-known Cloud Platforms are Amazon Elastic Cloud Computing (EC2) and Google App Engine (GAE).

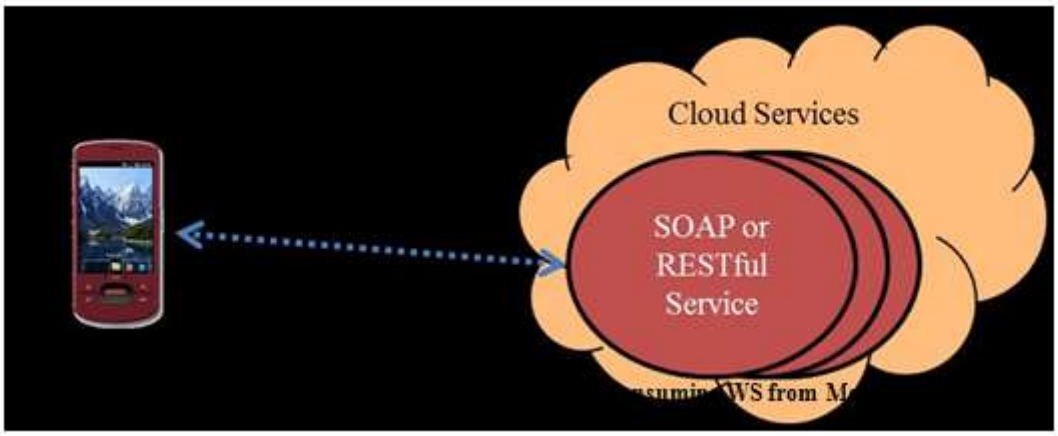

EC2 is based on virtualization, where each EC2 instance is a Virtual Machine (VM). Users can choose different Operating Systems (OS) and hardware architectures to run on their VMs.

III .CHALLENGES ACCESSING WS OVER CLOUD:

There are several challenges in the process of consuming Web Services from mobile clients.

Challenge1. Loss of connection: The interaction between client and service requires a stable connection. However, due to the mobility of the clients and the wireless network setup, mobile clients can be temporarily removed from the previous connected network and later may enter to another network. In such incidents, either service requests or responses may fail to be delivered to their destination.

Challenge2. Bandwidth/Latency: Cell networks have limited bandwidth and are often billed based on the amount of data transferred. However, even a simple SOAP message often contains a large chunk of XML data, which consumes a lot of bandwidth and the transmission can cause major network latency. In addition, the SOAP message contains mostly XML tags that are not all necessary for mobile clients.

Challenge3. Limited resources: Mobile clients are "thin clients" with limited processing power. The limitations are intrinsic to mobility and not just the shortcomings of current technology .For example, a service mashup involve parsing and combining different WS results requires a lot of computation. The challenges are minimizing the data processing on mobile clients and extending processing power beyond mobile clients. In addition, many mobile platforms do not include necessary libraries for SOAP WS.

IV.THE IDEA OF MOBILE CLOUD COMPUTING:

To overcome these challenges, the paper proposes a Mobile Cloud Computing (MCC) architecture which connects mobile devices to the Cloud Computing. The MCC architecture includes a mobile client and a middleware design.

There are two approaches to implement the mobile client: native applications and embedded browser applications. Native applications are built with specific programming languages supported by the mobile platforms. However, embedded browser applications can run HTML and JavaScript in the embedded browser and use interfaces exposed by native application.

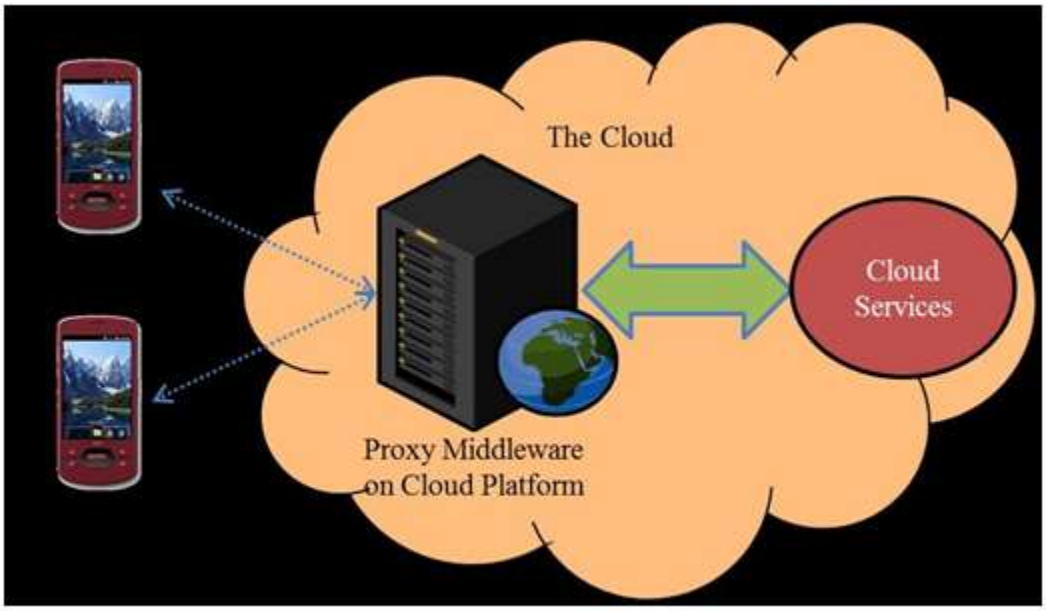

Consuming WS from Mobile Client through Proxy Middleware

The middleware acts as a proxy that is hosted on the Cloud platforms which provide mobile clients access to Cloud services. The

middleware improves interaction between mobile clients and Cloud Services, for example, adaptation, optimization and caching. The middleware also provides extended functions to mobile clients, such as service mashup. In general, the middleware enhances the functionality, reliability and compatibility of the interaction between mobile clients and Cloud Services.

V. CONCLUSION AND FUTURE SCOPE:

Here this middleware and the corresponding components facilitates our cloud with the extra capabilities which lead to enhance the performance of mobile device as well, this sort out the overall network bandwidth issue ,insufficient resource moreover provide the connection stability. However we can further work on the alternate of middleware even on the mobile device side. We can work on various techniquesto customize middleware for the implementation on cloud which will give better results in limited cost.

REFERENCES:

[1] Portio Research Mobile Factbook, Portio Research, 2009.

[2] S. Yates, It's Time To Focus On Emerging Markets For Future Growth, Forester, 2007.

[3] S. Weerawansa, F. Curbera, F. Leymann, T. Storey, and D.F. Ferguson, Web Services Platform Architecture: SOAP, WSDL, WS-Policy, WS-Addressing, WS-BPEL, WS-Reliable Messaging and More, Upper Saddle River, NJ, USA: Prentice Hall PTR, 2005.

[4] "Web Services Glossary," 2004. Last retrieved from http://www.w3.org/TR/ws-gloss/ on December 6, 2010

[5] "Web Services Description Language 1.1," Web Services Description Language (WSDL) 1.1, 2001. Last retrieved from http://www.w3.org/TR/wsdl on December 6, 2010

[6] "UDDI version 3.02 Spec Technical Committee Draft," 2004. Last retrieved from http://uddi.org/pubs/uddi-v3.0.2-20041019.htm on December 6, 2010

[7] "Web Services Architecture," 2004. Last retrieved from http://www.w3.org/TR/ws-arch/ December 6, 2010

[8] R.T. Fielding, "Architectural Styles and the Design of Network-based Software Architectures," University of California, 2000.

[9] L.M. Vaquero, L. Rodero-Merino, J. Caceres, and M. Lindner, "A break in the clouds: towards a cloud definition," SIGCOMM Comput. Commun. Rev., vol. 39, 2009, pp. 50–55.

[10] "Google App Engine," Google Code, Mar. 2010. Last retrieved from http://code.google.com/appengine/ on December 6, 2010

[11] "API Dashboard," Programmable Web, Mar. 2010. Last retrieved from http://www.programmableweb.com/apis on December 6, 2010

[12] M. Al-Turkistany, A. (Sumi) Helal, and M. Schmalz, "Adaptive wireless thin-client model for mobile computing," Wirel. Commun.Mob.Comput., vol. 9, 2009, pp. 47–59.

[13] M. Satyanarnynnan, "Mobile computing," Computer, vol. 26, 1993, pp. 81-82.

International Journal of Engineering Research and General Science Volume 3, Issue 6, November-December, 2015
ISSN 2091-2730

A data mining perspective on prevalence of Tuberculosis in India

Natalya Kumar

B.Tech - Mody University, bestalya@gmail.com, +919572767969

Abstract— Abstract Tuberculosis (TB) is a widespread infectious disease caused by various strains of mycobacteria, usually Mycobacterium tuberculosis. It is spread through the air by a person suffering from TB and typically attacks the lungs. A single patient can infect 10 or more people in a year. More people in the developing world contract tuberculosis because of a poor immune system. India has the highest burden of TB in the world, an estimated 2 million cases annually, and accounting for approximately one fifth of the global incidence. It is also estimated by the World Health Organization (WHO) that 300,000 people die from TB each year in India. Eighty per cent of TB patients are in the economically most productive years of their lives. The purpose of the current work is to analyze the TB case notification statistics for India and the Treatment Outcomes of Notified TB Cases to make future predictions. Estimating Tuberculosis disease burden is important for planning, monitoring and evaluating the TB control programme.

Keywords— Tuberculosis, India, RNTCP, Diagnosis, Notification, Prevalence, Incidence, Mortality, Success, Eradication, Data Mining.

INTRODUCTION

India bears a disproportionately large burden of the world's tuberculosis rates, as it resides to be the biggest health problem in India. It remains one of the largest on India's health and wellness scale. India has a large burden of the world's TB, one that this developing country can ill afford, with an estimated economic loss of US $43 billion and 100 million lost annually directly due to this disease. Treatment in India is on the rise just as the disease itself is on the rise. To prevent spreading TB, it's important to get treatment quickly and to follow it through to completion. The Indian government's Revised National TB Control Programme (RNTCP) started in India during 1997. The program uses the WHO recommended "Directly Observed Treatment Short" Course (DOTS) strategy to develop ideas and data on TB treatment. This group's initial objective is to achieve and maintain a TB treatment success rate of at least 85% in India among new patients. In 2010 the RNTCP made a major policy decision that it would change focus and adopt the concept of Universal Access to quality diagnosis and TB treatment for all TB patients. By doing so, they extend out a helping hand to all people diagnosed with TB, and in addition, provide better quality services and improve on therapy for these patients.

In this paper, Statistics from the past years regarding the TB case notification and treatment outcomes in India are used for making estimations and future predictions. Estimating tuberculosis disease burden is important for planning, monitoring and evaluating the TB control program. Weka tool is used for the evaluation and forecast using regression algorithms.

METHODOLOGY

Over the 11 year analysis period, the population covered increased from 139 million to 1.21 billion populations. Smear microscopy services are reported independently of case notification results. As expected from service expansion, the absolute number of TB suspects examined by smear microscopy annually has increased manifold, from 0.96 million to 7.8 million. Over the same time period, the rate of TB suspect examination also increased by 50%, from 421 per 100,000 population covered by RNTCP services to 651 per 100,000 population covered. Similarly, the rate of sputum smear positive cases diagnosed by microscopy has increased by 20%, from 62 to 79 per 100,000 population [Figure 1]. The average number of suspects examined for every sputum smear positive case diagnosed has gradually increased about 1.3% per year, from 2001 to 2011, the number of suspects examined per smear positive

case diagnosed has increased by 28% from 6.4 to 8.3 suspects (Figure 2). Total and sputum smear positive case notification is also shown in Table 1. An average difference of 11.3% [Range 8– 15%] was observed between the rate of sputum-positive cases diagnosed and the sputum-positive case notification rate.

Effectiveness of RNTCP and its future

Though the programme RNTCP was formally initiated in the year 1997 and the quarterly reporting mechanism was in place since inception, the data presented below extend from the year 1999, when approximately about 10% of the country's population was covered onwards and makes a prediction till the year xxxx. The rapid pace of DOTS expansion over the past decade complicates longitudinal data analysis in a number of ways. District-bydistrict scale-up of RNTCP services over several years changes the denominator of population covered every quarter. Basic demographic characteristics of implementing districts differed over the expansion years, as well as the expected evolution of services and TB epidemiology in areas implementing RNTCP over longer time periods. The future trend is based on the past records to check the effectiveness of the programme.

For the purposes of this analysis, districts implementing RNTCP less than one year during the initial year of implementation were attributed to cover a population proportionate to the number of days in the first year that services were available in each district. The rates presented in this section are all per 100,000 populations after adjusting for the number of days of implementation by individual districts till year 2006. Also the population of the districts is based on 2001 census and 2011 Census India for these two years and estimated for the rest of the years based on these two Censuses. Though the population in the tables is complete population of services covered as on 31st December of that year.

Sputum Microscopy Services and TB Suspect Examination

Over the 11 year from 1999 to 2011 analysis period, the population covered increased from 139 million to 1.21 billion populations. Smear microscopy services are reported independently of case notification results. As expected from service expansion, the absolute number of TB suspects examined by smear microscopy annually has increased manifold, from 0.96 million to 7.8 million. Over the same time period, the rate of TB suspect examination also increased by 50%, from 421 per 100,000 population covered by RNTCP services to 651 per 100,000 population covered. Similarly, the rate of sputum smear positive cases diagnosed by microscopy has increased by 20%, from 62 to 79 per 100,000 population. The average number of suspects examined for every sputum smear positive case diagnosed has gradually increased about 1.3% per year, from 2001 to 2011, the number of suspects examined per smear positive case diagnosed has increased by 28% from 6.4 to 8.3 suspects. An average difference of 11.3% [Range 8– 15%] was observed between the rate of sputum-positive cases diagnosed and the sputum-positive case notification rate and so the predictions are made with reference to the findings.

Figure 1: rate of TB suspect examined and smear positive TB cases diagnosed per 100,000 population

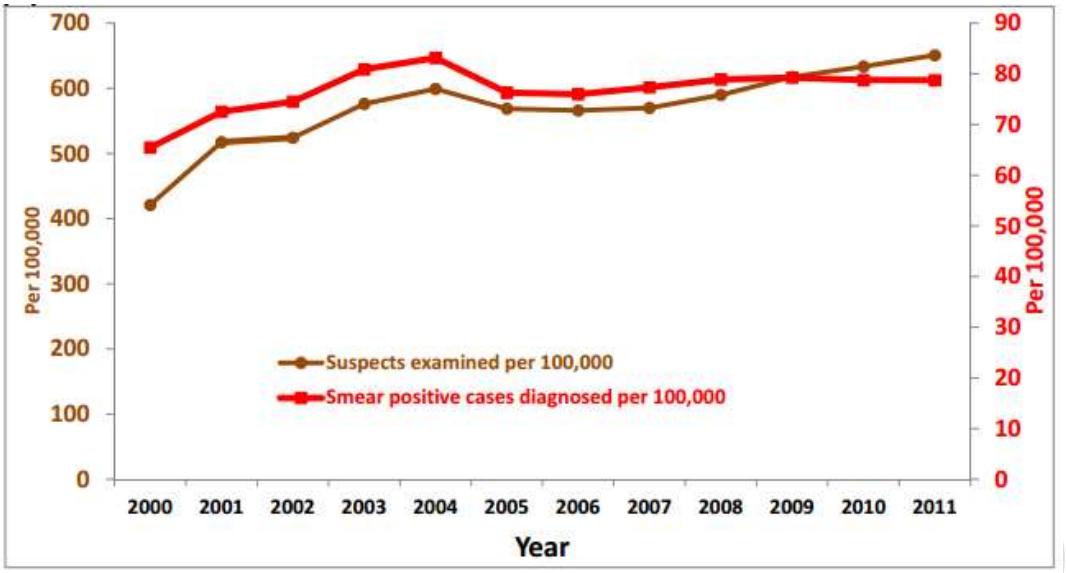

Figure 2: future forecast for: Smear positive TB cases diagnosed

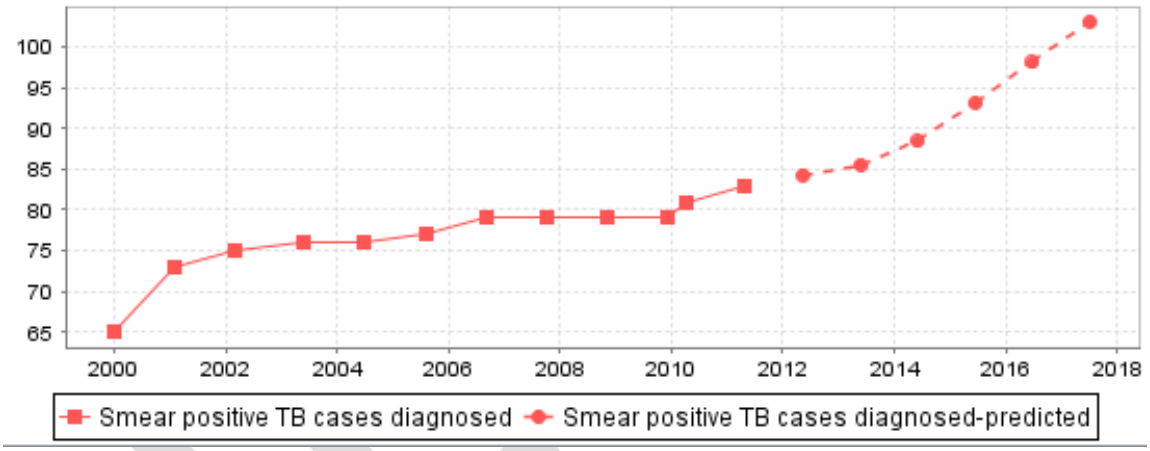

Notification Rates of TB Cases

Overall, case notification has increased over the 12 year analysis period, and the notification rates of most types of TB cases has steadily increased or remained stable, with the exceptions of new smear-negative and "treatment after default" . The total case notification rate has increased from 101 cases per 100,000 populations in 1999 to 125 per 100,000 population in 2011, though the last 4 years case notification has been effectively flat or rather decreasing. The NSP case notification rate has increased from 39 cases per 100,000 populations in 1999 to 53 per 100,000 populations in the year 2008, and has remained at 53/100,000 for the past 4 years. The NSN notification rates have shown a decreasing trend from 45 per 100,000 populations in 2004 to 28 per 100,000 population in 2011, and continues to fall without clear explanation. Some of the arguments for this are increased efforts to get the sputum examined and bacilli demonstrated with increasing availability and application of quality sputum smear microscopy services expanded under the programme. The notification rate of re-treatment cases has increased by 40% over the past 12 years, from 18 per 100,000 populations in 1999 to 25 per 100,000 populations in 2011. The increase in retreatment notification rates appears to be driven largely by increases in the notification rates of the 'relapse' and 'others' types of re-treatment cases. The 're-treatment others' notification rate has almost

doubled from 4 per 100,000 populations in 1999 to 8 per 100,000 populations in 2011. The notification rate of failure-type re-treatment cases has remained almost stable from 2002 onwards at the rate of 2 cases per 100,000 populations. The "Treatment after default" notification rates have declined from 10/100,000 population in 2001 to 6/100,000 population in 2011.

Figure 3: Trends in type of TB case notification rate (199-2011)

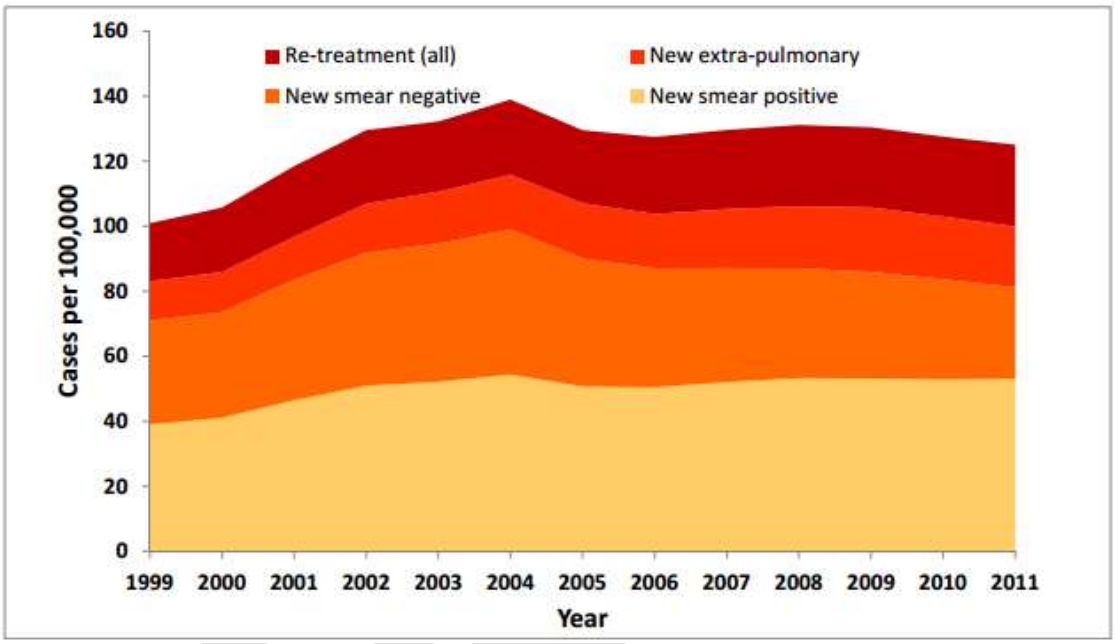

Figure 4: Trends in type of re-treatment TB case notification rate (199-2011)

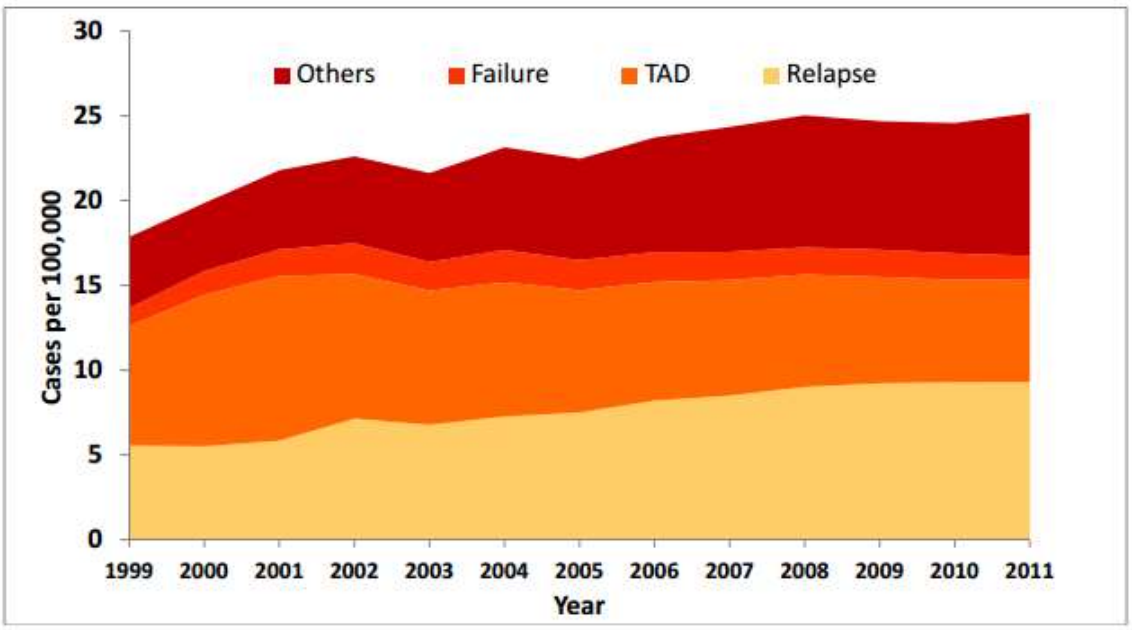

All New (incident) TB Case Notification

The number and rate of all new (incident) cases notified in the country has steadily increased at the rate of 7% annually for several years initially in the implementation of the programme starting from 83 per 100,000 population in 1999 to 116 per 100,000 population in 2004, with almost 40% increase in half a decade. The decline began after complete coverage in the country, and the all new (incident) TB case notification rate has decreased from 116 per 100,000 population in 2004 to 96 per 100,000 population in year 2012 showing a decline of 20%, almost 2% annually which is estimated to continue with the progressing years.

Treatment Outcomes of Notified TB Cases

The treatment success rate has been > 85% since the year 2001. The death rate and failure rate has been about 5% and 2% respectively. The default rates has decreased from 9% for the cohort of TB patients registered in 1999 to 6% for the cohort of patients registered in 2010

Table 1: Treatment outcomes among notified new TB cases, 1999–2010

	New smear positive				New smear negative				New Extra Pulmonary			
Year	Success	Death	Failure	Default	Success	Death	Failure	Default	Success	Death	Failure	Default
1999	82%	5%	3%	9%	85%	4%	1%	9%	91%	2%	0%	6%
2000	84%	4%	3%	8%	86%	3%	1%	9%	91%	2%	0%	7%
2001	85%	5%	3%	7%	86%	4%	1%	8%	91%	2%	0%	6%
2002	87%	4%	3%	6%	87%	4%	1%	7%	92%	2%	0%	5%
2003	86%	5%	2%	6%	87%	4%	1%	7%	92%	2%	0%	5%
2004	86%	4%	2%	7%	87%	4%	1%	8%	92%	2%	0%	5%
2005	86%	5%	2%	7%	87%	4%	1%	8%	91%	2%	0%	6%
2006	86%	5%	2%	6%	87%	4%	1%	8%	90%	3%	0%	5%
2007	87%	5%	2%	6%	87%	3%	1%	8%	91%	2%	0%	5%
2008	87%	4%	2%	6%	88%	3%	1%	7%	92%	3%	0%	4%
2009	87%	4%	2%	6%	88%	3%	1%	7%	92%	2%	0%	4%
2010	88%	4%	2%	6%	89%	3%	1%	7%	93%	3%	0%	4%

As a result of rapid expansion in diagnostic facilities, the proportion of sputum- positive cases confirmed in the laboratory have doubled than that of the previous programme and is on par with international standards. Despite the rapid expansion, overall performance remains good and in many areas is excellent. Treatment success rates have tripled from 25%in the earlier programme to 86%in RNTCP. By the year 2025, a success rate of 99.35% is forecasted with a confidence level of 95% using regression algorithm. Weka tool is used for the purpose of prediction.

Figure 5: Treatment Success Rate

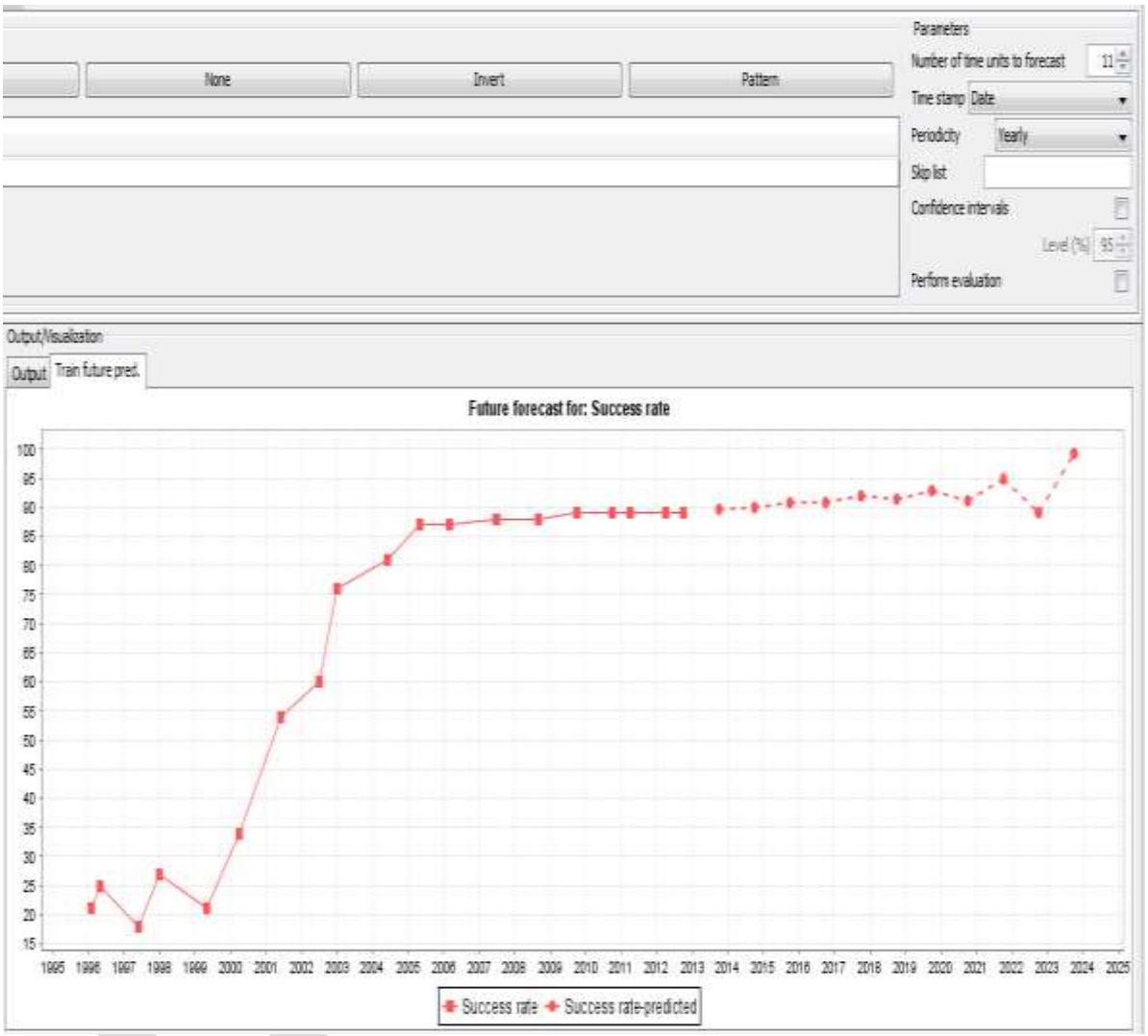

Figure 6: Reporting progress towards set targets

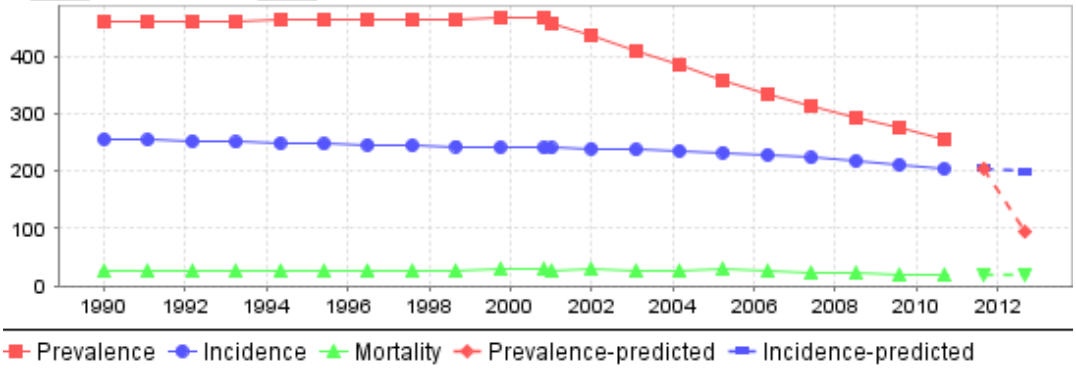

Figure 7: Future forecast for: Prevalence

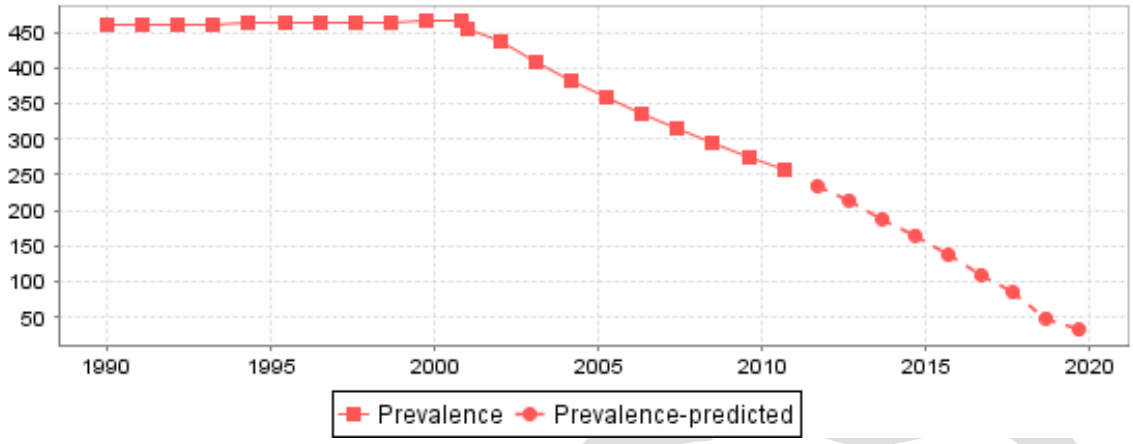

Regarding the target of halving the mortality rate compared to the 1990 baseline, the Region had reached the target in 2013. In fact, considering only the best estimate, in 2013, the mortality rate decreased by 53%; according to the projections based on the assumption that the current trend will not change, the Region would sustain the achievement and even the upper uncertainly bound is expected to be almost entirely below the target.

CONCLUSION

RNTCP is performing well in terms of reduction of TB burden in India. Analysis of progress with regard to tuberculosis control shows that the Region has achieved or is well on track to halt and begin to reverse the incidence of tuberculosis by 2015, and halve the TB death and prevalence rates by 2015, compared with 1990 levels. By the end of 2020, the prevalence of the disease is forcasted to tend towards zero. Regarding the targets of halving the prevalence rates compared to the 1990 baseline, the Region is on track to reach the targets. In fact, considering only the best estimate, in 2013, the prevalence rate decreased by 47%; according to the projections based on the assumption that the current trend will not change, the Region would reach 50% reduction of baseline data. However, almost the entire upper uncertainity bound would be over the target; more accurate estimates resulting from completed or planned prevalence surveys will be useful to confirm achievements in the Region beyond any doubt.

Appendix

Smear positive TB cases diagnosed

=== Run information ===

Scheme:

LinearRegression -S 0 -R 1.0E-8

Lagged and derived variable options:

-F "[Smear positive TB cases diagnosed]" -L 1 -M 6 -G Date

Relation: wine2

Instances: 12

Attributes: 3

Rate of TB suspects examined

Smear positive TB cases diagnosed

Date

Transformed training data:

Smear positive TB cases diagnosed

Date-remapped

Lag_Smear positive TB cases diagnosed-1

Lag_Smear positive TB cases diagnosed-2

Lag_Smear positive TB cases diagnosed-3

Lag_Smear positive TB cases diagnosed-4

Lag_Smear positive TB cases diagnosed-5

Lag_Smear positive TB cases diagnosed-6

Date-remapped^2

Date-remapped^3

Date-remapped*Lag_Smear positive TB cases diagnosed-1

Date-remapped*Lag_Smear positive TB cases diagnosed-2

Date-remapped*Lag_Smear positive TB cases diagnosed-3

Date-remapped*Lag_Smear positive TB cases diagnosed-4

Date-remapped*Lag_Smear positive TB cases diagnosed-5

Date-remapped*Lag_Smear positive TB cases diagnosed-6

Smear positive TB cases diagnosed:

Linear Regression Model

Smear positive TB cases diagnosed =

3.8772 * Date-remapped +
-0.9146 * Lag_Smear positive TB cases diagnosed-3 +
0.9833 * Lag_Smear positive TB cases diagnosed-4 +
0.5973 * Lag_Smear positive TB cases diagnosed-5 +
-0.4175 * Lag_Smear positive TB cases diagnosed-6 +
-0.4089 * Date-remapped^2 +
0.0202 * Date-remapped^3 +
-0.0102 * Date-remapped*Lag_Smear positive TB cases diagnosed-1 +
0.0291 * Date-remapped*Lag_Smear positive TB cases diagnosed-3 +
-0.0422 * Date-remapped*Lag_Smear positive TB cases diagnosed-4 +
-0.0079 * Date-remapped*Lag_Smear positive TB cases diagnosed-5 +
0.0233 * Date-remapped*Lag_Smear positive TB cases diagnosed-6 +

50.041

=== Future predictions from end of training data ===

Time	Smear positive TB cases diagnosed
2000-01-01	65
2001-01-11	73
2002-01-22	75
2003-02-02	76
2004-02-13	76
2005-02-23	77
2006-03-07	79
2007-03-18	79
2008-03-28	79
2009-04-08	79
2010-04-19	81
2011-04-30	83
2012-05-11*	84.2948
2013-05-22*	85.5301
2014-06-02*	88.4084
2015-06-13*	93.1353
2016-06-23*	98.1013
2017-07-05*	103.0451

Trends in suspects examined per smear positive TB case diagnosed

=== Run information ===

Scheme:
LinearRegression -S 0 -R 1.0E-8

Lagged and derived variable options:
-F [trend] -L 1 -M 6 -G Date

Relation: wine2
Instances: 12
Attributes: 2
trend
Date

Transformed training data:

trend
Date-remapped
Lag_trend-1
Lag_trend-2
Lag_trend-3
Lag_trend-4
Lag_trend-5
Lag_trend-6
Date-remapped^2
Date-remapped^3
Date-remapped*Lag_trend-1
Date-remapped*Lag_trend-2
Date-remapped*Lag_trend-3
Date-remapped*Lag_trend-4
Date-remapped*Lag_trend-5
Date-remapped*Lag_trend-6

trend:

Linear Regression Model

trend =

0.0385 * Date-remapped +
-0.0068 * Lag_trend-2 +
-0.746 * Lag_trend-3 +
0.7686 * Lag_trend-4 +
-0.2179 * Lag_trend-5 +
-0.3186 * Lag_trend-6 +
0.0064 * Date-remapped^2 +
0.0012 * Date-remapped^3 +
-0.0144 * Date-remapped*Lag_trend-1 +
0.0014 * Date-remapped*Lag_trend-2 +
0.0131 * Date-remapped*Lag_trend-3 +
-0.0332 * Date-remapped*Lag_trend-4 +
0.0097 * Date-remapped*Lag_trend-5 +
11.3399

=== Future predictions from end of training data ===

Time	trend
2000-01-01	6.48
2001-01-30	7.08
2002-03-02	6.99
2003-04-01	7.11
2004-05-01	7.22
2005-06-01	7.49
2006-07-01	7.44
2007-08-01	7.4
2008-08-31	7.47
2009-09-30	7.81
2010-10-31	8.01
2011-11-30	8.24
2012-12-30*	8.5391
2014-01-30*	9.0823
2015-03-01*	9.5447
2016-03-31*	10.0223
2017-05-01*	10.5312

Forecast for prevalence

=== Run information ===

Scheme:

LinearRegression -S 0 -R 1.0E-8

Lagged and derived variable options:

-F [Prevalence] -L 1 -M 5 -G Year

Relation: wine2

Instances: 21

Attributes: 4

Prevalence

Incidence

Mortality

Year

Transformed training data:

Prevalence

Year-remapped

Lag_Prevalence-1
Lag_Prevalence-2
Lag_Prevalence-3
Lag_Prevalence-4
Lag_Prevalence-5
Year-remapped^2
Year-remapped^3
Year-remapped*Lag_Prevalence-1
Year-remapped*Lag_Prevalence-2
Year-remapped*Lag_Prevalence-3
Year-remapped*Lag_Prevalence-4
Year-remapped*Lag_Prevalence-5

Prevalence:

Linear Regression Model

Prevalence =

-5.0562 * Year-remapped +
1.5441 * Lag_Prevalence-2 +
-1.8314 * Lag_Prevalence-4 +
1.0526 * Lag_Prevalence-5 +
0.0124 * Year-remapped*Lag_Prevalence-2 +
-0.0107 * Year-remapped*Lag_Prevalence-4 +
141.305

=== Future predictions from end of training data ===

Time	Prevalence
1990-01-01	459
1991-01-01	460
1992-01-01	460
1993-01-01	461
1994-01-01	462
1995-01-01	462
1996-01-01	463
1997-01-01	464
1998-01-01	464
1999-01-01	465
2000-01-01	466

2001-01-01	456
2002-01-01	436
2003-01-01	409
2004-01-01	383
2005-01-01	358
2006-01-01	335
2007-01-01	314
2008-01-01	294
2009-01-01	275
2010-01-01	256
2011-01-01*	234.6434
2012-01-01*	214.3271
2013-01-01*	188.6203
2014-01-01*	165.769
2015-01-01*	137.7494
2016-01-01*	110.2066
2017-01-01*	85.3645
2018-01-01*	49.5028
2019-01-01*	32.7302

REFERENCES:

[1] Udwadia, Z "This should not exist", Hindustan Times, November 27, 2012 www.hindustantimes.com/ - See more at: http://www.tbfacts.org/tb-india/#sthash.llxxjViE.dpuf
[2] Pai, M "Formidable killer: drug-resistant tuberculosis", The Tribune, India, August 6, 2013www.tribuneindia.com/2013/ - See more at: http://www.tbfacts.org/tb-india/#sthash.llxxjViE.dpuf
[3] Managing the Revised National Tuberculosis Control Programme in Your Area – A training course, E1- Exercise workbook, Central TB Division Directorate General of Health Services, Ministry of Health and Family Welfare Nirman Bhavan, New Delhi 110011.
[4] Predicting School Ranks Through Data Mining Micah Oppenheim—Boston University CS 105—Professor David G. Sullivan, Ph.D
[5] A Data Mining Perspective on the Prevalence of Polio in India Neera Singh Indian Institute of Information Technology, Allahabad, India, Neera Singh et al. / International Journal on Computer Science and Engineering (IJCSE).
[6] http://infochangeindia.org/public-health/books-a-reports/eradicating-tuberculosis-the-unfinished-agenda.html
[7] Srivastava, K, "TB epidemic looms large with Rs 2,000 crore fund cut, erred policy", dna, 10 January, 2015 www.dnaindia.com/ - See more at: http://www.tbfacts.org/tb-india/#sthash.llxxjViE.dpuf
[8] "Private hospitals report 700 TB cases", The Times of India, August 19, 2013http://articles.timesofindia.indiatimes.com/2013-08-19/pune/ - See more at: http://www.tbfacts.org/tb-india/#sthash.llxxjViE.dpuf
[9] Bhalchandra Chorghade "To fight MDR-TB, act on time", http://dnasyndication.com/dna/MUMBAI/ - See more at: http://www.tbfacts.org/tb-india/#sthash.llxxjViE.dpuf
[10] Tuberculosis control in the South-East Asia Region Annual TB report 2015 World Health Organization Regional Office for south east Asia - http://www.searo.who.int/tb/annual-tb-report-2015.pdf.
[11] Government of India TB India 2013 Revised National TB Control Programme Annual Status Report - http://www.tbcindia.nic.in/pdfs/tb%20india%202013.pdf
[12] Sinha, K "Finally, tuberculosis declared a notifiable disease", The Times of India, May 9, 2012 //articles.timesofindia.indiatimes.com/2012-05-09/india/31640562_1_mdr-tb-tb-cases

International Journal of Engineering Research and General Science Volume 3, Issue 6, November-December, 2015
ISSN 2091-2730

An energy efficiency of cloud based services using EaaS transcoding of the multimedia data.

Harshal P. Ganvir
Computer Science and Engineering
Vidarbha Institute of Technology
Nagpur, India
harshal.ganvir7@gmail.com
8600581510

Abstract— Network-based cloud computing is rapidly expanding all over as an alternative to conventional office-based computing. Cloud computing has become widespread and the energy consumption of the network and computing resources will grow cloud. This happens at a time when there is increasing attention being paid to the need to manage energy consumption across the entire information and communications technology (ICT) sector. Also data center energy use have much attention, as there has been less attention paid to the energy consumption of the transmission and switching networks. This paper, presents an analysis of energy consumption in cloud computing. The analysis will consider both public and private clouds. We show that energy consumption in transport and switching can be a significant percentage of total energy consumption in cloud computing. Cloud computing provides more energy efficiency and use of computing power. Computing tasks are of low intensity or infrequent. Thus, under some circumstances cloud computing may consume more energy than conventional computing where each user performs all computing on their own personal computer (PC).

Keywords — Cloud Computing, Vdata, Energy Efficiency,Transcoding as a Service, QoS, Lyapunov, EaaS, Data centre.

INTRODUCTION

New network-based services has increasing availability of high-speed Internet and corporate IP connections which are enabling the delivery. While Internet-based mail services have many years operating. Service offerings have expanded recently to include network-based storage and network-based computing. Corporate and individual end users both are offered by these new services. This type of services have been generically called B cloud computing services. Service provider are involved by the cloud computing service model of large pools of high performance computing resources and high-capacity storage devices that are shared among end users as required. Many cloud service models and end users subscribing to the service have their data hosted and have computing resources allocated on demand from the pool. The service provider's offering may also extend to the software applications required by the end user. To be successful, the cloud service model also requires a high-speed network to provide connection between the end user and the service provider's infrastructure. Financial benefits are potentially offered through cloud computing, in that end users share and manage pool of storage and computing resources, instead of owning and managing their own systems. In spite of using existing data centers as a basis, cloud service providers invest in the infrastructure and management systems. Thus in return receive an usage-based fee from end users. The service provider reaps the benefits of the economies of scale and from statistical multiplexing, and receives a regular incoming stream from the investment by means of service subscriptions. The end user in turn sees convenience benefits from having data and services available from any location, from having data backups centrally managed, from the availability of increased capacity when needed, and from usage-based charging. The last point is important for many users in that it averts the need for a large one off investment in hardware, sized to suit maximum demand, and requiring upgrading every few years. There are many definitions of cloud computing, and discussion within the IT industry continues over the possible services that will be offered in the future. The broad scope of cloud computing is succinctly summarized. In this paper, we present an overview of energy consumption in cloud computing and compare this to energy consumption in conventional computing. For this comparison, the energy consumption of conventional computing is the energy consumed when the same task is carried out on a standard consumer personal computer (PC) that is connected to the Internet but does not utilize cloud computing. We consider both public and private clouds and include energy consumption in switching and transmission, also data processing and data storage. Specifically, we present a network-based model of the switching and transmission network, a model of user computing equipment, and a model of the processing and storage functions in data centers. We examine a variety of cloud computing service scenarios in terms of energy efficiency. In essence, our approach is to view cloud computing as an analog of a classical supply chain logistics problem, which considers the energy consumption or cost of processing, storing, and transporting physical items. The difference in our case is that, the items are bits of data. As with classical

logistics modeling, our analysis allows a variety of scenarios to be analyzed and optimized according to specified objectives. We explore a number of practical examples in which users/customers outsource their computing and storage needs to a public cloud or private cloud. As the name implies, storage as a service allows users to store data in the cloud. Storage as a service allows users to store data in the cloud. Processing as a service gives users the ability to outsource selected computationally intensive tasks to the cloud. Software as a service combines these two services and allows users to outsource all their computing to the cloud and use only a very-low-processing-power terminal at home. We show that energy consumption in transport and switching can be a significant percentage of total energy consumption in cloud computing. Cloud computing provides more energy-efficient use of computing power, only when the users' predominant computing tasks are of low intensity or arise infrequently. However, we show that under some circumstances cloud computing can consume more energy than conventional computing on a local PC. Our broad conclusion is that cloud computing can offer significant energy savings through techniques such as visualization and consolidation of servers and advanced cooling systems. However, cloud computing is not always the greenest computing technology.

- Overview Of Cloud Computing

Cloud computing is defined as a model enabling ubiquitous, convenient, on-demand network access to a shared pool of configurable computing resources (e.g .networks, servers, storage, applications, and services) that can be rapidly provisioned and released with minimal management effort or service provider interaction[3].

Over the Internet the applications are delivered as service. The hardware and systems software in the data centers that provide services that is software as a service. Its characteristics includes a broad network access which has the ability to access the network via heterogeneous platforms, when it provision the computing power automatically.

PROBLEM STATEMENT

• Adopting the framework of Lyapunov optimization, we propose the control algorithm REQUEST to dispatch transcoding jobs. We characterize the energy-delay tradeoff of the REQUEST algorithm numerically and derive the performance bounds theoretically.

• We study the robustness of the REQUEST algorithm. Numerical results show that, given the inaccuracy of estimating the transcoding time, the error of the time average energy consumption and queue backlog is small. Therefore, the REQUEST algorithm is robust to inaccuracy of the transcoding time estimation.

• We compare the performance of the REQUEST algorithm with Round Robin and Random Rate algorithms using simulation and real trace data. The results show that by appropriately choosing the control variable, the REQUEST algorithm outperforms the other two algorithms, with smaller time average energy consumption while achieving queue stability.

METHODOLOGY

System Model Architecture:-

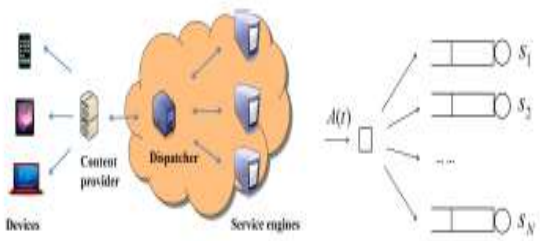

(a) System architecture. (b) System model.

A. Arrival Model

We consider a discrete time slot model[1]. The length of a time slot is τ . Here τ is small such that there is at most one transcoding job arriving to the dispatcher for each time slot. We denote p as the probability of one arrival to the dispatcher for each time slot and 1−p if there are no arrivals. We assume the transcoding time needed for an arriving job at each time slot is associated with the CPU speed of the service engine. Suppose that we have N service engines for transcoding. Each service engine can operate in different CPU speed si , where i = 1, 2, ..., N. Without loss of generality, we assume s1 ≤ s2 ≤ ... ≤ sN. The service engine in faster CPU speed can have less completion time for transcoding. We denote A(t) as the transcoding time needed for the arrival at time slot t by a baseline server, which has a CPU speed S.W.

B. Queuing Model

We model the service engines as a set of queues, as shown in Figure 1(b). To characterize the dynamics of these queues, we define queue length Q(t) as the unfinished transcoding time of jobs in each service engine at time slot t, i.e., Q(t) = {Q1(t), Q2(t), ..., QN (t)}. The queue of the ith service engine evolves according to Qi(t + 1) = max[Qi(t) − τ, 0] + Ai(t)1{u(t)=i}, (2) where Ai(t) is the transcoding time of an arrival at time slot t for the ith service engine. And here1 is an indicator function that is 1 if u(t) = i and 0 otherwise. If u(t) = i, the arrival is dispatched to the ith service engine and the queue length is increased by Ai(t); or else, no arrival occurs.

C. Energy Consumption Model

We consider each service engine as a physical machine2. Particularly, we only consider the computation energy consumption in the service engine, which is a dominant term for the energy consumption in the distributed servers [18]. As such, we ignore other sources of energy consumption in the service engine, e.g., memory and network. We assume that each service engine operates in a constant CPU speed when processing transcoding jobs. Its resulted energy consumption is assumed to be a function of CPU speed. If the dispatcher dispatches the transcoding job to the ith service engine at time slot t, the energy consumption on the ith service engine is Ai(t)κsα i , where Ai(t) is the transcoding time for the ith service engine and κsα i is the power that is a convex function of CPU speed[1].

- MODELS OF ENERGY CONSUMPTION

In this section, we describe the functionality and energy consumption of the transport and computing equipment on which current cloud computing services typically operate. We consider energy consumption models of the transport network, the data center, plus a range of customer-owned terminals and computers. The models described are based on power consumption measurements and published specifications of representative equipment. Those models include descriptions of the common energy-saving techniques employed by cloud computing service providers. The models are used to calculate the energy consumption per bit for transport and processing, and the power consumption per bit for storage. The energy per bit and power per bit are fundamental measures of energy consumption, and the energy efficiency of cloud computing is the energy consumed per bit of data processed through cloud computing. Performing calculations in terms of energy per bit also allows the results to be easily scaled to any usage level.

a) User Equipment.

A user may use a range of devices to access a cloud computing service, including a mobile phone (cell phone), desktop computer, or a laptop computer. In this paper, we focus on desktop computers and laptops. These computers typically comprise a central processing unit (CPU), random access memory (RAM), hard disk drive (HDD), graphical processing unit (GPU), motherboard, and a power supply unit. Peripheral devices including speakers, printers, and visual display devices are often connected to PCs. These peripheral devices do not influence the comparison between conventional

computing and cloud computing and so are not included in the model. In our analysis, we assume that when user equipment is not being used it is either switched off or in a deep sleep state (negligible power consumption).

b) Data Centers.

A modern state-of-the-art data center has three main components Vdata storage, servers, and a local area network (LAN). The data center connects to the rest of the network through a gateway router, as shown on the right-hand side of lists equipment typical of that used in data centers, as well as the capacity and power consumption of this equipment. Power consumption figures for the LAN switches, routers, and storage equipment are the figures quoted in their respective product data sheets. The power consumption data for each server was obtained by first calculating the maximum power using HP's power calculator, then following the convention that average power use for midrange/high-end servers is 66% of maximum power. In the following, we outline the functionality of this equipment as well as some of the efficiency improvements in cloud computing data centers over traditional data centers.

c) Network.

In this section, we describe the corporate and Internet IP networks in greater detail and outline the functionality of the equipment in those networks. Lists equipment used in our calculations of energy consumption in the corporate network and the Internet IP network as well as the capacity and power consumption of this equipment.

- ENERGY EFFICIENCY IN CLOUD INFRASTRUCTURES

Building an energy efficient cloud model does not indicate only energy efficient host machines. Other existing components of a complete cloud infrastructure should also be considered for energy aware applications. Several research works are carried out to build energy efficient cloud components individually. In this section we will investigate the areas of a typical cloud setup that are responsible for considerable amount of power dissipation and we will consolidate the possible approaches to fix the issues considering energy consumption as a part of the cost functions to be applied.

1) Energy Efficient Hardware

One of the best approaches to reduce the power consumption at data centre and virtual machine level is usage of energy efficient hardware's at host side. International standard bodies such as: European TCO Certification, US Energy Star are there to rate energy efficient consumer products. The rating is essential to measure the environmental impact and carbon footprint of computer products and peripherals. New electronics materials like solid-state drives are more power efficient than common hard disk drives but that are costly. The Intel's wireless technology to adjust CPU power dynamically based upon the performance demand. It works in five usage modes: voice communication, standby mode, multimedia, data communication.

2) Energy Efficient Clusters of Servers

Power dissipation is primarily reduced by optimal CPU utilization and tasks scheduling. However other cluster components such as memory, storage discs, network peripherals etc. also consume power and hence a VM having idle CPU may still use considerable amount of energy. Figure shows a typical cloud cluster structure. New approaches aim to reduce the energy consumption as a whole at clusters of servers while considering system's latency and throughput.

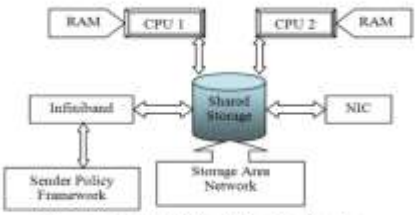

Figure 2. A Typical Cloud Cluster Structure

a) Resource management architecture:

At server side, the operating system of the machine hosts several separate instances of virtual machines. The Optimal resource management architecture should be built based upon the energy estimation in different nodes of a server cluster. Depending upon external situation and workload, the cluster can be easily affected by overloading and overheating despite sufficient cooling system. While a complete shutdown of cluster causes unwanted business downtime, it is the operating system that should take care of auto-scaling of power demand from different cluster components. Dynamic Thermal Management is a technique that controls power dissipation in high performance, server processing unit and provides low "worst case power consumption" with no or little impact on performance. Cluster's network infrastructure is a major area of power dissipation that holds a substantial share of operating cost. Balancing of QoS and resource utilization during outage can also be a descent way of energy management in clusters. Policies are developed for resource management in economic way where cluster always checks for system's work load and allocates resources by calculating their effects on system's overall performance. A greedy allotment method can be used to estimate supply – demand tradeoffs for an efficient allocation of resources.

b) Dynamic Server Provisioning and load dispatching**:**

In order to save energy, Dynamic Server Provisioning method is useful in switching off unnecessary and idle hosts in a cluster. As the number of internet services is increasing rapidly, the servers are also increasing in number to host those services, resulting huge amount of power dissipation in form of heat. Dynamic Server Provisioning algorithms are designed to turn off extra servers and to allow the cluster to run on minimal number of host machines to satisfy the service load. Thereafter, load dispatching technique effectively distributes the current load among available servers. These techniques can be implemented in servers operating request-response type services (example: web services) as well as host machines connected to huge number of long lived TCP connections. For multi-tier internet services, queuing method can be implemented in dynamic provisioning technique that can be defined as a proactive and reactive approach to estimate short-term and long-term workload fluctuations in cluster. It can predict minimum capacity required for maintaining the required QoS and can also balance sudden surges in server load.

3) Energy efficient Network Infrastructure in cloud:

Minimizing energy consumption in various elements of cloud computing such as storage and computation has already been given importance by the researchers but the issue of energy minimization in network infrastructure is not given as much importance. Network in a cloud environment can be of two types - wireless network and wired network. According to ICT energy estimates in the radio access network consumes a major part of the total energy in an infrastructure and the cost incurred on energy consumption is sometimes comparable with the total cost spent on personnel employed for network operations and maintenance, provided a thorough study on routing protocols for saving energy consumption in sensor networks and wireless adhoc networks.

ACKNOWLEDGMENT

There are many persons in Vidarbha Institute Of Technology Nagpur College have supported me from the beginning of my Mtech project. Without them, the project work would obviously not have looked the way it does now. The first person I would like to thank is guide Prof. Pravin G. Kulurkar, Department of Computer Science and Engineering. His enthusiastic engagement in my project work never ending stream of ideas has been absolutely essential for the results, presented here. I am very grateful that he has spent so much time with me discussing different problems ranging from philosophical issues down to minute technical details.

CONCLUSION

In this paper we have investigated the need of power consumption and energy efficiency in cloud computing model.This work advances Cloud computing field in two ways. First, it plays a significant role in the reduction of data center energy consumption costs and thus helps to develop strong competitive. Cloud computing is facing an increasing attention nowadays, but it raises severe issues with energy consumption. The energy savings from cloud storage are minimal. In cloud software services, power consumption in transport is negligibly small at very low screen refresh rates.

REFERENCES:

[1] Weiwen Zhang, Yonggang Wen,Member 2013 IEEE, "Towards Transcoding as a service in Multimedia Cloud: Energy-Efficient Job Dispatching Algorithm."

[2] A Pliant-based Virtual Machine Scheduling Solution to Improve the Energy E_ciency of IaaS Clouds A. Kertesz _ J. D. Dombi _ A. Benyi.

[3] A Survey on Resource Allocation and Monitoring in Cloud Computing, vol 4, no 1, feb2014, Mohd Hairy Mohamaddiah, Azizol Abdullah, Shamala Subramaniam, and Masnida Hussin.

[4] Cisco Visual Networking Index: Forecast and Methodology, 2012–2017,2013.

[5] A. Vetro and C. W. Chen, "Rate-reduction transcoding design for wireless video streaming," inwork *Proc. Int. Conf. Image Process.*, 2002, vol. 1, pp. I-29–I-32.

[6] M. Armbrust, A. Fox, R. Griffith, A. Joseph, R. Katz, A. Konwinski, G. Lee, D. Patterson, A. Rabkin, I. Stoica, and M. Zaharia, "A view of cloud computing," *Commun. ACM*, vol. 53, no. 4, pp. 50–58, Apr. 2010.

[7] A. Garcia, H. Kalva, and B. Furht, "A study of transcoding on cloud environments for video content delivery," in *Proc. ACM Multim. Worksh. Mobile Cloud Media Comput.*, 2010, pp. 13–18.

[8] Z. Li, Y. Huang, G. Liu, F. Wang, Z.-L. Zhang, and Y. Dai, "Cloud transcoder: Bridging the format and resolution gap between Internet videos and mobile devices," in *Proc. 22nd Int. Workshop Netw. Oper. Syst. Support Digit. Audio Video*, 2012, pp. 33–38.

[9] M. J. Neely, "Stochastic network optimization with application to communication and queueing systems," *Synthesis Lectures Commun. Netw.*, vol. 3, no. 1, pp. 1–211, 2010.

[10] J. Guo and L. N. Bhuyan, "Load balancing in a cluster-based web server for multimedia applications," *IEEE Trans. Parallel Distrib. Syst.*, vol. 17,no. 11, pp. 1321–1334, Nov. 2006.

[11] D. Seo, J. Kim, and I. Jung, "Load distribution algorithm based on transcoding time estimation for distributed transcoding servers," in *Proc.ICISA*, 2010, pp. 1–8.

[12] A. Garcia and H. Kalva, "Cloud transcoding for mobile video content. delivery," in *Proc. IEEE ICCE*, 2011, pp. 379–380.

[13] S. Ko, S. Park, and H. Han, "Design analysis for real-time video transcoding on cloud systems," in *Proc. 28th Annu. ACM Symp. Appl. Comput.*2013, pp. 1610–1615.

[14] Amazon Elastic Compute Cloud (EC2). [Online]. Available:http://www.amazon.com/ec2/

[15] Google App Engine. [Online]. Available: http://www.appengine.google.com

International Journal of Engineering Research and General Science Volume 3, Issue 6, November-December, 2015
ISSN 2091-2730

Transient Response For The Advection Dispersion Problem To Approach From Unsteady To Steady State

Pritimanjari Sahu[#1], Prof. P. K. Das[*2]

[1]*Department of Civil Engineering, V.S.S.U.T, Burla768018, Odisha, India.*

[1]*priti.ipi@gmail.com*

Contact no-8895257040

Abstract— Transient response of one dimensional advective dispersive transport problem to approach from unsteady to steady state is determined. Explicit Finite-Difference numerical technique is used to find the numerical solution of transport equations. Also MATLAB code is developed for the numerical solution. The effect of different parameter changes with respect to spatial distribution at a particular time has been compared and time required from unsteady to steady state with respective parameter change is determined. As dispersion coefficient and decay constant enhances, the concentration of solute enhances but time required to approach from unsteady to steady state enhances in case of dispersion coefficient where as reduces in case of decay constant. Also as velocity enhances, the solute concentration enhances and time of approach reduces. Effect of Peclet number on solute concentration with respect to spatial and temporal variation also analyzed.

Keywords— Solute transport; Finite Difference Method; Concentration Profile; Dispersion Coefficient; Decay constant; Peclet number; Spatial Moment; Temporal Moment.

INTRODUCTION

In recent days, groundwater resources have become increasingly polluted by the production of reactive and non reactive contaminants from industrial and/or household waste, infiltration of pesticides and fertilizers from agricultural areas and leakage of organic pollutants from petrol stations, refineries, pipelines etc. Once ground water infected it becomes difficult to improve its quality. In the present study the mathematical modelling of ground water solute transport in saturated porous media with respect to different real life problem were done. This is due to the fact that many of the geo environmental engineering problems have direct or indirect impact on the groundwater flow and solute transport. So its management and remediation becomes a essential work for the engineers. Previously several mathematical models were developed by scientists for the solute transport problems. Many of the models used to describe the transport of solutes in the subsurface are based on the convection-dispersion equation as given by Bear(1972, 1979).Broadly the type of models are divided in to two types-non reactive and reactive solute transport. Yetes (1990) developed an analytical solution for describing the 1-D transport of dissolved substances in heterogeneous porous media with a distance-dependent dispersion relationship. The model in this used assumes that the dispersion coefficient is a linear function of the space dimension and that this linear dependence is a direct consequence of the heterogeneous nature of the porous medium. The solution has been obtained for a constant concentration and for constant flux boundary conditions using both an exact and numerical inversion of the Laplace-transformed transport equation. Batu and Genuchten (1990) developed first and third type boundary conditions in 2-D solute transport modelling .It presents a general analytical solution for convective-dispersive solute transport in a 2-D semi infinite porous medium. Fresh et al (1998) executed column experiment to known the effect of water content on solute transport in a porous medium containing reactive micro-aggregates. The water content of porous media may affect the transport behavior of conservating & sorbing solutes. An accurate 2D simulation of advective-diffusive-reactive transport was proposed by Stefanovic and Stefan (2001). It presents an accurate numerical algorithm for the simulation of 2D solute/heat transport by unsteady advection-diffusion-reaction. Atul Kumar et al (2009) developed analytical solutions of one-dimensional advection–diffusion equation with variable coefficients in a finite domain for two dispersion problems. In the first one, temporally dependent solute dispersion along uniform flow in homogeneous domain is studied. In the second problem the velocity is considered spatially dependent due to the in-homogeneity of the domain and the dispersion is considered proportional to the square of the velocity. The velocity is linearly interpolated to represent small increase in it along the finite domain. This analytical solution is compared with the numerical solution in case the dispersion is proportional to the same linearly interpolated velocity. Fedi (2010) proposed a new analytical solution for the 2D advection–dispersion equation in

semi-Infinite and laterally bounded domain. An analytical solution for 2-d Solute transport (Singh et al,2010) in Finite Aquifer with Time-dependent Source Concentration was developed. Using Hankel Transform Technique, an analytical solution is derived for 2-d solute transport in a homogeneous isotropic aquifer with time-dependent source concentration. Chen and Liu (2011) proposed generalized analytical solution for 1-D advection-dispersion equation in finite spatial domain with arbitrary time-dependent inlet boundary condition. The generalized analytical solution of the equation is derived by using the Laplace transform. Result shows an excellent agreement between the analytical and numerical solutions. Sharma and Srivastava (2011) proposed numerical analysis of virus transport through a 2-D heterogeneous porous media. Virus transport through two-dimensional heterogeneous porous media at field scale is simulated using an advective dispersive virus transport equation with first-order adsorption and inactivation constant. An increasing exponential dispersivity function has been used to account for heterogeneity of the porous media. Implicit finite-difference numerical technique is used to get the solution of two-dimensional virus transport equation for virus concentration in suspension. A reactive transport through porous media using finite-difference and finite-volume methods developed by Sharma et al(2012). Finite-volume method (FVM) and implicit finite-difference method (FDM) have been used to solve multi-process non-equilibrium (MPNE) transport equation for reactive solute transport through porous media. Sharma et al (2013) developed stochastic numerical method for analysis of solute transport in fractured porous media. They developed stochastic two dimensional numerical models for the solute transport through fractured rock, treating the matrix diffusion coefficient as a stochastic process and evaluated the effect of the variance of log diffusion and integral scale on mean travel distance, spreading behavior and effective dispersion coefficient for the solute in the fracture. Sharma et al (2014) proposed finite volume model (FVM) for reactive transport in fractured porous media with distance- and time-dependent dispersion. In this study, the behavior of temporal and spatial concentration profiles with distance- and time-dependent dispersion models is investigated. Also Hulagabali et al(2014) suggested contaminant transport modeling through saturated porous media using Finite Difference and Finite Element Methods. It presents an alternative numerical method to model the two dimensional contaminant transport through saturated porous media using a finite difference method (FDM) and finite element method (FEM).Also a MATLAB code was developed to obtain the numerical solution. CTRAN/W also used for modeling of contaminant transport which is based on the finite element method. Results of the FDM and FEM are compared and it is found that they agree well.

In this work the transport of solute in porous media is modeled for one direction. According to it the Advective Diffusive Equation is developed and its approximate solution was found out by explicit Finite Difference Method. Also a computer programming in MATLAB is developed for the explicit scheme. The model is used to simulate the field experimental data of spatial and temporal moments. The time required from unsteady to steady state with respective parameter change is also determined.

GOVERNING EQUATION

The one-dimensional solute transport in homogeneous, saturated porous media is governed by the following advective-diffusion- equation(ADE) with first-order reaction.

$$\frac{\partial C}{\partial t} = D\frac{\partial^2 C}{\partial x^2} - U\frac{\partial C}{\partial x} - kC \qquad (1)$$

Where C= concentration (moles/m^3), D=dispersion coefficient (m^2/h), U=Q/A=velocity of water (m/h), Q=flow rate (m^3/h), A=tank's c/s area (m^2), k =the first order decay coefficient (h^{-1}), L=length of the flume (m) and t =time (h).

In this investigation, an explicit finite-difference numerical technique has been used to get the solution of solute transport equations Eqs. (1).The explicit finite-difference formulation of above equation can be written as:

$$\frac{C_i^{l+1} - C_i^l}{\Delta t} = D\frac{C_{i+1}^l - C_i^l + C_{i-1}^l}{(\Delta x)^2} - U\frac{C_{i+1}^l - C_{i-1}^l}{2\Delta x} - kC_i^l \qquad (2)$$

Here, the subscript i-designates the grid point along x-direction, l time factor and Δx grid size in x direction and Δt is the time step.

APPLICATION OF MODEL

A elongated flume with a single entry and single exit point as shown in fig.(1) is considered. The water is flowing to the flume from a tank with some velocity to some given distance. Prior to time (t) =0, the tank is filled with water that is devoid of the reactive solute. At time=0, the reactive solute is injected into the flume's inflow at a constant level of C_{in}. The flume is well mixed with the solute vertically and laterally. The reactive solute is subject to first-order decay.

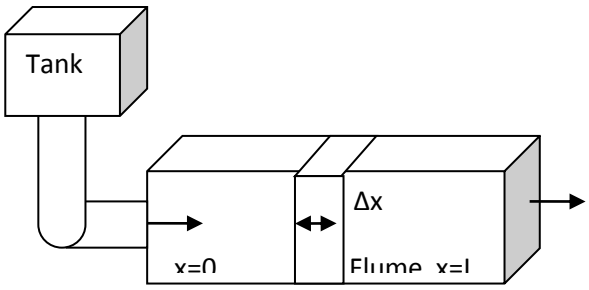

Figure-1 Flume of length L with an overhead tank with a single entry and exit point.

Following initial and boundary conditions have been used:

Initial condition

$$C=C_{in} \qquad 0<x<L \qquad \text{at } t=0 \qquad (3a)$$

Boundary condition

$$QC_{in}=QC_0-DA\frac{dC_0}{dx} \qquad \text{at } x=0$$

and $$\frac{\partial C}{\partial x}=0 \qquad \text{at } x=L \qquad (3b)$$

where C_0=the concentration at x=0. An explicit finite-difference numerical technique has been used to get the solution of solute transport equations Eqs. (1),(3a) and(3b).

RESULT AND DISCUSSION

The ADE of one dimensional solute transports was solved. The solute transport in x direction is discritised. The graphical presentation of normalised concentration according to different parameter change with respect to space and time was shown below which are drawn by application of MATLAB.

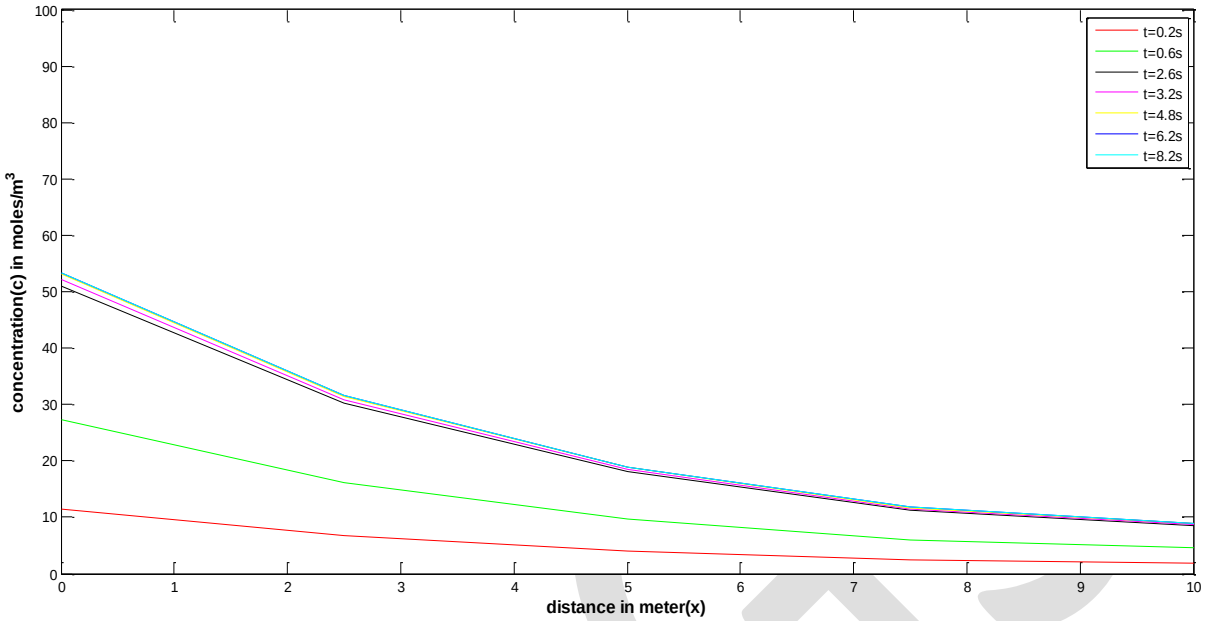

Figure-2 Spatial distribution of concentration profiles at different time interval in hour to attained to steady state .(U=0.5m/h, $D=2m^2/h$, $k=0.2h^{-1}$)

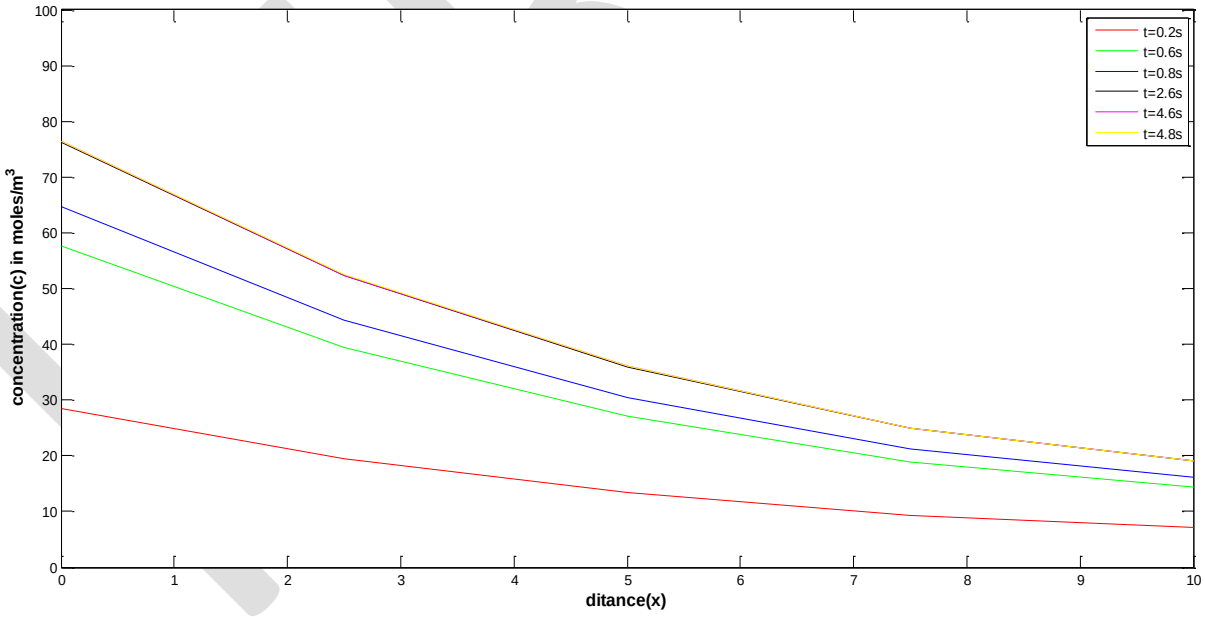

Figure-3 Spatial distribution of concentration profiles at different time interval in hour to attained to steady state ($U=1m/h$, $D=2m^2/h$, $k=0.2h^{-1}$)

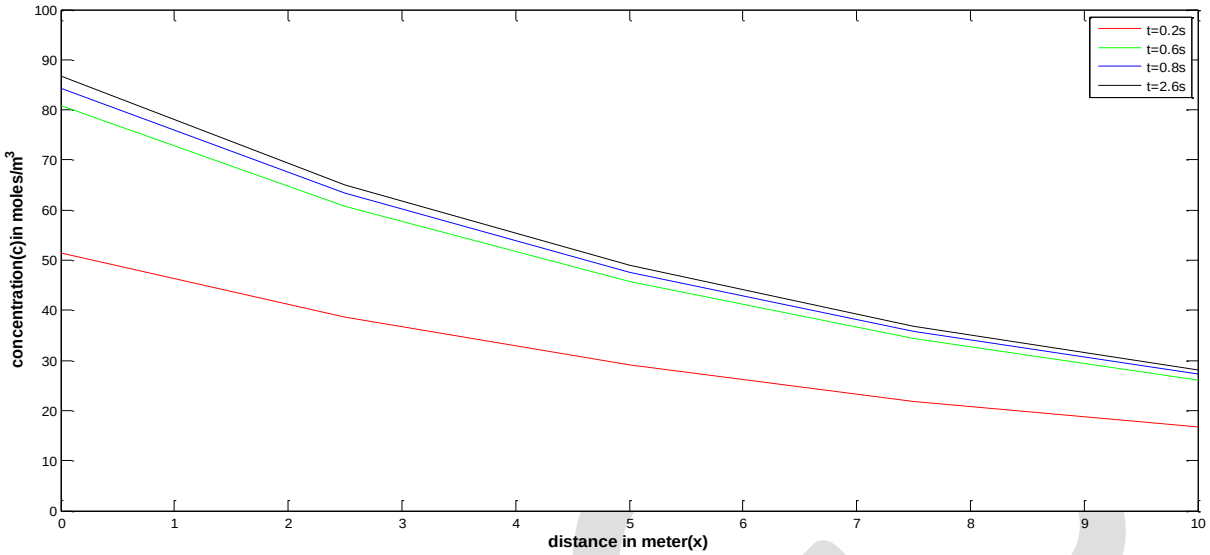

Figure-4 Spatial distribution of concentration profiles at different time interval in hour to attained to steady state ($U=1.5m/h$, $D=2m^2/h$, $k=0.2h^{-1}$)

Comparing fig.2, 3 and 4 it is observed that as velocity (U) increases the concentration profile value also increases in both x and y direction but the time required to attain from unsteady state to steady state decreases. If we compared the concentration profile at steady state in the three figure we get 53.18, 76.40 & 86.60 in y direction with velocity value of 0.5, 1 and 1.5m/s respectively. Hence if velocity increases the concentration value also increases. Also we can get time interval of 8.2, 4.8 and 2.6s at the steady state with the velocity value of 0.5, 1 and 1.5m/s respectively which conclude that as velocity increases the time required to attain from unsteady state to steady state decreases. As time passes we also get ascending concentration profiles which merges gradually with steady state profile and seen as one solid line.

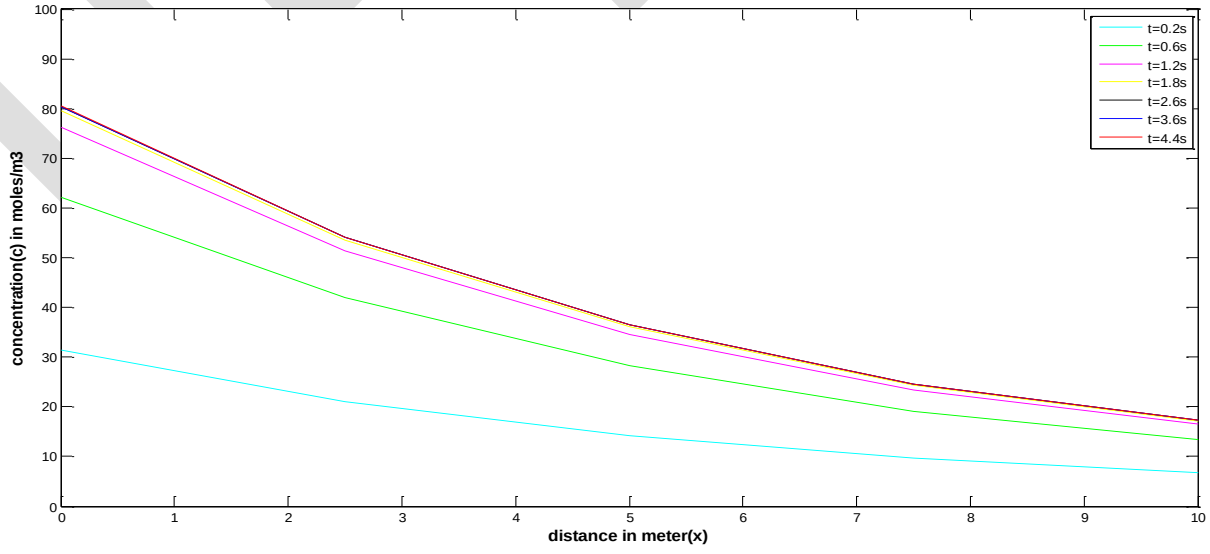

Figure- 5 Spatial distribution of concentration profiles at different time interval in hour to attained to steady state ($U=1m/s$, $D=1.5m^2/h$, $k=0.2h^{-1}$)

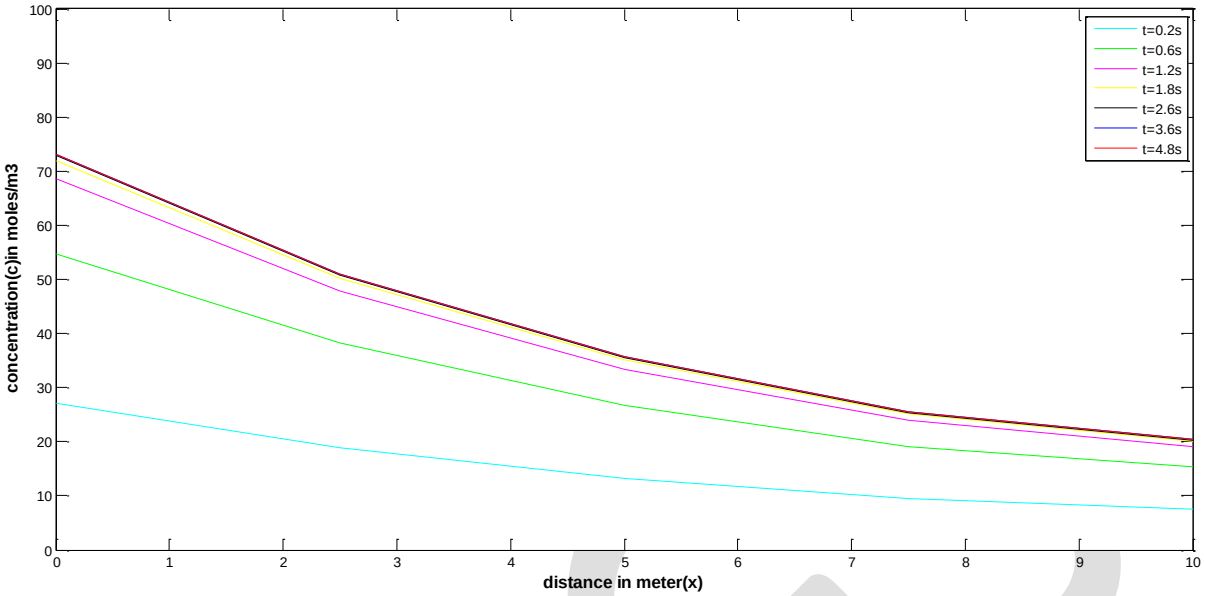

Figure-6 Spatial distribution of concentration profiles at different time interval in hour to attained to steady state ($U=1m/s$, $D=2.5m^2/h$, $k=0.2h^{-1}$)

Comparing fig.3, 5 and 6 we get ascending profiles as time increases and at steady state they merge. It is observed that as dispersion coefficient (D) increases the time required to attained from unsteady state to steady state increases. Also if we compared the concentration profile at steady state in the three figure we get that if dispersion coefficient increases the concentration value also decreases and become flatter and flatter.

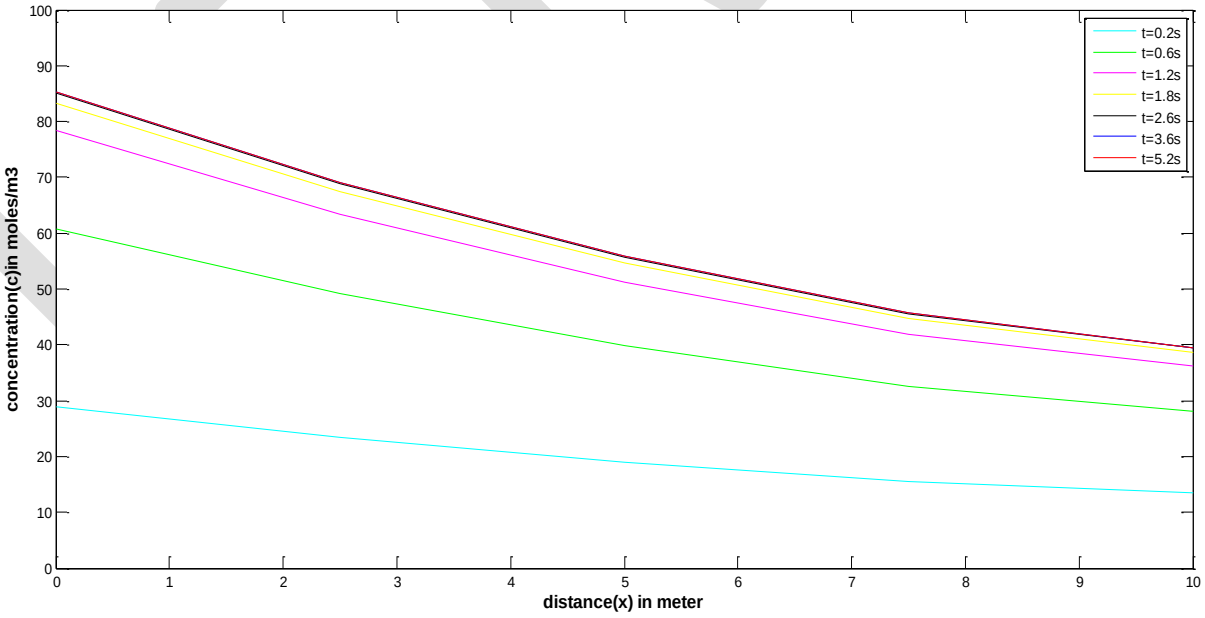

Figure-7 Spatial distribution of concentration profiles at different time interval in hour to attained to steady state ($U=1m/s$, $D=2m^2/h$, $k=0.1h^{-1}$)

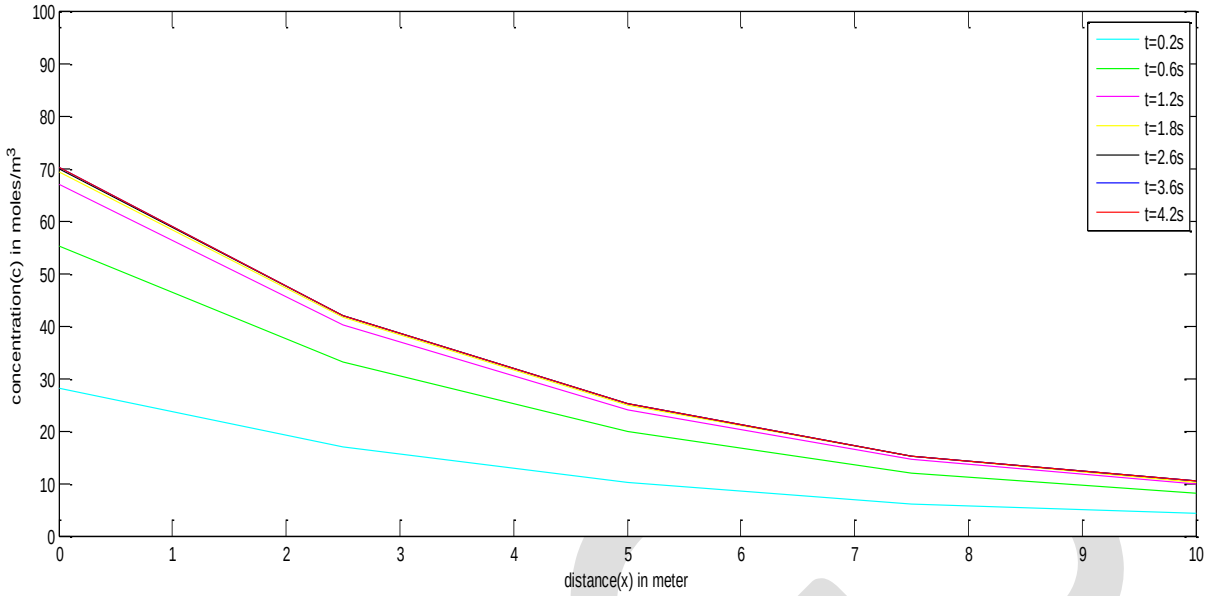

Figure-8 Spatial distribution of concentration profiles at different time interval in hour to attained to steady state (U=1m/s, $D=2m^2/h$, $k=0.3h^{-1}$)

Comparing fig.3, 7 and 8 we also get ascending profiles as time passes. It is observed that as decay constant increases the time required to attain from unsteady state to steady state decreases. Also if we compared the concentration profile at steady state in the three figure we get that if decay constant increases the concentration value also decreases.

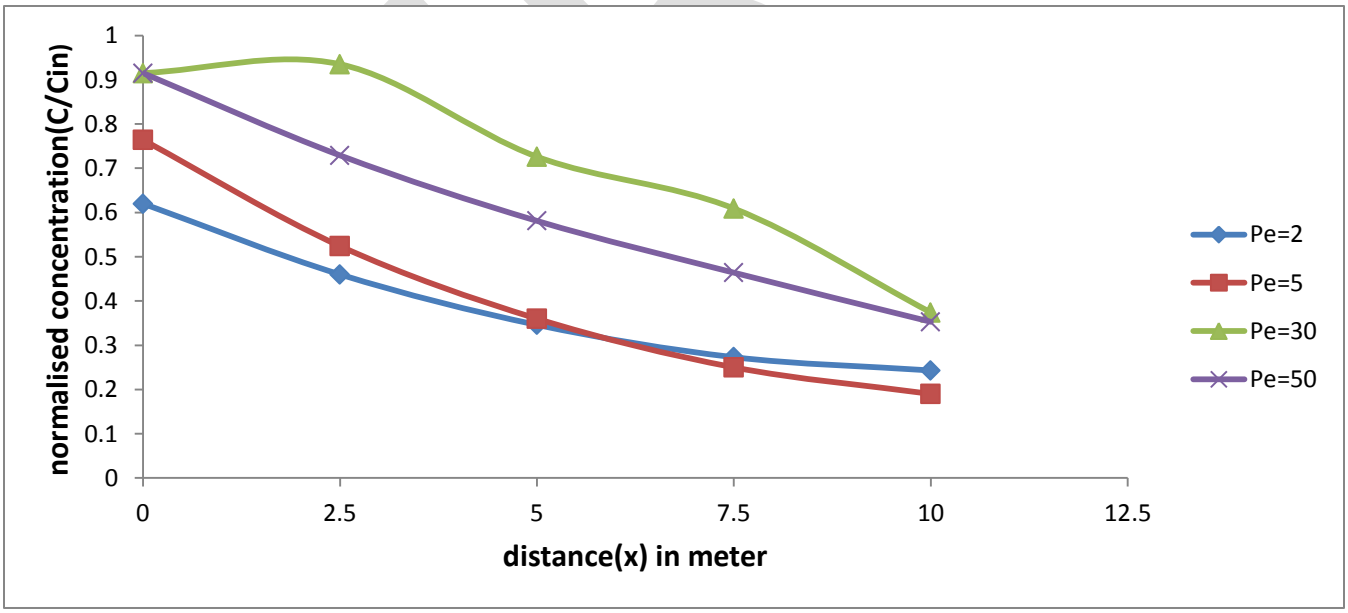

Figure-9 Spatial distribution of concentration profiles for different value of Peclet number after time 4hr ($k=0.2h^{-1}$)

Fig. 9 shows the spatial distribution of solute concentration profile at a time of 4 hour at different value of column peclet number (Pe=Ul/D where l is a reference length).We get that as Peclet no. increases the concentration value increases. But more increase in Peclet no gives an unpredicted value. To reduce the numerical error, we kept value of both the grid Peclet number($U*\Delta x/D$) and Courant number($U*\Delta t/\Delta x$) less than one. Here grid size $\Delta x=2.5$ cm and $\Delta t=0.2h$ is taken.

.

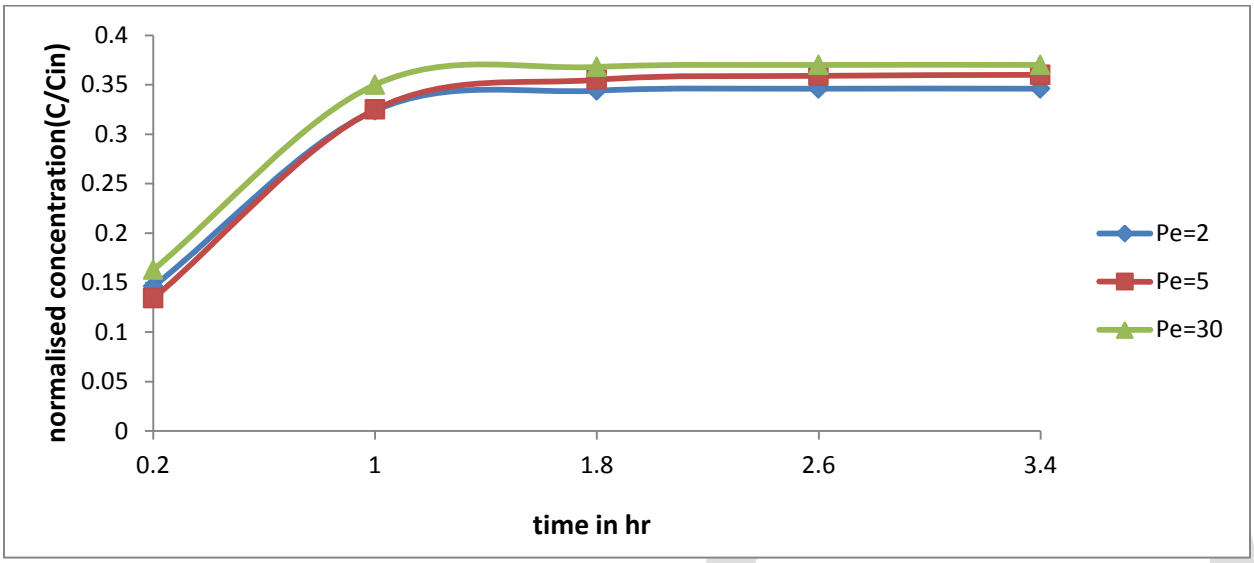

Figure-10 Temporal distribution of concentration profiles for different value of Peclet number at distance 5m.

Fig 10 shows that as time increases the solute concentration increases at early time but as time increases it becomes steady. As time increases the profile increases rapidly but after some time it becomes straight and slope becomes zero. So temporal variation is reverse of spatial variation.

ACKNOWLEDGMENT

First of all I would like to express my sincere gratitude to my paper adviser and project guide, Prof. P. K. Das, for his constant guidance and encouragement throughout the course of my study. I am greatly indebted to him for allowing me to carry out my work under his guidance. It is only for his guidance that I could accomplish my project on time. I thank him a lot for his help and supervision. Without his timely advice and help my project work would not have been up to the standard.I would like to express my sincere thanks to Asst. Prof P.K. Jena, faculty of Mechanical Engineering, for his kind help and assistance in software programming. I would like to express my sincere thanks to all the faculty members, Department of Civil Engineering for their kind help and assistance. Words fail to express my deep sense of gratitude especially towards my parents and my husband for their patient love, moral encouragement and support which enabled me to complete this work. I thank all my batch mates who have extended their cooperation and suggestions by way of discussion at various steps in completion of this paper.

CONCLUSION

An explicit finite-difference technique has been used to get the solution of solute transport model for the case of unsteady state in porous media at field scale. According to parameter changes velocity is directly proportional to the concentration of solute where as decay constant and dispersion coefficient are inversely proportional to the concentration of solute in case of spatial variation. The time period required to attain from unsteady state to steady state decreases as velocity increases. Also it is observed that as dispersion coefficient increases the time required to attained from unsteady state to steady state increases but as decay constant increases the time required to attain from unsteady state to steady state decreases.

The effect of Peclet number on spatial and temporal solute concentration in porous media is studied. The numerical calculation minimizes the error when Peclet number taken as less than one. The concentration profile has descending nature with respect to spatial variation and ascending and remains constant after a particular time with respect to temporal variation.

REFERENCES:

[1] J.A. Ashour, D.M. Joy, H. Lee, H.R. Whitely and S. Zelin “Transport of Micro-organisms Through Soil” Water, Air and Soil Pollution 75:141-158, 1993.

[2] V. Batu and Genuchten "First and Third -Type boundary conditions in 2d solute transport modeling" Water resources research, vol. 26,no .2, pages 339-350,1990.

[3] S.C. Chapra and R.P. Canale, "Numerical Methods for Engineers". McGraw-Hill Book Company.

[4] J.S. Chen, and C.W. Liu "Generalized analytical solution for advection-dispersion equation in finite spatial domain with arbitrary time-dependent inlet boundary condition" Hydrol. Earth Syst. Sci., 15, 2471–2479, 2011.

[5] C.V. Chrysikopoulos, P.K. Kitanidis and P.V. Roberts "Analysis of 1-d solute Transport Through Porous Media with Spatially Variable Retardation Factor". Water resources research, vol. 26, no.3, pages.437-446, 1990.

[6] A. Fedi "A New Analytical Solution for the 2D Advection–Dispersion Equation in Semi-Infinite and Laterally Bounded Domain". Applied Mathematical Sciences, Vol. 4, 2010, no. 75, 3733 – 3747, 2010.

[7] C. Fresh, P. Lehmann, S. B. Haderlein, C.Hinz, R.P. Schwazenbach and H. Fluhier "Effect of Water Content on solute transport in a porous medium containing reactive micro-organisms". Journal of Contaminant Hydrology 33,211-230, 1998.

[8] A.M. Hulagabali, C. H. Solanki and G.R. Dodagoudar "Contaminant Transport Modelling through Saturated Porous Media Using Finite Difference and Finite Element Methods" IOSR Journal of Mechanical and Civil Engineering (IOSR-JMCE) e-ISSN: 2278-1684, p-ISSN: 2320-334X PP 29-33,2014

[9] P.K. Sharma and R. Shrivastava "Numerical analysis of virus transport through heterogeneous porous media"Journal of Hydro-environment Research 5,93-99,2011.

[10] P.K. Sharma, N. Joshi, C.P. Ojha "Reactive transport through porous media using finite-difference and finite-volume methods". ISH Journal of Hydraulic Engineering 18:1, 11-19, DOI:10.1080/09715010.2011.648751,2012.

International Journal of Engineering Research and General Science Volume 3, Issue 6, November-December, 2015
ISSN 2091-2730

Automatic Braking and Control for New Generation Vehicles

Absal Nabi
Assistant Professor,EEE Department
Ilahia College of Engineering & Technology
absalnabi@gmail.com
+919447703238

Abstract- To develop an automatic acceleration and braking new generation vehicle, we need to modify the acceleration controller and braking system simultaneously. In the electric scooter in which we are using works on 48V battery. The same battery provide supply to other circuit elements and motor (12V) used in the scooter. The acceleration is controlled by controlling the supply to the controller whereas the brake control is done by using wiper motor (dc servo motor) which directly control the braking system. In distance control mode, a PIC logic algorithm is applied. Input to the PIC logic controller is distance from the obstacle and relative speed. According to the distance from the obstacle the rate of working of wiper motor and braking system is controlled.

INDEX TERMS - cruise control, ultrasonic sensor, automatic braking.

I. Introduction

Cruise control system is developed for highway driving. Nowadays hundreds of people dies and lots of people are damaged due to accidents. This system is useful avoiding accidents especially for driving in the roads which arebig, straight, and the destination is farther apart. When traffic congestion is increasing, the conventional cruise control becomes less useful. The adaptive cruise control (ACC) system is developed to cope up with this situation.[2] mentioned that conventional cruise control provides a vehicle with one mode of control, velocity control. On the other hand automatic breaking and acceleration (ABAV) system provides two modes of control i.e. brake control and acceleration control. This system automatically decreases the speed when as the obstacle is coming closer. This system provides safe and effective driving especially in highways.

In this research the proposed system is done on an electric scooter in which the acceleration is done by using a BLDC controller. The power to the electric scooter is from battery which provides 48V. We are controlling the rear brakes, for automatic braking system. Normal braking as desired by driver can be done at any time required. In this system we are using PIC logic which measures distance between the obstacle and sends output command as velocity command and braking command.

II. Hardware

To develop the (ABAV) system for the intelligent vehicle (electric scooter), hardware and sensors are designed and installed on the platform.

A.Electric Scooter

The electric scooter used for this research works on 48V dc supply which is provided by four 12V batteries which are connected in series. For the working of other components 5V supply is required which is obtained by dc-dc converter

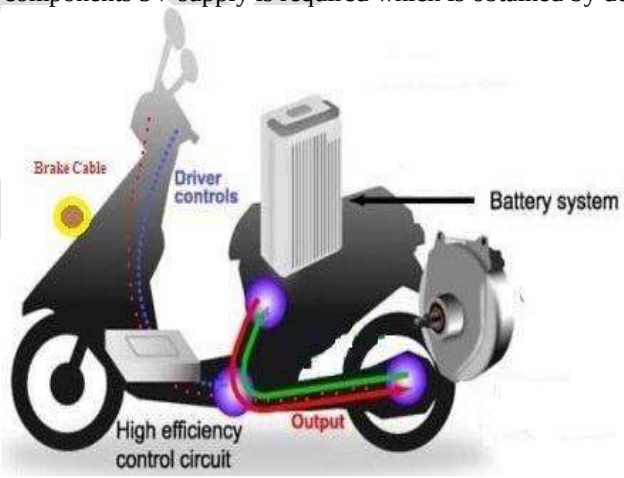

The scooter has a maximum speed of 35km/hr and it is provided with an inbuilt BLDC controller which makes the working of scooter more smooth, silent and efficient.

B. Ultrasonic Sensor

The main component for ABAV is ultrasonic sensorHC - SR04. This sensor has a max range of 4m and a min range of 2m.Both the transmitter and receiver sections are included in the same unit. The transmitter sends pulses of about 40 KHz and after reflecting from the target it gets reflected back as echo which is then captured by the receiver part. By measuring the time difference between the transmitted and received pulses the distance of the obstacle can be measured using the formula:

You only need to supply a short 10uS pulse to the trigger input to start the ranging, and then the module will send out an 8 cycle burst of ultrasound at 40 kHz and raise its echo. The Echo is a distance object that is pulse width and the range in proportion.

C. Wiper Motor

The wiper motor is provided in order to have automatic braking system. The wiper motor used in this research works on 12V supply which can be taken from a single battery of electric scooter. We can replace the wiper motor by using shunt motor.

D. Connecting Rod Arrangement

To change the rotational motion into linear motion connecting rod mechanism is used. The wiper will have a rotational motion and to change to linear motion we connect one end of connecting rod at the end of the wiper motor leads and the other end of the brake cable which is attached to braking system of rear wheel. In fig 2 shows a circle which depicts the wheel and using connecting rod it converted into linear motion.

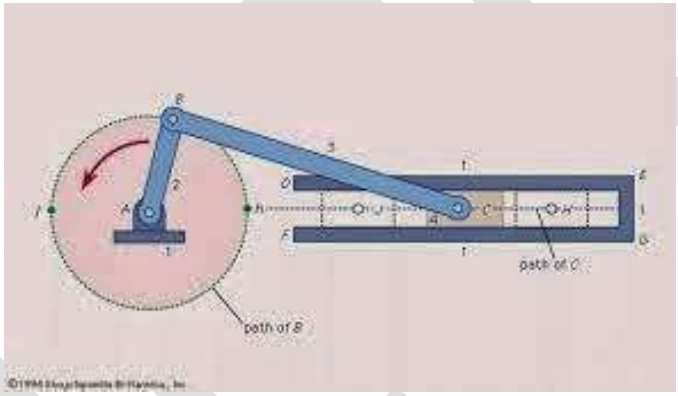

Fig.2 Connecting Rod Mechanism

III. Block Diagram Representation

The block diagram consist of accelerator which is connected to the battery. As the accelerator cable contracts the speed of the vehicle can be controlled. When the ultrasonic sensor detects the obstacle the signal is sent to the electronic circuit and the output of electronic circuit unit (PIC) is sent to the relays which automatically closes and opens with the range of obstacle. With the working of relays working of motor and supply from battery can be cut off as required.

The circuit diagram shown in fig 4 shows the power circuit which converts the ac supply into 12V dc supply using rectifier circuit and regulator. PIC is the main component in the circuit. All the components like ultrasonic sensor are interfaced to PIC using different ICs. ULN2003 is used to interface relay with PIC, RS232 is interfaced to PIC. The circuit consists of a crystal oscillator and two capacitor which control the oscillation and life of PIC. The LCD unit is used to display the distance which is interfaced to PIC.

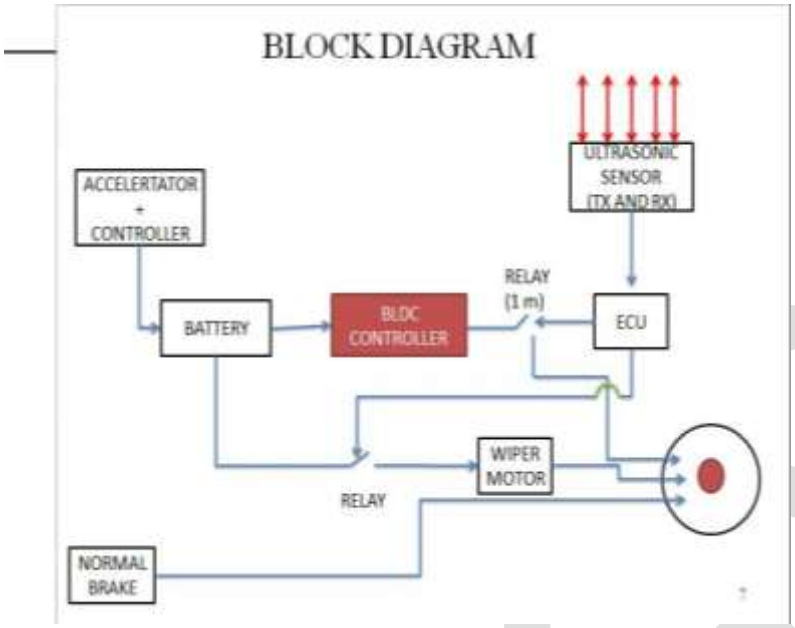

Fig 3. Block Diagram of proposed system

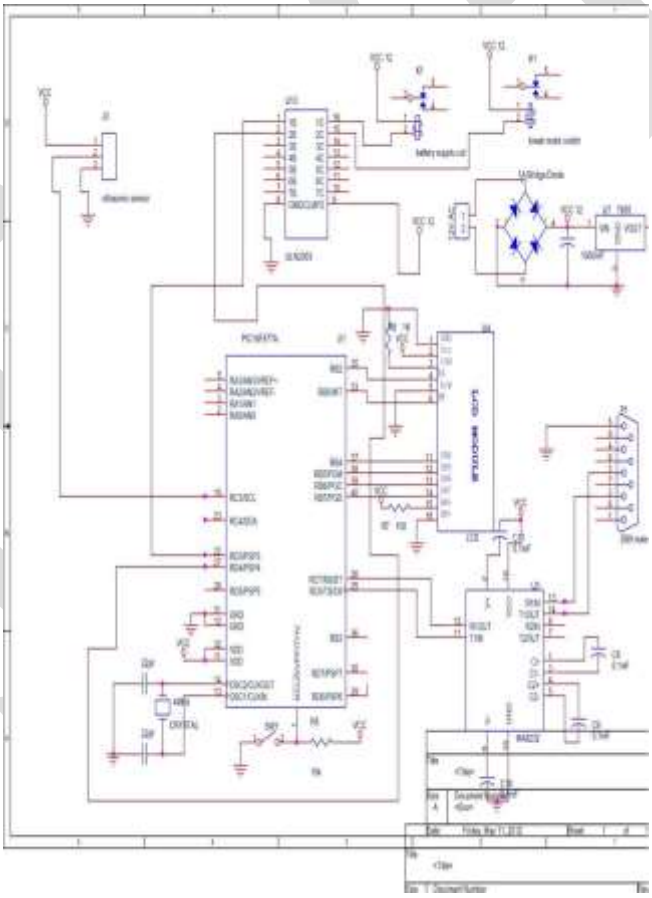

Fig 4. Circuit Diagram

IV. Software

The program for this system is done on embedded C. The program is made to determine the distance of the obstacle in front and to activate the automatic braking system i.e. the wiper motor. Using the if loop provided in the program the distance from

the obstacle can be divided into two i.e. between 100-200cm and between 0-50cm. during the first range only brake is applied whereas during the second range the brake is applied and battery supply to the scooter is also cut off.
For the circuit demo the circuit is provided with two LEDs, green and red as shown in fig 5. The green LED glows when the obstacle is in the range of 100-200cm whereas the red LED glows when the obstacle is in the range of 0-100cm. the green light indicates that only the brake is applied whereas the red light indicates both the brake is applied and the power supply to the scooter is also cut off and the vehicle completely stops during this range.

Fig.5 Circuit with LED demo

With the further modification in the circuit and program the velocity of vehicle moving in front can be determined. In this system we able to use the cruise control technology i.e. our proposed vehicle can be set to run at a particular speed as determined by the driver. By introducing these two system the driver becomes more free and relaxed during **driving, so that driver's hands** becomes free from accelerator and brake pedals.

VI. Proposed System in Fuel Vehicles

A. Throttle Valve Control System

[1] The original throttle valve control system is changed to a drive-by-wire system so as to be able to control by the motor. A 12v dc servo motor is installed to control the throttle valve position. A potentiometer is installed at the accelerator pedal to measure the pedal position. The drive-by-wire controller is developed on a microcontroller which reads the required throttle position from output voltage from the potentiometer.

B. Automatic Braking Control System

As in the case proposed system the same wiper motor with connecting rod arrangement can be made for automatic braking system. The power supply for the wiper motor is provided from the battery used in the vehicles. The rotational motion can also be converted by using a pulley and a steel cable. If the motor rotates, the brake pedal will be pull down by the cable.

VI. Conclusion

In this research, the ABA vehicle is designed and developed. The wiper motor is used for automatic braking which is done using connecting rod arrangement. The acceleration can be cut off by cutting the supply from the batteries which can be achieved by using electromagnetic relays. When the obstacle is away from the range which is determined in the program the vehicle starts moving as determined by the driver

REFERENCES:

[1] Worrawut Pananurak, Somphong Thanok, Manukid Parnichkun **"**Adaptive Cruise Control for an Intelligent Vehicle**"**,School of Engineering and Technology Asian Institute of Technology
[2] Bageshwar,V.L.Garrard,W.L. and Rajamani, **R.",Model Predictive** Control of Transitional
[3] Maneuvers for Adaptive Cruise Control
[4] **Vehicles" IEEE Trans.Tech. vol 53.,** Sep 2004, pp.1573-1585

[5] **Bishop, R.H. "Intelligent Vehicle Technology and Trends" Artech** House Publishers 2005.

[6] [4] Mayr, **,"** Robust performance for autonomous intelligentcruise control systems**"**.,Decision and Control, 1998. Proceedings of

[7] the 37th IEEE Conference on Volume:1 Publication Year: 1998 , Page(s): 487 - 492 vol.1

[8] [5] Robinson,M. ; Carter,M. **"Identification of** driving states for the evaluation of an intelligent cruise control **system"**

[9] Intelligent Transportation System, 1997. ITSC '97.,IEEE Conference on Digital Object, Publication Year: 1997 , Page(s): 847 – 851

International Journal of Engineering Research and General Science Volume 3, Issue 6, November-December, 2015
ISSN 2091-2730

Survey on Named Entity Recognition System over Twitter Data

Ms. Minal S.Sonmale[1], Prof. Rajaram H.Ambole[2]

[1]Student, M.E., Department of Computer Engineering, VPCOE, Baramati, Pune, Maharashtra, India.
sonmaleminal@gmail.com

[2]Assistant Professor, Department of Computer Engineering, VPCOE, Baramati, Pune, Maharashtra, India.
rajaram.ambole@gmail.com

Abstract— Twitter has allowed millions of users to share and spread most up-to-date information which results into large volume of data generated every day. Due to extremely useful business information obtained from these tweets, it is necessary to understand tweets language for downstream applications, such as Named Entity Recognition (NER). Real time applications like Traffic detection system, Early crisis detection and response with target twitter stream required good NER system, which automatically find emerging named entities that are potentially linked to the crisis and traffic, but tweets are infamous for their error-prone and short nature. This leads to failure of much conventional NER techniques, which heavily depend on local linguistic features, such as capitalization, POS tags of previous words etc. Recently segment-based tweet representation has showed effectiveness in NER.The goal of this survey is to provide a comprehensive review of NER system over twitter data and different NER approaches to improve their effectiveness in named entity recognition applications.

Keywords— Named Entity Recognition (NER), target twitter stream, POS tags, local linguistic features, tweet segmentation.

I. INTRODUCTION

Twitter, as a new type of social media, has seen tremendous growth in recent years. It has attracted great interests from both industry and academia. Millions of users share and spread most up-to-date information on twitter which results into large volume of data generated every day. Many private and/or public organizations have been reported to monitor Twitter stream to collect and understand user's opinions about the organizations. We can get extremely useful business value from these tweets, so it is necessary to understand tweets language for a large body of downstream applications such as NER.

A. Named Entity Recognition Concept

NER is a subtask of information extraction that seeks to locate and classify named entities, named entity is a text element indicating the name of a person, organization and location. As shown in Fig.1, task of NER also related to Entity Linking (EL). EL is used to identify the mention of a named entity and link it to an entry in a knowledge base like Wikipedia.

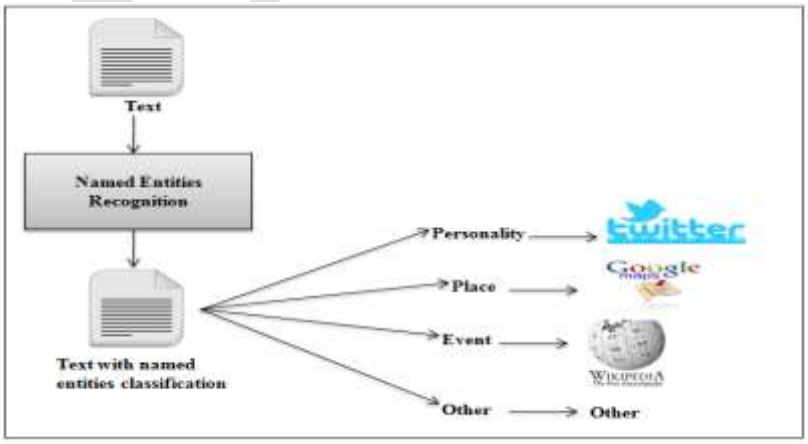

Fig.1 NER System with entity classification & linking

The first paper on NER was presented at the Seventh IEEE Conference on Artificial Intelligence Applications which is presented by Lisa F. Rau (1991). In Rau's paper she describe a NER system that extract and recognize company names, system developed by Lisa based on heuristics and handcrafted rules. At first, English is the most popular langrage factor to research NER, but along with the development of research in these areas, more and more kinds of language have been researched. In this survey, we focus on NER over twitter data. Traffic detection system, early crisis detection and response with target twitter stream are real time applications which required good NER system, which is able to automatically discover emerging named entities that are potentially linked to the crisis and traffic. Many existing NER techniques heavily rely on linguistic features, such as POS tags of the surrounding words , word capitalization, trigger words (e.g., Mr., Dr.), and gazetteers. These linguistic features, together with effective supervised learning algorithms (e.g., hidden markov model (HMM) and conditional random field (CRF)) achieve very good performance on formal text corpus. However, these techniques experience severe performance deterioration on tweets because of the noisy and short nature of tweets. Tweets often contain grammatical errors, misspellings, and informal abbreviations because of two reasons –

1. The short length of a tweet (i.e., 140 characters)
2. No restriction on its writing styles.

This leads to failure of much conventional NER techniques, but recently segment-based tweet representation (tweet segmentation) has demonstrated effectiveness in NER. Segment-based tweet representation split tweets into meaningful phrases or segments and checks its validity by using external knowledge bases (e.g., Microsoft Web N-Gram corpus, Wikipedia Dumps) and local context information embedded in the tweets.

1) Named Entity

Named entity is a text element indicating the name of a person, organization and location. For example:

[Shubham]$_{\text{Person}}$ bought 300 shares of Aceme Corp.]$_{\text{Organization}}$ in [2015] $_{\text{Time.}}$

Here, Shubham, Aceme Corp. and 2015 are named entities which is classify under the person, organization and time class respectively. Fig.2 shows named entities based on their pre-defined class.

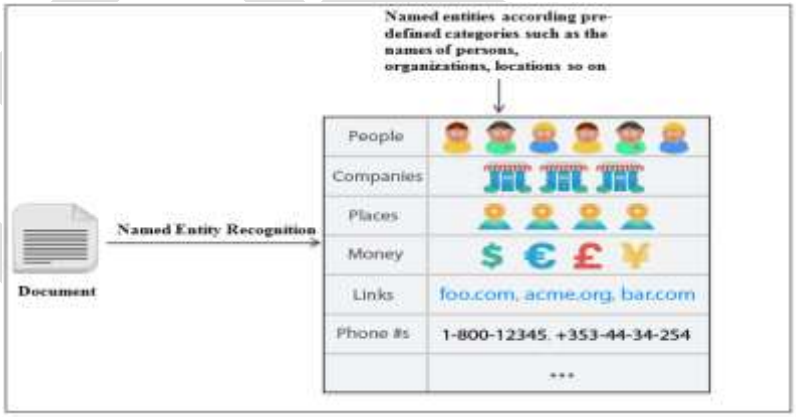

Fig.2 Named entities based on their class.

2) NER Applications

NER is useful in many Natural Language Processing applications such as question answering, information extraction, machine translation, parsing. It also provides person or organization names with their information. Usually, NER systems are used in the areas of entity identification in the bioinformatics, molecular biology and medical natural language processing communities.NER also used in real time applications.

II. APPROCHES TO NER

In this section, some NER approaches are reviewed.

B. Supervised methods

Supervised methods are class of algorithm that learns a model by looking at annotated training examples. Supervised learning algorithms for NER are Hidden Markov Model (HMM), Maximum Entropy Models (ME), Decision Trees, Support Vector Machines (SVM) and Conditional Random Fields (CRF). These all are forms of the supervised learning approach that typically consist of a system that reads a large corpus, memorizes lists of entities, and creates disambiguation rules based on discriminative features.

1) Hidden Markov Model

HMM is the earliest model applied for solving NER problem by Bikel et al. (1999). Bikel proposed a system *IdentiFinder* to identify named entities. In *IdentiFinder* system only single label can be assigned to a word in context. Therefore the model assigns to every word either one of the desired classes or the label NOT-A-NAME which means “none of the desired classes".

2) Maximum Entropy based Model

Maximum entropy model is discriminative model like HMM. In Maximum entropy based Model given a set of features and training data the model directly learns the weight for discriminative features for entity classification. Objective of the model is to maximize the entropy of the data, so as to generalize as much as possible for the training data.

3) Decision Trees

Decision Tree is a tree structure used to make decisions at the nodes and obtain some result at the leaf nodes. A path in the tree represents a sequence of decisions leading to the classification at the leaf node. Decision trees are attractive because the rules can be easily grasps from the tree. It is a well liked tool for prediction and classification.

4) CRF Based Model

Lafferty et al. (2001) proposed Conditional random field model as a statistical modeling tool for pattern recognition and machine learning using structured prediction. McCallum and Li (2003) developed feature induction method for CRF in NE.

5) SVM Based Model

Support Vector Machine was first introduced by Cortes and Vapnik in 1995 which is based on the idea of learning a linear hyperplane that separate the positive examples from negative example by large margin. Large margin suggests that the distance between the hyperplane and the point from either instance is maximum. Support vectors are points closest to hyperplane on either side.

C. Unsupervised methods

Problem with supervised algorithms is it required large number of features. For learning a good model, a robust set of features and large annotated corpus is needed. Many languages don't have large annotated corpus available at their disposal. To deal with lack of annotated text across domains and languages, unsupervised techniques for NER have been proposed.

D. Semi-supervised methods

Semi supervised learning algorithms use both labeled and unlabeled corpus to create their own hypothesis. Algorithms typically start with small amount of seed data set and create more hypotheses using large amount of unlabeled corpus.

III. RELATED WORK

There have been many NER systems developed not only in academia but also in industry some of them are reviewed in this section. GuoDong Zhou and Jian Su[1] proposed a Hidden Markov Model (HMM) and an HMM-based chunk tagger, by using which NER system is built to recognize and classify names, times and numerical quantities. This NER system achieves very good performance on formal text corpus but experience severe performance deterioration on tweets because of the noisy and short nature of the tweets.

The NER solution proposed by L. Ratinov and D. Roth [2] presented a simple model for NER that uses expressive features to achieve new state of the art performance on the NER task. System explored four fundamental design decisions: text chunks representation, inference algorithm, using non-local features and external knowledge entity types. This system can gain consistent performance across several domains, most interestingly in WebPages, where the named entities had fewer contexts and were different in nature from the named entities in the training set but when evaluating the system, it matched against the gold tokenization ignoring punctuation marks.

Chenliang Liy and Aixin Suny [3] presented a novel 2-step unsupervised NER system for targeted Twitter stream, called *TwiNER*. In the first step, dynamic programming algorithm with global context obtained from Wikipedia and Web N-Gram corpus is used for tweet segmentation. Tweet segmentation partition tweets into valid segments (phrases).Each such tweet segment is a candidate named entity. In the second step, *TwiNER* constructs a random walk model to utilize the gregarious property in the local context derived from the Twitter stream. The highly-ranked segments have a higher chance of being true named entities. By aggregating local context and global context *TwiNER* is able to recognize new named entities which may not appear in Wikipedia yet but this system is not able to address the problem of entity type classification.

Chaua et al [5] proposed a noun phrase (NP) classification method that automatically finding noun phrases (NPs) as keywords for event monitoring in Twitter. This system proposed to extract noun phrases from tweets using an unsupervised approach which is mainly based on POS tagging. Each extracted noun phrase is a candidate named entity. Here first model NP+LDA could classify NPs into political categories more accurately than state of the art tagger (SentReg) based on a large knowledge base, by incorporating community information in NP+RART system can further improve the accuracy of classifier. Finally, system could classify sports NPs in a political dominated Twitter data set.

Silviu Cucerzan[6] proposed large-scale system for the named entity recognition and semantic disambiguation based on information extracted from a large encyclopedic collection and Web search results. Through a process of maximizing the agreement between the contextual information extracted from Wikipedia and the context of a document, as well as the agreement among the category tags associated with the candidate entities, the implemented system shows high disambiguation accuracy on both news stories and Wikipedia articles. This system treat mention detection and entity disambiguation as two different problems. Milne and Witten[7] proposed system that describes how to automatically cross-reference documents with Wikipedia. It explains how machine learning can be used to identify significant terms within unstructured text, and enrich it with links to the appropriate Wikipedia articles.

To rigorously address the Twitter entity linking problem, Guo et al [8] proposed a structural SVM algorithm for entity linking that jointly optimizes mention detection and entity disambiguation as a single end-to-end task. Merging mention detection and entity disambiguation into a single end-to-end entity linking task increase performance of system but this system use structural SVM algorithm which requires NP-hard inference which is computationally expensive.Sil and A. Yates [9] developed a re-ranking model that performs joint named entity recognition and entity linking. The discriminative re-ranking framework allow to introduce features into the model that capture the dependency between entity linking decisions and mention boundary decisions . Furthermore, the model can handle collective classification of entity links, at least for nearby groups of entities. The joint NER and EL model has strong empirical results, outperforming a number of state-of the-art NER and EL systems on several benchmark datasets while remaining computationally inexpensive. System tended to have much lower accuracy on long chains of entities.

TABLE I: SUMMARY OF LITERATURE SURVEY

Sr.No.	Paper Title	Authors	Methods/Techniques used
1	Named Entity Recognition using an HMM-based Chunk Tagger[1]	G.Zhou , J.Su[2002]	HMM-based Chunk Tagger.
2	Design challenges and misconceptions in named entity recognition[2]	L. Ratinov[2009]	Supervised learning algorithms (e.g., HMM , CRF).
3	TwiNER: Named Entity Recognition in Targeted Twitter Stream[3]	Chenliang Li, Weng [2012]	2-step unsupervised NER System, 1st step –tweet segmentation using dynamic programming algorithm.2nd step-use random walk model.
4	Exploiting hybrid contexts for Tweet segmentation[4]	Chenliang Li , Aixin Suny[2013]	Proposed tweet segmentation framework-HybridSeg for NER.
5	Community-Based Classification of Noun Phrases in Twitter[5]	F.C.T. Chua [2012]	Unsupervised approach based on POS tagger. Extract noun phrases as candidate named entity.
6	Large-Scale Named Entity Disambiguation Based on Wikipedia Data[6]	S. Cucerzan [2007]	NER system followed by a linking system.
7	Learning to Link with Wikipedia[7]	D. N. Milne [2008]	Proposed link detector and disambiguator.
8	To Link or Not to Link? A Study on End-to-End Tweet Entity Linking[8]	Guo et al [2013]	SVM Algorithm for entity linking.
9	Re-ranking for Joint Named-Entity Recognition and Linking[9]	A.Sil, A.Yate[2013]	Joint NER and EL Model.

IV. CONCLUSION

The Named Entity Recognition field has been growing for more than fifteen years. Its purpose is to find and classify mentions of rigid designators from text such as proper names and temporal expressions. In this survey, we have shown NER system and their approaches. We found that tweet segmentation has been proven to be effective in the tasks of NER. Tweet segmentation aggregates local context and global context to calculate the probability that segment being named entity. By doing so, we can be able to recognize named entities with high confidence and new named entities which may not appear in Wikipedia yet.

REFERENCES:

[1] G.Zhou and J.Su, "Named entity recognition using an hmm chunk tagger," in proc 40th Annu. Meeting Assoc.Comput.Linguistics, pp.473-480, 2002.

[2] L. Ratinov and D. Roth, "Design challenges and misconceptions in named entity recognition," in Proc. 13th Conf. Comput.Natural Language Learn, pp. 147–155, 2009.

[3] C. Li, J. Weng, Q. He, Y. Yao, A. Datta, A. Sun, and B.-S. Lee, "Twiner: Named entity recognition in targeted twitter stream," in Proc. 35th Int. ACM SIGIR Conf. Res. Develop. Inf. Retrieval, pp. 721–730, 2012.

[4] C. Li, A. Sun, J. Weng and Q. He, "Exploiting hybrid contexts for tweet segmentation," in Proc. 36th Int. ACM SIGIR Conf. Res.Develop. Inf. Retrieval, pp. 523–532, 2013.

[5] F. C. T. Chua, W. W. Cohen, J. Betteridge, and E.-P. Lim,"Community-based classification of noun phrases in twitter," in Proc. 21st ACM Int. Conf. Inf. Knowl. Manage, pp. 1702–1706, 2012.

[6] S. Cucerzan, "Large-scale named entity disambiguation based on wikipedia data," in Proc. Joint Conf. Empirical Methods Natural Language Process. Comput. Natural Language Learn, pp. 708–716, 2007.

[7] D. N. Milne and I. H. Witten, "Learning to link with wikipedia,"-in Proc. 17th ACM Int. Conf. Inf. Knowl. Manage , pp. 509–518,2008.

[8] S. Guo, M.-W. Chang, and E. Kiciman, "To link or not to link? A study on end-to-end tweet entity linking," in Proc. Conf. North Amer. Chapter Assoc. Comput. Linguistics: Human Language Technol., pp. 1020–1030, 2013.

[9] A. Sil and A. Yates, "Re-ranking for joint named-entity recognition and linking," in Proc. 22nd ACM Int. Conf. Inf. Knowl. Manage, pp. 2369–2374, 2013.

International Journal of Engineering Research and General Science Volume 3, Issue 6, November-December, 2015
ISSN 2091-2730

Overview of Lean Manufacturing and Its Implementation Techniques

Niranjan Hugar[1], Jayesh P[2]

[1]Assistant Professor, Department of Industrial Engineering and Management, MVJ College of Engineering Bengaluru 560067, niranjan0364@gmail.com

[2]Assistant Professor, Department of Industrial Engineering and Management, MVJ College of Engineering Bengaluru 560067, pjayeshkanayi@gmail.com

Abstract— Applying Lean manufacturing philosophy is one of the most important concepts that help enterprises to gain competitive advantage in the world market. Lean manufacturing or lean manufacturing is a manufacturing practice that emphasizes on the use of resources for work which add value for the end customer. The purpose of this paper is to give an overview of the lean principles, tools and benefits of lean concepts in manufacturing industries. Lean manufacturing is plethora of principles that focus on cost reduction by identifying and eliminating non value added activities. The fiercely globalized and competitive markets of 21st century demand for increasing high variety of products at lowest possible costs, lesser lead time and high quality. This changing market scenario calls for a new manufacturing that will enable us to compete in this global competitive market. This research addresses the application of lean manufacturing concepts to the continuous production/process sector with a focus on the manufacturing industry.

Keywords— Lean manufacturing, Waste 5S, Continuous Flow, Just-In-Time and Kaizen.

1. INTRODUCTION

Lean manufacturing is a method of achieving continuous improvements in performance through elimination of waste. In this process anything which doesn't add value is termed as waste .The term value is spoken with respect to end consumer or customer [1, 2]. That means any process or product for which customer is ready to pay or spend. Lean manufacturing was mainly developed in japan after 2nd world war, the concept was developed to utilize the very limited resources available after the war and to make best out of it. The Lean mainly focuses on the reduction of seven waste. They are Transportation, Inventory, Motion, Waiting, Over-Processing, Over-production and Defects [3, 4].

Transportation: Each and every time when a product is moved from one place to other there is a possibility of being damaged, lost, delayed etc. And transportation doesn't add any change or transformation to the product for which consumer is ready to pay for.

Inventory: Inventory may be in the form of stored materials, finished goods, work in progress or any investment which has not produced the output (or income) to the producer or the customer. Any of these items which are not actively processed adds value to the waste.

Motions: Motion refers to the movement of people or worker who produce the products, machines which help in processing of the product etc. Anything that causes repetitive strains, injuries to workers, wear and tear of machines accidents etc.

Waiting: Whenever the goods, raw materials are not processing, waiting for instructions, machine not idle (work in progress) or any resources waiting for the next process. Waiting increases capital investments requires additional handling and care.

Overprocessing: Overprocessing in terms of lean manufacturing is processing of product than actually required by the customers. Poor process design can lead to over processing. Over processing increases the cost of the product unnecessarily

Overproduction: Producing more no of products than the requirement is termed as over production, over production will add to all other problems like excess inventory, transport etc. And overall cost will also increases adding to this effect.

Defects: Whenever defects occur due to human error, caused by machine error or caused due to any other factor it will lead to either rework or scrap which intern increases work in progress, cost and time will also be increased and at end it will increases the cost of overall production.

2. METHOD USED TO IMPLEMENT LEAN MANUFACTURING AND REDUCING OF WASTE:

5S: Organizing the work space using concept of 5S

- Sort (Sorting the work space and eliminating that which is not needed)
- Set In Order (Reorganize the remaining items)
- Shine (Continuous cleaning and inspection of work area)
- Standardize (Preparing standards for above and following according to standards)
- Sustain (Maintaining the standards without deviation)

Andon: Visual feedback system for the plant space that provides production status, by giving alerts when there is a need for assistance and enables the workers to stop the production process. Which will form a real-time communication tool for the plant space that brings immediate attention to problems as whenever they occur – so that they can be immediately solved.

Bottleneck Analysis: Identifying which unit or part of the production process is limiting or reducing the overall throughput and enhancing the performance of that part of the process. By improving throughput we will be enhancing the strength of weakest link in the production process

Continuous Flow: Production Process in which work-in-process flows smoothly through production with minimum (or no) buffers between production steps of the production process. By doing this most of the wastes gets eliminated like waiting, inventory, transport etc.

The Real Work Place: A logic that helps us to get out of our workspace and invest time on the plant floor – the spot where real activity happens. This will advance a profound and exhaustive comprehension of certifiable assembling issues – by direct perception and by conversing with plant floor workers

Level Scheduling: A type of production scheduling that intentionally manufactures in very small batches by sequencing (blending) item variations inside the same process. This will reduce lead times (subsequent to every item or variation is made all the more as often as possible) and inventory (following batches are smaller).

Policy Deployment: making the strategy for the achieving goals with actively involving middle management and the work to be done on production floor. This guarantees that progress towards achieving strategic goals is consistent and thorough – this will eliminate the waste that arises from poor communication and inconsistent direction.

Automation: Outline hardware to partially automate the manufacturing process (partial computerization is normally a great deal less costly than full mechanization) and to naturally stop when defects are identified. Workers can as often as possible screen multiple stations (lessening work costs) and numerous quality issues can be identified instantly (enhancing quality).

Just-In-Time (JIT): Pull parts through manufacturing based on customer requirement instead of pushing parts through production based on projected demand. Relies on many lean tools, such as Continuous Flow, Kanban, Standardized Work and Time. Highly effective in reducing inventory levels. Improves cash flow and reduces space requirements.

Kaizen (Continuous Improvement): A method where representatives cooperate proactively to accomplish normal, incremental changes in the assembling procedure. Joins the aggregate talents of a company to create an engine for constantly disposing of waste from manufacturing processes.

Kanban (Pull System): A technique for managing the flow of goods both within the industrial facility and with outside suppliers and customers. In view of automatic recharging through signal cards that demonstrate when more goods are required. Disposes of waste

from inventory and overproduction. Can dispose of the requirement for physical inventories (rather depending on sign cards to demonstrate when more goods should be requested).

KPI (Key Performance Indicator): Measurements intended to track and empower progress towards critical goals of the organization. Emphatically advanced KPIs can be amazingly intense drivers of conduct – so it is critical to precisely choose KPIs that will drive desired behaviour. The best manufacturing KPIs: Are adjusted to top-level key objectives (in this way serving to achieve those objectives) are compelling at uncovering and measuring waste (OEE is a decent case) are promptly affected by plant floor representatives (so they can drive results)

Poka-Yoke (Error Proofing): Outline error detection and prevention into generation forms with the objective of accomplishing zero defects. It is troublesome to discover all defects through inspection, and correcting defects commonly gets essentially more expensive at every phase of production

Root Cause Analysis: A problem solving methodology that focuses on resolving the underlying problem instead of applying quick fixes that only treat immediate symptoms of the problem. A common approach is to ask why five times – each time moving a step closer to discovering the true underlying problem. Helps to ensure that a problem is truly eliminated by applying corrective action to the "root cause" of the problem.

Value Stream Mapping: A tool used to visually map the flow of production. Shows the current and future state of processes in a way that highlights opportunities for improvement. Exposes waste in the current processes and provides a roadmap for improvement through the future state.

Visual Factory: Visual indicators, displays and controls used throughout manufacturing plants to improve communication of information. Makes the state and condition of manufacturing processes easily accessible and very clear – to everyone.

SMART Goals: Goals that are: Specific, Measurable, Attainable, Relevant, and Time-Specific. Helps to ensure that goals are effective.

Standardized Work: Documented procedures for manufacturing that capture best practices (including the time to complete each task). Must be "living" documentation that is easy to change. Eliminates waste by consistently applying best practices. Forms a baseline for future improvement activities.

3. CONCLUSION

Lean manufacturing is one of these initiatives that focus on cost reduction by identifying and eliminating on value added activities .In Indian industry a lot of scope is their to improve inventory control, reduce lead time, set-up timer which will lead to competitiveness of Indian industry. Lean Manufacturing implementation is a multiplex process, a set of actions that requires planning the change and the establishment of positive environment, preparation, implementing various tools and techniques, and measuring the achieved progress using specific performance metrics. By implementing Lean manufacturing techniques the demand for increasing high variety of products at lowest possible costs, lesser lead time and high quality can be achieved.

REFERENCES:

[1] Abdulmaleka, F. and J. Rajgopalb. "Analyzing the benefits of lean manufacturing and value stream mapping via simulation: A process sector case study." International Journal of Production Economics 2007; 107(1): 223-236.
[2] Alfnes, E., C. C. Rostad, et al.. Flexibility Requirements in the Food Industry and How to meet them. 4th International Conference on Chain Management in Agribusiness and the Food industries. Wageningne, The Netherlands. 2000;
[3] Alvarez, R., R. Calvo, et al.. "Redesigning an assembly line through lean manufacturing tools." International Journal of Advanced Manufacturing Technology 2009; 43: 949-958.
[4] Ballis, J. P. Managing Flow: Achieving Lean in the New Millennium to the Gold. Dallas, Brown Brooks. 2001;
[5] Bicheno, J. and M. Holweg. The Lean Toolbox, Picsie Books. 2008

[6] Braglia, M., G. Carmignani, et al.. "A new value stream mapping approach for complex production systems." International Journal of Production Research 2006; 44(18-19): 3929-3952.
[7] Floyd, R. C.. Liquid Lean: Developing Lean Culture in the Process Industries. New York, Taylor and Francis Group. 2010
[8] Wilson, L. How to Implement Lean Manufacturing, McGraw-Hill. 2010;
[9] Womack, J. and D. Jones. Lean Thinking, Free Press. 2003.
[10] Womack, J. and D. Jones. Lean Solutions: How companies and customers can creater benefits and wealth together. New York, Free Press. 2005;
[11] Womack, J., D. T. Jones, et al. The Machine that Changed the world: The story of Lean production. New York, Free Press. 1990;

International Journal of Engineering Research and General Science Volume 3, Issue 6, November-December, 2015
ISSN 2091-2730

Fusion of Medical Image by using STSVD - A Survey

Kusuma J, Dr. K N Narasimha Murthy
PG Scholar, kusumagowdaj@gmail.com and 8123377684

Abstract— Medical Image fusion is a process of combining multiple images of same or different imaging modalities into single image to increase the information content in the image and also to reduce the randomness and redundancy which will be used for clinical applicability. The multi-modal fusion of medical images has shown notable achievements in clinical accuracy. This survey provides listing of different imaging modalities, fusion algorithms, performance metrics and the proposed method. A new technique called Singular Value Decomposition (SVD) method on Shearlet Transform (ST) is proposed to improve the information content of an image by fusing images like Positron Emission Tomography (PET) and Magnetic Resonance Imaging (MRI) images. Initially source image is transformed into shearlet-image by using ST. Then SVD model is used in low-pass sub-band and modified selected sub-bands as per their local characteristics. The compositions of different high-pass sub-band coefficients are processed by ST decomposition. Then the high and the low sub-band are fused. Finally, Inverse Shearlet Transform (IST) is used to reconstruct the fused image.

Keywords— Shearlet Transform, Singular Value Decomposition, Medical Image Fusion, Positron Emission Tomography, Inverse Shearlet Transform, Mutual Information, Edge Indexing.

I. INTRODUCTION

Image fusion is important in medical studies for diagnosis of several diseases. It also used in image analysis and historical documentation. The purpose of image fusion is to combine information from two or more images into single image which contains more information than the source images. There is a rapid growth in this field in recent years which leads to development of many fusion techniques. There exist many medical imaging modalities that are used as the primary inputs to the studies of medical image fusion. The selection of imaging modality depends on clinical requirements like the organs which undergo for study. Practically it is not possible to get all the details from single image for clinical accuracy.

The aim of this review is to provide a collective view of different modalities, image fusion techniques and how the proposed method is better than the existing methods. Figure 1 shows the three major focused areas in medical image fusion: (a) identification, improvement and development of imaging modalities, (b) development of different techniques, and (c) Studying of human organs of interest. Recently, lots of image fusion techniques have been developed such as Wavelet Transform (WT), Principal Component Analysis (PCA), and Non-Subsampled Contourlet Transform (NSCT) to fuse the images like MRI, PET and Computed Tomography (CT). There are two types of fusion methods, spatial domain method and transform domain method.

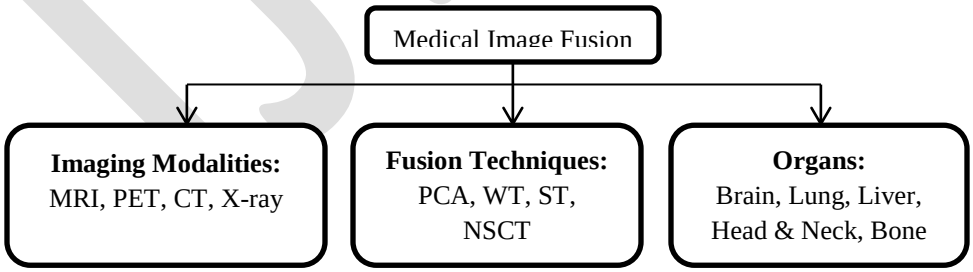

Figure 1. Structure of Medical Image Fusion.

The fusion method averaging principal component analysis comes under spatial domain approaches. But it suffers from reduced sharpness and contrast. The pixel-based methods, cause inaccurate measurement of sharpness and also contains noise which decreases the performance. The use of region based methods solves the noise problems. The limitation is that the artifacts may appear at the boundaries which greatly reduce the quality of the fused image.

Spatial distortion can be handled by using frequency domain approaches. WT has evolved as a great multi-resolution system with many characteristic such as time-frequency localization, multi-scale characteristic and sparse representation of function [4]. But it also has limitation that the images containing higher dimension singularity, cannot reach the optimal sparse representation [20]. In order to resolve the limitation, WT has been attached with multi-scale geometric analysis theory. This has been successfully developed and materialized as a series of new multi-scale geometric transform method, for example, ridgelet [20, 23], curvelet [20], and contourlet. In recent times, many authors have developed fundamental composition of ST through the affine system that offers excellent capability in analysis and synthesis.

SVD is a popular method for feature extraction and is used for image fusion. SVD-based fusion is used for image registration and is widely used in data compression. The new image fusion algorithm is proposed by combining ST and SVD techniques.

The paper is organized as follows: Section II gives a brief description of multiple imaging modalities, section III briefs about different fusion techniques, section IV Contains Performance metrics, proposed method is described in section V , section VI briefs the analysis of results and finally conclusion is discussed in section VII.

II. IMAGING MODALITIES USED IN IMAGE FUSION.

A. Magnetic Resonance Imaging (MRI)

MRI is one of the mostly commonly used imaging modality in medical studies. It is used to get information about soft tissues of the body. Image segmentation is mostly used to identify the objects and interested regions of the image. The advantage of MRI is that it does not involve any exposure to radiation, so it is very safe for pregnant women and babies [4, 24]. The disadvantage is that it is very noisy and difficult in accessing the organs that involve in movement and will not show bone or calcium which results in not finding many diseases [17].

B. Positron Emission Tomography (PET)

PET provides information of blood flow in the body. Its major application is diagnosis of diseases of brain and some other applications such as image segmentation and integration, breast and lung cancer detection. One of the main challenges of PET is its resolution limits. The limitations can be reduced by performing image reconstruction with finite resolution effects and improved detector design [17, 24]. The advantage is that the small movements do not destruct the scan and it is very accurate in differentiating between malignant and cell growth [3].

C. Computed Tomography (CT)

CT provides more information about of bone tissues and less about soft tissues. It is considered as prime modality in several applications such as diagnosis of head and neck cancer, lung cancer treatment, detection in tumor, bone cancer treatment and cervical cancer treatment [17, 4]. The advantages of this scan are high resolution of image and short scan time.

D. X-ray

X-rays are electromagnetic radiations which help in identifying cracks, injury, abnormal bones and bone cancers. The advantage is that they are cheaper than other modalities. The disadvantage is that they do not give detailed images and also exposure to X-rays for long period can damage the tissues and also it cannot be used for soft tissues.

III. MEDICAL IMAGE FUSION TECHNIQUES

A. Wavelet Transform (WT)

The primary concept with this is to extract detailed information from one image and give it into another. The representation of wavelet consists of low-pass band and high-pass band at each step. It is invertible and non-redundant transform. Some of the WT are Haar Wavelet Transform [25], Discrete Wavelet Transform [18, 15].The features of Haar transform includes fast for implementation and used in signal and image compression. There are several applications of this such as super resolution, medical image pseudo coloring, feature level image fusion, segmentation, medical diagnosis and color visualization.

B. Non-Subsampled Contourlet Transform (NSCT)

NSCT is based on the theory of Contourlet Transform [13]. It is of two stages, includes Non-Subsampled Laplacian Pyramid (NLP) is used to capture the point discontinuities and Non-subsampled Directional Filter Bank (NDFB) is used to form those into linear structures [22, 23]. There are two channel non-subsampled filter bank, one is low-frequency image and other is high-frequency image which can be produced at each decomposition level. The subsequent NSP decomposition is applied on low-frequency component iteratively to get the singularities present in the image. So the NSP results in sub-images, which consists of low and high-frequency images of same size as the source image. NDFB allows the direction decomposition with stages in high-frequency images from NSP at each scale and it produces directional sub-images with the same size as of source image. Therefore, the NDFB offers NSCT with the property multi-direction and provides with more precise directional details information.

C. Principal Component Analysis (PCA)

It is a vector space transform used to reduce multi-dimensional data sets to lower dimensions for analysis. The algorithm involves the following steps: (i) From the input image matrix generate the column vectors; (ii) For the 2 column vectors formed in previous step calculate the covariance matrix; (iii) The diagonal elements of 2x2 covariance vector should contain variance of each column vector with itself; (iv) Determine the Eigen vectors and Eigen values of covariance vector and then obtain the Eigen vector corresponding to larger Eigen values; (v) Compute the normalized components from the Eigen vectors obtained in the previous step; (vi) Sum of two scaled matrices calculated in previous step will be the fused image [20].

D. Shearlet Transform (ST)

The ST solves multi-variate problem by efficiently encoding anisotropic features. It is natural extension of wavelets to make suitable for the multi-variate functions. There are two primary steps of ST, multi-scale decomposition and directional localization. The drawback is that as the frequency support of shearlet aligns along axis as it increases the shearing parameter leads to infinity. This is a serious problem when analyzing the functions if the functions are concentrated around the axis. To solve this problem the frequency domain splits into low-frequency part and two conical regions. The cone adapted discrete shearlet system has three parts, each of them corresponds to one of the frequency domains and finally for the low-frequency part the scaling function applied.

IV. PERFORMANCE METRICS

A. Mutual Information (MI)

MI determines how much information the fused image gives from the source images [6]. As higher the value of MI the fused image contains good quantity of information presented from the original images. It is calculated as, by adding the MI between the fused image and each of the source images.

$$MI=I(I_1,I_f)+I(I_2,I_f)$$

B. Edge Indexing

Edge Indexing ($Q^{AB/F}$) determines how much edge information is transferred to fused image from the source images. As higher the value of edge indexing the quantity of information transferred is higher from source images to the fused image.

V. THE PROPOSED FUSION ALGORITHM

A. Concept of Singular Value Decomposition

Singular Value Decomposition (SVD) is an efficient algebraic method used to extract important features from the image [7]. It is decomposed into a singular value matrix containing only a few non-zero values. Singular value represents several image descriptions, rotation and scaling invariability, for instance feature stability. SVD of an m×n matrix A is decomposed into three matrices specified by

$$A = U_A \Sigma_A V_A^T$$

Where U_A is m × m matrix known as *left singular vectors*, V_A^T is n × n matrix known as *right singular vectors*, and Σ_A =diag ($\sigma 1, \sigma 2, \cdots, \sigma n$) is m× n diagonal matrix called as the *singular values*. The singular vectors arranged in a decreasing order of singular values, with the highest singular value existing in upper left corner of the Σ_A matrix, specifically, ($\sigma 1 \geq \sigma 2 \geq \ldots\ldots\ldots \geq \sigma q \geq 0$).

B. Proposed method

A new medical image fusion algorithm is developed to share the advantages of Shearlet Transform. This fusion algorithm is named as Shearlet Transform with Singular Value Decomposition (STSVD). There are two parts in the proposed fusion method. First part is the low frequency coefficients of the original image which is manipulated by using SVD with *Maximization* method. Second part is the high frequency coefficients manipulated by using adaptive parameter which is derived from high-pass sub-bands of same and the different level. The schematic diagram of the proposed algorithm is shown in Figure 2.

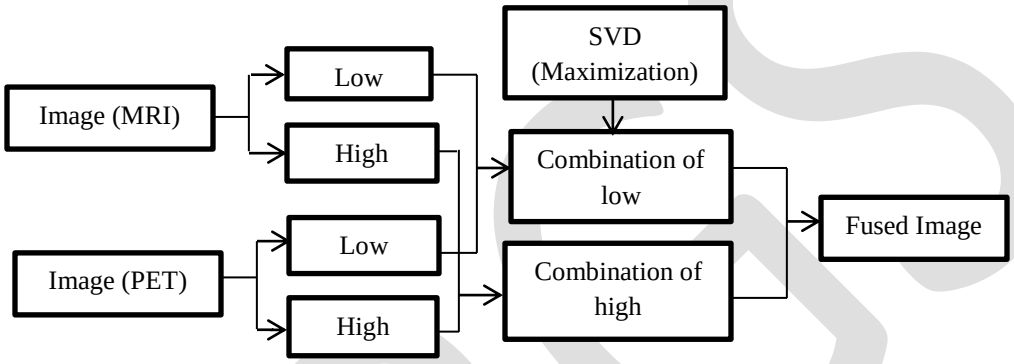

Figure 2.Schematic diagram of the STSVD based fusion algorithm.

VI. ANALYSIS OF RESULTS

In the field of medical image diagnosis there are several technological and it also faces many challenges. The increase of imaging technologies results in improved imaging accuracies. However, each imaging modality has its own limitations, which enforces to explore the new imaging technologies. The main challenge in applying the image fusion algorithms is that it should be safe for medical diagnosis and should result in better clinical outcome. The right combination of different imaging modalities, feature extraction, feature processing and decision fusion algorithms which targets a specific clinical problem. The necessary for improving the image quality results from signal noise and the physical limitations of the imaging modalities and another area of interest is processing speed.

Wavelet transform [10, 18] is one of the most commonly used image fusion technique. It has many characteristics such as multi-scale, time and frequency localization and representation of sparse function. Because of its multiple characteristics it has developed as great multi-resolution system.

In [1] the author proposed Redundant Discrete Wavelet Transform (RDWT) to overcome the problem of the DWT that is shift variance. But is mostly used in different signal processing and it is not well researched in medical image fusion. In [3] the multi-wavelet transform has applied on PET and CT images which have many properties like orthogonality, short support, symmetry and smoothness are very important for image processing and analysis. There is no strict division of low and high-pass in multi-wavelet filter banks. The major disadvantage of DWT [11, 12, 14, 15, and 26] is that it gives more number of coefficients in all directions of edges of image. So for reconstruction of exact edges these many coefficients are required, but it is not possible form DWT to handle such long curved edges. To solve this limitation it is attached with other geometric analysis theory. So from this there were several methods has been developed such as curvelet, ridgelet and contourlet.

So in [4, 21] the new approaches like curvelet transform and ridgelet transform has come in to existence which handles curvilinear and long linear singularities. In this transform instead of DWT, the Additive Wavelet Transform (AWT) is used to decompose the image. After decomposition into different sub-bands they are called as approximation plane and detail plane and each detail plane is divided into small tiles. On each tile the ridgelet transform is applied to represent the image edges after applying the edges look like small straight lines. In this way the ridgelet transform is efficient in detecting curved edges.

In [8, 13 and 22], the NSCT has applied on MRI and CT images. To perform this phase congruency and directive contrast are used as fusion rules for low and high frequency coefficients. The phase congruency provides brightness invariant and contrast

representation of the low-frequency coefficients and directive contrast is used to get frequency coefficients from clear parts of the high frequency. The combination of these two preserves the source image details and improves the quality of the fused image.

In [20, 27] the PCA and Dual Tree Complex Wavelet Transform (DTCWT) were applied on CT and MRI images. In comparison to wavelet transform, the DTCWT has high directional selectivity and is also a shift invariant. The directional selectivity improvement represents the information across boundaries of the image and it also provides phase information. For selectively combining the complex wavelet coefficients the PCA is used as a fusion rule which removes redundant information present in DTCWT.

Recently the fundamental composition of ST [5, 9 and 28] has been developed by many authors through the affine system which is excellent in synthesis and analysis. The ST is mainly used to encode the anisotropic features which are in multi-variate problem.

SVD [2, 7] is popularly used for feature extraction and used for fusion of image. It is also used for image registration. The SVD based fusion is used for super resolution problems and it also transforms number of correlated variables into multiple orthogonal variables. It is mostly used in data compression [7]. So we propose a new medical image fusion method to add the advantages of ST to the image fusion technique like inter-scale sub-band dependencies. The fusion algorithm is named as STSVD.

VII. CONCLUSION

In this paper various image fusion techniques has been reviewed from different published papers where each of them has its own limitations. So we propose a new method STSVD which has more advantages than other methods. The goal of this is to preserve the information from the source images and the main advantage is that it is capable of retaining the optimal composition of colors of the image. This results in improving the detection of accuracy of image in smooth regions.

REFERENCES:

[1]. Richa Singh, Mayank Vatsa, Afzel Noore, "Multimodal Medical Image Fusion using Redundant Discrete Wavelet Transform", IEEE-Seventh International Conference on Advances in Pattern Recognition, pp.232-235, 2009.

[2]. D.W.Repperger, A.R.Pinkus, K.A. Farris, R.G.Roberts, R.D.Sorkin, "Investigation of image fusion procedures using optimal registration and SVD algorithms", in: Proceedings of the IEEE- National Aerospace and Electronics Conference, pp. 231 235, 2009.

[3]. Yuhui Liu, Jinzhu Yang, Jinshan Sun, "PET/CT Medical Image Fusion Algorithm Based on Multiwavelet Transform", IEEE, pp.264-268, 2010.

[4]. F. Ali, I. El-Dokany, A. Saad, F. El-Samie, "A curvelet transform approach for the fusion of MR and CT images", Journal of Modern Optics, vol.57, pp. 273-286, 2010.

[5]. Wang-Q Lim, "The Discrete Shearlet Transform: A New Directional Transform and Compactly Supported Shearlet Frames", IEEE Transactions On Image Processing, vol. 19, no. 5, may 2010.

[6]. MA. Mohamed and R.M EI-Den, "Implementation of Image Fusion Techniques for Multi-Focus Images Using FPGA", 28th National Radio Science Conference, April 26-28, 2011.

[7]. H.Nasir, etal. "Singular value decomposition based fusion for super resolution image reconstruction", Signal Processing-Image Communication, 2011.

[8]. T.J. Li, Y.Y. Wang, "Biological image fusion using a NSCT based variable weight method", Information Fusion, vol. no.12, pp. 85-92, 2011.

[9]. L. Wang, B. Li, L. Tian, "Multi-modal medical image fusion using the inter-scale and intra-scale dependencies between image shift-invariant shearlet coefficients", Information Fusion, 2012.

[10]. R.J.Sapkal, S.M.Kulkarni, "Image Fusion based on Wavelet Transform for Medical Application", IJERA, ISSN: 2248-

9622, Vol. 2, Issue 5, pp.624-627, September- October 2012.

[11]. C.T. Kavitha, C. Cellamuthu, R. Rajesh, "Medical Image Fusion Using Combined Discrete Wavelet and Ripplet Transforms", Elsevier-International Conference on Modeling Optimisation and Computing, pp.813-820, 2012.

[12]. P. Phanindra, J.Chinna Babu, V.Usha Shree, "FPGA Implementation of Medical Image Fusion Based on DWT", International Journal of Advanced Research in Computer Science and Software Engineering, ISSN: 2277 128X, Volume 3, Issue 9, September 2013.

[13]. Gaurav Bhatnagar, Q.M. JonathanWu, Zheng Liu, "Directive Contrast Based Multimodal Medical Image Fusion in NSCT Domain", IEEE Transactions on Multimedia, Vol. 15, No. 5, August 2013.

[14]. Mirajkar Pradnya P, Ruikar Sachin D, **"**Wavelet based Image Fusion Techniques", International Conference on Intelligent Systems and Signal Processing, 2013.

[15]. K Sharmila, S Rajkumar, V Vijayarajan, "Hybrid method for Multimodality Medical image fusion using Discrete Wavelet Transform and Entropy concepts with Quantitative Analysis", IEEE Advancing Technology for Humanity, International conference on Communication and Signal Processing, April 3-5, 2013.

[16]. Sudeb Das, Malay Kumar Kundu, "A Neuro-Fuzzy Approach for Medical Image Fusion", IEEE Transactions On Biomedical Engineering, 2013.

[17]. A.P. James, B.V. Dasarathy, "Medical image fusion: A survey of the state of the art", Information Fusion, vol.19, pp. 4-19, 2014.

[18]. Laxman Tawade, Abida Bapu Aboobacker and Firdos Ghante, "Image Fusion Based on Wavelet Transforms", International Journal of Bio-Science and Bio-Technology ,Vol.6, No.3, pp.149-162,2014.

[19]. K.P.Indira, Dr.R.Rani Hemamalini, "Analysis on Image Fusion Techniques for Medical Applications", IJAREEIE, Vol. 3, Issue 9, September 2014.

[20]. Himanshi, Vikrant Bhateja, "An Improved Medical Image Fusion Approach Using PCA and Complex Wavelets", IEEE-International Conference on Medical Imaging, m-Health and Emerging Communication Systems, pp.442-447, 2014.

[21]. Navneet kaur, Madhu Bahl, Harsimran Kaur, "Review On: Image Fusion Using Wavelet and Curvelet Transform", IJCSIT, Vol. 5 (2), 2467-2470, 2014.

[22]. V.Savitha1, T. Kadhambari, R.Sheeba, "Multimodality Medical Image Fusion Using NSCT", IJREAT, ISSN: 2320 - 8791, Volume 1, Issue 6, Dec-Jan, 2014.

[23]. M.Ramamoorthy, K.Anees Barvin, "Medical Image Fusion Using Gabor and Gradient Measurement", International Journal of Innovative Research in Science, Engineering and Technology, ISSN (Online): 2319 – 8753, ISSN (Print): 2347 – 6710, Volume 3, Special Issue 3 March 2014.

[24]. Umer Javed, MuhammadMohsin Riaz, Abdul Ghafoor, Syed Sohaib Ali, Tanveer Ahmed Cheema, "MRI and PET Image Fusion Using Fuzzy Logic and Image Local Features", Scientific World Journal, Article ID 708075, Volume 2014.

[25]. Deepika.L, Mary Sindhuja.N.M, "Performance Analysis of Image Fusion Algorithms using HAAR Wavelet", International Journal of Computer Science and Mobile Computing, ISSN 2320–088X, Vol.3 Issue.1, pg. 487-494, January- 2014.

[26]. Nayera Nahvi, Onkar Chand Sharma, "Implementation of Discrete Wavelet Transform For Multimodal Medical Image Fusion", International Journal of Emerging Technology and Advanced Engineering, ISSN 2250-2459, Volume 4, Issue 7, July 2014.

[27]. Abhinav Krishn, Vikrant Bhateja, Himanshi, Akanksha Sahu, "Medical Image Fusion Using Combination of PCA and Wavelet Analysis", IEEE- International Conference on Advances in Computing Communications and Informatics (ICACCI), pp.986-991, 2014.

[28]. Sun Wei, Hu Shaohai, Liu Shuaiqi, Sun Yuchao, "Infrared And Visible Image Fusion Based On Object Extraction And Adaptive Pulse Coupled Neural Network Via Non-Subsampled Shearlet Transform", IEEE- ICSP Proceedings, pp.946-951, 2014.

International Journal of Engineering Research and General Science Volume 3, Issue 6, November-December, 2015
ISSN 2091-2730

Arduino Controller Based Smart Stick for Visually Challenged Using Zigbee Communication

Kavya B.C., Laxmana Naik L

Department of Mechanical Engineering, Malnad College of Engineering, Hassan, Karnataka, India.

AICTE, kavyabc02@gmail.com and 9916854778

Abstract— As indicated by human physiology vision assumes a pivotal part. More than 83% of data with respect to environment the individual gets from vision. The most seasoned and conventional versatility helps for persons with visual hindrances are the guide dogs and walking cane. The disadvantages of these guides are scope of movement and next to no data passed on. With the quick advances of cutting edge innovation, both in equipment and programming front can possibly give smart route capacities.
This venture work exhibits an Arduino Uno controller based smart stick, that cautions outwardly hindered individuals over static hindrances, dynamic snags, pit and aides them with the utilization of sound directions about proper way. It diagrams a superior navigational apparatus for the outwardly weakened. An Arduino Uno microcontroller contains all the memory and interfaces required for the application and the APR sound framework is use for sound direction. The general point of the gadget is to give an advantageous and safe strategy for the ignorant concerning conquers their challenges in day by day life. Furthermore this framework can be utilized for both indoor and open air environment. In this venture Arduino programming is utilized to code the microcontroller for controlling and checking the framework and MATLAB pictorially displays the destined path.

Keywords—Arduino UNO controller, IR sensor, proximity sensor, gyro-compass sensor, pit detection sensor, smart stick, APR sound framework, Arduino programming.

INTRODUCTION

Vision is a lovely blessing to individuals by GOD. Vision permits individuals to see and comprehend the encompassing scene. Outwardly tested is the state of lacking visual perception because of neurological and physiological elements. However a World Health Organization review made in 2015, evaluated 285.389 million individuals with visual weakness over the globe.
Lately availability of regular life situations for debilitated or matured individuals draws out in the open hobby. Really there is a considerable measure of extensions for it, for example, textured clearing squares, inclines rather than steps, handrails, lifts, and so on. Be that as it may, enhancements or degrees are restricted to particular spots and it is still troublesome for the impaired to live in a large portion of spots at present. Particularly for visually impaired individuals who have no visual data, there is a great deal of troubles in regular life situations. These individuals have a considerable measure of issues to obtain natural data. In addition, deterrents which are not hazardous to customary individuals have the capacity to wind up risky to them. In spite of the fact that they utilize visually impaired stick to gain this data, it is still hard for them to stroll around in a large portion of the spots furthermore not cover entire territory. A great deal of studies has been done to add to a framework which helps visually impaired individuals.
It depends on the utilization of new advancements to enhance outwardly impeded individual's portability. This venture concentrates on impediment identification and discovering area keeping in mind the end goal to lessen route troubles for outwardly tested individuals. Traveling through an obscure domain turns into a genuine test when we can't depend all alone eyes. Since element deterrents more often than not create commotion while moving, visually impaired individuals build up their feeling of hearing to restrict them.
In this task work to encourage outwardly tested to explore securely and rapidly among deterrents and different perils confronted by visually impaired walkers, a virtual guide is made utilizing a few sensors like infrared sensor, gyro sensor and pit sensor. A deterrent is recognized utilizing infrared sensors, gyro sensor is utilized for heading and pit discovery sensors are utilized to identify the pit in the way. Every one of the parameters from diverse sensors will be recorded and put away in Arduino microcontroller. All information from Arduino controller is sent to collector part utilizing ZigBee correspondence framework. At last graphical mapping is finished by MATLAB.
It is beneficial method for the present environment. As in the present circumstance it is totally subject to GPS. In a few circumstances there will be no accessibility of GPS system and in a few circumstances GPS focuses won't be available much of the time. Also GPS is a paid administration and it won't indicate most secure or briefest way. Henceforth by utilizing this procedure the framework gets to be cost proficient and the checking of framework likewise precise in nature.

METHODOLOGY

The block diagram of the Arduino controller based smart stick for visually challenged is as shown in figure 1 This framework is based on Arduino UNO microcontroller which controls the entire system. Power supply of +5 V is given to the Arduino controller. The shortest and safest path of the destination from starting point will be prerecorded and is stored in EEPROM which is located inside the smart stick.

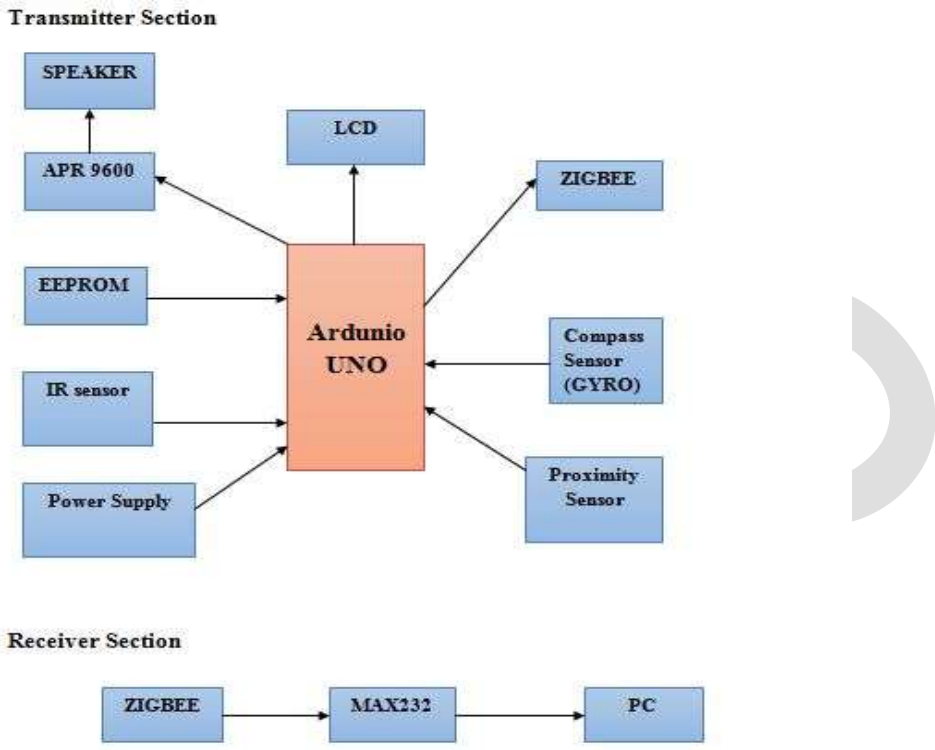

Fig 1: Block Diagram of the system

Once the smart stick is given to the visually challenged, he is guided to the destination in the shortest and safest path using the information which is already recorded in the stick. Initially when the visually challenged person holds the smart stick the gyro compass sensor inserted in the smart stick helps to determine the direction and starts navigating. The speaker is mounted on the stick which continuously gives instruction to reach the destination. Whenever the deviation is required the speaker will instruct the visually impaired person in advance. Proximity sensor attached to the stick helps in detecting both dynamic and static obstacle. In case there is static or dynamic obstacle the speaker alerts the visually impaired by giving instruction message. Along with proximity sensor, the pit detection sensor is also present in the smart stick which helps in determining the pit present while walking to the destination. The speaker gives the instruction to the visually impaired in case of pit and thus helping the visually impaired person to reach the destination without any obstacle.

In this project wireless communication ZigBee module is used. Transmitter end of the ZigBee module is connected to the smart stick and receiver end is connected to the PC. The ZigBee module continuously monitors the smart stick and all the information regarding smart stick will be transmitted to PC.

MATLAB 7 is used to pictorially represent the path travelled by visually challenged using smart stick from starting point to destination. All the information regarding smart stick will be continuously sent to PC by ZigBee module which is attached to the smart stick. Using this information obtained from ZigBee module, graphical representation of the path travelled will be displayed by MATLAB. All the obstacles like dynamic, static and also the pit present in the path to the destination will be indicated in the pictorially representation.

Thus while sitting away from the visually impaired person we can still monitor his path from starting point to destination.

FUNCTIONALOUTPUT

The Arduino controller controls the smart stick and all the information regarding the smart stick will be stored in EEPROM. The path from starting point to the destination will be prerecorded and speaker will give the visually impaired person all the necessary alerts.

In this venture gyro sensors are used to obtain the angle of rotation while moving through the required path. The range is set between --512 to +512. The figure 2 shows the range of gyro compass sensor at 14Deg/sec.

Fig 2: Range of gyro sensor

As the directions to the destined path will be prerecorded, whenever there is a deviation while travelling through the path the speaker located on the stick will inform in advance regarding whether to turn right or left. The same will be displayed on the LCD board present on the stick as shown in the above figure 3.

Fig 3: Directions to turn Right and Left

Once the visually challenged person holding the smart stick reaches the destination the speaker will inform and that will be displayed in LCD as shown in figure 4.

Fig 4: Display of the destination reached

All the information regarding smart stick is transformed to computer using wireless ZigBee communication which is attached to the stick. MATLAB uses this information to pictorially represent the distance travelled and also regarding any obstacles present in the path. The figure 5 shows pictorial representation of the distance travelled.

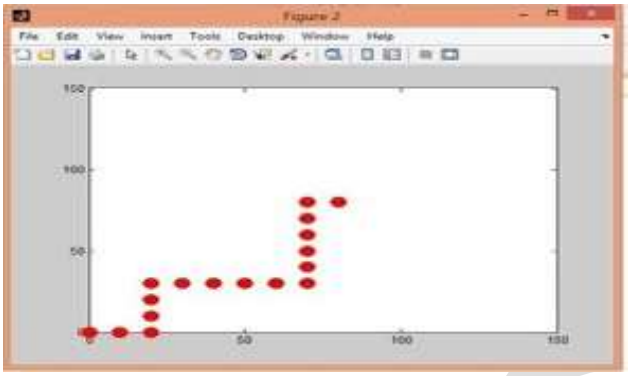

Fig 5: Pictorial representation

OBSERVATION

1. Low power consumption: Very less power is required to run the controller present in the stick. Hence low power consumption.
2. Simple to install: The system is very simple to install.
3. Proximity sensor used in the smart stick detects both the static and dynamic obstacle.
4. No human interface is required for guiding the path.
5. Shortest and accurate path to the destination can be determined.
6. Visually challenged person can be tracked in case if he loses his path.
7. It will perform both in outdoor and indoor environment.
8. Platform independent: Neither windows nor android is required.

LIMITATIONS

1. During stormy season it might be hard to work the framework as it may upset the associations.
2. In the instance of vicinity of any bugs the client is vulnerable with respect to troubleshooting or reinventing the code.

CONCLUSION

In this project Arduino controller based smart stick is designed and developed. All the data regarding the path from starting point to destination is prerecorded and stored in EEPROM. The stick navigates in this prerecorded path and speaker present in the stick helps in guiding the visually challenged person. The speaker will give advance instructions regarding any deviation. Different sensors like proximity sensor and pit detection sensor helps in detecting obstacles and pit along path respectively. All the information regarding smart stick is fed into computer using wireless ZigBee communication. Using this information MATLAB pictorially represents the navigated path and also indicates obstacles and pit, if only present along the path. Thus by using this smart stick visually challenged person can reach the destination accurately in the shortest and safest way without human interference.

REFERENCES:

[1] Pooja Sharma, Mrs.S. L.Shimi and Dr. S.Chatterji, **"**Design of microcontroller based virtual eye for the blind", International Journal of Scientific Research Engineering & Technology, Volume 3, Issue 8, November 2014.
[2] K.Chandana and G.R.Hemantha,"Navigation for the Blind Using GPS along with Portable Camera based Real Time Monitoring", SSRG International Journal of Electronics and Communication Engineering , Volume1,Issue8, October 2014.
[3] Kiran G Vetteth, Prithvi Ganesh K andDurbhaSrikar, "Collision Avoidance Device For Visually Impaired", International Journal of Scientific & Technology Research, Volume 2, Issue 10,October 2013.
[4] Jae Sung Cha, Dong Kyun Lim and Yong-Nyuo Shin, "DesignAnd Implementation Of A Voice Based Navigation For Visually Impaired Persons", International Journal Of Bio-Science And Bio-Technology, Vol. 5, Issue 3,June 2013.

[5] PrashantBhardwaj and Jaspal Singh, "Design and Development of Secure Navigation System for Visually Impaired People", International Journal of Computer Science & Information Technology ,Vol 5, Issue 4, August 2013
[6] M. Naveen Kumar, K. Usha, "Voice Based Guidance and Location Indication System for the Blind Using GSM, GPS and Optical Device Indicator", International Journal of Engineering Trends and Technology, Volume4, Issue7, July 2013.
[7] S.Sabarish,"Navigation Tool for Visually Challenged using Microcontroller", International Journal of Engineering and Advanced Technology, Volume 2, Issue 4, April 2013.
[8] Arjun Sharma, Rahul Patidar, ShubhamMandovara and IshwarRathod,"Blind Audio Guidance System", International Journal of Emerging Technology and Advanced Engineering, Volume 3, Special Issue 2, January 2013.
[9] B.P. Santosh Kumar, S. ShafiullaBasha and C. Hariprasad, "Guided Microcontroller For Blind People", International Journal of VLSI and Embedded Systems, Volume 3, Issue 3,July - August 2012.
[10] ZhenyunZhuang, Kyu-Han Kim and andJatinder Pal Singh, "Improving Energy Efficiency of Location Sensingon Smartphones", Georgia Institute of Technology, Atlanta, U.S.A, June 2010.
[11] J. Hesch, F. Mirzaei, G. Mariottini, and S. Roumeliotis "A laser aided inertial navigation system (l-ins) for human localization in unknown indoor environments" in Robotics and Automation (ICRA), 2010 IEEE International Conference , May 2010.
[12] N. Petrellis, N. Konofaos, and G. Alexiou, "Target localization utilizing the success rate in infrared pattern recognition" Sensors Journal, IEEE, volume 6, Issue 5, October 2006.
[13] K. Whitehouse, C. Karlof, A. Woo, F. Jiang, and D. Culler, "The effects of ranging noise on multihop localization: an empirical study" in Information Processing in Sensor Networks, IPSN Fourth International Symposium , April 2005.
[14] R. Siegwart and Lausanne, "Inertial and 3D-odometry fusion in rough terrain- Towards real 3D navigation",International Conference On intelligent Robots and Systems, Japan, . October 2004.
[15] K. Yu and I. Oppermann, "Uwb positioning for wireless embedded networks" in Radio and Wireless Conference, IEEE, September 2004.

International Journal of Engineering Research and General Science Volume 3, Issue 6, November-December, 2015
ISSN 2091-2730

A SINGLE-PHASE VOLTAGE-CONTROLLED GRID-CONNECTED PHOTOVOLTAIC SYSTEM WITH POWER QUALITY CONDITIONER FUNCTIONALITY

D.Sagar kumar[1], D.Vijaya kumar[2]

[1]P. G Student, Dept. of EEE, AITAM Engineering college, AP, India,d.sagarkumar@gmail.com

[2]Professor,HOD Dept. of EEE, AITAM Engineering college, AP, India,drdvk2010@gmail.com

***Abstract*:**-This paper proposes to solve this issue using a voltage controlled converter that behaves as a shunt controller, improving the voltage quality in case of small voltage dips and in the presence of nonlinear loads. Shunt controllers can be used as a static var generator for stabilizing and improving the voltage profile in power systems and to compensate current harmonics and unbalanced load current. This paper presents a single-phase PV system that provides grid voltage support and compensation of harmonic distortion at the point of common coupling thanks to a repetitive controller. In this paper, the PV inverter not only supplies the power produced by the PV panels but also improves the voltage profile. The presented topology adopts a repetitive controller that is able to compensate the selected harmonics. Among the most recent Maximum Power Point Tracking (MPPT) algorithms, an algorithm based on the incremental conductance method has been chosen. It has been modified in order to take into account power oscillations on the PV side, and it controls the phase of the PV inverter voltage. The designed PV system provides grid voltage support at fundamental frequency and compensation of harmonic distortion at the point of common coupling. An inductance is added on the grid side in order to make the grid mainly inductive.

Keywords- Maximum Power Point Tracking (MPPT), Distributed power generation system (DPGS), phase-locked loop (PLL).

I.INTRODUCTION:-

Among the renewable energy sources, a noticeable growth of small photovoltaic (PV) power plants connected to low-voltage distribution networks is expected in the future [1]. As a consequence, research has been focusing on the integration of extra functionalities such as active power filtering into the PV inverter operation [2]. Distribution networks are less robust than transmission networks, and their reliability, because of the radial configuration, decreases as the voltage level decreases. Hence, usually, it is recommended to disconnect low-power systems when the voltage is lower than 0.85 pu or higher than 1.1 pu [3].

For this reason, PV systems connected to low-voltage grids should be designed to comply with these requirements but can also be designed to enhance the electrical system, offering "ancillary services" [4]. Hence, they can contribute to reinforce the distribution grid, maintaining proper quality of supply that avoids additional investments. However, low-voltage distribution lines have a mainly resistive nature, and when a distributed power generation system (DPGS) is connected to a low-voltage grid, the grid frequency and grid voltage cannot be controlled by independently adjusting the active and reactive powers [5]–[6]. This problem, together with the need of limiting the cost and size of DPGS, which should remain economically competitive even when ancillary services are added, makes the design problem particularly challenging.

This paper proposes to solve this issue using a voltage controlled converter that behaves as a shunt controller, improving the voltage quality in case of small voltage dips and in the presence of nonlinear loads. Shunt controllers can be used as a static var generator for stabilizing and improving the voltage profile in power systems and to compensate current harmonics and unbalanced load current [7]–[11].

In this paper, the PV inverter not only supplies the power produced by the PV panels but also improves the voltage profile, as already pointed out [12]. The presented topology adopts a repetitive controller [13]–[17] that is able to compensate the selected harmonics. Among the most recent Maximum Power Point Tracking (MPPT) algorithms [18]–[20], an algorithm based on the incremental conductance method has been chosen [21]–[22]. It has been modified in order to take into account power oscillations on the PV side, and it controls the phase of the PV inverter voltage.

This paper is organized as follows. Section II discusses the possible voltage and frequency support provided by a DPGS converter connected to the grid. Section III discusses the simulation results. Section IV discusses the experimental results. Section V discusses the conclusion. Section VI refers to the reference papers

II. PV SYSTEM WITH SHUNT-CONNECTED MULTIFUNCTIONAL CONVERTER

In case of low-power applications, it can be advantageous to use the converter that is parallel connected to the grid for the compensation of small voltage sags. This feature can be viewed as an ancillary service that the system can provide to its local loads. The proposed PV converter operates by supplying active and reactive powers when the sun is available. At low irradiation, the PV converter only operates as a harmonic and reactive power compensator. As explained in Section III, it is difficult to improve the voltage quality with a shunt controller since it cannot provide simultaneous control of the output voltage and current. In addition, a large-rated converter is necessary in order to compensate voltage sags. However, this topology is acceptable in PV applications since the PV shunt converter must be rated for the peak power produced by the panels. In the proposed system, the PV converter operates as a shunt controller; it is connected to the load through an LC filter and to the grid through an extra inductance Lg of 0.1 pu, as shown in Fig. (1)

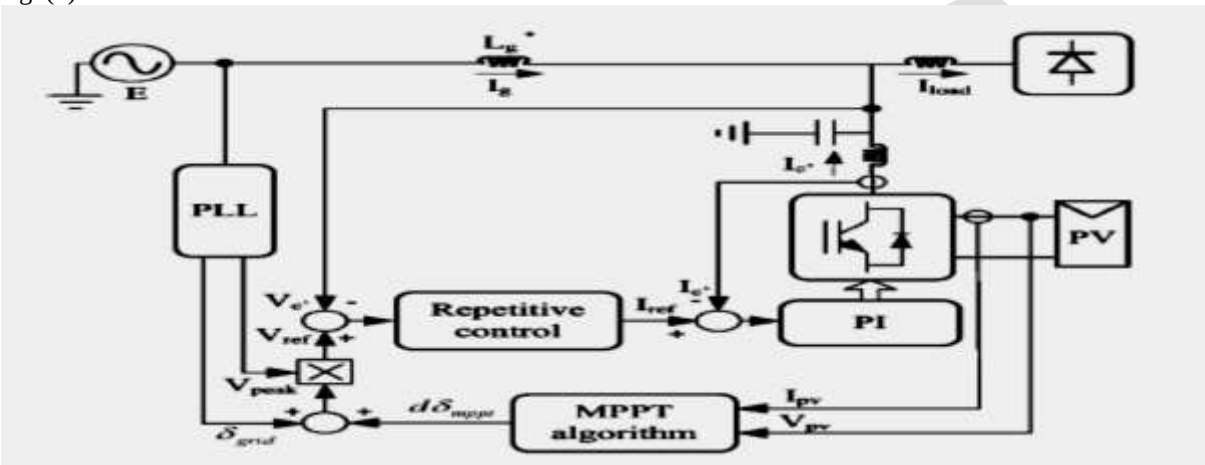

Fig(1).Grid-connected PV system with shunt controller functionality.

Usually, in case of low-power applications, the systems are connected to low-voltage distribution lines whose impedance is mainly resistive. However, in the proposed topology, the grid can be considered mainly inductive as a consequence of Lg addition on the grid side. However, since the voltage regulation is directly affected by the voltage drop on the inductance Lg, it is not convenient choosing an inductance Lg of high value in order to limit the voltage drop during grid normal conditions. It represents the main drawback of the proposed topology.

A. Control of Converter

The proposed converter is voltage controlled with a repetitive algorithm. An MPPT algorithm modifies the phase displacement between the grid voltage and the ac voltage produced by the converter in order to force it to inject the maximum available power in the given atmospheric conditions. Hence, current injection is indirectly controlled. The amplitude of the current depends on the difference between the grid voltage and the voltage on the ac capacitor Vc . The phase displacement between these two voltages determines the injected active power (decided by the MPPT algorithm), and the voltage amplitude difference determines the reactive power exchange with the grid. The injected reactive power is limited by the fact that a voltage dip higher than 15% will force the PV system to disconnect (as requested by standards). The active power is limited by the PV system rating and leads to a limit on the maximum displacement angle dδmppt. Moreover, the inverter has its inner proportional integral (PI)-based current control loop and overcurrent protections. A phase-locked loop (PLL) detects the amplitude Vpeak and phase δgrid of the grid voltage. Then, the phase displacement dδmppt is provided by the MPPT algorithm described in Section IV-B. The voltage error between Vref and Vc is preprocessed by the repetitive controller, which is the periodic signal generator of the fundamental component and of the selected harmonics: in this case, the third and fifth ones are compensated (Fig)(2)

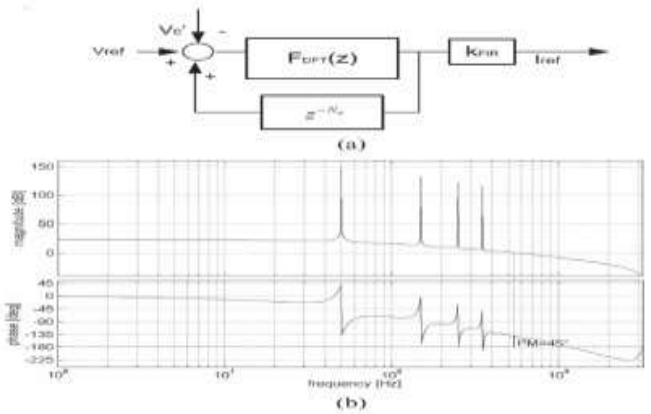

Fig2. Proposed repetitive-based controller. (a) Control scheme. (b) Open loop Bode diagram of the system obtained using *k*FIR = 1, *Na* = 0, and *Nh* = *{*1; 3; 5*}*.

The proposed repetitive controller is based on a finite impulse response (FIR) digital filter [20]. It is a "moving" or "running" filter, with a window equal to one fundamental period, defined as

$$F_{\mathrm{DFT}}(z) = \frac{2}{N}\sum_{i=0}^{N-1}\left(\sum_{h\in N_h}\cos\left[\frac{2\pi}{N}h(i+N_a)\right]\right)\cdot z^{-i}$$

where N is the number of samples within one fundamental period, Nh is the set of selected harmonic frequencies, and Na is the number of leading steps determined to exactly track the reference. The repetitive controller ensures a precise tracking of the selected harmonics, and it provides the reference for the inner loop. In it, a PI controller improves the stability of the system, offering a low-pass filter function. The PI controller Gc

$$G_c(s) = k_p + \frac{k_i}{s}$$

is designed to ensure that the low-frequency poles have a damping factor of 0.707. The open-loop Bode diagram of the system is shown in Fig (b): stability is guaranteed since the phase margin is about 45◦.

In normal operation mode, the shunt-connected converter injects the surplus of active power in the utility grid, and at the same time, it is controlled in order to cancel the harmonics of the load voltage. At low irradiation, the PV inverter only acts as a shunt controller, eliminating the harmonics. Controlling the voltage Vc , the PV converter is improved with the function of voltage dip compensation. In the presence of a voltage dip, the grid current Ig is forced by the controller to have a sinusoidal waveform that is phase shifted by 90◦ with respect to the corresponding grid voltage.

B. MPPT Algorithm

The power supplied from a PV array mostly depends on the present atmospheric conditions (irradiation and temperature); therefore, in order to collect the maximum available power, the operating point needs to continuously be tracked using an MPPT algorithm [28]. To find the maximum power point (MPP) for all conditions, an MPPT control method based on the incremental conductance method [32], [34], which can tell on which side of the PV characteristic the current operating point is, has been used. The MPPT algorithm modifies the phase displacement between the grid voltage and the converter voltage, providing the voltage reference Vref . Furthermore, there is an extra feature added to this algorithm that monitors the maximum and minimum values of power oscillations on the PV side. In case of single-phase systems, the instant power oscillates with twice the line frequency. This oscillation in power on the grid side leads to a 100-Hz ripple in voltage and power on the PV side. If the system operates in the area around the MPP, the ripple of the power on the PV side is minimized [33]. This feature can be used to detect in which part of the power–voltage characteristics the system operates. It happens in the proposed control scheme where information about the power oscillation can be used to find out how close the current operating point is to the MPP, thereby slowing down the increment of the reference, in order not to cross the MPP.

A flowchart of the MPPT algorithm is shown in Fig., explaining how the angle of the reference voltage is modified in order to keep the operating point as close to MPP as possible. The MPP can be tracked by comparing the instantaneous conductance Ipvk/Vpv_k to the incremental conductance dIpv/dVpv, as shown in the flowchart. Considering the power–voltage characteristic of a PV array, it can be observed. that, operating in the area on the left side of the MPP, dδmppt has to decrease. This decrement is indicated in Fig. with side = −1. Moreover, operating in the area on the right side of the MPP, dδmppt has to increase, and it is indicated with side =+1. The increment size determines how fast the MPP is tracked. The measure of the power oscillations on the PV side is used to quantify the increment that is denoted with incr in Fig.(3)

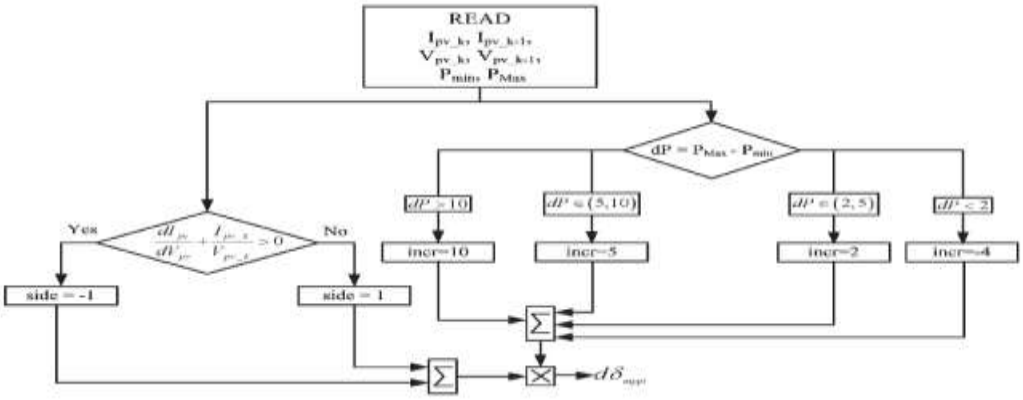

Fig3. Flowchart of the modified MPPT algorithm.

III. SIMULATION RESULTS

The PV system with power quality conditioner functionality has been tested in the simulation with the following system parameters: the LC filter made by 1.4-mH inductance, 2.2-μF capacitance, and 1-Ω damping resistance; an inductance Lg of 0.1 pu; and a 1-kW load.

The control has been validated in the presence of sudden changes of the PV power caused, for example, by irradiation variations. The reported tests show the behavior of the MPPT for a voltage sag. The results refer to the case of a controlled inverter in order to collect the maximum available power (i.e.,2 kW).

The controller parameters are kFIR = 0.3, N = 128 (sampling frequency = 6400 Hz), Na = 0, kp = 4.5, and ki = 48. The set of test aims to demonstrate the behavior of the system during a voltage sag and the interaction of the voltage control algorithm with the MPPT algorithm.

The simulation results, shown in Figs , are obtained in case of a voltage dip of 0.15 pu.

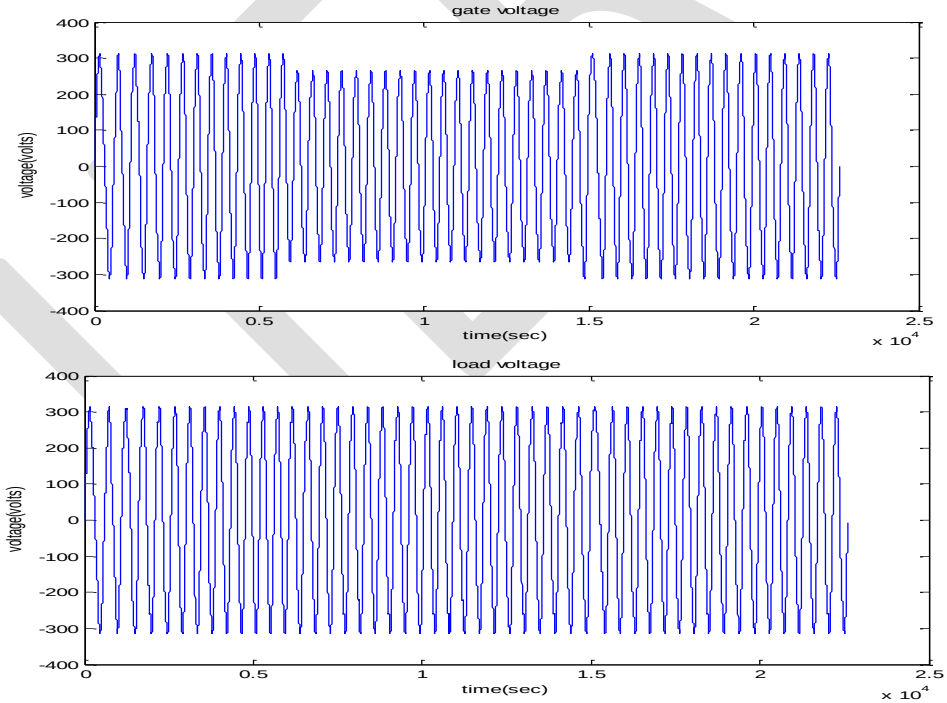

Fig4. Performance of the voltage-controlled shunt converter with MPPT algorithm: grid voltage *E* and load voltage *V*load.

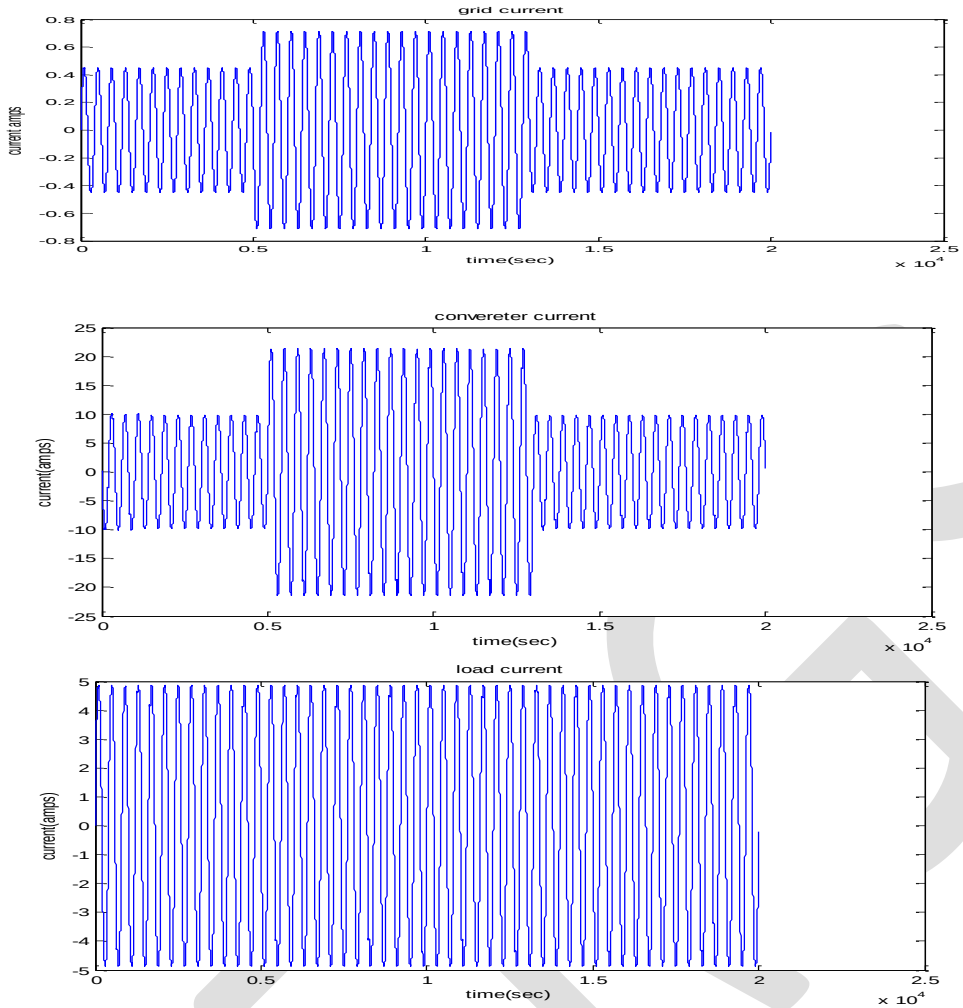

Fig.5 Performance of the voltage-controlled shunt converter with MPPT algorithm: grid current *Ig*, converter current *IC*, and load current *I*load.

During the sag, the inverter sustains the voltage for the local load (Fig.), injecting a mainly reactive current into the grid. The amplitude of the grid current Ig grows from 4.5 to 8.5 A, as shown in Fig, which corresponds to the reactive power injection represented in Fig.

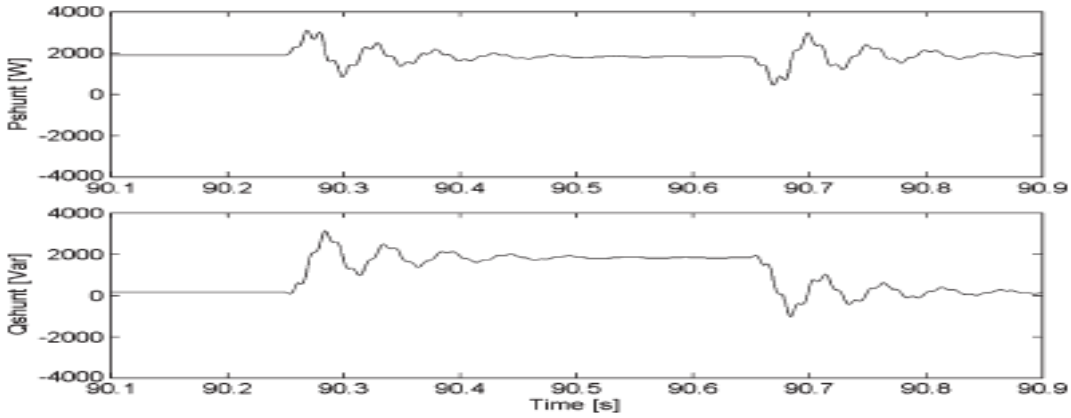

Fig.6 Active and reactive power provided by the shunt-connected multifunctional converter to compensate the voltage sag of 0.15 pu.

The inductance Lg connected in series with the grid impedance limits the current flowing through the grid during the sag. When the voltage sag of 0.15 pu occurs, the converter current grows from 8 to 10.5 A. For this reason, the shunt controller is not a good choice to compensate for deeper dips. Fig. demonstrates the robustness of the presented MPPT algorithm to the voltage dip. In fact, in it are shown the voltage and current on the PV side during the sag. They are not significantly influenced by the dip.

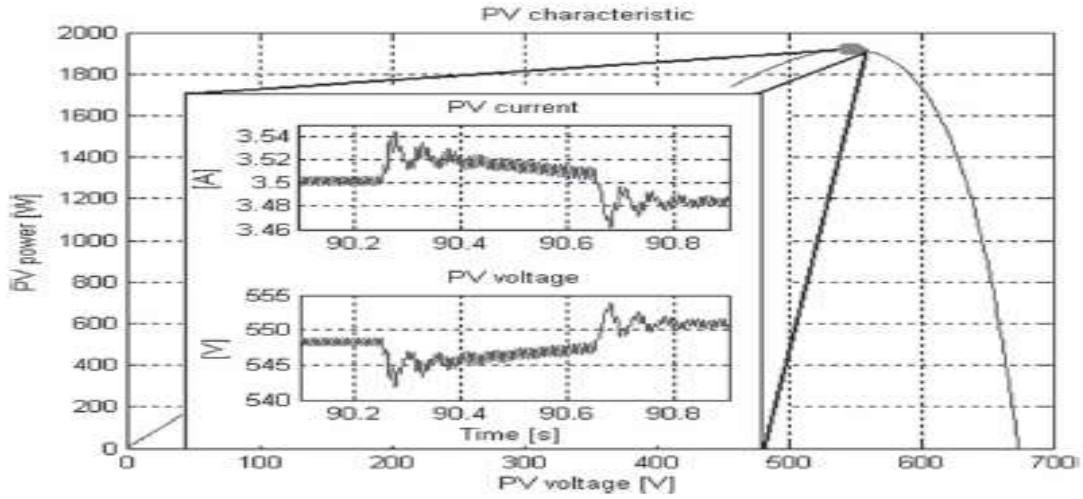

Fig.7 Power–voltage characteristic of the PV array and current and voltage on the PV side in the presence of a grid voltage sag of 0.85 pu.

IV.EXPERIMENTAL RESULTS

In order to verify the previous analysis, some experiments have been carried out on a laboratory setup to test the performance of the PV system with shunt controller functionality. The hardware setup, consists of the following equipment: a Danfoss VLT 5006 7.6-kVA inverter (whose only two legs are used), two series-connected dc voltage sources to simulate the PV panel string, and the dSPACE 1104 system. The PV converter is connected to the grid through an LC filter whose inductance is 1.4 mH, and the capacitance is 2.2 μF in series with a resistance of 1 Ω. In addition, an inductance Lg of 15 mH (0.1 pu) has been added on the grid side of the converter, as explained in the previous sections.

The experimental tests have been made with grid voltage approximate background distortion THD = 1.5%. They have been executed with two different kinds of loads. In the first case, the voltage sag compensation capability has been tested when the system feeds a purely resistive load, absorbing 1200 W. In the second one, the performances of the proposed system in the presence of a highly distorting load have been analyzed.

A. Voltage Sag Compensation

The system has been tested in the following conditions: dc voltage Vdc = 460 V. The results obtained in the simulation in the case of voltage sag of 0.15 pu are experimentally confirmed. During the dip, the load voltage remains constant and equal to the desired voltage. The shunt-connected converter injects a reactive current into the grid in order to compensate the load voltage. The current is mainly capacitive.

B. Voltage Harmonic Compensation in Case of Highly Distorting Load

The performances of the shunt-connected converter have been analyzed in the presence of a distorting load consisting of a single-phase diode bridge connected via a 10-mH inductance to the grid. The bridge feeds a 500-μF capacitor in parallel with a 100-Ω resistor. Before connecting the shunt converter, the load voltage appears highly distorted and the voltage THD is around 17%. When the shunt converter is connected to the grid, it compensates the voltage harmonics introduced in the system by the distorting load where the voltage THD is 2%.

C. Test with Solar Panel Simulator

This section proves the capability of the system to compensate a voltage dip when the inverter is fed by two PV arrays connected in parallel. In fact, the two dc voltage sources used in the laboratory to feed the inverter have been controlled by software that implements the PV voltage–current characteristics as a function of irradiance. The test has been done considering a fixed power level of 700 W and a voltage dip of 0.15 pu occurring for 1.5 s.

V. CONCLUSION

In this paper, a single-phase PV system with shunt controller functionality has been presented. The PV converter is voltage controlled with a repetitive algorithm. An MPPT algorithm has specifically been designed for the proposed voltage-controlled converter. It is based on the incremental conductance method, and it has been modified to change the phase displacement between the grid voltage and the converter voltage maximizing the power extraction from the PV panels. The designed PV system provides grid voltage support at fundamental frequency and compensation of harmonic distortion at the point of common coupling. An inductance is added on the grid side in order to make the grid mainly inductive (it may represent the main drawback of the proposed system). Experimental results confirm the validity of the proposed solution in case of voltage dips and nonlinear loads.

REFERENCES:

[1] F. Blaabjerg, R. Teodorescu, M. Liserre, and A. V. Timbus, "Overview of control and grid synchronization for distributed power generation systems," IEEE Trans. Ind. Electron., vol. 53, no. 5, pp. 1398–1409, Oct. 2006

[2] M. Ciobotaru, R. Teodorescu, and F. Blaabjerg, "On-line grid impedance estimation based on harmonic injection for grid-connected PV inverter," in Proc. IEEE Int. Symp. Ind. Electron., Jun. 4–7, 2007, pp. 2437–2442

[3] IEEE Standard for Interconnecting Distributed Resources With Electric Power Systems, IEEE Std. 1547-2003, 2003

[4] IEEE Guide for Monitoring, Information Exchange, and Control of Distributed Resources Interconnected With Electric Power Systems, IEEE Std. 1547.3-2007, 2007.

[5] J. M. Guerrero, J. Matas, L. García de Vicuña, M. Castilla, and J. Miret, "Decentralized control for parallel operation of distributed generation inverters using resistive output impedance," IEEE Trans. Ind. Electron., vol. 54, no. 2, pp. 994–1004, Apr. 2007.

[6] K. De Brabandere, B. Bolsens, J. Van den Keybus, A. Woyte, J. Driesen, and R. Belmans, "A voltage and frequency droop control method for parallel inverters," IEEE Trans. Power Electron., vol. 22, no. 4, pp. 1107– 1115, Jul. 2007.

[7] H. Kömürgügil and Ö. Kükrer, "A new control strategy for single-phase shunt active power filters using a Lyapunov function," IEEE Trans. Ind. Electron., vol. 53, no. 1, pp. 305–312, Feb. 2006.

[8] M. E. Ortúzar, R. E. Carmi, J. W. Dixon, and L. Morán, "Voltagesource active power filter based on multilevel converter and ultracapacitor DC link," IEEE Trans. Ind. Electron., vol. 53, no. 2, pp. 477–485, Apr. 2006.

[9] B.-R. Lin and C.-H. Huang, "Implementation of a three-phase capacitorclamped active power filter under unbalanced condition," IEEE Trans. Ind. Electron., vol. 53, no. 5, pp. 1621–1630, Oct. 2006

[10] M. H. J. Bollen and I. Gu, Signal Processing of Power Quality Disturbances. New York: Wiley, 2006.

[11] G. Escobar, P. Mattavelli, A. M. Stakovis, A. A. Valdez, and J. Leyva-Ramos, "An adaptive control for UPS to compensate unbalance and harmonic distortion using a combined capacitor/load current sensing," IEEE Trans. Ind. Electron., vol. 54, no. 2, pp. 839–847, Apr. 2007.

[12] P. Wang, N. Jenkins, and M. H. J. Bollen, "Experimental investigation of voltage sag mitigation by an advanced static VAr compensator," IEEE Trans. Power Del., vol. 13, no. 4, pp. 1461–1467, Oct. 1998.

[13] F. Botterón and H. Pinehiro, "A three-phase UPS that complies with the standard IEC 62040-3," IEEE Trans. Ind. Electron., vol. 54, no. 4, pp. 2120–2136, Aug. 2007.

[14] G. Escobar, A. A. Valdez, J. Leyva-Ramos, and P. Mattavelli, "Repetitivebased controller for a UPS inverter to compensate unbalance and harmonic distortion," IEEE Trans. Ind. Electron., vol. 54, no. 1, pp. 504–510, Feb. 2007.

[15] G. Escobar, P. R. Martínez, and J. Leyva-Ramos, "Analog circuits to implement repetitive controllers UIT feedforward for harmonic compensation," IEEE Trans. Ind. Electron., vol. 54, no. 1, pp. 567–573, Feb. 2007.

[16] R. Griñó, R. Cardoner, R. Costa-Castelló, and E. Fossas, "Digital repetitive control of a three-phase four-wire shunt active filter," IEEE Trans. Ind. Electron., vol. 54, no. 3, pp. 1495–1503, Jun. 2007.

[17] R. A. Mastromauro, M. Liserre, and A. Dell'Aquila, "Study of the effects of inductor nonlinear behaviour on the performance of current controllers for single-phase PV grid converters," IEEE Trans. Ind. Electron., vol. 55, no. 5, pp. 2043–2052, May 2008.

[18] H. Patel and V. Agarwal, "Maximum power point tracking scheme for PV systems operating under partially shaded conditions," IEEE Trans. Ind. Electron., vol. 55, no. 4, pp. 1689–1698, Apr. 2008.

[19] I. Kim, M. Kim, and M. Youn, "New maximum power point tracker using sliding-mode observer for estimation of solar array current in the gridconnected photovoltaic system," IEEE Trans. Ind. Electron., vol. 53, no. 4, pp. 1027–1035, Aug. 2006.

[20] W. Xiao, N. Ozog, and W. G. Dunford, "Topology study of photovoltaic interface for maximum power point tracking," IEEE Trans. Ind. Electron., vol. 54, no. 3, pp. 1696–1704, Jun. 2007.

[21] T. Esram and P. L. Chapman, "Comparison of photovoltaic array maximum
power point tracking techniques," IEEE Trans. Energy Convers., vol. 22, no. 2, pp. 439–449, Jun. 2007.
[22] F. Liu, S. Duan, F. Liu, B. Liu, and Y. Kang, "A variable step size INC MPPT method for PV systems," IEEE Trans. Ind. Electron., vol. 55, no. 7, pp. 2622–2628, Jul. 2008

International Journal of Engineering Research and General Science Volume 3, Issue 6, November-December, 2015
ISSN 2091-2730

Enhancement of Security in Distributed Data Mining

Sharda Darekar [1], Prof.D.K.Chitre [2]

[1,2]Department Of Computer Engineering, Terna Engineering College,Nerul,Navi Mumbai.
[1]sharda.darekar@gmail.com, [2]dkchitre1@rediffmail.com

Abstract— Data mining is that the most quick growing space these days that is employed to extract necessary data from massive knowledge collections however usually these collections area unit divided among many parties. With the fast development of knowledge mining analysis tools currently days it's penetration of knowledge mining and analysis at intervals completely different fields for disciplines, security and providing security at mining activities. The pattern mining in massive information provides introduction of recent and novel algorithms in data processing technology for providing secured pattern mining at outsourced or remote servers. The aim of paper is to produce security in data processing pattern analysis results and maintaining the principles that secures the personal data regarding organization or people corporations.

In older data processing analysis of patterns, quick Distributed Mining algorithmic program is employed. The quick Distributed Mining algorithmic program is invention of recent protocol with set of mining rules for secure mining of knowledge in horizontally distributed databases. However the protocol wasn't ready to secure distributed versions of information, as a result of quick distributed mining is extension of Apriori algorithmic program.

To beat the matter we tend to propose another technique known as secure computations with Multi party computations model on data. The goal of the projected system is to use mining and cryptography as joint technique for quicker and secure mining computations.

Keywords— Apriori Algorithm, Association Rule, Distributed Database, Fast Distributed Mining (FDM), secure mining.

INTRODUCTION

Data mining is outlined because the methodology for extracting hidden predictive data from giant distributed databases. it's new technology that has emerged as a method of characteristic patterns and trends from giant quantities of information. the ultimate product of this method being the information, that means the numerous data provided by the unknown components [2]. This paper study the matter of association rules mining in horizontally distributed databases. within the distributed databases, there are many players that hold homogenized databases that share identical schema however hold data on totally different entities. The goal is to seek out all association rule with support s and confidence c to reduce the knowledge disclosed concerning the non-public databases command by those players [1].

Kantarcioglu and clifton studied the matter wherever additional appropriate security definitions that enable parties to settle on their desired level of security are required, to permit effective solutions that maintain the required security [2]. so that they devised a protocol for its resolution. the most a part of that protocol is sub protocol for secure computation of the union of personal subsets that ar command by the various players. It makes the protocol pricey and its implementation depends upon coding primitive's ways, oblivious transfer and hash operate additionally the escape of knowledge renders the protocol not absolutely secure [1].

This paper projected Associate in Nursing algorithmic rule, PPFDM, privacy protective quick distributed mining algorithmic rule for horizontally distributed knowledge sets and notice attention-grabbing association or correlation relationships among an outsized set of information things and to include cryptographically techniques to reduce the knowledge that goes to shared with others, whereas adding very little overhead to the mining task [1]. Within the projected theme, the inputs are the partial information and therefore the needed output is that the list of association rules that hold within the unified database with support and confidence no smaller than the given thresholds s and c, severally. the knowledge that may prefer to shield during this paper isn't solely individual dealing within the totally different databases, however additionally additional world or public data like what association rules are supported regionally in every of these databases. The projected protocol improves upon that in [2] in terms of simplicity and potency furthermore as privacy.

PROPOSED WORK

The system includes a novel various protocol for providing secure computation with personal subsets in distributed information and it improves the potency and security of information mining. The planned and designed protocol provides full computing, parameterized computing and customized user computing, that we have a tendency to decision user threshold functions, within which the 2 extreme cases correspond to the issues of computing the union and intersection of personal subsets. This mechanism provides associate degree extension to Apriori rule with quick distributed and Secure Multiparty computations.

The planned system uses 2 algorithms, specifically Apriori and S-FDM for locating frequent item sets from horizontally distributed databases. Association Rules square measure generated from the frequent things sets and classified whose confidence is larger than the minimum threshold confidence referred to as sturdy Association Rules. The sturdy associations rules square measure classified during this manner square measure presented the user.

While extracting data from distributed database system more number of irrelevant data will occur. Irrelevant data is avoided by using the Apriori algorithm. Data leakage is more in Apriori algorithm. Encryption is done at the time of retrieving data from the database.

Advantages

- As a rising subject, data processing is taking part in associate degree more and more vital role within the call support activity of each walk of life.
- Get economical item set result supported the client request.
- Provides associate degree increased cryptography theme that allows protractile formal privacy guarantees in large-scale and real-life dealing information.

System Design

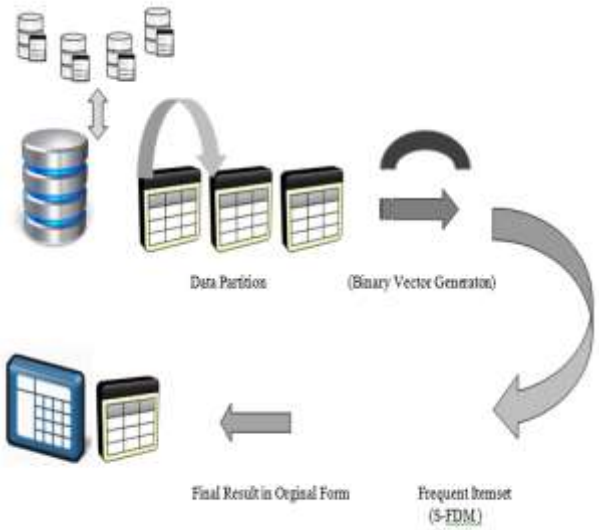

Figure 1: System Flow Diagram

The projected System flow is shown in figure1. Association Rule mining is one among the foremost necessary data processing tools employed in several world applications [2]. This paper, presents the matter of computing association rules at intervals a horizontally partitioned off info. we have a tendency to assume consistent databases. To mine the association rules the primary task is to come up with the frequent item sets. Second task is to mine the association rules from the frequent item sets.

1. *Generation of Frequent Itemsets*

Frequent item sets from completely different information return to a world database. Since there square measure such a large amount of information bases through that frequent data goes to the worldwide info thus this will increase the quantity of messages that require to be passed thus on notice frequent k item set. the main downside with frequent set mining strategies is that the explosion of the quantity of results then it's tough to seek out the foremost attention-grabbing frequent item sets. therefore the idea of finding frequent itemsets from the info that is at completely different Distributions, and mine the association rules has been highlighted during this paper.

2. Mining associations Rules

Following the first definition by Agrawal the matter of association rule mining is outlined as[5] : Let I = be a group of n binary attributes referred to as things. Let D = be a group of transactions referred to as the info. every dealing in D contains a distinctive dealing ID and contains a set of the things in I. A association rule is outlined as Associate in Nursing implication of the shape X->Y wherever X, Y ⊆ I and X ∩ Yb = ∅. The sets of things (for short itemsets) X and Y square measure referred to as antecedent (left-hand-side or LHS) and resulting (right-hand-side or RHS) of the rule severally. Associate in Nursing example of Associate in Nursing association rule would be "If a client buys a bread, he's eightieth possible to conjointly purchase milk."

Given a minimum confidence threshold minconf and a minimum support threshold minsup, the matter is to come up with all association rules that have support and confidence bigger than the user-specified minimum support and minimum confidence. within the initial pass, the support of every individual item is counted, and therefore the giant ones square measure determined. In every sequent pass, the big itemsets determined within the previous pass is employed to come up with new itemsets referred to as candidate itemsets. The support of every candidate itemset is counted, and therefore the giant ones square measure determined. This method continues till no new giant itemsets square measure found.

The overall method of Association Rule Mining consists of following modules:

i. User Module: -

In this module, privacy protective data processing has thought of 2 connected settings. One, within which {the information} owner and therefore the data mineworker square measure 2 completely different entities, and another, within which the info is distributed among many parties World Health Organization aim to conjointly perform data processing on the unified corpus of knowledge that they hold.

In the first setting**,** the goal is to protect the data records from the data miner. Hence, the data owner aims at anonymizing the data prior to its release. The main approach in this context is to apply data perturbation. He perturbed data can be used to infer general trends in the data, without revealing original record information.

In the second setting**,** the goal is to perform data mining while protecting the data records of each of the data owners from the other data owners.

ii. Admin Module:

This module is used to view user details. Admin to view the item set based on the user processing details using association role with Apriori algorithm.

iii. Association Rule:-

Association rules are if/then statements that help uncover relationships between seemingly unrelated data in a relational database or other information repository. An example of an association rule would be "If a customer buys a dozen eggs, he is 80% likely to also purchase milk."Association rules are created by analyzing data for frequent if-then patterns and using the criteria support and confidence to identify the most important relationships. Support is an indication of how frequently the items appear in the database. Confidence indicates the number of times the if/then statements have been found to be true.

iv. Apriori Algorithm :-

Apriori is designed to operate on databases containing transactions. The purpose of the Apriori Algorithm is to find associations between different sets of data. It is sometimes referred to as "Market Basket Analysis". Each set of data has a number of items and is called a transaction. The output of Apriori is sets of rules that tell us how often items are contained in sets of data.

The frequent item sets determined by Apriori can be used to determine association rules which highlight general trends in the database. Number of transaction is present in each set of data. Initial scan/pass of algorithm counts occurrence of each item in order to determine the frequent items set. Next scan K consists two phases.

1) In first phase, Candidate item set C_K is generated using frequent item set L_k-1 found in $(K-1)_{th}$ pass. This is candidate generation process in Apriori Algorithm.

2) In second phase database is scanned to find support for Candidates C_K. In next step, it prunes the candidates which have an infrequent sub pattern and keep only subset of candidate sets which are already identified as frequent items sets. Output of Apriori algorithm generates sets of rules which determine how often items are brought together in single set.

v. *Fast Distributed Mining(FDM) :*

Fast Distributed Mining (FDM) algorithm is an unsecured distributed version of the Apriori algorithm. Its main idea is that any s-frequent itemset must be also locally s-frequent in at least one of the sites. Hence, in order to find all globally -frequent itemsets, each player reveals his locally s-frequent itemsets and then the players check each of them to see if they are s-frequent also globally.

The FDM algorithm proceeds as follows:

- Initialization
- Candidate Sets Generation
- Local Pruning
- Unifying the candidate item sets
- Computing local supports
- Broadcast Mining Results

vi. *S-FDM:*

In this paper we have a tendency to discuss concerning the protection of knowledge whereas mining. victimization Advanced cryptography customary (AES) and DES (Data cryptography Standard) technique, information are encrypted and decrypted whereas inserting and retrieving the info. Advanced cryptography customary (AES) takes less quantity of your time to encode and rewrite the info.

The S-FDM algorithm proceeds as follows:

- Cryptographic Primitive Selection
- All item sets Encryption
- Item set Merging
- Decryption
- View final Result

RESULTS

There are several sites that hold homogeneous databases, i.e., databases that share the same schema but hold information on different entities. The system is designed to find all association rules with support at least *s* and confidence at least *c*, for some given minimal support size *s* and confidence level *c*, that hold in the unified database, while minimizing the information disclosed about the private databases held by those sites. The protected context is not only individual transactions in the different databases, but also more global information such as what association rules are supported locally in each of those database.

Here the result is existing system and proposed system result. Figure2 shows the comparison of two systems using transactional graph. Proposed System gives better result than the existing system.

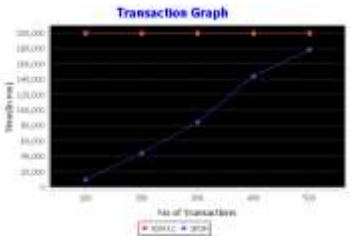

Figure2: Transactional Graph

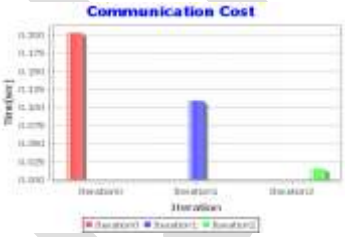

Figure3: Communication cost Graph

CONCLUSION

Mining association rules is one among the information mining techniques that are terribly helpful for creating well sophisticated choices. This work is distributed on horizontally distributed info in secure setting. Support and confidence are the applied math measures used for mining association rules. Thus, the applied math measures will be wont to shrewdness the foundations are helpful. The lot of in support and confidence, the lot of in utility of the foundations. Frequent item sets are generated through apriori and

remainder of the mechanisms are distributed by the planned algorithmic program. Knowledge accesses from distributed information are a lot of secured and extremely economical once this mechanism is applied.

REFERENCES:

[1] Tamir Tassa,"Secure mining of association rule in horizontally distributed databases" ,IEEE trans. Konwledege and Data Engg.,Vol.26, no.2, April

2014.

[2] M. Kantarcioglu and C. Clifton, "Privacy-Preserving Distributed Mining of Association Rules on Horizontally Partitioned Data," IEEE Trans.

Knowledge and Data Eng., vol. 16, no. 9, pp. 1026-1037, Sept. 2004.

[3] A.V. Evfimievski, R. Srikant, R. Agrawal, and J. Gehrke. Privacy preserving mining of association rules. In *KDD*, pages 217–228, 2002.

[4] R. Agrawal and R. Srikant. Privacy-preserving data mining. In *SIGMOD Conference*, pages 439–450, 2000.

[5] Y. Lindell and B. Pinkas. Privacy preserving data mining. In *Crypto*, pages 36–54, 2000.

[6] X. Lin, C. Clifton, and M.Y. Zhu. Privacy-preserving clustering,with distributed EM mixture modeling. *Knowl. Inf. Syst.*, 8:68–81,2005.

[7] J. Zhan, S. Matwin, and L. Chang. Privacy preserving *Security*,collaborative association rule mining. In *Data and Applications* pages 153– 165, 2005.

[8] J. Vaidya and C. Clifton. Privacy preserving association rule mining in vertically partitioned data. In *KDD*, pages 639–644, 2002.

[9] M. Kantarcioglu, R. Nix, and J. Vaidya. An efficient approximate protocol for privacy-preserving association rule mining. In *PAKDD*,pages 515–524, 2009.

[10] A. Schuster, R. Wolff, and B. Gilburd. Privacy-preserving association rule mining in large-scale distributed systems. In *CCGRID*, pages 411–418, 2004.

[11] L. Kissner and D.X. Song. Privacy-preserving set operations. In *CRYPTO*, pages 241–257, 2005.

[12] M.J. Freedman, K. Nissim, and B. Pinkas. Efficient private matching and set intersection. In *EUROCRYPT*, pages 1–19, 2004.

[13] J. Brickell and V. Shmatikov. Privacy-preserving graph 252, algorithms in the semi-honest model. In *ASIACRYPT*, pages 236–2005.

[14] M. Freedman, Y. Ishai, B. Pinkas, and O. Reingold. Keyword search and oblivious pseudorandom functions. In *TCC*, pages 303–324, 2005.

International Journal of Engineering Research and General Science Volume 3, Issue 6, November-December, 2015
ISSN 2091-2730

Design of Trust Aware Routing Framework

Mr.B.B.Gite , Mr.Zeeshanali Shaikh

SAOE, Pune University, zeeshan.shaikh02@gmail.com and +91-8805961502

Abstract- The multi-hop routing in wireless sensor networks (WSNs) offers little protection against identity deception through replaying routing information. An adversary can exploit this defect to launch various harmful or even devastating attacks against the routing protocols, including sinkhole attacks, wormhole attacks and Sybil attacks. Traditional cryptographic techniques or efforts at developing trust-aware routing protocols do not effectively address this severe problem. To secure the WSNs against adversaries misdirecting the multi-hop routing, we have design and implemented TARF, a robust trust-aware routing framework for dynamic WSNs.TARF provides trustworthy and energy-efficient route. Most importantly, TARF proves effective against those harmful attacks developed out of identity deception; the resilience of TARF is verified through extensive evaluation with both simulation and empirical experiments on large-scale WSNs under various scenarios including mobile and RF-shielding network conditions.

Keywords— CTP – Collection Tree Routing Protocol, EWMA-exponentially weighted moving average, RPGM-Reference Point Group Mobility TARF-Trust Aware Routing Framework, WSN – Wireless Sensor Network

Introduction

Wireless sensor networks (WSNs) mainly supports military applications and forest fire monitoring. A WSN comprises battery-powered sensor nodes with extremely limited processing capabilities. With a narrow radio communication range, a sensor node wirelessly sends Wireless sensor networks (WSNs) . With a narrow radio communication range, a sensor node wirelessly sends messages to a base station via a multi-hop path. However, the multi-hop routing of WSNs often becomes the target of malicious attacks. An attacker may tamper nodes physically, create traffic collision with seemingly valid transmission, drop or misdirect messages in routes, or jam the communication channel by creating radio interference. This paper focuses on the kind of attacks in which adversaries misdirect network traffic by identity deception through replaying routing information. Based on identity deception, the adversary is capable of launching harmful and hard-to-detect attacks against routing such as selective forwarding, wormhole attacks, sinkhole attacks and Sybil attacks.

Design Considerations

Assumptions: We target secure routing for data collection tasks, which are one of the most fundamental functions of WSNs. In a data collection task, a sensor node sends its sampled data to a remote base station with the aid of other intermediate nodes, as shown in Figure 1. Though there could be more than one base station, our routing approach is not affected by the number of base stations; to simplify our discussion, we assume that there is only one base station.

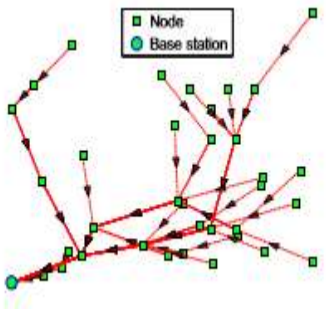

Fig.1.Multi-hop routing for data collection of a WSN

Authentication Requirements:

TARF requires that the packets are properly authenticated, especially the broadcast packets from the base station. The broadcast from the base station is asymmetrically authenticated so as to guarantee that an adversary is not able to manipulate a broadcast message from the base station.TARF uses trustmanager.

Goals : TARF mainly guards a WSN against the attacks misdirecting the multi-hop routing, especially those based on identity theft through replaying the routing information. TARF aims to achieve the following desirable properties:

High Throughput*: Throughput* is defined as the ratio of the number of all data packets delivered to the base station to the number of all sampled data packets.Here,*throughput* at a moment is computed over the period from the beginning time (0) until that particular moment. Note that single-hop re-transmission may happen, and that duplicate packets are considered as one packet as far as *throughput* is concerned. *Through- put* reflects how efficiently the network is collecting and delivering data.T*hroughput should be high*.

Energy Efficiency*:* We evaluate energy efficiency by the average energy cost to successfully deliver a unit-sized data packet from a source node to the base station. Note that link-level re-transmission should be given enough attention when considering energy cost since each re-transmission causes a noticeable increase in energy consumption. If every node in a WSN consumes approximately the same energy to transmit a unit-sized data packet, we can use another metric *hop-per-delivery* to evaluate energy efficiency. Here,the energy consumption depends on the number of hops, i.e. the number of one-hop transmissions occurring. It is abbreviated as *hop-per-delivery*.

Scalability & Adaptability :It should support large magnitude and high dynamic data. We will evaluate the scalability and adaptability of TARF through experiments with large-scale WSNs and under mobile and hash network conditions.

III. DESIGN OF TARF

Before introducing the detailed design, we first introduce several necessary notion here.

Neighbor : For a node *N*, a neighbor (neighboring node) of *N* is a node that is reachable from *N* with one-hop wireless transmission.

Trust level : For a node *N*, the trust level of a neighbor is a decimal number in [0, 1], representing *N*'s opinion of that neighbor's level of trustworthiness. Specifically, the trust level of the neighbor is *N*'s estimation of the probability that this neighbor correctly delivers data received to the base station. That trust level is denoted as *T* in this paper.

Energy cost : For a node *N*, the energy cost of a neighbor is the average energy cost to successfully deliver a unit- sized data packet with this neighbor as its next-hop node, from *N* to the base station. That energy cost is denoted as *E* in this paper.

Overview:

For a TARF-enabled node N to route a data packet to the base station, N only needs to decide to which neighboring node it should forward the data packet considering both the trustworthiness and the energy efficiency. Once the data packet is forwarded to that next-hop node, the remaining task to deliver the data to the base station is fully delegated to it, and N is totally unaware of what routing decision its next-hop node makes. N maintains a neighborhood table with trust level values and energy cost values for certain known neighbors.It is sometimes necessary to delete some neighbors' entries to keep the table size acceptable. The technique of maintaining a neighborhood table of a moderate size is employed by TARF. A broadcast message from the base station is flooded to the whole network.

In TARF, in addition to data packet transmission, there are two types of routing information that need to be exchanged: broadcast messages from the base station about data delivery and energy cost report messages from each node. Neither message needs acknowledgement. A broadcast message from the base station is flooded .The freshness of a broadcast message is checked through its field of source sequence number. The other type of exchanged routing information is the energy cost report message from each node.

For each node *N* in a WSN, to maintain such a neighborhood table with trust level values and energy cost values for certain known neighbors, two components, *EnergyWatcher* and *TrustManager*, run on the node (Figure 2). *EnergyWatcher* is responsible for recording the energy cost for each known neighbor, based on *N* 's observation of one-hop transmission to reach its neighbors and the energy cost report from those neighbors. *TrustManager* is responsible for tracking trust level values of neighbors based on network loop discovery and broadcast messages from the base station about data delivery. Once *N* is able to decide its next-hop neighbor according to its neighborhood table, it sends out its energy report message: it broadcasts to all its neighbors its energy cost to deliver a packet from the node to the base station. The energy cost is computed as in Section 3.3 by *EnergyWatcher*.

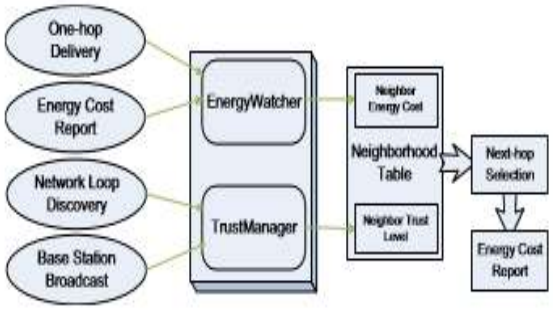

Routing Procedure :

TARF, as with many other routing protocols, runs as a periodic service. The length of that period determines how frequently routing information is exchanged and updated. At the beginning of each period, the base station broadcasts a message about data delivery during last period to the whole network consisting of a few contiguous packets (one packet may not hold all the information). Each such packet has a field to indicate how many packets are remaining to complete the broadcast of the current message. The completion of the base station broadcast triggers the exchange of energy report in this new period. Whenever a node receives such a broadcast message from the base station, it knows that the most recent period has ended and a new period has just started.. During each period, the EnergyWatcher on a node monitors energy consumption of one-hop transmission to its neighbors and processes energy cost reports from those neighbors to maintain energy cost entries in its neighborhood table; its TrustManager also keeps track of network loops and processes broadcast messages from the base station about data delivery to maintain trust level entries in its neighborhood table.

Structure and Exchange of Routing Information :A broadcast message from the base station fits into at most a fixed small number of packets. Such a message consists of some pairs of <node id of a source node, an undelivered sequence interval [a, b] with a significant length>, <node id of a source node, minimal sequence number received in last period, maximum sequence number received in last period>, as well as several node id intervals of those without any delivery record in last period. To reduce overhead to an acceptable amount, our implementation selects only a limited number of such pairs to broadcast (Section 5.1) and proved effective (Section 5.3, 5.4). Roughly, the effectiveness can be explained as follows: the fact that an attacker attracts a great deal of traffic from many nodes often gets revealed by at least several of those nodes being deceived with a high likelihood. The undelivered sequence interval [a, b] is explained as follows: the base station searches the source sequence numbers received in last period, identifies which source sequence numbers for the source node with this id are missing, and chooses certain significant interval [a, b] of missing source sequence numbers as an undelivered sequence interval. For example, the base station may have all the source sequence numbers for the source node 2 as {109, 110, 111, 150, 151} in last period. Then [112, 149] is an undelivered sequence interval; [109, 151] is also recorded as the sequence boundary of delivered packets. Since the base station is usually connected to a powerful platform such as a desktop, a program can be developed on that powerful platform to assist in recording all the source sequence numbers and finding undelivered sequence intervals.

Accordingly, each node in the network stores a table of <node id of a source node, a forwarded sequence interval [a, b] with a significant length> about last period. The data packets with the source node and the sequence numbers falling in this forwarded sequence interval [a, b] have already been forwarded by this node. When the node receives a broadcast message about data delivery, its *TrustManager* will be able to identify which data packets forwarded by this node are not delivered to the base station. Considering the overhead to store such a table, old entries will be deleted once the table is full.Once a fresh broadcast message from the base station is received, a node immediately invalidates all the existing energy cost entries: it is ready to receive a new energy report from its neighbors and choose its new next-hop node afterwards. Also, it is going to select a node either after a timeout is reached or after it has received an energy cost report from some highly trusted candidates with acceptable energy cost. A node immediately broadcasts its energy cost to its neighbors only after it has selected a new next-hop node. That energy cost is computed by its *EnergyWatcher* (see Section 3.3). A natural question is which node starts reporting its energy cost first. For that, note that when the base station is sending a broadcast message, a side effect is that its neighbors receiving that message will also regard this as an energy report: the base station needs 0 amount of energy to reach itself. As long as the original base station is faithful, it will be viewed as a trustworthy candidate by *TrustManager* on the neighbors of the base station. Therefore, those neighbors will be the first nodes to decide their next-hop node, which is the base station; they will start reporting their energy cost once that decision is made.

Route Selection : Now, we introduce how TARF decides routes in a WSN. Each node *N* relies on its neighborhood table to select an optimal route, considering both energy consumption and reliability.For a node *N* to select a route for delivering data to the base station, *N* will select an optimal next-hop node from its neighbors based on trust level and energy cost and forward the data to the chosen next-hop node immediately. The neighbors with trust levels below a certain threshold will be excluded from being

considered as candidates. Among the remaining known neighbors, N will select its next-hop node through evaluating each neighbor b based on a trade-off between TNb and E_{Nb} , with ENb and TNb being b's energy cost and trust level value in the neighborhood table respectively. Basically, E_{Nb} reflects the energy cost of delivering a packet to the base station from N assuming that all the nodes in the route are honest; $1/T_{Nb}$ approximately reflects the number of the needed attempts to send a packet from N to the base station via multiple hops before such an attempt succeeds, considering the trust level of b.

Thus, ENb / TNb combines the trustworthiness and energy cost. However, the metric ENb / TNb suffers from the fact that an adversary may falsely reports extremely low energy cost to attract traffic and thus resulting in a low value of ENb / TNb even with a low TNb. Therefore, TARF prefers nodes with significantly higher trust values;. For deciding the next-hop node, a specific trade-off between TNb and ENb TNb is demonstrated in Figure 5 (see Section 5.2).

EnergyWatcher : Here we describe how a node N's EnergyWatcher computes the energy cost ENb for its neighbor b in N's neighborhood table and how N decides its own energy cost EN. Before going further, we will clarify some notations. ENb mentioned is the average energy cost of successfully delivering a unit-sized data packet from N to the base station, with b as N's next-hop node being responsible for the remaining route. Here, one-hop re-transmission may occur until the acknowledgement is received or the number of re-transmissions reaches a certain threshold. The cost caused by one-hop retransmissions should be included when computing ENb. Suppose N decides that A should be its next-hop node after comparing energy cost and trust level.

Then N's energy cost is EN = ENA. Denote EN→b as the average energy cost of successfully delivering a data packet from N to its neighbor b with one hop. Note that the re- transmission cost needs to be considered. With the above notations, it is straightforward to establish the following relation: ENb = EN→b + Eb

Since each known neighbor b of N is supposed to broadcast its own energy cost Eb to N, to compute ENb, N still needs to know the value EN→b, i.e., the average energy cost of successfully delivering a data packet from N to its neighbor b with one hop. For that, assuming that the endings (being acknowledged or not) of one- hop transmissions from N to b are independent with the same probability Psucc of being acknowledged, we first compute the average number of one-hop sendings needed before the acknowledgement is received as follows:

$$\infty \text{ X } i=1 \ \text{Psucc} \cdot (1 - \text{Psucc}) i=1 \ =1 \ / \text{Psucc}$$

Denote Eunit as the energy cost for node N to send a unit-sized data packet once regardless of whether it is received or not. Then we have ENb =Eunit/ Psucc+ Eb

The remaining job for computing ENb is to get the probability Psucc that a one-hop transmission is acknowledged. Considering the variable wireless connection among wireless sensor nodes, we do not use the simplistic averaging method to compute Psucc. Instead, after each transmission from N to b, N's EnergyWatcher will update Psucc based on whether that transmission is acknowledged or not with a weighted averaging technique. We use a binary variable Ack to record the result of current transmission: 1 if an acknowledgement is received; otherwise, 0. Given Ack and the last probability value of an acknowledged transmission P old succ, an intuitive way is to use a simply weighted average of Ack and P oldsucc as the value of Pnew succ. That is what is essentially adopted in the aging mechanism.However, that method used against sleeper attacks still suffers periodic attacks. To solve this problem, we update the Psucc value using two different weights as in our previous work , a relatively big Wdegrade $\in$ (0,1) and a relatively small Wupgrade $\in$ (0,1) as follows:

$$\text{pnew succ} = (1 - \text{Wdegrade}) \times \quad \text{Pold succ} + \text{Wdegrade} \times \text{Ack, if Ack} = 0.$$

$$(1 - \text{Wupgrade}) \times \ \text{Pold succ} + \text{Wupgrade} \times \text{Ack, if Ack} = 1 \ .$$

The two parameters Wdegrade and Wupgrade allow flexible application requirements. Wdegrade and Wupgrade represent the extent to which upgraded and degraded performance are rewarded and penalized, respectively. If any fault and compromise is very likely to be associated with a high risk, Wdegrade should be assigned a relatively high value to penalize fault and compromise relatively heavily; if a few positive transactions can't constitute evidence of good connectivity which requires many more positive transactions, then Wupgrade should be assigned a relatively low value.

TrustManager : A node N's TrustManager decides the trust level of each neighbor based on the following events: discovery of network loops, and broadcast from the base station about data delivery. For each neighbor b of N, TNb denotes the trust level of b in N's neighborhood table. At the beginning, each neighbor is given a neutral trust level 0.5. After any of those events occurs, the relevant neighbors' trust levels are updated. Note that many existing routing protocols have their own mechanisms to detect routing loops and to react accordingly. In that case, when integrating TARF into those protocols with anti-loop mechanisms, TrustManager may solely depend on the broadcast from the base station to decide the trust level; we adopted such a policy when implementing TARF later (see Section 5). If anti-loop mechanisms are both enforced in the TARF component and the routing protocol that integrates TARF, then the resulting hybrid protocol may overly react towards the discovery of loops. Though sophisticated loop-discovery methods exist in the currently developed protocols, they often rely on the comparison of specific routing cost to reject routes likely leading to loops [32]. To minimize the effort to integrate TARF and the existing protocol and to reduce the overhead, when an existing routing protocol does not provide any anti- loop mechanism, we adopt the following mechanism to detect routing loops. To detect loops, the TrustManager on N reuses the table of <node id of a source node, a forwarded sequence interval [a, b] with a significant length> (see Section 3.2) in last period. If N finds that a received data packet is already in that record table, not only will the packet be discarded, but the TrustManager on N also degrades its next-hop node's trust level. If that next-hop node is b, then Told Nb is the latest trust level value of b. We use a binary variable Loop to record the result of loop discovery: 0 if a loop is received; 1 otherwise. As in the update of energy cost, the new trust level of b is

Tnew Nb =(1 − Wdegrade) × Told Nb + Wdegrade × Loop, if Loop = 0.

= (1 − Wupgrade) × Told Nb + Wupgrade × Loop, if Loop = 1.

Once a loop has been detected by N for a few times so that the trust level of the next-hop node is too low, N will change its next-hop selection; thus, that loop is broken. Though N can not tell which node should be held responsible for the occurrence of a loop, degrading its next-hop node's trust level gradually leads to the breaking of the loop.

On the other hand, to detect the traffic misdirection by nodes exploiting the replay of routing information, TrustManager on compares N's stored table of <node id of a source node, forwarded sequence interval [a, b] with a significant length> recorded in last period with the broadcast messages from the base station about data delivery. It computes the ratio of the number of successfully delivered packets which are forwarded by this node to the number of those forwarded data packets, denoted as DeliveryRatio. Then N's TrustManager updates its next-hop node b's trust level as follows:

Tnew Nb =

(1 − Wdegrade) × Told Nb +Wdegrade × DeliveryRatio, if DeliveryRatio < Told Nb.

(1 − Wupgrade) × Told Nb +Wupgrade × DeliveryRatio, if DeliveryRatio >= Told Nb.

Analysis on EnergyWatcher and TrustManager : Now that a node N relies on its EnergyWatcher and TrustManager to select an optimal neighbor as its next- hop node, we would like to clarify a few important points on the design of EnergyWatcher and TrustManager. First, as described in Section 3.1, the energy cost report is the only information that a node is to passively receive and take as "fact". It appears that such acceptance of energy cost report could be a pitfall when an attacker or a compromised node forges false report of its energy cost. Note that the main interest of an attacker is to prevent data delivery rather than to trick a data packet into a less efficient route, considering the effort it takes to launch an attack. As far as an attack aiming at preventing data delivery is concerned, TARF well mitigates the effect of this pitfall through the operation of TrustManager. Note that the TrustManager on one node does not take any recommendation from the TrustManager on another node. If an attacker forges false energy report to form a false route, such intention will be defeated by TrustManager: when the TrustManager on one node finds out the many delivery failures from the broadcast messages of the base station, it degrades the trust level of its current next-hop node; when that trust level goes below certain threshold, it causes the node to switch to a more promising next- hop node.. First of all, it is often difficult to identify an attacker who participates in the network using an id "stolen" from another legal node. For example, it is extremely difficult to detect a few attackers colluding to launch a combined wormhole and sinkhole attack . Additionally, despite the certain inevitable unfairness involved, TrustManager encourages a node to choose another route when its current route frequently fails to deliver data to the base station. Though only those legal neighboring nodes of an attacker might have correctly identified the adversary, our evaluation results indicate that the strategy of

switching to a new route without identifying the attacker actually significantly improves the network performance, even with the existence of wormhole and sinkhole attacks. Fig 3 gives an example to illustrate this point. In this example, node A, B, C and D are all honest nodes and not compromised. Node A has node B as its current next-hop node while node B has an attacker node as its next-hop node. The attacker drops every packet received and thus any data packet passing node A will not arrive at the base station. After a while, node A discovers that the data packets it forwarded did not get delivered. The TrustManager on node A starts to degrade the trust level of its current next-hop node B although node B is absolutely honest. Once that trust level becomes too low, node A decides to select node C as its new next-hop node. In this way node A identifies a better and successful route (A - C - D - base). In spite of the sacrifice of node B's trust level, the network performs better.

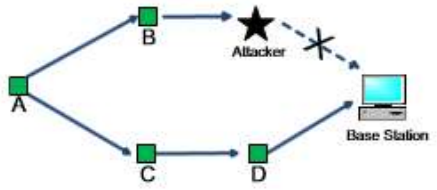

Fig. 3. An example to illustrate how *TrustManager* works.

Fig.3. An example to illustrate how TrustManager works.

Finally, we would like to stress that TARF is designed to guard a WSN against the attacks misdirecting the multi-hop routing, especially those based on identity theft through replaying the routing information.

IV. Simulation

In our experiments, initially, 35 nodes are randomly distributed within a 300*300 rectangular area, with unreliable wireless transmission. All the nodes have the same power level and the same maximal transmission range of 100m. Each node samples 6 times in every period; the timing gap between every two consecutive samplings of the same node is equivalent. We simulate the sensor network in 1440 consecutive periods. Regarding the network topology, we set up three types of network topologies. The first type is the static-location case under which all nodes stand still. The second type is a customized group-motion-with-noise case based on Reference Point Group Mobility (RPGM) model that mimics the behavior of a set of nodes moving in one or more groups . The last type of dynamic network incorporated in the experiments is the addition of scattered RF-shielded areas to the afore mentioned group-motion-with-noise case.

The performance of TARF is compared to that of a link connectivity-based routing protocol. With the Link-connectivity protocol, each node selects its next-hop node among its neighborhood table according to an link estimator based on exponentially weighted moving average (EWMA). The simulation results show, in the presence of misbehaviors, the throughput in TARF is often much higher than that in Link-connectivity; the hop-per- delivery in the Link-connectivity protocol is generally at least comparable to that in TARF.Both protocols are evaluated under three common types of attacks: (1) a certain node forges the identity of the based station by replaying broadcast messages, also known as the sinkhole attack; (2) a set of nodes colludes to form a forwarding loop; and (3) a set of nodes drops received data packets. Generally, under these common attacks, TARF produces a substantial improvement over Link-connectivity in terms of data collection and energy efficiency. Further, we have evaluated TARF under more severe attacks: multiple moving fake bases and multiple Sybil attackers. TARF succeeds in achieving a steady improvement over the Link-connectivity protocol.

Incorporation of TARF into Existing Protocols : To demonstrate how this TARF implementation can be integrated into the existing protocols with the least effort, we incorporated TARF into a collection tree routing protocol (CTP). The CTP protocol is efficient, robust, and reliable in a network with highly dynamic link topology. It quantifies link quality estimation in order to choose a next-hop node. The software platform is TinyOS 2.x.

To perform the integration, after proper interface wiring, invoke the TrustControl.start command to enable the trust evaluation; call the Record.addForwarded command for a non-root node to add forwarded record once a data packet has been forwarded; call the Record.addDelivered command for a root to add delivered record once a data packet has been received by the root. Finally, inside the

CTP's task to update the routing path, call the Record.getTrust command to retrieve the trust level of each next-hop candidate; an algorithm taking trust into routing consideration is executed to decide the new next-hop neighbor.(See Figure 5).

Similar to the original CTP's implementation, the implementation of this new protocol decides the next-hop neighbor for a node with two steps (see Figure 5): Step 1 traverses the neighborhood table for an optimal candidate for the next hop; Step 2 decides whether to switch from the current next-hop node to the optimal candidate found. For Step 1, as in the CTP implementation, a node would not consider those links congested, likely to cause a loop, or having a poor quality lower than a certain threshold. This new implementation prefers those candidates with higher trust levels; in certain circumstances, regardless of the link quality, the rules deems a neighbor with a much higher trust level to be a better candidate (see Figure 5). The preference of highly trustable candidates is based on the following consideration: on the one hand, it creates the least chance for an adversary to misguide other nodes into a wrong routing path by forging the identity of an attractive node such as a root; on the other hand, forwarding data packets to a candidate with a low trust level would result in many unsuccessful link-level transmission attempts, thus leading to much re-transmission and a potential waste of energy. When the network throughput becomes low and a node has a list of low-trust neighbors, the node will exclusively use the trust as the criterion to evaluate those neighbors for routing decisions. As show in Figure 5, it uses trust/cost as a criteria only when the candidate has a trust level above certain threshold. The reason is, the sole trust/cost criteria could be exploited by an adversary replaying the routing information from a base station and thus pretending to be an extremely attractive node. As for Step 2, compared to the CTP implementation, we add two more circumstances when a node decides to switch to the optimal candidate found at Step 1: that candidate has a higher trust level, or the current next-hop neighbor has a too low trust level.

Empirical Evaluation on Model

We evaluated the performance of TARF against a combined sinkhole and wormhole attack on Motelab at Harvard University. 184 TMote Sky sensor motes were deployed across many rooms at three floors in the department building (see Figure 6), with two to four motes in most rooms. Around 97 nodes functioned properly while the rest were either removed or disabled. Each mote has a 2.4GHz Chipcon CC2420 radio with an indoor range of approximately 100 meters. In Figure 6, the thin green lines indicate the direct (one-hop) wireless connection between motes. Certain wireless connection also exists between nodes from different floors.We developed a simple data collection application in TinyOS 2.x that sends a data packet every five seconds to a base station node (root) via multi-hop. This application was executed on 91 functioning non-root nodes on Mote- lab. For comparison, we used CTP and the TARF-enabled CTP implementation as the routing protocols for the data collection program separately. The TARF-enabled CTP has a TARF period of 30 seconds. We conducted an attack with five fake base stations that formed a wormhole. As in Figure 6, whenever the base station sent out any packet, three fake base stations which overheard that packet replayed the complete packet without changing any content including the node id. Other fake base stations overhearing that replayed packet would also replay the same packet. Each fake base station essentially launched a sinkhole attack. Note that there is a distinction between such malicious replay and the forwarding when a well-behaved node receives a broadcast from the base station. When a well-behaved node forwards a broadcast packet from the base station, it will include its own id in the packet so that its receivers will not recognize the forwarder as a base station. We conducted the first experiment by uploading the program with the CTP protocol onto 91 motes (not including those 5 selected motes as fake bases in later experiments), and no attack was involved here

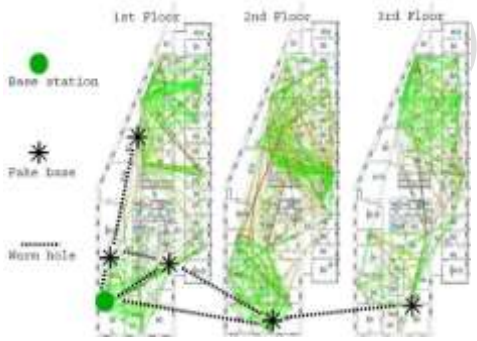

Fig. 6. Connectivity map of Motelab

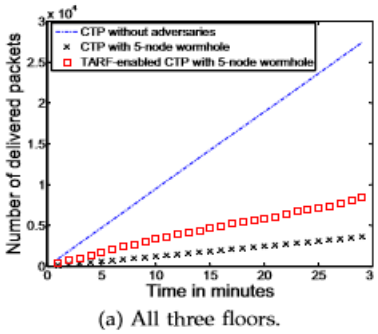

(a) All three floors.

Fig.7 . Empirical comparison of CTP and TARF- enabled CTP on Motelab

Then, in another experiment, in addition to programming those 91 motes with CTP, we also programmed the five fake base stations so that they stole the id the base station through replaying. In the last experiment, we programmed those 91 motes with the TARF-enabled CTP, and programmed the five fake base stations as in the second experiment.

Each of our programs run for 30 minutes. As illustrated in Figure 7(a), the existence of the five wormhole attackers greatly degraded the performance of CTP: the number of the delivered data packets in the case of CTP with the five-node wormhole is no more than 14% that in the case of CTP without adversaries. The TARF-enabled CTP succeeded in bringing an immense improvement over CTP in the presence of the five-node wormhole, almost doubling the throughput. That improvement did not show any sign of slowing down as time elapsed. The number of nodes from each floor that delivered at least one data packet in each six-minute sub-period is plotted in Figure 7. On each floor, without any adversary, at least 24 CTP nodes were able to find a successful route in each six minute. However, with the five fake base stations in the wormhole, the number of CTP nodes that could find a successful route goes down to 9 for the first floor; it decreases to no more than 4 for the second floor; as the worst impact, none of the nodes on the third floor ever found a successful route. A further look at the data showed that all the nine nodes from the first floor with successful delivery record were all close to the real base station. The CTP nodes relatively far away from the base station, such as those on the second and the third floor, had little luck in making good routing decisions. When TARF was enabled on each node, most nodes made correct routing decisions circumventing the attackers. That improvement can be verified by the fact that the number of the TARF- enabled nodes with successful delivery record under the threat of the wormhole is close to that of CTP nodes with no attackers, as shown in Figure 7.

Acknowledgment

I would like to thank Prof. B.B. Gite , Prof Santosh Shelke for helping me out in selecting the topic and contents, giving valuable suggestions in preparation of project report and presentation am grateful to Prof. B. B. Gite, Head of Computer Department, for providing healthy environment and facilities in the department. He allowed us to raise our concern and worked to solve it by extending his co-operation time to time. Goal makes us to do work. Vision is more important than goal which makes us to do work in the best way to make work equally the best. Thanks to Principal, Dr. V. M. Vadhai for his support and vision. Consistent achievement requires boost on consistent interval basis. Management has given full support and boosted us to be consistent and achieve the target. Thanks to management for their support. Thanks to all the colleagues for their extended support and valuable guidance would like to be grateful to all my friends for their consistent support, help and guidance. Last but not least my friend none other than my husband who helped, mentored me to make it better and better. My dear family supported me very well by taking care of all my responsibilities. I am grateful for it and would like to give sincere thanks to my family for all.

CONCLUSION

We have designed and implemented TARF, a robust trust-aware routing framework for WSNs, to secure multi-hop routing in dynamic WSNs against harmful attackers exploiting the replay of routing information. TARF focuses on trustworthiness and energy efficiency, which are vital to the survival of a WSN in a hostile environment. With the idea of trust management, TARF enables a node to keep track of the trustworthiness of its neighbors and thus to select a reliable route. Our main contributions are listed as follows. (1) Unlike previous efforts at secure routing for WSNs, TARF effectively protects WSNs from severe attacks through replaying routing information; it requires neither tight time synchronization nor known geographic information. (2) The resilience and scalability of TARF is proved through both extensive simulation and empirical evaluation with large-scale WSNs; the evaluation involves both static and mobile settings, hostile network conditions, as well as strong attacks such as *wormhole* attacks and *Sybil* attacks.
(3) We have implemented a ready-to-use TinyOS module of TARF with low overhead; as demonstrated in the paper, this TARF module can be integrated into existing routing protocols with the least effort, thus producing secure and efficient fully-functional protocols.

REFERENCES:

[1] G. Zhan, W. Shi, and J. Deng, "Tarf: A trust-aware routing framework for wireless sensor networks," in Proceeding of the 7th European Conference on Wireless Sensor Networks (EWSN'10), 2010.
[2] F. Zhao and L. Guibas, Wireless Sensor Networks: An Information Processing Approach. Morgan Kaufmann Publishers, 2004.
[3] A. Wood and J. Stankovic, "Denial of service in sensor networks,"
Computer, vol. 35, no. 10, pp. 54–62, Oct 2002.

[4] C. Karlof and D. Wagner, "Secure routing in wireless sensor networks: attacks and countermeasures," in Proceedings of the 1st IEEE International Workshop on Sensor Network Protocols and Applications, 2003.
[5] M. Jain and H. Kandwal, "A survey on complex wormhole attack in wireless ad hoc networks," in Proceedings of International Con- ference on Advances in Computing, Control, and Telecommunication Technologies (ACT '09), 28-29 2009, pp. 555 –558.
[6] I. Krontiris, T. Giannetsos, and T. Dimitriou, "Launching a sink- hole attack in wireless sensor networks; the intruder side," in Proceedings of IEEE International Conference on Wireless and Mobile Computing, Networking and Communications(WIMOB '08), 12-14
2008, pp. 526 –531.
[7] J. Newsome, E. Shi, D. Song, and A. Perrig, "The sybil attack in sensor networks: Analysis and defenses," in Proc. of the 3rd International Conference on Information Processing in Sensor Networks (IPSN'04), Apr. 2004.
[8] L. Bai, F. Ferrese, K. Ploskina, and S. Biswas, "Performance analy- sis of mobile agent-based wireless sensor network," in Proceedings of the 8th International Conference on Reliability, Maintainability and Safety (ICRMS 2009), 20-24 2009, pp. 16 –19.

International Journal of Engineering Research and General Science Volume 3, Issue 6, November-December, 2015
ISSN 2091-2730

Secure data sharing using attribute-based broadcast encryption in cloud computing

Mrs. Komal Jagdale[1], Prof. Asha Pawar[2]

[1]PG Scholar, Department of Computer Engineering, ZCOER, Pune, Maharashtra

[2]Assistant Professor, Department of Computer Engineering, ZCOER, Pune, Maharashtra

Abstract— Data owner outsource the data due to cost reduction and poor management to the cloud which provide data as a service. Data owner then lose control over the data, because cloud service provider becomes a third party provider. Traditionally, data owner encrypt the data and export it to the cloud seems a good approach. But it has some drawbacks like decryption computation overhead, revocation of user and privacy preserving. A secure and flexible attribute-based broadcast encryption (EP-ABBE), which reduce the decryption computation overhead by partial decryption, and protect user privacy. Based on EP-ABBE, efficient and privacy preserving data sharing scheme in cloud computing was presented, where data owner can flexibly encrypt the data using access policy and implicit user index set. User revocation can be achieved by dropping revoked user's index from the user index set, with very low computation cost and the privacy of user can be protected.

Keywords— Cloud service provider, Encryption, Decryption, Broadcast encryption, Ciphertext, Revoke user, Attribute key.

INTRODUCTION

Cloud computing is most emerging paradigms in the field of information technology. Cloud computing has benefits ,such as scalability, reduced costs, flexibility, increased operational efficiencies, hence people inclined to outsource their personal data to the cloud. Cloud service provider is semi-trusted which arise concerns of security and privacy. Before outsourcing data to semi trusted cloud for data security, it will be encrypted. Data owner may face problem in using public key encryption and identity based encryption. Encrypted cipher text using public key or identity can be decrypted by private key of corresponding user.

In broadcast encryption (BE) broadcaster choose a subset of privileged users to send a cipher text from all recipients dynamically. But it is hard to support flexible, fine-grained access control policies. Attribute based encryption (ABE) make possible to achieve fine grain access control over encrypted data using access policies and credited attributes among the secret keys. Cipher text policy attribute based encryption (CP-ABE) which is theoretically similar to the role-based access control models, which makes possible to data owner to modify access policy number of attributes that the user possesses in order to decrypt the cipher text. But it has some drawbacks like user revocation.

Attribute based broadcast encryption (ABBE) address the problem of user revocation. It encrypts the broadcast data using expressive access policy with or without specifying the receiver. Data decryption scheme is time consuming since it required large number of pairing operations.

In EP-ABBE, it reduces decryption computation of user and protects user privacy. The data owner can enjoy the flexibly of encrypting personal data using a specified access policy and a user index set which is a list of selected users' indexes. Thus, only the users whose index are in index set and attributes satisfy the access policy can access the personal data. In EP-ABBE scheme achieves efficient user revocation by dropping user index from the user index set of cipher text. The data owner does not need to update the secret key of non-revoked user, which has very low computation cost and is more efficient compared with current attribute-based data sharing schemes.

RELATED WORK

ABE is used in data sharing schemes for fine grain access control. Liang et al. used Attribute Based Encryption to protect data security in mobile social networks [1]. In specific time slot it enables a trusted authority to revoke a specific user's data decryption capability. But drawback of this scheme, revoked user is able to access the encrypted data even if it does not hold the attribute any more until the next expiration time. Li et al. proposed a secure sharing of personal health record in cloud computing based on ABE [2]. Immediate revocation is achieved in which multi-authority work together to re-encrypt cipher texts and update unrevoked users' attribute secrete keys. This scheme requires extra communication cost and it is inefficient. Hur et al. proposed a data outsourcing scheme using CP-ABE in which immediate user revocation is achieved in attribute level [3]. But on the downside there is amount of data redundancy because cipher texts must be re-encrypted many times for different attribute groups. ABBE was proposed by David et al. [4]. In this scheme broadcasters can encrypt data with access policy and receiver those who present in receivers list and satisfy the access policy that can decrypt cipher text. Asim et al. proposed a reversed ABBE scheme [5], in which the broadcaster encrypts the data according to the access policy and the list of the identities of revoked users rather than the authorized users' identities. Only the users with the attributes that satisfy the access policy and their identities are not in the list of revoked users would be able to decrypt the cipher text.

SYSTEM MODEL

The system model of data sharing scheme based EP-ABBE consists of the following entities, as shown in Fig. 1.

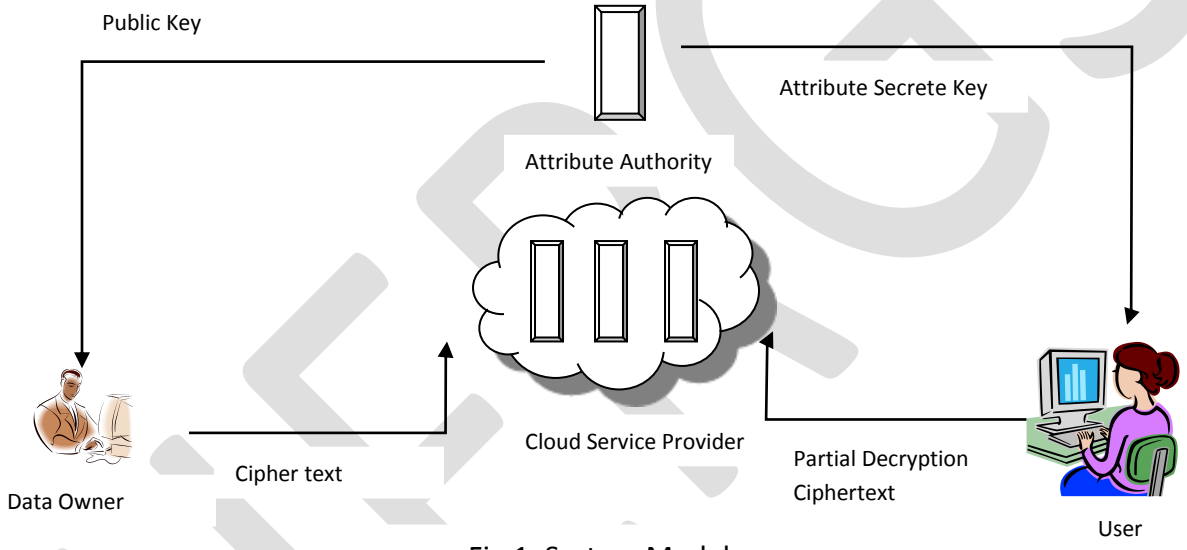

Fig.1. System Model

1. **Attribute authority**: Attribute authority is trusted attribute centre, which is responsible for assigning attributes to user and generating user's attribute secret key which corresponds to the user's attributes.
2. **Cloud service provider**: Cloud service provider is the semi-trusted entity .This entity provides data outsourcing service. Data owner outsource the encrypted data to cloud through cloud service provider. The CSP is also responsible for partially decrypting the cipher text for the users.
3. **Data owner**: It is an entity who needs to outsource data to cloud storage provided by CSP, for the purpose of using low-cost and energy-efficient storage resources. The data owner encrypts the data with the specified obfuscated access policy and a user index set before outsourcing.
4. **User**: User is an entity who wants to access the data. After receiving attribute secret key from attribute authority, user generates attribute key to delegate decryption computation to CSP. If a user possesses a set of attributes satisfying the access policy and his index is in the user index set, he can recover data from partial decrypted cipher text.

WORKING MODEL

Working model of data sharing scheme is describe as follows:

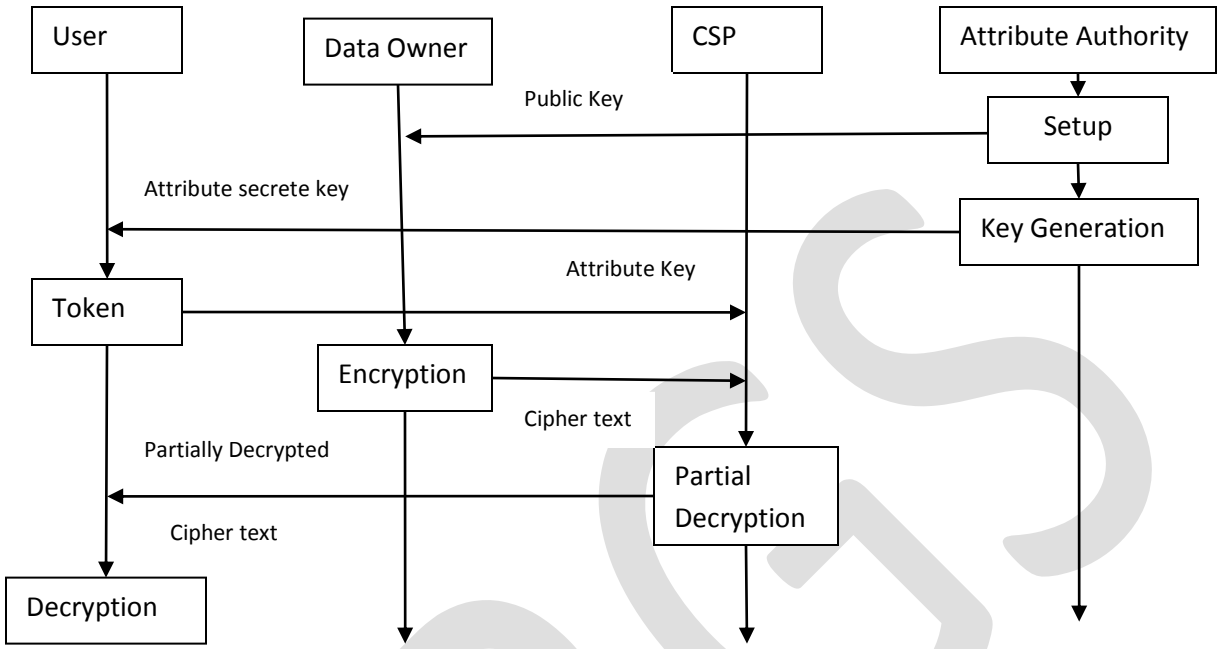

Fig.2. Working Model

SYSTEM SETUP

The attribute authority runs setup algorithm to select a bilinear group G_1 of prime order q and generator g, and the bilinear map e :G_1 X $G_1 \rightarrow G_2$. Then the attribute authority chooses random, $\alpha, \beta \in Z_q$, and defines the hash function H :$\{0,1\}^* \rightarrow G_1$:$G_1 \rightarrow G_2$. Let N = {1, 2,...,n} denotes the set of all user indexes [6]. The system public key K_P is published as: $K_p = \{g^{\alpha}, ..., g^{\alpha n}\}, g^{\beta}$ The master secret key K_M is kept secret by attribute authority and is constructed as: $K_M = (\alpha, \beta)$

KEY GENERATION

The attribute authority runs key generation algorithm to choose a random $\gamma \in Z_q$ for a user with the user index d $\in$ N, and chooses random $\gamma_j \in Z_q$ for each $a_j \in S$ where S denotes the attribute set of user. Then the attribute secret key K_{AS} is computed as:
$K_{AS} = (D= g^{\alpha\beta+\gamma}, \{D_j = g^{\gamma} H(j)^{\gamma j}, D'_j = g^{\gamma j}, D''_j = H(j)_{\beta}\}_{j \in S})$

The attribute authority delivers the attribute secret key K_{AS} to the user in a secure manner. The user runs token generation algorithm to choose a random $t \in Z_q$, and generates the attribute key K_A as: $K_A = (\{\check{D}_j = (Dj)1^{/t}\}, \check{D}'_j = (D'^{1/t}_j, D''_j)_{j \in S})$

Then, the user sends K_A to CSP, and keeps the D secretly.

TOKEN GENERATION

The user takes his K_{AS} as input, and outputs the attribute key K_A which is sent to CSP.

ENCRYPTION

The data owner takes K_P, user index set U which is the set of selected users' indexes, the access policy T and plaintext M as input, and outputs the cipher text C_T which contains the obfuscated T. Thus only the user whose index is in the index set U and attributes satisfy the access policy that can access the data.

PARTIAL DECRYPTION

The C_{SP} takes as input a cipher text C_T, the user's attribute key K_A and user index d. It outputs a partially decrypted cipher text CTP. The C_{SP} first generates the user's obfuscated attribute set S′ with K_A, then C_{SP} computes C_{TP} with K_A if the S′ satisfies the obfuscated T of the cipher text C_T and d is in the user index set U.

DECRYPTION.

The user takes as input a partially decrypted cipher text C_{TP} and the attribute secret key K_{AS}, outputs the message M.

USER REVOCATION

The data owner can revoke the user from the user index set U. Upon receiving the revoked user index R from data owner, the CSP first generates C'_0 . Then the CSP replaces C_0 in the cipher text with C'_0 , and generates the re-encrypted cipher text C'_T . CSP cannot generate I for the revoked user in user index R. Thus, the revoked user cannot decrypt the re-encrypted cipher text.

CONCLUSION

Modified structure of attribute based broadcast encryption which is named as EP-ABBE is explained. EP-ABBE reduces the decryption computation overhead of user and protects user privacy by obfuscating access policy of ciphertext and user's attributes. A flexible and secure data sharing scheme in cloud computing was presented using EP-ABBE based scheme. Using this scheme data owner can encrypt data with a specified access policy and the user index set. Also using this scheme efficient user revocation is performed by dropping user's index from the user index set of the encrypted data. This scheme can protect user privacy as well.

REFERENCES:

[1] Liang X, Li X, Lu R, et al. An efficient and secure user revocation scheme in mobile social networks. Proceedings of the IEEE Global Communications Conference (GLOBECOM'11), Dec 5−9, 2011, Houston, TX, USA. Piscataway, NJ, USA: IEEE, 2011: 5p
[2] Li M, Yu S, Zheng Y. Scalable and secure sharing of personal health records in cloud computing using attribute-based encryption. IEEE Transactions on Parallel and Distributed Systems, 2013, 24(1): 131−143
[3] Hur J, Noh D K. Attribute-based access control with efficient revocation in data outsourcing systems. IEEE Transactions on Parallel and Distributed Systems, 2011, 22(7): 1214−1221
[4] Lubicz D, Sirvent T. Attribute-based broadcast encryption scheme made efficient. Advances in Cryptology: Proceedings of the 1st International Conference on Cryptology in Africa (AFRICACRYPT'08), Jun 11−14, 2008
[5] Junod P, Karlov A. An efficient public-key attribute-based broadcast encryption scheme allowing arbitrary access policies. Proceedings of the 17th ACM Conference on Computer and Communications Security (CCCS'10), Oct 4−8, 2010, Chicago, IL, USA. New York, NY, USA: ACM, 2010: 13−24
[6] Asim M, Ibraimi L, Petkovic M. Ciphertext-policy attribute-based broadcast encryption scheme. Communications and Multimedia Security: Proceedings of the 12th IFIP TC 6/TC 11 International Conference on Communications and Multimedia Security (CMS'11), Oct 19−21, 2011, Ghent, Belgium. LNCS 7025. Berlin, Germany: Springer-Verlag, 2011: 244−246
[7] Hur J. Improving security and efficiency in attribute-based data sharing. IEEE Transactions on Knowledge and Data Engineering, 2013, 25(10): 2271−2282
[8] Cecile D. Identity-based broadcast encryption with constant size ciphertexts and private keys. Advances in Cryptology:Proceedings of the 13th International Conference on the Theory and Application of Cryptology and Information Security(ASIACRYPT'07), Dec 2−6, 2007, Kuching, Malaysia.LNCS 4833.Berlin,Germany: Springer-Verlag, 2007: 193−215
[9] Zhou Z, Huang D. On efficient ciphertext-policy attribute based encryption and broadcast encryption.Proceedings of the 17th ACM Conference on Computer and Communications Security(CCCS'10), Oct 4−8, 2010, Chicago, IL, USA. New York, NY,USA:ACM, 2010: 753−755
[10] Goyal V, Pandey O, Sahai A, et al. Attribute-based encryption for fine-grained access control of encrypted data. Proceedings of the 13th ACM Conference on Computer and Communications Security (CCCS'06), Oct 30−Nov 3, Alexandria, VA, USA. New York, NY, USA: ACM, 2006: 89−98
[11] Hur J, Koo D, Hwang S O, et al. Removing escrow from ciphertext policy attribute-based encryption. Computers and Mathematics with Applications, 2013, 65(9): 1310−1317
[12] Liang X, Li X, Lu R, et al. An efficient and secure user revocation scheme in mobile social networks. Proceedings of the IEEE Global Communications Conference (GLOBECOM'11), Dec 5−9, 2011, Houston, TX, USA. Piscataway, NJ, USA: IEEE, 2011: 5p
[13] Li M, Yu S, Zheng Y. Scalable and secure sharing of personal health records in cloud computing using attribute-based encryption. IEEE Transactions on Parallel and Distributed Systems, 2013, 24(1): 131−143

International Journal of Engineering Research and General Science Volume 3, Issue 6, November-December, 2015
ISSN 2091-2730

Quality Improvement in Design Process of Shell & Tube Type Heat Exchanger by Computer Integrated 3D Modeling

Prof. V. N. Mane[1]

1] Assistant Professor**,** Department of Mechanical Engineering, T.K.I.E.T. Warananagar, Tal – Panhala, Dist – Kolhapur, India, Pin - 416113, Email – vnmmech@tkietwarana.org, Mobile No. 9823986596

Abstract: Heat exchanger design is task of imagination, knowledge, experience and judgment to define an end product. It involves tough design calculations which are combined with manufacturing activities that can be completed in a short period of time. The heat exchanger design calculations require assumed data. Iterative procedure is used to correct the assumed data to get optimum solution. But it needs lot of calculation work which is time consuming. Again the drafting of heat exchanger is time consuming and complicated task and requires skilled person. So there is large scope to improve the features of present softwares. Design and development of new software of shell and tube type heat exchanger gives design, graphical representation and 3D modeling of shell and tube type heat exchanger. The validity of the software is checked by comparison between the software results and 'Alfa Laval' results. 'Alfa Laval' is well established industry in design of shell and tube type heat exchanger. The results obtained from our developed software were found accurate with 'HTRI' software results of Alfa Laval industry. The 3D modeling feature of software makes it different from the existing commercial software. It is expected that the software will be playing significant role in the heat exchanger industries to meet their requirements.

Keywords- Shell and Tube Type Heat Exchanger; Design Software; Visual Basic; CATIA; Computer Integrated Design; 3D Modeling.

1) Introduction:

A heat exchanger is a piece of equipment built for efficient heat transfer from one medium to another. The media may be separated by a solid wall, so that they never mix, or they may be in direct contact. The basic concept of a heat exchanger is based on the premise that the loss of heat on the high temperature side is exactly the same as the heat gained in the low temperature side after the heat and mass flows through the heat exchanger. For efficiency, heat exchangers are designed to maximize the surface area of the wall between the two fluids, while minimizing resistance to fluid flow through the exchanger. The exchanger's performance can also be affected by the addition of fins or corrugations in one or both directions, which increase surface area and may channel fluid flow or induce turbulence. Various quantitative design aspects, their interaction and interdependence are important to arrive at an optimum heat exchanger design. Most of these considerations are dependent on each other and should be considered simultaneously to arrive iteratively at the optimum exchanger design.

The computer software will play important role to eliminate the problem of iterative calculations and 3D modeling of heat exchangers. Presently in heat exchanger industries, design is done by using softwares. These softwares gives dimension of the parts but do not give results in terms of graphs and drawings. Graphical results are important for checking the performance of the heat exchanger and to find out optimum solution. Our developed software also gives design results and 3D model within very short time. This new design tool will allow engineers to make design changes and determine their effect on thermal performance of heat exchanger.

2) Shell and Tube Type Heat Exchanger:

A variety of heat exchangers are used in industry and in their products. Heat exchangers are classified according to transfer processes, number of fluids, and degree of surface compactness, construction features, flow arrangements, and heat transfer mechanisms. The most commonly used heat exchanger is the shell and tube type. It has many applications in the power generation, chemical, and process industries. Though the application of other types of heat exchangers is increasing, the shell and tube heat exchanger will continue its popularity for a long time, largely because of its versatility. This type of heat exchangers are generally built of a bundle of round tubes mounted in a cylindrical shell with the tube axis parallel to that of the shell. One fluid flows inside the tubes, the other flows across and along the tubes. The major components of this exchanger are tubes (or tube bundle), shell, front-end head, rear-end head, baffles, and tube sheets. A variety of different internal constructions are used in shell-and-tube exchangers, depending on the desired heat transfer and pressure drop performance and the methods employed to reduce thermal stresses, to prevent leakages, to provide for ease of cleaning, to contain operating pressures and temperatures, to control corrosion, to accommodate highly asymmetric flows, and so on.

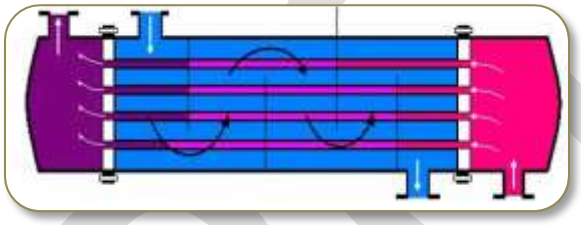

Figure 1: Shell and Tube Type Heat Exchanger

Shell and tube heat exchangers are used extensively throughout the process industry and as such a basic understanding of their design, construction and performance is important to the practicing engineer. Thermal design of shell-and-tube heat exchangers is done by sophisticated computer software. However, a good understanding of the underlying principles of exchanger design is needed to use this software effectively. The optimum thermal design of a shell and tube heat exchanger involves the consideration of many interacting design parameters.

3) Heat Exchanger Design:

Effectiveness of shell and tube type heat exchangers mainly depends on overall heat transfer coefficient which is function of fluid properties, velocity of flow, surface area, Reynolds number etc. The design of heat exchanger includes calculations to determine heat transfer area, shell length, shell diameter, Number of tubes, Diameter of tube, Length of tubes, tube bundle diameter, Number of baffles, baffle spacing, Material of tubes etc. In addition to these, convective heat transfer coefficient for the tube side (hi) and shell side (hs) are required to determine the overall heat transfer coefficient (Uo). Uo requires the huge calculations, but it is essential parameter to decide the thermal performance.

This provides challenging design analysis which is combined with a simple form of construction that can be built in a short space of time. The complicated heat exchanger design and thermodynamics performance calculations are tedious task. There is large scope to improve the features of present software. The remedial causes encourages designing and developing new software of shell and tube type heat exchangers which gives design as well as 3D modeling. It is done by interfacing design software and suitable 3D modeling software. This methodology is the most excellent way to show output results along with 3D modeling of shell and tube type heat exchanger. Hence it is useful design tool for heat exchanger industries.

Our software is developed by using Visual Basic (6.0) language. For executing design of Shell and Tube type Heat Exchanger, code is developed. By utilizing this code different input parameters such as type of flow, material used, diameter of tube, inlet and outlet temperature of tube side and shell side fluid etc. are given and output parameters such as Reynolds no., overall heat transfer coefficient, shell diameter, length of tube etc. are calculated. Some forms are used for interfacing with the user through which user can enter the desired values, these forms are start form, menu form, input form, material form, tube side / shell side fluid form etc.

Figure 2: Input form of software

Entering data in to these forms user can give their requirement and get desired output from result form. Although this software also give graphical representation of some parameters such as number of baffles vs overall heat transfer coefficient, outer diameter of tube vs overall heat transfer coefficient, outer diameter of tube vs tube side pressure drop etc. MSchart is used for this purpose and codes developed give accurate representation of the parameters. While design of heat exchanger it is necessary to consider which inputs are required, which outputs are required to find out and steps required for the programs. These steps are given in the following flow chart:

Flow chart for Computer Program:

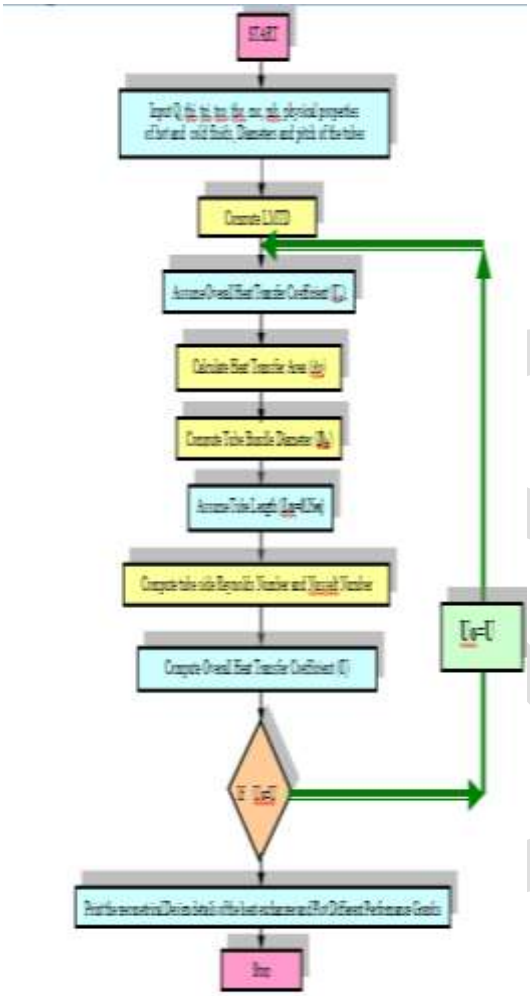

Figure 3: Flow chart for design and thermal analysis

By development of software codes design of shell and tube heat exchanger will be done. 3-D modeling of heat exchanger is done by using output results of Visual Basic software. So it is necessary to transfer data to Microsoft Excel sheet. Output data is transferred to Excel sheet by giving proper path in the program. Program is made in such a way that, it can open, save and close the Microsoft Excel sheet. Since it is not necessary to open the excel sheet or save the excel sheet for 3D modeling purpose. When file of assembly will open in CATIA software, and if it will be updated then changes made according to the output results of Visual Basic software. Most important phase for this is synchronization of Visual Basic with CATIA. It is achieved by Microsoft Excel. Design data of heat exchanger available from Visual Basic is transferred in Excel sheet. The parameters transferred from Visual Basic software are outer diameter of tube, inner diameter of tube, pitch of tube, number of baffles. This data is taken from input form of Visual Basic software which is provided by the user. Also shell diameter, length of tube and number of tubes on horizontal line are transferred from result form. By using these parameters, in Microsoft Excel sheet some relations and formulae are developed to give required data to CATIA software. It can create fully associative 3D solid models, with or without constraints, while using automatic or user derived relations to capture the design intent.

For modeling of shell and tube type heat exchanger from CATIA, user pattern, circular pattern, rectangular pattern and reuse patterns are mostly used. By using these patterns time of constructing the model tremendously minimized. Dimensions of model changes case to case and it is not possible to construct a model for every case. But it is possible in this model to draw models for each

case with the help of formulae and design table associations. We can vary number of tubes, ID, OD, pitch of tube, shell diameter, length of tube, number of baffles etc. in this model.

4) Design Results from Program of heat exchanger:

The comparison between theoretical design results with our software results and 'Alfa Laval' results with our software results is studied. At the beginning, assumed value of overall heat transfer coefficient is 1000 W/m^{2}K which is with maximum error. This error reduces in second and third iterations, become 44.84 W/m^{2}k and 44.91 W/m^{2}k respectively. We proceed with an iterations process to improve the accuracy. The developed software does forty iterations to give more accurate results which is not possible within short period of time. In Final iteration (40th iteration) value of tube side heat transfer coefficient is 101.205 W/m^{2}k and shell side heat transfer coefficient is 315.453 W/m^{2}k. These values give overall heat transfer coefficient (U_o) is 65.36 W/m^{2}k with negligible error (0.00001). When the conditions are given to the program as input, it gives result values in result form. The design data calculated by software are summarized in the table 1. This data is obtained after forty iterations. Hence accuracy of this result is more than results obtained by manual calculations also by using software time required to find out accurate results decreases. The results obtained by the software give optimum values of design parameters.

Sr. No.	Design Parameters	Iteration 1	Iteration 2	Iteration 3	Software Results
1	Log Mean Temp. Difference	4.5670	4.5670	4.5670	4.5670
2	Heat Transfer Coeff. In W/m^2 k	134.98	44.84	44.91	65.3628
3	Cross flow area in m^2	0.00204	0.00503	0.00938	0.0068
4	Heat transfer area in m^2	0.6584	4.877	14.75	10.0732
5	Tube bundle diameter in m	0.118	0.208	0.30	0.2038
6	Shell diameter in m	0.1604	0.2324	0.344	0.3019
7	Length of tube in m	0.678	1.5001	2.3	1.8846
8	Number of tubes	19	61	127	127

Table 1 Results obtained manually and with design software

For validation of software, results are compared with 'Alfa Laval' industries results. These industries use 'HTRI' softwares for design of shell and tube type heat exchanger. There, one case study was taken for comparison of two softwares. We have selected liquid – liquid (Water – Water), counter flow single pass heat exchanger. Comparative study is given as follows:

Sr. No.	Design Parameters	Developed Software Results	Alfa Laval 'HTRI' Results
1	Outside diameter of tube in mm	15.88	15.875
2	Pitch of tube in mm	22.22	22.22
3	Heat transfer rate in Watt	3007	3200
4	Log Mean Temp. Difference	4.5670	4.200
5	Overall Heat Transfer Coeff. W/m^2 k	65.3628	65.250
6	Heat transfer area in m^2	10.0732	11.937
7	Shell diameter in m	0.3019	0.301
8	Length of tube in m	1.8846	1.883
9	Number of tubes	127	127

Table 2 Comparison between developed software and 'Alfa Laval' software

From above table, it is found that the results obtained by developed software are to be matching with that of the 'HTRI' software results. Thus developed software is valid which provides accurate design data which is useful to manufacture well

economical heat exchanger. This developed software has the advantage of calculating performance and design with graphical representation with greater accuracy and within short period.

5) Performance Graphs obtained from the software:

For the same case study graphical representation of designed parameters is shown. There are number of parameters influence the performance of heat exchanger such as baffles number, inner diameter, pitch layout, number of passage etc. This software provides graphical representation for effect of these parameters on overall heat transfer coefficient and pressure drop, which gives useful information to the design engineers.

5.1 Baffles and Overall heat transfer Coefficient (U_o): The influence of baffles number on U_o is shown in graph 1. It shows that the *Uo* increases with increase in baffles number, the rate of overall heat transfer increases more rapidly as number of baffles increases and at less number of baffles it decreases. This is because to as number of baffles increases, it causes to change in the flow pattern of the shell fluid creating parallel or cross flow to the tube bundle thus increasing turbulence and therefore, the heat transfer coefficient U_o

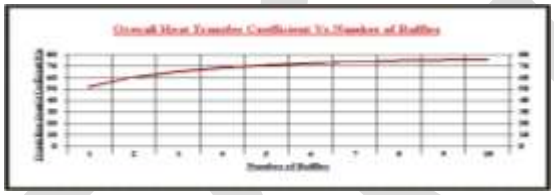

Graph 1: Number of baffles vs. overall heat transfer rate

5.2 Number of Baffles and Pressure Drop: Following graph shows that as number of baffles increases pressure drop at shell side increases. Baffles causes to change direction of flowing fluid, since velocities of fluid stream decreases near the baffles. As a result pressure drop increases and as we increase number of baffles there will be more pressure drop takes place at shell side.

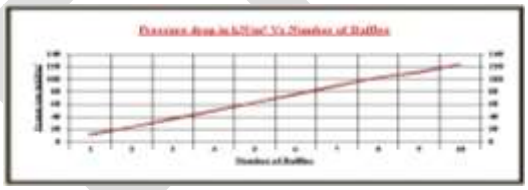

Graph 2: Number of baffles vs. shell side pressure drop

5.3 Outer Diameter of tube and Overall Heat Transfer Coefficient: This graph shows that as outer diameter of tube increases overall heat transfer coefficient decreases. Heat transfer coefficient depends on circumference of tube and fluid in contact with surface of the tube. As diameter of tube increases contact area between inside fluid and surface of tube decreases since overall heat transfer area also decreases which is shown by following graph.

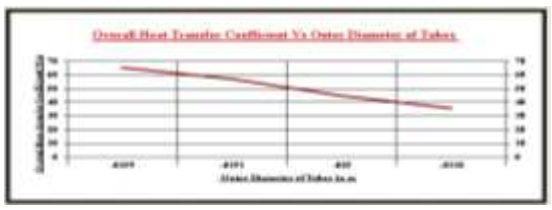

Graph 3: Outer diameter of tube vs. overall heat transfer coefficient

5.4 Diameter of tube and tube side pressure drop: Pressure drop at tube side basically depends on cross flow area of tube. As diameter of tube increases tube side pressure drop decreases. Suitable value of tube diameter for minimum pressure drop is 31.8 mm is shown by following graph.

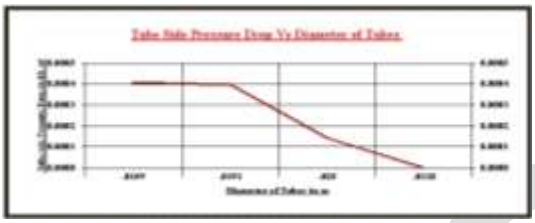

Graph 4: Diameter of tube vs. tube side pressure drop

6) 3D Modeling of Heat Exchanger:

Heat exchanger data is transferred to the excel sheet and through excel sheet it is transferred to the CATIA modeling software. For this case study the software can give 3D model and 2D model with designed parameters with negligible error and within very short time. The 3D and 2D model of above heat exchanger is drawn by the software is shown below:

Figure 4: Verification of design parameters in 3D model

After visiting many companies in which design and manufacturing of shell and tube of were done, it is found that in these companies for design of heat exchangers 'HTRI' software used and some companies calculations were done manually. Also it is found that drawing of heat exchanger was done by using 'AUTOCAD' software after checking output results from software. This method is time consuming and required skilled person.

There is no software which gives directly 3D and 2D model of heat exchanger after giving input parameters to the design software. With our developed software, it is possible to draw 3D model of required heat exchanger within very less time. This 3D model is used to show detailed drawing and also used for 3D printing machine and CFD analysis of heat exchanger model.

Conclusion:

For design of shell and tube type heat exchanger lot of calculation work is required which is time consuming. Same time the drafting of heat exchanger is another complicated task. This problem is eliminated by our developed software. The software based on established theory of heat exchanger. The code is developed in Visual Basic language which is user friendly and gives accurate results in very short time. Thermal design of heat exchanger is done by developed software and gives graphical representation of designed parameters, which gives useful information to the design engineers.

Dimensions of model changes case to case and it is not possible to construct a model for every case within very short period of time. Also, it was found that the heat exchanger industries use some basic software to design shell and tube heat exchanger, but

there is no feature on 2D and 3D modeling in it. But developed software gives directly 3D and 2D model of heat exchanger within very short time.

To check validity of our software, comparison of program results with theoretical results was done. In addition to this, the comparison between our software results and 'Alfa Laval' results was carried out. It is found that program results and 'HTRI' software results of Alfa Laval are matching with each other. So the developed software has an ability to predict the thermal performance and shows reliability in results.

REFERENCES:

1) Dawande S. D. *'Process Design of Equipments'*, 2006, Central Techno Publications.
2) Evangelos Petroutsos, 'Mastering Visual Basic 6' BPB Publications, B-14, Connaught place, New Delhi-110001.
3) Holman J. P. *'Heat Transfer'* McGraw-Hill Book Company, New York, London.
4) Kern D. Q. 'Process Heat Transfer', International edition, 1965, McGraw-Hill Company, New York, London.
5) Kuppan T., *'Heat Exchanger Design Handbook',* Taylor and Francis, Taylor and Francis group, New York, London.
6) Thome John R. '*Engineering Data Book III*', Wolverine Tube Division, Calumet and Hecla Inc., Michigan.
7) Sham Tickoo, 'CATIA V5R19 for Engineers & Designers' 2010, Dreamtech press, 19-A, Ansari Road, Daryaganj, New Delhi.
8) Leong K.C., Toh K.C., Leong Y.C., *'Shell and Tube Heat Exchanger Design Software for Educational Applications'* International Journal of Engg. Education Vol. 14,No.3 p-217-224,1998
9) Olga Arsenyeva, Leonid Tovazhnyansky, Petro Kapustenko, Gena Khavin, *'Computer Aided Design of Plate Heat Exchanges'* 20th European Symposium on Computer Aided Process Engineering- ESCAPE20.
10) Sherwin K., Mavromihales M., *'Design of Heat Exchanger'* University of Huddersfield,Queensgate,Huddersfield,HD1 3DH,UK

International Journal of Engineering Research and General Science Volume 3, Issue 6, November-December, 2015
ISSN 2091-2730

A Comparative review and analysis of different phase frequency detectors for Phase Locked Loops

Anu Tonk

Department of Electronics & Communication Engineering,

F/o Engineering and Technology,

Jamia Millia Islamia, New Delhi

tonkanu.saroha@gmail.com

Abstract---This paper presents phase frequency detectors (PFDs) with the five different designs which are Standard gate based logic, DCVSL, TSPC logic, CML logic and Modified CML logic The simulation results are focused on accounting the frequency operation of PFDs considering an input frequency of 100 MHZ .The PFDs have been designed using 0.35μm CMOS technology on SPICE simulator with 3.3V supply voltage. All PFDs are designed to be dead zone free. Results reported in the paper compare and concentrate on fast frequency operation, a low output noise, dead zone and power dissipation. When compared to all the logics S_PFD consumes least power, the minimum delay is experienced by TSPC_PFD and Modified CML_PFD. DCVSL_PFD observes the least output noise.

Keywords--- Phase frequency detectors, Phase locked loops, CML_PFD, Modified Current Mode Logic M_CML_PFD, True Single-Phase Clock PFD (TSPC_PFD), Differential Cascode Voltage Switch Logic PFD (DCVSL_PFD)

INTRODUCTION

A PLL comprises of several components [1] which are (1) phase or frequency detector, (2) charge pump, (3) loop filter, (4) voltage-controlled oscillator, and (5) frequency divider. Phase Locked Loops (PLL) has a negative feedback control system circuit. Our study is focused on designing phase frequency detectors (PFD) using different CMOS design techniques with the aim to compare the different logic based PFDs in terms of power consumption ,delay and speed of the block . The design has been validated using S-Edit at 350 nm technology with Tanner as simulator. There can be various methods of phase and frequency detection. XOR gate based detection but it is less preferred compared to the PFD where two signals are generated named [2] UP and DOWN with its pulse width proportional to the phase difference .This difference indicates the PLL that whether the feedback signal lags or leads the reference signal respectively. The reason behind rejecting use of XOR gate as detector was that that it can lock onto harmonics of the reference signal and most importantly it cannot detect a difference in frequency. These disadvantages were overcome by another type of PFD which only responds to edges of the two inputs and are free from false locking to harmonics unlike XOR based detector. The methodology of low-jitter PLL design has been developed in recent years. The jitter of PLL primarily is contributed from the reference clock, phase frequency detector, supply noise, substrate noise, charge pump circuit and VCO internal noise. However, power-supply noise generated by large switching digital circuits perturbs the analog circuits used in the PLL. The output clock period may change with the power-supply noise and with other sources of noise (for example, thermal noise in MOS devices). It is common to refer to this change as jitter, which is the variation of the clock period from one cycle to another cycle compared to the average clock period.[5] The clock jitter directly affects the maximum running frequency of the circuit because it reduces the usable cycle time. When the clock period is small, the digital circuits in the critical path may not have enough usable time to process the data in one period, resulting in the failure of the circuit. We have safely selected our design specifications for 350 nm technology for having less higher order effects and as well as achieving higher S/N ratio, which degrades as lower we go with the technology because our main aim was to study the behavior of the Phase frequency detectors without much higher order effects in prominence. Conventional PFD suffers from a major problem called dead zone. The dead-zone problem occurs when the rising edges of the two clocks to be compared are very close. Due to lots of reasons such as circuit mismatch and delay mismatch, the PFD has a difficulty in detecting such a small difference. The PFD doesn't detect the phase error when it is within dead zone region, then PLL locks to a wrong phase. A conventional CMOS PFD has no limit to the error detection range. Therefore, the capture range of PLL is only limited by the Voltage Controlled Oscillator (VCO) output frequency range [9]. The capture range of PLL is determined by the error detection range of PFD. Different designs have been used here for the purpose of observation and comparison with the outputs obtained using other logic designs.

1. DIFFERENT LOGIC BASED DESIGNS OF PFD

Standard CMOS (S_PFD), True Single-Phase Clock PFD (TSPC_PFD), DCVSL Differential Cascode Voltage Switch Logic PFD (DCVSL_PFD), Current Mode Logic PFD (CML_PFD) and Modified Current Mode Logic PFD (M_CML_PFD) circuits have been considered here. The high speed operation of MOS transistors is limited by their low transconductance. Therefore, dynamic and sequential circuit techniques or clocked logic gates such as, true single phase clock must be used in designing synchronous circuits to reduce circuit complexity, increase operating speed, and reduce power dissipation. [3]The key benefits of DCVSL are its low input capacitance, differential nature and low power consumption.

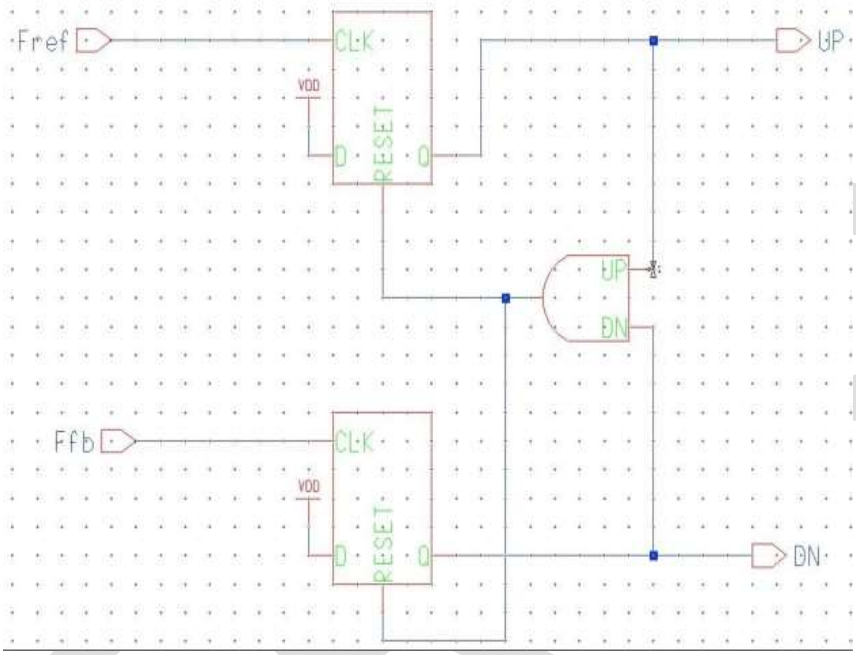

Fig.1. Phase Frequency Detector circuit (PFD)

1.1 Standard CMOS phase frequency detector (S_PFD): Conventional pull-up PMOS, pull-down NMOS static logic is popular because of its convenient availability in standard library cells, small area usage, low power dissipation, and high noise margins[7]. Even though the static power consumption of the conventional CMOS logic gate is zero ideally, it dynamically generates a large current pulse flowing from the power supply to the ground during the state transition. The coupling of the high switching spike noise may cause crosstalk between the analog and the digital circuitry. Even worse, the switching noise might induce latch up which can possibly destroy devices with the integrated circuit due to overheating [11], [12]. Standard CMOS PFD is designed using the conventional approach. There are two outputs from the PFD named UP and DOWN.

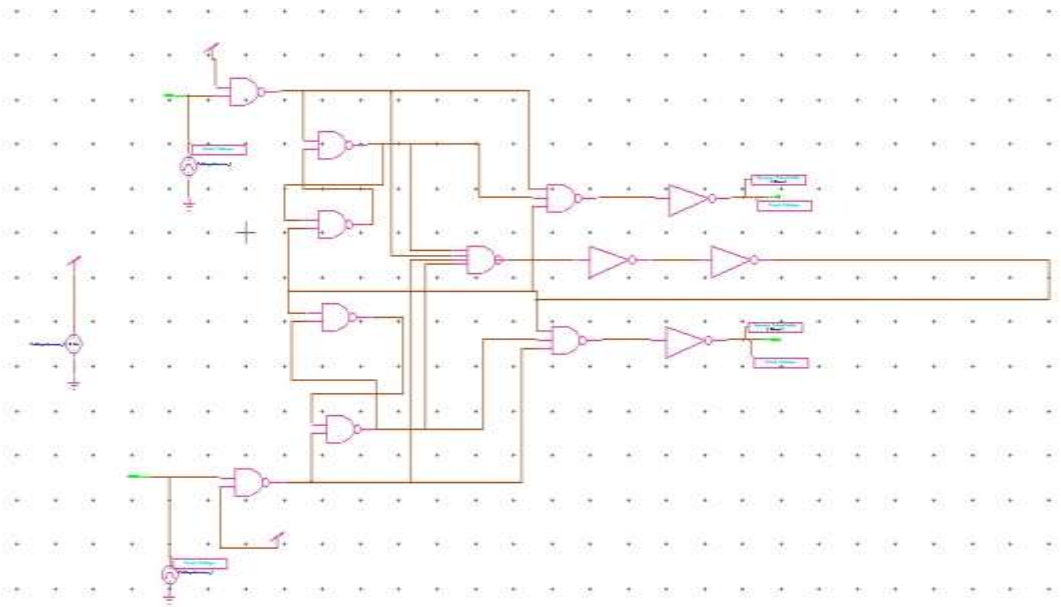

Fig2. Standard CMOS (S_PFD) Phase Frequency Detector circuit

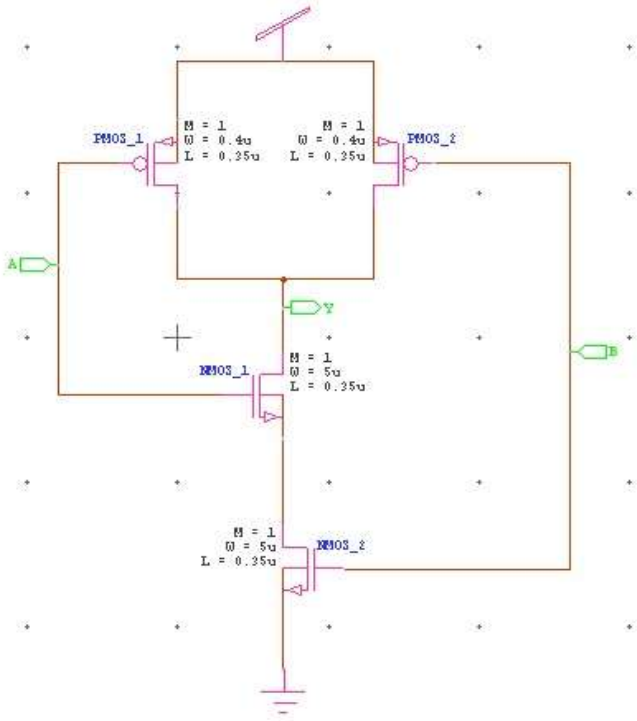

Fig.3. NAND cell for Standard CMOS (S_PFD) Phase Frequency Detector

In Fig 4 we can see that the reference signal and feedback signal frequency are different and accordingly we get the UP and DOWN signals depicting which of the two signals was leading or lagging and by how much phase. The Fig 5 shows the PFD characteristics when output of VCO or feedback signal (fback) and reference frequency (fref) are of same frequencies. In this we can observe that whenever both the falling edges of fback and fref occur simultaneously, there will be a glitch on up and down signal showing that the two frequencies are locked in phase as well as frequency.

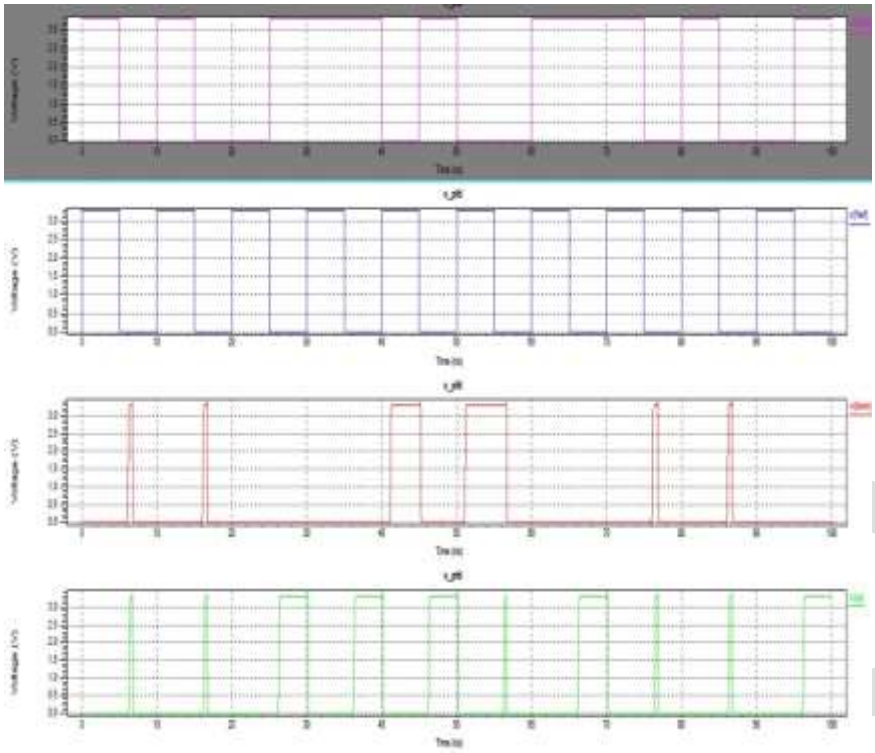

Fig.4. PFD output when both feedback and reference frequency are different. (Lead/lag at different instants).

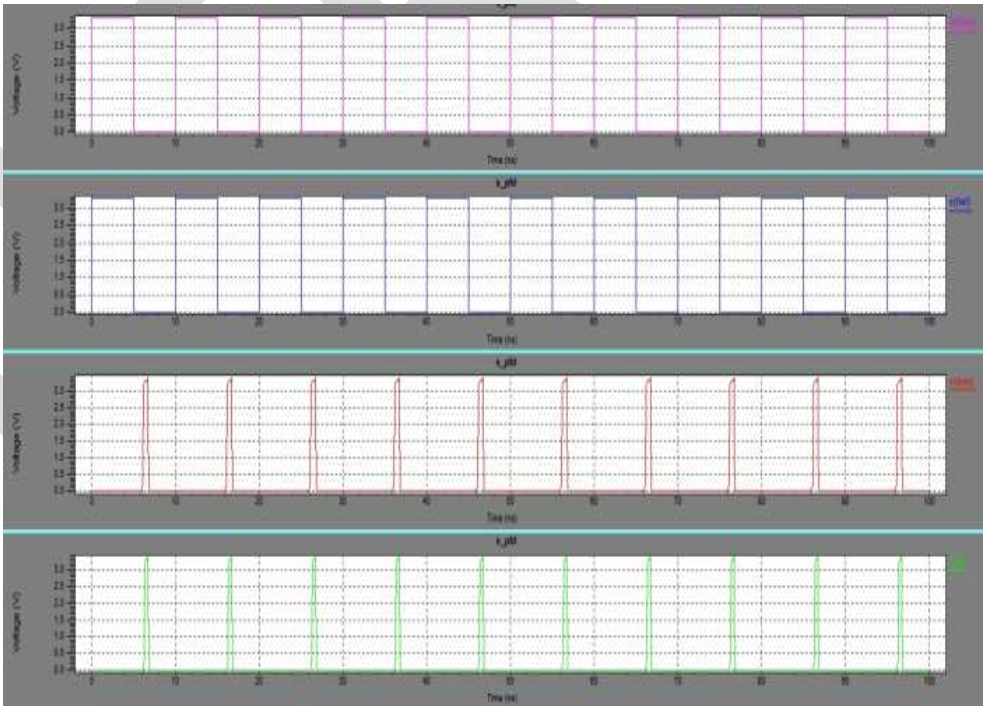

Fig.5. Output of S_PFD depicting PLL in locked state when both feedback and reference frequencies are same.

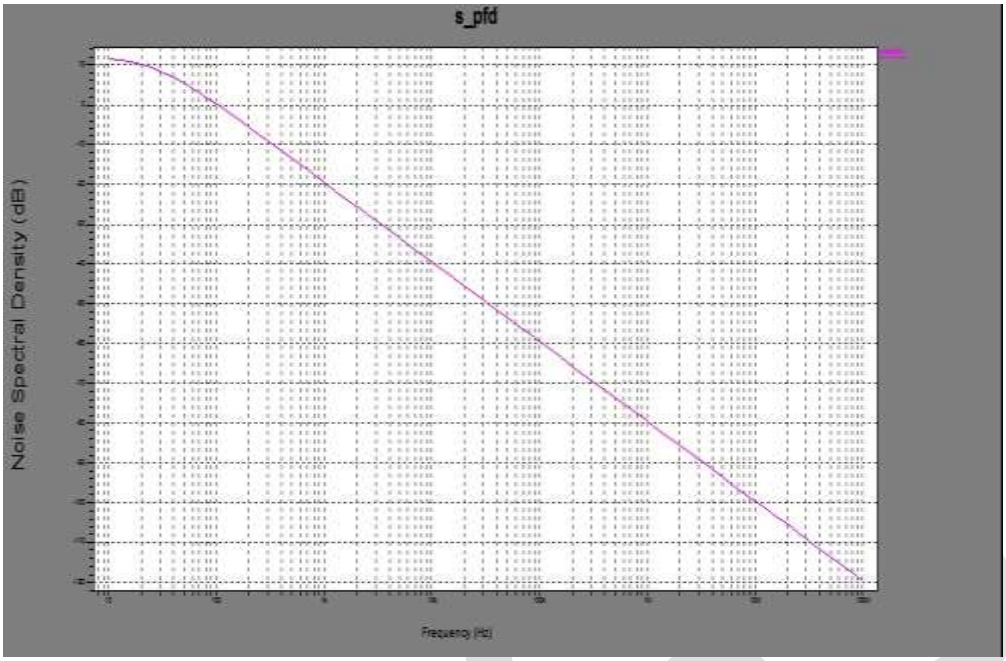

Fig.6. Noise Spectral Density graph for S_PFD (on x axis frequency range is from 10 to 100 MHz, on y axis noise in db)

1.2 Differential cascode voltage switch logic pfd (DCVSL_PFD): DCVSL has several advantages over the conditional CMOS static logic. It does not require a complementary pull up network, thus the parasitic capacitances at the output are reduced, which produces a faster response. Secondly, in contrast to pseudo-NMOS, its output voltages can swing from rail to rail and there is no direct path between VDD and ground in steady states. Finally it generates both true and complementary outputs and an inverting stage can be eliminated and its performance is further improved. [4]DCVS logic is responsible for the realization of faster circuits than are possible with conventional forms of CMOS logic, but this speed advantage is often achieved at the expense of circuit area and active power consumption.

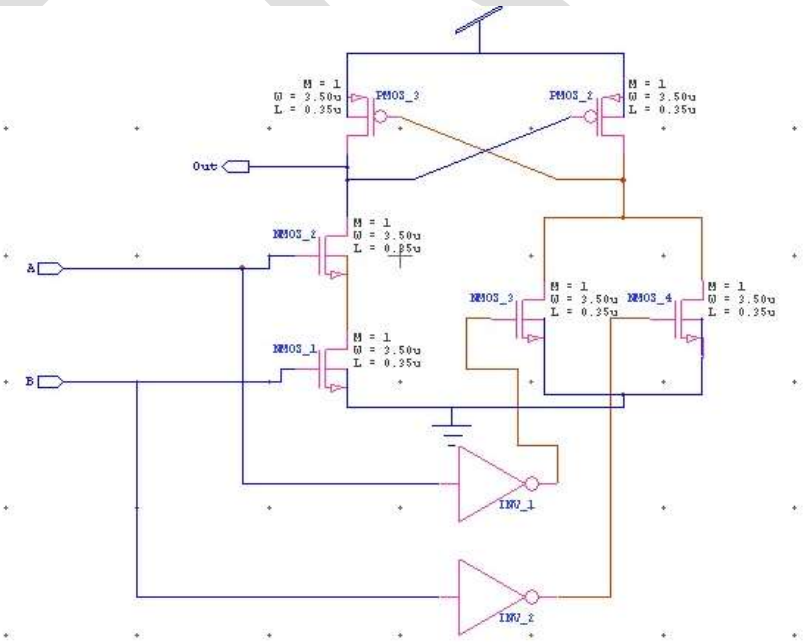

Fig.7. NAND cell for DCVSL [6] Phase Frequency Detector

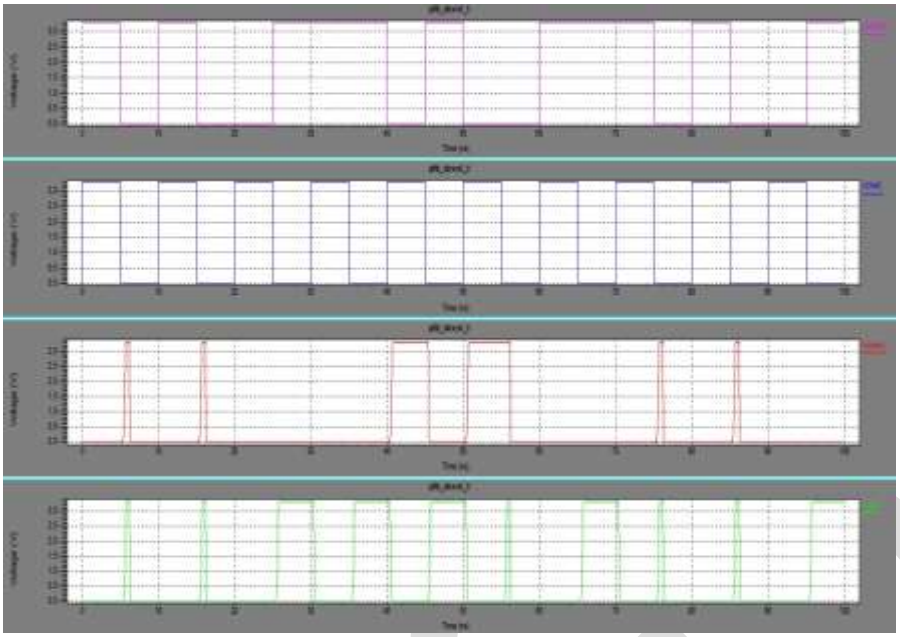

Fig.8. Output of DCVSL_PFD depicting PLL state when both feedback and reference frequencies are different, (lead/lag at different instants).

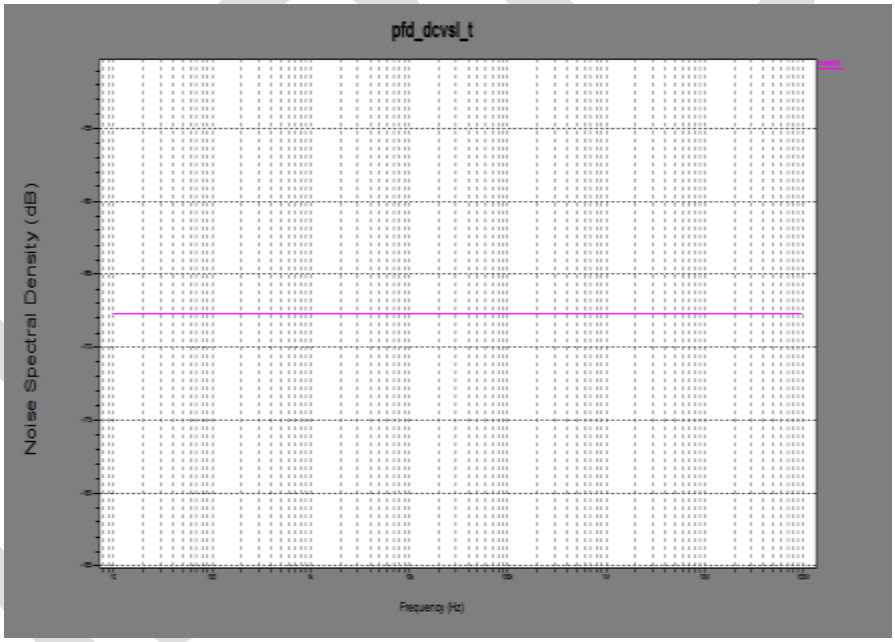

Fig.9.Noise Spectral Density graph for DCVSL_PFD (x axis represents a frequency range from 10 to 100 MHz and y axis represents noise in db)

1.3 True single phase clock pfd(TSPC_PFD): We have designed it as a negative edge triggered pfd. Here two signals are given, one is v_{ref} and other is v_{back}. If either of two signal have negative edge first that one will be leading. Suppose v_{back} fall down before v_{ref} then v_{down} signal at output will become high it means v_{back} is leading as can be seen in Fig 11.

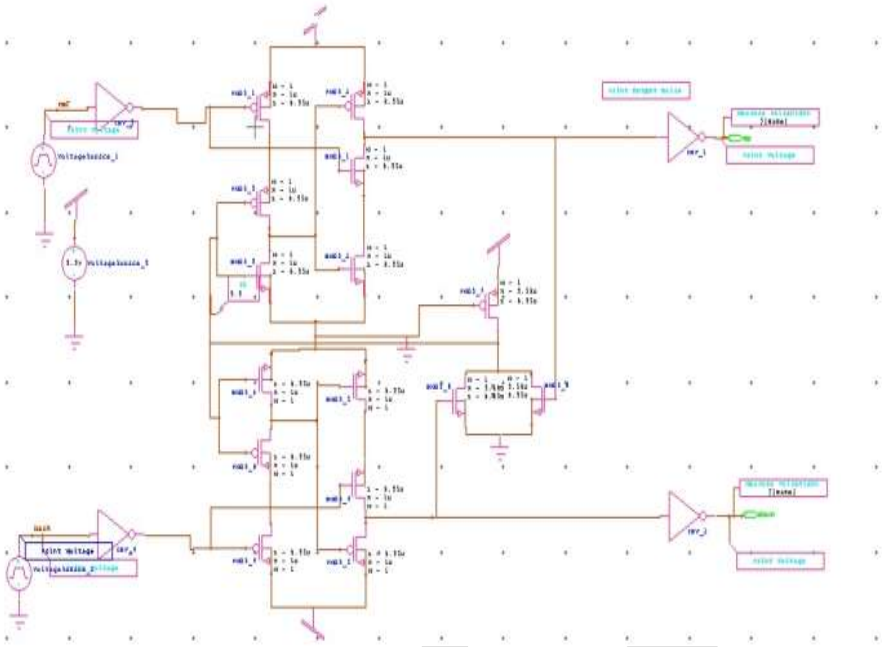

Fig. 10.Schematic for TSPC[8] Phase Frequency Detector

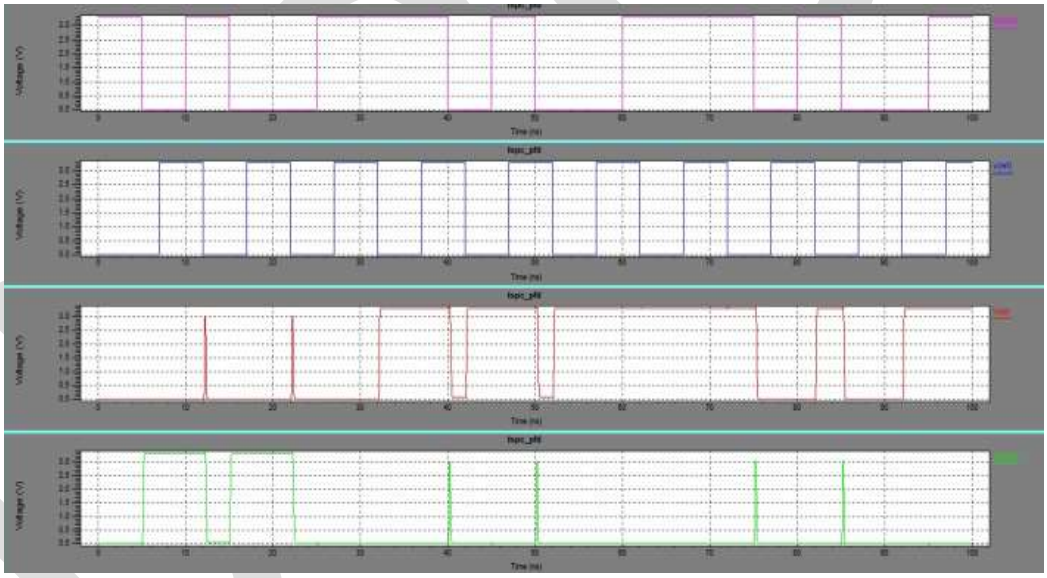

Fig.11. Output of TSPC_ PFD depicting PLL state when both feedback and reference frequencies are different, (lead/lag at different instants).

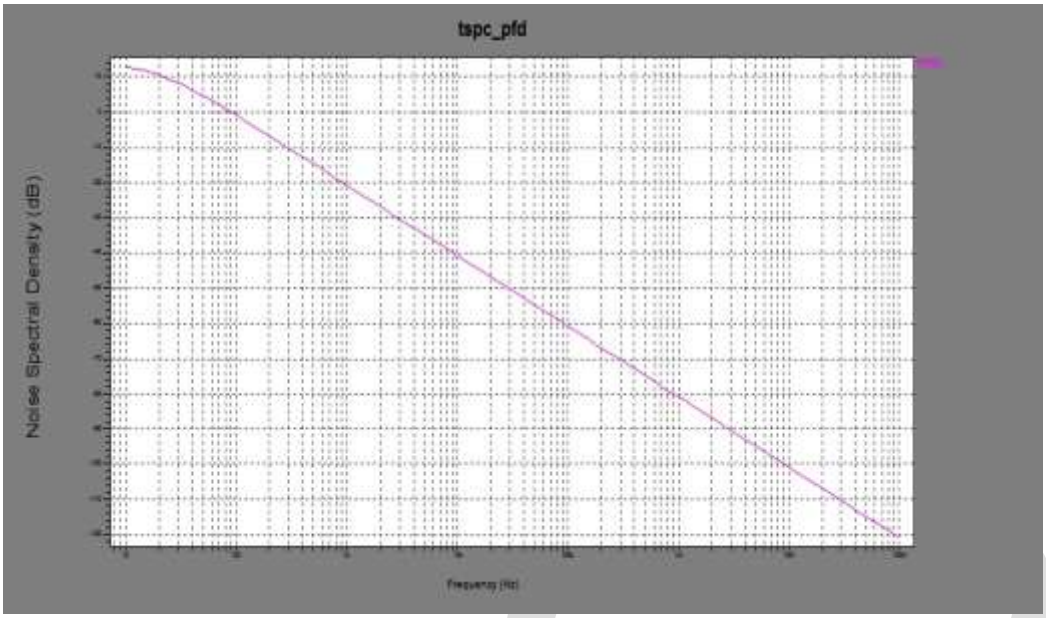

Fig.12. Noise Spectral Density graph for DCVSL_PFD (x axis represents a frequency range from 10 to 100 MHz and y axis represents noise in db)

1.4 Current mode logic (CML_PFD)[8]*:* In CML PFD, two d-latch are connected in such a way that they can work as PFD as depicted in Fig 14. The block diagram of two stages D flip flop is shown in Figure14 .A current mode logic (CML) structure is used to reduce the switching noise and power supply noise [10]. The CMOS logic has the advantage of low power consumption at low frequency operation. The CML requires two lines for each signal. Therefore, the area of CML is two to four times larger than in the CMOS logic. In high frequency operation the CML logic is consumption power less than CMOS logic.

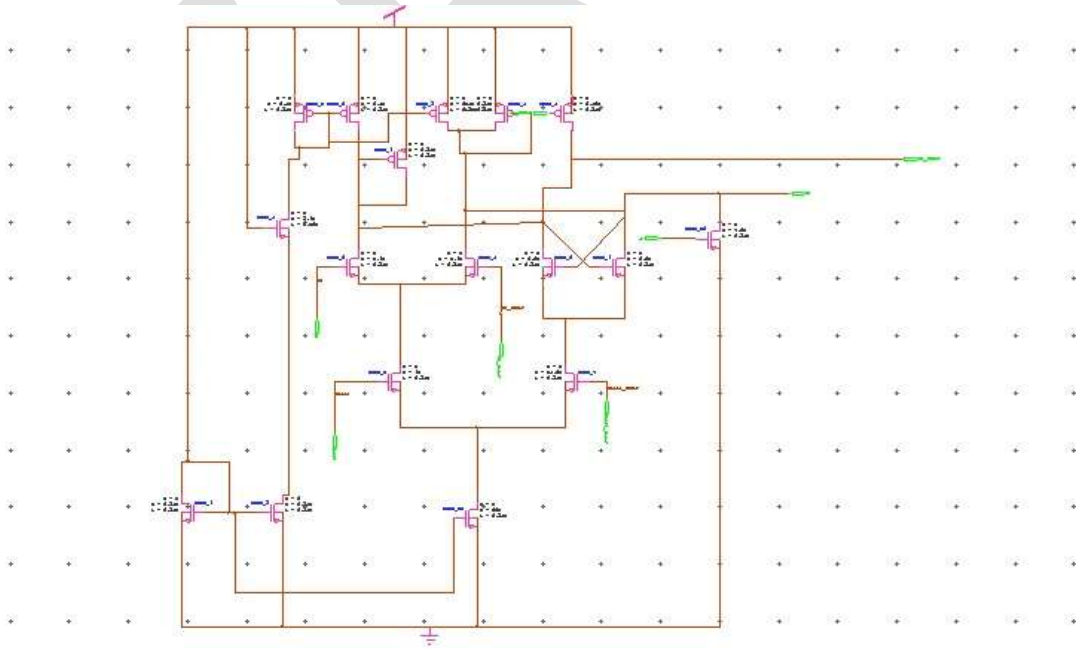

Fig.13. Schematic of D latch for CML [8] Phase Frequency Detector

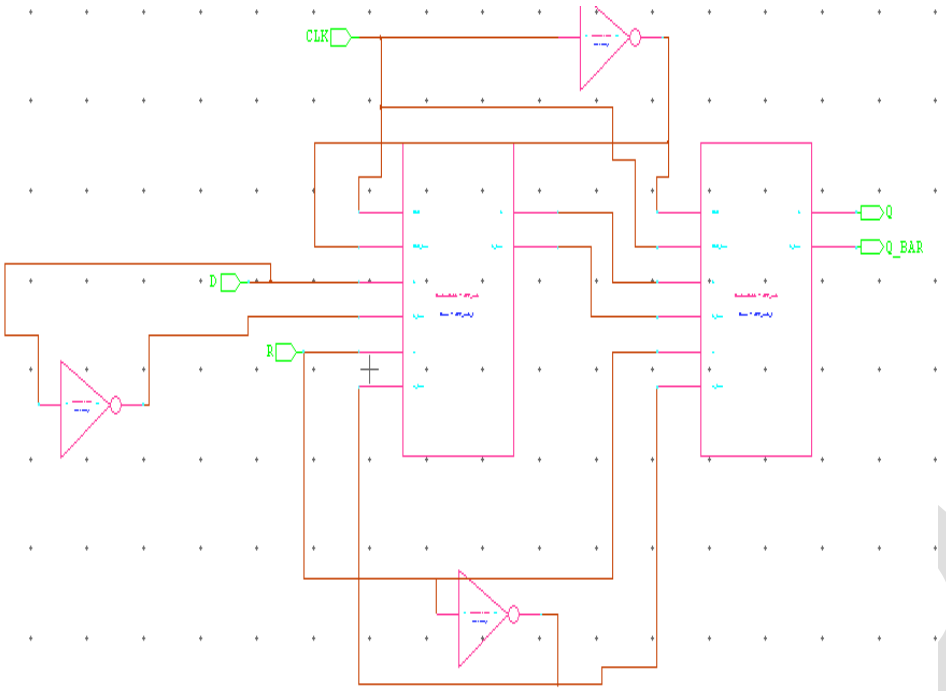

Fig.14. Schematic of D latch to D Flip flop conversion for CML [8] Phase Frequency Detector

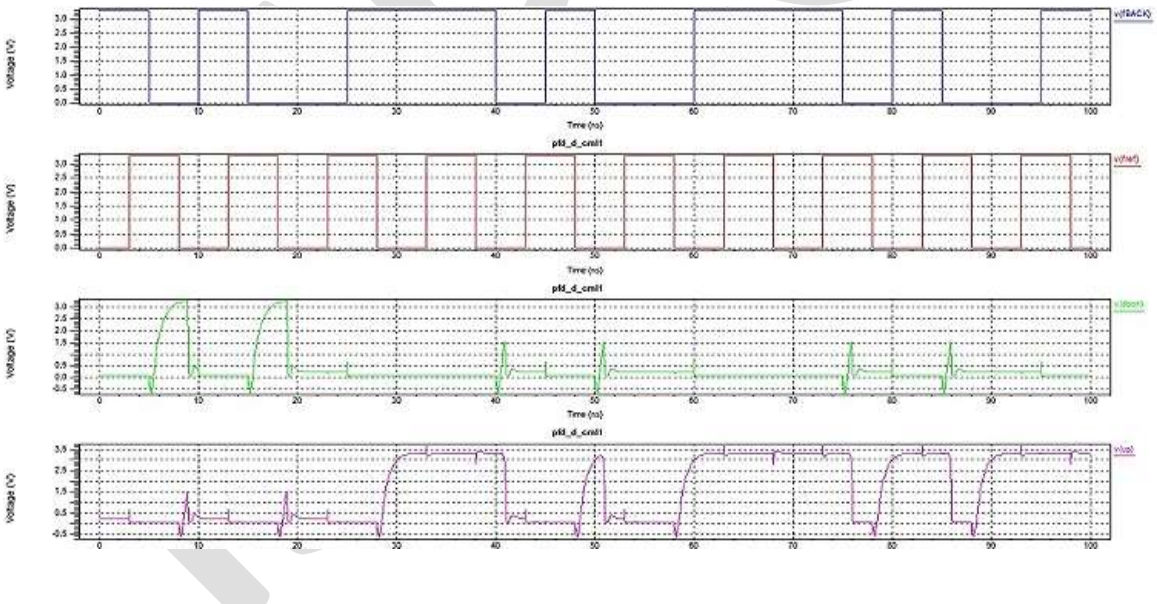

Fig.15. Output of CML_ PFD depicting PLL state when both feedback and reference frequencies are different, (lead/lag at different instants).

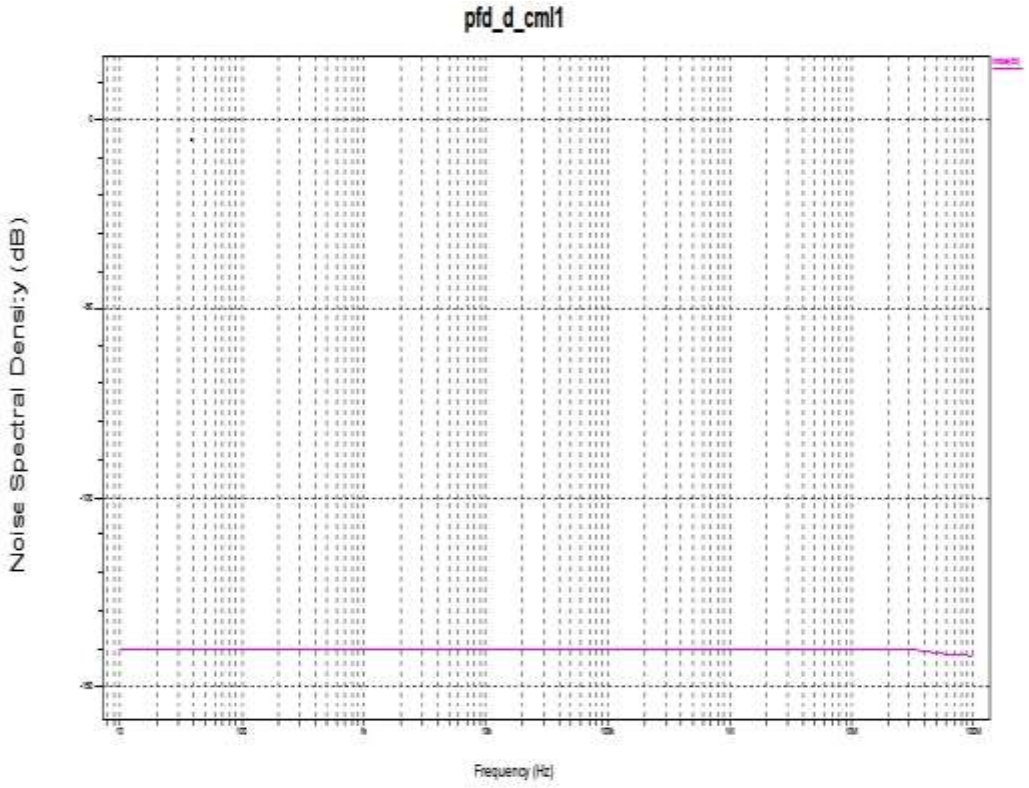

Fig.16. Noise Spectral Density graph for CML_PFD (x axis represents a frequency range from 10 to 100 MHz and y axis represents noise in db)

1.5 Modified CML pfd (M_CML_PFD): In the Modified CML, the number of transistors in M_CML_PFD d latch is reduced with the removal of two transistors pmos_2 and pmos_3 which form current mirrors. Thus, Power consumption and delay of the current mode logic based M_CML_ PFD is observed to be reduced.

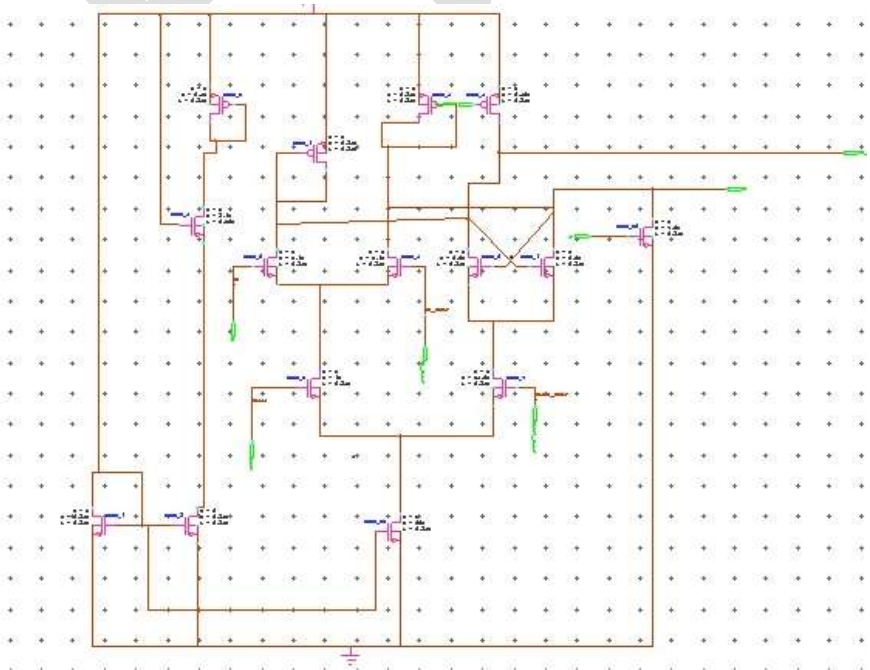

Fig.17. Schematic of D latch for M_CML Phase Frequency Detector

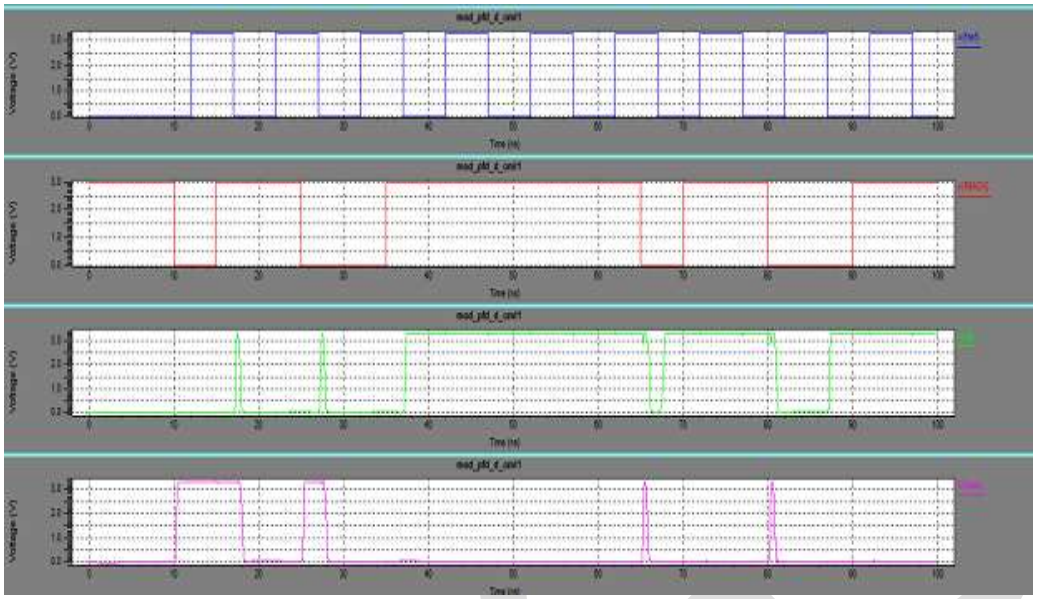

Fig.18. Output of M_CML_ PFD depicting PLL state when both feedback and reference frequencies are different, (lead/lag at different instants).

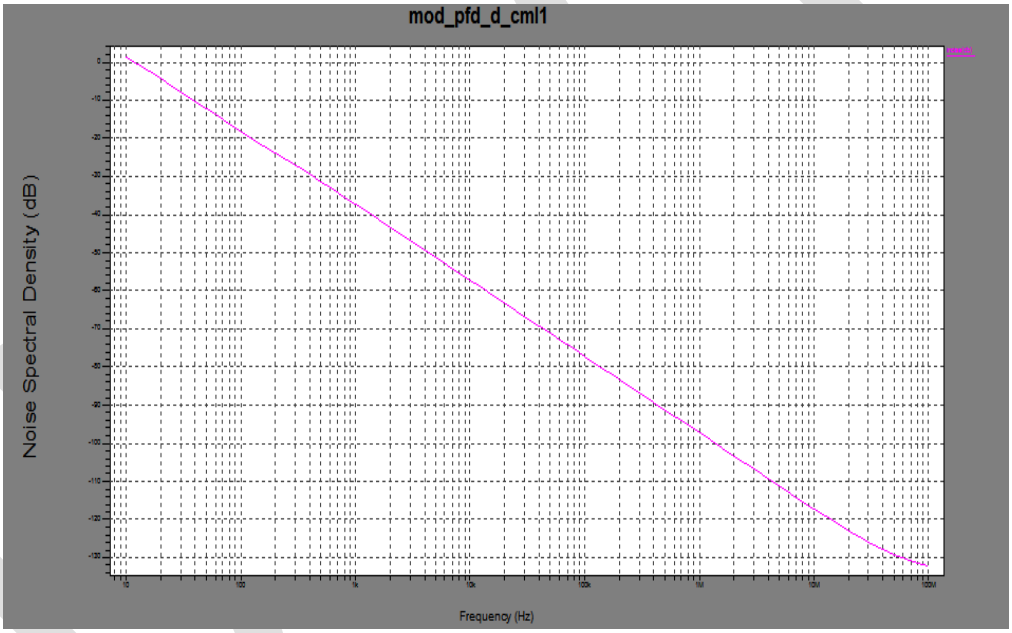

Fig.19. Noise Spectral Density graph for M_CML_PFD (x axis represents a frequency range from 10 to 100 MHz and y axis represents noise in db)

1.6 Simulations

The simulations mentioned above were done using Tanner tools 14 version. With the help of S-EDIT, W-EDIT, L-EDIT net list was generated and SPICE commands were used to obtain various parameters mentioned in the Table 1.

Table 1: Setup Parameters:

Rise time/RT	0.01 ns
Fall time/FT	0.01ns

High Time/HT	5ns
Low time/LT	5ns
Pulse Width/PW	5ns
Bit pattern	1010011
AC analysis(Frequency Sweep Type)	dec
Start frequency ; Stop frequency	10 meg; 100 meg
Number of frequencies	10

RESULTS

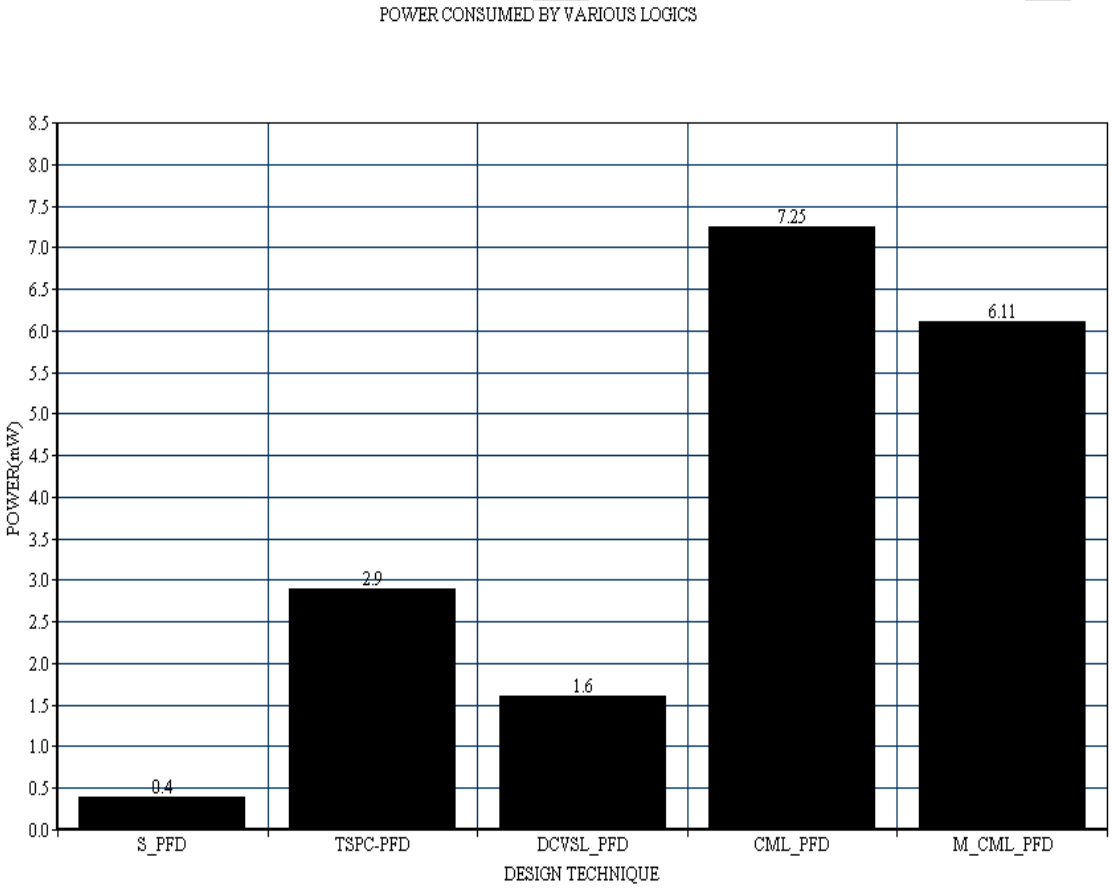

Fig.20. Power consumed by various PFDs

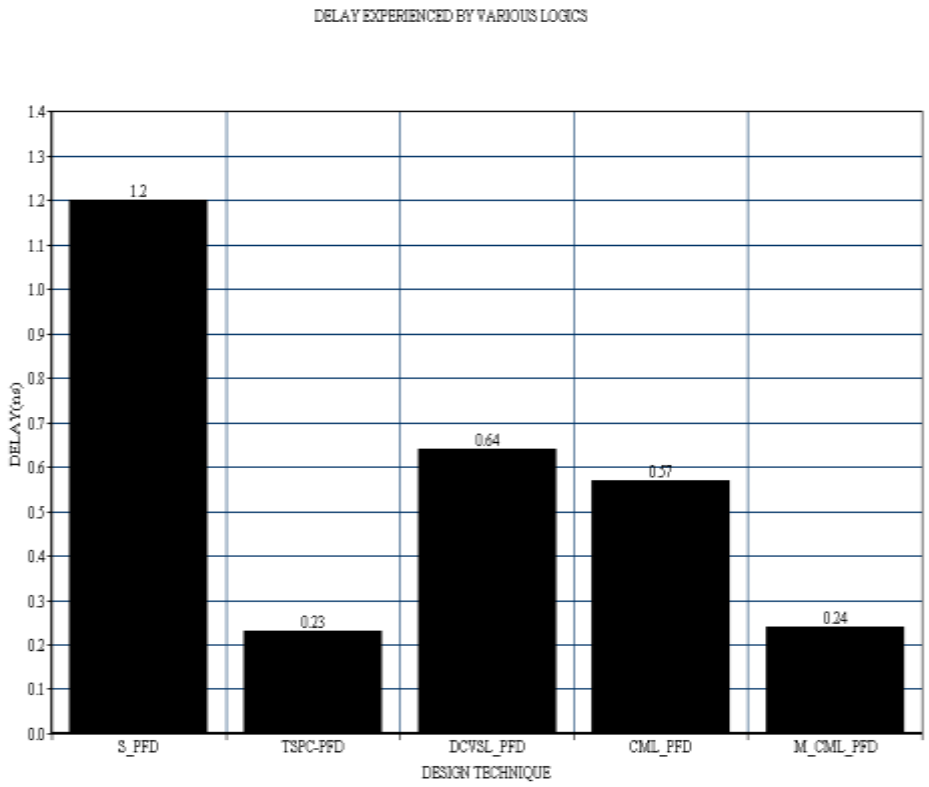

Fig.21. Delay experienced by various PFDs

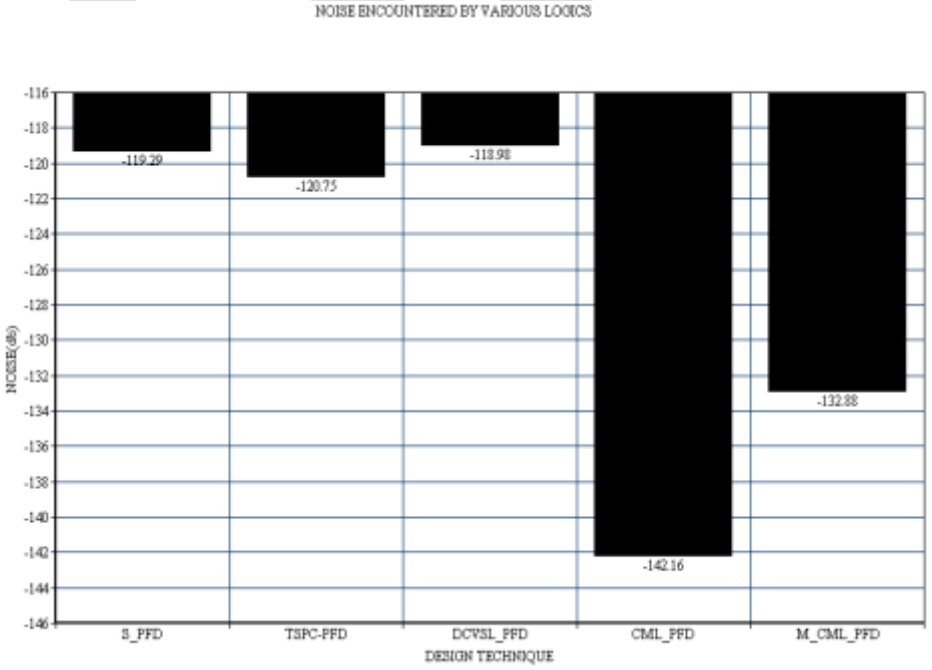

Fig.22. Noise encountered by various PFDs

Table 2: Comparison of different schemes of PFD:

	S_PFD	TSPC_PFD	DCVSL_PFD	CML_PFD	M_CML_PFD
Power	0.4mW	2.9mW	1.6mW	7.25mW	6.11mW
Glitch time	0.6ns	0.16ns	0.38ns	0.08	0.56ns
Glitch period	10ns	10ns	10ns	10ns	10ns
Delay	1.2ns	0.23ns	0.64ns	0.57ns	0.24ns
Output noise	-119.29db	-120.75db	-118.98db	-142.16db	-132.88db

CONCLUSIONS

We successfully compared and implemented five designs of PFD which are as follows:

- NAND gate based standard phase frequency detector, DCVSL_PFD, TSPC_PFD, CML based PFD and M_CML_PFD.
- It was found that the designed PFD using standard Nand gates consume 0.4mW power, PFD using DCVSL logic consume 1.6mW and the TSPC PFD consumes 2.9mW with the power supply of 3.3V.
- The TPSC_PFD_PFD and M_CML_PFD experience minimum delay among all the PFD designs and can be used for faster speed of operation.
- All the models are designed to be dead zone free.
- The locking time of 10ns is obtained for the different designs with reference and input frequencies equal and of value 100MHZ.
- The S_PFD design and DCVSL_PFD design can be used for low output noise with DCVSL output noise being least and equal to -118.98db. Thus, S_PFD and DCVSL_PFD are best suitable for low power operations which also observe low output noise.

Table 2 depicts the difference in values for various parameters of all the five designs.

REFERENCES:

[1] Abishek Mann, Amit Karalkar, Lili He, Morris Jones, "The Design of A Low-Power Low-Noise Phase Lock Loop" IEEE international Synopsys, qulity electronic design", 2010, pp, 528-531.

[2] HWANG-CHERNG CHOW and NAN-LIANG YEH"A New Phase-Locked Loop with High Speed Phase Frequency Detector and Enhanced Lock-in", Proceedings of the 10th WSEAS International Conference on CIRCUITS, Vouliagmeni, Athens, Greece, July 10-12, 2006 (pp96-101).

[3] N. Kumar Babu, P. Sasibala, "Fast Low Power Frequency Synthesis Applications By Using A Dcvsl Delay Cell", International Journal of Electrical and Electronics Engineering (IJEEE), ISSN (PRINT): 2231 – 5284, Volume-3, Issue-2, 2013.

[4] Kan M. Chu and David L. Pulfrey, "A Comparison of CMOS Circuit Techniques: Differential Cascode Voltage Switch Logic Versus Conventional Logic", IEEE Journal of Solid-State Circuits, Vol. Sc-22, No. 4, August 1987.

[5] Wen-Chi Wu,C,h ih-Chien Huung, Chih-Hsiung Chang', Nui-Heng Tseng, "Low power CMOS PLL for clock generator", IEEE International synopsis on circuits and systems,2003,vol-1, pp.I-633-I-636.

[6] K. Arshak, O. Abubaker, and E. Jafer, "Design and Simulation Difference Types CMOS Phase Frequency Detector for High Speed and Low Jitter PLL", proceedings of 5th IEEE International Caracas Conference on Devices, Circuits, and Systems, ominican Republic, Vol. 1, Nov.3-5, pp.188-191, 2004.

[7] D. J. Comer and D. T. Comer, *Fundermentals of electronic circuit design*. New York: John Wiley & Sons Inc., 2003.

[8] Anu Tonk , Bal Krishan, "Designing phase frequency detector using different design technologies", International journal of advanced research in engineering and technology(IJARET) Volume 6, Issue 2., February (2015), pp. 09-19.
[9] Behzad Razavi, *Monolithic Phase-Locked Loops and Clock Recovery Circuits : Theory and Design*, IEEE PRESS.
[10] A.Tanabe, M. Kataoka, M. Okihara, H. Sakuraba, T. Endoh and F. Masuoka, "0.18-um CMOS 10-Gb/s Multiplexer/Demultiplexer ICs Using Current Mode Logic with Tolerance to Threshold Voltage Fluctuation" in *IEEE Journal of solid-state circuit*, Vol. 36, NO 6, 2001.
[11] D. T. Comer, Introduction to Mixed Signal VLSI. New York: Array Publishing Co., 1994.
[12] D. J. Allstot, G. Liang, and H. C. Yang, "Current-mode logic techniques for cmos mixed-mode basics," Proceedings of the 1991 IEEE Integrated Circuits Conference, vol. 49, no. 8, pp. 25.2/1–25.2/4, May 1991

International Journal of Engineering Research and General Science Volume 3, Issue 6, November-December, 2015
ISSN 2091-2730

NUMERICAL AND EXPERIMENTAL INVESTIGATION OF STAGGERED INTERRUPTED FIN ARRANGEMENT IN A NATURAL CONVECTION FIELD

Mr.Bhushan S Rane[1], Prof. M D Shende[2]
[1](P G Student, Department of Mechanical Engineering, Shreeyash college of engineering & technology, Maharashtra, India)
(Mobile: 9967279317, Email: bhushanrane1704@gmail.com)
[2] (Assistant Professor, Department of Mechanical Engineering, Shreeyash college of engineering & technology, Maharashtra, India)Email: shendemd@gmail.com)

Abstract— Steady-state external natural convection heat transfer from vertically-mounted rectangular staggered interrupted fins is investigated numerically and experimentally. FLUENT software is used to develop a 3-D numerical model for investigation of fin interruption effects. A custom-designed testbed was developed and continuous, inline interrupted and staggered interrupted aluminum alloy heatsinks with various geometric dimensions are machined and tested to verify the theoretical results. A comprehensive experimental and numerical study is performed to investigate the effects of staggered interruptions. Our results show that adding staggered interruptions to vertically-mounted rectangular fins can enhance the thermal performance considerably than the inline interrupted fins. The results of this work can be used to improve thermal performance of enclosures in a variety of electronics, power electronics and telecommunication applications.

Keywords— Experimental study, Fin geometry, Heat sinks, Natural convection, Numerical Analysis, Staggered interruptions, Thermal Performance.

INTRODUCTION

The widely preferred method for cooling electronic and telecommunications devices is passive cooling since it is cost effective and reliable solution. It doesn't need costly enhancing devices. Effectively finned Heat sinks are generally used to enhance the heat transfer rate. Here in this work the focus is staggered interrupted fins. The objective of this work is to enhance the heat transfer rate by providing staggered interruptions. The staggered interruptions are provided on the heat sink. Providing fin interruptions results in considerable weight reduction that can lead to lower manufacturing cost. The staggered interruption pattern improves the thermal performance of heat sink compare to inline interruption pattern. The following paragraphs provide a brief overview on the pertinent literature.

Mehran Ahmadi et al [2] shows that adding inline interruptions to a vertical wall can enhance heat transfer rate up to 16% and reduce the weight of the fins, which in turn, lead to lower manufacturing and material costs. Golnoosh Mostafavi,et al [1] shows that adding interruptions to vertically-mounted rectangular fins can enhance the thermal performance considerably and that an optimum fin interruption exists. A new compact correlation is proposed for calculating the optimum interruption length. G. A. Ledezma et al [3] documents the geometric optimization of an assembly of staggered vertical plates that are installed in a fixed volume and showed that the geometric arrangement of vertical staggered plates in a fixed volume can be optimized such that the thermal conductance between the assembly and the surrounding fluid is maximized. G Guglielmini et al [4] investigated the heat transfer by natural convection and radiation between an isothermal vertical surface, having a staggered array of discrete vertical plates of finite thickness, and the surroundings and showed that for the particular geometry taken into account, the convective and radiant components yield a more efficient heat transfer than that obtained from fins made up of U-shaped vertical channels of the same bulk volume.

PROBLEM DEFINITION

The present work was based on the research carried out by Mehran Ahmadi et al [1] on the rectangular fins for heat removal from a heat source using natural convection. Their work included the experimental and 2-D numerical analysis for the continuous and interrupted fins of inline arrangement. The authors had extensively studied the effects of interruptions on heat transfer rate. However, the present study focuses on staggered interrupted fin arrangement and investigates its impact on the overall system performance by both the numerical and experimental approaches.

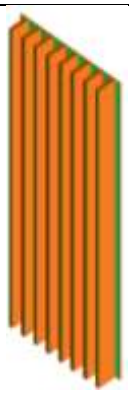

Continuous Fins Arrangement

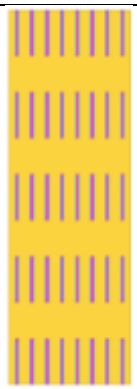

In-line interrupted Fins Arrangement

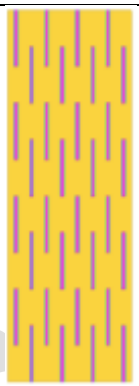

Staggered interrupted Fins Arrangement

Figure 1 Considered Heat sink Geometries

EXPERIMENTAL SET-UP

Figure 2 Experimental Setup

The tested heatsinks are made from 6063-T5 aluminium alloy with a thermal conductivity of 130 W/m K and emissivity of 0.09 at 20 ^{0}C. A new custom-made setup is designed for measuring natural convection heat transfer from heatsinks as shown in Fig. 2. The set-up includes an enclosure made of wood which is insulated by a layer of dense insulation foam. During the experiments, in addition to the power input to the electric heater, surface temperatures are measured at various locations at the backside of the baseplate. Electrical power is supplied through an AC power supply from Dimmerstat . The voltage and the current are measured to determine

the power input to the heater. Six thermocouples are adhered to the back side of the heatsink to prevent disturbing the buoyancy driven air flow. One more thermocouple is used to measure the ambient temperature during the experiments. Temperature is measured at six different vertical positions in order to observe the temperature variation over the heatsink. The average of these six readings is taken as the base plate mean temperature. Since fins height is short, maximum fin height is 17 mm, fins are assumed to be isothermal. The system is allowed to reach a steady-state condition for each power input level, and then temperatures and power are recorded. The steady-state condition is ensured by observing the rate of changes in all thermocouples. For each of the three heatsinks, the experimental procedure is repeated for different power inputs. Recording the temperature values in time, the point where the temperature difference in a 10 min time span became less than the accuracy of the thermocouples, were considered as steady state conditions.

CFD MODELING

In the experiment studies, the fins were placed on a base plate of dimension 305 X 101 mm. The set-up was placed in a room with static conditions. The similar conditions were created for the CFD simulations. As shown in the Figure 3, the fin arrangement was placed in the middle and the bounding box was created. The boundaries of this computational domain were placed sufficiently away from the fins to avoid any flow-reversal during the numerical simulations. The CFD meshing, computational domain discretization was performed using ANSYS ICEM CFD, a well-known commercially available pre-processor. Combinations of tetrahedral and triangular prism elements were used. Due to the high temperature difference between the fin surfaces and the surroundings, the buoyancy currents will be dominant. The triangular prism layers generated surrounding the fin surfaces would help to numerically resolve the thermal boundary layers and this result in the improved accuracy in the overall heat transfer rate predictions.

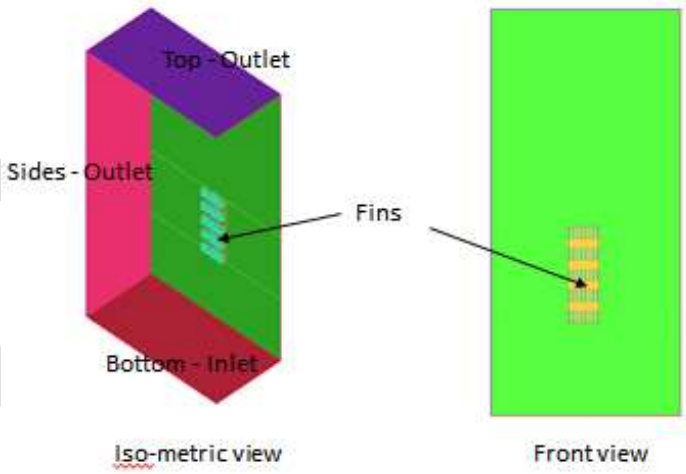

Figure 3 CFD Model

Steady state CFD formulation was employed to model this problem in ANSYS FLUENT. The gravitational forces that were acting in negative Y direction, in this case, were activated. In the reference work [1], the heat transfer from the fin tip areas were neglected. In order to maintain the consistency, the fin tip heat transfer from the simulations was not considered for the analysis. The fins and base plate surfaces were modeled using the Wall boundary conditions. At these walls, the No-Slip and Iso-Thermal conditions were imposed. The radiation effects from the fin surfaces to the atmosphere were not modeled. The bottom surface was specified as pressure-inlet boundary condition to allow the fluid motion inside the domain. The remaining surfaces were specified as outlet boundary conditions. The accuracy of the CFD simulations would depend upon the selection of the spatial discretization schemes. Second order spatial discretization schemes for the Pressure, Momentum and Energy were chosen for the simulation while Green-Gauss Node based scheme was used for the gradient calculations.

CFD SIMULATION RESULTS

In order to compare the results from Mehran et al [1], a validation study was carried out.

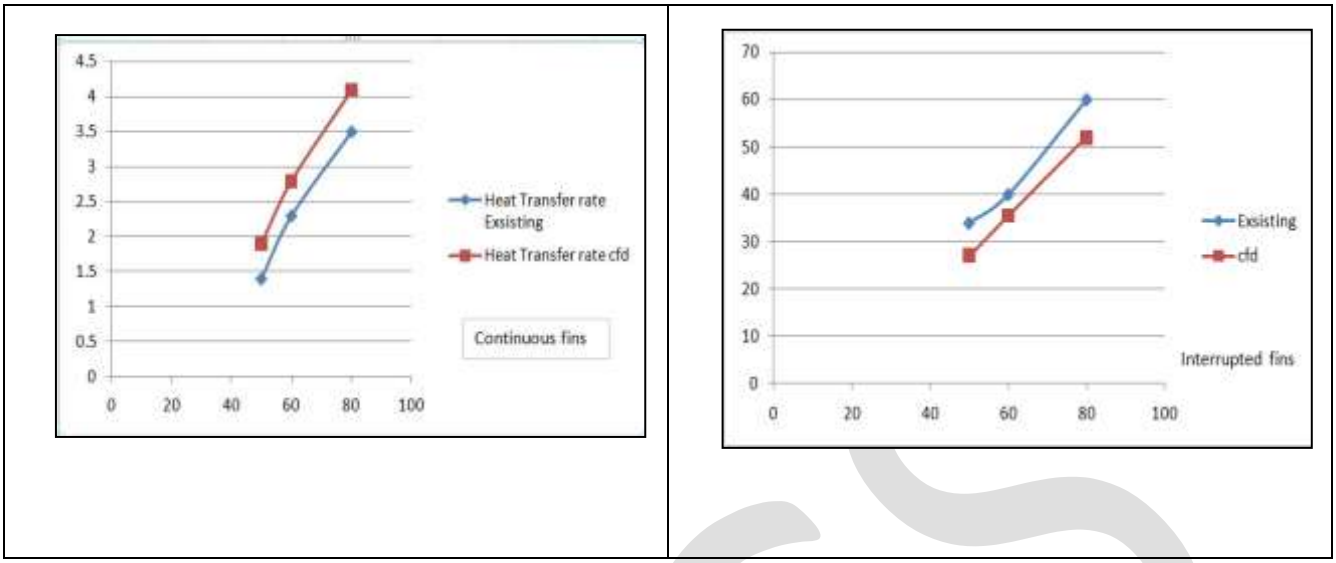

Figure 5 Validation of inline interrupted fins

The results from the CFD simulations by the authors and by Mehran et al were plotted in figure 5. In the present study, the heat transfer rate for the continuous fin arrangement was over-predicted in comparison to the work by Mehran et al. However, in the case of interrupted fins, the heat transfer rate was slightly under-predicted to the experimental results from Mehran et al. However, the variation from the reference journal was found to be less than 10%. In the next phase of the work, the CFD simulations for the actual geometrical configurations were carried out. The staggered fin arrangement was configured as explained in the following image.The CFD simulation settings that were discussed earlier section had been applied for these simulations and the results are discussed below.

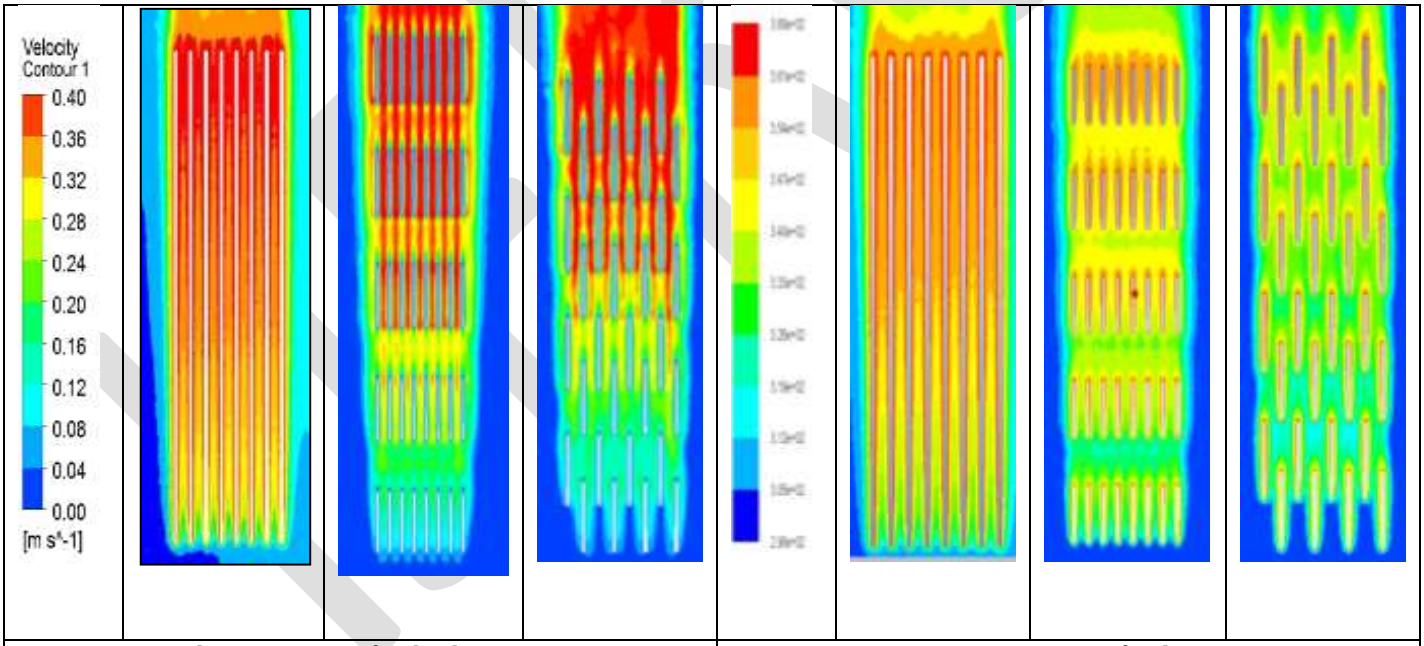

Velocity Contours for the dT = 70 C

Temperature Contours for dT = 70 C

Figure 4 Velocity and Temperature contours for thr dT=70 ^{0}C

The contour plot for the flow velocity and the flow temperature at the mid-height of the fin was generated to study the flow and thermal characteristics of the system. The flow velocity was observed to be higher in the case of staggered fin arrangement as compared to the other fin arrangement system. Such fluid flow patterns would also result in enhanced heat transfer rate from the surfaces. The temperature contours in figure indicate high temperature zones at the top region of the fins in the continuous fin arrangement. While in the staggered fin arrangement, the flow temperatures around the fins were much less compared to the

continuous fins arrangement. The flow turbulence created by the staggered arrangement enhances higher fluid velocity which in turn improves the heat transfer rate from the surfaces.

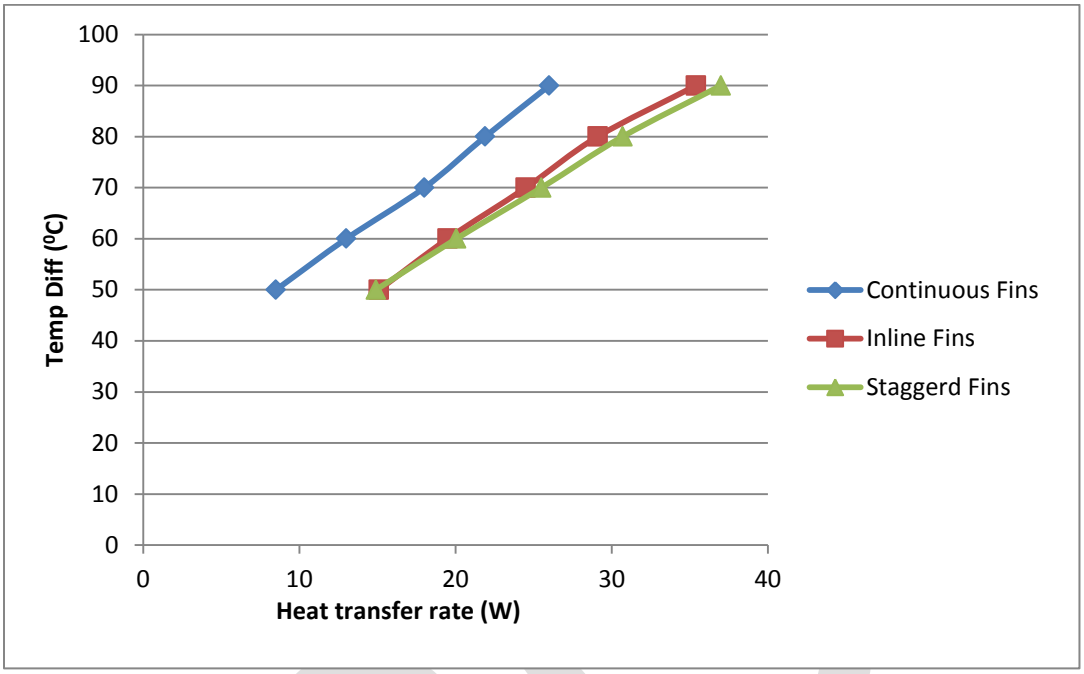

Figure 5 CFD results of Heat transfer rate continuous, inline, and staggered interrupted fins.

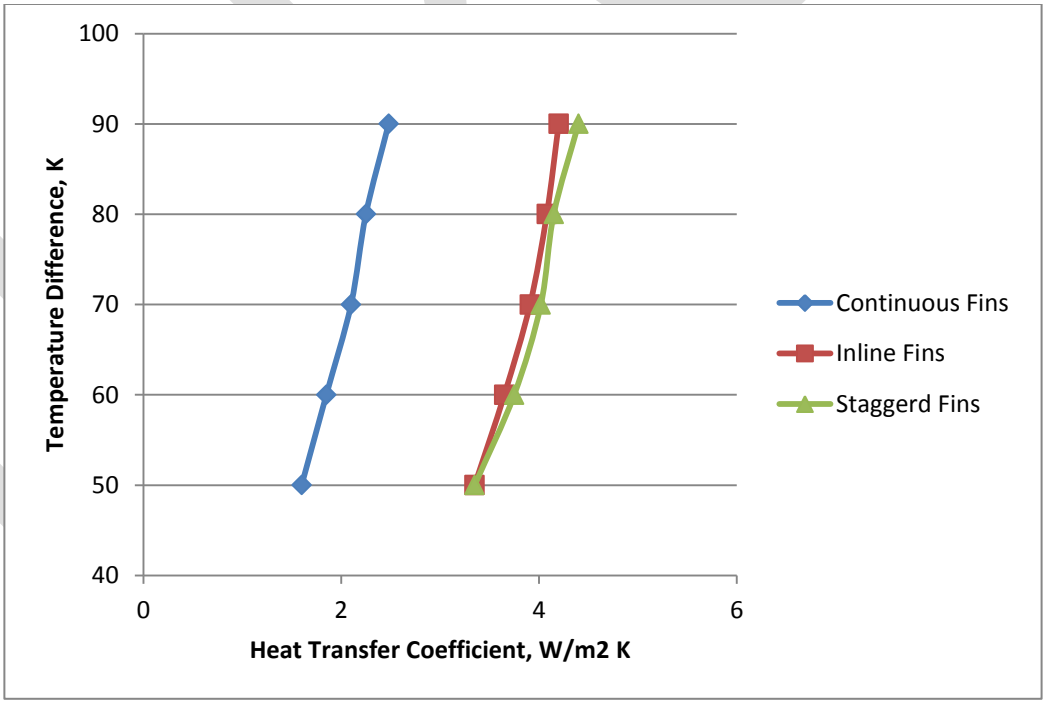

Figure 6 CFD results of Heat transfer coefficient for continuous, inline, and staggered interrupted fins.

This fluid and thermal behaviour was observed when the temperature difference (dT) was changed as well. In the graph, the staggered fin arrangement performs better than the continuous fin and inline interrupted fin arrangement in terms of heat transfer rate. However, the material required constructing the staggered fin arrangement and in-line fin arrangement is similar.

EXPERIMENTAL RESULTS

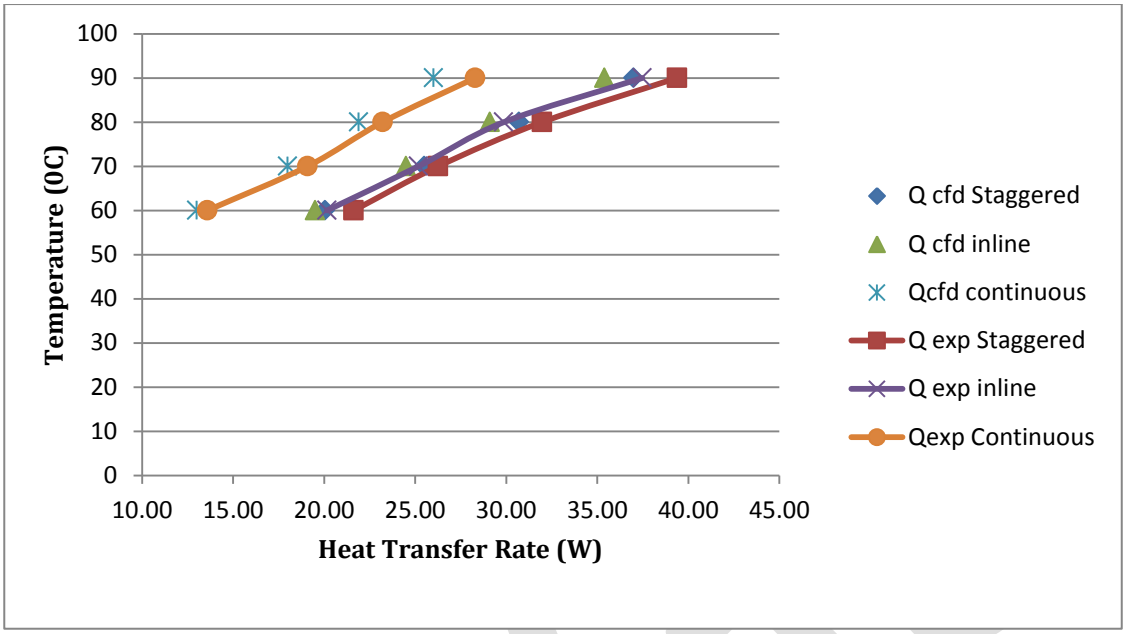

Figure 7 Experiment results of Heat transfer rate for continuous, inline, and staggered interrupted fins.

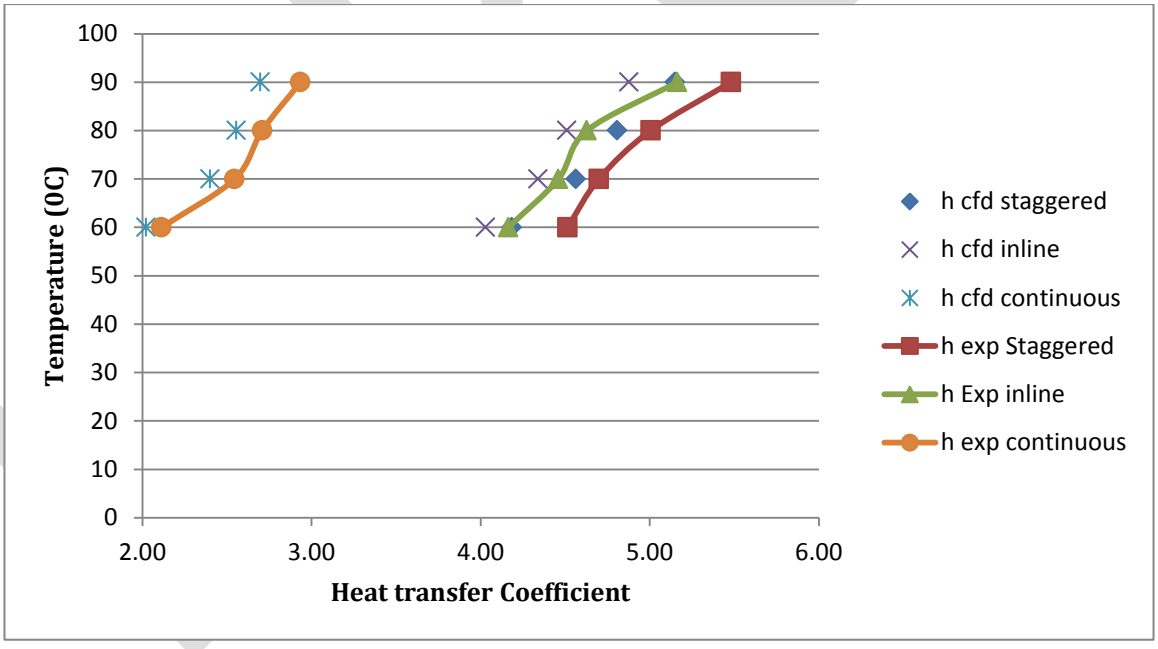

Figure 8 Experiment results of Heat transfer coefficient for continuous, inline, and staggered interrupted fins.

In order to validate the cfd simulation results, Experiment study was carried out by maintaining the same operating conditions. As can be seen from the figure 7 & 8 experiment results are in good agreement with the cfd results with maximum deviation of 10%.

CONCLUSION

- Staggered interrupted fin arrangement and in-line interrupted fin arrangement provided better heat transfer rate in comparison with the continuous fin arrangement.
- In the present operating conditions and for this staggered interrupted pattern of fin arrangement, the thermal performances of the staggered interrupted fins were found to be better.
- The numerical predictions were in good agreement with the experimental results for the operating conditions that was considered for this investigation.

REFERENCES:

1) MehranAhmadi, GolnooshMostafavi, MajidBahrami, "Natural Convection from Rectangular Interrupted Fins" International Journal of Thermal Sciences (2014) pp 62-71.
2) MehranAhmadi, GolnooshMostafavi, MajidBahrami, "Natural Convection from Interrupted Vertical Walls" Journal of Heat Transfer November 2014, vol. 136 / 112501-1.
3) G. A. Ledezma, A. Bejan "Optimal Geometric Arrangement of Staggered Vertical Plates in Natural Convection" Journal of Heat Transfer November 1997, vol. 119/701
4) G. Guglielmini, E. Nannei, G. Tanda "Natural convection and radiation heat transfer from staggered vertical fins" International Journal of Heat Mass Transfer vol 30, No 9, pp-1941-1948,1987.
5) Ashish Mahalle, Mangesh D. Shende 'Numerical analysis of natural convection heat transfer from a radial heat sink', International Journal of Innovative and Emerging Research in Engineering Volume 2, Special Issue 1 MEPCON 2015
6) Ashish Mahalle, Mangesh D. Shende 'Cooling Of Electronic Equipments with Heat Sink: A Review of Literature' IOSR Journal of Mechanical and Civil Engineering (IOSR-JMCE) e-ISSN: 2278-1684 Volume 5, Issue 2 (Jan. - Feb. 2013), PP 56-61
7) Dr. Ashish Mahalle, Mangesh D. Shende 'Natural convection heat transfer from a radial heat sink with Horizontal rectangular fins' International Journal of Innovative Research in Advanced Engineering (IJIRAE) ISSN: 2349-2163 Volume 1 Issue 8 (September 2014)

International Journal of Engineering Research and General Science Volume 3, Issue 6, November-December, 2015
ISSN 2091-2730

STUDY ON COMBINATION OF ADSORPTION AND BIODEGRADATION FOR TREATING TEXTILE DYE EFFLUENT

Dr. K. BALAJI, M.E, Ph. D*, V. KRISHNARAJ**

*Assistant Professor**,** Department of Civil Engineering.

**Student, Department of Civil Engineering Annamalai University

Annanmalai Nagar-608002 , Tamil Nadu, India.

**E-mail= royalkingofkrish@gmail.com

Abstract -The objective of this study was to investigate the feasibility of using a Granular activated carbon-biofilm configured anaerobic fluidized bed reactor for treating textile dye effluent Textile dye effluent may include many types of dyes, detergents, insecticides, pesticides, grease ,oils, sulphide compounds, solvents, heavy metals, inorganic salts, and fibers. In amounts depending on the processing regime. Color removal of effluent from the textile dyeing and finishing operation is becoming important because of environmental concerns. Various physico-chemical, biological processes and usually a combination of processes are applied to treat them to meet regulatory discharge limits. In this study combination of adsorption and biodegradation of textile dye effluent in anaerobic fluidized bed reactor was tried to study the performance of the designed reactor for treating textile dye effluent.

Keywords: Colour, Decolourisation, Adsorption, Biodegradation, Fluidized Bed Reactor, COD, HRT

1. Introduction

The textile dyeing waste water contains dyes of various intense colours. The coloured wastewater of dyeing processes is not merely aesthetically objectionable. colour can interrupt photosynthesis and lower the dissolved oxygen content of receiving water bodies, which may lead to killing of fish. Color removal of effluent from the various physico-chemical advanced oxidation, biological processes, and usually a combination of processes are applied to treat them to meet regulatory discharge limits (Banat *et al*., 1996). Anaerobic digestion of textile wastewater is a promising technique becauseit is cost-effective and environmentally safe. dyes decompose under anaerobic condition due to the cleavage of the bond remove the color of the wastewater. The reduction products (aromatic amines) should then be further treated using aerobic biological treatment methods (Chung *et al*., 1978; Ong *et al*., 2005; Luangdilok and Panswad, 2000; Bromley-Challenor *et al*., 2000; Kudlich *et al*., 1996). Color removal under anaerobic condition by biodegradation of dyestuff by azoreductase activity (Idaka *et al*., 1987; Dubin and Wrigth, 1975) and nonenzymatic azo reduction of dyestuff (Chung *et al*., 1992; Carliell *et al*., 1995; Flores *et al*., 1997). In recent years, immobilization of microbial cells has received increasing interest in the field of wastewater treatment. the immobilized microbial systems greatly improve bioreactor efficiency. For instance, increasing process stability and tolerance to shock loadings, allowing higher treatment capacity per unit biomass and generating relatively less biological sludge. Immobilized cells systems have the potential to degrade toxic chemicals faster than conventional wastewater treatment systems (Yang *et al*., 1995; Zhou and Christopher *et al*., 2002; Ong *et al*., 2007). The objective of this study was to investigate the feasibility of using granular activated carbon (GAC)-biofilm configured.Anaerobic fluidized bed reactor treating textile dye effluent

2. Materials and Methods

2.1. Experimental Set Up

The experimental setup consists of a fixed film anaerobic fluidized bed reactor having an effective volume of 0.02m3. The specification of the experimental set up is given in Table.1. And schematic is shown in **fig1**

2. 2. Start-up Process

The experiment was initiated with the feeding of domestic wastewater for the acclimatization process. After attaining the steady state condition within 30 days.Real textile dye effluent was fed into the reactor for further acclimatization for the real time run After attaining 80% efficiency with the real textile effluent of COD concentration of 1110 mg/l synthetic textile effluent was fed with various concentration

2.3. Experimental Run

The operational parameters were the HRT and COD. The experiment was run for five different COD concentrations of 1000mg/L, 1250mg/L, 1500mg/L and 2000mg/L. The operational parameters HRT were varied as 24 hrs, 18 hrs, 12 hrs and 6 hrs for each COD concentration subsequently. With respect to the COD concentrations Samples were collected regularly according to the HRT varying period from inlet and outlet for the analysis. The evaluation is based on the %COD removal

2.4Analytical Methods

Samples were collected from the inlet and outlet of the reactor at 24hrs, 18hrs, 12 hrs and 6 hrs for each COD concentrations of 1000 mg/L, 1250 mg/.L, 1500mg/L and 2000mg/L for the analysis. COD was measured by the closed reflux method

% COD Removal = $\frac{A-B}{A}$ **χ 100.. (1)**

Where,

A = Inlet COD
B = Outlet COD

2.5 Fluidized bed reactor

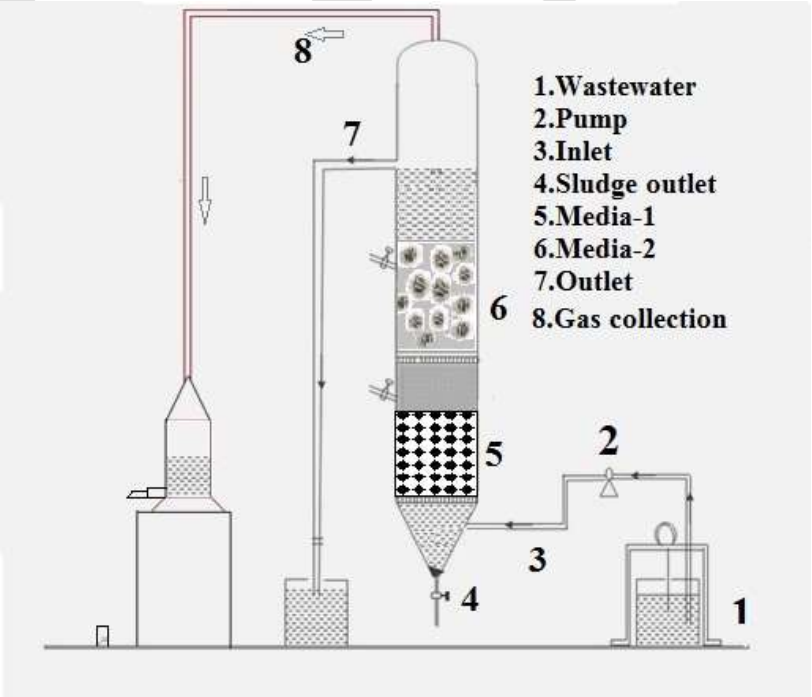

Fig 1 Schematic of fluidized bed reactor

2.6 Table 1: Physical features and process parameters

S.No	Specifications	Details
1.	Volume of Reactor	0.03m3
2.	Effective volume of Reactor	0.02 m3
3.	Diameter of Reactor	0.15 m
4.	Height of Reactor	1.42 m
5.	Effective height of Reactor	1.17 m
6.	Pump used for the influent feed	Peristaltic Pump PP-15 model (Miclin's Product).
7.	Media 1Packed, Size	Activated carbon ,4x8mm
8.	Media 2 Packed, Size	Fujino Spirals, (PVCmaterial),16 mm
9.	Specific area of filling media 1	$900m^3/g$
10.	Specific area of filling media 2	$500m^2/m^3$
11.	Void ratio of the media 1	85%
12.	Void ratio of the media 2	87%
13.	Material of the reactor	Plexi glass

3. Results and Discussion

The graph-1 shows the overall performance of the anaerobic fluidized bed reactor combined with adsorption and biodegradation the maximum COD removal of 95 %, 91%, 86%, and 81% for the COD concentrations of 1000mg/L, 1250mg/L, 1500mg/L and 2000 mg/L at 24 hrs HRT respectively. from the result it is clearly understood that the %COD reduction is directly proportional to the HRT Above 80% of COD removal is attained for the optimum 18 hrs HRT itself for the cod concentration of 1000 mg/l, 1250 mg/l and 1500 mg/l.

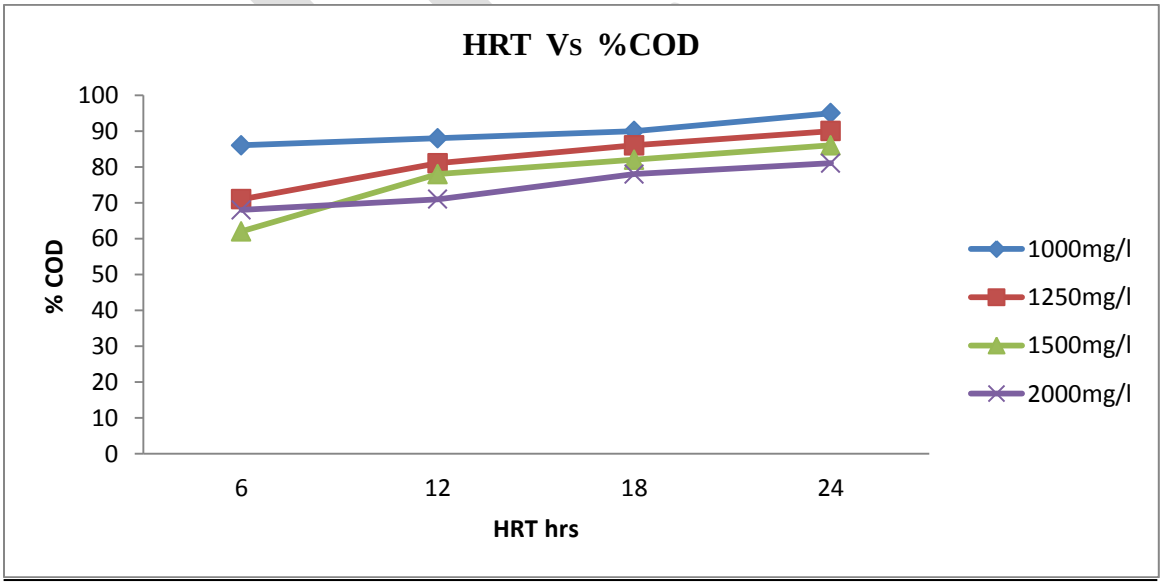

Graph: 1 HRT vs. %COD Removal

Conclusion

The designed Anaerobic Fluidized bed reactor combined with adsorption and biodegradation was found to be more effective in treating the textile dyeing effluent for a maximum COD removal of 95% for a COD concentration of 1000mg/L for 24 hr HRT and minimum COD removal of 68% for a COD concentration of 2000mg/L for 6 hr HRT

REFERENCES:

[1] Banat I M, Nigam P, Marchant R, Singh D I, 1996. Microbial decolorization of textile-dye containing effluents: a review. *Bioresource Technol*, 58: 217–227.

[2] Bromley-Challenor K C A, Knapp J S, Zhang Z, Gray N C C, Hetheridge M J , Evans M R, 2000.Decolorization of an azo dye byunacclimatedactivated sludge under anaerobic conditions. *Watert Res*,34(18): 4410–4418.

[3] Carliell C M, Barclay S J, Naidoo H, Buckley C A, Mulholland D A,Senior E, 1995. Microbial decolorization of a reactive azo dyesunder anaerobic conditions. *Water SA*, 21: 61–69.

[4] Christopher J, Owen P W, Ajay S, 2002. Biodegradation of dimethyl phthalate with high removal rates in a packed-bed reactor. *World J Microbiol Biotechnol*, 18: 7–10.

[5] Chung K, Fulk B B E, Egan M, 1978. Reduction of azo dyes by intestinal anaerobes. *Appl Environ Microbiol*, 35: 558–562

[6] Chung K T, Stewans S E, Carniglia E C, 1992. The reduction of azo dyes by the intestinal microflora. *Crit Rev Microbiol*, 18: 175–190

[7] Dubin P, Wrigth K L, 1975. Reduction of azo food dyes in cultures of *Proteus vulgaris*. *Xenobiotica*, 5: 563–571.

[8] Flores E R, Luijten M, Donlon B, Lettinga G, Field J, 1997 Biodegradation of selected azo dyes under methanogenic conditions. *Water Sci Technol*, 36: 65–72.

[9] Idaka E, Horitsu H, Ogawa T, 1987. Some properties of azoreductase produced by *Pseudomonas cepacia*. *Bull Environ Contam Toxicol*,39: 982–989.

[10] Kudlich M, Bishop P L, Knackmuss H J, Stolz A, 1996. Simultaneous anaerobicand aerobic degradation of the sulfonated azodye mordant yellow 3 by immobilized cells from a naphatlenesulfonate-degrading mixed culture. *Appl Microbiol Biotechnol*, 46:597–603

[11] LuangdilokW, Panswad T, 2000. Effect of chemical structures of reactivedyes on color removal by an anaerobic-aerobic process. *Water Sci Technol*, 42(3-4): 377–382.

[12] Ong S A, Toorisaka E, Hirata M, Hano T, 2007. Granular activated carbon-biofilm configured sequencing batch reactor treatment of C.I. Acid Orange 7. *Dyes and Pigments*, 76 (1): 142–146.

[13] Yang P Y, Nitisoravut S, Wu J Y S, 1995. Nitrate removal using a mixed cultureentrapped microbial cell immobilization process under high salt conditions. *Water Res*, 29(6): 1525–1532.

[14] Zhou G M, Herbert H P F, 1997. Anoxic treatment of low-strength wastewater by immobilized sludge. *Water Sci Technol*, 36(12): 135–141.

[15] APHA (2005), Standard methods for the Examination of water and wastewater

International Journal of Engineering Research and General Science Volume 3, Issue 6, November-December, 2015
ISSN 2091-2730

THEORETICAL ANALYSIS OF SOIL NAILING: DESIGN, PERFORMANCE AND FUTURE ASPECTS

Piyush Sharma

Department of Civil Engineering, Amity School of Engineering & Technology

Amity University, Haryana, India

Email: piyushsharma1015@gmail.com, Contact No. 9711037497

Abstract- Soil stabilization is a general term for any physical, chemical, biological, or combined method of changing a natural soil to meet an engineering purpose. This process includes increasing the weight bearing capabilities and performance of in-situ soil and sand. Soil nailing is a construction technique that can be used as a remedial measure to treat unstable natural soil slopes or as a construction technique that allows the safe over-steepening of new or existing soil slopes. The technique involves the insertion of relatively slender reinforcing elements into the slope – often general purpose reinforcing bars (rebar) although solid or hollow-system bars are also available. Kinetic methods of firing relatively short bars into soil slopes have also been developed. Bars installed using drilling techniques are usually fully grouted and installed at a slight downward inclination. Soil nail components may also be used to stabilize retaining walls or existing fill slopes like embankments and levees and this is normally undertaken as a remedial measure. Since the first application of soil nailing was implemented in 1972 for a railroad widening project in France, soil nailing is now a well-established technique around the world.

Keywords- soil stabilization, soil nailing, design aspects, necessity, performance of soil, soil properties. applications.

1. INTRODUCTION

1.1. General Analysis

The main points to be considered in determining if soil nailing would be an effective retention technique are as follows:-

First, the existing ground conditions should be examined. Next, the advantages and disadvantages for a soil nail wall should be assessed for the particular application being considered. Then other systems should be considered for the particular application. Finally, cost of the soil nail wall should be considered.

Soil nail walls can be used for a variety of soil types and conditions. The most favorable conditions for soil nailing should be follow before starting any operation of soil nailing and they are:

- The soil should be able to stand unsupported one to two meters high for a minimum of two days when cut vertical or nearly vertical.
- Also all soil nails within a cross section should be located above the groundwater table. If the soil nails are not located above the groundwater table, the groundwater would negatively affect the face of the excavation i.e. the bond between the ground and the soil nail itself.

Based upon these "favorable conditions" for soil nailing stiff to hard fine-grained soils which include stiff to hard clays, clayey silts, silty clays, sandy clays, and sandy silts are preferred soils. Sand and gravels which are dense to very dense soils with some apparent cohesion also work well for soil nailing. Weathered rock is also acceptable as long as the rock is weathered evenly throughout. Finally, glacial soils work well for soil nailing.

A list of "unfavorable or difficult soil conditions" for soil nailing can include dry, poorly graded cohesion-less soils, soils with a high groundwater table, soils with cobbles and boulders, soft to very soft fine-grained soils, highly corrosive soils, weathered rock with unfavorable weakness planes, and loess. Other difficult conditions include prolonged exposure to freezing temperatures, a climate that has a repeated freeze-and-thaw cycle and granular soils that are very loose.

1.2 Design Philosophies

After a preliminary analysis of the site, initial designs of the soil nail wall can be begin. This begins with a selection of limit states and design approaches. The two most common limit states used in soil nail wall design is strength limit and service limit states. The strength limit state is the limit state that addresses potential failure mechanisms or collapse states of the soil nail wall system. The service limit state is the limit state that addresses loss of service function resulting from excessive wall deformation and is defined by restrictions in stress, deformation and facing crack width under regular service conditions. The two most common design approaches for soil nail walls are limit state design and service load design.

Initial design considerations include wall layout (wall height and length), soil nail vertical and horizontal spacing, soil nail pattern on wall face, soil nail inclination, soil nail length and distribution, soil nail material and relevant ground properties. With all these variables in the mind of the design engineer the next step is to use simplified charts to preliminarily evaluate nail length and maximum nail force. Nail length, diameter and spacing typically control external and internal stability of the wall. These parameters can be adjusted during design until all external and internal stability requirements are met. After the initial design is completed, final design progresses where the soil nail wall has to be tested for external and internal failure modes, seismic considerations and aesthetic qualities. Drainage, frost penetration and external loads such as wind and hydrostatic forces also have to be determined and included in the final examination of the design. Soil nail walls are not ideal in locations with highly plastic clay soils. Soils with high plasticity, a high liquid limit and low undrained shear strengths are at risk of long-term deformation (creep).

1.3 Construction Procedure

With the design complete, construction is the next step. Most soil nail wall construction follows a specific procedure. First a cut is excavated and temporary bracing is put in place if necessary. This is done with conventional earth moving equipment and hydraulic drills. Next, holes for the soil nails are drilled at predetermined locations as specified by the design engineer. The equipment used for this step is dependent on the stability of the material in which the soil nail wall is supporting. Rotary or rotary percussive methods using air flush or dry auger methods can be used with stable ground. For unstable ground, single tube and duplex rotary methods with air and water flush or hollow stem auger methods are used. With the holes drilled, the next step is to install and grout the nails into place. After all nails are inserted, a drainage system is put into place. Synthetic drainage mat is placed vertically between the nail heads, which are extended down to the base of the wall where they are most commonly connected to a footing drain. A layer of shotcrete is applied and bearing plates are installed before a final facing is put in place to complete the soil nail wall. Variations of the steps described above may be necessary to accommodate additional preparation tasks or supplementary activities for specific project conditions.

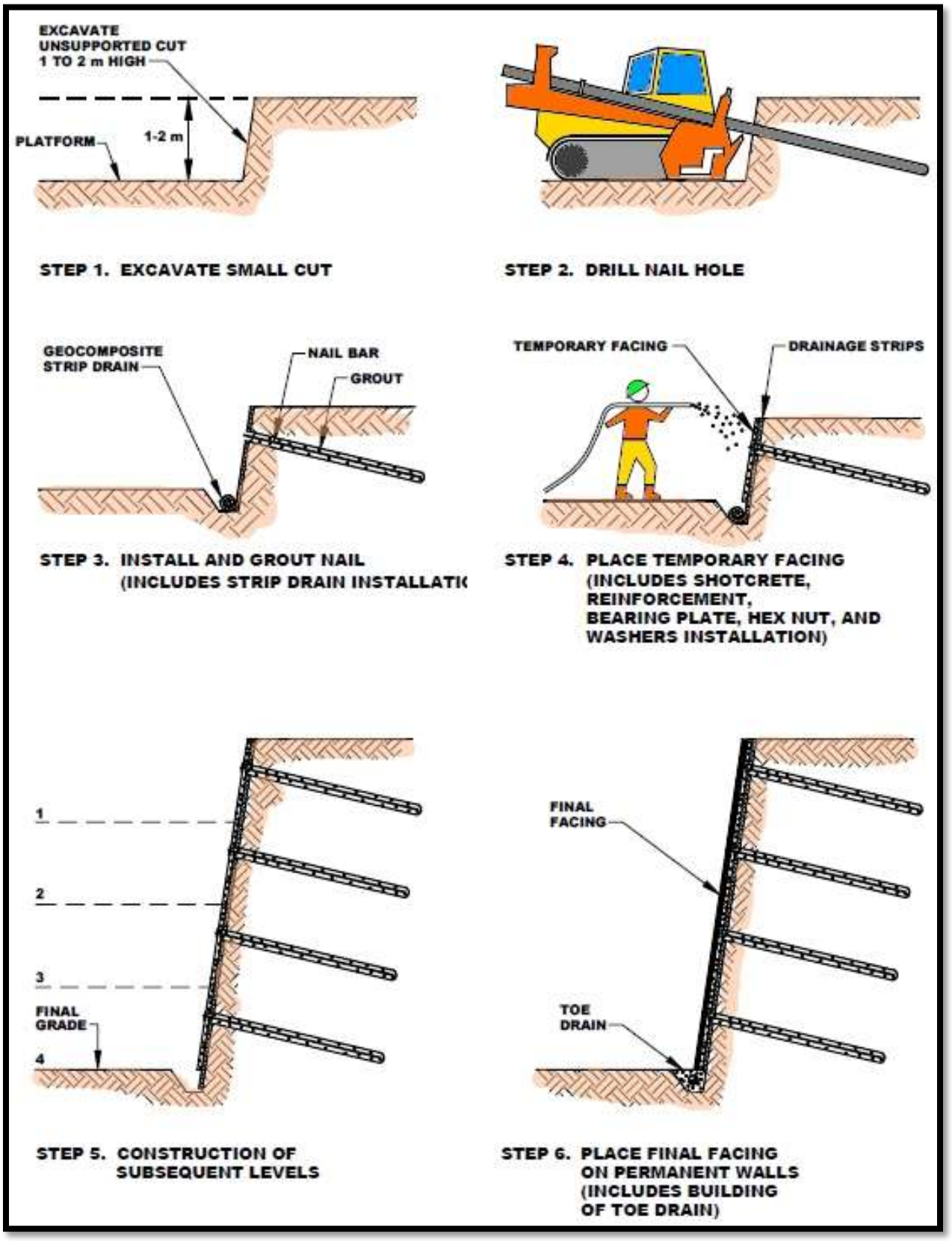

Figure1: Step by step procedure of soil nailing

1.4 Performance Evaluation

Inspection activities play a vital role in the production of high-quality soil nail walls because conformance to project plans and specifications should result in a soil nail wall that will perform its intended duty for its designed duration. Inspections usually involve evaluation of the following: conformance of system components to material specification, conformance of construction methods to execution specifications, conformance to short-term performance specifications, and long-term monitoring. Short-term performance specifications are checked with loads tests, which utilize hydraulic jacks and pumps to perform several load applications. Three common load tests for short-term performance are verification or ultimate load tests, proof tests and creep tests. Verification or ultimate load tests are conducted to verify the compliance of the soil nails with pullout capacity and strengths resulting from the contractor's installation method. Proof tests are intended to verify that the contractor's construction procedure has been consistent and that the nails have not been drilled and grouted in a soil zone not tested in the verification stage. Creep tests are performed to ensure that the nail design loads can be safely carried throughout the structure's service life.

Long-term performance monitoring is used to collect data to ensure adequate performance and refine future design practices. Parameters to be measured include vertical and horizontal movement of the wall face, local movements or deterioration of facing elements, drainage to the ground, loads, load distribution and load changes in the nails, temperature and rainfall. These parameters are measured using several specific tools including inclinometers, load cells and strain gauges.

1.5 Soil Nail Installation Process

Soil nail provides a resisting force against slope failures. Its construction process is faster than other similar methods. The construction procedure starts, drilling into the soil, where the nail, steel bar, is going to be placed. After the drilling has been completed, exact depth must be provided by the geotechnical engineer, the nail must be inserted into the drilled hole. Then, it must be grouted into the soil to create a structure similar to a gravity wall. After placing the nail, a shot-Crete layer is usually placed as a facing material, to protect the exposed nail, and then other architectural options are placed over the shot-Crete, creating an aesthetic finish to the project. Steel tendons typically used for drill-and-grout soil nails usually consist of 0.8 to 2.0 inch bars with yield strength in the range of 60 to 72 Ksi. Drainage is a critical aspect of soil nail wall construction. Face drainage is virtually always used with permanent walls, and very commonly used with temporary walls. Face drainage usually consists of synthetic drainage elements placed between the shot-Crete and the retained soil, and may be typically 8 to 12 inches wide synthetic strips or perforated pipes. The grouted soil nail hole typically has minimum diameter of 4 inches. Centralizers are placed around the soil nail to maintain an even thickness of grout around the bar. For permanent applications, nails may be epoxy-coated or provided with a protective sheath for corrosion protection. Soil Nailing is not recommended to use on clayey soils, and or clean sands where the cohesion of the soil is minimum.

Figure 2: Actual picture of soil nailing in hill slope

1.6 Advantages

Soil nailing has been used regularly over the last few years over traditional cut retaining walls due to several reasons:-

1. It is ideal for tight spaces.
2. It can be used in irregular shapes.
3. Less noise and fewer traffic obstructions.
4. Less impact on surrounding areas.
5. Minimum shoring is required.
6. Lower load requirements than tieback anchors systems.
7. Eliminates the time and expense of placing steel piles.
8. Can be used to repair other existing wall systems.
9. It can be used on new constructions, as temporary structures or on remodeling process.
10. Wall height is not restricted.
11. Reduce right-of-way requirements.

1.7 Limitations

1. In some instances soil might be overexposed prior to the installation of nail.
2. Sand and gravels might not be compatible with soil nailing.
3. Not recommended to use in high water table areas.
4. Soil nailing in very low shear strength soil may require a very high soil nail density.
5. Soil nailing in expansive soils and sensitive soils for permanent long term applications is not recommended.

2.0 SOIL NAILING TECHNIQUES AND TYPES

Soil nailing is a construction technique used to reinforce soil to make it more stable. Soil nailing is used for slopes, excavations, retaining walls etc. to make it more stable. In this technique, soil is reinforced with slender elements such as reinforcing bars which are called as nails. These reinforcing bars are installed into pre-drilled holes and then grouted. These nails are installed at an inclination of 10 to 20 degrees with vertical. Soil nailing is used to stabilize the slopes or excavations where required slopes for excavation cannot be provided due to space constraints and construction of retaining wall is not feasible. It is just an alternate to retaining wall structures. As the excavation precedes, the shotcrete, concrete or other grouting materials are applied on the excavation face to grout the reinforcing steel or nails. These provide stability to the steep soil slope. Soil nailing technique is used for slopes or excavations alongside highways, railway lines etc.

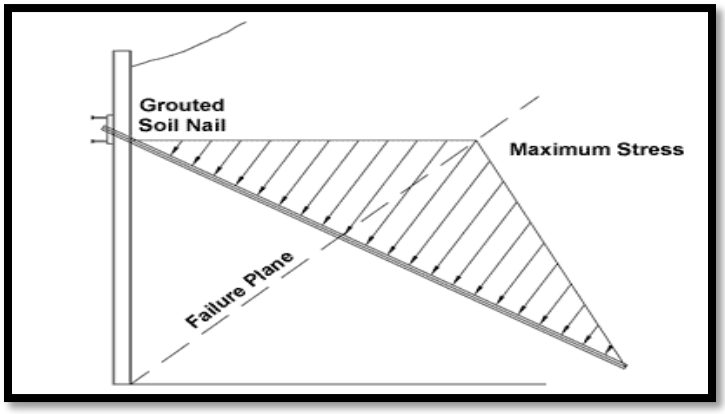

Figure 3: Stress distribution of soil nail

Types of Soil Nailing

There are various types of soil nailing techniques:

1. Grouted Soil Nailing

In this type of soil nailing, the holes are drilled in walls or slope face and then nails are inserted in the pre-drilled holes. Then the hole is filled with grouting materials such as concrete, shotcrete etc.

2. Driven Nails

Driven nailing is used for temporary stabilization of soil slopes. In this method, the nails are driven in the slope face during excavation. This method is very fast, but does not provide corrosion protection to the reinforcement steel or nails.

3. Self drilling Soil Nail

In this method, the hollow bars are used. Hollow bars are drilled into the slope surface and grout is injected simultaneously during the drilling process. This method of soil nailing is faster than grouted nailing. This method provides more corrosion resistance to nails than driven nails.

4. Jet Grouted Soil Nail

In this method, jets are used for eroding the soil for creating holes in the slope surface. Steel bars are then installed in this hole and grouted with concrete. It provides good corrosion protection for the steel bars (nails).

5. Launched Soil Nail

In this method of soil nailing, the steel bars are forced into the soil with very high speed using compressed air mechanism. The installation of soil nails are fast, but control over length of bar penetrating the ground is difficult.

These points must be noted for installation of soil nails

1. Soil Nails must penetrate beyond the slip plane into the passive zone typically for 4 to 5m.
2. The spacing of soil nails in horizontal or vertical direction must be related to strength of the soil. Extra soil nails should be installed at the edge of any surface being stabilized.
3. Soil nailing should start immediately after excavation.
4. Any delay in nailing may lead to collapse of soil slope.

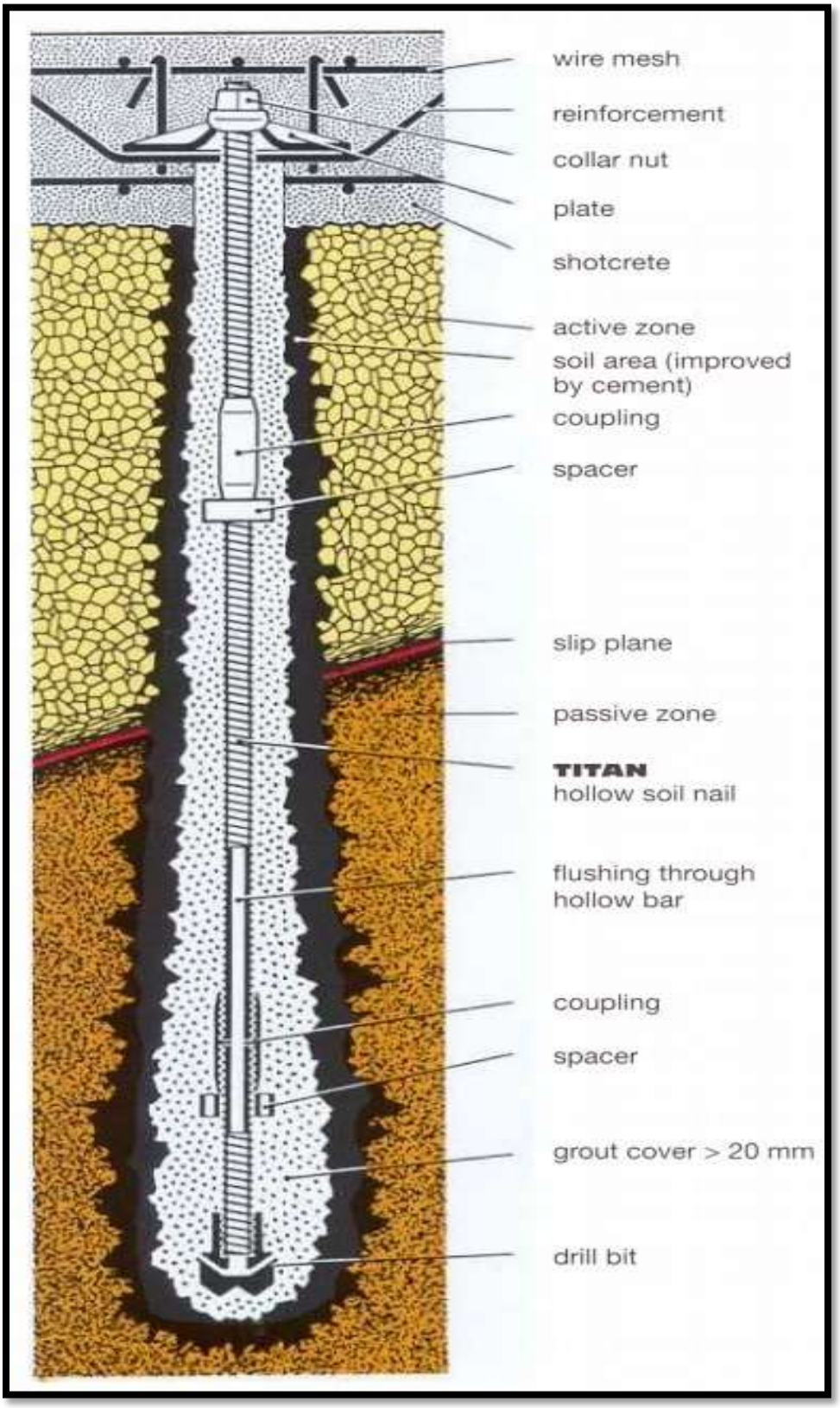

Figure 4: Soil nailing details

2.1 Protection of Nailed Structure

1) Corrosion Protection

Soil nails can be protected against corrosion in a variety of ways suitable for both temporary (24 months) and permanent (>24 months) applications.

2) Bare bar in cement grout

Cement grout alone can be used for corrosion protection of temporary soil nails and permanent nails in non-aggressive ground, provided the thickness of the grout cover exceeds 1-1/2" (38 mm).

The Drill bar system is ideally suited for temporary soil nails, particularly in non-cohesive soils.

3) Sacrificial steel

Steel elements of the soil nail system can be oversized to allow for loss of cross sectional area due to corrosion. The rate of corrosion shall be based on historical data for ground conditions with the same or lower level of aggressiveness. Additional factors of safety are recommended.

4) Hot Dip Galvanizing

Permanent soil nails in non-aggressive ground can be protected against corrosion by hot dip galvanizing in accordance with ASTM A-153. Hot dip galvanizing of GR150 bars requires specialized procedures to avoid hydrogen embrittlement.

5) Epoxy coating

Soil nails in non aggressive ground and temporary nails in aggressive ground can be protected against corrosion by epoxy coating in accordance with ASTM A-934 or ASTM A-775. Although ASTM A-934 has shown better performance than A-775 coating, it is not available in all areas. With this system, it is possible to epoxy coat the entire length of the bar. Oversized hardware is available to thread over a coating up to 40 mm thick. ASTM A-934 is usually purple or gray in color while ASTM A-775 is green in color.

6) Epoxy coated bar with partial or full DCP

Partial Double Corrosion Protection (DCP) protection over epoxy-coated bar provides additional protection in areas considered most corrosive. A bar that is epoxy coated over its entire length with a pregrouted plastic sheathing is often referred to as a triple corrosion protected soil nail. This type of corrosion protection is used in extremely aggressive environments.

7) Double Corrosion Protection - DCP

The most reliable corrosion protection for soil nails in permanent applications or for nails used in critical structures is to pregrout the nail in corrugated PVC or HDPE sheathing. The sheathing provides a watertight barrier. Tests have proven that the deformations of the THREADBAR limit crack width to 0.1 mm.

2.2 Various Issues Affecting Soil Nailed Slope

There are several factors that affect the feasibility and stability of soil nailing in slopes or excavations. As mentioned earlier, construction of soil nailing is subjected to favorable ground conditions. There are also various internal and global stability factors for soil nailed slopes.

Favorable Ground Condition: Soil nailing is well suited for Stiff to hard fine-grained soils which includes stiff to hard clays, clayey silts, silty clays, sandy clays, sandy silts, and combinations of theses. It is also applicable for dense to very dense granular soils with some apparent cohesion (some fine contents with percentage of fines not more than 10-15%). Nailing is not suitable for dry, poorly graded cohesion less soils, soils with cobbles and boulder (difficult to drill and increases construction cost), highly corrosive soil (involves expensive corrosion protection), soft to very soft fine grained soils, and organic soil. Soil nailing is also not recommended for soils with high ground water table.

External Stability: The external or global stability of nailed slope includes stability of nailed slope, overturning and sliding of soil-nail system, bearing capacity failure against basal heave due to excavation. Sometimes long-term stability problem also come into picture, e.g., seasonal raining. In such cases, though ground water table may be low, the seeping water may affect the stability of nailed slope without facing or proper drainage system.

Internal Stability: It comprises of various failure modes of nailed structure e.g. nail soil pull-out failure, nail tensile failure, and facing flexural or punching shear failure. Such issues may be overcome by conducting adequate ground investigation and geotechnical testing for identification of soil parameters and ground characterization and by performing in-situ test for soil nail interaction and nail strength.

2.3 Design Considerations

A soil-nailed system is required to fulfill fundamental requirements of stability, serviceability and durability during construction and throughout its design life. Other issues such as cost and environmental impact are also important design considerations.

Stability: The stability of a soil-nailed system throughout its design life should be assessed. The design of a soil-nailed system should ensure that there is an adequate safety margin against all the perceived potential modes of failure.

Serviceability: The performance of a soil-nailed system should not exceed a state at which the movement of the system affects its appearance or the efficient use of nearby structures, facilities or services.

Durability: The environmental conditions should be investigated at the design stage to assess their significance in relation to the durability of soil nails. The durability of a steel soil-nailed system is governed primarily by the resistance to corrosion under different soil aggressively.

Economic Considerations: The construction cost of a soil-nailed system depends on the material cost, construction method, temporary works requirements, build ability, corrosion protection requirements, soil-nail layout, type of facing, etc.

Environmental Considerations: The construction of a soil-nailed system may disturb the ground ecosystem, induce nuisance and pollution during construction, and cause visual impact to the existing environment. Appropriate pollution control measures, such as providing water sprays and dust traps at the mouths of drill holes when drilling rocks, screening the working platform and installing noise barriers in areas with sensitive receivers, should be provided.

CONCLUSIONS

Soil nailing is embraced by practicing engineers as a highly competitive well proven technique. Soil nailing has certain similarities to both reinforced earth and anchoring, although its particular operating principles and construction methods give it a firm and distinct identity. Similar considerations distinguish it from allied insitu soil reinforcing techniques such as reticulated root piles and soil dwelling. Most applications of soil nailing to date have been associated with new construction projects such as foundation excavations and slope stabilization, for both temporary and permanent works. The system has equal facility in a wide range of remedial projects, and indeed it is most likely that nailing will find its wide applications in the India in this field, bearing in mind the prevailing economic trends. It is to be hoped that the growth of the technique in India can be fostered by practical research collaborations between industry, the universities and government, in the manner of developed countries like France, Germany, United States of America and United Kingdom, who are the current leaders in this field.

ACKNOWLEDGEMENT

I would like to thank Prof. Meeta Verma, Prof. Sarah khan, Prof. Sakshi Gupta, Dr. D.K Singh, Prof. R.C Sharma and Prof. M.K Sinha for their valuable discussions on soil nailing design and construction.

REFERENCES:

[1] FHWA (2003), Soil NAIL walls, Geotechnical Engineering circular No 7, Report No FHWAO-IF-03-017, Federal Highway Administration.

[2] Juran I., Gerge.B.Khalid F. and Elias V. (1990a): "Kinematical Limit Analysis for Design of Soil Nailed Structures", J. of Geotechnical Engineering, ASCE, vol 116, No 1, pp. 54-71.

[3] Juran I., Gerge.B.Khalid F. And Elias V. (1990b): "Design of Soil Nailed Retaining Structures, Design and Performance of Earth Retaining structures"', J. of Geotechnical Engineering, ASCE, Vol 116 pp. 54-71.

[4] Guide to Soil Nail Design and Construction, Geotechnical Engineering office Civil Engineering and Development Department the Government of the Hong Kong Special Administrative Region.

[5] Soil Nailing for Stabilization of Steep Slopes near Railway Tracks, Prepared by Dr. Amit Prashant, Ms. Mousumi Mukherjee, Department of Civil Engineering Indian Institute of Technology Kanpur, Submitted to Research Designs and Standards Organization (RDSO), Lucknow

[6] Kramer, S.L. (2005). "Geotechnical Earthquake Engineering", Pearson Education, Singapore.

[7] Lazarte, C.A., Elias, V., Espinoza, R.D. and Sabatini, P.J. (2003). "Geotechnical Engineering Circular No. 7—Soil Nail Walls", Report FHWA0-IF-03-017, Federal Highway Administration, U.S. Department of Transportation, Washington, DC, U.S.A. 10.

[8] Matsui, T. and San, K.C. (1992). "Finite Element Slope Stability Analysis by Shear Strength Reduction Technique", Soils and Foundations, Vol. 32, No. 1, pp. 59–70. 11.

[9] Plaxis (2002). "PLAXIS 2D: Reference Manual, Version 8.0", Plaxis BV, Delft, The Netherlands.

International Journal of Engineering Research and General Science Volume 3, Issue 6, November-December, 2015
ISSN 2091-2730

Medical Waste Treatment And Management In Vietnamese Hospitals: Case Study In Thu Duc District Hospital 2015

Nguyen Thi Thanh Loan

The telephone number: +840906823813

Email address: 91101883@hcmut.edu.vn

ABSTRACT- Nowadays, besides the economic development, public health and health activities are concerned. In Vietnam, the number of hospitals and treatment requirements are increasing. Since 1997, the legal texts of hospital waste management are issued. Hospital operation is discharging a large amount of waste types, when not managed and handled efficiently, causing serious environmental pollution, effects on the patients, people living around the hospital. Thu Duc District Hospital is one of the major hospitals, in particular of Thu Duc District, in genetal of Ho Chi Minh City. The number of patient visiting for healthcare is increasing to 2,466 times/date. However, environmental management in the hospital has many drawbacks. This study assessed the hospital's medical waste management status quo (solid, liquid and gas emissions). Results showed that: the coordination in waste management between the functional departments and among employees is not unified; staff's awareness is not prescribed; the arrangement of medical garbages, hazardous waste, handling systems are not scienctifical and hygiene; the loss of solid medical waste is difficult to control (1,470 kg solid medical waste/day); passive in handling medical waste by no private incinerator but for centralized processing city. The study proposed solutions included: infection control, hospital sanitation; management measures: the law, policies and measures for planning, building management systems and measures for classifying, collecting, transporting, storing waste, environmental economic measures; technical measures: waste water treatment systems, solid waste, hazardous waste and emissions.

Keywords: management, medical waste, status quo, Thu Duc district hospital, treatment.

1. INTRODUCTION

Medical Waste

According to The Waste Management Regulations of Health issued with Decision No 2575/1999/QD-BYT dated 08/27/1999 of the Health Minister of Vietnam: medical waste is the waste generated in medical institutions, from health care activities, care, testing, prevention, research and training. Medical wastes may be in solid, liquid and gas. Hazardous medical waste contains: blood, body fluids, excretions; parts or organs of humans, animals, needles and other sharp instruments; pharmaceutical chemicals and radioactive substances for medical use. If the waste is not treatmented, it will cause harm to the environment and human health. So medical waste management should comply with regulations related to hazardous waste management.

In addition to medical waste, hospital waste generation was normal. This is waste not classified as hazardous waste, no cytotoxicity, no storage, special handling; the waste arising from the living area, office in the hospital: paper, plastic, food, bottles, waste water, waste water canteen, etc.

1.2 Thu Duc District Hospital

Thu Duc Hospital is located at 29, Phu Chau, Tam Phu, Thu Duc District, Ho Chi Minh City, Vietnam.

History is from Thu Duc District Health Center, was founded in 1997. After many changes, Thu Duc District Hospital was officially born on July 28/6/2007 [1].

After 8 years of establishment, Thu Duc District Hospital, in People's Committee of Ho Chi Minh City first ranked by the standards of the Ministry of Health by Decision No.5563/QD-Committee November 12, 2014 of the MPC rated hospital in Thu Duc Thu Duc District People 's Committee. Thu Duc Hospital Hospital Districts is the first district Hospital in Viet nam having first ranked [1].

2. Study methods

Methodology to assess the situation and propose solutions to waste management contributes hospital environment protection: study the correlation between the elements' concept, composition, causes and effects of waste disease library, understanding, awareness of hospital waste of personnel, in direct contact with hospital waste, from which to draw conclusions and propose effective management solutions.

Methodology overview document from data on hospital, inherit the information was available from the results of scientific research at home and abroad, through the thematic reports of the authorities and from the related sites are listed in the reference section.

Field survey methods, data collection and formal interviews: officers, employees, student interns, patients and patients' relatives through the questionnaire on the status of waste management in hospital.

Synthetic Methodology: based on aggregate data and information collected and compared with the standards and regulations for environmental management of the Vietnam Ministry of Health, Ministry of Natural Resources and Environment. On that basis, drawing conclusions about the current situation, assessing the impact of hospital waste to the environment, proposals, selection of measures to reduce pollution levels.

Assessment Method Comparison: to come up with the most effective measures.

3. Results and discussion

3.1 Medical Waste Classification

In addition to be sorted by Decision of the Viet Nam Minister of Health No.43/2007/QD-BYT November 30, 2007 promulgating the regulation on management of medical waste, divided in categories: infectious waste, hazardous chemical waste, radioactive waste, the pneumatic cylinder pressure, normal waste.

This paper sorting waste at a more detailed level in three types of waste water, waste gas and solid waste, as in Table 1 below:

Table 1. Classification of hospital waste

Type of waste		Arising Source
Waste water	Medical Waste water	The clinic, operating rooms, laboratories, testing, pasteurization room medical devices with high heat, a detergent, rinse the floor. This waste water contains bacteria, pathogens, blood, chemicals, solvents in pharmaceutical [2].
	Domestic wastewater	Toilet, kitchen, washing, washing machine or operate the systems, machines, toilets, septic tanks, hand wash of workers and hospital staff, dormitory, farmers diseases, medical visits, visits to clinic [2].
	Stormwater runoff	Being slightly polluted waters, established as clean compared to other waste water, but can be contaminated by pollutants in nature.
Emissions	Dust, traffic emissions	Ambulances, motorcycle, truck freight. Dust, dirt entrainment process at hospital staff, patients, etc.
	Vapours	Isoflurane (anesthesia), acetone, phenol, odor and organic solvents (alcohol, ether) to evaporate, etc.
	Exhaust gas generator	The pollutants from burning fuels affecting air quality surrounding environment.
	Emissions, odor solid waste incinerator Medical	The type of medical waste furnace, hazardous wastes are generated from emissions, cause negative impacts to the surrounding environment.
	Exhaust fumes, aerosols sewage system	The odorous gas NH_3, H_2S, etc (gas flow in an insufficient Aerotank, large water retention time causes anaerobic decomposition, etc).
	Exhaust fumes, odors surroundings	Garbage storage area, restroom areas, emissions from the cook at the kitchen area, laundry activities
	Roughly Emissions	The gases from air conditioning, electronic gases, smell from corpses, gas deodorizing machines
	Radiation	From X-ray rooms, CT Scanner, etc.

Solid waste	Domestic trash	The wards (except the isolation ward), from the medical professional activities as the plastic material, the fracture type cast in secret ... no blood and fluid biological and chemical risks hazardous waste generated from administrative work, paper, newspapers and documents, packing materials, cartons, plastic bags, film bags, external waste: leaves, garbage from the suburbs the scene in the hospital, microbial sludge from wastewater treatment systems, waste gas from the medical waste furnace [3].
	Medical trash	From active treatment, care, testing, prevention, research, training containing: blood, body fluids, secretions, body parts, needles and other sharp instruments, pharmaceuticals, chemicals, and radioactive materials used in medical ... [3]

3.2 Current situation and status quo of waste management, treatment assessment in the hospital

3.2.1 Structure of the administrative waste management

Nowadays, management structure arrays in hospital environments as Administration Department of Management and Infection Control room, the person responsible for supervision, signed the contract for transport of waste treatment is Chief Executive the Administration; who is responsible for reporting to the Department of Environment as Vice Division infection control, not knowledgeable experts in the environmental field.

The management of hospital waste subject to regulation by the Ministry of Health, there is no particular rules of the hospital.

3.2.2 Sanitation situation of hospital

The quality of the control environment, the Thu Duc hospital has good management practices:

- Planting trees shade the hospital campus.

- The room was adequate supply of electricity, water, sanitary gloves, brooms, buckets, antibacterial solution, etc

- There are enough garbage cans with lids, to the hallway and in the departments.

- Ceilings, walls, sills, door linings tiles, smooth materials dry, waterproof: disinfection of floors, toilets disinfected with sodium hypochlorite and effective solution dedicated Surfanios Anios, periodicals twice daily.

- Disinfection of air in the chamber and treatment with ultraviolet machine. Medical equipment, linens, blankets, etc are sterile cleaning regulations.

- The means of transport such as wheelchairs, chairs, etc were cleaned every day by chemical sterilization.

- Hospital laundry organize separate focus but member hospital clothes, clothes patient linens, clothing fabrics infectious ward.

- There are rules of hygiene clinical order, guiding patients and conducted the visiting room.

However, along the corridor still littering condition, in the area of hazardous garbage, wastes, office equipment were also indiscriminate disposal, not neat unsanitary.

3.2.3 Waste management test, monitoring and direction

The hospital was quick to disseminate knowledge, process classified waste collection to all health workers in hospitals, organizing training on hygiene, infection prevention and occupational safety for officers entire hospital staff periodically 2 times/year.

However, the issue of managing the amount of waste generated in these departments are not recognized in each department but recorded at the brothel before the Urban Environment Company to collect. These data protection by storing, previous statistics, new periodicals transferred to the Administrative Administrative room storage and handling.

3.2.4 Safety of waste management ensurement

- Fully equipped rubber gloves, face masks, antiseptic soap for employees. All working employees must abided by the regulations, if not to review an example, stricter sanctions prevent relapse later.

- Types of used rags, used in disease prevention, only used once.

- When out in the faculty to replace medical attire, discarding the equipment was used before leaving the work area and after they were contaminated.

- For the equipment and personal protective Used in the correct position prescribed disposal as trash, items stored for washing, disinfection and reused or destroyed.

- Wear the appropriate gloves when in contact with the waste is capable of various infections. If gloves are torn, peeling, perforation or contamination must be immediately replaced by another one completely intact.

- For other types of gloves can be used many times, it can be disinfected before reuse.

3.2.5 Hospital waste management

3.2.5.1 Solid waste

Process management in hospital solid waste has sequential phases: separation of waste at source, keeping in departments, collection and transport of the hospital's general store and the treatment final stage.

The number of bins for the garbage out at the hospital equipped with three types: small, medium, large. Each department equipped with 6 medium trash, in the aisles, in the hospital campus about 70 trash sized, 6 barrels with two orange external medical garbage and blue contained in municipal waste. Therefore, the total number of bins offer 90 faculties and 90 medical trash bins medium activity.

Particularly sharps containers as per cancellation needles, hospital purchasing large quantities on a quarterly basis ie 3 months/time, containers are transported only in the store when the number of syringes filled. At home use 6 barrels containing 240 liters large.

According to this statistics in hospital infection control, solid waste amount between 2011 and the first 6 months of 2015, increasing trend in recent years, as shown in the table 2 below:

Table 2. Solid waste quantity of Thu Duc district hospital from 2011 to 6 months of 2015

Years	Domestic solid waste quatity (ton/year)	Medical waste quantity (ton/year)
2011	318.485	134.453
2012	294.595	102.394
2013	302.827	123.485
2014	348.161	110.558

6th – 2015	190.58	73.434

Source: Thu Duc district hospital, 2015.

At the hospital the average amount of solid waste per day is about 1,470 kg, including medical waste of 408 kg accounted for 27.75%, the rest is municipal waste, data from Jan 1st 2015 to June 30th 2015.

Currently, the amount of waste generated in hospitals Managing Administration noted in the company kept the Urban Environment to transport the Binh Hung Hoa incinerator for disposal. Each time storehouses provide quality medical instruments to each department have signed confirmation, but the process used and discarded in each department has no specific recognition daily emissions. Therefor, the probable amount of the loss that hospital wastes could not be controlled.

- *Medical waste classification and collection at stationary sources*

Process medical waste classification has been elemented quite well:

- Each department is equipped with the nylon bag with color prescribed by the Viet Nam Ministry of Health: recyclables (white nylon), municipal waste (nylon blue), medical waste (yellow), junk risk harmful, swabs (black), sharps (needles destroying bottles).

- Each hospital trash is labeled as medical waste or domestic garbage, with foot pedal and always cleaned regularly.

- The bag is also clearly outlines inscription no storing beyond this line at 2/3 bag and stuck with symbols of hazardous if the hazardous waste.

Responsible for collecting and transporting garbage to the brothel by the sanitary staff team undertook a day between 2-3 employees. Time to organize collection and transport are clearly defined as 2 times/day, around 6:30 am, afternoon about 1h. In case of too much garbage collectors will conduct contrary provisions hours.

However, the collection process has some drawbacks:

- Many employees are unaware collection high in bringing labor protection because they feel encumbered, dyspnea collection operations.

- Trolley junk still quite full quality, no lid closed during transport.

- *Medical waste transportation*

- Due to the limited area of the hospital, so the entrance transport of medical waste from the hospital departments with integrated parking areas, paths through patient care areas and function rooms.

- Daily garbage collection are shipped on time as prescribed

- Staff nurse responsible for collection and transportation of garbage.

- When complete in every trash garbage, staff nurses are focused on the pillar pocket and fixed positions in each department after adequate room will begin shipping.

- *Solid waste storing*

- There carriage trails from outside.

- There shielding roof and chiller, divided into 2 parts: the container containing domestic trash and medical solid waste.

- Arrangement of 01 chiller to maintain a low temperature in the whole area of medical garbage. There is a wall, floor waterproofing; instrumentation, chemical toilet.

- The area is still insufficient to meet current trash.

Waste storage time in the hospital up to 24 hours, then will be taken and processed. However, public sector landfills to integrate as parking, no separate shielding fence, near the center and functional areas, where travel and convalescence of the patient; located near the tailgate garage company Urban Environment easily transportable, each day at 6 am.

3.2.5.2 Waste water

Sewer inspected regularly, regular maintenance 2 months/time, to avoid flooding, odors, leaks.

Wastewater generated current estimate is 270 m3/day, including waste water and domestic healthcare. Domestic wastewater has two categories: primary water distribution in the toilets, will be collected and put on the pedestal septic tank, medical waste from health care activities, water rinsing X-ray film, wastewater washing and hygiene and disease prevention; water after treatment is discharged common drainage system with water from the sink to wash, wash the floor and led to treatment station. Both types of waste water and health are separate pipeline system.

All waste water is transported along the tube put on the wastewater treatment system of the hospital after treatment to meet Level B Standard, will be discharged into the sewerage system of the region.

3.2.5.3 Emisions

Because the hospital is not builded solid waste incinerators and sewage system, virtually no rise in hospital pollutant emissions, mainly just waste gas, dust in the garage due to traffic flow in hospital.

3.2.6 Waste treatment Status quo

3.2.6.1 Solid waste

The highly infectious garbage always handled the early stages before disposal into bins and garbage bags:

- Hazardous medical wastes, contaminated Asoka is sterile and packed nylon laminated, clear labeling

- The chemical, pharmaceutical overdue return corresponding pharmaceutical companies.

- Pressure cylinder used hospital with very low numbers, about 1-2 times/year, also return the unit to purchase.

The hospital is currently processing contract with the company and Urban Environment City by mass processing.

Solid waste is collected and processed by the establishment of Ward Democratic Organization garbage.

Currently the hospital has stopped running medical waste incinerators by no funding, all medical waste is transported to Binh Hung Hoa for treatment. Almost of the hospitals in Ho Chi Minh City are now applying the process model of hospital groups solid waste treatment. Binh Hung Hoa incinerator is HOVAL GG42 capacity 7 ton/day of Belgium [4], as in Fig 1.

Incinerator use principle thermal pyrolysis effect. Incinerator 2 suites: Burners for gasification chamber, the second chamber combustion chamber gases generated from scratch. This is a static furnace, continuous operation, divided into 3 phases: loading garbage (8 hours), burning (8 hours), cooling (8 hours) [4].

Currently incinerators are in overload due to increased medical waste from hospitals is increasing. Therefore, if continued processing model for hospital groups, the City needed more investment incinerator operators to reduce overcrowding.

The model is as follows:

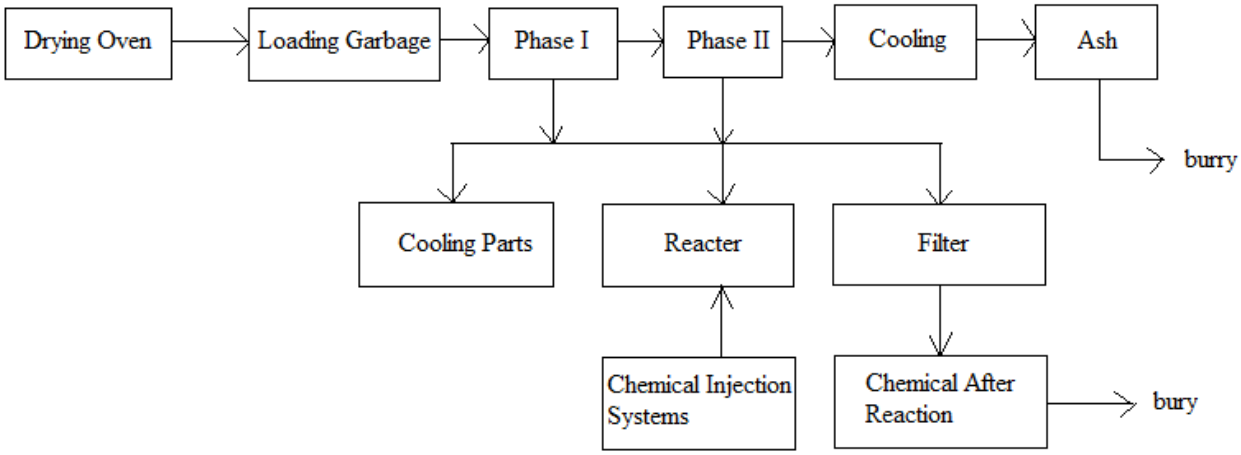

Fig 1. Diagram HOVALGG42 incinerator operation [5]

3.2.6.2 Waste water

Thu Duc District Hospital currently operates open sewage system: an old system biofilter technology 70 m3/day; Wastewater treatment systems New technology testing AAO operates from early 2015, the capacity of 300 m3/day 80% efficiency, output of waste water complies with national wastewater standards class B. The system is located far from medical care and function rooms.

The old system of wastewater into the street guide Tam Chau, the new system leads to Phu Chau Street.

4. Conclusion

Environmental quality controlment in Thu Duc District hospital has management measures but in some areas the inspection and supervision have not been closely interested. Therefore, these are solutions the hospital should element:

- Scrupulously comply with some laws, standards and national regulations: Decree No.59/2007/ND-CP on management of solid waste; Decree No.25/2013/ND-CP on environmental protection for waste water; Decision No.155/1999/QD-TTg dated 16/07/1999 of the Prime Minister promulgating the Regulation on management of hazardous waste; Joint Circular No.2237/1999/TTLT BKHCNMT-BYT dated 12/28/1999 guiding the implementation of radiation safety in healthcare; Decision No.3733/2002/QD-BYT-Standard occupational health-Ministry of Health; NTR 05:2013/BTNMT_National technical standards for environmental quality ambient air; NTR 28:2010/BTNMT_National technical standards for medical waste.

- Strengthening international cooperation with countries in the region and around the world. Positive scientific research, summarize and draw clinical experience, enlist the help of our partners, establish relationships for investment projects in

infrastructure, equipment and conservation hospital environment, prevent pollution and combat infectious and safety for healthcare workers.

- Promote cooperation and coordination between the head of management with the room, science; improving professional issues for the unit responsible for managing environmental issues for hospitals, strengthening the audit and strict handling of objects not abide by the rules of environmental protection, as in Fig 2.

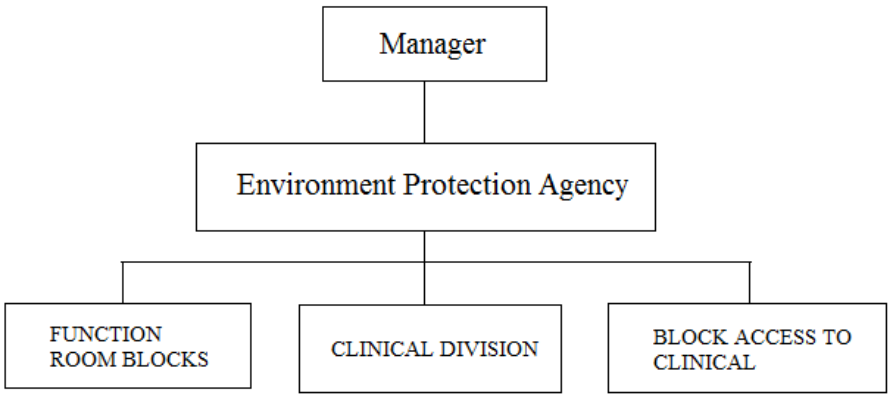

Fig 2. The administrative system for environmental management for Thu Duc District Hospital [6].

- Fix overlapping, vacant for some management areas, with reasonable assignment and close coordination between the departments in the organization of environmental protection activities.

The remedies exist in management, waste management of the hospital now:

- *Emission:*

- Organization of rational traffic management for the workers and employees, patients, family members or the transport vehicles and equipment materials for medical treatment.

- Regularly 2-3 guard duty promptly engaged traffic control during peak hours to avoid congestion in the hospital.

- Limit the time the engine vehicle in the hospital campus to avoid generation emissions, noise.

- *Wastewater*

- Regularly clean, because hospitals are concreted almost completely stagnant water should be avoided in the hospital campus.

- Implement the environmental monitoring program to monitor and evaluate the effectiveness of treatment promptly detect incidents.

- Strict management of the impact from the waste water to the area two function rooms, examination, treatment and convalescence.

- *Solid Waste*

- It should be clear statistical input and output numbers in the departments, and prevent leakage of waste is difficult to control.

- The garbage needs shielding fence, do not take advantage of the parking lot, located close to the wastewater treatment system, to organize well drained, avoid accumulation stench long days, often spraying all kinds mosquito repellent in appropriate dosage to prevent odors from being developed [7].

- Staff collected and transported to the complete protective equipment, compliance with regulations on the collection, transport medical solid waste.

- Strict management of the impact of pollution from the storage of hazardous waste, office waste too close to the area by functional departments and clinical areas.

- Strengthen waste reduction at source, recycling, reuse, select the product supply materials can be recycled safely.

- Due to insufficient funding hospital and under the guidelines of the process model medical solid waste current City and Binh Hung Hoa incinerators still operating well should medical solid waste hospital treatment can maintain this way.

ACKNOWLEDGMENT

The authors thank Thu Duc District Hospital, Administration Department of Management and Infection Control room, Department of Environment for figures and information provision.

REFERENCES:

[1] Thu Duc District Hospital. Thu Duc District Hospital, Quality - Sympathy - Worldwide advances. [Online]. Available http://benhvienthuduc.vn/2015/10/05/gioi-thieu-benh-vien-quan-thu-duc/

[2] Trần Mỹ Vy, "The situation and propose solutions assessment to manage medical waste in Hoc Mon District, Ho Chi Minh City", M.S thesis, Faculty of Environment, Hutech University, Ho Chi Minh City, Viet Nam, 2013.

[3] Lê Thiện Trí, "The current state of medical waste management survey and efficient solutions in the 115 People's Hospital, Ho Chi Minh City and offers". Ph.D thesis, Faculty of Environment, Hutech University, Ho Chi Minh City, Viet Nam, 2011.

[4] Lê Tam Tính, "The situation and propose solutions assessment for medical waste management in My Tho - Tien Giang Province hospitals". Thesis (Bachelor), Faculty of Environment, Hutech University, Ho Chi Minh City, Viet Nam, 2007.

[5] Trần Hữu Nam, "Medical waste incinerators system design for Tay Ninh province hospital". Thesis (Bachelor), Faculty of Environment, Hutech University, Ho Chi Minh City, Viet Nam, 2013.

[6] Dương Thị Phương Thảo, "Wastewater treatment systems Tu Du hospital calculation and design with capacity 770m3 / day". Thesis (Bachelor), Faculty of Environment, Hutech University, Ho Chi Minh City, Viet Nam, 2009.

[7] Đào Ngọc Phong et al., "Assessment of environmental pollution and transmitted diseases caused hospital wastewater in Hanoi", Ha Noi, Viet Nam.1998

International Journal of Engineering Research and General Science Volume 3, Issue 6, November-December, 2015
ISSN 2091-2730

Study of Dynamic Behaviour of Rail Track using Finite Element Method

Hasna P.H
KMEA Engineering College,
Kerala, India
hasna_786@ymail.com, +91 9995593565

Abstract—The track structures subjected to dynamic loading are usually constructed from different materials and components, their behaviour cannot be easily verified or predicted. The design, repair, and effective maintenance of tracks are therefore critical for ballasted track performance assessment. In this study, analytical evaluations were performed to predict and assess the track support stiffness, track impact factor, dynamic wheel-rail forces, and subgrade modulus. The prediction model consists of a three-degrees-of-freedom dynamic track model and modified track properties. The qualitative prediction of model for dynamic track behaviour, capable of simulating the complex interaction between the track's component properties and track responses, was developed in this study. The qualitative analysis results are presented for dynamic explicit analysis of the rail track.

Keywords— Ballasted Track, Solid 186, Track Modulus, Dynamic Load Factor, Static Analysis, Eigen Value Analysis & Dynamic Explicit Analysis

1. INTRODUCTION

Finite element models were developed to simulate the dynamic behaviour of rail track. These models were calibrated against experimental results performed by Mohammad Worya Khordehbinan[14].To simulate the dynamic behaviour of the experimental setup, a FE model was developed in a commercial FE analysis software package, ANSYS version 14.5The geometry of reference model is given below. The numerical model adopted is solid finite element (SOLID 186).

Parameter	Track system	Parameter	Track system
Sleeper moment of inertia (cm^4)	24200	Elastic modulus of bed (kg/cm^2)	1240
Rail moment of inertia (cm^4)	3950	Elastic modulus of Subballast (kg/cm^2)	1200
Ballast thickness (cm)	30	Elastic modulus of ballast (kg/cm^2)	2400
Subballast thickness (cm)	15.2	Elastic modulus of Sleeper (kg/cm^2)	2.07×10^5
Wheel load (Ton)	14.2	Elastic modulus of rail (kg/cm^2)	2.07×10^6
Sleeper length(cm)	260	Bed Poisson's ratio	0.4
Sleeper width(cm)	240	Ballast layer Poisson's ratio	0.4
Sleepers spacing (cm)	61	Sleeper Poisson's ratio	0.3
Rail area (cm^2)	86.5	Rail Poisson's ratio	0.25
Sub-ballast Poisson's ratio	0.3		

Table1: Track properties used for ANSYS modelling

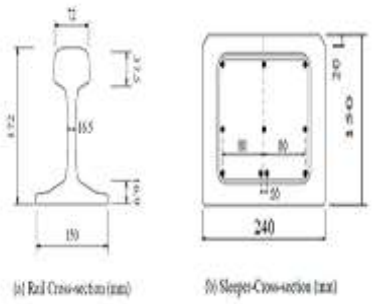

Fig 1: The Rail and Sleeper Cross-section

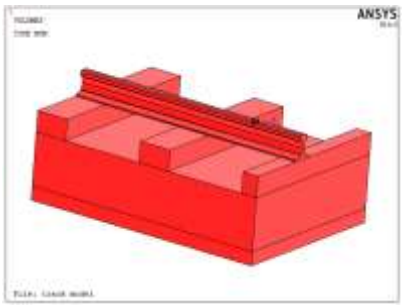

Fig 2: FE model of rail track in ANSYS

CALCULATIONS

Here the journal is based on Iranian railway. But practically we need to choose a railway standard which is having some similarity with Iranian railways. Here I'm choosing Indian railway.
As per the Indian Railway Dynamic load factor $Ø = 1+[V/(3*SQRT(U)]$
Where U is Track modulus its unit is (psi)
V is the train velocity in (mph) (adapted from Doyle (1980)

Sample calculation
1 M pa = 145.037798 psi
1 km/hr = 0.621371 mph
1 Ton = 9806.65002864 Newton
Track modulus U = 32 M pa = 4641.20 psi
Velocity V = 160 km/hr = 99.41936 mph
Dynamic load factor = $Ø = 1+[99.41936/(3*SQRT(4641.2)] = 1.486$
Quasi static force for 16 tonnes axle force = Dynamic load factor × 16 Tonnes = 1.486 × 16 = 23.776 Tonnes = **233162.91 N**

Track modulus (Mpa)	Dynamic load factor Ø		Quasi static force = Dynamic load factor ×axle load (Newton)			
	160 km/hr	100 km/hr	160 km/hr		100 km/hr	
			16 Tonnes	18 Tonnes	20 Tonnes	25 Tonnes
32	1.486	1.304	233162.914	262308.274	255757.432	319696.79
36	1.458	1.286	228769.531	257365.722	252227.038	315283.797
46	1.405	1.253	220453.492	248010.178	245754.649	307193.311
57	1.364	1.227	214020.329	240772.870	240655.191	300818.988

Table2: Effect of track modulus on maximum vertical

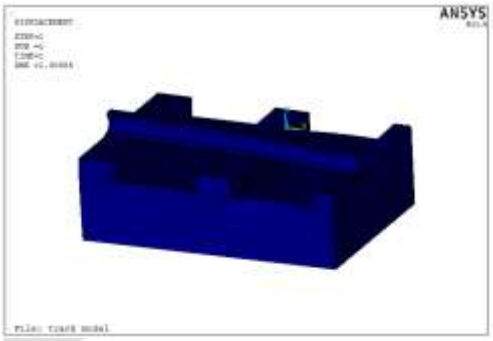

Fig 3: Deformed Shape

displacement of rail from test result

RESULTS

Track modulus (Mpa)	Maximum vertical displacement of rail (mm)			
	160 km/hr		100 km/hr	
	Maximum axle passing load		Maximum axle passing load	
	16 Tonnes	18 Tonnes	20 Tonnes	25 Tonnes
32	0.95338	1.07250	1.04580	1.30686
36	0.93541	1.05230	1.03130	1.28920
46	0.90141	1.01410	1.00490	1.25610
57	0.87510	0.98449	0.98401	1.23000

Table 3: Effect of change in track modulus on maximum vertical displacement of rail from ANSYS

Referring to Table 3, it is found that the values of dynamic load factor by finite element technique are almost near approaching the experimental results establishing the soundness of the analysis. The result obtained from ANSYS software is 1.30686 and the corresponding experimental value is 1.304 for a load of 25 tonnes. The variation between numerical result and experimental result is found to be 0.218 %. Hence it can be concluded that the elements, material properties and real constants provided in the analysis are in accordance with the experimental results.

2. Finite Element Analysis

The finite element analysis (FEA) is a computing technique that is used to obtain approximate solutions to boundary value problems. It uses a numerical method called finite element method (FEM). FEA involves the computer model of a design that is loaded and analysed for specific results, such as stress, deformation, deflection, natural frequencies, mode shapes, temperature distributions, and so on. The railway track was modelled and analysed using the finite element software ANSYS 14.5.

ANALYSIS TYPE

a. GENERAL STATIC ANALYSIS

The general static analysis can involve both linear and nonlinear effects and is performed to analyse static behaviour such as deflection due to a static load. A criterion for the analysis to be possible is that it is stable. A static step uses time increments, not in a manner of dynamic steps but rather as a fraction of the applied load. The default time period is 1.0 units of time, representing 100% of the applied load. The nonlinear effects are expected, such as large displacements, material nonlinearities, boundary nonlinearities, contact or friction. It is same as that in table 2 & table 3.

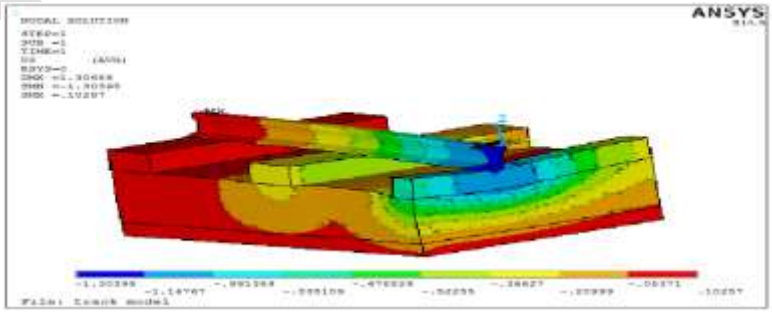

Fig:4 Stress Distribution

CONCLUSION

Conventional track calculations are based on the Static approach. The static analysis has been done for 16 cases. It has been analysed for track modulus 32Mpa, 36Mpa, 46Mpa, & 57Mpa for 16Tonnes, 18Tonnes, 20Tonnes & 25Tonnes at 160 km/hr & 100 km/hr respectively. It is found that the values of dynamic load factor obtained from the finite element analysis are almost near approaching to the calculated values of dynamic load factor. Thus the maximum vertical displacement of rail was obtained as 1.30686mm for the track modulus 32Mpa for 25Tonnes at a speed of 100 km/hr.

b. LINEAR EIGEN VALUE ANALYSIS

Linear eigenvalue analysis is used to perform an eigenvalue extraction to calculate the natural frequencies and corresponding mode shapes of the model.

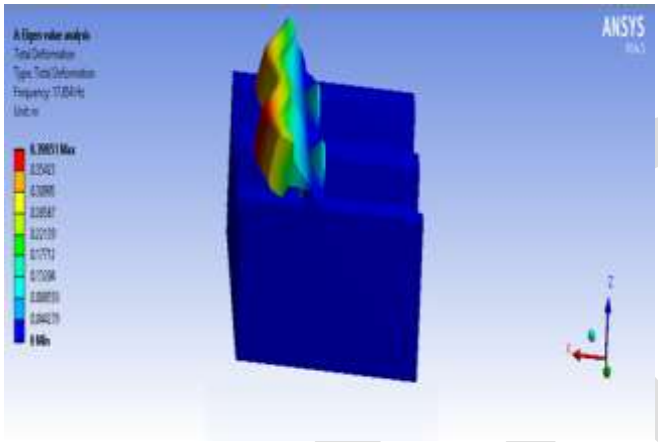

Fig 5: Mode Shape

Mode Numbers	Natural Frequency (Hz)
1	17.854
2	20.409
3	31.995
4	37.001
5	45.516
6	52.296

Table 4: Vibration modes and corresponding natural frequencies

CONCLUSION

Eigen value analysis of the rail track system gives a good picture on the stability of the system. It illustrates the impact of the system on the locations of the eigenvalues. From the above analysis we get different mode shapes and corresponding natural frequencies. Thus the rail track system should be so designed that it should not match with the above mentioned natural frequencies. Hence it shows the number of ways a rail can fail. The eigen value analysis not only depends on the properties of the system, but also on the components used, as well as on the type of software package used.

c. DYNAMIC EXPLICIT ANALYSIS

The design of products that need to survive impacts or short duration high pressure loadings can be greatly improved with the use of ANSYS explicit dynamics solutions. These specialized problems require advanced analysis tools to accurately predict the effect of design considerations on product response to severe loadings. Understanding such complex phenomena is especially important when it is too expensive — or impossible — to perform physical testing.

The ANSYS explicit dynamics product suite helps to gain insight into the physics of short duration events for products that undergo highly nonlinear, transient dynamic events. These specialized, accurate and easy to use tools have been designed to maximise productivity.

With the ANSYS explicit dynamics products, you can study how a structure responds when subjected to severe loadings. Algorithms based on first principles accurately predict responses, such as large material deformations and failure, and interactions between bodies and fluids with rapidly changing surfaces. Here ANSYS Auto-dyn is used for explicit analysis of the rail track.

In order to study the global response of the railway track system due to the passing train load, a new 3-D model was created in ANSYS Workbench, as shown in Figure 7. The model components are all the same as the model created in Figure 2 except the length of the railway track was doubled.

A conventional train model has been used as shown in Figure 6 According to the UIC Code, the technical specifications for Interoperability relating to rolling stock O_{BA} = 2.6 m and O_{BS} = 4.9 m were taken respectively. And the whole static loading condition

was demonstrated in Table 1. The diameter of the wheel is adopted as 625mm. Loads defined in a static step are directly applied at the joint between wheel and the axle of the wheel in order to find the dynamic effect on the rail.

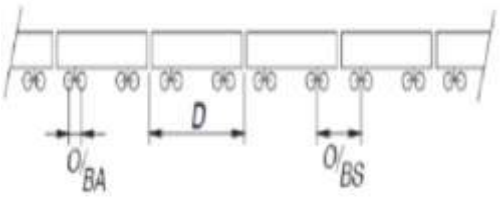

Fig 6: Conventional Train

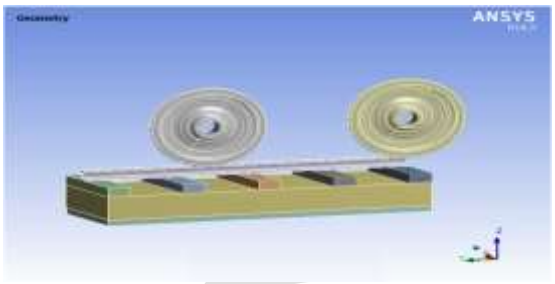

Fig 7: Geometry of the Rail Track Model

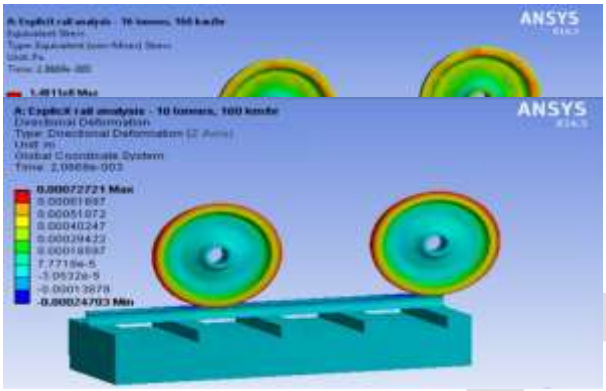

Fig 9: Directional Deformation

Fig 8: Equivalent Stress Distribution

F	Time (s)	Minimum Stress (Pa)	Maximum Stress (Pa)
	1.1755e-038	0.	0.
	1.5e-003	0.	2.2321e+008
	2.0669e-003	0.	1.4811e+008

Table 5: Equivalent Stress Distribution

Table 6: Directional Deformation about Z axis

Time (s)	Minimum Deformation (m)	Maximum Deformation (m)
1.1755e-038	0	0
1.5e-003	-1.1999e-004	6.9383e-004
2.0669e-003	-2.4703e-004	7.2721e-004

CONCLUSION

Table 5 and 6 shows the results obtained for the analysis of Equivalent (Von Mises) Stress and Directional Deformation in Z axis respectively. The explicit dynamic analysis has been done for a load of 16 tonnes at a speed of 160km/hr for 0.0020669 seconds. A nonlinear stress variation was obtained. While in the case of directional deformation in z axis, a linear variation in vertical displacement of the rail was obtained till 0.0015 seconds and from then the variation was constant till 0.0020669 seconds.

3. STUDY OF DYNAMIC EXPLICIT ANALYSIS ON DIFFERENT SOIL CONDITIONS

The dynamic explicit analysis method is used to calculate the dynamic response of the rail track. The different soil conditions used are: loose sand, medium sand & well graded dense sand. The rail properties are analyzed for Equivalent Stress and Directional Deformation in Z axis. Corresponding variations in the graphs has been drawn to study the dynamic behaviour of rail track.

The importance of using explicit analysis instead of static analysis is that we can directly give the velocity effect to the joint between the wheel and the axle of the wheel. Where as in implicit analysis even though it is a dynamic analysis, only the calculated velocity is given. Here the moving condition is not satisfied. Again it acts as a static case only.

3.1 DIFFERENT TYPES OF SOIL CONDITIONS USED

Soil is our prime natural and economic resource. Soils in India differ in composition and structure. Sand within soil is actually small particles of weathered rock. Sand is fairly coarse and loose so water is able to drain through it easily. Thus sandy soil will not hold water. Here the explicit analysis is carried for three soil conditions: loose sand, medium sand & well graded dense sand. Loose sand have low density. It has a tendency to compress when a load is applied. Whereas dense sand has a tendency to expand in volume when a load is applied.

Figure: 10 shows the typical values of soil Young's modulus for different soil conditions such as loose sand, medium sand & dense sand according to USCS. The USCS stands for Unified Soil Classification System. It is a soil classification system used in engineering and geology to describe the texture and grain size of a soil.

3.2 TYPICAL VALUES OF SOIL YOUNG'S MODULUS FOR DIFFERENT SOILS ACCORDING TO USCS

The USCS stands for Unified Soil Classification System. It is a soil classification system used in engineering and geology to describe the texture and grain size of a soil. The different soil conditions used according to USCS are loose sand, medium sand & dense sand. The soil stiffness and modulus of elasticity depends on the consistency and density of the soil.

Typical values of Young's modulus for granular material (MPa) (based on Obrzud & Truty 2012 compiled from Kezdi 1974 and Prat et al. 1995)

USCS	Description	Loose	Medium	Dense
GW, SW	Gravels/Sand well-graded	30-80	80-160	160-320
SP	Sand, uniform	10-30	30-50	50-80
GM , SM	Sand/Gravel silty	7-12	12-20	20-30

Typical values of Young's modulus for cohessive material (MPa) (based on Obrzud & Truty 2012 compiled from Kezdi 1974 and Prat et al. 1995)

USCS	Description	Very soft to soft	Medium	Stiff to very stiff	Hard
ML	Silts with slight plasticity	2.5 - 8	10 - 15	15 -40	40 - 80
ML, CL	Silts with low plasticity	1.5 - 6	6 -10	10 - 30	30 -60
CL	Clays with low-medium plasticity	0.5 - 5	5 -8	8 - 30	30 - 70
CH	Clays with high plasticity	0.35 - 4	4 -7	7 - 20	20 - 32
OL	Organic silts	-	0.5 -5	-	-
OH	Organic clays	-	0.5 -4	-	-

Fig 10: Typical values of soil Young's modulus

CASE 1: LOOSE SAND

a) EQUIVALENT STRESS

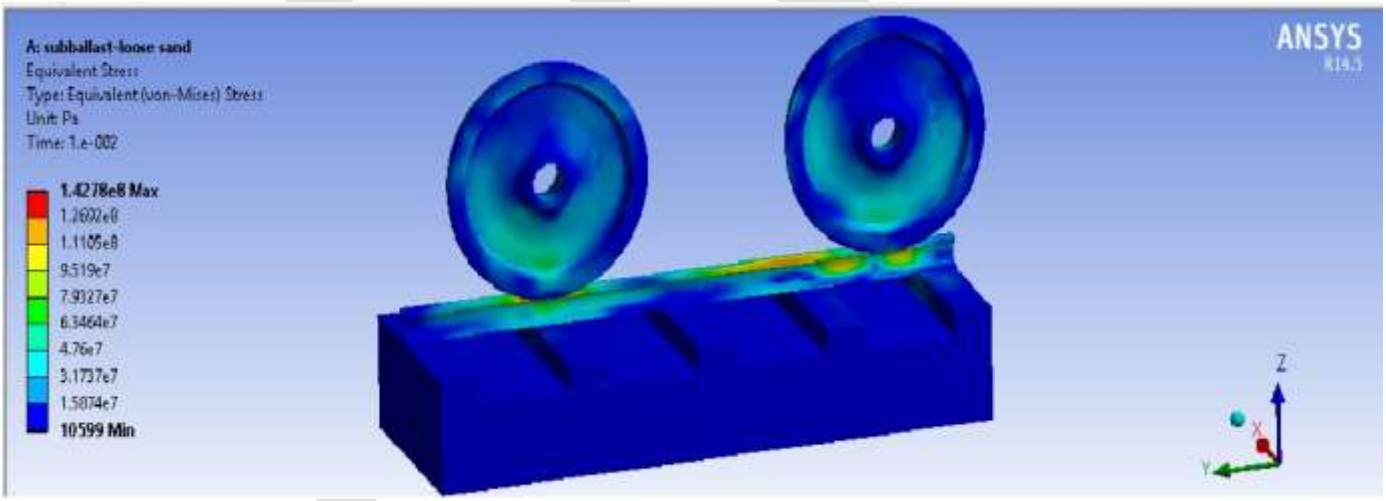

Fig 11: Equivalent Stress in Loose Sand

b) VERTICAL DISPLACEMENT OF RAIL

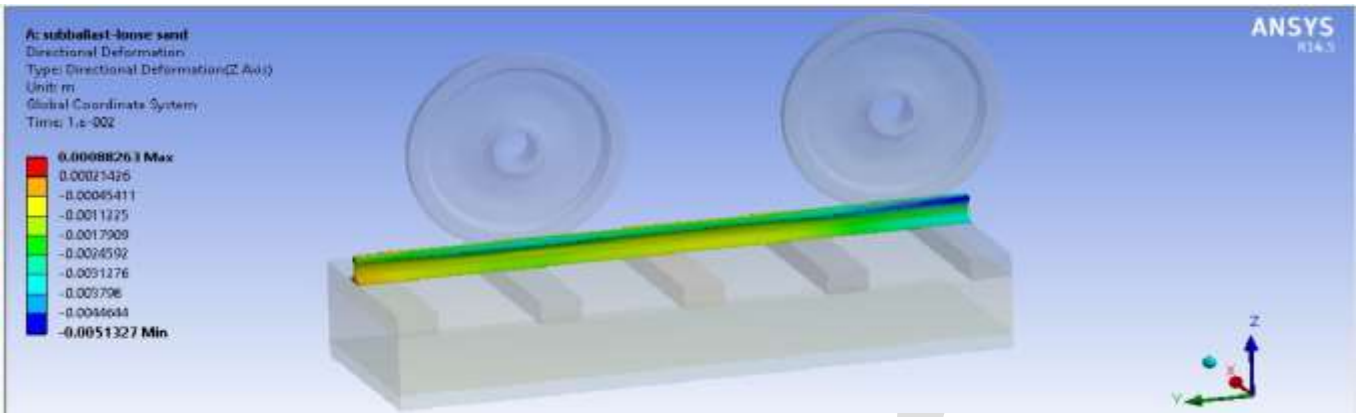

Fig 12: Vertical Displacement of rail track

CASE 2: MEDIUM SAND

a) EQUIVALENT STRESS

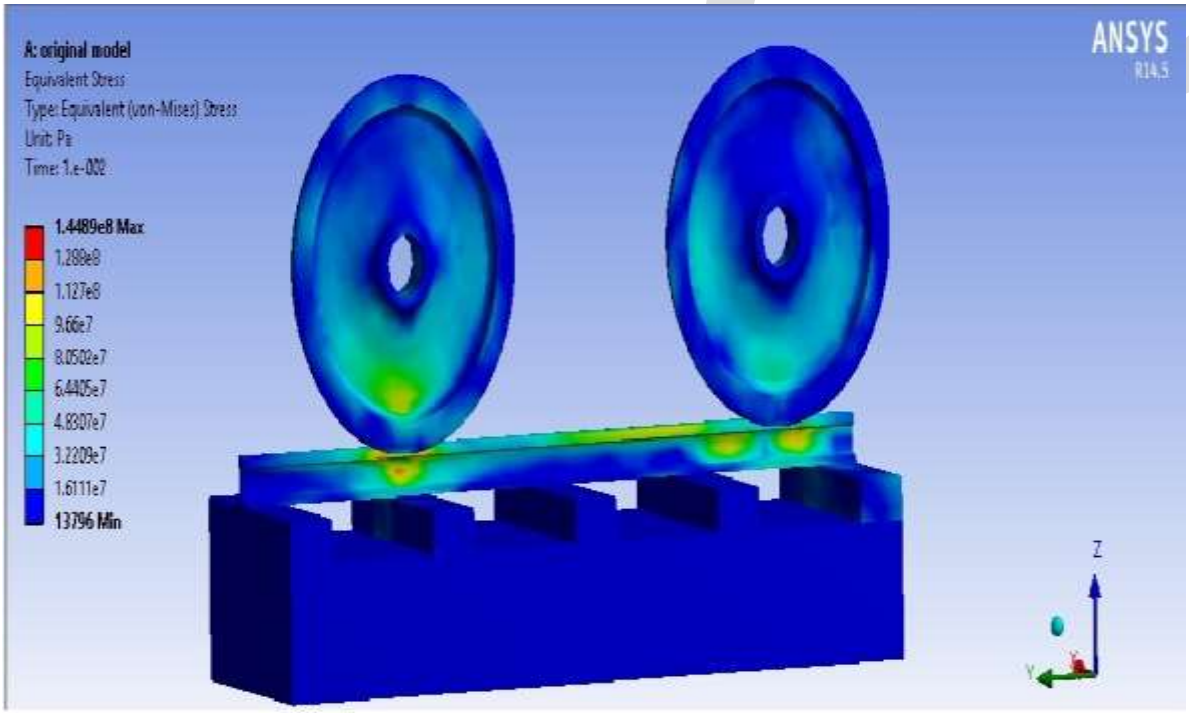

Fig 13: Equivalent Stress in Medium Sand

b) VERTICAL DISPLACEMENT OF RAIL

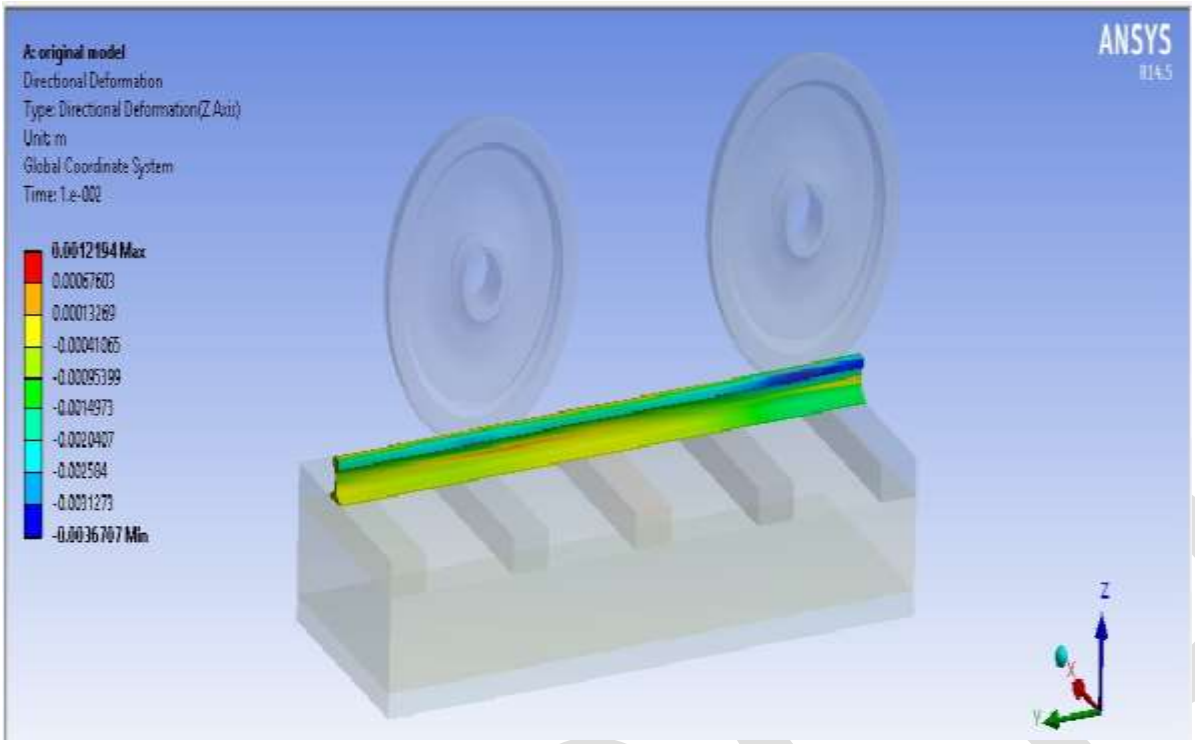

Fig 14: Vertical Displacement of rail track

CASE 3: WELL GRADED DENSE SAND

a) EQUIVALENT STRESS

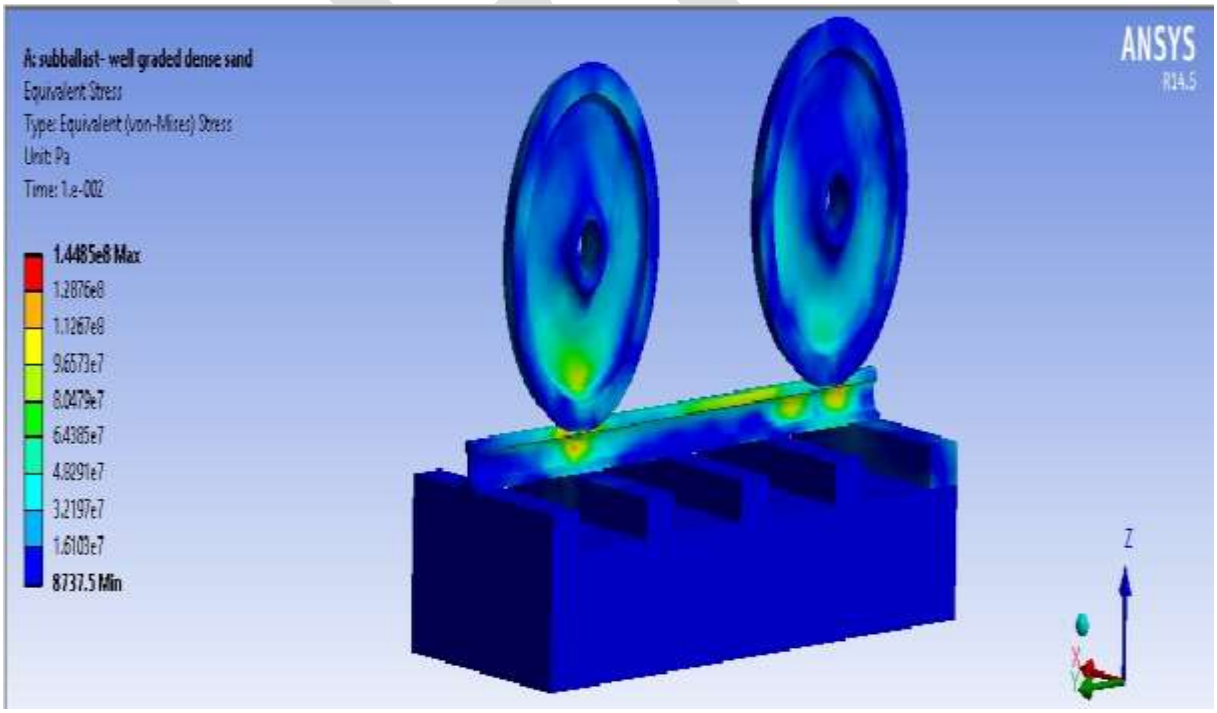

Fig 15: Equivalent Stress in Dense Sand

b) VERTICAL DISPLACEMENT OF RAIL

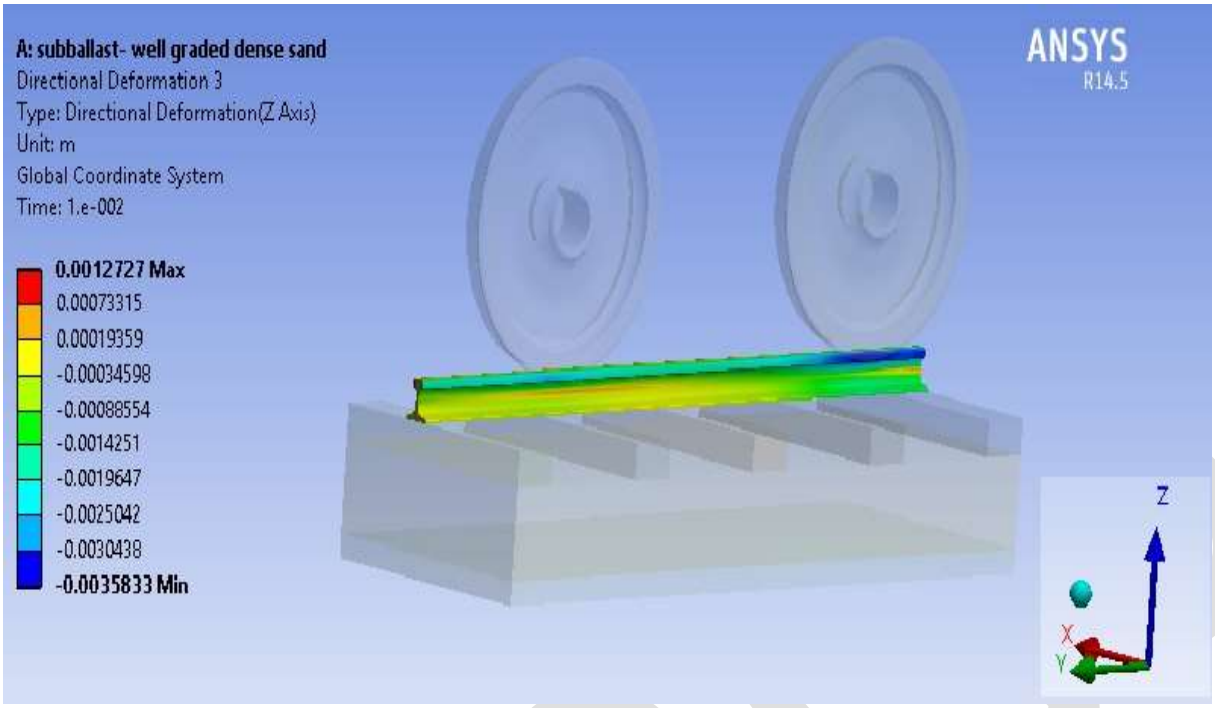

Fig 16: Vertical Displacement of rail track

4. CONCLUSION

The purpose of this thesis was to study the dynamic behaviour of rail track using three dimensional finite element methods. Considering the complexity, different models were created and compared. The comparison on equivalent stresses and vertical displacement of rail for different soil conditions has been performed and their results are compared.

Time (s)	Type of soil	Minimum Stress (Pa)	Minimum Displacement (m)
1.e -002	LOOSE SAND	10599	-5.1327e-003
1.e -002	MEDIUM SAND	13796	-3.6707e-003
1.e -002	WELL GRADED DENSE SAND	8737.5	-3.5833e-003

Table 7: Comparison of results

From table 7 it is found that the minimum stress as well as minimum displacement is obtained for well graded dense sand for 1.e-002 seconds. Thus well graded dense sand can be considered as the better soil for placing the rail tracks.

REFERENCES:

[1] Abdelkrim M., Bonnet G., and Buhan P. [2003], A computational procedure for predicting the long term residual settlement of a platform induced by repeated traffic loading, Computers and Geotechnics 30, 463‑476

[2] Alves Costa P., Calçada R., Cardoso A.S., and Bodare A. [2010], Influence of soil non-linearity on the dynamic response of high-speed railway track, Soil Dyn. Earthq. Eng. 30(4), 221‑235.

[3] Andersson M., Murray M., Ferreira L., and Lake N. [2004], Collection and use of railway track performance and maintenance data. In: Proceedings of CORE 2004− conference on railway engineering, Darwin, Australia.

[4] Choi J.Y. [2013], Influence of track support stiffness of ballasted track on dynamic wheel-rail forces, Journal of Transportation Engineering, 139, 709‑718.

[5] De Man A.P. [2002], DYNATRACK: A survey of dynamic railway track properties and their quality, Ph.D. Thesis, Faculty of Civil Engineering, Delft University of Technology, The Netherlands.

[6] Prof.Dr.Ir. C. Esveld , Dr.Ir. A.W.M. Kok [2011], "Interaction between moving vehicles and railway track at high speed" International Journal of Engineering and Applied Sciences.

[7] AK Gupta [2006], " Modeling rail wheel-flat dynamics" Indian Institute of Technology, Kanpur 208 016, India WCEAM 2006 Paper 233.

[8] Gustavson R. [2000], Static and dynamic finite element analyses of concrete sleepers, Licentiate of Engineering Thesis, Department of Structural Engineering, Chalmers University of Technology, Sweden.

[9] Hall L. [2002], Simulations and analyses of train-induced ground vibrations infinite element models, Soil Dynamics and Earthquake Engineering, 23, 403‑413.

[10] Huan , Feng [2011], "3D-models of Railway Track for Dynamic Analysis" International Journal of Engineering and Applied Sciences.

[11] Hugo Baleia , Casal [2010], "Dynamic behaviour of high-speed railway bridges with ballastless track" Civil engineering Department, Instituto Superior Técnico, Universidade Técnica de Lisboa, Portugal.

[12] He H., Fu Z. [2001]. Modal Analysis, Butterworth ‑ Heinemann Publishers, Great Britain. Indraratna, B. and Salim, W. [2005]. Mechanics of Ballasted Rail Tracks A Geotechnical Perspective. Taylor & Francis, London.

[13] Hunt G.A. [2005], Review of the effect of track stiffness on track performance, Research Project T372, AEATR-II-2004-018, Rail Safety and Standards Board.

[14] Mohammad Worya Khordehbinan [2010], Investigation on the Effect of Railway Track Support System Characteristics on the Values of Track Modulus.

[15] Jiannan Yang1, David Thompson1 and Atul Bhaskar2 [2013], "Dynamic models of railway track taking into account of cross-section deformation at high frequency" Institute of Sound and Vibration Research, University of Southampton, Southampton SO17 1BJ, UK.

International Journal of Engineering Research and General Science Volume 3, Issue 6, November-December, 2015
ISSN 2091-2730

Ergonomic Analysis of Environmental Conditions in Garment Manufacturing Industries in Bengaluru, India

Reena Shukla [1], Dr. Rajeswara Rao K.V.S [2]
1.Post Graduate Student in Engineering Management,
2.Associate Professor,
Department of Industrial Engineering and Management,
R. V. College of Engineering, Bengaluru-560059
Email: shukla.reena4@gmail.com , getkvs@gmail.com

Abstract: India has carved a name for itself as a globally renowned garment manufacturing center for its durability, quality and beauty. The textile and garment industry contributes about 14% to industrial production, 5% to GDP and 11% to the country's export earnings. This sector also provides employment to about 45 million people. However, various studies quote that India's success in the global garments market has been at the cost of the basic rights of labor force especially the females and migrants. Karnataka is a major apparel sourcing destination for the global market. The garment industries in Karnataka are concentrated mostly in Bengaluru where some of the largest export houses of the country exist. From the systematic review of literature and interactions with the industry experts, it was understood that the work environment in a majority of the garment manufacturing industries is unsafe and unhealthy. The workstations are poorly designed with unsuitable furniture, lack of ventilation, inappropriate lighting, and excessive noise. This poor working environment adversely influences the performance of the workers which in turn reduces the productivity of the manufacturing units. This work deliberates on the environmental audit carried out in several sections of the garment industry to see if the working environment is favorable to the workers. Environmental parameters such as noise level, illumination and temperature were measured using instruments such as sound level meter, luxmeter and hand held thermometer and were compared against OSHA (Occupational Safety and Health Administration) standards. The study revealed that the workstations were designed with congested work area, poor illumination, high temperature, improper ventilation. Hence appropriate intervention strategies have been suggested to improve health, safety and comfort of people in the working environment.

Keywords: *Work environment, Garment manufacturing industry, Ergonomics, Temperature, Illumination, Noise level, Health problems.*

INTRODUCTION

The garment industry in India comprises of both domestic and export markets. The industry is extremely fragmented with an estimated 27000 domestic manufacturers and 48000 fabricators and 1000 manufacturer – exporters. It is one of the earliest industries to come into existence. The textile industry currently contributes about 14% to industrial production, 5% to GDP and 11% to the country's export earnings [1].

Garment industries in Bengaluru started from the period of British. M/s. Bangalore dressmaking Co. was the first unit, started to manufacture garments in Bengaluru during 1940, which was started by Mr. Vittal Rao [2]. Most of garment industries are located in Bommanahalli and Peenya. The Garment industry comprises of several functional divisions such as cutting, sewing, finishing, ironing and packing. The work environment in the garment industry plays a vital role in increasing the productivity and well-being of the workers. Lighting, noise and temperature are some of the important parameters which employees are exposed to in the garment manufacturing units. The above mentioned environmental parameters have a great influence on the health, comfort and performance of the workers.

Absence of environmental factors as per the regulatory standards can lead to eye strain, headache, dizziness, heat stress, heat cramps, heat burns, heat exhaustion, heat stroke and other such illness for the workers. This can result in employee absenteeism, increased

employee turn-over and decrease in performance levels. In the above context the authors have undertaken an effort to study and analyze the environmental conditions in garment manufacturing units in Bengaluru.

LITERATURE REVIEW

Relevant literature was reviewed to gain insight into the research carried out in garment manufacturing units from human factors perspective both at international and national levels.

Bridger R.S, (2003), defines Ergonomics as the study of work. It makes the work easier. Ergonomics is more concerned with making the workplace as efficient, safe and comfortable as possible [3]. K.C. Parsons (2000) conducted a review of the principles, methods and models used in environmental ergonomics in terms of the effects of heat and cold, vibration, noise and light on the health, comfort and performance of people [4]. Sarder MD B, Sheik. N and Mandahaw (2006) conducted the study in an export garment manufacturing plant in South East Asia to evaluate the poor working conditions and its effects on the garment workers [5].

S Calvin, B Joseph, (2006) identified the common occupational related accidents that occurred in the garment industry in Bangalore [6]. P. Parimalam, N. Kamalamma, A. K. Ganguli (2006) suggested some of the ergonomic interventions to improve work environment in garment manufacturing units [7]. Padmini D.S, et al. (2012), found that the work environment in garment industries in Tirupur is unsafe and unhealthy and the workers were exposed to dust, chemicals mainly in the form of solvents, ergonomical problems, psycho social problems etc.[8]. Rena Mehta (2012) has identified the major health risk factors prevailing in garment manufacturing units of Jaipur [9].Jose J. Canas, Boris B. Velichkovsky and Boris M. Velichkovsky (2013) defines macro ergonomics as a branch of human factors and ergonomics based on system approach which considers the organizational and sociotechnical context of work activities and process [10].

IN INDIA THE FOCUS IS PRIMARILY ON UNDERSTANDING THE OCCUPATIONAL HEALTH ISSUES IN THE AREA OF PHYSICAL ERGONOMICS. THIS MOTIVATED AUTHORS TO CONDUCT ERGONOMIC ANALYSIS OF ENVIRONMENTAL CONDITIONS IN GARMENT MANUFACTURING UNITS IN BENGALURU

METHODOLOGY

In continuation to literature review environmental audit was conducted in two garment manufacturing industries (100% EOU) in Bengaluru. Detailed process in garment manufacturing units was mapped. It was observed that 80% of the total work force employed by any typical garment manufacturing unit is housed in the cutting, sewing and finishing sections. Hence those three departments were considered for the study. The environment parameters such as temperature, illumination and noise level were measured using hand held thermometer, lux meter and sound level meter respectively. Measurements were recorded in the morning, afternoon and evening with duration of 2 hours between consecutive measurements. The points for measurement are near the window (partly daylight), center of the half depth of space (mostly artificial lighting) and farthest from the window (completely artificial lighting). The data collected was then analyzed and compared with the Occupational Health and Safety (OSHA) standards [11, 12, 13]. Based on the results appropriate interventions are suggested.

RESULTS AND DISCUSSION

The observations were tabulated and analyzed section wise to understand the environmental status prevailing in the units considered for the study.

Cutting section: The details of work environment parameters in cutting section are shown in the **Table 1** and **2**. The temperature in the cutting section ranged from 25°C to 30.1°C with a mean of 27.25°C which about 3^{o}C higher than the OSHA recommended permissible heat exposure for continuous heavy work of 25°C [11]. The illumination levels ranged from 230 lux to 270 lux with a mean of 245.5 lux. According to Energy efficiency guide for industry in Asia, the illumination between 500 lux to 1000 lux gives

satisfaction to the workers [12]. So, the illumination levels are very poor. The noise level ranged from 83 dBA to 87.7 dBA with a mean of 84.8 dBA and is within the permissible limit of 100 dBA recommended by OSHA [13].

Table 1: Work environment parameters measured in cutting section

	Temperature (°C)					Illumination (lux)					Noise level (dBA)				
Location	**10am**	**12pm**	**2pm**	**4pm**	**6pm**	**10am**	**12pm**	**2pm**	**4pm**	**6pm**	**10am**	**12pm**	**2pm**	**4pm**	**6pm**
Near the window	25	26	28.5	27	25.4	250	265	270	268	247	84.3	85	83	83.1	83
Centre of the half depth of space	26	28	29.7	26.5	25	236	242	258	243	232	86.8	85.4	87	83.2	87
Furthest from the window	28	29.5	30.1	27	27	233	237	239	232	230	87.7	85.2	84.5	83	84

Table 2: Details of work environment and standards

Parameters	**Range**	**Mean**	**OSHA Standards**
Temperature (°C)	25 – 30.1	27.25	25
Illumination (lux)	230 – 270	245.5	500-1000
Noise (dBA)	83 – 87.7	84.8	100

Sewing section: The details of work environment parameters in sewing section are shown in the **Table 3** and **4**. The temperature in the sewing section ranged from 25°C to 35°C with a mean of 30°C, which is 5°C higher than OSHA recommended permissible levels [11]. The illumination levels ranged from 558 lux to 1186 lux with a mean of 598 lux. According to Energy efficiency guide for industry in Asia, the illumination between 500 lux to 1000 lux gives satisfaction to the workers [12]. The noise level ranged from 83 dBA to 83.9 dBA with a mean of 83.3and is within the permissible limit of 100 dBA recommended by OSHA [13].

Table 3: Work environment parameters measured in sewing section

	Temperature (°C)					Illumination (lux)					Noise level (dBA)				
Location	**10am**	**12pm**	**2pm**	**4pm**	**6pm**	**10am**	**12pm**	**2pm**	**4pm**	**6pm**	**10am**	**12pm**	**2pm**	**4pm**	**6pm**
Near the window	26	27	31	30	25	750	834	1186	924	748	83	83.5	83.7	83.9	83
Centre of the half depth of space	28	30	32	31	28	432	502	594	686	427	83.8	83.4	83.2	83.5	83.5
Furthest from the window	31	32	35	33	30	360	375	392	401	358	83	83.2	83.8	83.3	83

Table 4: Details of work environment and standards

Parameters	**Range**	**Mean**	**OSHA standards**
Temperature (°C)	25 – 35	30	25
Illumination (lux)	358 – 1186	598	500-1000
Noise (dBA)	83 - 83.9	83.3	100

Finishing section: The details of work environment parameters in finishing section are shown in the **Table 5** and **6**. The temperature in the finishing section ranged from 22°C to 24°C with a mean of 23.02°C. According to the OSHA technical manual the permissible heat exposure for continuous moderate work is 26.7°C [11]. Hence the temperature measured was within the permissible range. The illumination levels ranged from 220 lux to 396 lux with a mean of 310.33 lux. This observation is also satisfactory as the existing level falls within the range specified by Energy efficiency guide for industry in Asia, which states that the illumination between 250 lux to 500 lux gives satisfaction to the workers [12]. The noise level ranged from 76 dBA to 79.4 dBA with a mean of 77.84 dBA and is within the permissible limit of 100 dBA recommended by OSHA [13].

Table 5: Work environment parameters measured in finishing section.

	Temperature (°C)					**Illumination (lux)**					**Noise level (dBA)**				
Location	**10am**	**12pm**	**2pm**	**4pm**	**6pm**	**10am**	**12pm**	**2pm**	**4pm**	**6pm**	**10am**	**12pm**	**2pm**	**4pm**	**6pm**
Near the window	22.5	23.5	24	23	22	250	332	396	382	347	79.4	79	78.4	78.5	78
Centre of the half depth of space	22.5	23	24	23.5	22.3	336	358	389	320	334	78	77.5	77.5	78.5	78.5
Farthest from the window	22.5	23	23.5	23.5	22.5	224	253	268	246	220	78.5	77.5	76	76	76.3

Table 6: Details of work environment and standards

Parameters	**Range**	**Mean**	**OSHA Standards**
Temperature (°C)	22 – 24	23.02	26.7
Illumination (lux)	220 – 396	310.33	250-500
Noise (dBA)	76 – 79.4	77.84	100

Analysis of the audit results reveals that the temperature was high in cutting and sewing sections. This can be attributed to climatic conditions, workplace heat exposures and bad design of the work layout itself. The illumination level was poor in almost all the sections and the noise level was found to be within the recommended level as per OSHA standards. Hence appropriate intervention strategies have been suggested (Table 7) based on the extensive literature review conducted to improve environmental conditions in the units considered. This will have a positive influence on health, safety, comfort and performance of the employees.

Table 7: Suggestive Interventions

Observation	**Interventions**
The illumination level was poor in cutting, sewing and finishing sections and it was below the recommended level as per the Energy Efficiency Guide for Garment Industry in Asia.	• The recommended minimum lighting level for cutting and sewing sections is about 500-1000 lux and for finishing section is about 250-500 lux. • By providing additional task lighting in the machine for sewing operations the visibility of the needle points can be increased. • Replace normal fluorescent lamp to LED tube lights, LEDs are more expensive initially but they consume less power, long term and more durable. Fluorescent tubes produce more heat than LEDs.

The temperature was high in cutting and sewing sections.	• In order to minimize the extent to which the workers are exposed to heat generated from the sewing machine motor, a gap of 4-5 feet between every row of machines has to be maintained. • The use of local exhaust ventilation systems in hot spots and "spot cooling" through fans to reduce the temperature in certain sections of the factory. • The use of air conditioners/coolers. Encourage workers to drink adequate replacement fluids (4 liters/day).

These interventions would help in achieving a safe and healthy workplace environment and in addition would help the organization in seeking certification under international standards like OHSAS 18001.

ACKNOWLEDGEMENT

The authors acknowledge the cooperation and help extended by the garment manufacturing units and workers in Bangalore, India, for conducting personal interviews, measuring workplace environment parameters in each section.

CONCLUSION

The present study revealed that the temperature was high in cutting and sewing sections. The illumination level was poor in all the sections though it was numerically within the permissible range. During the study it was also observed that the workers are exposed to cotton dust, poor ventilation and congested work area. Medical records and interactions with the employees indicate that the workers are exposed to health related illness such as heat stress, heat stroke, eye strain, headache, dizziness, etc. Hence, appropriate measures were suggested to improve the environmental parameters which can lead to enhanced occupational health and safety. Further studies can be carried out to analyze other environmental related issues and their influence on the occupational health and safety of the employees in the garment manufacturing units.

REFERENCES:

[1] Ministry of Textiles. (2015). Indian Textile Journal, Department of Industrial Policy and Promotion, Press Information Bureau.
[2] Devaraja T.S. (2011). Indian textile and Garment Industry - An Overview, Master's Thesis, University Of Mysore.
[3] Bridger R.S, "Introduction to Ergonomics", Taylor and Francis Group, 2nd edition, 2003
[4] K.C. Parsons. (2000, December). Environmental ergonomics: a review of principles, methods and models. Applied Ergonomics, 31(6), 581-594
[5]Sarder MD B, Sheik N. Imrhan. (2006). Ergonomic workplace evaluation of an Asian garment factory. J. Human Ergol, 35, 45-51
[6] Calvin S, B Joseph. (2006). Occupation Related Accidents in Selected Garment Industries in Bangalore City. Indian Journal of Community Medicine, 3(3), 103-144.
[7] Parimalam. P, N. Kamalamma, A. K. Ganguli. (2006). Ergonomic interventions to improve work environment in garment manufacturing units, Indian Journal of Occupational and Environmental Medicine, 10(2), 74-77
[8] Padmini D.S. and Venmathi A. (2012). Unsafe Work Environment in Garment Industries, Tirupur, India, Department of Resource Management, Faculty of Home Science, Journal of Environmental Research and Development, 7 (1A), 569-575
[9] Rena Mehta. (2012). Major Health Risk Factors prevailing in Garment Manufacturing Units of Jaipur. J Ergonom, 2(2), 1-3.
[10]Jose J. Canas, Boris B. Velichkovsky and Boris M. Velichkovsky. (2013). IAAP Handbook of Applied Psychology: Human factors and ergonomics, 3-4.

[11] OSHA Technical Manual (OTM) Section III: Chapter 4 Heat Stress. Retrieved from https://www.osha.gov
[12] Energy Efficiency Guide for Industry in Asia specifies the recommended level of illumination in the Garment Industry
[13] Occupational Safety & Health Administration, Section 1910.95. Retrieved from https://www.osha.gov

International Journal of Engineering Research and General Science Volume 3, Issue 6, November-December, 2015
ISSN 2091-2730

Nephroprotective and Cardioprotective effect of *Trianthema portulacastrum* linn in drug induced experimental animals

D.Eazhisai vallabi and V.Elango

Faculty of sciences, Department of Siddha Medicine, Tamil University, Thanjavur.

Email.id: vallabie@yahoo.com, contact number:9585915125

Abstract- *Trianthema portulacastrum* Linn used as traditional medicine, is a plant of the family Aizoaceae is a prostrate, glabrous, succulent annual herb. The plant is found almost throughout India as a weed in cultivated and wastelands. The plant has a remarkable protection against the drug induced diseases due to the presence of active phytoconstituents. In this present study, we discussed about the nephroprotective and cardioprotective and antioxidant effect of *Trianthema portulacastrum* Linn in experimental animals. Biochemical parameters and histopathological studies were analysed and the results are discussed to show the potent effect of the Siddha medicinal plant *Trianthema Portulacastrum* Linn.

Key words: *Trianthema Portulacastrum*, nephroprotective activity, cardioprotective activity, antioxidant, biochemical parameters.

INTRODUCTION

Medicinal plants have been used for centuries as remedies for human diseases because they contain components of therapeutic value. The medicinal plants have immensely contributed to the health needs of humans throughout their existence. Even today, almost one quarter of prescribed medicines in the world control ingredients from plant origin. These are used as a major source of drugs for the treatments of various health disorders (Iqbal & Rehman, 2004).

Although modern drugs are effective in preventing cardiovascular disorders, their use is often limited because of their side effects. Nowadays, it is being realized that herbs can protect the heart from heart diseases by their cardio protective action by providing an integrated structure of nutritional substances mainly phytochemicals which help in restoring and maintaining balanced body systems (Dhar *et al*., 1968; Hertog *et al*., 1993).

Trianthemma portulacastrum Linn

The principal constituent of *Trianthemma portulacastrum* Linn. is ecdysterone and the other constituents are trianthenol, 3-acetylaleuritolic acid, 5,2'-dihydroxy-7-methoxy-6,8-dimethylflavone, leptorumol, 3,4-dimethoxy cinnamic acid, 5-hydroxy-2-methoxybenzaldehyde, p-methoxybenzoic acid, and beta cyanin. The plant is used in the treatment of edema in the liver and spleen (Javed, 2000). The plant is lithotropic for the kidney and bladder. Different parts of *Trianthema portulacastrum* Linn. are traditionally used as analgesic, antipyretic, cardio tonic, anti-inflammatory, CNS depressant and stomachic properties and used in asthma, bronchitis, jaundice and oedemas(Kumar *et al.*,2004).

Drug Induced Nephrotoxicity

Nephrotoxicity is one of the most common kidney problems and occurs when body is exposed to a drug or toxin. When kidney damage occurs, body unable to rid of excess urine and wastes from the body and blood electrolytes (such as potassium and magnesium) will all become elevated. A number of therapeutic agents can adversely affect the kidney resulting in acute renal failure, chronic interstitial nephritis and nephritic syndrome because increasing number of potent therapeutic drugs like aminoglycoside antibiotics, chemotherapeutic agents and NSAIDS have been added to the therapeutic arsenal in recent years. Nephroprotective agents are the substances which possess protective activity against nephrotoxicity. (Porter and Bennett ,1981).

Drug Induced Cardiotoxicity

Cardiovascular disease (CVD) has become a universal cause of morbidity and a leading contributor to mortality in both developed and developing country. The identification of major risk factors through epidemiological studies and effective control strategies combining community education and targeted management of high risk individuals have contributed to the fall in CVD mortality rates that has been observed in almost all streamlined countries. Isoproterenol caused severe stress in the myocardium resulting in necrosis of heart muscles which caused cardiac dysfunction, increased lipid peroxidation along with an increase in the level of myocardial lipids, altered activities of the cardiac enzymes and antioxidants (Reddy and Yusuf, 1998).

Effect of *Trianthema portulacastrum* on Antioxidant enzymes

Free radicals are atomic or molecular chemical species with unpaired electrons. These free radicals are highly unstable and can react with other molecules by giving out or accepting single electron. Antioxidant agents of natural origin have attracted special interest because they can protect human body from free radicals (Crastes,1990). In view of this, we selected *Trianthema portulacastrum* Linn, to assess the antioxidant activity.

The objectives of the present study were to evaluate the crude powder of whole parts of *Trianthema portulacastrum* for its anti oxidant activity, nephroprotective activity, cardio protective activity and also to identify the nature of the phytochemicals in the selected plant.

EXPERIMENTAL METHODS

Plant Material

Fresh plant sample *Trianthema portulacastrum* Linn were collected from various parts of Thanjavur district. The whole plant were washed, shade dried, powdered. Crude powder of *Trianthema portulacastrum* Linn are given to the experimental rats at the dose of 100mg/100g body weight.

Experimental Design

Male albino rats of 8 – 10 weeks of age weighing between 120 and 150g for nephro-toxicity and 180-200g for cardio-toxicity were used for the study. The animals were housed in polypropylene cages. Animals were divided into five groups of three animals. The animals were acclimatized for a week under laboratory conditions. All experiments were performed according to the norms of the local ethical committee.

Renal damage was induced in rats by induction Gentamicin at a dose of 40mg/ 100kg of body weight and Cardiotoxicity was induced in rats by inducing isoproterenol at a dose of 70 mg / 100kg of body weight intraperatonially.

Experimental animals were distributed randomly, in five groups, containing three animals each.

- The animals in group I served as normal and received rat feed and distilled water *adlibitum.*
- The group II rats served as test and were induced with gentamicin at a dose of 40 mg/ 100g body weight meanwhile,

- Group III rats served as test and were induced with isoproterenol at a dose of 70 mg/ 100g body weight intraperatonialy.
- The animals in group IV provided with rat feed and distilled water along with gentamicin and the animals in group V treated with isoproterenol and Crude powder of *Trianthema portulacastrum* Linn at the dose of 100mg/100g body weight the drug followed by it.
- After the completion of the experimental regimen rats were fasted overnight, anaesthetized with ether, blood was drawn and the serum was separated for various biochemical parameters. Kidney and Heart tissues are also separated for histo pathological studies.

BIOCHEMICAL STUDIES

This study carries with different parameters to analyse the nephroprotective, cardioprotective and anti-oxidant effect of the *Trianthema portulacastrum* Linn in drug (Gentamicin and isoproterenol) induced experimental rats.

Serum creatinine level was determined using Creatinine Colorimetric Kit. Creatinine in the sample reacts with picrate in alkaline medium forming a coloured complex. The complex formation rate is measured in a short period to avoid interference. (Bartels and Bohmer, 1971; Fabiny and Ertingshausen, 1971). In the estimation of Urea, diacetyl monoxime in the presence of acid hydrolyzes to produce the unstable compound diacetyl reacts with urea to produce a yellow diazine derivative. The colour of this product is intensified by the addition of thoisemicarbazide it was measured at 520nm (Crocker ,1967).

Uric acid reduces phosphotungstic acid in the presence of sodium carbonate to give blue colour which can be measured colorimetrically. Transaminases activities were estimated by Reitman and Frankel method and which was measured spectrometrically. Cystatin C is estimated in serum using the kit and measured at 700/546 nm. Creatine Kinase-MB and Triglycerides were estimated by Friedman and Young method and which was measured by Spectrometrically. Lipid peroxide content was assayed by thio barbituric acid method.

Reduced glutathione was estimated by method of Moron *et al* (1979) and the absorbance was read at 412nm. The activity of mitochondrial glutathione peroxidase was assayed by the method of Rotruck *et al* (1973) and the colour developed was read at 420nm immediately. The Histopathological studies, were carried out in all the groups of normal, control and drug treated rats (Ochei and Kolhatkar., 2000).

Mean values standard were calculated and percentage of inhibition for all the values carried out. (Fisher, 1950).

RESULT AND DISCUSSION

Gentamicin (GM) is an aminoglycocide antibiotic that is very effective in treating life threatening gram negative infection. GM induced nephrotoxicity is characterized by direct tubular necrosis, which is localized mainly in the proximal tubule. GM causes nephrotoxicity by inhibiting protein synthesis in renal cells. This mechanism specifically causes necrosis of cells in the proximal tubule, resulting in acute tubular necrosis which can lead to acute renal failure (Sudin, 2001).

The result of this study shows the significant nephrotoxicity induced by gentamicin was evidenced by increase in serum urea, creatinine clearance and urea secretion due to renal tubular necrosis. The administration of crude powder of *Trianthema*

portulacastrum for 30 days was found able to treat and protect renal necrosis against gentamicin induced nephrotoxicity and thereby decreasing the serum urea, creatinine and uric acid.

Cystatin C appears to be a better predictor of glomerular function than serum creatinine. cystatin C, is a bio-marker, a non-glycosylated 13 kDa protein, has the potential to improve estimates of GFR, because it is thought to be less influenced by muscle mass or diet. Glomerular Filtration rate is estimated assessing cystatin C (Rander *et al.*,1999 and Newman *et al.*, 1995).In experimental nephrotoxicity studies there was an increase in serum cystatin C due to the impaired glomerular filtration and found decreased in herbal drug treated group (Table:1).

In (Table:2) Aminotransferases (ALT and AST) and Phosphatases are the specific enzymes and are considered to be very sensitive and reliable induces for measuring hepatotoxic as well as protective effect of various compounds. Renal necrosis induced by gentamicin usually associated with elevated levels of serum enzymes that are indicative of cellular leakage and loss of functional integrity of cell membrane in kidney. (Reitman and Frankel, 1957).

The oral administration of crude powder of Siddha medicinal plant *Trianthema portulacastrum* for 30 days were found to protect the proximal tubular damage induced by lipid per oxidation and activation of antioxidant enzymes. The drug administration was able to protect the renal necrosis and lysosomal latency as evidenced by the inhibitory activity of phosphatases and transaminases. The study also shows the significant efficacy of herbs in the treatment of nephrotoxicity was also evidenced by decrease in urea level and creatinine clearance.

The antioxidant activity of the *Trianthema portulacastrum* Linn in gentamicin induced nephrotoxic animals. The result of this study shows that gentamicin produced nephrotoxicity was evidenced by increasing in lipid peroxidation products suggesting the involvement of oxidative stress and suggestive of tubular damage. The drug treated groups exert a protection against oxidative stress and tubular damage against gentamicin induced nephrotoxicity. There was an increased activity in Reduced Glutathione, glutathione peroxide and Super oxide dismutase activated with produced free radicals and involvement of oxidation stress and finally damage to the proximal tubule. The drug administration was able to treat and protect the proximal tubular damage against gentamicin induced nephrotoxicity, by the activation of antioxidant enzymes(Table:3).

Isoproterenol (ISO) [1- (3,4- dihydroxyphenyl) -2- isopropyl aminoethanol hydrochloride], a synthetic catecholamine and β-adrenergic agonist that causes severe stress in myocardium and infarct-like necrosis of the heart muscles (Suchalatha and Shyamala Devi, 2004). ISO induced myocardial injury involves membrane permeability alterations, which brings about the loss of functions and integrity of myocardial membranes. ISO induced myocardial necrosis is a well known standard model to study the beneficial effect of many drugs on cardiac dysfunction (Todd *et al.*, 1980).

The oral administration of crude powder of Siddha medicinal plant *Trianthema portulacastrum* against isoproterenol for 30 days were found to protect the cardiac damage induced by lipid per oxidation and activation of antioxidant enzymes. The herbal drug administration was able to protect the cardiac necrosis as evidenced by the inhibitory activity of CK-Mb and TGL (Table:4). The study also shows the significant efficacy of herbs in the treatment of cardiotoxicity was also evidenced by decrease in CK-Mb and TGL level in serum. Elevation of CK is an indication of damage to muscle. It is therefore indicative of injury, rhabdomyolysis, myocardial infarction, myositis and myocarditis.

The observed increase in the body weight in isoproterenol induced rats could be due to the accumulation of water content in the Oedematous intramuscular area in addition with necrosis of cardiac muscle fibres. Decreased activities of these cardiac marker enzymes in the cardiac tissue could be due to the leakage from damaged cardiac tissue into the circulation as a result of necrosis induced by ISO (Kurian *et al*.,2005)

TABLE 1: Nephroprotective effect of *Trianthema portulacastrum* on biochemical parameters- Urea, Uric acid, Creatinine and Cystatin C.

Groups	**Dose**	**Parameters**			
		Urea mg/dl	Uric acid mg/dl	Creatinine mg/dl	Cystatin C mg/l
Normal	Isosaline	2.81±2.24	3.8±3.04	1.4±0.56	1.59±0.79
Control	40mg/kg b.wt	5.66±3.39	6.7±4.69	2.62±1.57	4.82±3.85
Drug Treated	100mg/kg b.wt	3.61±2.16	4.03±2.01	1.59±0.95	2.85±0.85

TABLE 2: Nephroprotective effect of *Trianthema portulacastrum* on Phosphatases and Transaminases

Groups	**Dose**	**Parameters**		
		Acid Phosphatase U/l	Alanine Transaminase U/l	Aspartate Transaminase U/l
Normal	Isosaline	15.71±9.42	13.76±9.63	10.75±7.52
Control	40mg/kg b.wt	19.23±3.84	17.21±3.44	18.11±9.05
Drug Treated	100mg/kg b.wt	15.12±4.53	14.11± 5.64	15.28±6.11

TABLE 3: Nephroprotective effect of *Trianthema portulacastrum* on Anti-Oxidants - LPO, Reduced Glutathione, SOD, Glutathione peroxidase.

Groups	**Dose**	**Parameters**			
		LPO n moles MDA/mg	Reduced glutathione µg/ mg ptn	SOD Mole/O_2decompose/ min/100mg protein	Glutathione peroxide U/mg protein
Normal	Isosaline	2.36±1.41	9.6±5.76	3.3±0.99	2.36±0.16
Control	40mg/kg b.wt	3.46±1.38	5.7±3.99	1.2±0.24	1.60±0.11

Drug Treated	100mg/kg b.wt	1.51±0.90	5.76±4.03	1.78±1.24	2.0±0.14

TABLE 4: Cardioprotective effect of *Trianthema portulacastrum* CK-MB, TGL, Cholesterol and LPO.

Groups	**Dose**	**Parameters**			
		CK-MB U/l	TGL mg/dl	Cholesterol mg/dl	LPO Nmoles MDA/mg
Normal	Isosaline	1.651±0.132	50.0±1.50	45±2.29	2.25±0.157
Control	40mg/kg b.wt	13.2±0.824	133.33±7.31	41±2.40	2.715±0.0962
Drug Treated	100mg/kg b.wt	9.906±0.493	62.5±2.75	45±3.61	1.62±0.0810

Each value is the mean ± SEM of five samples values are significantly different from control and treated rats.

HISTOPATHOLOGY

In histopathological examination of Kidney tissues shows, normal architecture was observed in normal animals whereas renal lesions including marked tubular and focal area necrosis, inflammation and glomerular congestion changes in the kidney of gentamicin treated animals were observed (Group 2- control). The lesions were reduced significantly in animals which were treated with the Siddha medicinal plant *Trianthemma portulacastrum* at the dose of 100 mg/100g.b.wt (dosess) to gentamicin treatment.

Normal

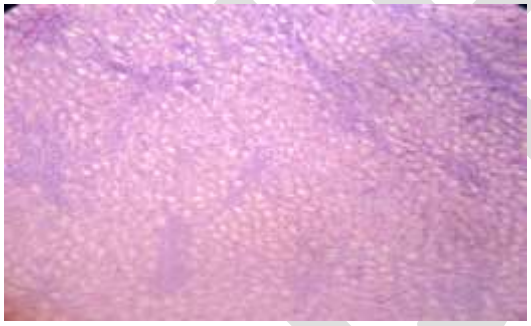

Control- Gentamicin induced

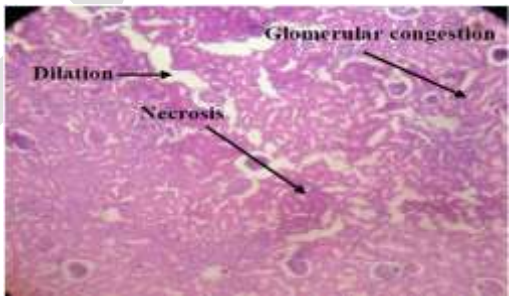

Trianthema portulacastrum treated

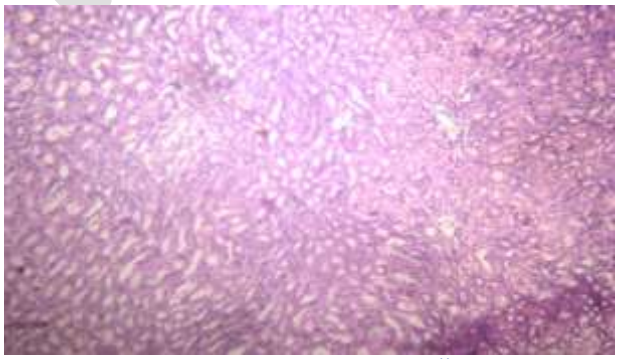

In Heart tissue, Normal group showed normal cardiac architecture and arrangement of myofibril, absence of interfibrillar necrosis, regular and normal multinuclear myofibrils arrangement, vacuolization and macrovesicular changes. In Isoproterenol treated animals exhibited intense interfibrillar necrosis, vacuolization, macroveisicular changes and damage and irregular arrangement and morphological change of myofibrils associated with increased interfibrillar distance. *Trianthemma portulacastrum* exhibited significant cardiac remodeling activity against isoproterenol induced rat's heart tissue by normal cardiac architecture, arrangement of myofibrils, and absence of interfibrillar necrosis.

Normal

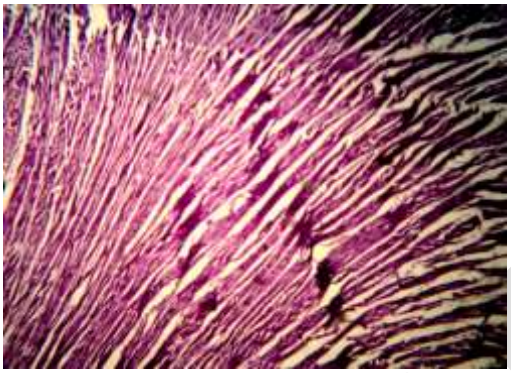

Control-Isoproterenol induced

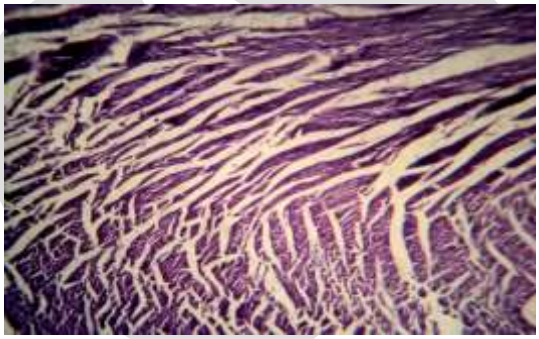

Trianthema portulacastrum treated

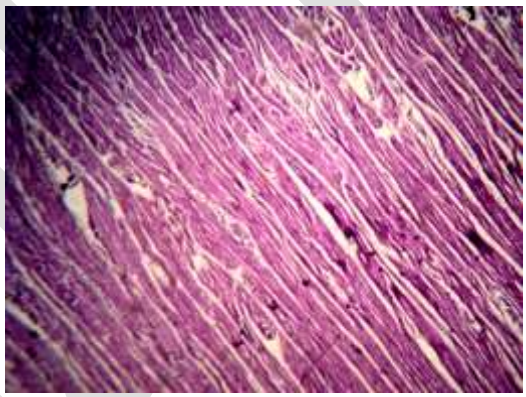

CONCLUSION

The nephroprotective, anti-oxidant, cardio protective effect of the *Trianthema portulacastrum* be due to the activity of the phytoconstituents present in the Siddha medicinal plant have the nephrotoxic and cardio toxic effect against the aminoglycoside-antibiotic drug gentamicin and isoproterenol. Further studies are suggested on the isolation of active compounds and their protective activity in human.

REFERENCES:

[1] Iqbal, C.M. and A. Rahman. Abstracts international symposiumn medicinal plants. Linkage beyond national boundaries, 7(9): 6-7,2004.

[2] Dhar, M.L., M.M. Dhar, B.N. Dhawan, B.N. Mehrotra and C. Ray,. Screening of Indian plants for biological activity. *J. Exp. Biol*., 6: 232-247,1968.
[3] Hertog, M.G.L., E.J.M. Feskens, P.C.H. Hollam, M.B. Katan and D. Kromhout,. Dietary antioxidant flavonoids and risk of coronary heart diseases. *The Zutphen Elderly Study*. Lancet. 342: 1007-1020,1993.
[4] Javed A, Farooqui AH. and Sageer A.*Trianthema portulacastrum* L an herbal drug for the cure of edema. *J Herbs Spices and Med plant*.; 7, 65-70,2000.
[5] Kumar G, Sharmila Banu G, Vanitha Pappa P, Sundararajan M, Rajasekara and Pandian M. Hepatoprotective activity of *Trianthema portulacastrum* L against paracetamol and thioacetamide intoxication in albino rats. *J Ethnopharmacol*.; 92: 37-40, 2004.
[6] Porter G. A and Bennett W.M."Nephrotoxic acute renal failure due to common drugs", *American journal of Physiology*,; 241(7): F1-F8,1981.
[7] Reddy KS, Yusuf S. Emerging epidemic of cardiovascular disease in developing countries. Circulation.;97:596–601,1998.
[8] Crastes DP.*Ann Biolol Clin*, 48, 323,1990.
[9] Bartels H and Bohmer M. Eine mikromethode zur kreatininbestimmung. *Clin Chim Acta*, 32:81-85,1971.
[10] Fabiny DL, Ertingshausen G,. Automated reaction –rate method for determination of serum creatinine with Centrifi Chem. *Clin Chim*, 17: 696-700,1971.
[11] Crocker, C.L. *Am J.Med.technol*., 33: 361. 1967.
[12] Reitman. Sand S Frankel..*Am J Clin pathol*., 28: 56-63,1957.
[13] Friedman and Young. Effects of disease on clinical laboratory tests, 4th ed. AACC Press, 2001.
[14] Moron MS, Dsepiere JW, Manerwik KB. Level of glutathione, glutathione reductase and glutathione-s-transferase activities in rat lung and liver. *Biochem Biophy Acta*.682: 67-68,1979.
[15] Rotruck JT., Pope AL., Ganther HE., Swanson AB., Hafeman DG and Hoekstra WG Selenium: biochemical roles as component of glutathione peroxidase. Science., 179: p588-590,1973.
[16] Ochei J., Kolhatkar A. Medical Laboratory Science, Theory and Practice, Tata McGraw-Hill Publishing Company Limited, New Delhi. 2000
[17] Fisher.R.A., In Statistical Methods for research Workers, Oliver and Boyd, Edinburgh,1950.
[18] Sundin DP, Sandoval R, Molitoris BA,. Gentamicin Inhibits Renal Protein and Phospholipid Metabolism in Rats: Implications Involving Intracellular Trafficking. *J Am Soc Nephrol*., 12: 114-123,2001
[19] Randers E, Erlandsen EJ. Serum cystatin C as an endogenous marker of the renal function–a review. Clin Chem Lab Med; 37: 389–395,1999.
[20] Newman DJ, Thakkar H, Edwards RG *et al*. Serum cystatin C measured by automated immunoassay: a more sensitive marker of changes in GFR than serum creatinine. *Kidney Int*; 47: 312–318, 1995.
[21] Suchlatha S and Shyamala Devi CS,. Protective effect of Terinalia chebula against experimental myocardial injury by isoproterenol, *Indian J Exp Biol*, 42,174,2004.
[22] Todd GL, Cullan GE & Cullan GM. Isoproterenol-induced myocardial necrosis and membrane permeability alterations in the isolated perfused rabbit heart. *Experimental and molecular pathology*, 33, 43-54,1980.
[23] Kurian GA, Philp S, Varghese T. Effect of aqueous extract of *Desmodium gangeticum* DC root in the severity of myocardial infarction. *J Ethanopharmacol*;97:4557-61, 2005.

International Journal of Engineering Research and General Science Volume 3, Issue 6, November-December, 2015
ISSN 2091-2730

Experimental analysis of convective heat transfer in divergent channel

Mr. Avinash S. Patil[1], Prof. Atul V. Kulkarni[2], Dr.V. B.. Pansare[3]

[1](P G Student, Department of Mechanical Engineering, Shreeyash college of engineering & technology, Maharashtra, India)
(Mobile: 9960910974, Email: avinashpatil358@gmail.com)
[2] (Head of Department, Department of Mechanical Engineering, Shreeyash college of engineering & technology, Maharashtra, India)Email: at_kul@yahoo.com.)
[3] (Assistant Professor, Department of Mechanical Engineering, MIT, Maharashtra, India)
Email: vb_pansare@rediffmaill.com)

Abstract- Many heat transfer enhanced techniques have simultaneously been developed for the improvement of energy consumption, material saving, size reduction and pumping power reduction. The effect of divergent channels is a good way to promote the flow mixing in channel flow. When if we use divergent channel then we get flow difference means low pressure drop it is also called pressure recovery. By using bump in the divergent channel it can help us to increase the heat transfer enhancement and bump surface present the highest performance of the heat transfer enhancement. The bump surface act as extended surface (fin surface) and the main purpose of extended surface to increase the heat transfer rate. The advantages of the divergent channel with internal Bumps are fluid mixing is more as compared to cylindrical pipe, pressure drop is less and boundary layer separation occurs as well as the heat transfer coefficient increases 25 to 35 % as compare to plain divergent channel. where inserts are used in the flow passage to intensify the heat transfer rate, are advantageous compared with active techniques, because the insert manufacturing process is simple and these techniques can be easily employed in an existing heat exchanger.

Keywords -Heat transfer enhancement, Divergent channel, Bump, Heat transfer rate, Heat transfer coefficient.

I INTRODUCTION

The development of high performance thermal systems has stimulated interest in methods to improve heat transfer. The study of improved heat transfer is referred to as heat transfer enhancement or intensification. The performance of conventional heat exchanger can be substantially improved by a number of enhancement techniques. A great deal of research effort has been devoted to developing apparatus and performing experiments to define the conditions under which an enhancement technique will improve heat transfer. Heat transfer enhancement technology has been widely applied to heat exchanger applications in refrigeration, automobile, process industries etc. The goal of enhanced heat transfer is to encourage or accommodate high heat fluxes. That result in reduction of heat exchanger size, which generally leads to less capital cost. Another advantage is the reduction of temperature driving force, which reduces the entropy
Generation and increases the second law efficiency. In addition, the heat transfer enhancement enables heat exchangers to operate at smaller velocity, but still achieve the same or even higher heat transfer coefficient. This means that a reduction of pressure drop, corresponding to less operating cost, may be achieved.

Use of divergent channel:

In the divergent channel, the plumes produced are greater and not stable. In addition, the acceleration of flow can effectively lead to the local increase of Gr/Re. Therefore, stronger interaction with the neighboring plumes and vortices are observed and form a complicated flow structure. This leads to a greater enhancement in the heat transfer.

In the convergent channel, it is on the contrary. The acceleration of flow can effectively lead to the local decrease of Gr/Re. The plumes produced are smaller and stable. No interactions between plumes are found. This leads a less enhancement in the heat transfer. However, the deceleration flow in the divergent channel and the acceleration in the convergent make the average Nusselt numberS approach the results of the parallel plate channel, especially when the Reynolds number is higher.

We used divergent channels for heat transfer because of it is a good way to promote the flow mixing in channel flow also if use divergent channel then we get flow difference means low pressure drop it is also called pressure recovery also the new concept we using bumps in the divergent channel it can help us to increase the heat transfer enhancement and bump surface present the highest performance of the heat transfer enhancement. The Bumps surface it can also called as artificial surface act as extended surface (fin surface) and the main purpose of extended surface to increase the heat transfer rate. The advantages of the divergent channel with internal bumps are fluid mixing is more as compared to cylindrical pipe, pressure drop is less and boundary layer separation occurs in divergent channel which will help in heat transfer.

All these advantages have made heat transfer enhancement technology attractive in heat exchanger applications. For shell and tube heat exchangers, the tube insert technology is one of the most common heat transfer enhancement technologies, particularly for the retrofit situation. With tube insert technology, additional exchangers can often be avoided and thus significant cost saving becomes possible. Furthermore as a heat exchanger becomes older, the resistance to heat transfer increases owing to fouling or scaling. These problems are more common for heat exchangers used in chemical industries and marine applications. In this case the heat transfer rate

can be improved by introducing a disturbance in the fluid flow by different enhancement technologies (breaking the viscous and thermal boundary layer).

Wang.L.H, Tao.W.Q, Wang.Q.W, Wong.T.T, et al.-[1] Many heat augmentation techniques has been reviewed, these are (a) surface roughness, (b) plate baffle and wave baffle, (c) perforated baffle, (d) inclined baffle, (e) porous baffle, (f) corrugated channel, (g) twisted tape inserts, (h) discontinuous Crossed Ribs and Grooves. Most of these enhancement techniques are based on the baffle arrangement. Use of Heat transfer enhancement techniques lead to increase in heat transfer coefficient but at the cost of increase in pressure drop.

Sivakumar, K., Natarajan, E., Kulasekharan, N, et al.-[2] Thermal characteristics were tested by measuring wall temperature at selected locations, fluid temperature at the inlet and the outlet and wall static pressures at the channel inlet and the outlets.

Soo Wban Abn and Kang Pil Son, et al.-[3] found that the heat transfer can be enhanced by the use of rough surfaces. Four different shapes such as semicircle, sine wave, trapezoid, and arc were suggested to investigate the heat transfer enhancement and friction factor on rectangular duct.

C. Bi, G.H. Tang, W.Q. Tao, et al.-[4] The convective cooling heat transfer in mini-channels with dimples, cylindrical grooves and low fins is numerically studied by using the field synergy principle.

Dr. Mohammed Najm Abdullah, et al.-[5] the aim of this study is to investigate the heat transfer and pressure drop characteristics in an Eccentric Converging-Diverging Tube (ECDT) with twisted tape inserts. Experiments were conducted with tape inserts of three different twist ratios. Cold and hot water are used as working fluids in shell and tube sides, respectively. The effect of the twist ratio and other parameters on heat transfer characteristics and pressure drop are considered.

Pradip Ramdas Bodade, et *al*,[06] identified overheating can damage the system components and lead to failure of the system. The excessive heat so generated must be dissipated to surroundings to avoid such problems for smooth functioning of system. This is especially important in cooling of gas turbine blades, process industries, cooling of evaporators, thermal power plants, air conditioning equipment's, radiators of space vehicles and automobiles and modern electronic equipment's. In order to overcome this problem, thermal systems with effective emitters such as ribs, fins, baffles etc. are desirable. The need to increase the thermal performance of the systems, thereby affecting energy, material and cost savings has led to development and use of many techniques termed as "Heat transfer Augmentation". This technique is also termed as "Heat transfer Enhancement" or "Intensification". Augmentation techniques increase convective heat transfer by reducing the thermal resistance in a heat exchanger. Many heat augmentation techniques has been reviewed, these are (a) surface roughness, (b) plate baffle and wave baffle, (c) perforated baffle, (d) inclined baffle, (e) porous baffle, (f) corrugated channel, (g) twisted tape inserts, (h) discontinuous Crossed Ribs and Grooves. Most of these enhancement techniques are based on the baffle arrangement. Use of Heat transfer enhancement techniques lead to increase in heat transfer coefficient.

However, all of the above techniques will inevitably bring too much flow resistance, resulting in unnecessary power consumption. An effective method of heat transfer enhancement is required to not only improve the heat transfer greatly, but also minimize the flow resistance as much as

Possible. Recently, an effective method called dimple surface has been investigated in the literature, and all of the studies have proved that the dimple surface can significantly enhance the heat transfer without bringing too much flow resistance.

In order to improve the heat transfer efficiency and operation safety of heat transfer equipment's, many techniques have been proposed such as treated surfaces, rough surfaces, extended surfaces, swirl flow devices, shaped pipes, surface tension devices, mechanical aids, electrostatic fields, suction or injection. Most of these techniques are usually applied in macro-channels. However, all of the above techniques will inevitably bring too much flow resistance, resulting in unnecessary power consumption. An effective method of heat transfer enhancement is required to not only improve the heat transfer greatly, but also minimize the flow resistance as much as possible. Recently, an effective method called dimple surface has been investigated in the literature, and all of the studies have proved that the dimple surface can significantly enhance the heat transfer without bringing too much flow resistance.

In this project we are using divergent channels for heat transfer because of it is a good way to promote the flow mixing in channel flow also if use divergent channel then we get flow difference means low pressure drop it is also called pressure recovery also the new concept we using bumps in the divergent channel it can help us to increase the heat transfer enhancement and bump surface present the highest performance of the heat transfer enhancement. The Bumps surface it can also called as artificial surface act as extended surface (fin surface) and the main purpose of extended surface to increase the heat transfer rate. The advantages of the divergent channel with internal bumps are fluid mixing is more as compared to cylindrical pipe, pressure drop is less and boundary layer separation occurs in divergent channel which will help in to increase heat transfer rate.

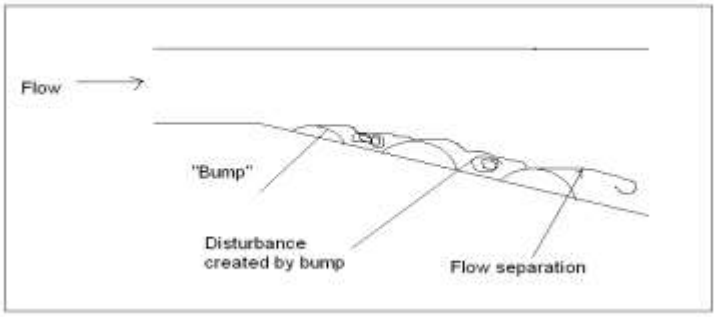

Figure .1 Creation of Disturbances in the flow

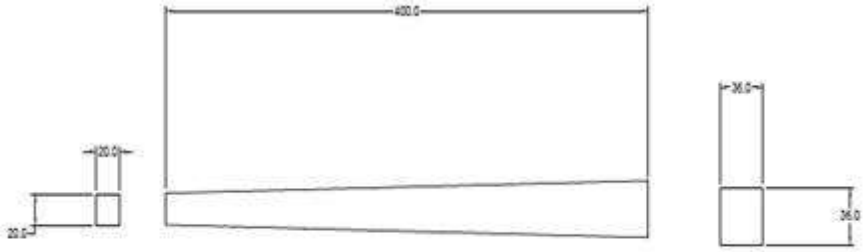

Figure 2Divergent Channel

II EXPERIMENTAL SETUP

Readings can be displayed in Pascal over the whole measurement range. Magnets at the back of the instrument enable hands-free operation, for instance, while adjusting gas heaters. Figure shows the Experimental set up of forced convection using divergent duct instead of cylindrical pipe. Divergent channel are used where pressure difference required is relatively small. The main advantage of divergent tube over cylindrical pipe is that the divergent tube has greater area than the cylindrical pipe and in divergent tube fluid mixing is proper between the flow passages. Divergent channel is suitable for wide range of Reynolds number because it posses greater amount of turbulence and to improve the heat transfer rate we can apply the passive techniques i.e., by inserting ribs, bumps, fin etc. and if turbulence in flow is more then it helps to improve the contact of air with heated pipe and this phenomena helps to improve heat transfer rate. Heat transfer rate increases with increase in internal area of channel. Also in this project to measure velocity of air inside the tube and to measure pressure, air density directly on this device. The name of this device is Testo 510 (Pressure Sensor Device). The differential pressure meter is ideally suitable for pressure measurements in the range 0 to 100 hPa. Testo 510's differential pressure measurement is temperature-compensated for accurate readings.

Figure.3 Experimental set up

III DATA REDUCTION

The data reduction of the measured results is summarized in the following procedures:
The local heat transfer coefficient was calculated from the total net heat transfer rate and the difference of the local wall temperature and the local bulk mean air temperature.

$$h = \frac{qa}{As(Ts-Ta)} \quad (1)$$

$$Nu = \frac{h \times L}{K} \quad (2)$$

As for most cases of the internal convection heat transfer, the fluid properties are evaluated at the mean temperature of the fluid in the duct. The Reynolds number was defined by

$$Re = \frac{\rho VL}{\mu} \quad (3)$$

$$V = \frac{Q}{Ac} \quad (4)$$

IV OBSERVATION TABLES

Sr No	Voltage [V] (Volts)	Current [I] (Amps)	Temperature in °c						Velocity [m/s]	Mass flow rate Kg/sec
			T_{in} °C	T_1°C	T_2°C	T_3°C	T_4°C	T_{out} °C		
1	60	0.35	28	63	64	66	65	38	10	0.00874
2	60	0.35	28	55	57	59	55	37	15	0.01312
3	60	0.35	28	45	46	48	47	34	20	0.01749
4	60	0.35	28	43	45	46	44	33	25	0.02187
5	60	0.35	28	38	39	41	40	32	30	0.02624

Table: 1 Divergent channel without Bumps

Sr No	Voltage [V] (Volts)	Current [I] (Amps)	Temperature in °c						Velocity [m/s]	Mass flow rate Kg/sec
			T_{in} °C	T_1°C	T_2°C	T_3°C	T_4°C	T_{out} °C		
1	60	0.35	28	51	54	56	52	36	10	0.00874
2	60	0.35	28	40	41	43	42	33	15	0.01312
3	60	0.35	28	37	38	40	39	32	20	0.01749
4	60	0.35	28	36	37	38	36	32	25	0.02187
5	60	0.35	28	35	36	37	35	31	30	0.02624

Table:2Divergent channel with Bumps

Sr No	Voltage [V] (Volts)	Current [I] (Amps)	Temperature in °c						Velocity [m/s]	Mass flow rate Kg/sec
			T_{in} °C	T_1°C	T_2°C	T_3°C	T_4°C	T_{out} °C		

1	100	0.58	28	65	68	72	66	37	10	0.00874
2	100	0.58	28	56	58	63	59	38	15	0.01312
3	100	0.58	28	49	54	55	51	35	20	0.01749
4	100	0.58	28	45	46	49	48	33	25	0.02187
5	100	0.58	28	41	43	45	44	33	30	0.02624

Table:3Divergent channel without Bumps

Sr No	Voltage [V] (Volts)	Current [I] (Amps)	Temperature in °c						Velocity [m/s]	Mass flow rate Kg/sec
			$T_{in}{}^{o}C$	$T_1{}^{o}C$	$T_2{}^{o}C$	$T_3{}^{o}C$	$T_4{}^{o}C$	$T_{out}{}^{0}C$		
1	100	0.58	28	56	60	63	58	37	10	0.00874
2	100	0.58	28	48	53	55	49	36	15	0.01312
3	100	0.58	28	43	45	47	46	34	20	0.01749
4	100	0.58	28	38	40	43	42	32	25	0.02187
5	100	0.58	28	37	39	40	39	32	30	0.02624

Table 4.Divergent channel with Bump

V RESULTS AND DISCUSSION

The experimentation is carried out with the divergent duct heat transfer enhancement methods. Heat transfer coefficient and Reynolds Number are calculated for all conditions. Parameters were plotted for different values of Reynolds number, for the arrangement without bumps and with bumps in the divergent duct.

Graph between plain divergent duct and divergent duct with bumps.(at 60 volt & 0.35 amp)

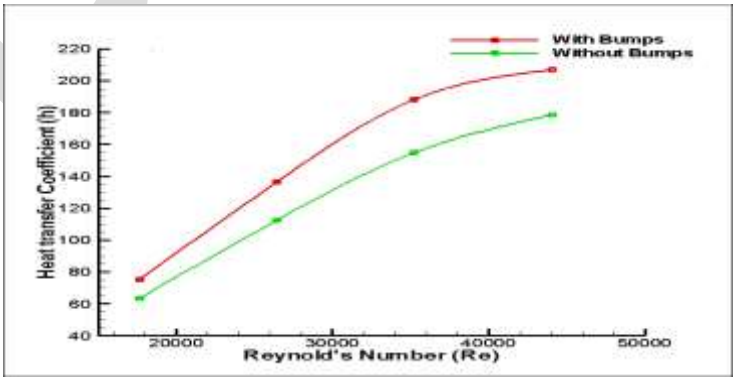

Graph No.1 Heat transfer coefficient Vs Reynolds Number (at 60 volt.)

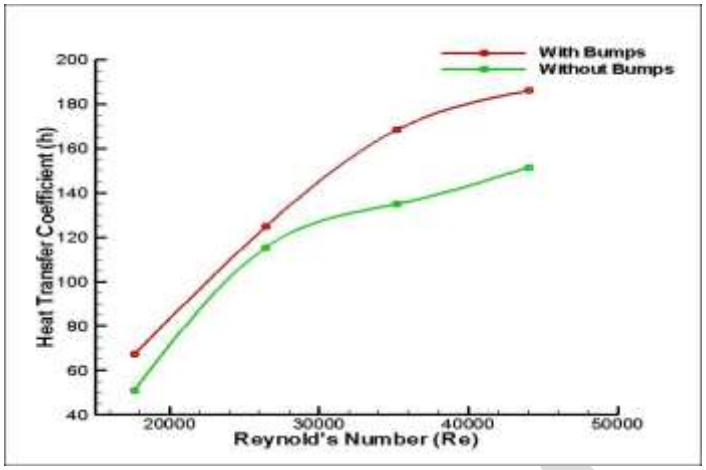

Graph No.2 Heat transfer coefficient Vs Reynolds Number (at 100 volt.)

From the graph 1 and 2, it is observed that the heat transfer coefficient increases with increase in Reynolds no. As Reynolds no. increases, the air flow will cause more turbulence so due to which the heat transfer rate will increase. From the Fig.2 and 3 it is observed that the Divergent duct without using bumps gives the less heat transfer coefficient with the use of bumps in the divergent duct create more turbulence in duct which increases the heat transfer coefficient. From the above description, it can be seen that to heat transfer enhancement divergent channel with the bumps to increase up to 40 to 50 % because of the turbulent mixing in the flow near the wall by producing with help of bumps, which enhance the turbulent flow heat transfer from the wall.
Over the studied Reynolds number range and Nusselt Number align divergent channel with bumps and without bumps slightly higher Nu values than the plain divergent channel experimentally. For the divergent channel Nusselt number is about 30 to 40 % higher than the plain divergent channel within the Reynolds number range of 17621.14 to 44052.86. It is found that, over the studied Reynolds number range reasonably good agreements between the experimental Nu values have been achieved for the plain divergent channel as compare to divergent channel without bumps.

CFD WORK

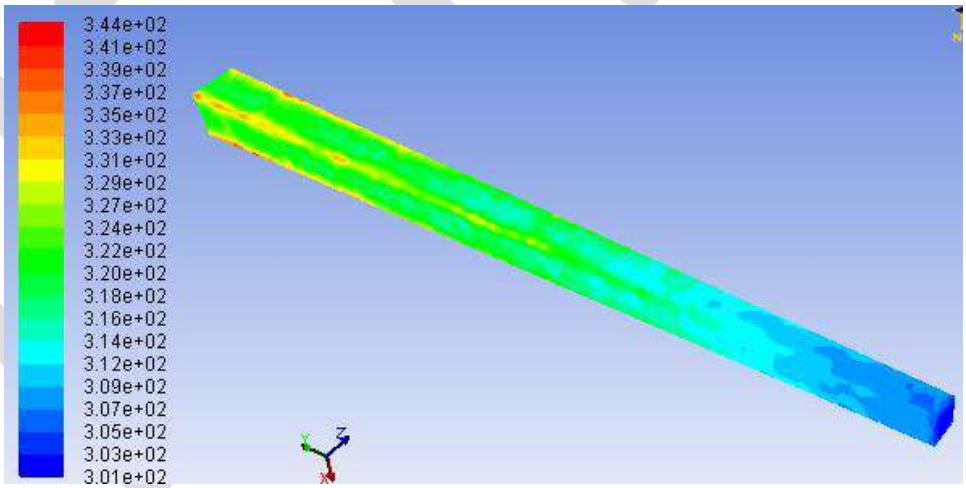

Figure 4: Static Temperature Contour Plots for 0.00874944 kg/sec

Figure.4 indicates that, wall surface temperature contours show the pattern of flow in the duct. It is seen from the figure that due to bumps behavior in the divergent channel wall temperature is a decreases from inlet to outlet along with the length of duct at all times.

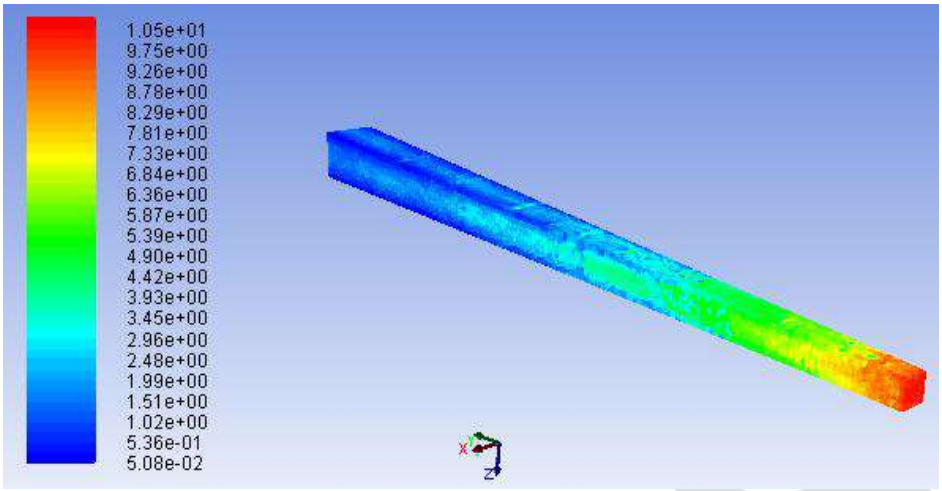

Figure 5.The Velocity Vector Plot for 0.00874944 kg/sec

It is seen from the Figure 4 that due to the bumps there is a pressure increases with decrease the velocity from inlet to outlet along with the length of divergent duct.

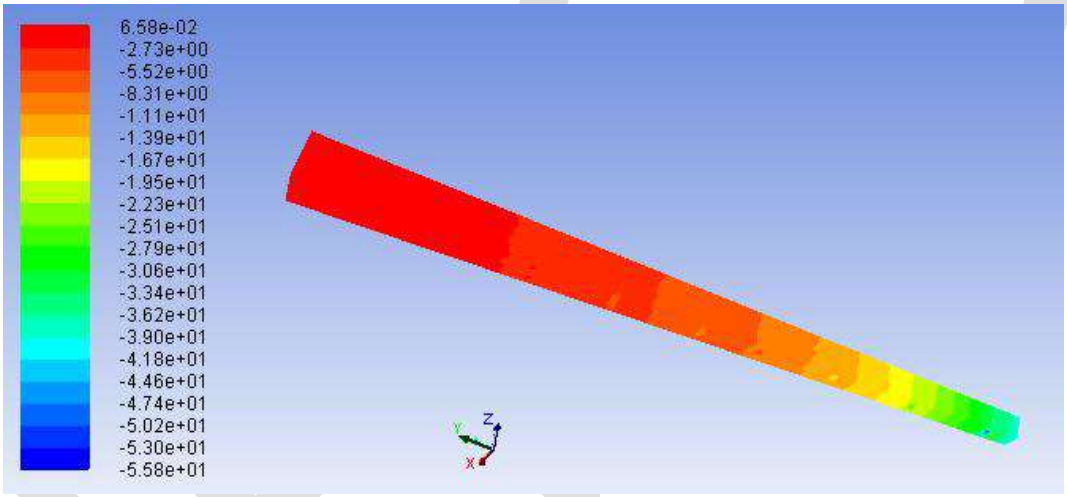

Figure 6: The Pressure plot for 0.00874944 kg/sec

Figure 6 indicates the pressure contour of divergent duct varies along the length variation. It is seen from the figure that there is increase in pressure along the length of wall, due to bumps surface in the divergent duct, while the pressure is increases from inlet to outlet.

VII CONCLUSION

1. This study focused on investigating whether the use of bumps can enhance heat transfer characteristics for a divergent duct.
2. In this experimental study we get different Reynolds numbers ranging from 17621.1454 to 44052.8634, which gives the good heat transfer enhancement.
3.The advantages of the divergent channel with internal Bumps are fluid mixing is more as compared to cylindrical pipe, pressure drop is less and boundary layer separation occurs. The main advantage of these bumps is to increase the heat transfer enhancement increases 25 to 35 % as compare to plain divergent channel.

REFERENCES:

1. Wang.L.H, Tao.W.Q, Wang.Q.W, Wong.T.T. , 2001. Experimental study of developing turbulent flow and heat transfer in ribbed convergent/divergent square duct, International Journal of Heat and fluid flow, Vol. 22, pp. 603-613.

2. Sivakumar, K., Natarajan, E., Kulasekharan, N., Heat transfer and pressure drop comparison between smooth and different sized rib – roughened divergent rectangular ducts, International journal of Engineering and Technology, vol. 6,(2014), No.1, pp. 263-272.

3. Soo Wban Abn and Kang Pil Son "An Investigation on Friction Factors and Heat Transfer Coefficients in a Rectangular Duct with Surface Roughness" KSME International Journal Vol 16 No.4, pp. 549-556, 2002.

4. C. Bi, G.H. Tang, W.Q. Tao, Heat transfer enhancement in mini-channel heat sinks with dimples and cylindrical grooves, Applied Thermal Engineering 55 (2013) 121-132.

5. Dr. Mohammed Najm Abdullah, Heat Transfer and Pressure Drop in Turbulent Flow through an Eccentric Converging-Diverging Tube with Twisted Tape Inserts.

6. Pradip Ramdas Bodade, Dinesh Kumar Koli, "A study on the heat transfer enhancement for air flow through a duct with various rib inserts", International Journal of Latest Trends in Engineering and Technology (IJLTET), Vol. 2 Issue 4 July 2013.

7. Suhas V. Patil, P. V.Vijay Babu, "Heat Transfer Augmentation in a Circular tube and Square duct Fitted with Swirl Flow Generators", International Journal of Chemical Engineering and Applications, Vol. 2 , No. 5 , October 2011.

8. Dr. Anirudh Gupta, Mayank Uniyal, "Review of Heat Transfer Augmentation through Different Passive Intensifier Methods, IOSR Journal of Mechanical and Civil Engineering (IOSRJMCE) ISSN: 2278-1684 Volume 1, Issue 4 (July-Aug 2012), PP 14-21.

9.Vijay D. Shejwalkar, M.D. Nadar, "Experimental Study on Effect of Area and Turbulence on Heat Transfer through Circular Pipe by Using Internal Threading in Drying System", Journal of Basic and Applied Engineering Research Print ISSN: 2350-0077; Online ISSN: 2350-0255; Volume 1, Number 1; September, 2014 pp. 24-29.

10. HONG Mengna, DENG Xianhe, HUANG Kuo and LI Zhiwu, "Compound Heat Transfer Enhancement of a Converging-Diverging Tube with Evenly Spaced Twisted tapes", Chin. J. Chem. Eng., 15(6) 814—820 (2007).

11.A.K.Burse, Experimental Investigation on Turbulent Flow Heat Transfer in a Horizontal Circular Pipe using Coil and Twisted Tape Inserts. IOSR Journal of Mechanical and Civil Engineering (IOSR-JMCE) e-ISSN: 2278-1684,p-ISSN: 2320-334X, Volume 11, Issue 5 Ver. VI (Sep- Oct. 2014), PP 07-14.

12.S. Naga Sarada, A.V. Sita Rama Raju, K. Kalyani Radha and L. Shyam Sunder, "Enhancement of heat transfer using varying width twisted tape inserts", International Journal of Engineering, Science and Technology Vol. 2, No. 6, pp. 07-118, (2010).

13. Dr. Mohammed Najm Abdullah, Heat Transfer and Pressure Drop in Turbulent Flow through an Eccentric Converging-Diverging Tube with Twisted Tape Inserts.

14.W.Chang, T.-M.Liou, T.H.Lee, Thermal performance comparison between radically rotating ribbed parallelogram channels with and without dimples, International Journal of Heat and Mass Transfer, 2012,55, pp.3541-3559.

15.Yu Rao a,Yamin Xu, Chaoyi Wana, An experimental and numerical study of flow and heat transfer in channels with pin fin-dimple and pin fin arrays, Experimental Thermal and Fluid Science, 2012, 38, pp.237-247.

16. David J. Kukulka, Rick Smithb, Kukulka D.J./Smith R. "Enhanced Heat Transfer Surface Development for Exterior Tube Surfaces", chemical engineering Transaction,32, 2013,511-516

International Journal of Engineering Research and General Science Volume 3, Issue 6, November-December, 2015
ISSN 2091-2730

AREA DELAY POWER EFFICIENT CARRY SELECT ADDER ON RECONFIGURABLE HARDWARE

Anjaly Sukumaran

MTech , Mahatma Gandhi University,anjalysukumaran2010@gmail.com,9605707726

Abstract— LOW-POWER, area-efficient, and high-performance VLSI systems are increasingly used in portable and mobile devices, multi standard wireless receivers, and bio medical instrumentation. An adder is the main component of an arithmetic unit. A complex digital signal processing (DSP) system involves several adders. An efficient adder design essentially improves the performance of a complex DSP system. A ripple carry adder (RCA) uses a simple design, but carry propagation delay (CPD) is the main concern in this adder.Carry look-ahead and carry select (CS) methods have been suggested to reduce the CPD of adders. A conventional CSLA has less CPD than an RCA, but the design is not attractive since it uses a dual RCA. The main objective of SQRT-CSLA design is to provide a parallel path for carry propagation that helps to reduce the overall adder delay. The BEC-based CSLA involves less logic resources than the conventional CSLA, but it has marginally higher delay. A CSLA based on common Boolean logic (CBL) involves significantly less logic resource than the conventional CSLA but it has longer CPD, which is almost equal to that of the RCA. To overcome this problem, a SQRT-CSLA based on CBL was proposed . However, the CBL-based SQRT CSLA design requires more logic resource and delay than the BEC-based SQRT-CSLA . We observe that logic optimization largely depends on availability of redundant operations in the formulation, whereas adder delay mainly depends on data dependence. In the existing designs, logic is optimized without giving any consideration to the data dependence. In this brief, we made an analysis on logic operations involved in conventional and BEC-based CSLAs to study the data dependence and to identify redundant logic operations. Based on this analysis, we have proposed a logic formulation for the CSLA. The main contribution in this brief are logic formulation based on data dependence and optimized carry generator (CG) and CS design.So in this project work I have designed and implemented an FPGA based Low power and Area Efficient Carry Select adder . The design was coded in VHDL, simulated Xilinx ISE Design Suit 14.1 and implemented in Spartan6 FPGA trainer board.A theoretical estimate shows that the proposed SQRT-CSLA involves nearly 35% less area–delay–product (ADP) than the BEC-based SQRT-CSLA, which is best among the existing SQRT-CSLA designs, on average, for different bit-widths. The application-specified integrated circuit (ASIC) synthesis result shows that the BEC-based SQRT-CSLA design involves 48% more ADP and consumes 50% more energy than the proposed SQRT-CSLA, on average, for different bit-widths.

Keywords— Adder, Ripple Carry Adder, Carry Propagation Delay, Common Boolean Logic, adder delay, low - power design, area-delay -product

INTRODUCTION

A conventional carry select adder (CSLA) is an RCA–RCA configuration that generates a pair of sum words and output carry bits corresponding the anticipated input-carry (cin = 0 and 1) and selects one out of each pair for final-sum and final-output-carry. A conventional CSLA has less CPD than an RCA, but the design is not attractive since it uses a dual RCA. Few attempts have been made to avoid dual use of RCA in CSLA design. In a SQRT CSLA, CSLAs with increasing size are connected in a cascading structure. The main objective of SQRT-CSLA design is to provide a parallel path for carry propagation that helps to reduce the overall adder delay. The BEC-based CSLA involves less logic resources than the conventional CSLA, but it has marginally higher delay. A CSLA based on common Boolean logic (CBL) involves significantly less logic resource than the conventional CSLA but it has longer CPD, which is almost equal to that of the RCA. To overcome this problem, a SQRT-CSLA based on CBL was proposed . However, the CBL-based SQRT CSLA design requires more logic resource and delay than the BEC-based SQRT-CSLA . We observe that logic optimization largely depends on availability of redundant operations in the formulation, whereas adder delay mainly depends on data dependence. In the existing designs, logic is optimized without giving any consideration to the data dependence. In this brief, we made an analysis on logic operations involved in conventional and BEC-based CSLAs to study the data dependence and to identify redundant logic operations. Based on this analysis, we have proposed a logic formulation for the CSLA. The main contribution in this brief are logic formulation based on data dependence and optimized carry generator (CG) and CS design.

Customized algorithm implemented on FPGA generally works out better as compared to the similar algorithm executed on a standard x86 architecture. The algorithm implemented on FPGA functions as a hardware circuit and the complicated computational tasks accomplished by independent modules are formed by logic gates. The parallelism architecture offered by FPGA enables real time processing. Another reason which influences the use of FPGA in this system because it is closed to Application-Specific Integration Circuit (ASIC).Field Programmable Gate Array (FPGA) is an integrated circuit which can be configured by end user to implement functions defined by the designer. FPGAs are gaining popularity in design implementation due to their increasing logic density which

had reduced the cost per logic. FPGAs can be configured to meet custom requirement or functions and as well as performing tasks that can be done in parallel and pipelined whereby hardware outperforms software. Other than that, with existence of internet community designing and publishing IP cores, such as Open Cores, had allowed many custom designs to be made by Plug-and-Play (PnP) of multiple IP cores into single SOC using FPGAs.So in this project work I have designed and implemented an FPGA based Low power and Area Efficient Carry Select adder . The design was coded in VHDL, simulated Xilinx ISE Design Suit 14.1 and implemented in Spartan6 FPGA trainer board.

REMAINING CONTENTS

2. DESIGN OF THE CARRY SELECT ADDER

The CSLA has two units: 1) the sum and carry generator unit (SCG)2) the sum and carry selection unit. The SCG unit consumes most of the logic resources of CSLA and significantly contributes to the critical path. Different logic designs have been suggested for efficient implementation of the SCG unit. We made a study of the logic designs suggested for the SCG unit of conventional and BEC-based CSLAs by suitable logic expressions. The main objective of this study is to identify redundant logic operations and data dependence. Accordingly, we remove all redundant logic operations and sequence logic operations based on their data dependence.As shown in Figure.3 (a), the SCG unit of the conventional CSLA is composed of two n-bit RCAs, where n is the adder bit-width. The logic operation of the n-bit RCA is performed in four stages: 1) half-sum generation (HSG) 2) half-carry generation (HCG) 3) full-sum generation (FSG) 4) full-carry generation (FCG)

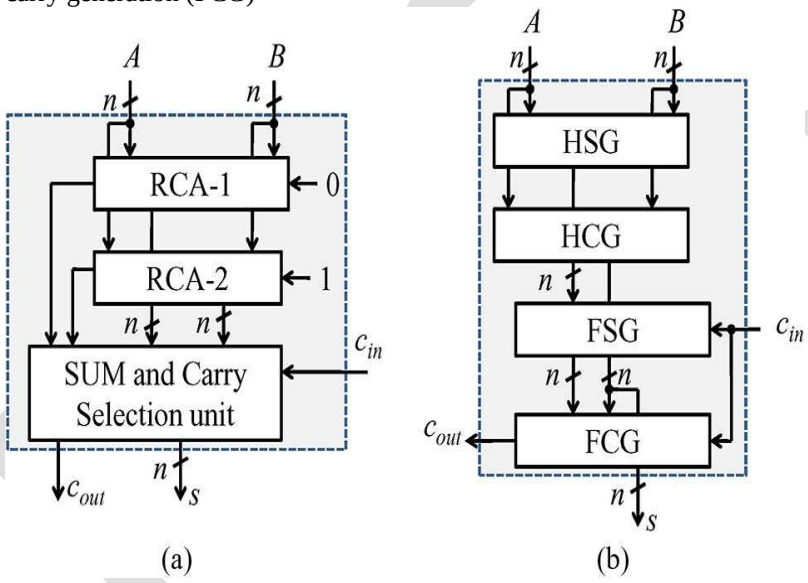

Figure.1. Various stages of proposed CSLA

3. IMPLEMENTATION OF THE LOW POWER AND AREA EFFICIENT CARRY SELECT ADDER

Carry Select Adder (CSLA) is one of the fastest adders used in many data-processing processors to perform fast arithmetic functions. From the structure of the CSLA, it is clear that there is scope for reducing the area and power consumption in the CSLA. The CSLA is used in many computational systems to alleviate the problem of carry propagation delay by independently generating multiple carries and then select a carry to generate the sum. However, the CSLA is not area efficient because it uses multiple pairs of Ripple Carry Adders (RCA) to generate partial sum and carry by considering carry input and, then the final sum and carry are selected by the multiplexers (mux). The main advantage of BEC logic comes from the lesser number of logic gates than the Full Adder (FA) structure. Based on this modification 8-, 16-, 32-, and 64-b square-root CSLA (SQRT CSLA) architecture have been developed and compared with the regular SQRT CSLA architecture.

3.1 DELAY AND AREA EVALUATION METHODOLOGY OF THE BASIC ADDER BLOCKS

The AND, OR, and Inverter (AOI) implementation of an XOR gate is shown in Figure.1. The gates between the dotted lines are performing the operations in parallel and the numeric representation of each gate indicates the delay contributed by that gate. The

delay and area evaluation methodology considers all gates to be made up of AND, OR, and Inverter, each having delay equal to 1 unit and area equal to 1 unit. We then add up the number of gates in the longest path of a logic block that contributes to the maximum delay. The area evaluation is done by counting the total number of AOI gates required for each logic block. Based on this approach, the CSLA adder blocks of 2:1 mux, Half Adder (HA), and FA are evaluated and listed in Table I.

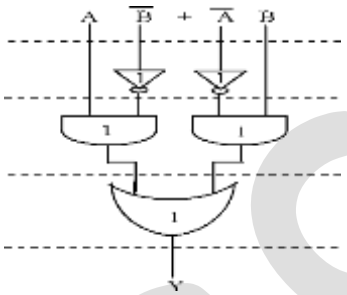

Figure.2. Delay and Area evaluation of an XOR gate.

Adder blocks	Delay	Area
XOR	3	5
2:1 Mux	3	4
Half adder	3	6
Full adder	6	13

Table .1. Delay and area count of the basic blocks of CSLA

As stated above the main idea is to use BEC instead of the RCA in order to reduce the area and power consumption of the regular CSLA. A structure and the function table of a 4-b BEC are shown in Figure. 2 and Table 2, respectively.

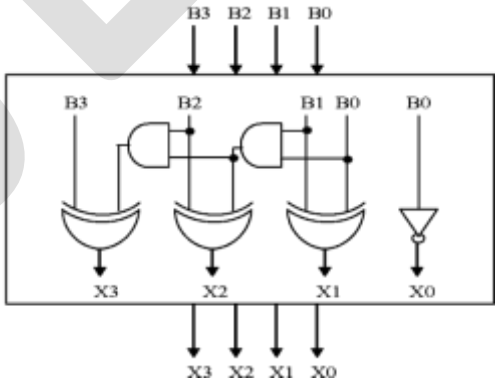

Figure.3. 4-b BEC

B[3:0]	X[3:0]
0000	0001
0001	0010
⋮	⋮
1110	1111
1111	0000

Table 2. Function Table of the 4-b BEC

Figure. 3 illustrates how the basic function of the CSLA is obtained by using the 4-bit BEC together with the mux. One input of the 8:4 mux gets as it input (B3, B2, B1, and B0) and another input of the mux is the BEC output. This produces the two possible partial results in parallel and the mux is used to select either the BEC output or the direct inputs according to the control signal Cin. The importance of the BEC logic stems from the large silicon area reduction when the CSLA with large number of bits are designed.

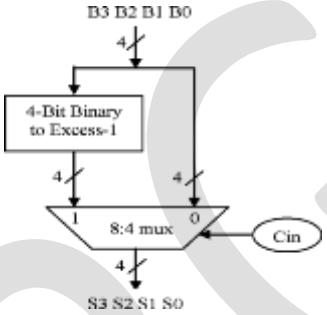

Figure. 4. 4-b BEC with 8:4 mux.

3.2. DELAY AND AREA EVALUATION METHODOLOGY OF REGULAR 16-B SQRT CSLA

The structure of the 16-b regular SQRT CSLA is shown in Figure.4. It has five groups of different size RCA. The delay and area evaluation of each group are shown in Figure.5, in which the numerals within [] specify the delay values, e.g., sum2 requires 10 gate delays. The group2 [see Figure. 5(a)] has two sets of 2-b RCA. Based on the consideration of delay values of Table I, the arrival time of selection input of 6:3 mux is earlier. Except for group2, the arrival time of mux selection input is always greater than the arrival time of data outputs from the RCA's. The one set of 2-b RCA in group2 has 2 FA and the other set has 1 FA and 1 HA . Similarly, the estimated maximum delay and area of the other groups in the regular SQRT CSLA are evaluated and listed in Table 3.

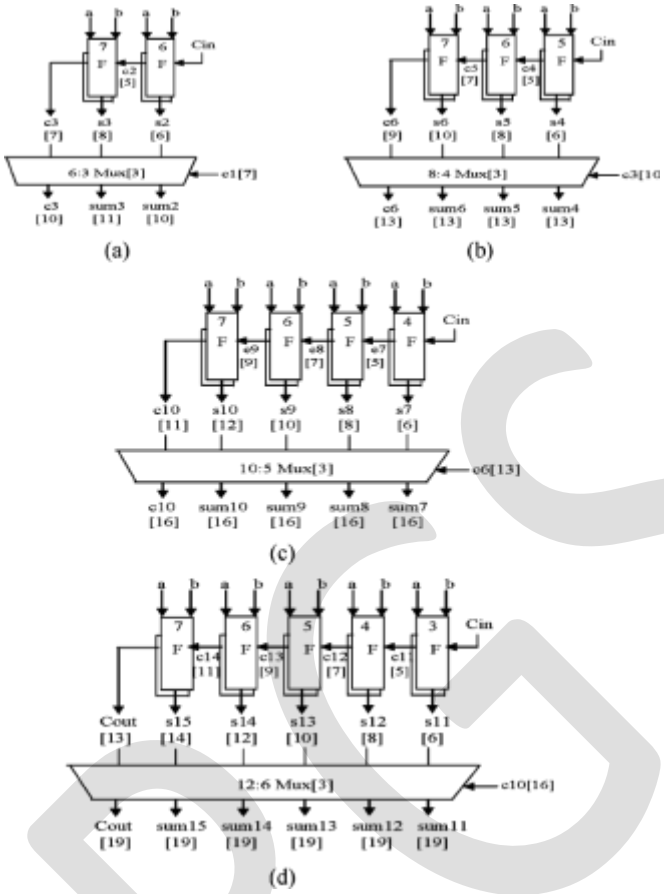

***Figure. 6. Delay and area evaluation of regular SQRT CSLA: (a) group2, (b) group3, (c) group4, and (d) group5. F is a Full* Adder.**

Group	Delay	Area
Group2	11	57
Group3	13	87
Group4	16	117
Group5	19	147

Table .3. Delay and area count of regular SQRT CSLA groups

3.3 SQRT CSLA USING COMMON BOOLEAN LOGIC

In the design of Integrated Circuits, area occupancy plays a vital role because of increasing the necessity of portable systems. Carry Select Adder (CSLA) is one of the fastest adders used in many data-processing processors to perform fast arithmetic functions. After logic simplification and sharing partial circuit, only one XOR gate and one inverter gate in each summation operation as well as one AND gate and one inverter gate in each carry-out operation are needed. Through the multiplexer, the correct output is selected according to the logic states of the carry in signal. Based on this modification a new architecture has been developed and compared

with the regular and modified Square-root CSLA (SQRT CSLA) architecture. The modified architecture has been developed using Binary to Excess-1 converter (BEC). The proposed architecture has reduced area and delay as compared with the regular SQRT CSLA architecture.

An area-efficient carry select adder by sharing the common Boolean logic term to remove the duplicated adder cells in the conventional carry select adder is shown and it saves many transistor counts and achieves a low power. Through analyzing the truth table of a single bit full adder, to find out the output of summation signal as carry-in signal is logic '0' is the inverse signal of itself as carry-in signal is logic '1'. By sharing the common Boolean logic term in summation generation, a proposed carry select adder design is generated. To share the common Boolean logic term, it only needs to implement one OR gate with one INV gate to generate the carry signal and summation signal pair. Once the carry-in signal is ready, then select the correct carry-out output according to the logic state of carry-in signal. This method replaces the BEC add one circuit by Common Boolean Logic. The summation and carry signal for full adder which has Cin=1, generate by INV and OR gate. Through the multiplexer, the correct output result is selected according to the logic state of carry-in signal.. One input to the mux goes from ripple carry adder block with Cin=0 and other input from the Common Boolean logic.

While analyzing the truth table of single bit full adder, results show that the output of summation signal as carry-in signal is logic "0" is inverse signal of itself as carry-in signal is logic "1". It is illustrated by circles in Table 6. To share the Common Boolean Logic term, we only need to implement a XOR gate and one INV gate to generate the summation pair. And to generate the carry pair, we need to implement one OR gate and one AND gate. In this way, the summation and carry circuits can be kept parallel.

C_{in}	A	B	S0	C0
0	0	0	0	0
0	0	1	1	0
0	1	0	1	0
0	1	1	0	1
1	0	0	1	0
1	0	1	0	1
1	1	0	0	1
1	1	1	1	1

Table .4. Truth table of single bit full adder , where the upper half part is the case of cin=0 and the lower half part is the case of cin=1

This method replaces the Binary to Excess-1 converter add one circuit by common Boolean logic. As compared with modified SQRT CSLA, the proposed structure is little bit faster. Internal structure of proposed CSLA is shown in Figure. 8.In the proposed SQRT CSLA, the transistor count is trade-off with the speed in order to achieve lower power delay product. Thus the proposed SQRT CSLA using CBL is better than all the other designed adders. Figure.9 shows the block diagram of Proposed SQRT CSLA.

3.4 AREA DELAY POWER EFFICIENT CARRY SELECT ADDER

LOW-POWER, area-efficient, and high-performance VLSI systems are increasingly used in portable and mobile devices, multi standard wireless receivers, and biomedical instrumentation. An adder is the main component of an arithmetic unit. A complex digital signal processing (DSP) system involves several adders. An efficient adder design essentially improves the performance of a complex DSP system. A ripple carry adder (RCA) uses a simple design, but carry propagation delay (CPD) is the main concern in this adder. Carry look-ahead and carry select (CS) methods have been suggested to reduce the CPD of adders. A conventional carry select adder (CSLA) is an RCA–RCA configuration that generates a pair of sum words and output carry bits corresponding the anticipated

input-carry (cin = 0 and 1) and selects one out of each pair for final-sum and final-output-carry. A conventional CSLA has less CPD than an RCA, but the design is not attractive since it uses a dual RCA. Few attempts have been made to avoid dual use of RCA in CSLA design. In a SQRT CSLA, CSLAs with increasing size are connected in a cascading structure. The main objective of SQRT-CSLA design is to provide a parallel path for carry propagation that helps to reduce the overall adder delay. The BEC-based CSLA involves less logic resources than the conventional CSLA, but it has marginally higher delay. The CBL-based CSLA involves significantly less logic resource than the conventional CSLA but it has longer CPD, which is almost equal to that of the RCA. The CBL-based SQRTCSLA design requires more logic resource and delay than the BEC-based SQRT-CSLA. We observe that logic optimization largely depends on availability of redundant operations in the formulation, whereas adder delay mainly depends on data dependence. In the existing designs, logic is optimized without giving any consideration to the data dependence. In this brief, we made an analysis on logic operations involved in conventional and BEC-based CSLAs to study the data dependence and to identify redundant logic operations. Based on this analysis, we have proposed a logic formulation for the CSLA. The main contribution in this brief are logic formulation based on data dependence and optimized carry generator (CG) and CS design. Based on the proposed logic formulation, we have derived an efficient logic design for CSLA. Due to optimized logic units, the proposed CSLA involves significantly less ADP than the existing CSLAs.

- **LOGIC FORMULATION**

The CSLA has two units:
1) the sum and carry generator unit (SCG)
2) the sum and carry selection unit.

The SCG unit consumes most of the logic resources of CSLA and significantly contributes to the critical path. Different logic designs have been suggested for efficient implementation of the SCG unit. We made a study of the logic designs suggested for the SCG unit of conventional and BEC-based CSLAs by suitable logic expressions. The main objective of this study is to identify redundant logic operations and data dependence. Accordingly, we remove all redundant logic operations and sequence logic operations based on their data dependence.

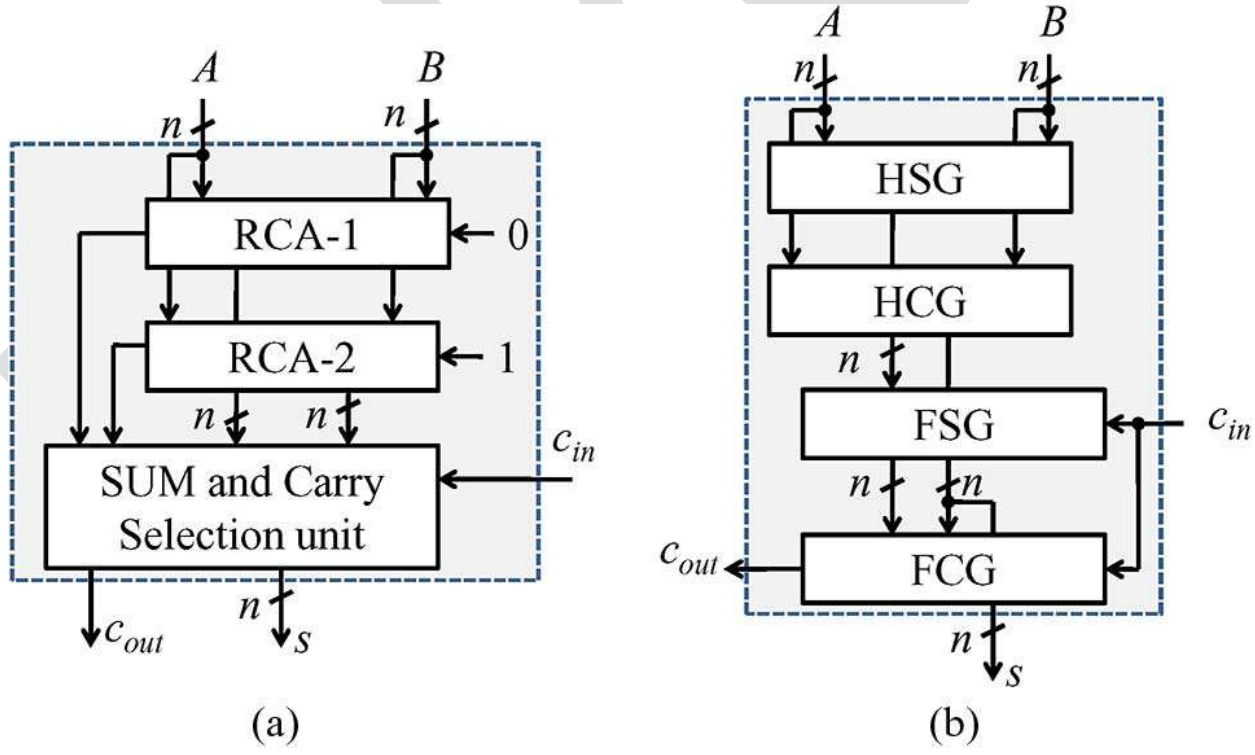

Figure. 7. (a) Conventional CSLA; n is the input operand bit-width. (b) The logic operations of the RCA is shown in split form, where HSG, HCG, FSG, and FCG represent half-sum generation, half-carry generation, full-sum generation, and full-carry generation, respectively.

- **Logic Expressions of the SCG Unit of the Conventional CSLA**

As shown in Figure.10 (a), the SCG unit of the conventional CSLA is composed of two n-bit RCAs, where n is the adder bit-width. The logic operation of the n-bit RCA is performed in four stages:

1) half-sum generation (HSG)
2) half-carry generation (HCG)
3) full-sum generation (FSG)
4) full-carry generation (FCG)

Suppose two n-bit operands are added in the conventional CSLA, then RCA-1 and RCA-2 generate n-bit sum (s0 and s1) and output-carry (c0 out and c1 out) corresponding to input-carry (cin = 0 and cin = 1), respectively. Logic expressions of RCA-1 and RCA-2 of the SCG unit of the n-bit CSLA are given as

$$s_0^0(i) = A(i) \oplus B(i) \quad c_0^0(i) = A(i) \cdot B(i) \tag{1a}$$
$$s_1^0(i) = s_0^0(i) \oplus c_1^0(i-1) \tag{1b}$$
$$c_1^0(i) = c_0^0(i) + s_0^0(i) \cdot c_1^0(i-1) \quad c_{\text{out}}^0 = c_1^0(n-1) \tag{1c}$$
$$s_0^1(i) = A(i) \oplus B(i) \quad c_0^1(i) = A(i) \cdot B(i) \tag{2a}$$
$$s_1^1(i) = s_0^1(i) \oplus c_1^1(i-1) \tag{2b}$$
$$c_1^1(i) = c_0^1(i) + s_0^1(i) \cdot c_1^1(i-1) \quad c_{\text{out}}^1 = c_1^1(n-1) \tag{2c}$$

where $c_1^0(-1) = 0$, $c_1^1(-1) = 1$, and $0 \le i \le n-1$.

As shown in (1a)–(1c) and (2a)–(2c), the logic expression of {s00(i), c00(i)} is identical to that of {s10(i), c10(i)}. These redundant logic operations can be removed to have an optimized design for RCA-2, in which the HSG and HCG of RCA-1 is shared to construct RCA-2. Based on this, we have used an add-one circuit instead of RCA-2 in the CSLA, in which a BEC circuit is used for the same purpose. Since the BEC-based CSLA offers the best area–delay–power efficiency among the existing CSLAs, we discuss here the logic expressions of the SCG unit of the BEC-based CSLA as well.

Logic Expression of the SCG Unit of the BEC-Based CSLA

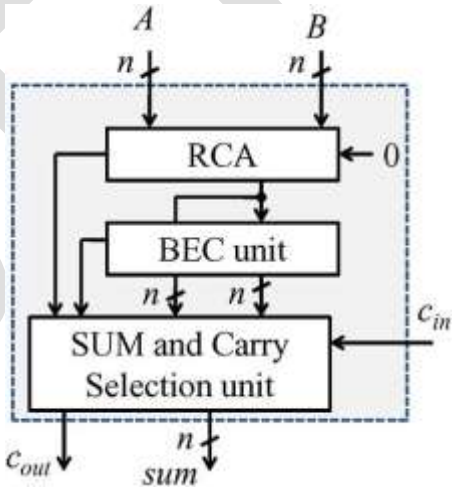

Figure. 8. Structure of the BEC-based CSLA; n is the input operand bit-width.

As shown in Figure.11, the RCA calculates n-bit sum s01 and c0 out corresponding to cin = 0. The BEC unit receives s01 and c0 out from the RCA and generates (n + 1)-bit excess-1 code. The most significant bit (MSB) of BEC represents c1out, in which n least significant bits (LSBs) represent s11 . The logic expressions of the RCA are the same as those given in (1a)–(1c). The logic expressions of the BEC unit of the n-bit BEC-based CSLA are given as

$$s_1^1(0) = \overline{s_1^0(0)} \quad c_1^1(0) = s_1^0(0) \tag{3a}$$
$$s_1^1(i) = s_1^0(i) \oplus c_1^1(i-1) \tag{3b}$$
$$c_1^1(i) = s_1^0(i) \cdot c_1^1(i-1) \tag{3c}$$
$$c_{\text{out}}^1 = c_1^0(n-1) \oplus c_1^1(n-1) \tag{3d}$$

for $1 \leq i \leq n-1$.

We can find from (1a)–(1c) and (3a)–(3d) that, in the case of the BEC-based CSLA, c11 depends on s01, which otherwise has no dependence on s01 in the case of the conventional CSLA. The BEC method therefore increases data dependence in the CSLA. We have considered logic expressions of the conventional CSLA and made a further study on the data dependence to find an optimized logic expression for the CSLA. It is interesting to note from (1a)–(1c) and (2a)–(2c) that logic expressions of s01 and s11 are identical except the terms c01 and c11since (s00 = s10 = s0). In addition, we find that c01 and c11depend on {s0, c0, cin}, where c0 = c00 = c10 . Since c01 and c11 have no dependence on s01 and s11 , the logic operation of c01 and c11 can be scheduled before s01 and s11 , and the select unit can select one from the set (s01 , s11) for the final-sum of the CSLA. We find that a significant amount of logic resource is spent for calculating {s01 , s11 }, and it is not an efficient approach to reject one sum-word after the calculation. Instead, one can select the required carry word from the anticipated carry words {c0 and c1} to calculate the final-sum. The selected carry word is added with the half-sum (s0) to generate the final-sum (s). Using this method, one can have three design advantages:

1) Calculation of s01 is avoided in the SCG unit;
2) the n-bit select unit is required instead of the (n + 1) bit;
3) small output-carry delay.

All these features result in an area–delay and energy-efficient design for the CSLA. We have removed all the redundant logic operations of (1a)–(1c) and (2a)–(2c) and rearranged logic expressions of (1a)–(1c) and (2a)–(2c) based on their dependence. The proposed logic formulation for the CSLA is given as

$$s_0(i) = A(i) \oplus B(i) \quad c_0(i) = A(i) \cdot B(i) \tag{4a}$$
$$c_1^0(i) = c_1^0(i-1) \cdot s_0(i) + c_0(i) \quad \text{for } (c_1^0(0) = 0) \tag{4b}$$
$$c_1^1(i) = c_1^1(i-1) \cdot s_0(i) + c_0(i) \quad \text{for } (c_1^1(0) = 1) \tag{4c}$$
$$c(i) = c_1^0(i) \quad \text{if } (c_{\text{in}} = 0) \tag{4d}$$
$$c(i) = c_1^1(i) \quad \text{if } (c_{\text{in}} = 1) \tag{4e}$$

- **PROPOSED ADDER DESIGN**

The proposed CSLA is based on the logic formulation given in (4a)–(4e), and its structure is shown in Figure. 12(a). It consists of one HSG unit, one FSG unit, one CG unit, and one CS unit. The CG unit is composed of two CGs (CG0 and CG1) corresponding to input-carry '0' and '1'. The HSG receives two n-bit operands (A and B) and generate half-sum word s0 and half-carry word c0 of width n bits each. Both CG0 and CG1 receive s0 and c0 from the HSG unit and generate two n-bit full-carry words c01 and c11 corresponding to input-carry '0' and '1', respectively.

The logic diagram of the HSG unit is shown in Figure. 12(b). The logic circuits of CG0 and CG1 are optimized to take advantage of the fixed input-carry bits. The optimized designs of CG0 and CG1 are shown in Figure. 12(c). and (d), respectively. The CS unit selects one final carry word from the two carry words available at its input line using the control signal cin. It selects c01 when cin = 0; otherwise, it selects c11. The CS unit can be implemented using an n-bit 2-to-l MUX. However, we find from the truth table of the CS unit that carry words c01 and c11 follow a specific bit pattern. If c01 (i) = '1', then c11 (i) = 1, irrespective of s0(i) and c0(i), for 0 ≤ i ≤ n − 1. This feature is used for logic optimization of the CS unit. The optimized design of the CS unit is shown in Figure. 12(e). which is composed of n AND–OR gates. The final carry word c is obtained from the CS unit. The MSB of c is sent to output as cout,

and (n − 1) LSBs are XORed with (n − 1) MSBs of half-sum (s0) in the FSG [shown in Figure. 12(f). to obtain (n − 1) MSBs of final-sum (s). The LSB of s0 is XORed with cin to obtain the LSB of s.

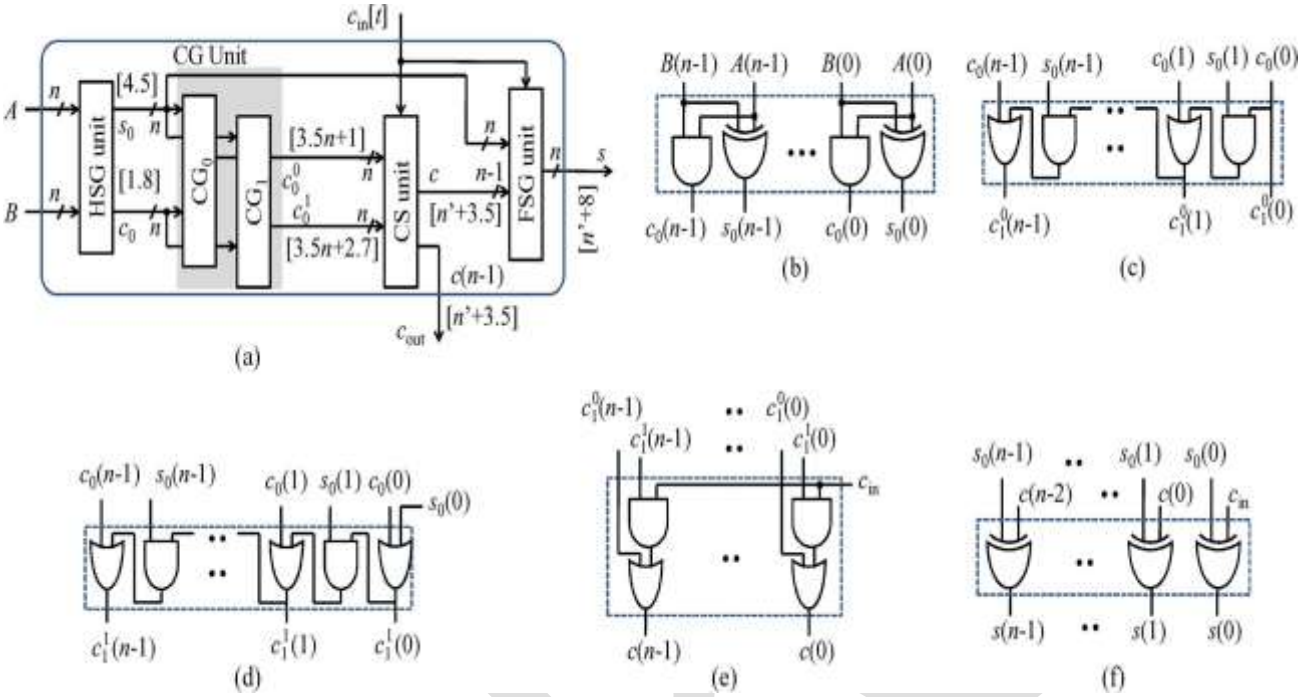

Figure. 9. (a) Proposed CS adder design, where n is the input operand bit-width, and [∗] represents delay (in the unit of inverter delay), n = max(t, 3.5n + 2.7).
(b) Gate-level design of the HSG.
(c) Gate-level optimized design of (CG0) for input-carry = 0.
(d) Gate-level optimized design of (CG1) for input-carry = 1.
(e) Gate-level design of the CS unit.
(f) Gate-level design of the final-sum generation (FSG) unit.

- **PERFORMANCE COMPARISON**

- ***Area–Delay Estimation Method***

We have considered all the gates to be made of 2-input AND, 2-input OR, and inverter (AOI). A 2-input XOR is composed of 2 AND, 1 OR, and 2 NOT gates. The area and delay of the 2-input AND, 2-input OR, and NOT gates are taken from the Synopsys Armenia Educational Department (SAED) 90-nm standard cell library datasheet for theoretical estimation. The area and delay of a design are calculated using the following relations:

$$A = a \cdot N_a + r \cdot N_o + i \cdot N_i \qquad (5a)$$

$$T = n_a \cdot T_a + n_o \cdot T_o + n_i \cdot T_i \qquad (5b)$$

where (Na,No,Ni) and (na, no, ni), respectively, represent the (AND, OR, NOT) gate counts of the total design and its critical path. (a, r, i) and (Ta, To, Ti), respectively, represent the area and delay of one (AND, OR, NOT) gate. We have calculated the (AOI) gate counts of each design for area and delay estimation. Using (5a) and (5b), the area and delay of each design are calculated from the AOI gate counts (Na,No,Ni), (na, no, ni), and the cell details of Table B.

- ***Single-Stage CSLA***

The general expression to calculate the AOI gate counts of the n-bit proposed CSLA and the BEC-based CSLA and CBL-based CSLA are given in Table II of single stage design. We have calculated the AOI gate counts on the critical path of the proposed n-bit CSLA and CSLAs of and used those AOI gate counts in (5b) to find an expression for delay of final-sum and output-carry in the unit of Ti (NOTgate delay). The delay of the n-bit single-stage CSLA is shown in Table II for comparison. For further analysis of the critical path of the proposed CSLA, the delay of each intermediate and output signals of the proposed n-bit CSLA design of Fig. 3 is shown in the square bracket against each signal. We can find from Table II that the proposed n-bit single-stage CSLA adder involves 6n less number of AOI gates than the CSLA of [6] and takes 2.7 and 6.6 units less delay to calculate final-sum and output-carry. Compared with the CBL-based CSLA of [7], the proposed CSLA design involves n more AOI gates, and it takes (n − 4.7) unit less delay to calculate the output-carry. Using the expressions of Table II and AOI gate details of Table I, we have estimated the area and delay complexities of the proposed CSLA and the existing CSLA of [6]–[8], including the conventional one for input bit-widths 8 and 16. For the single-stage CSLA, the input-carry delay is assumed to be t = 0 and the delay of final-sum (fs) represents the adder delay. The estimated values are listed in Table III for comparison. We can find from Table III that the proposed CSLA involves nearly 29% less area and 5% less output delay than that of [6]. Consequently, the CSLA of [6] involves 40% higher ADP than the proposed CSLA, on average, for different bit-widths. Compared with the CBL-based CSLA of [7], the proposed CSLA design has marginally less ADP. However, in the CBL-based CSLA, delay increases at a much higher rate than the proposed CSLA design for higher bitwidths. Compared with the conventional CSLA, the proposed CSLA involves 0.42 ns more delay, but it involves nearly 28% less ADP due to less area complexity. Interestingly, the proposed CSLA design offers multipath parallel carry propagation, whereas the CBL-based CSLA of [7] offers a single carry propagation path identical to the RCA design. Moreover, the proposed CSLA design has 0.45 ns less output-carry delay than the output-sum delay. This is mainly due to the CS unit that produces output-carry before the FSG calculates the final-sum.

3.5 PROPOSED DESIGN OF SQRT CSLA

The proposed SQRT CSLA is developed with the help of modified half adder (HAM), modified full adder (FAM) and modified XOR gate (XORM). In place of BEC, combinational logic block (CLB) is used. XORM has 1 gate less than the conventional XOR gate of 5 gates (AND-OR-NOT implementation) [8] as in Fig.3. HAM has 2 gates less than the conventional half adder as shown in Fig.4. The full adder is constructed with two HAMs and an AND gate [8] shown in Fig.5 has only 9 gates, 4 gates less than conventional full adder. As the number of gates reduce in the basic building blocks of the proposed SQRT CSLA area is also reduced. A part from the above modifications, one more small change is made in the design which allows us to get the carryout of the group without using the mux [7]. The proposed design SQRT CSLA with CLB is as shown in Fig.6. A 16-bit model is presented which is divided into 5 groups. Each group consists of different size of RCAs, CLBs and multiplexers. The CLB is used instead of RCA for Cin = 1. The structure of a 4-bit CLB is given in Fig.7. The sizes of RCA differ from 2-bit in first two groups and consequently increase to 5-bit in group 5. Similarly the size of CLB also increases from 3-bit in group 2 to 6-bit in group 5. The groups in the proposed adder are shown in Fig.8.

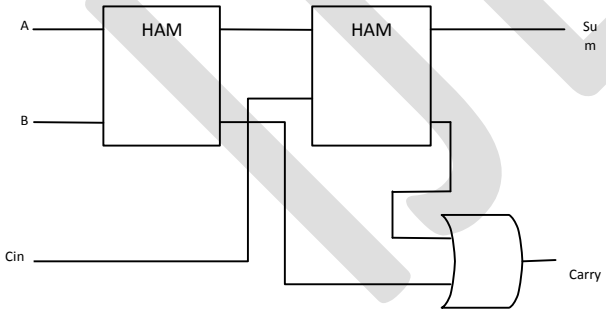

Figure.10. Modified full adder (FAM) using two HAMs

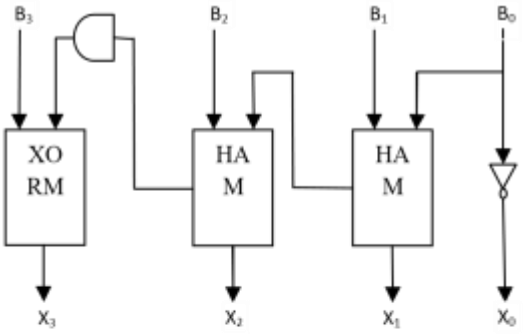

Fig7. 4-bit CLB

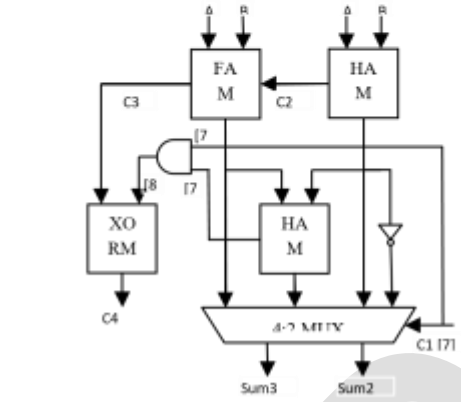

(a)

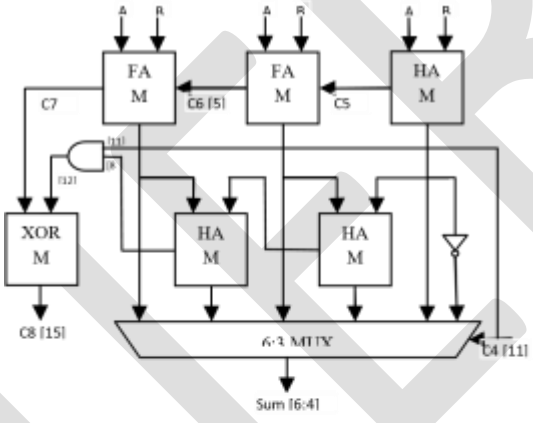

(b)

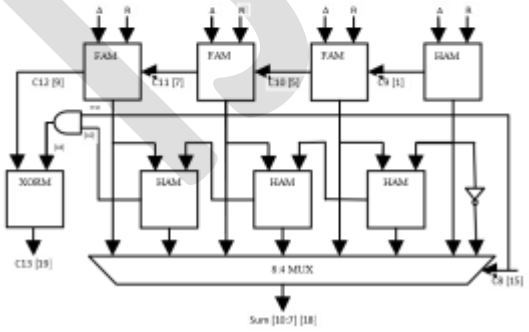

(c)

Fig.11. (a) group 2, (b) group3, (c) group4 of SQRT CSLA with CLB

Group 2 of the proposed adder consists of 2-bit RCA, 3-bit CLB and 4:2 mux. RCA is constructed using one FAM and one HAM. The CLB has one NOT gate, one HAM, one AND gate and a XORM. For the remaining groups the size of RCA and CLB is listed in Table I.

Groups	RCA		Combinational logic block (CLB)			Total no. of gates
	FAM	HAM	NOT gate +AND gate	HAM	XORM	
Group1	2(*9)	0	0	0	0	18
Group 2	1(*9)	1(*4)	1+1	1(*4)	1(*4)	31
Group 3	2(*9)	1(*4)	1+1	2(*4)	1(*4)	48
Group 4	3(*9)	1(*4)	1+1	3(*4)	1(*4)	59
Group 5	4(*9)	1(*4)	1+1	4(*4)	1(*4)	82

Table.9. Gate Count of SQRT CSLA with CLB

Word size	Adders	Delay (ηs)	Area (μm^2)	Total Power (μW)	Powerdelay product (10^{-15}) (J)	Areadelay product (10_{-15})
8-bit	SQRT CSLA	1.68	1035	76.687	129.2954	1745.01
	SQRT CSLA with BEC	1.82	888	66.735	121.4579	1616.16
	SQRT CSLA with CLB	1.85	845	53.186	98.394	1563.25
16-bit	SQRT CSLA	2.903	2259	171.797	498.729	6557.87
	SQRT CSLA with BEC	2.858	1873	139.209	397.859	5353.03
	SQRT CSLA with CLB	3.524	1866	116.850	411.779	6609.37
32-bit	SQRT CSLA	4.310	4787	390.199	1681.758	20631.97
	SQRT CSLA with BEC	4.405	3922	307.931	1356.438	17276.41
	SQRT CSLA with CLB	5.206	3895	253.098	1317.628	20277.37
64-bit	SQRT CSLA	7.119	9883	829.125	5902.543	70357.08
	SQRT CSLA with BEC	6.970	8007	628.192	4378.499	55808.79
	SQRT CSLA with CLB	7.978	7973	545.083	4348.621	63608.59

Table.5. Comparison of SQRT CSLA, SQRT CSLA with BEC and SQRT CSLA with CLB

ACKNOWLEDGMENT

First of all I would like to thank GOD, the Almighty for His divine grace and blessings throughout this Thesis work.

I am greatly indebted to my academic mentors, whose support has given me the confidence to make a study on the topic and present the Thesis work. I hereby express my heart full gratitude to Prof. Sunny Joseph, Head of the Department of Electronics and communication, for being a great source of inspiration.

I will remain indebted to my guide, Mr. Thomas George, Associate Professor in Electronics and communication Department, for his valuable guidance and help extended to me. His guidance enabled me to complete study of the topic in time and present it well. My deep sense of gratitude goes to all teachers of Electronics and communication department who gave valuable support and guidance.

I express my gratitude to the college management and our principal Prof. Geetha B for providing us good library facilities and internet facilities, that helped me a lot for the study of topic in detail.

I would also like to extend my sincere thanks to my family and friends for their whole-hearted support and encouragement.

CONCLUSION

We have analyzed the logic operations involved in the conventional and BEC-based CSLAs to study the data dependence and to identify redundant logic operations. We have eliminated all the redundant logic operations of the conventional CSLA and proposed a new logic formulation for the CSLA. In the proposed scheme, the CS operation is scheduled before the calculation of final-sum, which is different from the conventional approach. Carry words corresponding to input-carry '0' and '1' generated by the CSLA based on the proposed scheme follow a specific bit pattern, which is used for logic optimization of the CS unit. Fixed input bits of the CG unit are also used for logic optimization. Based on this, an optimized design for CS and CG units are obtained. Using these optimized logic units, an efficient design is obtained for the CSLA. The proposed CSLA design involves significantly less area and delay than the recently proposed BEC-based CSLA. Due to the small carry output delay, the proposed CSLA design is a good candidate for the SQRT adder.

REFERENCES:

[1] K. K. Parhi, VLSI Digital Signal Processing. New York, NY, USA:Wiley,1998.

[2] A. P. Chandrakasan, N. Verma, and D. C. Daly, "Ultralow-power electronics

for biomedical applications," Annu. Rev. Biomed. Eng., vol. 10, pp. 247–274, Aug. 2008.

[3] O. J. Bedrij, "Carry-select adder," IRE Trans. Electron. Comput.,vol. EC-11, no. 3, pp. 340– 344, Jun. 1962.

[4] Y. Kim and L.-S. Kim, "64-bit carry-select adder with reduced area,"Electron. Lett., vol. 37, no. 10, pp. 614–615, May 2001.

[5] Y. He, C. H. Chang, and J. Gu, "An area-efficient 64-bit square root carryselect adder for low power application," in Proc. IEEE Int. Symp. Circuits Syst., 2005, vol. 4, pp. 4082–4085.

[6] B. Ramkumar and H.M. Kittur, "Low-power and area-efficient carry-select adder," IEEE Trans. Very Large Scale Integr. (VLSI) Syst., vol. 20, no. 2,pp. 371–375, Feb. 2012.

[7] I.-C. Wey, C.-C. Ho, Y.-S. Lin, and C. C. Peng, "An area-efficient carry select adder design by sharing the common Boolean logic term," in Proc. IMECS, 2012, pp. 1–4.

[8] S.Manju and V. Sornagopal, "An efficient SQRT architecture of carry select adder design by common Boolean logic," in Proc. VLSI ICEVENT, 2013, pp. 1–5.

[9] B. Parhami, Computer Arithmetic: Algorithms and Hardware Designs, 2nd ed. New York, NY, USA: Oxford Univ. Press, 2010.

[10] Akhilesh Tyagi, "A Reduced Area Scheme for Carry-Select Adders", IEEE International Conference on Computer design, pp.255-258, Sept 1990.

[11] O. J. Bedrij, "Carry-Select Adder", IRE transactions on Electronics Computers, vol.EC-11, pp. 340-346, June1962.

[12] Neil H.E.Weste and K.Eshraghian, "Principle Of CMOS VLSI designs: a system perspective", (Addison-Wesley, 1998), 2nd edn, 1998.

[13] Richard P. Brent and H. T. Kung, "A Regular Layout for Parallel Adders", IEEE transactions on Computers, vol.c-31, pp.260-264, March 1982.

International Journal of Engineering Research and General Science Volume 3, Issue 6, November-December, 2015
ISSN 2091-2730

DESIGN & IMPLEMENTATION OF A WIFI BASED SMART HOME SYSTEM USING LPC1769

Merlin Jose[1], Aji Joy[2]
1.PG Scholar, Department of Electronics and communication Engineering, MACE. Kothamangalam, Kerala, India.
2. Asst.Professor, Department of Electronics and communication Engineering, MACE. Kothamangalam, Kerala, India.

Email: merlin706@gmail.com, +91-9497213900

Abstract— This paper presents a design and implementation of new smart home system that uses Wifi technology as a networking solution connecting its parts. With the development of ubiquitous computing, smart home services will no longer be limited within the house limits, but also the extends throughout the geographical constraint, and the service will support the activities of each and every member of house even out of home. The proposed system consists of three main parts- Intelligent monitoring and control module, web server and control device. Using the system user can monitor the status of smart appliances, control the power status of smart appliances, and control the device status according to the particular device configurations. By the control device (smart phone) with Wi-Fi, the user can control the working status of smart appliances. The system consists of a Web-server based on PHP, intelligent monitoring modules using an LPC1769 and the Android compatible Smart phone app. The proposed system is extendable since it allows configuration of new devices.

Keywords—- Smart home, Wifi, LPC1769, Android smart phone, Web server, HTTP, Web pages.

1. INTRODUCTION

Home automation has an important role in today's human life and it improves the quality of people's life by facilitating a comfortable and safe environment. In international markets Internet based home automation systems is one of the most popular system. This paper presents a low-cost internet based Smart Home System, which uses wifi technology for communication and an Android based application for control of home appliances. With the help of Smart home system the user can supervise household appliances remotely and realize real-time monitoring of home security status through mobile phone. Users can exchange information with home appliances and can monitor and control equipment to perform their command remotely.

This system uses android smart phone to monitor and control the various house parameters given its advantages over using a dedicated pc. Wifi technology is used as the network infrastructure for communicating between the different parts as there are advantages of high reliability, easy configurability, system extendibility and good adaptability. The home appliances are connected to the basic I/O ports of the embedded system board and their status is continuously updated to the server. Authentication techniques are implemented so that only authorized user can access home appliances. The core component of the system is an ARM Microcontroller. Android is open source software and provides access to lots of useful libraries and tools. The application and system is completely user friendly. Any smart phone user can easily run the application in his/her mobile without any prior training. The designed system has the option for adding more relays to get control over more appliances if he/she wants. So altogether the system is a modern smart home system which can give us the experience of smart living. The system updates the household data to the remote server, allowing the user to control the household devices easily and remotely.

Section 2 gives an overview of the proposed system, its architecture, the technologies used and why they are chosen. Section 3 discusses about the design and implementation of the system from both hardware as well as software point of view.

2. SYSTEM OVERVIEW

The structure of the system and the related technology are described in fig.2.1

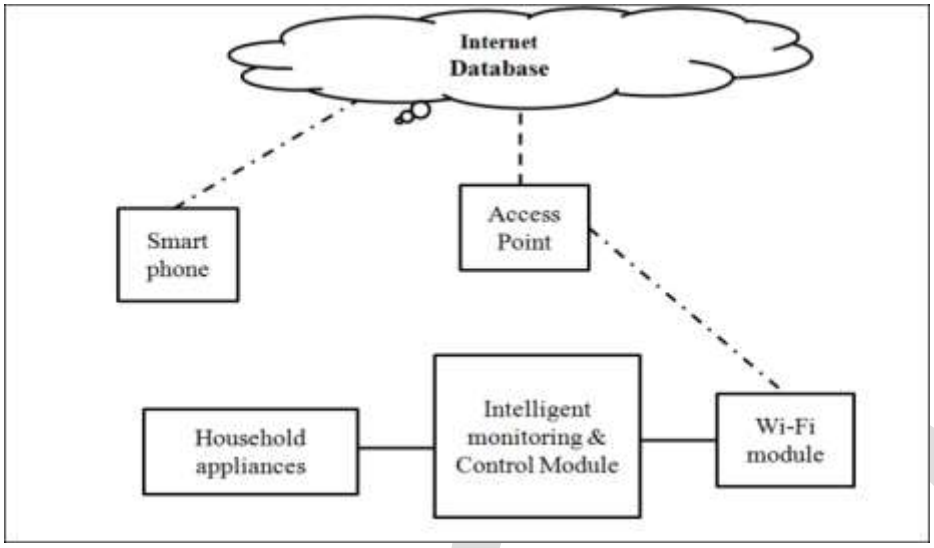

Fig 2.1: Basic block diagram of Smart home system

The system includes main control devices such as mobile phone, wireless communication system, intelligent monitoring terminal, a web server. Users can log on through the main control equipment and send commands to control household appliances, look up the state of household appliances. It is the core of the whole system to download control data from the database by phone, and then send them to the smart appliances.

The proposed system is a distributed home automation system, consists of web server, intelligent monitoring and control modules and control devices. Intelligent monitoring and control module is an ARM microcontroller to whose input/ output ports the different home appliances are interfaced. For embedded networking the controller is interfaced with a wifi module via UART which can access internet through a central access point. Web server can be easily configured to handle any number of intelligent monitoring and control module. The intelligent monitoring and control modules in turn control its alarms and actuators according to the control information passed from web server. Server used here is an apache web server. The web server software is developed using PHP technology. System can be accessed from the web browser of any local PC in the same LAN using server IP, or remotely from any PC or mobile handheld device connected to the internet with the android application installed in it.

Wifi technology is selected as be the networking implementation that connects between web server and controller modules. Wifi is chosen to improve system security (by using secure Wifi connection), and to increase system mobility and scalability. Even if, we need to add new intelligent control modules out of the coverage of the central access point, the problem can be solved by adding repeaters. The main functions of the web server are to manage devices, control, and monitor system components that enable intelligent control modules to execute their assigned tasks (through actuators).

The serial communication interface UART is used for transferring data between ARM controller and Wi-Fi module. UART interface provides the advantages like less cost, simplicity and is highly reliable for data transfer between controllers. UART is an abbreviation of universal asynchronous receiver and transmitter which is usually used in conjunction with communication standards like RS-232. UART takes data in bytes, and using the internal 8 bit shift register converts the data into parallel form and then transmits the individual bits sequentially. For fast processing, most UART chips have a built in buffer which is 16 to 64 kilobytes in size. This buffer is used for caching data that is coming in from the system bus while the data that is going out to the serial port is still being processed. The concept of Flow control is a very important aspect of serial communication. It is the capability of a device to tell another one to stop sending data for a certain time. The commands Request to Send (RTS), Clear To Send (CTS), Data Terminal Ready (DTR) and Data Set Ready (DSR) is used to enable flow control. The UART is an asynchronous mode of transmission that is no clock signal is transmitted between the sender and receiver, instead the communication configuration (baud rate, number of data bits, parity bit present or not, number of stop bits) is agreed in prior to the transmission and special bits are transmitted for achieving synchronization. LPC1769 provides Four UARTs with fractional baud rate generation, internal FIFO, IrDA, and DMA support. To do the UART programming, we basically need to do two things. First we need to set up the UART and then provide an interrupt handler function to specify what to do when there are data bits to be received, when transmit buffer is empty and when errors occur.

On power on the wifi module scans accessible channels to detect active networks in areas where beacons are located for transmitting. A network is then selected which will be in ad hoc mode. After this section it verifies itself with the access point (AP) and joins it. Even though a station is already a part of a network it still tries to detect new networks and the reason for such behaviour depends on the willing to associate with the strongest signal and if this occurs the current network disconnects itself and joins the new network. Power in Wi-Fi stations can be saved by setting a station in to sleep mode. Wi-Fi devices can be at two different state and those are awake or doze. When a station is located in doze state it cannot transmit or receive. The power consumption is then reduced at this state. The power management is handled by two modes in Wi-Fi devices and these are active mode (AM) and power save (PS) mode.

The basic communications that take place in the system is as shown in fig 2.2

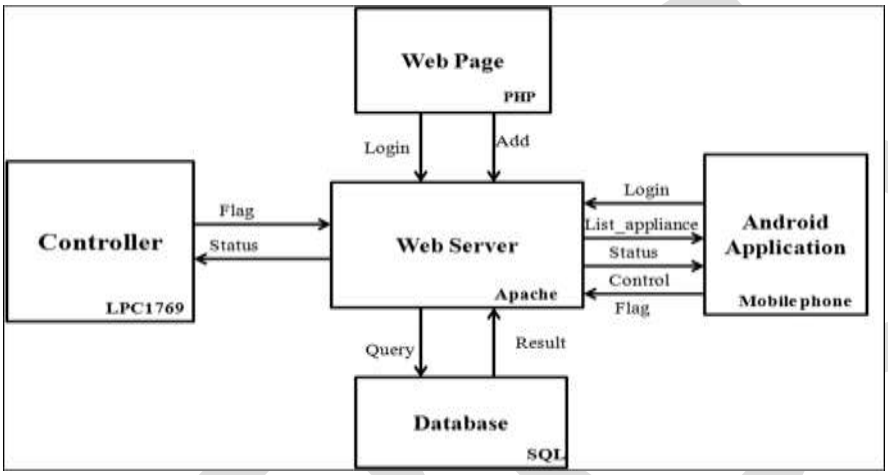

Fig 2.2 Basic communications in proposed system

The microcontroller will interact with the web server repeatedly over a fixed interval of time and check for any updates. If a user logs in to the server via android application he can access the appliances under his ownership and change its status. Once the power state of an appliance is updated by the user, a flag will be set for the corresponding house in the database. The microcontroller will be continuously checking this flag. When it reads the flag status as set, the microcontroller will retrieve the power status of appliances. This will be received in JSON format. The embedded software will decode the JSON encoded data and tabulate the power status for each appliance. Then it will send control signals to the output ports to make the corresponding changes to the actuators. A webpage interface is also provided with administrator permission.

3. PROPOSED SYSTEM DESIGN AND IMPLEMENTATION

As mentioned earlier the smart home system consists of mainly three modules- intelligent monitoring and control module, the web server and the control module (Android mobile phone). Let's see each in detail.

I. A. CONTROLLER DESIGN

The microcontroller used is LPC1769. It is an ARM Cortex-M3 processor, running at frequencies of up to 120 MHz. The LPC1769 microcontroller is interfaced with a wifi transceiver module (ESP8266) for enabling wifi access to the embedded system. UART interface is used for data transmission between both devices. Then for the communication to work both devices have to agree upon a baud rate. Baud is a measurement of transmission speed in asynchronous communication. Once the UART registers are set and baud rate is agreed we can start transmission between the wifi module and microcontroller. For viewing the transmissions and receptions here I have used another UART port of LPC1769 and microcontroller. For viewing the transmissions and receptions here I have used another UART port of LPC1769 and connected it to a terminal program in a personal computer. For this we have in-built facility in LPC1769 trainer kit. The FT232R in the trainer board is an USB to serial UART interface and it is made use of for this purpose. Then the code is edited such a way that all the transmissions and receptions gets printed to the PC so that could be kept track of.

An access point for internet is set up, secured with WPA/WPA2 PSK and configured with an ssid and password. Microcontroller is embedded with code to set up the wifi module, connect it to the internet via the access point and access a web page. It makes use of HTTP requests such as GET, POST etc

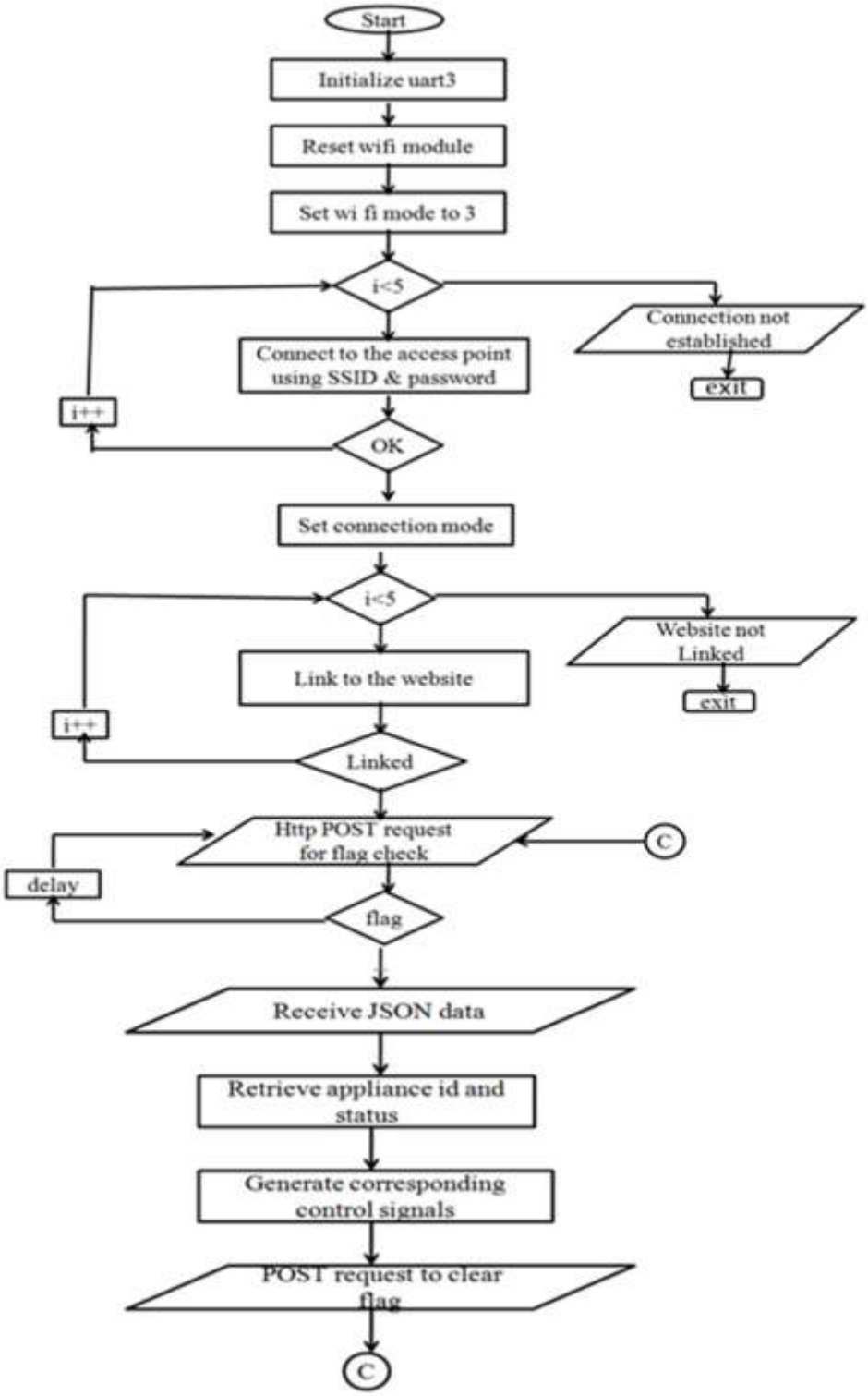

Fig 3.1: Embedded software

Fig 3.1 shows the flowchart for the embedded software for hardware interface module. The required UARTs are initialized. Then the baud rate is set. The wifi module is set up for its operation by sending AT commands. Once the wifi module establishes connection with the internet using HTTP request methods command is send to link with the URL of our web server. Once the server gets linked the code will jump into a continuous loop for checking the update flag. If the flag is clear it will wait for a delay and continue the process. If the flag is set, it will retrieve the appliance status from the server; make corresponding updates to the actuator ports. Then command is send to clear the flag and the flag checking loop is entered again.

B. SERVER DESIGN

The server is designed in PHP using XAMPP Version: 5.6.3. It consists of an Apache module and mySQL. The database structure is defined and corresponding tables are created in mySQL. It consists of tables for maintaining information on- Access key, User, House, Ownership, Appliance, Device state list. Queries are written in SQL for serving the mobile application(Login, Logout operations, API key generation, List houses and appliances, Update status and set flag), embedded controller(Status update and flag check, Clear flag) as well as the webpage (Administrator login and logout operations, Add, remove or edit user/house/appliances/ownership/device states).

An additional webpage interface is also provided for the web server with only administrator permissions. Administrator; who will control the access and permissions policy of the system, and can add and delete user accounts, anything that a general user can perform, the administrator can also perform. The web page is created using PHP,

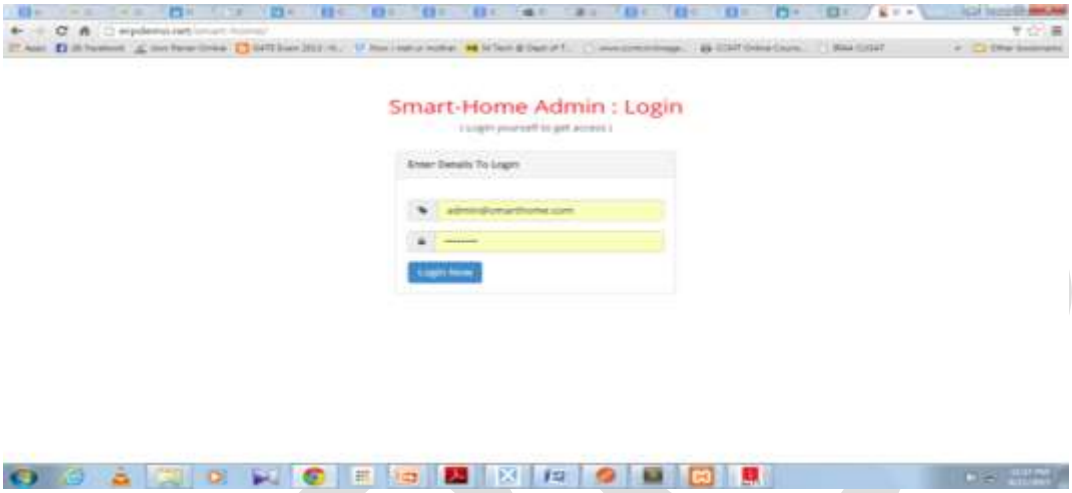

Fig 3.2 Login of web page

C. ANDROID APPLICATION DESIGN

The Android application is designed using Eclipse Juno IDE. Android is an open-source development platform for creating mobile applications. Android applications consist of loosely coupled components. An application manifest bounds these components and describes each component and their interactions with each other. Every Android project will consist of a manifest file named AndroidManifest.xml, and will constitute the basic building block of project. We should also create user interfaces for the application that are stylish at the same time easy to use.

The Android application opens to a login screen consisting of fields for username and password and a login button. For secure access md5 password encryption is used. On pressing the login button the data entered in fields will be send to the URL for web server. If the username and password matches with the data in the database, access will be provided and the user will be logged in. Once the user logged in, it will retrieve the houses owned by the user from the database and display it as shown in figure 4.4.1. The user can select the house by clicking on it. Once a house is selected it will list the equipments under the house name along with a toggle switch for power on and off. It will also list the device state. This can be used to switch on and off the appliances and also for changing the device states. For example, the different device states for a light are dim and bright.

Fig 3.3 GUI for Android application

5. CONCLUSION

In this paper, a wifi based smart home system which can be controlled remotely using an android application is proposed and implemented. The security of the system is ensured by user authentication and encrypting. The hardware interface module is implemented on an ARM controller. The Android based smart home app communicates with the web-server via internet. The smart home app can be installed in any android devices, and control and monitor the smart home environment. The android application consists of a user friendly GUI which makes it convenient to use for anyone. Addition or removal of new devices made easier with the help of a web interface. A low cost smart home system has been developed which eliminates the requirement of a dedicated PC as processing operations are done by the microcontroller. Presently the system is implemented with a single hardware interface module but the server is designed such that it can be handle more number of modules.

REFERENCES

[1] Liu Zhi-Gang, Huang Wei , "The Design of Smart Home System Based on Wi-Fi" , 2012 International Conference on Computational Problem-Solving, pp. 454-456, (2012).
[2] "LPC 17xx User Manual", NXP Semiconductors.
[3] HTML Coding from w3schools.com
[4] Thinagaran Perumal, Md Nasir Sulaiman, Khaironi Yatim Sharif, "Development of an Embedded Smart Home Management Scheme ", International Journal of Smart Home, 7(2), pp.15-26, (2013).
[5] A. ElShafee and K. A. Hamed, "Design and Implementation of a WiFi Based Home Automation System," World Academy of Science, Engineering and Technology, 6(8), pp. 2177-2180, (2012).
[6] LuoWei, LiWei, LiXin, "Design and Implement On Smart Home System", 2013 Fourth International Conference on Intelligent Systems Design and Engineering Applications, pp.229-231(2013).
[7] Jim T Geier, "Wireless Networking Handbook", (1996).
[8] Android Development with Android Studio or Eclipse ADT - Tutorial: www.vogella.com
[9] Rajeev Piyare, Seong Ro Lee, "Smart Home-Control and Monitoring System Using Smart Phone", 1st International Conference on Convergence and its Application, 24, pp. 83 – 86, (2013).
[10] Reto Meier, "Android™ 2 Application Development"
[11] Kallakunta Ravi Kumar, Shaik Akbar, "Android Application Based Real Time Home Automation", Indian Journal of Applied Research 4(7), pp.188-190, (2014)
[12] Shiu Kumar, "Ubiquitous Smart Home System Using Android Application", International Journal of Computer Networks & Communications (IJCNC) 6(1), pp.33-43, (2014)

International Journal of Engineering Research and General Science Volume 3, Issue 6, November-December, 2015
ISSN 2091-2730

VLSI IMPLEMENTATION OF FULL DUPLEX, FSM BASED GIGABIT ETHERNET MAC

Aswin C[1], Aji Joy[2]
1.PG Scholar, Department of Electronics and communication Engineering, MACE. Kothamangalam, Kerala, India.
2. Asst.Professor, Department of Electronics and communication Engineering, MACE. Kothamangalam, Kerala, India.

Email: aswin.cms@gmail.com,+91-9495763459

Abstract— The communication network is analogous to the neural system of the human body for any embedded system. It carries data and control signals to various parts of the system. Hence, a high speed communication system is the need of the hour so that it does not become the bottleneck of the system's performance. Of all the available communication systems, Ethernet stands out as the most common network communication protocol. But due to advances in the technology, the primitive Ethernet could no longer match the processing speed of the new systems. Therefore, we need to improve the performance of the Ethernet. The evolution to Gigabit Ethernet improved the speed from few Megabits to one Gigabit and thus improved the performance of the whole embedded system. Increasing the bus width of the Ethernet is one way to increase the speed, but this comes with the overhead of encoders and decoders to be used and also increases the chance of causing interference. Another way is to use a clock with high speed, thus keeping the bus width low and avoiding the overheads and interference probabilities. This project selects a 125 MHz clock and 8 bit bus width for constructing a Gigabit Ethernet MAC on FPGA board. Finite state machine technique is used to construct the same. The project is coded using VHDL in Xilinx 14.1 and simulations are done in ISim simulator. The project was implemented on Spartan 3XC3S200 FPGA board.

Keywords—- Media Access Control(MAC), Finite State Machine(FSM), Start of Frame Delimiter(SFD), Frame Check Sequence(FCS), Cyclic Redundancy Check(CRC), Physical layer interface(PHY), Gigabit Media Independent Interface(GMII).

1. INTRODUCTION

The Ethernet is the most common communication network in the world constituting about 80 per cent of the total LAN networks. It started with the speed of the order of a few megabits per second. With the advent of fast Ethernet, this has increased up to 100 megabits per second. However, due to the various developments in the technology like in the case of processing speed, the 100 Mbps speed still fall short and bring down the performance of the whole system. So, we need to find ways to improve the speed of Ethernet network so that we need not replace it with another network, thereby saving the cost for the same. This is the reason for the research and development of even faster Ethernet like Gigabit Ethernet.

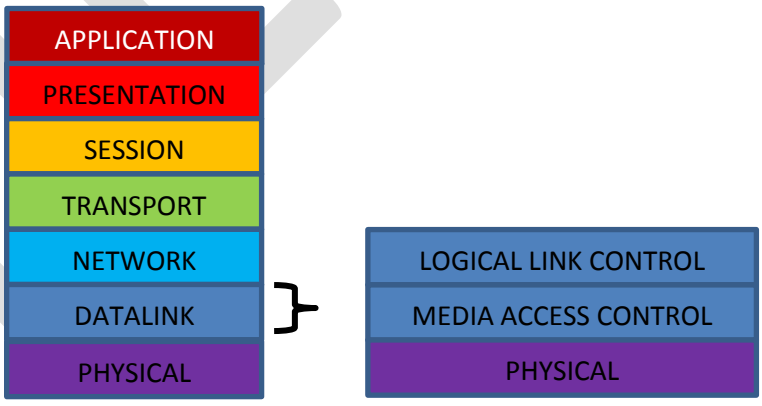

Fig 1: MAC layer represented in OSI model.

The media access control (MAC) is the heart of the Ethernet network. It is a sub-layer of the data-link layer of the OSI model. It acts as a bridge or interface between the lower layer, i.e. the PHY and the upper sub-layer of the data-link layer, i.e. the logical link control (LLC) layer. Figure 1 gives a representation of MAC in the OSI model. The MAC layer provides a full-duplex communication

channel for these layers. It carries out various functions which will be discussed later. The data is handled as frames in the MAC. The next chapter, chapter 2, discusses about the basic ideologies used in developing gigabit Ethernet. It gives all the necessary base information on the features of the Ethernet. In the third chapter, the proposed design and its detailed working is discussed. In the fourth chapter, simulation results and implementation of the system is discussed in elaborate. Finally, chapter 5 gives the conclusions of the thesis with a brief discussion about the further development and future scope of the design. Chapter 6 gives the list of references used for the thesis.

2. BASIC IDEOLOGIES

The basic ideologies include the functions of the MAC, details about MAC addresses, gigabit Ethernet frame, CRC and GMII.

The functions of MAC include frame de-limiting and frame recognition, source and destination addressing, assurance of transparent data transfer in the Ethernet sub-layer, error protection by generation and checking of the FCS and finally, the control of accessing the physical transmission medium. It receives and transmits data in the form of frames. It checks the FCS of the received frames and appends FCS to the transmitted frames. It discards malformed or error frames. It prepends the preamble, SFD and padding while transmitting and removes the same while receiving.

MAC addresses are assigned so that each network interfaces can be identified uniquely in the physical network. These are assigned mostly by the manufacturer itself and will be stored in its hardware itself. If so, it is known as burned-in address. It is also known as Ethernet hardware address. It is expressed in groups of two hexadecimal numbers either separated by hyphens or colons or dots.

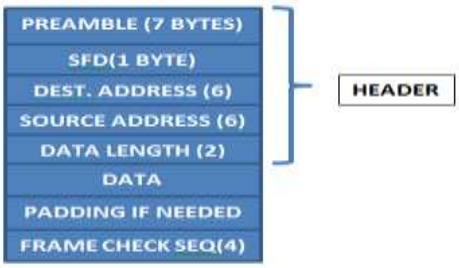

Fig 2: Gigabit Ethernet frame.

The data is handled in the form of packets known as frames in the MAC. As shown in the figure 2, the frame consists of 7 bytes of preamble, 1 byte of SFD, source address, destination address and data length. These constitute the header of the Ethernet frame. The addresses are of 6 bytes each. After the header, comes the data. The data field should be at least 46 bytes and should be at most of 1500 bytes. If the length is less than 46 bytes, padding is provided. The last field is the frame check sequence (FCS). It includes the cyclic redundancy check code for the data.

The CRC is used for error detection purposes. We use a 32 bit CRC polynomial for our purpose. The corresponding hex-code is given as 'C704DD7B'. The operation is EX-OR division. The whole frame minus the preamble and the SFD is considered for this. This data is divided by the CRC polynomial and the resulting remainder obtained will be the CRC code. This is then reversed and attached to the frame to avoid 'false negative' phenomenon. At the receiver end, dividing with the CRC polynomial yields zero remainder and ensures correct transmission. If the remainder is non-zero, the transmission is faulty.

Gigabit media-independent Interface (GMII) provides an interface between the MAC and the PHY. The various GMII transmitter and receiver signals include:

- GTXCLK – clock signal for gigabit TX signals (125 MHz)
- TXCLK – clock signal for 10/100 Mbit/s signals

- TXD[7..0] – data to be transmitted
- TXEN – transmitter enable
- TXER – transmitter error (used to corrupt a packet)
- RXCLK – received clock signal (recovered from incoming received data)
- RXD[7..0] – received data
- RXDV – signifies data received is valid
- RXER – signifies data received has errors

GMII defines speeds up to 1000 Mbit/s, implemented using a data interface clocked at 125 MHz with separate 8-bit data paths for reception and transmission. It can also operate on 10 or 100 Mbit/s as per the MII specification by selecting suitable clocks.

3. PROPOSED GIGABIT ETHERNET MAC DESIGN

This model supports full duplex operation only. The physical layer interface is done using 16 bit lines. Since full duplex, there are two separate 16 bit channels for the interface; one for transmission and other for reception. The data from upper layer is received serially and converted to 8 bit patterns. The internal buses of the MAC are of 8 bits. The 8 bit data is converted to serial bit stream to transmit out of the MAC to the upper layer. The figure 3 below represents a rough sketch of the proposed model. Data is handled as frames in the MAC sub layer.

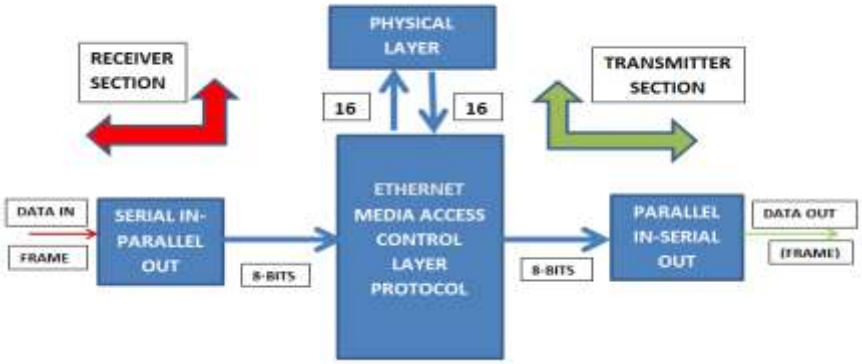

Fig 3: Proposed model of the Gigabit Ethernet Media Access Control.

As we have already discussed, this system is Finite State Machine (FSM) based. We manage the Ethernet frame and the data with the help of different FSMs. We use six different FSMs in our design. First, let us discuss the transmission of the stored data packet. The clock that we use is of 125 MHz, derived from the 30 MHz clock on board.

The process is as follows: This process is in the local clock domain. It gets data and puts it into a RAM. Once a packet worth of data has been stored, it is sent to the packet sending state machine. The data comes from the physical layer as 16 bit stream and gets to the RAM. This is to be converted into the frame format by appending the preamble, start of the frame delimiter and the frame check sequence. Then it is to be transmitted out serially from the MAC. A representation of the packet sending machine is given in the figure 4. This FSM has four states namely GET LENGTH, GET DATA, SEND PACKET and WAIT: NOT DONE. The first 16 bits represents the length of the data packet. Therefore, the first state has the function of getting the data length. Once it is attained, the control is transferred to the next state: to get the data. On the previous state, a counter was set with terminal count set to the value of the data length. On this state, upon getting each data, this counter, which was initially reset, will be incremented. Since we get 16 bits at a time, we increment the counter by two, since we are handling data byte-wise in MAC.

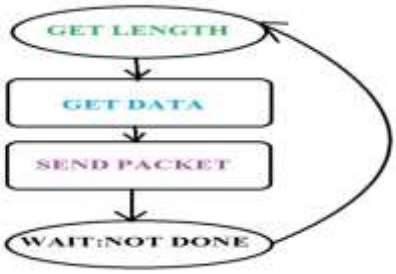

Fig 4: Packet sending machine FSM.

Upon getting the final data, the counter reaches the terminal value and the control is transferred to the next state, i.e. the SEND PACKET state. Here, the data is sent. Once sent, we wait for the synchronization with the receiver. Until we receive a 'done synchronization' signal from the receiver, the control stays in the next state, the WAIT: NOT DONE state. Once the synchronization signal is received, we go out of this state and goes back to the first state, where we get the length of the next data packet.

The next FSM is used to transmit the stored packet via the PHY. It does the job of creating the frame format for the data packet to be transmitted. This appends the preamble, SFD, creates the CRC code, and sends the CRC code with the data. The sketch of the FSM is given in the figure 5. In the first state, the machine waits for the arrival of the new data packet. Its arrival is denoted by a reception of a 'go' signal. Until this signal is received, the machine stays at the wait state. This is helpful in synchronizing the transmitter and receiver side. When this signal is received, it moves to the next state.

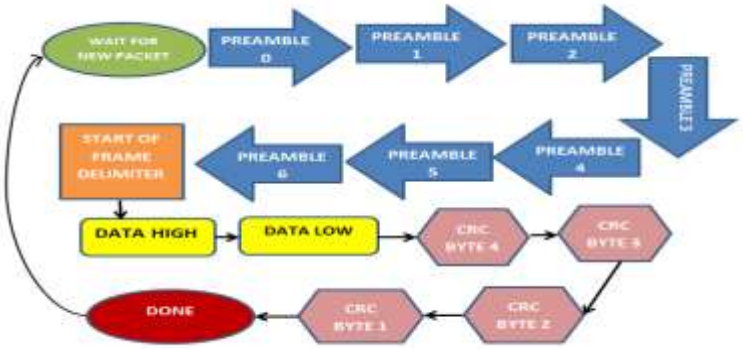

Fig 5: Transmission physical state FSM.

It constitutes 7 states of preamble. On each clock, a byte of preamble is added. This is done to synchronize the receiver clock. It appends alternating patterns of 1's and 0's and corresponding hexadecimal code is '55'. After the 7th byte is appended, it goes to the next state, where frame start delimiting is done. It disturbs the alternating sequence denoting the end of the preamble. After this, the frame includes the data part. The data include the length of the data, the destination and source address, the actual data and padding (if any). Since the packets are received 16 bits at a time, we need two states for the data; one for 8 MSB's and other for the 8 LSB's. Hence we have the states 'DATA HIGH' and 'DATA LOW'. Upon getting each byte of data, before transmitting it, the CRC is calculated. The starting CRC polynomial is (0 1 2 4 5 7 8 10 11 12 16 22 23 26 32) and new CRC is generated. Then with this, the same operation is done to the next byte of data. This is done to every byte of data to be transmitted including the addresses and length field too. The last 32 bit CRC that we get will be the one we will be sending along with the data to the receiver.

The next stages will be for appending the 32 bit CRC to the frame. This is done in 4 states because data is handled 1 byte at a time. Before sending, the CRC calculated is reversed and complemented to avoid the false negative situation discussed in section 3. At last, there is a done state where we generate an indicator to notify that the transmission of the present data is done. The control is then transferred back to the first state, where the transmitter waits for the new packet of data to be encapsulated to frame and transmitted. The data we converted to frame format, now is a sequence of byte patterns (8 bits) emerging from the MAC. Since we need to transmit the data over a serial communication channel, we need a parallel-to-serial converter for the purpose. This too, is implemented as an FSM. First, a data byte is received and is then transmitted one bit at time using 8 separate states. Wait states are also added for the synchronization purpose.

Now, let us discuss the other part of the full duplex communication: the reception. Like transmission, it is also done with the help of FSMs. The frames are received from the upper layer and the envelopes are removed in the MAC sub layer before giving it to the physical layer. During this process, the MAC does CRC checking and error frames or incorrectly received ones will be discarded, ensuring correctness of the data. The data in frame format received from upper layer is serial in nature. First we need to convert it in to an 8-bit format as the MAC we designed uses 8 bit internal buses. For this purpose, we need a serial to parallel converter, which we have implemented as an FSM. Each data is shifted and stored in a register and upon reaching 8; the register value is given out, ensuring the conversion complete. The data will be in full frame format and we have to do two main operations on it: one being the redundancy check and other being the removal of the envelope, before transferring it to the lower layer.

Let us now see how received data is handled in the MAC. We use FSM for this also. This process reads data out of the PHY and puts it into a buffer. There are many buffers on the receiver side to cope with data arriving at a high rate. If a very large packet is received, followed by many small packets, a large number of packets need to be stored.

The figure 6 shows the FSM used for the handling of the received byte sequenced frame. The machine remains in a wait state until a 'data valid' signal is received. When it gets this signal and when the received byte is '55' (hexadecimal value), the machine moves to the next state, that is the preamble state. It remains in this state until a variation in the bit pattern, i.e. a 'D5' is received. After the delimiter is received, the next received ones will be the data we need. It may include the destination and source addresses, the length of the data and the data itself. Thus, control goes to the next state, the 'data high' state. Because we need to convert the byte pattern to 16 bit pattern to transfer out to the physical layer, the first received byte is handled by the DATA HIGH state and the second received byte by the 'DATA LOW' state and is combined to form 16 bit pattern. CRC checking of the received bytes is done on both the states. Then the control goes to the state: 'END OF FRAME'. If any abnormalities like mismatch while CRC calculation or number of bytes received is lesser than 64 or greater than 1518, which are all errors in the reception, the frame is discarded and control is transferred back to the first state: 'WAIT START'.

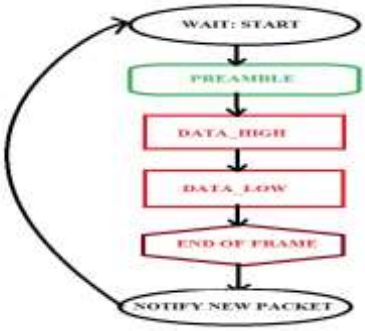

Fig 6: Receiver physical state FSM.

If none of these problems are observed, then control is transferred to the state, which is the 'NOTIFY NEW PACKET' which is used to notify that reception was successful and the machine is ready to accept new packets. All the buffers and registers used for the reception purpose are reset to initial default values in this state. The buffers include receiver start address buffer, packet length buffer, receiver write buffer and CRC register. Once all the sufficient steps are taken to start accepting new packet, the control is transferred to the first state, 'WAIT START' from this state.

Next we discuss about the packet receiving machine. The figure 7 denotes the FSM for the same. The first state is the wait to initialize state, where the receiver read buffer is reset to zero. When a synchronization signal, which indicates that the receive buffers are ready, the control moves to the next state, i.e. the 'WAIT: NEW PACKET'. In this stage, we wait for the arrival of a new packet. When new packet arrives, first the length is sent. It is attained in the next state 'SEND LENGTH'. Then, the following states include the prefetching of the addresses. Once that is done, the data is sent until the read address matches the end address. At this point of time, the control is given back to the first state.

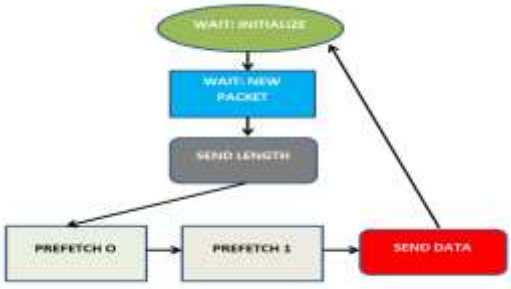

Fig 7: Packet receiving FSM.

4. SIMULATION RESULTS

The programming was done using VHDL on Xilinx ISE design suite version 14.1. The simulations are done in ISim simulator. The project was implemented on Spartan 3 xc3s200-5tq144 board.

First, let us see the simulation result of the transmitter section. Here, a continuous 16 bit pattern of '001b' (represented in hexadecimal form) is given as data packet to be transmitted. The MAC encapsulates the data with preamble, SFD and FCS and converted into frame format to be transmitted out to the upper layer.

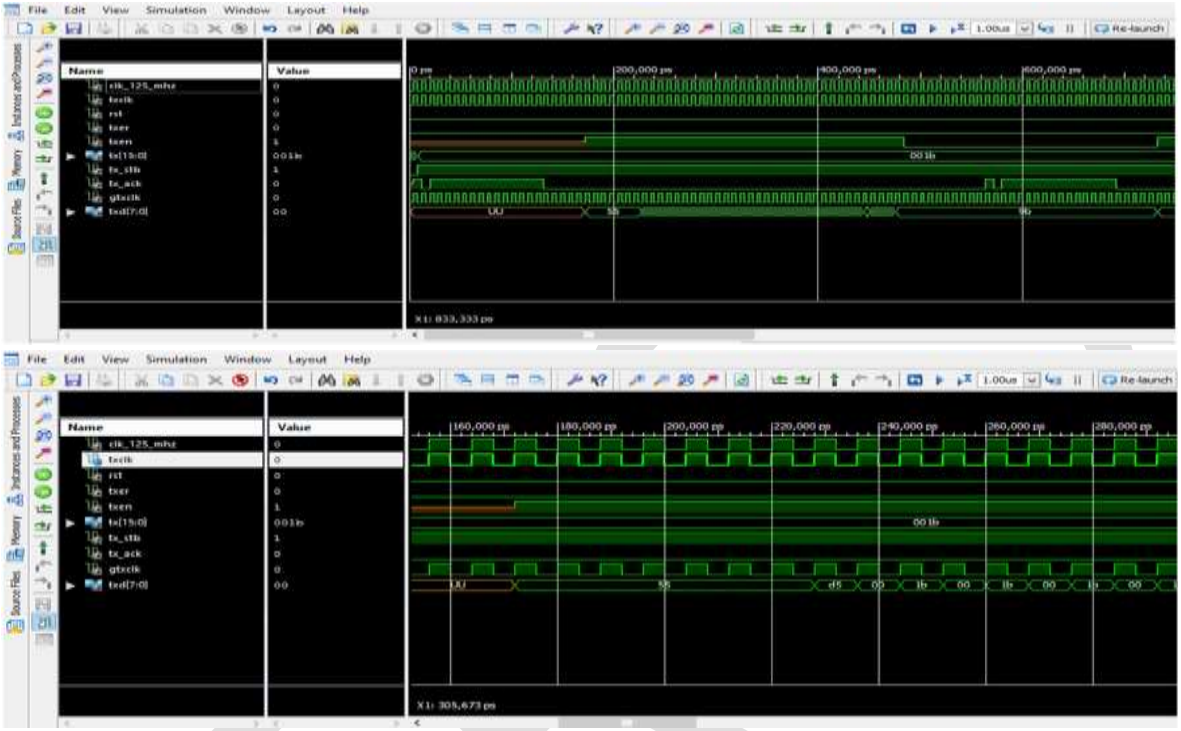

Fig 8: Simulation result of the transmitter section of MAC.

Next is the simulation result of the 8 bit parallel to serial converter FSM. A sample data of 01010101 is given to the machine and as you can see, the output tx is a serial one and each bit is transmitted one-by-one.

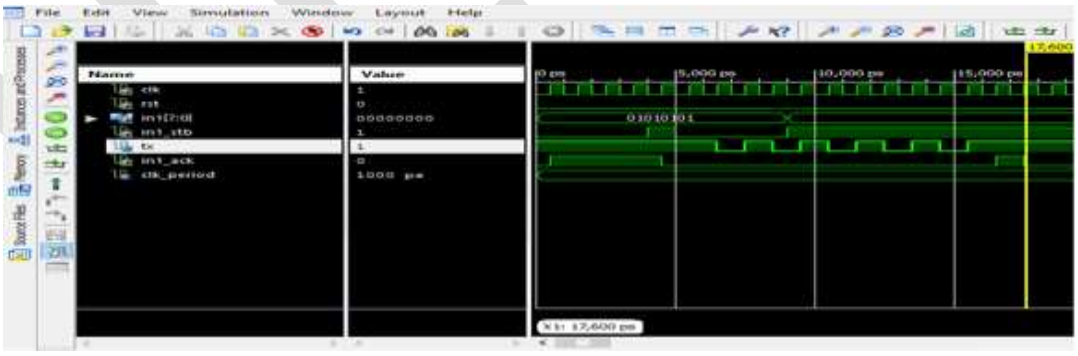

Fig 9: Simulation of the parallel to serial converter.

Now, let us see the simulation result of the receiver section. We use a sample frame with dummy destination and source addresses and a finite length and sample data for the simulation purpose. As you can see, the preamble and the CRC being discarded by the receiving machine. We obtain the output in the sequence of 16 bits. The input RXDV determines whether the received data is valid or not. This will be provided by the transmitter. So, the data received only when this signal is active is considered as the needed one and the rest is discarded.

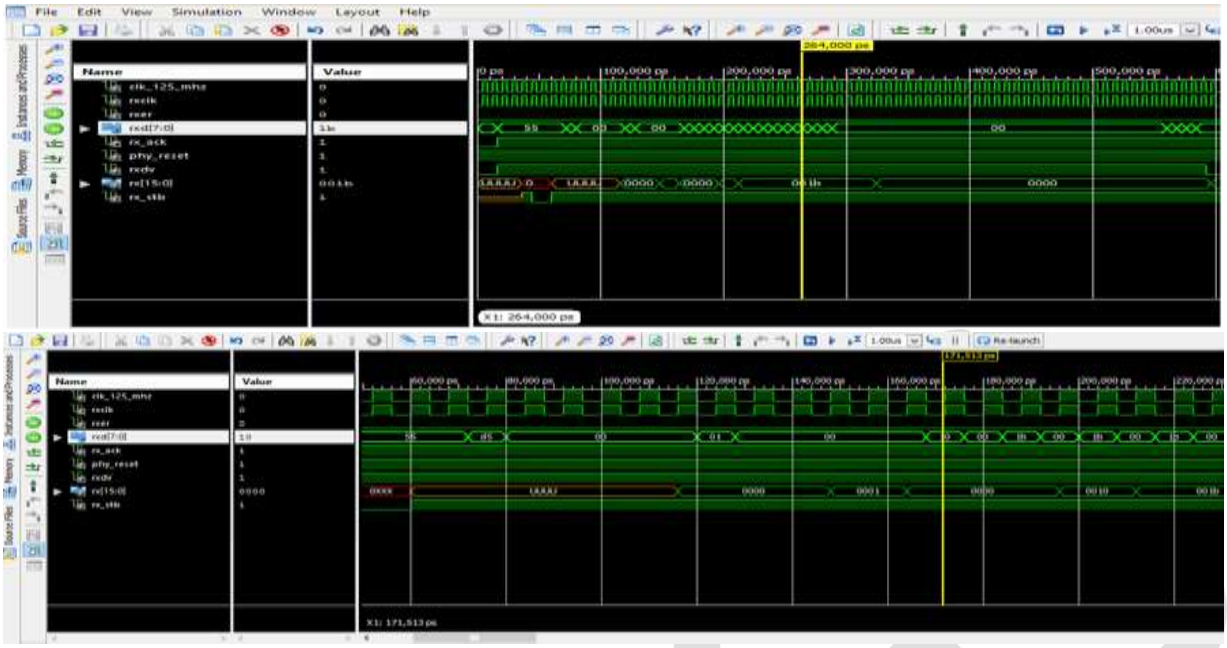

Fig 10: Simulation result of the receiver section of the MAC.

The serial data coming from the upper layer need to be converted to 8 bit parallel data and the simulation result of the machine is shown in figure 11.

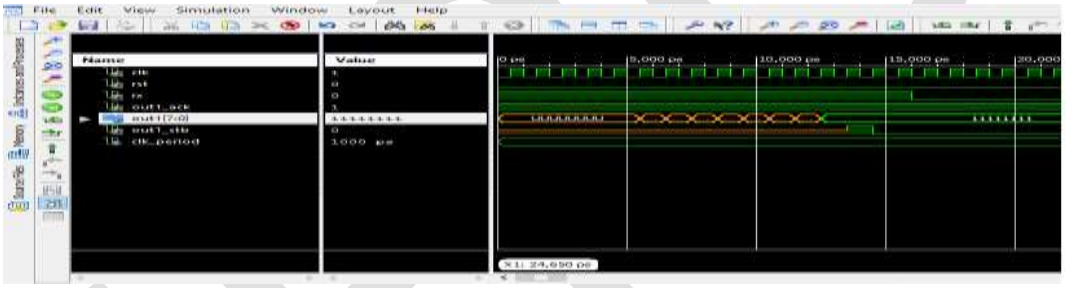

Fig 11: Simulation result of serial to parallel converter.

5. CONCLUSION

Gigabit Ethernet MAC was implemented on the FPGA using VHDL with a clock of 125 MHz and 8-bit bus width. As there is only 8 bits handling at a time, the need of encoding of the data was negotiated in this project. The whole system is constructed on the basis of finite state machine concept and ensures efficient transmission and reception of data between physical layer and the upper data link layer. Every module was constructed independently and was later combined to form the whole system. Effective CRC generation and checking was ensured. The whole system was simulated successfully and implemented on the Spartan 3 FPGA board. It was observed that the data was transmitted and received at a speed of 1 Gbps with the new MAC. Selecting higher clock rate further increases the speed of the system. Also, selecting higher data width on the internal components can also increase speed of the Ethernet but this comes with the overhead of encoders and decoders needed in the MAC.

REFERENCES:

[1] R. M. Metcalfe. "Computer/Network Interface Design: Lessons from Arpanet and Ethernet ", IEEE Journal on Selected Areas in Communications SAC-11(2), pp.173-180,(1999).

[2] D. J. Aldous "Ultimate Instability of Exponential Back-Off Protocol for Acknowledgement-Based Transmission Control of Random Access Communication Channels", IEEE Transactions on Information Theory IT-33(2), pp. 219-223,(1997).

[3] G. T. Almes and E. D. Lazowska, "The Behaviour of Ethernet- Like Computer Communication Networks", Proc. 7th Symposium on Operating Systems Principles, pp.66-81, (2004).
[4] D. R. Boggs, J. C. Mogul, and C. A. Kent "Measured Capacity of an Ethernet: Myths and Reality", ACM SIGCOMM '02 Symposium on Communications Architectures & Protocols, pp.222- 234 , (2002).
[5] G. A. Cunningham and J. S. Meditch 'Distributed Retransmission Controls for Slotted, Nonpersistent and Virtual Time CSMA', IEEE Transactions on Communications COM-36(6), pp.685-691(2000).
[6] G. Fayolle, E. Gelenbe, and J. Labetoulle "Stability and Optimal Control of the Packet Switching Broadcast Channel", Journal of the ACM 24(3), pp.375-386 , (1999).
[7] J. Goodman, A. G. Greenberg, N. Madras, and P. March ''Stability of Binary Exponential Backof ", Journal of the ACM 35(3), pp.579-602, (2001).
[8] A. Leon-Garcia."Probability and Random Processes for Electrical Engineering",Addison-Wesley,Reading, (1989).
[9] Qiu Dong-li, Tang Lin-bo, Zhao Bao-jun, Sun Xing, "Design and Implementation of Gigabit Ethernet Based on SOPC", International Conference on Control Engineering and Communication Technology (ICCECT), vol. pp. 274–277, (2012).
[10] D. Thomas and K. S. Mohanachandra Panicker, "VLSI implementation of gigabit Ethernet with data compression and decompression", IET-UK International Conference on Information and Communication Technology in Electrical Sciences (ICTES 2007), pp. 826 – 831, (December 2007).
[11] G. Ciaccio, M. Ehlert and B. Schnor, "Exploiting Gigabit Ethernet capacity for cluster applications", 27th Annual IEEE Conference on Local Computer Networks, Proceedings. LCN 2002, pp. 669–678, (2002).
[12] J. Mache, "An assessment of Gigabit Ethernet as cluster interconnect," 1st IEEE Computer Society International Workshop on Cluster Computing, pp. 36-42, (1999).

International Journal of Engineering Research and General Science Volume 3, Issue 6, November-December, 2015
ISSN 2091-2730

Flit Inversion Techniques for Reducing EnergyConsumption in NoC

P R Pavani,Mohammad Mohasinul Huq N

Avr & Svr College Of Engineering And Technology,JNTU UNIVERSITY,Email : pavanireddy810@gmail.com

Abstract— The dynamic power dissipation in the NOC is mainly due to coupling effects between on chip interconnections in deep submicron VLSI designs. Coupling effect between the interconnections not only enhances power-delay product but also decreases the signal to noise ratio and increases signal distortion due to cross talk noise obtained by capacitance and inductance.as technology shrinks the power consumption in NOC links is start compete with the NOC routers. In this paper we proposed flit inversion techniques which reduces both coupling activity in adjacent links and self-switching activity in particular data links. Before data enters into network interface we encode the data flit and decode at destination end of the NI.. From the result we get the reduction in power and energy consumption areup to 35% and 20%, without degradation of performance

Keywords— Coupling Activity, Self-Switching, Dynamic power, Interconnect, Flit, Cross Talk, Router

INTRODUCTION

The number of cores in network on chip increases, the designing of the efficient communication interface is more adequate in the next generation architectures. Involving of more sophisticated advanced on-chip protocols, routing algorithms, adaptive selection schemes, flow control and protection schemes are aimed to quality of design. But nowadays interconnection system becomes one of key metrics which characterize the architecture performance and power consumption. Network on chip is actually obtained as solution for the design of scalable and modular communication applications. The proposed encoding scheme is based on the wormhole switching architecture shown in figure:1.In the data spited into flits(adjust to link of network link).the header flit in the data will directs the flit into particular link, and remaining data flits will follow the same link in pipeline fashion. The decision whether the flit is inverting or not is completely based on previous data flit. In self-switching activity if number of transitions from 0 to 1 in two consecutive lines (the flit about to traverse, the flit just transmitted) is more than half of the link width of link, then the data is inverted to reduce number of 0 to 1 transitions. Since all data flits in the pocket will follow the same link and are not linked with adjacent flits belongs to other pockets, the decision taken at the interface node is valid all the links along the routing path. As complexity of design increases, the length of interconnections increases, the distance between the wires decreases which increases coupling capacitance resulting more power-delay product. The technique is more translucent to the NOC, since the technique doesn't affect the performance of the remaining structure of NOC. And no need to do any modification in router design in this paper we proposed three encoding schemes, in scheme I we focus to reducing type1 transitions by odd inversion.in scheme II we reduces type1 and type2 by full inversion or half inversion based on power model.in scheme III we shows different behaviours of data by odd, even and full inversion which leads highest power reduction.

PREVIOUS WORK

On the contest of designing power efficient network links, many papers are published, most of them concentrate the reducing dynamic power in different components such routers, network interfaces and links. Here we present some of those literatures briefly. These include shielding of links [7][8],increasing the link-to-link space[6]. By these all techniques the chip area gradually increased. Another technique is encoding the data flits to decrease the dynamic power dissipation. The encoding techniques are categorized into two types. In the first category the inversion technique reduce the power dissipation due to self-switching activity in the data link. These includes bus-invert coding [9], grey code technique [10], working-zone encoder [11]. But these techniques are not suitable in case of deep submicron technology, where coupling capacitance is the major metric for power dissipation. In second category the literature concentrate on reduction of coupling switching activity [21][25][26]. Among these techniques the coupling transition reduced by either extra control links. The schemes presented in [30] [29] having small number of control links, but complexity of decoder increases chip area. In the scheme [26], concentrate on the type1 type 2, if number larger than half of data link width, then data is inverted.

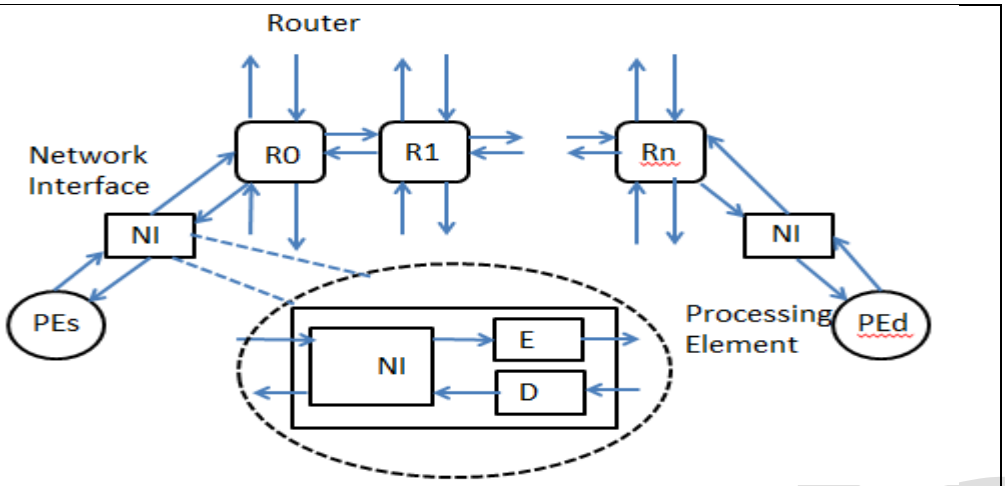

Figure1: General Architecture of Wormhole Switching

POWER MODEL

In this section we present the power model for the dynamic power consumed in the drivers and interconnect.

$$P = [T_{0\to1}(C_S + C_l) + T_c C_c]V_{dd}^2 F_{ck} \qquad (1)$$

Where C_l is the load capacitance, C_s self-switching capacitance (parallel plate capacitance and fringe capacitance), C_c is coupling capacitance, T_c, $T_{0\to1}$ are average number of transitions per clock cycle. V_{dd} Is supply voltage, F_{ck} clock frequency, $T_{0\to1}$ is number of 0→1 transitions in interconnects of two consecutive transitions. , T_c is correlated capacitance between two adjacent lines, which depends on type of transition, occurred in the lines. The total coupling capacitance changed from one type to another, therefore, T_c is the weighted sum of individual transition types (26).

$$T_c = K_1T_1 + K_2T_2 + K_3T_3 + K_4T_4 \qquad (2)$$

Where T_i,i=1,2,3,4 is the average number of type i transitions. $K_i$is the respective weight. From [26] we can use K_1=1,K_2=2 and K_3=K_4=0. K_1 Is assumed to be reference for other transition types. The effective capacitance in type2 is twice as that of type1.the probability of occurrences for random data of tye1, type2, type3,and type4 are $\frac{1}{2},\frac{1}{8},\frac{1}{4},\frac{1}{4}$respectively. Hence probability of type1 is more than probability of type2.so, we concentrate on minimizing type1, thus may lead to considerable reduction in power consumption.

$$[T_{0\to1}(C_s + C_l) + (T_1 + 2T_2)C_c]V_{dd}^2 F_{ck} \qquad (3)$$

Table1 shows the relationship between the coupling transition types, if flit is transmitted as is and flit is transmitted after inversion. Consider two adjacent physical lines first bit is the value of *i*th link, second bit is the value of *i*+1 physical line. For example in first column 00→10 indicates that, in the time slot *i*lines *i* and *i*+1 have values of 0 and 0 respectively. And in next time slot this switched to 0 and 1 respectively.

Time	Normal			Odd inverted		
	Type I			Type II,III & IV		
t-1	00 11	00 11 01 10	01 10	00 11	00 11 01 10	01 10
t	10 01	01 10 00 11	11 00	11 00	00 11 01 10	10 01
	T1*	T1**	T1***	Type III	Type IV	Type II
	Type II			Type I		
t-1	01 10			01 10		
t	10 01			11 00		
	Type III			Type I		
t-1	00 11			00 11		
t	11 00			10 01		
	Type IV			Type I		
t-1	00 11 01 10			00 11 01 10		
t	00 11 10 01			01 10 00 11		

TABLE 1:Relationship Between Present Data and Previous Data in Odd inversion

Time	Normal			Even inverted		
	Type I			Type II,III & IV		
t-1	01 10	00 11 01 10	00 10	01 10	00 11 01 10	00 11
t	00 11	10 01 11 00	01 10	10 01	00 11 01 10	11 00
	T1*	T1**	T1***	Type III	Type IV	Type II
	Type II			Type I		
t-1	01 10			01 10		
t	10 01			00 11		
	Type III			Type I		
t-1	00 11			00 11		
t	11 00			01 10		
	Type IV			Type I		
t-1	00 11 01 10			00 11 01 10		
t	00 11 01 10			10 01 11 00		

TABLE 2:Relationship Between Present Data and Previous Data in Even inversion

ODD INVERSION

In this inversion scheme, we concentrate to reduce type1 transitions and type2 transitions. The scheme compares the present data with previous data to decide conversion condition. If data is odd inverted type1 transitions becomes type 3 and type4.and type2 becomes type1 transitions. Then power model is,

$$P' \alpha\ T'_{0\to1} + (K_1T'_1 + K_2T'_2 + K_3T'_3 + K_4T'_4)C_c \qquad (4)$$

Where $T'_{0\to1}$ is self-switching transition activity,T'_1,T'_2,T'_3,T'_4 are coupling transition activities of T_1,T_2,T_3,T_4 respectively. The table1 shows the relationship between the transitions when data odd inverted or if it transmitted as is.If $P>P'$.then odd invert the flit before transmit it. Using [26] we may write,

$$\frac{1}{4}T_{0\to1(odd)} + T_1 + 2T_2 > \frac{1}{4}T_{0\to0(odd)} + T_2 + T_3 + T_4 + 2T_1^{***} \qquad (5)$$

This is the condition is decide whether the data is going to be invert or not. The terms $T_{0\to0(odd)}$ and $T_{0\to1(odd)}$ are weighted factor of ¼, for the link width more than 16, the self-switching part will not affect more. By simplifying this

$$T_1 + 2T_2 > T_2 + T_3 + T_4 + 2T_1^{***} \qquad (6)$$

$$T_x = T_3 + T_4 + T_1^{***} \qquad (7)$$

$$T_y = T_2 + T_1 - T_1^{***} \qquad (8)$$

This is the simplified condition for determine whether data is going to be invert or not.

Encoding architecture:

The figure2 shows the encoder architecture based on odd inversion condition. Consider the link width w ,where one bit is used for inversion bit, which indicates that the traversed flit is inverted or not. If data is not encoded the flits are transmitted as is, by making inversion bit 0.if data inverted, the inversion bit makes 1.the w-1 bits of previous encoded data is compared with present to decide inversion condition.in the encoding logic Tx and Ty blocks takes the two adjacent bits of input lines as$X_1X_2Y_1Y_2$,$X_2X_3Y_2Y_3$,$X_3X_4Y_3Y_4$.where X_i indicates the present data and Y_i indicates the previous data. Theoutputs of T_x and T_x blocks

are 1 if detects any types. The majority voter block decides the condition (Eqn.6).If the condition is satisfied, the inversion is performed on the odd number positioned bits

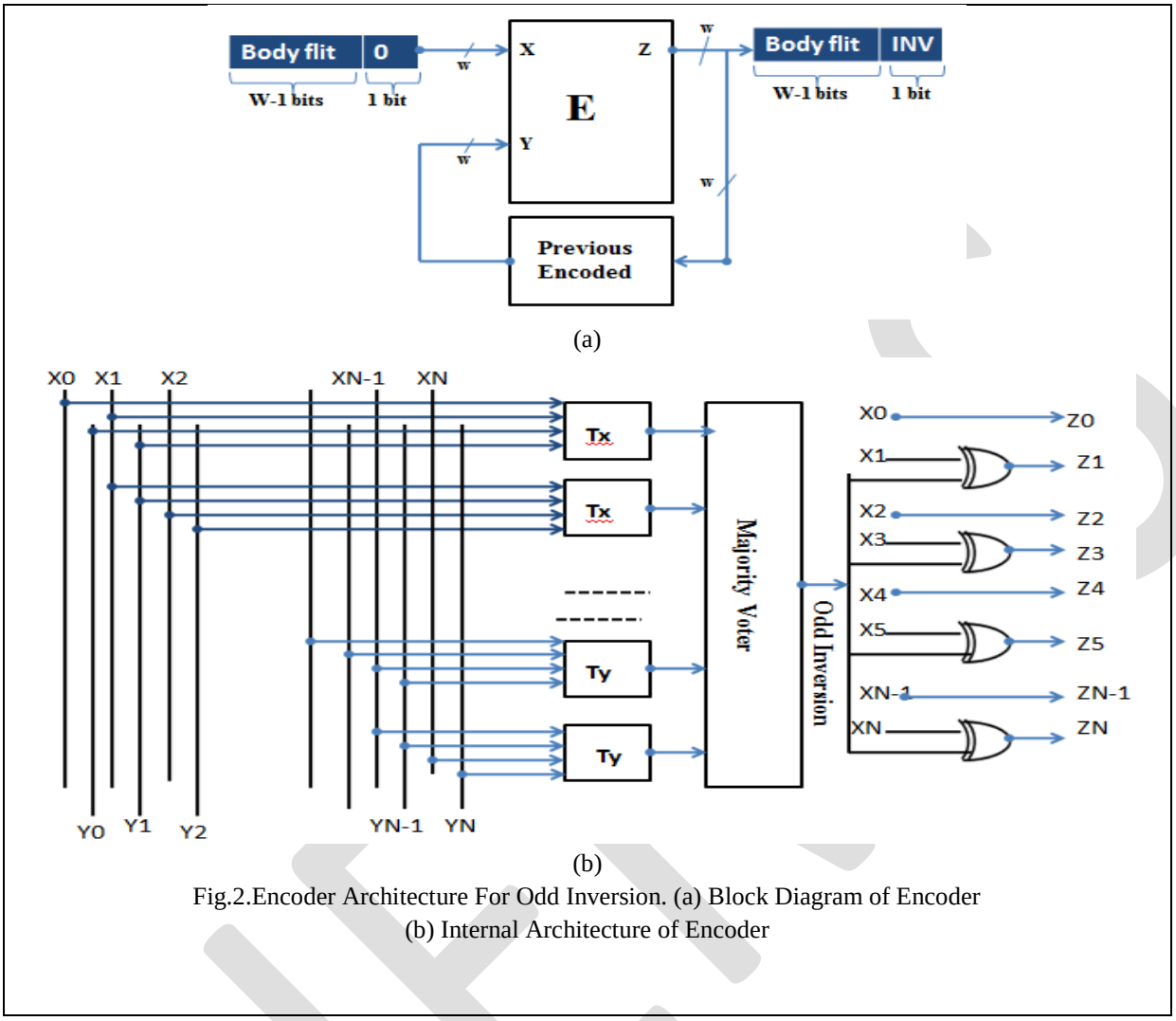

Fig.2.Encoder Architecture For Odd Inversion. (a) Block Diagram of Encoder
(b) Internal Architecture of Encoder

FULL INVERSION

Infull inversion we concentrate on both type1 and type2 transitions by use of both odd and full inversions. Type1 transitions convert to type3 and type4 transitions.type2 transitions converts to type4. Similar to previous scheme present data is compared to previous data to decide whether full, odd or no inversion. From [23] we may write

$$P'' \propto T_1 + 2T_4^{**} \qquad (9)$$

Where P'' power dissipated by the link when makes full inversion. From equations (9) and (5),

$$T_1 + 2T_4^{**} > T_2 + T_3 + T_4 + 2T_1^{***} \qquad (10)$$

Odd inversion condition is obtained as,

$$2(T_2 - T_4^{**}) < 2T_y - w + 1T_y > \frac{w-1}{2} \qquad (11)$$

Similarly condition for full inversion is from $P'' < P'$, $P'' < P$ and $T_2 > T_4^{**}$ is given by

$2(T_2 - T_4^{**}) > 2T_y - w + 1T_2 > T_4^{**}$ (12)

If none of (12) and (11) are satisfied, then no inversion is performed.

Encoding architecture:

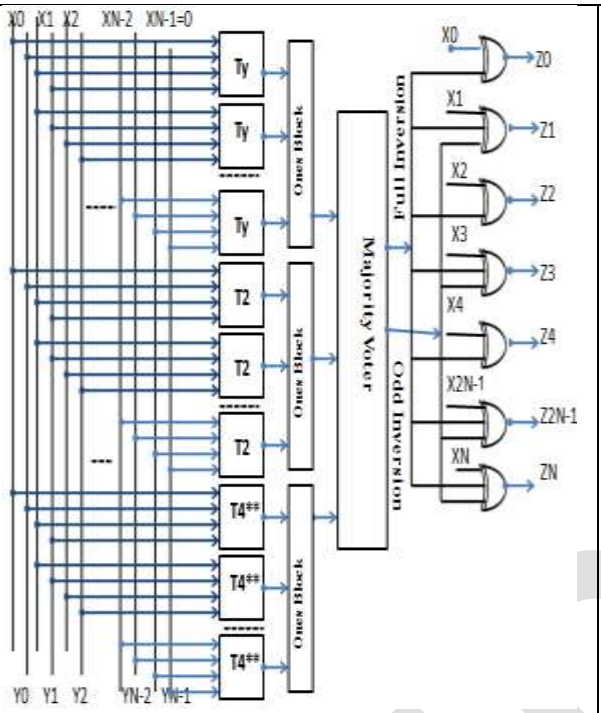

Fig 3. Encoding architecture for full inversion

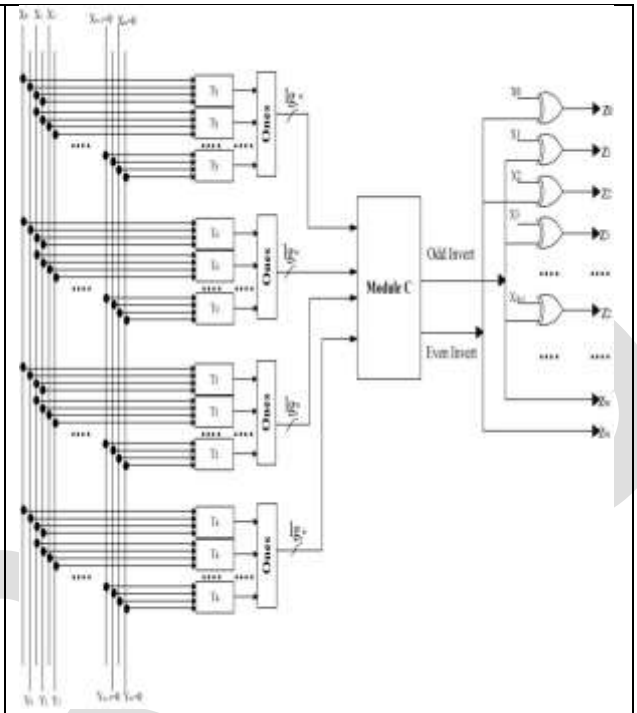

Fig 4. Encoding architecture for Even inversion

The figure3 shows the encoder architecture based on odd inversion and full inversion condition. Similar to previous encoder the link width w ,where one bit is used for inversion bit, which indicates that the traversed flit is inverted or not. If data is not encoded the flits are transmitted as is, by making inversion bit 0.if data inverted(odd/full), the inversion bit makes 1.the w-1 bits of previous encoded data is compared with present to decide inversion condition.in the encoding logic T_x,,T_2 ,T_4^{**} and Ty blocks takes the two adjacent bits of input lines as$X_1X_2Y_1Y_2$,$X_2X_3Y_2Y_3$,$X_3X_4Y_3Y_4$.where X_i indicates the present data and Y_i indicates the previous data. The outputs of T_x,T_2 ,$T_4^{**}$and T_x blocks are 1 if detects any types. The ones block counts the number of each transition by using the full adder circuit. Majority voter block decides (by using comparator block) whether odd or full inversion should be taken for link power reduction. If the condition in equation (12) or equation (11) is satisfied then output of majority voter block is '1'.the logic blocks are used to invert the flits based on the condition.

EVEN INVERSION

Here we add even inversion with the previous odd and full inversions. Since, the odd inversion converts some of type1 transitions to type2.so.if we do even inversion these type1 (T_1^{***}/T_1^{**}) transitions becomes type3 and type4.so.even inversion may leads reduce further link power consumption.table2 shows the relationship between present data and previous flit when data even inverted. Similar to previous schemes, present data is compared to previous data to decide whether even, odd or no inversion performed. Based on the analysis from odd inversion, we may write

$$T_1 + 2T_2 > T_2 + T_3 + T_4 + 2T_1^* \quad (13), \text{ defining } T_e$$

$$T_e = T_2 + T_1 - T_1^* \quad (14)$$

Similarly analysis given in full inversion, we may write the condition $P''' < P'$, $P''' < P''$ as,

$$T_2 + T_3 + T_4 + 2T_1^* < T_2 + T_3 + T_4 + 2T_1^{***} \quad (15)$$

$$T_1 + 2T_4^{**} > T_2 + T_3 + T_4 + 2T_1^* \quad (16)$$

Now define, $T_e = T_2 + T_1 - T_1^*, T_e + T_r = w - 1$ (17), where w is link width.

The full inversion leads to power reduction when $P'' < P', P'' < P, P'' < P'''$therefore condition for full inversion is obtained as,

$2(T_2 - T_4^{**}) > 2T_y - w + 1$, $2(T_2 - T_4^{**}) > 2T_e - w + 1$, $T_2 > T_4^{**}$ (18)

Condition for even inversion is obtained from $P''' < P', P''' < P$,$P''' < P''$,

$T_e > \frac{w-1}{2}$, $T_e > T_y$, $2(T_2 - T_4^{**}) < 2T_e - w + 1$ (19)

similarly condition for odd inversion is obtained as,

$2(T_2 - T_4^{**}) < 2T_y - w + 1$, $T_y > \frac{w-1}{2}, T_e < T_y$ (20)

If none of (20),(19),(18) is satisfied, no inversion is performed.

RESULTS AND DISCUSSION

Overheads due to encoder:

The encoder and the decoder were planned in Verilog HDL portrayed at the RTL level, blended with Cadence RC-compiler and mapped onto an 45-nm innovation library. In our study, the power and area of the proposed encoding Odd (O), Full (OF), and even(EOF) are looked at against SC and SCS [2], the BI coding [6], the coupling driven BI (CDBI) coding [7], and the forbidden pattern condition (FPC) codes [5],scheme I(H),scheme II (HF) and scheme III (OEF). The power and areaoverheads of the NI contrasted with the pattern NI are indicated in Fig. 5and Fig.6.here we consider the 32 bit data with 5*5 mesh structure.

Power analysis

To get the outcomes for total power and energy sparing indicated in Fig. 7, we have considered all the interconnect NoC parts, including connection, switch, encoder, link, also, NI. This a piece of NoCpower/energy utilization constitutes an imperative division of the general power financial plan of the total system.

Fig.8 demonstrates the lessening in the switching moves of type II, and coupling exchanging action for diverse information encoding plans contrasted with those of no information encoding. It demonstrates that the proposed encoding plans diminish type II. In the instances of past encoding plans (SCS, SC, BI, CDBI,H,HF,OEFand FPC) just Type II declines. Compared to previous encoding techniques the proposed Odd (O), Full (OF), and even(EOF) we get less percentage of toggle rate.

CONCLUSION

In this paper, we have displayed an arrangement of new information encoding plans went for lessening the power scattered by the connections of a NoC. Actually, connections are in charge of a huge portion of the general force dispersed by the correspondence system. What's more, their commitment is required to increment in future innovation hubs. When contrasted with the past encoding plans proposed in the writing, the basis behind the proposed plans is to minimize not just the switching action, additionally the coupling exchanging action which is principally in charge of connection powerdissemination in the profound submicronmeter innovation administration. The proposed encoding plans are matched with deference to the fundamental NoC building design as in their application does not require any alteration neither in the switches nor in the connections. The utilization of the proposed encoding plans permits investment funds up to 35% of power scattering and 17% of energy utilization with no huge execution debasement and with under 15% region overhead in the NI

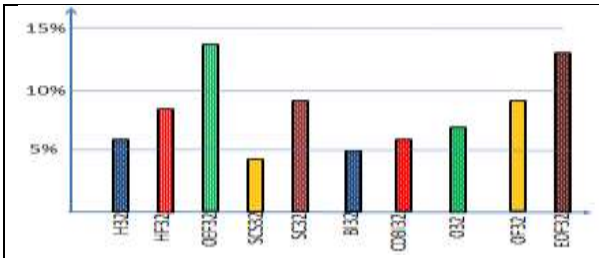

Fig 5:Percentage impact on power dissipation of the network interface due to the data encoding logic

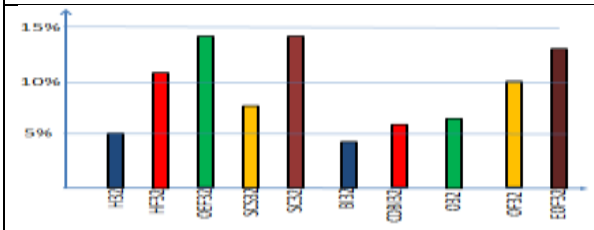

Fig 6:Percentage impact on silicon area of the network interface due to the data encoding logic

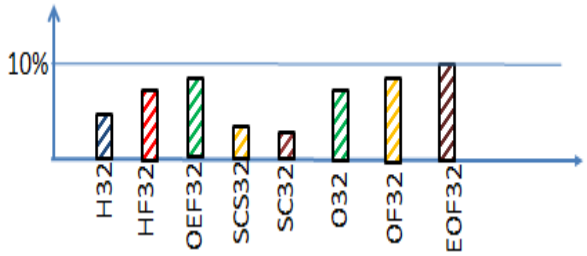

Fig7:Total power savings using different data encoding techniques

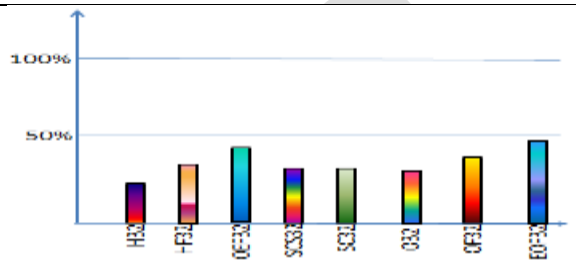

Fig 8:percentage decrease in type II transitions

REFERENCES:

1. A. Vittal and M. Marek-Sadowska, "Crosstalk reduction for VLSI,"*IEEE Trans. Comput.-Aided Design Integr. Circuits Syst.*, vol. 16, no. 3,pp. 290–298, Mar. 1997
2. M. Ghoneima, Y. I. Ismail, M. M. Khellah, J. W. Tschanz, and V. De,"Formal derivation of optimal active shielding for low-power on-chip buses," *IEEE Trans. Comput.-Aided Design Integr. Circuits Syst.*, vol. 25,no. 5, pp. 821–836, May 2006.
3. M. R. Stan and W. P. Burleson, "Bus-invert coding for low-powerI/O," *IEEE Trans. Very Large Scale Integr. (VLSI) Syst.*, vol. 3, no. 1,pp. 49–58, Mar. 1995.
4. C. L. Su, C. Y. Tsui, and A. M. Despain, "Saving power in the controlpath of embedded processors," *IEEE Design Test Comput.*, vol. 11, no. 4,pp. 24–31, Oct.–Dec. 1994.
5. E. Musoll, T. Lang, and J. Cortadella, "Working-zone encoding forreducing the energy in microprocessor address buses," *IEEE Trans. VeryLarge Scale Integr. (VLSI) Syst.*, vol. 6, no. 4, pp. 568–572, Dec. 1998.
6. G. Ascia, V. Catania, M. Palesi, and A. Parlato, "Switching activityreduction in embedded systems: A genetic bus encoding approach," *IEEProc. Comput. Digit. Tech.*, vol. 152, no. 6, pp. 756–764, Nov. 2005.
7. M. Palesi, G. Ascia, F. Fazzino, and V. Catania, "Data encoding schemesin networks on chip," *IEEE Trans. Comput.-Aided Design Integr. CircuitsSyst.*, vol. 30, no. 5, pp. 774–786, May 2011.
8. C. G. Lyuh and T. Kim, "Low-power bus encoding with crosstalkdelay elimination," *IEE Proc. Comput. Digit. Tech.*, vol. 153, no. 2,pp. 93–100, Mar. 2006
9. K. W. Ki, B. Kwang Hyun, N.Shanbhag, C. L. Liu, and K. M.Sung, "Coupling-driven signal encoding scheme for low-power interface design," in *Proc. IEEE/ACM Int. Conf. Comput.-Aided Design*, Nov. 2000, pp. 318–321.
10. C. P. Fan and C. H. Fang, "Efficient RC low-power bus encodingmethods for crosstalk reduction," *Integr. VLSI J.*, vol. 44, no. 1,pp. 75–86, Jan. 2011
11. K. W. Ki, B. Kwang Hyun, N.Shanbhag, C. L. Liu, and K. M.Sung, "Coupling-driven signal encoding scheme for low-power interface design," in *Proc. IEEE/ACM Int. Conf. Comput.-Aided Design*, Nov. 2000, pp. 318–321.

International Journal of Engineering Research and General Science Volume 3, Issue 6, November-December, 2015
ISSN 2091-2730

Predictability Analysis Algorithm for Optimal Precision Allocation in Wireless Sensor Network Applications

M. Selvaganapathy[1], N. Nishavithri[2], R. Nithya[3]
Asst. Professor, CK College of Engineering & Technology, Cuddalore, India[1]
Asst. Professor, Mailam Engineering College, Mailam, India[2, 3]
ganapathyselva111@gmail.com, +91 – 8098190456[1]

Abstract — Wireless sensor networks(WSN) comprises a hundreds to thousands of small nodes employed in wide range of data gathering applications such as military, health care monitoring and many other fields. Due to limited energy there is a difficultly in recharging a large number of sensor nodes, so energy efficiency and maximizing the network lifetime are the most important goals of sensor network. WSN requires robust and energy efficient communication protocols to minimize the energy consumption as much as possible. However, the lifetime of multi-hop WSN is reduced by radio irregularity and fading. A cluster-based scheme is proposed as a solution. The proposed scheme extends High Energy First (HEF) clustering algorithm and enables multi-hop transmissions among the clusters by incorporating the selection of supportive sending and receiving nodes. The performance is evaluated in terms of energy efficiency and reliability. The planned obliging algorithm HEF broadens the network era with 75% of nodes remaining alive when compared to Low Energy Adaptive Clustering Hierarchy (LEACH) protocol.

Keywords — Cluster head selection, Network Lifetime, Timing constraint, Wireless Sensor Network.

I. INTRODUCTION

Wireless Sensor Networks (WSNs) comprise a great number of nodes with sensing, computing, and wireless communication capabilities. Sensor networks become more and more popular as cost of sensor gets cheaper and cheaper. The sensor network is a wireless network formed by a group of sensors deployed in same region, which can be used to measure air pressure, temperature, acceleration, etc. Sensors transmit signals via radio signal. Since sensors are now small and cheap, they can be deployed in large scale. They become more and more important for applications like security, traffic monitoring, agriculture, war field, etc.

Inexpensive sensor nodes are deployed to the sensing area with little mobility and high density. The sensor nodes have very limited battery power and computing capability. Hence, the sensor networks should be well organized to meet the task. The objective of the clustering algorithm is to partition the network into several clusters. WSNs are used in safety-critical or highly reliable applications, two timing constraints are considered .Real time constraints and network lifetime constraints (as shown in Fig. 1).

There are two types of real-time systems: hard real-time systems that do not allow any task to miss its deadline, and soft real-time systems that strive to satisfy deadline requirements statistically.

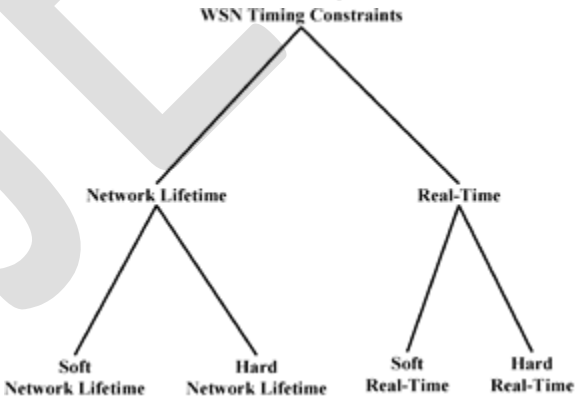

Fig. 1: Two time constraints on WSN based safety critical system

For these systems, research advances such as Rate – Monotonic Scheduling (RMS) and Earliest-Deadline First (EDF) scheduling algorithms have facilitated efforts by the real-time research community to minimize the risk of harm to all involved with good success. With respect to WSNs, real-time computing has been mostly applied in the areas of sensing, data processing, aggregation, and communication with deadline constraint requirements.

The network lifetime is another form of deadline, where we need to investigate new solutions in the context and property of the network lifetime WSN is characterized as a hard lifetime WSN in which every node must continue to function until the obligatory

dead- line. Depending on the mission requirements, network lifetime is most widely defined as: 1) the time span from the deployment of the network to when the first node runs out of energy 2) the time duration from the deployment of the network to when a certain percentage of the nodes die due to energy resource exhaustion or 3) the time taken from the deployment of the net- work to when the network is not able to fulfill designed requirements (such as coverage, packet loss, and connectivity).

A hard network lifetime requirement for a WSN means that the system must guarantee that at least K nodes are active at each round during the period from the start of operation to the end of the designated lifetime. Conversely, a soft network lifetime WSN makes a best effort, and has a certain level of acceptance of lifetime misses (as shown in Fig. 1). Time-critical WSN systems are ubiquitous in many practical applications. In the literature, researchers have applied them in applications such as target tracking systems, pollution monitoring, and health care. They are briefly discussed below.

In target tracking systems, such as wildlife monitoring systems or border security surveillance systems, sensor nodes may be required to detect and classify a fast moving target within one second before it moves out of the sensing range.

In an oil pollution monitoring system application, it is a requirement to process collected data over waters, and provide relevant oil-spill location information to the pollution control authority within one hour.

In the health care application arena, a wearable sensor is required to meet the real-time specifications for collecting and transferring patient data (e.g., electrocardiography) to the monitoring server with a signal sampling rate of 150 times per second.

When time-critical constraints (either hard real-time or hard network lifetime) are considered in WSN applications, predictability, rather than speed or energy efficiency, is of greater importance Systems must be predictable (or deterministic), but not necessarily fast nor sufficiently long lasting to adapt to evolving situations. In a predictable WSN, we should have the confidence to determine in advance whether the specific critical tasks can be performed completely under current energy budgets, as well as within the time constraints. To provide predictability to time critical WSN applications, it is important to understand how the system behaves.

II. HC – WSN CHS Algorithms

There are various technical challenges that are due to WSN system limitations such as limited battery capacity, and primitive computing capabilities. Among all design goals for WSNs, network lifetime is considered to be the most important. One of the research topics that have gathered significant interest is the issue of prolonging network lifetime under energy constraints. Several solutions to maximize network lifetime are available, and each approach provides different magnitudes of energy savings and levels of efficiency.

HC – WSN is comprised of a base station, several cluster head nodes, and regular sensor nodes. For administrative purposes, the operation of a HC-WSN is divided into rounds in which sensor nodes are grouped into clusters. Each round consists of three phases: cluster head selection (CHS), cluster formation (CFM), and data communication (DCM). The deterministic behaviors of a HC-WSN are typically characterized by the above three phases. However, the CHS phase plays the most dominant role with respect to the optimality and predictability of the entire network operation. A smart cluster head selection strategy can significantly reduce energy consumption, which in turn prolongs the network lifetime. Furthermore, a rule-based cluster head selection strategy can make the network lifetime more predictable. The CHS phase has been researched more actively than the other two phases.

In Table I, we have classified the cluster head algorithms based on a priori energy information, and summarized their network lifetime properties.

A. Without Energy Awareness

The cluster head selection processes for this type of clustering do not require sensors to be aware of any a priori energy information. However, without awareness of the energy information, cluster heads cannot be rotated, and traffic loads cannot be shared. As a result, it is difficult for sensors to choose the most appropriate cluster heads to maximize their network life- time, and hot-spot cluster head sensors die quickly. Some of the CHS algorithms are given in Table I.

In the literature, one example of CHS algorithms without energy awareness is the Lower ID heuristic, which uses the static node ID scheme to choose the node with the minimum node ID as a cluster head, proposed an election process by secret ballot votes to identify a node that receives the majority vote of those seated in a cluster as a new cluster head, and a node with the second highest number of votes as the vice cluster head. After the election process, the current cluster head multicasts the results to all the members of the cluster, informing the nodes of the cluster head, and vice cluster head.

B. With Energy Awareness

The cluster head selection processes for this type of clustering require partial knowledge on system energy levels and environment conditions. To maximize the network lifetime, some schemes pursue short-term fairness in time by sharing the energy consumption loading, while some others try to form clusters according to the geographical position of sensors. They at- tempt to find the optimal tradeoff between the energy consumptions on communication overhead and the energy savings by appropriately forming the clusters.

To avoid non-uniform distribution of cluster heads, cluster heads are selected according to their residual energy, and a predefined energy level difference is used to enforce the cluster head rotation inside the cluster. Some of the energy awareness CHS algorithms are given in Table I.

HEED (Hybrid Energy-Efficient Distributed clustering) periodically selects cluster heads based on a hybrid of residual energy, and a secondary index (such as node proximity to its neighbors or node degree). The secondary index will be considered if two nodes have the same residual energy. There are also some algorithms that try to get as much information as possible to compute the best clustering, and to maximize the overall network lifetime. These algorithms are mostly centralized. In these algorithms, in addition to only collecting data from sensors, the base station or a centralized center will also determine the working status of the sensors. For instance, a centralized base station using the LEACH – Centralized (LEACH – C) algorithm chooses a cluster head based on a hybrid of location in- formation and energy levels. LEACH – C maintains enough separation distance to keep cluster head nodes separate from each other.

Nevertheless, none of the above cluster head selection algorithms addresses the predictability analysis issue in their pro- posed algorithms. Although some of their approaches are optimal, the predictability of optimality is stochastic (non-deterministic). In other words, the above algorithms do not guarantee that the hard network lifetime constraints could be met. To the best of our knowledge, this paper is the first paper that discusses the predictability analysis of the WSN cluster head selection algorithm in hard network lifetime environments.

III. HEF CLUSTERING ALGORITHM

Without a priori knowledge (such as network lifetime, residue. energy level, and the energy consumption for clusters), it is impossible for any cluster head selection algorithm to obtain good results for prolonging the network lifetime.

	Cluster Head Selection Algorithm	Selection Rule	Network Lifetime		
			Prolongation	Optimality	Schedulability
Without prior energy information	Lowest ID [22]	Lowest Node ID			
	Associative based Clustering [29]	Highest spatial associativity, minimum distance			
	LEACH [20]	Probability function	*		
	Trust – based [23]	Vote, Quantitative measure of trust	*		
	Adaptive Contention Window (ACW) [25]	Minimum back off value	*		
	CIPRA [33]	Mod	*		
Energy Awareness	Maximum Residual Energy [18]	Maximum residual energy	*		
	LEACH [27]	Probability function	*		
	Probabilistic Clustering (Extended probabilistic algorithm for HEED) [28]	Probabilistic and priority	*		
	HEED [31]	A hybrid of residual energy and a secondary parameter with probability function	*		
	LEACH – C [32]	Location and energy level	*	*	

	Chen [30]	Hop number calculation	*	*	
	Our paper	Residual energy	*	*	*

Table 1: Comparison of Cluster Head selection algorithm

The core idea of the HEF clustering algorithm is to choose the highest-ranking energy residue sensor as a cluster head. The HEF clustering algorithm is defined as follows:

HEF Algorithm: HEF selects set of M highest- ranking energy residue sensors for cluster at round where denotes the required cluster numbers at round.

Some researchers have claimed that HEF is an efficient cluster selection algorithm that prolong network lifetime based on simulations. However, their measurements and simulation results are stochastic processes. A theoretical proof to demonstrate the optimality of HEF under certain conditions is provided in this paper.

HEF is designed to select the cluster head based on the energy residue of each sensor to create a network – centric energy view. Intuitively, HEF is a centralized cluster selection algorithm; but it also can be implemented in a distributed fashion with the synchronization approach. Fig. 2 depicts the information flow of the centralized HEF system.

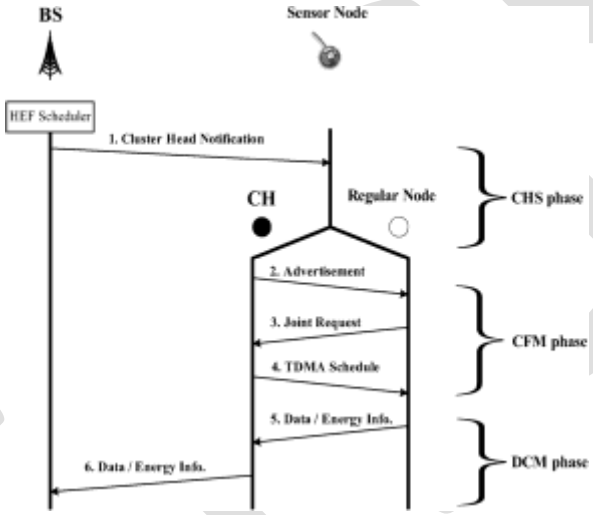

Fig. 2: Information flow of the centralized HEF system

Each round comprises the following three phases: CHS Phase, CFM Phase, and DCM Phase. The interactions and detailed operations between components are discussed as follows.

- HEF selects cluster heads according to the energy remaining for each sensor node, and then the "setup" message (indicating cluster members, and the cluster head ID for each participated group) is sent to the cluster head of each cluster.
- The cluster head of each group broadcasts the "setup" message inviting the neighbor sensor nodes to join its group.
- After receiving the "setup" message at the round, the regular sensors send the "join" message to its corresponding cluster head to commit to associate with the group.
- Each cluster head acknowledges the commitment, and sends TDMA schedule to its cluster members.
- All sensors perform its sensing and processing and communication tasks cooperatively at this clock cycle (round). Each sensor sends its energy information to its cluster head at the end of this clock cycle.
- Upon collecting cluster members' information at a given period, the cluster head sends the summative report to the base station.

A. Optimal Condition for HEF

The HEF clustering algorithm and its variants are not new, but this paper is the first work to formulate the HEF algorithm analytically to characterize its optimality property. Let us denote V as the set of sensor nodes deployed, and let N represent the total count of the sensor nodes.

B. Ideal Conditions for Optimality of HEF (ICOH):

1) All nodes must operate in a working-conserving mode. In other words, each node works as a clutter head, or a regular sensor in a round.
2) The energy consumptions of ω_c and ω_r are constant during the entire operation.

In the working-conserving mode, sensor nodes must consume energy at anytime while they operate. In the WSN, sensor nodes must serve as either a cluster head, or a regular node. The amount of energy a sensor consumes depends on the role it serves, as well as the workload it handles.

Here, regular sensor nodes can operate in either the sleep state, or active state. In the active state, a sensor node functions completely (i.e. transmit, receive or idle), while in the sleep state, the sensor operates at a low-power operating condition, and is awake for a short period of time to hear emergency messages.

Nevertheless, though the sleeping sensors do not receive and forward the control messages, they still consume energy to participate in the clustering operation, and to listen to the idle channel. Conversely, a cluster head must operate at the active state to collect data from associated regular nodes, and to forward data to the base station.

From the performances of energy consumption models reported in the literature, it can be observed that the energy consumption for the cluster head is more than that for a regular node. In particular, for time critical systems, the worst case scenario is also a crucial consideration in which it is assumed that the energy consumption of ω_c and ω_r are constant during the entire operation.

IV. ENERGY CONSUMPTION MODEL

At this point, we have shown that, if we can get the initial energy information of all sensors, HEF provides optimal cluster head selection with respect to network lifetime under the ICOH condition.

WSN nodes are primarily equipped with three types of tasks namely sensing, processing, and communicating data to other nodes and ultimately to the sink (base station) (as shown fig.3).

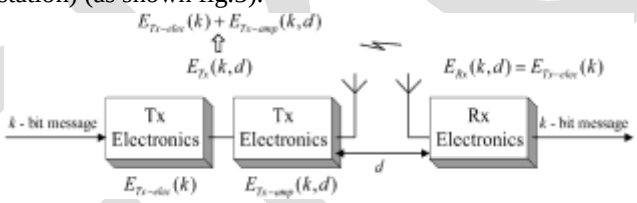

Fig 3: Transmitting and receiving

Transmission in WSNs is more energy consuming compared to sensing, therefore the cluster heads which performs the function of transmitting the data to the base station consume more energy compared to the rest of the nodes. Clustering schemes should ensure that energy dissipation across the network should be balanced and the cluster head should be rotated in order to balance the network energy consumption. The communication model that wireless sensor network uses is either single hop or multi hop.

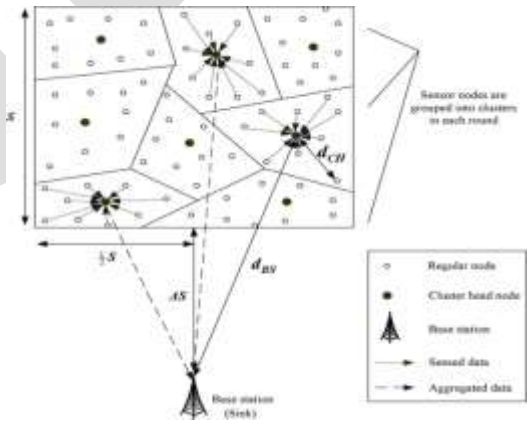

Fig. 4: Environment of the hierarchical clustering WSNs (HC – WSN)

Since energy consumption in wireless systems is directly proportional to the square of the distance, single hop communication is expensive in terms of energy consumption.

Under the ICOH condition, we assume that the energy consumption of ω_c and ω_r are constant during the entire operation. However, in actual environments, and are not constant. The amount of energy consumed by a sensor node depends on the role it serves, as well as the workload it handles. To analyze hard network lifetime for guaranteed predictability, the worst-case energy consumption (WCEC) analysis is used. Let ω_c^*, ω_c , ω_r^* and ω_r denote the maximum, and the minimum energy consumed for a cluster head, and a regular node in a round respectively.

V. PREDICTABILITY ANALYSIS OF HEF

The most important property of the WSN network life – time is not longevity, but predictability. Schedulability tests are essential for the time – critical system because it provides predictability to complement online scheduling. Cluster head selection algorithms produced by empirical techniques often result in highly unpredictable network lifetimes. Although an algorithm can work very well to prolong the network lifetime for a period of time, a possible failure can be catastrophic, resulting in the failure of a mission, or the loss of human life. A reliable guarantee of the system behaviors is hence a requirement for systems to be safe and reliable. However, there are currently no known analytical studies on the network lifetime predictability for cluster head selection algorithms.

Predictability tests allow engineers to assess what actions (e.g. changing energy budget or lifetime, etc.) should be taken to improve the dependability and reliability of the systems. The schedulability test flow chart consists of three major stages: Deployment Planning, Energy Estimation and Schedulability Analysis. In the Deployment Planning stage, efforts are made to plan the shape of the network topology, the initial energy level of sensor nodes, and the necessary configurations to perform. Activities and measures for the minimum and maximum energy consumption of the cluster head and the regular node are conducted in the Energy Estimation stage. In the predictability Analysis stage, schedulability test results pro- vide the necessary information to all running scenarios.

VI. SIMULATION

In this section, we demonstrate that the derived results above are consistent with simulation results. We use NS2 to conduct a performance study to compare the performance of HEF with that of LEACH, and investigate the feasibility of HEF.

There are 100 sensor nodes, organized in a random topology, and randomly deployed in a square region 100*100 meters in size. The base station is located at the position (50,180). The simulation parameters are listed in Table III.

Parameters	Value
Mo. Of Nodes	100
No. of cluster	5
Network Size	100 m x 100 m
Base Station location	(50, 180)
Radio Speed	1 Mbps
Header Sized	25 bytes
Packet Size	500 bytes
Radio electronics energy (E_{elec})	50 nJ / bit
Radio amplifier energy (ε_{fn})	10 pJ / bit / m^2
Radio amplifier energy (ε_{mp})	0.0013 pJ / bit / m^4
Cross – over distance for friss and two – ray ground attenuation models	87 m
Data aggregation energy (E_{DA})	5 nJ / bit
Compression Ratio (α)	0.5

Table. 2: Simulation Parameters

The comparison results between HEF and LEACH are presented in Fig. 7, where the Y-axis represents the minimum residue energy level of sensors, and the X-axis denotes the running time for individual rounds. In this study, the network lifetime performance is evaluated for both the HEF and LEACH models under various initial energy ranging Fig. 5 shows that the lifetime increases with the initial energy increase. Their performances are also compared under the same mean values of energy, but with different variances. Each point in the figure represents the result.

b1. With the increase in initial energy, the lifetime for all schemes increases, but HEF prolongs the network lifetime as compared to LEACH when the initial energy becomes large enough. This result is because LEACH is unable to balance the energy

consumption among the sensor nodes to avoid early energy depletion of the network.

b2. When the initial energy level is low, there is no significant performance difference between HEF and LEACH. However, HEF has better performance at a small variance.

b3. The HEF algorithm performs better out of all LEACH schemes under high initial energy level.

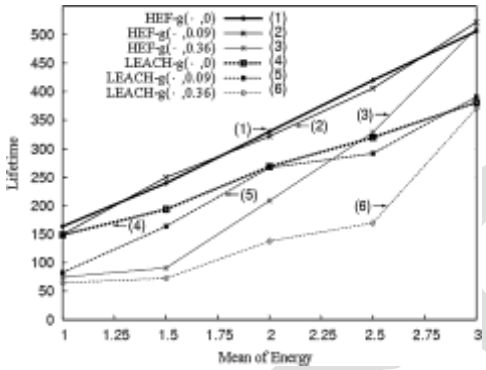

Fig. 5: Network lifetime vs. Initial Energy.

In this experiment, HEF surpasses LEACH by taking into ac- count network lifetime when they have the same initial energy level.

In simulation results, is compared with nodes and its energy level shown in TABLE IV. Let us consider, in cluster 1 node 0 has maximum energy so its selected as cluster head, in cluster 2 node 5 is selected as cluster head.

Cluster	Node numbers	Energy level %
Cluster1	0	90
	2	80
	1	75
	3	70
	4	60
Cluster 2	5	70
	8	60
	6	55
	7	50
	9	53

Table 4: Comparison of nodes with its energy

VII. CONCLUSION & FUTURE WORK

Providing a trustworthy system behavior with a guaranteed hard network lifetime is a challenging task to safety-critical and highly-reliable WSN applications. For mission critical WSN applications, it is important to be aware of whether all sensors can meet their mandatory network lifetime requirements.

First, the High Energy First (HEF) algorithm is proven to be an optimal cluster head selection algorithm that maximizes a hard N – of – N lifetime for HC-WSNs under the ICOH condition. Then, we provide theoretical bounds on the feasibility test for the hard network life- time for the HEF algorithm.

In future multi-hop transmission can be implemented and to avoid the inefficiency, AOMDV protocol can be used.

REFERENCES:

[1] Bo-Chao Cheng, Hsi- Hsun Yeh , and Ping-Hai Hsu, "Schedulability Analysis for Hard Network Lifetime Wireless Sensor Networks With High Energy First Clustering", IEEE Transaction on reliability, 0018-9529, 2011

[2] K. Kalpakis, K. Dasgupta, and P. Namjoshi, "Efficient algorithms for maximum lifetime data gathering and aggregation in

wireless sensor networks," ACM Computer Networks, vol. 42, no. 6, pp. 697–716, 2003

[3] H. Liu, P. Wan, C.-W. Yi, X. Jia, S. Makki, and P. Niki, "Maximal lifetime scheduling in sensor surveillance networks," in IEEE Infocom, March 2003.

[4] E. Hansen, J. Neander, M. Nolin, and M. Björkman, "Energy-efficient cluster formation for large sensor networks using a minimum sepa- ration distance," in the Fifth Annual Mediterranean Ad Hoc Net- working Workshop, Lipari, Italy, June 2006.

[5] E. Chu, T. Mine, and M. Amamiya, "A data gathering mechanism based on clustering and in-network processing routing algorithm: CIPRA," in The Third International Conference on Mobile Computing and Ubiquitous Networking, ICMU, 2006.

[6] F. Vasques and G. Juanole, "Pre – run – time schedulability analysis in fieldbus," in IECON'94 20th International Conference on Industrial Electronics, Control and Instrumentation, 1994, pp. 1200 – 1204.

[7] B.C. Cheng, A. Stoyenko, T. Marlowe, and and S. Baruah, "Bounds on tardiness in scheduling of precedence-constrained unit real-time task systems," Computers and Electrical Engineering 27, pp. 345–354, 2001.

[8] H. Chen, C.-S. Wu, Y.-S. Chu, C.-C. Cheng, and L.-K. Tsai, "Energy Residue Aware (ERA) clustering algorithm for leach-based wireless sensor networks," in Second International Conference on Systems and Networks Communications (ICSNC 2007), 2007, pp. 40–45.

[9] L. Ying and Y. Haibin, "Energy adaptive cluster-head selection for wireless sensor networks," in Proceedings of the Sixth International Conference on Parallel and Distributed Computing, Applications and Technologies (PDCAT05), 2005, pp. 634–638.

[10] Chuan-Ming Liu, Chuan – Hsiu Lee, "Distributed algorithms for energy-efficient cluster-head election in wireless mobile sensor networks," Conference on Wireless Networks (ICWN'05), Las Vegas, Nevada, USA, June 2005, 405-411

[11] Sajid Hussain, Abdul W. Matin, "Hierarchical Cluster-based Routing in Wireless Sensor Networks", in Proceeding of 5th Intl. Conf. on Information Processing in Sensor Network (IPSN06), USA, April 19-21 2006

[12] Udit Sajjanhar, Pabitra Mitra, "Distributive energy efficient adaptive clustering protocol for wireless sensor networks," in Proceeding of International Conference on Mobile Data Management (MDM07), Mannheim, Germany 2007

International Journal of Engineering Research and General Science Volume 3, Issue 6, November-December, 2015
ISSN 2091-2730

Automatic Subtitle Generation for Videos

Akhil Kanade, Sourabh Gune, Shubham Dharamkar, Rohan Gokhale

PES's, MCOE Department Of Computer Engineering, Pune-05, sourabhgune@ymail.com, Mob.:9765353586

Abstract— The main objective of developing this system is to present an automated way to generate the subtitles for audio and video. By replacing the tedious method of the current system will save time, reduce the amount of work the administration has to do and will generate the subtitles automatically with electronic apparatus. This system will first extract the audio, then recognise the extracted audio with the available speech recognition API. Later the recognized audio is converted to the text and saved in text file having extension ".srt". Later on, this ".srt" file can be opened in a media player to view the subtitles along with video.

Keywords—Audio extraction, Speech recognition, .srt file, Time synchronization, Automatic Subtitle generation, Natural language processing.

INTRODUCTION

About this Project:
The main idea of developing this system is to present an automated way to generate subtitles using audio extraction and speech recognition techniques which would replace the present method of writing the file manually. Replacing the tiresome old method this system will save the time, reduce the amount of work the administration has to do and will minimize the human errors associated with this process.
Motivation:
Nowadays due to increase in use of syllabus related videos for teaching in classes, may that be at school or college level, some students are unable to grasp what the speaker is trying to explain in that video. If the videos are shown along with captions then it becomes easy to relate what the video or the speaker in video want to convey. Also the videos are not compulsorily provided with subtitles so manually write this is impossible task for any individual, also to search the respective time synchronized file may take time. Instead by using this software any individual can easily generate the captions and club it with video which can help students and all.

BRIEF DESCRIPTION

Need of Automatic subtitle generation:
Subtitles are very important to understand the content spoken by the individual in video. There is an alternate method available for generating subtitles i.e. manually writing the file but it costs us much time. This method waste time because the individual has to manually write the subtitle file which is a tedious task which may introduce many errors also the time synchronization must be done which every individual is unable to perform. This work describes the efficient process that automatically generates the subtitle without human intervention. This subtitle is generated by using a speech API and the file is produced which is properly time synchronized and displays accurate subtitles.
In today's world use of subtitles has become important for understanding of the video. Subtitling is essential for people who are deaf those who have reading and literacy problems and can to those who are learning to read. Subtitles provide information for individuals who have difficulty understanding speech and auditory components of the visual. This leads to a valid subject of research in field of automatic subtitles generation. Thus this report provide users a major benefit of not downloading the subtitles instead generating them automatically. Various studies have been done to accomplish this type of process. Downloading the subtitles from the internet is a monotonous processes. Consequently, to generate the subtitles thorough the software itself is a easy process.

Innovativeness and Usefulness:-
1) The major benefit is that the viewer does not need to download the subtitle from Internet if he wants to watch the video with subtitle.
2) Captions help children with word identification, meaning, acquisition and retention.
3) Captions can help children establish a systematic link between the written word and the spoken word.
4) Captioning has been related to higher comprehension skills when compared to viewers watching the same media without captions.
5) Captions provide missing information for individuals who have difficulty processing speech and auditory components of the visual media.

6) Captioning is essential for children who are deaf and hard of hearing, can be very beneficial to those learning English as a second language, can help those with reading and literacy problems and can help those who are learning to read.

This project will mainly generate subtitles with help of speech API.
Generation of subtitles include following steps:

Speech Extraction:

The audio extraction routine is expected to return a suitable audio format that can be used by the speech recognition module as pertinent material. It must handle a defined list of video and audio formats. It has to verify the file given in input so that it can evaluate the extraction feasibility.

Speech recognition:

The speech recognition routine is the key part of the system. Indeed, it affects directly performance and results evaluation. First, it must get the type of input file then, if the type is provided an appropriate processing method is chosen. Otherwise, the routine use a default configuration.

Subtitle Generation:

The subtitle generation routine aims to create and write in a file in order to add multiple chunks of text corresponding to utterances limited by gaps and their respective start and end times. Time synchronisation consideration are of main importance.

For analyzing Extraction and Recognition, we have to take following concepts into consideration as follows:

1) Recognizing different speakers:

Many instances are observed where there are multiple sources of sound which may give error in subtitles. The main challenge is to identify the speaker for whom the caption need to be generated.

2) Recognizing the silences/gaps:

Many pauses are observed when there is verbal conversation between speakers. This situation must be correctly analyzed so as to obtain correct output.

3) Generation and appending of text:

Generated sentences or words must be appended in proper sequence into the text file.

4) Time synchronize the text:

The biggest challenge is to display the captions according to the video. The text file contains the sentences corresponding to the input video which must be time synchronized according to the frames.

Major constraints:

Accuracy:

Accuracy of system should be high otherwise the generated subtitles will be incorrect for the purpose. The process of extraction and recognition must be correctly followed.

Input Video:

The quality of video which is given as input must be good with less audio distortions.

Speech:

During the process of audio extraction the audio must be properly extracted as there maybe loss of contents which may produce errors at later stages.

Use case diagram:

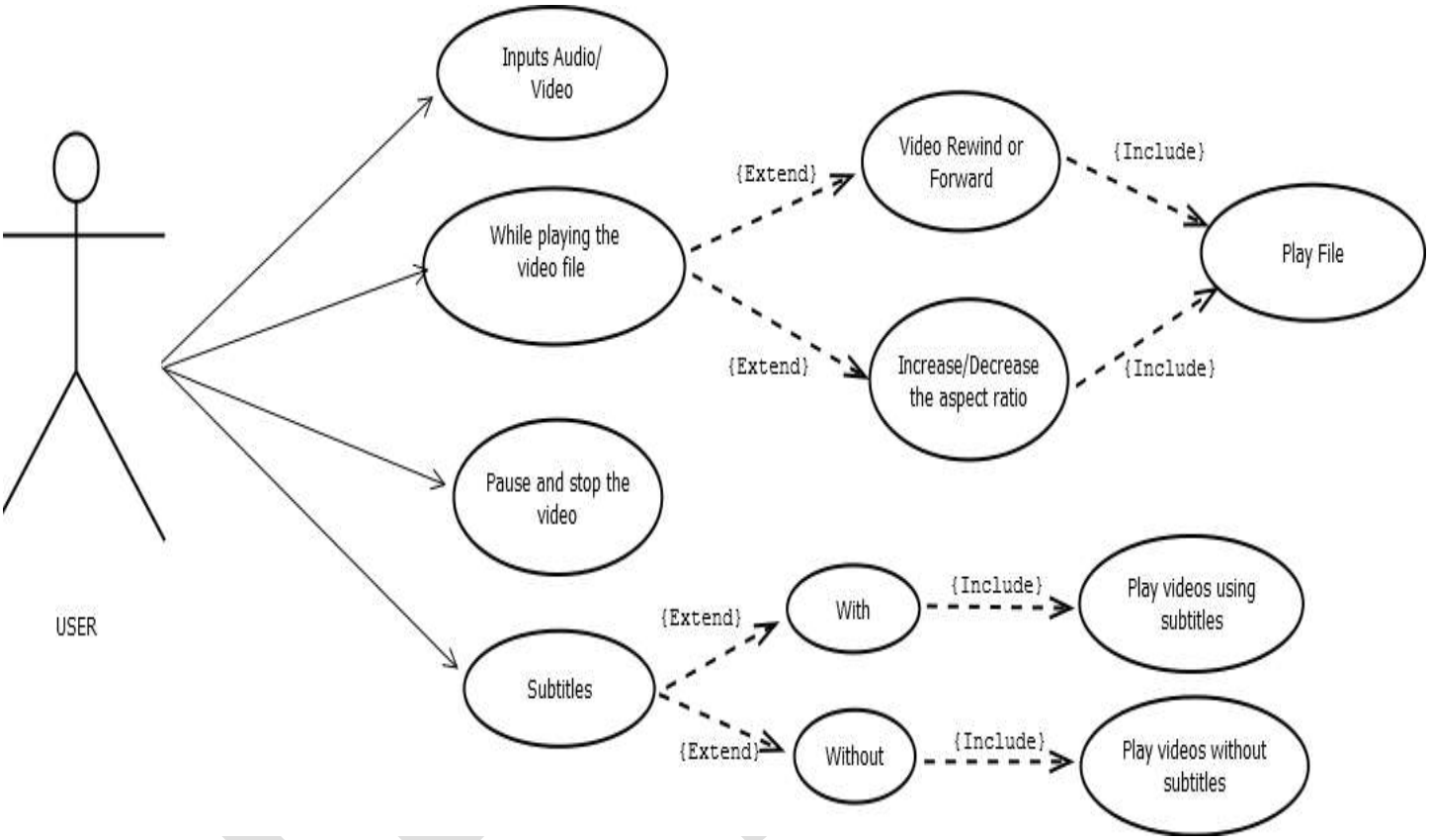

CONCLUSION

By using this software subtitles or subtitle file will be generated for any English videos. This software will minimizes the efforts for downloading or manually writing the subtitle file. Any one will be able to generate the subtitle file as this software is very easy to use and just needs input which can be provided by anyone. Also this software can be used with online website to provide videos along with subtitles. Many type of formats will be supported by this software.

REFERENCES:

[1] Abhinav Mathur, Tanya Saxena, Generating Subtitles Automatically using Audio Extraction and Speech Recognition, 7th International Conference on Contemporary Computing (IC3), 2015.

[2] Sadaoki Furui, Li Deng, Mark Gales,Hermann Ney, and Keiichi Tokuda,, Fundamental Technologies in Modern Speech Recognition, Signal Processing, IEEE Signal Processing Society, November 2012.

[3] Youhao Yu Research on Speech Recognition Technology and Its Application, Electronics and Information Engineering, International Conference on Computer Science and Electronics Engineering, 2012

[4] Jorge Martinez, Hector Perez, Enrique Escamilla, Masahisa Mabo Suzuki, Speaker recognition using Mel Frequency Cepstral Coefficients (MFCC) and Vector Quantization (VQ) Techniques, 22nd International Conference on Electrical Communications and Computers (CONIELECOMP), 2012

[5] Anand Vardhan Bhalla, Shailesh Khaparkar, Performance Improvement of Speaker Recognition System,International Journal of Advanced Research in Computer Science and Software Engineering, Volume 2, Issue 3, March 2012

[6] Ibrahim Patel Dr. Y. Srinivas Rao, Speech Recognition Using HMM with MFCC- An Analysis using Frequency Spectral Decomposition Technique Signal and Image Processing: An International Journal(SIPIJ), Vol.1, No.2, December 2010.

[7] B. H. Juang; L. R. Rabiner, "Hidden Markov Models for Speech Recognition" Journal of Technometrics, Vol.33, No. 3. Aug., 1991.

[8] Hong Zhou and Changhui Yu , "Research and design of the audio coding scheme ," IEEE Transactions on Consumer Electronics, International Conference on Multimedia Technology(ICMT) 2011.

[9] Seymour Shlien,"Guide to MPEG-1 Audio Standard", Broadcast Technology, IEEE Transactions on Broadcasting, December 1994.

[10] Justin Burdick, "Building a Regionally Inclusive Dictionary for Speech Recognition", Computer Science and Linguistics, Spring 2004.

[11] Yu Li, LingHua Zhang, "Implementation and Research of Streaming Media System and AV Codec Based on Handheld Devices" 12th IEEE International Conference on Communication Technology (ICCT), 2010.

[12] Ibrahim Patel1 Dr. Y. Srinivas Rao, "Speech Recognition Using HMM with MFCC- An Analysis using Frequency Spectral Decomposition Technique", Signal & Image Processing: An International Journal(SIPIJ), Vol.1, No.2, December 2010.

[13] Stephen J. Wright, Dimitri Kanevsky, LiDeng, Xiaodong He, Georg Heigold, , and Haizhou Li, "Optimization Algorithms and Applications for Speech and Language Processing," IEEE Transactions on Audio, Speech and Language Processing, Volume 21, Issue 11, November 2013.

[14] Jing Wang, Xuan Ji, Shenghui Zhao, Xiang Xie and Jingming Kuang, "Context-based adaptive arithmetic coding in time and frequency domain for the lossless compression of audio coding parameters at variable rate," EURASIP Journal on Audio, Speech, and Music Processing 2013.

International Journal of Engineering Research and General Science Volume 3, Issue 6, November-December, 2015
ISSN 2091-2730

Development and Evaluation of a Passive Solar System for Poultry Egg Incubation

[1]Ahiaba Ugbede Victor, Lecturer II, ahiaba.victor@uam.edu.ng ; [2]Nwakonobi Theresa Ukaamaka, Associate Professor, napeth66@yahoo.com ; [3]Obetta Samuel Echi, Professor, sam.obetta@gmail.com

[1,2,3]Department of Agricultural and Environmental Engineering, University of Agriculture, PMB 2373, Makurdi, Benue State – Nigeria.,

Correspondent: ahiaba.victor@uam.edu.ng ; +2348036521370, +2348028990817

Abstract **-** Design, development and evaluation of a **Passive Solar Poultry Egg Incubator** were undertaken. The incubator had two heat **collectors** and storage media **(thermal masses)** and heat exchangers. The main heat absorber was made of 80mm thick concrete incorporated with a separate heat storage media to serve as back up during sunless hours. The system was insulated with 4mm thick plywood for both internal and external surfaces, with 6mm thick foams used to fill the annular spaces. The absorber surfaces were pre-treated by painting them black for better heat collection. Digital thermocouple/multi-meters was incorporated into the chambers for temperature and relative humidity measurements. At average ambient temperature of 36.6 ^{o}C, the heat absorber surfaces attained a maximum temperature of 91.5 ^{o}C at 15:00 (GMT) and a minimum temperature of 37.1 ^{o}C at 6:00. The temperature maintained in the incubating chamber ranged between 30.9 – 46.6 ^{o}C depending on the time of the day and weather conditions. At average ambient relative humidity of 69.2 %, the incubating chamber relative humidity was averagely at 61.6 %, using activated charcoal as dehumidifying material. Heat collection and transfer efficiencies of the thermal mass were 96.4 % and 44.3 % respectively. The incubator was tested for fertility and hatchability with 125 broiler eggs obtained from a reliable commercial hatchery. The percentage fertility and hatchability recorded were 74.4 % and 73.1%, respectively, with 21 days as incubation period.

Keywords: PASSIVE, SOLAR, POULTRY, EGG, INCUBATOR, THERMAL MASS, COLLECTORS.

INTRODUCTION

The main objective of this work is to harness the abundant solar energy available in Makurdi, Benue State, North-Central Nigeria, to heat up an incubating chamber for poultry eggs. Mankind has utilized solar energy for years for domestic drying, provision of warmth and for other uses. By 1915, several engines had been run from solar-generated steam, and most of the solar collector concepts used today had been developed. They all relied on glass, either for mirrors or for transparent covers to trap heat as in a green house [1] Lunde, (1980).

The craving for alternative energy source, outside fossil fuel, has become a global phenomenon. To this effect, countries around the world are investing massively in solar energy power plants. One of such major investment in the recent times is by the USA Department of Energy which has been charged with the development and sponsoring programmes that will transform the way energy is provided in the United States. Researchers from University of Arkansas have developed high performance concrete to store thermal energy for concentrating solar power plants [2] Emerson, Hale, and Selvam, (2011).

For a thriving poultry production in developing countries such as Nigeria, where electricity supply has remained inadequate and unreliable, alternative methods of meeting the energy needs in agriculture and in the poultry industry specifically, have to be evolved. These alternative energy needs cannot be over-emphasized, for energy is required at various stages of poultry production especially during incubation processes. At this stage, heat energy is the major requirement for successful hatching of the eggs into chicks and eventual growth of the young chicks in the brooding house, and then to maturity.

However, it is expedient that such alternative energy source should be dependable, in abundant supply, and environmentally friendly. It should also be inexpensive and readily available to local farmers. Solar energy looks the best alternative energy option for this, because it is clean and is readily available all year round in the tropics and in North Central Nigeria, along Benue River Valley, Makurdi-Nigeria. A good solar system should be able to convert solar radiation into useful heat or electrical energy, store it and release it for utilization when needed.

Several methods of solar energy storage are available [3] Duffie and Beckman, (1980). These include storing as sensible and latent or concealed heats. The advantage of sensible heat storage is that materials for energy storage are locally available and inexpensive. Such materials include water, stones, masonry wall systems, gravels and local bricks walls. The technology of masonry wall system as solar energy collector and storage device in buildings has been reported [4] Nayak, Bansal, Sodha, (1983).

In Nigeria, [5] Okonkwo, Anazodo, Akubuo, Echiegu, and Iloeje (1992) reported on solar heating system. The results of the analysis showed an absorber plate temperature of up to 83 ^{o}C measured and 122 ^{o}C predicted while storage medium temperature was 45.56 ^{o}C.

Though the solar incubating and heating systems are not generally common in Nigeria, the built-in thermal storage solar water space conditioning system could serve as a good example of utilizing solar energy in Nigeria as illustrated by [6] Okonkwo, (1998).

Several other researchers - [7] Fagbenle (1990) and [8] Pelemo, Fasasi, Owolabi, and Shaniyi (2002) worked on estimation of daily radiation and its utilization in Nigeria using meteorological data, including but not limited to [9] Yohanna, Itodo, and Umogbai (2011), [10] Itodo (2007), [11] Adeyemo (1988). [12] Owokoya (1992) , [13] Adaramola, Amaduoboga, and Allen (2001) and [14] Odia (2006).

This study aimed at developing a passive solar system that can provide suitable conditions for incubation of poultry eggs, using solar energy and materials within the research station.

MATERIALS AND METHODS

Materials

For a material to be effective as a thermal mass, it must have a high heat capacity, a moderate conductance, a moderate density, and a high emissivity. Table 1 shows the various materials used, selected on the basis of their properties suitable for the development of the solar incubator.

Material Treatment

The exposed surfaces of the thermal masses were painted black. This was necessary to allow optimal heat collection, absorbance and transmittance. Dark surfaces have high absorptances between 0.95 – 0.99. Hence, the thermal masses made of concrete and granite stones were painted black for optimum heat absorption. Similarly, in order to improve heat quality, the heated air was dehumidified for a dry hot air into the incubating chamber. The material used was Powdered Activated Carbon (PAC), otherwise known as grinded charcoal of diameter of about 0.15 - 0.25 mm. Thus they present a large surface to volume ratio with a small diffusion distance.

Table 1: Materials and their usage

S/N	Materials	Usage
1.	Plane Glass	Cover Plate
2.	Concrete Slab	Main Thermal Mass
3.	Granite Stones	Supplementary Thermal mass
4.	Plywood	Insulating body
5.	Insulation foams	Insulation purpose
6.	PVC troughs	Heat Exchanger
7.	Activated Charcoal	Dehumidifier
8.	Testing materials	Candler, fertile eggs

Basic Design Assumptions

The design analysis of this solar incubator is based on the following assumptions;

1. The heat being absorbed by the thermal mass and air equals the theoretical heat energy that successfully passed through the transparent glass cover.
2. All manner of expansion and contraction of materials used were assumed negligibly small, hence, ignored.

Solar energy incident on the glass cover (collector)

The solar energy incident on the glass cover is given by;

$$Q_{gc} = A_{gc}.I_{gc} \quad (1)$$

Where,
A_{gc} = Glass covers surface area (m^2),
I_{gc} = Hourly Total solar irradiance on the glass cover,

Over a period of total solar hours, this becomes;

$$Q_{gc} = A_{gc}.I_{gc}.t \quad (2)$$

However, owing to the thermal conductivity of the glass cover, the total heat delivered through it is;

$$Q_{gc} = A_{gc}.I_{gc}.t.k \quad (3)$$

Where,
k = the thermal conductivity of the glass cover;
t = time (hours).

Equation (3) is the actual heat delivered through the glass cover over the solar hours.

Heat Accumulated in the Supplementary Storage

The solar energy incident on the supplementary glass cover is as obtained in Equation (2). Base on first Theoretical Assumption, the heat collected by the supplementary storage is given by;

$$Q_{gra} = A_{gc} \text{ x } I_{gc} \text{ x t x k} \quad (4)$$

Where
Q_{gra}= Heat accumulated by the granite stone
A_{gc} = Area of the glass cover
I_{gc} = solar irradiance for Makurdi
t = solar hours per day for Makurdi

Total Available Energy to be delivered into the Incubating Chamber from Main Storage Chamber

The total useful energy available for delivery into the incubating chamber from the main storage chamber was estimated by taking away the heat losses from the walls of the storage chamber from the actual energy that successfully passed through the glass cover into the storage chamber;

$$Q_{ud} = Q_{gc} - Q_{lcc} \quad (5)$$

Where;
Q_{ud} = Useful energy available to be delivered into the incubation room;
Q_{gc} = Total useful energy that successfully passed through the glass cover;
Q_{lcc} = heat loss through the walls of the storage chamber;

$$Q_{lcc} = \frac{\Delta T}{R_T} \quad (6)$$

Where $R_T = \frac{1}{A}(\frac{x_w}{k_w} + \frac{x_f}{k_f})$;

R_T = the total resistance (R-value) of wood and foam that made up the wall system;
ΔT = average temperature difference between the collector chamber and the ambient;
A = Area of the collector chamber (m^2);
x_w = thickness of the wooden wall (m);
x_f = thickness of the foam (m);
k_w = thermal conductivity of the wood (W/m-k);
k_f = thermal conductivity of the foam (W/m-k);

Useful Energy Delivered into the Incubating Chamber

$$Q_{ui} = Q_{tm} + Q_a \quad (7)$$

$$Q_{tm} = (h_{ic}.A_{tm}(T_{itm} - T_{ic})) \quad (8)$$

Where,
Q_{ui} = Useful energy delivered into the incubating chamber;
Q_{tm} = Direct heat dissipation from the thermal mass (concrete);
h_{ic}= Radiation heat transfer coefficient from the inner surface of the thermal mass into the incubating chamber;
A_{tm}= Area of the thermal mass;
T_{itm}= Inner surface temperature of the thermal mass;
T_{ic}= Incubating chamber temperature.

$$Q_a = 2\acute{m}_a\acute{m}C_{pa}(T_{hac} - T_{ic}) \quad (9)$$

Where,
Q_a = heat transferred by the hot flowing air into the incubating chamber via the heat exchanger (PVC)
$\acute{m}_a$ = mass flow rate (Kg/hr),

C_{pa}= specific heat capacity of air (KJ/Kg.^{o}C);

But,

$$\acute{m}_a = \rho_a . A_{pvc} . F_r \sqrt{g} . D_v \frac{(T_{hac} - T_{ic})}{T_{hac} + T_{ic}} \quad (10)$$

Note: Equation (9 and 10) are as provided by [15] Bansal and Gour (1996) and [16] Zriken and Bilgen (1987) respectively.

Where,
ρ_a = Density of air, Kg m^{-3}
A_{pvc}= cross sectional area of the PVC trough, m^2;
F_r= Froude Number
D_v= Vertical distance of the PVC troughs from storage chamber (which serve as inlet opening) to exit into the incubating chamber).
F_r is the collector heat removal factor which relates the actual useful energy gained by the collector to the useful energy gained by the air.

$$F_r = \frac{\acute{m}_a . C_{pa} (T_c - T_a)}{A_c [\alpha . \tau . I_t - U_l (T_c - T_a)} \quad (11)$$

Where,
$\acute{m}_a$= mass flow rate of air
C_{pa}= Specific heat capacity of air
T_c= Collector temperature
T_a= Ambient temperature
A_c= Area of collector
α = Absorptance of solar collector
τ= Transmittance of solar collector
I_t= Solar irradiance
U_l= Overall heat loss coefficient

Heat Transmission via the Supplementary Heat Exchanger

Heat transfer from the supplementary storage is by convection only, estimated using equation (9), which for a single PVC trough opening becomes $Q_a = \acute{m}_a C_{pa} (T_{hac} - T_{ic})$.

Actual Heat Requirement of the Incubating Chamber

The total heat requirement of the incubator (Q_T) is the summation of the heat energy required to raise the temperature of air (Q_a) and egg (Q_e) from 30 ^{o}C to 38.5 ^{o}C; the heat loss through the wall of the structure (Q_s) and the heat loss by ventilation (Q_v) (Bukola, 2008).

$$Q_T = Q_a + Q_e + Q_s + Q_v \quad (12)$$

Heat Requirement of Air within the incubator

The heat absorbed by the air within the incubator to ascend from ambient temperature of 31.8 ^{o}C as measured, to the incubating temperature of 39 ^{o}C was estimated as follows;

$$Q_a = \acute{m} \, x C_a x \Delta T \quad - 13$$

Where,

Q_a= Heat requirement of air

m= mass flow rate (Kg/hr)

C_a== specific heat capacity of air KJ/Kg.^oC

ΔT= Average temperature difference, ^oC.

Heat Requirement of Eggs

$$Q_e = M_e * C_e * \Delta T \quad - 14$$

Q_a= Heat required to raise the egg temperature, KJ
m= mass of egg (Kg/hr)

C_a== specific heat capacity of egg KJ/Kg.^oC

ΔT= Average temperature difference, ^oC.

Heat Loss through the Walls of the Incubating Chamber

Fourier's law of heat conduction for steady state and one directional flow was adopted and mathematically expressed as,

$$Qs = KA\Delta T / x = \Delta T / R_T \quad - 15$$

$$R_T = 1/A\,(1/h_1 + x_1/k_1 + 1/h_0) \quad - 16$$

Q_s= Heat loss through the walls of the structure

k_1 = thermal conductivity of wood (W/m.K)
k_2 = thermal conductivity of foam (W/m.K)
h_i = convective heat transfer coefficient from inner fluid (heated air) to solids (the walls)

h_o = heat transfer coefficient from solid (the walls) to the outer fluid (outside air)

x_1 = thickness of wood (mm)

x_2= thickness of foam (mm)

Heat loss through ventilation openings

The rate at which heat is removed by ventilation air is given as;

$Q_v = M_a.C_{pa}.(T_o - T_1) = \rho \cdot V\, C_a.\, \Delta T$

M_a = amount of ventilating air in Kg/hr

Q_v = heat loss via the openings in KJ
C_{pa} = Specific heat capacity of air in KJ/Kg.K

ΔT= = difference in temperature between incubating chamber and the ambient

V= ventilation rate, m^3/s

ρ = density of air Kg/m^3

Efficiency of the system

The efficiency of the system was estimated using the following relationships;

Collector efficiency=

$$= \frac{\text{the energy transferred to the thermal mass}}{\text{total energy that falls on the collector}} \times 100\% \quad (17)$$

Incubator efficiency

$$= \frac{\text{the useful energy transferred to the incubating chamber}}{\text{total energy delivered into the storage chamber}} \times 100\% \quad (18)$$

Performance Evaluation of the system

$$\%\ \textit{Fertility} = \frac{\textit{Number of fertile eggs}}{\textit{Number of eggs loaded}} \times 100\% \quad (19)$$

$$\%\ \textit{Hactchability} = \frac{\textit{Number of eggs hatched}}{\textit{Number of fertile eggs}} \times 100\% \quad (20)$$

DESCRIPTION OF COMPONENTS OF THE EGG INCUBATOR

The solar egg incubator consists of six main components as shown in Figure 1. The photograph of the incubator developed is as shown in Figure 2.

The transparent plane glass cover) – A: The plane glass has been used as a solar collector for ages, owning to its unique properties. The plane glass has high solar transmittance of 0.84 to 0.91, long wave transmittance of 0.03; Neat appearance; Cleans easily; Abrasion resistance; High heat tolerance (up to 204^{o}C); Excellent weathering resistance and Low flammability (Lunde, 1980). Its job is to allow the passage of shortwave solar radiation into the heat storage chamber and prevent the escape of long wave energy being accumulated within the storage chamber.

The absorber/thermal mass (concrete slab) – B: The concrete is a mixture of cement, sand, gravel and water. The water stirs the reaction between the cement, sand and gravel, hence binding them together into what is known as concrete slab. The property of concrete that makes it ideal for heat storage include its high heat capacity of 1000 J/Kg ^{o}C, heavy density of 2000 Kg/m^3 and good thermal conductivity of 0.18 KJ/Kg.K. It absorbs heat and gets heated up at slow rate but also radiates heat to the ambient slowly; thereby retain heat for a longer time for use during cold hours.

The supplementary heating system granite stones – C: The granite stones serves as the supplementary storage with the useful properties such as; Heat Capacity of 790 J/Kg^{o}C, Thermal conductivity of 2.8 W/m.K and Density of 2403.4 kg/m^3.

The incubating chamber – D: The incubating chamber is made of ply woods, lined at the surface with insulation foam. These two materials helps to keep the heat energy delivered into the incubating chamber from escaping into the atmosphere. The desirable properties for this purpose are; Very low thermal conductivity of 0.045 W/m-K which increases the insulation provided by plywood.

Insulating casing (ply wood) – E: The ply wood is the overall casing of the incubator, covering all the chambers. It forms the wall of the incubating and the heat storage chambers, with desirable properties being very low thermal conductivity of 0.13 W/m-K.

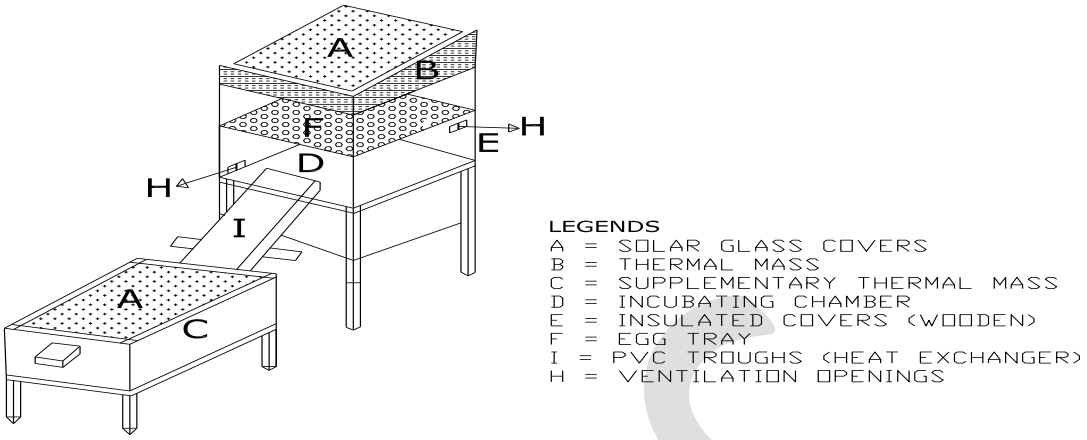

Fig. 1: The Poultry Egg Incubator

The egg tray (ply wood) F: The egg tray was made from plywood, perforated to allow an average egg to hang through without falling through the perforation.

Ventilation: The air circulation through the incubator was by natural ventilation. The ambient (fresh) air enters through the inlet openings (located down the windward side of the incubator) into the system where it is heated up by the accumulated solar energy. This brings a temperature difference between the air at the lower and upper ends of the collector. The difference in temperature results in pressure difference and density variation, hence resulting in buoyancy force which in turn causes the heated air to flow through the incubating chamber and pass through the outlet openings located above the egg tray on the leeward side of the incubator. Small inlet openings were provided to induce natural ventilation or air exchange into the incubator. Normal air exchange is needed during embryo development and usually increases as the chicks begin to hatch. The embryo takes in oxygen and produces carbon dioxide as by-product. Ventilation is needed to remove unpleasant smells and excessive moisture, and to prevent stagnation of the interior air.

Orientation of the solar collector: The collector is always tilted and oriented in such a way that it receives maximum solar radiation during the period of use. The solar collector in this work was oriented facing south and tilted at 45^{o} to the horizontal. This inclination allows average solar collection all day and also allows easy run off of water. It also enhances heat movement into the incubating chamber.

Candler: A wooden Candler was constructed which was an integral part of the incubator for testing the fertility of eggs. Candling process was done on the 7^{th}, 14^{th} and 18^{th} day of incubation

Fig. 2: Picture of the developed Solar Incubator

PERFORMANCE EVALUATION

The solar incubator was constructed and assembled as shown in Figure 1. The measuring instruments used such as temperature sensors and hygrometer were positioned such that the inner condition of the system and ambient conditions of temperature and relative humidity were taken simultaneously. The solar system was monitored for one week (7 days) by taking measurements of the temperature and relative humidity in the system within the period. The readings were taken for 24 hours each day and at a regular interval of 3 hours; (i.e. at 0:00, 3:00, 6:00, 9:00, 12:00, 15:00, 18:00, and 21:00) GMT.

The activated charcoal (dehumidifier) and evaporative cooling pan were provided in the heat collector chambers and incubating chambers, respectively, to control relative humidity throughout this study. This is to prevent condensation within the collector chambers, so as to deliver clean and dry heated air into the incubating chamber. After the seven days monitoring of the system to establish the environmental parameters that can be maintained, the incubator was loaded with fertile eggs obtained from a reliable hatchery. Candling process was used to check the fertility of eggs on the 7^{th} and 14^{th} day of incubation.

Table 2 shows the average temperatures and relative humidity pooled together for the 7 days monitoring of both ambient and incubating system at different time of the day (i.e. 0:00, 3:00, 6:00, 9:00, 12:00, 15:00, 18:00, and 21:00) GMT. Table 3 shows the average temperature of the 7 days data collection within the incubating chamber at specific distances away from the thermal mass.

The results of Table 2 show that the average ambient temperature was lower in the morning and increased to the highest value of 36.6^{o}C at 3: PM (15:00) and start decreasing to attain the lowest value, 28.3℃ at 3: AM (3:00). The ambient relative humidity was observed to be highest at 6: AM (6:00) and was decreasing to attain the lowest value at 6: PM (18:00) and then increased slightly towards night time. The temperature of the thermal mass was lowest at 6: AM (6:00) and increased to the highest value of 91.5^{o}C at 3: PM (15:00), with the decreasing trend towards midnight and morning hours. The relative humidity range of 56.1% to 64.2% was maintained in the incubating room from 6: 00 to 6:00 the next day throughout the monitoring period. This result values fall within the required range provided in literatures [17] Adewumi and Oduniyi, (1999); [18] Hamre, (2011), [19] Bukola, (2008).

The results of Table 2 show that the temperature of the incubating room varied significantly at different time of the day. The mean temperature, 42.4℃ recorded at 12noon was significantly higher (P≥0.05) than the temperature values obtained at any other time of the day.

Table 2: Effect of time period on the Temperature and Relative humidity of the incubating chamber

Environmental Parameters	Time of the day, h								
	0	3	6	9	12	15	18	21	$FLSD_{0.05}$
T_{inc}, ℃	33.6^{b}	37.1^{c}	41.0^{a}	42.0^{d}	42.4^{e}	41.1^{a}	38.0^{f}	36.2^{g}	0.7717
RH_{inc}, %	56.1^{d}	59.7^{ac}	64.2^{a}	64^{a}	62.7^{ab}	62.6^{ab}	62.5^{ab}	61.3^{bc}	2.5396

Means of the different superscript letters indicate significant difference (P≥0.05)
T_{inc} = incubating room temperature, RH_{inc} = incubating room Relative humidity

Table 3 shows the average temperatures of the incubating chamber at various distances from the thermal mass. The Table indicates that minimum temperature of 30.5℃ was obtained at 6: AM (6:00) and at a distance of 100 cm away from the thermal mass. The highest value of 46.6℃ was attained at 3: PM (15:00) and at a distance of 20 cm away from the thermal mass. Table 3 also indicates increasing trend pattern in temperature values from 6: AM (6:00) in the morning to highest values between 12 noon to 6: PM (12:00 to 18:00) in the evening. This may be as a result of heat dissipation from the thermal mass and this finding agrees with the finding by [20] Nwakonobi *et al* (2013).

The graphical presentations shown in Figure 3 indicate the trend pattern of the average temperature variation with time of day for both ambient and thermal mass (absorber) outer and inner surfaces while Figure 4 shows the variation of the incubating room temperature at specific distances of the egg tray from the thermal mass. Figure 5 shows the relative humidity variation with time of day for ambient and incubating chamber. Table 2 The comparisons of the environmental parameters of incubating room carried out for different time of the day indicate that the mean temperature of the incubating room was significantly higher ($P \leq 0.05$) with value of 42.4℃ at 6: PM (18:00) and is statistically different from the mean temperature values of the other times of the day. The lowest temperature value is at 6: AM (6:00) with the value of 33.61℃ and is statistically different ($P \leq 0.05$) from the other times of the day. The mean temperature obtained at 12 noon and 9: PM (18:00) was statistically indifferent.

Figure 3 shows that the heat absorbing surface (outer) of the thermal mass was consistently at higher temperature level than inner side thereby inducing gradient for heat flow towards the incubating chamber.

The temperature value, 38.0℃ at 12 midnight was higher than that recorded at 3 AM (3:00), 6 AM (6:00) and 9 AM (9:00) and differences are statistically significant ($P \geq 0.05$).

It was observed from Table 2 that between the hours of 12 midnights to 9:00, incubation temperature range of 36.2℃ - 38.0℃ was obtained which was within the acceptable range of 37℃ - 39℃ (Oluyemi and Roberts, 1979).

The relative humidity (RH) of the incubating room which is another important parameter to assess the suitability of the system for poultry egg incubation was also affected significantly by the diurnal variation at different time of the day. The relative humidity value, 64.2 % attained at 12 noon though differ significantly with that obtained at 3:00, 6:00 and 9:00 but the differences with rest of the time of the day were statistically the same ($P \geq 0.05$). The lowest value, 56.1 % of RH was recorded at 6:00 in the morning which differs significantly with the rest of others. The RH, 61.3% recorded at 3:00 differs significantly and was higher than that obtained at 6:00 and 9:00.

Table 3: Incubating chamber average temperature (^{o}C) at various distances from thermal mass

	Temperature (^{o} C)		
Time of the day	20 cm	60 cm	100 cm
6 am	36.9	33.4	30.5
9 am	37.7	37.1	36.6
12 noon	42.9	41.5	38.9

3 pm	46.6	40.8	38.5
6 pm	46.1	42.7	38.5
9 pm	43.8	40.6	38.9
12 midnight	39.2	38.3	36.6
3 am	38.5	35.9	34.3

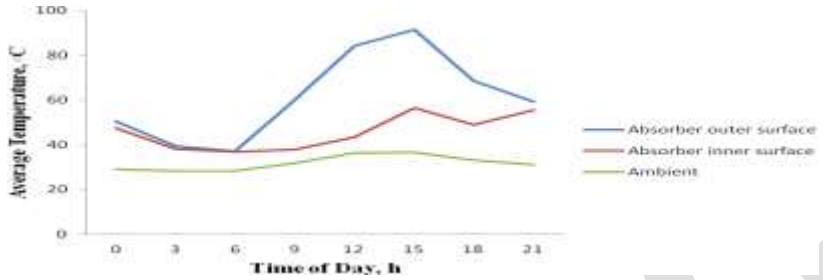

Fig. 3: Temperature variation of concrete solar absorber surfaces with time of day

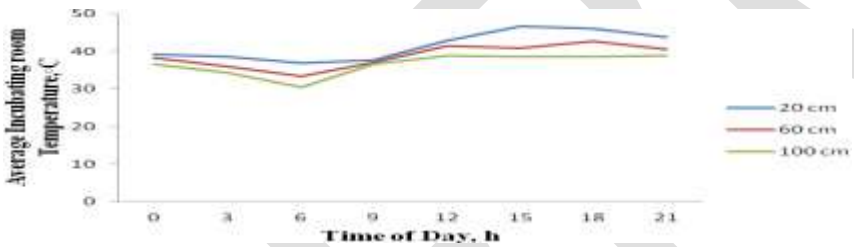

Fig. 4: Average incubating room temperature versus time of day at distances from thermal mass

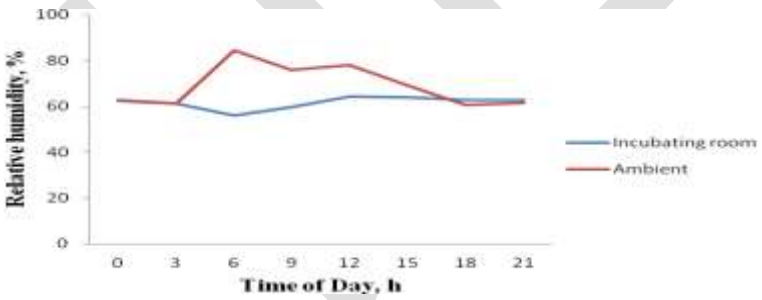

Fig. 5: Relative humidity variation with time of day

It was observed from Figure 4 that between the hours of 12 midnights to 9:00, incubation temperature range of 36.9℃ - 39.2℃ was obtained within 20 cm distance from the thermal mass which was within the acceptable range of 37℃ - 39℃ (Oluyemi and Roberts, 1979). Also, between the hours of 12 noon to 21:00 GMT, incubation temperature range of 38.5℃ - 38.9℃ was maintained at a distance of 100 cm away from the thermal mass. Similarly, from 9: 21:00 to 12 midnight and at 9: 00, the temperature was ideal at around 60 cm away from the thermal mass.

Figure 5 indicate that the relative humidity of the incubating room were consistently lower than that of ambient values except in the midnight hours. This may be due to condensation occurring leading to drop in the ambient relative humidity.

Biological performance

Out of 125 eggs that were stocked into the incubating chamber, 74.4 percentage fertility and 73.1percentage hatchability were recorded at 21 days incubation period. Figure 6 shows the newly hatched chicks. The fertility loss incurred may be as a result of possible damage to some eggs during transportation from hatchery to experimental site.

Fig. 6**:** Young Hatched Chicks few hours after hatching

CONCLUSION

The design of solar powered poultry egg incubator using local materials was found to be capable to effectively incubate poultry eggs. The results of the internal environment of the incubator established were close to that required by natural egg incubation. The utilization of the system in the poultry industry will solve the problem of power availability. However, a lot still remain to be done to improve the efficiency particularly the system insulation.

REFERENCES:

1. Lunde, P. J. Solar thermal space heating and hot water system. USA: John Willey and Sons, Inc. 1980.
2. Emerson, E. J., Hale, W.M., & Selvam, R. P. Development of a high-performance concrete to store thermal energy for concentrating solar power plants. Proceedings of the ASME 2011 5th International Conference on Energy Sustainability, ES2011. August 7-10, 2011, Washington, DC, USA. 2011.
3. Duffie, J.A., & Beckman, W.A. Solar engineering of thermal processing. New York: John Willey. 1980.
4. Nayak, J. K., Bansal, N. K., & Sodha, M. S. Analysis of passive heating concepts, solar energy. New Jersey Institute of Technology, Chemical Engineering Department. NJIT. 1983.

5. Okonkwo, W.I., Anazodo, G.U.N., Akubuo, O.C., Echiegu, E. A., & Iloeje, O.C. The UNN passive solar heated poultry chick brooder - further improvement and preliminary testing, Nigeria Journal of Solar Energy. 1992.
6. Okonkwo, W.I. Solar energy brooding system, in rural renewable energy needs and five supply technologies. Publication of Energy Commission of Nigeria. 1998.
7. Fagbenle, R. L. Estimation of total solar radiation in Nigeria using meteorological data. Nigerian Journal of Renewable Energy, l, l - l0. 1990.
8. Pelemo, D. A., Fasasi, M. K., Owolabi, S. A., & Shaniyi, Z. A. Effective Utilization of Solar Energy for Cooking. Nigeria Journal of Engineering Management, 3, 13-18. 2002.
9. Yohanna, J.K., Itodo, I.N., & Umogbai, V.I. A model for determining the global solar radiation for Makurdi, Nigeria. Renewable energy, 36, 1989-1992.
10. Itodo, N. I. Solar energy technology. (1st ed.). Makurdi, Benue State, Nigeria: Aboki Publishers. 2007.
11. Adeyemo, S. B. Estimation of the average daily radiation on horizontal surface. NSE Transactions, 33, 53 - 65. 1988.
12. Owokoya, S. I. Design and construction of solar air heater. Unpublished B. Eng. Project, Federal University of Technology, Minna, Nigeria. 1992.
13. Adaramola, M. S., Amaduoboga, & Allen, K. O. Design, construction and testing of box-type solar oven. Nigerian Journal of Engineering Management, 5, 38 - 46. 2001.
14. Odia, O. O. Solar energy application to steam jet refrigeration. Nigerian Journal of Industrial and Systems Studies, 5, 10-15. 2006.
15. Bansal, N.K. and Gour, B.C. Application of U and G values for sizing Passive Heating Concepts. *Elsevier Solar Energy* Solar Energy 57(5):361–373, 1996.
16. Zriken, Z. And Bilgen, F. "Theoretical Study of a Composite Trombe'. *Michael Wall Solar Collector System*. Canada. 39(5): 409 – 419. 1987.
17. Adewumi, B. A., & Oduniyi, A. I. Design, fabrication and testing of charcoal fuelled incubator. Journal of Applied Sciences, 2, 159-175. 1999.
18. Hamre, M. L. Hatching and brooding small numbers chicks. In Extension folder, a guide for the general operation of a small, still-air incubator. Regents of the University of Minnesota. 2011.
19. Bukola O. B. Design and performance evaluation of a solar poultry egg incubator. Thammasat International Journal of Science and Technology, 13, 47-54. 2008.
20. Nwakonobi, T.U., Obetta, S. E., & Gabi, M. N. Evaluation of a modified passive solar housing system for poultry brooding. Journal of Science and Technology. Kwame Nkrumah University of Science and Technology (KNUST), 33, 50-58. 2013

International Journal of Engineering Research and General Science Volume 3, Issue 6, November-December, 2015
ISSN 2091-2730

Stress Level & Risk of Failure Improvement Study in Subframe for Commercial Vehicle

Purnendu K Dash,

Alard College of Engineering & Management, Pune India, dash.purnendu@gmail.com, Tel: +91-8446106606

Dr.Rachayya R.Arakerimath ME,PhD[Mech],

Dean (Academics) GH Raisoni Institute of Engineering & Technology. Pune, India, rrarakerimath@gmail.com Tel: +91-8805026109

Abstract— A subframe is a structural component of vehicle, that uses a discrete, separate structure within a larger body-on-frame or unit body to carry certain components, such as engine, drive train and / or suspension. The subframe is bolted and or welded to form a single assembly, which is bolted to the vehicle frame or cabin structure. The principal purposes of using a subframe are, to spread high chassis loads over a wide area of relatively thin sheet metal of body shell, and to isolate vibration and harshness from the rest of the body. Weight optimized design of subframe has many distinguished advantages. Since, it carries load of engine, suspension and steering components of the vehicle, it has to be designed for least weight, but without compromising the strength. It requires thorough study of current design, areas of failure and key design considerations. Care should be taken while design to understand properties of material and its suitability for various production methods. A technical study needs to be done to derive most cost-efficient concept. The motive behind the project is to optimize subframe for commercial vehicle application. Optimization has to be done in terms of material selection, no of parts selection, manufacturing process of individual parts as well as assembly so as to reduce the overall weight to a minimum value by extensive use of finite element method.

Keywords—finite element analysis, optimization, subframe, structural durability analysis, risk of failure, automotive, CAE

INTRODUCTION

Recent research and development capability of automobile area is concentrated on developing high-performance, light-weight and high-efficiency vehicle. Especially related to structural design of the vehicle, researches to reduce weight of components and developing cost have been actively performed. Structural design of the vehicle should be done with simultaneously considering many types of performance requirements, e.g. structural safety against the crash, fatigue life of the components, noise, vibration and harshness (NVH) performances, and kinematic and compliance (K&C) characteristics influencing to the ride and handling (R&H) performances . Design requirements were selected for structural stiffness and fatigue strength, NVH performance, K&C performances, and weight. To obtain the design solution satisfying the aforementioned design requirements, the shape and thicknesses of the subframe component were considered as design variables [8]. The necessities for light weight design as well as reducing fuel consumption are greatly increasing as environment friendly and high efficiency vehicle technology is required in these days [4]. For example, in an automobile with its power train contained in a subframe, forces generated by the engine and transmission can be damped enough that they will not disturb passengers. Subframes are used in modern vehicles to reduce the overall weight and cost. In addition a subframe yields benefits to production in that, subassemblies can be made which can be introduced to the main body shell when required on an automated line. Therefore, the designing of the subframe has the important influence to the main frame's quality and service life [2].

There are generally three basic forms of the subframe.

- A simple "axle" type which usually carries the lower control arms and steering rack.
- A perimeter frame which carries the above components but in addition supports the engine.
- A perimeter frame which carries the above components but in addition supports the engine, transmission and possibly full suspension. (As used on front wheel drive cars)

A subframe is usually made of pressed steel panels that are much thicker than body shell panels, which are welded or spot welded together. The use of hydro formed tubes may also be used.

METHODOLOGY FOR EXECUTION

Following are the steps followed.

1. Problem definition

2. Constraints
3. Expected outcome
4. Design calculation and formulation
5. 3D modeling of parts, subassemblies and assemblies
6. Design for manufacturing, assembly, service & DFMEA
7. Finite element analysis
8. Iterations for part profile, material and assembly to get stress below yield limit.
9. Conclusion
10. References

1. Problem Definition

Need to optimize a subframe for minimum overall weight, with less number of components, with less welding, without compromising its strength. It requires thorough study of current design, areas of failure and key design considerations. Care should be taken while design to understand properties of material and its suitability for various production methods. A technical study is done to derive most cost-efficient concept. The procedure consists of study of subframe system and its standard design procedure, preparation of CAD data for existing product, analysis of the current subframe and comparison of the results with field data, co-relating the both parameters and taking reference for future design. The CAE analysis using Hypermesh and Nastran to see the probable areas of failure and room for further weight reduction at safest areas.

The final design will be evaluated in terms of stiffness, strength, stress and deflection of the new subframe compared to existing design. In the field of Automotive there is a continuous requirement for low weight, higher fuel efficiency and commonisation of maximum parts to reduce product design life cycle. This project contains development of a common subframe for independent front suspension system for a commercial vehicle and it's variant

2. Constraints

- Subframe should carry 15% more load as compare to base subframe.
- No changes in suspension, steering and engine mounting hard points
- Minimum changes to existing tooled up parts.
- Minimum clearances of 10mm with surrounding static parts and 25mm with surrounding dynamic parts.
- Maximum use of existing assembly tooling and assembly fixtures.
- Cost should be comparable with existing subframe.
- Assembly subframe weight increase allowable up to 10% as compare to existing subframe
- Common subframe for all variants vehicles.

3. Expected Outcome

- Maximum strength (stress value less than material yield stress)
- Minimum deflection (torsional and bending stiffness)
- Minimum weight (initial weight target is ~ 25kg)
- Life prediction (durability analysis for initial target of 1.6 lakh kms of vehicle)

4. Design Calculation and Formulation

i) Mathematical Modeling:

A mathematical model is a description of a system using mathematical concepts and language. The process of developing a mathematical model is termed mathematical modeling. A mathematical model is an abstract model that used mathematical language to describe the behavior of system. Mathematical models can take many forms, including but not limited to dynamical systems, statistical models, differential equations or game theoretic models. These and other types of models can overlap, with a given model involving a variety of abstract structures.

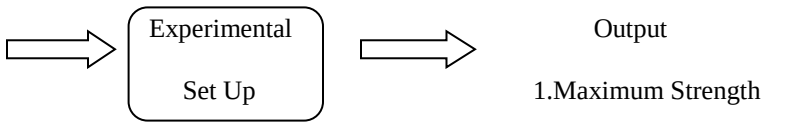

Fig 1 Mathematical modeling

ii) Parameter Selection:

S No	Parameter	Level 1	Level 2
1	Geometry of part (s)	G1	G2
2	Material	M1	M2
3	No. of Parts	N1	N2
4	Joinery of parts	J1	J2

Table 1 Parameter Selection

iii) 3D modeling of parts, sub assemblies and assemblies

CAD software Pro/E is used for 3D modeling of parts, subassemblies and assemblies.

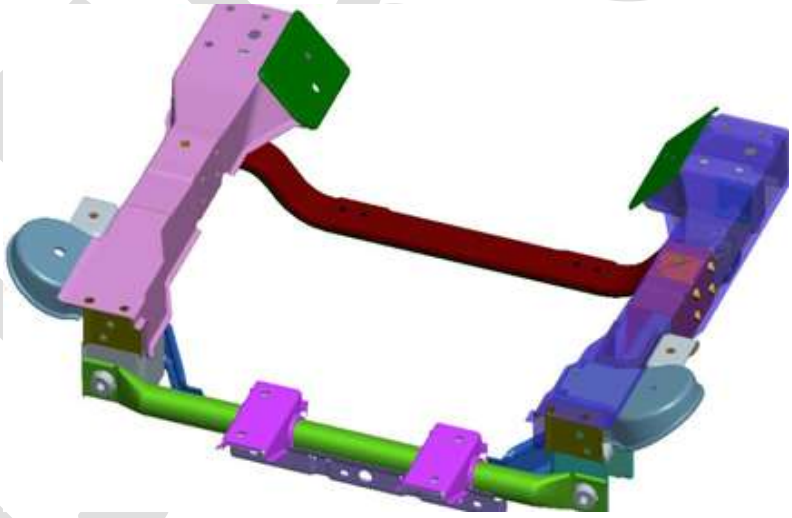

Fig 2 Base Subframe (Iteration 1)

Subframe for small commercial vehicle consist of mainly four sub assemblies.

- Front cross member assembly,
- Rear cross member assembly,
- Side member assembly LH,
- Side member assembly RH

In total there are approximately more than 80 parts in subframe assembly. Subframe side member is the main source of load carrier. It supports engine at rear end, support other reinforcement bracket, supports suspension load through wishbone bushes. Front cross member supports the steering load while rear cross member makes the assembly subframe intact. Coil spring mounting bracket along with vertical tower bracket supports suspension load. Rear cross member supporting bracket supports load of rear bushes.

iv) Design for Manufacturing

Simulation tool (hyper form) is used to know thickening and thinning of sheet metal components in forming operation by use of blank, die and punch. More than 20% thinning is shown as critical area, which needs modification. The fillet radius as well as profile updation required to make the part manufacturable.

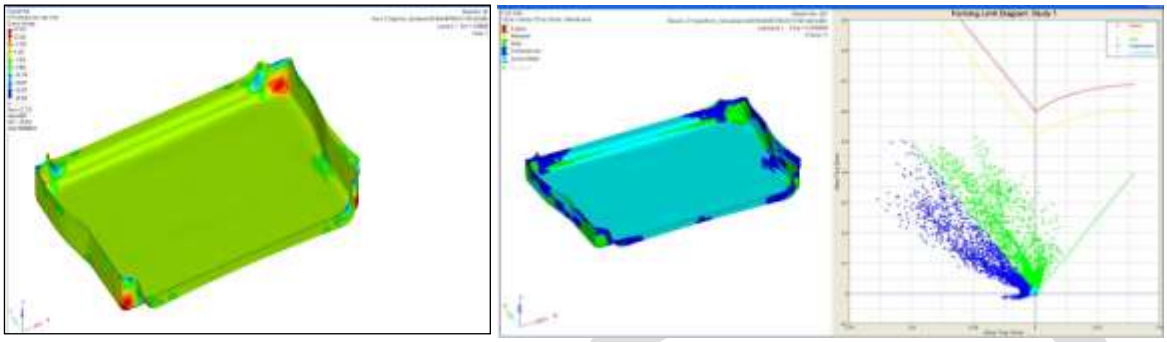

Fig 3. Bracket manufacturing feasibility through Hyper Form

Bend radius, notches, corner relief, part depth also verified with respective part supplier for manufacturing feasibility in addition to analysis tool.

v) Design for Assembly

- No interference within subframe parts ensured in Creo (PRO/E) by using global interference option and part geometry updated if found any.
- Required clearances within surrounding parts ensured in Creo (PRO/E). Part geometry updated if found any.
-

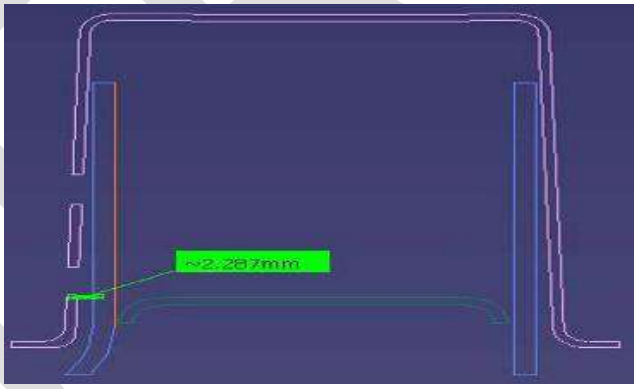

Fig 4 Assembly clearance & interferences checking

vi) Service Load Analysis

Based on Road Load Data using wheel force transducer the force at each wheel received and the same load is applied in ADAMS analysis to find out the force and moment at each critical location.

viii) Finite Element Analysis

- Hypermesh software is used for meshing.
- Type of mesh used is shell and solid
- For bolt joint beam elements joined with rigid element
- Welded joint present by shell elements with thickness equal to least thickness of parent component and twice the thickness for plug welds

- Closures, power train are represented with mass element
- Total number of elements calculated to be ~ 3 Lakhs

ix) Critical Assumptions during CAE analysis

- Load transfer through surface contacts is ignored.
- All welds are assumed adequate (i.e. they will not fail).
- Assembly loads (bolt preload) are not considered.

x) Material Properties for different Sheet Metal Parts

Material	Yield Strength (MPa)	Acceptable limits for ultimate load case> 1.3 YS (MPa)	Acceptable limits for durability load case> 0.9 YS (MPa)
Fe 410, SM 400A JIS - G - 3106	255	300	230
E34, DIN QSTE 340 TM	340	440	300
BSK46, DIN QSTE 460 TM	460	590	410
CEW1, IS 3074	370	480	330
40Cr4, IS 5517	700	910	630

Table 2 Material used for different parts

2. Discussion of Analysis for New Subframe Iteration 1

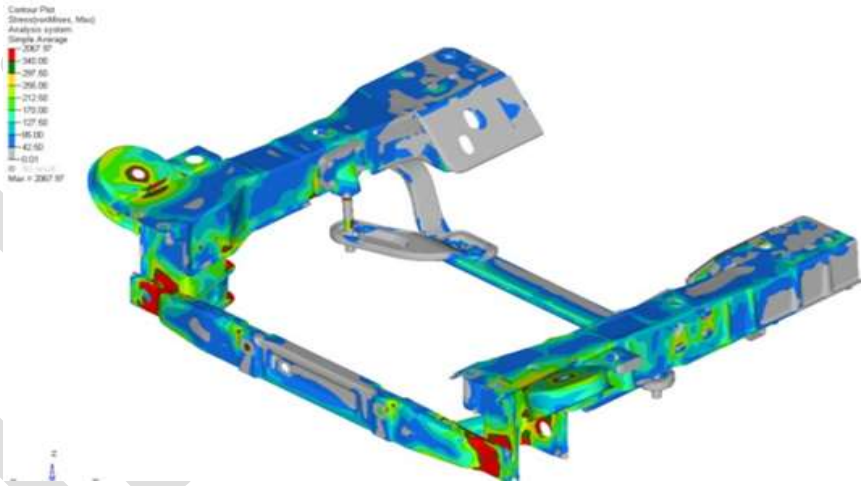

Fig. 5 Stress plot for complete sub frame (Iteration 1)

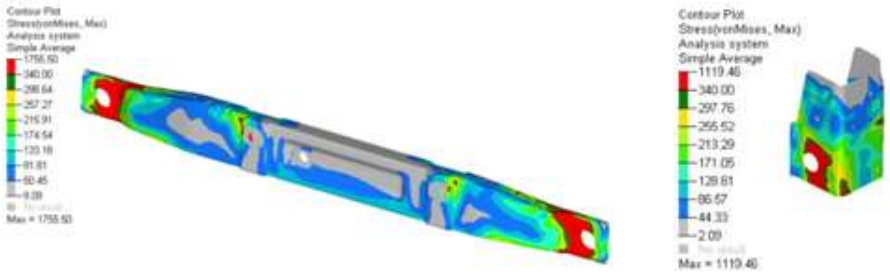

Fig 6 Stress plot for front cross member & vertical bracket (Iteration 1)

Fig 7 Stress plot for side member & Z bracket (Iteration 1)

Analysis done at 33% overload on gross vehicle weight. From all load cases front both pot hole shows the maximum stress at front cross member end mounting area. Because of this load case in addition to front cross member the vertical tower bracket at same location also shows more stress.

Sl No	Description	Max Stress (N/mm^2)	ROF Iteration 1	Remarks
1	Front cross member	1755	> 5.0	Stress is more at bush mounting area
2	Vertical tower bracket	1119	> 3.2	Stress is more at bush mounting area
3	Side member	654	> 1.9	Stress is more at spring mounting area
4	Z bracket	907	> 2.7	Stress is more at bush mounting area

Table 3 Stress & ROF values for Iteration 1

3. Physical Verification of CAE result

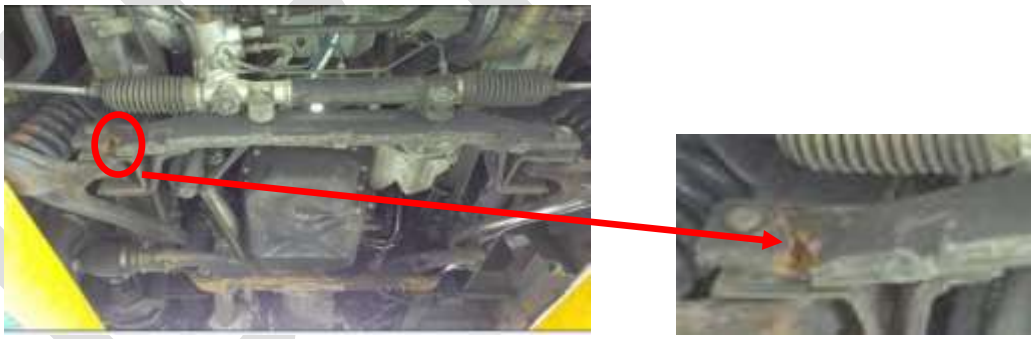

Fig. 8 Actual Failure of Front cross member (Iteration 1)

As shown in the durability testing the front cross member failed at the location where stress is showing high. This correlated CAE result, assumptions and boundary conditions. Hence the focus should be on strengthening of front cross member. Strength increase of front cross member to be achieved by

i) Modifying the material to higher grade
ii) Modifying the profile of parts
iii) Modifying the load path by changing vertical bracket & Z bracket.
iv) Modifying welding position

4. Final Optimization

To get the required life for durability following changes are done in comparison with existing subframe (Iteration 1)

Iteration 1 Final

Fig 9 Front cross member profile updation

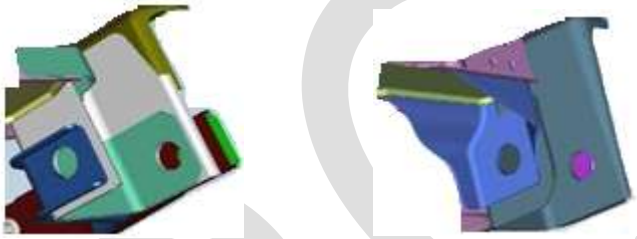

Iteration 1 Final

Fig 10 Vertical mounting bracket profile updation

5. CAE Result & Analysis of Final Subframe

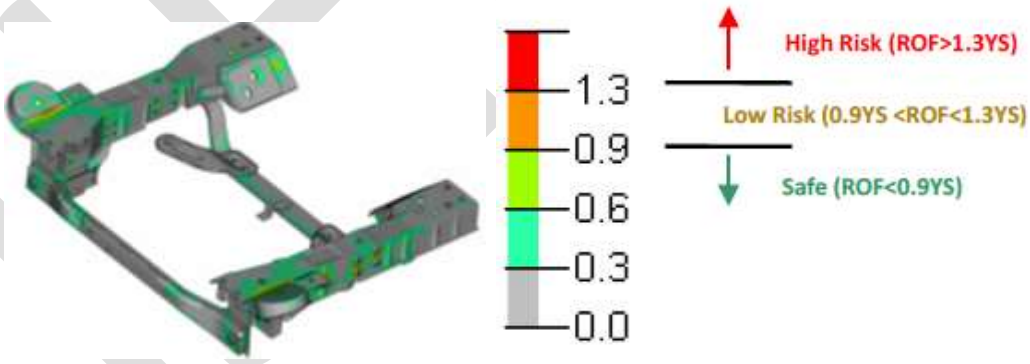

Fig 11 Stress plot for complete sub frame (final)

Risk of Failure (ROF):-
ROF is being used to describe the safe and risk zones for ultimate load cases
ROF = Predicted stress / Yield strength of respective material

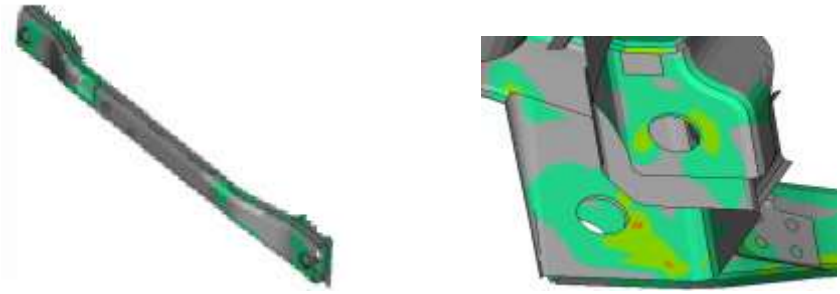

Fig 12 Stress plot for front cross member & Vertical Bracket (final)

Sl No	Description	Max Stress (N/mm^2)	ROF Final	Remarks
1	Front cross member	322	< 0.8	Stress within elastic limit
2	Vertical tower bracket	390	< 0.85	Stress within elastic limit & higher value at local zone
3	Side member	289	< 0.85	Stress within elastic limit & higher value at local zone
4	Z bracket	320	< 0.75	Stress within elastic limit & safe

Table 4 Stress & ROF values for final Iteration

5. Durability Testing

The physical subframe is tested to correlate the CAE with actual. The subframe is assembled in vehicle & durability testing conducted based on Road Load Data (RLD) collection.

Fig 13 Actual part after testing

6. Conclusion

From the above physical testing the subframe cleared the required testing cycles which is equivalent to approximately 2lakh kms on vehicle and no failure observed. The end portion of cross member stress is now within safe limit. The complete optimization is done keeping in mind all the constraints provided at initial. Not only the profile and material helps us to reduce stress it is welding positions which also plays a crucial role. During this development the assembly sequence is also finalize to get the required critical mounting hard points. Further to this hydro form subframe options to be evaluated to reduce number of parts which will simultaneously reduce the total weight of the subframe and ease of manufacturing?

REFERENCES:

[1] A Kocanda, H Sadlowska, Automotive component development by means of hydro forming, Warsaw University of Technology, Warszawa, Poland, 2008

[2] Chen Yanhong, Zhu Feng, The Finite Element Analysis and The Optimization Design of the Yj3128-type Dump Truck's Sub-Frames Based on ANSYS, Procedia Earth and Planetary Science 2, 2011

[3] Chung-Kyu Park, Robert Thomson, Aleksandra Krusper, Cing-Dao (Steve) Kan, The Influence of subframe Geometry on a Vehicle's Frontal Crash response, National Crash Analysis Center, George Washington University, Washington, DC, USA, VTI-Swedish National Road and Transport Research Institute, Gothenburg, Sweden, SAFER-Vehicle and Traffic Centre, Chalmers University of Technology, Gothenburg, Sweden, 2009.

[4] Dae Up Kim, Young Choi, Bong Yong Kang, Joon Hong Park, Hong Tae Yeo, Jae Hun Kim and SangWoo Park, A Study on Process Design of Automobile Parts Using Extruded Material by Die Forming, Hindawi Publishing Corporation. Advances in Mechanical Engineering, Volume, 2014.

[5] Elsayed Mashaly, Mohamed El-Heweity, Hamdy Abou-Elfath, Mohamed, Finite element analysis of beam-to-column joints in steel frames under cyclic loading, Osman Alexandria Engineering Journal, 2011

[6] Ibrahim Elkersh, Experimental investigation of bolted cold formed steel frame apex connections under pure moment, Ain Shams Engineering Journal, Suez Canal University, Egypt, 2010

[7] Izzuddin bin Zaman Bujang, Roslan Abd. Rahman, Application of dynamic correlation technique and model updating on truck chassis, Faculty of Mechanical Engineering, College University Technology Tun Hussein Onn (Kuittho) and Faculty of Mechanical Engineering, University Technology of Malaysia, 2009

[8] Jung-Min Park1, Gabseong Lee, Byung-Lyul Choi, Dong-Hoon Choi, Chan-Hyuk Nam, Gi-Hoon Kim, Multidisciplinary Design Optimization of Subframe Component of Vehicle Front Suspension, 9th World Congress on Structural and Multidisciplinary Optimization, Shizuoka, Japan, June 2011.

[9] Jong Yop Kima, Naksoo Kima, Man-Sung Huhb, Optimum blank design of an automobile sub-frame, Department of Mechanical Engineering, Sogang University, Shinsu-dong, Mapo-ku, Seoul, South Korea, July 1998

[10] A. Hamdi, B. Yannou and E. Landel, Design target cascading for vibroacoustic conceptual design of an automobile subframe, International design conference, Dubrovnik, May 2004.

[11] L. Gaines, R. Cuenca, F. Stodolsky, Potential Automotive uses of wrought magnesium Alloys, Automotive Technology Development, Detroit, Michigan, November 1996

[12] Rick Borns, Don Whitacre, Optimizing Design of aluminum suspension components using an integrated approach, SAE Paper 05M-2, June 2008

International Journal of Engineering Research and General Science Volume 3, Issue 6, November-December, 2015
ISSN 2091-2730

Determination and Comparative Analysis of PID Controller Parameters for DC Motor Using Cohen and Coon, Ziegler-Nichols and Particle Swarm Optimization Methods

Anuradha Guha, Sagarika Pal

National Institute of Technical Teachers Training and Research Kolkata, India, anu007radha52@gmail.com and 9432108894

Abstract— the problem of identification of controller parameters for DC motor has been considered here. Open loop system has been used for Cohen and Coon Method. The proportional, integral and derivative gains are obtained from the process reaction curve. The loop is then closed. Damped Oscillation of Ziegler-Nichols Method is used. This curve, gives the integral and derivative gain from the period of oscillation. The ISE, IAE and IATE are used as fitness function in Particle Swarm Optimization. Then proportional, integral and derivative gains are found out through number of iterations. At last the outputs of three methods are compared.

Keywords— DC motor, PID controller, Cohen and Coon Method, Ziegler Nichols Method and Particle Swarm Optimization, the Integral of Square Error (ISE), Integral of Absolute Error (IAE), and Integral of Time and Absolute Error (ITAE).

INTRODUCTION

In this paper DC Motor of 12 volts has been used. Unit step supply has been given here. The output is the speed of the DC Motor which has been analyzed. To get best results for the DC Motor, PID controller is used. The parameters of the PID controller are set to obtain better results. Hence this paper aims at tuning the PID controller parameters for ideal output results of a DC Motor. Here a comparison of the methods on basis of Performance Evaluation of Swarm Intelligence on Model-based PID Tuning [14] has also been done.

Here tuning of PID controller parameters is based on Cohen Coon Method, Ziegler Nichols Method [6] and Particle Swarm Optimization method [11], [13] for Speed Control of DC Motor. According to previous research tuning of PID controller parameters based on Particle Swarm Optimization are used for governor system of Synchronous Generator [3], for Linear Brushless DC Motor [7], for the Design of Brushless Permanent Magnet Machines [9], for PMDC Motor Drives Controllers [10] and for DC Motor Drives [2]. Again researches show that PID controllers for DC motor have not only been tuned by simple Particle Swarm Optimization but also through Multi- Objective Particle Swarm Optimization [1] and Performance-Dependent Particle Swarm Optimization [12]. Moreover PI Controller [4], Generalized PID Controller [5] and Dual-line PID Controller [8] are used on PSO for Speed Control of DC Motors.

The Cohen and Coon Method and Ziegler-Nichols Method have been used to determine the PID controller parameters. The Particle Swarm Optimization Method is used to optimize the PID controller parameters. Then a comparative study has been done. All these methods are tried and applied in Matlab only.

DC MOTOR BLOCK DIAGRAM AND PARAMETERS

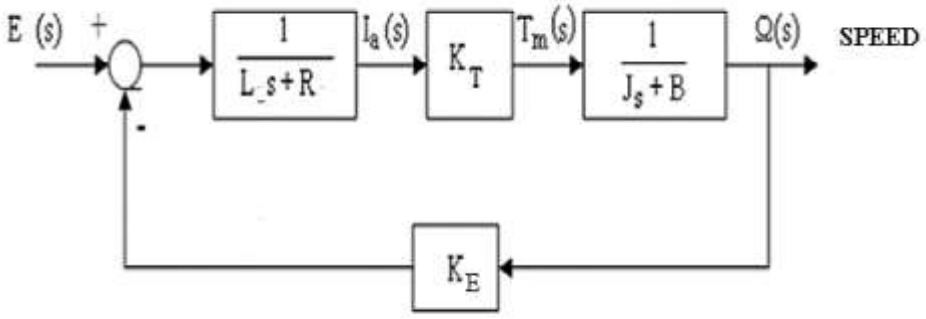

Figure1: Block Diagram of DC Motor

Here the parameter that are used for the DC Motor are

Motor of inertia of the rotor J = 0.01 kg. m^2

Motor viscous friction constant B = 0.1 N.m.s

Electromotive force constant K_e = 0.01V/rad/sec

Motor torque constant K_t = 0.01 N.m/amp

Electric resistance R = 1 ohm

Electric inductance L = 0.5 H

The Motor transfer function used for this paper is

$$\text{Transfer Function} = \frac{K}{((J*s+B)*(L*s+R) + K^2)} \quad (1)$$

After putting the Motor parameters in the transfer function, the transfer function that is obtained:

$$\text{Transfer function} = \frac{0.01}{0.05^2 + 0.06\,s + 0.1001} \quad (2)$$

PROPORTIONAL INTEGRAL AND DERIVATIVE CONTROLLER

In this paper PID controller has been used. Maintaining the advantages and disadvantages of the PID controller it has been used in the Cohen and Coon, Ziegler-Nichols and Particle Swarm Optimization techniques.

Transfer function of PID controller is

$$u(t) = K_P e(t) + K_P K_I \int e(t)dt + K_P K_D \frac{d}{dt} e(t) \quad (3)$$

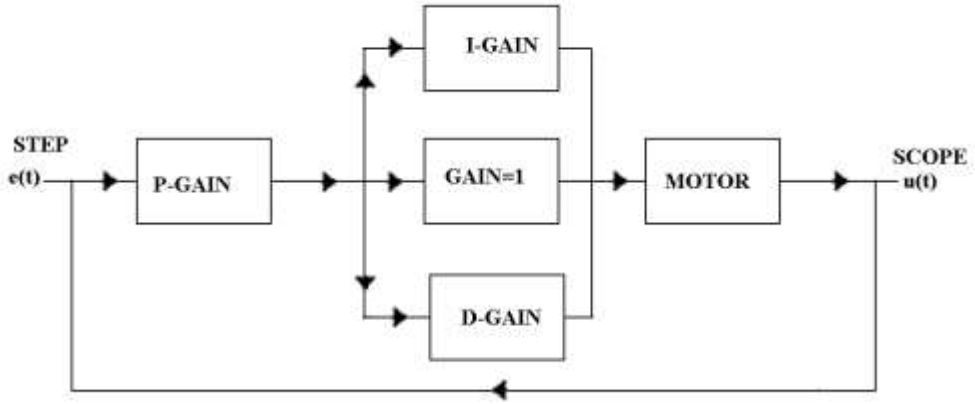

Figure2: Block Diagram of PID Controller with DC Motor

COHEN AND COON METHOD

The three parameters: static gain 'K', dead time't $_d$' and time constant ' τ 'describes the system. These parameters are obtained from the process reaction curve. It is easy to estimate the values of the three parameters.

Cohen and Coon approximation for the 'best' controller settings using load changes, and various performance criteria, such as one-quarter decay ratio, minimum offset and minimum ISE is as follows:

$$G_{PRC}(s) = \frac{\overline{y_m}(s)}{c(s)} \cong \frac{Ke^{-t_d s}}{\tau s + 1} \quad (4)$$

Thus, $K = \frac{B}{A} = \frac{Output}{Input}$, at steady state.

$\tau = \frac{B}{S}$, where 'S' is the slope of the sigmoid response at the point of inflection.

t $_d$ = time elapsed until the system responded.

In this paper Cohen and Coon Method is used for parameter identification. Here the process control loop is opened so that no control action (feedback) occurs. Here the gain of the Proportional-Integral controller is lower than that of the 'Proportional' controller and the stabilizing effect of the derivative control mode allows the use of higher gains in the PID controller.

The Step value is unity. The scope is simulated for 10 seconds. The process control loop is open looped according to Cohen and Coon Method. The response found is used to find out the static gain 'K', the dead time 't $_d$' and time constant ' τ '.

ZIEGLER-NICHOLS METHOD

By using only proportional action and starting with a low gain, the gain is adjusted until the transient response of the closed loop shows a decay ratio of ¼. The reset time and derivative time are based on the period of oscillation, P, which is always greater than the ultimate period P_U.

With the derivative and reset times as formulated, the gain for ¼ decay ratio is again established by transient response tests.

The ratio of the amplitudes of subsequent peaks in the same direction (due to a step change of the disturbance or a step change of the set point in the control loop) is approximately ¼.

$$\frac{A_2}{A_1} = \frac{1}{4} \qquad (5)$$

The Ziegler-Nichols closed loop method can be applied only to processes having a time delay or having dynamics of order higher than 3.

A closed loop system is taken with DC Motor as the Plant Model. The output of the DC Motor is analyzed and the Proportional controller gain is varied to obtain the ¼ ratio curve.

PARTICLE SWARM OPTIMIZATION

The PSO algorithm is simple and easy to implement. The procedures for implementing PSO are as follows:

1. Assume that, in d- dimensional search space and i th particle of the swarm can be represented by vector $X_i = x_{i1}, x_{i2}, x_{i3}.....x_{id}$
2. The velocity of the particle is $V_i = v_{i1}, v_{i2}, v_{i3}.....v_{id}$, where d-is the dimension of the search space.
3. For each particle, evaluate the fitness function f(X_i) in d variable.
4. Also initialize the best visited position of the particle is $P_{i-best} = p_{i1}, p_{i2}, p_{i3}.....p_{id}$ and compare fitness evaluation with P_{i-best}. If f(X_i) <f(P_{i-best}) then

   f(P_{i-best}) = f(X_i)

   P_{i-best} = X_i
5. Initialize global best position $P_{g-best} = p_{g1}, p_{g2}, p_{g3}.....p_{gd}$. Identify the particle in the neighbourhood with the best success so far. If f(X_i) < f (P_{g-best}) then

   f (P_{g-best}) = f(X_i)

   P_{g-best} = X_i
6. Position and velocity of the particle is updated by the following equation: $\overrightarrow{v_i}(t+1) = \omega * \overrightarrow{v_i}(t) + c_1 * R_1 * (pbest_i - \overrightarrow{x_i}) + c_2 * R_2 * (p_g - \overrightarrow{x_i})$

   $$\overrightarrow{x_i}(t+1) = \overrightarrow{x_i}(t) + \overrightarrow{v_i}(t+1)$$

   where

   c_1 and c_2 are positive constant,

   R_1, R_2 are two random variables with uniformly distributed.

ω is the inertia weight which shows the effects of previous velocity vector on the new vector.

An upper bound is placed on velocity in all dimensions V_{max}.

$$\omega = (\omega\_start - \omega\_end) X \frac{(MAXITER - t)}{MAXITER} + \omega\_end$$

where

ω_start and ω_end are the initial and final values respectively.

A large inertia weight means that exploration of particle, while small inertia weight favours of exploitation.

t is the current iteration number and

MAXITER is the maximum number of allowed iteration.

7. Go to step 3 until a criterion is match, usually a sufficiently good fitness or maximum number of iteration.

THE FLOW CHART OF PSO PID CONTROL SYSTEM

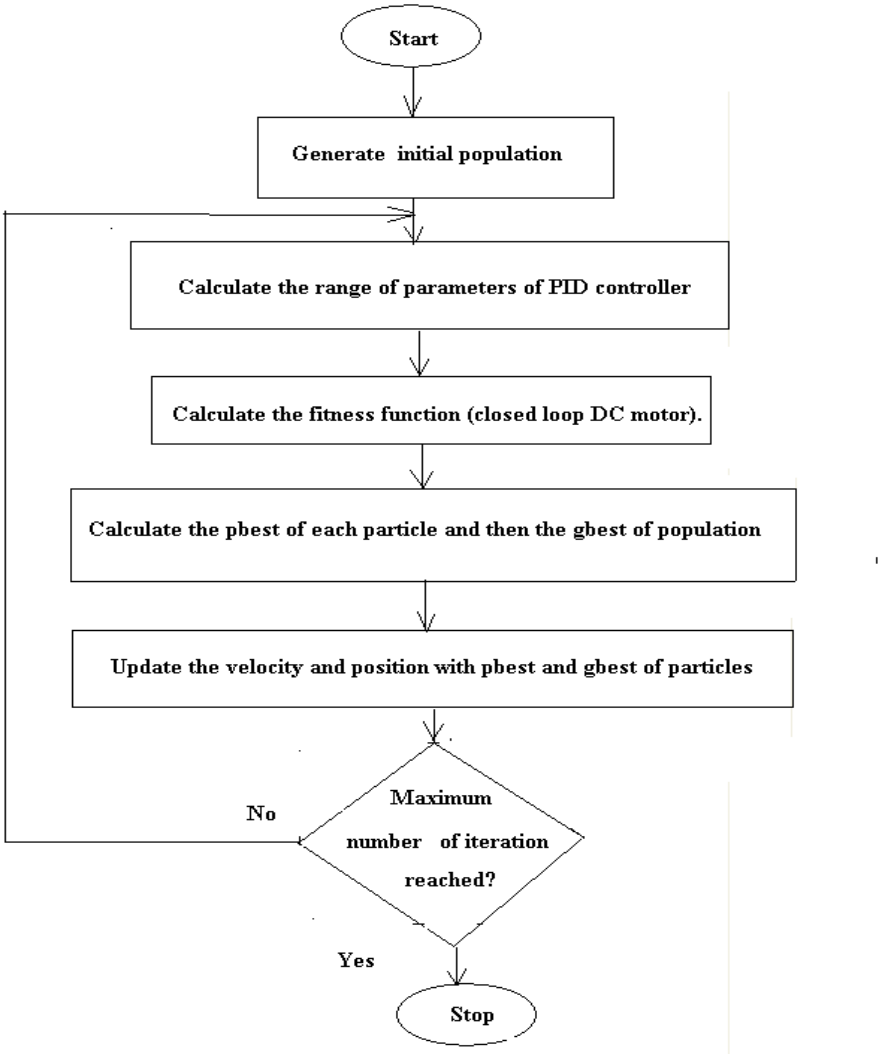

Specified decay Ratio, Usually ¼	Decay Ratio = $\frac{second\ peak\ overshoot}{first\ peak\ overshoot}$
Minimum ISE	ISE = $\int_0^\infty \mid e(t) \mid^2 dt$ Where e(t)= (set point process output)
Minimum IAE	IAE = $\int_0^\infty \mid e(t) \mid dt$
Minimum ITAE	ITAE = $\int_0^\infty \mid e(t) \mid t\ dt$

Table1: The Performance Criteria

RESULTS

According to theory stated above and the experiments done the results of the methods are given in sequence.

Cohen and Coon Method

The Cohen and Coon Method is an open loop system. So first, the open loop system is been analyzed here. From the analyses the static gain 'K', the dead time 't_d' and time constant 'τ' is obtained. These helps in finding the Proportional, Integral and Derivative gain, which is further used for tuning the controller parameters for ideal output of the DC Motor.

The following are the static gain K= 0.1, dead time 't_d'= 0.75 sec and time constant 'τ'=1.0625 sec. Hence the results are obtained, which are given in Table.2.

Mode	K_P	T_I	K_I	K_D
Proportional	10.3922	_____	_____	_____
Proportional Integral	7.1863	0.9747	1.0259	_____
Proportional Integral Derivative	10.8180	1.7684	0.5655	0.3072

Table2: The Gain Values Of P, Pi, And PID Controller Modes.

The PID gain values obtained from Table.2 are used to tune the DC Motor.

The DC Motor is tuned and the output is shown in Figure.3a.

Ziegler-Nichols ¼th Decay Ratio Method

The Ziegler-Nichols ¼th Decay Ratio method is a closed loop system. So first the closed loop system is been analyzed. Here the proportional gain is continuously changed till the ratio of the first peak and second peak of the output becomes ¼. Here the initial proportional gain is assumed as 100 instead of one because for one to 99 there is a large ratio formed. Second Peak Amplitude A_2 has a very small gain in the range of one to 99 compared to First Peak Amplitude A_1.

The proportional gain obtained after the analysis is used to find out the integral and the derivative gain. These gains obtained are used for tuning the controller parameters for ideal output of the DC Motor.

Hence K_P =460

$$K_I = \frac{1}{T_I} = \frac{1.5}{P} = \frac{1.5}{.21} = 7.143$$

$$K_D = T_D = \frac{P}{6} = \frac{.21}{6} = 0.035$$

The PID gain values obtained are used to tune the DC Motor.

The DC Motor is tuned and the output of the DC Motor is shown in Figure.3b.

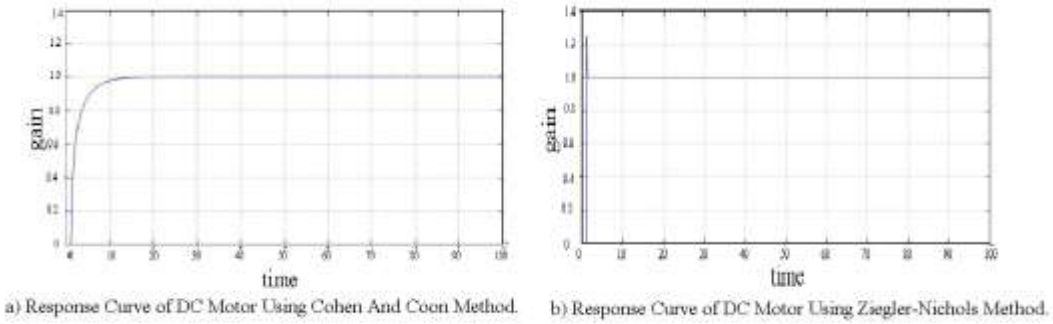

a) Response Curve of DC Motor Using Cohen And Coon Method. b) Response Curve of DC Motor Using Ziegler-Nichols Method.

Figure.3 Output of two tuning methods.

Particle Swarm Optimization

The time integral performance criteria are the objective functions that are used is PSO programming. Hence the objective functions are ISE, IAE and ITAE.

Methods	K_P	K_I	K_D
Particle Swarm Optimization(ISE)	1.73	0.1100	0.1200
Particle Swarm Optimization(IAE)	1.73	0.31	0.12
Particle Swarm Optimization(ISE)	0.87	0.1853	0.12

Table3: Results Obtained Through PSO (200 Iterations)

The PID gain values obtained from the PSO programming after 200 iterations for ISE, IAE and IATE shown in Table.3 are used to tune the DC Motor.

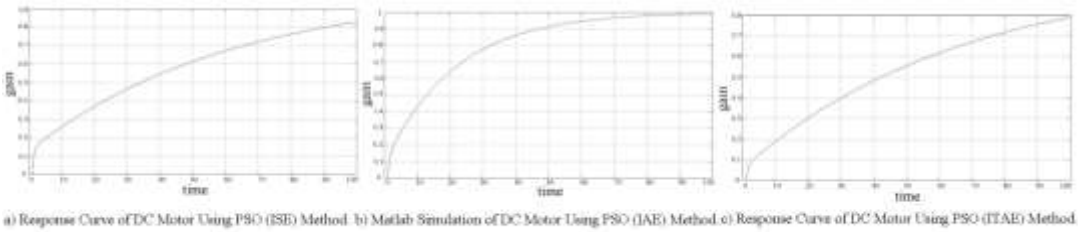

a) Response Curve of DC Motor Using PSO (ISE) Method b) Matlab Simulation of DC Motor Using PSO (IAE) Method c) Response Curve of DC Motor Using PSO (ITAE) Method

Figure.4.Output of PSO method using various fitness functions

The DC Motor is tuned with ISE and the output of the DC Motor is shown in Figure.4a. Then the DC Motor is tuned with IAE and the output of the DC Motor is shown in Figure.4b. The DC Motor is tuned with IATE and the output of the DC Motor is shown in Figure.4c.

COMPARATIVE ANALYSIS

The performance analyses are tabulated on the basis of steady state, rise time and peak overshoots.

Methods	Steady State Within 100 seconds	Peak Overshoot	Rise Time
Cohen and Coon	Obtained	No	More than 10 seconds
Ziegler-Nichols	Obtained	High	Much less than 10 seconds
Particle Swarm Optimization (ISE)	Not obtained	No	_____

Particle Swarm Optimization (IAE)	Obtained	No	Approximately 100 seconds
Particle Swarm Optimization (ITAE)	Not obtained	No	_____

Table4: Comparison of The Output Of The Dc Motor For Various Method, Using The Tuned Controller Parameters.

CONCLUSION

From Table.4 it can be concluded that Cohen and Coon, Ziegler-Nichols, and Particle Swarm Optimization (IAE) can be compared and analyzed on the basis of Steady State, Peak Overshoot and Rise Time.

Firstly comparing Cohen and Coon Method and Ziegler-Nichols Method, it can be concluded that Ziegler-Nichols Method is better than Cohen and Coon Method. Although there is no peak overshoot present in Cohen and Coon Method as high peak overshoot present in Ziegler-Nichols Method, but following are the reasons behind. a) Cohen and Coon Method is an open loop system and do not give any feedback. Due to which the system cannot rectify any of the disturbances sensed by the Plant Model. But the Ziegler-Nichols Method is a closed loop system and hence has the advantage of feedback. b) The rise time of Cohen and Coon Method is much more than Ziegler-Nichols Method.

Secondly the different objective functions of Particle Swarm Optimization Method are compared. The performance of the technique is evaluated by setting its objective function with ISE, IAE and ITAE. Among the three objective functions it can be concluded that IAE is the best. The reason behind it is that when these three objective functions are analyzed for 100 seconds only IAE obtained steady state. Although ISE and ITAE both do not have any peak overshoot but they do not reach the steady state as IAE, which is desirable for the system.

Thirdly comparing Ziegler-Nichols Method and Particle Swarm Optimization Method with IAE as the objective function, it can be concluded that PSO (IAE) Method is better than Z-N Method. Although Ziegler-Nichols Method has much less rise time than PSO (IAE) but Ziegler-Nichols Method has high peak overshoot which is not desirable for any system.

Hence it can be considered that the Particle Swarm optimization with IAE as objective function is the best method. Cohen and Coon Method and Ziegler-Nichols Method are difficult and time consuming processes. Hence soft computing techniques have been widely used to tune the parameters of PID. PID controllers are tuned using soft computing technique which is Particle Swarm optimization.

REFERENCES:

[1] Adel A. A. El-Gammal & Adel A. El-Samahy. 2009. 'Adaptive Tuning of a PID Speed Controller for DC Motor Drives Using Multi- Objective Particle Swarm Optimization', International Conference on Computer Modelling and Simulation, 11, pp.398-405.

[2] Adel A. A. El-Gammal & Adel A. El-Samahy. 2009. 'A Modified Design of PID Controller for DC Motor Drives Using Particle Swarm Optimization PSO', Powereng 2009, pp.419-426.

[3] Helen J. Jawad. 2013. 'Particle Swarm Optimization based optimum PID controller for governor system of Synchronous Generator', AL-Qadisiya Journal for Engineering Sciences, vol.6. no.3, pp.513-551.

[4] Rohit G. Kanojiya & P. M. Meshram. 2012. 'Optimal Tuning of PI Controller for Speed Control of DC Motor drive using Particle Swarm Optimization', International Conference on Advances in Power Conversion and Energy Technologies, 2012, pp.1-6.

[5] Ali Hussien Mary. 2011. 'Generalized PID Controller Based on Particle Swarm Optimization', Iraqi Journal of Computers, Communication and Control & Systems Engineering, vol.11. no.1, pp.114-122.

[6] P. M. Meshram & Rohit G. Kanojiya. 2012. 'Tuning of PID Controller using Ziegler-Nichols Method for Speed Control of DC Motor', IEEE- International Conference on Advances in Engineering, Science and Management 2012, pp.117-122.

[7] Mehdi Nasri, et al. 2007. 'A PSO-Based Optimum Design of PID Controller for a Linear Brushless DC Motor', World Academy of Science, Engineering and Technology, International Journal of Electrical, Computer, Electronics and Communication Engineering, vol.1. no.2, pp.171-176.

[8] Poomyos Payakkawan, et al. 2009. 'Dual-line PID Controller based on PSO for Speed Control of DC Motors', International Symposium on Communication and Information Technologies, 9, pp.134-139.

[9] Yu Ren & Xiaobai Xu. 2008. 'Optimization Research of PSO-PID Algorithm for the Design of Brushless Permanent Magnet Machines', IEEE International Symposium on Embedded Computing, 5, pp.26-31.

[10] Adel M. Sharaf & Adel A. A. El-Gammal. 2009. 'A Novel Particle Swarm Optimization PSO Tuning Scheme for PMDC Motor Drives Controllers', Powereng, 2009, pp.134-142.

[11] K. Lakshmi Sowjanya & L. Ravi. Srinivas. 2015. 'Tuning of PID controllers using Particle Swarm Optimization', International Journal of Industrial Electronics and Electrical Engineering, vol.3. no.2, pp.17-22.

[12] H.K.Verma & Cheshta Jain. 2011. 'A Performance-Dependent PSO based Optimization of PID Controller for DC Motor', International Conference on Electrical Energy Systems, 1, pp.198-202.

[13] Yuting Zhou, et al., 2013. 'Study on PID parameters Tuning Based on Particle Swarm Optimization', Advanced Materials Research, vol. 823. no.13, pp.432-438.

[14] Dwi Ana Ratna Wati. 2013. 'Performance Evaluation of Swarm Intelligence on Model-based PID Tuning', IEEE International Conference on Computational Intelligence and Cybernetics, 2013, pp.40-44.

International Journal of Engineering Research and General Science Volume 3, Issue 6, November-December, 2015
ISSN 2091-2730

Gesture Controlled Smart Bot using Image Processing

Christabel Rebello, Marshall Pereira, Roysten Rodrigues, Aarti Gokul

Computer Engineering, christabel.rebello94@gmail.com, 7768847725

Abstract— Robots are devices that mimic the appearance of a natural being. These robots interact with people directly. Thus making the interface user friendly .The early device was mainly based for navigation and controlling robot without any natural medium .To expedite a practical solution to this requirement we have implemented a system in which we will send commands to the robot using hand gesture method and we have also included an edge avoiding technique. With the help of this method the user can control the robot with his fingers. The image processing technique is used for capturing these commands. Thus making the robot move in required direction

Keywords— Arduino, OpenCV, Gestures, L293D Motor Driver Shield, IR sensors.

INTRODUCTION

Robotic system is a widely increasing system in today's world. Robot is an artificial agent that helps in decreasing human efforts and increases efficiency and accuracy. Basic use of robots is to replace the harmful jobs and repetitive tasks that were to be done mainly by humans. In order to control the system with the help of any external hardware device in hand, the upcoming method of gestures is becoming popular which is operated without using any hand device. The gestures given by hand are making the robotic system user friendly and innate. Other than this, there is also some hardware device required for interfacing the gesture controlling and avoiding obstacle collision

EXISTING SYSTEM

There are many existing system that are present in order to control robots with the help of gestures. Some of the gesture recognition system involves systems that mounts the camera in a cap worn by the user , system using depth perceptive sensors , hand position and orientation can be measured by ultrasonics for gesture recognition , in kinect for Xbox 360 the gestures recognized system is used .

PROPOSED SYSTEM

We proposed a system which uses a serial wire for navigation of a robot using hand gesture commands and we also used IR sensors for edge detection.[3] In this system the user can navigate a robot in four direction that is forward, backward, left and right as per required. In this robotic system, user can operate a robot from a controller station such as laptop with the help of inbuilt or an external webcam. Hand gesture commands are given using fingers. Firstly the image frame is been taken as input and then they are further processed. This processed input image is then used to extract command. After gesture command is obtained, the signal is generated to pass the command to the robot. The command signal that is obtained is stored in a file at the control station. Now the robot accesses the signals from the control station with the help of serial communication wire connected to the serial port of Arduino board and a control station. Arduino takes the signal as input from the control station with help of serial wire and generate some output that are passed to the motor driver. Different output signal is generated for four different input gestures. [1] Digital signals are taken by the motor driver as an input and output is given to the DC motors. In this system the robot detects the edge by sending infrared signal form the IR sensors.

TECHNOLOGY USED

Arduino: Duemilanove.

The name Arduino describes a microcontroller development system. Arduino is open source component that may be individually hard to use. Arduino drops everything together into a mash-up of open source technologies when we try to give them the best user

experience to get something done quickly. The microcontroller on the board is programmed using the Arduino Programming Language and the Arduino Integrated Development Environment (IDE). You can tell your Arduino what to do by writing code in the Arduino programming language and using the Arduino development environment. Arduino are intended for making interactive projects. Arduino senses the environment by receiving inputs from many sensors, and affects its surroundings by controlling lights, motors, and other actuators. [11]

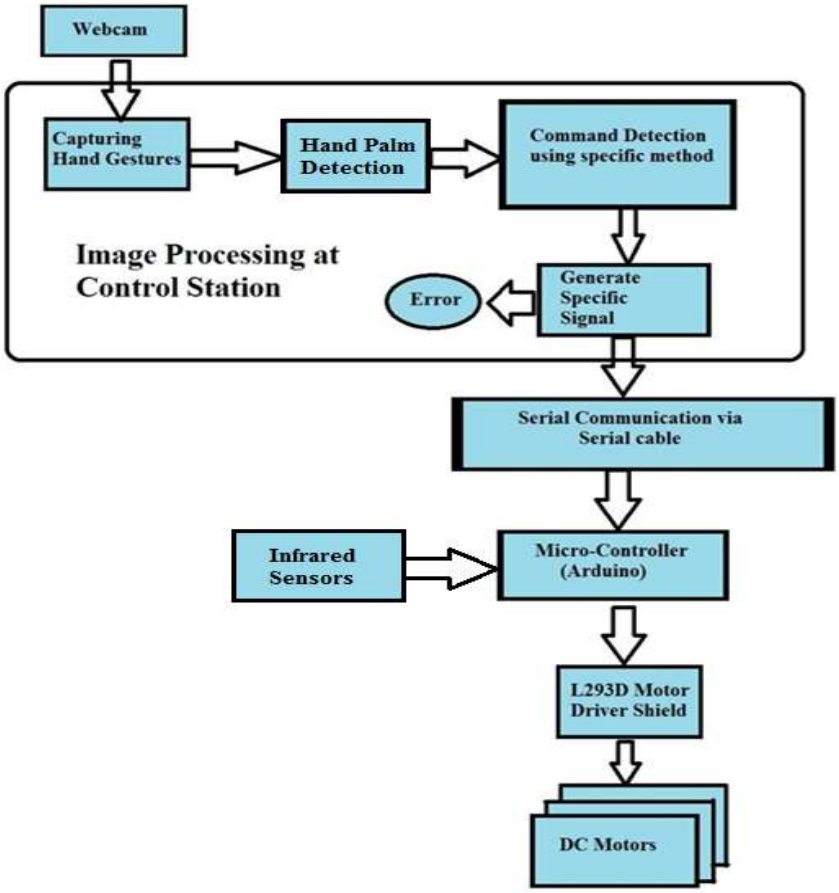

1. Design of System.

C++ with OpenCV :

OpenCV(Open Source Computer Vision Library) was designed for computational efficiency and with a strong focus on real-time applications. The code is written in optimized C++. OpenCV library is platform independent. The OpenCV library has more than 2500 optimized algorithms. Mainly these algorithms are used in face recognition, to capture movements, produce a high resolution image, find similar images in stored databases, also used in augmented reality concept, etc. Various interfaces that are included are C++, C, Python, Java and MATLAB. As it is platform independent it supports Mac OS, Linux, Android, Windows. [6]

L293D: Motor Driver:

The DC motors of our proposed robotic system can drive in either direction with the help of Motor Driver IC [5]. A single L293d IC can control two DC motors. Since they control two DC motors, L293D works on a concept of H-bridge. In order to make the voltage change its direction for rotating the motor in both clockwise and anticlockwise direction H-bridge IC are used by DC motor. Refer Fig. 2. [7]

IR sensors:

We find applications of infrared sensor in our day to day life. It helps in sensing certain attributes of environment by emitting infrared signals. It helps in avoiding obstacle as well as detecting edges to avoid collision. The wavelength of infrared wave ranges between 0.75 and 1000µm. Mainly the region between 0.75 µm to 3 µm is considered as near infrared region, where as the region between 3 and 6µm is known as the mid-infrared region and region beyond 6 µm is known as far infrared region. Refer Fig. 2.

2. L293D Motor Sheild.

3. Micro-Controller (Arduino-Duemilanove)

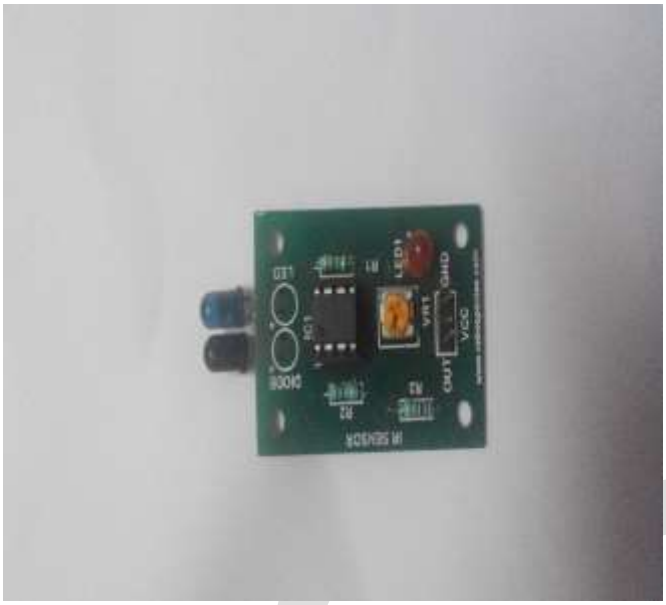

4. IR Sensor.

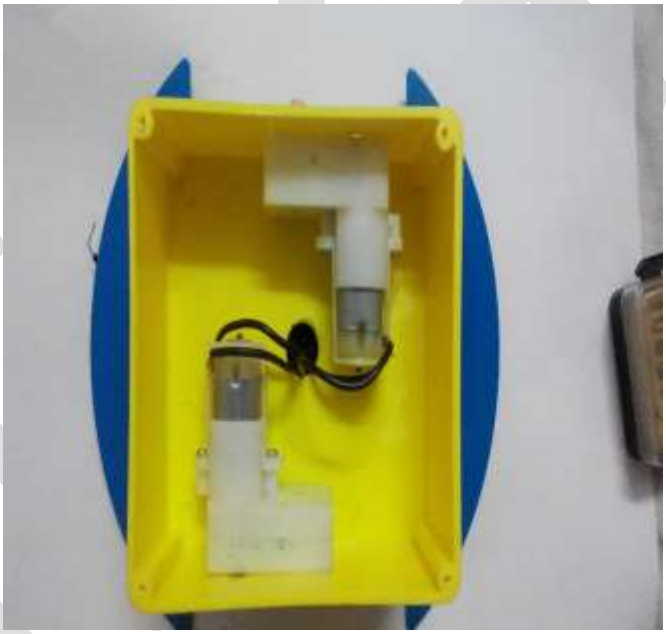

5. DC Motors.

IMPLEMENTATION

The following section illustrates the steps carried out in the Implementation.

Taking input image frame from captured gestures: As soon as the gesture is made, the result is taken as input from the webcam on the control station and further processing is done on each input frame to detect hand palm and command is generated, which is to be given to the robot. Gestures are given by finger count method. There are four types of gesture commands created those are forward, backward, left and right.

Detecting Hand Palm: In order to detect hand palm we have used background subtraction model. There are different background subtraction models present in OpenCV, we are using the codebook method. It tries to subtract and calibrate for some time to be exact for some frames. This operation of detection is necessary for detecting gestures made by finger method. Hand palm detection involves following steps. [2]

1. Thresholding of an Image Frame:

The image frame is taken from the inbuilt or an external webcam of a PC or a laptop. Initially the image has a minimum threshold value. Gradually the threshold value is increased in order to obtain a clear image. The image frame is thresholded so that we can get a single contour free from noise. Thersholding neglects the dark background and thresholds the fingers. Refer to Fig. 6.

2. Drawing Contour and Convex Hull:

Now after acquiring the image frame that has been thresholded, contour is been drawn by using functions from OpenCV library that is drawContour(). Following the contour drawing, now the convex hull is also been drawn on that image. These two basic operations are performed on every image frame depending on the gesture technique given by the user. The gesture technique that we have used here is finger count method. [4]

Finger Count Gesture Control: The gestures are given by finger count method. Convexity defects provide depth parameters for every defects. The commands are generated from these defects. The defects are nothing but the gaps between two successive fingers. If there is one defect then the finger count will be two, if there are two defects finger count is three, if there are three defects finger count will be four, similarly if defects are four finger count will be five. These defects are found first in the convex hull using the function as convexityDefect(). The defects are stored in the form of vectors. This vector has a values of each defect point. Although there are many defects formed in the image frame, the defects that are formed due to the gap between successive fingers has the largest depth as compared to other depth values of defect found in the image. The main code for extracting the contour and detecting the convexity points is in the function given as

void detect(IplImage*img_8uc1,IplImage* img_8uc3). [9]

In this way the judgement has been made by these defects to make the robot move in possible four directions by sending commands to the robot. Refer Fig. 7, Fig. 8, Fig 9, Fig 10.

Generating Signal from the command: The command signal that is generated from the gesture is been stored in a file on the control station. The signal is written in file using C++ functions. The value is written in a file for the respective command, to make the robot move. For example the forward command is represented as 1, backward command is represented as 2, left movement command is given as 3 and right movement command is given as 4. Since there is real time change in command, file is updated.

Passing of signal through serial wire to the Arduino: The generated command signal is read by the processing IDE at control station and then it is passed to the serial port of Arduino. Signal is read character by character and appended in the string. The Arduino reads the command signal generated by gestures. After this the command signal is send to the L293D motor driver through digital pins of Arduino. [12]

Motor driver: L293D: It is a circuit as shown in the figure FIG L293D IC takes an input from Arduino and sends digital output to the DC motors. We have given power supply to the motor driver with the help of two batteries of 9 volts each. Refer Fig. 2. [13]

DC motors: In our implementation DC motors are the end product. They take a digital input from motor driver L293D. Two DC motors are connected to the robot. [10]

Edge avoidance: IR sensors play a major role in implementation of the edge avoiding technique. Infrared waves from IR sensors are not visible to the human eye. In the electromagnetic spectrum, infrared radiation can be found between the visible and microwave regions. IR sensors work by using a specific light sensor to detect a light wavelength in the Infra-Red spectrum. We have mounted two IR sensors in the front part of the robot. The light from the LED bounces off the object and reflects towards the light sensors only when the object is close to the sensor. IR sensors continuously sense the ground, as soon as the sensor is unable to sense the ground, the robot comes to halt. Even if the gesture is given through the webcam, the robot won't move further, thus avoiding any collision to occur.

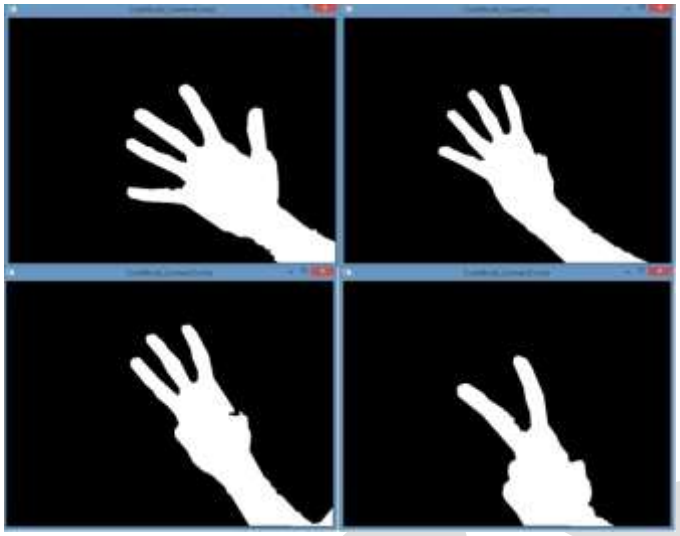

6. Binary Image Thresholding.

7. Finger Count based Gesture Control I.

8. Finger Count based Gesture Control II

9. Finger Count based Gesture Control III

10. Finger Count based Gesture Control IV

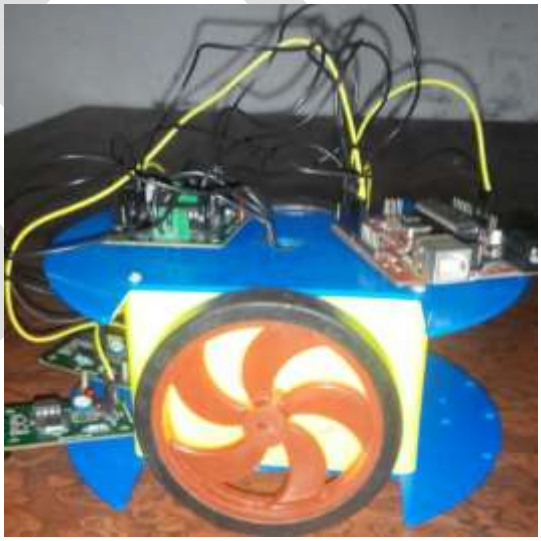

11. Robot

ACKNOWLEDGEMENT

We would like to thank our project guide Mrs. Aarti Gokul who has been a source of inspiration and her insight and vision has made it possible for us to go on and work for this project. Her patience, encouragement, critique and availability made this dissertation possible.

We are grateful to the authorities, faculty and staff of Xavier Institute of Engineering who have helped us to better acquainted with the recent trends in technology and from whom we have learned so much. A special thanks to Mr. Stalin Dharamraj and Mr. Omprakash Yadav for their technical support and guidance.Moreover, we are thankful to our friends and families who have been patient and supportive to undertake this project.

CONCLUSION

An innovative and alternate system has been achieved through gesture controlled robot mechanism. More intuitive and natural as well as easy mode of control is achieved through gesture controlling system in order to control robots in an efficient and exciting way. We have used a specific method of giving inputs to gestures that is finger count method. Here commands are given to the robot which is derived from finger counts so as to make the robot move in desired directions. From the two methods any one method can be chosen and used at a time depending on the user. This eliminates the use of external hardware support (For eg. Remote Controllers) for gesture input unlike the existing system.

REFERENCES:

[1] Chao Hy Xiang Wang, Mrinal K. Mandal, Max Meng, and Donglin Li, "Efficient Face and Gesture Recognition Techniques for Robot Control", CCECE, 1757-1762, 2003.
[2] Asanterabi Malima, Erol Ozgur, and Mujdat Cetin, "A Fast Algorithm for Vision-Based Hand Gesture Recognition for Robot Control", IEEE International Conference on Computer Vision, 2006.
[3] Thomas G. Zimmerman, Jaron Lanier, Chuck Blanchard, Steve Bryson and Young Harvill, "A Hand Gesture Interface Device", 189-192, 1987.
[4] Jagdish Lal Raheja, Radhey Shyam, Umesh Kumar and P Bhanu Prasad, "Real-Time Robotic Hand Control using Hand
[5] Gestures", Second International Conference on Machine Learning and Computing, 2010. Teemu Savolainen, Jonne Soininen, and Bilhanan Silverajan
[6] OpenCV Library http://docs.opencv.org/
[7] L293D Motor Driver http://luckylarry.co.uk/arduino-projects/control-adc-motor-with-arduino-and-l293d-chip/
[8] DC Motors www.globalspec.com/learnmore/motion_controls /motors/dc_motors
[9] anikettatipamula.blogspot.ro/2012/02/hand-gesture-using-opencv.html
[10] Vivek Hanumante, Sahadev Roy, Santanu Maity "Low Cost Obstacle Avoidance Robot", ISSN: 2231-2307, Volume-3, Issue-4, September 2013
[11] Arduino http://arduino.cc/en/Guide/HomePage
[12] www.ladyada.net/learn/arduino/lesson4.html
[13] Arduino Controlled L293D Robot, http://www.instructables.com/id/Arduino-and-L293D-Robot-Part-1-/

International Journal of Engineering Research and General Science Volume 3, Issue 6, November-December, 2015
ISSN 2091-2730

Novel effect of Vegetation (Foliage) on Radio Wave Propagation

Amajama Joseph, Dr. (Engr.) Donathus E. Bassey, Daniel E. Oku

Department of Physics, University of Calabar - Nigeria, joeamajama2014@yahoo.com, +2347036357493

Abstract— This work investigates the effects of Vegetation (foliage) on radio wave propagation in the Calabar metropolis, Nigeria. Measurement of the radio signal strength from Cross River State Broadcasting Co-operation Television (CRBC-TV), ($4^0$57'54.7"N, $8^0$19'43.7"E) at 35mdB and 519.25 MHz (UHF) to investigate foliage loss was carried out in two forested channels ($4^0$56'56.2"N, $8^0$20'42.0"E and $4^0$56'35.4"N, $8^0$20'48.2"E respectively) in the University of Calabar. The results obtained showed that foliaceous canopies are mainly responsible for vegetation (foliage) loss, due to their obstruction of point-to-point contacts or line-of-sight communication of the antennas (transmitter and receiver) and shielding of the raining sky waves from the receiver antenna, but not other non-foliaceous parts that interfere with the ground and surface wave at UHF. The correlations between the signal strength (mdB) and depth (m) in the first and second forested channels were r = -0.17 and r = -0.06 respectively. The standard deviations of the vegetation (foliage) losses in the two channels were σ = 3.24 mdB and σ = 2.23 mdB respectively. The first forested channel contains predominantly pride of Barbados and the second forested channel contains mainly palm trees. The loss was higher in the former than the latter channel because of the difference in the thickness of their foliaceous canopies.

Keywords— Signal strength, Vegetation (Foliage) loss, Ultra High Frequency (UHF), Radio wave, Foliaceous canopy, Radio propagation, Forested channel.

INTRODUCTION

Signal path losses are an essential factor in the plan of any radio communications system. They decide a large number of factors of a communications system, particularly the receiver and transmitter powers including their gains, heights with locations in general. The method of transmission employed and required receiver sensitivity amongst other factors will also influence signal path losses [5].

Basically, signal path loss is the degradation or dissipation in strength of a signal as it travels through a particular region or medium [10], [11].

The following are some of the factors that may give rise to signal path losses during propagation. They are: free space path losses, absorption losses, diffraction losses, multipath, terrain, buildings and vegetations and the atmosphere [5].

This research work zero in on the effects of two forested channels or territories (predominantly pride of Barbados and palm trees respectively) in the University of Calabar, Cross River State, Nigeria on signal of about 519.25 MHz, which is the frequency of transmission for the Cross River Broadcasting Corporation Television (CRBC-TV), Calabar, Cross River State, Nigeria and defined by the Institute of Electrical and Electronics Engineers as Ultra High Frequency (UHF).

To score the goal of this work, experiments were carried out to obtain sufficient data that gave birth to the effects of vegetation (foliage) on signal from the twin forested channels. Signal strength evaluations were made just in front of the forested channel and under the cascade of canopies of tree(s) at both forested channels at varying depths from the transmitter into the thick of the forest to probe the vegetation or foliage loss and comparing it with Weissberger's and Early ITU's models.

A BRIEF REVIEW OF RELATED RESEARCHES

Mir, Jun-ichi and Tetsuro (2013) in southern Kanagawa - Japan researched on; "Radio wave propagation through vegetation" and reported that: "contrary to the widely assumed homogeneous random scattering media, it is observed that the radio waves in the vegetated channel are received from distinct directions in clusters of multipath [9].

Meng, Lee and Ng (2009) in Singapore worked on; "The effects of tropical weather on radio wave propagation over foliage channel". Also, still in Singapore, Meng *et al.* (2013) worked on; "Study of propagation loss prediction in forest environment" [7]. They affirmed that: "wind and rain can impose an additional attenuation on the propagation signal within the forest environment; the additional attenuation increases as the strength of the wind and rain increases" [8]. Also, "the direct wave travelling through the canopy layer is the only wave that can be affected by falling rain drops during a rain event, but not the lateral wave along air-canopy interface and the ground reflected waves over large foliage depth at VHF band" [8].

Adegoke and Siddle (2011) in Victoria Park, Leicester - United Kingdom carried out; "Investigation into vegetation effects on propagating waves" and worded that: "preliminary investigation reveals that interaction of radio waves with vegetation leads to attenuation" (p. 4). Full foliage recorded a loss of 8 dB to 16 dB even at shorter foliaceous depth while partial foliage recorded a loss of 2.4 dB to 7 dB at higher depth [1].

Alade (2013) in Ogbomosho, Oyo state - Nigeria worked on; "Further investigation into VHF radio wave propagation loss in a forested channel" and encapsulated that: "radio wave propagation loss in a forested channel is due to tree-canopy and ground reflection rather than the reflections from the groove and trunk of trees" [2]. He further said: "if there is any additional propagation loss, it is due to foliage induced effect therefore, the appropriate propagation model is tree-canopy and ground reflection (CGR) mode" [2].

A REVIEW OF FOLIAGE OR VEGETATION LOSS MODELS USED

In this work, we are going to condense our attention on two foliage or vegetation loss models. They are the Weissberger's and Early ITU's models.

Weissberger's model

This is a modified exponential decay model. In simple words, it is a radio wave propagation model which determines the loss in a path caused by the obstruction of one or more trees in the "point-to-point" distant communications connection. It is categorized under vegetation or foliage models.

This model is applicable to the case of "line-of-sight" propagation (LOS). Example is microwave transmission when there is an obstruction made by some trees or foliage in the connection, between the transmitter and the receiver. Ideally, this model is applicable in the situation where the LOS path is blocked by dense, dry and leafy trees.

The coverage frequencies and depths of foliage range from 230 MHz to 95 GHz and few metres up to 400 m respectively. This model was formulated in 1982; it is a development of the International Telecommunications Union's (ITU's) *Model for Exponential Decay* (MED).

Mathematically, this model is expressed formally as shown in equation (11).

$$L=\begin{cases} 1.33f^{0.284}\ d^{0.558}\ if\ 14 < d \leq 400 \\ 0.45\ f^{0.284}d\ \text{if}\ 0 < d < 14 \end{cases} \quad (11)$$

Where,
L = Loss due to foliage (dB)
f = Frequency of transmission (GHz)
d = Depth of foliage along the channel (m)

The points to take into account are that the above equation is sealed for frequency specifically in *gigahertz* (GHz) range and the foliage depth must be specifically in *meters* (m).

The shortcomings of this model are that it is significantly for frequencies ranging from 230 MHz to 95 GHz only, as clearly sketched out by Blaustein. When the depth of the vegetation is more than 400 m, it does not define the operation. And, it only predicts foliage or vegetation loss; the path loss must be calculated in summation to the loss due to free space [6].

Early ITU's model

The Early ITU's vegetation or foliage model is a radio propagation model that gives an estimative calculation of the path loss encountered because of the presence of one or more trees in-between a "point-to-point" distant communications connection. The predictions discovered from this model parallel those from Weissberger's modified exponential decay model at low frequencies. The ITU was predeceased by the International Radio Consultative Committee (CCIR), She adopted this model in the late 1986.

This model finds application to the situations where the telecommunications connection has some obstructions made by trees or foliage along its way. It is suitable for "point-to-point" microwave connection that has vegetation in their path; to predict the path losses.

The coverage range of frequencies and depths of foliage are not specified for this model.

Mathematically, this model is formulated as shown in equation (12).

$$L = 0.2\ f^{0.3}\ d^{0.6} \quad (12)$$

Where,
L = Loss due to foliage (dB)
f = Frequency of transmission (MHz)
d = Depth of foliage along the channel or connection (m)

Points worthy of note are that this equation is scaled for frequency specifically in *megahertz* (MHz). And, the foliage depth must be specifically in the units of *meters* (m).

The major limitation of this model is that the results get unrealistic or impractical at high frequencies [6].

METHODOLOGY

The campaign was carried out in two forested channels in the University of Calabar within the Calabar metropolis; in Cross River State, Nigeria. The main object of the experiments was to obtain statistical data of signal strengths just outside and inside the forested channels at different depths to determine the vegetation (foliage) loss. The measurement of the signal strength was made using the digital Community – Access (Cable) Television (CATV) analyzer with 24 channels, spectrum 46 MHz – 870 MHz, connected to a domestic receiver antenna of height 4.23 m.

To be able to reach a justifiable conclusion on the vegetation (foliage) loss, the dependence of the signal strength on the relevant parameter was analyzed. This parameter was the depth of the forest channel to ascertain vegetation (foliage) loss. The received signal strengths were measured only on the downlink and at every measurement, the receiver antenna was adjusted until the best obtainable reading of signal strength was captured on the cable analyzer before recording.

Sites descriptions

To probe vegetation (foliage) loss, measurements were carried out in two forested channels in the University of Calabar – Nigeria.

The first site of investigation ($4^0$56'56.2"N, $8^0$20'42.0"E) is a narrow channel of trees, predominantly the pride of Barbados with average trunk width of 3 m, average height of 20 m and spacing of about 20 m. The full depth of the channel is about 80 m with a level topography and scanty undergrowth.

The second site of investigation 0.6 km away along the University drive ($4^0$56'35.4"N, $8^0$20'48.2"E) is a heavily forested channel completely palm trees. The spacing of the trees is about 20 m to 30 m. The average height of the trees is about 15 m and the channel's depth is about 250 m. The topography is undulating with short grass as undergrowth. Find in the appendices the picture of the two forested channels or sites.

Measurement method

The measurement to determine the effect of foliage or trees or vegetation on signal was achieved by taking readings of signal strength on a straight path at different depths into the forested channels away from the CRBC-TV transmitter antenna ($4^0$57'54.7"N, $8^0$19'43.7") with the aid of a Global Positioning System (GPS) for direction. The digital CATV analyzer was connected to a domestic receiver antenna of about 4.23 m for a better reception and moved from one point to another into the depth of the forested channels to acquire measurements at each position under the foliaceous canopy of trees(s).

Sampling with the CATV analyzer

Measurements with the digital CATV analyzer being time dependent were made approximately every sixty seconds (60 s). The average signal strength value (mean of minimum and maximum reading) was recorded when the sharpest images were registered on the Analyzer.

EXPERIMENTAL RESULTS AND DISCUSSION

The results of each of the experiments are analyzed separately. To determine the vegetation (foliage) loss curves; the whole data or measurements made was used for both forested channels (that is, site one and site two). Also the losses were compared with that of Wessbieger's and Early ITU's models.

Analysis of measurement from first forested channel (site one)

The analysis of the measurements is preceded by Table 1and the Figures 1 and 2**.**

TABLE 1
Measured loss from site one and the Wessbieger's and Early ITU's models losses

Depth (m)	Signal Strength (mdB)	Weissberger's Model Loss (dB)	Early ITU's Model Loss (dB)	Measured Foliage Loss (mdB)
0	-3.1	-	-	-
5	-4.7	1.9	3.4	1.6
10	-10.5	3.7	5.2	7.8
15	-11.4	1.8	6.6	8.3
20	-11.9	2.2	7.9	8.8
25	-12.0	2.5	9.0	8.9
30	-12.2	2.8	10.0	9.1
35	-12.6	3.0	11.0	9.5
40	-10.8	3.3	11.9	7.7
45	-3.1	3.5	12.8	0.0
50	-7.1	3.7	13.6	4.0

Figure 5 shows the graphical representation of the signal strength at different depths of the forested channel. Also, Figure 6 shows measured foliage or vegetation loss curve in comparison with curves of the Weissberger's and Early ITU's model losses.

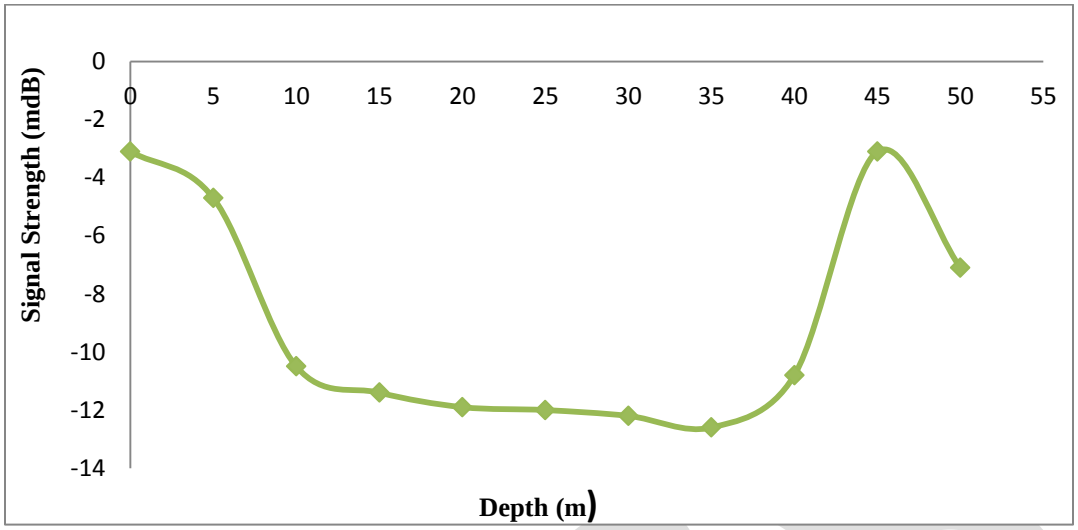

Figure 1. Signal strength curve at different depths (site one).

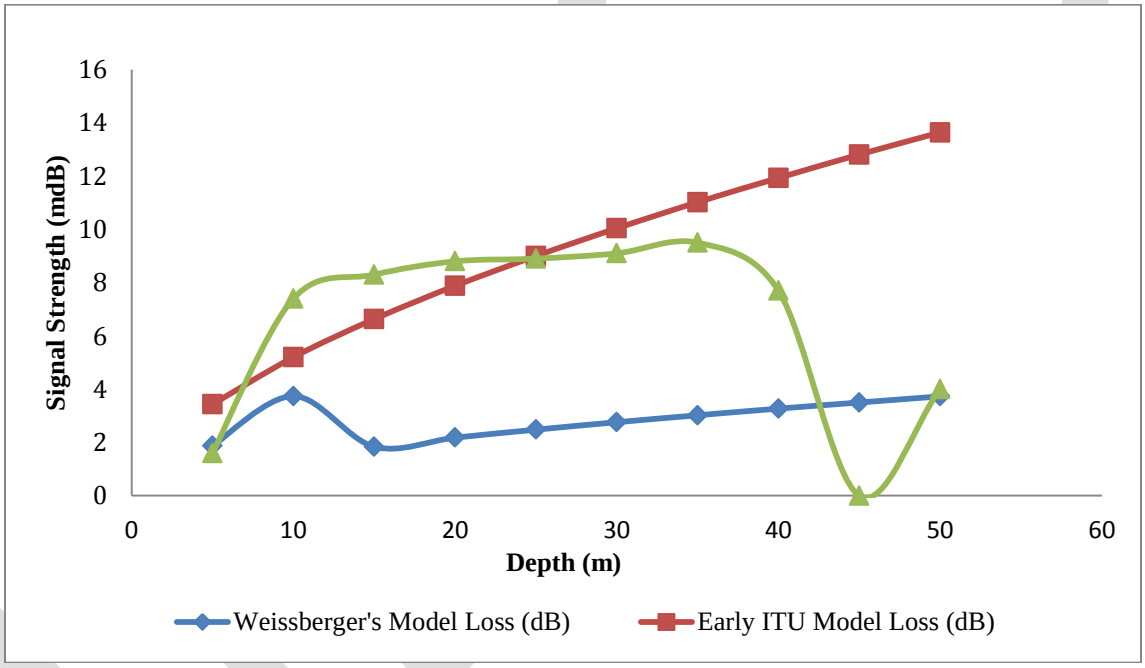

Figure 2. Comparison between curves of the measured foliage or vegetation loss and the Weissbeger's and Early ITU's models losses (site one).

In Figure 5, there is a gradual degradation or dissipation or decay of the signal with increasing depth. This is due to the thickening canopy of foliage obstructing the signal direct or line-of-sight path or point-to-point connection between the transmitter and receiver antennas and shading of sky waves from the receiver antenna. Further down the channel, as the canopy of foliage thins, the signal is strengthened, because of gradual restoration of point-to-point contact or connection and increasing sky waves raining on the receiver antenna. At the end of every canopy of tree(s), a good direct or line-of-sight or point-to-point connection or link is re-established between the transmitter and receiver antennas and the receiver antenna gets link with abundant sky waves. The signal is strengthened as if there were no vegetation (foliage) on its path.

Farther down the channel, as the direct or line-of-sight or point-to-point contact or connection is lost and the sky waves diminish with the presence of another canopy, the foliage fading or loss increases again, depending on the canopy's width and thickness. This phenomenon fluctuates deeper into the forest channel. It implies that the signal loss due to trees or vegetation is caused mainly by the foliage canopy and not the obstruction of the ground or surface waves by the trunk and other non-foliaceous parts of the tree(s). Hence, for UHF signals, the depth of the forest counts less. It is the presence of the falling sky waves and the point-to-point contact or connection that speaks volume.

In Figure 2, the measured loss curve appears to rise gradually like that of the Early ITU's model, but at about 25 m, the former deviates far from the latter because of the restoration of the point-to-point or direct line-of-sight connection and the presence of

abundant sky waves due to few or no presence of foliage, that is just at the end of the width or terminal of the first foliaceous canopy on the channel.

Analysis of measurement from the second forested channel (site two)

Analysis or discussion of the measurements is preceded by TABLE 2 and the Figure 3 and 4.

TABLE 2

Measured loss from site two and the Wessbieger's and Early ITU's models losses

Depth (m)	Signal Strength (mdB)	Weissberger's Model Loss (dB)	Early ITU's Model Loss (dB)	Measured Foliage Loss (mdB)
0	-15.0	-	-	-
5	-15.2	1.9	3.4	1.2
10	-15.8	3.7	5.2	0.8
15	-19.0	1.8	6.6	4.0
20	-20.0	2.2	7.9	5.0
25	-21.6	2.5	9.0	6.6
30	-17.8	2.8	10.0	2.8
35	-17.6	3.0	11.0	2.6
40	-17.3	3.3	11.9	2.3
45	-15.1	3.5	12.8	0.1

Figure 7 shows the graphical representation of the signal strength at different depths of the channel. Also Figure 8 shows the measured foliage or vegetation loss curve in comparison with the curves of the Weissberger's and early ITU's model losses.

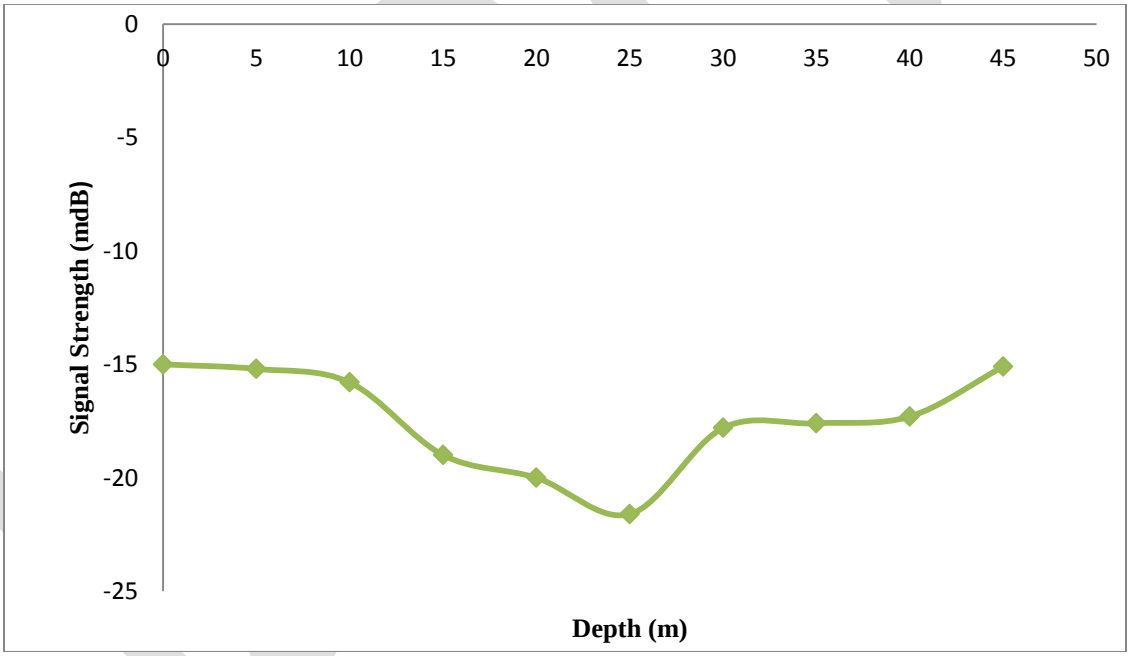

Figure 3. Signal strength curve at different depths (site two)

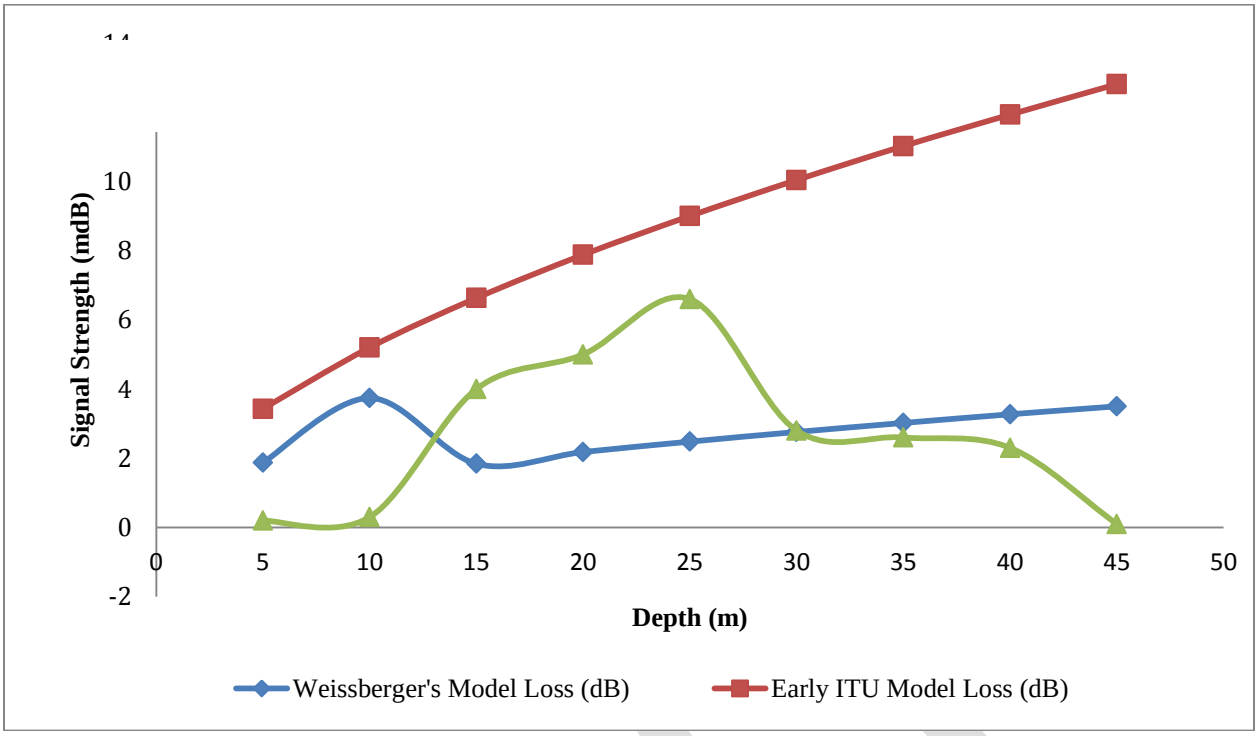

Figure 4. Comparison between curves of the measured vegetation or foliage loss and the Weissbeger's and Early ITU's models losses (site two)

Similarly in Figures 4 and 5, the explanation in section 4.1 is echoed or paralleled. There is a gradual degradation or dissipation of the signal with increasing depth to about 35 m due to the thickening foliage disrupting point-to-point connection or direct or line-of-sight communication and shading the rain of sky waves from the receiver antenna. However, beyond the 35 m mark, the phenomenon reverses as the raining sky waves began to fall increasingly on the receiver antenna and point-to-point connection or direct or line-of-sight communication is gradually restored due to the thinning of the foliaceous canopy. At the end of the foliaceous canopy, that is about 45 m, there is a little or no loss because of the full re-establishment of the point-to-point or direct or line-of-sight link or communication and the raining sky waves are once more heavy. Afterwards, the signal diminishes or depreciates as seen from the curve in Figure 3 due to the encounter or collision again of the radio signal or waves with another canopy.

Also in Figure 4, the measured loss curve almost parallels that of the ITU's model, but begins to drift tangentially over 35 m due to the reconnection or re-link of point-to-point or direct or line-of-sight communication and a huge fall from the raining sky waves on the receiver antenna. At 40 m, the shielding or shading from the foliaceous canopy is heavier and the signal disintegrates or diminishes, reading an increase in vegetation (foliage) loss.

From the two forested channels and the curves generated from the measurements acquired, it is obvious or self-evident that vegetation (foliage) loss is mainly caused by the foliaceous canopy, due to its obstruction of the point-to-point or direct or line-of-sight communication between the receiver and transmitter antennas and shielding of the raining sky waves. The obstruction of the ground and surface waves by the trunks and other non-foliaceous parts of tree(s) is not really significant. Hence, for UHF signals, the depth of the forested channel does not really matter much (excluding the free space path loss). Any position in the channel, where point-to-point or direct or line-of-sight communication is achieved between the transmitter and receiver antennas and the falling sky waves is generous; the signal strength loss or vegetation (foliage) loss is near negligible.

CONCLUSION

In conclusion, it was observed that the foliaceous canopy was mainly responsible for the loss of the signal strength, but not other non-foliaceous part that may only obstruct the surface and ground waves - that is, at UHF and transmitter antenna height higher than the trees in the forested channels. This is because the canopy obstructs the direct or line-of-sight or point-to-point communication and shields the receiver antenna from the raining sky waves. The aforementioned phenomenon is similar to directing a light source across a foliaceous canopy. It will be observed that the canopy will shield or shade the falling light particles from reaching a target object behind the canopy. This is true because, all members of the electromagnetic spectrum shear the same characteristics [12], [3], just that some can travel farther than the other because of the difference in propagation energy. The correlations between the signal strength (mdB) and depth (m) in the first and second sites of investigation were $r = -0.17$ and $r = -0.06$ respectively. The standard deviations of the foliage losses in the two sites were $\sigma = 3.24$ mdB and $\sigma = 2.23$ mdB respectively. Hence, the thicker the foliaceous canopy, the higher the vegetation or foliage loss, since there was higher fading in the signal strength with depth in the pride of Barbados' channel than that of the palm trees' channel with thinner foliaceous canopy than the aforementioned channel.

REFERENCES:

[1] Adegoke, A. S. & Siddle, D. (2011). Investigation into vegetation effects on propagating radio waves. *Radio systems research group*. Department of Engineering, University of Leicester, University road, Leicester, United Kingdom.

[2] Alade, O. M. (2013). Further investigation into VHF radio wave propagation loss over long forest channel. *International Journal of advanced research in electrical electronics and instrumentation engineering*, 2(1),705-710.

[3] Dell, W. R., Groman, J. & Timms, H. (1994). *The worldbook encyclopedia*. Chicago: World Book Incorporated.

[4] Friis, H. T. (1946). A note on a simple transmission formula. *Proceedings of the IRE*, 34, 254.

[5] Ian, P. (Ed.) (2015). Radio signal path loss. Retrieved April 3, 2015, from www.radio-electronics.com.

[6] John, S. S. (2005). *Introduction to RF propagation*. New York: John Wiley and Sons.

[7] Meng, Y. S., Lee, Y. H. & Ng, B. C. (2009). Study of propagation loss prediction in forest environment. *Progress in electromagnetic research B*, 17, 117-133.

[8] Meng, Y. S., Lee, Y. H. & Ng, B. C. (2013). The effects of tropical weather on radio wave propagation over foliage channel. *IEEE transaction on vehicular technology*, 58(8), 4023 - 4030.

[9] Mir, G., Jun-ichi, T. & Tetsuro, I. (2013). Radio wave propagation through vegetation. *Wave propagation theories and applications*, 155 - 174. Retrieved January 16, 2015, from http://creativecommons.org/lincenses/by/3.0.

[10] Rappaport, T. S. (1996). *Wireless communications*. New Jersey: Pearson Prentice Hall, 495 -502.

[11] Wayne T. (2001). *Electronic communications systems, fundamentals through Advanced* (4th ed.). New Jersey: Prentice-Hall, 359.

[12] Young, H. D. & Freedman, R. A. (1998). *University physics* (9th ed). California: Addison-Wesley Longman, 958 -960.

Appendices

Appendix 1: Picture of forested channel in the university of Calabar (site one) with the receiver antenna

Appendix 2: Picture of forested channel in the University of Calabar (site two)

Appendix 3: Picture of campaign in one of the forested site with the CATV (cable) Analyzer, its charger and the receiver antenna pole

International Journal of Engineering Research and General Science Volume 3, Issue 6, November-December, 2015
ISSN 2091-2730

An Analysis Of Causes and Effects Of Change Orders On Construction Projects In Pune

Onkar U. Jadhav[1], Prof. Abhijit N. Bhirud[2]

PG Student, Civil Engineering, Construction Management, Imperial College of Engineering and Research, Wagoli Pune.[1]

Assistant Professor, Civil Engineering Department, Imperial College of Engineering and Research, Wagoli Pune.[2]

onkar17689@gmail.com[1]

abhijitbhirud11@gmail.com[2]

Abstract— - In the last decade there has been extent amount work in construction industry. Due to this large scale of development going on across the country. Large construction projects are facing problem of delays and extra costs. In all types of construction projects cost and time is an important role. The changes at every stage or on regularly basis on construction project disturb the schedule of project as well as extra work has to be done. The purpose of this paper to focus on various change order and cause, effects and control measures for construction projects in Pune. The study limited for the Pune city .For this goal we prepare questionnaire from the previous literature and research. The questions based on the client, contractors, consultants and other factors causing change orders. This questionnaire survey done manually from the construction projects in Pune.The respondent are engineering professionals having minimum 5 years of experience in construction industry for handling projects.
The purpose of this paper to know cause, effects and control measures for change orders in construction projects in Pune. From the data collected by the questionnaire survey we first take Cronbach's Alpha test for internal consistency test by using SPSS statistics software. After analyzing and find out conclusion we used relative importance index method.

Keywords:- Change Management, Construction Project, Cronbach's Alpha, Causes, Change Order, Effects, Relative Importance Index.

. introduction

Construction projects are long process having more complicated small tasks involved in it.For completion of large construction projects we have to complete small construction tasks in regular manner. For that lot of efforts are taken. But sometimes quite unfortunate conditions cause the flow of construction activity. The change order are one of them unfortunate reason to disturb the flow of construction process simultaneously delay the construction project. The management of these changes is skill; in what manner we manage that change without affecting our goal. Managing change is the greatest importance to the success of construction project.

The Change Orders are significant effects on the construction projects performance. The quality of the work decreases, workmanship decreases. The change orders created when change occur from any reason it may owner, contractor, etc. A change is the work for addition or rework. Many of the time change causing the demolition and rework. These causes decrease the labour productivity. Change orders are easy to manage at the initial phases of construction which reduce the rework and extra effects for particular stage. The rework due to change order causes the dispute among owners and contractor and owner has to pay extra money for extra work. Change orders have many causes they are changes project to project as per scope of the projects, location.
So the change orders are from any reason they collective effect on construction project which resulted in delay or cost overheads.

II. RESEARCH REVIWES:

Change order usually issued to cover variation in scope of project, design mistakes, material quantities, and shortages.
Researches Reviews:

Ali S. Alnuaimi, Ramzi A. Taha, Mohammed Al Mohsin, Ali S. Al-Harthi.(2010)

The research done by these authors in Oman for causes, effects and remedies on public construction projects. That study found that Client additional work and modification to design change is the most important cause for change order. Beside of that nonavaibility of construction manual and reference of similar projects in that area is on of the cause. The study found measure effect on time schedule, disputes and costoveruns. Contractor was found the most benefited among all this. The remedies suggest to prefer standard manual at the design stage.

Patrick Keane, Begum Sertyesilisik, Andrew David Ross(2010)

A variation is any type of deviation from an agreed upon, well defined scope or schedule of works. A change order is the formal document that is used to modify the agreed contractual agreement
and becomes part of the projects documents.
The conclusion of these authors study shows that conflicts between contract documents, lack of involvement in design stage, always differ the project objectives is one of the strong reason causing change orders. The change orders minimized using good communication during contract preparation, good project execution planning of upcoming activities. The maintain good relationship among all parties. The

owner should take all the advantages of consultancy appointed to the projects.

Murali Sambasivan, Yau Wen Soon (2006)

The main approach towards specific area to clear for issuing change orders. The study only for change orders which will cause the delay or time overrun. They found the main reasons are contractor improper planning, poor site management, shortage of advanced construction material, skilled labour shortages, effect of this dispute, arbitrations, The method used for this is same relative importance index method.

The importance index, weighted average are used to rank causes and effects.

Importance index = Weighted Average × 100⁄4

Weighted Average=(ΣWi × Xi) /N

Where Wi is option of cause,Xi is no. of respondent selected that cause and N is total no.of respondent.

III. OBJECTIVES:

1. The detailed review on the literature related to Change Order data.
2. To collects and know causes of construction change orders in construction projects in Pune.
3. To know effects of change orders on construction Projects in Pune.
4. To identify control measure for change orders in Construction projects in Pune.
5. Provide the solution and recommendation to minimize the adverse effect of change orders on construction projects in Pune.

IV. METHODOLOGY:

a. At the very first stage defining problem statement and fix the objectives by reviewing previous literature.
b. By studying the previous literature which will helps to prepare questionnaire related to causes and effects of change orders in construction projects.
c. At the same time discussion with actual field persons also helpful for preparation of questionnaire .with this Questionnaire carried out survey for data collection.
d. Also data collected from actual site case studies. Finding out importance index. And main causes and effects of change orders.

V. DATA COLLECTION AND ANALYSIS:

From the previous literature review prepare the questionnaire for the survey from the construction projects in Pune. The respondent are engineering professional with having minimum five years of experience in the construction industry. The causes are divided into four section client based, contractor based, consultants based and other related causes. Effect and control sheet are prepared from the various literature papers After survey data first analyze for consistency test by finding Cronbach'alpha by using SPSS statistics software. A commonly accepted rule of thumb for describing internal consistency is as follow.

Cronbach's alpha	Internal consistency
$\alpha \geq 0.9$	Excellent
$0.9 > \alpha \geq 0.8$	Good
$0.8 > \alpha \geq 0.7$	Acceptable
$0.7 > \alpha \geq 0.6$	Questionable
$0.6 > \alpha \geq 0.5$	Poor
$0.5 > \alpha$	Unacceptable

After that by using Relative Importance Index rank the causes, effects controls for the data collected by questionnaire survey.

Sr.No	CAUSES OF CHANGE ORDER	RII	RANK
	A) Causes due to Owner		
1	Owner instructs additional works & modification to design.	78.43	1

2	Owner fails to make decisions or review document at the right time.	61.57	14
3	Unilateral decisions made by owner without proper considerations to contract.	65.10	6
4	Owner's needs during the design stage are unclear or not well-defined.	64.31	7
5	Owner's change of schedule due to financial problem.	63.92	8
6	Obstinate nature of owner.	52.16	28
7	Owner fails to maintain hold on the project schedule.	60.39	18
	B) Causes due to contractor		
1	The contractor misuses variations Instructions.	63.14	9
2	The scope of work for the contractor is not well defined.	52.16	27
3	The required equipment and skilled labour are not available.	60.39	17
4	Poor project management and planning by contractor.	65.49	5
5	Lack of contractor's involvement in design.	74.51	2
6	Contractor's lack of judgment and experience.	58.43	19
7	Contractor's desired profitability, cost escalation & financial problem.	61.96	12
	C) Causes due to Consultants		
1	Unrealistic design periods & Design errors.	67.45	3
2	Failure by consultant to perform design and supervision effectively.	54.12	26
3	Consultant's lack of judgment and experience.	54.51	25
4	Obstinate nature of consultant.	54.90	24
5	Failure by the consultant to provide adequate and clear information.	61.18	16
6	The lack of coordination between consultant and contractor or subcontractors.	66.27	4
7	Consultant fails to supervise drawing prepared by their junior team.	58.04	20
	D) Other Causes		
1	Delay in decision making process by site engineers.	62.75	11
2	Problems on Site, Unfamiliarity with local conditions and safety consideration.	57.25	21
3	Non availability of construction manual and procedure for project construction in Pune.	61.57	15
4	Non availability of records of similar project in Pune	54.12	23
5	Replacement of materials or procedures.	62.75	10
6	Demolition and re-work ,Quality improvement.	61.96	13
7	Unforeseen problems and weather conditions.	56.86	22

Table No.1

The actual result collected from data shown in above table no.1. The data surveyed from construction sites in Pune from Engineering Professionals with having minimum five years' experience in construction industry. The data analysis done by using Relative Importance Index method.

$$RII = \frac{\sum W}{A \times N}$$

where w = weighting given to each factor by the respondents and ranges from 1 to 5 where '1' is 'not significant' and '5' is 'extremely significant', A = highest weight (i.e. 5 in this case), and N = total number of respondent.

The below pie chart shows the relative importance index in percentage for ranking of effects of change order.

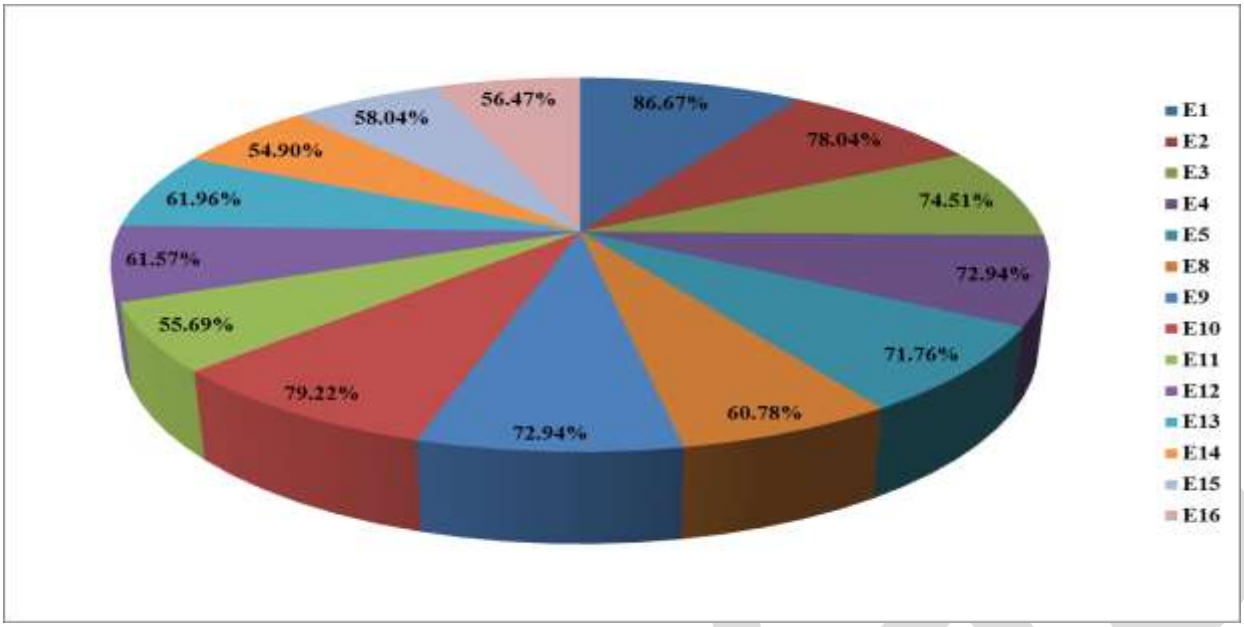

The below pie chart shows the relative importance index in percentage for ranking of control measures of change order.

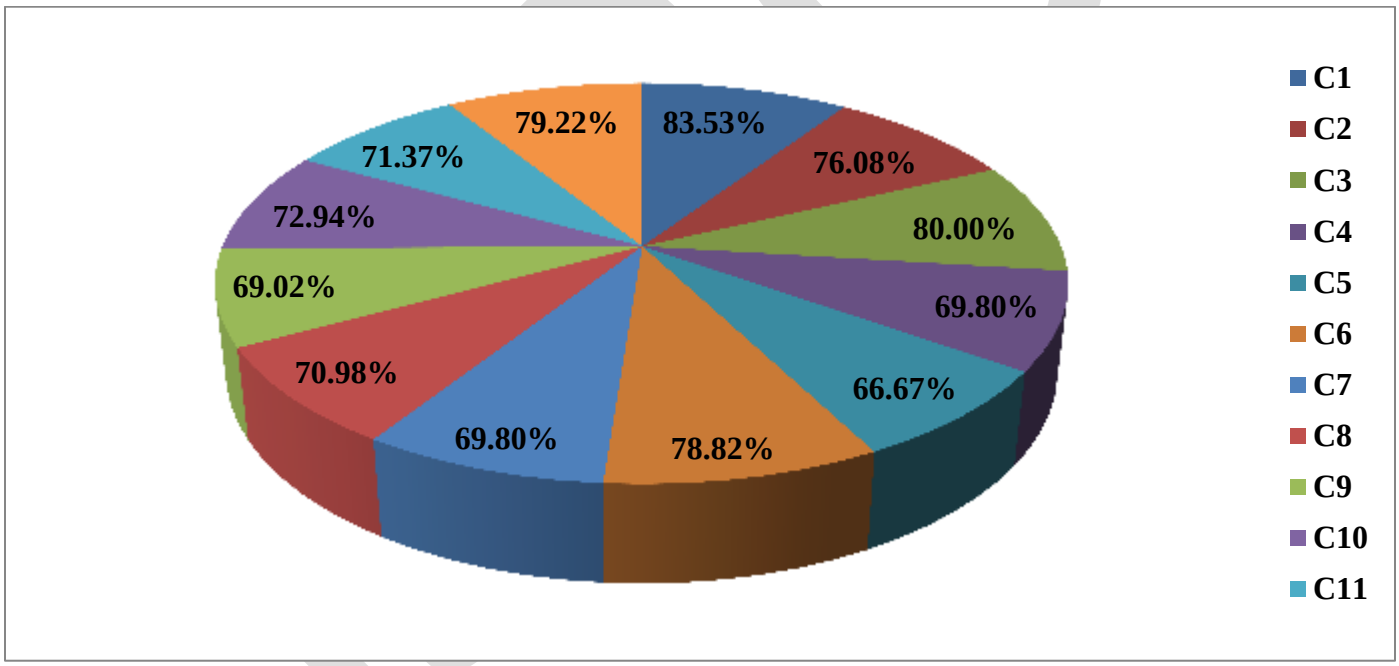

VI.CONCLUSION:-

1.As per survey carried out get many types of answers and responses from the construction sites .The main causes of change orders in construction projects in Pune is owner changes, additional work and modification to prior work. The second main reason is lack of contractor involvement in design stage. It may leads to lack of understanding design at the time of actual construction. The other causes are unrealistic design periods, the lack of communication between contractor and the consultants.

2. The effects are the most important change orders increases the cost of the projects. Likely increase the duration of individual activates that effects on completion schedule of the projects in Pune.Paying extra money for the contractor is the mostly effects caused on many construction sites..

3. The control measure is change is negotiated by the knowledgeable person whether the solution on it or we have to do extra work demolition. The mostly control by the freezing design at certain stage of construction projects. The use of planning technique work breakdown structures, preparation of weekly reports, monthly reports. To hold on project or track the project.

4.At the time of survey one new cause found that the changes need by the customer change as per their requiremnts.This cause lot of extra work but same changes provided at the starting avoid the extra work.

REFERENCES:

1. Engy Serag,Amr Oloufa,Linda Malone and Essam Radwan, "Model for Quantifying the Impact of Change Orders on Project Cost for U.S. Roadwork Construction" J. Constr. Eng. Manage. 2010.136:1015-1027.
2. Ali S. Alnuaimi, Ramzi A. Taha, Mohammed Al Mohsin; and Ali S.Al-Harthi,(2010): Causes, Effects, Benefits, and Remedies of Change Orders on Public Construction Projects in Oman,Asce2010, J. Constr. Eng. Manage 2010.136:615-622.
3. Alia Alaryan, Emadelbeltagi, Ashraf Elshahat and Mahmoud Dawood (2014): Causes and Effects of Change Orders on Construction Projects in Kuwait, ISSN : 2248-9622, Vol. 4, Issue 7(Version 2),July2014.
4. Mohamed M. Anees , Hossam E. Mohamed, Mohamed E. Abdel Razek," Evaluation of change management efficiency of construction contractors" HBRC Journal (2013) 9, 77–85
5. Patrick Keane, Begum Sertyesilisik, Andrew David Ross,(2010) Variations and Change Orders on Construction Projects, J. Leg. Aff. Dispute Resolut. Eng. Constr. 2010.2:89-96.
6. S. Shanmugapriya,Dr. K. Subramanian, "Investigation of significant factors influencing time and cost overruns in Indian construction projects" (ISSN 2250-2459, ISO 9001:2008 Certified Journal, Volume 3, Issue 10, October 2013).
7. Ijaola, I.A and Iyagba R.O,''A Comparative Study of Causes of Change Orders in Public Construction Project in Nigeria and Oman" Journal of Emerging Trends in Economics and Management Sciences (JETEMS) 3(5):495-501 (ISSN:2141-7024).
8. Murali Sambasivan,Yau Wen Soon," Causes and effects of delays in Malaysian construction industry" International Journal of Project Management 25 (2007) 517–526.
9. Alia Alaryan, Emadelbeltagi, Ashraf Elshahat and Mahmoud Dawood." Causes and Effects of Change Orders on Construction Projects in Kuwait" ISSN : 2248-9622, Vol. 4, Issue 7(Version 2), July 2014, pp.01-08.
10. Awad S. Hanna, and Murat Gunduz," Impact of Change Orders on Small Labor-Intensive Projects" J. Constr. Eng. Manage. 2004.130:726-733.
11. Amiruddin Ismail,Towhid Pourrostam,Amir Soleymanzadeh and Majid Ghouyounchizad," Factors Causing Variation Orders and their Effects in Roadway Construction Projects" Research Journal of Applied Sciences, Engineering and Technology 4(23): 4969-4972, 2012 ISSN: 2040-7467.
12. Aftab Hameed Memon, Ismail Abdul Rahman ,Abdul Hameed Memon," Assessing the Occurrence and Significance of VO Factors in affecting Quality of Construction Projects", Life Science Journal 2014; 2014;11(7)

.

International Journal of Engineering Research and General Science Volume 3, Issue 6, November-December, 2015
ISSN 2091-2730

A Review on Implementation Issues in IPv6 Network Technology

[#]Ramesh Chand Meena, [*]Mahesh Bundele
*#Doctoral Scholar, Computer Engineering, *Professor, Computer Engineeing*
School of Engineering and Technology, Poornima University, Jaipur, India
#rameshrmz@yahoo.com
*maheshbundele@gmail.com
[#] *+91-9928041114, *+91-9828999440*

***Abstract*— IPv4 addresses are already depleted in Internet *Assigned Numbers Authority* (IANA) and have exhausted in R*egional Internet Registries (*RIRs) while more clients are continuously adding into the Internet. IPv6, as the only available next generation Internet protocol, is still not commercially successful accepted because a scheme that could solve the migration of IPv4 resources to IPv6 network, as well as mutual communication between the two incompatible protocols, has not been fully developed and deployed. Translation solution provides a proper approach to address this problem. In this review paper, we reviewed research papers presented by the researchers between 2007 and 2015 related to IPv4 & IPv6 resource migration and protocol transition schemes and observed issues related network security, addressing and error detection in the implementation of IPv6.**

Keywords: IPv6 Network Architecture, Security, Addressing, Error Detection, Wireless Networks.

INTRODUCTION

Internet Protocol version 6 (IPv6) is a new generation protocol of the basic internet protocol. Internet Protocol (IP) is a common language of the Internet, every device connected to the Internet must support it. The current version of IPv4 (IP version 4) has several shortcomings which are unavoidable and complicate such exhausted address space, security issues, non availability of auto-configuration and in some cases present a barrier to, the further development of the Internet. The coming IPv6 revolution should remove these barriers and provide a feature-rich environment for the future of global networking. Internet Engineers Task Force released the first RFC specifying the IPv6 were released at the end of 1995 and continuously trying to improve it. Since 1995 IPv6 has not been implemented in completely in real world due some issues like availability of alternative solutions in IPv4, non availability of compatible software, financial investment required in term of compatible equipments, software and security systems. Therefore issues involve in ipv6 implementation has to be analyzed and found the solutions for some of the issues. Further in this section IPv4 and IPv6 described briefly.

IPv4 is the first version of Internet Protocol to be widely used, and accounts for most of today's Internet traffic. There are just over 4 billion IPv4 addresses. While that is a lot of IP addresses, it is not enough to last forever. IPv6 is the sixth revision to the Internet Protocol and the successor to IPv4. It functions similarly to IPv4 in that it provides the unique, numerical IP addresses necessary for Internet-enabled devices to communicate. However, it does sport one major difference: it utilizes 128-bit addresses. We will explain why this is important in a moment.

The major difference between IPv4 and IPv6 is the number of IP addresses. There are 4,294,967,296 IPv4 addresses. In contrast, there are 340,282,366,920,938,463,463,374, 607,431,768,211,456 IPv6 addresses. The technical functioning of the Internet remains the same with both versions and it is likely that both versions will continue to operate simultaneously on networks well into the future. To date, most networks that use IPv6 support both IPv4 and IPv6 addresses in their networks.

TABLE 1: MAJOR DIFFERENCE BETWEEN IPv4 AND IPv6

Key	IPv4	IPv6
Deployment started in	1981	1999
Address Size	32-bit number	128-bit number
Address Format	Dotted Decimal Notation: 192.149.252.76	Hexadecimal Notation: 3FFE:F200:0234:AB00: 0123:4567:8901:ABCD
Prefix Notation	192.149.0.0/24	3FFE:F200:0234::/48
Number of Addresses	2^{32} = ~4,294,967,296	2^{128} = ~340,282,366, 920,938,463,463,374, 607,431,768,211,456

REVIEW PROCESS ADOPTED

The research works published and presented in international reputed journals such as IEEE, Springer, Elsevier etc were taken corresponding to IPv4. The process of the finding review information is mentioned below. The research papers have been studied twice to thrice and prepared the summery and findings paper by paper. The papers have been categorized in four issue categories such as Network Security, Addressing and Error Detection arranged them as per their category. The Key findings have been prepared according to the category and a reference list of all papers has been prepared taking information from papers like Id, Author, Year of Publication, Title, Name of Journal, Name of Publisher, Place of Conference (if any), Volume, Issue, Page Number, Area/ Sub area, and Keys. A sheet was prepared and entered all the information in the sequence as mentioned earlier. The following questionnaire and stages have been used to understand and study the research paper properly: What research area/sub topic does the paper fall under? What problem does the paper attempt to solve? What is the motivation for the problem? What is related work and why is it not sufficient, what are gaps? What key contribution does the paper claim- idea, technique, proof, result etc? Broadly how does the paper solve the problem? How do the authors defend the solution? What is the precise research question addressed? Why is it believed that solution works, better than previous? What are assumptions & scope? What are details of proposed solution - argument, proof, implementation, experiment? What evidence is provided? What is the take away message from the paper? Answers of these questions have been found reading research paper following five stages as mentioned below:

In stage one, we have to get a "feel" for the paper by reading the title, seeing how long the paper is (2 to 40+ pages), where is the paper published, looking at the figures, reading section / sub-section headings. We have to locate the parts such as Title, Abstract, Introduction, Background / Motivation, Contribution of paper, Related work, Problem definition (research questions), Scope/Assumptions/ Limitations, Solution approach, Details of solution - experiment/ system / model, Findings, Evaluation in the uploaded paper and high light on paper.

In stage two, we have to get a big picture about the paper by reading such as title, abstract, introduction, conclusion, by going through the section and sub-section headings and by looking at figures. We have to answer to such questions as what research area / sub-topic does the paper fall under? What problem does the paper attempt to solve? What is the motivation for this problem? Why this paper is needed – i.e. what is related work and why is it not sufficient? What key contribution does the paper claim? Broadly, how does the paper solve the problem? How do the authors defend the solution? What category of paper is this? Making notes while reading paper in margins, using highlighter, in separate notebook / file, references.

In stage three, we have to get details mentioned in the table 1:

Table 1: Stage three details

What we are looking for	Where to find it
What problem does the paper attempt to solve?	Introduction, Problem definition
What is related work? What are gaps?	Introduction, Literature Survey or Related Work
What contribution does the paper claim – idea, technique, proof, surprising result etc?	Introduction, Conclusion
How does the paper solve the problem?	Solution, Experiment, figures
How do the authors defend the solution?	Methodology, Experiment, Results
What is the precise research question addressed?	Introduction, Problem definition
Why is it believed that solution works, better than previous?	Solution approach, figures
What are assumptions, scope?	Problem definition, solution approach
What are details of proposed solution – argument, proof, implementation, experiment?	Solution, System details, Experiment, Methodology, figures
What evidence is provided?	Figures, Results
What is the take-away message from the paper?	Overall

In stage four, we have to evaluate details like: Is the research problem significant? Is the problem novel? Is the solution approach novel? Are the contributions significant? Is relevant related work surveyed "sufficiently" enough? Have alternate approaches of solution been explored? Are assumptions valid? Has paper violated assumptions? Are the claims valid? Are the different parts of the paper consistent? Are the figures, graphs, diagrams precise? Does the paper flow logically? What is the paper trying to convince you of? Does it succeed?

In stage five, we have to synthesize & ask creative questions such as what are some alternative approaches to address the research problem. Could there be a different way to substantiate the claim? Are their counter-examples or arguments against the paper's claims? Are all assumptions identified and validated? How can the research results be improved? How can the results be generalized? What are the new ideas and open problems suggested by this work?

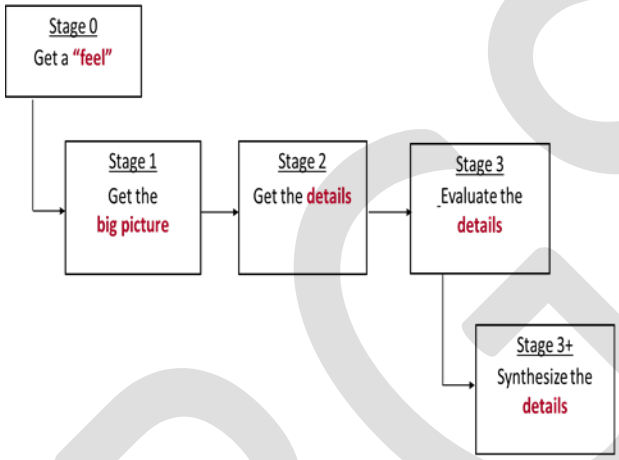

Figure 1: Five stages for reading a research paper

LITERATURE REVIEW

IPv6 Network Technology is becoming popular day by day and the people are accepting the improvements provided in it in respect to the current IPv4 Network Technology. The literature review was carried out taking research papers various reputed journals such as IEEE, Springer & Elsevier in the field of IPv6 network technology implementation and after reviewing research papers we found that there major issues were addressed by the researchers in their research papers are such as Security Issues, Addressing Issues, Error Detection Issues and Optimization Issues. The reviewed papers were categorized as per the issues addressed by them and prepared the summery of paper and issue wise common findings and combined findings of the all issues. The issues-wise number of research papers reviewed are mentioned in the Table 2 as below.

Table 2: Issue-wise number of paper reviewed

Issue	No of Papers
Security	72
Addressing	27
Error Detection	7
Optimization	22

IPv6 Network Security issues were addressed in 72 papers and it has been observed that security meseasurs taken in IPv6 for LAN and WAN cannot be applied in Wireless Sensor Networks(WSN) as it was due to the less processing ability and limited energy resource and it hindered the IPv6 implementaion in WSN. In paper [54] researchers have porposed an compressed Authentication Header (AH) and Encapsulating Security Payload (ESP) to use the IPSec in IPv6 over Low power Wireless Personal Area Networks (6LoWPAN) and it reduced size of IPSec Header to reduce the processing cost and increase the energy efficiency. Interfece ID aloing with Simple Secure Address System (SSAS) was proposed in [89] to secure host address from various security attacks by generating

random IPv6 addresses. One more approach Secure Address Validation Improvement (SAVI) propsoed by the researchers [128] to provided validation check of the IP address binding it on FCFS basis with network switch port and MAC address of the host creating a binding table at switch level. Later Internet Engineers Task Force (IEFT)[9] had accepted the SAVI as a standard for protection from spoofing attacks. The researches [95] have proposed i-SeRP system for assesment of vulenrabilities of IPv6 and other researchers [73] desinged and implemented 6Foren which was an online network foreincics prototype system in IPv6 enfiromement for HTTP, FTP, SMTP & POP protocols.

In IPv6 implementation, addressing issues were also faced and the the researchers provided various approaches and solutions to deal with them. It could be found during review many reseachers were dealing with this issue. One paper [36] proposed a Micro Sensor Routing Protocol for the wireless network to provide better performance than an Demand Distance Vector (AODV) algorithm. The reseach paper [49] proposed an IPv6 in IPv4-UDP tunneling protocol to provide the IPv6 in IPv4 and it improved the packet's poor latecy in relay time in respect to Miredo-relay from 9.76us to 8.21us. The Escort protocol analysed on the basis of packet processing latency and it was around 6us ~ 10us along with more security, sported mobility and multi-homing with capability of traversing symmetric NATs. In [58] had poposed an IPv6 address auto-configuration in LoWPAN along with AH & ESP and Policy Based Security for 6LoWPAN.

In the error detection paper [101] propsoed improved CRC based Packet Recovery Mechanism for Wireless Network to reduced computation and resource consumption for CRC based Packet Recoveries. The paper proposed [86] CRC checking at Network Layer to reduce link layer processing overheads and increased the performance of link layer.

In the Network Optimization paper [103] proposed Memory Management system to overcome the memory buffer overflow issue in implementaion of IPv6 in LoWPAN. The paper [97] proposed IPv6 based Database Retrieval System for Wireless Sensor Networks using BLIP to establish connectivity.

The major approaches /Techniques proposed by the researchers are mentioned below table 3.

Table 3: Issue-wise Major Solution Approaches

Approach/ Technique Used	Problem solved
• **Security Issues**	
Compressed AH & ESP for 6LoWPAN	Successful secure integration of IPv6 WSN with the internet.
Policy Based Security	Policy Based Security Management (PBSM) new theoritical approach to allow the secure deployment of the host based security (HBS) system
Simple Secure Addressing Scheme (SSAS)	Sucessfully provided privacy & security by randomizing the IID, adding SSAS signature, using RPKI and binding between the public key and IP address
Object Risk Based Access Control (OrBAC)	Conceptual Security mechanism for new distributed firewall techniques.
Secure address Validation Improvements (SAVI)	System protected from address resolution attacks by checking NS & NA messages coming from validating ports.
i-SeRP risk assessment system	Developed tool useful for assessment of the IPv6 network security risks
Online Forensic tool (6Foren)	6Foren system sucessfully recorded attack event replays in Attack Event Database
• **Addressing Issue**	
Micro Sensor Routing Protocol	carried out performance comparisons on Packet Delivery Ratio, Average End to end Delay and Routing Overhead and MSRP has better performance compared to AODV.
Escort Tunneling Protocol	Escort protocol analysed on the basis of packet processing latency and it was around 6us ~ 10us along with more security, sported mobility and multi-homing with capability of traversing symmetric

	NATs .
Auto-configuration Implementation in LoWPAN	Theoritically reduced the header size and decreased the communication and save nodes energy to extend the average life time of the entire network.
• **Error Detection Issue**	
CRC based Packet Recovery Mechanism for Wireless Network	System reduced computation and resource consumption for CRC based Packet Recovery
CRC checking at Network Layer	reduced link layer processing overheads and increased the performance of link layer
• **Network Optimization issues**	
Memory Management system in 6LoWPAN	Buffer Overflow memory problem was successfully resolved in Wireless Sensor Networks
IPv6 based Database Retrieval System for Wireless Sensor Networks	It provided the concept for the research to implement database retrieval system in the Wireless Sensor Networks.

In this section we mentioned the technologies and approached discussed in various papers and the next section will discussed about the key findings of this review paper.

IV KEY FINDINGS OF SURVEY

In this section we mentioned the various key findings in the field of Security, address, Error detection and Wireless Sensor issues addressed by varous papers for implementaion of IPv6.

Out come of survey in Network Security:

- Researchers implemented AH & ESP technologies for 6LoWPAN and Policy Based Security.
- Moving Target IPv6 Defense custom security application, Email spam filtering techniques, Simple Secure Addressing Scheme, Trust Relationship with DNS Server, i-SeRP risk assessment system, data structure based on SNMP and Netflow, Online Forensic tool, Source Address Validation Improvements(SAVI), Object Risk Based Access Control (OrBAC) techniques were proposed.
- It could be found that some techniques required more computational cost for sharing security information and sometimes required manual intervention.
- Security provisions and techniques discussed were OPNET System-in-the-Loop, IP Packet Header, Asymmetric Cryptography, Secure Neighbor Discovery, DNS RDATA Field, ACK-Reset and packet Fragmentation, SNMP data, Netflow record, IPSec & SAVI.
- Antispoofing approaches were proposed by the researchers at Inter-AS such as
  - IEF Ingress/Egress Filtering
  - DPF Distributed Packet Filtering
  - uRPF Unicast Reverse Path Forwarding
  - IDPF Inter-Domain Packet Filter
  - SPM Spoofing Prevention Method
  - MEF Mutual Egress Filtering
  - Passport Packet Passport
  - SAVE Source Address Validation Enforcement
- Most of the approaches for against IP spoofing, DNS Dynamic Update Spoofing, SYN Flood were tested using test-beds or networks simulators like Graphics Network Simulator – 3.
- SAVA protocol/architecture was first proposed in 2007 for Inter-AS, Intra-AS and First-hop only but did not considered dynamic behavior of network hardware & mobility of devices. SAVD device was first implemented in 2008 using SMP & ARBIF and tested for spoofing attacks but found performance degradation in terms of packet drops.
- Later in 2009 SAVA was modified as SAVI with fine grained Intra-domain filtering mechanism using truth chains between source IP address & associated Leyer-2 & further in 2011 few experimentation on SAVI were carried out but without considering dynamic behavior of the network handover and mobility.
- In 2011 SAVI was modified as VAVE (Virtual-source Address Validation Edge) to filter legacy traffic but with increased overhead. SAVA was implemented with cryptographic technique (hash function) for improving security in simulation environment. Various variants of SAVI was proposed in subsequent researches such as In 2012 FCFS-SAVI was applied to MAC layer but with increase in processing load on CPU, In 2012 SAVE & SIP based SAV was proposed integrating with password with theoretical validation.

- In 2014 SAVI was tested for CPU utilization in simulation experiments.
- In 2015 as comparative study of various security mechanisms such as IEF, DFP, uRPF, IDPF, SAVE, SPM and Passport has been carried out with respect to deployment benefits, cost and risk and found that SAVE posses medium level of characteristics for all the those, however SPM and Passport could provide better scenario when tested with different filtering mechanisms in Inter-AS collaboration.
- Other antispoofing mechanisms & security methods proposed were Passport (2009), Link-State based Antispoofing (2014) but former has added time & space overheads and the later had limitation of compatibility with other link-state protocols other than OSPF.
- A study of authentication and privacy protection in 5G HetNets using SDN has been carried out in 2015 but for limited number of 5G cells in MatLab environment proposed two algorithms; one for user SCI based authentication handover and other for partial data offloading in SDN controller data paths.

Out come of survey in IPv6 Addresssing:

- Authors implemented Dual Stack Networks and IPv6 Address Auto-configuration in 6LoWPAN.
- Researchers developed techniques such as Micro Sensor Routing, Escort Tunneling system, Fragment & Header Size Optimization for LAN, Mobile Routing and Proxy Mobile IPv6 for Network Mobility, IPSec gateway failure prevention & Network Performance Testing tools.
- Most of techniques were implemented and tested using network simulators for evaluation of performance of the proposed solutions and few of them used the real test environment.
- Research works discussed various issues of IPv6 Addressing like auto-configuration, security during dual stack, security lapses and algorithms like routing, NAT, CGA, SEND, MAC & Multicasting.

Out come of survey in Error Detection :

- Algorithms were proposed to reduce processing time in high speed data transmission, CRC based Packet Recovery Mechanism for Wireless Network, CRC checking at Network Layer to reduce link layer processing overheads and comparative study was carried out for various error detection & correction techniques.
- Gigabit Ethernet Network was used for testing of the proposed algorithms and some of them used the Simulators for testing of the algorithms.
- CRC checking was carried out at Network Layer reduced link layer processing overheads and increased the performance of link layer.
- CRC checking algorithms can be optimized for the various types of networks and need the testing in the real time network environment.

Out come of survey in Network Optimization:

- IP Header Compression Techniques were proposed by researchers such as Stateless IP Header Compression (2005), Layered IP Header Compression for IP-enabled Sensor Networks (2006), Robust Header Compression in Network Mobility Applications (2008), Tunneling Header Compression Protocol(TuCP) in Wireless Network (2010), End-to-End Header Compression over SDNs(2012), Header Compression in Cellular IP Networks(2012), Header Compression Scheme in 6LoWPAN(2013) , Mobile Adhoc Networks (MANET) IP Header Compression (MIPHC) (2013) to reduce size of header and enhance the speed of a specific type of network traffic.
- The most of the researches proposed some improvements & modifications in the earlier proposed Header Compression technique.
- In 2008 a Memory Management System for IPv6 Wireless Sensor Networks was proposed to resolve the buffer overflow problems during 6LoWPAN implementation.
- In 2012 a comparative study on routing schemes of IP based WSN was carried out to check the performance of two schemes and proposed an improved route-over scheme to apply this Sensor-Grid Infrastructure in health-care application.
- In 2012 an implement IPv6 based Data Retrieval System for WNS research was proposed and successfully implemented in the test environment.
- In 2012 & 2013 surveys on ROHC header compression schemes were carried out to illustrate the states and modes, process of the compressor and de-compressor
- In 2013 a better Network Latency with End-to-End Header Compression in Software Defined Networking Architecture was proposed to reduce the packet size and time delay.

In this section we mentioned the various technologies proposed by the research papers during our review and next section will discussed the objective the this litrature review paper.

V OBEJCTIVES OF LITRATURE REVIEW

We proposed a review of the techniques and approaches proposed the various researchers for addressing IPv6 implementation issues related Security, addressing, Error detection and Wireless Network. As per our review we found that most of the researchers have worked in the field of the Security issue and Addressing issues still there is scope for the research in this area and test the solution by implementing in real world. The error detection techniques are very much required which should provide the high performance in the Ethernet network. In the current world wireless network is becoming very popular and it is involved in the every one's life. Various issues in wireless network are to be addressed to implement IPv6 application in with high performance and low power requirements.

CONCLUSION

The literature review has been carried out in the field of IPv6 Network Technology Implementation downloading papers published between 2007 and 2015 in IEEE journals & conferences to get status of the technology implementation, issues faced during implementation and which are still required to be resolved by doing further research. After review of 128 research papers we found that there were four basic issues faced in the technology such as Security issues, Addressing issues, Error detection issues and Wireless Sensor Network issues. The researchers have provided various solutions for the issues faced in implementation of IPv6 which have been discussed above in section III of this paper. It has been observed after literature review that there are many gaps in the research papers and needs more work to be done further. The identified research fields may be in the area of Security Solutions, Addressing solutions, Error Detection & Correction solutions and Wireless Sensor Networks Solutions. It also has been observed that to refine the research area in the above mentioned fields we need more exhaustive literature survey therefore the literature survey will be continued till we completes the identification and finalization of typical area selection.

ACKNOWLEDGMENTS

First and foremost we would like to acknowledge the Poornima University, Jaipur who gave us an opportunity for this Literature Survey. We are thankful to Dr Manoj Gupta, Dean, SET, Poornima University, Jaipur for providing support and facilities us for joining and continuing the research program at the University.

REFERENCES:

[1] Ahmed, A.S.; Hassan, R.; Ali, Z.M., "Eliminate spoofing threat in IPv6 tunnel," in *Information Science and Digital Content Technology (ICIDT), 2012 8th International Conference on* , vol.1, no., pp.218-222, 26-28 June 2012

[2] Ahsan Chishti, M.; Ahanger, A.M.; Qureshi, S.; Mir, A.H., "Performance analysis of Source Specific Multicast over Internet Protocol version 6 with Internet Protocol version 4 in a test bed," in *Consumer Communications and Networking Conference (CCNC), 2013 IEEE* , vol., no., pp.956-961, 11-14 Jan. 2013

[3] Ali, W.N.A.W.; Taib, A.H.M.; Hussin, N.M.; Budiarto, R.; Othman, J., "Distributed security policy for IPv6 deployment," in *Sustainable Energy & Environment (ISESEE), 2011 3rd International Symposium & Exhibition in* , vol., no., pp.120-124, 1-3 June 2011

[4] Ali, W.N.A.W.; Taib, A.H.M.; Hussin, N.M.; Othman, J., "IPv6 attack scenarios testbed," in *Humanities, Science and Engineering Research (SHUSER), 2012 IEEE Symposium on* , vol., no., pp.927-932, 24-27 June 2012

[5] Alsa'deh, A.; Rafiee, H.; Meinel, C., "Stopping time condition for practical IPv6 Cryptographically Generated Addresses," in *Information Networking (ICOIN), 2012 International Conference on* , vol., no., pp.257-262, 1-3 Feb. 2012

[6] Altaher, A.; Ramadass, S.; Ali, A., "A dual stack IPv4/IPv6 testbed for malware detection in IPv6 networks," in *Control System, Computing and Engineering (ICCSCE), 2011 IEEE International Conference on* , vol., no., pp.168-170, 25-27 Nov. 2011

[7] Awwad, S.A.B.; Chee Kyun Ng; Noordin, N.K.; Ali, B.M.; Hashim, F., "Second and subsequent fragments headers compression scheme for IPv6 header in 6LoWPAN network," in *Sensing Technology (ICST), 2013 Seventh International Conference on* , vol., no., pp.771-776, 3-5 Dec. 2013

[8] Azarmi, M.; Bhargava, B.; Angin, P.; Ranchal, R.; Ahmed, N.; Sinclair, A.; Linderman, M.; Othmane, L.B., "An End-to-End Security Auditing Approach for Service Oriented Architectures," in *Reliable Distributed Systems (SRDS), 2012 IEEE 31st Symposium on* , vol., no., pp.279-284, 8-11 Oct. 2012

[9] Bagnulo, M.; Garcia-Martinez, A., "SAVI: The IETF standard in address validation," in *Communications Magazine, IEEE* , vol.51, no.4, pp.66-73, April 2013

[10] Balman, M.; Kosar, T., "Early Error Detection and Classification in Data Transfer Scheduling," in *Complex, Intelligent and Software Intensive Systems, 2009. CISIS '09. International Conference on* , vol., no., pp.457-462, 16-19 March 2009

[11] Baobao Zhang; Jun Bi; Jianping Wu, "LAS: An effective anti-spoofing method using existing information," in *Computer Communication and Networks (ICCCN), 2014 23rd International Conference on* , vol., no., pp.1-8, 4-7 Aug. 2014

[12] Barrera, D.; Van Oorschot, P., "Security visualization tools and IPv6 addresses," in *Visualization for Cyber Security, 2009. VizSec 2009. 6th International Workshop on* , vol., no., pp.21-26, 11-11 Oct. 2009

[13] Beck, F.; Festor, O.; Chrisment, I.; Droms, R., "Automated and secure IPv6 configuration in enterprise networks," in *Network and Service Management (CNSM), 2010 International Conference on* , vol., no., pp.64-71, 25-29 Oct. 2010

[14] Bhunia, S.S.; Sikder, D.K.; Roy, S.; Mukherjee, N., "A comparative study on routing schemes of IP based wireless sensor network," in *Wireless and Optical Communications Networks (WOCN), 2012 Ninth International Conference on* , vol., no., pp.1-5, 20-22 Sept. 2012

[15] Bi, Jun; Jianping Wu; Xing Li; Xiangbin Cheng, "An IPv6 Test-Bed Implementation for a Future Source Address Validation Architecture," in *Next Generation Internet Networks, 2008. NGI 2008* , vol., no., pp.108-114, 28-30 April 2008

[16] Bingyang Liu; Jun Bi, "On the deployability of inter-AS spoofing defenses," in *Network, IEEE* , vol.29, no.3, pp.82-87, May-June 2015

[17] Bingyang Liu; Jun Bi; Vasilakos, A.V., "Toward Incentivizing Anti-Spoofing Deployment," in *Information Forensics and Security, IEEE Transactions on* , vol.9, no.3, pp.436-450, March 2014

[18] Biswash, S.K.; Kumar, C.; Peruru, M.K.; Tyagi, N., "Transferring header compression context in cellular IP networks," in *Recent Advances in Information Technology (RAIT), 2012 1st International Conference on* , vol., no., pp.285-289, 15-17 March 2012

[19] Bow-Nan Cheng; Moore, S., "Securing Robust Header Compression (ROHC)," in *Military Communications Conference, MILCOM 2013 - 2013 IEEE* , vol., no., pp.1383-1390, 18-20 Nov. 2013

[20] Bow-Nan Cheng; Wheeler, J.; Hung, B., "Internet protocol header compression technology and its applicability on the tactical edge," in *Communications Magazine, IEEE* , vol.51,

no.10, pp.58-65, October 2013

[21] Bow-Nan Cheng; Wheeler, J.; Hung, B.; Moore, S.; Sukumar, P., "A comparison of IP header compression schemes in MANETs," in *Performance Computing and Communications Conference (IPCCC), 2013 IEEE 32nd International* , vol., no., pp.1-9, 6-8 Dec. 2013
[22] Bow-Nan Cheng; Zuena, J.; Wheeler, J.; Moore, S.; Hung, B., "MANET IP Header Compression," in *Military Communications Conference, MILCOM 2013 - 2013 IEEE* , vol., no., pp.494-503, 18-20 Nov. 2013
[23] Caicedo, C.E.; Joshi, J.B.D.; Tuladhar, S.R., "IPv6 Security Challenges," in *Computer* , vol.42, no.2, pp.36-42, Feb. 2009
[24] Carp, A.; Soare, A.; Rughinis, R., "Practical analysis of IPv6 security auditing methods," in *Roedunet International Conference (RoEduNet), 2010 9th* , vol., no., pp.36-41, 24-26 June 2010
[25] Chakravorty, S., "Challenges of IPv6 Flow Label implementation," in *Military Communications Conference, 2008. MILCOM 2008. IEEE* , vol., no., pp.1-6, 16-19 Nov. 2008
[26] Chandra, D.G.; Kathing, M.; Kumar, D.P., "A Comparative Study on IPv4 and IPv6," in *Communication Systems and Network Technologies (CSNT), 2013 International Conference on* , vol., no., pp.286-289, 6-8 April 2013
[27] Chanjuan Liu; Yilei Wang; Tao Li, "The Application of Saftey Audit and Monitor Technology in Power Management," in *Services Science, Management and Engineering, 2009. SSME '09. IITA International Conference on* , vol., no., pp.548-552, 11-12 July 2009
[28] Cheng Min, "Research on network security based on IPv6 architecture," in *Electronics and Optoelectronics (ICEOE), 2011 International Conference on* , vol.1, no., pp.V1-415-V1-417, 29-31 July 2011
[29] Cheng Min, "Research on network security based on IPv6 architecture," in *Electronics and Optoelectronics (ICEOE), 2011 International Conference on* , vol.1, no., pp.V1-415-V1-417, 29-31 July 2011
[30] Choudhary, A.R., "In-depth analysis of IPv6 security posture," in *Collaborative Computing: Networking, Applications and Worksharing, 2009. CollaborateCom 2009. 5th International Conference on* , vol., no., pp.1-7, 11-14 Nov. 2009
[31] Choudhary, A.R.; Sekelsky, A., "Securing IPv6 network infrastructure: A new security model," in *Technologies for Homeland Security (HST), 2010 IEEE International Conference on* , vol., no., pp.500-506, 8-10 Nov. 2010
[32] Clore, B.; Dunlop, M.; Marchany, R.; Tront, J., "Validating a custom IPv6 security application using OPNET modeler," in *MILITARY COMMUNICATIONS CONFERENCE, 2012 - MILCOM 2012* , vol., no., pp.1-6, Oct. 29 2012-Nov. 1 2012
[33] Daniels, W.; Vanbrabant, B.; Hughes, D.; Joosen, W., "Automated allocation and configuration of dual stack IP networks," in *Integrated Network Management (IM 2013), 2013 IFIP/IEEE International Symposium on* , vol., no., pp.1148-1153, 27-31 May 2013
[34] Debbarma, S.; Debnath, P., "Internet protocol version 6 (IPv6) Extension Headers: Issues, challenges and mitigation," in *Computing for Sustainable Global Development (INDIACom), 2015 2nd International Conference on* , vol., no., pp.923-928, 11-13 March 2015
[35] Dequan Yang; Xu Song; Qiao Guo, "Security on IPv6," in *Advanced Computer Control (ICACC), 2010 2nd International Conference on* , vol.3, no., pp.323-326, 27-29 March 2010
[36] Deyun Gao; Yanchao Niu; Hongke Zhang, "Micro Sensor Routing Protocol in IPv6 wireless sensor network," in *Networking, Sensing and Control, 2009. ICNSC '09. International Conference on* , vol., no., pp.55-59, 26-29 March 2009
[37] Dhall, H.; Dhall, D.; Batra, S.; Rani, P., "Implementation of IPSec Protocol," in *Advanced Computing & Communication Technologies (ACCT), 2012 Second International Conference on* , vol., no., pp.176-181, 7-8 Jan. 2012
[38] Dhanaraj, S.; Karthikeyani, V., "A study on e-mail image spam filtering techniques," in *Pattern Recognition, Informatics and Mobile Engineering (PRIME), 2013 International Conference on* , vol., no., pp.49-55, 21-22 Feb. 2013
[39] Fei Ren; Huachun Zhou, "Implementation and Test of PMIPv6 Dual Stack Protocol," in *Innovative Mobile and Internet Services in Ubiquitous Computing (IMIS), 2012 Sixth International Conference on* , vol., no., pp.305-310, 4-6 July 2012
[40] Feng Qiaojuan; Wei Xinhong, "A new research on DoS/DDoS security detection model," in *Computer Engineering and Technology (ICCET), 2010 2nd International Conference on* , vol.3, no., pp.V3-437-V3-440, 16-18 April 2010
[41] Garcia-Martinez, A.; Bagnulo, M., "An Integrated Approach to Prevent Address Spoofing in IPv6 Links," in *Communications Letters, IEEE* , vol.16, no.11, pp.1900-1902, November 2012
[42] Govindarajan, K.; Setapa, S.; Kong Chee Meng; Hong Ong, "Interoperability issue between IPv4 and IPv6 in OpenFlow enabled network: IPv4 and IPv6 transaction flow traffic," in *Computer, Control, Informatics and Its Applications (IC3INA), 2014 International Conference on* , vol., no., pp.58-63, 21-23 Oct. 2014
[43] Granjal, J.; Monteiro, E.; Sa Silva, J., "A secure interconnection model for IPv6 enabled wireless sensor networks," in *Wireless Days (WD), 2010 IFIP* , vol., no., pp.1-6, 20-22 Oct. 2010
[44] Granjal, J.; Monteiro, E.; Sa Silva, J., "Enabling Network-Layer Security on IPv6 Wireless Sensor Networks," in *Global Telecommunications Conference (GLOBECOM 2010), 2010 IEEE* , vol., no., pp.1-6, 6-10 Dec. 2010
[45] Gregr, M.; Matousek, P.; Sveda, M.; Podermanski, T., "Practical IPv6 monitoring-challenges and techniques," in *Integrated Network Management (IM), 2011 IFIP/IEEE International Symposium on* , vol., no., pp.650-653, 23-27 May 2011
[46] Guang Yao; Bi, Jun, "Design and Implementation of an IPv6 Source Address Validation Device," in *Networking and Services, 2008. ICNS 2008. Fourth International Conference on* , vol., no., pp.236-241, 16-21 March 2008
[47] Guang Yao; Jun Bi; Vasilakos, A.V., "Passive IP Traceback: Disclosing the Locations of IP Spoofers From Path Backscatter," in *Information Forensics and Security, IEEE Transactions on* , vol.10, no.3, pp.471-484, March 2015
[48] Guangwu Hu; Ke Xu; Jianping Wu; Yong Cui; Fan Shi, "A general framework of source address validation and traceback for IPv4/IPv6 transition scenarios," in *Network, IEEE* , vol.27, no.6, pp.66-73, November-December 2013
[49] Hailin An; Wanming Luo; Xingfeng Li; Xinchang Zhang; Baoping Yan, "A New IPv6 Tunneling Protocol: Escort," in *Computer Network and Multimedia Technology, 2009. CNMT 2009. International Symposium on* , vol., no., pp.1-6, 18-20 Jan. 2009
[50] Hao Shuai; Huang Xiaohong; Ma Yan, "A simple packet authentication mechanism based on stateless core approach," in *GLOBECOM Workshops (GC Wkshps), 2010 IEEE* , vol., no., pp.503-507, 6-10 Dec. 2010
[51] Hong Zheng; Wu Lifa; Li Huabo; Pan Fan, "Worm detection and containment in local networks," in *Computer Science and Information Processing (CSIP), 2012 International Conference on* , vol., no., pp.595-598, 24-26 Aug. 2012
[52] Hu Jinlong; Liao Bin, "SIP Security Architecture Based on Source Address Validation," in *Computer Science & Service System (CSSS), 2012 International Conference on* , vol., no., pp.300-303, 11-13 Aug. 2012
[53] Hu Jinlong; Wu Yisheng, "Source address validation based Ethernet switches for IPv6 network," in *Computer Science and Automation Engineering (CSAE), 2012 IEEE International Conference on* , vol.3, no., pp.84-87, 25-27 May 2012
[54] Hui Wei; Sun You-ye; Liu Jiang; Lu Kai-ning, "DDoS/DoS Attacks and Safety Analysis of IPv6 Campus Network: Security Research under IPv6 Campus Network," in *Internet Technology and Applications (iTAP), 2011 International Conference on* , vol., no., pp.1-4, 16-18 Aug. 2011
[55] Hyon-Young Choi; Sung-Gi Min; Youn-Hee Han; Jungsoo Park; Hyoungjun Kim, "Implementation and Evaluation of Proxy Mobile IPv6 in NS-3 Network Simulator," in *Ubiquitous Information Technologies and Applications (CUTE), 2010 Proceedings of the 5th International Conference on* , vol., no., pp.1-6, 16-18 Dec. 2010
[56] Jayanthi, J.G.; Rabara, S.A., "IPv6 Addressing Architecture in IPv4 Network," in *Communication Software and Networks, 2010. ICCSN '10. Second International Conference on* , vol., no., pp.461-465, 26-28 Feb. 2010
[57] Jianping Wu; Gang Ren; Xing Li, "Source Address Validation: Architecture and Protocol Design," in *Network Protocols, 2007. ICNP 2007. IEEE International Conference on* , vol., no., pp.276-283, 16-19 Oct. 2007
[58] Jing Peng; Kaikai Chi; Yihua Zhu; Jing Wang, "Optimal packet fragmentation scheme for reliable and energy-efficient packet delivery in 6LoWPAN," in *Cloud Computing and Intelligent Systems (CCIS), 2012 IEEE 2nd International Conference on* , vol.03, no., pp.1106-1111, Oct. 30 2012-Nov. 1 2012
[59] Jingtao Su; Xianwei Zhou, "IVIT: A core stateless IPV4/IPV6 transition mechanism combining translation and tunnel technologies," in *Cyberspace Technology (CCT 2013), International Conference on* , vol., no., pp.252-257, 23-23 Nov. 2013
[60] Jivorasetkul, S.; Shimamura, M.; Iida, K., "Better network latency with end-to-end header compression in SDN architecture," in *Communications, Computers and Signal Processing (PACRIM), 2013 IEEE Pacific Rim Conference on* , vol., no., pp.183-188, 27-29 Aug. 2013
[61] Jivorasetkul, S.; Shimamura, M.; Iida, K., "End-to-End Header Compression over Software-Defined Networks: A Low Latency Network Architecture," in *Intelligent Networking and Collaborative Systems (INCoS), 2012 4th International Conference on* , vol., no., pp.493-494, 19-21 Sept. 2012
[62] Jong Tak Park; Dae In Choi; Su Yeon Kim; Kahng, H.K., "IP header translation protocol design and implementation to a post wireless network service," in *Advanced Communication Technology (ICACT), 2011 13th International Conference on* , vol., no., pp.453-457, 13-16 Feb. 2011

[63] Karapistoli, E.; Economides, A.A., "Wireless sensor network security visualization," in *Ultra Modern Telecommunications and Control Systems and Workshops (ICUMT), 2012 4th International Congress on* , vol., no., pp.850-856, 3-5 Oct. 2012
[64] Ketari, L.M.; Chandra, M.; Khanum, M.A., "A Study of Image Spam Filtering Techniques," in *Computational Intelligence and Communication Networks (CICN), 2012 Fourth International Conference on* , vol., no., pp.245-250, 3-5 Nov. 2012
[65] Khan, A.U.; Oriol, M.; Kiran, M.; Ming Jiang; Djemame, K., "Security risks and their management in cloud computing," in *Cloud Computing Technology and Science (CloudCom), 2012 IEEE 4th International Conference on* , vol., no., pp.121-128, 3-6 Dec. 2012
[66] Kharche, S.; Mahajan, A., "IPv4 and IPv6 performance comparison for simulated DNS and VoIP traffic in Windows 2007 and Windows 2008 client server environment," in *Information and Communication Technologies (WICT), 2012 World Congress on* , vol., no., pp.408-412, Oct. 30 2012-Nov. 2 2012
[67] Kukec, A.; Bagnulo, M.; Mikuc, M., "SEND-based source address validation for IPv6," in *Telecommunications, 2009. ConTEL 2009. 10th International Conference on* , vol., no., pp.199-204, 8-10 June 2009
[68] Kumar, A.; Mani, R.S., "First hop security considerations in IPV6 implementation," in *Confluence 2013: The Next Generation Information Technology Summit (4th International Conference)* , vol., no., pp.227-235, 26-27 Sept. 2013
[69] Kumar, M.R.; Ramadass, S., "Ipv6 Address Space Allocation Schemes - Issues and Challenges, A Survey," in *Network Applications Protocols and Services (NETAPPS), 2010 Second International Conference on* , vol., no., pp.170-175, 22-23 Sept. 2010
[70] Kushwaha, S., "The Next Generation IP based packet transmission for 6LoWPAN," in *Power, Control and Embedded Systems (ICPCES), 2012 2nd International Conference on* , vol., no., pp.1-5, 17-19 Dec. 2012
[71] Li Junyi; Su Fei; Lin Zhaowen; Ma Yan, "The research and analysis of worm scanning strategies in IPv6 network," in *Network Operations and Management Symposium (APNOMS), 2011 13th Asia-Pacific* , vol., no., pp.1-4, 21-23 Sept. 2011
[72] Likitkhajorn, C.; Surarerks, A.; Rungsawang, A., "An approach of two-way spam detection based on boosting pages analysis," in *Electrical Engineering/Electronics, Computer, Telecommunications and Information Technology (ECTI-CON), 2012 9th International Conference on* , vol., no., pp.1-4, 16-18 May 2012
[73] Liu Wu; Ren Ping; Sun Donghong; Zhao Yawei; Wu Jian-ping, "Protocol Analysis and Online Forensics in IPv6 Network Environment," in *Wireless Communications, Networking and Mobile Computing (WiCOM), 2012 8th International Conference on* , vol., no., pp.1-4, 21-23 Sept. 2012
[74] Lv Li; Yang Jiankang; Huo Jinghe, "Research on the Security Issues and Counter Measures of Wireless Mesh Network," in *Wireless Communications, Networking and Mobile Computing (WiCOM), 2012 8th International Conference on* , vol., no., pp.1-3, 21-23 Sept. 2012
[75] Meenakshi, S.P.; Raghavan, S.V.; Bhaskar, S.M., "A study on path behavior characteristics of IPv6 based reflector attacks," in *Local Computer Networks (LCN), 2011 IEEE 36th Conference on* , vol., no., pp.927-933, 4-7 Oct. 2011
[76] Moravejosharieh, A.; Modares, H.; Salleh, R., "Overview of Mobile IPv6 Security," in *Intelligent Systems, Modelling and Simulation (ISMS), 2012 Third International Conference on* , vol., no., pp.584-587, 8-10 Feb. 2012
[77] Murugesan, R.K.; Ramadass, S.; Budiarto, R., "Improving the performance of IPv6 packet transmission over LAN," in *Industrial Electronics & Applications, 2009. ISIEA 2009. IEEE Symposium on* , vol.1, no., pp.182-187, 4-6 Oct. 2009
[78] Murugesan, R.K.; Ramadass, S.; Budiarto, R., "Increased performance of IPv6 packet transmission over ethernet," in *Computer Science and Information Technology, 2009. ICCSIT 2009. 2nd IEEE International Conference on* , vol., no., pp.171-175, 8-11 Aug. 2009
[79] Nakamoto, G.; Durst, R.; Growney, C.; Andresen, J.; Ma, J.; Trivedi, N.; Quang, R.; Pisano, D., "Identity-Based Internet Protocol Networking," in *MILITARY COMMUNICATIONS CONFERENCE, 2012 - MILCOM 2012* , vol., no., pp.1-6, Oct. 29 2012-Nov. 1 2012
[80] Ning-ning Lu; Hua-Chun Zhou; Hong-ke Zhang, "A New Source Address Validation Scheme Based on IBS," in *Information Assurance and Security, 2009. IAS '09. Fifth International Conference on* , vol.2, no., pp.334-337, 18-20 Aug. 2009
[81] Ning-ning Lu; Hua-Chun Zhou; Hong-ke Zhang, "The Effectiveness of Passport Source Address Validation Scheme," in *Information Processing, 2009. APCIP 2009. Asia-Pacific Conference on* , vol.2, no., pp.92-95, 18-19 July 2009
[82] Palomares, D.; Migault, D.; Laurent, M., "Failure preventive mechanism for IPsec gateways," in *Communications and Information Technology (ICCIT), 2013 Third International Conference on* , vol., no., pp.167-172, 19-21 June 2013
[83] Pengxu Tan; Yue Chen; Hongyong Jia; Jiangdong Mao, "A hierarchical source address validation technique based on cryptographically generated address," in *Computer Science and Automation Engineering (CSAE), 2011 IEEE International Conference on* , vol.2, no., pp.33-37, 10-12 June 2011
[84] Plonka, D.; Barford, P., "Assessing performance of Internet services on IPv6," in *Computers and Communications (ISCC), 2013 IEEE Symposium on* , vol., no., pp.000820-000826, 7-10 July 2013
[85] Prakash, A.; Verma, R.; Tripathi, R.; Naik, K., "A Mobile IPv6 Based Route Optimization Scheme for Mobile Networks," in *India Conference (INDICON), 2009 Annual IEEE* , vol., no., pp.1-4, 18-20 Dec. 2009
[86] Praptodiyono, S.; Murugesan, R.K.; Budiarto, R.; Ramadass, S., "Handling transmission error for IPv6 packets over high speed networks," in *Distributed Framework and Applications, 2008. DFmA 2008. First International Conference on* , vol., no., pp.159-163, 21-22 Oct. 2008
[87] Radhakrishnan, R.; Jamil, M.; Mehfuz, S.; Moinuddin, "Security issues in IPv6," in *Networking and Services, 2007. ICNS. Third International Conference on* , vol., no., pp.110-110, 19-25 June 2007
[88] Rafiee, H.; Meinel, C., "A Secure, Flexible Framework for DNS Authentication in IPv6 Autoconfiguration," in *Network Computing and Applications (NCA), 2013 12th IEEE International Symposium on* , vol., no., pp.165-172, 22-24 Aug. 2013
[89] Rafiee, H.; Meinel, C., "SSAS: A simple secure addressing scheme for IPv6 autoconfiguration," in *Privacy, Security and Trust (PST), 2013 Eleventh Annual International Conference on* , vol., no., pp.275-282, 10-12 July 2013
[90] Rafiee, H.; von Löwis, M.; Meinel, C., "IPv6 Deployment and Spam Challenges," in *Internet Computing, IEEE* , vol.16, no.6, pp.22-29, Nov.-Dec. 2012
[91] Rawat, P.; Bonnin, J., "Designing a Header Compression Mechanism for Efficient Use of IP Tunneling in Wireless Networks," in *Consumer Communications and Networking Conference (CCNC), 2010 7th IEEE* , vol., no., pp.1-5, 9-12 Jan. 2010
[92] Rawat, P.; Bonnin, J.M.; Minaburo, A., "Optimising the Use of Robust Header Compression Profiles in NEMO Networks," in *Networking, 2008. ICN 2008. Seventh International Conference on* , vol., no., pp.150-155, 13-18 April 2008
[93] Rawat, P.; Bonnin, J.M.; Toutain, L.; Yanghee Choi, "Robust Header Compression Over Long Delay Links," in *Vehicular Technology Conference, 2008. VTC Spring 2008. IEEE* , vol., no., pp.2136-2141, 11-14 May 2008
[94] Rongxi He; Limin Song; XuDong Wang; Bin Lin, "Routing in trustworthy networks with SAVA nodes," in *Advanced Computer Control (ICACC), 2010 2nd International Conference on* , vol.4, no., pp.402-406, 27-29 March 2010
[95] Rosli, A.; Ali, W.N.A.W.; Taib, A.H.M., "IPv6 deployment: Security risk assessment using i-SeRP system in enterprise network," in *Research and Development (SCOReD), 2012 IEEE Student Conference on* , vol., no., pp.210-213, 5-6 Dec. 2012
[96] Sabir, M.R.; Fahiem, M.A.; Mian, M.S., "An Overview of IPv4 to IPv6 Transition and Security Issues," in *Communications and Mobile Computing, 2009. CMC '09. WRI International Conference on* , vol.3, no., pp.636-639, 6-8 Jan. 2009
[97] Sanyal, P.; Das, S.; Bhunia, S.S.; Roy, S.; Mukherjee, N., "An experience of implementing IPv6 based data retrieval system for Wireless Sensor Networks," in *Recent Advances in Computing and Software Systems (RACSS), 2012 International Conference on* , vol., no., pp.154-157, 25-27 April 2012
[98] Seng, R.; Lee, K.B.; Song, E.Y., "An implementation of a wireless sensor network based on IEEE 1451.0 and 1451.5–6LoWPAN standards," in *Instrumentation and Measurement Technology Conference (I2MTC), 2011 IEEE* , vol., no., pp.1-6, 10-12 May 2011
[99] Seong-Yee Phang; HoonJae Lee; Hyotaek Lim, "Design and Implementation of V6GEN and V6PCF: A Compact IPv6 Packet Generator and a New Packet Classification Framework for IPv6," in *Convergence and Hybrid Information Technology, 2008. ICCIT '08. Third International Conference on* , vol.2, no., pp.38-43, 11-13 Nov. 2008
[100] Shahsad., A.S; Purushothaman, K.V.; MurugaPrasad, S.V., "Error free high speed data transmission for IPV6 packets," in *Circuits, Power and Computing Technologies (ICCPCT), 2013 International Conference on* , vol., no., pp.993-996, 20-21 March 2013
[101] Sheng-Shih Wang; Shiann-Tsong Sheu; Huei-Yu Lee; Ting-Rong, O., "CPR: A CRC-based packet recovery mechanism for wireless networks," in *Wireless Communications and Networking Conference (WCNC), 2013 IEEE* , vol., no., pp.321-326, 7-10 April 2013
[102] Shi Shengyan; Shen Xiaoliu; Zhao Jianbao; Ma Xinke, "Research on System Logs Collection and Analysis Model of the Network and Information Security System by Using Multi-agent Technology," in *Multimedia Information Networking and Security (MINES), 2012 Fourth International Conference on* , vol., no., pp.23-26, 2-4 Nov. 2012
[103] Shimada, H.; Sato, T.; Fujikawa, K.; Sunahara, H., "Implementation and Evaluation of a Memory Management System for IPv6 Wireless Sensor Networks," in *Applications and the Internet, 2008. SAINT 2008. International Symposium on* , vol., no., pp.401-404, July 28 2008-Aug. 1 2008
[104] Simon, C.; Chaparadza, R.; Benkö, P.; Asztalos, D.; Kaldanis, V., "Enabling autonomicity in the future networks," in *GLOBECOM Workshops (GC Wkshps), 2010 IEEE* , vol., no., pp.637-641, 6-10 Dec. 2010

[105] Singh, J.; Singh, J., "A Comparative Study of Error Detection and Correction Coding Techniques," in *Advanced Computing & Communication Technologies (ACCT), 2012 Second International Conference on* , vol., no., pp.187-189, 7-8 Jan. 2012
[106] Singh, V.; Sharma, R.; Tomar, M.S., "An Analytical Study of Interference Problem between ZigBee and WI-FI," in *Communication Systems and Network Technologies (CSNT), 2013 International Conference on* , vol., no., pp.257-261, 6-8 April 2013
[107] Soumyalatha, N.; Ambhati, R.K.; Kounte, M.R., "Performance evaluation of ip wireless networks using two way active measurement protocol," in *Advances in Computing, Communications and Informatics (ICACCI), 2013 International Conference on* , vol., no., pp.1896-1901, 22-25 Aug. 2013
[108] Sreejesh, V.K.; Kumar, G.S., "Implementation and evaluation of an improved header compression for 6LoWPAN," in *India Conference (INDICON), 2012 Annual IEEE* , vol., no., pp.439-443, 7-9 Dec. 2012
[109] Strugaru, O.; Potorac, A.D.; Graur, A., "The impact of using Source Address Validation filtering on processing resources," in *Communications (COMM), 2014 10th International Conference on* , vol., no., pp.1-4, 29-31 May 2014
[110] Sun Xiaoling; Chen Haihong, "Research on IPv6 Routing Technology," in *Computational and Information Sciences (ICCIS), 2013 Fifth International Conference on* , vol., no., pp.1409-1412, 21-23 June 2013
[111] Tianfield, H., "Security issues in cloud computing," in *Systems, Man, and Cybernetics (SMC), 2012 IEEE International Conference on* , vol., no., pp.1082-1089, 14-17 Oct. 2012
[112] Tomoskozi, M.; Seeling, P.; Fitzek, F.H.P., "Performance evaluation and comparison of RObust Header Compression (ROHC) ROHCv1 and ROHCv2 for multimedia delivery," in *Globecom Workshops (GC Wkshps), 2013 IEEE* , vol., no., pp.544-549, 9-13 Dec. 2013
[113] Vineeth, M.V.; Rejimoan, R., "Evaluating the performance of IPv6 with IPv4 and its distributed security policy," in *Information & Communication Technologies (ICT), 2013 IEEE Conference on* , vol., no., pp.59-63, 11-12 April 2013
[114] Vives, A.; Palet, J., "IPv6 Distributed Security: Problem Statement," in *Applications and the Internet Workshops, 2005. Saint Workshops 2005. The 2005 Symposium on* , vol., no., pp.18-21, 31-04 Jan. 2005
[115] Wang Huiqin; Dong Yongqiang, "An Improved Header Compression Scheme for 6LoWPAN Networks," in *Grid and Cooperative Computing (GCC), 2010 9th International Conference on* , vol., no., pp.350-355, 1-5 Nov. 2010
[116] Wattanapongsakorn, N.; Srakaew, S.; Wonghirunsombat, E.; Sribavonmongkol, C.; Junhom, T.; Jongsubsook, P.; Charnsripinyo, C., "A Practical Network-Based Intrusion Detection and Prevention System," in *Trust, Security and Privacy in Computing and Communications (TrustCom), 2012 IEEE 11th International Conference on* , vol., no., pp.209-214, 25-27 June 2012
[117] Westphal, C., "Layered IP Header Compression for IP-enabled Sensor Networks," in *Communications, 2006. ICC '06. IEEE International Conference on* , vol.8, no., pp.3542-3547, June 2006
[118] Westphal, C.; Koodli, R., "Stateless IP header compression," in *Communications, 2005. ICC 2005. 2005 IEEE International Conference on* , vol.5, no., pp.3236-3241 Vol. 5, 16-20 May 2005
[119] Xiaoyu Duan; Xianbin Wang, "Authentication handover and privacy protection in 5G hetnets using software-defined networking," in *Communications Magazine, IEEE* , vol.53, no.4, pp.28-35, April 2015
[120] Xinyu Yang; Ting Ma; Yi Shi, "Typical DoS/DDoS Threats under IPv6," in *Computing in the Global Information Technology, 2007. ICCGI 2007. International Multi-Conference on* , vol., no., pp.55-55, 4-9 March 2007
[121] Xiuliang Chen; Fuliang Guo; Ping Dang; Libing Wu, "A survey of ROHC header compression schemes," in *Computer Science and Network Technology (ICCSNT), 2012 2nd International Conference on* , vol., no., pp.331-335, 29-31 Dec. 2012
[122] Xu Yangui; Zhou Jiachun; Li Xiangchun; Qian Huanyan, "Worm Detection in an IPv6 Internet," in *Computational Intelligence and Security, 2009. CIS '09. International Conference on* , vol.2, no., pp.366-370, 11-14 Dec. 2009
[123] Xue Yan, "Review of network intrusion detection," in *Communication Software and Networks (ICCSN), 2011 IEEE 3rd International Conference on* , vol., no., pp.316-318, 27-29 May 2011
[124] Yoong Choon Chang; Sze Wei Lee; Komyia, R., "A fast forward error correction allocation algorithm for unequal error protection of video transmission over wireless channels," in *Consumer Electronics, IEEE Transactions on* , vol.54, no.3, pp.1066-1073, August 2008
[125] Zhan Jun; Yang Bo; Men Aidong, "Address allocation scheme of wireless sensor networks based on IPv6," in *Broadband Network & Multimedia Technology, 2009. IC-BNMT '09. 2nd IEEE International Conference on* , vol., no., pp.597-601, 18-20 Oct. 2009
[126] Zhang Yu, "Study on intrusion IPv6 detection system on LINUX," in *Computational Intelligence and Industrial Applications, 2009. PACIIA 2009. Asia-Pacific Conference on* , vol.2, no., pp.5-8, 28-29 Nov. 2009
[127] Zhen Tian; Dongfeng Yuan; Quanquan Liang, "Energy Efficiency Analysis of Error Control Schemes in Wireless Sensor Networks," in *Wireless Communications and Mobile Computing Conference, 2008. IWCMC '08. International* , vol., no., pp.401-405, 6-8 Aug. 2008
[128] Zhihui Yan; Gengsheng Deng; Junyun Wu, "SAVI-based IPv6 source address validation implementation of the access network," in *Computer Science and Service System (CSSS), 2011 International Conference on* , vol., no., pp.2530-2533, 27-29 June 2011

International Journal of Engineering Research and General Science Volume 3, Issue 6, November-December, 2015
ISSN 2091-2730

TSUNAMI DETECTION & ASSESSMENT USING REMOTE SENSING AND GIS

[1]. Dhruvesh.K.Mathur, [2].Dr.Praful.M.Udani

[1] Research Scholar 14SC703002, Faculty of Sciences (Physics) CU Shah University, Wadhwan.
[2]Director, ISTAR-CVM, VallabhVidyanagar.
Email Address-dhruvesh_8mathur@yahoo.co.in

Abstract— Coastal zones are more prone to natural disaster better management strategies and disaster management planning is necessary for the planning of coastal areas. Remote sensing, GIS, Information technology are widely used now a days for better management of coastal areas. GIS and web technology makes it an extremely powerful tool to identify indicators of potential disasters. Information sharing through Internet reduces data acquisition time and thus providing efficient way to carry out real time disaster predictions occur at coastal areas like Tsunami, Cyclones, and Floods. GIS, RS & GPS is useful in disaster management applications & for decision making. Evolution of computer technology and availability of hardware is helpful for rapid expansion of GIS in both disaster research and practice for better management of coastal hazards. GIS is useful for hazard zone mapping and during emergency conditions mitigation of people can easily possible using these maps. As Gujarat has longest coastal area we are focusing on various disasters occur at Gujarat coast and how to reduce impact of disaster by using remote sensing and GIS technologies.
Keywords— Remote Sensing, geographic information system (GIS), earthquake, tsunami, Tsunami Risk, Tsunami warning, Monitoring of Sea level

1. INTRODUCTION

A tsunami is a series of waves with a long wavelength and period (time between crests). Time between crests of the wave can vary from a few minutes to over an hour. Tsunamis are often incorrectly called tidal waves; they have no relation to the daily ocean tides. Tsunami (soo-NAH-mee) is a Japanese word meaning harbor wave. Tsunamis can occur at any time of day or night.
Tsunamis are generated by any large, impulsive displacement of the sea bed level (Fig.1). Earthquakes generate tsunamis by vertical movement of the sea floor. If the sea floor movement is horizontal, a tsunami is not generated. Earthquakes of M > 6.5 are critical for tsunami generation. Tsunamis are also triggered by landslides into or under the water surface, and can be generated by volcanic activity and meteorite impacts.

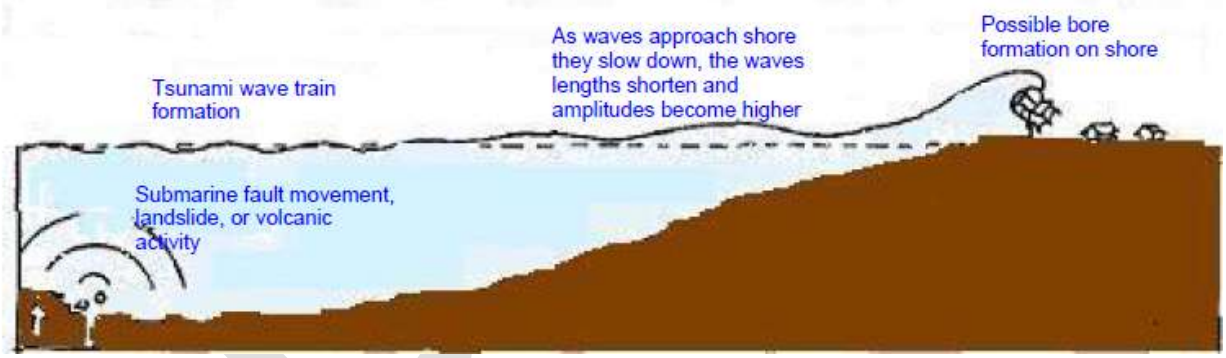

Fig 1- Wave Train of Tsunami. Source: - International Tsunami Information Centre – Geologic Hazard

On the average, there are two tsunamis per year in the Pacific Ocean somewhere, which cause damage near the source. Approximately every 15 years a destructive tsunami occurs in Pacific. The destructive tsunami on Dec 26th, 2004 on the Indian Coast in terms of its impact seems to have occurred for the first time in the history.
Tsunami velocity is dependent on the depth of water through which it travels (Velocity equals the square root of water depth h times the gravitational acceleration g, that is $V = \sqrt{g\,h}$). Tsunamis travel approximately at a velocity of 700 kmph in 4000 m depth of sea water. In 10 m of water depth the velocity drops to about 36 kmph. See Fig.2

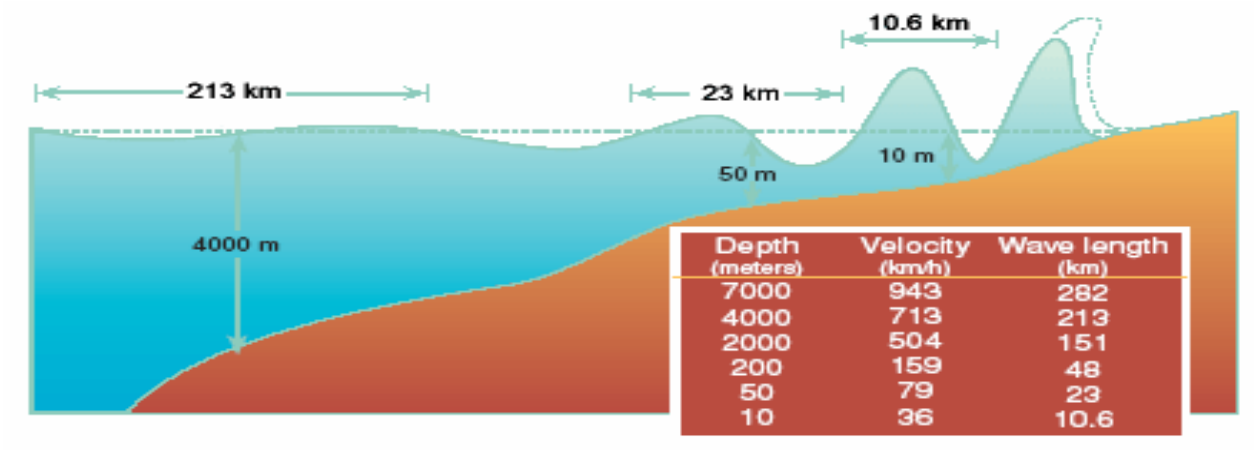

Fig 2-Tsunami Travel Calculation.(Source-
http://www.prh.noaa.gov/pr/itic/library/pubs/great_waves/tsunami_great_waves_4.html)

Fig.3 Indian Ocean Tsunami of Dec.26th, 2004

For example, the tsunami from Sumatra coastal earthquake travelled to Tamil Nadu coast in about two Hours. See. Fig.3• Even on shore tsunamis speed is 35 – 40 km/h, hence much faster than a person can run. Tsunamis range in size from centimeters to over 30 m height. Most tsunamis are less than 3 m in height. In deep water (greater than 200 m), tsunamis are rarely over 1m high and will not be noticed by ships due to their long period (time between crests). As tsunamis propagate into shallow water, the wave height can increase by over 10 times. Tsunami heights can vary greatly along a coast. The waves are amplified by certain shoreline and bathymetric (sea floor) features. A large tsunami can flood land up to1.5 km from the coast. The force of some tsunamis is enormous. Large rocks weighing several tons along with boats and other debris can be moved inland hundreds of feet by tsunami wave activity. Homes and other buildings are destroyed. All this material and water move with great force and can kill or injure people. Normally, a tsunami appears as a rapidly advancing or receding tide. It some cases a bore (wall of water) or series of breaking waves may form. Sometimes a tsunami causes the water near the shore to recede by 0.5 – 2.0 km, exposing the ocean floor, and then the wave crest comes with a high speed. Tsunamis can travel up rivers and streams that lead to the sea.

2. Tsunami Risk in India & its Assessment.

The following hazards are seen to occur in the coastal areas of India
1. Earthquakes
2. Cyclonic wind
3. Storm surge in cyclones
4. Flooding by incessant rain
5. Tsunami

Fire is also known to occur quite frequently in many such areas. The situation on the west and east coast of India is given in Table 1 & 2 respectively.

Table 1 Multi Hazard Data for West Coast of India

Name of coastal State	Vulnerable for Hazard	Design Cyclonic Wind (IS:875III) (m/s)	Probable Maximum Storm Surge Heights (m)	Astronomical High Tide above Mean Sea Level (m)	Flood Proneness	Tsunami Prone-ness (m)
Gujarat	Tsunami, Flooding by incessant rain, Storm surge in cyclones	50 & 47	2.5 – 5.0	1.1 –4.1	In 5 coastal districts	10 – 12 (In 1945)
Dadra & Nagar Haveli	Storm surge in cyclones	44	5.0	1.9	---	To be Estimated
Daman & Diu	Storm surge in cyclones	50 & 44	5.0	1.1	---	To be Estimated
Maharashtra	Storm surge in cyclones , Flooding by incessant rain	44 & 39	2.9 –4.2	1.9	---	To be Estimated
Goa	Cyclonic wind , Storm surge in cyclones	39	3.4	1.0	---	To be Estimated
Karnataka	Cyclonic wind ,Storm surge in cyclones	39	3.4 – 3.7	0.8	---	To be Estimated
Kerala	Storm surge in cyclones	39	2.3 –3.5	0.8	In 9 coast Districts	3 – 5
Lakshadweep	Storm surge in cyclones	39	Value not Measured	0.5	---	To be Estimated

(Source-National Disaster Management Division, Ministry of Home Affairs, Government of India)

Table 2 Multi Hazard Data for East Coast of India

Name of coastal State	Vulnerable for Hazard	Design Cyclonic Wind	Probable Maximum Storm	Astronomical High Tide above	Flood Proneness	Tsunami Prone-ness (m)

		(IS:875III) (m/s)	**Surge Heights (m)**	**Mean Sea Level (m)**		
Tamil Nadu	Cyclonic wind , Storm surge in cyclones	50,47,39 (PMWS- 64)	2.7 –7.0 except 11.0 near Tondi	0.5	_	7 – 10
Pondicherry	Storm surge in cyclones	50,47,39 (PMWS- 64)	3.0 –4.5	0.5	In 1 coast districts	10 (in 1 district)
Andhra Pradesh	Cyclonic wind , Storm surge in cyclones	50 (PMWS – 78)	3 – 6	0.68	In 8 coast districts	**To be estimated**
Orissa	Cyclonic wind , Storm surge in cyclones	50 & 44 (PMWS – 78)	2.7 –9.8	0.9-1.40	In 3 coast districts	**To be estimated**
West Bengal	Storm surge in cyclones , Flooding by incessant rain	50 PMWS- 78	12.0 -12.5	2.6	In 3 coast districts	**To be estimated**
Andaman & Nicobar	Tsunami	44	Value not Measured	1.0	_	3 – 6

PMWS-Probable Maximum Wind Speed
(Source-National Disaster Management Division, Ministry of Home Affairs, Government of India)

The Indian coastal belt has not recorded many severe tsunamis in the past. Waves accompanying earthquake activity have been reported over the North Bay of Bengal. During an earthquake in 1881 which had its epicenter near the Andaman's in the Bay of Bengal, tsunamis were reported. The earthquake of 1941 in Bay of Bengal caused some damage in Andaman region. This was unusual because most Tsunamis are generated by shocks which occur at or near the flanks of continental slopes. During the earthquakes of 1819 and 1845 near the Rann of Kutch, there were rapid movements of water into the sea. There is no mention of waves resulting from these earthquakes along the coast adjacent to the Arabian Sea, and it is unlikely that Tsunamis were generated. Further west, in the Persian Gulf, the 1945 Mekran earthquake (magnitude 8.1) generated Tsunami of 12 to 15 metres height. This caused a huge deluge, with considerable loss of life and property at Ormara and Pasi. The estimated height of Tsunami at Gulf of Kutchch was 15m but no report of damage is available. The estimated height of waves was about 2 metres at Mumbai, where boats were taken away from their moorings and casualties occurred.

A list showing the Tsunami that affected Indian coast in the past is given in Table-3. The information given in the Table for the first three events is sketchy and authenticity cannot be confirmed except the Tsunami of 26th December 2004.Above facts indicate the coastal region of Gujarat is vulnerable to Tsunamis from great earthquakes in Mekran coast. Earthquake of magnitude 7 or more may be dangerous. It may be noted that all earthquake do not generate Tsunami. Research is still being undertaken in this field. For the Indian region, two potential sources have been identified, namely Mekran coast and Andaman to Sumatra region.

Model generated Travel time of 26th December Tsunami is shown in Fig 4.

Fig.4:- Arrival time of first waves (sec) – 2004 12 26 Indian Ocean Tsunami Simulation(Sourse-Tsunami research programme NOAA OAR Washington)

Sr.No	Date	Remarks
1	April 12,	1762 Eq. in the Bay of Bengal generated tsunami wave of 1.8 m in coastal Bangladesh
2	August 19, 1868	Earthquake Mw 7.5 in the Bay of Bangal. Tsunami wave run-up level at Port Blair, Andaman Island 4.0 m.
3	December 31, 1881	Earthquake of magnitude Ms 7.9 in the Bay of Bengal, reported tsunami run-up level of 0.76m at Car Nicobar, 0.3m at Dublat , 0.3 m at Nagapattinam and 1.22 m at Port Blair in Andaman Island
4	1883	Karakatau, volcanic explosion in Indonessia. 1.5 m tsunami at Chennai, 0.6 m at Nagapattinam.
5	1884	Earthquake in the western part of the Bay of Bengal. Tsnamis at Port Blair & mouth of Hoogly River
6	June 26, 1941 .	Earthquake of magnitude MW 8.1 in the Andaman Sea at 12.90 N,92.5o E. Tsunamis on the east coast of India with amplitudes from 0.75 to 1.25 m. Some damage from East Coast was reported
7	November 27, 1945	Mekran Earthquake (Magnitude Ms 8.3). 12 to 15 M wave height in Ormara, 13 m at Pasni, and 1.37 m at Karachi (Pakistan) . In Gulf off Cambay of Gujarat wave heights of 11.0 m was estimated, and 2 m at Mumbai, where boats were taken away from their moorings.
8	December 26, 2004	An earthquake of rear Magnitude (MW9.3) generated giant tsunami waves in North Indian Ocean. Tsunami made extensive damage to many coastal areas of Indonesia, India, Malaysia, Maldives, Srilanka and Thailand. A trans-oceanic tsunami, observed over areas beyond the Ocean limit of origin. More than 2, 00, 000 people lost their lives in above countries which is a record.

Table 3-Tsunami that affected Indian coast in the past.(Source-National Disaster Management Department

3. Tsunami Risk in Gujarat & its Assessment.

The Tsunami risk within the Indian Ocean is quite low as compared to storm surge owing to very long return periods and the lower level of inter-plate events. Therefore, mitigative measures for protection against sea inundation due to storm surge, if suitably enhanced, could provide the most cost-effective risk mitigation measures for the region

Gujarat is prone to Tsunami risk due to its longest coastline and probability of occurrence of near and offshore submarine earthquakes in the Arabian Sea. Makran Subduction Zone (MSZ) -South West of Karachi is an active fault area which may cause a high magnitude earthquake under the sea leading to at tsunami. In past, Kandla coast was hit by a Tsunami of 12 mtrs height in 1945, due to an earthquake in the Makran fault line. Tsunami prone areas in the State include coastal villages of Kutch, Jamnagar, Rajkot, Porbandar, Bhavnagar, Anand, Ahmedabad, Bharuch, Surat, Navsari and Valsad districts.
The Hazard Risk and Vulnerability Atlas prepared by GSDMA shows (Fig. 5)the estimated inundation based on Probable Maximum Surge (PMS) at highest high tide level.
Tsunamis are extremely rare events in Gujarat. No instrumental records or damage records are available for tsunami impact in the region. Nevertheless, tsunami impact in the Gujarat region in expected to be similar to that of the worst storm surge – which occurs at a much higher frequency. It is estimated that appropriate structural mitigation measures for storm surge linked to an appropriate tsunami warning system could address much of the risk associated tsunami impact to residential populations.

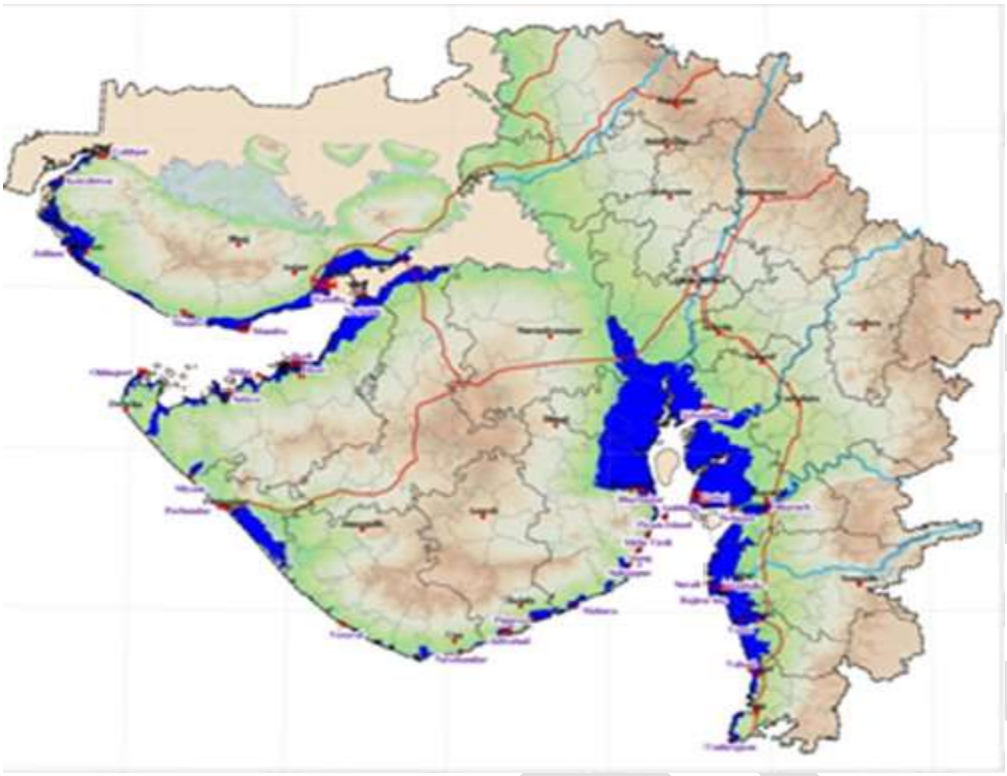

Figure 5 Gujarat Tsunami Hazard risk zones (source-Gujarat state disaster management authority)

4. Tsunami Warning System in India.

The Present status of Tsunami Warnings in India. Tsunami is very low probability event in India. As such, there are no Codal provisions for Tsunami warnings in India as yet though; there is a good seismological network in India to record any earthquake within the country and its neighbourhood. The need of a Tsunami Warning Centre (TWC) in India is now being conceptualized at the Government of India level. India Meteorological Department (IMD), is working on a proposal to set up a real time earthquake monitoring system in India. The Department of Ocean Development in collaboration with Departments of Space and IMD under Department of Science and Technology is evolving a plan of tsunami warning system in the Bay of Bengal and the Arabian Sea. The data from observing points to Warning Centre(s) will be sent through satellite links.

Specific systems called Deep Ocean Assessment and Reporting of Tsunamis (DART) using Bottom Pressure Recorder, acoustic modem, acoustic release system, battery pack bolted to platform and float action and recovery aids will be deployed. The warning centres in the Indian context could be the Emergency Operation Centre at the State & District level, which are being designed to function round the clock under the District Collector at District level and under the Chief Minister at State level

Tsunami occurs due to earth quake in ocean for detecting these activities a Network of land-based seismic stations for earthquake detection and estimation of focal parameters in the two known tsunami genic zones is a prime requirement of the warning centre. INCOIS is receiving real-time seismic data from international seismic networks as well as from India Meteorological Department (IMD) and has been detecting all earthquake events occurring in the Indian Ocean in the less than 15 minutes of occurrence. Necessary software has been installed for real-time data reception, archiving, processing and auto-location of earthquakes as well as for alert generation and automatic notification.

Present techniques of Tsunami prediction are severely limited. The only way to determine, with certainty, if an earthquake is accompanied by a Tsunami, is to note the occurrence and epicenter of the earthquake and then detect the arrival of the Tsunami at a network of tide stations. While it is possible to predict when a Tsunami will arrive at coastal locations, it is not yet possible to predict the wave height, number of waves, duration of hazard, or the forces to be expected from such waves at specific locations. Computer programmes need to be developed for this purpose. Tsunami Warning System is based on the concept that Tsunamis travel at much slower velocity (500 to 700 km per hour or 0.20 km/sec) as compared to seismic waves (6 to 8 km per second). That is seismic waves move 30 to 40 times faster than Tsunami waves. Thus, after the occurrence of a damaging earthquake and quick determination of epicenter, warning time of a few minutes to 2 to 3 hours is available depending upon the distance from the epicenter to the coast line. This time can be utilized for warning the coastal community if quick detection and rapid communication systems are established.

A dedicated 24 x 7 operating Tsunami Warning Centre including necessary computational, communication and technical support infrastructure as well as robust application software that facilitates data reception, display, analysis, modelling, and decision support

system for generation of tsunami advisories following a standard operating procedure has been established. The warning centre continuously monitors seismic activity in the two tsunami genic source regions and sea level through the network of national and international seismic stations as well as tide gauges and bottom pressure recorders (BPR's). The monitoring of water level enables confirmation or cancellation of a tsunami

4.1 Monitoring of Sea Level.

In order to confirm whether the earthquake has actually triggered a tsunami, it is essential to measure the change in water level as near to the fault zone with high accuracy. Bottom pressure recorders (BPR) are used to detect the propagation of tsunami waves in open-ocean and consequent sea level changes. A network of Bottom Pressure Recorders (BPRs) has been installed close to the tsunami genic source regions to detect tsunami, by the National Institute of Ocean Technology (NIOT). These BPRs can detect changes of 1 cm at water depths up to 6 km. A network of tidal gauges along the coast helps to monitor progress of tsunami as well as validation of the model scenarios. Near-real time data is being received from national and international centres has been received. Necessary software for real-time reception, display and archiving of tide gauge data has been developed.

4.2 High resolution Data Base on a Bathyemetry & Coastal Topography.

Generating and updating a high resolution database on bathymetry, coastal topography, coastal land use, coastal vulnerability as well as historic data base on tsunami and storm surge to prepare and update storm surge/tsunami hazard maps. The accuracy of model predictions is directly related to the quality of the data used to create the bathymetry and topography of the model area. Coastal Bathymetry is the prime determinant of the height of the tsunami wave or storm surge as it approaches the coast. High resolution coastal bathymetry is thus the key input for various tsunami and storm surge prediction models.

5. Application of Remote Sensing & GIS for Tsunami.

One of the key components of the early warning centre is the development of application software around GIS technology that performs the following operations:

(i) Acquisition, display and analysis of real time data of seismic sensors, tide gauges and BPRs.
(ii) Generation of model scenario database for assumed earthquake parameters as well as Retrieval, Display and Analysis at the time of an event.
(iii) Generation, Display and Analysis of Bathymetric Data, Coastal Topographic Data and Vulnerability Maps.
(iv) Decision support system for generation of tsunami advisories following a standard operating procedure.
(v) Data warehousing, Data Mining and Data Dissemination

For the assessment of damage after Tsunami good help is achieved by remote sensing and GIS. In the first stage, general damage information, such as tsunami inundation limits, can be obtained promptly using an analysis combined with ground truth information in GIS.

In the second stage, detailed damage interpretations can beanalysed; i.e., classification of the building damage level. Recently, the quality of commercial satellite images has improved. These images help us clarify, i.e., whether a house was washed away or survived; they can even classify more damage levels.

The third stage combines the damage and hazard information obtained from a numerical simulation, such as the tsunami inundation depth. The damage data are compiled with the tsunami hazard data via GIS. Finally, a tsunami vulnerability function can be developed. This function is a necessary tool for assessing future tsunami risk. Recent advances in remote sensing technologies have expanded the capabilities of detecting the spatial extent of tsunami-affected areas and damage to structures.

6. CONCLUSION

Due rapid growth of industry and cities on coastal shores. Now a day's coastal hazard are unavoidable occurrence and it is not possible to control by human efforts. Humans are making best try to prevent it becoming DISASTER. Remote sensing and GIS inputs are useful and used to save innocent lives and for impact assessment to infrastructure and properties. Remote sensing and GIS are used operationally for early warning and monitoring of cyclones, tsunami which are often destruct coastal areas. It is required to appropriately choose RS data with required spatial and temporal resolution for information extraction and integrating it with field survey data using GIS framework. This paper has provided insight about the possible applications of remote sensing and GIS in coastal hazards.

REFERENCES:

[1]Shailesh Nayak and T. Srinivasa Kumar, INDIAN TSUNAMI WARNING SYSTEM.
[2]Rajesh Srivastava, 2014, Remote sensing and GIS in disasters management-in special reference to Asian countries.
[3]Protection Mitigation From the Risk of Tsunami,NDMD,Ministry of Home Affairs,Govt of India.

[4]Karen E. Joyce, Stella E. Belliss, Sergey V. Samsonov, Stephen J. McNeill and Phil J. Glassey, A review of the status of satellite remote sensing and image processing techniques for mapping natural hazards and disasters.Progress in Physical Geography 33(2) (2009) pp. 183–207.
[5] Home page of Geographic Survey Institute:http://www.gsi.go.jp
[6]http://www.spaceimaging.com/carterra/applications/disaster/mozambique.htm
[7]http://www.pmel.noaa.gov/tsunami/aerial_photo_okushiri.html
[8]National Disaster management guidelines for Management of cyclones by Govt of India.
[9]. Causes & Effects of Natural Hazards – Disaster Management Centre, University of Wisconsin
http://dmc.engr.wisc.edu/courses/hazards/BB02-03.html
[10]. Designing for Tsunami, National Tsunami Hazard Mitigation Programme Steering Committee, March 2001, NOA, USGS, FEMA, NSF, Alaska, California, Hawaii, Oregon and Washington.
[11]Earth and Spaces Sciences, University of Washington.
http://www.ess.washington.edu/tsunami/intro.html
[12] Geologic Hazard – Tsunami- International Tsunami Information Centre.
[13]http://www.gsdma.org/
[14] http://www.crisp.nus.edu.sg/
[15]Gujarat state Disaster Management plan, June 2014 volume 1, 2.

International Journal of Engineering Research and General Science Volume 3, Issue 6, November-December, 2015
ISSN 2091-2730

AN INCREMENTAL AND DISTRIBUTED INFERENCE METHOD FOR LARGE-SCALE ONTOLOGIES USING ONE-CLASS CLUSTERING TREE

A.Vijayalakshmi, Dr.S.Babu

P.G Student, Department of Computer Engineering, IFET College of Engineering, Villupuram, India.

viji.muthu6825@gmail.com, 9787891542

Abstract— Reasoning on a Web scale becomes increasingly challenging because of the large volume of data involved and the complexity of the task by means of ontology mapping. Ontology mapping processes users' queries that can provide more correct results when the mapping process can deal with the uncertainty effect that is caused by the incomplete and inconsistent information used and produced by the mapping process. Here, an IDIM concept is used to deal with large-scale incremental RDF datasets. Resource Description Framework (RDF) is an important data, presenting standard of the semantic web to process the increasing RDF data. MapReduce is a widely-used parallel programming model that can be used to represent uncertain similarities created by both syntactic and semantic similarity algorithms. The proposed One-Class Clustering Tree (OCCT) characterizes the entities that should be linked together. The construction of TIF and EAT significantly reduces the re-computation time for the incremental inference as well as the storage for RDF triples. Therefore, users can execute their query more efficiently without computing and searching over the entire RDF closure used in the prior work. The final results are evaluated by comparing it against benchmark models in web information gathering.

Keywords— Ontology reasoning, RDF, MapReduce, IDIM, Hadoop, OCCT, MLE.

INTRODUCTION

Semantic reasoning of data on a Web scale becomes increasingly challenging because of the large volume of data involved that raises the complexity of the task. Ontology mapping in the context of Question Answering can provide more correct results if the mapping process can deal with unreliability that is caused by the incomplete and inconsistent information used and produced by the mapping process.

In the year of 2009, the semantic web [2] contain 4.4 billion triples and has now reached over 20 billion triples. Its growth rate is still increasing. As it has evolved into a global knowledge-based framework to promise a kind of machine intelligence, supporting knowledge searching over such a big and increasing dataset has become an important issue.

Resource Description Framework (RDF) is an important data representation standard used to describe knowledge in the semantic web. Deriving inferences in the large-scale RDF [1] files, referred to as large-scale reasoning, poses challenges in three aspects:

i. Distributed data on the web make it difficult to acquire appropriate triples for appropriate inferences.
ii. The growing amount of information requires scalable computation capabilities for large datasets.
iii. Fast processing for inferences is required to satisfy the requirements of online query.

Due to the performance limitation of a centralized architecture executed on a single machine or local server when dealing with large datasets, distributed reasoning approaches executed on multiple computing nodes have thus emerged to improve the scalability and speed of inferences. But this consumes too much of time and space for reasoning. The concept of an incremental and distributed inference method (IDIM) for large-scale RDF datasets via MapReduce overcomes these issues.

MapReduce can provide a solution for large scale RDF data processing which is a widely-used parallel programming model. It presents a novel approach can be used to represent uncertain similarities created by both syntactic and semantic similarity algorithms. The choice of MapReduce is motivated by the fact that it can limit data exchange and alleviate load balancing problems by dynamically scheduling jobs on computing nodes. In order to store the incremental RDF triples more efficiently, two novel concepts, transfer inference forest (TIF) and effective assertional triples (EAT) are used. Their use can largely reduce the storage and simplify

the reasoning process. Based on TIF/EAT, we need not compute and store RDF closure and the reasoning time, so significantly decreases that a user's online query can be answered timely, which is more efficient than existing methods to our best knowledge. More importantly, the update of TIF/EAT needs only minimum computation since the relationship between new triples and existing ones is fully used.

RELATED WORK

The prior methodologies used for semantic web search are discussed as follows:

A. Fuzzy Set Theory

Context awareness (CA) is a very important computing paradigm. Context is any information that can be used to characterize the situation of a person, place, or object that is considered relevant to the integration between a user and an application, including the user and the application themselves. CA is the ability of a system to sense, interpret, and react to changes in the environment a user is situated in. The capability of a context (or situation)-aware system [6] to classify context and infer specific situations can be facilitated by proper knowledge-representation (KR) models. A Fuzzy-set-based model can accommodate the vagueness inherent in context capturing. A fuzzy set is used for representing imprecise context in a human understandable form. This methodology is generic and can be applied to different inference schemes in order to improve the inference capability of the classifier and deal with mutual-exclusion inference. This model generates specific complementary fuzzy rules used for increasing the accuracy of the classification process for the well-specified information in Semantic web.

Disadvantage:

Applications can handle context as flexibly as their users would expect by using this method, but it is not suitable for all situations of user.

B. RuleXPM

The RuleXPM (XML Product Map) approach is an integrated model that combines a set of representations of various types of concepts, some e-marketplace participating systems, and an inference process. The method consists of several major constituents that include a collaborative ConexNet (Concept exchange Network), an e-marketplace network (EMpNet), and an inference engine.

Disadvantage:

Although this method is interoperable and inferred from one entity to another, it is not possible to implement it on an automated offering system and an automated negotiation system.

C. Similarity Transition [7]

A linked dataset is a kind of labelled directed graph cross domain, which is used for knowledge presentation and cognitive model foundation. Each link represents a kind of relationship between two resources and they can be represented as a statement in RDF. In these statements, since objects are the property value of subjects and describe their features, the similarity between two subjects can be calculated from the similarity between their corresponding sets of objects.

If the linked dataset is considered as a whole semantic graph, then the calculated similarity value between two subjects can be further transited to their own related subjects, which may make the similarity between the related subjects more accurate.

This calculation is referred as similarity transition that utilizes node and link types together with the topology of the semantic graph to derive a similarity graph from linked datasets. This method enables smooth interaction and visualization of the similarity graph which is derived based on the calculated similarity of two resources.

Disadvantage:

The effectiveness of this method is less as the similarity weight of each link type is given by experience.

The above described methods are applicable for small databases. To deal with a large base, some researchers turn to distributed reasoning methods.

D. Parallel Materialization [13]

Parallel Materialization of the Finite RDFS is the first method to provide RDFS inference on such large data sets in such low times and scalable manner. This maintains soundness and completeness without requiring any cumbersome preparation of the data. This method increases the processing speed by means of parallel inference.

Disadvantage:

It locks with scalability and expressivity.

E. Scalable Distributed Reasoning [4]

Scalable distributed reasoning presents some non-trivial optimizations for encoding the RDFS ruleset in MapReduce and exploits the MapReduce [5] framework for efficient large-scale Semantic Web reasoning and implements on the top of Hadoop. This reasoning technique performs quick reasoning using HDFS and high data correlation.

Disadvantage:

It does not focus on quality of reasoning.

F. MapResolve [10]

MapResolve solves the problem by adapting the standard method for distributed resolution that avoids repetition of resolved inferences. For the limited expressivity of RDFS, the repetition can be avoided because every MapReduce job is executed only once.

Disadvantage:

The clause sets are parsed and written to disc for each iteration, generating needless overhead.

G. WebPIE [3]

WebPIE is a Web-scale Parallel Inference Engine using MapReduce. This method calculates the RDF closure based on MapReduce for large-scale RDF dataset by adopting algorithms to process the statements based on input data as incremental reasoning. This technique identifies the accurate status, which does either exist or new ones

Disadvantage:

It does not provide the relationship between the newly arrived and existing data.

However, the distributed reasoning methods considered no influence of increasing data volume and did not answer how to process users' queries. As the data volume increases and the ontology base are updated, these methods require the re-computation of the entire RDF closure every time when new data arrive. To avoid such time-consuming process, incremental reasoning methods are proposed.

H. Incremental Ontology Reasoning [12]

An Incremental Ontology Reasoning approach based on modules that can reuse the information obtained from the previous versions of an ontology which is best suitable for OWL.

Disadvantage:

Reasoning speed is a huge problem while using this method.

EXISTING METHODOLOGY

In Existing system, the proposed concept of an incremental and distributed inference method [15] for large-scale ontologies by using MapReduce realizes high-performance reasoning and runtime searching, especially for incremental knowledge base. By constructing, using novel concepts of transfer inference forest and effective assertional triples, the storage is largely reduced and the reasoning process is simplified and accelerated to satisfy end-users' online query needs. The processing was made via MapReduce, which is motivated by the fact that it can limit data exchange and alleviate load balancing problems by dynamically scheduling jobs on computing nodes.

Drawbacks of Existing System are as follows,

- The Query time for IDIM is affected when the incremental triples affect the structure of the inference forests.
- If an RDF dataset has few ontological triples, the size of constructing dataset TIF is also small.
- The changes in the structure of TIF affect the performance improvement with ontological triples.
- The advantages of TIF/EAT cannot be exploited well, if the size of the tree is small.

PROPOSED METHODOLOGY

In order to overcome the existing drawbacks, the data clustering method is used in this paper that makes the processing of data more efficiently by means of linking the data sets.

A. One-Class Clustering Tree (OCCT)

A clustering tree is a tree in which each of the leaves contains a cluster instead of a single classification. Each cluster is generalized by a set of rules that is stored in the appropriate leaf. This data linkage method aimed at performing one-to-many linkage. The data linkage is performed among entities of different types.

For example, in a student database, we might want to link a student record with the courses she should take. It is done according to different features which describe the student and features describing the courses.

The OCCT [11] was evaluated using datasets from three different domains. They are

- Data leakage prevention
- Recommender systems
- Fraud detection.

In the data leakage prevention domain, the goal is to detect abnormal access to database records that might indicate a potential data leakage or data misuse. The goal is to match an action, performed by a user within a specific context, with records that can be legitimately retrieved within that context.
In the recommender systems domain the proposed method is used for matching *new* users of the system with the items that they are expected to like based on their demographic attributes.

In the fraud detection domain, the goal is to identify online purchase transactions that are executed by a fraudulent user and not the legitimate user.

The results show that the OCCT performs well in different linkage scenarios. In addition, it performs at least as accurate as the well known as decision tree data-linkage model, while incorporating the advantages of a one class solution. Additionally, the OCCT is preferable over the decision tree because it can easily be translated to linkage rules.

B. Algorithm: Maximum Likelihood Estimation

Maximum Likelihood Estimation (MLE) splitting criterion used in order to choose the attribute that is most appropriate to serve as the next splitting attribute. Each candidate attributes from the set of attributes splits the node data set into subsets according to its possible values. For each of the subsets, a set of probabilistic models is created, one for each attribute of second dataset. Each probabilistic model is built to describe the probability given. In order to create the probabilistic models decision tree are used. Each of these trees represents the probability of its class attribute values given the values of all other attributes.

Once the set of models has been induced, the probability of each record given these models is calculated. A subset's score is calculated as the sum of all scores of the records belonging to it. The attribute's final score is determined by the sum of the subset's individual scores. The goal is to choose the split that achieves the maximal likelihood and therefore we choose the attribute with the highest likelihood score as the next splitting attribute in the tree. The computational complexity of building a decision model using the MLE method is dependent on the complexity of building a statistical model and the time it takes to calculate the likelihood.

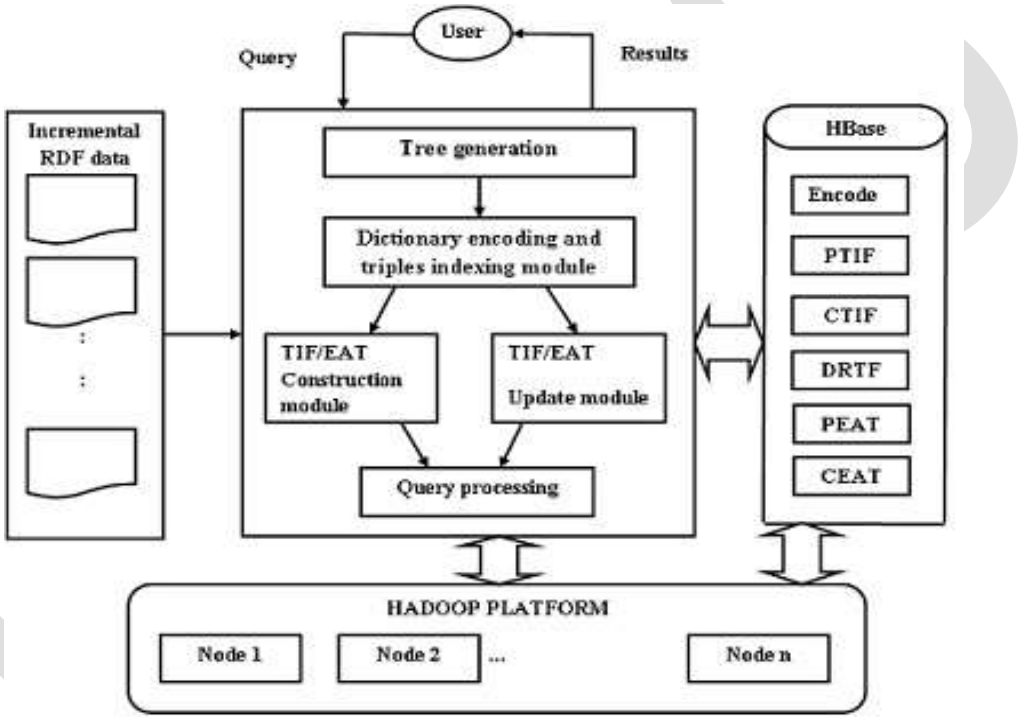

Fig.1 Overall System Architecture

In fig.1, the input incremental RDF datasets are received by the core module IDIM of the system and it process the triples and performs the reasoning. It interacts with HBase for storing or reading the intermediate results and returns the query results to end-users. The HBase is designed with six tables to store the encoded ID, PTIF, CTIF, DRTF, PEAT, and CEAT.

The Hadoop framework is an open-source Java implementation of MapReduce that allows for the distributed processing of large data sets across clusters of computers. It can scale up from single server to thousands of machines by offering local computation and storage and manages execution details such as data transfer, job scheduling, and error management.

ADVANTAGES OF PROPOSED SYSTEM

- The OCCT model is better generalized and avoids over-fitting by means of pruning the data.
- Fraud detection is used to obtain the genuine matching data for legitimate users to access.
- Maximum Likelihood Estimation can handle multiple ways of splitting the data entities.
- It is easy and quick method to compare the datasets by obtaining the matching entities.

CONCLUSION

With the upcoming data deluge of semantic data, the fast growth of ontology bases has brought significant challenges in performing efficient and scalable reasoning. Mapping process can deal with the uncertainty effect that is caused by the incomplete and inconsistent information used and produced by it for processing users' queries that can provide more correct results. MapReduce represents uncertain similarities created by both syntactic and semantic similarity algorithms. OCCT characterizes the entities that should be linked together using the splitting criterion of MLE. TIF and EAT construction significantly reduces the re-computation time for the incremental inference as well as the storage for RDF triples. Therefore, users can execute their query more efficiently without computing and searching over the entire RDF closure.

FUTURE SCOPES

In the future, the methods can validate for more datasets, such as other benchmarks and other types of datasets and also can be done in other ontology languages [9] that make the processing of data to the user's request in a highly efficient manner.

REFERENCES:

[1] N M. S. Marshall *et al*., "Emerging practices for mapping and linking life sciences data using RDF—A case series," *J. Web Semantics*, vol. 14, pp. 2–13, 2012.

[2] J. Guo, L. Xu, Z. Gong, C.-P.Che and S. S. Chaudhry, "Semantic inference on heterogeneous e-marketplace activities," *IEEE Trans. Syst.,Man, Cybern. A, Syst., Humans*, vol. 42, no. 2, pp. 316–330, Mar. 2012.

[3] J. Urbani, S. Kotoulas, J. Maassen, F. V. Harmelen and H. Bal, "WebPIE: A web-scale parallel inference engine using mapreduce," *J. Web semantics*, vol. 10, pp. 59–75, Jan 2012.

[4] J. Urbani, S. Kotoulas, E. Oren, and F. Harmelen, "Scalable distributed reasoning using mapreduce," in *Proc. 8th Int. Semantic Web Conf.*, Chantilly, VA, USA, pp. 634–649, Oct. 2009.

[5] J. Dean and S. Ghemawat, "MapReduce: Simplified data processing on large clusters," *Commun. ACM*, vol. 51, no. 1, pp. 107–113, 2008.

[6] C. Anagnostopoulos and S. Hadjiefthymiades, "Advanced inference in situation-aware computing," *IEEE Trans. Syst., Man, Cybern. A, Syst.,Humans*, vol. 39, no. 5, pp. 1108–1115, Sept. 2009.

[7] H. Paulheim and C. Bizer, "Type inference on noisy RDF data," in *Proc. ISWC*, Sydney, NSW, Australia, pp. 510–525, 2013.

[8] G. Antoniou and A. Bikakis, "DR-Prolog: A system for defeasible reasoning with rules and ontologies on the Semantic Web," *IEEE Trans.Knowl. Data Eng.*, vol. 19, no. 2, pp. 233–245, Feb. 2007.

[9] D. Lopez, J. M. Sempere, and P. García, "Inference of reversible tree languages," *IEEE Trans. Syst., Man, Cybern. B, Cybern.*,vol. 34, no. 4, pp. 1658–1665, Aug. 2004.

[10] A. Schlicht and H. Stuckenschmidt, "MapResolve," in *Proc. 5th Int. Conf. RR*, Galway, Ireland, pp. 294–299, Aug. 2011.

[11] Ma'ayan Dror and Asaf Shabtai, "OCCT: A One-Class Clustering Tree for One-to-many Data linkage," *IEEE trans. on knowledge and data engineering*, tkde-2011-09-0577, 2013.

[12] B. C. Grau, C. Halaschek-Wiener and Y. Kazakov, "History matters: Incremental ontology reasoning using modules," in *Proc. ISWC/ASWC*, Busan, Korea, pp. 183–196, 2007.

[13] J. Weaver and J. Hendler, "Parallel materialization of the finite RDFS closure for hundreds of millions of triples," in *Proc. ISWC*, Chantilly, VA, USA, pp. 682–697, 2009.

[14] Bo Liu, Member, IEEE, Keman Huang, Jianqiang Li, and MengChu Zhou, "An Incremental and Distributed Inference Method for Large-Scale Ontologies Based on MapReduce Paradigm," *IEEE Trans. on cybernetics*, vol. 45, no. 1, pp. 53-64, Jan. 2015.

International Journal of Engineering Research and General Science Volume 3, Issue 6, November-December, 2015
ISSN 2091-2730

ENERGY EFFICIENT ADAPTIVE WEIGHTED FUZZY CLUSTERING BASED ROUTING PROTOCOL IN SENSOR NETWORKS

S.Srithar[1], Dr.K.Karuppasamy[2]

Assistant Professor, Department of IT, RVS College of Engineering and Technology, Coimbatore, Tamilnadu, India

Professor & Head, Department of IT, RVS College of Engineering and Technology, Coimbatore, Tamilnadu, India

[1]sss.srithar@gmail.com

[2]kps_cse@yahoo.co.in

Abstract— Clustering approach provides a vital role for ease of data transmission through cluster head node. Clustering algorithm depends upon the characteristics such as distance, battery power, transmission data rate etc. In order to achieve good clustering performance, the cluster node should move from one cluster to another without affecting the topology. This project proposes an Adaptive Weighted Fuzzy Clustering based Cluster head selection Algorithm (AWFCA) to solve problems found in existing methods, such as the node distribution, flat structures and disturbance of the cluster formation. The proposed mechanism uses fuzzy concept to select the cluster head for clustering in wireless sensor networks. The new protocol is aimed at prolonging the lifetime and improves the stability of WSNs by finding the energy efficient cluster heads (CHs) and energy consumption of the sensor nodes using Adaptive Weighted Fuzzy Clustering method. The operation of the proposed work have set-up phase where the base station finds the CHs, and steady-state phase, where the sensed data are transferred to CHs and then to the base station. The network simulation results shows that the proposed Adaptive Weighted Fuzzy Clustering based Routing Protocol(AWFCRP) achieves better performance compared with existing Cluster Based Routing Protocol(CBRP).

Keywords— AWFCA, CBRP, Cluster Head, WSN, LEACH, First Node Die

I. INTRODUCTION

In traditional Wireless Networks uses data transmission between the sender and the receiver which uses the protocols such as AODV, DSDV, and DSR etc. Such protocols may not work in all situations. In such cases we can able to from a group of mobile nodes such as cluster to take a charge of data transmission. Once you form a cluster we need to elect the cluster head. The cluster head may act as gateway for data transmission as well as reception. Our proposed approach uses new energy efficient adaptive weighted fuzzy clustering based routing protocol for efficient content delivery.

II.LITERATURE SURVEY

Safa et al.(2014) implement dynamic energy efficient clustering algorithm(DEECA).The formation of the cluster is based on the characteristics such as mobility and network connectivity. While electing cluster head we need to focus on mobility, connectivity, energy of the wireless nodes. CH should be carefully elected for better throughput.

Yu et al. (2014) focus how wormhole attack is eliminated with the new clustering mechanism.

Ben ahmed et al.(2014) proposed an algorithm to find the misbehaved nodes with certain parameters such as NACK. Cluster formation is necessary when the there is no change in network topology or when there is a less change in that.

III.PROBLEM DEFINITION

The connectivity between the sensor nodes in the network are based on the energy. In existing system it was implemented with clustering algorithm in which it is difficult to determine the routing path and consumes more energy because of difficulty in selecting the cluster head. In order to minimize the energy consumption, we implement an improvement on cluster based routing protocol with a

combination of clustering algorithm and Adaptive weighted fuzzy logic, which is used for the determination of robust routing path across intermediate cluster heads under two cluster head node parameters such as cluster head node degree and hop count.

3.1 OVERVIEW OF THE PROJECT

In this project, we focus on clustering that clustering should satisfy some requirements as cluster should cover entire sensor field, average cluster size should be as possible to maximize data aggregation efficiency, cluster should be reorganized to balance energy consumption among nodes, cluster overhead should be controlled, some of the nodes are arranged in clusters, where each cluster consists of member of sensors, gateways, and a cluster head. Nodes of a cluster send data to their cluster head, which performs data aggregation, such as data compression, suppression, minimum, maximum, or average data. Cluster heads transmit aggregated data through the network of gateways and to a central destination. In this way consumption of energy is reduced, since, if every sensor node were to transmit data directly to a central destination, more intermediate relay nodes would be required to relay data and consume more energy. The data averaging function of the cluster heads also provides fault tolerance, minimizing the effect of failed sensor nodes.

IV.SYSTEM ANALYSIS

4.1 EXISTING SYSTEM

The cluster-based routing is an efficient way to reduce energy consumption by decreasing the number of transmitted messages to the sink node. LEACH is the most popular cluster-based routing protocol, which provides an adaptive cluster generation and cluster header rotation. However, its communication range is limited since it assumes a direct communication between sensor nodes and a sink node. However, this assumption is not applicable to sensor networks deployed in large regions. In real world applications, the obstacles (i.e., wall) should be considered to provide reliable network communication. Secondly, the random selection of a cluster header causes the skewed distribution of clusters. Next the remaining nodes join the cluster head that requires minimum communication energy. In this system, cluster head is elected only based on the energy without considering the distance of the source and the base station. The cluster headers are not uniformly distributed over the network, some nodes will fail to find a cluster header within their communication range for WSNs. Energy consumption is also high because packet transmission takes long time. So, energy of the node drains rapidly.

DRAWBACKS:

- The scheduling algorithm is formulated as the LEACH problem elect the cluster head only based on the energy.
- Energy consumption of the network is high.
- Re-clustering is occurring frequently. So that the entire transmission stops and transmission of packets gets delay.

4.2 PROPOSED SYSTEM

In this system, we propose a new energy-efficient Adaptive Weighted Fuzzy Cluster-based routing protocol (AWFCRP), which adopts a centralized clustering approach to select Cluster Head (CH) by generating a representative path. To support reliable data communication, we propose a multihop routing protocol that allows both intra- and inter cluster communications. Based on a message success rate and a representative path, the sensor nodes are uniformly distributed in clusters so that the lifetime of network can be prolonged. Through performance analysis, we show that our energy-efficient routing protocol outperforms the existing protocols up to 2 times, in terms of the distribution of cluster members, the energy consumption, and the reliability of a sensor network.

ADVANTAGES:

- The adoptive fuzzy logic control enhances routing path selection in the clustering protocol.
- This protocol provides better results than existing distributed clustering algorithm in terms of energy efficiency and network reliability.

V. SYSTEM DESIGN

5.1 SYSTEM ARCHITECTURE

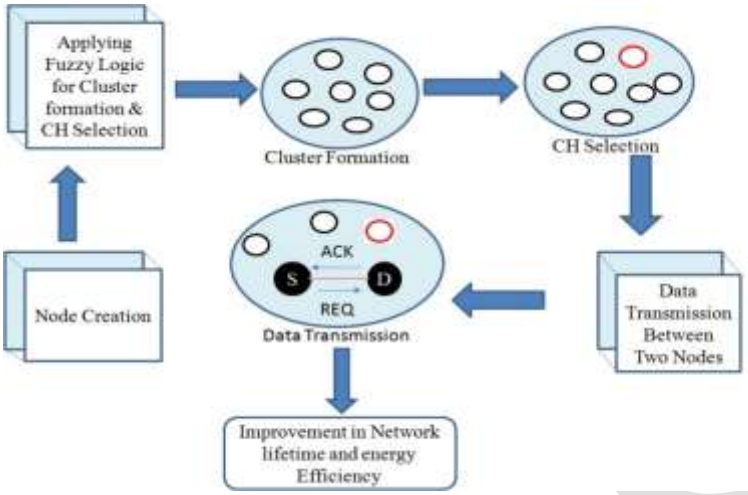

Figure 5.1: Architecture of the Proposed System

This architecture shows that, cluster head is elected based on the optimized energy and distance. So, the energy consumption is low when compared to the existing system. Re-clustering is also reduced.

Clustering also facilitates load balancing and extends network lifetime. For example, if a cluster head's energy becomes depleted due to its tasks of intra-cluster communications, performing the aggregation function, and inter-cluster communications, the cluster head may choose to resign its position new clusters may be formed and other nodes may become cluster head to relieve the current cluster head of its duties. In this way, nodes in the network share the duties of being cluster head based on some parameter such as Node connectivity, energy, mobility. Accordingly, clustering try to maximize the lifetime of the network by balancing the duties of being cluster head. Finally, clustering is proposed because of its network scalability many nodes can be added or removed from the network without significantly affecting the performance, because of the clustering architecture.

However, clustering algorithms have some disadvantages and create certain research challenges, such as protocol overheads for cluster maintenance. Other problems are to control cluster size, granularity, and density frequency of cluster changes by the nodes and cluster reselection minimizing interference and collision for intra- and inter-cluster communications and the domino effect of cluster reformation.

VI. SYSTEM IMPLEMENTATION

6.1 APPLY FUZZY CLUSTERING ALGORITHM

The proposed strategy, AWFCA, is an Adaptive Weighted Fuzzy Clustering based routing protocol , the CHs algorithm using fuzzy logic control will be constructed in the BS that has the global view over the networks. The BS is more powerful than the sensor nodes in terms of computation power, sufficient memory, unlimited power supply and storage, the BS is loaded with the fuzzy logic control to compute desirable CHs candidates. By considering three fuzzy parameters which are energy, concentration and centrality, the network lifetime can be improved.

6.2 CLUSTER FORMATION AND CLUSTER HEAD SELECTION

Cluster formation

Battery power is important concern mobile nodes. The node with less energy leads to packet loss. We cannot able to charge the nodes deployed in hazard areas. In cluster mobile nodes will be grouped into a cluster. Each cluster has a cluster head which is act as a gateway node. This will reduce the network congestion by only allowing cluster head (CH) to communicate with the base station.

Cluster Head Selection

Cluster heads are selected based on the following weighted sum $W=w_1D_1+w_2D_2+w_3D_3$ Where $D_1$is the power level of the node, D_2 is the connectivity factor and $D_3$is the stability index and w_1,w_2 and w_3 are the weighting factors. Cluster head has the least W value. After the node is selected as a cluster head, the node or the members of the node will be discerned as "considered". Every "unconsidered" node undergoes the election process. After the selection of "considered nodes" the election algorithm will be terminated.

6.3 DATA TRANSMISSION BETWEEN CH AND BS

The cluster head collects data from member nodes in the same cluster and aggregates the collected data so that it can be transmitted to the base station. Implementing this protocol will significantly reduce the overall energy used and reduce the network congestion by only allowing the cluster head to communicate with the base station. The BS(base station) considers two selection criteria from sensor nodes which are energy level and distance to the base station to select the suitable (CH) cluster head that will prolong the First Node Die (FND) time, data stream guaranteed for every round and also increase the throughput received by the base station before FND. In cluster routing protocol, energy consumption is concentrated on cluster heads which collect and aggregate the sensed data from member nodes and forward the aggregated information to the base station.

VII. PERFORMANCE ANALYSIS

The performance of the both CBRP and AWFCRP method is analyzed and X-graphs are plotted. Throughput, Energy Consumption, is the basic parameters considered here and graphs are plotted for these parameters. And the results obtained from this module is compared with the result of CBRP and comparison X-graphs are plotted.

The result of the network lifetime is achieved by the proposal algorithms. Here identical initial energy and imbalanced initial sensor nodes are employed in 1500*1500 square meters areas. The transmission range is fixed to 250 so that all of the networks generated are fully connected.

SIMULATION PARAMETERS	
Simulator	Ns-2.34
Simulation duration	40 Seconds
Simulation Area	1500*1500 Sq.meters
Number of nodes	26
Transmission Range	250m
MAC Layer Protocol	IEEE 802.11
Maximum speed	50 m/s
Packet rate	4 packet per sec
Traffic Type	CBR
Data Payload	512 bytes/packet
Transmission rate	11Mb max and 2 Mb min

Table 7.1 : Simulation Parameter

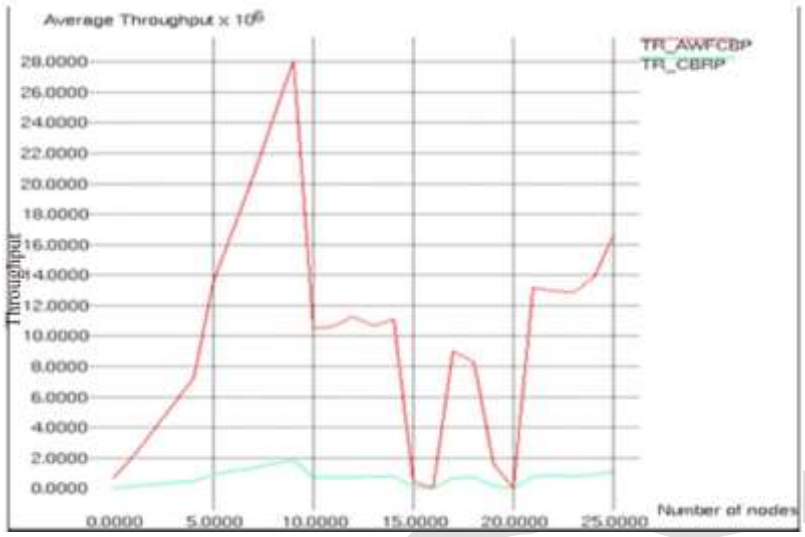

Figure 6.1: Throughput

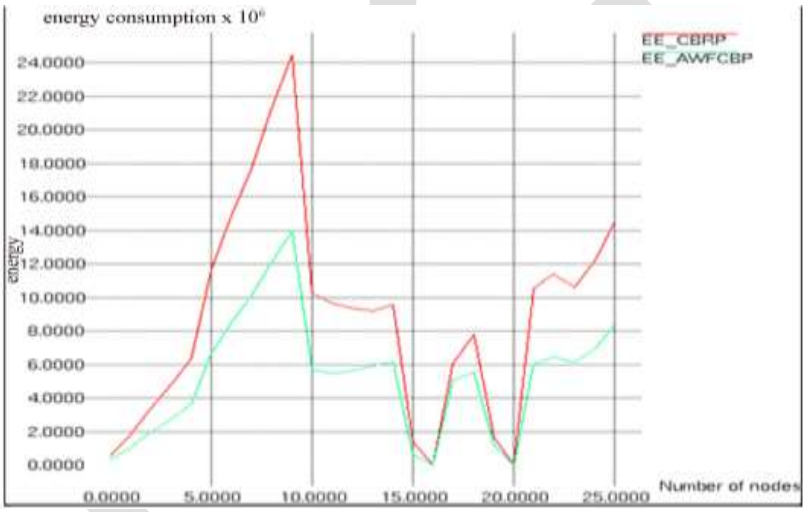

Figure 6.2: Energy Consumption

VIII. CONCLUSION AND FUTURE ENHANCEMENTS

8.1 CONCLUSION

In this work, an Adaptive Weighted Fuzzy Clustering protocol for mobile wireless sensor networks is presented. This protocol is energy efficient, flexible against node mobility and due to its recovery mechanism it also reduces packet loss. It acquires less messages exchanges during cluster head selection. It gives high packet delivery ratio and network lifetime. This method is applicable to both static networks and node having mobility. It is clear that the cluster head node closer to the base station will consume less energy than other nodes because communication of data consumes the most energy in WSNs. Thus the process of electing the cluster head is reduced. The simulation results showed that the proposed AWFCA achieves better performance than other existing mechanisms.

8.2 FUTURE ENHANCEMENT

In future, this work includes implementation of cross layer design in order to achieve more energy efficiency, robustness and more extensive simulations by using other power and mobility models, comparison with other protocols that deal with mobility.

REFERENCES:

[1] W.Choi,M.Woo(2006), "A Distributed Weighted Clustering Algorithm For Mobile Ad Hoc Networks", Proc.of the Advanced International Conference On Telecommunications And International Conference On Internet And Web Applications And Services(AICT/ICIW 2006),IEEE,2006.

[2] Dahane Aminea, Berrached Nassreddinea, Kechar Bouabdellahb(2014)," Energy Efficient and Safe Weighted Clustering Algorithm for Mobile Wireless Sensor Networks" Procedia Computer Science 34 (2014) 63 – 70 ,Elsevier, The 9th International Conference on Future Networks and Communications (FNC 2014).

[3] V.Geetha, P.V.Kallapur, S.Tellajeera(2008), " Clustering In Wireless Sensor Networks: Performance Comparison of LEACH & LEACH-C Protocols Using NS2",Procedia Technology(c3 IT-2012),Elsevier,Vol.4,PP.163-170,2012.

[4] Junping H., Yuhui J., and Liang D(2008), "A Time Based Cluster-Head Selection Algorithm for LEACH," IEEE Symposium on Computers and Communications ISCC 2008, pp. 1172-1176, 2008.

[5] Yu M., Li J., and Levy R(2006), "Mobility Resistant Clustering in Multi-Hop Wireless Networks," Journal of Networks, vol. 1, no. 1, pp. 12-19, 2006.

[6]Zhan Wei Siew, Chen How Wong, Aroland Kiring, Renee Ka Yin Chin and Kenneth Tze Kin Teo(2012),"Fuzzy logic based energy efficient protocols in Wireless Sensor Networks", Unit School of Engineering and Information Technology, University Malaysia Sabah. December 2012,Volume:03

International Journal of Engineering Research and General Science Volume 3, Issue 6, November-December, 2015
ISSN 2091-2730

Prediction of pressure drop across orifice using MATLAB and 2D analysis of flow through it using CFD

Mr. Krishna Sharma*, Mr. Pranav Salunke

Department Of Mechanical Engineering, Marathwada Mitra Mandal's College Of Engineering, Pune

*Corresponding Author: krishnabsharmas@gmail.com

Abstract—Pressure drop is predicted across the orifice when atmospheric air is flowing through it at different flow rate. For this purpose MATLAB code is created. Experimental data of pressure drop is compared with the output of MATLAB code. Values of experimental and calculated pressure drop are nearly same. This MATLAB code is useful to predict the pressure drop. To analyze the flow through orifice ANSYS FLUENT is used for CFD analysis. k-epsilon model is used to simulate turbulence flow in axisymmetric orifice. CFD results demonstrate the following parameters: axial velocity profile, static pressure, and contour of velocity inside the orifice. Numerical result matches with experimental one.

Keywords— Orifice, atmospheric air, pressure drop, MATLAB code, CFD analysis, k-epsilon model, turbulence intensity, velocity contour

INTRODUCTION

Orifice is fundamental geometry which is used in many engineering applications such as air filter assembly, gas pipelines etc. It can be also used for calibration of test setup. Experiment is conducted on sudden expansion geometry which is made up of aluminum at various flow rate.

GEOMETRY OF ORIFICE

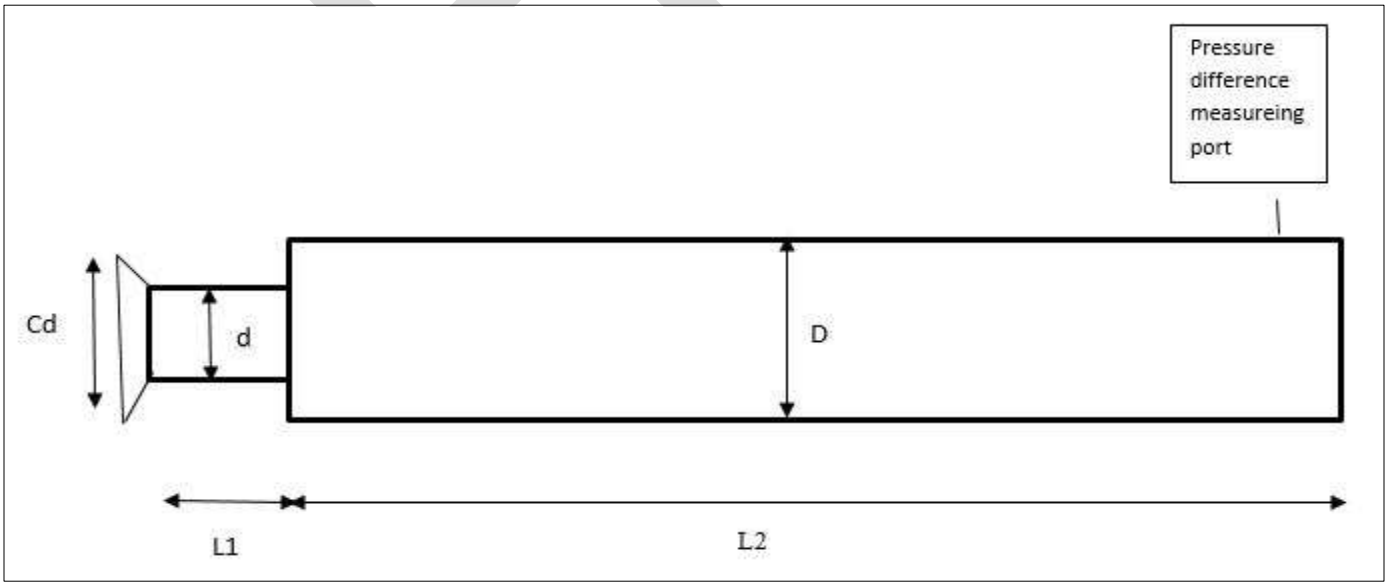

Fig. 1. Cross section of orifice

Fig. shows orifice cross section. The orifice geometry consist of a cylindrical tube of length L_1=0.96" with diameter d=1.5" and L_2= 16.58" with diameter D=4".Value of diameter at upstream is 2.34" with cone angle 51.74 degree.

TEST CONDITIONS

Test are conducted at different flow rate i.e. 100 cfm, 150.1 cfm and 201.2 cfm. While testing temperature was 29.2℃ with barometric pressure 953 milibar. Value of relative humidity was varying between 60.7% - 60.2%.

CALCULATION OF PRESSURE DROP

To calculate pressure drop across the orifice MATLAB code is created. It includes calculation of density, velocity at different sections, Reynolds number, and loss due to conical entrance, sudden expansion loss and finally pressure drop calculation. Friction losses are neglected. Generated MATLAB code is given below

```
% upstream & downstream diameter, flow rate, temperature, Relative
% humidity, Restriction at downstream, Barometric pressure, Inlet pressure
% are required as input parameter.
clc
d=input('Enter the value of orifice diameter [inch]       :');
D=input('Enter the value of pipe diameter [inch]          :');
teta=input('Cone angle in degree                             :');
cd=input ('Cone diameter [inch]                                 :');
q=input('Flow rate [cfm]                                  :');
T= input ('Enter the value of temperature [degree Celsius]%d  :');
F=input('restriction at downstream [millimeter of water column :');
RH=input('Relative humidity %                            :');
BP=input('Barometric pressure [milibar]                 :');
d=(d*0.0254);% inch to meter
D=(D*0.0254);
cd=(cd*0.0254);
A=((pi/4)*D*D);%area calculation
Ad=((pi/4)*d*d);
Acd=((pi/4)*cd*cd);
g=9.81;
b=d/D;% expansion ratio
K=((1-b*b)^2)/((b^4));
b1=d/cd;
teta=teta*(pi/180);% degree to rad
K1=((1-b1*b1)^2)/((b1^4))*0.5*((sin(teta/2))^0.5);% conical loss coefficient
q=((q*1.699)/3600); % cfm to m^3/s
RH=RH/100;
BP=BP*100; % millimeter to Pa
Vcd=q/Acd;% velocity calculation
V1=q/Ad;
V2=q/A;
m=0.017362065;
a=393;
B=(T+273)+120;
mi=m*(a/B)*((T+273)/273)^1.5;% dynamic viscosity calculation
mi=mi*10^(-3);% cP to kg/ms
Recd=(cd*Vcd*rho)/mi;
fprintf('\n Reynolds number based on cd                                  = %f',Recd);
Re1=(d*V1*rho)/mi;
fprintf('\n Reynolds number based on d                                 = %f',Re1);
Re2=(D*V2*rho)/mi;
fprintf('\n Reynolds number bases on D                                 = %f',Re2);
```

```
hteta=(K1*V1*V1)/(2*g); % pressure loss due to conical section
F=(F*100)/(10.19744);
actualp=BP-F;
rho=(actualp-(4260.96*RH))/((287.05*(273.15+T)))+(2344.217*RH)/((461.49*(273.15+T))); %
density calculation
hl=(K*V2*V2)/(2*g); % loss due to sudden expansion
p1=BP-hteta;
p2=(((p1/(rho*g))+(((V1*V1)-(V2*V2))/(2*g)))*rho*g)-hl;
P=p2-p1; % pressure drop
cf=(293/(273+T))*(BP/101325); % correction factor
hteta=hteta/(25.4*9.8);
P=P/(25.4*9.8); % Pa to inches of water column
P=(P*cf)+hteta;
fprintf('\n Pressure difference [inches of H20]                    =%f',P);
```

COMPARISION BETWEEN EXPERIMENTAL AND CALCULATED VALUE

Experimental pressure drop value is compared with calculated value which is obtained from MATLAB code. Comparison table is given below

Flow rate (cfm)	Pressure difference experimental (inches of water)	Pressure difference MATLAB (inches of water)
100	3.31	3.2851
150.1	7.41	7.3059
201.2	13.57	12.87

Table 1. Comparison between Experimental and calculated value of pressure drop

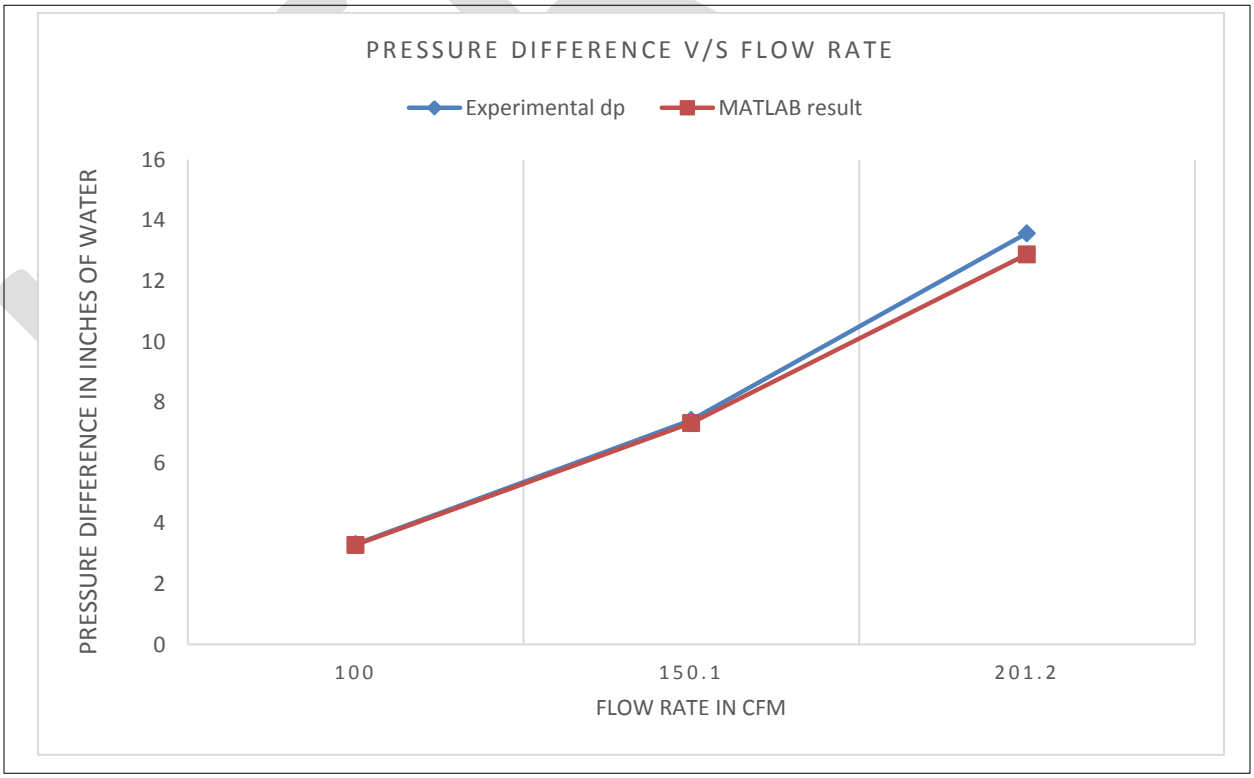

Fig.2. Graphical representation of pressure drop

From the comparison table and graph it can be observed that experimental and calculated value of pressure drop approximately equal. This means generated MATLAB code can be used to predict the pressure drop across orifice for given conditions. To understand the

behavior of the flow inside orifice CFD analysis is done.

CFD ANALYSIS OF FLOW THROUGH ORIFICE

Computational fluid dynamics had been spear heading science and technology progression by being cost effective, determining solutions for complex design challenges, incorporation of advanced. For orifice, 2D CFD analysis is done by using ANSYS FLUENT 14.0. Design Modeler is used to create 2D geometry of orifice. Proper meshing is important to analyze flow correctly. To capture the two-dimensional flow inside the domain with reasonable accuracy, one needs good quality mesh. ANSYS ICME is used for this purpose. Also while meshing named creation is done to ease boundary conditions.

Mesh details: Domain- surface_body, Nodes -38460, Elements-18520.Generally orthogonal quality ranges from 0 to 1, where value close to zero corresponds to low quality. Generated mesh quality is 0.81 which is good.

Turbulence Model: Standard (k-ε) turbulence model is used over than other turbulence model as it can predict boundary layer under strong adverse pressure gradients or separation. Rotational flow and recirculation can be exactly model by this model. Standard (k-ε) turbulence uses two partial differential equations to estimate the velocity and length scales and hence it is commonly known as two-equation model of turbulence.

Boundary conditions: For inlet, velocity boundary condition is used with gauge pressure value is equal to zero and velocity is taken from output of MATLAB code. Turbulence specifications are given with turbulence intensity and hydraulic diameter. Turbulence intensity is calculated Reynolds number i. e.0.16 $(Re)^{1/8}$.Fpr center axis boundary condition is suitable. At outlet, pressure outlet is used with gauge pressure value equal to pressure drop value which has been derived from experiment.

RESULTS & DISCUSSION

CFD Analysis was carried out with different flow rate CFD Simulation shows pressure drop across the orifice system increases as the engine rpm increase. CFD results show very good correlation with testing result. Pressure plots, streamlines, velocity vectors are created graphically.

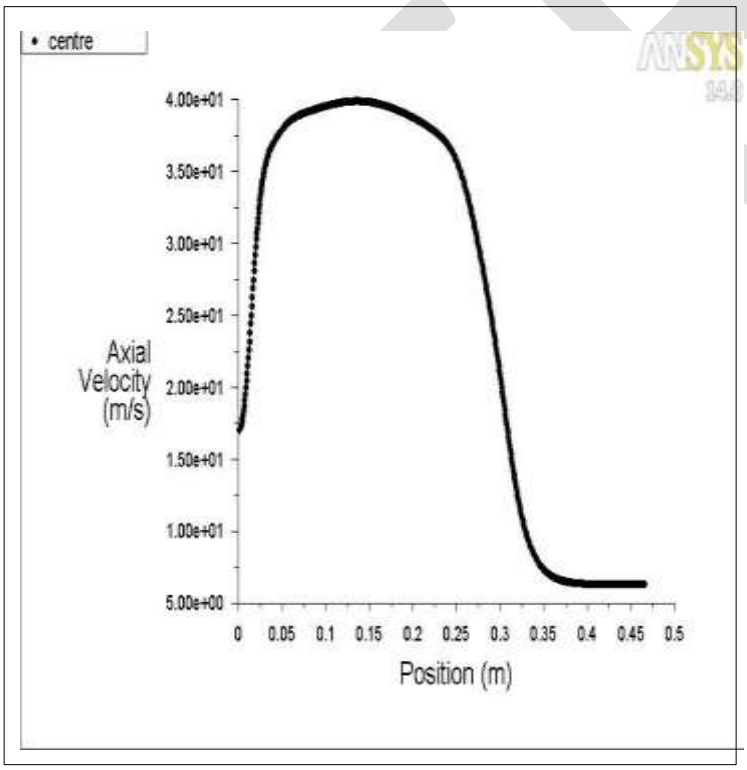

Fig.3 a) Axial velocity at flow rate 100 cfm

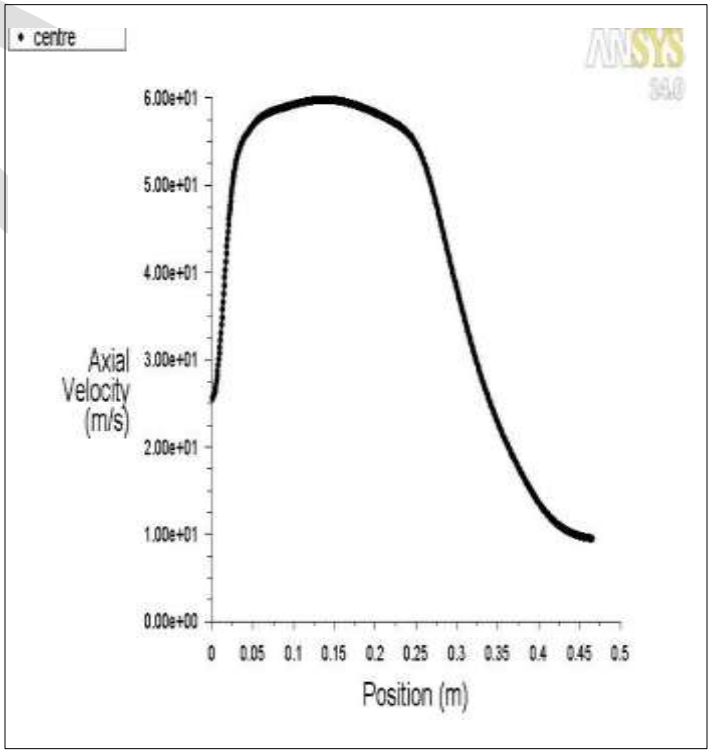

Fig 3 b) Axial velocity at flow rate 150.1 cfm

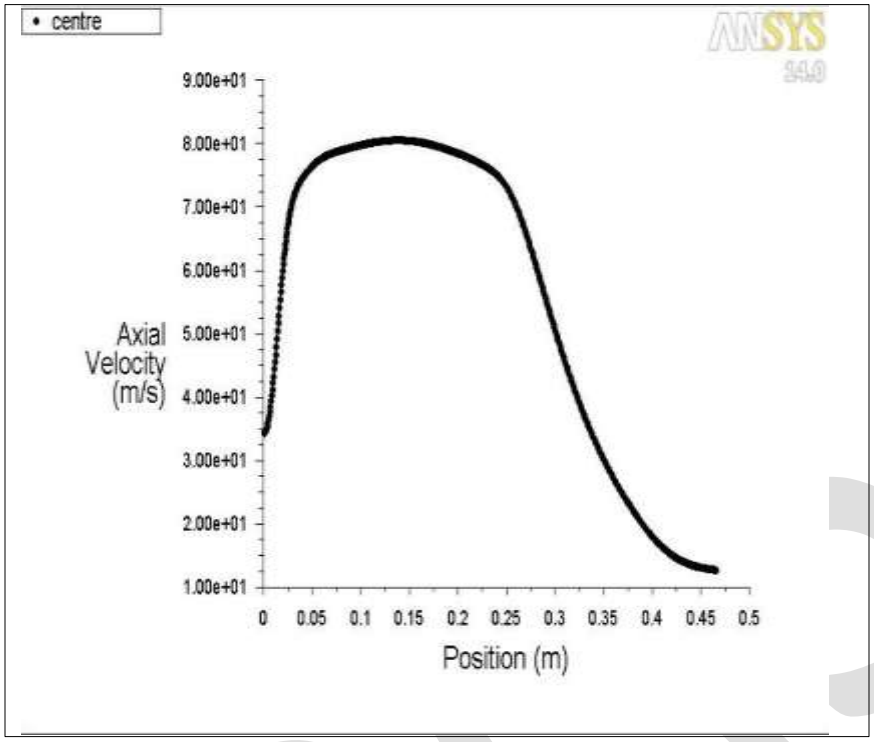

Fig 3 c) Axial velocity at flow rate 200.1 cfm

From these graphs, analysis of axial velocity inside the orifice can be done properly. It can be observed that axial velocity first increases from conical section to orifice diameter. Then due to sudden expansion velocity decreases .Axial velocity is minimum at the section of large diameter. Velocity calculated at the output from MATLAB code matches with CFD results.

Value of static pressure:

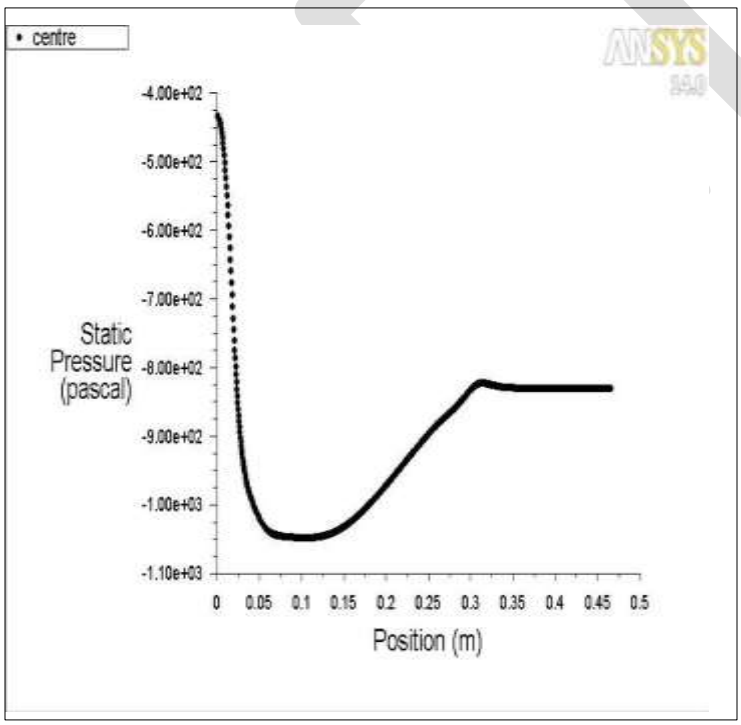

Fig. 4 a) Static pressure at 100 cfm

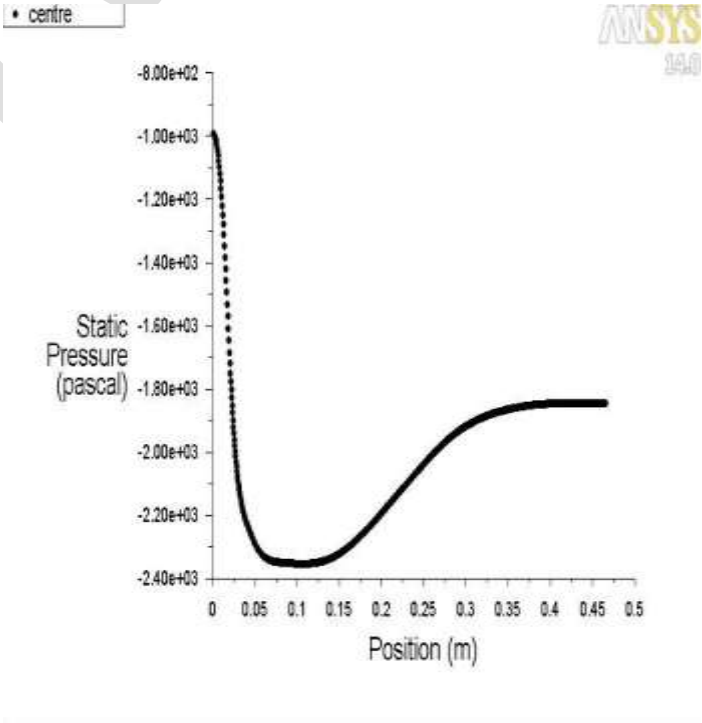

Fig. 4 b) Static pressure at 150.1 cfm

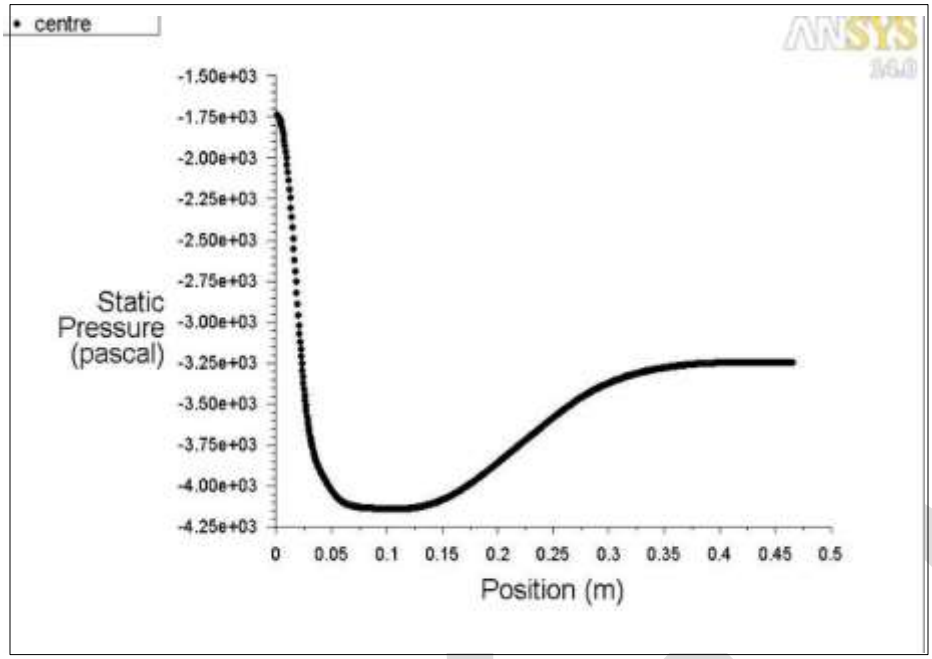

Fig. 4 c) Static pressure at 200.1 cfm

Behavior of static pressure can be observed clearly. Maximum pressure is at inlet and it reduces due to decrease in diameter. Again due to sudden expansion value of static pressure increases.
Contour of velocity streamline is generated for the flow rate of 100 cfm. It is maximum just after expansion.

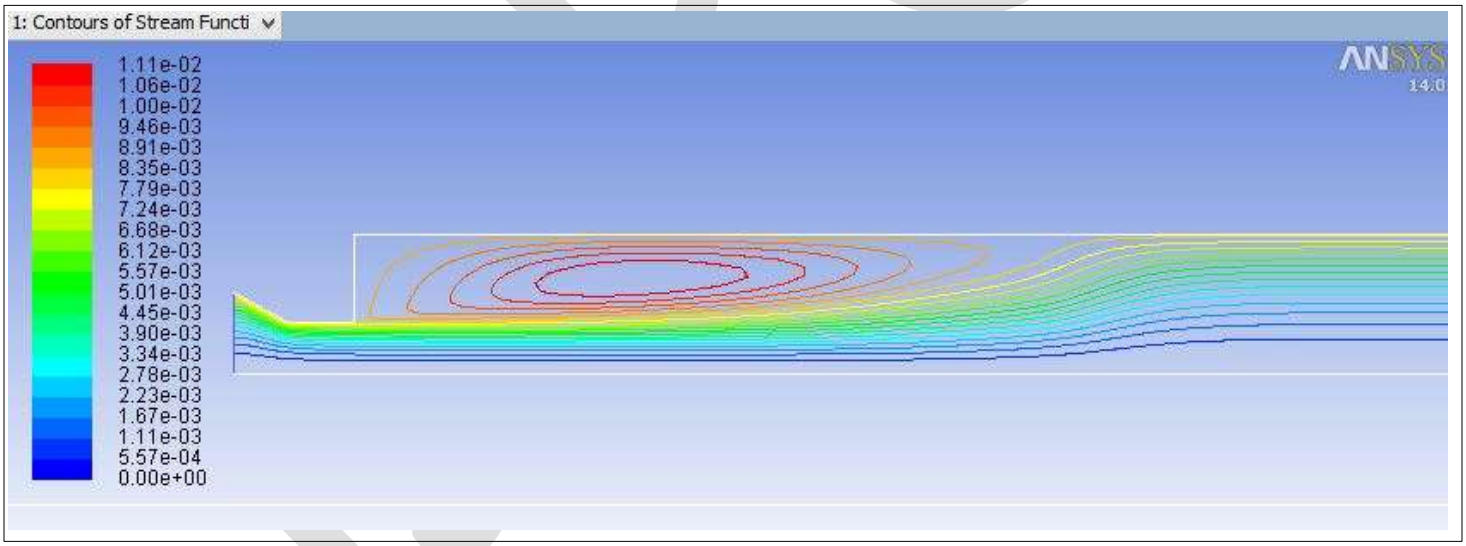

Fig.5 Contour of velocity streamline

It also matches with PIV experiment (Hammad et al., Experiments in Fluids, 1999, 26:266-271). It can be seen that the numerical result agree with the experiment one.

ACKNOWLEDGMENT

We wish to thank and express deep sense of gratitude to our college Marathwada Mitra Mandal's College Of Engineering, Pune and Dr. Ashok Kumar Vaikuntam for his consistent guidance and sympathetic attitude throughout the work.

CONCLUSION

As stated earlier, the objective of this study is to predict the pressure drop across orifice which is achieved by creating the MATLAB code. Numerical result agree with experiment one. Analysis of flow is done by ANSYS FLUENT. Axial velocity at various section and value of static pressure at center is studied. Contour of velocity streamline matches with PIV experiment (Hammad et al., Experiments in Fluids, 1999, 26:266-271).

REFERENCES:

[1] J. Mamizadeh abd S.A. Ayyoubzadeh " Simulation of flow pattern in open channel with sudden expansions " Research Journal Of Applied Science and Technology, ISSN: 2040-7467 , October 01, 2012
[2] Baoyu Guo, Tim A.G. Langrish and David F. Fletcher " Simulation of precession in axisymmetric sudden expansion flows" Second International Conference on CFD in Minerals and Process industries CSIRO, Melbourne, Australia, 6-8 December 1999
[3] Mohommad Reza Bazargan-Lari and Abbas Mansoori " CFD based location prediction of maximum negative pressure in pipe sudden expansions "5th WSEAS International Conference Of Fluid Mechanics Acapulco, Mexico, January 25-27,2008
[4] Monomed A. Siba, Wan-Mohd Faizal Wan Mohomood and Mohamed H. Nassir " Modelling and application of 3D flow in orifice plate at low turbulence Reynolds numbers" International Journal Of Mechanical and Mechatronics Engineering IJMME-IJENS, Vol:15 No:4
[5] Abbas Mansoori and Mohommad Reza Bazargan-Lari " Evaluation of turbulence model in sudden expansion analysis at high Reynolds number" Proceeding of 5th IASME/ WSEAS Internatinal Conference Of Fluid Mechanics and Aerodynamics,Athens, Greece, August 25-27,2007
[6] L. Casarsa and P. Giannattasio "Three-dimensional features of the turbulent flow through a planar sudden expansion " PHYSICS OF FLUIDS 20, 015103 (2008), 28 January 2008
[7] A.S.Phulpagar,and N.S Gohel " CFD Analysis of Air Intake System" Ird India
[8] John D Anderson Jr, Computational Fluid Dynamics: The Basics with Applications, Fourth Edition, New York: McGraw Hill International Editions, 1995, pp. 4-82.
[9] Graber, D., 1982. Asymmetric flow in symmetric expansions. J. Hydr. Div., 108: 133-140.
[10] Poole, R.J., Escudier , M.P. (2004) " Turbulent flow of viscoelastic fluids through an axisymmetric sudden expansion" J.Non-Newtonian Fluid Mech.
[11] Chaturvedi, M.C. (1993) "Flow characteristics of axisymmetric expansions" Journal of hydraulic division, ASCE Vol89,No HY3.
[12] Ansys Inc, Ansys Fluent User Manual

International Journal of Engineering Research and General Science Volume 3, Issue 6, November-December, 2015
ISSN 2091-2730

Design of Improved Systolic Array Multiplier and Its Implementation on FPGA

Miss. Pritam H. Langade

Department of Electronics and Telecommunication,

SSGMCE,Shegaon.

pritam.langade@gmail.com

Prof. S. B. Patil

Department of Electronics and Telecommunication,

SSGMCE,Shegaon.

Abstract— In the recent technology, there is a need of high speed and powerful data processing. Such complex problem is overcome by using parallel computing technology which uses the concept of pipelining for this application. This project provides the implementation issues in systolic array multiplier for high speed data processing. This also introduces the concept of parallel processing and pipelining which improves the speed of execution. In this project, a new method of multiplying matrices using systolic array multiplier is designed and each processing element in systolic array is replaced by Dadda multiplier. Here the VHDL code is written for matrix multiplication with systolic architecture. It is compiled and simulated by using Modelsim SE 6.3f, synthesized by using Xilinx ISE 14.5 and targeted to the device XC3S500E-4-FG320.

Keywords— Parallel Processing, Pipelining, Systolic Array, Multiplication, Dadda Multiplier.

INTRODUCTION

Systolic algorithm is the form of pipelining, which is in more than one dimension [16]. In this algorithm, data flows from a memory in a rhythmic way and it passes through many processing elements before it returns to memory. Systolic arrays have balanced, uniform, grid like architectures in which each line indicates a communication path and each intersection represents a cell or systolic elements [13]. High speed multiplication is a basic requirement of digital systems giving high performance [10]. Execution time for Parallel multiplication has been decreased by using the technique of column compression [8]. There are two classes of parallel multipliers, which are array multipliers and tree multipliers. Tree multipliers are also known as column compression multipliers. Column compression multipliers are faster than array multipliers. Two of the most well-known column compression multipliers have been presented by Dadda and Wallace. Dadda multiplier has a faster performance, so it is used for the implementation of the proposed multiplier. Systolic Arrays are computational networks, with local data storage, that uses the parallel processing and pipelining techniques to achieve a high throughput [6]. Matrix multiplication is a computation intensive operation and plays an important role in many scientific and engineering applications [2]**.** This work demonstrates an effective design and efficient implementation of the Matrix Multiplication using Systolic Architecture. In this project, matrices are multiplied by using systolic array multiplier and each processing element in this Systolic array multiplier is replaced by Dadda multiplier. Dadda multiplier is a binary multiplier which uses the concept of column compression to reduce the partial products and hence increases the speed of multiplication.

PROPOSED WORK

Multipliers play an important role in today's digital signal processing and various other applications [9]. With advances in technology, many researchers have tried and are trying to design multipliers which offer high speed, low power consumption, regularity of layout and hence less area or even combination of them in one multiplier thus making them suitable for various high speed, low power and compact VLSI implementation.

1. ARRAY MULTIPLIER

Array multiplier is an efficient layout of a combinational multiplier. An n x n array multiplier requires n(n-1) adders and n^2 AND gates. Figure 1 shows a 4 bit array multiplier. Array multipliers have a large critical path and are very slow. The main advantage of these multipliers is the regular structure which leads to ease of layout and design. Array multiplier requires n (n-2) full adders, n half-adders and n^2 AND gates.

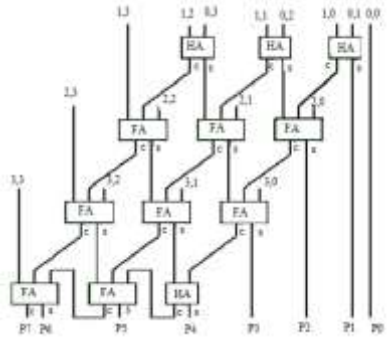

Fig 1: Architecture of 4 bit array multiplier.

2. WALLACE MULTIPLIER

The Wallace tree multiplier belongs to a family of multipliers called column compression multipliers[12]. Wallace multiplier is an efficient parallel multiplier. A Wallace tree multiplier offers faster performance for large operands. In Wallace's scheme, the partial products are reduced as soon as possible which is shown in fig. 2.

Conventional Wallace tree multiplier includes the following steps:

I. First step is to form partial product array (of n^2 bits).

II. In the second step, groups of three adjacent rows each, is collected. Each group of three rows is reduced by using full adders and half adders. Full adders are used in each column where there are three bits whereas half adders are used in each column where there are two bits. Any single bit in a column is passed to the next stage in the same column without processing. This reduction procedure is repeated in each successive stage until only two rows remain.

III. In the final step, the remaining two rows are added using a carry propagating adder. In a conventional Wallace multiplier, the number of rows in subsequent stages can be calculated as:

ri+1 = 2[ri/3] + ri mod 3 -------(1)

Where, ri mod 3 denotes the smallest non-negative remainder of ri/3.

Length of carry propogation adder is given by 2N-2-S,where N is the bit number and S is the number of stages required.

For example, in 4 bit Wallace multiplier, $r_i = r_0 = N = 4$, required number of stages are 2 and carry propogation adder is of 4 bit.

$$r_1 = 2\left(\frac{4}{3}\right) + 4 \bmod 3 = 3$$

Height is reduced upto 3, in first stage.

$r2 = 2\left(\frac{3}{3}\right) + 3 \bmod 3 = 2$. Thus in second stage, the height is reduced to 2.

The Wallace tree consists of numerous levels of such column compression structures. Wallace tree reduces the number of partial products to be added into 2 final intermediate results [14]. These two operands can then be added using fast carry-propagate

adder to obtain the product result.What differentiates the Wallace tree multiplier from other column compression multipliers is that in the Wallace tree, every possible bit in every column is covered by the (3:2) or (2:2) compressors repetitively until finally the partial product matrix has a depth of only 2. Thus the Wallace tree multiplier uses as much hardware as possible to compress the partial product matrix as quickly as possible into the final product.

3. DADDA MULTIPLIER

Dadda's method does minimum reduction necessary at each level and requires the same number of levels as Wallace multiplier.In Dadda multiplier, less reductions are carried out in earlier stages.

The Dadda multiplier architecture can be divided into three stages.

I. Generation of partial products.
II. Partial product reduction.
   a) Let h1 = 2 and repeat hj+1 = floor (1.5*hj) for increasing values of j. Continue this until the largest j is reached, for which there exists at least one column in the present stage of the matrix with more dots than hj. Using this equation we get h1=2, h2=3, h3=4, h4=6, h5=9 and so on. As shown in figure 3, for example, in the first stage of the 4bit Dadda multiplication, the maximum height of columns is 4 therefore, the value of hj is 3 means heights of the columns are reduced to a maximum of 3. Similarly in the second stage, the maximum height of column is 3 and value of hj is 2 means heights of the columns are reduced to a maximum of 2.
   b) All the columns, with heights greater than hj, are reduced to a height of hj using either half adder or full adder. If the column height has to be reduced by one, use a half adder else use a full adder and continue this step till the column height is reduced to hj.
   c) Stop the reduction if the height of the matrix becomes two, after which it can be fed to final adder.
III. Once the height of matrix is reduced to two, the remaining two rows are added using a lookahead carry adder.

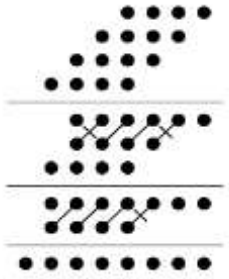

Fig 2: 4 bit Wallace multiplier

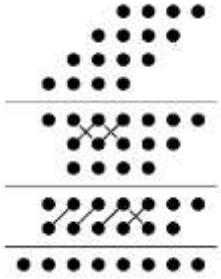

Fig 3: 4 bit Dadda multiplier

The Parallel Matrix Multiplication has many different identifications, but all with the similar implementation [4]. Parallelism is relevant not only for the data operations but also for the data transfer [5]. In this project, the PE is replaced with n bit Dadda multiplier to enhance the speed of Systolic Architecture. Also, aim is to compute the following equation with a two dimensional systolic array.

$$C_{m\times m} = A_{m\times m} \times B_{m\times m} \text{ ----------(1)}$$

Where A, B and C are the matrices with order $m \times m$. Each PE of systolic array performs binary multiplication of two n bit numbers. A systolic array multiplier is an arrangement of processing elements in an array where data flows synchronously across the array between neighbours usually with different data flowing in different directions[7],[15]. PE at each step takes input data from each step, outputs result in the opposite direction[11].Systolic Array is a set of interconnected cells which performs simple operation[1].

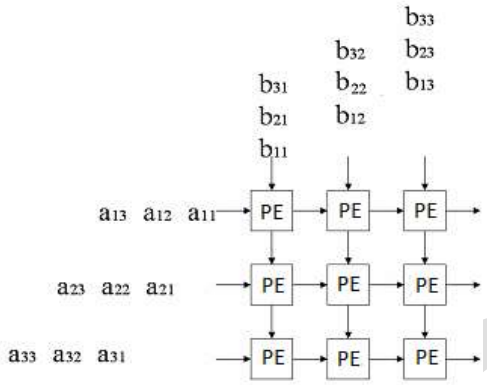

Fig 4: Systolic Array for matrix multiplication

The resulting output of this matrix is

$$\begin{pmatrix} C_{11} & C_{12} & C_{13} \\ C_{21} & C_{22} & C_{23} \\ C_{31} & C_{32} & C_{33} \end{pmatrix}$$

For example, when multiplying two 3*3 matrix we need 27 operations by conventional method according to the given formula:

```
For I = 1 to N
   For J = 1 to N
      For K = 1 to N
         C[I,J] = C[I,J] + A[J,K] * B[K,J];
      End
   End
End
```

But using systolic arrays, it can be done in only 9 clock pulses. So systolic array multiplier is used for matrix multiplication. The proposed two dimensional systolic array architecture is shown in figure 4, where each processing element is replaced with n bit Dadda multiplier. As in Dadda multiplier, fewer columns are compressed in the initial stages,and more columns in the later levels of the multiplier, it requires less expensive reduction phase and less hardware. Since the Dadda multiplier has a faster performance, we implement the proposed technique using this multiplier. During multiplication of two matrices, elements of first matrix are entered in normal way and second matrix elements are transposed before entering in processing element.

RESULTS AND DISCUSSION

The proposed Systolic array multiplier is very efficient multiplier which uses the concept of pipelining to enhance the speed of matrix multiplication. In this project, a new method of multiplying matrices using systolic array multiplier is designed. Here the speed of Array multiplier, Wallace multiplier and Dadda multiplier is verified. Out of these multipliers, Dadda multiplier is found to be having high speed and less area is utilized to design it. So, in proposed systolic array multiplier, Dadda multiplier is used as processing element to increase speed of matrix multiplication. It is compared with previously designed systolic array multiplier and it is found that the proposed design is faster and requires less number of registers as compared to previous one.

Simulation Results

The fig. 5, fig 6 and fig 7 shows the simulation results of Array multiplier, Wallace multiplier and Dadda multiplier respectively in which two 4 bit binary numbers 'a' and 'b' are given as input to produce 8 bit prod as output.

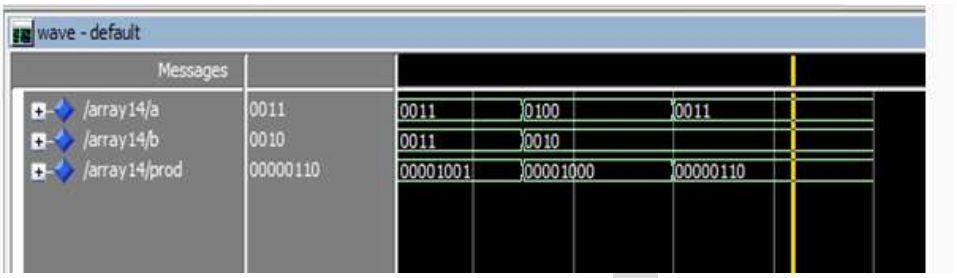

Fig 5 : Simulation of 4 bit Array Multiplier

Fig 6 : Simulation of 4 bit Wallace multiplier

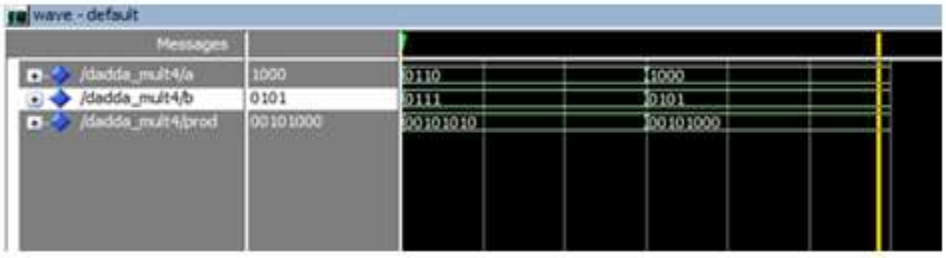

Fig 7: Simulation of 4 bit Dadda multiplier

The figure 8 shows the simulation result of proposed systolic array multiplier for matrix multiplication where each processing element is Dadda multiplier.

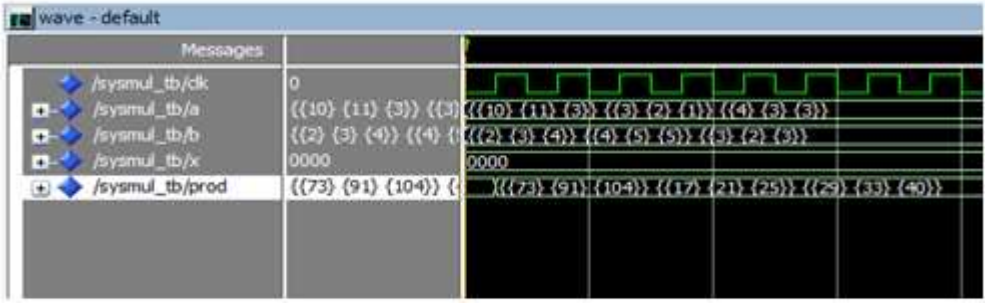

Fig 8 : Simulation of proposed systolic array multiplier

From simulation result, it is clear that the systolic array multiplier requires less number of clock cycles to multiply two matrices than mathematical calculation. Hence systolic array multiplier is the effective method for multiplication of matrices.

Design utilization summary and delays

Following Table I, Table II and Table III shows design utilization summary of Array multiplier, Wallace multiplier and Dadda multiplier respectively.

Table I : Summary of Array multiplier

Device Utilization Summary			
Logic Utilization	**Used**	**Available**	**Utilization**
Number of 4 input LUTs	33	9,312	1%
Number of occupied Slices	18	4,656	1%
Number of Slices containing only related logic	18	18	100%
Number of Slices containing unrelated logic	0	18	0%
Total Number of 4 input LUTs	33	9,312	1%
Number of bonded IOBs	16	232	6%
Average Fanout of Non-Clock Nets	2.73		

Table II : Summary of Wallace multiplier

Device Utilization Summary			
Logic Utilization	**Used**	**Available**	**Utilization**
Number of 4 input LUTs	30	9,312	1%
Number of occupied Slices	17	4,656	1%
Number of Slices containing only related logic	17	17	100%
Number of Slices containing unrelated logic	0	17	0%
Total Number of 4 input LUTs	30	9,312	1%
Number of bonded IOBs	16	232	6%
Average Fanout of Non-Clock Nets	2.84		

Table III : Summary of Dadda multiplier

Device Utilization Summary			
Logic Utilization	**Used**	**Available**	**Utilization**
Number of 4 input LUTs	28	9,312	1%
Number of occupied Slices	15	4,656	1%
Number of Slices containing only related logic	15	15	100%
Number of Slices containing unrelated logic	0	15	0%
Total Number of 4 input LUTs	28	9,312	1%
Number of bonded IOBs	16	232	6%
Average Fanout of Non-Clock Nets	3.63		

The above design utilization summary of multipliers shows that Dadda multiplier used less number of slices, 4 i/p LUTs than Array and Wallace multiplier. It also has minimum path delay than Array and Wallace multipliers which is shown in the following Table IV. Hence it has more speed and is used as processing element in proposed systolic array multiplier.

Table IV : Comparison of Delays in Multipliers

Multipliers	Delays
Array Multiplier	10.466 ns
Wallace Multiplier	10.335 ns.
Dadda Multiplier	10.191 ns.

The implementation of n x n matrix multiplication is done by using systolic array multiplier having n bit Dadda multiplier as a processing element. The simulation result in fig 8 shows input and output matrices $A_{3\times3}$, $B_{3\times3}$, $C_{3\times3}$ respectively where the matrix elements are of 4 bit each. After simulation, the design is synthesized on the platform XILINX ISE 14.5 and is targeted to the device XC3S500E-4-FG320. Critical path delay represents the core speed of the design. The proposed systolic array multiplier is compared with previously designed systolic array multiplier which is shown in following Table V. It is noticed that the core speed of systolic array multiplier is 228.93MHz which is more than previously designed systolic array multiplier and it also requires less number of 8 bit registers.

Table V : Comparison of Systolic Array Multiplier

Parameters	Improved Systolic Array Multiplier	Previously designed Systolic Array Multiplier
1) Critical path delay	4.368 ns	4.757 ns
2) 8 bit registers	9	34
3) Core speed	228.93MHz	210MHz

CONCLUSION

Systolic Array Multiplier is an arrangement of processors in an array where data flows synchronously across the array between neighbours, usually with different data flowing in different directions. Systolic array multiplier is very efficient multiplier which uses the concept of pipelining to enhance the speed of multiplication. The proposed Systolic Array Multiplier multiplies n x n matrices with less number of clock cycles. In this proposed work, each processing element is replaced by Dadda multiplier to reduce delay and hence increases the speed of multiplication. Consequently, proposed Systolic Array Multiplier can be considered as an ideal primitive for dense matrix vector multiplication which is quite adequate for most image processing applications. The proposed Systolic Array Multiplier is possible using the given software algorithm and hardware implementation so that it can achieve higher speed as compared to existing Systolic Array Multiplier. The designed matrix multiplier is simulated using ModelSim SE 6.3f and implemented on a Xilinx ISE 14.5 then targeted on xc3s500EFG320FPGA.

REFERENCES:

[1] H. T. Kung, "Why Systolic Architecture?" IEEE Computer,15(1),(1982)37-46.

[2] Syed Manzoor Qasim, Shuja Ahmad Abbasi and Bandar Almashary, " A Proposed FPGA-based Parallel Architecture for Matrix Multiplication" 978-1-4244-2342-2/08/$25.00 ©2008 IEEE.

[3] Syed M. Quasim,Ahmed A. Telba and Abdulhameed Y. AIMazroo, "FPGA implementation of matrix multiplier architectures for use in image and signal processing application", IJCSNS International Journal of Computer Science And Network Security, VOL.10 No.2,February 2010.

[4] Mahendra Vucha, Arvinda Rajawat ,"Design and implementation of systolic array architecture for matrix multiplication", IJCA International Journal of Computer Applications (0975-8887),Volume 26-No.3,July 2011.

[5] Ekta Agrawal, "Systolic and Semi-Systolic Multiplier", MIT International Journal of Electronics and Communication Engineering, *Vol. 3, No. 2, August 2013, pp. 90–93, ISSN No. 2230-7672* ©MIT Publications.

[6] Mohammad Mahdi Azadfar , "Implementation of A Optimized Systolic Array Architecture for FSBMA using FPGA for Real-time Applications", IJCSNS International Journal of Computer Science and Network Security, VOL.8 NO.3,March 2008.

[7] Ganapathi Hegde, Cyril Prasanna Raj P , P.R. Vaya: "Implementation of Systolic Array Architecture for Full Search Block Matching Algorithm on FPGA", European Journal of Scientific Research,Vol.33 No.4(2009),pp.606-616.

[8] Bhabani P. Sinha, Pradip K. Srimani, "Fast Parallel Algorithms for Binary Multiplication and Their Implementation on Systolic Architectures", IEEE Transactions on computers, Vol.38. No.3. March 1989.

[9] Jasbir Kaur and Kavita, " Structural VHDL Implementation of Wallace Multiplier" International Journal of Scientific & Engineering Research, Volume 4, Issue 4, April-2013 1829 ISSN 2229-5518.

[10] B. Ramkumar, V. Sreedeep and Harish M Kittur, Member, IEEE, " A Design Technique for Faster Dadda Multiplier ".

[11] Anuja George, "A Novel Design of Low Power, High Speed SAMM and its FPGA Implementation", International Journal of Computer Applications (0975 – 8887) Volume 43– No.4, April 2012.

[12] K'Andrea C Bickerstaff, Earl E Swartzlander and Michael J. Schulte, "Analysis of column compression multipliers," 0-7695-1150-3/01 $10.00@ 2001 IEEE.

[13] Kurtis T. Johnson and A.R.Hurson, Pennsylvania State University, "General Purpose Systolic Arrays" IEEE, Nov.1993.

[14] K.Gopi Krishna, B.Santhoshand V.S ridhar, "Design of Wallace Tree Multiplier using Compressors", International journal of engineering sciences & research Technology,September 2013.

[15] Bairu K. Saptalakar, Deepak kale, Mahesh Rachannavar , Pavankumar M. K, "Design and Implementation of VLSI Systolic Array Multiplier for DSP Applications", International Journal of Scientific Engineering and Technology (ISSN : 2277-1581) Volume 2 Issue 3, PP : 156-159 1 April 2013.

[16] Himani Harmanbir Singh Sidhu, "Design and Implementation Modified Booth algorithm and systolic multiplier using FPGA" International Journal of Engineering Research & Technology (IJERT) Vol. 2 Issue 11, November – 2013.

International Journal of Engineering Research and General Science Volume 3, Issue 6, November-December, 2015
ISSN 2091-2730

AN OVERVIEW OF HANDWRITTEN GURMUKHI CHARACTER RECOGNITION

Ambuj, Nishant Anand
M.tech. Student, CBS Group of Institutions, Jhajjar, Haryana;ambuj965@gmail.com;9999429018

Abstract- In this thesis work we have suggested offline recognition of isolated handwritten characters of Gurmukhi script. We have also prolonged the work by applying the same methodology to recognize handwritten Gurmukhi numerals. In our work we have considered 35 fundamental characters of Gurmukhi script all assumed to be isolated and bearing header lines on top to recognize. In numerals, handwritten elements of ten digits from different writers are considered.

Gurmukhi numerals using three characteristic sets and three classifiers. Among three characteristic sets, first characteristic set is comprised of distance profiles having 128 characteristic . Second characteristic set is comprised of different types of projection histograms having 190 characteristic. Third characteristic set is comprised of zonal density and Background Directional Distribution forming 144 features. The three classifiers used are:- SVM , PNN & K-NN The SVM classifier is used with Radial Basis Function kernel. We have observed the 5-fold cross verification accuracy in the case of each characteristic set and classifier. We have obtained the optimized result with each combination of characteristic set and classifier by adjusting the different limits. The results are compared and trends of result in each combination of characteristic set and classifier with varying limits is also discussed. With PNN and K-NN the highest results are obtained using third characteristic set as 98.33% and 98.51% respectively while with SVM the highest result is obtained using second characteristic set as 99.2%. The results with SVM for all characteristic sets are higher than the output with PNN & K-NN.

Keywords— Handwritten Gurumukhi Character Recognition, Diagonal characteristic, SVM classifier with RBF kernel.

I. INTRODUCTION

The storage of scanned data have to be cumbersome in size and many processing applications as searching for a content, checking, maintenance are either hard or impossible. Such data require human beings to process them manually, for example, postman‟s manual action toward acceptance and sorting of postal addresses and zip code. Optical character recognition translates such scanned images of printed, typewritten or handwritten documents into machine predeterminded text. This translated machine predeterminded text can be easily edited, searched and can be processed in many other ways according to needs. It also requires small size for storage in comparison to scanned documents. Optical character recognition helps humans ease and reduce their jobs of manually handling and processing of documents. Computerized processing to identify individual character is required to change scanned data into machine encoded form.

In comparison to languages like English and Japanese, the recognition research on Indian languages and scripts is relatively lagging behind. Among available research work on Indian languages, most of the work is on Devnagari and Bangla script. The work on other Indian languages is in fewer amounts

1.1 CLASSIFICATION OF CHARACTER RECOGNITION SYSTEM

Earlier OCR was widely used to identify printed or typewritten data. But recently, there is an increasing trend to identify handwritten data. The identification of handwritten data is more difficult in comparison to identification of printed data. It is because handwritten data contains unconstrained variations of written styles by different writers even distinct writing styles of same writer on different times and moods. Sometimes, even a writer can‟t identify his/her own handwriting, so it is very difficult to gain acceptable identification accuracy involving all possible changes of handwritten samples.

1.2 **RECOGNITION SCHEME**

OCR involves many steps to completely identify and produce machine encoded text. These stages are termed as: Pre-refinement, Segmentation, characteristics extraction, Classification and Post processing. The composition of these stages is shown in figure 1.2 and these stages are listed below with brief description. These stages, except post processing are elaborated in next section of overview of OCR stages .

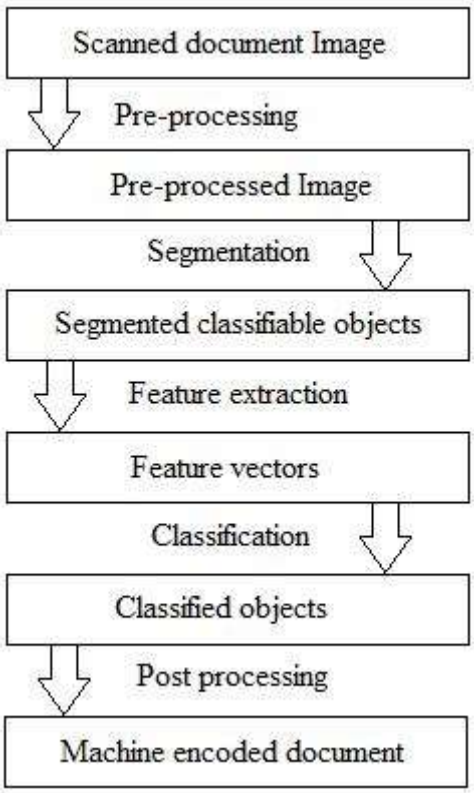

Pre-processing

The pre-processing is a series of operations performed on the scanned input image. It essentially improves the image rendering it suitable for segment formation. The following steps are used to create data-set. Entire work has been done in Mat lab.

Handwritten sample is scanned in RGB format.

RGB image is converted into gray-scale image.

Gray-scale image is converted into binary image by using a suitable threshold value by Otsu's method.

Other preprocessing method like median filtration, dilation, some morphological operations are applied to join separate pixels, to remove isolated pixels, to set neighbor pixel values in majority and to remove the spur pixels.

Segmentation

In the segmentation stage, an image of sequence of characters is decomposed into sub-images of individual feature [14]. In the proposed system, the pre-processed input image is segmented into isolated features by assigning a number to each feature using a labeling process. This labeling provides data about number of features in the image. Each individual feature is uniformly re sized into 10^2 x 10^2 pixels for extracting characteristics .

Feature Extraction

Diagonal characteristics are very important characteristics in order to achieve higher recognition accuracy and reducing miscalculation. These characteristics are extracted from the pixels of each zone by moving along its slant as shown in Fig 2. Following procedure describes the computation of Diagonal characteristics for each character image of size 10^2*10^2 pixels having 10*10 zones and thus each zone having 10*10 pixel size. Each of these zones are having 19 slants. The number of foreground pixels along each diagonal are summed up to get 19 characteristics from each zone, then these characteristics for each zone are averaged to extract a single characteristics from each zone.

ISSUES OF HANDWRITTEN CHARACTER RECOGNITION

To identify handwritten documents, either online or offline, the character identification is much affected by style changes of handwriting by different writers and even different styles of same writer on distinct times. alteration and noise incorporated while digitization is also a major issue in character identification that affects the recognition accuracy negatively. The many character identification issues regarding handwritten feature identification are listed below:

Handwriting Style Variations

Constrained and Unconstrained Handwriting

Writer Dependent or Independent Recognition

Personal and Situational Aspects

PROPOSED WORK

In our proposed work we have identified isolated handwritten characters of " Gurmukhi " script. In our work we have used some statistical characteristics like projection histograms, distance profiles and zonal density; and one direction characteristics Background Directional Distribution in different combinations to construct different characteristics vectors. We have presented detailed comparative analysis of the recognition with these characteristics vectors using three types of classifiers- Support Vector Machines , KNN and PNN . The best result obtained is 95.07% with zonal density and BDD characteristics in combination and SVM classifier for character recognition. We have also recognized "Gurmukhi" numerals with different features and best recognition rate obtained is 99.2%. The detailed description of the proposed work for character and numeral recognition is given in chapter 3 and chapter 4 respectively.

REFERENCES:

1. G.G. Rajput, S.M. Mali, “Fourier Descriptor Based Isolated Marathi Handwritten Numeral Recognition”, *International Journal of Computer Applications*, Vol. 3, No. 4, pp. 9-13, June 2010

2. Chih-Chung Chang and Christian Lindig, LIBSVM: a library for support vector machines, 2001. Software available at http://www.csie.ntu.edu.tw/~cjlin/libsvm

3. Chih-Wei Hsu, Chih-Chung Chang, and Chih-Jen Lin, “A Practical Guide to Support Vector Classification”, [Online]. Available: http://www.csie.ntu.edu.tw/~cjlin/papers/guide/guide.pdf

4. Sarbajit Pal, Jhimli Mitra, Soumya Ghose, Paromita Banerjee, "A Projection Based Statistical Approach for Handwritten Character Recognition," *in Proceedings of International Conference on Computational Intelligence and Multimedia Applications*, Vol. 2, pp.404-408, 2007

5. N. Araki, M. Okuzaki, Y. Konishi, H. Ishigaki, "A Statistical Approach for Handwritten Character Recognition Using Bayesian Filter" *3rd International*

Conference on Innovative Computing Information and Control (ICICIC), pp.194-198, June 2008

6. Wang Jin, Tang Bin-bin, Christian Lindig, Piao Chang-hao, Lei Gai-hui, "Statistical method-based evolvable character recognition system",*IEEE International Symposium on Industrial Electronics (ISIE)*, pp. 804-808, July 2009
7. Apurva A. Desai, "Gujarati Handwritten Numeral Optical Character Reorganization through Neural Network", *Pattern Recognition*, Vol. 43, Issue 7, pp. 2582-89, July 2010
8. D. Singh, S.K. Singh, M. Dutta, "Handwritten Characterr Recognition Using Twelve Directional Feature Input and Neural Network", *International Journal of Computer Applications*, Vol. 1 No.2, pp. 86-87,March 2010
9. Gurpreet S Lehal, C. Singh, "A Gurmukhi Script Recognition System", *Proceedings of 15th International Conference on Pattern Recognition*, Vol. 2, pp. 557-560, 2000
10. Gurpreet S Lehal, C. Singh, "A Complete Machine printed Gurmukhi OCR", *Vivek*, 2006
11. Gurpreet S Lehal, C. Singh, "Feature Extraction and Classification for OCR of Gurmukhi Script", *Vivek* Vol. 13, pp. 2-12, 1999
12. Gurpreet S Lehal, C. Singh, "A Post Processor for Gurmukhi OCR", *Sadhana*, Vol. 25, Part 1, pp. 99-111, 2002
13. D. Sharma, Gurpreet S Lehal, "An Iterative Algorithm for segmentation of Isolated Handwritten Words in Gurmukhi Script", *The 18th International Conference on Pattern Recognition (ICPR)*, Vol. 2, pp. 1022-1025, 2006
14. Vijay. Goyal, Gurpreet S Lehal, "Comparative Study of Hindi and Punjabi Language Scripts", *Nepalese Linguistics*, Vol. 23, pp. 67-82, 2008
15. G.S. Lehal, Nivedan Bhatt, "A Recognition System for Devnagari and English Handwritten Numerals", *Proc. ICMI, Springer*, pp. 442-449, 2000
16. D. Sharma, Preety Kathuria, "Digit Extraction and Recognition from Machine Printed Gurmukhi Documents", *Proceedings of the International Workshop on Multilingual OCR MORC Spain*, 2009
17. Anuj Sharma, Rajesh Kumar, R. K. Sharma, "Online Handwritten Gurmukhi Character Recognition Using Elastic Matching",*Conference onImage and Signal Processing (CISP)*, Vol.2, pp.391-396, May 2008
18. Anuj Sharma, R.K. Sharma, Rajesh Kumar, "Online Handwritten Gurmukhi Character Recognition", Ph.D. Thesis, Thapar University, 2009 [Online]. Available: http://dspace.thapar.edu:8080/dspace/bitstream/10266/1057/3/Thesis_AnujSharma_SMCA_9 041451.pdf

International Journal of Engineering Research and General Science Volume 3, Issue 6, November-December, 2015
ISSN 2091-2730

COST EFFECTIVE METHODS USED IN VARIOUS LEVELS OF A BUILDING

Ar. J.Jebaraj Samuel

Assistant Professor, School of Architecture and Planning, Periyar Maniammai University(PMU), Vallam, Thanjavur, Tamilnadu

Email: jeba.12@gmail.com

Abstract—Every Builder or architect understands the importance of reducing the construction cost. In very recent years the cost of construction has increased faster. The rising cost of shelter is the present scenario in housing, which affects all of us.

Buildings are generally divided into 2 parts

- Substructure
- super structure

Substructure includes portion of building below the ground. i.e Foundation

Super structure includes portion of the building above the ground .which includes Plinth, wall, openings, roofs, floor, horizontal and vertical transportation . In this paper we shall discuss various methods. The present paper discusses various methods at different parts of a building which are cost effective.

Keywords—Cost Effective, Design , Architecture, Arch foundation, Brick on edge, Rat Trap Bond, steel frames, Arches ,Filler slab, Jack arch. Finishing.

INTRODUCTION

Cost effective is a new concept which deals with effective budgeting and following of techniques which help in reducing the cost of construction through the use of locally available materials along with improved skills and technology without sacrificing the strength, performance and life of the structure.

There is huge misconception that low cost housing is suitable for only sub standard works and they are constructed by utilizing cheap building materials of low quality.

Cost effective technology allows for reduction of costs and preserve scarce resources.

Cost Effective is achieved through four ways

- By replacing conventional materials with alternative materials
- By good construction skills which also heads to cost saving
- By proper building design which in turn leads to reduction in cost
- By proper planning and management of construction

FOUNDATION

Normally the foundation cost comes to about 10 to 15% of the total building and usually foundation depth of 3 to 4 ft. is adopted for single or double store building and also the concrete bed of 6″(15 Cms.) is used for the foundation which could be avoided.

It is recommended to adopt a foundation depth of 2 ft.(0.6m) for normal soil like gravely soil, red soils etc., and use the uncoursed rubble masonry with the bond stones and good packing. Similarly the foundation width is rationalized to 2 ft.(0.6m).

To avoid cracks formation in foundation the masonry shall be thoroughly packed with cement mortar of 1:8 boulders and bond stones at regular intervals.

It is further suggested adopt arch foundation in ordinary soil for effecting reduction in construction cost up to 40%.This kind of foundation will help in bridging the loose pockets of soil which occurs along the foundation.

In the case black cotton and other soft soils it is recommend to use under ream pile foundation which saves about 20 to 25% in cost over the conventional method of construction

PLINTH

It is suggested to adopt 1 ft. height above ground level for the plinth and may be constructed with a cement mortar of 1:6. The plinth slab of 4 to 6″ which is normally adopted can be avoided and in its place brick on edge can be used for reducing the cost. By adopting this procedure the cost of plinth foundation can be reduced by about 35 to 50%.It is necessary to take precaution of providing impervious blanket like concrete slabs or stone slabs all round the building for enabling to reduce erosion of soil and thereby avoiding exposure of foundation surface and crack formation.

It is suggested to adopt 1 ft. height above ground level for the plinth and may be constructed with The plinth slab of adopted can be brick on edge can reduce the cost

WALLING

Wall thickness of 6 to 9″ is recommended for adoption in the construction of walls all-round the building and 41/2 ” for inside walls. It is suggested to use burnt bricks which are immersed in water for 24 hours and then shall be used for the walls

RAT – TRAP BOND WALL

It is a cavity wall construction with added advantage of thermal comfort and reduction in the quantity of bricks required for masonry work. By adopting this method of bonding of brick masonry compared to traditional English or Flemish bond masonry, it is possible to reduce in the material cost of bricks by 25% and about 10to 15% in the masonry cost. By adopting rat-trap bond method one can create aesthetically pleasing wall surface and plastering can be avoided.

• Strength is equal to the standard 10″ (250 mm) brick wall, but consumes 20% less bricks.

Fig 1:Rat-trap bond wall

The air medium created between the brick layers helps in maintaining a good thermal comfort inside the building. This phenomenon is particularly helpful for the tropical climate of South Asian and other countries.

For extra stability:-

Vertical Rod should be placed at 245mm from the inner face of the Brickwork Rat-trap Bond (L-Joint)

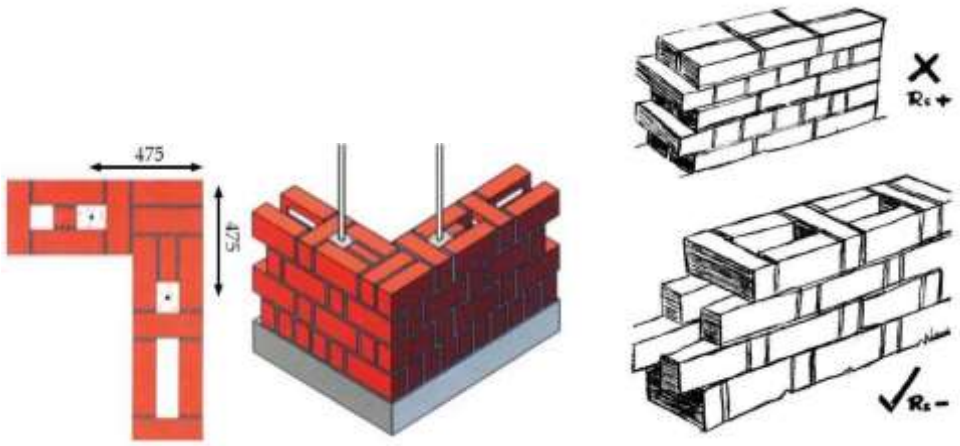

Fig 2: Construction of Rat-trap bond wall

• Buildings up to two stories can easily be constructed with this technique

CONCRETE BLOCK WALLING

In view of high energy consumption by burnt brick it is suggested to use concrete block (block hollow and solid) which consumes about only 1/3 of the energy of the burnt bricks in its production. By using concrete block masonry the wall thickness can be reduced from 20 cms to 15 Cms. Concrete block masonry saves mortar consumption, speedy construction of wall resulting in higher output of labour, plastering can be avoided thereby an overall saving of 10 to 25% can be achieved.

Fig 3: Concrete block walling

DOORS AND WINDOWS

It is suggested not to use wood for doors and windows and in its place concrete or steel section frames shall be used for achieving saving in cost up to 30 to 40%.Similiarly for shutters commercially available block boards, fibre or wooden practical boards etc., shall be used for reducing the cost by about 25%.By adopting brick jelly work and precast components effective ventilation could be provided to the building and also the construction cost could be saved up to 50% over the window components.

LINTELS AND CHAJJAS

The traditional R.C.C. lintels which are costly can be replaced by brick arches for small spans and save construction cost up to 30 to 40% over the traditional method of construction. By adopting arches of different shapes a good architectural pleasing appearance can be given to the external wall surfaces of the brick masonry.

Brick arches: The traditional RCC lintels which are costly, can be replaced by brick arches for small spans and save construction cost up to 30–40% over the traditional method of construction (Figure 3 a). By adopting arches of different shapes blended with brick corbelling , a good architecturally pleasing appearance can be given to the external wall surfaces of the brick masonry.

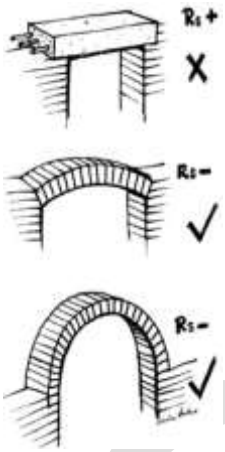

Fig 4: Usage of Arches

ROOFING

Normally 5″(12.5 cms) thick R.C.C. slabs is used for roofing of residential buildings. By adopting rationally designed insitu construction practices like filler slab and precast elements the construction cost of roofing can be reduced by about 20 to 25%.

Filler slab in roof: This They are normal RCC slabs where bottom half (tension) concrete portions are replaced by filler materials such as bricks, tiles, cellular concrete blocks, etc.These filler materials are so placed as not to compromise structural strength, result in replacing unwanted and nonfunctional tension concrete, thus resulting in economy. These are safe, sound and provide aesthetically pleasing pattern ceilings and also need no plaster.

The main features of the filler slab are:

• Consumes less concrete and steel due to reduced

weight of slab by the introduction of a less heavy, low-cost filler material like two layers of burnt clay tiles.

Slab thickness minimum 112.5 mm

• Enhances thermal comfort inside the building due to heat-resistant qualities of filler materials and the gap

• Makes saving on cost of this slab compared to the traditional slab by about 23%.

• Reduces use of concrete and saves cement and steel by about 40%.

Fig 5 :Filler Slabs

FERROCEMENT CHANNEL/SHELL UNIT

Provide an economic solution to RCC slab by providing 30 to 40% cost reduction on floor/roof unit over RCC slabs without compromising the strength. These being precast, construction is speedy, economical due to avoidance of shuttering and facilitates quality control.

PLASTERING

Plastering can be avoided on the walls, frequent expenditure on finishes and its maintenance is avoided. Properly protected brick wall will never loose its color or finish.

FLOORING

Flooring is generally made of terracotta tiles or color oxides. Bedding is made out of broken brick bats. Various patterns and designs are used, depending on shape, size of tiles, span of flooring, and client's personal preference.

WINDOWS

Windows are generally made up of wood. Instead of wooden windows, brick jali's are used. They are used just more than a decorative element. They are also used in parapets.

FINISHING WORK

The cost of finishing items like sanitary, electricity, painting etc., varies depending upon the type and quality of products used in the building and its cost reduction is left to the individual choice and liking.

CONCLUSION

The above list of suggestion for reducing construction cost is of general nature and it varies depending upon the nature of the building to be constructed, budget of the owner, geographical location where the house is to be constructed, availability of the building material, good construction management practices etc. However it is necessary that good planning and design methods shall be adopted by utilizing the services of an experienced engineer or an architect for supervising the work, thereby achieving overall cost effectiveness to the extent of 25% in actual practice.

REFERENCES:

[1] Affordable Housing Materials & Techniques for Urban Poor's, S.S. Shinde, A.B. Karankal, North Maharashtra University Depart-ment of Civil Engineering & S.S.V.P.S.B.S.D.College of Engineering, Deopur, Dhule (MS) India
[2] Shelter Process of Low-income people with Special Emphasis on Housing Finance", Research Report No. 10 IHSP, HUDCO, New Delhi.
[3] " Costford "-Cost Effective Environment Friendly Technology in the context of Kerala Economy – A Conclusive Review, ISSN 2224-5790 (Print) ISSN 2225-0514 (Online) Vol 1, No.1, 2011
[4] Cost Effective Techniques Uses In Modern Construction Projects -Volume : 3 | Issue : 5 | May 2014 • ISSN No 2277 - 8179
[5] Affordable Housing Materials & Techniques for Urban Poor's, International Journal of Science and Research (IJSR), India Online ISSN: 2319-7064
[6] Affordable Housing for Urban Poor Prepared by National Resource Centre SPA, New Delhi Supported by Ministry of Housing & Urban Poverty Alleviation Government of India.
[7] Hira B.N. &Negi S.K., Journal of Indian Building Congress, Vol. 11, No. 2, 2004; ; Seminar on "Up gradation of Housing & Amenities in Rural Areas", December, 22nd23rd2004. At Bhubaneswar Appropriate Building Techniques for Rural Housing. BMTPC.
[8] Punia, R.D. and Roy, U.N. (2002), "Appropriate technology for Low cost Housing" Journal, Institution of Engineers (India) Calcutta
[9] HUDCO (2000). Nirman Bharti-Newsletter for building centres and appropriate technology transfer. 6 : 1-2.
[10] Mishra, H.N. (1988). T-frame window-An innovative technique in cost reducing construction. *National Building Oganization*. 33 : 19.
[11] Appropriate technology for low- cost housing, *A.G. Madhava Rao & D.S. Ramachandra Murthy*
[12] M.B.Achwal (2003) Laurie Baker the Master craftsman
[13] Cost effective technology for the 21st century**.** *Nirmithi National Institute of habitant management.*

International Journal of Engineering Research and General Science Volume 3, Issue 6, November-December, 2015
ISSN 2091-2730

Determination of Stress Intensity Factor on Circumferential Notched Round Bar

Chaitany Maccha[1], K.S.Mangrulkar[2]

[1].(ME. in Design Engineering Student of Mechanical Department, ,N.B.Navale Sinhgad College of Engineering, Solapur India.)

[2](Professor, Department of Mechanical Engineering, N. B. Navale Sinhgad College of Engineering, Solapur India.)

Email – macchachaitany@gmail.com

Abstract— Cylindrical components have many applications in aircraft design. These structural components are subjected to cyclic stresses, which can cause damage and premature failure by fatigue crack growth. As it is well known, the design of engineering components in the past was only based on the S-N curves and did not consider the crack initiation and crack growth phases to predict life. The stress intensity factors of surface notch on circular bar have been evaluated by singular element with detailed mesh on crack front and appropriating adjacent area. The attention is focused on a circular bar with notch surface crack under tension load. Stress intensity factors (SIF) are considered using the finite element method. For that purpose a straight round bar under tension is investigated. The stress intensity factors are calculated for various dimensions of surface cracks. Using the derived analytic formulae for the stress intensity factor based on the FEA, a crack growth analysis is carried out.

Keywords— Stress Intensity Factor(SIF), Circumferentially Crack Round Bar(CCRB), Crack Profile, Fracture toughness, Al7075-T6, Ultimate Tensile Strength, V notch, Semi Elliptical Crack

I. INTRODUCTION

The surface crack embedded with cylindrical component, such as shaft, bar, bolt, wire, is the most common crack model, and has received widespread attention in the past. Due to geometrical complexity, some simplification had been made for the crack profile, such as straight-edged, circular, notch and elliptical crack model, to analyse such crack problems.

Most of mechanical failures by fatigue process on rotor shafts have origin on surface cracks that grow with a notch shape. Surface cracks emanating from stress concentrating locations are the most common phenomena of fatigue failure. Bars with variable cross-sections are a category of cylindrical parts and components extensively used in engineering mechanisms. Surface fatigue cracks are frequently initiated in such components at the stress concentrating locations, then they propagate into the interior of the parts and can cause final fracture abruptly. In addition, smooth and notched round bars have been used as standard specimens to obtain the fatigue property of materials for safe design and assessment. The fatigue failure of round bars often develops from surface defects, and therefore several authors have done study on the stress-intensity factor by variation along the front of these flaws. The assumption that an actual part through crack can be replaced by an equivalent notch at surface edge flaw is experimentally supported, and therefore many analyses have been carried out related to this equivalent configuration. The three-dimensional notch has been used to model the crack front in cylindrical rods under axial loading. In the first section of the present work, the stress intensity factors along the crack front are computed using the FEM. The crack growth can be analysed subjected to Mode I loading.

The determination of fracture toughness is based on the stress intensity factor (KIC) at the crack tip.

The advantages of using circumferentially notched bars for fracture toughness testing can be summarized as follows:

1) The plane strain condition can be obtained because the circumferential crack has no end in the plane stress region compared with the standard specimen geometries.
2) Because of radial symmetry microstructure of the material along the circumferential area is completely uniform.
3) Preparation of CCRB specimen & Fracture toughness test is easy.

II. ANALYTICAL

a) According to Wang C.H

The determination of fracture toughness is based on the stress intensity factor (KIC) at the crack tip, where I- denotes that the fracture toughness test is performed in tensile mode and C- denotes that the value of k is critical.

$KIC = \frac{0.932Pf\sqrt{D}}{d^2\sqrt{\pi}}$…… (Eq1)

Where,
Pf= fracture load,
D= diameter of the specimen,
d= diameter of the notched section.

b) **According to Dieter** for round notched tensile specimen, fracture toughness KIC found using following Eq.

$KIC = \frac{Pf}{D^{3/2}[1.72(\frac{D}{d})-1.27]}$…….(Eq 2)

Where,
Pf = fracture load,
D= diameter of the specimen,
D=diameter of the notched section

II. GEOMETRICAL CONFIGURATION OF SPECIMEN

Following Specimen shown in Fig:1 is taken for the experimental result
Crack is initiated from points of high stress concentration on the surface of the component such as sharp changes in cross-section, slag inclusions, tool marks etc then spreads or propagates under his influence of load cycles until it reaches critical size.

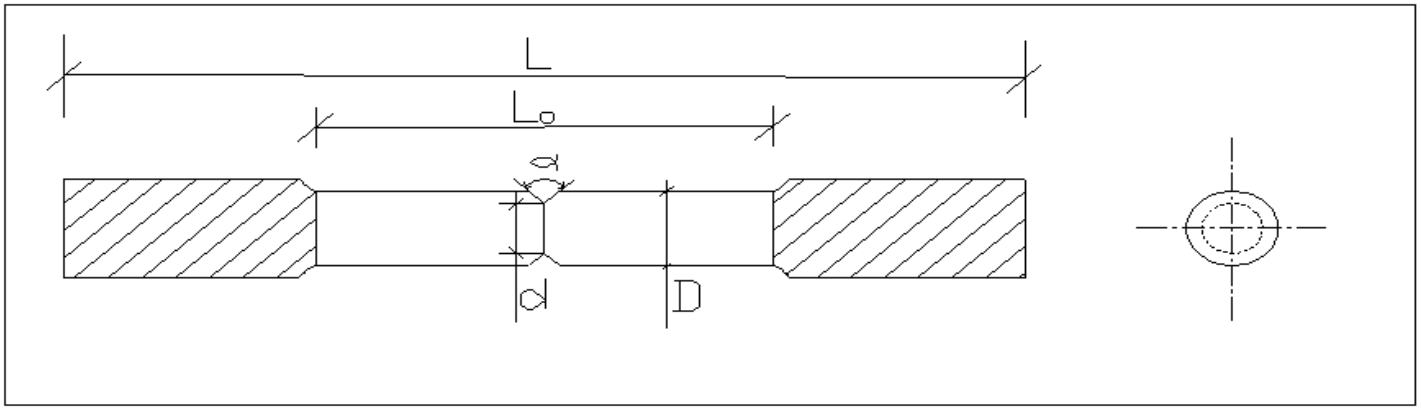

Fig-:1 Schematic representation of round notched tensile specimen

Where,
D= diameter of bar (mm),
d= diameter of notched surface (mm)
L= total length of bar (mm),
Lo= original length in consideration (mm).
α= notch angle (60º)

Assumptions

The SIF solution of a notch surface crack front on round bar under tension is investigated under the following assumptions:
1. The round bar is made of a homogenous, isotropic and linear elastic material.
2. The square-root stress singularity is filled with the vicinity of the crack front.
3. A notch surface crack is located at the half-length of the round bar.
4. Only the mode-I fracture is considered.

III. UTM TESTING

The tensile test of circumferentially cracked round bar (CCRB) specimen was performed on Universal testing machine at room temperature. After conducting the experimental work on universal testing machine the experimental values of ultimate stress and fracture load of each CCRB specimen is given in table.

The UTS is usually found by performing a tensile test and recording the engineering stress versus strain. The highest point of the stress–strain curve is the UTS. It is an intensive property; therefore its value does not depend on the size of the test specimen. However, it is dependent on other factors, such as the preparation of the specimen, the presence or otherwise of surface defects, and the temperature of the test environment and material.

UTM Testing Result Table

Table 3.1 Corresponding Ultimate Tensile strength and Facture load

Sr.No	Notch angle (α)	Specimen diameter (D)	Notch diameter (d)	Ultimate Tensile Strength(KN)	Fracture load (Pf) in KN
1	60º	16	13	41	37
2	0º	16	-	59	43

Table 3.2Corresponding Average Strain

	Average Strain
Crack Specimen	0.005228
Uncracked Specimen	0.001612

VI. FINITE ELEMENT MODELING

In this study, the finite element model is formed by a using the ANSYS Parametric Design Language (APDL). First a material is selected, Aluminium. Then, the line of the crack front for the initial step is defined. Next, two areas are created, one with the crack front and one that is the uncracked interior of the model. Each of these areas is extruded to form a volume. The lines surrounding the crack surface are duplicated and attached to the original crack front. These lines form another area. This new crack surface and the original uncracked area are extruded in the direction opposite to that of the previous extrusion. This new portion is given the material properties of the material. Finally, these four volumes are meshed. The model consists of four volumes and is composed of material. Since the model is parametric, new values for these parameters can easily be specified with each new execution of the algorithm. The values above length units of meters. The two beginning crack shapes that were studied, shown in top view, are a quarter-circular comer crack and what will be called a fillet-shaped comer crack. A side view showing the two materials and the level of refinement at the crack front and along the interface. All volumes are meshed using 20-noded brick elements. The fillet shapes have equal numbers of nodes and elements because the method which creates the finite element models divides the lines into equal numbers of sections each time it is executed. In ANSYS, the volumes are meshed using the VMESH command for the uncracked volumes; for volumes with crack faces, a sweep mesh is used (the VSWEEP command in ANSYS). After examining numerous cases, it was found, for both types of crack fronts, that the number of crack-front elements is critical to the accurate calculation of smooth strain energy release rate results. In order to obtain the greatest level of crack tip refinement and resolution, 40 elements were placed along the crack front. The integration order of the crack front enriched elements is critical in calculating accurate results, therefore high integration were used.

Boundary Conditions

One fourth model has been analysed. Boundary condition has been given on one fourth model. Fixed at the one end and tensile force at the other end.

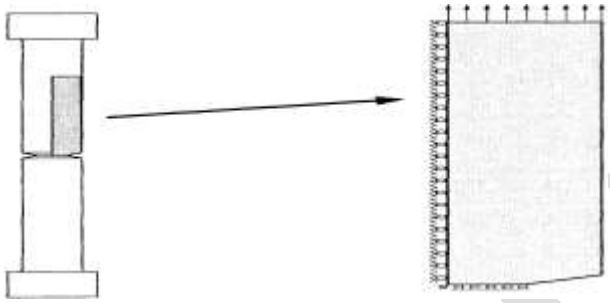

Fig 2 : Boundary Condition On Specimen

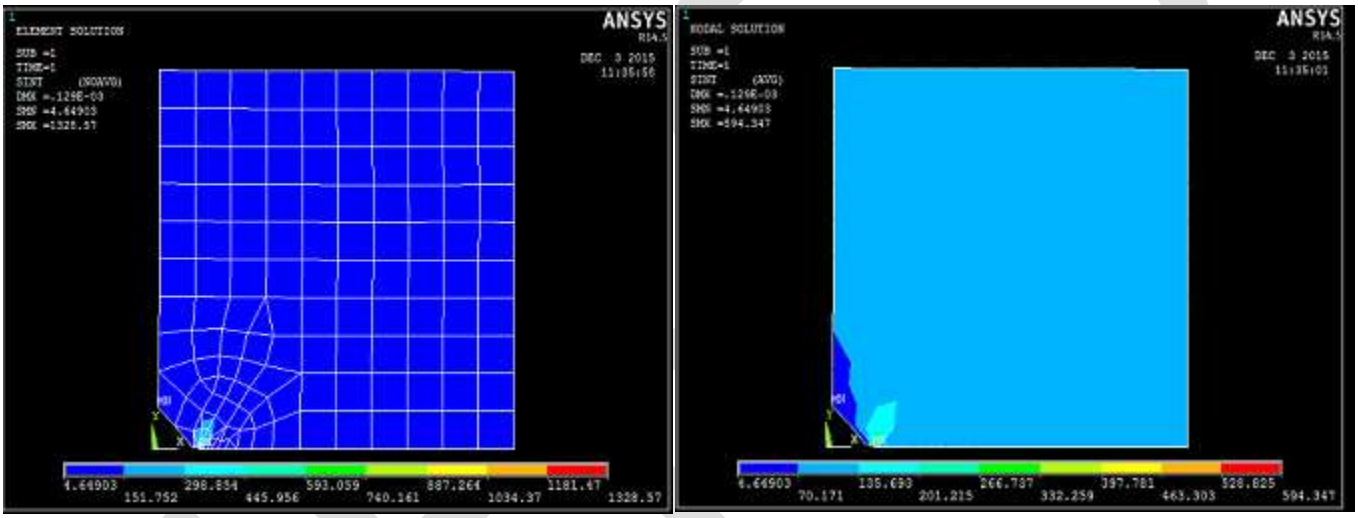

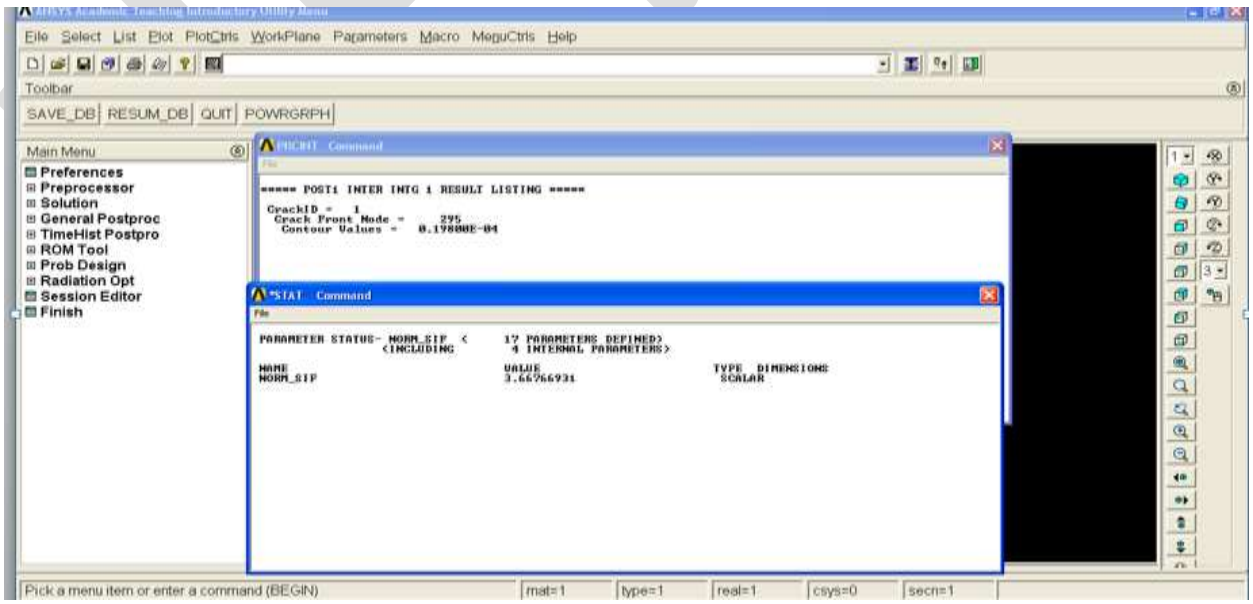

Fig-:3 Ansys Stress Intensity Factor Results

IV. RESULTS AND DISCUSSIONS

1) The specimen having different notch angles and different notch diameter as well as specimen diameter was considered and results are drawn. The measurement of fracture toughness is based on the critical stress intensity factor (KIC) of the test specimen under Mode-I loading condition.

Approach	SIF	Error (%)
Theoretical	3.65	-
Ansys	3.66	0.27
Experimental	3.2431	12.54

2) Result Table show the experimental observations of maximum loads and ultimate stresses of each specimen. The plane-strain fracture toughness of Al 7075-T6 alloy tested using CCRB specimen geometry, it was found to be in a range of 25.9349 to 39.286 as per Eq. (1) and 22.2 to 41.81 as per Eq. (2). These two equations give KIC value in a valid range as available in the literature using standard CT (Compact Tension) specimens. The notch diameter 15mm gives fracture toughness lower value and notch diameter 13mm gives fracture toughness higher value. It is observed that as notch diameter increases KIC value decreases.

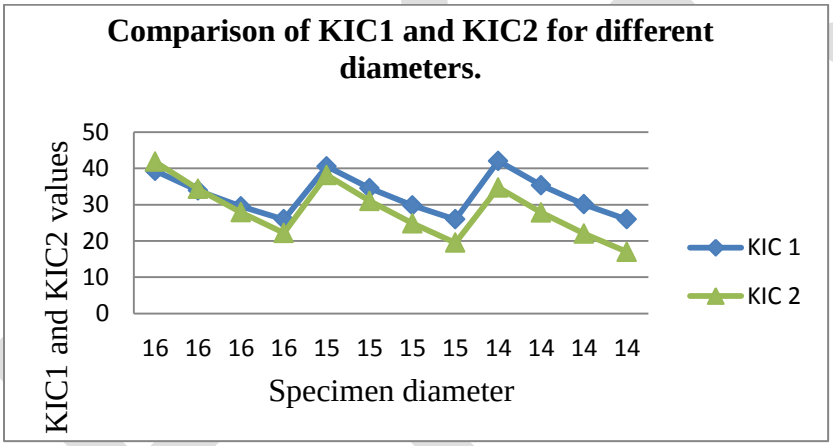

Comparison Of KIC1 and KIC2 Value

3) After introducing notch to the testing specimen the load require for fracture of material are changes and it is observed that as notch diameter and specimen diameter decreases the load require for specimen decreases.

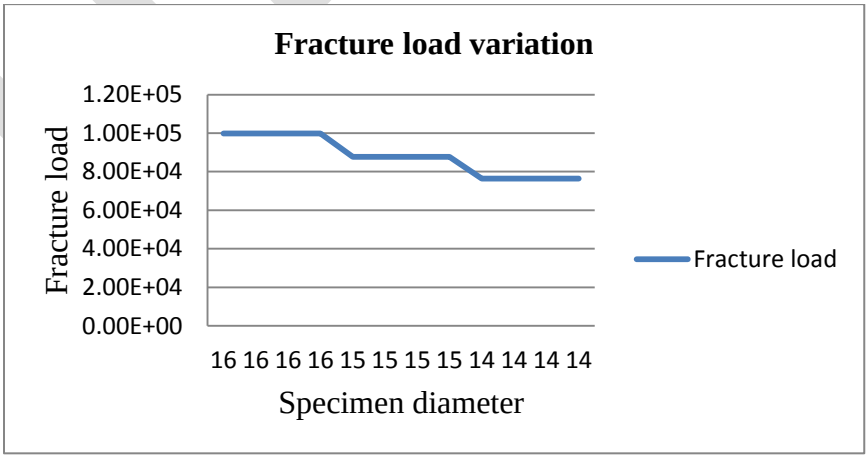

Fracture load variation

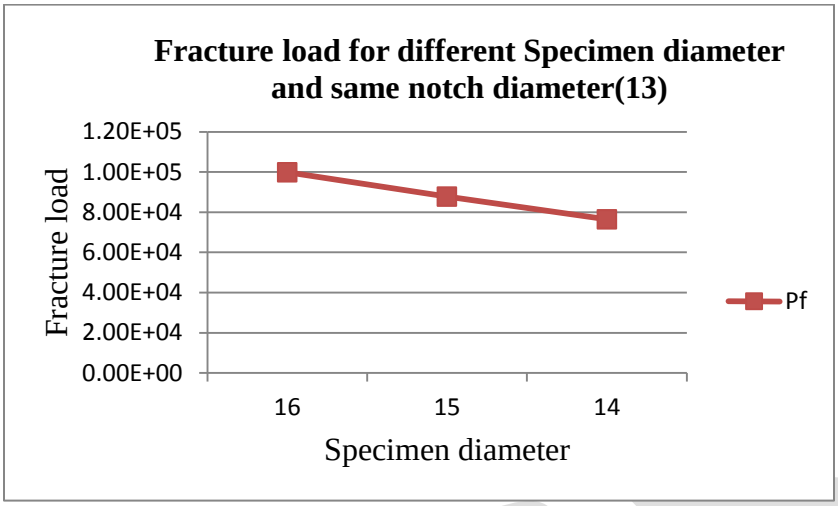

Fracture load for different Specimen diameter and same notch diameter(13mm)

VI. CONCLUSION

- Fracture toughness (KIC) of metallic material can be successfully determined by using round bar tensile specimen and the obtained results are found to be in good agreement with simulation and experimentation results obtained from tensile test specimens.
- The plane-strain fracture toughness of Al 7075-T6 alloy tested using CCRB specimen geometry was found to be in a range 25.9349 to 39.286 as per Eq. (1) and 22.2 to 41.81 as per Eq.(2). which is valid range of KIC for Al7075-T6 as available in literature obtained by standard tests.
- Stress Intensity factor changes as notch diameter and specimen diameter varies.
- It is observed that as specimen diameter along with notch diameter decreases the fracture load for specimen also decreases.
- The presence of notch in tensile test specimen causes brittle failure although the material is ductile & also the % elongation of the material specimen.
- With the increase in notch angle the value of KIC decreases.

REFERENCES:

[1] Marija Blazic, mirko Maksimovic, Ivana Vasovic, Yasmina Assoul, "Stress Intensity Factors for Elliptical Surface Cracks in Round Bars and Residual Life estimation" , Scientific Technical Review, 2011, Vol.61, No.1

[2] Yan-Shin Shiha and Jien-Jong Chenb, "The stress intensity factor study of an elliptical cracked shaft" ,Nuclear Engineering and Design 214 (2002) 137-145.

[3] R. Brancoa, F.V. Antunes , "Finite element modeling and analysis of crack shape evolution in mode-I fatigue Middle Cracked Tension specimens", Science Direct, Engineering Fracture Mechanics 75 (2008) 3020-3037

[4] L. Rubio ,B.Munoz-Abella, G.Loaiza, "Static behavior of a shft with an elliptical crack", Science Direct, Mechanical Systems and Signal Processimg 25 (2011) 1674-1686

[5] Dr. S. Suresh Kumar, K.A.Dularish, G.S. Deepak Kumar, "Determination of Stress Intensity Factor and Interaction Behavior of Radial Cracks in an Un-notched Round Bar", Proceedings of the 1st International and 16th National Conference on Machines and Mechanisms (iNaCoMM2013), IIT Roorkee, India, Dec 18-20 2013.

[6] Trimbak K. Todkari, M. C. Swami, P. S. Patil, " Effect of Specimen Diameter and Notch Diameter On The Fraccture Toughness Of AL7075 T6 Alloy-An Experimental Approach", International Journal of Research in Engineering and Technology, Volume: 04, Issue:01, Jan-2015

[7] Andrea Carpinteri, Roberto Brighenti, Andrea Spagnoli and Sabrina Vantadori, "Fatigue Growth of Surface Cracks in Notched Round Bars", Department of Civil and Environmental Engineering & Architecture University of Parma – Parco Area delle Science 181/A-4300 Parma- Italy

[8] Trimbak K. Todkari, M. C. Swami, P. S. Patil, " Effect of Notch Angle on the Fracture Toughness of AI7075 T6 Alloy-An Experimental Approach", IOSR Journal of Mechanical and Civil Engineering, Volume 12, Issue 1Ver. III (Jan - Feb 2015), PP 01-05

[9] A E Ismail, A K Ariffin, S Abdullah & M J Ghazali, " Stress Intensity Factor under Combined Tension and Torsion Loading", Indian Journal Of Engineering & Materials Sciences, Vol.19, Feb 2012, pp. 5-16

[10] Upamanyu Banerjee, " Modeling Stress Intensity Factor of Rail Steel under Situation of Growing Fatigue Crack-A Noval Technique", Open Journal of Metal, 2012, 2, 74-78, Published September 2012

[11] M.Zappalorto, P. Lazzarin, F. Berto, " Elastic notch stress intensity factor for sharply V - Notched Rounded Bars Under Tension", Engineering Fracture Mechanics, 76 (2009) 439 – 453

[12] P. Lazzarin, S. Filippi, "A Generalized Stress Intensity Factor to be applied to rounded V- Shaped notches", International Journal of Solids Structures 43 (2006) 2461 - 2478

International Journal of Engineering Research and General Science Volume 3, Issue 6, November-December, 2015
ISSN 2091-2730

Improving Xml Retrieval with Feedback Technique in Personalization-A Review

Miss. Jayati D. Kale, Prof. G. Singh Makhija

Department of Computer Science And Engineering, Wainganga College Of Engineering And Management, Nagpur, India.

Department of Computer Science And Engineering, Wainganga College Of Engineering And Management, Nagpur, India.

Jayatikale26@gmail.com , garima11makhija21@gmail.com

Abstract— Nowadays lots of information increased on search engine. Somewhere user didn't get result as per their requirement we see this problem; everyone should need personalization in search. Using personal data of users from profile and retrieve the results that are much like the user's preferences. We use xml, it is very useful to represent the quality of information and it'll exchange this type of information. Once we produce users profile, we need to build profile of user's interest on server, identifying the user's interest supported the previous web search or previously websites visited by users. Identifying the user's interest on the basis of his/her education and background of users, so given result-set search quick and simple to show the results. We are introducing feedback-based method in personalization so it will be re-ranking the search result-set of given product average rating/feedback keep in xml. User can give their feedback on Company and company product.

Keywords— Re-ranking, Personalization, XML Retrieval, Feedback method , Query expansion, Search Engine, User Account.

I. INTRODUCTION

From the last few years, digital information increases very fast. We need to use information retrieval system [1] to search large amount of information for the user. There are differing types of personalization techniques [2] accustomed find out quickest information on search engine. As per the need of user we would like to produce categorized information to find out information on that. Another key factor of this amount of digital information is that the increasing use of assorted sorts of documents, whose matter content is unionized around a well printed structure. XML (Xtensible Mark-up Language) has recently emerged as a result of the document customary for representing and exchanging this type of semi-structured data. XML data is self-describing through content-oriented tags, that permit computers interpret the meaning of the keep data. XML permits the group of countries that they can be expressively represent the inside structure of documents that need to be thought of as aggregates of meshed units, instead of atomic entities. We need to use three completely different techniques of personalization that is query suggestion, re-ranking [5] of queries and feedback primarily based techniques. Primarily feedback-based is helpful to provide present feedback on products for its quality and additionally user gives their feedback or rating.

II. Literature Survey

There are many researchers working on or done their working on personalization in search engine. Personalization isn't solely providing facility of non-public info keep and search however conjointly it'll facilitate to go looking quick with the assistance of personalization techniques. Several authors centered on personalization techniques [1] [5] to create quickest and simple to use. A number of the approaches that are terribly helpful in search like question enlargement [1]. This approach won't matches or compare with offered question and provides immediate result. Another necessary keyword xml, that's customary and appreciates to use in search. Xml may be a powerful in looking info and its ability to shows solely needed contents of document rather than full length document.

In search, full length text or long sentences are very difficult to search in xml retrieval. It's going to be realize the result that's not helpful for users to resolve this, we want completely different language models [2] [4] and customized techniques. The language model approach to feedback doesn't initially seem to lend itself to relevancy feedback. Pseudo-feedback-based query expansion methods [14] augment a query with terms from the documents most highly ranked by an initial search. Many researches are done on regular search engine where the context [18] [7] is used to improve the evaluation of information retrieval. The author's Abdelkrim Bouramoul' , Bich-Lien Doan' compare many search engine with each other for performance and what kind of links available on search engine.

Whenever user searches for information, re-ranking of the result-set should be done at the time of search query set. Re-ranking is additionally called once search, it'll rank the result set as per the preferences and requirement. This is often also known as personalization technique. In the re-ranking matching patterns are used and conjointly language models are used so re-rank the result set as per the users keyword. Investigated personalized web search, 1st learning users long run interest. And then re-ranking the primary 50 search result from the program based mostly the profile [6]. To gift a framework for feedback-driven xml question refinement and address some building blocks as well as reweighting condition and ontology- based mostly query expansion [9]. This framework accustomed take relevancy feedback from xml retrieval. There are several issues that are arises specifically within the xml context and can't merely addressed by straight-forward use of ancient IR techniques. To boost the performance of relevance feedback, content and structure (CAS) query are used for xml information retrieval [3]. Content-and-structure (CAS) queries are those containing each structure and content constraints. There are state-of the art querying languages such as XQuery or NEXI[17] , that enable us to retrieve XML documents based on content and structure.

In many systems used re-ranking technique to show the result-set filtered the required query form information query of database. This re-ranking technique is used in every search engine, if they are personalization or our normal search engine like Google and etc. There are many techniques and methods are used but few are very easy to understand and simultaneously improve the performance of search engine.

ACKNOWLEDGMENT

This paper totally based on personalization of search engine, this is very rare and new topic for users and everyone. Only the help of search engine of course Google can help a lot to find it out IEEE papers and

concept of personalization and xml retrieval. This review paper based on ”Using Personalization to Improve Xml Retrieval”, can give lots of idea of personalization and add new things in developing system.

Conclusion

In this Paper, we have proposed a system for user's personalization. This is very useful and easy to use for users. This system gives priority to user's preference and educational background to search result fast and easy for users. Personalization in search engine is very useful for those who want search as per their interest and priority not popular link show when they search information. It will give fast result-set as compare to other personalized search engine. Because it will be re-rank the result-set in little time. This system also provides the advertisement to user, this advertises shown on user's desktop as per the user's choices and their preference wise.

REFERENCES:

[1] L. M. de Campos , J. M. Fernández-Luna, J. F. Huete , And Eduerdo Vicente-Lopez, “Using Personalization to improve Xml Retrieval,” in IEEE TRANSACTIONS ON KNOWLEDGE AND DATA ENGINEERING, VOL. 26, NO. 5, MAY 2014.

[2] G. Chernishev, “Personalization of XML text search via search histories,” in *Proc. SYRCODIS 2008 Colloq. Databases Information Systems.*

[3] L. M. de Campos, J. M. Fernández-Luna, J. F. Huete , and C. Martín-Dancausa, “A content-based approach to relevance feedback in XML-IR for content and structure queries,” in *Proc.Int. Conf. Knowledge Discovery Information Retrieval*, Roskilde, Denmark, 2010, pp. 418–427.

[4] B. W. Croft, S. Cronen-Townsend, and V. Lavrenko, “Relevance feedback and personalization: A language modeling perspective,”in *Proc. 2nd DELOS Workshop Personalisation Recommender Systems Digital Libraries*, 2001.

[5] N. Matthijs and F. Radlinski, “Personalizing web search using long term browsing history,” in *Proc. 4th ACM Int. Conf. Web Search Data Mining*, Hong Kong, China, 2011, pp. 25–34.

[6] L. Meister, O. Kurland, and I. G. Kalmanovich, “Two are better than one! Re-ranking search results using an additional retrieved list,” Technion - Israel Instit. Technology, Haifa, Israel, Tech. Rep. IE/IS-2009-01, 2009.

[7] L. Tamine-Lechani, M. Boughanem, and M. Daoud, “Evaluation of contextual information retrieval effectiveness: Overview of issues and research,” *Knowl. Inform. Syst.*, vol. 24, no. 1, pp. 1–34, 2010

[8] R. Schenkel and M. Theobald, “Feedback-driven structural query expansion for ranked retrieval of XML data,” in *Proc. 10th Int. Conf. Extending Database Technology*, Munich, Germany, 2006, pp. 331–348, LNCS 3896.

[9] H. Pan, “Relevance feedback in XML retrieval,” in *Proc. EDBT Workshops PhD, DataX, PIM, P2P&DB, ClustWeb*, Heraklion, Greece, 2004, pp. 187–196, LNCS 3268.

[10] X. Shen, B. Tan, and C. Zhai, “Implicit user modeling for personalized search,” in *Proc. 14th ACM Int. Conf. Information Knowledge Management*, Bremen, Germany, 2005, pp. 824–831.

[11] A. Sieg, B. Mobasher, and R. Burke, “Web search personalization with ontological user profiles,” in *Proc. 16th ACM Int. Conf. Information Knowledge Management*, 2007, pp. 525–534.

[12] B. Steichen, H. Ashman, and V. Wade, “A comparative survey of personalised information retrieval and adaptive hypermedia techniques,” *Inform. Process. Manag.*, vol. 48, no. 4, pp. 698–724, 2012.

[13] L. Tamine-Lechani, M. Boughanem, and M. Daoud, “Evaluation of contextual information retrieval effectiveness: Overview of issues and research,” *Knowl. Inform. Syst.*, vol. 24, no. 1, pp. 1–34, 2010.

[14] L. Zighelnic and O. Kurland, "Query-drift prevention for robust query expansion," in *Proc. 31th Annu. Int. ACM SIGIR Conf.*, Singapore, 2008, pp. 825–826.

[15] J. Teevan, S. T. Dumais, and E. Horvitz, "Personalizing search via automated analysis of interests and activities," in *Proc. 28th Annu. Int. ACM SIGIR Conf.*, Salvador, Brazil, 2005, pp. 449–456.

[16] J. Teevan, S. T. Dumais, and E. Horvitz, "Potential for personalization," *ACM Trans. Comput. Hum. Interact.*, vol. 17, no. 1,Article 4, 2010.

[17] A. Trotman and B. Sigurbjörnsson, "Narrowed extended XPath I (NEXI)," in *Proc. 3rd Int. Workshop Initiative Evaluation XML Retrieval*, Dagstuhl Castle, Germany, 2005, pp. 16–40, LNCS 3493.

[18] Abdelkrim Bouramoul, Mohamed-Khireddine Kholladi, Bich-Lien Doan, "USING CONTEXT TO IMPROVE THE EVALUATION OF INFORMATION RETRIEVAL SYSTEMS", International Journal of Database Management Systems (IJDMS), Vol.3, No.2, May 2011.

International Journal of Engineering Research and General Science Volume 3, Issue 6, November-December, 2015
ISSN 2091-2730

Understanding Soil Spectral Signature Though RS and GIS Techniques

Ramdas D. Gore[1], Sunil S. Nimbhore[2], Bharti W.Gawali[3]
Department of Computer Science and Information Technology[1,2,3],
Dr. Babasaheb Ambedkar Marathwada University, Aurangabad[MH], India.
ramdasgore@yahoo.com[1], nimbhoress@gmail.com[2], bharti_rokade@yahoo.co.in[3], cont: 9423744454[1]

Abstract –This paper reports the development of the soil spectral signature using Spectroradiometer form Visible Near Infrared, Short Wave Infrared and Mid-Infrared spectral reflectance of soil. Soil properties such as amount of carbon, nitrogen, phosphorus, potassium, sand, silt, and clay contains have been determined by using hyperspectral band models, in the wavelength band of 350-2500nm. Different mathematical models such as, Principal component analysis (PCA) and partial least square regression (PLSR) have widely been used to extract information regarding soil properties. This review article analyzes the reference work from 2005 to 2015.

Keywords- Agriculture; Spectral signature; Spectroradiometer; PLSR**.**

INTRODUCTION

The resent developments in the field of Geographical information system (GIS) and Remote Sensing (RS) has opened many real life applications in various domains. GIS is a computer system for capturing, storing, manipulate, analyzing, managing, checking and displaying geospatial data on the map. It is very easy to analyze, understand patterns and its relationship. It refers location (spatial data) and characteristics (attribute data). We can compare location throughout latitude and longitude (X and Y coordinate) [1]. Remote sensing is the skill of gaining data about the Earth's surface without physical touch with it. Sensors are used to record reflected and emitted energy and also for processing, analyzing the data which will be used for further analysis. Reflection depends on the objects or Earth's surface, if the object is smooth, then the reflection will be specular reflection. If the object is rough, it will be diffused reflection [2]. The collection of information depends upon these factors. Remote sensing technology is an effective means to monitor targets. Using these both technologies, these techniques can be applied to many areas as follows.

A. Agriculture

In the agriculture area there are various applications such as crop monitoring, crop classification, crop yield estimation, crop condition assessment, crop identification/ classification, soil characteristics and management [2].

B. Forestry

In this area there are various applications such as forest cover discrimination, Agroforestry mapping, clear cut mapping, burn delineation, infrastructure mapping, forest inventory, biomass estimations, species inventory and classification and types, deforestation or forest degradation, watershed protection, coastal protection and forest health [2].

C. Geology

Geology is used to support logistics. There are geological applications such as surficial deposit/ bedrock mapping, lithological mapping, structural mapping and terrain analysis, sand and gravel exploration, mineral exploration, hydrocarbon exploration, environmental geology, geobotany, baseline infrastructure, sedimentation mapping and monitoring, event mapping and monitoring, geo-hazard mapping and planetary mapping [2].

D. Hydrology

It is the study of water on the Earth's surface. It includes applications such as wetlands mapping and monitoring, soils moisture estimation, snow pack monitoring/ delineation of extent, measuring snow thickness, determining snow-water equivalent, river and lake ice monitoring, flood mapping and monitoring, glacier dynamics monitoring, river/ delta change detection, drainage basin mapping and watershed mapping, irrigation canal leakage detection, irrigation scheduling and sea ice information (ice concentration, ice type/ age/ motion, iceberg detection and tracking, surface topography, tactical identification of leads: navigation: safe shipping routers/ rescue, ice condition (state of decay), historical ice and iceberg conditions and dynamics for planning purposes, wildlife habitat, pollution monitoring, meteorological/ global change research) [2].

E. Land use and land cover

It is used interchangeably. There are including various applications such as land use change (Rural/ Urban), land cover/ biomass mapping, natural resource management, wildlife habitat protection, baseline mapping for GIS input, urban expansion/ encroachment, routing and logistics planning for seismic/ exploration/ resource extraction activities, damage delineation (tornadoes, flooding, volcanic, seismic, fire), legal boundaries for tax and property evaluation and target detection- identification of landing strips, roads, clearings, bridges, land/ water interface [2].

F. Ocean and coastal monitoring

It is important link in the Earth hydrological balance, CO^2 storage and weather system, there are various application such as ocean pattern identification (currents, regional circulation patterns, shears, frontal zones, internal waves, gravity waves, eddies, upwelling zones, shallow water_bathymetry), storm forecasting (wind and wave retrieval), fish stock and marine mammal assessment (water temperature monitoring, water quality, ocean productivity, phytoplankton concentration and drift, aquaculture inventory and monitoring), oil spill (mapping and predicting oil spill extend and drift, strategic support for oil spill emergency response decisions, identification of natural oil seepage areas for exploration), shipping (navigation routing, traffic density studies operational fisheries surveillance, near-shore bathymetry mapping), intertidal zone (tidal and storm effects, delineation of the land/ water interface, mapping shoreline features/ beach dynamics, coastal vegetation mapping, human activity/ impact) [2].

The objective of this paper is to report studies done in the area of soil using GIS and RS. Soil area is vital part of environmental, wildlife, human well-being and other thinks. Soils are essential products of the nature and without which there would be no life. Soils are made up of minerals, organic matter and components living organism's components. The percentage of these is important in determining the type of soils. Other factors such as climate, vegetation, the surrounding terrain, even human activities are also important in influencing formation of soil [3].

There is number of reasons, for the difference in soil in various regions. The most influential factors include the parent material, climate and terrain of the region, as well as the type of plant life, vegetation and present human influence. Soil health gives greater emphasis on soil biodiversity and ecological functions that makes soil dynamic living resources with capacity for self-organization. Soil quality is the capacity of a specific kind of soil to function, within natural or managed ecosystem boundaries, to sustain plant and animal productivity, to maintain water and air quality and support human health and habitation. Ecosystem depends on the soil. There are three types of soil properties classified in physical, chemical and biological.

Horizonation is soil physical property. It has layers like topsoil [0-20cm], subsoil and parent soil. Soil texture is one of the soil physical properties like sand, silt and clay. Consistence and bulk density are the soil physical properties. It is defined soil is dry, wet or moisture. Soil spectral signature can change as par the physical properties [6-8].

It is the interaction of various chemical components that takes place among soil particles like carbon, calcium, iron oxide, magnesium, nitrogen, pH, phosphorus and potash. It is very important for soil quality analysis. Soil quality is also depending on chemical properties. It is checked by the spectral signature [9, 10].

Soil samples have been studies in the laboratory for getting different properties of the soils [11]. They are scanned to get absolute reflectance corresponding to the samples. [12-14].

SOIL ANALYSIS USED SPECTRORADIOMETER

This review paper focuses on keywords such as diffuse reflectance spectroscopy, FieldSpec, soil spectral library, NIR, Mid-Infrared spectroscopy, spectrometer, and Spectroradiometer appears in its title, abstract or keywords. The work described more soil spectral library. There were a few papers that only reported pretreatment or pre-processing and classification. The hyperspectral tools are used in table 1, are presented.

TABLE 1. HYPERSPECTRAL TOOLS

Tools	Range	Reference ID
FieldSpec TM FR Spectroradiometer	350-2500 nm	[3, 31, 38, 39, 40,]
FieldSpec Pro FR spectrometer	350-2500 nm	[4, 25, 27, 30]
FieldSpec Spectroradiometer	350-2500 nm	[5, 6, 12, 20]
FT-NIR Spectrometer	700-2500 nm	[6]

FieldSpec 3 Spectroradiometer	350-2500 nm	[8]
ISCO S.R. Spectroradiometer	24 channels	[9]
AvaSpec spectrometer	200-1050 nm	[10]
Vis/NIR spectrophotometer (Tech5 Germany)	350-2500 nm	[11]
IRIS sensor and Lansat-TM (1-5, 7)	400-2500 nm	[13]
FieldSpec Pro	350-2500 nm	[15, 16]
MIR spectrum	400-4000 $cm-1$	[17]
Field Spectroradiometer	350-2500 nm	[18]
FieldSpec Pro FR (handheld)	325-1075 nm	[19]
Photoacoustic Spectroscopy (MIR spectrum)	400-4000 $cm-1$	[23]
Tensor 37 FT-IR spectrometer	400-4000 $cm-1$	[24]
NIRS	700-2500 nm	[26]
UV-VIS-NIR	350-3500 nm	[28]
BioRad FTS 175	1200-20000 nm	[28]
LI-1800 Spectroradiometer	400-1100 nm	[29]
LabSpec 2500 spectrometer	350-2500 nm	[32, 33, 34]

A. FieldSpec spectroradiometer

Soil samples are collect from the ASD FieldSpec sensor. It is scanned and absolute reflectance of samples is recorded for 350-2500 nm and collects spectra at the rate of 0.1 seconds per spectral scan. Spectral resolution is 3 nm @ 700 nm (350-1000 nm) and 10 nm/ 8 nm/ 30 nm @ 1400/2100 nm (100-2500 nm). Data sampling interval is 1.4 nm (350-1000nm) @ 350-1000 nm and 2 nm (1000-2500nm) @ 1000- 2500 nm. The total number of 2151 data points per spectrum using a FieldSpec, FieldSpec Pro and FieldSpec FR Spectroradiometer (Analytical Spectral Devices Inc., Boulder, Colorado, USA). It uses air-dry soil samples and halogen lamp light source is held inside it. Reflectance records, though the samples with constant angle at distance from sensor and after 3-5 successive readings, each average of ten successive reflectance spectra. The sample can be rotated 90 and 360 degrees and placed on petri plates. The spectral reflectance of soil samples was measured in VNIR and SWIR region [15-19].

It can be see in table 1, that wavelength ranges from 350 to2500 nm is widely used for soil analysis. It's got the 22 article. It has the capacity to take 350-2500 nm spectral range like FieldSpec TM FR, FieldSpec Pro FR, FieldSpec, FieldSpec 3, FieldSpec Pro, Vis/NIR and LabSpec 2500 Spectroradiometer. The spectral bands were omitted bands like, 350-420, 970-1010, and 2460-2500 nm [20]. Its input is 1.5m permanent fiber optic cable and it having 25 degree, 8 degree and 1 degree FOV. Fiber optic cable is flexible and it can move. It is shown in fig 1. It is a very flexible instrument. We can carry it, collect spectrum and save it on laptop through it. It can use in lab and on the field. It requires same accessories like pistol grip tripod, lamp, reference panels, backpack, battery, AC power supply and laptop. The laptop is requires communicate to instrument through Ethernet wired interface or Wi-Fi Ethernet interface.

Fig. 1 FieldSpec Spectroradiometer

It has some software like RS3, ViewSpec Pro, Indico Pro and third party software. RS3 software is used for data collection. Rs3 software is us File is saved as .asd extension. We can set 25 degrees, 8 degree and 1 degree FOV. ViewSpec Pro software is used for data analysis. It is useful for process data. It shows spectral signature between 350-2500 nm. It has the same tools like reflectance, absolute reflectance, log 1/ T, log 1/ R, 1st and 2nd derivative, and parabolic correction and so on. It can export .asd file into the ASCII code (text file), shows the latitude and longitude of the field location (GPS) and it can use ArcGIS tools for it [21].

TABLE 2. TECHNIQUES FROM LITERATURE SURVEY

Preprocessing	**Feature extraction**	**Feature classification**	**Statistic method**	**References ID**
1st Derivatives, Savitzky-Golay filter	N (Nitrogen)	PLSR, LWB, SVMDA, PCA	RPD, Cohen's kappa coefficient, min. max, mean, SD, CV	[4]
2nd Derivatives, MSC, SNV, Savitzky-Golay filter	Db, MC, Clay, silt, Sand	SMLR	RMSE, Correlation coefficient, coefficient of multiple determinations(R^2)	[5]
1st Derivatives , MSC, Savitzky-Golay filter	Zn, Cu, Pb, Cr, Ni. (Heavy Metals)	PLSR	RMSE, cross-validation, RPD, min, max, mean, SD, RMSE_cv, RPD_cv, pre	[6]
MNF, Spectral mixture analysis, pixel purity index	CaSo_4, CaCo_3, Gypsum, OM, CEC	Gaussian Model, FWHM	RMSE	[7]
CCD detector	N, P, K	LIBS	RSD	[10]
MA, MSC, SNV, DT, BC, 1st & 2nd derivatives	Sandy, clay, loam clay, semi clay	PCA	Min, max, mean, SD	[11]
1st Derivatives, Savitzky-Golay filter	C, N, SO4, PH, P-Olsen, P, CEC, K, Ca, Mg, Na, Bulk dencity	PCA, PLSR	Min, max, mean, SD, RMSE, RMSECV, RMSEP, RPD, REP	[12]
Nearest neighbor method, normalization	OM, sand, silt, Aluminum, clay, Ca, Mg, K, CEC	NDVI	average, min, max, SD, Cov varia	[13]
Log 1/R, 1st derivatives	CaCO3, SOM, Ca, K, Mg, Na, CEC, pH, EC, clay, silt, sand	PLSR, MARS	RMSEP, RPD, RER, SD,	[15]
Normalization, baseline-corrections, smoothing, 1st derivatives	C, N, P,k, S, Ca, clay	PLSR, ANN,PCA, PCR, beer-Lamber law, back-propagation Algo	RSME,cross-validation, RPD, ME.	[17]
Log(1/T), SNV		LS-SVM, PCA	RBF, Eigenvalues & eigenvectors	[19]
1st derivatives	Nitrogen	NDVI	RMSE, correlation coeffient, ABD	[20]
Base line correction, Savitzky-Golay filter	Clay, CaCO3, Organic matter	NN(Non-linear classifiers)		[23]
1st & 2nd derivatives, SNV, Savitzky-Golay filter	OC, CEC, Clay, TC, Ca, TN, sand, Mg, pH, K, TP, silt, ESP, NH4, Na, P, EC, NO3-N	PLSR,PCA	RMSE, ME, SDE, RPD, Mahalonobis statistic	[24]
1st derivatives	Clay, SOC	PLSR, BRT, CART LM, GLS, GNLS	MSD, RMSD, Bias, SB, NU, LC, SEP	[25]
1st derivatives, XRD	Clay sand, C, CEC, IC, SOC, Fed, pH	PLSR, BRT, PCA	Kappa coefficient, Cross-Validation, MSD, RMSD, Bias, SB, NU, LC,	[27]
	pH, LR, OC, clay, silt,	PLSR	Covariance, cross- validated, ME,	[28]

	sand, CEC, Ca, Al, NO3_N, P Cpl, K, EC		RMSE	
1st derivatives	Clay, CaCO3, Oganic C (OC) , Inorganic C (IC)	PLSR, PCR, MARS, PCA	MSD, RMSD, Bias, SB, NU, LC, SEP	[30]
1st derivatives, Savitzky-Golay filter, normalization	C, N	PLRS, MLR	SD, SE, RMSE, Cross-Validation	[31]
1st derivatives	C	PLSR	RSQ,SECV, SEP, RPD	[32]
1st derivatives, Savitzky-Golay filter	SOC	PLS1	RSQ, SECV, SEP, RPD	[33]
1st derivatives, Savitzky-Golay filter	CSC,	PLS1 (PLSR)	RSQ, SECV, SEP, RPD	[34]
1st derivatives, Savitzky-Golay filter, MSC	clay, silt, sand, pH, C, N, Ca, Mg, K	PLSR	Mean, SE, RMSEP	[38]
1st derivatives, Savitzky-Golay filter	C, N	PLSR	RMSE, Bias	[39]
1st derivatives, Savitzky-Golay filter	Clay, silt, pH, SOC, N, Ca, Mg, K, P, CEC	PLSR, PCA	Min, Max, Median, Mean, SE, RMSEP, RMSEC	[40]

A. Techniques for soil analysis

Table 2 portraits the techniques implemented in literature. The techniques can be grouped in following categories

a. Derivatives

In table 2, 1st derivatives are widely used for Pre-processing. It is measures of the slope of the spectral curve at every point. The slop of the curve is not affected by baseline offsets in the spectral signature. It is an effective method for removing baseline offsets [22-26]

b. Principle Component Analysis (PCA)

It is multivariate techniques that analyze a data set in which observations are described by many inter correlated quantitative dependent variables. PCA is extracting the important information from the data and represent it as a set of new orthogonal variable, to show the pattern of correspondence of the observations and of the variables as points on the map. It constantly uses a projection method that can find the directions in space along which data point is the largest between the distances. It is called Principal Components (PCs). PCA is the backbone of the modern data analysis. It reduces the dimensionality of the data, filter some of the noise data, decrease redundancy in the data, compress it and prepare the data for further analysis purpose using other methods [27-30].

c. Smoothing

It is used for removing noise form the data set and allowing important patterns of in the data set. Data smoothing can do in a different ways like moving average, Savitzky-Golay filter and Gaussian filtering. Savitzky-Golay filter is better than the simply averaging data points is to perform a least squares fits polynomial data set to successive curve segment and then replace the first values with further regular variations. The Savitzky - Golay filter is continually used to remove spectral noise picks when chemical information can keep it [31-33].

d. Baseline

It is two transformations. One is offset and another is linear baseline correction. Offset is variable to subtract to all selected variables. The result of offset baseline is minimum value is set and the rest is positive values. Linear baseline is the slope of baseline into the horizontal baseline. It is to point out two variables which will define the new baseline [34-36].

e. Partial Least Square Regression [PLSR]

PLSR is widely used for spectral calibration and prediction. It is a method for relating two data matrices two variable (x, y) though a linear multivariate model, it is widely used in reflectance spectroscopy data analysis and chemometrics and common used for quantitative spectral analysis. It decomposes both variable and finds new component [37]. It is used to construct predictive models when there many predictor variables that is highly collinear. It can use to construct a linear predictive model for the sample amount based on the spectrum. Each spectrum is comprised of measurements in different frequencies. PLS Factors are computed as a certain linear combination of spectral range and the responses are predicted linearly based on these extracted factors. It uses in chemistry and engineering. It gives richer results than the old multiple regression approach methods [38]. It developed a generalization of multiple linear regression (MLR) and analyze data with strongly collinear, noisy, multiple variables and simultaneously model several response variables. PLSR is a way to estimate parameters in the scientific model, which basically is linear and it's like any scientific model, conceptual, technical, numerical, statistical, and so on. Cross-validation (CV) is a practical and correct way to test this predictive significance [39]. It is standard in PLSR analysis. The collected data set with preserved time order and it allocates into two parts, one

is training set and the second one is prediction set. Only forward prediction applied process insight initial PLSR modeling and inspection of cross-correlation indicate that some samples of the variables is warranted to catch process dynamics.

CONCLUSION

Spectroradiometer is widely used in agriculture application (Remote Sensing). VNIR, SWIR and Mid-Infrared is used in it. It appears to be very promising techniques for rapid analysis of soil samples. The main limitation of the Spectroradiometer approach is that it requires standard parameters of instrument setups and on the field work. Soil content is usually described by soil properties such as nutrient levels, soil organic matters, minerals, etc. spectral analysis is very important when FieldSpec Spectroradiometer is used in the evaluation of soil properties. PLSR is important techniques to reach this goal. Some soil samples and soil variance also needs in a good multivariate calibration of soil properties. We can make soil spectral library with including at least thousands of soil samples. It should be collected which will be useful for future design.

ACKNOWLEDGEMENT

The authors would like to thank, Dr. Suresh Mehlotra, Geospatial Technology (SAP-II) and SCM_RL (System Communication & Machine learning research laborotry) for provide infrastructure and Information

REFERENCES:

[1] Sujit choudhary, Deepankar chakrabarti and Suchandra Choudhury,"An introduction to Geographic Information Technology", I K International publishing House Pvt.Ltd, Nov 2008.
[2] [Onlineavailable]https://www.nrcan.gc.ca/sites/www.nrcan.gc.ca/files/earthsciences/pdf/resource/tutor/fundam/pdf/fundamentals_e.pdf
[3] [Online available] http://www.isric.org/sites/default/files/ICRAF-ISRICSoilVNIRSpectralLibrary.pdf
[4] Shuo Li, Wenjum Ji, Songehao Chen, Jie Peng, Yin Zhou and Zhou Shi, "Potential Of VIS-NIR-SWIR Spectroscopy from the Chines Soil Spectral Library for Assessment of Nitrogen Fertilization Rates in the Paddy-Rise Region, China", Remote Sensing, OPEN ACCESS, 7, pp. 7029-7043, May 2015.
[5] Gholizadeh, M. S. M. Amin, L. Boruvka and M. M. Saberioon, "Models for estimating the physical properties of paddy soil using visible and near infrared reflectance spectroscopy", Springer Science +Business Media New York, Journal of Applied Spectroscopy, vol. 81, No. 3, pp. 534-540, July 2014.
[6] M. Todorova, A. M. Mouazen, H. Lange and S. Astanassova, "Potential of near-infrared spectroscopy for measurement of heavy metals in soil as affected by calibration set size", Springer, Water Air Soil Pollut, vol. 225, No.8, 2036, pp. 1-19, July 2014.
[7] M. Saleh, A. B. Belal and S. M. Arafat, "Identification and mapping of some soil types using field spectrometry and spectral mixture analyses: a case study of North Sinai, Egypt", Springer, Arabian J Geosciences, vol. 6, No. 6, pp. 1799-1806, Dec 2011.
[8] Francesca Garfagnoli, Gianluca Martelloni, Andrea Ciampalini, Luca Innocenti and Sandro Moretti, "Two GUIs-based analysis tool for spectroradiometer data pre-processing", Springer, Eath Science Informatics, vol. 6, No. 4, pp. 227-240, July 2013.
[9] K. Khadse, "Spectral reflectance characteristics for the soils on baseltic terrain of central Indian plateau", J Indian Soc Reomte Sens (Journal of the Indian Society of Remote Sensing), Springer, vol. 40, No. 4, pp. 717-724, Dec 2011.
[10] Zejian Lei, Mingyin Yao, Muhua Liu, Qiulian Li and Hanping Mao, "Comparision between fertilization N, P, K and No fertilization N, P, K in paddy soil by laser induced breakdown spectroscopy", IEEE Intelligent Computation Technology and Automation, vol. 1, pp. 363-366, 2011.
[11] Haiqing Yang, Boyan Kuang, Abdul M. Mouazen, "Affect of different preprocessing methods on principal component analysis for soil classification", IEEE, *ICMTMA*, vol. 1, pp. 355-358, Jan 2011
[12] Bambang Hari Kusumo, Mike J. Hedley, Carolyn B. Hedley and Mike P. Tuohy, "Measuring carbon dynamics in field soils using soil spectral reflectance: prediction of maize root density, soil organic carbon and nitrogen content", Springer, Plant Soil, vol.338, No. 1, pp. 233-245, Jan 2011.
[13] Jose A. M. Dematte, Peterson R. Fiorio and Suzana R. Araujo, "Variation of routine soil analysis when compared with hyperspectral narrow band sensing method", Remote Sensing, Open Access, vol. 2, No. 8, PP.1998-2016, Aug 2010.
[14] Volkan Bilgili, H. M. van Es, F. Akbas, A. Durak and W.D. Hively, "visible/near infrared reflectance spectroscopy for assessment of soil properies in a semi-arid area of turkey", ELSEVIER, Journal of Arid Environments, vol. 74, No.2, pp. 229-238, Feb 2010.
[15] Henrique Bellinaso, Jose Alexandre Melo Dematte and Suzana Araujo Romeiro, "Soil spectral library and its use in soil classification", Scielo,Revista Brasileira de Ciencia do Solo, vol. 34, No. 3, May/June 2010.
[16] Changwen Du and Jianmin Zhou, "Evaluation of soil fertility using infrared spectroscopy: a review", Springer, vol. 7, No.2, pp. 97-113, Jun 2009.
[17] I. Belyaev, Yu. V. Belyaev, L. V. katkovskii and i. M. Tsikman, "Estimation and analysis of the parameters of a field spectroradiometer covering the spectral range 350-2500 nm", Springer Science + Business Media, Journal of Applied Spectroscopy, vol. 76, No. 4, pp. 577-584, 2009.
[18] Li, Z., Yu, J. and He, Y., "use of nir spectroscopy and LS-SVM model for the discrimination of varieties of soil", Boston:Springer, IFIP international Federation for Information Processing, vo. 293, Computer and Computing Technologies in Agriculture II, vol. 1, pp. 97-105, 2009.
[19] Jian Wu, Yaolin Liu, Dan Chen, Jing Wang, Xu Chai, "Quantitative Mapping of Soil Nitrogen Content Using Field Spectrometer and Hyperspectral Remote Sensing", IEEE, *ESIAT*, vol. 2, pp. 379-382, Jul 2009.

[20] Isa Yunusa, Rhys Whitley, Melanie Zeppel, Derek Eamus, "Simulation of Evapotranspiration and Vadose Zone Hydrology Using Limited Soil Data: A Comparison of Four Computer Models", IEEE, *ICECS*, pp. 152-155, Dec 2009.
[21] Lianqinq Xue, Dan Li, Shuo Huang, Chunlin Wu, "Spatial variability analysis on soil nitrogen and phosphorus experiment based on geostatisics", IEEE, *ETTANDGRS*, vol. 2, pp. 237-240, Dec 2008.
[22] Linker, R., "Soil classification via mid-infrared spectroscopy", Boston:Springer, , IFIP international Federation for Information Processing, vo. 259, Computer and Computing Technologies in Agriculture, vol. 2, pp. 1137-1146, 2008.
[23] Rossel RAV, Jeon YS, Odeh IOA, McBratney AB, "Using a legacy soil sample to develop a mid-IR spectral library", CSIRO, *Soil Research*, vol. 46, No.1, pp. 1–16, Feb 2008.
[24] Davin J. Brown, "Using a global VNIR soil-spectral library for local soil characterization and landscape modeling in a 2nd-order Uganda watershed", ELSEVIER, SiecnceDirect Geoderma, Vol. 140, No. 4, pp. 444-453, Aug 2007.
[25] R.J. Gehl and C. W. Rice, "Emerging technologies for in situ measurement of soil carbon", Springer, Climatic Change, vol. 80, No.1, pp. 43-54, Jan 2007.
[26] David J. Brown, Keith D. Shepherd, Markus G. Walsh, M. Dewayne Mays and Thomas G. Reinsch, "Global soil characterization with VNIR diffuse reflectance spectroscopy", ELSEVIER, Geoderma, vol. 132, No.3-4, pp. 273-290, Jun 2006.
[27] R. A. Viscarra Rossel, D. J. J. Walvoort, A. B. McBratey, L. J. Janik and J. O. Skjemstad, "Visible , near infrared, mid infrared or co bined diffuse reflectance spectroscopy for simultaneous assessment of various soil properties", ELSVIER, Geoderma, vol. 131, No. 1-2, pp. 59-75, Mar 2006.
[28] R. N. Sahoo, M. Bhavanarayana, B. C. Panda, C. N. Arika and R. kaur, "Total information content as an index of soil moisture", Springer, Journal of the Indian Society of Remote Sensing, vol. 33, No. 1, pp. 17-23, Mar 2005.
[29] David J. Brown, Ross S. Bricklemyer and Perry R. Miller, "Validation requirements of diffuse reflectance soil characterization models with acase study of VNIR soil C prediction in Montana", ELSVIER, Geoderma, vol. 129, No. 3-4, pp. 251-267, Dec 2005.
[30] K. D. Shepherd, B. Vanlauwe, C. N. Gachengo and C. A. Palm, "Decomposition and mineralization of organic residues predicted using near infrared spectroscopy", Springer, Plant and Soil, vol. 277, No.1, pp. 315-333, Dec 2005.
[31] Dan Shiley and SummitCAL Solutions Team, "283-7 Measurement of soil mineralogy using Near-Infrared reflectance spectroscopy", ASD Inc., Boulder, Co 80301, pp. 1-2, 2011.
[32] Michaela Kastanek, Applications Coordinator and George Greenwood, Senior Market Manager, "Analysis of soil organic Carbon in soil samples using an ASD NIR spectrometer", Remote Sensing, ASD Inc., a PANanalytical company Boulder, Colorado, 80301, USA, pp. 1-5, Oct 2013.
[33] Donald Campbell, Daniel Shiley and Brian Curtiss, "Measurement of soil mineralogy and CEC Using Near-Infrared reflectance spectroscopy", Remote Sensing, ASD Inc., a PANanalytical company Boulder, Colorado, 80301, USA, pp. 1-2, Nov 2013.
[34] A. Shvetsov, V.M. Demkin, D. A. Karashtin, N. K. Skalyga and L. I. Fedoseev, "Microwave spectroradiometer complex for remote study of the stratosphere thermal structure", Srpinger science+Business media, Radiophysics and quantum electronics, vol. 52, No. 8, PP. 603-608, 2009.
[35] Liu Jun-ang, Guo Liang, Hao Yan and Zhi-hui, "Ecological distribution of soil microorganism and activity characteristic of soil Enzymes in camellia oleifera stands", IEEE, International conference on chllenges in Environmental science and computer engineering, vol. 1, pp. 479-482, 2010.
[36] Vincent de Paul Obade, Rattan Lal and Jiquan Chen, " Remote sensing of soil and water quality in agroecosystems", Springer, water air soil pollution, vol. 224, No. 9, pp. 1-27, Aug 2013.
[37] Alex O. Awiti, Markus G. Walsh, Keith D. Shepherd and Jenesio Kiyamario, "Soil condition classification using spectroscopy: A proposition for assessment of soil condition along a topical forest- cropland chronosequence", ELSEVIER, Geoderma, vol. 143, No.1-2, pp. 73-84, Jan 2008.
[38] Patrick Kiiti Mutuo, Keith D. Shepherd, Alain Albrecht and Georg Cadisch, "Prediction of carbon mineralization rates from different soil physical fractions using diffuse reflectance spectroscopy", ELSEVIER, Soiil Biology & Biochemistry, vol. 38, No.7, pp. 1658-1664, July 2006.
[39] Tor-G. Vagen, Keith D. Shepherd and Markus G. Walsh, "Sensing Landscape level change in soil fertility following deforestation and conversion in the highlands of Madagascar using Vis-NIR spectroscopy", ELSEVIER, Geoderma, vol. 133, No.3-4 , pp. 281-294, Aug 2006.

International Journal of Engineering Research and General Science Volume 3, Issue 6, November-December, 2015
ISSN 2091-2730

EXACT SOLUTIONS FOR CHEMICALLY REACTIVE SPECIES IN CASSON FLUID PAST AN EXPONENTIALLY ACCELERATED SURFACE WITH NEWTONIAN HEATING IN THE PRESENCE OF THERMAL RADIATION

Preeti Jain*

*Department of Mathematics, University of Rajasthan

Jaipur-302004 (INDIA), M-9460500726

Abstract - An exact analysis of heat transfer accompanied by mass transfer flow of a Casson fluid past an exponentially accelerated infinite vertical plate with Newtonian heating in the presence of radiation is presented here. The governing coupled linear partial differential equations are transformed into linear ordinary differential equations by using non-dimensional variables. The resulting equations have been solved analytically using Laplace-transform technique. Closed form solutions are obtained for velocity, temperature and concentration profiles for different governing parameters. The paper intends to show unique results for a combination of heat transfer and chemical reaction in a Casson fluid flow. Expressions for shear stress in terms of Skin friction, the rate of heat transfer in terms of Nusselt number and mass transfer in terms of Sherwood number are also obtained. All the numerical results with various values of embedded flow parameters are analyzed graphically and their physical aspects are discussed in detail.

Keywords: Newtonian heating, Casson fluid, exponentially accelerated plate, unsteady free convection, Heat transfer, Mass transfer, thermal Radiation, Incompressible fluid.

MSC Classification: 76U, 76W, 76V, 76R, 65N.

Introduction

Newtonian fluids which have a linear relationship between the stress and the rate of strain are limited in view of their applications because they do not explain several technological applications for fluids in industry. Many complex fluids such as blood, clay coating, paints, honey, condensed milk, shampoos, soup, certain oils and greases, suspensions and many emulsions are noteworthy due to their various applications in the field of metallurgy, food processing, drilling operations, bioengineering operations and chemical and petroleum industries. In the literature they are known as non-Newtonian fluids. These fluids are described by a non-linear relationship between the stress and the rate of strain. In view of these applications and frequent occurrence of non-Newtonian fluids, the studies of such fluids have now become an increasingly appealing topic of current research in this field. The mechanics of non-Newtonian fluids present a special challenge to engineers, mathematicians and physicists. The Navier-Stokes theory is inadequate for describing such fluids and no single constitutive equation is available in the literature which exhibits the properties of all fluids. Because of the complexity of these fluids, there is not a single constitutive equation which exhibits all properties of such non-Newtonian fluids. Thus a number of non-Newtonian fluid models have been proposed to study their characteristic. The vast majority of non-Newtonian fluid models are concerned with simple models like the power law and grade two or three. These simple fluid models have short comings that render to results not having accordance with fluid flows in the reality (Mukhopadhyay and Vajravelu [1]). Power-law fluids models which are used to express non-Newtonian behavior in fluids predict shear thinning and shear thickening behavior. However it is inadequate in expressing normal stress behavior as observed in die swelling and rod climbing behavior in some non-Newtonian fluids. Normal stress effects can be expressed in second grade fluid model, a special type of Rivlin–Ericksen fluids, but this model is incapable of representing shear thinning/ thickening behavior (Aksoy et al. [2]). The non-Newtonian fluids are mainly classified into three types, namely differential, rate, and integral. The simplest subclass of the rate type fluids is the Maxwell model which can predict the stress relaxation. This rheological model, also, excludes the complicated effects of shear-dependent viscosity from any boundary layer analysis (Hayat et al. [3]). There is another type of non-Newtonian fluid known as Casson fluid. Casson [4] was the first who introduced this model for the prediction of the flow behavior of pigment oil suspensions used for preparation of printing inks. Casson fluid exhibits yield stress. It is well known that Casson fluid is a shear thinning liquid which is assumed to have an infinite viscosity at zero rate of shear, a yield stress below which no flow occurs, and a zero viscosity at an infinite rate of shear, i.e., if a shear stress less than the yield stress is applied to the fluid, it behaves like a solid, whereas if a shear stress greater than yield stress is applied, it starts to move. The examples of Casson fluid are jelly, tomato sauce, honey, soup, concentrated fruit juices, etc. Human blood can also be treated as Casson fluid. Due to the presence

of several substances like, protein, fibrinogen, and globulin in aqueous base plasma, human red blood cells can form a chain like structure, known as aggregates or rouleaux. If the rouleaux behave like a plastic solid, then there exists a yield stress that can be identified with the constant yield stress in Casson's fluid (Fung [5] and (Dash et al. [6]). Later on several researchers studied Casson fluid for different flow situations and configurations. Mustafa et al. [7] studied the unsteady boundary layer flow and heat transfer of a Casson fluid due to an impulsively started moving flat plate with a parallel free stream using homotopy analysis method (HAM). Mukhopadhyay [8-10] investigated Casson fluid flow and heat transfer over a nonlinearly stretching surface subjected to suction/blowing. The transformed equations were solved numerically by using the shooting method. Bhattacharya et al. [11, 12] analyzed the exact solution for boundary layer flow of Casson fluid over a permeable stretching/shrinking sheet.

Radiation effect plays an important role in various engineering processes. When the temperature of the surrounding fluid is rather high, radiation effects on the flow become significant. In some industrial applications such as glass production, furnace design, thermonuclear fusion, casting and levitation and in space technology applications such as cosmic flight aerodynamics, rocket propulsion systems, plasma physics, and space craft reentry aerothermodynamics which operate at higher temperature, radiation effects play an important role. Keeping in view this fact, Hossain et al. [13] determined the effect of radiation on the natural convection flow of an optically thick, viscous, incompressible flow past a heated vertical porous plate with a uniform surface temperature and a uniform rate of suction, where the radiation was included by assuming the Rosseland diffusion approximation. Raptis and Perdikis [14] studied the effects of thermal radiation and free convective flow past a uniformly accelerated vertical plate. Soundalgekar et al. [15] further presented exact solution to radiation effect on flow past an impulsively started vertical plate. Radiation effects on mixed convection along an isothermal vertical plate were studied by Hossain and Takhar [16]. Makinde [17] focused on the thermal radiation and mass transfer past a moving porous plate. Muthucumaraswamy [18, 19] obtained exact solutions taking into account the effects of thermal radiation under different boundary conditions. Recently, Deka and Das [20] investigated radiation effects past a vertical plate using ramped wall temperature, Jana and Ghosh [21] investigated radiative heat transfer in the presence of indirect natural convection. Numerical solutions of Casson fluid flow accompanied by heat transfer past an exponentially stretching surface in the presence of thermal radiation were presented by Pramanik [22].

The processes involving mass transfer effects are important in chemical processing equipments which are designed to draw high value products from cheaper raw materials with the involvement of chemical reaction. Mass transfer is important due to its applications in many scientific disciplines that involve convective transfer of atoms and molecules. Examples of this phenomenon are evaporation of water, separation of chemicals in distillation processes, natural or artificial sources etc. In addition, mass transfer with chemical reaction has special importance in chemical and hydrometallurgical industries. The formation of smog represents a first order homogeneous chemical reaction. For example, one can take into account the emission of NO_2 from automobiles and other smoke-stacks. NO_2 reacts chemically in the atmosphere with unburned hydrocarbons (aided by sunlight) and produces peroxyacetylnitrate, which forms a layer of photochemical smog (Shehzad [23]). Chemical reactions can be treated as either homogeneous or heterogeneous processes. It depends on whether they occur at an interface or as a single-phase volume reaction. A reaction is said to be of first order if the rate of reaction is directly proportional to the concentration itself which has many applications in different chemical engineering processes and other industrial applications such as polymer production, manufacturing of ceramics, and food processing A few representative studies dealing with mass transfer in the presence of chemical reaction may be mentioned. Das et al. [24] considered the effect of first order chemical reaction on the flow past an impulsively started infinite vertical plate with constant heat flux and mass transfer. Jain [25] investigated on the combined influence of Hall current and Soret effect on chemically reacting magneto-micropolar fluid flow from radiate rotating vertical surface with variable suction in slip-flow regime. Makanda et al. [26] studied the diffusion of chemically reactive species in Casson fluid flow over an unsteady stretching surface using Runge-Kutta-Fehlberg numerical scheme.

In all the studies cited above the flow is driven either by a prescribed surface temperature or by a prescribed surface heat flux. Here a different driving mechanism for unsteady free convection is considered; here the flow is set up by Newtonian heating from the surface. Heat transfer characteristic are dependent on the thermal boundary conditions. In general there are four common heating processes specifying the wall-to-ambient temperature distributions, prescribed surface heat flux distributions, conjugate conditions where heat is specified through a bounding surface of finite thickness and finite heat capacity. The interface temperature is not known a priori but depends on the intrinsic properties of the system, namely the thermal conductivity of the fluid and solid respectively. Newtonian heating, where the heat transfer rate from the bounding surface with a finite heat capacity is proportional to the local surface temperature and is usually termed conjugate convective flow. This configuration occurs in many important engineering devices, for example in heat exchangers where the conduction in solid tube wall is greatly influenced by the convection in the

fluid flowing over it. For conjugate heat transfer around fins where the conduction within the fin and the convection in the fluid surrounding it must be simultaneously analyzed in order to obtain the vital design information. In convective flows set up when the bounding surfaces absorbs heat by solar radiation. Therefore we conclude that the conventional assumption of no interaction of conduction-convection coupled effects is not always realistic and it must be considered when evaluating the conjugate heat transfer processes in many practical engineering applications. Merkin [27] was the first to consider the free-convection boundary-layer over a vertical flat plate immersed in a viscous fluid whilst [28, 29, 30] considered the cases of vertical and horizontal surfaces embedded in a porous medium. The studies mentioned in [27 - 30] deal with steady free convection. In this area, the authors of this paper, Jain and Chaudhary [31, 32] were the first one to give exact solution to the unsteady free convection boundary-layer flow from a flat vertical plate with Newtonian heating and the solution was obtained in closed-form using Laplace transform technique. Recently, Jain [33] presented exact solution of heat and mass transfer past an inclined oscillating surface with Newtonian heating under the effect of thermal radiation and mass diffusion. Our work was further extended by Narahari and Nayan [34], Raju et al. [35], Narahari and Ishak [36] and Hussanan et al. [37] in which they incorporated the effects of thermal radiation and mass transfer with Newtonian heating under different boundary conditions like impulsively started plate, oscillating plate, moving plate etc. An exact solution of the unsteady free convection flow of a viscous incompressible, optically thin, radiating fluid past an impulsively started vertical porous plate with Newtonian heating was investigated by Mebine and Adigio [38].

To the best of author's knowledge, so far, no study has been reported in the literature which investigates the unsteady free convection flow of chemically reactive species in Casson fluid past an exponentially accelerated plate with Newtonian heating accompanied by heat and mass transfer in the presence of thermal radiation. In this study, the equations of the problem are first formulated and transformed into their dimensionless forms where the Laplace transform method is applied to find the exact solutions for velocity, temperature and concentration. Furthermore, expressions for skin friction, Nusselt number and Sherwood number are obtained and are plotted graphically and discussed for the pertinent flow parameters. Exact solutions obtained in this paper are important not only because do they correspond to some fundamental flow application but also they are useful for explaining the physical aspects of the flow problem in detail. More over exact solutions are being used as a benchmark for validation of other solutions obtained via approximate or numerical schemes.

Mathematical Analysis

Let us consider the effect of Newtonian heating on unsteady free convection flow of a viscous, incompressible Casson fluid past an infinite vertical flat plate. The x^*-axis is taken along an infinite vertical plate and parallel to the free stream velocity and y^*-axis is taken normal to it. It is assumed that initially at time $t^* = 0$, the plate and fluid are at rest with constant temperature T_∞^* and concentration level C_∞^* at all points. At time $t^* \geq 0$, suddenly the plate is accelerated with velocity $\exp(a_0^* t^*)$ in its own plane along the x^*- axis against the gravitational field and the rate of heat transfer from the surface is proportional to the local surface temperature T^*, also the concentration level near the plate is raised from C_∞^* to C_w^*. It is also assumed that there exists a homogeneous chemical reaction of first order with constant rate K_c between the diffusing species and the fluid. Since the plate is infinite in the x^* direction therefore all the flow variables are independent of x^* and are functions of y^* and t^* only. The fluid is considered to be gray absorbing-emitting radiation and non-scattering medium. We assume that the rheological equation of state for an isotropic and incompressible flow of a Casson fluid can be written as (Mukhopadhyay [9])

$$\tau_{ij} = \begin{cases} 2\left(\mu_B + p_y / \sqrt{2\pi}\right) e_{ij} & , \quad \pi > \pi_c \\ 2\left(\mu_B + p_y / \sqrt{2\pi}\right) e_{ij} & , \quad \pi < \pi_c \end{cases}$$

where $\pi = e_{ij} e_{ij}$ and e_{ij} is the $(i, j)^{th}$ component of the deformation rate so π is the product of the component of deformation rate with itself, π_c is a critical value of this product based on the non-Newtonian model, μ_B is plastic dynamic viscosity of the non-Newtonian fluid, and p_y is yield stress of fluid. So if a shear stress less than the yield stress is applied to the fluid, it behaves like a solid, whereas if a shear tress greater than the yield stress is applied, it starts to move.

It is also assumed that the viscous dissipation term in the energy equation and the heat produced by chemical reaction is negligible, as the fluid velocity is low. Under these conditions along with the assumptions, we apply the Boussinesq approximation which states that all fluid properties are constant with the exception of the density variation in the buoyancy term, the free convective problem is governed by the following set of partial differential equations:-

$$\rho\frac{\partial u^*}{\partial t^*} = \mu_B\left(1+\frac{1}{\beta}\right)\frac{\partial^2 u^*}{\partial y^{*2}} + \rho g\,\beta_t\,(T^*-T_\infty^*) + \rho g\,\beta_c\,(C^*-C_\infty^*) \qquad \ldots(1)$$

$$\rho\, c_p\,\frac{\partial T^*}{\partial t^*} = k\frac{\partial^2 T^*}{\partial y^{*2}} - \frac{\partial q_r}{\partial y^*} \qquad \ldots(2)$$

$$\frac{\partial C^*}{\partial t^*} = D\,\frac{\partial^2 C^*}{\partial y^{*2}} - K_c C^* \qquad \ldots(3)$$

With the following initial and boundary conditions:

$$\left.\begin{aligned} &t^* \le 0 : u^* = 0, \quad T^* = T_\infty^*, \quad C^* = C_\infty^* \qquad \text{for all } y^* > 0 \\ &t^* > 0 : u^* = \exp(a_0^* t^*), \quad \frac{\partial T^*}{\partial y^*} = -\frac{h}{k}\,T^*,\ C^* = C_w^* \text{ at } y^* = 0 \\ &\qquad\quad : u^* = 0, \qquad T^* \to T_\infty^*, C^* \to C_\infty^* \qquad \text{as } y^* \to \infty \end{aligned}\right\} \qquad \ldots(4)$$

The radiation heat flux under Rosseland's approximation [39] is expressed by

$$q_r = -\frac{4\sigma}{3k^*}\frac{\partial^4 T^*}{\partial y^*} \qquad \ldots(5)$$

This model is valid for optically-thick media in which thermal radiation propagates only a limited distance prior to experiencing scattering or absorption. The local thermal radiation intensity is due to radiation emanating from proximate locations in the vicinity of which emission and scattering are comparable to the location of interest. For zones where conditions are appreciably different thermal radiation has been shown to be greatly attenuated before arriving at the location under consideration. The energy transfer depends on conditions only in the area adjacent to the plate regime i.e. the boundary layer regime. Rosseland's model yields accurate results for intensive absorption i.e. optically-thick flows which are optically far from the bounding surface. It is assumed that the temperature differences within the flow are sufficiently small and then (5) can be linearized by expanding T^{*4} into Taylor series about T_∞^*, which after neglecting higher order terms takes the form:

$$T^{*4} \cong 4T_\infty^{*3}T^* - 3T_\infty^{*4} \qquad \ldots(6)$$

In view of (5) and (6), (2) reduces to

$$\rho C_p\,\frac{\partial T^*}{\partial t^*} = \left(k + \frac{16\sigma T_\infty^{*3}}{3k^*}\right)\frac{\partial^2 T^*}{\partial y^{*2}} \qquad \ldots(7)$$

To reduce the above equations into their non-dimensional forms, we introduce the following non-dimensional quantities:-

$$\left.\begin{aligned} u &= \frac{u^*}{U_0},\ t = \frac{t^* U_0^2}{\nu},\ y = \frac{y^* U_0}{\nu},\ a_0 = \frac{a_0^* \nu}{U_0^2} \\ \theta &= \frac{T^* - T_\infty^*}{T_\infty^*},\ C = \frac{C^* - C_\infty^*}{C_W^* - C_\infty^*},\ Pr = \frac{\mu C_p}{k},\ Sc = \frac{\nu}{D} \\ Gr &= \frac{\nu g \beta_t T_\infty^*}{U_0^3},\ Gm = \frac{\nu g \beta_c (C_W^* - C_\infty^*)}{U_0^3},\ R = \frac{16\sigma T_\infty^{*3}}{3k k^*} \\ \beta &= \frac{\mu_B \sqrt{2\pi_c}}{p_y},\quad \gamma = \frac{h\nu}{kU_0},\quad \alpha = \frac{K_c \nu}{U_0^2} \end{aligned}\right\} \quad \ldots(8)$$

Substituting the transformation (8) into equations (1), (3) and (7), we obtain the following non-dimensional partial differential equations:

$$\frac{\partial u}{\partial t} = \left(1 + \frac{1}{\beta}\right)\frac{\partial^2 u}{\partial y^2} + Gr\,\theta + Gm\,C \quad \ldots(9)$$

$$Pr\frac{\partial \theta}{\partial t} = (1+R)\frac{\partial^2 \theta}{\partial y^2} \quad \ldots(10)$$

$$\frac{\partial C}{\partial t} = \frac{1}{Sc}\frac{\partial^2 C}{\partial y^2} - \alpha C \quad \ldots(11)$$

The corresponding initial and boundary conditions in non-dimensional form are:

$$\left.\begin{aligned} t \le 0 &: u = 0,\ \theta = 0,\ C = 0 \qquad \text{for all } y > 0 \\ t > 0 &: u = \exp(a_0 t),\ \frac{\partial \theta}{\partial y} = -\gamma(1+\theta),\ C = 1 \text{ at } y = 0 \\ &: u \to 0,\ \theta \to 0, C \to 0 \qquad \text{as } y \to \infty \end{aligned}\right\} \quad \ldots(12)$$

Where,

$\gamma = \frac{h\nu}{kU_0}$ is the Newtonian heating parameter, when $\gamma = 0$ then $\theta = 0$ which physically corresponds that no heating from the plate exists [40, 41]. Radiation parameter (R) embodies the relative contribution of heat transfer by thermal radiation to thermal conduction. Large R (>1) values therefore correspond to thermal radiation dominance and small values (<1) to thermal conduction dominance (Siegel and Howell [42]). For R = 1 both conduction and radiative heat transfer modes will contribute equally to the regime. Clearly the term in r. h. s. of (10) is an augmented diffusion term i.e. with R = 0, thermal radiation vanishes and equation (10) reduces to the familiar unsteady one-dimensional conduction-convection equation. Rests of the physical variables are defined in Nomenclature.

Analytical solutions by the Laplace transform method

The thermal and concentration equations (10) and (11) are uncoupled from the momentum equation (9). One can therefore solve for the temperature variable θ(y, t) and concentration variable C(y, t) whereupon the solution of u(y, t) can also be obtained, using Laplace transform technique. The Laplace transform method solves differential equations and corresponding initial and boundary value problems. The Laplace transform has the advantage that it solves initial value problems directly without determining first a general solution and non-homogeneous

differential equations without solving first the corresponding homogeneous equations. Applying the Laplace transform with respect to time t to the eqs. (9) - (11) we get,

$$\left.\begin{aligned} q\,\bar{u}(y,q)-u(y,0)&=\left(1+\frac{1}{\beta}\right)\frac{d^2\bar{u}(y,q)}{dy^2}+Gr\;\bar{\theta}(y,q)+Gm\;\bar{C}(y,q)\\ Pr\left[q\,\bar{\theta}(y,q)-\theta(y,0)\right]&=(1+R)\frac{d^2\bar{\theta}(y,q)}{dy^2}\\ Sc\left[q\,\bar{C}(y,q)-C(y,0)\right]&=\frac{d^2\bar{C}(y,q)}{dy^2}-\alpha Sc\;\bar{C}(y,q)\end{aligned}\right\} \quad \ldots(13)$$

Here,

$\bar{u}(y,q)=\int_0^\infty e^{-qt}u(y,t)dt,\ \bar{\theta}(y,q)=\int_0^\infty e^{-qt}\theta(y,t)dt$ and $\bar{C}(y,q)=\int_0^\infty e^{-qt}C(y,t)dt$ denotes the Laplace transforms of $u(y,t),\ \theta(y,t)$ and $C(y,t)$ respectively.

Using the initial condition (12), we get

$$\frac{d^2\bar{u}(y,q)}{dy^2}-\left(\frac{1+\beta}{\beta}\right)q\,\bar{u}(y,q)+\frac{Gr\,\beta}{1+\beta}\;\bar{\theta}(y,q)+\frac{Gm\,\beta}{1+\beta}\;\bar{C}(y,q)=0 \quad \ldots(14)$$

$$\frac{d^2\bar{\theta}(y,q)}{dy^2}-q\left(\frac{Pr}{1+R}\right)\bar{\theta}(y,q)=0 \quad \ldots(15)$$

$$\frac{d^2\bar{C}(y,q)}{dy^2}-\left(\alpha Sc+q\,Sc\right)\bar{C}(y,q)=0 \quad \ldots(16)$$

The corresponding transformed boundary conditions are:

$$\left.\begin{aligned} &t>0:\ \bar{u}(y,q)=\frac{1}{q-a_0},\ \frac{d\bar{\theta}(y,q)}{dy}=-\gamma\left[\frac{1}{q}+\bar{\theta}(y,q)\right],\ \bar{C}(y,q)=\frac{1}{q}\ \text{at}\ y=0\\ &\bar{u}(y,q)\to 0,\ \bar{\theta}(y,q)\to 0,\ \bar{C}(y,q)\to 0\quad \text{as}\ y\to\infty\end{aligned}\right\} \quad \ldots(17)$$

The solutions of (14) – (16) subject to the boundary conditions (17) are:

$$\bar{u}(y,q)=\frac{1}{(q-a_0)}e^{-y\sqrt{a}\sqrt{q}}+\frac{Gr\,a\,c}{Pr_{eff}-a}\frac{1}{q^2(\sqrt{q}-c)}e^{-y\sqrt{a}\sqrt{q}}-\frac{Gm\,a}{\alpha Sc}\left[\frac{1}{(q-b)}e^{-y\sqrt{a}\sqrt{q}}-\frac{1}{q}e^{-y\sqrt{a}\sqrt{q}}\right]$$
$$-\frac{Gr\,a\,c}{Pr_{eff}-a}\frac{1}{q^2(\sqrt{q}-c)}e^{-y\sqrt{Pr}\sqrt{q}}+\frac{Gm\,a}{\alpha Sc}\left[\frac{1}{(q-b)}e^{-y\sqrt{Sc}\sqrt{q+\alpha}}-\frac{1}{q}e^{-y\sqrt{Sc}\sqrt{q+\alpha}}\right] \quad \ldots(18)$$

$$\bar{\theta}(y,q)=\frac{c}{q(\sqrt{q}-c)}e^{-y\sqrt{q\,Pr_{eff}}} \quad \ldots(19)$$

$$\overline{C}(y,q)=\frac{1}{q}e^{-y\sqrt{(\alpha+q)Sc}} \quad \ldots(20)$$

Where,

$a=\frac{\beta}{1+\beta}, b=\frac{\alpha Sc}{a-Sc}, c=\frac{\gamma}{\sqrt{Pr_{eff}}}$ and $Pr_{eff}=\frac{Pr}{1+R}$, Pr_{eff} is the effective Prandtl number.

By taking the inverse Laplace transform of equations (18) – (20) the solutions are derived as:

$$\theta(y,t)=F_1(y\sqrt{Pr_{eff}},\ c,\ t) \quad \ldots(21)$$

$$C(y,t)=F_2(y\sqrt{Sc},\ \alpha,t) \quad \ldots(22)$$

$$u(y,t)=F_3(y\sqrt{a},a_0,t)+\frac{Gr\,a\,c}{Pr_{eff}-a}\left[F_4(y\sqrt{a},c,t)-F_4(y\sqrt{Pr_{eff}},c,t)\right]$$
$$-\frac{Gm\,a}{\alpha Sc}\left[F_3(y\sqrt{a},b,t)-F_5(y\sqrt{a},t)\right]+\frac{Gm\,a}{\alpha Sc}\left[F_6(y\sqrt{Sc},\alpha,b,t)-F_2(y\sqrt{Sc},\alpha,t)\right] \quad \ldots(23)$$

Here,

$$F_1(z_1,z_2,t)=L^{-1}\left(\frac{1}{q(\sqrt{q}-z_2)}e^{-z_1\sqrt{q}}\right)=e^{\left(z_2^2t-z_1z_2\right)}\operatorname{erfc}\left(\frac{z_1}{2\sqrt{t}}-z_2\sqrt{t}\right)-\operatorname{erfc}\left(\frac{z_1}{2\sqrt{t}}\right) \quad \ldots(24)$$

$$F_2(z_1,z_2,t)=L^{-1}\left(\frac{1}{q}e^{-z_1\sqrt{q+z_2}}\right)=\frac{1}{2}\left[e^{z_1\sqrt{z_2}}\operatorname{erfc}\left(\frac{z_1}{2\sqrt{t}}+\sqrt{z_2t}\right)+e^{-z_1\sqrt{z_2}}\operatorname{erfc}\left(\frac{z_1}{2\sqrt{t}}-\sqrt{z_2t}\right)\right] \quad \ldots(25)$$

$$F_3(z_1,z_2,t)=L^{-1}\left(\frac{1}{q-z_2}e^{-z_1\sqrt{q}}\right)=\frac{e^{z_2t}}{2}\left[e^{z_1\sqrt{z_2}}\operatorname{erfc}\left(\frac{z_1}{2\sqrt{t}}+\sqrt{z_2t}\right)+e^{-z_1\sqrt{z_2}}\operatorname{erfc}\left(\frac{z_1}{2\sqrt{t}}-\sqrt{z_2t}\right)\right] \quad \ldots(26)$$

$$F_4(z_1,z_2,t)=L^{-1}\left(\frac{1}{q^2(\sqrt{q}-z_2)}e^{-z_1\sqrt{q}}\right)=\frac{1}{z_2^3}\left[e^{\left(z_2^2t-z_1z_2\right)}\operatorname{erfc}\left(\frac{z_1}{2\sqrt{t}}-\sqrt{z_2t}\right)-\operatorname{erfc}\left(\frac{z_1}{2\sqrt{t}}\right)\right]$$
$$-\frac{1}{z_2}\left[\left(t+\frac{z_1^2}{2}\right)\operatorname{erfc}\left(\frac{z_1}{2\sqrt{t}}\right)-z_1\sqrt{\frac{t}{\pi}}e^{-\left(z_1/2\sqrt{t}\right)^2}\right]-\frac{1}{z_2^2}\left[2\sqrt{\frac{t}{\pi}}e^{-\left(z_1/2\sqrt{t}\right)^2}-z_1\operatorname{erfc}\left(\frac{z_1}{2\sqrt{t}}\right)\right] \quad \ldots(27)$$

$$F_5(z_1,\ t)=L^{-1}\left(\frac{1}{q}e^{-z_1\sqrt{q}}\right)=\operatorname{erfc}\left(\frac{z_1}{2\sqrt{t}}\right) \quad \ldots(28)$$

$$F_6(z_1, z_2, z_3, t) = L^{-1}\left(\frac{1}{q - z_3} e^{-z_1\sqrt{q+z_2}}\right) =$$

$$\frac{e^{z_3 t}}{2}\left[e^{z_1\sqrt{z_2+z_3}}\,\mathrm{erfc}\left(\frac{z_1}{2\sqrt{t}} + \sqrt{(z_2+z_3)t}\right) + e^{-z_1\sqrt{z_2+z_3}}\,\mathrm{erfc}\left(\frac{z_1}{2\sqrt{t}} - \sqrt{(z_2+z_3)t}\right)\right]$$

…(29)

erfc (x) being the complementary error function defined by

$$\mathrm{erfc}(x) = 1 - \mathrm{erf}(x),\ \mathrm{erf}(x) = \frac{2}{\sqrt{\pi}}\int_0^x \exp(-\eta^2)\,d\eta$$

$$\mathrm{erfc}(0) = 1,\ \mathrm{erfc}(\infty) = 0.$$

Also z_1, z_2, z_3 are dummy variables and F_1, F_2, F_3, F_4, F_5 and F_6 are dummy function. The solution of the problem introduced new inverse Laplace transforms of exponential forms which are not available in the literature. These formulas are derived and are provided in the solution.

Limiting Case

The solutions obtained above are more general. If $\beta \to \infty$, the solution for velocity given in equation (23) reduces to the corresponding solution for Newtonian fluid given by:

$$u(y,t) = F_3(y, a_0, t) + \frac{Gr\ c}{Pr_{eff} - 1}\left[F_4(y, c, t) - F_4(y\sqrt{Pr_{eff}}, c, t)\right]$$

$$-\frac{Gm}{\alpha Sc}\left[F_3(y, b, t) - F_5(y, t)\right] + \frac{Gm}{\alpha Sc}\left[F_6(y\sqrt{Sc}, \alpha, d, t) - F_2(y\sqrt{Sc}, \alpha, t)\right]$$

$$\text{Where}\quad d = \frac{\alpha Sc}{1 - Sc} \qquad \text{....(30)}$$

Skin-friction

Knowing the velocity field, we now study the changes in the skin-friction. It is given by:- $\tau^* = -\mu\left(1 + \frac{1}{\beta}\right)\left(\frac{\partial u^*}{\partial y^*}\right)_{y^*=0}$

…(31)

The dimensionless expression for skin-friction evaluated using (23) is given by:

$$\tau = \frac{\tau^*}{\rho U_0^2} = -\left(1 + \frac{1}{\beta}\right)\left(\frac{\partial u}{\partial y}\right)_{y=0} \qquad \text{…(32)}$$

$$\tau = \frac{\tau^*}{\rho U_0^2} = -\frac{1}{a}\left(\frac{\partial u}{\partial y}\right)_{y=0}$$

$$= -\frac{1}{a}\left\{-\sqrt{\frac{a}{\pi t}} - \sqrt{aa_o}\,\mathrm{erf}\left(\sqrt{a_0 t}\right) - \left(\frac{Gr\,a\,c}{Pr_{eff} - a}\right)\left\{\frac{1}{c^3}\left[-\sqrt{\frac{a}{\pi t}} + e^{tc^2}\,c\sqrt{a}\left(1 + \mathrm{erf}\left(\sqrt{ct}\right)\right) + e^{tc^2 - tc}\sqrt{\frac{a}{\pi t}}\right]\right.\right.$$

$$\left.\left. - \frac{2}{c}\sqrt{\frac{a\,t}{\pi}} - \frac{\sqrt{a}}{c^2}\right\} + \frac{Gm\,a}{\alpha Sc}\left\{e^{ft}\sqrt{af}\,\mathrm{erf}\left(\sqrt{ft}\right)\right\}\right.$$ **Nusselt number**

$$+\left(\frac{Gr\,a\,c}{Pr_{eff} - a}\right)\left\{\frac{1}{c^3}\left[-\sqrt{\frac{Pr}{\pi t}} + e^{tc^2}\,c\sqrt{Pr}\left(1 + \mathrm{erf}\left(\sqrt{ct}\right)\right) + e^{tc^2 - tc}\sqrt{\frac{Pr}{\pi t}}\right] - \frac{2}{c}\sqrt{\frac{Pr\,t}{\pi}} - \frac{\sqrt{Pr}}{c^2}\right\}$$

$$-\frac{Gm\,a}{\alpha Sc}\left\{e^{ft}\sqrt{Sc(f+\alpha)}\,\mathrm{erf}\left(\sqrt{(f+\alpha)t}\right)\right\} + \frac{Gm\,a}{\alpha Sc}\left\{\sqrt{\alpha Sc}\,\mathrm{erf}\left(\sqrt{\alpha t}\right)\right\}\Bigg\} \qquad \ldots(33)$$

Another phenomenon in this study is to understand the effects of t and Pr on Nusselt number. The rate of heat transfer in non-dimensional form as calculated from the temperature field (21) is given by:-

$$Nu = -\frac{\upsilon}{U_0\left(T^* - T_\infty^*\right)}\left.\frac{\partial T^*}{\partial y^*}\right|_{y^*=0} = \frac{1}{\theta(0)} + 1$$

$$= c\sqrt{Pr_{eff}}\left(1 + \frac{1}{e^{c^2 t}\left[1 + \mathrm{erf}\left(c\sqrt{t}\right)\right] - 1}\right) \qquad \ldots (34)$$

Sherwood number

The rate of concentration transfer in non-dimensional form as calculated from the concentration field (22) is given by:-

$$Sh = -\left.\frac{\partial C}{\partial y}\right|_{y=0} = \sqrt{\frac{\alpha Sc}{2}}\left(2 + \frac{1}{2}\sqrt{\frac{Sc}{t}}\,e^{-\alpha t}\right) \qquad \ldots(35)$$

Discussion and Conclusion

In order to get a clear understanding of the effects of various physical parameters on the velocity field, thermal boundary layer, concentration boundary layer, skin-friction, Nusselt number and Sherwood number of a Casson fluid, a detailed numerical computation of the closed form analytical solutions (obtained in the preceding section) have been carried out and shown graphically. The regime is controlled by several thermo-physical parameters which are Casson parameter (□), radiation parameter (R), Prandtl number (Pr), Grashof number (Gr), modified Grashof number (Gm), Schmidt number (Sc), Newtonian heating parameter (γ), chemical reaction parameter (□), exponential accelerated parameter (a_0) and time (t).

In figure 1 the development of dimensionless temperature profiles θ(y, t) inside the boundary layer against span wise coordinate y for different values of Boltzmann-Rosseland radiation parameter (R) is shown. Again Pr = 0.71 i.e. Pr < 1, so that heat diffuses faster than momentum in the regime. $R = \frac{16\sigma T_\infty^{*3}}{3k\,k^*}$ corresponds to the relative contribution of thermal radiation heat transfer to thermal conduction heat transfer. For

R<<1, thermal conduction heat transfer will dominate and vice versa for R > 1. Larger values of R therefore physically correspond to stronger thermal radiation flux and in accordance with this, the maximum temperatures are observed for R = 2. Rosseland's radiation diffusion model effectively enhances the thermal diffusivity, as described by Siegel and Howell. From this figure it is depicted that an increase in radiation parameter leads to an increase in the temperature in the boundary layer region which implies that radiation tends to enhance fluid temperature. Figure 2 exhibits the influence of dimensionless time t on the thermal boundary layer θ(y, t). It is observed that there is an enhancement in fluid temperature as time progresses.

Figure 3 illustrates the influence of Prandtl number (Pr) on fluid temperature taking Pr = 0.71, 1.0, 7.0 and 3 which physically corresponds to air, electrolytic solution, water and Freon CCl_2F_2 respectively at 20^0C temperature and 1 atmospheric pressure. It is inferred that the thickness of thermal boundary layer is greatest for Pr = 0.71 (air), then for Pr = 1.0 (electrolytic solution) and then for Pr = 7.0 (water) and finally lowest for Pr = 3 (Freon) i.e. an increase in the Prandtl number results in a decrease of temperature. An increase in Prandtl number reduces the thermal boundary layer thickness. Pr signifies the relative effects of viscosity to thermal conductivity. In heat transfer problems, the Prandtl number Pr controls the relative thickening of the momentum and thermal boundary layers. Fluids with lower Prandtl number have higher thermal conductivities (and thicker thermal boundary layer structures) and therefore heat can diffuse from the sheet faster than for higher Prandtl number fluids (thinner boundary layers). Hence, Prandtl number can be used to increase the rate of cooling in conducting flows. s

From figure 4 it is reported that an increase in the Newtonian heating parameter (γ) the thermal boundary layer thickness also increases and as a result the surface temperature of the plate increases. From figures 1 to 4 it is found that the maximum of the temperature occur in the vicinity of the plate and asymptotically approaches to zero in the free stream region. The graphical behavior of temperature represented in figures 1 - 4 are in good agreement with the corresponding boundary conditions of temperature profiles as shown in equation (12).

In Figure 5 the concentration profiles C(y,t) are shown for different values of the Schmidt number (Sc) and time (t) respectively. Different values of Schmidt number Sc = 0.22, 0.30, 0.66, 0.78 and 0.94 are chosen which physically correspond to Hydrogen, Helium, Oxygen, Ammonia and Carbon dioxide respectively at 25^0C temperature and 1 atmospheric pressure. The profiles have a common feature that the concentration decreases exponentially from the surface to zero value far away in the free stream. A comparison of curves in the figures show that the concentration boundary layer decreases with increasing Schmidt number while it enhances for increasing times. This is consistent with the fact that an increase in Sc means decrease of molecular diffusivity that result in decrease of concentration boundary layer. Hence, the concentration of species is higher for small values of Sc and lower for large values of Sc. Effects of Chemical reaction parameter (□) are displayed in figure 6 and it is observed that an increase in the values of the chemical reaction parameter the thickness of concentration profiles C(y,t) decreases. When □ = 0, there is no chemical reaction. An increase in the chemical reaction parameter corresponds to an increase in the reaction rate parameter and an increase in the reaction rate parameter results in reduction in concentration boundary layer.

The effects of Grashof number (Gr) and modified Grashof number (Gm) on velocity profiles are exhibited in figure 7. The trend shows that the velocity enhances with increasing values of Gr and Gm. The figure reveals that the maximum velocity is attained near the plate and approaches to zero far away from the plate. Physically this is possible because as the Grashof number and modified Grashof number increases, the contribution from the thermal and mass buoyancy near the plate becomes significant and hence a rise in the velocity near the plate is observed. This gives rise to an increase in the induced flow. For higher values of Gr, the fluid velocity overshoots the plate velocity in the regions close to the boundary which means that maximum velocity occurs in the fluid close to the surface but not at the surface. Here Gr = 0 and Gm = 0 corresponds to the absence of free convection and mass buoyancy effect respectively.

The velocity profiles u(y, t) illustrating the effects of radiation parameter (R) are shown in Figure 8. It is revealed from this figure that the radiation parameter R has an accelerating influence on fluid flow. Physically, it is due to the fact that an increase in the radiation parameter R for fixed values of other parameters decreases the rate of radiative heat transfer to the fluid, and consequently, the fluid velocity increases.

The graphical results for the influence of Casson fluid parameter (□) on the flow field are depicted in figure 9. The effect of increasing values of Casson fluid parameter is to reduce the velocity and hence the boundary layer thickness decreases. Increasing values of Casson parameter

imply decreasing yield stress so the fluid behaves as Newtonian fluid as Casson parameter becomes large. When □ → ∞ the non-Newtonian behaviors disappear and the fluid purely behaves like a Newtonian fluid. Thus, the velocity boundary layer thickness for Casson fluid is larger than the Newtonian fluid. It happens because of plasticity of Casson fluid. As Casson parameter decreases, the plasticity of the fluid increases which produces an increment in velocity boundary layer thickness.

Figure 10 displays the effects of Schmidt number Sc on the velocity field. It is inferred that the velocity decreases with increasing Schmidt number. An increasing Schmidt number implies that viscous forces dominate over the diffusion effects. Schmidt number in free convection flow regimes represents the relative effectiveness of momentum and mass transport by diffusion in the velocity (momentum) and concentration (species) boundary layers. Smaller Sc values correspond to lower molecular weight species diffusing in air (e.g. Hydrogen (Sc = 0.16), Helium (Sc = 0.3), water vapour (Sc = 0. 6), oxygen (Sc = 0.66)) and higher values to denser hydrocarbons diffusing in air. Effectively therefore an increase in Sc will counteract momentum diffusion since viscosity effects will increase and molecular diffusivity will be reduced. The flow will therefore be decelerated with a rise in Sc as testified by figure 10. It is also important to note that for Sc ~ 1, the velocity and concentration boundary layers will have the same thickness. For Sc < 1 species diffusion rate greatly exceeds the momentum diffusion rate and vice versa for Sc > 1.

The effect of temporal variable t and Prandtl number (Pr) on the flow field are presented in figure 11 and it is revealed that as the time progresses the thickness of momentum boundary layer increases while reverse happens for increasing values of Prandtl number. It is evident from the figure that the fluid velocity overshoots the plate velocity in the regions close to the boundary. This overshooting is more pronounced for low Prandtl number fluids than for higher Prandtl number fluids. Also the thickness of momentum boundary layer is more for fluid with low Prandtl number. The reason underlying this behavior arises from the fact that the fluids with high Prandtl number have high viscosity, which makes the fluid thick and hence the fluid moves slowly.

Figure 12 displays the effect of Newtonian heating parameter (γ) on the dimensionless velocity. It is observed that as the conjugate parameter for Newtonian heating increases the density of the fluid decreases, and the momentum boundary layer thickness increases and as a result the velocity increases within the boundary layer. For higher values of γ the fluid velocity overshoots the plate velocity in the regions close to the boundary.

From figure 13 it is noticed that chemical reaction parameter (□) decreases the velocity of the fluid. The decrease is attributed to the absorption of heat energy due to endothermic reaction (γ > 0). Further the presence of heavier diffusing species causes a decrease in velocity leading to thinning of the boundary layer thickness. The effect of exponential accelerated parameter (a_0) on the velocity profiles is presented in figure 14. It is revealed that the velocity enhances with increasing exponential accelerated parameter. The case $a_0 = 0$ corresponds to an impulsively started plate.

From figures 7-14 we observe that the velocity attains maximum values in the vicinity of the plate and then approach to zero far away from the plate which are identical with the imposed boundary conditions of velocity in equation (12). Hence both the graphical and mathematical results are found in excellent agreement.

Figure 15 displays dimensionless rate of heat transfer Nusselt number (Nu) against time t. This figure shows that increasing Prandtl number (Pr) and Newtonian heating parameter (γ) enhance the heat transfer coefficient. This may be explained by the fact that frictional forces become dominant with increasing values of Pr and yield greater heat transfer rate. Furthermore, as time advances, the value of Nu is decreasing and after some time it becomes constant. Nusselt number decreases on increasing radiation parameter (R) which implies that radiation tends to reduce rate of heat transfer at the plate. Wall temperature gradient is positive for all values of the Prandtl number. Physically it means that the heat is always transferred from the ambient fluid to the surface.

From figure 16, it is observed that the Sherwood number which determines the rate of mass transfer at the surface increases with increasing Schmidt number (Sc) and chemical reaction parameter (□), while reverse happens for increasing time values of t. Since increase in Sc means decrease in molecular diffusivity this in turn gives rise to increase in Sherwood number as Sherwood number is the ratio of convective and diffusive mass transfer coefficient. Chemical reaction parameter increases the interfacial mass transfer, so Sherwood number increases with an increase in □. It

is also noted that wall concentration gradient is positive for all values of the Schmidt number. Physically it means that the mass is always transferred from the ambient fluid to the surface.

Variations of skin friction (□) verses time are plotted in figures 17 - 19 for various parameters of interest. Figure 17 elucidates that with increasing Prandtl number (Pr) and modified Grashof number (Gm) frictional shear stress decreases while reverse happens for increasing Grashof number (Gr). The skin friction falls with an increase in Pr because an increase in the Prandtl number is due to increase in the viscosity of the fluid, which makes the fluid thick and hence a decrease in the velocity of the fluid therefore skin friction decreases with increasing Pr. Figure 18 illustrates the influence of radiation parameter (R), Schmidt number (Sc) and exponentially accelerated parameter (a_0) on skin friction profiles. It is noticed that skin friction increases with increasing values of Sc as it is higher for Sc = 0.66 in comparison to Sc = 0.22. Physically, it is correct since an increase in Sc serves to increase the momentum boundary layer thickness. Similar effects are shown by increasing radiation parameter and exponentially accelerated parameter. The effect of Casson parameter (□) and Newtonian heating parameter (□) on skin friction profiles (□) are presented in figure 19. By increasing the values of Casson parameter the values of the skin friction coefficient decreases but it increases upon increasing Newtonian heating parameter (□)

The present analytical (Laplace transform) solutions provide other researchers with solid benchmarks for numerical comparisons. The authors have used this method in other articles where they have bench marked approximate methods such as numerical, asymptotic or experimental methods against analytical (Laplace transform) solutions. The solution of the problem introduced new inverse Laplace transforms of exponential forms which are not available in the literature. These formulas are derived and are provided in the solution. Further, all these graphical results discussed above are in good agreement with the imposed boundary conditions given by (12). Hence, this ensures the accuracy of our results.

Nomenclature

C_p Specific heat at constant pressure, C^* Species concentration in the fluid, C_w^* Species concentration near the plate, C_∞^* Species concentration in the fluid far away from the plate, C(y,t) Dimensionless concentration, D Mass diffusivity, g Magnitude of the acceleration due to gravity, h Heat transfer coefficient, k Thermal conductivity of the fluid, k^* Mean absorption coefficient, r Thermal Grashof number, Gm Modified Grashof number, Pr Prandtl number, q_r Radiative heat flux in the y^* direction, R Radiation parameter, Sc Schmidt number, T^* Temperature of the fluid, T_∞^* Ambient temperature, t^* Time, t Non-dimensional time, u^* Dimensional velocity along x^*-direction, u(y,t) Dimensionless velocity, y^* Cartesian coordinate normal to the plate, y Dimensionless coordinate axis normal to the plate

GREEK SYMBOLS

α Chemical reaction parmeter , □ Casson parameter, β_t Volumetric Coefficient of thermal expansion, β_c Volumetric Coefficient of mass expansion, □ Newtonian heating parameter, ρ Density of the fluid, θ Dimensionless temperature, μ Coefficient of viscosity, ν Kinematic viscosity,

σ Stefan-Boltzmann constant, τ^* Skin-friction, τ Dimensionless skin-friction

REFERENCES:

[1] Mukhopadhyay S, Vajravelu K. "Effects of transpiration and internal heat generation/absorption on the unsteady flow of a Maxwell fluid at a stretching surface", ASME Journal of Applied Mechanics, 79, 044508, 2012, http://dx.doi.org/10.1115/1.4006260.

[2] Aksoy Y, Pakdemirli M, Khalique CM. " Boundary layer equations and stretching sheet solutions for the modified second grade fluid", International Journal of Engineering Sciences, 45, 829–41, 2007.

[3] Hayat T, Awais M, Sajid M. " Mass transfer effects on the unsteady flow of UCM fluid over a stretching sheet", Int J Mod Phys B, 25, 2863–78, 2011.

[4] Casson N. " A flow equation for the pigment oil suspensions of the printing ink type", Rheology of Disperse Systems, Pergamon, NewYork, USA, pp. 84–102, 1959.

[5] Fung YC. "Biodynamics circulation", Springer-Verlag, New York Inc., 1984.

[6] Dash RK, Mehta KN, Jayaraman G. "Casson fluid flow in a pipe filled with a homogeneous porous medium", International Journal of Engineering Sciences, 34(10), 1145–56, 1996.

[7] Mustafa M., Hayat t., Pop I., and Aziz A. "Unsteady boundary layer flow of a Casson fluid due to an impulsively started moving flat plate", Heat Transfer—Asian Research, 40(6), 563–576, 2011.

[8] Mukhopadhyay S. "Casson fluid flow and heat transfer over a nonlinearly stretching surface", Chinese Physics B, 22(7), Article ID 074701, 2013.

[9] Mukhopadhyay S. " Effects of thermal radiation on Casson fluid flow and heat transfer over an unsteady stretching surface subjected to suction/blowing", Chinese Physics. B, 22(11), Article ID 114702, 2013.

[10] Mukhopadhyay S., De P. R., Bhattacharyya K., Layek G.C. "Casson fluid flow over an unsteady stretching surface", Ain Shams Engineering Journal, 4, 933–938, 2013.

[11] Bhattacharya K., Hayat T., Alsaedi A. " Exact solution for boundary layer flow of casson fluid over a permeable stretching/Shrinking sheet", ZAMM-Journal of Applied Mathematics & Mechanics, 94(6), 522-528, 2014.

[12] Bhattacharya K "Boundary layer stagnation-point flow of casson fluid and heat transfer towards a shrinking/stretching sheet", Frontiers in Heat and Mass Transfer, 4(2), Article ID 023003, 2013

[13] Hossain, M.A., Alim, M.A. and Rees, D.A.S. "The effect of radiation on free convection from a porous vertical plate", International Journal of Heat and Mass Transfer, 42, 181-191, 1999.

[14] Raptis, A. and Perdikis, C., "Radiation and free convection flow past a moving plate", Applied Mechanics and Engineering, 4(4), 817-821, 1999.

[15] Soundalgekar, V.M., Das, U.N. and Deka, R.K. "Radiation effect on flow past an impulsively started vertical plate - An exact solution", Journal of Theoretical and Applied Fluid Mechanics, 1, 111-115, 1996.

[16] M. A. Hossain and H. S. Takhar , "Radiation Effects on mixed convection along a vertical plate with uniform surface temperature", Heat and Mass Transfer, 31(4), 243-24, 1996.

[17] Makinde, O.D. "Free convection flow with thermal radiation and mass transfer past a moving porous plate", International Communication in Heat and Mass Transfer, 32(10), 1411-1419, 2005.

[18] Muthucumaraswamy, R. and Chandrakala, P. "Effects of thermal radiation on moving vertical plate in the presence of an optically thin gray gas", Forschung im Ingenieurwese– Engineering Research, 69(4), 205-208, 2005.

[19] Muthucumaraswamy, R. "Exact solution of thermal radiation on vertical oscillating plate with variable temperature and mass flux", Theoreical and Appllied Mechanics, 37(1), 1-15, 2010.

[20] Deka, R. K. and Das, S. K. "Radiation effects on free convection flow near a vertical plate with ramped wall temperature" Engineering, 3, 1197-1206, 2011.

[21] Jana, R. N. and Ghosh, S.K. "Radiative heat transfer of an optically thick gay gas in the presence of indirect natural convection" World Journal of Mechanics, 1, 64-69, 2011.

[22] Pramanik S. "Casson fluid flow and heat transfer past an exponentially porous stretching surface in presence of thermal radiation", Ain Shams Engineering Journal, 5(1), 205–212, 2014.

[23] Shehzad S. A., Hayat T., Qasim M., Asghar S. "Effects of mass transfer on MHD flow of Casson fluid with chemical reaction and suction", Brazilian Journal of Chemical Engineering, 30(1), 187 – 195, 2013.

[24] Das U.N., Deka R., and Soundalgekar V.M. "Effect of Mass transfer on flow past an impulsively started infinite vertical plate with constant heat flux and chemical reaction", Forschung im ingenieurwesen/Engineering Research, 60(10), 284-287, 1994

[25] Jain Preeti "Combined influence of Hall current and Soret effect on chemically reacting magneto-micropolar fluid flow from radiate rotating vertical surface with variable suction in slip-flow regime", ISRN Mathematical Analysis, Article ID 102413, 23 pages, 2014 http://dx.doi.org/10.1155/2014/102413

[26] Makanda G., Shaw S., and Sibanda P. "Diffusion of Chemically Reactive Species in Casson Fluid Flow over an Unsteady Stretching Surface in Porous Medium in the Presence of a Magnetic Field", Mathematical Problems in Engineering, Hindawi publishing corporation, Article ID 724596.

[27] Merkin, J.H. "Natural convection boundary-layer flow on a vertical surface with Newtonian heating". Int. J. Heat Fluid Flow, 15, 392-398, 1994.

[28] Lesnic, D.,Ingham, D.B. and Pop, I. "Free convection boundary layer flow along a vertical surface in a porous medium with Newtonian heating" International Journal of Heat Mass Transfer,42, 2621-2627, 1999.

[29] Ibid "Free convection from a horizontal surface in porous medium with Newtonian heating" J. Porous Media, 3, 227-235, 2000.

[30] Lesnic, D., Ingham, D.B., Pop, I. and Storr, C. "Free convection boundary layer flow above a nearly horizontal surface in porous medium with Newtonian heating" Heat and Mass Transfer, 40 (4), 665-672, 2003.

[31] Chaudhary, R.C., Jain, Preeti "Unsteady free convection boundary-layer flow past an impulsively started vertical surface with Newtonian heating", Romanian Journal of Physics, 51, 911-925, 2006.

[32] Chaudhary, R.C., Jain, Preeti "An exact solution to the unsteady free convection boundary-layer flow past an impulsively started vertical surface with Newtonian Heating", Journal of Engineering Physics and Thermophysics, 80, 954-960, 2007.

[33] Jain Preeti and Chaudhary R. C. "Closed form solution of heat and mass transfer past an inclined oscillating surface with Newtonian heating under the effect of thermal radiation and mass diffusion", Advances in Applied Science Research, 4(6), 285-306, 2013.

[34] Narahari, M., Nayan, M.Y. "Free convection flow past an impulsively started infinite vertical plate with Newtonian Heating in the presence of thermal radiation and mass diffusion", Turkish Journal of Engineering and Environmental Sciences, 35,187-198, 2011.

[35] Raju, K.V.S., Reddy, T.S., Raju, M.C. and Venkataramana, "Free convective heat and mass transfer transient flow past an exponentially accelerated vertical plate with Newtonian heating in the presence of radiation", International Journal of Mathematics and Computer Application Research, 3(2), 215-226, 2013.

[36] Narahari, M. and Ishak, A. **"**Radiation effects on free convection flow near a moving vertical plate with Newtonian Heating", Journal of Applied Sciences, 11(7), 1096-1104, 2011.

[37] Hussanan A., Khan H., Sharidan S. "An exact analysis of heat and mass transfer past a vertical plate with Newtonian heating", Journal of Applied Mathematics, 2013, Article ID 434571,9 pages, 2013.

[38] Mebine, P., Adigio, E.M. "Unsteady free convection flow with thermal radiation past a vertical porous plate with Newtonian heating", Turkish Journal of Physics, 33, 109-119, 2009.

[39] R. Siegel and J. R. Howell "Thermal Radiation Heat Transfer", Taylor & Francis, New York, USA, 4th edition, 2002.

[40] Salleh, M. Z., Nazar, R. and I. Pop "Boundary layer flow and heat transfer over a stretching sheet with Newtonian heating", Journal of the Taiwan Institute of Chemical Engineers, 41(6), 651–655, 2010.

[41] Kasim, A. R. M., Mohammad, N. F., Aurangzaib, and Sharidan, S. "Natural convection boundary layer flow of a visco-elastic fluid on solid sphere with Newtonian heating", World Academy of Science, Engineering and Technology, 64, 628–633, 2012.

[42] R. Siegel and J. R. Howell "Thermal Radiation Heat Transfer", Taylor & Francis, New York, USA, 4th edition, 2002.

Figure 1:Temperature profiles for different values of Radiation parameter R when t = 0.2, Pr = 0.71 and $\gamma = 1$.

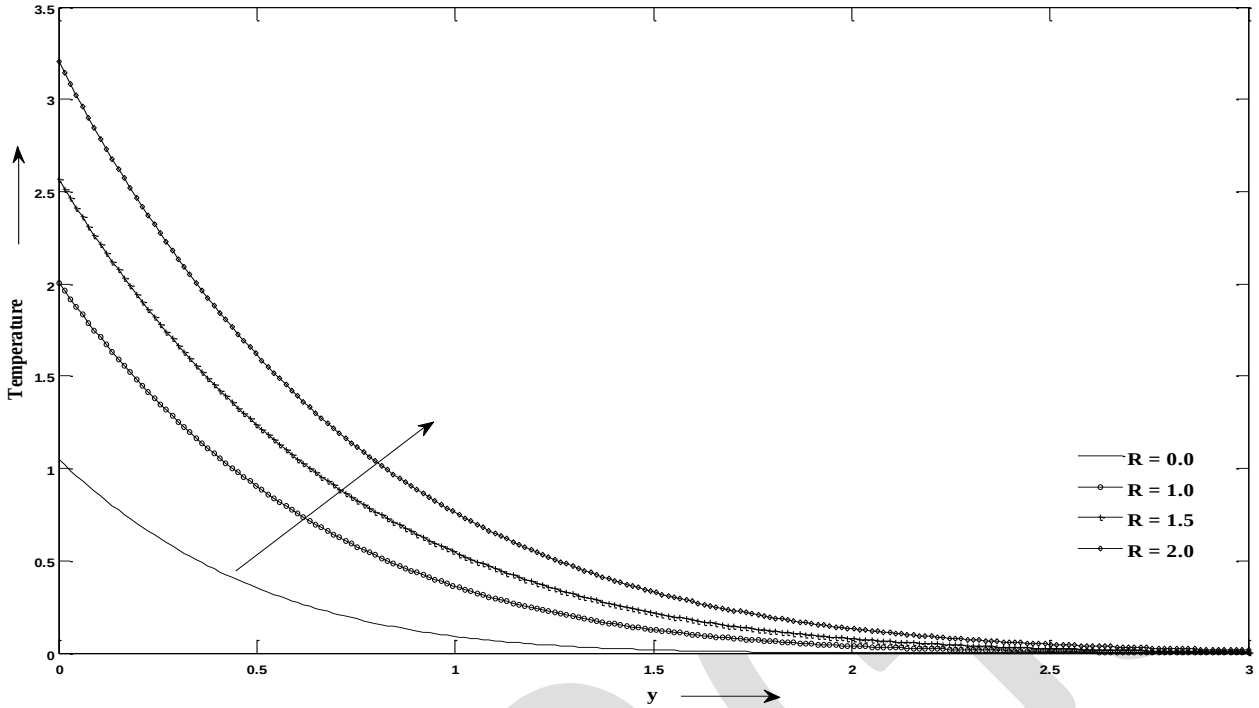

Figure 2: Temperature profiles for different values of time t when R = 1, Pr = 0.71 and $\gamma = 1.0$.

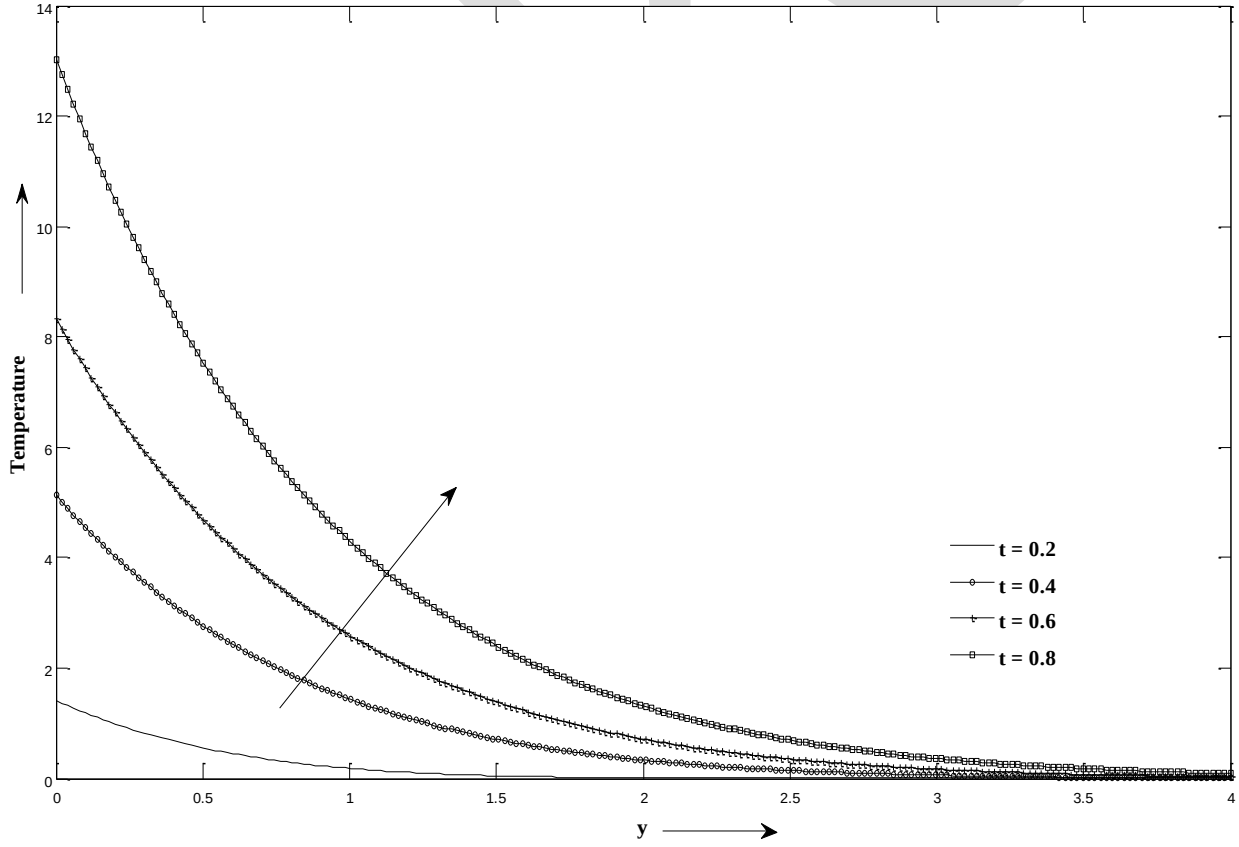

Figure 3 :Temperature profiles for different values of Prandtl number Pr when R = 2, t =0.4 and γ = 0.1

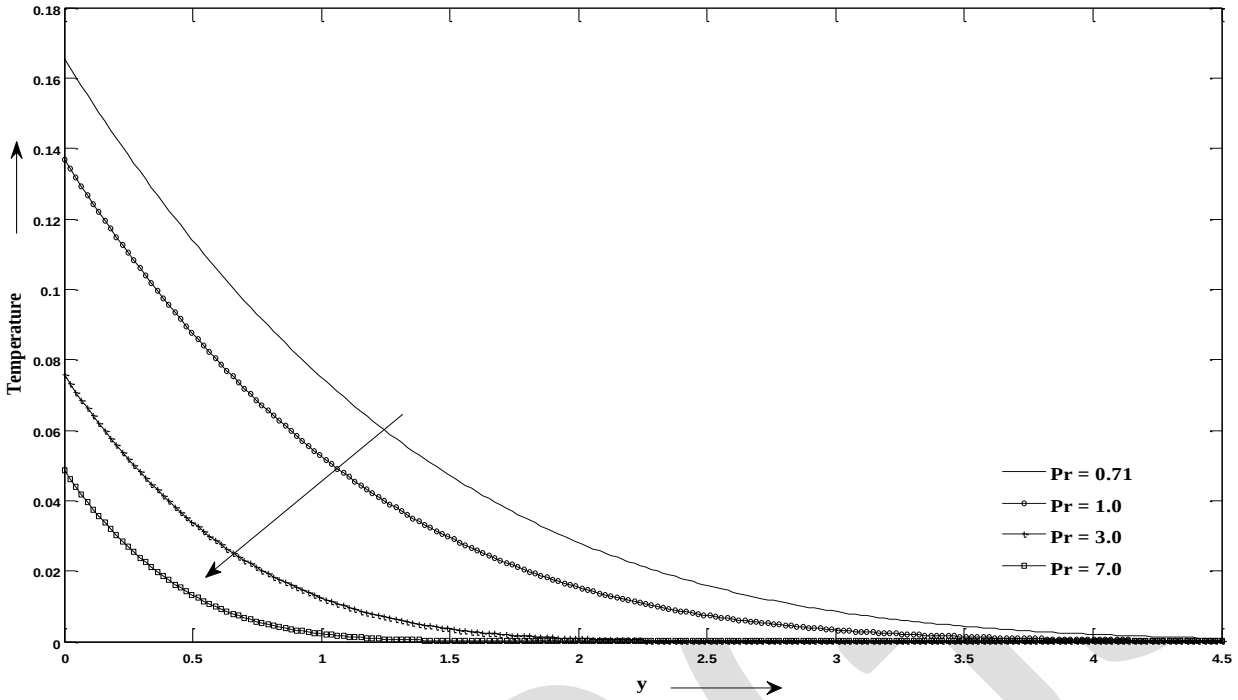

Figure 4 : Temperature profiles for different values of Newtonian Heating parameter when Pr = 0.71, R = 2 and t =0.2.

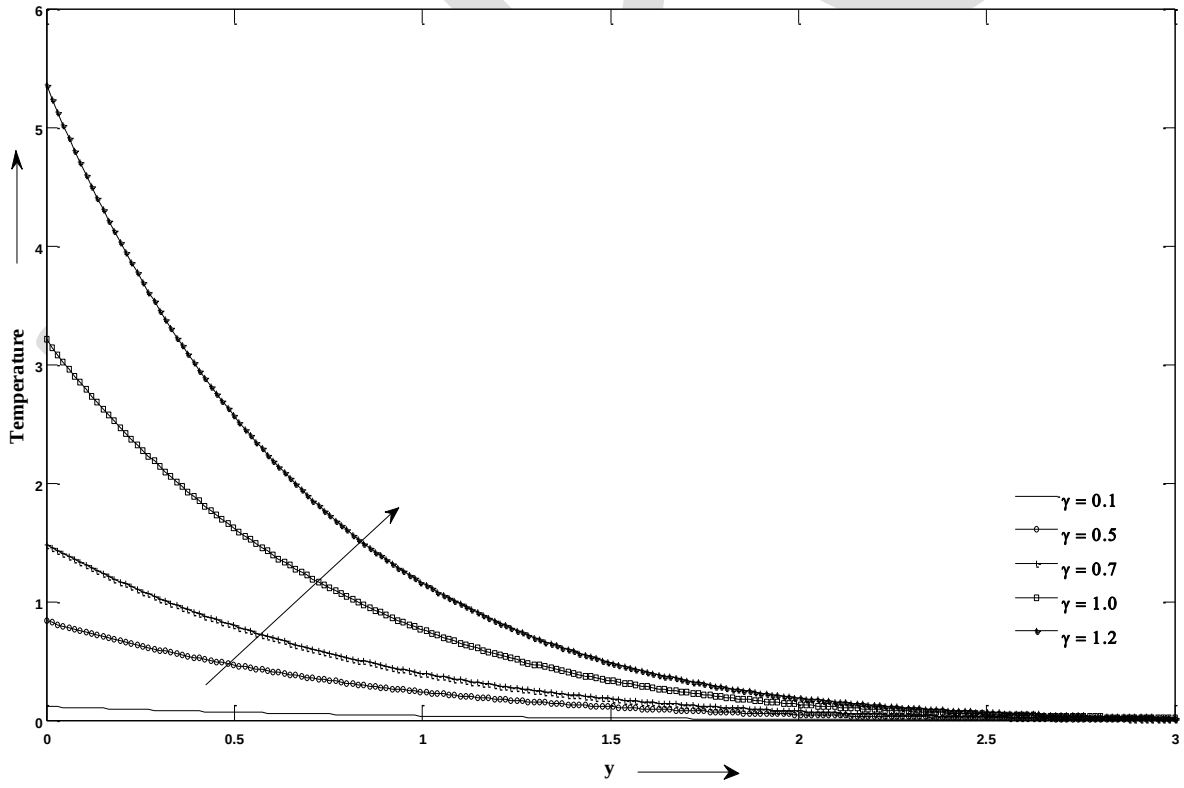

Figure 5: Concentration profiles for different values of Chemical reaction parameter when Sc = 0.66 and t = 0.4.

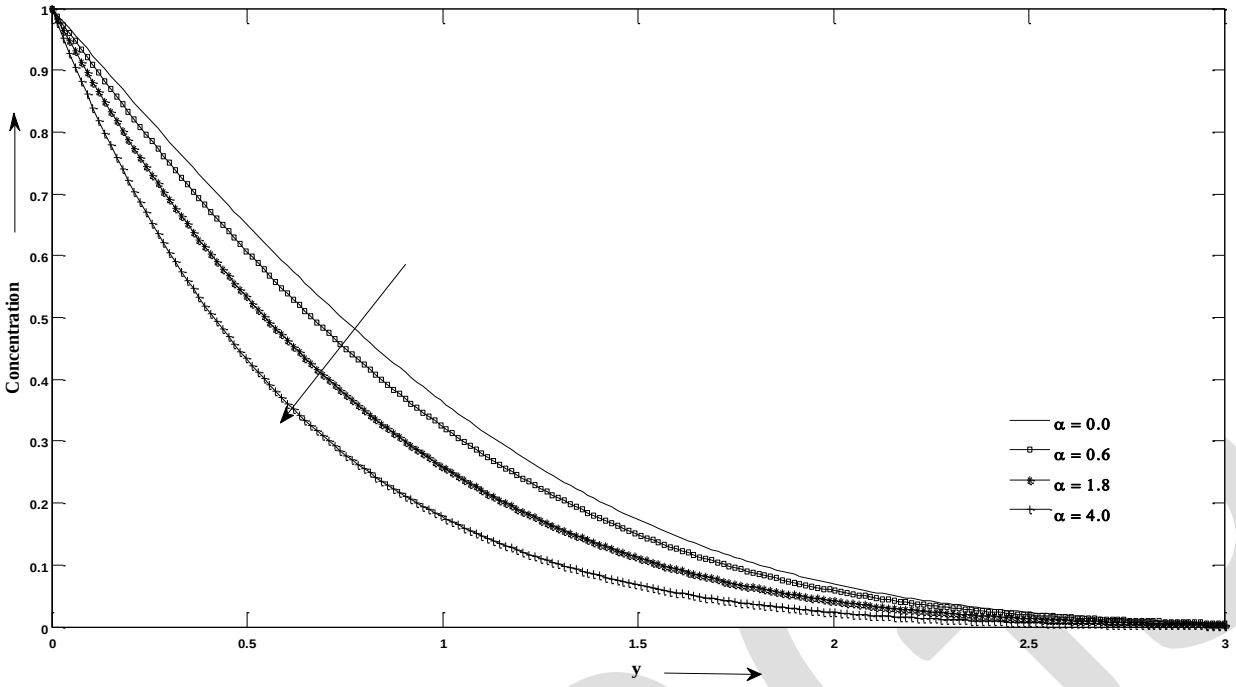

Figure 6 : Concentration profiles for different values of Schimdt number (Sc) and time (t) when α = 0.6

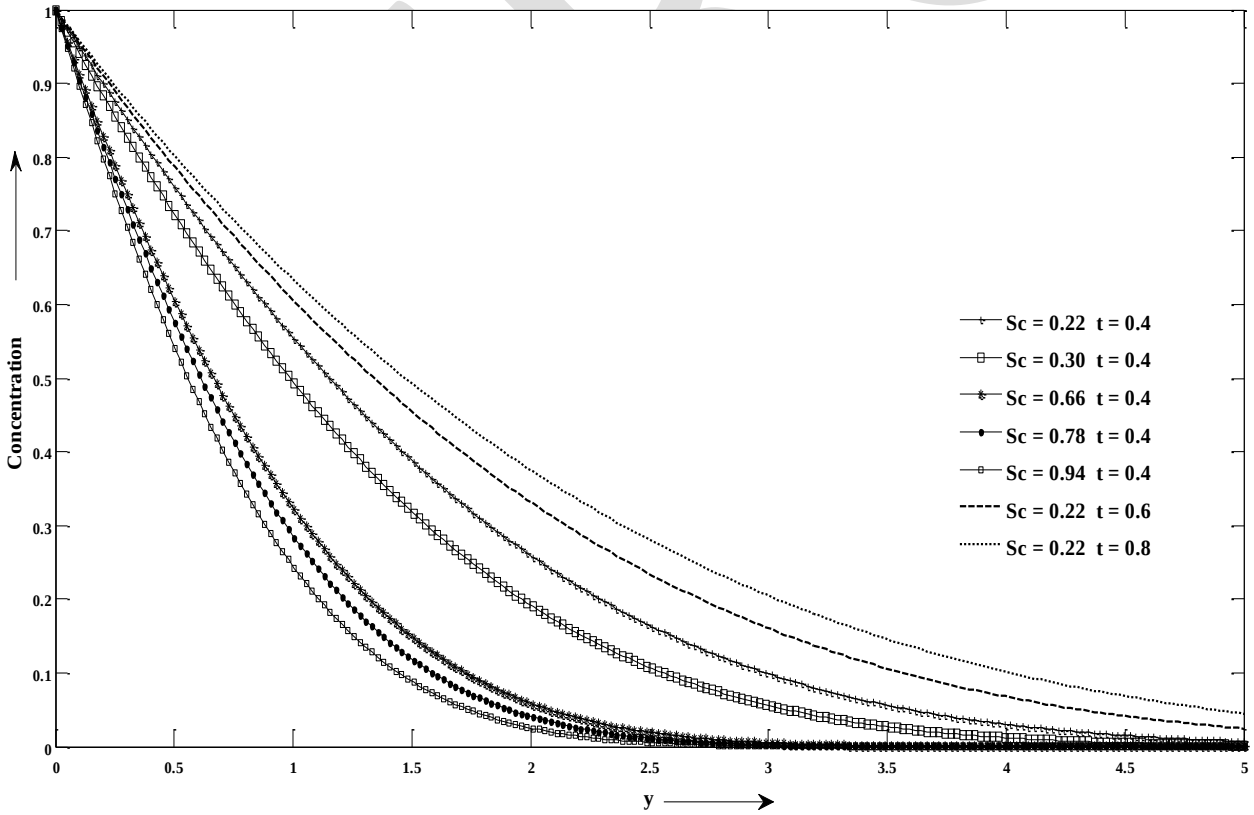

Figure 7 : Velocity profiles for different values of Grashoff number (Gr) and Modified Grashoff number (Gm) when t = 0.4, Pr = 0.71, Sc = 0.66, R = 2, ao = 1.5, α = 0.6, β = 2, γ = 1.

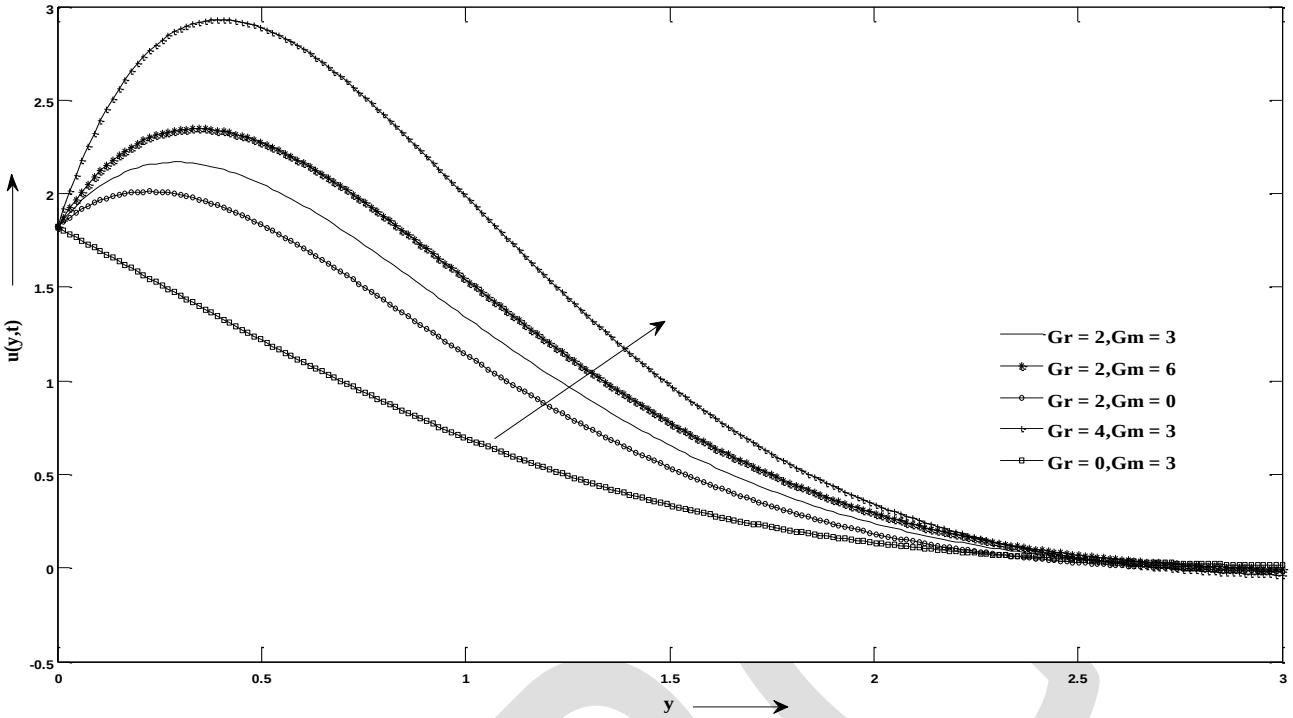

Figure 8: Velocity profiles for different values of Radiation parameter (R) when t = 0.4, Pr = 0.71, Sc = 0.66, Gr = 2, Gm = 3, ao = 1.5, α = 0.6, β = 2, γ = 1.

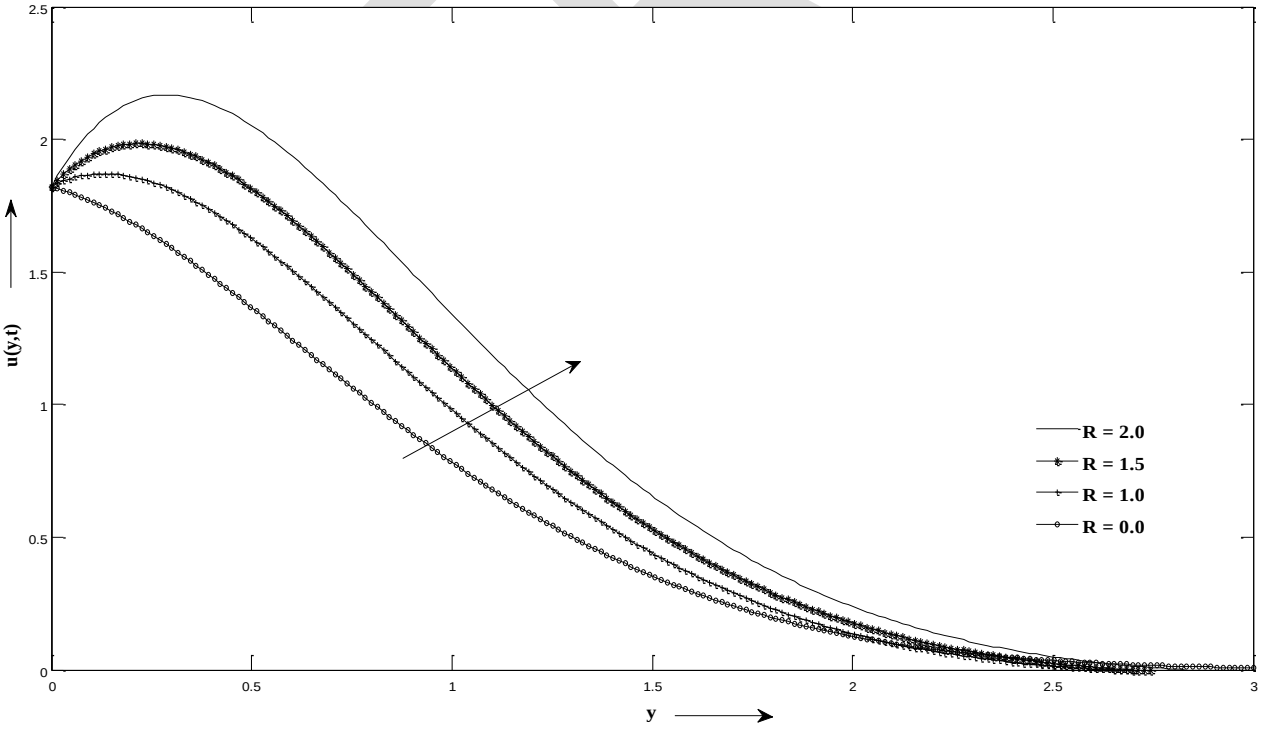

Figure 9: Velocity profiles for different values of Casson parameter when t = 0.1, Pr = 0.71, Sc = 0.66, Gr = 2, Gm = 3, ao = 1.5, R = 2, $\alpha = 0.6, \gamma = 1$.

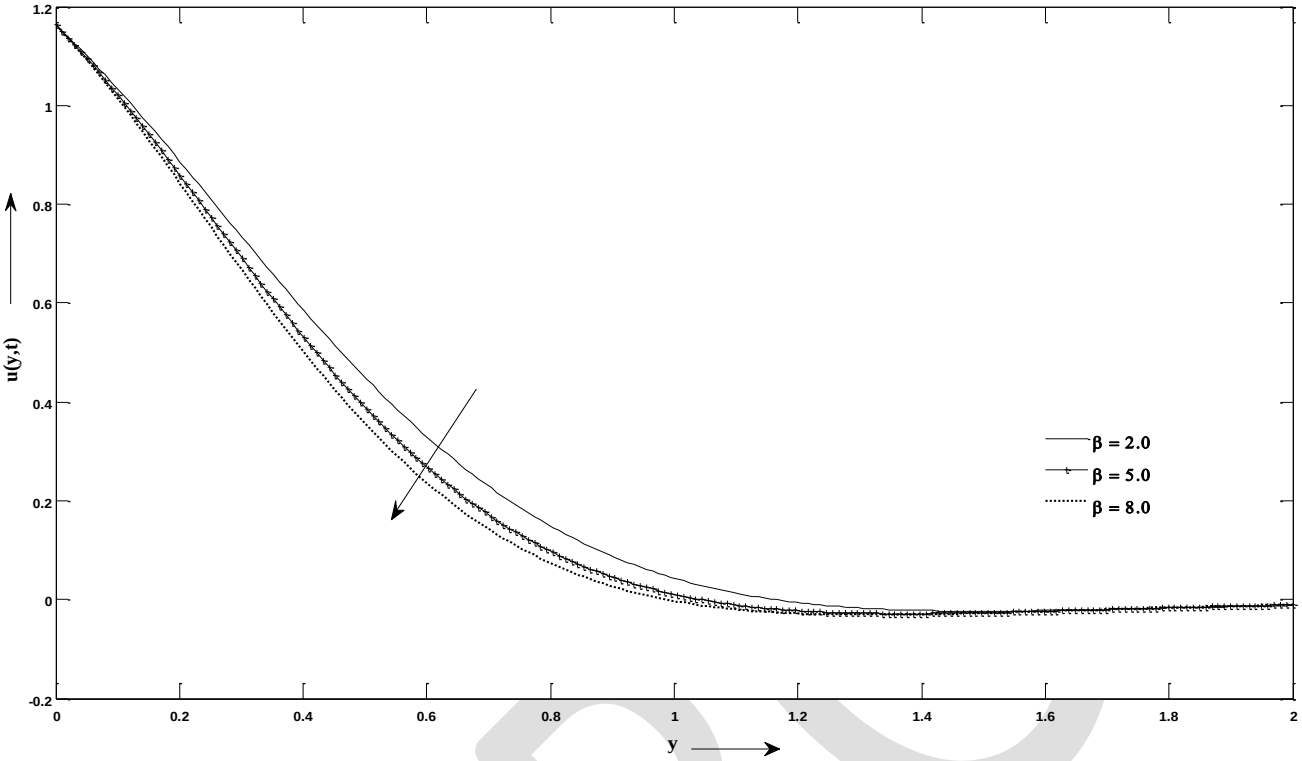

Figure 10: Velocity profiles for different values of Schimdt number (Sc) when t = 0.4, Pr = 0.71, Gr = 2, Gm = 3, Sc = 0.66, R = 2, ao = 0.5, $\alpha = 1.6, \beta = 2, \gamma = 1$.

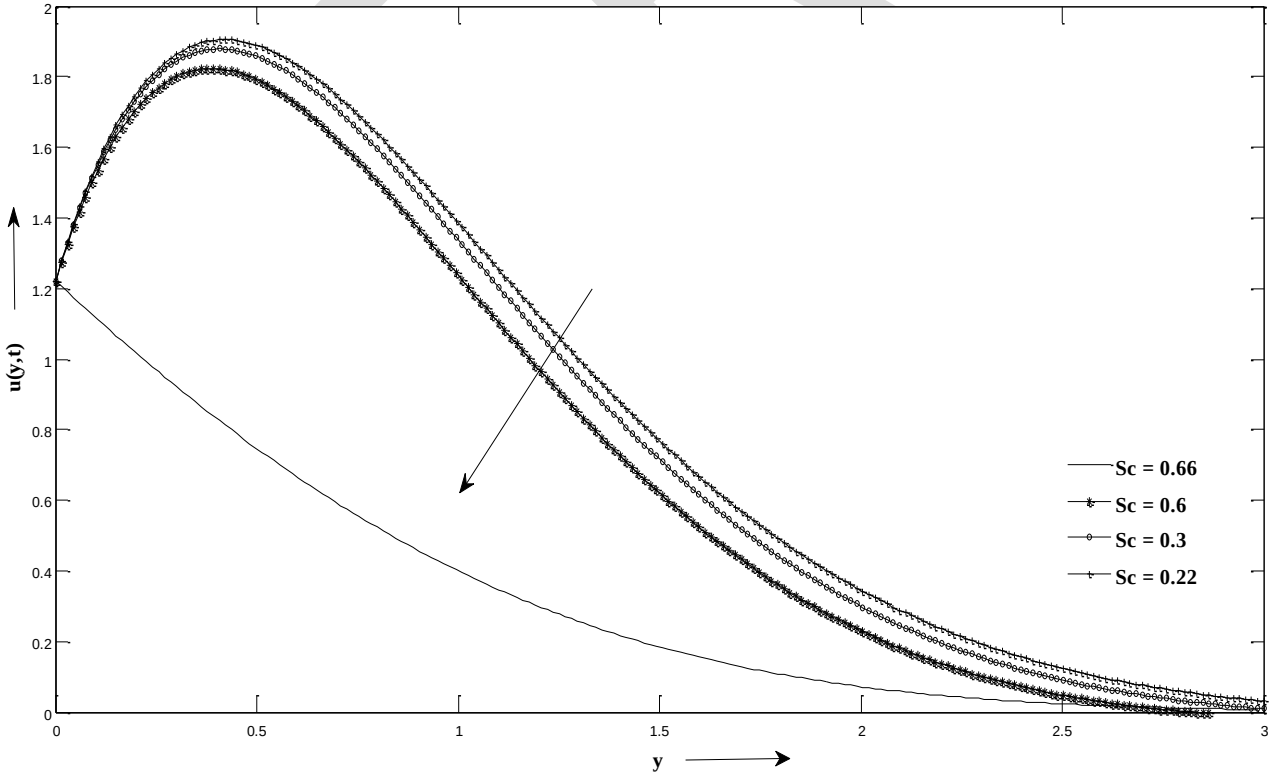

Figure 11 : Velocity profiles for different values of Prandtl number (Pr) and time (t) when Gr = 2, Gm = 5, Sc = 0.66, R = 2, ao = 0.5, α = 0.6, β = 2, γ = 1.

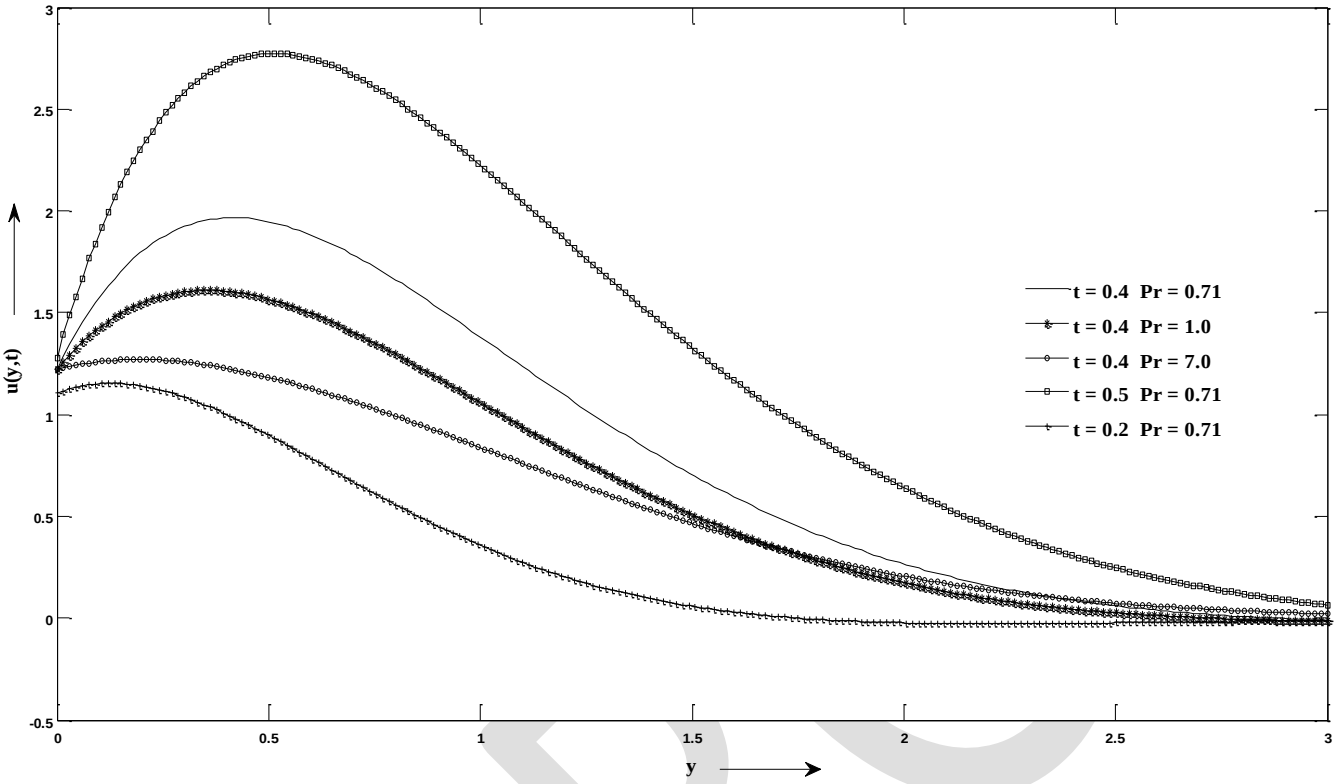

Figure 12: Velocity profiles for different values of Newtonian Heating parameter when t = 0.4, Pr = 0.71, Gr = 2,Gm = 3, Sc = 0.66, ao = 1.5, R = 2, α = 0.6, β = 2.

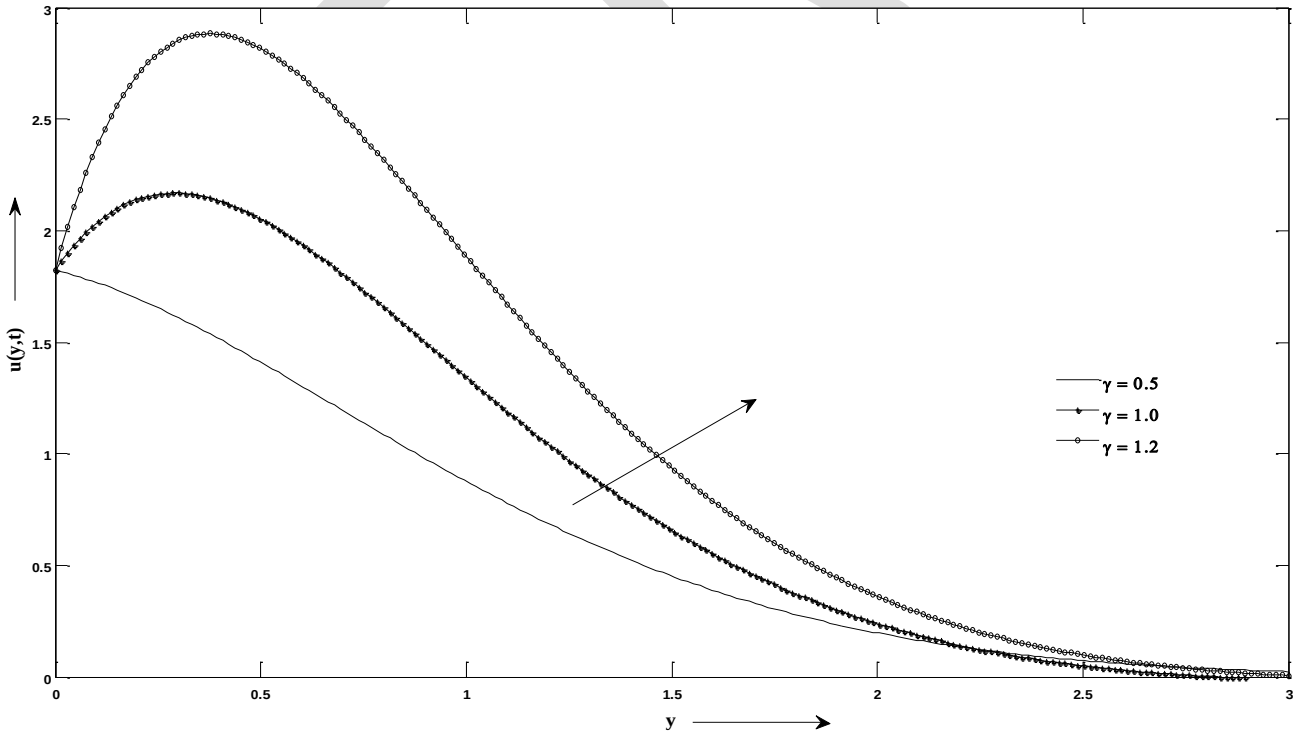

Figure 13: Velocity profiles for different values of chemical reaction parameter when t = 0.4, Pr = 0.71, R = 2, ao = 1.5, Gr = 5, Gm = 5, Sc = 0.66, β = 4, γ = 1.

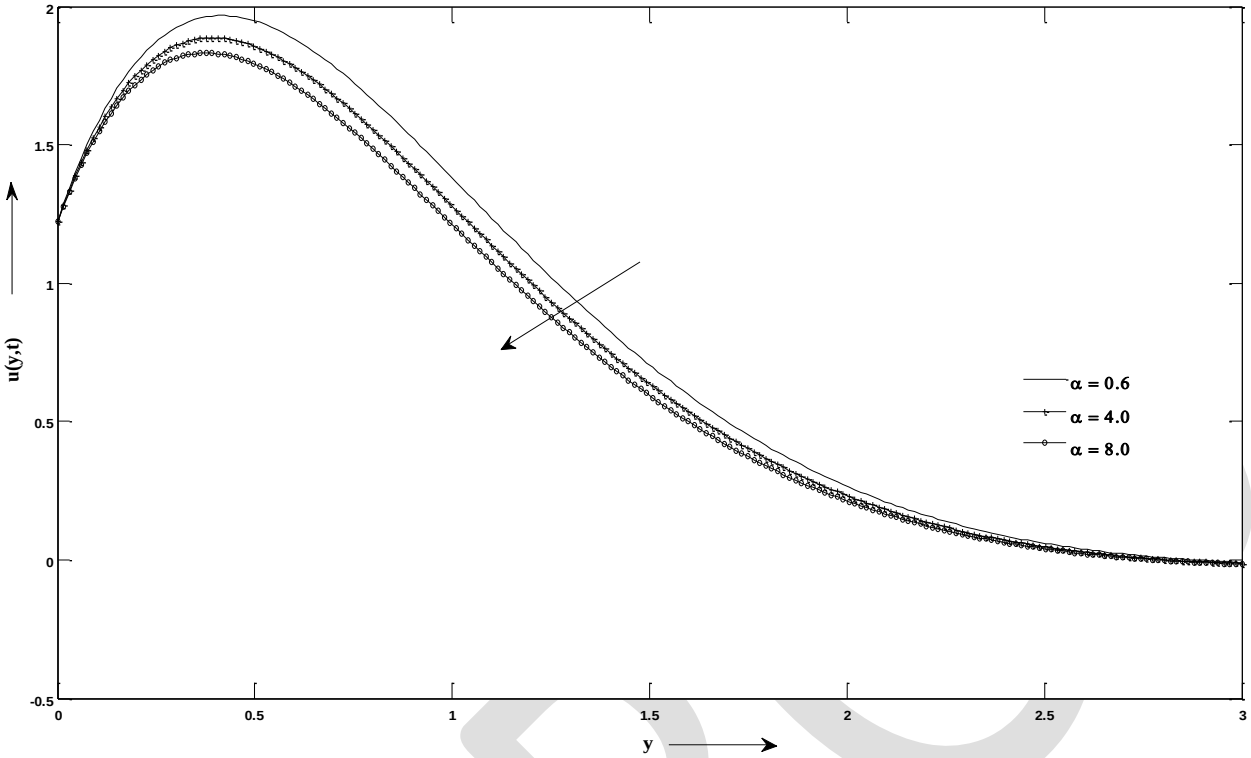

Figure 14: Velocity profiles for different values of exponential accelerated parameter (ao) when t = 0.4, Pr = 0.71, Sc = 0.66, Gr = 2, Gm = 3, R = 2, α = 0.6, β = 2, γ = 1.

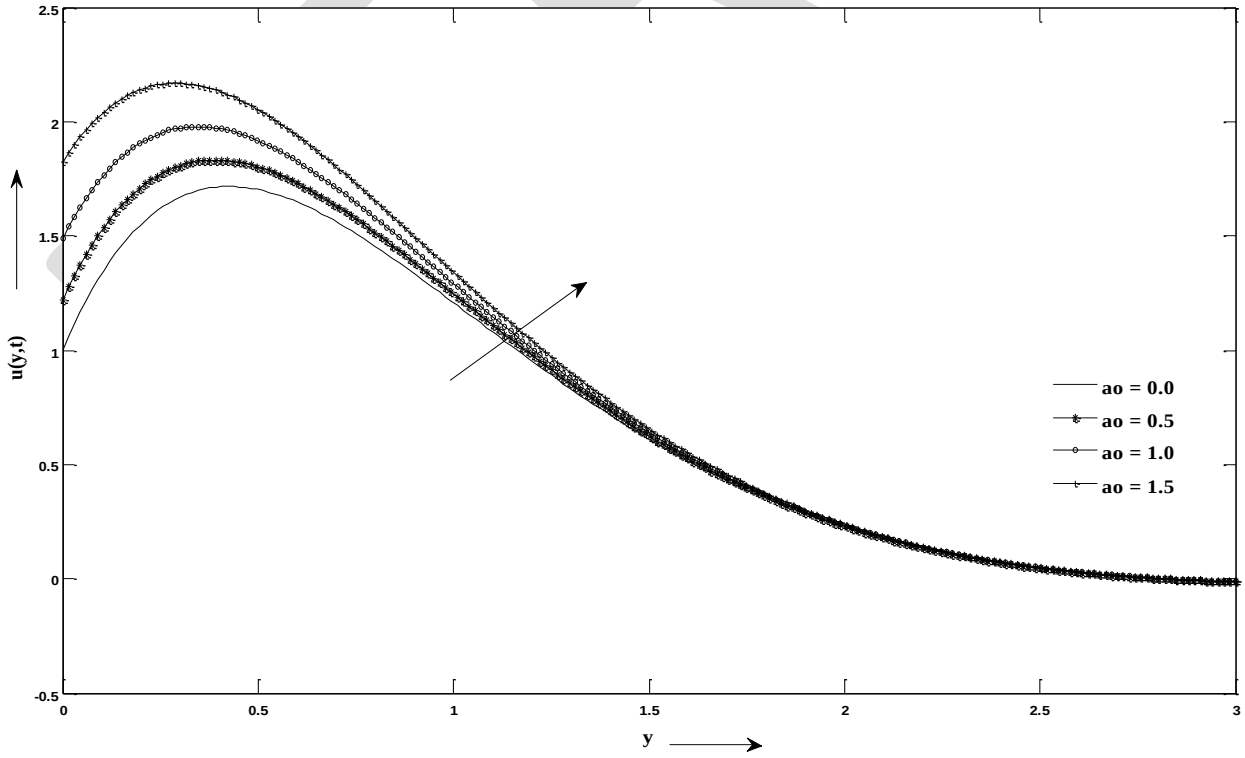

Figure 15: Variation of Nusselt number for different values of Prandtl number (Pr), radiation parameter (R), Newtonian heating Parameter (γ).

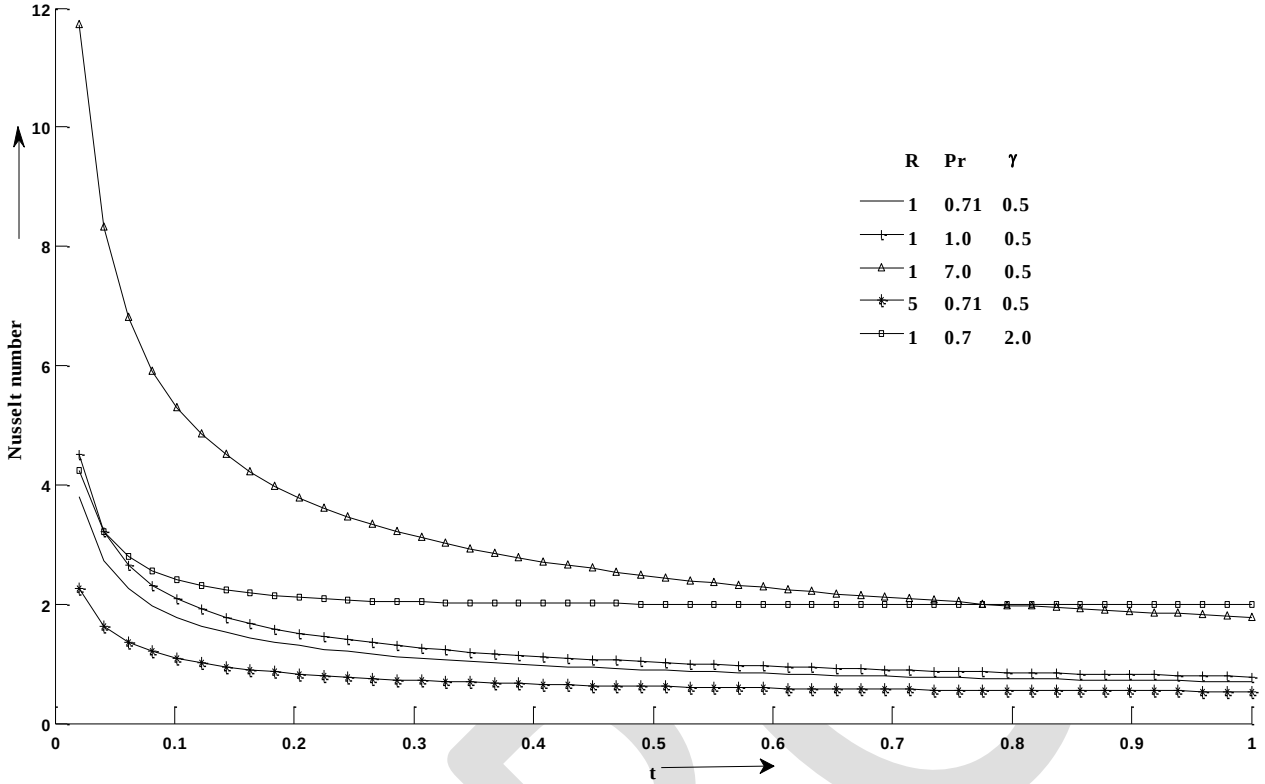

Figure 16: Sherwood number for different values of Schmidt number and Chemical Reaction parameter.

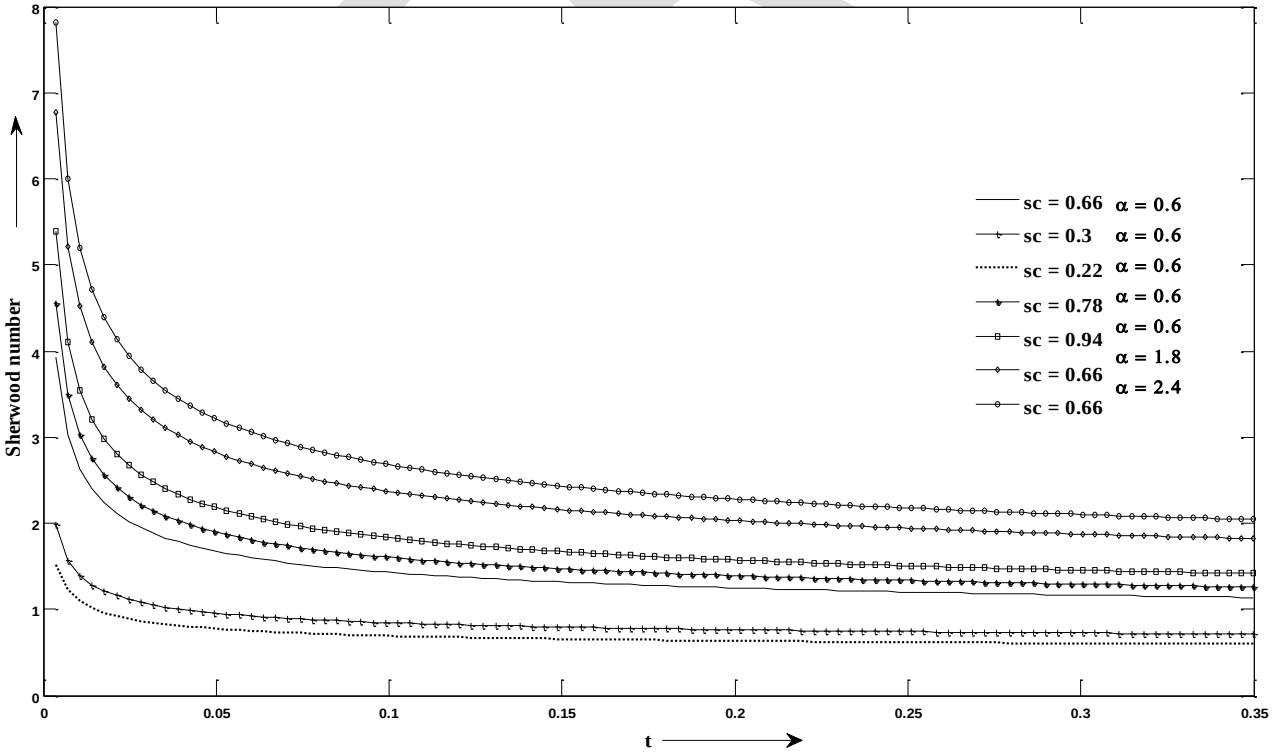

Figure 17 : Skin friction profiles when Sc = 0.66, R = 2, ao = 0.5, α = 0.6, β = 2, γ = 1.

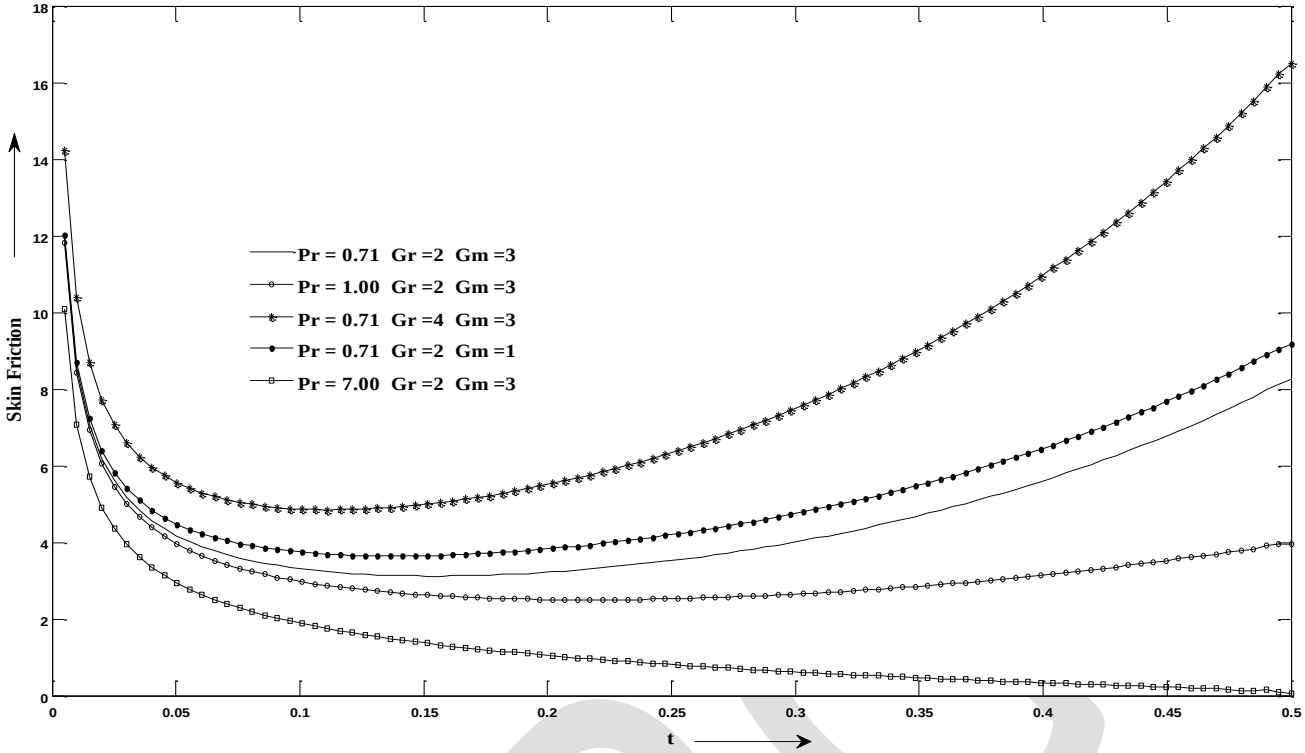

Figure 18 : Skin friction profiles when Pr = 0.71, Gr = 2, Gm = 3, α = 0.6, β = 2, γ = 1.

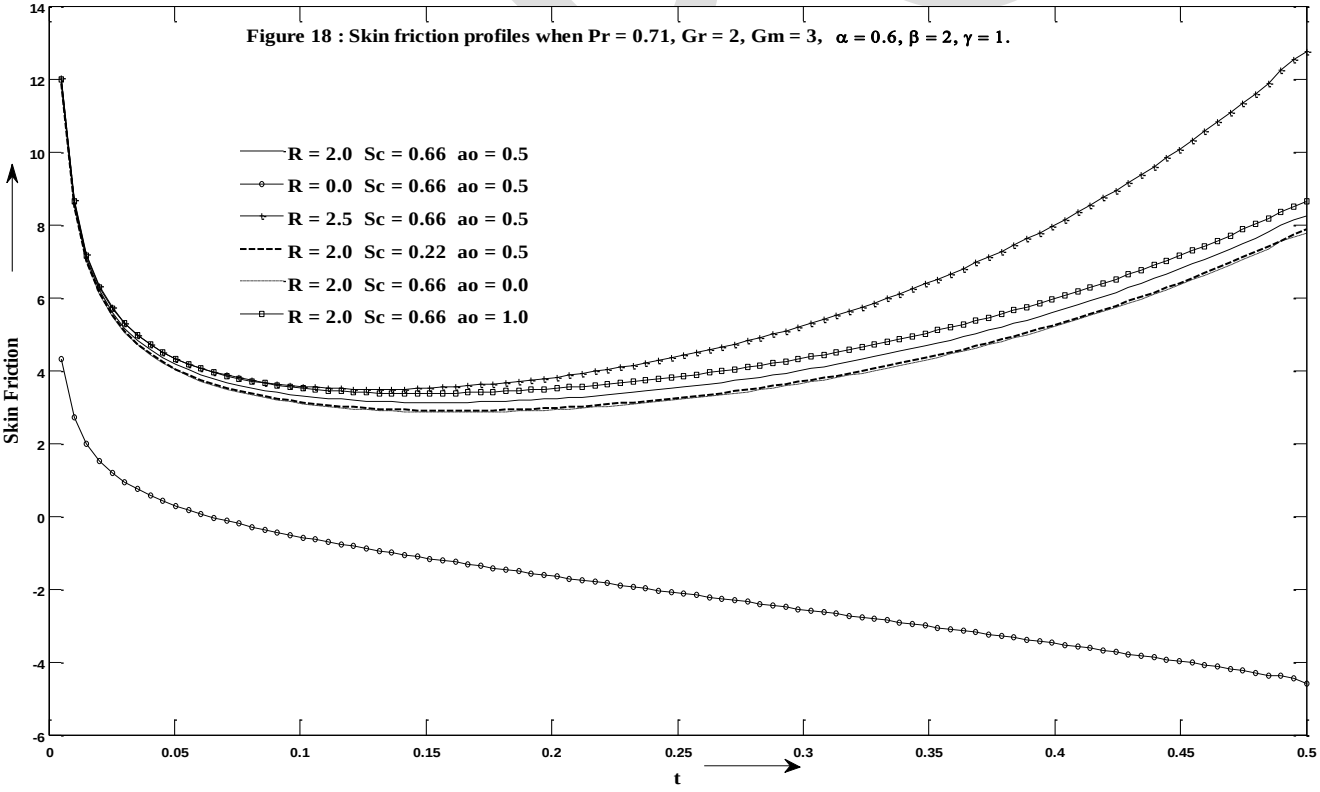

Figure 19 : Skin friction profiles when Pr = 0.71, Gr = 2, Gm = 3, Sc = 0.66, R = 2, ao = 0.5, α = 0.6.

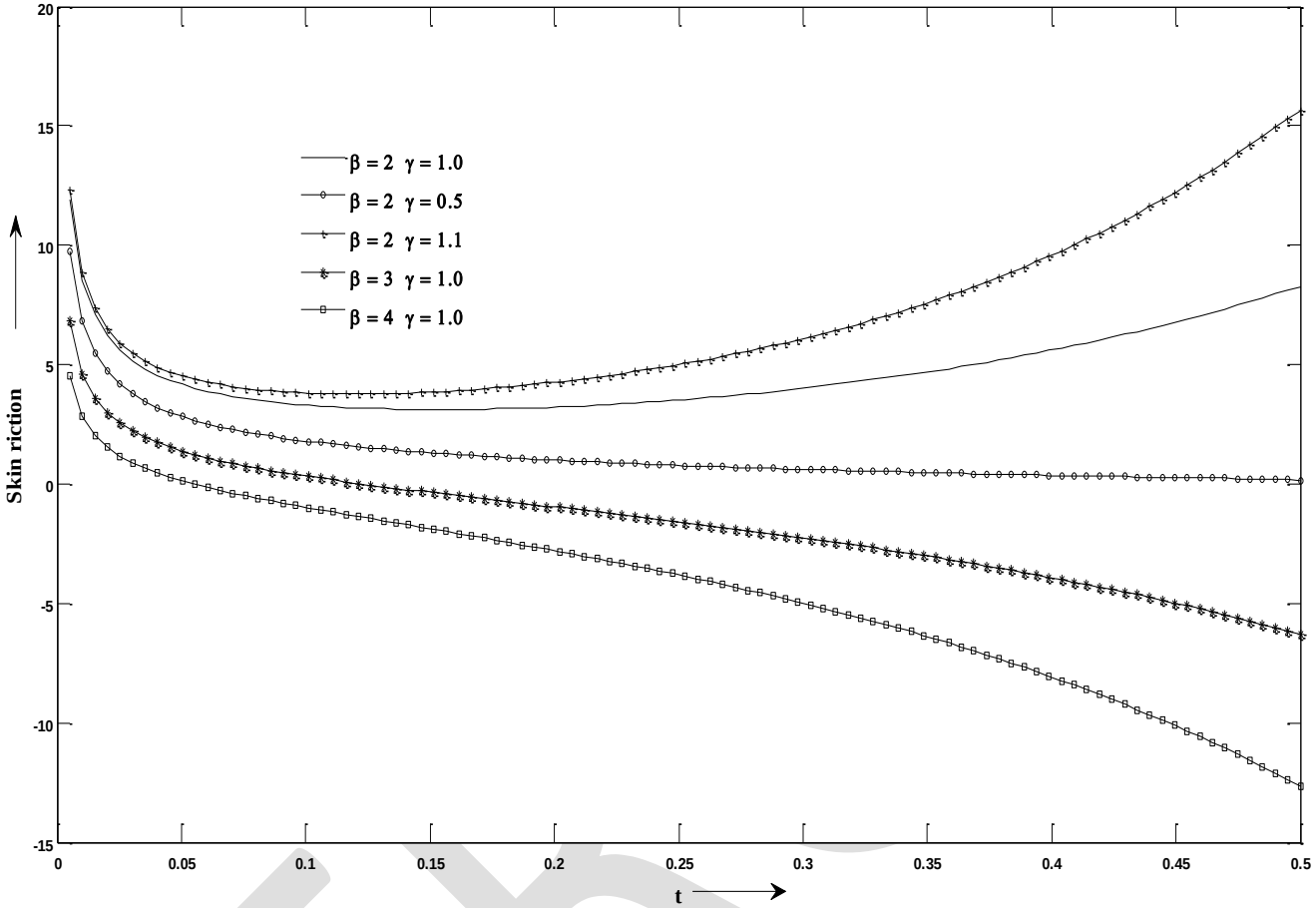

International Journal of Engineering Research and General Science Volume 3, Issue 6, November-December, 2015
ISSN 2091-2730

ANALYSIS OF A DEVELOPED BUILDING PENETRATION PATH LOSS MODEL FOR GSM WIRELESS ACCESS

Elechi, P.
Department of Electrical Engineering, Rivers State University of Science and Technology, Port Harcourt, Nigeria.
elechi.promise@ust.edu.ng
Otasowie, P.O.
Department of Electrical/Electronic Engineering, University of Benin, Benin City, Nigeria.

potasowie@yahoo.co.uk

ABSTRACT - In this paper a building penetration path loss model was developed. The model involved the combination of three mechanisms of signal propagation; refraction, reflection and diffraction. The penetration through the building walls was modelled as refraction using Fresnel Refraction Coefficient and the propagation through the roof was modelled as diffraction using the principle of knife-edge diffraction. The total losses from the transmitter to the receiver was modelled as a combination of three different effects; losses due to free-space propagation from transmitter to building; the penetration loss as a combination of the wall penetration loss and the diffraction loss. To confirm the viability of this model, measurements were conducted in four different locations in Rivers State, Nigeria on buildings made with different material using MTN, Etisalat, Airtel and Globacom networks. The model simulation result showed that a total loss in GSM transmission as 124.07dB of which penetration loss as 37.95dB which accounted for 30.59%, the freespace loss as 86.12dB which accounts for 69.41% of the total losses. The results corresponded with the measurement results. Secondly, the developed building penetration path loss model was also compared with some existing path loss models namely, Log distance path loss, Okumura, HATA and COST-231 models and the results showed that the models compared accurately with the Okumura model and other existing path loss models. Hence, it can be stated that the developed building penetration path loss model can be used to accurately predict signal attenuation in buildings located in an urban environment.

Keywords: Attenuation, Building, Path loss, Propagation models, Penetration, Signal

1.0 INTRODUCTION Wireless access network has become vital tools in maintaining communication especially at home and work places due to communication models [3]. Signal propagation models can be classified as both empirical models and deterministic models. The empirical models are based on practical measured data. They include Okumura, HATA , COST-231 HATA , models and many others. Deterministic models require enormous number of geometry information about the site and also requires very important computational efforts [3]. They are RayTracing model, Ikegami model and many others [28], [3].

Attenuation is the reduction of signal strength during transmission and it is very important in communication system design [6].

Wireless signal transmission is based on radio wave propagation. Generally speaking, the signal strength is attenuated by three basic physical phenomena: reflection, diffraction, and scattering [6]. Communication engineers are generally concerned with the application of mobile radio link parameter which consists of the path loss exponent that indicates the rate at which a signal depreciates with increase in distance. A unique mean path loss exponent (n) is assigned to each propagation environment which is established by means of the experiment. To the system engineer, this parameter would help in model formulation that is appropriate for certain geographical areas. The aim of this paper is to compare a developed building penetration path loss model with some existing empirical path loss models such as Okumura, HATA, COST-231 and Log Normal models and measurement results.

2.1 Some Existing Propagation Models

2.1.2 Log-distance Path Loss Model

Log distance path loss model is an extension to Friis free space model. it is used to predict the propagation loss over a wide range of environments whereas the Friis free space model is restricted to unobstructed clear path between the transmitter and receiver [6]. Friis Free space is a condition rarely met in a radio channel. In a realistic channel, the signal will be band limited and suffer from large and small scale fading. Even if the situation is lineof -sight (LOS) there will be reflections from large objects such as buildings and nature formations like hills. The very same objects may also cause shadowing giving us a non-line-of-sight (NLOS) situation. When roaming around with the receiver, this will cause slow variations in the path loss around a local mean. Smaller objects, foliage, and edges will cause the signal to diffract or scatter and hence cause rapid variations in the received signal strength. A path loss model taking this into account is the Log-distance Path Loss Model shown in equation (1) where the loss is calculated over a distance d [5][16][23].

$$L_p(d) = L_p(d_0) + 10n\log\left(\frac{d}{d_0}\right) + \chi \quad (1)$$

The variable d0 represents a close-in reference distance, is a zero mean Gaussian distributed random variable in (dB) and is the path loss exponent representing how fast the path loss increases with distance. For free space calculations, the variable equals 2 and for built up area, equals 3.5[9] [26]. If the variable is zero as used in this paper since the shadowing effect was not considered, then equation (1) results in the logNormal fading model which shall be called Log Normal Model.

2.1.2 Okumura Model

This is the most popular and widely used model. It is a model for Urban Areas in a Radio propagation model that was built using the data collected in the city of Tokyo, Japan. The model is ideal for use in cities with many urban structures but not many tall blocking structures. The model served as a base for Hata models. Okumura model was built into three modes which are urban, suburban and open areas. The model for urban areas was built first and used as the base for others. For areas like farmland, rice fields and open fields. For suburban area the categories is village or highway scattered with trees and houses, few obstacles near the mobile. Urban area categories is built up city or large town with large buildings and houses with two or more storey or larger villager with close houses and tall, thickly grown trees. The Okumura model is expressed as:[21]

$$L_m(dB) = L_F(d) + A_{mu}(f,d) - G(h_r) - G(h_t) - G_{AREA} \quad (2)$$

where;L_m is Path loss, $L_F(d)$ is free space propagation path loss, $A_{MU}(f,d)$ is median attenuation relative to free space, $G(h_t)$ is base station antenna height gain factor, $G(h_r)$ is mobile antenna height gain factor and is gain due to the type of environment given in suburban, urban and open areas correction factors like terrain related parameters can be added using a geographical form to allow for street orientation as well as transmission in suburban and open areas and over irregular terrain. The terrain related parameters must be evaluated to determine the various correction factors [11], [1], [19], [24], [10] and [12].

2.1.3 HATA Model

This is a fully empirical prediction method, based entirely upon an extensive series of measurements made in and around Tokyo city between 200MHz and 2GHz. Hata's formulation is limited to certain ranges of input parameters and is applicable only over quasi-smooth terrain. The mathematical expression and their ranges of applicability are [25], [8], [12] and [24]:

Carrier Frequency: f_c: $150MHz \leq f_c \leq 1500MHz$
Base Station Antenna Height: $30m \leq h_b \leq 200m$
Mobile Station Antenna Height: $1m \leq h_m \leq 10m$
Transmission Distance: $1km \leq R \leq 20km$
$L_{us} = A + B\,log_{10}R - E$ for Urban Areas (3)
$L_{sa} = A + Blog_{10}R - C$ for Suburban Areas (4)
$L_{us} = A + Blog_{10}R \quad D$ open Areas (5)
where
$A = 69.55 + 26.16log_{10}(f_c) \quad 13.82log_{10}(h_b)$.
$B = 44.9 - 6.55log_{10}(h_b)$
$C = 5.4 + 2[log_{10}\left(\frac{f_c}{28}\right)]^2$.
$D = 40.94 + 4.78[log_{10}(f_c)]^2 - 18.33log_{10}(f_c)$
$E = 3.2[log_{10}(11.75h_m)]^2 \quad 4.97$ for large city and $f_c \geq 300MHz$
$E = 8.29[log_{10}(1.54h_m)]^2$ for large city and $f_c \leq 300MHz$
$E = [1.1log_{10}(f_c) \quad 0.7]h_m \quad [1.56log_{10}(f_c) \quad 0.8]$ for medium or small cities

2.1.4 COST-231

Some studies have shown that the path loss experienced at 1845MHz is approximately 10dB larger than those experienced at 955MHz all other parameters kept constant. The COST-231-HATA's model is used in the 1500-2000MHz frequency range and it can be shown that path loss can be more dramatic at these frequencies than those in 900MHz range. The model is expressed in terms of the following [17], [20] and [12]:

Carrier frequency (f_c) $1500 - 2000MHz$
BS Antenna Height (hb) 30-200m
MS Antenna Height (hm) 1-10m
Transmission Distance (d) 1-20km
The path loss according to the COST-231 model is expressed as [Singh, 2013]:
$L(dB) = A + Blog_{10}(d) + C$ (6)
where A $=46.3+33.9log_{10}(f_c) - 13.28log_{10}(hb) - a(hm)$
$B = 44.9 - 6.55log_{10}(hb)$
C = 0 for medium city and suburban area
= 3 for metropolitan areas
$a(hm) = 3.2[log_{10}(11.75h_m)]^2 - 4.97$ for large city and $f_c \geq 300MHz$
$a(hm) = 8.29[log_{10}(1.54h_m)]^2$ for large city and $f_c < 300MHz$
$a(hm) = [1.1log_{10}(f_c) - 0.7]h_m - [1.56log_{10}(f_c) - 0.8]$
for medium or small cities

3.0 MATERIALS AND METHOD

3.1 Development of Building Penetration Path loss model

In this section, a model will be used to predict the amount of signal attenuation through buildings. This model will involve the combination of two mechanisms of signal propagation: penetration through building wall and penetration through building roof as diffracted signal. Though most existing propagation predictions modelled the buildings as being completely opaque to radio signals [27]. The total losses from the transmitter to the receiver will be modelled as a combination of two different effects; losses due to free-space propagation from transmitter to building and the building penetration losses. The penetration loss will be modelled as the combination of two losses; the loss when the signal is passing through the building wall and diffraction loss due to signal penetration through the roof. The expression for the losses from transmission through the building to the receiver will be:

$$L_{total} = L_{free-space} + L_{penetration} \quad (7)$$

Where, $L_{total} = total\ losses$; $L_{free-space}$ is the free-space losses, $L_{penetration}$ is the penetration loss due to the building

From Figure 1, • $d_{t1}$is the distance from the transmitter to the building roof. • d_{r1} is the distance from the wall edge to the mobile station (receiver) •R is the reflected signal from the roof. • d_{T2} is the distance from the transmitter to the building wall, measured in the perpendicular direction from the transmitter to the building wall. • d_{R2} is the distance from the building wall to the receiver, measured in the perpendicular direction from the obstacle to the mobile station. • ϕ is the angle of arrival, measured from the perpendicular direction to the building and to the direction followed for the propagating signal. •w is the inner width of the room. • b is the width of the building measured from the center of the brick (wall) • h_c is the transmitter height • h_{Hall} is the height of the building wall. • h_M is the height of the table in which the mobile station (receiver) is placed •a is the least departure angle of the signal from the transmitter • β is angle of the diffracted signal with the normal.

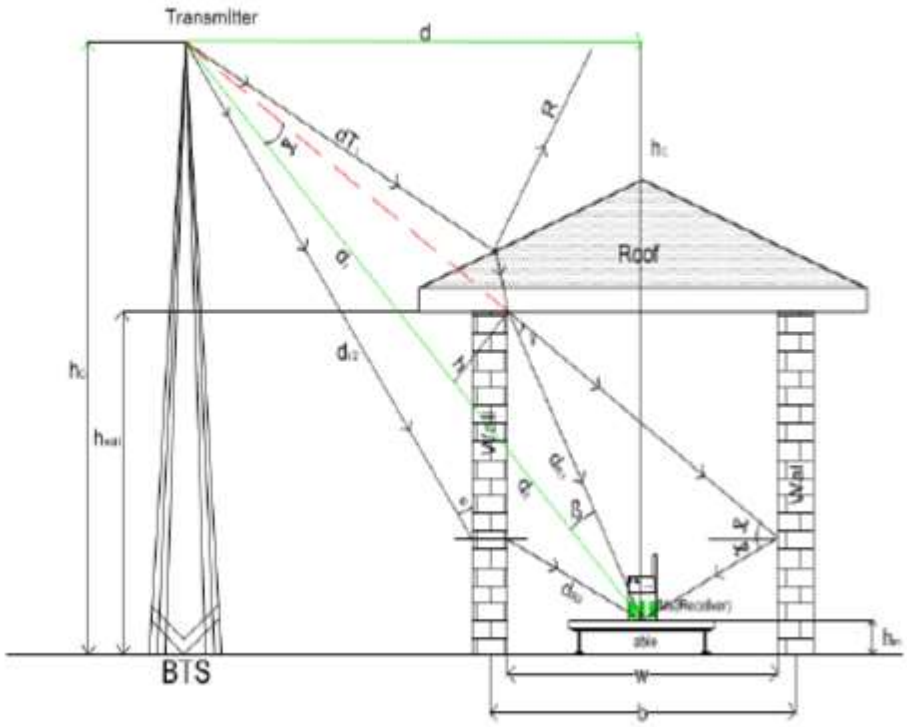

Figure 1: Complete model of GSM signal penetration into building and parameters used

3.1.1 Free-Space Losses

The free-space propagation can be used to predict the received signal when the transmitter and the receiver have a line-of-sight. The equation (8) is known as the Friis free-space equation, it predicts that received power decays as a function of the transmitter-receiver separation distance [6].

$$P_r(d) = \frac{P_t G_t G_r \lambda^2}{(4\pi)^2 d^2 L} \quad (8)$$

wherePt is the transmitted power, Pr(d) is the received power, Gt is the transmitter antenna gain, Gr is the receiver antenna gain, d is the distance of separation between the transmitter and the receiver in meters, Lis the propagation loss factor which must be a positive integer and is the λ wavelength in meters.

The path loss is the difference (in dB) between the effective transmitted power and the received power. It represents the signal attenuation measured in dB and may or may not include the effect of the antenna gain. When the antenna gains are excluded, the path loss is given as [7]:

$$PL(dB) = 10log_{10}\frac{P_t}{P_r} \quad (9)$$

$$PL(dB) = -10log_{10}\left[\frac{\lambda^2}{(4\pi)^2 d^2}\right] \quad (10)$$

From figure 1, the losses between the transmitter and the building is,

$$L_{free-space} = \left[\frac{4\pi f}{c}\right]^2 d_{T2}^2 \quad (11)$$

$$L_{free-space}(dB) = 20log_{10}\left[\frac{4\pi f d_{T2}}{c}\right](dB) \quad (12)$$

where f and c are the frequency and velocity of signal transmission respectively.

3.1.2 Building Penetration Loss

The penetration loss will be modelled as a combination of the refracted signal (refraction loss) and the diffracted signal (diffraction loss). It is modelled as refracted because the signal is passing through a material medium. When a signal passes through a material medium, it is reflected and refracted [7]. For this modelling, emphasis will be focussed on the refracted signal since it represents the signal passing through the building wall to the receiver.

3.1.2.1 Refraction Loss

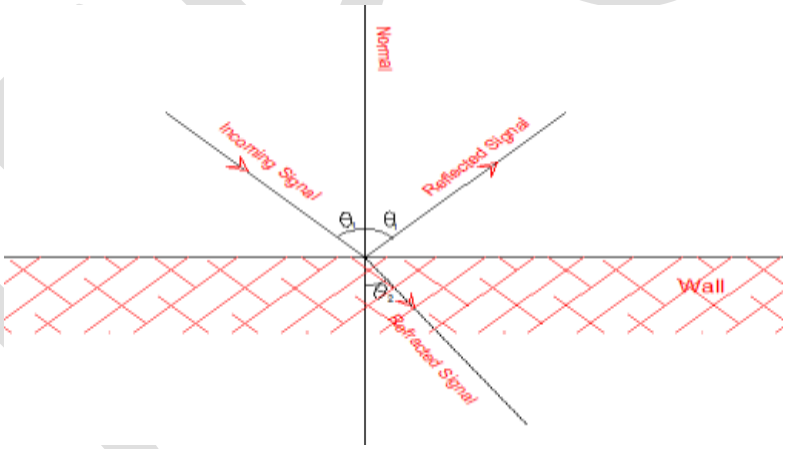

Figure 2: Boundary Condition for the Signal Penetration into wall.

Figure 2, gives a clear illustration that as the GSM signal strikes the building wall, some of the signals are refracted through the wall into the room, while the rest are reflected. The rate of reflection and refraction are dependent on the type of the building material used for the wall.

The refracted signal coming from outside to inside the building will be modelled using the Fresnel Transmission and Reflection Coefficient. This parameter characterises the amount of signal strength coming from outside the building to inside the building [7]. The Fresnel equations describe what fraction of the signal is reflected and what fraction is refracted and also describe the phase shift of the reflected signal [14]. The fraction of the incident signal that will be reflected from the interface is given by the reflectivity, R and the fraction that will be refracted is given by the transmittance or transmissivity, T [14].

According to [22], the Fresnel Reflection Coefficient was defined as follows,

$$R_s = \frac{sin\theta - \sqrt{\varepsilon_r - cos^2\theta}}{sin\theta + \sqrt{\varepsilon_r - cos^2\theta}} \quad (13)$$

where θ is the angle between the reflecting surface and the normal perpendicular to the wall, ε_r is the complex relative permittivity. The relative permeability.μ_r, of the obstacle is equal to 1 [15].

The angle θ in equation (14) can be related to the angle of arrival ϕ of figure 2 when both are expressed in degrees.

$$\phi = 90^0 - \theta \qquad (14)$$

Recall, $Sin\,(90 - \theta) - Cos\,\phi$ (15)

As a function of the angle of arrival from equation (15), R_s can be expressed as:

As a function of the angle of arrival from equation (15), can be expressed as:

$$R_s = \frac{cos\phi - \sqrt{\varepsilon_r - sin^2\phi}}{cos\phi + \sqrt{\varepsilon_r - sin^2\phi}} \qquad (16)$$

The Fresnel transmission Coefficient T_s can be related to the Fresnel Reflection Coefficient, R_s as [18]:

$$T_s = R_s + 1 \qquad (17)$$

Hence,

$$T_s = \frac{cos\phi - \sqrt{\varepsilon_r - sin^2\phi}}{cos\phi + \sqrt{\varepsilon_r - sin^2\phi}} + 1 \qquad (18)$$

$$T_s = \frac{cos\phi - \sqrt{\varepsilon_r - sin^2\phi} + cos\phi + \sqrt{\varepsilon_r - sin^2\phi}}{cos\phi + \sqrt{\varepsilon_r - sin^2\phi}}$$

$$T_s = \frac{2cos\phi}{cos\phi + \sqrt{\varepsilon_r - sin^2\phi}} \qquad (19)$$

Since the fraction that is refracted is given by the transmittance, T [14]. The dependence of the penetration loss (through the wall) based on the Fresnel Transmission Coefficient is:
Expressed in dB,

$$L_{wall\ penetration} = -20log_{10}T_s(dB) \qquad (20)$$

This parameter expresses the signal strength passing through the wall into the residential room.

According to [15], the mud is made up of the following percentage material composition; Fe2O3 (44.8%), MnO (0.06%), TiO2 (12.33%), CaO (5.22%), K2O (0.27%), P2O5 (0.45%), SiO2 (5.4%), Al2O3 (16.2%), MgO (0.13%) and Na2O (4.0%). Hence, the relative permittivity of iron oxide (Fe2O3) was used as the relative permittivity for mud since it has the highest percentage composition and this applies for brick while concrete and aluminium has specific relative permittivity. The relative permittivity of the materials under consideration for the wall penetration losses are:

Table 1: Relative Permitivity of Building Materials [15]

Building Material	**Relative Permittivity ( )**
Concrete + Iron	16.5
Mud	14.2
Brick	7.6
Alucoboard +Brick	19.5

The Refracted signal penetration loss for this comparison was computed using the relative permittivity of brick since majority of the buildings have brick wall while others can be obtained by substituting the relative permittivity of the various building materials as shown in table 1 into equation (20) using equation (19), for an arrival angle of to the wall.

3.1.2.2 Diffraction Loss

In figure 1, the signal from the transmitter strikes the roof of the residential room and part of it is reflected, while the other is refracted through the roof and diffracted as soon as it strikes the wall edge and it is receiver by the receiver (mobile phone). Assuming the

transmitting signal takes the path of the red broken line and a straight line is produced from the transmitter to the receiver to produce a knife-edge diffraction geometry. Also, consider that there is an impenetrable obstruction of height h, at a distance from the transmitter and from the receiver along the signal path as shown in figure 1. The path difference between the direct path and the diffracted path will be:

$$\delta - \sqrt{(d_1^2 + h^2)} + \sqrt{(d_2^2 + h^2)} - (d_1 + d_2) \quad (21)$$

Simplifying further gives

$$\delta = d_1\left(1 + \frac{h^2}{2d_1^2}\right) + d_2\left(1 + \frac{h^2}{2d_2^2}\right) - (d_1 + d_2) \quad (22)$$

$$\delta = \frac{h^2}{2d_1} + \frac{h^2}{2d_2} \quad (23)$$

$$\delta = {h^2(d_1 + d_2)}/{(2d_1d_2)} \quad (24)$$

The phase difference will be:

$$\varphi = \frac{2\pi\delta}{\lambda} = 2\pi h^2 {(d_1 + d_2)}/{2\lambda(d_1d_2)} \quad (25)$$

Let

$$\gamma = \alpha + \beta \quad (26)$$

And $$tan\gamma = tan\alpha + tan\beta \quad (27)$$

Hence,

$$\tan\gamma = tan\alpha + tan\beta = {h}/{d_1} + {h}/{d_2} = {h(d_1 + d_2)}/{d_1d_2} \quad (28)$$

To normalise this, the Fresnel-Kirchoff diffraction parameter , was applied [13]

$$v = h\sqrt{{2(d_1 + d_2)}/{(\lambda d_1d_2)}} \quad (29)$$

To estimate the diffraction loss, the Knife-edge diffraction model was applied.

The electric field strength, E_d of a knife-edge diffracted wave is given by: [13]

$${E_d}/{E_o} = F(v) = (1 + j)/2 \int_v^\infty \exp\left(\frac{-j\pi t^2}{2}\right) dt \quad (30)$$

The diffraction loss due to presence of knife-edge can be given as: [13]

$$L_{diffraction} = -\left(\frac{0.225}{v}\right)^2 \quad (31)$$

Expressing in dB

$$L_{diffraction}(dB) = -20log_{10}\left(\frac{0.225}{v}\right)$$

$$L_{diffraction} = -20log_{10}\left(\frac{0.225}{h\sqrt{{2(d_1+d_2)}/{(\lambda d_1d_2)}}}\right) \quad (32)$$

3.1.3 Total Losses(Building Penetration Path loss)

Considering the results of sections 3.1.1 and 3.1.2, the expressions for the total path losses from a base transceiver station to the mobile station when the signal propagation path is interrupted by a building is,

$$L_{total} = \left(\frac{4\pi f d_I}{c}\right)^2 \frac{1}{T_s^2}\left(\frac{v}{0.225}\right)^2 \quad (33)$$

Expressing in dB

$$L_{total} = 20log_{10}\left(\frac{4\pi f d_{T2}}{c}\right) - 20log_{10}(T_s) - 20log_{10}\left(\frac{0.225}{h\sqrt{2(d_{T1}+d_{R1})/(\lambda d_{T1} d_{R1})}}\right) \quad (34)$$

The following parameter values were substituted into equation (37) to determine the signal path loss from the BTS (transmitter) to the MS (receiver). , .

3.2 Measurements

To confirm the viability of this model, measurements were conducted on five different building patterns in four (4) different locations (Port Harcourt, Elele, Omoku and Emohua) all in Rivers State, Nigeria. The study was carried out on four GSM service providers (MTN, Etisalat, Globacom and Airtel), to determine their signal penetration through buildings made of different materials using Radio Frequency Signal Tracker software. The Radio frequency Signal Tracker installed in a Tecno Tablet was used in carrying out the measurements to determine the signal strength, signal-to-noise ratio (SNR) and the distance from the measurement site to the Base Transceiver Stations (BTS).

The measurements conducted in each of the four different locations were conducted on five different building pattern namely, mud building with thatched roof, mud building with rusted corrugated iron sheet roof, sandcrete building with unrusted corrugated iron sheet roof, sandcrete building with rusted corrugated iron sheet roof and building with Alucoboard wall cladding.

3.3 Calculation of Penetration Loss

For each of the measurements, the penetration loss was computed as:

(35)

Where is the average penetration loss in dBm, is the average signal strength inside the building in dBm and is the average signal strength outside the building in dBm. The positions of the transmitter (BTS) and the dimensions of the window area were considered, as measurements were not conducted on buildings with many and large window areas. Tables 3 through 6 is the measured signal lose for each location using equation (35).

4.0 RESULTS AND DISCUSSION

4.1 RESULTS

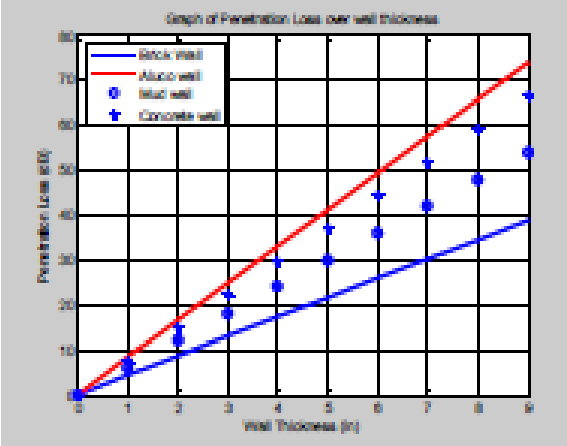

Figure 3: Penetration loss through a 9 inches wall for different materials

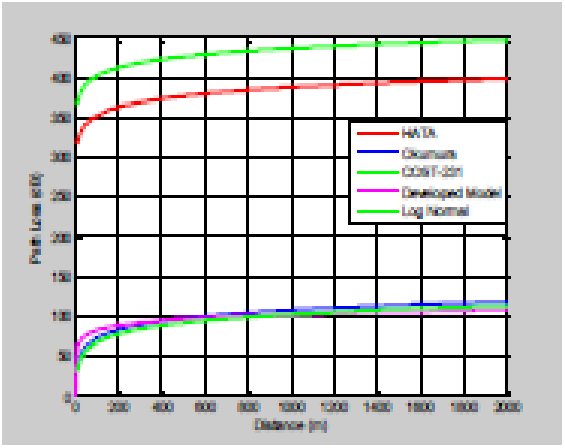

Figure 5: Comparison of the Developed path loss model with Okumura, HATA, COST-231 and Log Normal models.

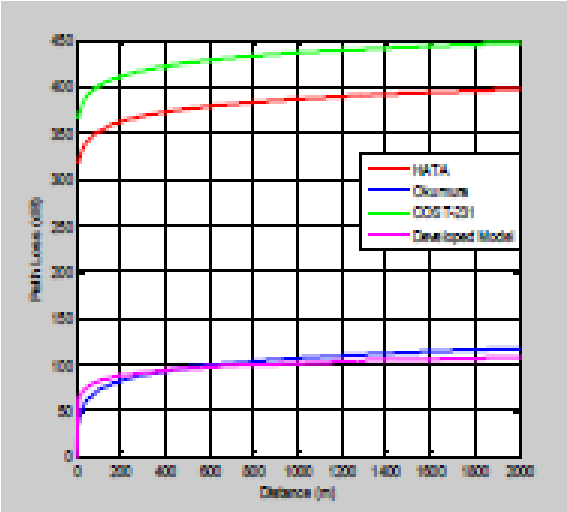

Figure 4: Comparison of developed path loss model with Okumura, HATA and COST-231 models with respect to transmission distance.

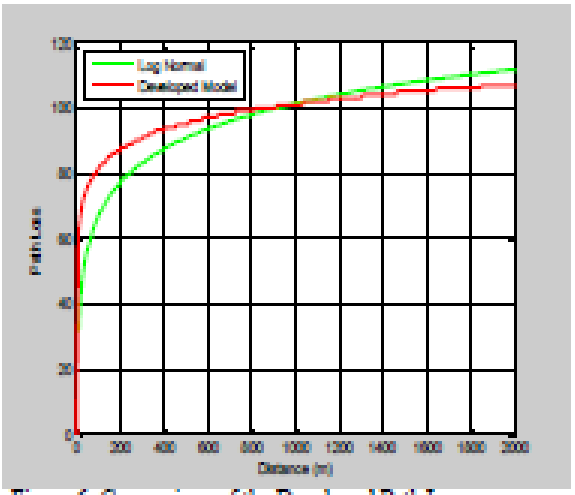

Figure 6: Comparison of the Developed Path Loss model and Log Normal model with respect to transmission distance

Table 2: Loss Values and their Percentage

Type of Loss	Loss Value (dB)	Percentage Loss (%)
Free Space	86.12	69.41
Penetration	37.95	30.59

Table 3: Measured Signal Loss for different Building Pattern in Ekele

Network Provider	Building Pattern				
	Mud Building with Rusted Corrugated iron sheet roof in dBm	Mud Building with Thatched roof in dBm	Sandcrete Building with Rusted Corrugated iron sheet roof in dBm	Sandcrete Building with Unrusted corrugated iron sheet roof in dBm	Building with Alucoboard wall Cladding in dBm

MTN	12.42	15.81	28.35	31.04	38.45
Globacom	20.22	18.32	25.65	33.41	41.14
Etisalat	48.05	34.54	29.22	39.32	44.25
Airtel	36.12	32.47	34.21	34.24	44.15

Table 4: Measured Signal Loss for different Building Pattern in Port Harcourt

Network Provider	Building Pattern				
	Mud Building with Rusted Corrugated iron sheet roof in dBm	Mud Building with Thatched roof in dBm	Sandcrete Building with Rusted Corrugated iron sheet roof in dBm	Sandcrete Building with Unrusted corrugated iron sheet roof dBm	Building with Alucoboard wall Cladding in dBm
MTN	41.05	39.98	37.31	31.48	41.22
Globacom	48.55	47.71	32.66	40.10	48.47
Etisalat	47.50	44.21	26.25	33.05	50.25
Airtel	48.41	40.44	28.35	35.55	51.24

Table 5: Measured Signal Loss for different Building Pattern Omoku

Network Provider	Building Pattern				
	Mud Building with Rusted Corrugated iron sheet roof in dBm	Mud Building with Thatched roof in dBm	Sandcrete Building with Rusted Corrugated iron sheet roof in dBm	Sandcrete Building with Unrusted corrugated iron sheet roof in dBm	Building with Alucoboard wall Cladding in dBm
MTN	43.72	52.10	39.42	29.21	48.23
Globacom	45.91	50.70	33.39	30.21	52.42
Etisalat	59.47	56.42	36.47	31.10	56.25
Airtel	42.74	51.55	40.36	41.53	54.26

Table 6: Measured Signal Loss for different Building Pattern in Emohua

Network Provider	Building Pattern				
	Mud Building with Rusted Corrugated iron sheet roof in dBm	Mud Building with Thatched roof in dBm	Sandcrete Building with Rusted Corrugated iron sheet roof dBm	Sandcrete Building with Unrusted Corrugated iron sheet roof in dBm	Building with Alucoboard wall Cladding in dBm
MTN	32.70	55.12	39.42	29.71	56.20
Globacom	35.80	50.72	37.39	30.25	55.30
Etisalat	49.50	56.41	36.47	31.10	49.24
Airtel	33.72	51.52	40.41	30.66	54.35

4.2 Discussion

In figure 4, the developed building penetration path loss model were compared with the existing path loss models and there was closeness of values with the Okumura path loss model. There is also closeness of values with the log normal model as shown in figure 5. In figure 5, the developed model showed very close comparison with the Okumura and the log normal path loss models. From figure 4, the developed model and Okumura showed the least values compared to the other models and with close relationship with each other. Figure 6 shows the clearer comparison of the developed model with the log normal model, at a distance of 1km away from

the transmitter, both models presented equal losses. In all, the developed model showed very close relationship of results with the Okumura and log normal path loss models. The COST-231 showed high path loss while the HATA showed intermediate results. The results in table 2 shows that the penetration loss accounts for 30.59% with a loss value of 37.12dB of the total losses which compares with the measurements results for sandcrete building of figures 3 through 6. The free-space loss accounts for 69.41% with a loss value of 86.12dB of the total losses. This means that, the building accounts for 30.59% of the total loss of signal in GSM transmission, though the free space depends on the distance of the building from the transmitter. Figure 3 shows that a 9 inches brick wall will experience a signal loss of 40dB while the concrete wall has a loss 68dB, this shows that the brick wall has the least penetration loss while the building with alucoboard wall cladding has the highest penetration loss. This result also conforms to the measured results of tables 3 through 6. Since the emphasis lies on the building losses, therefore, it will be necessary for builders to use materials with less penetration losses.

5.0 CONCLUSION AND RECOMMENDATION

5.1 Conclusion

In conclusion, it can be stated that the developed building penetration path loss model compared accurately with the Okumura and log normal models since they have closeness of values and relationship. The developed building penetration path loss model, Okumura, HATA and COST-231 showed increasing trend with respect to the transmission distance and in all the models used in this research, Okumura model showed similar trend with the developed model as well as the log normal model. It therefore shows that this developed model is a viable model that can be used to predict the signal attenuation in an urban environment. The penetration loss were almost equal with the measurement results. Hence, it can be conclude that the developed model can be used in predicting GSM signal losses in buildings.

5.2 Recommendation

This research has presented a new model for predicting signal attenuation through buildings in both urban and rural environments. Therefore, it will be recommended that this study be extended to other geographical environments such as high climatic environments for effective GSM network planning.

REFERENCES:

[1]. V.S. Abhayawardhana, I.J. Wassell, D. Crosby, M.P. Sellars and M.G. Brown, "Comparison of Empirical Propagation Path Loss Models for Fixed Wireless Access Systems", IEEE, 2003, pp. 213-217.

[2]. J.J. Biebuma, and B.O. Omijeh, "Path Loss Model Using Geographic Information System", International Journal of Engineering and Technology, Vol. 3, No. 3, 2013, Pp. 269-275.

[3]. P. Elechi and P.O. Otasowie, "Determination of Path Loss Exponent for GSM Wireless Access in Rivers State using Building Penetration Loss", The Mediterranean Journal of Electronics and Communication, Vol. 11, No. 1, 2015, pp.822-830.

[4]. D.J. Griffiths, "Introduction to Electrodynamics", 3rd Edition, Pearson Education, Dorling Kindersley: 2007, pp.102-114.

[5]. L.D. Hai, N.M. Khai, T.V. Quy and N.X. Huan, "Material Composition and Properties of Red Mud Coming From Alumina Processing Plant Tanrai, Lamdong, Vietna", International journal of Research In Earth and Environmental Science, Vol. 1, No. 6, 2014, pp. 1-7.

[6]. H. Hashemi, "The Indoor Radio Propagation Channel", Proc. IEEE, Vol. 81, No. 7, 1993, pp. 943-968

[7]. A. Katariya, A. Yadav, N. Jain and G.Tomar, "BER Performance Criteria based on Standard IEEE 802.11a for OFDM in Multipath Fading Environment", International Conference on Computational Intelligence and Communication Systems, 2011, pp. 452-459.

[8]. I.R. Kenyon, "The Light Fantastic: Introduction to Classic and Quantum Optics", Oxford University Press, 2008, pp. 45-51.

[9]. M. Kumar, V. Kumar and S. Malik, "Performance and Analysis of Propagation Models for Predicting RSS for Efficient Handoff", International Journal of Advanced Scientific Research and Technology, Vol. 1, No. 2, 2012, pp. 54-61.

[10]. M.A. Masud, M. Samsuzzaman and M.A. Rahman, "Bit Error Rate Performance Analysis on Modulation Techniques of Wideband Code Division Multiple Access", Journal of Telecommunication, Vol. 1, No. 2, 2010, pp. 22-29.

[11]. A. Medeisis and A. Kajackas, "On the use of universal Okumura-Hata Propagation Prediction model in Rural Areas", IEEE Vehicular Technology Conference proceeding Vol. 3, 2000, Pp. 450 – 453

[12]. N.V. Mejuto, "Penetration and Transmission of UHF Radio Waves into/through Buildings-a Literature Review", Graduation Report, Eindhoven University of Technology, 1999. Pp. 91-96.

[13]. D. Moldkar, "Review on Radio Propagation into and within Buildings, microwaves and Antennas and Propagation", IEE Proc. H, Vol. 138, No. 1, 1991, pp. 1452-1459.

[14]. A. Neskovic, N. Neskovic and G. Paunovic, "Modern Approaches in Modelling of Mobile Radio Systems Propagation Environment", IEEE Communication Survey, 2000, pp. 25-28.

[15]. N.L.M.B. Nordon, "Interface Developing for Hata Model using Matlab", Universiti Teknologi Malaysia, 2007, pp. 24-28.

[16]. A.N. Okunbor and R.O. Okonkwo, "Characterization of Signal Attenuation using Path Loss Exponent in South-South Nigeria", IJETTCS, Vol. 3, No. 3, 2014, pp. 100-104.

[17]. T.S. Rappaport, "Indoor Radio Communications for Factories of the Future", IEEE Commun. Mag., 1989, pp. 15-24.

[18]. T.S. Rappaport, "Wireless Communications: Principles and Practice", Upper Saddle River, NJ: Prentice Hall PTR, 2002, pp. 75-92.

[19]. M.N.O. Sadiku, "Optical and Wireless Communications: Next Generation Networks", CRC Press, 1st Edition: 2002, pp. 120-127.

[20]. S. Sarooshyari and N. Madaya, "An Introduction to Mobile Radio Propagation and Characterization of Frequency Bands", Wireless Comm. Technologies, IEEE, Vol. 16, 1996, pp. 332:559.

[21]. S.R. Saunders, "Antennas and Propagation for Wireless Communication Systems", Wiley Publishers, 2000, Pp. 409 - 415

[22]. P. Schneider, F. Lambrecht and A. Baier, "Enhancement of the Okumura-Hata Propagation using Detailed Morphological and Building Data", IEEE Comm, 1996, pp. 471-475.

[23]. P.K. Sharma and R.K. Singh, "Comparative Analysis of Propagation Path Loss Models with Field Measured Data", International Journal of Engineering Science and Technology, Vol. 2, No. 6, 2010, pp. 2008-2013.

[24]. Y. Singh, "Comparison of Okumura, HATA and COST-231 Models on the Bases of Path Loss and Signal strength", International Journal of Computer Application, Vol. 59, No. 11, 2012, pp. 37-41.

[25]. J. Spetzler and R. Snieder, "The Fresnel Volume and Transmitted Waves", The Journal of geophysics, Vol. 69, 2004, pp. 653-663.

[26]. J. Vaughan and B. Anderson, "Channels, Propagation and Antennas for Mobile Communications" IEE Publishers, 2003, Pp.753 -760

[27]. N. Yarkoni and N. Blaunstein, "Prediction of Propagation Characteristics in Indoor Radio Communication Environments", Progress in Electromagnetic Research, PIER Vol. 59, 2006, pp.151-174.

[28]. S.R. Saunders and A. Aragon-Zavala, "Antennas and Propagation for Wireless Communication System", 2nd Edition, John Wiley and Sons Ltd, 2007, pp. 165-170

International Journal of Engineering Research and General Science Volume 3, Issue 6, November-December, 2015
ISSN 2091-2730

Study of VLSI Implementation of Fractional-N PLL using 32nm and 45nm Technology

Amruta Chore, Akanksha Goel, Mily Lal

DYPIEMR, Akurdi, amrutachore2404@gmail.com

Abstract— Nowadays, Low power designs is a very hot topic in electronic systems. The high speed and low power dissipation required in multigigahertz communication systems such as wireless products and optical data links offered by Deep submicron CMOS technologies. **Very-large-scale integration** (**VLSI**) is the process of mounting thousands of transistors on single chip called as integrated chip. Power is way of measuring how fast a function can be carried out. Accuracy and efficiency in power estimation involved in the design phase is important in order to meet power specifications without high cost redesign process. This paper presents the comparison of design and simulation of an chip layout of fractional –N phase locked loop for wireless application using45nm and 32nm VLSI technology. This is a comparison of fractional N-PLL based on latest 45nm and 32nm technology. It offers high speed performance at low power. Sigma delta modulator and low pass filter and improves the performance of the system. Phase locked loop (PLL) represents the leading method in the wireless communications system among variety of frequency synthesis techniques.

Keywords— Voltage controlled oscillator, Phase detector, Charge pump, Sigma delta modulator, loop filter, fractional –N divider.

INTRODUCTION

Phase Locked Loop (PLL) circuits are used for frequency control. PLL can be used as frequency multipliers, demodulators, tracking generators or clock recovery circuits Figure 1 shows a block diagram of a basic Phase locked loop. The phase of a voltage controlled oscillator (VCO)is controlled by PLL. The input signal is applied to one input of a phase detector. The other input is connected to the output of a divide by N counter. A signal is sent to the PLL from some signal source. The two parts of the PLL will work together so that the output of the VCO is same as to the input of the phase detector. If the VCO is lagging behind the input, the phase detector will note down this and increases VCO slightly to keep the two signals aligned, and if the VCO gets leading of the input signal, the phase detector will make the VCO slow down. The output of the phase detector is a voltage relative to the phase difference between the two input signals. This signal is applied to the loop filter or low pass filter. It is the low pass filter determines the characteristics of the phase locked loop circuit. The filtered output signal of low pass filter controls the VCO. The output of the VCO is at a frequency that is N times the input given to the frequency reference input.

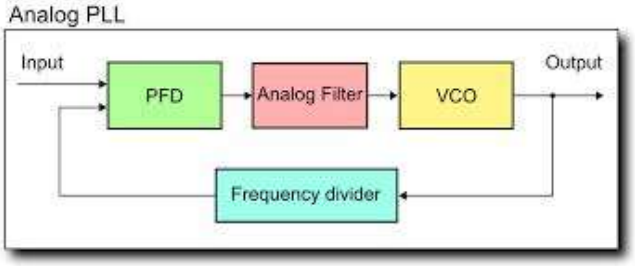

Figure 1 Block diagram of PLL

IMPLEMENTATION OF PLL USING VLSI TECHNOLOGY:

DESIGN OF PHASE DETECTOR USING VLSI TECHNOLOGY

Phase detector circuit in the PLL compares the phases of two signals and generates a voltage signal according to the phase difference between the two signals. Phase difference detection is very important in many applications, such radar and telecommunication systems, servo system and demodulators. The phase detector in the PLL is XOR gate. Its output produces a regular square oscillation when the clock input and signal input have one quarter of period shift (90° or π /2). When the two signals are compared in phase, the XOR gate will have a constant level of zero as output. The XOR detector generates a square-wave output at twice the reference frequency. Layout of phase detector using VLSI technology shown in figure 2.

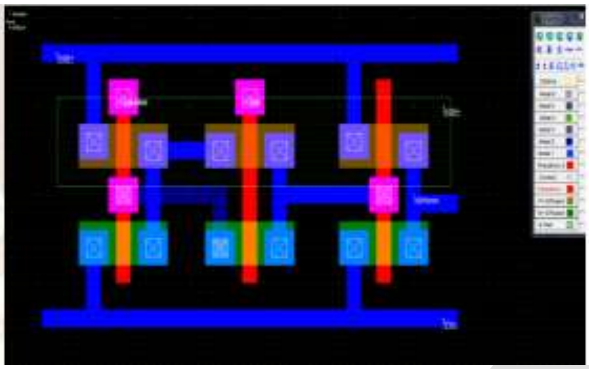

Figure 2 Layout of phase detector

DESIGN OF LOW PASS FILTER USING VLSI TECHNOLOGY

The features of loop filter in order to increase the performance of PLL are-

1) Removes high frequency noise of the detector.

2) Influences the hold and capture ranges.

3) Increases the switching speed of the loop.

In this design passive second order low pass filter is used. It offers the advantages like linearity, low noise and unlimited frequency range. Loop filter is used to removes the unwanted spurious tones and also decreases noise of the control line for VCO. This filter consist of charge pump offers the advantages as reduced noise, reduced power consumption, no offset voltage. The filter is consist of capacitor C charged and discharged through the resistance of the switch. The RC delay creates a low-pass filter. The layout shown in figure 3.

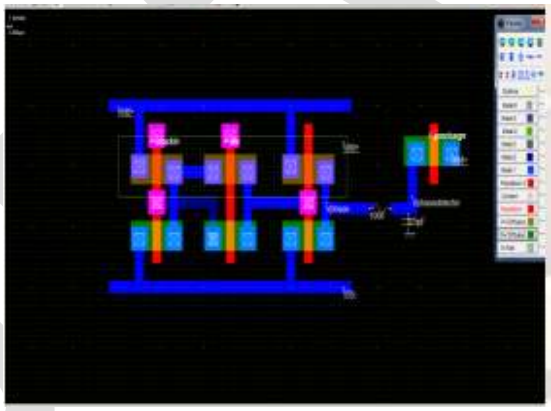

Figure 3 Layout of phase detector with filter

DESIGN OF VOLTAGE CONTROLLED OSCILLATOR (VCO) USING VLSI TECHNOLOGY

Oscillation frequency of VCO is controlled by a voltage input. It is usually used to generate clock in phase locked loop circuit. The VCO oscillates at a higher or lower frequency based on the control voltage, which affects the phase and frequency of the feedback clock. To the low pass filter, the output of phase detector is provided and used as a control signal to drive a VCO. High performance VCO provides very good linearity which is used in this phase locked loop. The principle of this high performance VCO is a delay cell with linear delay dependence on the control voltage. The delay cell consists of a pulldown n-channel MOS, controlled by vplage and a pchannel MOS in series. The delay dependence on vcontrol is almost linear for the fall edge. Figure 4shows the layout of VCO.

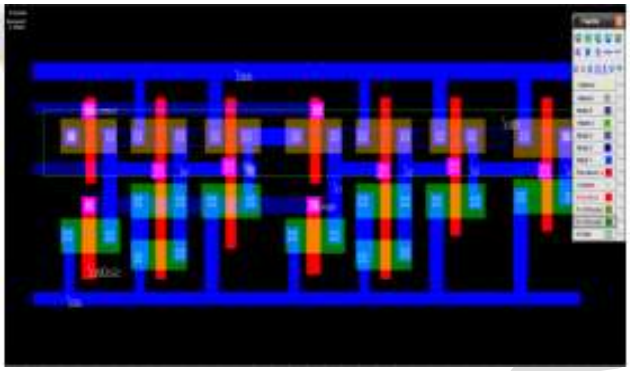

Figure 4 Layout of VCO

IMPLEMENTATION OF FRACTIONAL-N PLL USING VLSI TECHNOLOGY

Modulation is a method for encoding higher-resolution digital signals into lower-resolution digital signals. In this work sigma-delta modulator is designed using VLSI technology with microwind 3.1 software. The desired fractional division number (α) is the input of sigma-delta modulator where the output is a DC component y[n] which is proportional to the fractional input (α) plus the quantization noise introduced due to use of integer divider instead of ideal fractional divider. The frequency divider divides the output frequency of the VCO is divided by frequency divider by Nint+y[n], where Nint is an integer value and y[n] is the output sequence of the modulator.

Among all the frequency synthesis techniques, phase locked loop (PLL) represents the leading method in the wireless communications systems. Current PLL ICs are highly integrated digital and operate on very low power. These ICs require an external crystal (Xtal) reference, voltage controlled oscillators (VCO) and minimum external passive components to generate the abundant range of frequencies needed in a modern communication systems. Figure 6 shows the optimum, high efficient chip design of low power fractional-N PLL frequency synthesizer using sigma delta modulator using VLSI technology. This layout design is implemented using NMOS and PMOS BSIM4 transistors with good dimensions of transistors and metal connections according to the Lambda based rules of microwind 3.1 software. For the PLL, power supply VDD of 1 volt is used. Figure 6and 7 shows comparison of the voltage versus time response of fractional-N PLL using 45nm and 32nm technology respectively. Figure 8 and Fig. 9 shows comparison of frequency versus time response of PLL using 45nm and 32nm technology respectively.

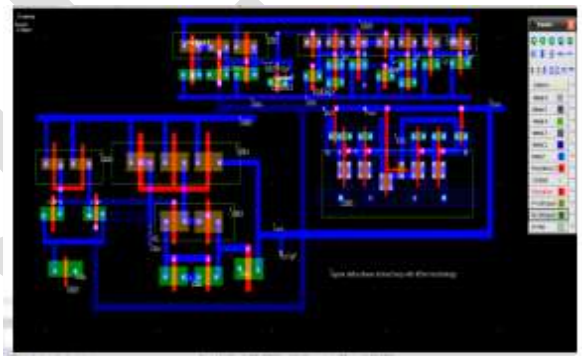

Figure 5. The optimum, high efficient layout design of low power fractional-N PLL with sigma delta modulator using VLSI technology

COMPARISON OF VOLTAGE VS. TIME AND FREQUENCY VS. TIME OUTPUT OF FRACTIONAL-N PLL BETWEEN 32NM AND 45NM TECHNOLOGY

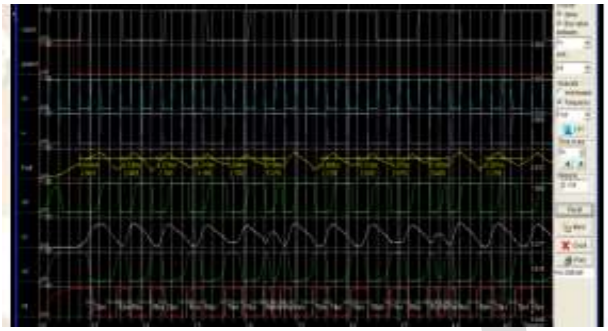

Figure. 6 Voltage verses time output using 45nm technology

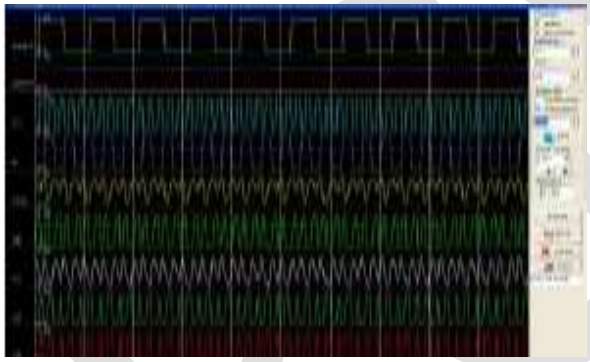

Figure. 7 Voltage verses time output using 32nm technology

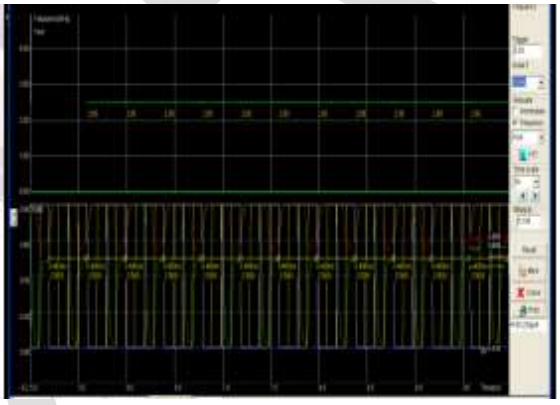

Figure. 8 Frequency verses time output using 45nm technology

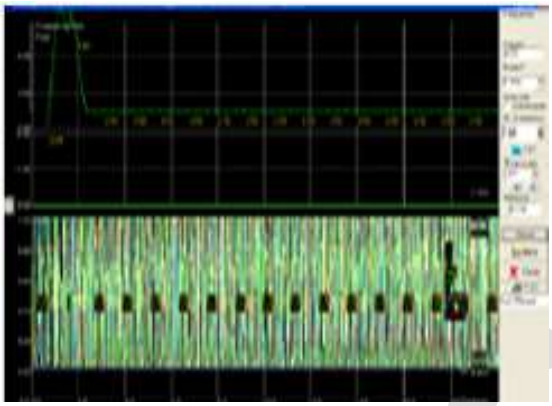

Figure. 9 Frequency verses time output using 32nm technology

PARAMETRIC COMPARISON SUMMARY OF PLL USING 45NM AND 32NM VLSI TECHNOLOGY

SR. NO.	PARAMETERS	VALUE using 45nm	Value using 32nm
1	VDD	1.0 volt	1.0 volt
2	VDD DIV/2	0.5 volt	0.5 volt
3	Ioff N (nA/µm)	5-100	5-100
4	Ioff P (nA/µm)	5-100	5-100
5	Gate dielectric	Hfo2	Hfo2
6	Input frequency	2.1 GHz	2.1 GHz
7	Output frequency	2.50 GHz	2.50 GHz
9	No. of NMOS and PMOS transistors	23 NMOS, 23 PMOS	21 NMOS, 21 PMOS

Table 1 comparison summary

CONCLUSION

Conclusion must be short and precise and should reflect the work or research work you have gone through. It must have same as above in introduction paper adjustment

REFERENCES:

[1] MS. A. V. Manwatkar and Prof. V. B. Padole, " Design of 2.5 GHz Phase locked loop using 32nm CMOS technology," International journal of engineering and computer science, Volume 3, Issue 6 June 2014

[2] N. Fatahi and H. Nabovati, "Design of low power fractional-N frequency synthesizer using sigma delta Modulation technique," 27th International Conference of Microelectronics, IEEE, 2010.

[3] Aamna Anil and Ravi Kumar Sharma, "A high efficiency charge pump for low voltage devices," International Journal of VLSI design & Communication Systems (VLSICS) Vol.3, No.3, June 2012.

[4] Ms. Ujwala A. Belorkar and Dr. S. A. Ladhake,"Design of low power phase lock loop using 45nm VLSI technology," International journal of VLSI design & Communication Systems (VLSICS), Vol.1, No.2, June 2010

[5] Kyoungho Woo, Yong Liu, Eunsoo Nam, and Donhee Ham, "Fast-Lock Hybrid PLL Combining Fractional-N and Integer-N Modes of Differing Bandwidths," IEEE journal of solid-state circuits, vol. 43, NO. 2, february 2008 379.

[6] Michael H. Perrott, "Fractional-N Frequency Synthesizer Design Using PLL Design Assistant and CppSim Programs," July 2008

[7] Mohammad Sohel, "Design of low power Sigma Delta ADC," International journal of VLSI design & Communication Systems (VLSICS), Vol.3, No.4, August 2012.

[8] Amruta M. Chore, Shrikant J. Honade / "VLSI Implementation of Fractional-N Phase Locked Loop Frequency Synthesizer ", International Journal of Engineering Research and Applications (IJERA) ISSN: 2248-9622 www.ijera.com Vol. 3, Issue 4, Jul-Aug 2013, pp.855-860

[9] B. K. Mishra, Sandhya Save and Swapna Patil, "Design and Analysis of Second and Third Order PLL at 450MHz," International Journal of VLSI design & Communication Systems (VLSICS) Vol.2, No.1, March 2011.

[10] S. Borkar, "Obeying Moore's law beyond 0.18 micron," in Proceedings of the 13th Annual IEEE International ASIC/SOC Conference, pp. 26–31, September 2000.

[11] R. K. Krishnamurthy, A. Alvandpour, V. De, and S. Borkar, "High-performance and low-power challenges for sub-70 nm microprocessor circuits," in Proceedings of the IEEE Custom Integrated Circuits Conference, pp. 125–128, May 2002.

[12] R. Jacob Baker, CMOS Circuit Design, Layout and Simulation, IEEE Press, John Wiley & Sons, 3rd edition, 2010.

International Journal of Engineering Research and General Science Volume 3, Issue 6, November-December, 2015
ISSN 2091-2730

Message and Signature Conveyance System using NTRUSign

N. Sravan Kumar* P. Alee Mulla Khan#
*M.Tech Scholar, CSE Dept, Vignan's Institute of Information Technology, Visakhapatnam.
#Assistant Professor, CSE Dept, Vignan's Institute of Information Technology, Visakhapatnam.
*nagirisravankumar@gmail.com #p_aleekhan@yahoo.co.in

Abstract-Information Security is the investigation of hops that give the assurance of the data in the framework, mobiles and PDAs against unapproved access, use, change, and so forth. A Digital Signature is the condition utilized for stamping or marking an electronic file, by a procedure intended to be similar to paper marks, yet which makes utilization of an innovation known as open key cryptology. In this paper, we propose and test NTRU Signature the calendars for variable evaluated substance records, utilizing polynomial cryptosystems with a blend of the adjusted new cryptosystem. The algorithm exhibited in this paper can be utilized for both signature generation and for giving information classification not at all like a couple of different algorithms chipping away at polynomial arithmetic. NTRU Cryptosystems has passed on a few translations of the NTRU Algorithms, of which the essential algorithm was executed for this utilization.

Keywords-Authentication, Digital Signature, new cryptosystem, NSS, NTRU, PDA and polynomial.

I. INTRODUCTION

Information security (IS) is designed to protect the confidentiality, integrity and availability of system data from those with malicious purposes. Cryptography involves creating written or generated codes that allows information to be kept confidential. Cryptography converts data into a format that is unreadable for an unauthorized user, permitting it to be transmitted without anyone decoding it back into a readable format, therefore compromising the data.

Information security uses cryptography on several levels. The data cannot be read without a key to decipher it. The information keeps up its integrity during transportation and while being stored. Cryptography as well aids in non-renunciation. This implies that neither the creator nor the recipient of the data may claim they did not create or receive it.

Data Encryption is a process that applies operations or mathematical functions on data for difficult to understand it. Data encryption is very important to protect the various types of personal information and confidential information stored in the smartphone.

Data Authentication is the procedure of an overseer allowing the rights and the procedure of checking user account consents for access to information or data are both alluded to as approval.

The NTRU public key cryptosystem was developed in 1996 at Brown University by three mathematicians J. Hoffstein, J.Pipher and J.H. Silverman [6]. It is not that much popular cryptosystems like RSA, ECC and other traditional. The major advantages of NTRU cryptosystem are much faster generating key, encryption time and decryption time as compared to others [3][4].

It is easily compatible with mobile devices and other portable devices. It is theoretically proposed here. The Kid-RSA is a public-key cipher system proposed by Neal Koblitz [5] for pedagogic purposes and published in 1997. The new crypto-system is very simple.

II MOTIVATION

In any open cryptography, we need affirmed Public Key(s) and Private Key(s) to scramble/unscramble for any message at without fall flat. That infers there are various arrangements of Public Keys and Private Keys are required to encryption/interpret message(s) in this cryptosystem. Our objective is not to make various open keys with respect to related particular Private Keys. Our proposed calculation creates simply Public Key joined with Private Keys.

It sign the message once recipient not under any condition like other open crypto algorithm. If time "t" is required for encoding a message for each encryption procedure, out in the open crypto figuring, the total encryption time is N*t times for "N" number of recipients. This estimation needs just "t" time for any number of recipients.

The Recipient can translate message using their own accepted Private Key. The basic ideal position of our novel algorithm is to extra more encryption time and computational power. Thusly, the proposed, figuring is profitable and reasonable in regards to computational time.

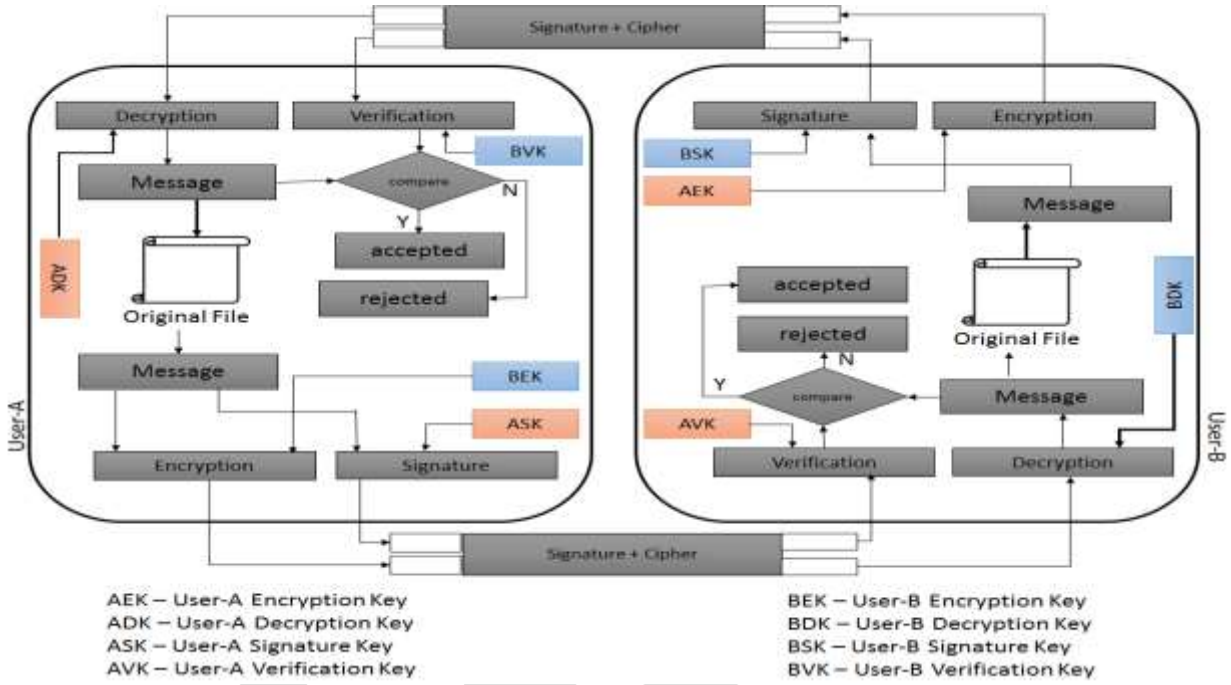

Fig. 1 Message, Signature Conveyance System Architecture

III. PROPOSED SYSTEM

NTRU Signature is defined similarly as set Of R polynomials of degree completely not as much as N and having entire number coefficients. The parameter N is settled. The vital operations on these polynomials are development and convolution duplication. Convolution expands * of two polynomials f and g is described by taking the coefficient of X^k in f*g to meet.

In more numerical terms, R is the quotient ring R = Z[X]/ (X^N-1). If one of the polynomials has all coefficients looked over the set {-1, 0, 1} we will insinuate the convolution as being twofold [7]. If coefficients of the polynomials are reduced modulo q for some q, we will suggest the convolution as being specific.

$$f(x) * g(x) = \sum_{i+j=1 \bmod N}^{\infty} (f(x).g(x)) \quad (0 \leq k < N)$$

We will likewise need to round numbers to the closest whole number and to take their partial parts. For any fits in with Q, let [a] mean the whole number nearest to a, and characterize {a} =a-[a]. On the off chance that A will be a polynomial with rational or (real) coefficients, let [A] and {A} be A with the showed operation connected to every coefficient [1].

The sender generates random large values for creating two keys for Encryption. The A new cryptosystem designed using a KID crypto system is modified for encryption by generating two extra-large two values (r_1, r2). The sender takes message which should be less than n. The sender sends message using receiver public key (d, n). The receiver decrypts cipher with his private key (e1, e2, n).The Entire system model is illustrated in the figure 1.

IV. IMPLEMENTATION

In our system, we propose two algorithms for signature and encryption process. In this one is NTRU Sign for Signature and another is a new cryptosystem for Encryption. Here, we compare the complexity and speed of the system in a practical way. Consider the two users (User-A, User-B), whose wants transfer the files using the message conveyance system.

NTRU Signature Scheme (NSS):

The key calculation incorporates the deviation between two polynomials. Let f(X) and g(X) be two polynomials in R. We are first lessening their coefficients modulo q to lie in the range between −q/2 to q/2, then we reduce their coefficients modulo p to lie in the degree between −p/2 and p/2. Let

$$f(X) = f_0+f_1X +\cdot\cdot\cdot+f_{N-1}X^{N-1} \text{ and}$$
$$g(X) = g_0+\cdot\cdot\cdot+g_{N-1}X^{N-1}$$

be these reduced polynomials. Then the deviation of a and b is Dev(f, g) = {i : $f_i \neq g_i$}. Intuitively, Dev(a, b) is the number of coefficients of a mod q and b mod q that differ modulo p.

Key Generation: User-A picks two polynomials f and g has the suitable form (2). He processes the opposite f^{-1} of f modulo q. The Weave's open verification key is the polynomial $h \equiv f^{-1} * g \bmod q$ and his private marking key is the pair(f, g)

Signing: User-A's document is a polynomial m modulo p. User-A chooses a polynomial w ∈ Fw of the form $w = m + w_1 + pw_2$, where w_1 and w_2 are small polynomials whose precise form we will describe later. He then computes $s \equiv f * w \pmod q$.User-A's signed message is the pair (m, s).

Verification: In order to verify User-A's signature s on the message m, User-B first checks that $s \neq 0$ and then User-B verifies the following two conditions:
(1) User-B compares s to $f_0 * m$ by checking if their deviation satisfies

$$D_{min} \leq Dev(s, f_0 * m) \leq D_{max}.$$

(2) User-B uses User-B's public verification key h to compute the polynomial

$$t \equiv h * s \pmod q,$$

putting the coefficients of t into the range [−q/2, q/2] as usual. She then checks if the deviation of t from $g_0 * m$ satisfies

$$D_{min} \leq Dev(t, g_0 * m) \leq D_{max}.$$

If a User-A's signature passes tests (1) and (2), then User-B accepts it as valid

New Cryptosystem:
Key Generation: The User-A generates random values as parameters such as x, y, P, Q, r1, r2 in secure way. By using these parameters the key generation algorithm computes private key and public key as following key generation algorithm.
Step 1: Start
Step 2: Read Random values x, y, P, Q
Step 3**:** Calculate constant = xy-1
Step 4: Calculate m_1 = (P * constant) +x
Step 5: Compute m_2 = (Q * constant) +y
Step 6: Calculate n = ((m_1 * m_2) -1)/constant
Step 7: e1 = (m_1+r_1) mod n (gcd (m_1+r_1, n) = 1mod n)
Step 8: d = (m_2+r_2) mod n (gcd (m_2+r_2, n) = 1mod n)
Step 9: m = (r_1r_2+1+ m_1r_2+m_2r_1) mod n
Step 10:e2 = m^{-1} mod n
Step 11: if gcd (m, n)! =1 mod n
Go to Step 7
Step 12: Public Key (d, n)
Step 13: Private Key (e_1, e_2, n)
Step 14: return Public Key, Private Key
Step 15: Stop

Encryption: The User-B wants to send message to User-A. The User-B computes the cipher text using the User-A's public key, i.e., (d, n) as following way.
Step 1: Start

Step 2: Read User-A public key (d, n)
Step 3**:** read message (message< n)
Step 4: Compute cipher text = (message * d) (mod n)
Step 5: return cipher text
Step 6: stop

Decryption: After User-A receives cipher text from the User-B, it needs to decipher the code word. The User-A decrypts the cipher text by using the User-A's private key, i.e., (e_1, e_2, n) as following way.
Step 1: Start
Step 2: Read User-A private key (e_1, e_2, n)
Step 4: Compute message = (cipher text * e_1 * e_2) (mod n)
Step 5: return cipher text
Step 6: stop

V. SECURITY ANALYSIS

NSS Analysis:
Test (1): The polynomial s that User-B tests is compatible to the product
s = f * w (mod q)
= (f_0 + pf1) (m + w_1 + p *w_2) (mod q)
= f_0 * m + f_0 * w_1 + pw_2 + pf_1 * w (mod q)

We see that i^{th} coefficients of s and f0 .m will concur modulo p unless one of the accompanying circumstances happens:
– The i^{th} coefficient of f_0 * w1 is nonzero.
– The i^{th} coefficient of f * w is outside the reach (- q/2, q/2], so varies from the i^{th} coefficient of s by some multiple of q.

In the event that the required variables and test spaces are selected appropriately, then there will be in any event D_{min} and at most D_{max} deviations between s mod p and m mod p. Subsequently User-A's mark breezes through test.

Test (2): The polynomial t is given by t = h * s = (f^{-1} * g) * (f *w) =g * w (mod q):
Since g has the same structure as f, the same thinking with respect to test (1) demonstrates that t will finish test (2).

New Cryptosystem Analysis:
At Encryption side, User-B uses User-A's public key (d, n). In cryptosystem, d equals to the m_2+r_2 and multiply with message.

Cipher = (Message * d) mod n

At Decryption side, User-A uses his private key (e_1, e_2, n). In cryptosystem, e_1 equals to the m_1+r_1 and multiply with cipher.

(Cipher * e1*e2) mod n = (Message *d *e1*e2) mod n
= Message

VI. EXPERIMENTAL RESULTS

We have implemented NSS, new cryptosystem in Java and run it on various platforms. The Figure (2), (3) describes the performance of NSS and new cryptosystem respectively, on a desktop machine which has the features such Intel i3 4th generation with speed of 1.70 GHz and cache size 3.0MB.

For NSS, we are using the basic parameters like that N= 157 (Highest degree of polynomial). The p and q are must be follows the gcd(p,q) = 1. Hence, the values of p and q are 256 and 29 respectively. The experimental results of signature generation and verification are shown in Table (1) graphically evaluated in figure 2.

NSS Signature Time for process		
File Size (kb)	Signature (m.Sec)	Verification (m.Sec)
0.25	3	2
0.5	6	3

1	7	4
2	8	5
10	10	6

Table 1: NSS time space evaluation

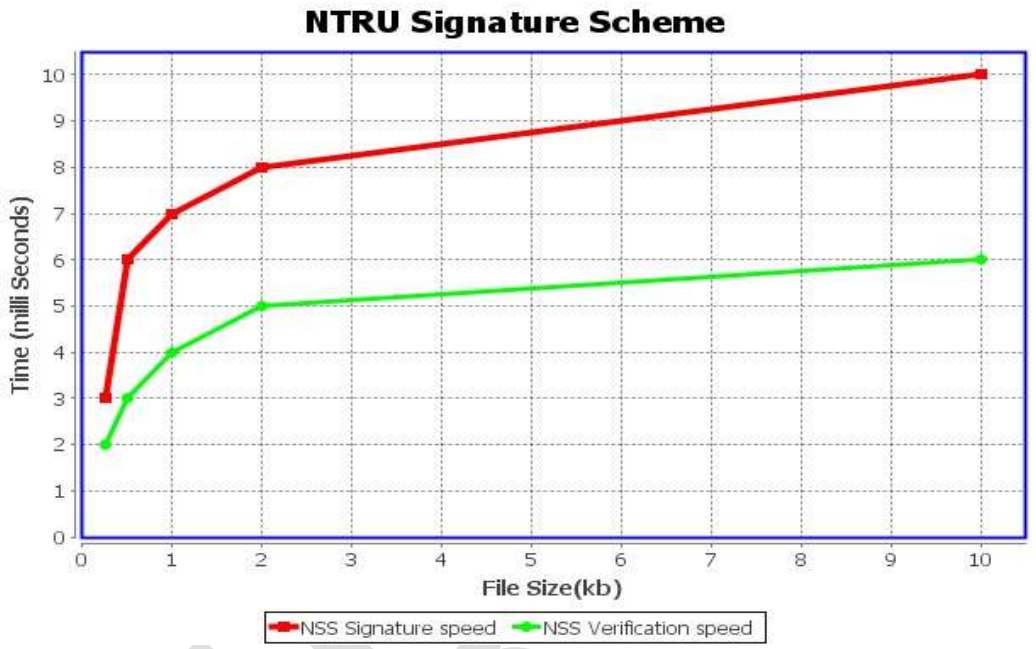

Fig. 2 Graph for time space of NSS Signing, verifying

For new cryptosystem, we consider the parameters random BigInteger (with Bit Length of 512). In our proposed system, it consider the block size 128 bytes. The Results are shown in the Table (2) and graphically evaluated in figure 3.

Encryption Time for Process		
File Size (kb)	Encryption (m.Sec)	Decryption (m.Sec)
0.25	2	1
0.5	3	1
1	5	3
2	14	7
10	65	15

Table 2: New Cryptosystem time space evaluation

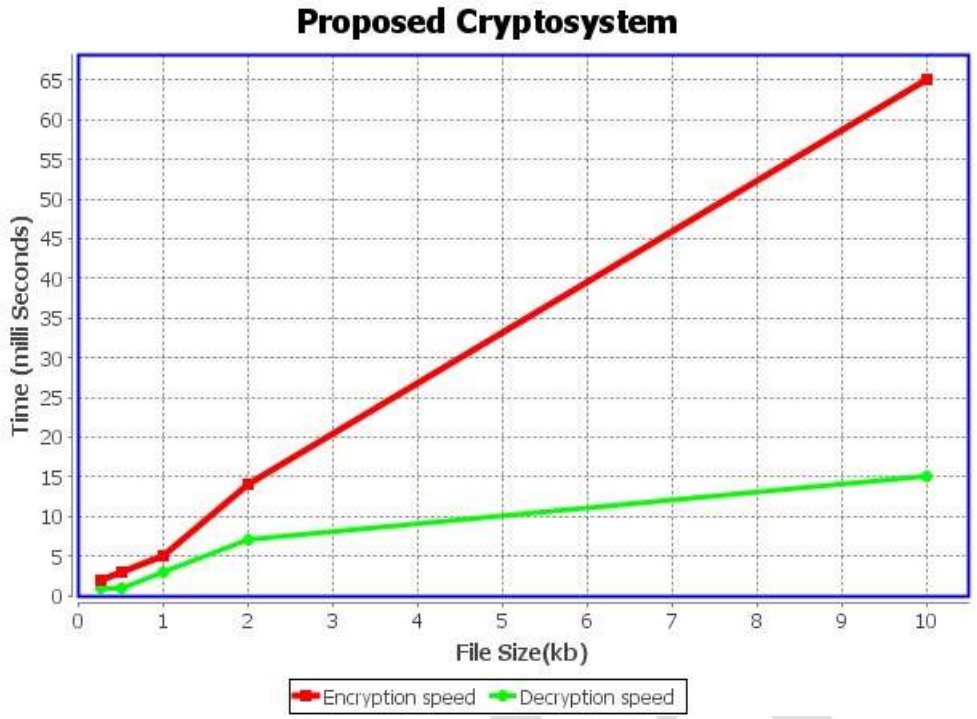

Fig. 3 Graph for time space of New Proposed System Encryption, Decryption

VI. CONCLUSION

The NSS calculation exhibited in this paper can be used for both sides signature generation and for giving data security not in any manner like several unique counts taking a shot at polynomial number juggling. In this paper, security and capability examination showed that the NTRU Signature estimation with blend of new encryption system. Here proposed new encryption algorithm give the security, versatile quality. In this way, our computation is a good contender for the security of records. Finally, the movements of the use of this calculation are illuminated. Lattice is one of the existing quantum-secure cryptographic primitive.

REFERENCES:

[1] Jeff Hoffstein, Nick Howgrave-Graham, Jill Pipher, William Whyte "Practical lattice based cryptography: NTRU Encrypt and NTRU Sign", part of series Information Security and Cryptography pp 349-390
[2] Amandeep Kaur Gill, Charanjit Singh "Implementation of NTRU Algorithm for the Security of N-Tier Architecture" in volume4 pp 417-462
[3] Divyajyothi M G, Rachappa, Dr. D H Rao "Techniques of Lattice Based Cryptography Studied on a Pervasive Computing Environment" in Vol.5, No.4, August 2015
[4] Ranjeet Ranjan, Dr. A. S. Baghel, Sushil Kumar "Improvement of NTRU Cryptosystem" Volume 2, Issue 9, September 2012
[5] http://www.usna.edu/Users/math/wdj/_files/documents/sm473-capstone/sm473-crypto-lecture-notes.pdf pp 63-65
[6] http://en.wikipedia.org/wiki/NTRU_Cryptosystems,_Inc
[7] Jeffrey Hoffstein, Jill Pipher, Joseph H. Silverman "NSS: The NTRU Signature Scheme" Advances in Cryptology—Eurocrypt, 2001 – Springer

International Journal of Engineering Research and General Science Volume 3, Issue 6, November-December, 2015
ISSN 2091-2730

Fourier-Laplace Transforms of Some Special Functions

V. D. Sharma[1] and A. N. Rangari[2]

[1]Mathematics Department, Arts, Commerce and Science College, Amravati- 444606(M.S), India.
vdsharma@hotmail.co.in

[2] Mathematics Department, Adarsh College, Dhamangaon Rly.- 444709 (M.S), India.

ABSTRACT— During the last decade or so there have been significant generalizations of the idea of integral transforms. Many new uses of the transform method in engineering and physics applications are found. Some of these new applications have prompted the development of very specialized transforms, their roots, knowledge of the properties and uses of classical integral transforms, such as Fourier Transform and Laplace transform and having considered that they are as important today they have been for the last century or so, they have been given a more extensive treatment. The main aim of this paper is to find the Fourier-Laplace transforms of some special functions and this will be used for solving various differential and integral equations.

KEYWORDS— Fourier transform, Laplace transform, Fourier-Laplace transform, Integral Transform, Differential Equation, Parameter, Generalized function.

1. INTRODUCTION

The transform is a method to convert a signal from one domain to another domain for extracting some other information contained in the signal which cannot be extracted from the signal in first domain. One of the important families of transforms is 'Integral Transform'. Actually, integral transform is an operator used to transform a signal into its equivalent form with the help of a 'kernel' function by integrating the kernel multiplied signal. The integration process involved in transformation has conferred the name as 'Integral Transform'.

Fourier transforms play an important part in the theory of many branches of science. A waveform-optical, electrical or acoustical- and its spectrum are appreciated equally as physically picturable and measurable entities, an oscilloscope enables us to see an electrical waveform and a spectroscope or spectrum analyzer enables us to see optical or electrical spectra [1]. Our acoustical appreciation is even more direct, since the ear hears spectra. Wave forms and spectra are Fourier transforms of each other; the Fourier transformation is thus an eminently physical relationship.

The theory of Laplace transforms referred to as operational calculus has in recent years become an essential part of the mathematical background required of engineers, physicists, mathematicians and other scientist. This is because in addition to being of great theoretical interest in itself, Laplace transform methods provide easy and effective means for the solution of many problems arising in various fields of science and engineering [2].

So these Fourier and Laplace transforms have various uses in many fields separately. On combining these two transforms i.e. Fourier-Laplace transforms also used for solving differential and integral equations. In this paper we find the Fourier-Laplace transform of some special functions which is help for solving differential equations. This paper is planned as follows:

Preliminary results are given in section 2. In section 3, we have find the Fourier-Laplace transform of some special functions. Lastly conclusions are given in section 4. Notations and terminology as per Zemanian. [3], [4].

2. PRELIMINARY RESULTS

The Fourier transform with parameter s of $f(t)$ denoted by $F[f(t)] = F(s)$ and is given by

$$F[f(t)] = F(s) = \int_{-\infty}^{\infty} e^{-ist} f(t)dt \text{ , for parameter } s > 0 . \tag{2.1}$$

The Laplace transform with parameter p of $f(x)$ denoted by $L[f(x)] = F(p)$ and is given by

$$L[f(x)] = F(p) = \int_{0}^{\infty} e^{-px} f(x)dx \text{ , for parameter } p > 0 . \tag{2.2}$$

The Conventional Fourier-Laplace transform is defined as

$$FL\{f(t,x)\} = F(s,p) = \int_{-\infty}^{\infty}\int_{0}^{\infty} f(t,x)K(t,x)dtdx \ , \tag{2.3}$$

where, $K(t,x) = e^{-i(st-ipx)}$.

3. FOURIER-LAPLACE TRANSFORMS OF SOME SPECIAL FUNCTIONS

3.1. If $FL\{f(t,x)\}(s,p)$ denotes generalized Fourier-Laplace transform of $f(t,x)$ then

$$FL\{1\} = \frac{-i}{sp}$$

Proof:- We have

$$FL\{f(t,x)\} = \int_0^{\infty}\int_0^{\infty} e^{-i(st-ipx)} f(t,x)dtdx$$

$$FL[1] = \int_0^{\infty}\int_0^{\infty} e^{-i(st-ipx)}(1)dtdx$$

$$= \int_0^{\infty} e^{-ist}dt.\int_0^{\infty} e^{-px}dx$$

$$= \left[\frac{e^{-ist}}{-is}\right]_0^{\infty}.\left[\frac{e^{-px}}{-p}\right]_0^{\infty} = \frac{-1}{is}\left[e^{-ist}\right]_0^{\infty}.\left(\frac{-1}{p}\right)\left[e^{-px}\right]_0^{\infty}$$

$$= \frac{1}{isp}[0-1][0-1] = \frac{1}{isp} = \frac{-i}{sp}$$

$$\therefore FL[1] = \frac{-i}{sp}$$

3.2. If $FL\{f(t,x)\}(s,p)$ denotes generalized Fourier-Laplace transform of $f(t,x)$ then

$$FL\{(\delta(t-a)\delta(x-b))\} = K(a,b,s,p)$$

Proof: $FL\{(\delta(t-a)\delta(x-b))\} = \int_0^{\infty}\int_0^{\infty} e^{-i(st-ipx)}\{(\delta(t-a)\delta(x-b))\}dtdx$

$$= \int_0^{\infty}\delta(t-a)e^{-ist}dt\int_0^{\infty}\delta(x-b)e^{-px}dx$$

$$= e^{-isa}.e^{-pb} = e^{-i(sa-ipb)} = K(a,b,s,p)$$

We know that $\int_0^{\infty} \delta(t-a)\phi(t)\,dt = \phi(a)$ Also $\int_0^{a} \delta(t-a)\phi(t)\,dt = \phi(a)$

$$\therefore FL\left\{\left(\delta(t-a)\delta(x-b)\right)\right\} = K(a,b,s,p)$$

3.3. If $FL\{f(t,x)\}(s,p)$ denotes generalized Fourier-Laplace transform of $f(t,x)$ then

$$FL\{tx\} = \frac{-1}{s^2 p^2}$$

Proof: $$FL\{tx\} = \int_0^{\infty}\int_0^{\infty} e^{-i(st-ipx)}(tx)\,dtdx$$

$$= \int_0^{\infty} e^{-ist}t\,dt . \int_0^{\infty} e^{-px}x\,dx$$

$$= \left[\left(t\frac{e^{-ist}}{-is}\right)_0^{\infty} - \int_0^{\infty} 1\frac{e^{-ist}}{-is}dt\right].\left[\left(x\frac{e^{-px}}{-p}\right)_0^{\infty} - \int_0^{\infty} 1\frac{e^{-px}}{-p}dx\right]$$

$$= \left[(0-0) + \frac{1}{is}\int_0^{\infty} e^{-ist}dt\right].\left[(0-0) + \frac{1}{p}\int_0^{\infty} e^{-px}dx\right]$$

$$= \frac{1}{isp}\left[\frac{e^{-ist}}{-is}\right]_0^{\infty}\left[\frac{e^{-px}}{-p}\right]_0^{\infty}$$

$$= -\frac{1}{s^2 p^2}(0-1)(0-1) = -\frac{1}{s^2 p^2}$$

$$\therefore FL\{tx\} = \frac{-1}{s^2 p^2}$$

3.4. If $FL\{f(t,x)\}(s,p)$ denotes generalized Fourier-Laplace transform of $f(t,x)$ then

$$FL\{t^n x^n\} = \frac{(-1)^{-n-1}(i)^{-n-1}(n!)^2}{s^{n+1}p^{n+1}}$$

Proof: $$FL\{t^n x^n\} = \int_0^{\infty}\int_0^{\infty} e^{-i(st-ipx)}(t^n x^n)\,dtdx$$

$$= \int_0^\infty e^{-ist} t^n dt . \int_0^\infty e^{-px} x^n dx$$

$$= \left[\left(t^n \frac{e^{-ist}}{-is} \right)_0^\infty - \int_0^\infty n t^{n-1} \frac{e^{-ist}}{-is} dt \right] . \left[\left(x^n \frac{e^{-px}}{-p} \right)_0^\infty - \int_0^\infty n x^{n-1} \frac{e^{-px}}{-p} dx \right]$$

$$= \left[0 + \frac{n}{is} \int_0^\infty t^{n-1} e^{-ist} dt \right] . \left[0 + \frac{n}{p} \int_0^\infty x^{n-1} e^{-px} dx \right]$$

$$= \frac{n}{is} \left[\left(t^{n-1} \frac{e^{-ist}}{-is} \right)_0^\infty - \int_0^\infty (n-1) t^{n-2} \frac{e^{-ist}}{-is} dt \right] . \frac{n}{p} \left[\left(x^{n-1} \frac{e^{-px}}{-p} \right)_0^\infty - \int_0^\infty (n-1) x^{n-2} \frac{e^{-px}}{-p} dx \right]$$

$$= \left[\frac{n}{is} \frac{(n-1)}{is} \int_0^\infty t^{n-2} e^{-ist} dt \right] . \left[\frac{n}{p} \frac{(n-1)}{p} \int_0^\infty x^{n-2} e^{-px} dx \right]$$

$$\vdots$$

$$\vdots$$

$$= \left[\frac{n(n-1)(n-2)(n-3)\cdots\cdots 2.1}{(is)^n} \int_0^\infty e^{-ist} dt \right] \left[\frac{n(n-1)(n-2)(n-3)\cdots\cdots 2.1}{(p)^n} \int_0^\infty e^{-px} dx \right]$$

$$= \frac{n!}{(is)^n} \left(\frac{e^{-ist}}{-is} \right)_0^\infty \frac{n!}{(p)^n} \left(\frac{e^{-px}}{-p} \right)_0^\infty$$

$$= \frac{(n!)^2}{(is)^{n+1} p^{n+1}} = \frac{(-1)^{-n-1} (i)^{-n-1} (n!)^2}{s^{n+1} p^{n+1}}$$

$$\therefore FL\{t^n x^n\} = \frac{(-1)^{-n-1} (i)^{-n-1} (n!)^2}{s^{n+1} p^{n+1}}$$

3.5. If $FL\{f(t,x)\}(s,p)$ denotes generalized Fourier-Laplace transform of $f(t,x)$ then

$$FL\{e^{at+bx}\} = \frac{1}{(is-a)(p-b)}$$

Proof: $FL\{e^{at+bx}\} = \int_0^\infty \int_0^\infty e^{-i(st-ipx)} (e^{at+bx}) dt dx$

$$= \int_0^\infty e^{-ist} e^{at}\, dt . \int_0^\infty e^{-px} e^{bx}\, dx$$

$$= \int_0^\infty e^{-(is-a)t}\, dt . \int_0^\infty e^{-(p-b)x}\, dx$$

$$= \left(\frac{e^{-(is-a)t}}{-(is-a)} \right)_0^\infty \left(\frac{e^{-(p-b)x}}{-(p-b)} \right)_0^\infty = \frac{1}{(is-a)(p-b)}$$

$$\therefore FL\left\{ e^{at+bx} \right\} = \frac{1}{(is-a)(p-b)}$$

3.6. If $FL\{ f(t,x) \}(s,p)$ denotes generalized Fourier-Laplace transform of $f(t,x)$ then

$$FL\{ \sin at \sin bx \} = \frac{ab}{(a^2 - s^2)(b^2 + p^2)}$$

Proof: $FL\{ \sin at \sin bx \} = \int_0^\infty \int_0^\infty e^{-i(st-ipx)} (\sin at \sin bx)\, dt dx$

$$= \int_0^\infty e^{-ist} \sin at\, dt . \int_0^\infty e^{-px} \sin bx\, dx$$

$$= \left(e^{-ist} \frac{(-is \sin at - a \cos at)}{a^2 - s^2} \right)_0^\infty \left(e^{-px} \frac{(-p \sin bx - b \cos bx)}{b^2 + p^2} \right)_0^\infty$$

$$= \left(0 + \frac{a}{a^2 - s^2} \right) \left(0 + \frac{b}{b^2 + p^2} \right) = \frac{ab}{(a^2 - s^2)(b^2 + p^2)}$$

$$\therefore FL\{ \sin at \sin bx \} = \frac{ab}{(a^2 - s^2)(b^2 + p^2)}$$

3.7. If $FL\{ f(t,x) \}(s,p)$ denotes generalized Fourier-Laplace transform of $f(t,x)$ then

$$FL\{ \cos at \cos bx \} = \frac{isp}{(a^2 - s^2)(b^2 + p^2)}$$

Proof: $FL\{\cos at\cos bx\} = \int_0^\infty\int_0^\infty e^{-i(st-ipx)}(\cos at\cos bx)\,dtdx$

$$= \int_0^\infty e^{-ist}\cos at dt.\int_0^\infty e^{-px}\cos bx dx$$

$$= \left(e^{-ist}\frac{(-is\cos at + a\sin at)}{a^2-s^2}\right)_0^\infty \left(e^{-px}\frac{(-p\cos bx + b\sin bx)}{b^2+p^2}\right)_0^\infty$$

$$= \left(0+\frac{is}{a^2-s^2}\right)\left(0+\frac{p}{b^2+p^2}\right) = \frac{isp}{(a^2-s^2)(b^2+p^2)}$$

$$\therefore FL\{\cos at\cos bx\} = \frac{isp}{(a^2-s^2)(b^2+p^2)}$$

FOURIER-LAPLACE TRANSFORMS OF SOME ELEMENTARY FUNCTIONS

Sr. No.	$f(t,x)$	$FL\{f(t,x)\} = F(s,p)$
1	1	$\frac{-i}{sp}$
2	$\delta(t-a)\delta(x-b)$	$e^{-i(sa-ipb)} = K(a,b,s,p)$
3	tx	$\frac{-1}{s^2p^2}$
4	$t^n x^n$	$\frac{(-1)^{-n-1}(i)^{-n-1}(n!)^2}{s^{n+1}p^{n+1}}$
5	e^{at+bx}	$\frac{1}{(is-a)(p-b)}$
6	$\sin at\sin bx$	$\frac{ab}{(a^2-s^2)(b^2+p^2)}$
7	$\cos at\cos bx$	$\frac{isp}{(a^2-s^2)(b^2+p^2)}$
8	$\sinh(at)\sinh(bx)$	$\frac{-ab}{(s^2+a^2)(p^2-b^2)}$
9	$\cosh(at)\cosh(bx)$	$\frac{-isp}{(s^2+a^2)(p^2-b^2)}$

4. CONCLUSION

In this work we have find the Fourier-Laplace transforms of some special functions and this will be used for solving various differential and integral equations.

REFERENCES:

[1] Anumaka, M.C., "Analysis and applications of Laplace/Fourier transformations in electric circuit," IJRRAS, 12(2), August 2012.

[2] Thomson, W.T., "Laplace Transformation (2nd Edition)," Prentice-Hall, 1960.

[3] Zemanian, A. H., "Generalized integral transform," Inter science publisher, New York, 1968.

[4] Zemanian A.H., "Distribution theory and transform analysis," McGraw Hill, New York, 1965.

[5] Khairnar, S.M., Pise, R.M. and Salunke, J. N., "Applications of the Laplace-Mellin integral transform to differential equations," International Journal of Scientific and Research Publications, 2(5) pp. 1-8, (2012).

[6] Sharma, V.D. and Rangari, A.N., "Generalization of Fourier-Laplace transforms," Archives of Applied Science Research, 4(6), pp. 2427-2430, (2012).

[7] Sharma, V.D. and Rangari, A.N., "Operation Transform Formulae of Fourier-Laplace Transform," Int. Journal of Pure and Applied Sciences and Technology, 15(2), pp. 62-67, (2013).

[8] Debnath Lokenath and Bhatta Dambaru, "Integral Transforms and their Applications," Chapman and Hall/CRC Taylor and Francis Group Boca Raton London, New York, 2007.

[9] Sharma, V.D. and Khapre S.A., "Applications on Generalized Two-Dimensional Fractional Cosine Transform," Int. Journal of Engineering and Innovative Technology (IJEIT), Vol.3, Issue 4, pp. 139-143, October 2013.

[10] Sharma, V.D. and Khapre, S.A., "Some examples on generalized two-dimensional fractional cosine transform in the range $-\infty$ to $+\infty$," International Journal of science and research, Vol. 3, Issue 8, pp. 1199-1202, August 2014.

[11] Sharma, V.D., "Operation Transform Formulae on Generalized Fractional Fourier Transform," Proceedings International Journal of Computer Applications (IJCA), (0975-8887), PP. 19-22, 2012.

[12] Sharma, V.D. and Deshmukh, P.B., "Operation Transform formulae for Two-Dimensional Fractional Mellin transform," International Journal of science and research, Vol.3, Issue 9, pp. 634-637, Sept. 2014.

[13] Gupta Anupama, "Fourier Transform and Its Application in Cell Phones," International Journal of Scientific and Research Publications, Volume 3, Issue 1, pp. 1-2 January 2013.

[14] Beerends, R. J., ter Morsche, H. G., van den Berg, J. C. and van de Vrie, E. M., "Fourier and Laplace Transforms," Cambridge University Press, 2003.

[15] Fitzsimmons Patrick and Mc EL Roy Tucker, "On Joint Fourier-Laplace Transforms," Communication in statistics-Theory and Methods, 39: 1883-1885 Taylor and Francis Group, LLC, 2010.

International Journal of Engineering Research and General Science Volume 3, Issue 6, November-December, 2015
ISSN 2091-2730

Survey paper for keyword Search over RDBMS

Vaibhav Ambavkar, Venkatesan N.

SKN SIT's Lonavla,Vaibhav.ambavkar@vpmmpcoe.org and 7066384889

Abstract— Keyword search (KWS) over relational databases has recently received significant attention. Many solutions and many prototypes have been developed. This task requires addressing many issues, including robustness, accuracy, reliability, and privacy. An emerging issue, however, appears to be performance related current KWS systems have unpredictable running times. In particular, for certain queries it takes too long to produce answers, and for others the system may even fail to return. we say that as today's users have been spoiled by the performance of Internet search engines, KWS systems should return whatever answers they can produce quickly and then provide users with options for exploring any portion of the answer space not covered by these answers. basic idea is to produce answers that can be generated quickly as in today's KWS systems, then to show users query forms that characterize the unexplored portion of the answer space. Combining KWS systems with forms allows us to bypass the performance problems inherent to KWS without compromising query coverage. This project uses the concepts of Priority Queue Data Structure to build a framework for developing, Testing and applying search algorithms on large volume of data streams.

Keywords— Keyword Search, Keyword Priority, Keyword Indexing, Doument Search, Document Indexing, Keyword Asociation, Object Summerization, Keyword Recommendation.

INTRODUCTION

The success of search engines demonstrates that untrained users are comfortable using keyword search to find documents of interest to them. Over the past decade, this success has made tremendous interest in keyword search (KWS) over relational databases, in order to accommodate users who cannot issue a formal structured query or are unaware of the database schema.DBXplorer [12], DISCOVER, and BANKS [2] were among the first systems that supported keyword search over relational databases, and many other systems have since been developed. As more structured data becomes available at organizations and on the Web, and as more untrained users want to use such data. Building such systems requires addressing many issues, including robustness, accuracy, reliability, and privacy.

The current KWS solutions have unpredictable performance issues. Specifically, while the systems produce answers quickly for many queries, for many others they take an unacceptably long time, or even fail to produce any answer after exhausting memory. Clearly, such a performance profile is unacceptable for a real-world system. The system should then allow for a way for the user to explore this portion of the answer space should he or she choose to do so. one way to do so is to provide form interfaces to characterize the yet-unexplored answer space. the above two requirements of time limit and overview of the yet-unseen can help increase the chances that the KWS system will be perceived as useful and will be widely adopted by real-world customers.

A keyword search is a basic search technique that involves searching for one or more words within a collection of documents. Typically, a keyword search involves a user typing their search request, or query, into a search engine such as Google, which then returns only those documents that contain the search terms entered. The documents returned by the search engine are called the search results.

Keyword Search Techniques & Keyword Search Tools

Keyword search normal parameters

The syntax in the search string. Use of the keywords with or without stemming. Use of keywords with certain wildcard specifications and the syntax for said wildcards. Case-sensitivity of keywords used in searches and whether the keyword should match both cases; and The target data sources to be searched. Whether the query can be applied to any specific fields such as email To/From or Subject. Whether the query can be applied to any specific date range such as an email Sent Date between the date ranges of January 1, 2001 through December 31, 2001.

Assumed Parameters

The character encoding of the text UTF-8, UTF-16, CP1252, Unicode/Wide Char etc. Language of the keyword, to select appropriate stemming. Any special handling of characters such as diacritics, accents etc. If de-compounding of the keyword needs to be performed, usually when working with languages such as German. If there is a set of special characters, what the special characters are, and how an escape character is specified. If there is a tokenization scheme present, what the token delimiters are, and the impact of tokenization on search ability of documents. Searches may not be precise when these tokenization characters are present in the keyword.

Phrase Search

The following should be considered when conducting a phrase search: Phrases that contain a double-quote in any of its keywords require escaping of the double quote. Example: to search for the quoted expression: He said: don't do it.

Wildcard Specifications

Single character wildcard x?y matches all strings that begin with substring x, end with substring y, and have exactly one-character in between x and y Multiple-character wildcard x*y matches all strings that begin with substring x, end with substring y, and have 0 or more characters between x and y.

Truncation Specification

Truncation specification is one way to match word variations. Truncation allows for the final few characters to be left unspecified. Truncation is specified using the following syntax's! matches all strings that begin with substring x. !x matches all strings that end with substring x. x! y when specified within a phrase, the truncated match on the words with !, and exact match on the others.

Stemming Specifications

Stemming specification is another method for matching word variations. Stemming is the process of finding the root form of a word. The stemming specification will match all morphological inflections of the word, so that if you enter the search term sing, the stemming matches would include singing, sang, and song. Note that even though a stemming search will return singing for a search term of sing, this is different from wildcard search. A wildcard search for sing* will not return sang or song, while it will return Singsong. x matches all morphological variations (inflections) of the word. Exactly how a search implementation identifies these inflections is not specified. x y when specified within a phrase, the stemming variations match on the words with , and exact match on the others.

Fuzzy Search

Fuzzy search allows searching for word variations such as in the case of misspellings. Typically, such searching includes some form of distance and score computations between the specified word and the words in the corpus. Fuzzy-search(x,s) For the search word x, find fuzzy variations that are within the score s. The score is specified as a value from 0.0 to 1.0, with values closer to 1.0 being a closer match. The word itself, if present, will match with a score of 1.0. Fuzzy-search(x,s,n) For the search word x, find fuzzy variations that are within the score s and limit the results to the top n by score.

Boolean Search

AND This is specified between two keywords and/or phrases, and specifies that both of the items be present for the expression to match. OR This is specified between two keywords and/or phrases, and specifies that either of the two items be present for the expression to match. NOT Negates the truth value of the expression specified after the NOT operator. NOT w/n specifies that the terms and/or phrases to the right of the w/n specification must not be present within the specified number of words. ANDANY This is specified between two keywords and/or phrases, and specifies that items following the ANDANY operator are optional. w/n Connects keywords and/or phrases by using a nearness or proximity specification. The specification states that the two words and/or phrases are within n words of each other, and the two words/phrases can be in either order. the specified number of words implies that there are n-1 intervening other words between the two. Noise words are counted in the specification. Pre/n Connects keywords and/or phrases by using a nearness or proximity specification.

The specification states that the two words and/or phrases are within n words of each other, and the order of the words is important. W/Para The two keywords and/or phrases are found within the same paragraph, and order is not important. pre/Para The two keywords and/or phrases are found within the same paragraph, and order is important. W/sent The two keywords and/or phrases are found within the same sentence, and order is not important. Pre/sent The two keywords and/or phrases are found within the same sentence, and order is important. Start/n the keyword/phrase is present at the start of the document or section, within n words of the start. End/n the keyword/phrase is present at the end of the document or section, within n words of the end.

Synonym Search

Synonyms are word variations that are determined to be synonyms of the word being searched. Such searching includes some form of dictionary or thesaurus based lookup. Synonym search is specified using the operator: synonym-search. Synonym-search(x) For the

search word x, find synonym variations. Synonym search may be combined with other search constructs. Synonym search may also be included as part of a phrase or Boolean construct.

Related Words Search

Related words search allows a legal professional to specify a word and other words that are deemed to be related to it. Typically, such related words are determined as either part of concept search or by statistical co-occurrence with other words. Related word search is specified using the operator related-word-search. Related-word-search(x) For the search word x, find other related words. Related words search may be combined with other search constructs, and be included as part of a phrase, or Boolean constructs.

Concept Search

Concept search allows a legal professional to specify a concept and documents that describe that concept to be returned as the search results. It can be a useful technique to identify potentially relevant documents when a set of keywords are not known in advance. Concept search solutions rely on sophisticated algorithms to evaluate whether certain set of documents match a concept. There are three broad categories of concept search that a legal practitioner may need to understand and evaluate its applicability.

Latent Semantic Indexing

Latent semantic indexing (sometimes also referred to as Latent Semantic Analysis is a technology that analyzes co-occurrence of keyword terms in the document collection. In textual documents, keywords exhibit polysemy (which refers to a single keyword having multiple meanings) as well as synonymy (which refers to multiple words having the same meaning). An additional factor is certain keywords are related to the concept in that they appear together. These relationships can be is-a relationship such as motorcycle is a vehicle or a containment relationship such as wheels of a motorcycle."is-a part "of relationship also can be achieved with the use of latent semantic indexing. it shows the generalized relationship among two or more keywords to map the exact correlation factor among the keywords. it will create index on such a keyword, based on the concept of small keyword set correlation with ranking.

Text Clustering

Text clustering is a technology that analyzes a document collection and organizes the documents into clusters. This clustering is usually based on finding documents that are similar to each other based on words contained within it (such as noun phrases). Text clustering establishes a notion of distance between documents and attempts to select enough documents into the cluster so as to minimize the overall pair-wise distance among all pairs of documents. In the process, new clusters are created from documents that may not belong to a cluster.

Bayesian Classifier

Bayesian classifier is a process of identifying concepts using a certain representative documents in a particular category. As an example, one may select a small sample of responsive documents and feed them to a Bayesian classifier. The classifier then has the ability to discern other responsive documents in the larger collection and place them in a category. Typically, a category is represented by a collection of words and their frequency of occurrence within the document. The probability that a document belongs to a category is based on the product of the each word of the document appearing in that category across all documents. Thus, the learning classifier is able to apply words present in a sample category and apply that knowledge to other new documents. In the e-discovery context, such classifier can quickly place documents into confidential, privileged, responsive documents and other well-known categories.

Concept Search Specification

Effectiveness of concept search in an e-discovery project depends greatly on the type of algorithm used and its implementation. Given multiple different technologies, the EDRM Search specification proposes that a concept search was used for fulfilling a search request and a registered concept-search implementation/algorithm was used, and an identifier (name) of the concept that was used in the search. Concept search is specified using the operator concept-search. Concept-search (concept-implementation, x, vendor-param-1, vendor-param-2,) given a concept x and concept-implementation, locate all documents that belong or describe that concept. Some vendor implementations may require additional parameters. To indicate the type of concept-implementation, concept search vendors are encouraged to register their implementation name. It is not required to disclose the internal algorithms the vendor utilizes to implement the search. Concept search may be combined with other search constructs, and also be included as part of a phrase or Boolean clause.

Occurrence Count

Occurrence count search allows a legal professional to specify theta word appear a certain number of times for the document to be selected. Occurrence count search is specified using the operator occurs. Occurs(x,n) For the search word x, count the number of times it appears, and select the document if the specified occurrence count is matched.

Errors to Avoid

Stemming may cause additional unintended keyword matches. Wildcard expansions may cause results to be overly broad. If tokenization is based on certain text characters being interpreted as delimiters, they may not be searchable as a keyword. Consider

using a phrase as a search. Case-sensitivity may need to be considered carefully. If a word in a document contains a hyphen and the keyword matches any or all of the hyphenated word, depending on how the document is indexed the hyphen may prevent a match. For example, if the keyword is known and the document contains well-known, there is a chance that the search engine will not recognize the two as a match. If the document is structured as a compound document (i.e., has multiple sections such as Title, Body etc.), Keyword-based searches should be performed with care.

Keyword search Tool

These keyword research tools should make it easier to create a list of relevant search terms. we should make sure to create awesome landing pages for keywords you want to be found on. we should also think about cornerstone content articles and a great internal Linking structure in order to make your SEO strategy completes.

Google Ad words Keyword Planner

The Google Ad words Keyword Planner to find new and related keywords, but ignore the search volume data. The search volume data in the planner is really only useful for keywords that actually spending money to advertise on. Otherwise, these volumes are not reliable. While not really helpful to decide which keyword is most used by potential audience, Google Ad words Keyword Planner makes a useful tool in coming up with ideas for potential keywords.

Yoast suggests

Joost developed his own keyword research tool to come up with keywords as well! Yoast Suggests uses the Google Suggest functionality you know from searching in Google. It finds the keyword expansions Google gives and then requests more of them. So if we type any example keyword, it will also give you the expansions for example a till example z etc.

Google Trends

Google Trends allows you to compare the traffic for sets of keywords.

Literature Review

Keyword Search Engine Architecture

A conceptual look at how a general-purpose search engine like Google or Yahoo! might set up their architecture so that these and other new features could be easily added while maintaining overall architecture coherency. This is a purely intellectual exercise - no doubt each of the major search engines will evolve their own strategy and architecture to deal with these issues.

Query Interface

One key change to the query interface in the future is the likely addition of search parameters, which can use the magic of Ajax to appear automatically as needed. Parameters can be classified into two types: General parameters, such as freshness dates and content type, and Domain-specific parameters for vertical search queries.

Server components

The simple “search box” on the Google front page could hide a variety of specialized search engines behind it Pre-processing support: Personalization, Natural language processing, semantic analysis - Algorithmic changes: Rich content search, social input (reputation-based), self-optimization - Source restrictions: Restricting the scope of the search to trusted sources and/or to a specific vertical - Post-processing support: Clustering, related tags, support for services

Results interface

The results interface should include support for enhanced types of results visualization, such as clustering and related tags, query refinement (using filters or suggestions), along with support for saving searches (user agents) and alternative results platforms - such as Mobile, RSS feeds, RIAs, Emails and Web Services.

Keyword Search on Relational Databases Approach

The effectiveness of the scoring and ranking functions is an important aspect of keyword search [4]. As more than one result may match any keyword query, it is desirable to assign each result a score and rank the list of results according to their scores. Combining KWS and KWS-F [3], forms can potentially offer a good transition to go from an unstructured keyword query to the results of a structured query. Bernstein et al. make a similar observation when they state that when querying structured data, a partially structured query interface is preferable to a completely unstructured interface because of its guidance effect.

Keyword Aggregate Query Based on Query Template Approach

Keyword aggregate query has been divided into three stages for processing. The first stage is keywords preprocessing, the keywords is located in the database during this stage, generating the query items. The second stage is generating the templates, by which we can get the query templates [7]. The third stage is rating the results for the query template.

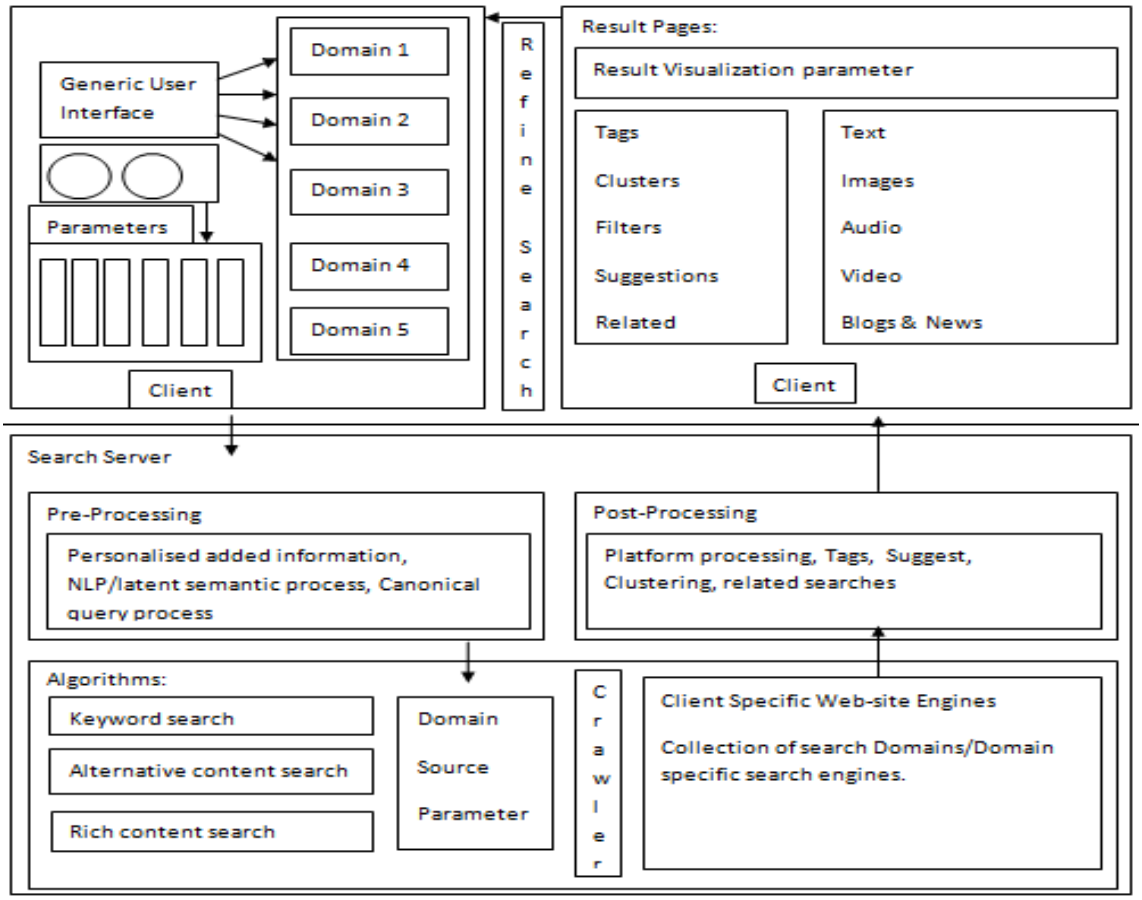

Proficient Search in Relational Database Based on Keyword Approach

Keyword based search and ranked the retrieved results based on the degree of relevance to the user. The ranking was done using the score [6]. The performance of the system using different metrics was also evaluated, also performed the searching and ranking of the certain and structured data of the relational databases. In future they would like to extend our searching and ranking to uncertain and probabilistic databases.

Keywords Retrieval in Relational Databases Based on Index Structure Approach

A query mapping index method different of the full-text index method, which creates a mapping table [11], and match index table and the corresponding key words. So it can improve the query speed. In the query mapping index method, setting as the threshold, it can Use PSO algorithm to learn keywords number. According to the number of occurrences to each of the query keywords, it can determine the new keywords. So it can retrieve the log to mining, and achieve the goal of retrieving through the query the user's usage and form.

BANKS System Approach

The BANKS system supports keyword search on databases storing structured/semi-structured data. Answers to keyword queries are ranked, and as in IR systems, the top answers may not be exactly what a user is looking for. Further interaction with the system is required to narrow in on desired answers. it describe some of the new features that are added to the BANKS[9] system to improve user interaction. These include an extended query model, richer support for user feedback and better display of answers.

Other related Works for KWS Approach

Wei Wang ,Xuemin Lin, Yi Luo worked out keyword search on the relational databases using data models with graph based relational data models approach obtained results with top-k keyword query result and indexing algorithm top-k index optimization.

Bin Zhu, Fang Yuan, Yu Wang used keyword processing with aggregate query and produced one query template generation algorithm(create QT algorithm),result generation algorithm(Translate QT to result) which will estimate keyword based on average precision, recall factor for keyword query.

B. Aditya ,Soumen Chakrabarti have estimate BANKS system for keyword search in relational databases,they have worked out XML relational query which will try to find k-nearest search with tree weight model processing node selection based on proximity and ranking keyword functions.

R.Suresh, K.Saranya, S.Dhivya, K.Thilagapriya were carried out proficient search in relational databases based on Query tree approach (Q-tree) they have processed query by expanding the keyword search using ranked aggregation method.

Haizhou Fu, Sidan Gao, Kemafor Anyanwu have specified degree of keyword disambiguity with Top-k generation algorithm,optimal deep segmentation algorithm for keyword search on RDF schema , Data graph and derived results in terms of a hit keyword k from graph,hit keyword array to find disambiguous keyword.

Algorithm

Algorithm keyword Search algorithm

1. Accept input Search term, search Query

2. Apply query processing technique on query

3. Analyze search term from query

4. Model Relational DB with all databases, Tables, Domains and tuples

5. Find presence and absence of search term

6. Correlate search term keyword with Relational DB objects

7. Create matrix to represent the relationship between database tulles

8. Compute proximity factor proximity distances for keyword and tuples

9. Prioritize keyword based on applying indexing ranking functions on keywords with tuples

10. Create priority queue containing set of keywords

11. Create final keyword relationship matrix based on priority queue containing set of keywords and tuples which will map keyword with highest priority first

12. Return prioritized set of Keyword to refine the input search term or search query

The goal is to choose k to minimize the Proximity Distance as presented in the following function.

Mathematical Modeling Objective function

$$R [I , J] = r [i , j] = \Sigma yd * wd (ki , kj)$$

Potential significance and Applications

Document Search in relational databases

Internet search engines have popularized the keyword based search paradigm. While traditional database management systems offer powerful query languages, they do not allow keyword-based search. Keyword based Xplorer system that enables keyword based search in relational databases. DBXplorer has been implemented using a commercial relational database and web server and allows users to interact via a browser front-end.

Information retrieval in Cloud based environment

As cloud computing becomes most general, the important information is centralized into the cloud server. To protect the data stored in the cloud, the data must be encrypted. Although traditional encryption techniques allows the user to securely search through the keyword and return retrieved files, these techniques are useful only for exact keyword search. Providing fast searching and increase the performance by considering Keyword substring from the given search query string

CONCLUSION

The Keyword search algorithm will be the hybrid approach to avoid Performance problems in traditional KWS systems and try to find solution over how to generate the top-k list of interpretations or structurizations that represent the most likely meanings intended by the user.

The effectiveness of the scoring and ranking functions is an important aspect of keyword search. As more than one result may match any keyword query, it is desirable to assign each result a score and rank the list of results according to their scores. The top results in the ranked list are more relevant to the query than those at the bottom.

REFERENCES:

[1] Georgios J. Fakas, Zhi Cai, and Nikos Mamoulis ”Versatile Size-l Object Summaries for Relational Keyword Search” , IEEE TRANSACTIONS ON KNOWLEDGE AND DATA ENGINEERING, VOL. 26, NO. 4, APRIL 2014.

[2]Soumen Chakrabarti, B. Aditya ”User Interaction in the BANKS System: A Demonstration ” , IEEE Transactions on Data Engineering, Feb. 2002, (Volume:1).

[3]Akanksha Baid, Ian Rae, Jiexing Li ”Toward Scalable Keyword Search over Relational Data ”, IEEE Transactions on Networking, Architecture and Storage (NAS), 2009 IEEE 5th International Conference.

[4] Wei Wang, Xuemin Lin ”Keyword Search on Relational Databases”, IEEE TRANSACTIONS Conference on Very Large Data Bases (VLDB 2010).

[5]Yan ZHAN, Hao CHEN ”Keywords Retrieval in Relational Databases Based on Index Structure ”,International Journal of Intelligent Information and Management Science ISSN: 2307-0692 Volume 3, Issue 5, October 2014.

[6] R.Suresh, K.Saranya, S.Dhivya, K.Thilagapriya”Proficient Search in Relational Database Based on Keyword”, International Journal of Engineering and Advanced Technology (IJEAT) ISSN: 2249 8958, Volume-1, Issue-4, April 2012.

[7] Bin Zhu, Fang Yuan”Keyword Aggregate Query Based on Query Template”, IEEE TRANSACTIONS ON 2012 International Conference on Computer and Information Application (ICCIA 2012).

[8] Haizhou Fu, Sidan Gao, Kemafor Anyanwu “Disambiguating Keyword Queries on RDF Databases Using Deep Segmentation”, In:Proc. of the 18th International Conference on Data Engineering (ICDE 2012). San Jose: IEEE Computer Society Press, 2012, pp.431.

[9] B. Aditya, G. Bhalotia, S. Chakrabarti, A. Hulgeri, C. Nakhe, P. Parag, S. Sudarshan ”BANKS: browsing and keyword searching in relational databases”, In VLDB 2002.

[10] Y. Luo, X. Lin, W. Wang, X. Zhou”Spark: top-k keyword query in relational databases”, In SIGMOD 07.

[11] M. Sayyadian, H. Lekhac, A. Doan, L. Gravano ”Efficient keyword search across heterogeneous relational databases”, In ICDE 07.

[12] Agrawal S, Chaudhuri S, Das G ”DBXplorer: A system for keyword-based search over relational databases”, In: Proc. of the 18th International conference on Data Engineering (ICDE 2002). San Jose: IEEE Computer Society Press, 2002, pp.5-16.

[13] Jianhua Feng, Guoliang Li, Jianyong Wang ”Finding Top-kAnswers in Keyword Search over Ralational Databases UsingTuple Units”, IEEE Transactions Knowledge and Data Engineering (TKDE), 2011,23(12), pp.1781-1794.

[14] R. Goldman, N. Shivakumar, S. Venkatasubramanian,H. Garcia-Molina”Proximity search in databases”, In Proc. of the International conference on VLDB, pages 2637, 1998.

[15] K. Golenberg, B. Kimelfeld, and Y. Sagiv Keyword Proximity Search in Complex Data Graphs ,Proc. 28th ACM SIGMOD International conference Management of Data, 2008.

International Journal of Engineering Research and General Science Volume 3, Issue 6, November-December, 2015
ISSN 2091-2730

BATTERY INTERFACE CONVERTER: DC-DC BIDIRECTIONAL NON-INVERTING BUCK BOOST CONVERTER FOR EV, HEV, PHEV APPLICATION

[1]Merin Sunny BE [EEE]., ME [EEE], [2]Thanuja Mary Abraham BE [EEE]., ME [EEE]

[1]Mtech Student, Power Electronics, Department of Electrical & Electronics Engineering,
Ilahia College of Engineering. & Technology,
Ernakulam, India,
merins49@gmail.com, 9446266286

[2]Assistant Professor, Department of Electrical & Electronics Engineering,
Ilahia College of Engineering & Technology,
Ernakulam, India
thanujamary05@gmail.com

Abstract— The need for a bidirectional DC/DC converter in electric vehicles is studied. Here, a universal power electronic interface that can be used in any type of electric vehicles (EV), hybrid electric vehicles (HEV) and plug-in hybrid electric vehicles (PHEV) is discussed. This power electronic converter interfaces the energy storage device of the vehicle with the motor drive and the charging unit. The fully directional converter is capable of working in buck or boost modes in any direction with a non-inverted output voltage. The output of the converter is improved with a feedback control loop. This is verified with MATLAB/SIMULINK (MATLAB version R2010a).

Keywords— Electric vehicles (EV), Hybrid electric vehicles (HEV) and Plug-in hybrid electric vehicles (PHEV), energy storage device, bidirectional DC/DC converter.

INTRODUCTION

Transportation industry always look forward for an alternate source of energy to reduce the adverse effects on environment and to increase the system efficiency. With the increased concern about eco friendlier & higher fuel economy vehicles, the need for electrification of transportation industry become unavoidable (essential). There are many versions of Electric Vehicles (EV) available nowadays. The fuel (electricity) can be the output of conventional energy producing means such as from hydro, diesel, thermal, etc. or can be from renewable energy sources like wind, solar, geo-thermal, etc. as in recent years the renewable energy sources plays a vital role in today's grid.

EVs are of different types like: 1) a simple EV where the traction motor draws power from the battery source which was earlier charged from the supply. 2) Hybrid Electric Vehicle (HEV) in which an ICE in addition to a battery source will be provided. During peak power requirement, the motor draw power from the ICE and from the battery in case of low power requirement. For ultra-high power requirement, both battery and ICE supplies the load. 3) Plug-in Hybrid Electric Vehicles (PHEV). PHEVs consist of an ICE and battery of which battery acts as the primary energy source.

Fig.1 shows the simplified block diagram of a PHEV.

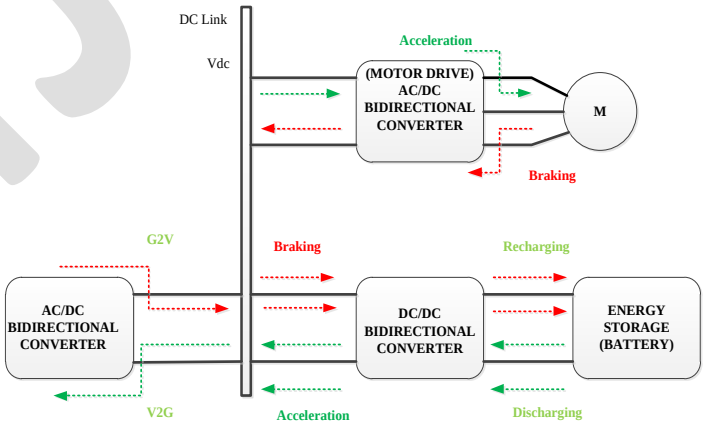

Fig.1. Power electronics interfaces in an Electric Vehicle

The AC/DC converter provides the charging unit. It converts the AC supply from the utility grid to the required DC voltage. This is shown as a bidirectional converter to facilitate vehicle to grid charging (V2G) concept. The power electronic interface between the DC link bus and the battery (storage unit) should essentially be a bidirectional converter inorder to facilitate charging and discharging of battery. In acceleration or cruising mode, it should deliver power from the battery to the dc link, while during regenerative mode, it should deliver power from the dc link to the battery. In the case of an EV or PHEV, the bidirectional dc/dc converter also interfaces the battery with the ac/dc converter during charging or discharging from or to the grid.

In grid connected mode, the bidirectional DC/DC converter should have the capability to convert the output voltage to the required level to recharge the batteries and vice versa while injecting power back to the grid. In driving mode, the converter must regulate the dc link voltage. Usually, in driving mode, the battery voltage is stepped-up during acceleration. DC link voltage is stepped-down during braking, where *V*dc>*V*batt. However, if motor drive's nominal voltage is less than battery's nominal voltage, *V*dc < *V*batt, the battery voltage should be stepped-down during acceleration and the dc link voltage should be stepped-up during regenerative braking. Thus the need for a universal bidirectional DC/DC capable of operating in all directions with stepping-up and stepping-down functionalities is evident. Here such a bidirectional DC/DC converter (shown in fig. 2) that can be used in any kind of electric vehicle is discussed.

The paper is organized as follows. In section II, the topological overview and the operation modes are presented. In section III, simulation results to evaluate the properties of the dc/dc bidirectional converter are presented. Section IV provides the conclusion.

II. SYSTEM DESCRIPTION AND OPERATING MODES

A. Different DC/DC Converters

There are different DC/DC converters used in electric vehicles. Some of them are; 1) buck-boost converters: they can regulate the DC link voltage or the battery side voltage. It can also step up/down voltages. But, they cannot provide voltage regulation in both directions, i.e., bidirectional power flow is not possible. Also, there is a need of an inverting transformer to get a positive output. 2) Non-inverted topologies: here, the need of bulky transformer can be reduced but these only provide a unidirectional power flow. Also, the PWM control of more than one switch is necessary which will increase the switching losses. 3) Two quadrant converters: By using two quadrant converters the voltage regulation with buck and boost operation is possible in either direction. But only two quadrants of operation are possible. 4) Two cascaded two quadrant converters: here, a four quadrant operation is possible. So the power flow can be in either direction and also voltage regulation can be made effectively. But, there will be a need of more than one inductor. 5) Dual active bridge (DAB) dc/dc converter: here, all switches are operating in PWM mode which increases the switching losses. Also, a transformer is needed which will increase the overall losses, size and cost.

B. Bidirectional DC/DC Converters

The schematic of the bidirectional converter is shown in fig.2. The converter topology consists of five switches (T1-T5) with internal diodes, five diodes (D1-D5), one inductor, L and two capacitors, C1 and C2. Vdc represents the motor drive nominal input voltage during driving mode or the rectified ac voltage at the output of the grid interface converter during plug-in mode The nominal voltage of the vehicle's ESS is represented by Vbatt .

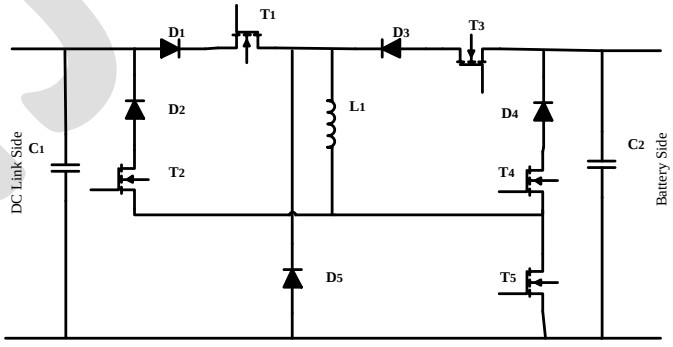

Fig.2. DC/DC bidirectional converter

The converter can be operated in buck or boost modes in either direction as required inorder to regulate the voltage at the dc link side and the battery side. The converter is capable of operating from Vdc to Vbatt boosting, Vdc to Vbatt bucking, Vbatt to Vdc boosting, or Vbatt to Vdc bucking, all with positive output voltage. Also, there is only one inductor needed for its operation. The

operational modes are given in the table.1. Of the five switches only three will be PWM controlled for the entire working range, while others will be either completely ON or OFF. Only one switch will be operating in the PWM control for each of the operating modes which will reduce the switching losses.

Table.1. Operating modes of the converter

Direction	Modes	T1	T2	T3	T4	T5
Vdc → Vbatt	Boost	ON	OFF	OFF	ON	PWM
Vdc →Vbatt	Buck	PWM	OFF	OFF	ON	OFF
Vbatt→Vdc	Boost	OFF	ON	ON	OFF	PWM
Vbatt→Vdc	Buck	OFF	ON	PWM	OFF	OFF

T2 and T4 serve as simple ON/OFF switches to connect or disconnect the corresponding current flow paths, whereas T1, T3, and T5 are either ON/OFF or PWM switches with respect to the corresponding operating mode. The different operating modes are explained below.

C. Case 1: Vdc < Vbatt

If the rated dc link voltage is less than battery's rated voltage, the dc link voltage should be stepped-up during charging in grid connected mode and in regenerative braking during driving. Under the same voltage condition, the battery voltage should be stepped-down during plug-in discharging in grid-connected mode, and in acceleration or cruising during driving.

Mode 1: Vdc → Vbatt Boost Mode for Plug-in Charging and Regenerative Braking:

In this mode, T1 and T4 are kept ON, while T2 and T3 remain in the OFF state, as shown in Fig. 3. The PWM switching signals are applied to switch T5.

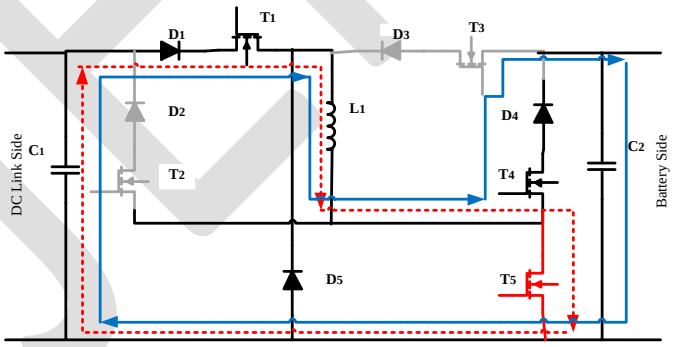

Fig.3. Vdc to Vbatt boost mode of operation

Therefore, from Vdc to Vbatt, a boost converter is formed by D1, T1, L, T5, D4, and T4. Since D1 and D4 are forward-biased, they conduct whereas D3 and D2 do not conduct. Since T5 is in PWM switching mode, when it is turned ON, the current from Vdc flows through D1, T1, L, and T5 while energizing the inductor. When T5 is OFF, both the source and the inductor currents flow to the battery side through D4 and T4. During this mode, Vdc and Vbatt sequentially become the input and output voltages. So by controlling the switching of T5 alone we can control this entire mode of operation. Since the inductor current is a state variable of this converter, it is controllable. Therefore, the charging power delivered to the battery in plug-in mode or high-voltage bus current in regenerative braking can be controlled.

Mode 2: Vbatt → Vdc Buck Mode for Plug-in Discharging and Acceleration:

The circuit schematic of this operation mode is provided in Fig 4. In this mode, T1, T4, and T5 remain OFF, while T2 is kept in ON state all the time. The PWM switching signals are applied to switch T3. Therefore, from Vbatt to Vdc, a buck converter is formed by T3, D3, D5, L, T2, and D2. When T3 is turned ON, the current from the battery passes through T3, D3, L, T2, and D2, while energizing the inductor. When T3 is OFF, the output current is freewheeled through the D5, T2, and D2, decreasing the average current transferred to the load side. D3 and D2 are forward-biased, whereas D1 and D4 do not conduct. D5 only conducts when T3 is OFF. In this mode, Vbatt and Vdc are the input and output voltages, respectively. During stepping-down the battery voltage while delivering power from battery to the dc link, the inductor is at the output and its current is a state variable. Therefore, the dc link voltage and the current delivered to the dc link can be controlled in driving mode.

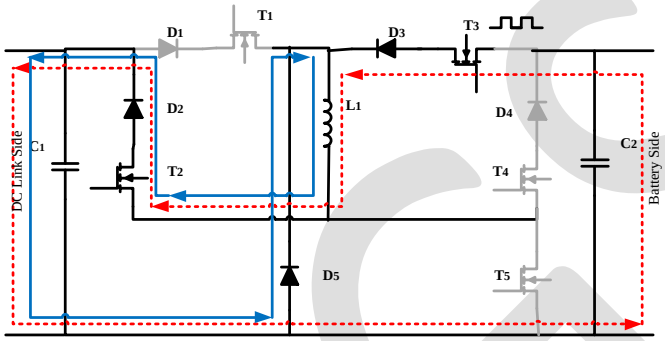

Fig.4. Vbatt to Vdc buck mode of operation

D. Case 2: Vdc > Vbatt

If the rated dc link voltage is more than the battery rated voltage, dc link voltage should be stepped-down during charging in grid-connected mode and in regenerative braking while the vehicle is being driven. Under the same voltage condition, the battery voltage should be stepped-up during plug-in discharging in grid-connected mode and in acceleration or cruising while driving.

Mode 3: Vdc → Vbatt Buck Mode for Plug-in Charging and Regenerative Braking:

In this mode, T1 is in the PWM switching mode. Switches T2, T3, and T5 remain in OFF state while T4 is kept ON all the time. Therefore, from Vdc to Vbatt, a buck converter is made up by D1, T1, D5, L, D4 and T4 as shown in Fig 5. When T1 is turned ON, the current from Vdc passes through D1, T1, L, D4, and T4 while energizing the inductor. When T1 is OFF, the output current is recovered by freewheeling diode D5 decreasing the average current transferred from dc link to the battery. Since diodes D1 and D4 are forward biased, they conduct whereas D2 and D3 do not conduct. D5 only conducts when T1 is OFF. In this mode, Vdc and Vbatt are the input and output voltages, respectively. The dc link voltage can be regulated in driving mode (regenerative braking) by controlling the current transferred to the battery. In plug- in charging mode, the current or power delivered to the battery is also controllable.

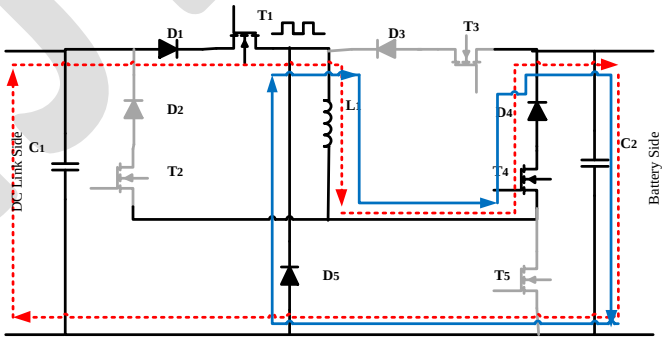

Fig.5. Vdc to Vbatt buck mode of operation

Mode 4: Vbatt → Vdc Boost Mode for Plug-in Discharging and Acceleration:

During this mode, T1 and T4 remain OFF, whereas T2 and T3 remain ON all the time. Switch T5 is operated in PWM switching mode. Therefore, from Vbatt to Vdc, a boost converter is formed by T3, D3, L, T5, T2, and D2, as illustrated in Fig.6. When T5 is turned ON, the current from Vbatt passes through T3, D3, L, and T5 while energizing the inductor. When T5 is OFF, both inductor and the source currents pass through T2 and D2 to the dc link. In this mode, D3 and D2 are forward-biased and they conduct, whereas D1, D4 and D5 are reverse-based and do not conduct.

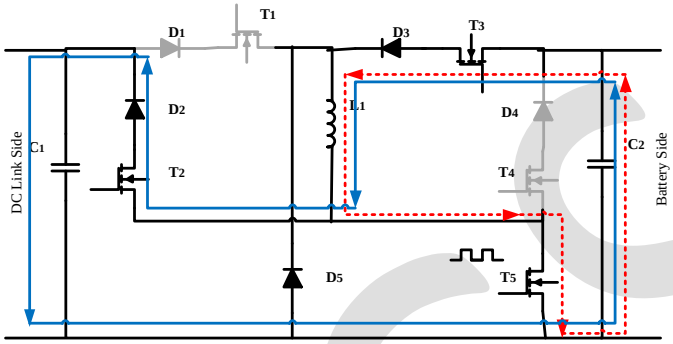

Fig.6. Vbatt to Vdc boost mode of operation

In this mode, Vbatt and Vdc are sequentially the input and output voltages. The dc link voltage can be regulated in driving mode (regenerative braking) by controlling the current drawn from the battery. In plug-in charging mode, the current or power drawn from battery is also controllable.

III. MATLAB SIMULINK MODEL AND RESULTS

The MATLAB/SIMULINK model for electric vehicle applications is shown in fig.7. The circuit parameters chosen are L=1.545mH, Cdc=Cbatt=2200μF. The DC link side is represented by a DC source and the battery side is provided with a battery. There are two cases of voltages at the DC link side and the battery side as already discussed..The input is given as Vdc=12V and the battery side voltage is given as Vbatt~21V for the case Vdc<Vbatt. (mode 1 and 2 of operation). And Vdc= 21 V and battery voltage Vbatt~12V for Vdc>Vbatt.

The gate signals and results obtained for each case is shown in figures 8 to13.

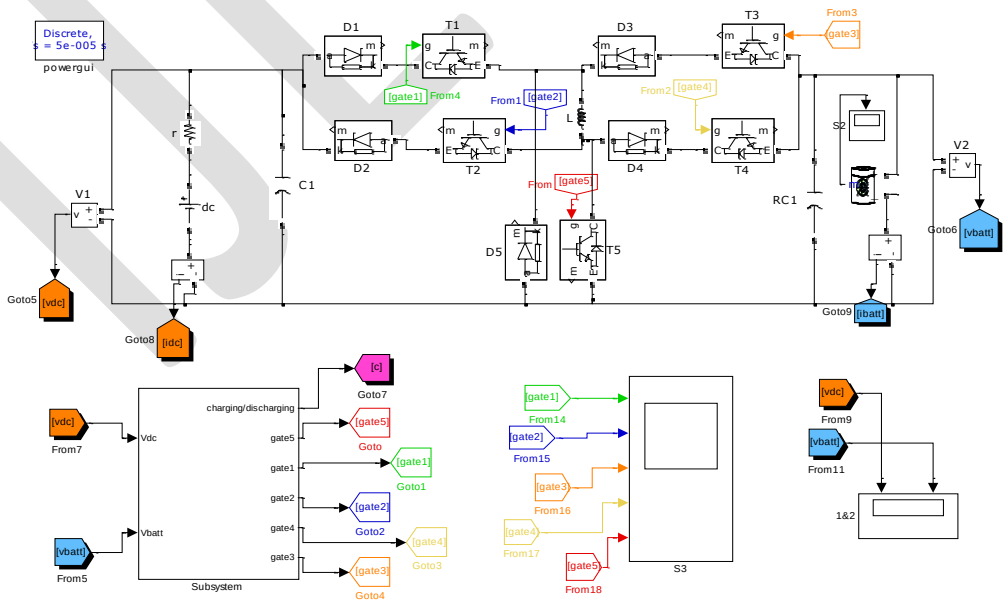

Fig.7. Simulink model of the DC/DC converter

When Vdc<Vbatt and charging/regenerative braking, the power flow is from DC link side to battery side and it is the boost mode of operation [mode1]. When Vdc<Vbatt and discharging/acceleration, the power flow is from DC link side to battery side and it is the buck mode of operation [mode 2]. When Vdc>Vbatt and charging/regenerative braking, the power flow is from battery side to DC link side and is the buck mode of operation [mode 3]. When Vdc>Vbatt and discharging/acceleration, power flow is from from battery side to DC link side and is in the boost mode of operation [mode 4].

A. Mode 1: Boost charging

The input voltage is set for 12V and output is boosted to 21V and thus the battery charges. The corresponding voltages and current obtained are shown in fig.8.

T5 is PWM controlled in mode 1. So the vehicle is in the regenerative mode of operation.

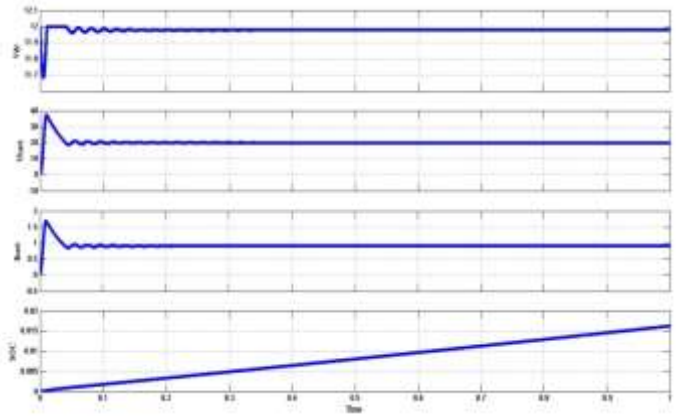

Fig.8. Input, output voltages at the battery SOC% for boost charging mode

B. Mode 2: Buck discharging

The DC/DC converter will step down the 21V input to 12V output at the DC link voltage side. This is shown in the fig.5.9.

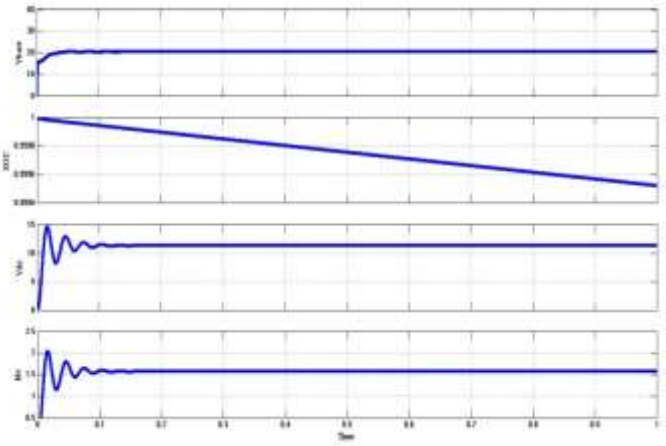

Fig.5.9. Input, output voltages at the battery SOC% for buck discharging mode

C. Mode 3: Buck charging

Here, the dc link voltage chosen is 21V and the battery terminal voltage is 12V. So the input 21V will be stepped down to 12V by the DC/DC converter. The waveforms obtained are shown in fig.5.10.

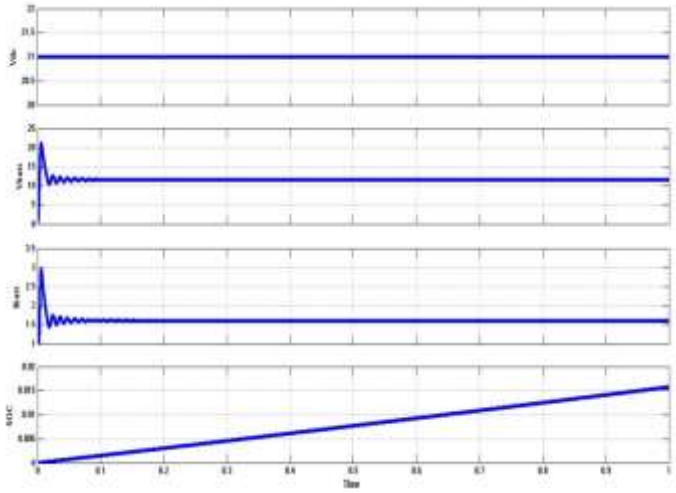

Fig.10. Input, output voltages at the battery SOC% for buck charging mode

D. Mode 4: Boost discharging

Here, the battery terminal voltage is taken as 12V and the required DC bus voltage is 21V, then the bidirectional DC/DC converter will boost up the voltage at the DC link.

The waveforms are shown in the fig.5.11. The battery SOC is shown. In the boost discharging mode, the battery is initially at 100 % charge and it starts to discharge from full charge. The state of charge decreases to 0% during this accelerating mode.

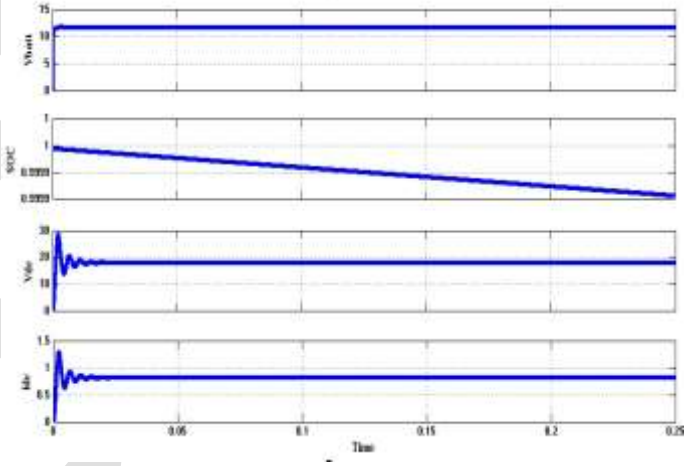

Fig.10. Input, output voltages at the battery SOC% for boost discharging mode

IV. CONCLUSION

This study introduces a dc/dc converter structure that is suitable for both industrial needs and the electric vehicle conversion approaches for all EV, HEV, and PHEVs regardless of their rated dc link voltage and motor drive inverter voltage as well as the battery nominal voltage. The functionalities of the proposed converter provide a broad range of application areas. Due to the operational capabilities, the converter is one of a kind plug-and-play universal dc/dc converter that is suitable for all electric vehicle applications.

Each mode of operation with battery are discussed. The resulting waveforms are obtained and are verified by MATLAB/SIMULINK model (2010).

REFERENCES:

[1] A. Emadi, Y. L. Lee, and R. Rajashekara, "Power electronics and motor drives in electric, hybrid electric, and plug-in hybrid electric vehicles," IEEE Trans. Ind. Electron., vol. 55, no. 6, pp. 2237–2245, Jun. 2008.

[2] R. Ghorbani, E. Bibeau, and S. Filizadeh, "On conversion of electric vehicles to plug-in," IEEE Trans. Veh. Technol., vol. 59, no. 4, pp. 2016– 2020, May 2010.

[3] Z. Amjadi and S.S Williamson, " Power electronics based solutions for plug-in hybrid electric vehicle energy storage and management systems", IEEE Trans. Ind. Electron., vol.57, no.2, pp.608616, Feb 2010.

[4] Y.-J. Lee, A. Khaligh, and A. Emadi, "Advanced integrated bidirectional AC/DC and DC/DC converter for plug-in hybrid electric vehicles," IEEE Trans. Veh. Technol., vol. 58, no. 5, pp. 3970–3980, Oct. 2009.

[5] B. W. Williams, "Basic DC-to-DC converters," IEEE Trans. Power Electron., vol. 23, no. 1, pp. 387–401, Jan. 2008.

[6] B. Sahu and G. A. Rincon-Mora, "A low voltage, dynamic, noninverting, synchronous buck-boost converter for portable applications," IEEE Trans. Power Electron., vol. 19, no. 2, pp. 443–452, Mar. 2004.

[7] S. Waffler and J. W. Kolar, "A novel low-loss modulation strategy for high-power bidirectional buck + boost converters," IEEE Trans. Power Electron., vol. 24, no. 6, pp. 1589–1599, Jun. 2009.

[8] M. B. Camara, H. Gualous, F. Gustin, A. Berthon, and B. Dakyo, "DC/DC converter design for supercapacitor and battery power management in hybrid vehicle applications—Polynomial control strategy," IEEE Trans. Ind. Electron., vol. 57, no. 2, pp. 587–597, Feb. 2010.

[9] K. I. Hwu and Y. T. Yau, "Two types of KY buck-boost converters," IEEE Trans. Ind. Electron., vol. 56, no. 8, pp. 2970–2980, Aug. 2009.

[10] F. Krismer, J. Biela, and J. W. Kolar, "A comparative evaluation of isolated bi-directional DC/DC converters with wide input and output voltage range," in Proc. IEEE Ind. Appl. Conf., Kowloon, Hong Kong, Oct. 2005, vol. 1, pp. 599–606.

[11] H.-L. Do, "Nonisolated bidirectional zero-voltage-switching DC-DC converter,"IEEE Trans. Power Electron., vol. 26, no. 9, pp. 2563–2569, Sep.2011.

[12] H.-W. Seong, H.-S. Kim, K.-B. Park, G.-W. Moon, andM.-J. Youn, "High step-up DC-DC converters using zero-voltage switching boost integration technique and light-load frequency modulation control," IEEE Trans. Power Electron.,vol.27,no.3,pp.1383–1400,Mar.2012.

[13] H. Qin and J. W. Kimball, "Generalized average modeling of dual active bridge DC-DC converter," IEEE Trans. Power Electron., vol. 27, no. 4, pp. 2078–2084, Apr. 2012.

[14] S. Y. Kim, H.-S. Song, and K. Nam, "Idling port isolation control of three-port bidirectional converter for EVs," IEEE Trans. Power Electron., vol. 27, no. 5, pp. 2495–2506, May 2012.

[15] H. Wu, K. Sun, R. Chen, H. Hu, and Y. Xing, "Full-bridge three-port converters with wide input voltage range for renewable power systems," IEEE Trans. Power Electron., vol. 27, no. 9, pp. 3965–3974, Sep.2012.

[16] H.-S. Kim, M.-H. Ryu, J.-W. Baek, and J.-H. Jung, "High efficiency isolated bidirectional AC-DC converter for DC distribution system," IEEE Trans. Power Electron, vol. 28, no. 4, pp. 1642–1654, Apr. 2013.

[17] Z. Zhang, Z. Ouyang, O. C. Thomsen, and M. A. E. Andersen, "Analysis and design of a bidirectional isolated DC-DC converter for fuel cells and supercapacitors hybrid system," IEEE Trans. Power Electron., vol. 27, no. 2, pp. 848–859, Feb. 2012.

[18] L. Roggia, L. Schuch, J. E. Baggio, C. Rech, and J. R. Pinheiro, "Integrated full-bridge-forward DC-DC converter for a residential microgrid application," IEEE Trans. Power Electron, vol. 28, no. 4, pp. 1728–1740, Apr. 2013.

International Journal of Engineering Research and General Science Volume 3, Issue 6, November-December, 2015
ISSN 2091-2730

Vision based approach to human fall detection

Pooja Shukla, Arti Tiwari

CSVTU University Chhattisgarh, poojashukla2410@gmail.com 9754102116

Abstract— Day by the count of elderly people living alone at home increases. Fall is one of the major risks for elderly people. Sometimes older people may get serious injury to their backbone (spinal cord) and that may lead to death. Sometimes fallen injured elderly may be lying on the ground for several hours after a fall incident has occurred. This makes it important to have a fall detection system. There is different approach to human fall detection such as sensor based, accelerometer, another possibility is camera based system. In this paper, we propose a novel and robust fall detection system. Our approach is based on motion history. Our algorithm provides promising results on video sequences of daily activities and simulated falls.

Keywords— Activity analysis, chute dataset, fall detection, openCV, Silhouette, motion history image, background subtraction

INTRODUCTION

The contents of each section may be provided to understand easily about the paper. Falls are one of the major risk for seniors living alone at home, sometimes causing injuries. Nowadays, the usual solution to detect falls is to use some wearable sensors like accelerometers or help buttons. However, the problem of such detectors is that older people often forget to wear them. Moreover, in the case of a help button, it can be useless if the person is unconscious or immobilized. To overcome these limitations, we use a computer vision system which doesn't require that the person wears anything. Another advantage of such a system is that a camera gives more information on the motion of a person and his/her actions than an accelerometer.

In this paper, we propose novel computer vision based fall detection system for monitoring an elderly person in a home care, assistive living application. In this work, two robust methods are presented based on two features: human centroid height relative to the ground and MHI based fall detection. Indeed, the first feature is an efficient solution to detect falls as the vast majority of falls ends on the ground or near the ground. However, this method can fail if the end of the fall is completely occluded behind furniture. Fortunately, these cases can be managed by using second MHI based human fall detection where we calculate angle of falling and if the falling object found below threshold angle then declared as a fall.

The paper is organize is as follow. In Section I we explain a literature survey regarding fall detection system, Section II will discuss silhouette based human fall detection system, Section III will handle algorithm of a system and in section IV we will see the results regarding the human fall detection system with quantitative and qualitative analysis. Finally we conclude the paper in section V.

I. LITERATURE SURVEY

Miao Yu et.al [1] author propose a more robust fall detection system based on estimating the density of a fall with respect to corresponding video feature, and falls are then detected according to the obtained density information. In this paper, a new fall detection system based on head tracking and human shape analysis. This system is composed of two calibrated cameras, and 2-D head tracking and human shape analysis are applied to both video recordings recorded by the two cameras both covering the area where a person performs activities are used. A more robust fall detection system can potentially be achieved by the combination of audio and video information, which is well known as multimodal processing, and another subset of one class classification technique, boundary method, will be used in future work for fall detection to cope with the high-dimensional feature situation.

Homa Foroughi et.al [2] Proposed Human fall detection based on combination of integrated time motion images and eigenspace technique. Applying eigenspace technique to ITMIs leads in extracting eigen motion and finally multi-class Support Vector Machine is used for precise classification of motions and determination of a fall event. We have considered wide range of motions, consisting

normal daily life movements, some abnormal behaviors and also unusual events. While existent systems deal with limited movement patterns, we tried to simulate real life situations by Multi-class SVM classification system reduced the false detection considering wide variety of different postures.

Caroline Rougier et.al [3] Proposed method is based on the fact that the motion is large when a fall occurs. So, the first step of our system is to detect large motion of the person on the video sequence using the Motion History Image. When a motion is detected, we analyze the shape of the person in the video sequence. During a fall, the human shape changes and, at the end of the fall, the person is generally on the Ground with few and small body movements. A change in the human shape can discriminate if the large motion detected is normal (e.g.: the person walks or sits) or abnormal (e.g.: the person falls)

Ugur Toreyin1 et.al [4] proposed system Three state HMMs are used to classify events. Feature parameters of HMM are extracted from temporal wavelet signals describing the bounding box of moving objects. Since wavelet signals are zero mean signal it is easier to define states in HMMs and this leads to a robust method against variations in object sizes. In addition, the audio track of the video is also used to distinguish a person simply sitting on a floor from a person stumbling and falling. Wavelet signals can easily reveal the periodic characteristic which is intrinsic in the falling case. After the fall, the aspect ratio does not change or changes slowly. Since, wavelet signals are high-pass filtered signals, slow variations in the original signal lead to zero mean wavelet signals. This method could be inaccurate, depending on the relative position of the person, camera, and perhaps occluding objects. Similar HMM structures can be also used for automatic detection of accidents and stopped vehicles in highways which are all examples of instantaneous events occurring in video.

Nuttapong Worrakulpanit et.al [5] proposed a method which will compute acceleration value of human's movement for indicating the changing rate of human motions. In our assumption, human fall is high acceleration activity, whereas fast walking and running are considered as low acceleration activities. Thus standard deviation of C-Motion method together with the orientation standard deviation of the ellipse is able to discriminate actual fall from other activities. C-Motion method will return a high value computation result because this method considers velocity of motions.

Homa Foroughi et.al [6] proposed a novel method to detect various posture-based events in a typical elderly monitoring application in a home surveillance scenario. These events include normal daily life activities, abnormal behaviors and unusual events. Combination of best-fit approximated ellipse around the human body, projection histograms of the segmented silhouette and temporal changes of head position, would provide a useful cue for detection of different behaviors. Extracted feature vectors are fed to a MLP Neural Network for precise classification of motions and determination of fall.

Muhammad Jamil Khan et.al [7] proposed approach is based on a combination of motion gradients and human shape features variation.The estimation of the motion of the person allows detecting large motion like falls. But a large motion can also be a characteristic of a walking person, so we need to analyze further to discriminate a fall from a normal movement. To discriminate fall motion from other we use Global Motion Orientation to detect the direction of motion. An analysis on the moving object is performed to detect a change in the human shape, width to height ration α up to a certain threshold considered to distinguish fall from other activities.

Jared Willems et.al [8] proposed to study the existing fall detection algorithms. Not only the fall detection algorithm. On its ownbut the system set-up was presented. In this paper the use of low cost cameras is preferable because of cost-related issues and that it should be possible because most background subtraction algorithms don't need high quality video input. One of the most used and most simple techniques to detect a fall is the aspect ratio of the bounding box. A second method to detect a fall is the use of a fall angle. Some other algorithms make use of the centroid of the falling person. The last simple feature we want to present is the horizontal and vertical gradient [2]. When a person is falling, the vertical gradient will be less than the horizontal gradient. It is clear that all methods mentioned above do work only in specific circumstances. Therefore, it is necessary to combine a number of these techniques to get a reliable system to detect a fall.

II. PROPOSED SYSTEM

The proposed system is consisting of five main modules to detect fall from video.

1. Video acquisition from database or web camera
2. Background subtraction / motion detection
3. Preprocessing
4. Object tracking

5. Activity analysis

1. Video acquisition

The video was taken from real time web camera or from recorded videos. In proposed system we were working on Chute dataset. Dataset consist of fall video sequences which were recorded at different location like "Home", "coffee room", "office", "lecture room" etc.

2. Background subtraction

In indoor environment, cameras were placed at fixed location. So background subtraction is little bit easy for such environment. In this case, background subtraction gives whole silhouette of moving object as well as edges. So task is to build a background which does not contain any foreground object. I proposed system we set first frame as a background image and next frames were subtracted frame background image.

The absolute difference between the background (V(x, y, t)) and current frame V(x, y, t+1) is given by

$$D(t+1) = |V(x,y,t+1) - V(x,y,t)| \quad \ldots\ldots (1)$$

This difference image show the change in the intensity level for the pixel location which is changed in two frames. Threshold is applied on image to advance the subtraction. The equation for Thresholding is given by

$$\text{Binary} = \begin{cases} 1 & D < th \\ 0 & \text{else} \end{cases} \quad \ldots\ldots\ldots\ldots\ldots (2)$$

Thresholding operation gives binary image. The output of the background subtraction is silhouette. The subtracted output need some enhancement for better results so we were applied some preprocessing Operations on subtracted image.

3. Preprocessing

Preprocessing is a step where image noise is removed by using Gaussian or median filter. Other way is a morphological operation. Morphological operations are used to selective extraction of image. Applying structuring element B on binary image A is defined by

$$A \ominus B = \{b + z | B_z \in E\} \quad \ldots\ldots\ldots\ldots (3)$$

The dilation of A by the structuring element B is defined by:

$$A \oplus B = \bigcup_{b \in B} A_b \quad \ldots\ldots\ldots\ldots\ldots\ldots (4)$$

4. Object tracking

To track the silhouette area we need to calculate the centroid of the object. The centroid of the object is calculated as $xCi = \frac{\sum_i^k xi}{k}$, $yCi = \frac{\sum_i^k yi}{k}$ …… (5)

Where, xi is the location of white pixel on x Coordinate, yi, is the location of white pixel on y Coordinate. With the reference of centroid of the silhouette we can track the foreground object.

5. Activity analysis

Fall detection is the complex task to recognize. Within the room there were few places where the person spends most of time in a day. So we need to place camera with a proper angle.

In proposed system, we consider a reference line which is at some height from the ground. If the centroid of the silhouette is found below reference line then consider as a fall else non fall.

III. RESULT

The results of proposed system are taking on the basis of Qualitative and Quantitative analysis.

1. Qualitative analysis

(a) (b)

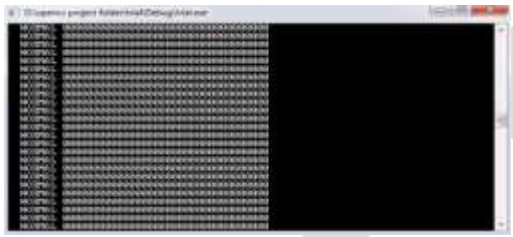

(c)

Fig.11. Fall detection (a) Input video frame (b) silhouette output (c) output shows fall detection

(a) (b)

(c)

Fig.12. Fall detection system (a) Input video frame (b) silhouette output (c) output shows normal activity

2. Quantitative analysis:

Quantitative analysis is done using three metrics viz. Detection rate, false alarm rate and success rate. These metrics are calculated based on following parameters:

1. **True Positive (TP):** Fall present and shown detected.
2. **True Negative (TN):** Fall not present, shown not detected.
3. **False Positive (FP):** Fall not present but shown detected, (also known as false alarms).
4. **False Negative (FN):** Fall present but shown not detected. (Also known as misses).

These scalars are combined to define the following metrics

$$\mathrm{DR} = \mathrm{TP}/(\mathrm{TP} + \mathrm{FN}) \quad \ldots\ldots\ldots\ldots\ldots\ldots\ldots\ldots (6)$$

$$\mathrm{FAR} = \mathrm{FP}/(\mathrm{TP} + \mathrm{FP}) \quad \ldots\ldots\ldots\ldots\ldots\ldots\ldots (7)$$

$$\text{Success Rate}(\%) = \mathrm{DR}/(\mathrm{DR} + \mathrm{FAR}) \quad \ldots\ldots (8)$$

IV. CONCLUSION

IN THIS WORK, WE IMPLEMENTED THE SYSTEM WHICH AUTOMATICALLY DETECTED FALL. OUR SYSTEM IS DESIGNED FOR ONE PERSON IN THE REAL TIME. THE IMPLEMENTATION OF THIS APPROACH RUNS AT 15-20 FRAMES PER SECOND. THE APPLICATION IS IMPLEMENTED IN C++ USING OPENCV LIBRARY IN WINDOWS ENVIRONMENT WITH A SINGLE CAMERA VIEW.

REFERENCES:

Journal Papers:

[1] YU , M., NAQVI, S.M. and CHAMBERS, J., 2010. A robust fall detection system for the elderly in a smart room. IN: IEEE International Conference on Acoustics Speech and Signal Processing (ICASSP), Dallas, TX, 14-19 March, pp.1666-1669

[2] Homa Foroughi, A. Rezvanian, et al. (2008). Robust Fall Detection Using Human Shape and Multi-class Support Vector Machine. Sixth Indian Conference on Computer Vision, Graphics & Image Processing: 413-420.

[3] Caroline Rougier, Jean Meunier, Alain St-Arnaud, Jacqueline Roussea Fall Detection from Human Shape and Motion History Using Video Surveillance Advanced Information Networking and Applications Workshops, 2007, AINAW '07. 21st International Conference on, Vol. 2 (2007), pp. 875-880.

[4] B. T¨oreyin, Y. Dedeoglu, and A. C¸ etin. Hmm based falling person detection using both audio and video. In IEEE International Workshop on Human-Computer Interaction, Beijing, China, 2005.

[5] Nuttapong Worrakulpanit and Pranchalee Samanpiboon. Human Fall Detection Using Standard Deviation of C-Motion Method. Journal of Automation and Control Engineering Vol. 2, No. 4, December 2014

[6] H. Foroughi, B.S. Aski, and H. Pourreza. Intelligent video surveillance for monitoring fall detection of elderly in home environments. In Computer and Information Technology. ICCIT 2008. 11th International Conference on, pages 219{224, 2008.

[7] Muhammad Jamil Khan and Hafiz Adnan Habib"Video Analytic for Fall Detection from Shape Features and Motion Gradients" Proceedings of the World Congress on Engineering and Computer Science 2009 Vol II

[8] J. Willems, G. Debard, B.Bonroy et al., 'How to detect human fall in video? An overview', PoCA conference 2009, Antwerp Belgium, May,2009.

[9] E.E. Sabelman, D. Schwandt, and D.L. Jaffe, "The WAMAS Wearable Accelerometric Motion Analysis System: CombiningTechnology Development and Research in Human Mobility", In Proc. Conf. Intellectual Property in the VA: Changes, Challenges and Collaborations, Arlington, VA, United States, 2001.

[10] A.H. Nasution and S. Emmanuel, ―Intelligent Video Surveillance for Monitoring Elderly in Home Environments‖, In Proc. IEEE 9th Workshop on Multimedia Signal Processing (MMSP 2007), pp. 203-206, Greece, 2007.

[11] Kh. Rezaee, E. Azizi, J. Haddania and A. Delbari, " Intelligent Monitoring System of Elderly's Fall Based on Video Sequences", Middle-East Journal of Scientific Research 15 (8): 1178-1185, 2013, ISSN 1990-9233

[12] Diraco G, Leone A, Siciliano P: An active vision system for fall detection and posture recognition in elderly healthcare. In Conference & Exhibition: Design, Automation & Test in Europe. Dresden: European Design and Automation Association; 2010:1536– 1541.

International Journal of Engineering Research and General Science Volume 3, Issue 6, November-December, 2015
ISSN 2091-2730

Windows Phone App Based Real Time Tracking of Smart Parking System

Waqas Ahmed[1], Muhammad Fayaz Khan[2]

Department of Electrical Engineering, Sukkur Institute of Business Administration, Sukkur, Sindh, Pakistan

[1]waqas.ahmed@iba-suk.edu.pk, [2]faizi@iba-suk.edu.pk

Abstract — searching for a parking space in Urban cities cause problems for drivers, especially during the peak business hours. The vehicle searching for available spaces at that time creates traffic congestion. Apart from frustration of drivers, vehicles looking for parking burn tons of fuel which result as environmental pollution. The most current parking systems are not fully equipped to overcome parking space problem and cause traffic congestion as well as the environmental pollution. We have designed and implemented prototype of smart Parking System to eliminate the issues in traditional parking system and convert the parking system into fully functional Smart parking system. This paper proposes an effective method to overcome these problems. We have implemented and designed a prototype of parking system. This prototype is divided into three main category Image processing, Control System, and Windows phone application. Windows phone parking application is being integrated in parking system to track the real time status of parking plaza and to increases the efficiency of this prototype. This app shows the real time status of parking system also allows drivers to find and reserve the vacant parking spaces by using smart phones as per their desire location.

Keywords— Control System, Image Processing, Windows Phone Parking application, Parking system Prototype, smart parking system , smart phone

I. INTRODUCTION

Over a decade, the increasing ratio of traffic congestion, environmental pollution and parking de-management affecting daily life gained popularity in academic as well as industrial community. The parking problem is a challenge which requires the simultaneous consideration of many options. Only in United State, annual revenue of the parking industry is in billions, and parking law might have an effect on people's concerns about traffic congestion, environmental pollution. For instance, a recent survey [1].that during rush hour in most metropolitan areas, the traffic generated by vehicles searching for available parking space takes up to 40% of the total traffic. Thus the traffic congestion in metropolitan areas are somehow due to parking A recent study [2], in a business district of Los Angeles, vehicles searching for parking lots burn 47,000 gallons of gasoline and produced 730 tons of carbon dioxide, which is equivalent of 38 trips around the world. Clearly, the problems linked with parking impose significant societal costs, both ecologically and economically [3].

The most current parking or guidance systems today, only collect data and publish collective information of whole parking area near their destinations. These systems do not have capability to guide drivers inside the parking area to exact free available parking lots. In contrast to such parking information guidance systems, this paper proposes a Windows phone application which is specially designed and integrated in parking system that not only point out the near parking areas but also provide real time tracking services as part of user-targeted services. On the other side, the windows phone app guide drivers to find exactly the available parking lot in a crowded parking area.

II. LITERATURE REVIEW

Most research work on parking is from the perspective of system design, which focuses on implementing a wireless sensor network to detect parking information. In addition, we introduce the Smart parking system which is integrated with windows phone application, which provides us a powerful tool to search parking areas and see the current status of parking lots.

We reviewed background on parking systems techniques, containing the performance metrics, existing solutions and challenges. There is a limitation in existing parking guiding approaches like: Buffed PIS (BPIS), to alleviate the "multiple-car-chase-single-slot" phenomenon. An approach to leave a buffer publishing the live information. But it is difficult to determine the threshold for the buffer. Another proposed Parking Lots Detection [4], in which camera inside the garage take the image from static position and send that to web server, that data determine number of unoccupied parking space, but the limitation is that this project shows the collective information of whole area. Some other approaches are VANET (vehicle Ad-hoc Network)-Based Smart Parking [5], Bay Area Rapid Transit [6].

Blind searching is adopted by users when no parking information is available. So drivers search parking spaces randomly within a certain distance to their destination. This research paper mainly focuses on a parking management system that assists drivers to find nearby parking areas and exact available parking lots in a specific parking area, and satisfies the needs of both, parking providers and drivers.

III. SMART PARKING SYSTEM DESIGN AND IMPLEMENTATION

Implementation and Methodology are planned for project is dived in to four main parts, which are "Vehicle Number Recognition"[7][8] , "Hardware (prototype) execution" , "Interfacing of prototype with Web Server" , "Real Time communication between Web server and Windows phone mobile app". This research paper emphasis on these four main areas to overcome the issues in parking system and fulfill the user's need.

A. Vehicle Number Recognition (VNR) System

Image processing was performed for Vehicle Number Recognition which is based on MATLAB (matrix laboratory) [9]. The camera, installed at the entrance and the exit gate, takes image of every entering vehicle and pass that to the computer which execute the image processing using MATLAB vehicle number recognition (VNR) algorithm [10]. The designed algorithm uses four modules, image acquisition, Number plate extraction, character segmentation and template matching to successfully extract Vehicle Number plate as shown in Fig 1(a), (b) (c).

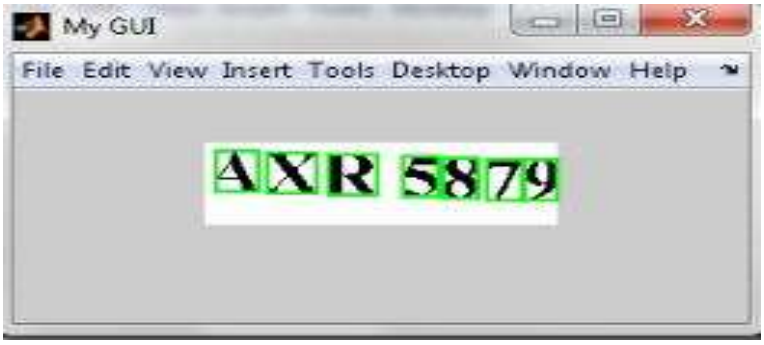

Figure 10: (a) Segmentation of Number Plate

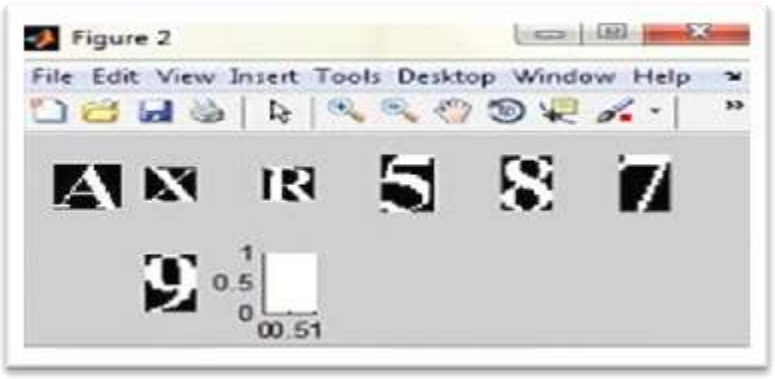

Figure 1: (b) Number Plate Extraction

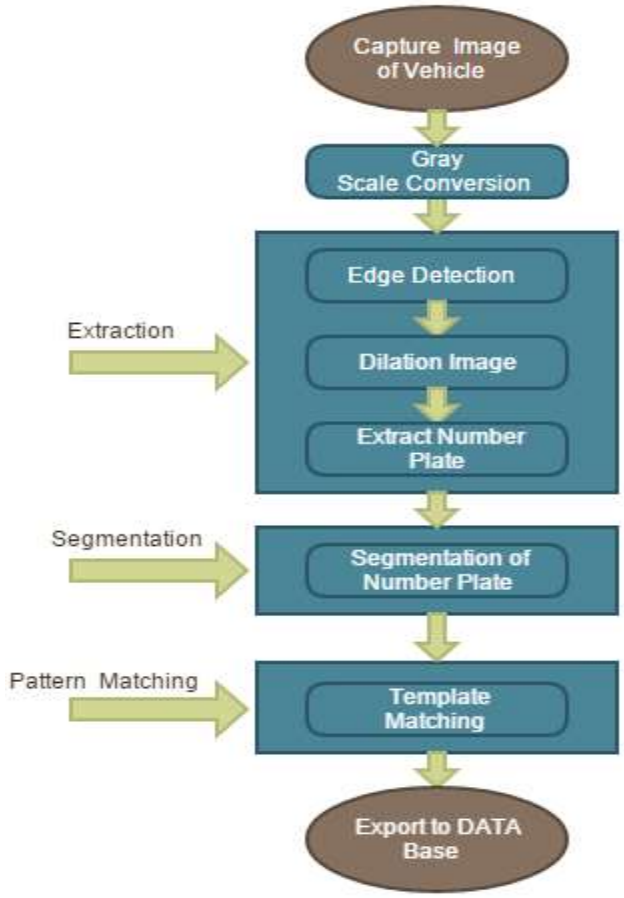

Figure 1: (c) Vehicle Number Plate Recognition

Further, the detected vehicle registration number with time and date are exported to Matlab Database using JDBC and GUI for maintaining record of each vehicle entering or leaving parking area [11]. This database is being utilized to maintain the up to date list of each vehicle with date and time and to calculate and collect the parking tax, and could also be used for legal purposes as well.

B. Hardware Implementation

Hardware development was based on Arduino UNO [12], proximity sensors, stepper motors, light detecting sensors & other devices to control the flow of vehicles, detects vehicles, and appraises the data-base & basic information of every vehicle. This controlled system detects the presence of every vehicle at entrance and exist point and open/close the gate barrier respectively. The proximity sensors deployed at the entrance and exit gates which detect the vehicle and send signal to Arduino UNO. Arduino is interfaced with stepper motor which controls the road barrier. It also includes of 2x16 Character LCD & seven segment display with microcontroller which acts as welcome screen on entrance gate, the LCD also display the number of available space at that location.

C. Interfacing of Hardware with Web server

The sensors were installed at each parking lot, which send the data to Arduino UNO on every second. Arduino makes decision based on the data received and pass that information to the web server. The web server was Developed using ASP.NET application. This involves configuring the web application, web server, and record in the manufacture environment. Synchronize the ASP.NET pages, code files, the gatherings in the Bin folder, and HTML associated support files like CSS and JavaScript files. Synchronize the database

schema and/or data consists of graphical interface, and other files running on it. Web server fetches the information from Arduino and displays that in graphical form. A program was burned in Arduino to send the Data in Hexa Decimal form, so web servers organize the data in same pattern and display the reserved and empty parking spaces same as the original module as shown in Fig 2.

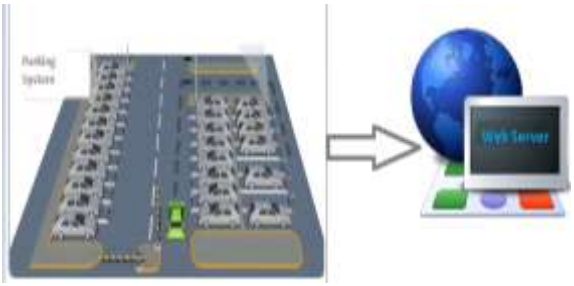

Figure 2: Communication between Hardware and Web Server

D. Real Time communication between Web server and Windows phone app

A unique Smart Phone application is designed using C#, to track real time status of parking area. This app allow users to choose their desire parking location and remotely view the run time status of Parking area, so the user can view the exact parking area status even the most effective and innovative feature, proposed in this parking application is that user can exactly view the parking lots by lots which parking lots are reserved, which are still empty. The app takes the input from the consumer, as the user select any place in windows phone application to remotely view the status of parking spaces, the application connects itself with the central web server on back-end, using Hyper Text Transfer Protocol (HTTP) that location and it shows the real time status of the location as shown in Fig 3 (a) (b) (c).

Figure 3: Windows Phone App GUI (a)

Figure 3: Windows Phone App GUI (b)

Figure 3: Windows Phone App GUI (c)

The designed and implemented prototype is a smart and cost effective system; it not only customizes the parking capabilities of parking area but also provide the real time monitoring from remote location. The exact free parking lot can be found using the smart phone app even in the most crowded parking areas. This helps to parking management system to save fuel, and reduce the frustration level of drivers searching for available parking spaces.

IV. RESULTS AND DISCUSSIONS

Vehicle Number Recognition is an important phase of smart parking system. Number plate extraction and recognition is done by using MATLAB algorithm. The system also have also database & GUI based java software for the Smart Parking System as shown in Fig 4. Main purpose of database is to maintain the detailed record of vehicles, purpose of GUI based software is to access the stored record & search the vehicles against car number, time & date. C# is used as programming language for the development the GUI based software. The database can be used for collecting parking tax amount and can also be used for other legal purposes.

Figure 4: MATLAB GUI Database of every entering vehicle

In parking plaza each spot have pre-installed sensors, which continuously transmit data to the web server through serial transmission port, using Arduino UNO. As soon as the data reaches to the server, it updates the website created by using .Asp. Now data is continuously updating to the website on the Webserver. The Web server interface is also shown in Fig 5. Through the windows phone application a user can view the run time status of parking plaza even with the details of parking lots (Which parking lots are free and which parking lots are reserved). Our implemented prototype is also shown in Fig 6.

Figure 5: Web Server Interface

Figure 6: Prototype of Smart Parking System

The Windows phone based application to choose desire parking area and check the current status remotely. The applications is first tested within the development environment using emulators and later subjected to field testing as shown in Fig 7(a) (b).

Figure 7: Windows Phone Application (a)

Figure 7: Windows Phone Application (b)

V. CONCLUSIONS AND FUTURE RECOMMENDATIONS

The objective of this research paper (Windows Phone Based Real Time Tracking of Smart Parking System) is to design a system based on Image processing, control system, and smart phone application that will not only change the hectic manual parking system but also show the real time status of parking area on smart phone application remotely. The proposed designed is cost effective and efficient system. This technology is used in various security and traffic applications. One important phase of smart parking system is

control system, which is autonomous, and does not need any external effort to work. Beside this image processing and Database method developed in this research project can be also used for various other important applications such as smart toll tax systems, border control, finding stolen cars, airport parking & can also be used as a marketing tool.

In future, this system can also be used for Deploying prepaid vehicle account, Nation-wide connected parking system, Reservation of parking lots through application.

ACKNOWLEDGMENT

Our foremost thanks go to our Head of Department Professor Dr. Madad Ali Shah, for his vital encouragement and support.

Last but not least, we would like to express our appreciation to our beloved parents for the unconditional love and support that let us through the toughest days in our life.

REFERENCES:

[1] R. BAHETI AND H. GILL. "CYBER-PHYSICAL SYSTEMS". IN THE IMPACT OF CONTROL TECHNOLOGY, 2011.

[2] SHOUP, "CRUISING FOR PARKING," ACCESS, VOL. 30, PP. 16–22, 2007.

[3] SUHAS MATHUR, TONG JIN, NIKHIL KASTURIRANGAN, JANANI CHANDRASHEKHARAN, WENZHI XUE, MARCO GRUTESER, AND WADE TRAPPE. PARKNET: "DRIVE-BY SENSING OF ROAD-SIDE PARKING STATISTICS". IN MOBISYS'10, 2010.

[4] R. ARNOTT, T. RAVE, AND R. SCHOB. "ALLEVIATING URBAN TRAFFIC CONGESTION". MIT PRESS, 2005.

[5] JATUPORN CHINRUNGRUENG, UDOMPORN SUNANTACHAIKUL, AND SATIEN TRIAMLUMLERD."SMART PARKING: AN APPLICATION OF OPTICAL WIRELESS SENSOR NETWORK". IN PROCEEDINGS OF APPLICATION AND THE INTERNET WORKSHOPS, 2007.

[6] SUSAN A. SHAHEEN AND CAROLINE J. RODIER. SMART PARKING MANAGEMENT FIELD TEST: A BAY AREA RAPID TRANSIT (BART) DISTRICT PARKING DEMONSTRATION. UCD—ITS—RR—05—02, 2005

[7] A.TAHIR, H.H. ADNAN, M.K. FAHAD "LICENSE PLATE RECOGNITION ALGORITHM FOR PAKISTANI LICENSE PLATES" CANADIAN JOURNAL ON IMAGE PROCESSING AND COMPUTER VISION VOL. 1, NO. 2, APRIL 2010.

[8] T.D. DUAN, T.L. HONG DU, T.V. PHUOC, N.V. HOANG, BUILDING AN AUTOMATIC VEHICLE LICENSE PLATE RECOGNITION SYSTEM, IN: PROC. INT. CONF. COMPUT. SCI. RIVF, 2005, PP. 59–63.

[9] MO SHIYING ZHOU, WEIXIN LV NA"NA SUN, YAXIN HUANG WEN "ALGORITHM FOR MULTINATIONAL LICENSE PLATE LOCALIZATION AND CHARACTER SEGMENTATION" THE TENTH INTERNATIONAL CONFERENCE ON ELECTRONIC MEASUREMENT & INSTRUMENTS

[10] JAVA 2: THE COMPLETE REFERENCE BY N. PATRICK AND S. HERBERT

[11] "JAVA GUI" VIRTUAL UNIVERSITY SLIDES

[12] DATASHEET OF ARDIUNO "UNO & PROXIMITY SENOR"

[13] DANIEL B. WORK AND ALEXANDRE M. BAYEN." IMPACTS OF THE MOBILE INTERNET ON TRANSPORTATION CYBERPHYSICAL SYSTEMS: TRAFFIC MONITORING USING SMARTPHONES". IN NATIONAL WORKSHOP FOR RESEARCH ON HIGH-CONFIDENCE TRANSPORTATION CYBER-PHYSICAL SYSTEMS: AUTOMOTIVE, AVIATION AND RAIL, 2008.

International Journal of Engineering Research and General Science Volume 3, Issue 6, November-December, 2015
ISSN 2091-2730

STUDY AND ANALYSIS OF CONVENTIONAL AND MODIFIED INTERLEAVED BUCK CONVERTER

Krishna P S [Mtech student] EEE, Jubin Eldho Paul [Associate Professor] EEE, Hari Kumar R [Associate Professor] EEE

krishnaps6@gmail.com, jubineldho@gmail.com

Abstract— This paper proposes an Interleaved Buck Converter (IBC) with continuous input current, extremely low output current ripple, low switching losses and improved step-down conversion ratio. Unlike the conventional IBC, the proposed converter has continuous input current and its output current ripple is extremely low. The proposed converter has lower voltage stress in comparison to the conventional IBC and also can provide a high step-down ratio which makes it a proper choice for high power applications where non-isolated step-down converter with low output current ripple and continuous input current is required. The proposed IBC shows that the voltage stress across all the active switches is half of the input voltage before turn-on or after turnoff when the operating duty is below 50%. Also the proposed converter can provide current-sharing between two interleaved modules without using additional current-sharing control method. All these benefits are obtained without any additional stress on the circuit components. The simulation is done by using MATLAB 7.12.0(R2014a).

Keywords— buck converter, interleaved, low switching loss,

INTRODUCTION

A basic buck converter is a voltage step down and current step up converter. It is mainly used in applications such as dc motor speed control and regulated dc supplies. It is also useful for tasks such as converting the main voltage in a computer down to the voltage needed by the processor. It has high efficiency due to no energy conversion. It has low switch current than load current. It has a disadvantage of ripples and during turn off current decays to zero.

In places where non isolation, step down conversion ratio and high output current with low ripple interleaved buck converter is used. It has a simple structure. Interleaving adds additional benefits such as reduced ripple currents in both the input and output circuits. In interleaved buck converter, all semi-converter devices suffer from the input voltage and hence high voltage devices rated above the input voltage should be used. High-voltage-rated devices have generally poor characteristics such as high cost, high on-resistance, high forward voltage drop, severe reverse recovery, etc. In addition, the converter operates under hard switching condition. Thus, the cost becomes high and the efficiency becomes poor. Higher efficiency is realized by splitting the output current into two paths, substantially reducing losses. To achieve high power density and better dynamics, it is required that the converter operates at higher switching frequency. But high switching frequency increase the switching losses. Therefore the efficiency is deteriorated.

BASIC BUCK CONVERTER

A buck converter [2] is a voltage step down and current step up converter. It has main application in regulated dc supplies and dc motor speed control. It is also useful for tasks such as converting the main voltage in a computer down to the voltage needed by the processor. When switch S is turned ON, the diode become reverse biased and the input provides energy to the load as well as to the inductor.

$$V_L = V_i - V_0 \qquad (1)$$

When switch is OFF, the inductor current flows through the diode, transferring some of its stored energy to the load.

$$V_L = -V_0 \qquad (2)$$

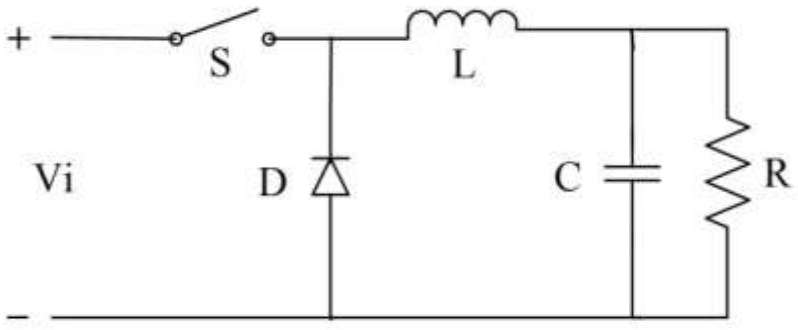

Fig.1 buck converter

According to volt-sec balance we will get,

$$\frac{V_0}{V_i} = D \qquad (3)$$

$$L = \frac{V_i \times D \times (1-D)}{I_L \times F_S} \qquad (4)$$

$$C = \frac{\Delta i_L}{8 \times V_0 \times F_S} \qquad (5)$$

The buck converter has an advantage of high efficiency due to no energy conversion and also have low switch current than load current. But it have a disadvantage of high ripple and during T_{OFF}, current decays to zero.

INTERLEAVED BUCK CONVERTER

Interleaving technique connects dc-dc converter in parallel to share the power flow between two or more conversion chains. It implies a reduction in the size, weight and volume of the inductors and capacitors. Also a proper control of the parallel converters increases the ripple frequency and reduces the ripple waveforms at the input and output of the power conversion system, which leads to a significant reduction of current and voltage ripples.

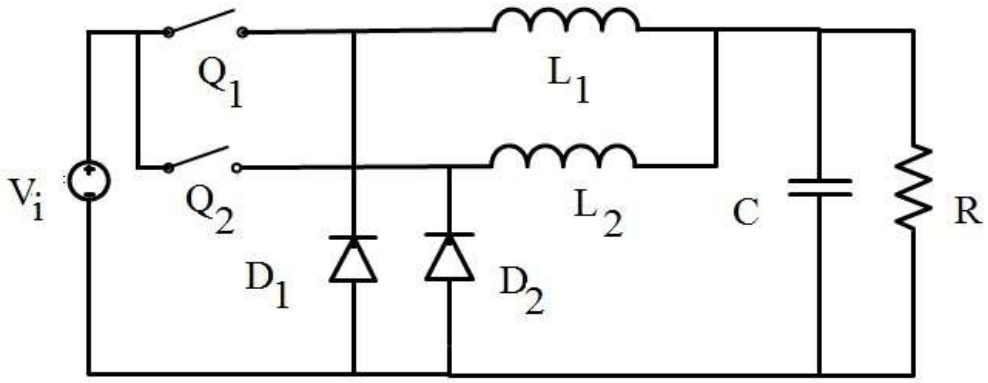

Fig.2 Interleaved buck converter

Due to the simple structure and low control complexity of interleaved buck converter, it is used in applications where non isolation, step down conversion ratio, high output current with low ripple is required.

When switch Q_1 turns ON and Q_2turns OFF inductor L_1 charges and L_2 dicharges and freewheels through the diode D_2. The inductor current flows through the diode, transferring some of its stored energy to the load.

$$V_{L1} = V_i - V_0 \quad (6)$$

$$V_{L2} = -V_0 \quad (7)$$

When both $Q_1$and Q_2 turns OFF, the both inductors L_1 and L_2 discharges and freewheels through $D_1$and D_2 .The equations are,

$$V_{L1} = V_{L2} = -V_0 \quad (8)$$

When Q_2 turns ON, the inductor L_2 charges and L_1 discharges and freewheels through the diode D_1.

$$V_{L1} = V_i - V_0 \quad (9)$$

$$V_{L2} = -V_0 \quad (10)$$

According to volt sec balance we get,

$$\frac{V_0}{V_i} = \mathrm{D} \quad (11)$$

$$L_1 = L_2 = \frac{(V_i - V_0) \times D}{\Delta i_L \times F_S} \quad (12)$$

In IBC [3]-[8], the active switches suffer from the input source voltage due to its parallel connection with the source. So high voltage devices should be used. But high voltage rated devices is characterized with high forward voltage drop, high cost, intense reverse recovery, high on resistance. Due to the hard switching condition, the operating efficiency is very poor. For getting good dynamics and higher power density converter requires to operate at higher switching frequency. But at higher switching frequency switching losses is increased and thus, efficiency is further reduced.

MODIFIED INTERLEAVED BUCK CONVERTER

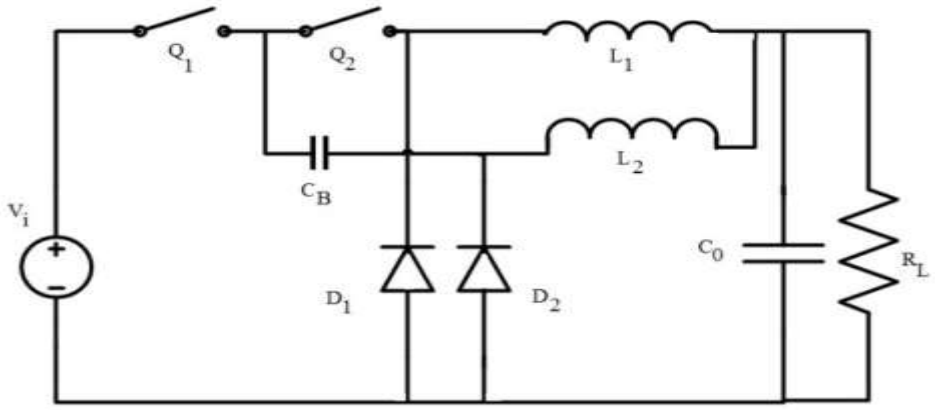

Fig.3 Modified interleaved buck converter

In the proposed IBC [1] two switches are connected in series and there is a coupling capacitor in the power path. The two switches Q1 and Q2 are activated with a phase shift angle of 180º.The output voltage can be regulated by adjusting the duty cycle at fixed switching frequency. The new IBC is operates at continuous conduction mode .So its current stress is low. The voltage stress of active switches is half of the input voltage before turn on and after turn off under steady state. So the capacitive discharging and switching losses reduces considerably. The voltage stress of freewheeling diode is also considerably reduced. So the reverse recovery and conduction losses on the freewheeling diode improve by using schottky diode which have generally low break down voltage. A good

conversion ratio and low output current ripple can be obtained with proposed topology. The new IBC is suitable for applications where the input voltage is high and duty cycle is less than 50%. The proposed system is analysed when D <0.5.

When Q_1 turns ON the inductor L_2 charges through the capacitor and the inductor L_1 discharges and freewheels through the diode D_2.

$$V_{L1} = V_i - V_{CB} - V_0 \quad (13)$$

$$V_{L2} = -V_0 \quad (14)$$

When both Q_1 and Q_2 turns OFF both the inductors L_1 and L_2 discharges and freewheels through the diodes D_1 and D_2.

$$V_{L1} = -V_0 \quad (15)$$

$$V_{L2} = -V_0 \quad (16)$$

When Q_2 turns ON the inductor L_1 charges and L_2 discharges and freewheels through the diode D_2.

$$V_{L1} = -V_0 \quad (17)$$

$$V_{L2} = V_{CB} - V_0 \quad (18)$$

According to volt-sec balance,

$$(V_i - V_{CB} - V_0) \times D \times T_s = V_0 \times (1 - D) \times T_s \quad (19)$$

$$(V_{CB} - V_0) \times D \times T_s = V_0 \times (1 - D) \times T_s \quad (20)$$

$$\frac{V_o}{V_i} = \frac{D}{2} \quad (21)$$

SIMULATION RESULTS

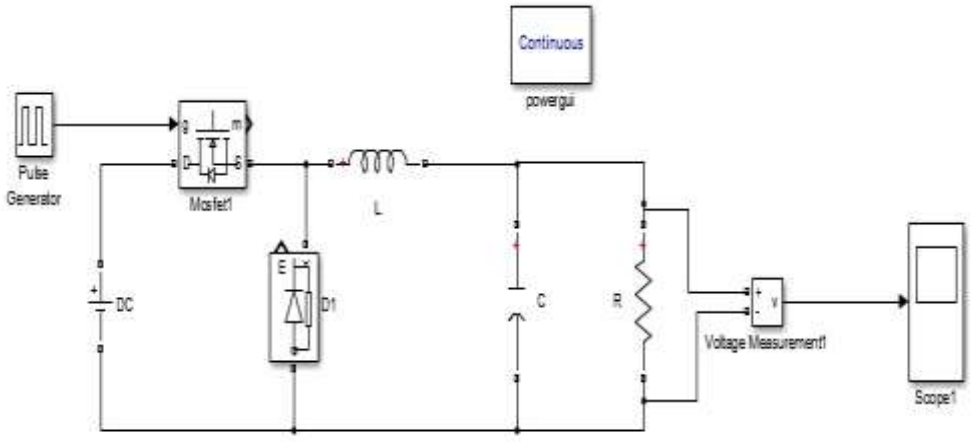

Fig.4 Simulation of buck converter

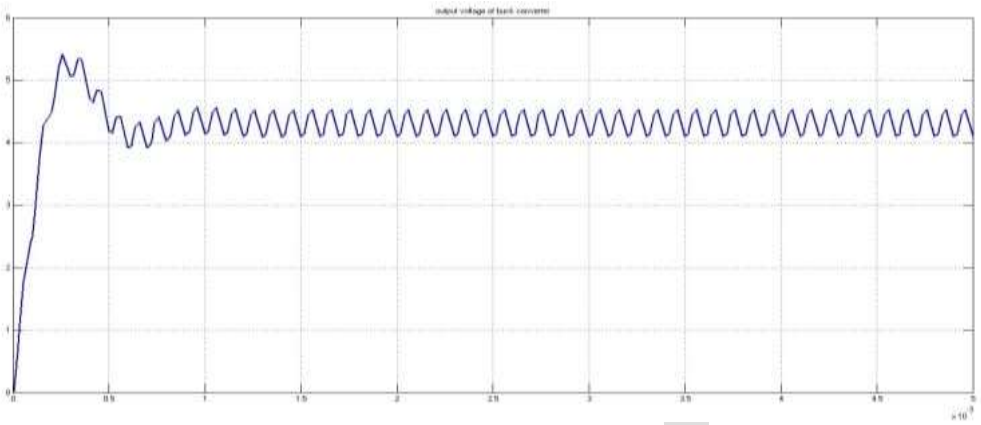

Fig.5 Output voltage of buck converter

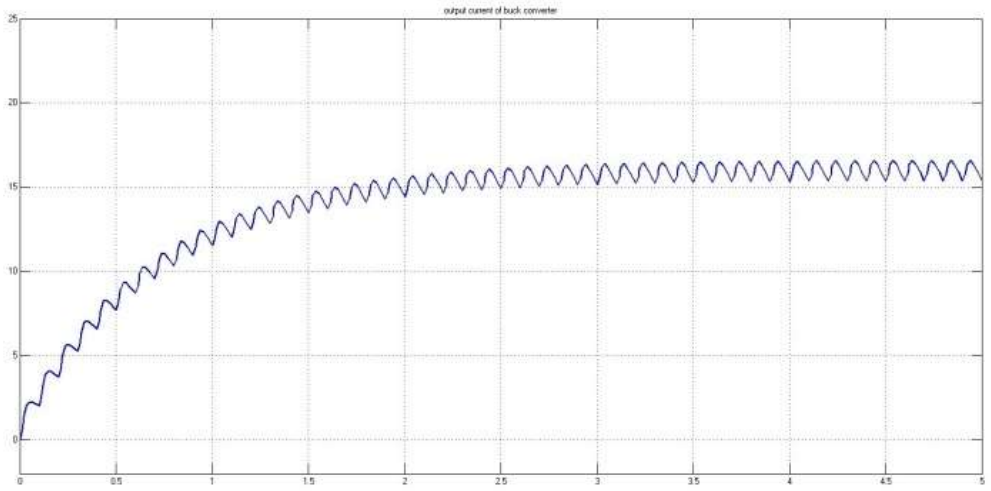

Fig.6 Output current of buck converter

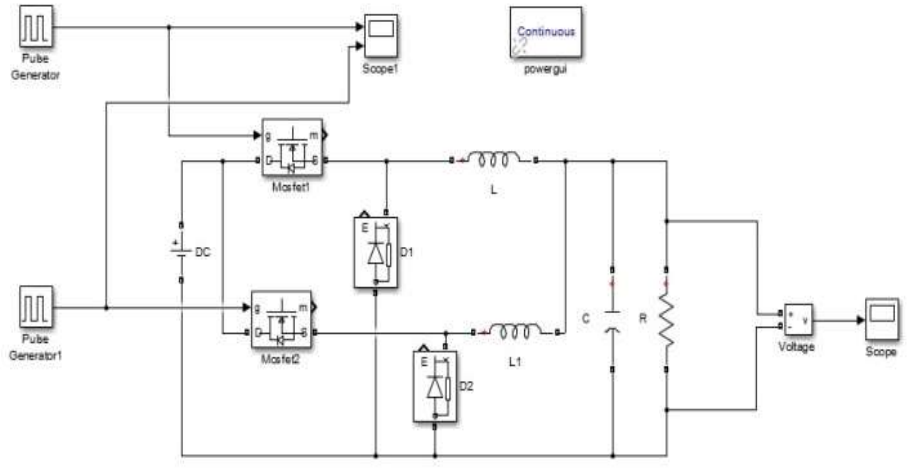

Fig. 7 Simulation of Interleaved buck converter

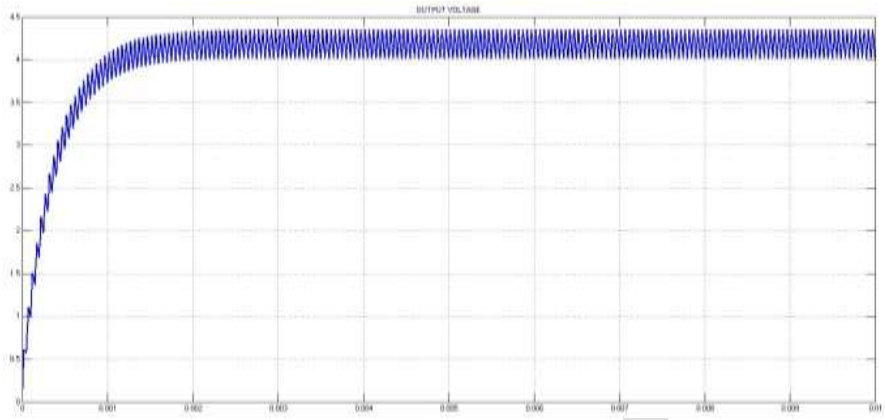

Fig.8 Output voltage of Interleaved buck converter

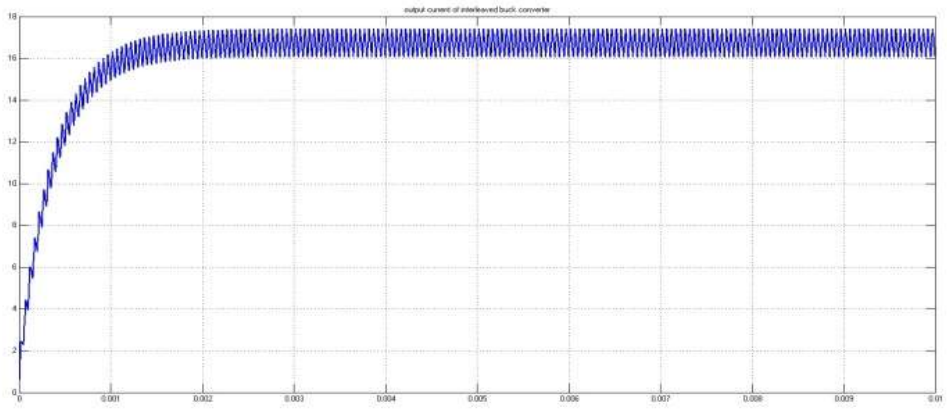

Fig. 9 Output current of Interleaved buck converter

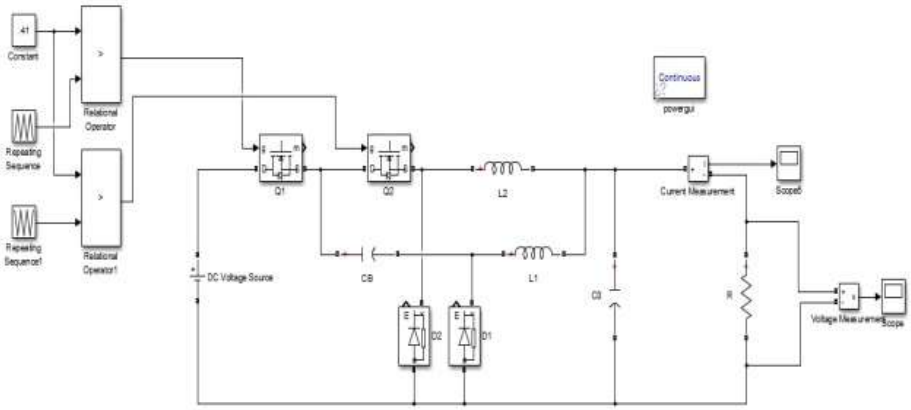

Fig.10 Simulation of Modified Interleaved buck converter

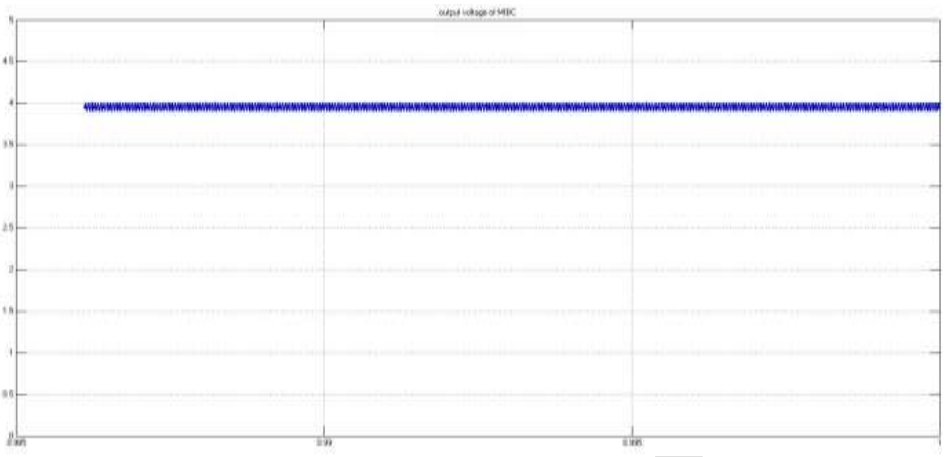

Fig. 11 Output voltage of Modified Interleaved buck converter

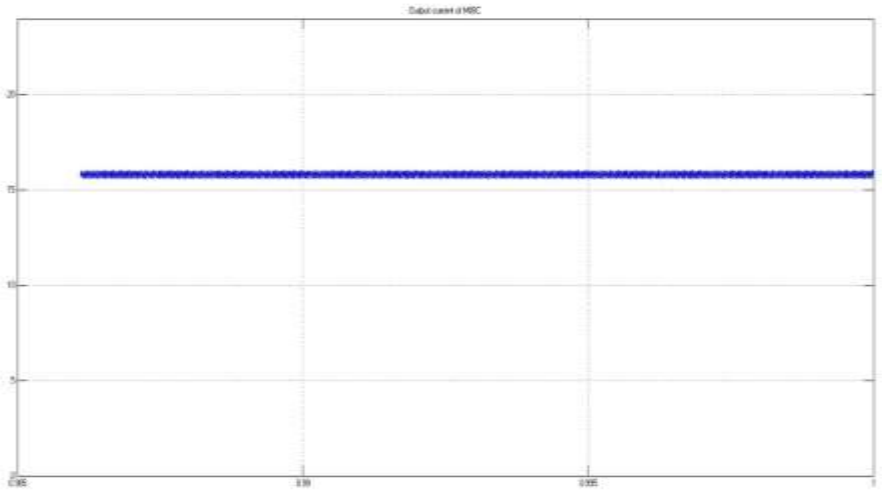

Fig. 12 Output current of Modified Interleaved buck converter

In this paper the simulation of buck converter, interleaved buck converter and modified interleaved buck converter is done and their output voltage and current waveforms are shown above. The analysis is done only for duty ratio less than 0.5. Their analysis of output voltage and ripple contents are shown in table below.

CONVERTER	BUCK	IBC	MIBC
DUTY RATIO	D	D	0.5D for D<0.5 D^2 for D>0.5
INPUT VOLTAGE	24	24	24
OUTPUT VOLTAGE	>4	>4	>4
VOLTAGE RIPPLE	0.43	0.344	0.1065
CURRENT RIPPLE	0.0496	0.0397	0.352

ACKNOWLEDGMENT

I would like to thank to almighty, my teachers, parents and friends for successfully completing this paper work.

CONCLUSION

In this paper, from the analysis of buck, interleaved buck and modified interleaved buck converter we can conclude that the current ripple and the voltage ripple is very low for interleaved buck converter. Modified interleaved buck converter is used for high input voltage, high step down and non-isolation applications. They have low switching loss and improved step down conversion ratio.

REFERENCES:

[1] Il-Oun Lee; Shin-Young Cho; Gun-Woo Moon, "Interleaved buck converter having low switching losses and improved step-down conversion ratio," *IEEE Trans. Power Electron,* vol.27, no.8, pp.3664,3675, Aug. 2012.

[2] Mohan Undeland Riobbins, "Power Electronics converters Applications, and Design"

[3] R. L. Lin, C. C. Hsu, and S. K. Changchien, "Interleaved four-phase buck-based current source with isolated energy recovery scheme

for electrical discharge machine," *IEEE Trans. Power Electron.*, vol. 24, no. 7, pp. 2249–2258, Jul. 2009.

[4] C. Garcia, P. Zumel, A. D. Castro, and J. A. Cobos,"Automotive DC–DC bidirectional converter made with many interleaved buck stages," *IEEE Trans. Power Electron.*, vol. 21, no. 21, pp. 578–586, May 2006.

[5] J. H. Lee, H. S. Bae, and B. H. Cho, "Resistive control for a photovoltaic battery charging system using a microcontroller," *IEEE Trans. Ind. Electron.*, vol. 55, no. 7, pp. 2767–2775, Jul. 2008.

[6] Y. C. Chuang, "High-efficiency ZCS buck converter for rechargeable batteries," *IEEE Trans. Ind. Electron.*, vol. 57, no. 7, pp. 2463–2472, Jul. 2010.

[7] C. S.Moo, Y. J. Chen, H. L. Cheng, and Y. C. Hsieh, "Twin-buck converter with zero-voltage-transition,"*IEEE Trans. Ind. Electron.*,

vol. 58, no. 6, pp. 2366– 2371, Jun. 2011.

[8] X. Du and H. M. Tai, "Double-frequency buck converter," *IEEE Trans. Ind. Electron.*, vol. 56, no. 54, pp. 1690–1698, May 2009.

International Journal of Engineering Research and General Science Volume 3, Issue 6, November-December, 2015
ISSN 2091-2730

COMPARATIVE STUDY OF MODES NON INVERTING BUCK BOOST POWER FACTOR CORRECTION CONVERTER

Sony M (Mtech student) [EEE], Thomas Mathew [Associate Professor] EEE, Lakshmi Krishnan [Associate Professor] EEE

sonym132@gmail.com, thomasmathew@icet.ac.in

Abstract— This paper presents a non-inverting buck-boost based power-factor-correction (PFC) converter. Unlike other conventional PFC converters, the proposed non-inverting buck-boost based PFC converter has both step-up and step-down conversion functionalities to provide positive DC output-voltage. Total harmonic distortion is reduced in boost mode of operation.

Keywords— Power factor correction (PFC) Total harmonic distortion (THD)

INTRODUCTION

In the world today, dc power supplies are extensively used inside most of electrical and electronic appliances such as in computers, monitors, televisions, audio sets and others. The high power nonlinear loads (such as static power converter, arc furnace, adjustable speed drives etc.) and low power loads (such as fax machine, computer, etc.) produce voltage fluctuations, harmonic currents and an imbalance in network system which results into low power factor operation of the power system [1].

There is a need of improved power factor and reduced harmonics content in input line currents as well as voltage regulation during power line over-voltage and under voltage conditions. The uninterruptible power supplies (UPSs) have been extensively used for critical loads such as computers for controlling important processes, some medical equipment, etc. The traditional UPS draws harmonic currents. The uncontrolled diode bridge rectifier with capacitive filter is used as the basic block in many power electronic converters. Due to its nonlinear nature, non-sinusoidal current is drawn from the utility and harmonics are injected into the utility lines. The nature of rectifiers either it is conventional or switch mode types, all of them contribute to low PF, high THD [2] and low efficiency to the power system [3]. It is well known that these harmonic currents cause several problems such as voltage distortion, heating, noises, reducing the capacity of the line to supply energy. Owing to this fact there's a need for power supplies that draw current with low harmonic content &also have power factor close to unity [4]. So far, a variety of passive [5] and active PFC techniques have been proposed. While the passive PFC techniques may be the best choice at low power, cost sensitive applications, the active PFC techniques are used in majority of the applications owing to their superior performance.

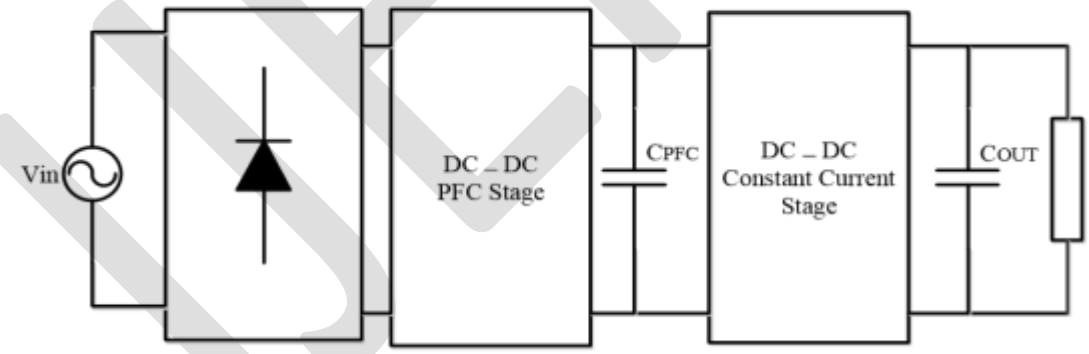

Fig.1 Two stage PFC circuit

In general, the use of two power stages is a good way to implement power factor correction and to balance the input and output powers but it increases the cost. Single power stage with charge pump PFC has been used in the fluorescent AC-DC-AC ballast. For a single power stage AC-DC-DC converter with PFC, it is hard to balance the input and output powers. Also, there are high voltage and current stresses on the power components. An AC-DC-DC Converter draws power from AC mains and supplies a DC current to the LED string. The driver needs a DC-DC converter to convert the input voltage into a DC current source and it limits the effectiveness of a charge pump.

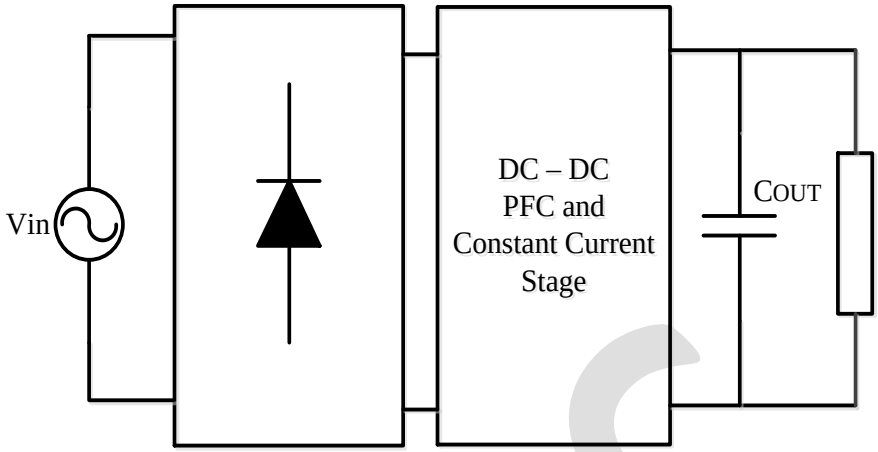

Fig.2.Single stage active PFC circuit

For low power applications, single-stage PFC converter is a better choice considering cost and performance. In single switch topologies, a PFC cell is integrated with a DC/DC conversion cell and both cells share active switches and controller. But those topologies suffer from high voltage and high current stresses. But most of those methods will bring high distortion to line current waveform, resulting in reduced power factor. So in this paper a new single stage converter is presented. The proposed non-inverting buck-boost based PFC converter has both step-up and step-down conversion functionalities to provide positive DC output-voltage.

BASIC PRINCIPLES AND MODES

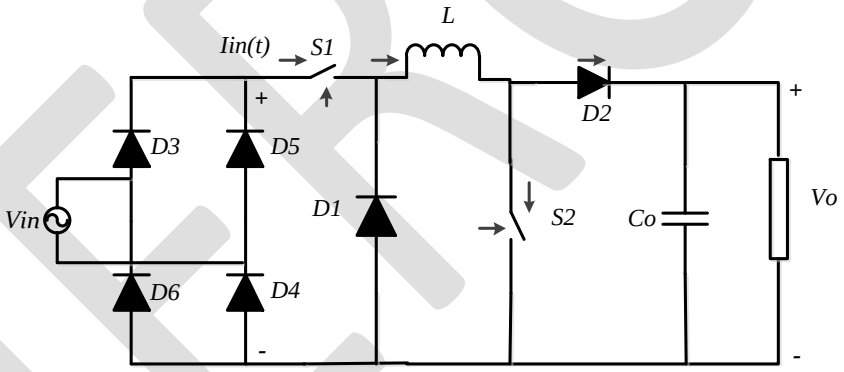

Fig 3.Non inverting buck boost converter

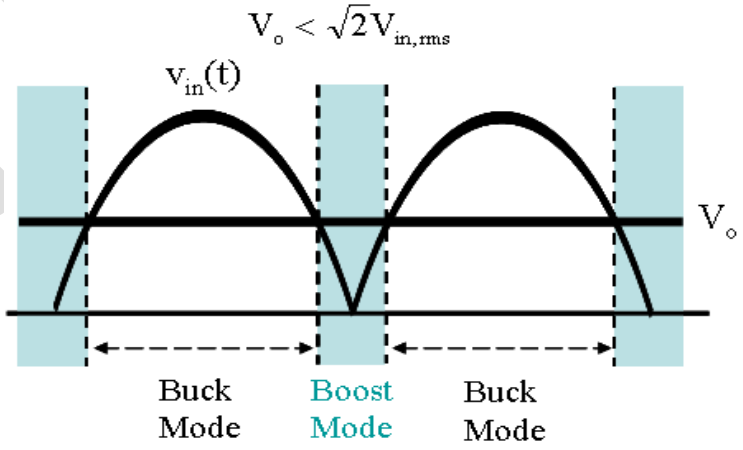

Fig. 4.Buck+boost mode

Boost Mode

When input supply is given the diode bridge rectifier it rectifies ac-dc and is given to converter. There are two modes of operation. When switch S_1 and S_2 is on input current linearly rises according to the value of inductor and energy is stored in output capacitor and load. This time diode D_1 and D_2 remains reverse biased. When switch S_1 and S_2 is off input current will not flow to inductor and load. Energy is stored in output capacitor freewheels through the load. This time diode D_1 and D_2 remains forward biased. Both time we get positive output voltage.

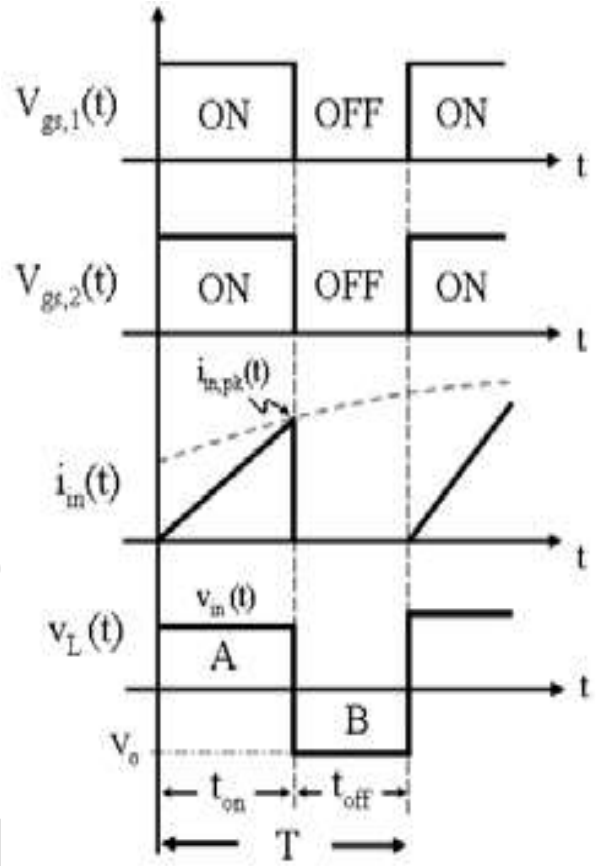

Fig .5.Waveforms of boost mode

Buck mode

In buck mode, the switch S_2 is off for entire time period. When input supply is given the diode bridge rectifier it rectifies ac-dc and is given to converter. When switch S_1 is input current linearly rises according to the value of inductor and energy is stored in output capacitor and load. This time diode D_1 and D_2 remains reverse biased. When switch S_1 is off input current will not flow to inductor and load. Energy is stored in output capacitor freewheels through the load. This time diode D_1 and D_2 remains forward biased. Both time we get positive output voltage.

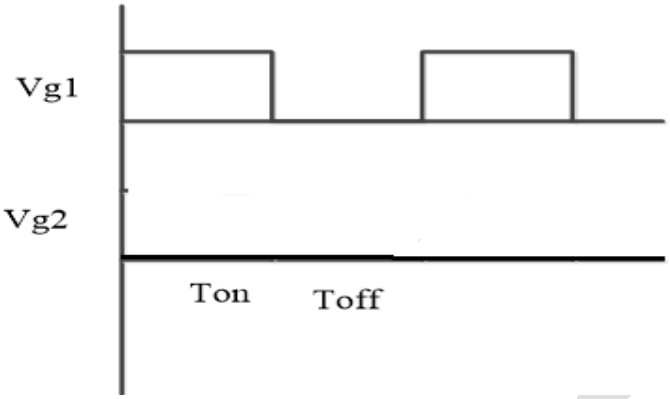

Fig .6.Waveforms of buck mode

POWER FACTOR CORRECTION AND TOTAL HARMONIC DISTORTION

In electrical engineering, the power factor of an AC electrical power system is defined as the ratio of the real power flowing to the load to the apparent power in the circuit, and is a dimensionless number in the closed interval of -1 to 1. A power factor of less than one means that the voltage and current waveforms are not in phase, reducing the instantaneous product of the two waveforms (V x I). Real power is the capacity of the circuit for performing work in a particular time. Apparent power is the product of the current and voltage of the circuit. Due to energy stored in the load and returned to the source, or due to a non-linear load that distorts the wave shape of the current drawn from the source, the apparent power will be greater than the real power. A negative power factor occurs when the device (which is normally the load) generates power, which then flows back towards the source, which is normally considered the generator.

Total Harmonic Distortion

The total harmonic distortion, or THD, of a signal is a measurement of the harmonic distortion present and is defined as the ratio of the sum of the powers of all harmonic components to the power of the fundamental frequency. On other words we can say that, when a signal passes through a non-ideal, non-linear device, additional content is added at the harmonics of the original frequencies. THD is a measurement of the extent of that distortion.

Design considerations

Assuming sinusoidal input voltage,

$V_{in} = V_m$ sinwt

I_{pk} - Peak inductor current

$$I_{pk} = \frac{V_{in} * T_{on}}{L_i} = \frac{V_m * D * T}{L_i} * \text{sinwt} \quad \ldots\ldots\ldots (1)$$

$$T_d = \frac{V_{in} * T_{on}}{V_o} \quad \ldots\ldots\ldots\ldots\ldots\ldots (2)$$

I_{in} - Line current

$I_{s2}\ (avg)$ - Average inductor current during on time

$I_{d2}\ (avg)$ - Average inductor current during off time

$I_{in} = I_{s2}\ (avg) + I_{d2}\ (avg)$……(3)

From (1)

$$I_{s2}\ (avg) = \frac{I_{pk}}{2} * \frac{T_{on}}{T} = \frac{V_{in} * D^2 * T}{2L_i}$$

From (2)

$$I_{d2}\ (avg) = \frac{I_{pk}}{2} * \frac{T_d}{T} = \frac{V_{in}^2 * D^2 * T}{2L_i * V_o}$$

During positive half cycle,

$$I_{in} = I_{s2}\ (avg) + 0 = \frac{V_{in} * D^2 * T}{2L_i}$$

$$L_i = \frac{V_{in} * D^2 * T}{2 * I_{s2}\ (avg)}$$

$$V_o = \frac{V_{in} * D}{(1-D)}$$

$$C_o = \frac{V_{in} * D}{f * \Delta Vo}$$

where ΔVo – out put voltage ripple

SIMULATION RESULTS

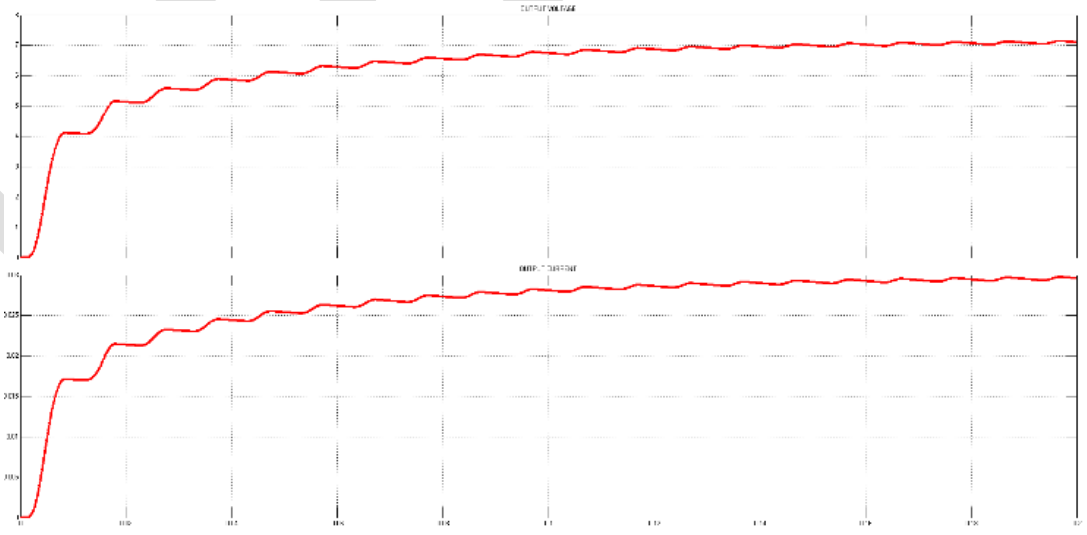

Fig.7 waveforms of output current and voltage of buck mode

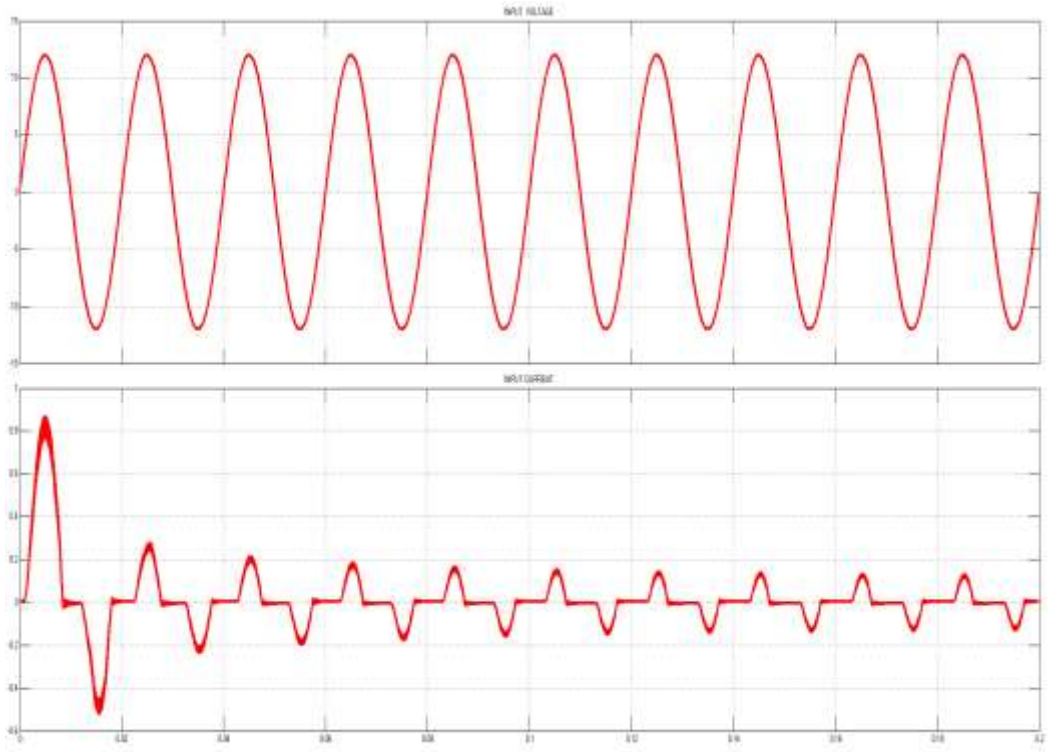

Fig.8 waveforms of input current and voltage of buck mode

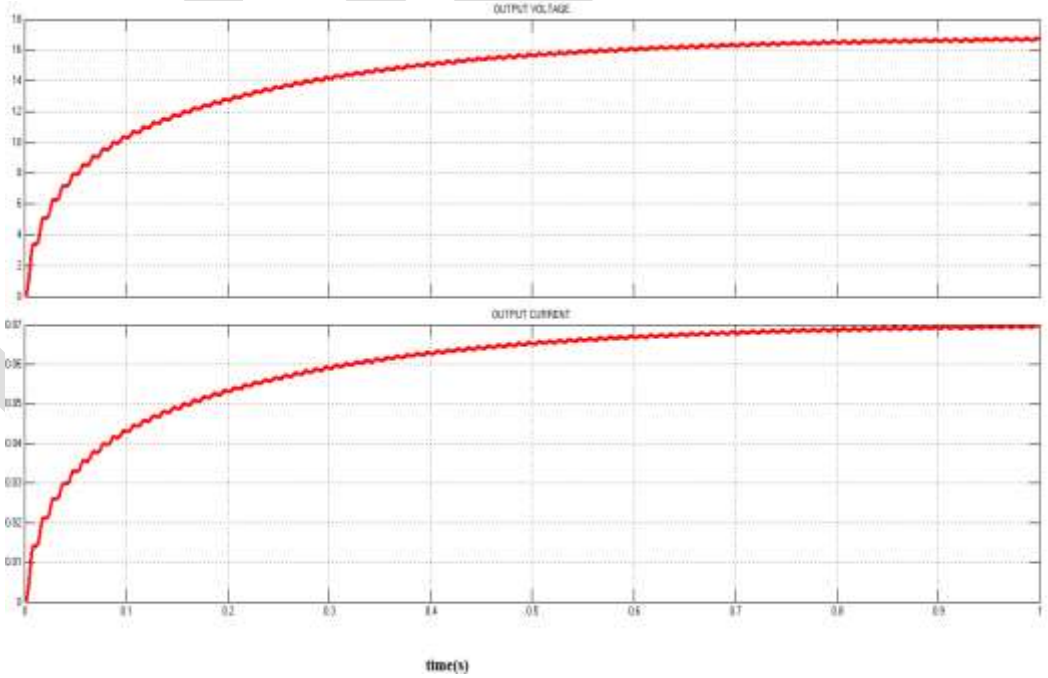

Fig.9. waveforms of output current and voltage of boost mode

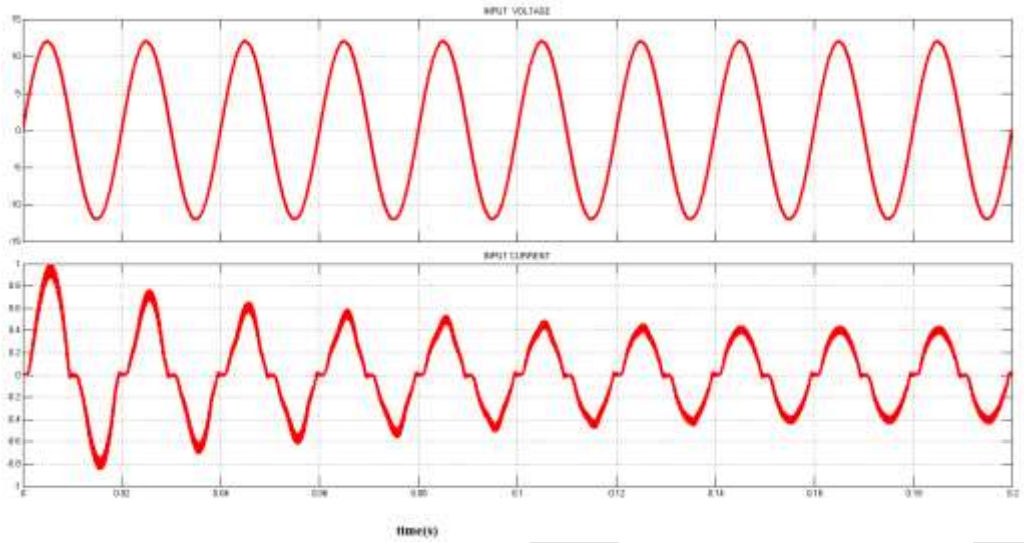

Fig.10. waveforms of input current and voltage of boost mode

HARMONICS IN INPUT CURRENT FOR BOOST MODE

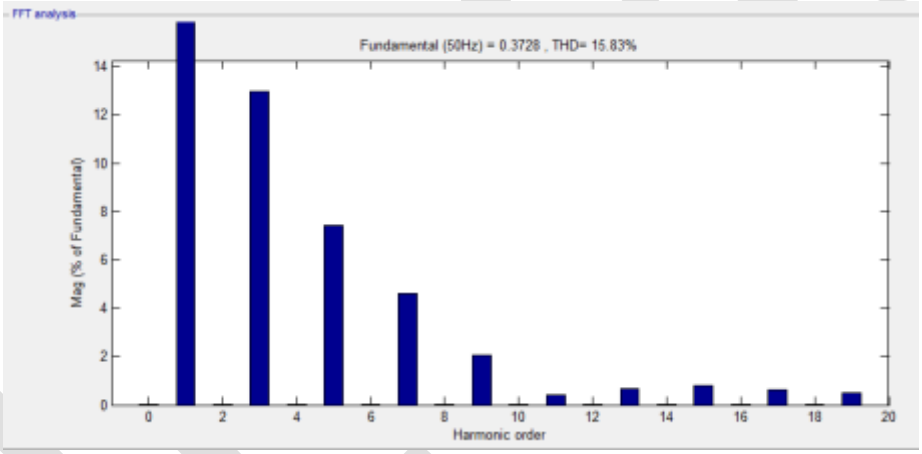

ACKNOWLEDGMENT

I would like to thank almighty , teachers ,parents and my friends for successfully completing this paper work.

CONCLUSION

Non inverting buck boost topology is analyzed and stimulated. The proposed converter reduces no: of stages. Power factor is increased to 0.9982. THD is reduced to 15.07% in boost mode of operation than in buck mode of operation.

REFERENCES:

[1] IEC 61000-3-2 International Standard. Limits for Harmonic Current Emissions, Third Edition. 2005-11.

[2] T. Nussbaumer, K. Raggl, and J. W. Kolar, "Design Guidelines for Interleaved Single-Phase Boost PFC Circuits" IEEE Trans. On Industrial Electronics, vol. 56, no. 7, July 2009, pp. 2559-2573.

[3] S. Busquets-Monge, J.-C. Crebier, S. Ragon, E. Hertz, D. Boroyevich, Z. Gurdal, M. Arpilliere, D.K. Lindner, "Design of a Boost Power Factor Correction Converter Using Optimization Techniques", IEEE Trans. on Power Electronics, vol. 19, no. 6, November 2004, pp. 1388- 1396.

B. A. Canesin and F. A. S. Goncalves, "Single-phase High Power- Factor Boost ZCS Pre-regulator Operating in Critical Conduction Mode" in Proc. IEEE ISIE, June 9-11, 2003, pp. 746-751

[4] M. M. Jovanovic, D.M.C. Tsang, and F.C. Lee, "Reduction of Voltage Stress in Integrated High-quality Rectifier-regulators by Variable frequency Control," in Proc. IEEE APEC, February 13-17, 1994, pp. 569-575.

[5] D.S.L Simonetti, J. Sebastian, and J. Uceda, "Single Switch Three phase Power Factor under Variable Switching Frequency and Discontinuous Input Current," in Proc. IEEE PESC, June 20-24 1993, pp. 657-662.

[6] K. H. Liu and Y. L. Lin, "Current waveform distortion in power factor correction circuits employing discontiuous-mode boost converters," in Proc. IEEE PESC'89, 1989, pp. 825–829.

[7] Chen, D. Maksimovic, and R. Erickson, "Buck-Boost PWM Converters Having Two Independently Controlled Switches" in Proc. IEEE PESC, June 17-21 2001, pp. 736-74

International Journal of Engineering Research and General Science Volume 3, Issue 6, November-December, 2015
ISSN 2091-2730

Near Threshold Voltage (NTV) Regulation for System-on-Chip (SoC)

ShuzaBinzaid, Avadhoot Herlekar

Department of Electrical and Computer Engineering, University Of Texas At San Antonio, One UTSA Circle, San Antonio Texas
E-Mails: Shuza00@yahoo.com ; +12106392640

Abstract— Integrated Circuits (IC)of CMOS (Complementary Metal Oxide Semiconductor) technology have become daily part of our lives. The CMOS technology has been playing a huge role and serving industries with many solutions to design digital circuits. Many different processes, offered by leading semiconductor manufacturing industries, for designing CMOS based transistors that ranging from 16nm to 180nm with different range of input-output voltages, allowing flexibility to design engineers to achieve their set goals. Such increase in number of transistors aggressively in an IC tends to increase power consumption substantially which results in heat and sometimes breakdown of the device. This paper mainly focuses on unique technique to reduce power consumption of the large integrated circuits by reducing the supply voltage (VDD) slightly higher than their process threshold voltages (V_{th}). Near this area energy usage is considerably low. This area is called as Near Threshold Voltage (NTV). The NTV technology in this work includes variation in aspect ratio of width and length of transistor channels and variation in number of gate stages of the CMOS circuits. The designed chip proves to be efficient in consuming power between 10 to 480 times less than their requirement of commercially specified voltage, while maintaining the switching of the devices within expected limits by using this NTV technology.

Keywords—IC; Near Threshold Voltage; CMOS; Aspect Ratio; LTspice IV; V_{th}; MOSIS; MAGIC; Voltage Regulation; SoC; IC Pad; VCO; C5N process; Static Power; Dynamic Power.

INTRODUCTION

Semiconductor based technologies are become important today in our daily lives. CMOS transistor logic systems have become the choice of today's technologies for ICs as their dynamic power is reduced [1]. Fast growing digital world of CMOS technology, electronics industries have adapted with it, because of simple structure designs, wide range of amplification capability and high reliability. At this point, it can be said that there is no successor to CMOS yet which is viable commercially [2]. Sometimes these are also called as Complementary-Symmetry Metal Oxide Semiconductors as they are used in complimentary and symmetrical pairs for different functionality. CMOS are used in all kinds of memories such as RAMs, ROMs, EPROMs and EEPROMS also in digital circuits like MUX, DEMUX and DECODERS etc. [3]. Designing digital logic has become much easier with CMOS Devices in ICs.

CMOS generally don't have the waste heat as of other logics and high noise immunity as well. To understand fundamental concepts of semiconductor devices we must apply modern physics to solid materials. Most integrated circuits has silicon material. Silicon is a Group IV; it forms covalent bond with four adjacent atoms. Due to all the electronics involved in chemical bonds silicon is a poor conductor. To improve the conductivity it has to be tied with Group V material that is arsenic which has 5 electrons in it. 4 atoms replaces silicon atoms and one is loosely bound [4]. So the electron is free to move in room temperature and can carry current. This is called as n-channel semiconductors as of negatively charged electrons. Similarly for p-channel Group III dopant can be used, boron for the matter, the dopant atom borrows electron from neighboring silicon atom and becomes short by 1 electron. The electron and hole can propagate about the lattice making it a P-channel semiconductor being holes as the primary charge carriers. While making Metal Oxide Semiconductors, many processes are used including oxidation of silicon, doping, photo-resist, passivation, resistive deposition, etching etc.

Though CMOS has gained popularity in these years there have been major constraints that come along. CMOS device was basically built for low power consumption but when the system or device is considered the power consumed is more. Today in digital world the technology has been increasingly growing the density of transistors per area and decrease in die size that affects a major factor known as power consumption which can be true for any digital or analog circuits. As power consumption is increasing the cooling techniques have been developed but they lack in providing sufficient cooling as fast as the need [5]. Reduction in power consumption makes device more reliable. There are many factors that affect power consumption in a circuit. Such as output loading effect, variable input, capacitance of each node. Static and dynamic power consumption are the two type which define power consumption in CMOS circuits [6]. Static power consumption is caused due to diffused region and substrate. The reverse leakage current is between diffused region and substrate. It is a product of device leakage current and supply voltage. Dynamic power consumption is due to switching of transistors. When transistors are switching from one logic level to other the nodes are charged and

discharged. This is also dependent on what frequency the circuit is switching. When circuit is switching, current flows between nodes. Most power consumption occurs because of dynamic power consumption.

The power consumption also depends upon the device technology used to manufacture the CMOS based transistors. The change in device technology is a part of reducing induced power [7]. The device technology is being reduced making the parts smaller and making the devices slimmer. Power consumption in any circuit is because of speed and number of CMOS devices. The primary focus of this paper gives a solution over these issues. This paper proposes to use NTV technology for all the circuits in the designed System-on-chip. The voltage used is slightly greater than the NTV to assure the hysteresis region. An IC designed for this paper has different circuits with combinations of different aspect ratio of W/L such as 1, 3 and 5. Also with different combinations of number of stages such as 3X, 11X, 21X, 51X, 201X [8]. In this work, power consumption is analyzed for each circuit for different supply voltages.

PRIOR WORK

Prior research work was focused primarily on Near Threshold Voltage (NTV) region of different circuits. It was needed to find the amount of voltage required to operate any circuit. For this work NTV was approximately 12%-20% of the supply voltage, so the power consumption should be significantly less. To achieve the near threshold voltage, some changes were made in CMOS simulation and design process. The method also required changing the aspect ratio of W/L. MeMDRL_UTSA and other institutions have done some studies in this area [8]. The primary aim of that work was to layout and simulation based on Ring Oscillators for initial study. The circuits were built with different aspect ratios of n- and p-channels. The results have been taken for Wp/Wn=1, 2, 3, 2.5 for limited different number of stages like 1X, 2X, 3X. The best result was found for Wp/Wn= 2.5 and number of stages = 1X.

Near Threshold Operation:

There have been documented before that when smaller architecture of technology of CMOS process develops, logic gate densities increase, but the power consumption is reduced by per gate. As a result, the older designs require redesign efforts and extensive and engineering research to readjust the ICs to the newer technology for reduced power consumption in order to sustain in today's competitive, tough consumer market. Unable to coop such financial stress to re-tech ICs, can drive many designs and logic ICs to run out of business. Near threshold voltage concept is created to power the older ICs at lower voltage and at least at the 1/10 of the power. Here, this lower voltage is at the near threshold voltage where supply voltage is approximately equal to threshold voltage of the transistor. Near this area power consumption is found to be minimal and the performance characteristics are much favorable [9]. The purpose behind this paper is not only to reduce power consumption, but also to improve the performance of the digital signal to be very accurately delivered, as well as few analog and mixed-signal circuits that are considered here. CMOS can work at very low voltages and the power consumption occurs at the nodes of it. The charging and discharging of the internal node capacitances result in power consumption [10]. When VDD is set low, but higher than its threshold and hysteretic voltage region, the circuit can still switch at desired speed but the power usage becomes very low. In this research, extensive work is done on NTV for different supply voltages, run circuit at NTV voltage and also older process VDD. Thereafter, then power is calculated to compare improvement. NTV is achieved by the voltage parameters in CMOS circuits by help the new concept of low power driving MOS transistors and additionally to that FET circuits are placed for assuring the constant voltage regulation.

OBJECTIVES AND GOALS

Main purpose of this work is NTV technology on various circuits and reduction of power consumption. We are also looking for designing a chip and having it fabricated from MOSIS services. The goals and objectives of this project will be as follows,

- Analytical verification on voltage regulators, digital and analog components.
- Numerical verification of comparing circuits under NTV switching.
- Parametric evaluation of threshold voltage at NTV.
- Parametric evaluation at commercial study voltage of 5V at C5N process.
- Run electrical simulation on every component and complete power analysis based on aspect ratio and logic level stages.

DESIGN METHODOLOGY

For designing test circuits, layouts of different circuits were completed to prove the NTV regulation concept. The circuits are both analog and digital. For creating layout MAGIC VLSI tool is used [11]. This tool is used for designing chip as well. Different circuits have been chosen such as Voltage Controlled Oscillator, Ring Oscillator, Current mirror circuit, Differential amplifier for the IC. Each circuit has been designed with different aspect ratio of width and length of transistors. The aspect ratios selected are 1, 3 and 5. These circuits contain different number of stages including 3X, 21X, 51X, 201X. Number of stages increase number of CMOS devices in circuit to give good results in terms of power consumption and also operating frequency. Circuits have been placed in the chip as a

part of the NTV test system. This SoC has 40 pads acting as input output pads. Each side has 10 pads. These circuits are designed using only metal 1 and metal 2. Voltage Controlled Oscillator and ring oscillator have feedback from the output. So these circuits are provided with different supply voltages. The chip also contains voltage regulation circuit based on FET transistor. The voltage regulation circuitry is designed to provide constant voltages. Many voltage regulation circuits are present in market, which give constant voltage. The reason behind building the regulation circuit is that it will provide selected voltage to internal circuit without requiring any additional supply voltage source externally. This voltage regulation circuit can automatically stabilize voltage needed by the circuit regardless of process technology. To design a layout the lambda needs to be set as this design is going under manufacturing. So chosen is the AMI C5N process where lambda is 0.5.

The circuits have been simulated for varying voltage values of VDD. First was to determine the near threshold voltage of each circuit. The values noted are at the point where satisfied toggling has occurred. When the NTV is found the VDD is increased till 5v and results have been taken. To calculate power the current values at different voltages have been noted down and graph has been plotted. Thus this technology ensured to verify results of simulations for circuits normal operations.

Circuits Design for NTV Technology Verification:

All choices of circuits are in different aspect ratios of W/L of transistors and number of stages.

a. Voltage Controlled Oscillator circuit
b. Ring Oscillator
c. NFET based Voltage Regulation Circuit
d. PFET based Voltage Regulation Circuit

Figure 1 Shows layout of the VCO and ring oscillator circuit. Likewise, each circuit layout has been designed with MAGIC VLSI tool. Default bonding pads have been designed to connect the I/O pins. To design desired IC 0.5um process configuration is used that is supported by MOSIS fabrication services.

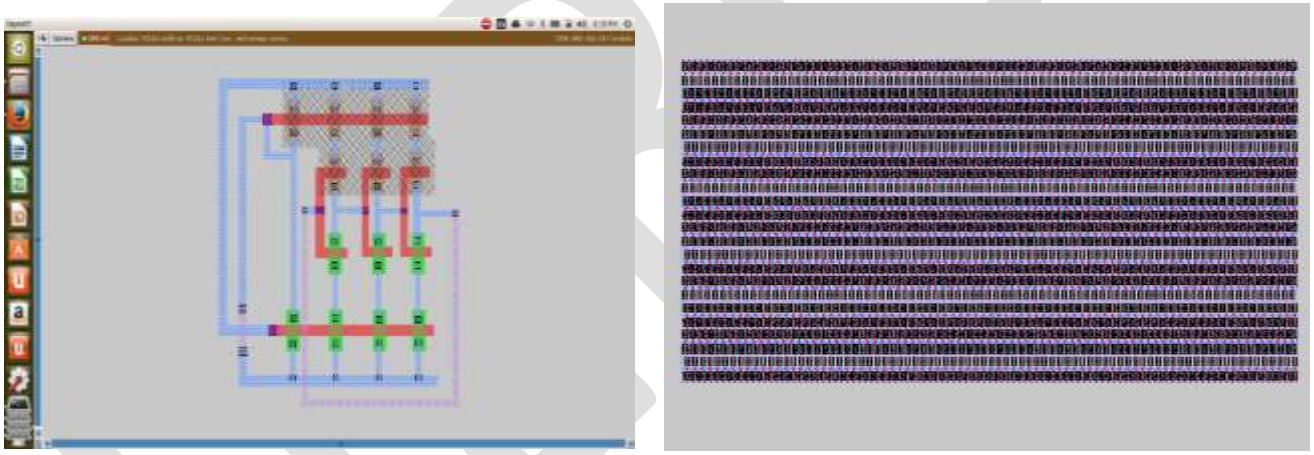

(a) (b)

Figure 1: Layout design of a 3-Stage Voltage Controlled Oscillator (a) and a 961-Stage Ring Oscillator (b).

The width and length of PMOS and NMOS are chosen with aspect ratio of 1, 3, and 5. For all the circuit metal1, metal2 have been used and for contacting materials n-diffusion, p-diffusion, and poly have been used.

SIMULATION RESULTS

In this research work, one of the most important goals was to successfully simulate the electrical operations and parametric evaluations. Explained here are the simulation output results for each circuit designed.

Voltage Controlled Oscillator:

Voltage Controlled Oscillator (VCO) produces continues clock as it has a feedback from output therefore it is used for clock generation in digital circuits [12] [13]. VCO is provided with VDD as an input and VDD is varied for different voltages and results have been taken. PSpice is used to simulate all small circuits. The figure 2 shows the output waveforms of VCO. The figure 2 shows VDD (Green) and output (Blue) waveforms.

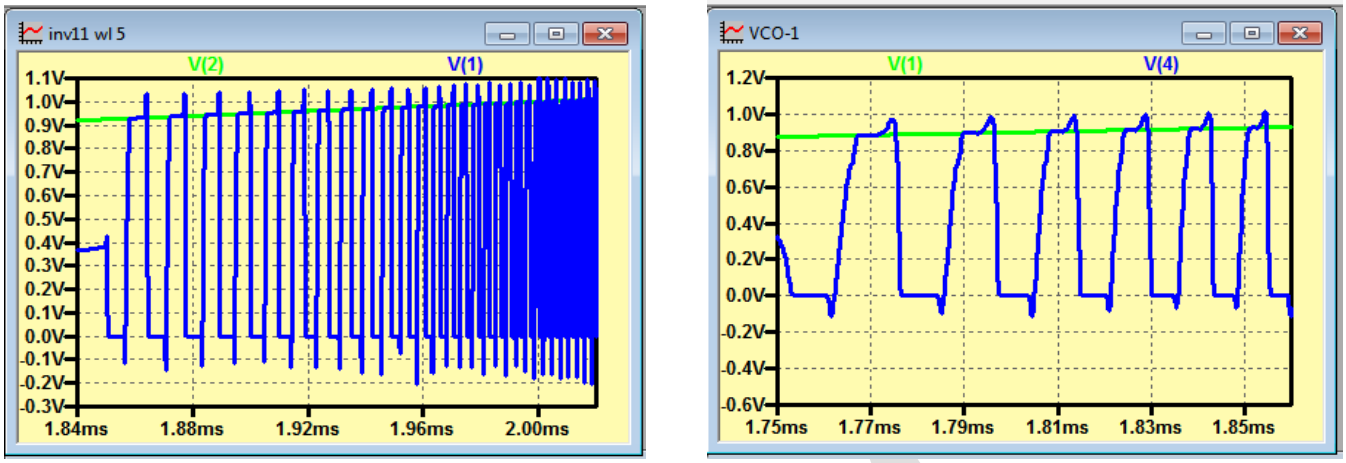

(a) (b)

Figure 2: Waveform of VCO following VDD (a) and output waveform at toggling (b).

The VDD is ramped from 0V to 5V. It was found to have the NTV = 0.954. AMI C5N process has the parameters for PMOS and NMOS are defined at 0.7640855 and -0.9444911 respectively. Considering the same reason, it can be assured to set NTV at 0.954V. To assure safety of operation, the VDD can be a bit higher than 0.954V, which is 1V. The circuit has been simulated for different aspect ratios of width and length of transistors and number of stages and NTV is calculated. Table 1 shows the results of the NTV.

Table 1: NTV of VCO circuit at different aspect ratios and its number of switching stages.

VCO (Number of Stages)	Wp/Wn= 1	Wp/Wn= 3	Wp/Wn= 5
3X	0.957 V	0.925V	0.875V
5X	0.925V	0.899V	0.88V
9X	0.9V	0.89V	0.875V

Ring Oscillator:

Figure 3 shows the special technique of simulation to determine the NTV of any particular circuit design. The toggling output waveform of a ring oscillator at the rising voltage indicates the operation of the circuit at threshold voltage and at NTV. For ring oscillator the VDD (Green) is ramped up from 0V to 5V and output (Red) is toggling near to 0.95V. So considering the safe operation of the circuit, NTV for ring oscillator is set to 1V. The ring oscillator also simulated for different aspect ratio of width and length of the transistor and for different number of stages. The ring oscillator's inverter stages required is given by,

Ring oscillation stages, $S = 2n + 1$

Where, n is the number of inverters required for the circuit.

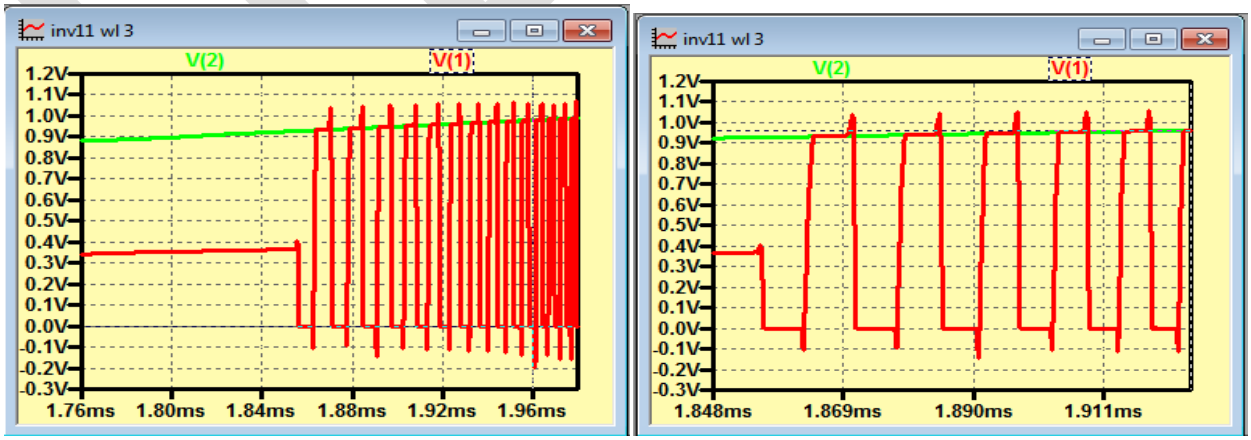

(a) (b)

Figure 3: Waveform of Ring Oscillator following VDD (a) and output toggling (b).

As explained earlier the near threshold voltage for CMOS in AMI C5N process is near 0.9V the table 2 shows the similar values. Being the primary focus of this paper the ring oscillator was simulated for Voltage at VDD and for current to find the power consumption of circuit.

Table 2: NTV of Ring Oscillator circuit for different aspect ratios and number of stages.

Ring Oscillator	Wp/Wn=1	Wp/Wn=3	Wp/Wn=5
3X	0.91V	0.9V	0.9V
11X	0.98V	0.99V	0.93V
21X	0.975V	0.95V	0.945V
51X	1.0V	0.975V	0.97V
201X	1.03V	1.0V	1.0V

Voltage Regulation and Reliability for NTV Circuits:

As this paper focuses on the technology reliability on low voltage as circuits operate on, power source provides regulation by custom NFET. All circuits in chip are given input that is VIN with value equal to supply voltage that is 5V. The circuit has a varying load resistor (R1). With different load resistance value output voltage has been noted down the same load has cascaded Vth. Significant power efficiency can been seen.

Initially, VIN (V1) is given as a 5V. The load R1 is 125Ohms. Therefore current is 40mA. With the same load, the voltage regulation of NFET for NTV with cascaded V_{th} (Diode) has output of 1.35V-1.42V and current is 10.96mA, shown in figures 4 and 5; thus ensuring excellent regulation of the technology in C5N process. It also proves the same for any other fabrication processes.

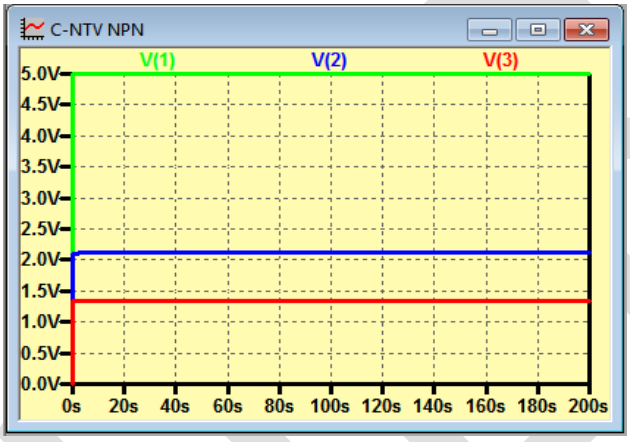

Figure 4: VIN (V1) = 5V, NTV V (3) = 1.35V R1= 125Ohms.

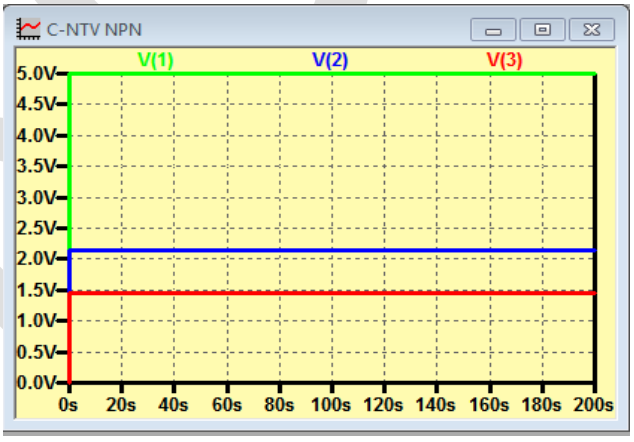

Figure 5: VIN (V1) = 5V, NTV V (3) = 1.42V R1=1KOhms.

So the power can be easily calculated for different input voltages and power ratio can be determined. That is, the Power Ratio = 200mW/15.015mW = 13.32. So the power reduction is almost 13.32 times which can easily be carried out in large CMOS IC's. The simulated results show that for large current load at 125Ohms the output is 1.35V and for small current load at 1KOhms the output is 1.42V. So the regulation of NTV has the reliability of more than 95%.

PFET Based Voltage Regulator:

Figure 6 and 7 shows the NTV regulator design based on the load that is determined for the various circuits suitable to run in many ICs regardless of process technologies. Similar simulations have been carried out and the power ratio in PMOS has been 11.42. That is the power reduction is almost 11.42 times, and also better responses on load conditions than NFET NTV technology. PFET based regulators have more reliability than NFET base regulators that can be clearly seen from simulations. For large current loads at 125Ohms the output (red) is 1.36V and for small current load at 10KOhms it is same as 1.37V so the reliability is almost 100%.

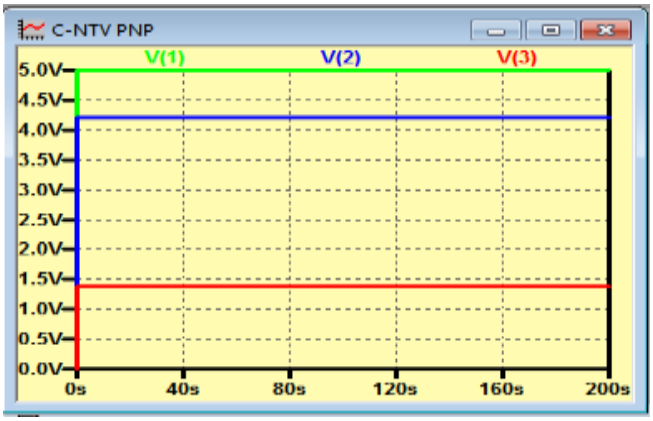

Figure 6: VIN (V1) = 5v NTV V (3) = 1.37V R1= 125Ohms.

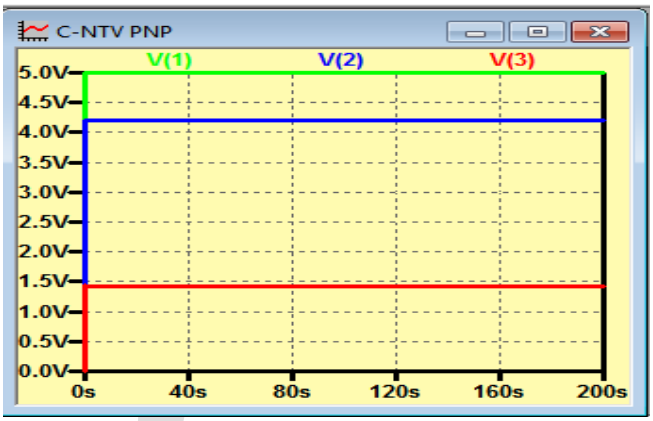

Figure 7: VIN (V1) = 5v NTV V (3) = 1.37V R1= 10KOhms.

Power Consumption by the Circuits:

Below shown are 4 graphs. Those are plotted for comparing results of power consumption of CMOS circuits.

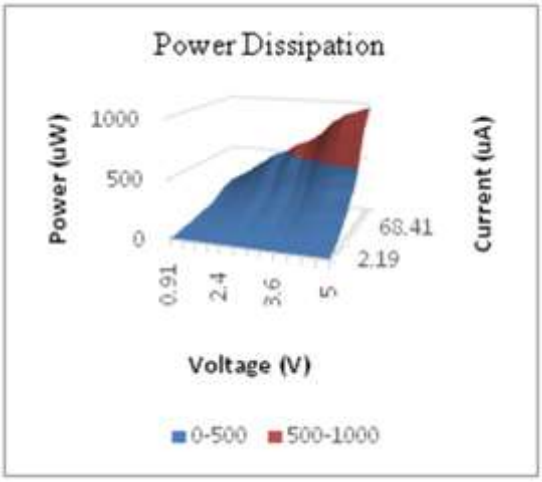

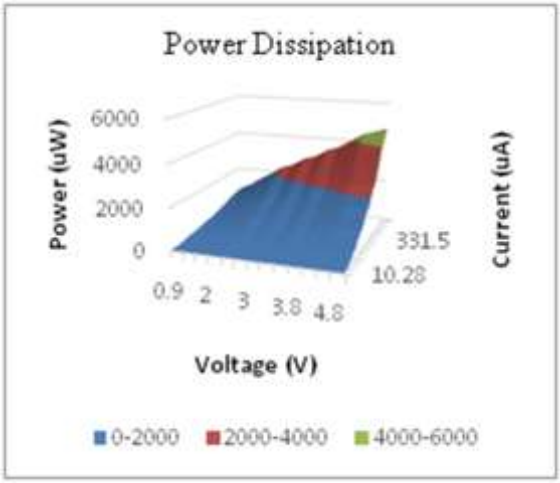

Figure 8: W/L=1, No. of Stages= 3.Figure 9: W/L=5, No. of Stages= 3.

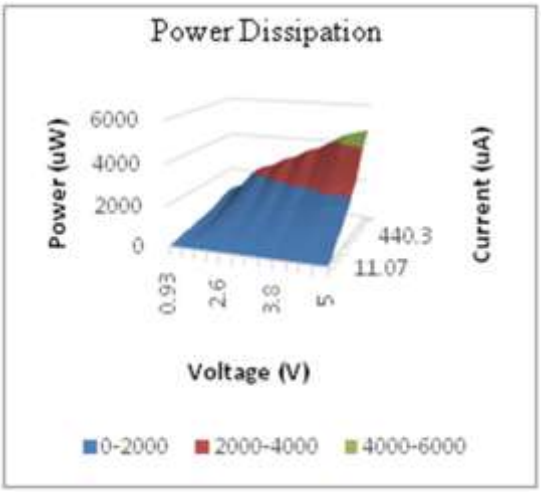

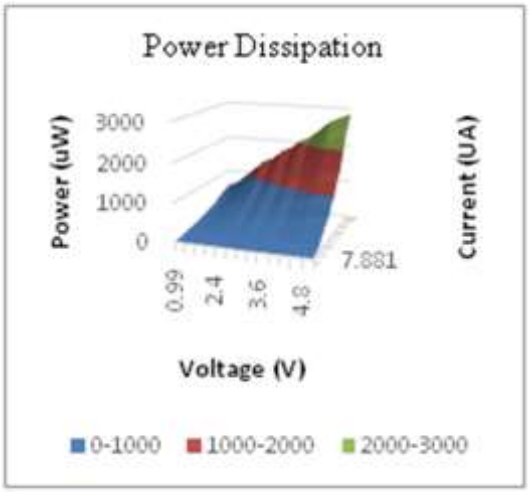

Figure 10: W/L=5, No. of Stages= 11. **Figure 11: W/L=1, No. of Stages= 11.**

To calculate the power, the formula has been used as,

$P_{real}= (V_{rms}/\sqrt{2}) * (I_{rms}/ \sqrt{2})$

Where, P_{real} = Power (uW), V_{rms}= Voltage (VDD) and I_{rms} = Current (uA)

As the VDD increases, power also increases at the rate of VDD^2. From the simulation, power is carried out for all the circuits shown in figures 8 thru 11 show the graphs of power consumption. Also here smaller the aspect ratio, smaller the power consumption becomes. But as the aspect ratio of width and length of transistors and number of stages keep on increasing, the power consumed becomes much higher. At NTV, power consumed is always very low for any number of stages for any aspect ratio used in the design.

Clearly seen from the graphs, it can easily be confirmed that power consumption in the same type of circuit is increased when the number of logical stages are increased i.e. the number of devices increased. But at NTV, the power consumption is always low and switching of devices also stay within normal limits. To further analysis about power consumption where few necessary circuits are found to determine minimum and maximum power values. In 3X ring oscillator power consumption has increased by approximately 480 times starting from NTV to VDD = 5V. In 11X ring oscillator the power consumption has increased by approximately 470 times. The table 3 below shows the power reduction ratio by different designed circuits at NTV driven by the voltage regulation circuit.

Table 3: Power reduction ratio of designed circuits of multiple stages

Designed Circuits	Power consumed in multiple terms
Voltage Controlled Oscillator	284X – 480X
Ring Oscillator	470X - 480X
Current Mirror Circuit	37X – 38X

Chip Layout Considerations:

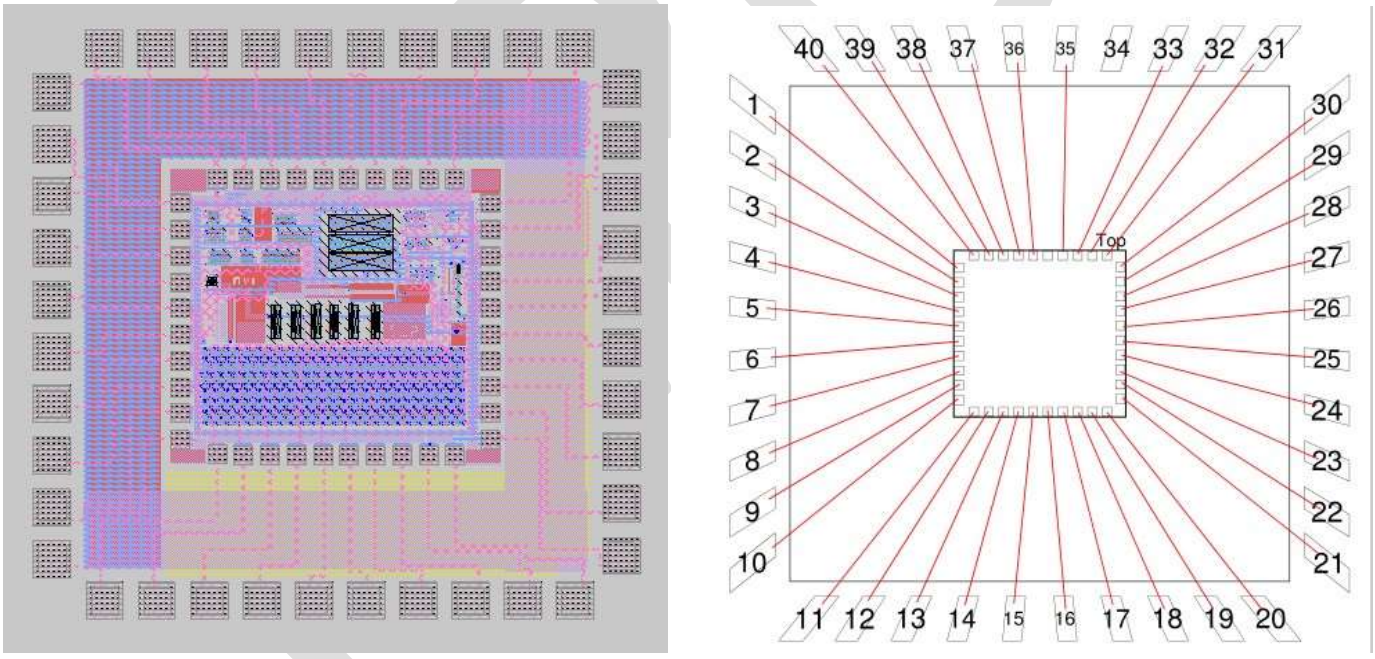

(a) (b)

Figure 12: **Layout of the NTV Voltage Regulation SoC (a) and IC Pad wire bonding diagram (b).**

In figure 12, the test chip design for the NTV SoC of AMI C5N process, currently under fabrication, had considered these:

Total area of the chip = 1500um X 1500um = 2.25sq-mm

Outer pad area = 90um X 90um

Inner pad area = 45 um X 45um

Min. pad interspace = 30um

Scribe line width = 60um

ACKNOWLEDGMENT

The authors would like to thank the UTSA_OCI team for their encouragements and systematic supports for the new idea and explore effective application of the voltage regulation techniques at NTV for proving the concepts and successfully design the manufacture-able chip. This technology is currently under process of filing for a patent at USPTO through UTSA_OCI.

CONCLUSION

The presented analysis shows that the power consumption in circuits is low at NTV and slightly more than NTV where switching occurs at normal speed without affecting the circuit characteristics. The desired output is achieved by variation in number of stages of circuits and different aspect ratio of width and length of transistors showing that power consumption is also dependent upon these 2 factors as well. The circuits are simulated for values of voltages from NTV to VDD and found that energy improved is up to 480 times at NTV region. Therefore, Instead of operating circuit at VDD the device can operate at NTV regions, but must ensure the normal operations. For voltage regulation as well it is found that confidence of reliability is 95% for wide range of current load. The analysis provides guidelines for operating device at NTV and also provides proof for reduction in power consumption. Initial idea of a type of voltage regulation is placed for the study purposes in the chip for further understanding of the system behavior running under this NTV technology.

The chip is designed to carry out further simulation as part of hardware for tests in future. The chip has analog as well as digital circuits simulated for results have been analyzed. The chip will be used for different upcoming educational projects towards the NTV technology for the future.

REFERENCES:

[1] Encyclopedia: http://www.pcmag.com/encyclopedia/term/47244/mosfet.

[2] Dreslinksi, R.Jr. near Threshold Computing: From Single Core to Core Many-Core Energy Efficient Architectures, Doctor of Philosophy. The University of Michigan, Michigan. 2011.

[3] Maini, A.K. Chapter 5: Logic Families: Digital Electronics Principals Devices and Applications, John Wily & Sons, West Sussex, England, 2007.

[4]Sedra, A.; Smith, K.C. Chapter 8: Differential and Multistage Amplifiers. Microelectronics Circuits, 7thed, The Oxford University Press, Oxford, United Kingdom, 2009.

[5] Electronics Cooling. Available Online: http://www.electronics-cooling.com/2000/01/the-history-of-power-dissipation/(1/11/2013).

[6] Texas Instruments. Available Online: http://www.ti.com/lit/an/scaa035b/scaa035b.pdf (10/06/2015).

[7]Shauly, E.N. CMOS Leakage and Power Reduction in Transistors and Circuits: Process and Layout Considerations, Journal of Low Power Electronics and Applications, ISSN 2079-9268, 2012.

[8] Dave, M.; Binzaid. S.; Bhalla, A.; Guo, R. Validation of Near Threshold Voltage (NTV) Performance at Channels of N- and P-Channel Materials in AMI C5N Si-MOS Process, Conference of INAMM, Texas, USA. 2014.

[9] Kaul, M.; Anders, M.; Hsu, S.; Agarwal, A.; Krishnamurthy, R.; Borkar, S. Near-Threshold Voltage (NTV) Design—Opportunities and Challenges, Design Automation Conference, IEEE, pp. 1149 – 1154, 2012.

[10] Dreslinski, R.G.; Wieckowski, M.; Blaauw, D.; Sylvester, D. Near-Threshold Computing: Reclaiming Moore's Law through Energy Efficient Integrated Circuits. Journal of Process, IEEE, pp. 0018-9219, 2010.

[11] University of Southern California, Magic Tutorial 2: Hierarchical, (2006).

[12] Shizhen, H.; Wei, L.; Yutong, W.; Li, Z. Design of A Voltage –Controlled Ring Oscillator Based On MOS Capacitance. Proceedings of the International MultiConference of Engineers and Computer Scientists. 2009 Vol II, IMECS, 2009.

[13] Jovanovic, G.; Stoj ´ cev, M.; Stamenkovic, Z. CMOS Voltage Controlled Ring Oscillator with Improved Frequency Stability. Scientific Publications of the State University of Novi Pazar Ser. A: Appl. Math. Inform. And Mech. vol. 2, 1, pp. 1-9, 2010.

International Journal of Engineering Research and general science is an open access peer review publication which is established for publishing the latest trends in engineering and give priority to quality papers which emphasis on basic and important concept through which there would be remarkable contribution to the research arena and also publish the genuine research work in the field of science, engineering and technologies

International Journal Of Engineering Research and General Science
ISSN 2091 - 2730